ATMOSPHERIC AND OCEANIC FLUID DYNAMICS

FUNDAMENTALS AND LARGE-SCALE CIRCULATION

Geoffrey K. Vallis

ATMOSPHERIC AND OCEANIC FLUID DYNAMICS

Fundamentals and Large-Scale Circulation

Geoffrey K. Vallis

Last updated on September 28, 2005.

The cover is a photograph from space of eddies in the Oyashio Current. the western boundary current of the North Pacific subpolar gyre, off the Kamchatka Peninsula, in March, 1992. The flow is baroclinically unstable, and sea-ice provides flow visualization. Snow cover (white) covers the thicker ice flows just to the right of the center of the image. Courtesy of NASA.

Contents

An asterisk indicates more advanced, but usually uncontroversial, material that may be omitted on a first reading. A dagger indicates material that is still a topic of research or that is not settled. *Caveat emptor.*

We must be ignorant of much, if we would know anything.
Cardinal John Newman (1801–1890).

Preface

THESE ARE MY INCOMPLETE NOTES on the fluid dynamics of the atmosphere and ocean, which is part of the larger field of geophysical fluid dynamics (GFD). It is an incomplete draft, it almost certainly contains errors, and many sources are not properly referenced. There are four parts to the book: basic GFD (chapters 1–5); waves, instabilities and turbulence (chaps 6–10); atmospheric circulation (chaps 11–13); and ocean circulation (chaps 14–16). The concentration in these notes is on the fluid dynamics relevant to the large-scale, extra-tropical general circulation of the atmosphere and ocean, typically involving scales of motion at and larger than the first baroclinic radius of deformation. Furthermore, the chapters on the circulation focus on the steady and statistically steady circulation and perforce a number of important topics are omitted — climate variability, equatorial phenomena, the spin-up of the ocean circulation, the quasi-biennial oscillation. Thus, although the book may appear rather large it is focussed on a limited and hopefully coherent range of material.

I have tried to keep the overall treatment of topics as straightforward and as clear as possible and in practice this means that the level should be appropriate for graduate students. There is a fair amount of repetition in these notes, and some (but not all) of this will be cleaned up as things progress. However, I think that some books have too *little* repetition, so that important things appear once, just like many unimportant things. Repetition can serve both to emphasize the important things, and to keep chapters and sections reasonably self-contained so the reader can jump around if s/he wishes. Obviously the chapters are intellectually linked — for example, heat transport in the atmosphere depends on baroclinic instability, but hopefully the reader already familiar with the latter will be able to read about the former without too much cross-referencing, and will regard the repetition that is present as a 'feature' and not a 'bug'!

The treatment generally is fairly physical and phenomenological, and rigour in the mathematical sense is absent — we treat the derivatives of integrals and of infinitesimal quantities rather informally, for example. An asterisk, *, next to a section means that

it may be omitted on first reading; it may be a little more advanced and is not essential for most of the subsequent material. A dagger, †, next to section means that the section discusses topics of research and may be controversial or even wrong. Roughly speaking, an asterisk typically indicates there is more advanced *manipulation* of the equations, whereas a dagger typically indicates there is *approximation* of the equations. If the asterisk or dagger is applied to a section it applies to all the subsections within. and if a dagger or asterisk appears within a section that is already so-marked, the warnings are even more emphatic. Problems marked with diamonds may be difficult, and I do not know the solutions to all of them. Good answers to some of them are probably publishable and I would appreciate hearing about any such work. Qui docet discit.

Please send your comments, questions and criticism to me at gkv@princeton.edu.

Acknowledgements

NOTATION

Mathematical style generally follows ISO standard practice, as described for example by Beccari (1999). Variables are normally set in italics, differential operators in roman, vectors in bold italics, and tensors in slanting sans serif. A subscripts denotes a derivative only if the subscript is a coordinate, such as x, y or z; a subscript 0 generally denotes a constant reference value (e.g., ρ_0). The components of a vector are denoted by superscripts. The list below contains only the more important variables, or instances of non-obvious notation. Distinct meanings are separated with a semi-colon.

Variable	Description
x, y, z	Cartesian coordinates, usually in zonal, meridional and vertical directions
t	Time
ϑ, λ	Latitude, longitude
$\mathbf{i}, \mathbf{j}, \mathbf{k}$	Unit vectors in (x, y, z) directions
p	Pressure
Z	Log-pressure, $-H \log p/p_0$
L, H	Horizontal length scale, vertical (height) scale
S	Salinity; source term on right-hand side of evolution equation
T	Temperature
θ	Potential temperature
ϕ	Pressure divided by density, p/ρ; passive tracer
b	Buoyancy, $-g\delta\rho/\rho_0$ or $-g\theta'/\theta_0$
u, v, z	Components of velocity in x, y, z or λ, ϑ, z directions
$\boldsymbol{v}$	Three-dimensional velocity, (u, v, z)
$\boldsymbol{u}$	Two-dimensional, horizontal velocity (u, v)
$\boldsymbol{\omega}$	Vorticity
ζ	Vertical component of vorticity
ψ	Streamfunction
m	Angular momentum about the earth's axis of rotation
$\Omega, \boldsymbol{\Omega}$	Rotation rate of earth and associated vector
f, f_0	Coriolis parameter, and its reference value
β	Rate of change of f with latitude, $\partial f/\partial y$
β_T, β_S	Coefficient of expansion with respect to temperature, salinity
N	Buoyancy, or Brunt-Väisälä, frequency
Q	Potential vorticity (in particular Ertel PV)
q	Quasi-geostrophic potential vorticity
$\dot{Q}$	Rate of heating
$\boldsymbol{\mathcal{F}}$	Eliassen Palm flux, $(\mathcal{F}^y, \mathcal{F}^z)$
$\mathcal{A}$	Wave activity
$\boldsymbol{\tau}$	Wind stress
τ	Zonal component or magnitude of wind stress; eddy turnover time
α	Inverse density, or specific volume
ρ	Density
ρ_θ	Potential density

Variable	Description
Re	Real part of expression; Reynolds number, UL/ν
Ra	Rayleigh number
Ro	Rossby number, U/fL
Pr	Prandtl ratio, f_0/N
h	Layer thickness (in shallow water equations)
σ	Layer thickness (in isentropic coordinates); Prandtl number
η	Specific entropy; perturbation height; enstrophy cascade or dissipation rate
$\boldsymbol{c}_g$	group velocity, (c_g^x, c_g^y, c_g^z)
c_p, c_v	Heat capacities at constant pressure and volume
g	Acceleration due to gravity
ν	Kinematic viscosity
v	Meridional component of velocity
κ	Diffusivity; the ratio R/c_p
γ	Vorticity gradient, $\beta - u_{yy}$; the ratio c_p/c_v
ϵ	Generic small parameter ('epsilon')
ε	Cascade or dissipation rate of energy ('varepsilon')
$\mathcal{K}$	Kolmogorov or Kolomogorov-like constant
$\left(\dfrac{\partial a}{\partial b}\right)_c$	Derivative of a with respect to b at constant c.
$\dfrac{\partial a}{\partial b}\bigg|_{a=c}$	Derivative of a with respect to b evaluated at $a = c$.
∇_z	Gradient operator at constant value of z, $\mathbf{i}\,\partial_x + \mathbf{j}\,\partial_y$, and similarly for ∇_x, ∇_y
$\nabla_z\cdot$	Divergence operator at constant value of z, i.e., $\partial_x + \partial_y$, and similarly for $\nabla_x\cdot, \nabla_y\cdot$
curl_z	Vertical component of $\nabla\times$ operator, $\mathrm{curl}_z A = \mathbf{k}\cdot\nabla\times A = \partial_x A^y - \partial_y A^x$
$\dfrac{\mathrm{D}}{\mathrm{D}t}$	Material derivative (generic)
$\dfrac{\mathrm{D}_3}{\mathrm{D}t}$	Material derivative in three dimensions, for example $\partial/\partial t + \boldsymbol{v}\cdot\nabla$.
$\dfrac{\mathrm{D}_2}{\mathrm{D}t}$	Material derivative in two dimensions, for example $\partial/\partial t + \boldsymbol{u}\cdot\nabla$.
$\dfrac{\mathrm{D}_g}{\mathrm{D}t}$	Material derivative using geostrophic velocity, for example $\partial/\partial t + \boldsymbol{u}_g\cdot\nabla$.

FUNDAMENTALS OF GEOPHYSICAL FLUID DYNAMICS

Are you sitting comfortably? Then I'll begin.
Julia Lang, *Listen With Mother,* BBC radio program, 1950–1982.

CHAPTER 1

Equations of Motion

T HIS CHAPTER establishes the fundamental governing equations of motion for a fluid, with particular reference to the fluids of the earth's atmosphere and ocean.[1] Our approach in many places is quite informal, and the treatment of the standard topics of viscosity and pressure is quite brief.

1.1 TIME DERIVATIVES FOR FLUIDS

The equations of motion of fluid mechanics differ from those of rigid-body mechanics because fluids form a continuum, and because fluids flow and deform. Thus, even though both classical solid and fluid media are governed by the same relatively simple physical laws (Newton's laws and the laws of thermodynamics), the expression of these laws differs between the two. To determine the equations of motion for fluids we must clearly establish what the time derivative of some property of a fluid actually means, and that is the subject of this section.

1.1.1 Field and material viewpoints

In solid-body mechanics one is normally concerned with the position and momentum of identifiable objects — the angular velocity of a spinning top or the motions of the planets around the sun are two well-worn examples. The position and velocity of a particular object is then computed as a function of time by formulating equations of the general form

$$\frac{\mathrm{d}x_i}{\mathrm{d}t} = F(\{x_i\}, t) \tag{1.1}$$

where $\{x_i\}$ is the set of positions and velocities of all the interacting objects and the operator F on the right-hand side is formulated using Newton's laws of motion. For

example, two massive point objects interacting via their gravitational field obey

$$\frac{\mathrm{d}\boldsymbol{r}_i}{\mathrm{d}t} = \boldsymbol{v}_i, \quad \frac{\mathrm{d}\boldsymbol{v}_i}{\mathrm{d}t} = -\frac{Gm_j}{(\boldsymbol{r}_i - \boldsymbol{r}_j)^2}\widehat{\boldsymbol{r}}_{i,j}, \qquad i = 1, 2; \; j = 3 - i. \qquad (1.2)$$

We thereby predict the positions, $\boldsymbol{r}_i$ and velocities, $\boldsymbol{v}_i$ of the objects given their masses, m_i and the gravitational constant G, and where $\widehat{\boldsymbol{r}}_{i,j}$ is a unit vector directed from $\boldsymbol{r}_i$ to $\boldsymbol{r}_j$.

In fluid dynamics such a procedure would lead to an analysis of fluid motions in terms of the positions and momenta of particular fluid elements, each identified by some label, which might simply be their position at an initial time. We call this a *material* point of view, because we are concerned with identifiable pieces of material; it is also sometimes called a *Lagrangian* view (after J.-L. Lagrange). The procedure is perfectly acceptable in principle, and if followed would provide a complete description of the fluid dynamical system. However, from a practical point of view it is much more than we need, and it would be extremely complicated to implement. Instead, for most problems we would like to know what the values of velocity, density and so on are at *fixed points* in space as time passes. (A weather forecast we might care about tells us how warm it will be where we live, and if we are given that we don't particularly care where a fluid parcel comes from.) Since the fluid is a continuum, this knowledge is equivalent to knowing how the fields of the dynamical variables evolve in space and time, and this is often known as the *field* or *Eulerian* viewpoint (after L. Euler).[2] Thus, whereas in the material view we consider the time evolution of identifiable fluid elements, in the field view we consider the time evolution of the fluid field from a particular frame of reference. That is, we seek evolution equations of the form

$$\frac{\partial}{\partial t}\phi(x, y, z, t) = F, \qquad (1.3)$$

where the field $\phi(x, y, z, t)$ is a dynamical variable (e.g., velocity, density, temperature) which gives the value at any point in space-time, and F is some operator to be determined from Newton's laws of motion and appropriate thermodynamic laws.

Although the field viewpoint will turn out to be the most practically useful, the material description is invaluable both in deriving the equations and in the subsequent insight it frequently provides. This is because the important quantities from a fundamental point of view are often those which are associated with a given fluid element: it is these which directly enter Newton's laws of motion and the thermodynamic equations. It is thus important to have a relationship between the rate of change of quantities associated with a given fluid element and the local rate of change of a field. The material or advective derivative provides this relationship.

1.1.2 The material derivative of a fluid element

A *fluid element* is an infinitesimal, indivisible, piece of fluid — effectively a very small fluid parcel. The material derivative is the rate of change of a property (such as temperature, or momentum) of a particular fluid element. It is also known as the 'substantive

derivative' (the derivative associated with a parcel of fluid substance), the 'advective derivative' (because the fluid property is being advected), the 'convective derivative' (convection is a slightly old-fashioned name for advection, still used in some fields), or the 'Lagrangian derivative'. It is just the total time derivative of a property of a piece of fluid.

Let us suppose that a fluid is characterized by a (given) velocity field $\boldsymbol{v}(\boldsymbol{x}, t)$, which determines its velocity throughout. Let us also suppose that it has another property ϕ, and let us seek an expression for the rate of change of ϕ of a fluid element. Since ϕ is changing in time and in space we use the chain rule:

$$\delta\phi = \frac{\partial\phi}{\partial t}\delta t + \frac{\partial\phi}{\partial x}\delta x + \frac{\partial\phi}{\partial y}\delta y + \frac{\partial\phi}{\partial z}\delta z = \frac{\partial\phi}{\partial t}\delta t + \delta\boldsymbol{x}\cdot\nabla\phi. \qquad (1.4)$$

This is true in general for any δt, δx, etc. Thus the total time derivative is

$$\frac{\mathrm{d}\phi}{\mathrm{d}t} = \frac{\partial\phi}{\partial t} + \frac{\mathrm{d}\boldsymbol{x}}{\mathrm{d}t}\cdot\nabla\phi. \qquad (1.5)$$

If this is to be a material derivative we must identify the time derivative in the second term on the right-hand side with the rate of change of position of a fluid element, namely its velocity. Hence, the material derivative of the property ϕ is

$$\frac{\mathrm{d}\phi}{\mathrm{d}t} = \frac{\partial\phi}{\partial t} + \boldsymbol{v}\cdot\nabla\phi. \qquad (1.6)$$

The right-hand side expresses the material derivative in terms of the local rate of change of ϕ ($\partial\phi/\partial t$), and a contribution arising from the spatial variation of ϕ, experienced only as the fluid parcel moves. Because the material derivative is so common, and to distinguish it from other derivatives, we denote it by the operator $\mathrm{D}/\mathrm{D}t$. Thus, the material derivative of the field ϕ is

$$\boxed{\frac{\mathrm{D}\phi}{\mathrm{D}t} = \frac{\partial\phi}{\partial t} + (\boldsymbol{v}\cdot\nabla)\phi}. \qquad (1.7)$$

The brackets in the last term of this equation are helpful in reminding us that $(\boldsymbol{v}\cdot\nabla)$ is an operator acting on ϕ.

Material derivative of vector field

The material derivative may act on a vector field $\boldsymbol{b}$, in which case

$$\frac{\mathrm{D}\boldsymbol{b}}{\mathrm{D}t} = \frac{\partial\boldsymbol{b}}{\partial t} + (\boldsymbol{v}\cdot\nabla)\boldsymbol{b}. \qquad (1.8)$$

In Cartesian coordinates this is

$$\frac{\mathrm{D}\boldsymbol{b}}{\mathrm{D}t} = \frac{\partial\boldsymbol{b}}{\partial t} + u\frac{\partial\boldsymbol{b}}{\partial x} + v\frac{\partial\boldsymbol{b}}{\partial y} + w\frac{\partial\boldsymbol{b}}{\partial z}, \qquad (1.9)$$

and for a particular component of $\boldsymbol{b}$,

$$\frac{\mathrm{D}b_x}{\mathrm{D}t} = \frac{\partial b_x}{\partial t} + u\frac{\partial b_x}{\partial x} + v\frac{\partial b_x}{\partial y} + w\frac{\partial b_x}{\partial z}, \tag{1.10}$$

or, in Cartesian tensor notation,

$$\frac{\mathrm{D}b_i}{\mathrm{D}t} = \frac{\partial b_i}{\partial t} + v_j\frac{\partial b_i}{\partial x_j} = \frac{\partial b_i}{\partial t} + v_j\partial_j b_i. \tag{1.11}$$

where the subscripts denote the Cartesian components and repeated indices are summed. In coordinate systems other than Cartesian the advective derivative of a vector is not simply the sum of the advective derivative of its components, because the coordinate vectors change direction with position; this will be important when we deal with spherical coordinates (and see problem 2.5). Finally, we note that the advective derivative of the position of a fluid element, $\boldsymbol{r}$ say, is its velocity, and this may easily checked by explicitly evaluating $\mathrm{D}\boldsymbol{r}/\mathrm{D}t$.

1.1.3 Material derivative of a finite volume

The volume that a given, unchanging, mass of fluid occupies is deformed and advected by the fluid motion, and there is no particular reason why it should remain constant. Indeed, the volume will change as a result of the movement of each element of its bounding material surface, and will in general change if there is a non-zero normal component of the velocity at the fluid surface. That is, if the volume of some fluid is $\int \mathrm{d}V$, then

$$\frac{\mathrm{D}}{\mathrm{D}t}\int_V \mathrm{d}V = \int_S \boldsymbol{v}\cdot\mathrm{d}\boldsymbol{S}, \tag{1.12}$$

where the subscript V indicates that the integral is a definite integral over some finite volume V, although the limits of the integral will be functions of time if the volume is changing. The integral on the right-hand side is over the closed surface, S, bounding the volume. Although intuitively apparent (to some), this expression may be derived more formally using Leibnitz's formula for the rate of change of an integral whose limits are changing (problem 1.2). Using the divergence theorem on the right-hand side, (1.12) becomes

$$\frac{\mathrm{D}}{\mathrm{D}t}\int_V \mathrm{d}V = \int_V \nabla\cdot\boldsymbol{v}\,\mathrm{d}V. \tag{1.13}$$

The rate of change of the volume of an infinitesimal fluid element of volume ΔV is obtained by taking the limit of this expression as the volume tends to zero, giving

$$\lim_{\Delta V\to 0}\frac{1}{\Delta V}\frac{\mathrm{D}\Delta V}{\mathrm{D}t} = \nabla\cdot\boldsymbol{v}. \tag{1.14}$$

We will often write such expressions informally as

$$\frac{\mathrm{D}\Delta V}{\mathrm{D}t} = \Delta V\nabla\cdot\boldsymbol{v}, \tag{1.15}$$

with the limit implied.

Consider now the material derivative of a property, ϕ, of an infinitesimal fluid element; that is, ϕ is the amount per unit volume of $\phi-$stuff — it might, for example, be mass density or density of a dye, per unit volume, in a fluid, and ϕ might be a vector. Then we have

$$\frac{\mathrm{D}}{\mathrm{D}t}(\phi \Delta V) = \phi \frac{\mathrm{D}\Delta V}{\mathrm{D}t} + \Delta V \frac{\mathrm{D}\phi}{\mathrm{D}t}. \qquad (1.16)$$

Using (1.15) this becomes

$$\frac{\mathrm{D}}{\mathrm{D}t}(\phi \Delta V) = \Delta V \left(\phi \nabla \cdot \boldsymbol{v} + \frac{\mathrm{D}\phi}{\mathrm{D}t} \right), \qquad (1.17)$$

and the analogous result for a finite fluid volume is just

$$\frac{\mathrm{D}}{\mathrm{D}t} \int_V \phi \, \mathrm{d}V = \int_V \left(\phi \nabla \cdot \boldsymbol{v} + \frac{\mathrm{D}\phi}{\mathrm{D}t} \right) \mathrm{d}V. \qquad (1.18)$$

This expression is to be contrasted with the Eulerian derivative for which the volume, and so the limits of integration, are fixed and we have

$$\frac{\mathrm{d}}{\mathrm{d}t} \int_V \phi \, \mathrm{d}V = \int_V \frac{\partial \phi}{\partial t} \, \mathrm{d}V. \qquad (1.19)$$

Now consider the material derivative of the integral of fluid property χ multiplied by the mass density, ρ. This arises, for example, in the derivation of the momentum equation, where the momentum of a fluid element is $\rho \boldsymbol{v} \Delta V$. In general the material derivative of $\chi \rho \Delta V$ is given by

$$\frac{\mathrm{D}}{\mathrm{D}t}(\chi \rho \Delta V) = \rho \Delta V \frac{\mathrm{D}\chi}{\mathrm{D}t} + \chi \frac{\mathrm{D}}{\mathrm{D}t}(\rho \Delta V) \qquad (1.20)$$

But $\rho \Delta V$ is just the mass of the fluid element, and that is constant — it is how a fluid element is defined. Thus the second term on the right-hand side vanishes and

$$\frac{\mathrm{D}}{\mathrm{D}t}(\chi \rho \Delta V) = \rho \Delta V \frac{\mathrm{D}\chi}{\mathrm{D}t} \qquad \text{and} \qquad \frac{\mathrm{D}}{\mathrm{D}t} \int_V \chi \rho \, \mathrm{d}V = \int_V \rho \frac{\mathrm{D}\chi}{\mathrm{D}t} \, \mathrm{d}V, \qquad (1.21\text{a,b})$$

where (1.21b) applies to a finite volume. That expression may also be derived more formally using Leibnitz's formula for the material derivative of an integral, and the result also holds when χ is a vector. The result is quite different from the corresponding Eulerian derivative, in which the volume is kept fixed; in that case we have:

$$\frac{\mathrm{d}}{\mathrm{d}t} \int_V \chi \rho \, \mathrm{d}V = \int_V \frac{\partial}{\partial t}(\chi \rho) \, \mathrm{d}V. \qquad (1.22)$$

Various material and Eulerian derivatives are summarized in the shaded box on the following page.

Material and Eulerian Derivatives

The material derivative of a scalar (ϕ) and a vector ($\boldsymbol{b}$) field are given by:

$$\frac{\mathrm{D}\phi}{\mathrm{D}t} = \frac{\partial \phi}{\partial t} + \boldsymbol{v} \cdot \nabla \phi, \qquad \frac{\mathrm{D}\boldsymbol{b}}{\mathrm{D}t} = \frac{\partial \boldsymbol{b}}{\partial t} + (\boldsymbol{v} \cdot \nabla)\boldsymbol{b}. \qquad \text{(D.1)}$$

Various material derivatives of integrals are:

$$\frac{\mathrm{D}}{\mathrm{D}t} \int_V \phi \, \mathrm{d}V = \int_V \left(\frac{\mathrm{D}\phi}{\mathrm{D}t} + \phi \nabla \cdot \boldsymbol{v} \right) \mathrm{d}V = \int_V \left(\frac{\partial \phi}{\partial t} + \nabla \cdot (\phi \boldsymbol{v}) \right) \mathrm{d}V, \quad \text{(D.2)}$$

$$\frac{\mathrm{D}}{\mathrm{D}t} \int_V \mathrm{d}V = \int_V \nabla \cdot \boldsymbol{v} \, \mathrm{d}V, \qquad \text{(D.3)}$$

$$\frac{\mathrm{D}}{\mathrm{D}t} \int_V \rho \phi \, \mathrm{d}V = \int_V \rho \frac{\mathrm{D}\phi}{\mathrm{D}t} \, \mathrm{d}V. \qquad \text{(D.4)}$$

These formulae also hold if ϕ is a vector. The Eulerian derivative of an integral is:

$$\frac{\mathrm{d}}{\mathrm{d}t} \int_V \phi \, \mathrm{d}V = \int_V \frac{\partial \phi}{\partial t} \, \mathrm{d}V, \qquad \text{(D.5)}$$

so that

$$\frac{\mathrm{d}}{\mathrm{d}t} \int_V \mathrm{d}V = 0 \quad \text{and} \quad \frac{\mathrm{d}}{\mathrm{d}t} \int_V \rho \phi \, \mathrm{d}V = \int_V \frac{\partial \rho \phi}{\partial t} \, \mathrm{d}V. \qquad \text{(D.6)}$$

1.2 THE MASS CONTINUITY EQUATION

In classical mechanics mass is absolutely conserved, and in solid-body there is usually no need for any separate equation to explicitly describe its effects. However, in fluid mechanics fluid flows into and away from regions, and fluid density may change, and an equation that explicitly accounts for the flow of mass is one of the 'equations of motion' of the fluid.

1.2.1 An Eulerian derivation

We will first derive the mass conservation equation from an Eulerian point of view; that is to say, our reference frame is fixed in space and the fluid flows through it. First we give an elementary derivation in Cartesian coordinates (refer to Fig. 1.1). Consider the infinitesimal, rectangular parallelepiped, control volume $\delta V = \delta x \delta y \delta z$ that is fixed in space. Fluid moves into or out of the volume through its surface S, including through its face in y–z plane, of area $\delta A = \delta y \delta z$ at coordinate x. The fluid flow through this
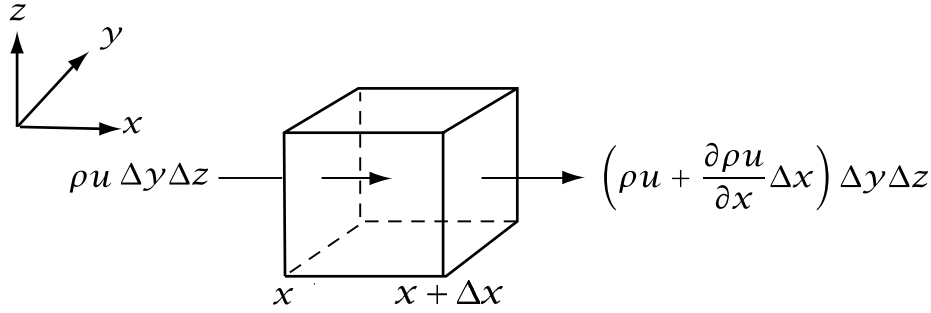
Fig. 1.1 Mass conservation in a cubic Eulerian control volume.

face, into the control volume, is

$$(\rho u)_x \times \text{Area} = (\rho u)_x \delta y \delta z \tag{1.23}$$

where u is the component of velocity in the x-direction, and the subscript x here denotes the coordinate of the argument. A small distance to the right the flow out of the control volume is

$$(\rho u)_{x+\delta x} \delta y \delta z. \tag{1.24}$$

Thus, the accumulation of fluid within the control volume, due to motion in the x-direction only, is

$$\delta y \delta z[(\rho u)_x - (\rho u)_{x+\delta x}] = -\frac{\partial(\rho u)}{\partial x}\delta x \delta y \delta z. \tag{1.25}$$

To this must be added the effects of motion in the y- and z-directions, namely

$$-\left[\frac{\partial(\rho v)}{\partial y} + \frac{\partial(\rho w)}{\partial z}\right]\delta x \delta y \delta z. \tag{1.26}$$

This net accumulation of fluid must be accompanied by a corresponding increase of fluid mass within the control volume. This is

$$\frac{\partial}{\partial t}(\text{Density} \times \text{Volume}) = \delta x \delta y \delta z \frac{\partial \rho}{\partial t}, \tag{1.27}$$

because the volume is constant. Thus, because mass is conserved, (1.25), (1.26) and (1.27) give

$$\delta x \delta y \delta z \left[\frac{\partial \rho}{\partial t} + \frac{\partial(\rho u)}{\partial x} + \frac{\partial(\rho v)}{\partial y} + \frac{\partial(\rho w)}{\partial z}\right] = 0. \tag{1.28}$$

Because the control volume is arbitrary the quantity in square brackets must be zero zero and we have the *mass continuity equation:*

$$\frac{\partial \rho}{\partial t} + \nabla \cdot (\rho \boldsymbol{v}) = 0. \tag{1.29}$$

$$\text{Fluid loss} = \int_S \rho \boldsymbol{v} \cdot \mathrm{d}\boldsymbol{S}$$

$$= \int_V \nabla \cdot (\rho \boldsymbol{v}) \, \mathrm{d}V$$

Surface element
points outward

Mass increase

$$= \int_V \frac{\partial \rho}{\partial t} \, \mathrm{d}V$$

Figure 1.2 Mass conservation in an arbitrary Eulerian control volume V bounded by a surface S. The mass gain, $\int_V (\partial \rho / \partial t) \, \mathrm{d}V$ is equal to the mass flowing into the volume, $-\int_S (\rho \boldsymbol{v}) \cdot \mathrm{d}\boldsymbol{S} = -\int_V \nabla \cdot (\rho \boldsymbol{v}) \, \mathrm{d}V$.
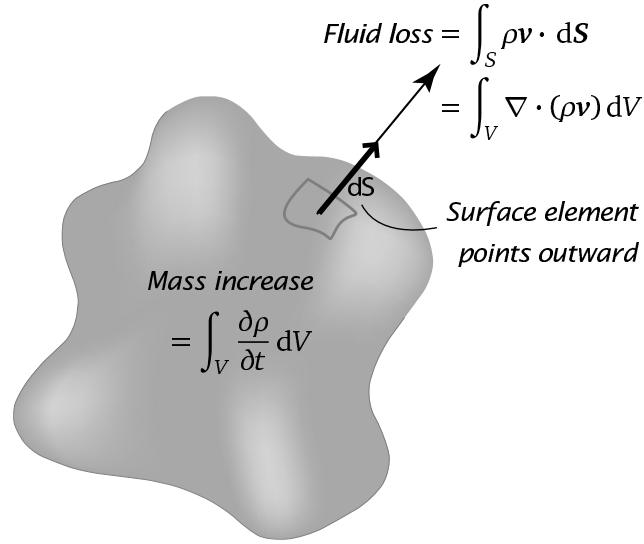
Vector derivation

Consider an arbitrary control volume V bounded by a surface S, fixed in space, with by convention the direction of $\boldsymbol{S}$ being toward the outside of V, as in Fig. 1.2. The rate of fluid loss due to flow through the closed surface S is then given by

$$\text{Fluid loss} = \int_S \rho \boldsymbol{v} \cdot \mathrm{d}\boldsymbol{S} = \int_V \nabla \cdot (\rho \boldsymbol{v}) \, \mathrm{d}V \tag{1.30}$$

using the divergence theorem. This must be balanced by a change in the mass M of the fluid within the control volume, which, since its volume is fixed, implies a density change. That is

$$\text{Fluid loss} = -\frac{\mathrm{d}M}{\mathrm{d}t} = -\frac{\mathrm{d}}{\mathrm{d}t} \int_V \rho \, \mathrm{d}V = -\int_V \frac{\partial \rho}{\partial t} \, \mathrm{d}V. \tag{1.31}$$

Equating (1.30) and (1.31) yields

$$\int_V \left[\frac{\partial \rho}{\partial t} + \nabla \cdot (\rho \boldsymbol{v}) \right] \mathrm{d}V = 0 \tag{1.32}$$

Again, because the volume is arbitrary, the integrand must vanish and we recover (1.29).

1.2.2 Mass continuity via the material derivative

We now derive the mass continuity equation (1.29) from a material perspective. This is the most fundamental approach of all since the principle of mass conservation states simply that the mass of a given element of fluid is, by definition of the element, constant. Thus, consider a small mass of fluid of density ρ and volume ΔV. Then conservation of mass may be represented by

$$\frac{\mathrm{D}}{\mathrm{D}t} (\rho \Delta V) = 0 \tag{1.33}$$

Both the density and the volume of the parcel may change, so

$$\Delta V \frac{\mathrm{D}\rho}{\mathrm{D}t} + \rho \frac{\mathrm{D}\Delta V}{\mathrm{D}t} = \Delta V \left(\frac{\mathrm{D}\rho}{\mathrm{D}t} + \rho \nabla \cdot \boldsymbol{v} \right) = 0 \qquad (1.34)$$

where the second expression follows using (1.15). Since the volume element is arbitrary, the term in brackets must vanish and

$$\frac{\mathrm{D}\rho}{\mathrm{D}t} + \rho \nabla \cdot \boldsymbol{v} = 0. \qquad (1.35)$$

After expansion of the first term this becomes identical to (1.29). This result may be derived more formally by re-writing (1.33) as the integral expression

$$\frac{\mathrm{D}}{\mathrm{D}t} \int_V \rho \, \mathrm{d}V = 0. \qquad (1.36)$$

Expanding the derivative using (1.18) gives

$$\frac{\mathrm{D}}{\mathrm{D}t} \int_V \rho \, \mathrm{d}V = \int_V \left(\frac{\mathrm{D}\rho}{\mathrm{D}t} + \rho \nabla \cdot \boldsymbol{v} \right) \mathrm{d}V = 0. \qquad (1.37)$$

Because the volume over which the integral is taken is arbitrary the integrand itself must vanish and we recover (1.35). Summarizing, equivalent partial differential equation representing conservation of mass are:

$$\boxed{\frac{\mathrm{D}\rho}{\mathrm{D}t} + \rho \nabla \cdot \boldsymbol{v} = 0, \qquad \frac{\partial \rho}{\partial t} + \nabla \cdot (\rho \boldsymbol{v}) = 0} . \qquad (1.38\text{a,b})$$

1.2.3 A general continuity equation

The derivation of continuity equation for a general scalar property of a fluid is similar to that for density, except that there may be an external source or sink, and potentially a means of transferring the property from one location to another than by fluid motion, for example by diffusion. If ϕ is the amount of some property of the fluid per unit volume (commonly known as the *concentration* of that property), and if the net effect per unit volume of all nonconservative processes is denoted by $Q[\phi]$, then the continuity equation for concentration may be written:

$$\frac{\mathrm{D}}{\mathrm{D}t} (\phi \Delta V) = Q[\phi] \Delta V \qquad (1.39)$$

Expanding the left hand side and using (1.15) we obtain

$$\frac{\mathrm{D}\phi}{\mathrm{D}t} + \phi \nabla \cdot \boldsymbol{v} = Q[\phi] \qquad (1.40)$$

or equivalently

$$\frac{\partial \phi}{\partial t} + \nabla \cdot (\phi \boldsymbol{v}) = Q[\phi]. \qquad (1.41)$$

If we are interested in a tracer that is normally measured per unit mass of fluid (which is typical when considering thermodynamic quantities) then the conservation equation would be written

$$\frac{\mathrm{D}}{\mathrm{D}t}(\xi\rho\Delta V) = Q[\xi]\rho\Delta V, \tag{1.42}$$

where ξ is the tracer *mixing ratio* — that is, the amount of tracer per unit fluid mass — and $Q[\xi]$ represents nonconservative sources (per unit mass). Then, since $\rho\Delta V$ is constant we obtain

$$\frac{\mathrm{D}\xi}{\mathrm{D}t} = Q[\xi]. \tag{1.43}$$

The source term $Q[\xi]$ is evidently equal to the rate of change of ξ of a fluid element. When this is so, it is common to write it simply as $\dot{\xi}$, so that

$$\frac{\mathrm{D}\xi}{\mathrm{D}t} = \dot{\xi}. \tag{1.44}$$

A tracer obeying (1.44) with $\dot{\xi} = 0$ is said to be *materially conserved*. If the tracer is materially conserved in the absence of nonconservative sources then it is sometimes said to be 'semi-materially conserved'.

1.3 THE MOMENTUM EQUATION

The momentum equation is a partial differential equation that describes how the velocity or momentum of a fluid responds to internal and imposed forces. We will derive it using material methods and initially without paying any attention to the those forces, and then we will examine the influences of momentum sources, informally deducing the terms representing the pressure, gravitational and viscous forces.

1.3.1 Advection

Let $\boldsymbol{m}(x, y, z, t)$ be the momentum-density field (momentum per unit volume) of the fluid. Thus, $\boldsymbol{m} = \rho\boldsymbol{v}$ and the total momentum of a volume of fluid is given by the volume integral $\int_V \boldsymbol{m}\,\mathrm{d}V$. Now, for a fluid the rate of change of a momentum of an identifiable fluid mass is given by the material derivative, and by Newton's second law this is equal to the force acting on it. Thus,

$$\frac{\mathrm{D}}{\mathrm{D}t}\int_V \rho\boldsymbol{v}\,\mathrm{d}V = \int_V \boldsymbol{F}\,\mathrm{d}V \tag{1.45}$$

Now, using (1.21b) (with χ replaced by $\boldsymbol{v}$) the left-hand side is

$$\frac{\mathrm{D}}{\mathrm{D}t}\int_V \rho\boldsymbol{v}\,\mathrm{d}V = \int_V \rho\frac{\mathrm{D}\boldsymbol{v}}{\mathrm{D}t}\,\mathrm{d}V, \tag{1.46}$$

and (1.45) becomes

$$\int_V \left(\rho\frac{\mathrm{D}\boldsymbol{v}}{\mathrm{D}t} - \boldsymbol{F}\right)\mathrm{d}V = 0. \tag{1.47}$$

Because the volume is arbitrary the integrand itself must vanish and we obtain

$$\rho\frac{\mathrm{D}\boldsymbol{v}}{\mathrm{D}t} = \boldsymbol{F}. \tag{1.48}$$

Expanding the material derivative, this may be written

$$\frac{\partial\boldsymbol{v}}{\partial t} + (\boldsymbol{v}\cdot\nabla)\boldsymbol{v} = \frac{\boldsymbol{F}}{\rho} \tag{1.49}$$

We have thus obtained an expression for how a fluid accelerates if subject to known forces. These forces are however not all external to the fluid itself; a stress arises from the direct contact between one fluid parcel and another, giving rise to pressure and viscous forces, sometimes referred to as *contact* forces. Because a complete treatment of these would be very lengthy, and is available elsewhere, we treat both of these very informally and intuitively.

1.3.2 The pressure force

Within or at the boundary of a fluid the pressure is the normal force per unit area due to the collective action of molecular motion. Thus

$$\mathrm{d}\boldsymbol{F}_p = -p\,\mathrm{d}\boldsymbol{S}. \tag{1.50}$$

where p is the pressure, $\boldsymbol{F}_p$ is the pressure force, and $\mathrm{d}\boldsymbol{S}$ an infinitesimal surface element. If we grant ourselves this intuitive notion, it is a simple matter to assess the influence of pressure on a fluid, for the pressure force on a volume of fluid is the integral of the pressure over the its boundary and so

$$\boldsymbol{F}_p = -\int_S p\,\mathrm{d}\boldsymbol{S}. \tag{1.51}$$

The minus sign arises because the pressure force is directed inward, whereas $\boldsymbol{S}$ is a vector normal to the surface and directed outward. Applying a form of the divergence theorem to the right-hand side gives

$$\boldsymbol{F}_p = -\int_V \nabla p\,\mathrm{d}V \tag{1.52}$$

and so the pressure force per unit volume is just $-\nabla p$. Inserting this into (1.49) we obtain

$$\frac{\partial\boldsymbol{v}}{\partial t} + (\boldsymbol{v}\cdot\nabla)\boldsymbol{v} = -\frac{\nabla p}{\rho} + \boldsymbol{F}' \tag{1.53}$$

where $\boldsymbol{F}'$ includes only viscous and body forces, per unit mass.

Table 1.1 Experimental values of viscosity for air, water and mercury at room temperature and pressure.

	μ (kg m^{-1} s^{-1})	ν (m^2 s^{-1})
Air	$1.8\ 10^{-5}$	$1.5\ 10^{-5}$
Water	$1.1\ 10^{-3}$	$1.1\ 10^{-6}$
Mercury	$1.6\ 10^{-3}$	$1.2\ 10^{-7}$

1.3.3 Viscosity and diffusion

Viscosity, like pressure, is a force due to the internal motion of molecules. The effects of viscosity are apparent in many situations — the flow of treacle or volcanic lava are obvious examples. In other situations, for example large-scale flow the atmosphere, viscosity is to a first approximation negligible. However, for a constant density fluid viscosity is the *only* way that energy may be removed from the fluid, so that if energy is being added in some way viscosity must ultimately become important if the fluid is to reach an equilibrium where energy input equals energy dissipation. When tea is stirred in a cup, viscosity is the mechanism whereby the fluid eventually stops spinning after we have removed our spoon.

A number of textbooks[3] show that, for most Newtonian fluids, the viscous force per unit volume is equal to $\mu \nabla^2 \boldsymbol{v}$, where μ is a coefficient of diffusivity. Although not exact, this is an extremely good approximation for most liquids and gases. With this term, the momentum equation becomes,

$$\frac{\partial \boldsymbol{v}}{\partial t} + (\boldsymbol{v} \cdot \nabla)\boldsymbol{v} = -\frac{1}{\rho}\nabla p + \nu \nabla^2 \boldsymbol{v} \tag{1.54}$$

where $\nu \equiv \mu/\rho$ is the *kinematic viscosity*. For gases, dimensional arguments suggest that the magnitude of ν should be given by

$$\nu \sim \langle \text{mean free path} \times \text{mean molecular velocity} \rangle \tag{1.55}$$

which for a typical molecular velocity of $300\,\text{m s}^{-1}$ and a mean free path of 7×10^{-8} m gives the not unreasonable estimate of $2.1 \times 10^{-5}\,\text{m}^2\,\text{s}^{-1}$, within a factor of two of the experimental value (table 1.1). Interestingly, the kinematic viscosity is less for water and mercury than it is for air.

1.3.4 Hydrostatic balance

The vertical component — meaning the component parallel to the gravitational force — of the momentum equation is

$$\frac{\mathrm{D}w}{\mathrm{D}t} = -\frac{1}{\rho}\frac{\partial p}{\partial z} - g \tag{1.56}$$

where w is the vertical component of the velocity. If the fluid is static the gravitational term is balanced by the pressure term and we have

$$\frac{\partial p}{\partial z} = -\rho g, \tag{1.57}$$

and this is known as *hydrostatic balance.* It is clear that the pressure at a point is given by the weight of the fluid above it, provided $p = 0$ at the top of the fluid. It might also appear that (1.57) would be a good *approximation* to (1.56) provided vertical accelerations, $\mathrm{D}w/\mathrm{D}t$, are small compared to gravity, which is nearly always the case in the atmosphere and ocean. While this statement is true if we need only a reasonably accurate representation of the pressure at a point or in a column, the satisfaction of this condition is not sufficient to ensure that (1.57) provides an accurate enough pressure to determine the *horizontal* pressure gradients responsible for producing motion. We return to this point in section 2.7.

1.4 THE EQUATION OF STATE

In three dimensions the momentum and continuity equations provide four equations, but contain five unknowns — three components of velocity, density and pressure. Obviously other equations are needed, and an *equation of state* relates the various thermodynamic variables to each other. The conventional equation of state is an expression that relates temperature, pressure, composition (salinity), and density, and we may write

$$p = p(\rho, T, S). \tag{1.58}$$

where S is the salinity (see below). An equation of this form is not the most fundamental equation of state from a thermodynamic perspective (an issue we visit later) but it connects readily measurable quantities. For an ideal gas we have

$$p = \rho R T, \tag{1.59}$$

where R is the gas constant for air and T is temperature. (R is related to the universal gas constant R_u by $R = R_u/m$ where m is the mean molecular weight of the constituents of the gas. Also, $R = nk$ where k is Boltzmann's constant and n is the number of molecules per unit mass.) For dry air, $R = 287 \,\mathrm{J\,kg^{-1}\,K^{-1}}$. Air has virtually constant composition, except for variations in water vapour content. A measure of this is the water vapour mixing ratio, $w = \rho_w/\rho_d$ where ρ_w and ρ_d are the densities of water vapour and dry air, respectively, and in the atmosphere w varies between 0 and 0.03. This variation makes the gas constant in the equation of state a weak function of water vapour mixing ratio; that is, $p = \rho R_{\mathrm{eff}} T$ where $R_{\mathrm{eff}} = R_d(1 + wR_v/R_d)/(1 + w)$ where R_d and R_v are the gas constants of dry air and water vapour. Since $w \sim 0.01$ the variation of R_{eff} is quite small and is often ignored, especially in theoretical studies.[4]

For a liquid such as seawater no such analytic expression is easily derivable, and semi-empirical equations are usually resorted to. One complication is the presence of salinity: seawater is in fact a solution of many ions in water — chloride ($\approx 1.9\%$ by weight) sodium (1%), sulfate (0.26%), magnesium (0.13%) and so on, with a total average concentration of about 35‰ (ppt, or parts per thousand). The ratio of the fractions of these salts is more-or-less constant throughout the ocean, and their total concentration may be parameterized by a single measure, the *salinity*, S. Given this, the density of seawater is a function of three variables — pressure, temperature, and salinity. For

pure water in a laboratory setting the temperature effect dominates and a reasonable approximation of the equation of state is

$$\rho = \rho_0[1 - \beta_T(T - T_0)], \tag{1.60}$$

where ρ_0 and T_0 are constant reference values, and β_T is a thermal expansion coefficient. Even for pure water, this equation is only valid for small variations around a reference state — note, for example, that pure water generally expands when heated, but that it contracts as its temperature rises from $0°\,$C to $4°\,$C, so that β_T cannot be constant.

In the ocean both pressure and salinity affect the density of seawater and the conventional equation of state has the general form $\alpha = \alpha(T, S, p)$, where $\alpha = 1/\rho$ is the specific volume and S the salinity. Small variations around a reference value can be obtained by using

$$\begin{aligned}
\mathrm{d}\alpha &= \left(\frac{\partial\alpha}{\partial T}\right)_{S,p}\mathrm{d}T + \left(\frac{\partial\alpha}{\partial S}\right)_{T,p}\mathrm{d}S + \left(\frac{\partial\alpha}{\partial p}\right)_{T,S}\mathrm{d}p \\
&= \alpha(\beta_T\,\mathrm{d}T - \beta_S\,\mathrm{d}S - \beta_p\,\mathrm{d}p),
\end{aligned} \tag{1.61}$$

where the second line serves to define the thermal expansion coefficient β_T, the saline contraction coefficient β_S, and the compressibility coefficient β_p (equal to α divided by the bulk modulus). These are in general not constants, but for small variations around a reference state they may be treated as such and we have

$$\alpha = \alpha_0\left[1 + \beta_T(T - T_0) - \beta_S(S - S_0) - \beta_p(p - p_0)\right]. \tag{1.62}$$

Typical values of these parameters, with variations typically encountered through the ocean, are: $\beta_T \approx 2\,(\pm1.5) \times 10^{-4}\,\mathrm{K}^{-1}$ (values increase with both temperature and pressure), $\beta_S \approx 7.6\,(\pm0.2)\times10^{-4}\,\mathrm{ppt}^{-1}$ (ppt = parts per thousand), $\beta_p \approx 4.1\,(\pm0.5)\times 10^{-10}\,\mathrm{Pa}^{-1}$. Since the variations around the mean density are small (1.62) can also be written

$$\rho = \rho_0\left[1 - \beta_T(T - T_0) + \beta_S(S - S_0) + \beta_p(p - p_0)\right]. \tag{1.63}$$

A linear equation of state for seawater is *not* accurate enough for quantitative oceanography; the β parameters in (1.62) themselves vary with pressure, temperature and (more weakly) salinity so introducing nonlinearities to the equation. The most important of these are captured by an equation of state of the form

$$\alpha = \alpha_0\left[1 + \beta_T(1 + \gamma^*p)(T - T_0) + \frac{\beta_T^*}{2}(T - T_0)^2 - \beta_S(S - S_0) - \beta_p(p - p_0)\right]. \tag{1.64}$$

The starred constants β_T^* and γ^* capture the leading nonlinearities: γ^* is the *thermobaric* parameter and β_T^* is the second thermal expansion coefficient. Even this expression has quantitative deficiencies and more complicated semi-empirical formulae are often used if high accuracy is needed.[5] More discussion is to be found in section 1.8.2.

Clearly, the equation of state introduces, in general, a sixth unknown, temperature,

and we will have to introduce another physical principle — the first law of thermodynamics or the principle of energy conservation — to obtain a complete set of equations. However, if the equation of state were such that it linked only density and pressure, without introducing another variable, then the equations would be complete; the simplest cases of all being constant density fluids for which the equation of state is just $\rho = $ constant. A fluid for which the density is a function of pressure alone is called a *barotropic fluid*; otherwise, it is a *baroclinic fluid*. Equations of state of the form $p = C\rho^{\gamma}$ are sometimes called polytropic.

1.5 THE THERMODYNAMIC EQUATION

The thermodynamic equation embodies the principle of the conservation of energy, and in fluids in which the equation of state involves temperature (and not just density and pressure) then the thermodynamic equation is necessary to obtain a closed system of equations.[6]

1.5.1 A few fundamentals

A fundamental postulate of thermodynamics is that the internal energy of a system in equilibrium is a function of its extensive properties volume, entropy, and the mass of its various constituents. (Extensive means that their value depends of the amount of material present, as opposed to an intensive quantity such as temperature.) For our purposes it is more convenient to divide all of these by the mass of fluid present, so expressing the internal energy per unit mass, I, as a function of the specific volume (or inverse density) $\alpha = \rho^{-1}$, the specific entropy η, and the mass fractions of its various components, or its chemical composition, which we parameterize as its salinity S. Thus we have

$$I = I(\alpha, \eta, S), \tag{1.65a}$$

or an equivalent equation for entropy,

$$\eta = \eta(I, \alpha, S). \tag{1.65b}$$

Given the functional forms on the right-hand sides, either of these constitutes a complete description of the macroscopic state of a system in equilibrium, and we call them the *fundamental equation of state*. The first differential of (1.65a) gives, formally,

$$dI = \frac{\partial I}{\partial \alpha} d\alpha + \frac{\partial I}{\partial \eta} d\eta + \frac{\partial I}{\partial S} dS. \tag{1.66}$$

We will now ascribe physical meaning to these differentials.

Conservation of energy states that the internal energy of a body may change because of work done by or on it, or because of a heat input, or because of a change in its chemical composition. We write this as

$$dI = dQ - dW + dC \tag{1.67}$$

where dW is the work done *by* the body, dQ is the heat input *to* the body, and dC accounts for the change in internal energy caused by a change in its chemical composition (e.g., its salinity). This is the first law of thermodynamics. It is applicable to a definite fluid mass, so we can regard dI as the change in internal energy per unit mass, and similarly for the other quantities. Let us consider the causes of variations in these quantities.

Heat Input: The heat input dQ is not the differential of any quantity, and we cannot unambiguously define the heat content of a body as a function of its state. However, the second law of thermodynamics provides a relationship between the heat input and the change in the entropy of a body, namely that in an (infinitesimal) quasi-static or reversible process, with constant composition,

$$T\,d\eta = dQ, \tag{1.68}$$

where η is the *entropy* of the body. The entropy *is* a function of the state of a body and is, by definition, an adiabatic invariant. It is an extensive quantity, meaning that if we double the amount of material then we double the entropy. Here we will be dealing with the amount of a quantity per unit mass, so that η is the specific entropy.

Work done: The work done by a body is equal to the pressure times the change in its volume. That is

$$dW = p\,d\alpha, \tag{1.69}$$

where $\alpha = 1/\rho$ is the specific volume of the fluid and p is the pressure.

Composition: The change in internal energy due to compositional changes is related to the change in salinity by

$$dC = \mu\,dS, \tag{1.70}$$

where μ is the *chemical potential* of the solution. The salinity of a parcel of fluid is conserved unless there are explicit sources and sinks, such as precipitation and evaporation at the surface and molecular diffusion. When these effects do occur the internal energy of a fluid parcel changes by (1.70). However, these effects are usually small, and most important effect of salinity is that it changes the density of seawater. In the atmosphere the composition of a parcel of air primarily varies according to the amount of water vapour in it; however, the main importance of water vapour is that when condensation or evaporation occurs, heat is released (or required) which provides an entropy source in (1.68).

Collecting equations (1.67) – (1.70) together we have

$$\boxed{dI = T\,d\eta - p\,d\alpha + \mu\,dS}. \tag{1.71}$$

We refer to this (often with $dS = 0$) as *the fundamental thermodynamic relation.* The fundamental equation of state, (1.65), describes the properties of a particular fluid, and the fundamental relation, (1.71), expresses the conservation of energy. Much of classical thermodynamics follows from these two expressions.

1.5.2 * More thermodynamic relations

From (1.71) it follows that

$$T = \left(\frac{\partial I}{\partial \eta}\right)_{\alpha,S}, \qquad p = -\left(\frac{\partial I}{\partial \alpha}\right)_{\eta,S}, \qquad \mu = \left(\frac{\partial I}{\partial S}\right)_{\eta,\alpha}. \qquad (1.72\text{a,b,c})$$

These may be regarded as the defining relations for these variables; it is because of the use of (1.71), and not just the formal expression (1.66), that the pressure and temperature defined this way are indeed related to the internal motion of motion of the molecules that constitute the fluid. Note that if we write

$$\mathrm{d}\eta = \frac{1}{T}\mathrm{d}I + \frac{p}{T}\mathrm{d}\alpha - \frac{\mu}{T}\mathrm{d}S, \qquad (1.73)$$

it is also clear that

$$p = T\left(\frac{\partial \eta}{\partial \alpha}\right)_{I,S}, \qquad T^{-1} = \left(\frac{\partial \eta}{\partial I}\right)_{\alpha,S}, \qquad \mu = -T\left(\frac{\partial \eta}{\partial S}\right)_{I,\alpha}. \qquad (1.74\text{a,b,c})$$

In the following derivations, we will unless noted suppose that the composition of a fluid parcel is fixed, and drop the suffix S on partial derivatives unless ambiguity might arise.

Because the right-hand-side of (1.71) is equal to an exact differential, the second derivatives are independent of the order of differentiation. That is,

$$\frac{\partial^2 I}{\partial \eta \partial \alpha} = \frac{\partial^2 I}{\partial \alpha \partial \eta} \qquad (1.75)$$

and therefore, using (1.72)

$$\left(\frac{\partial T}{\partial \alpha}\right)_{\eta} = -\left(\frac{\partial p}{\partial \eta}\right)_{\alpha}. \qquad (1.76)$$

This is one of the *Maxwell relations,* which are a collection of four similar relations which follow directly from the fundamental thermodynamic relation (1.71) and simple relations between second derivatives. A couple of others will be useful.

Define the *enthalpy* of a fluid by

$$h \equiv I + p\alpha \qquad (1.77)$$

then, for a parcel of constant composition, (1.71) becomes

$$\mathrm{d}h = T\mathrm{d}\eta + \alpha\mathrm{d}p. \qquad (1.78)$$

But h is a function only of η and p so that in general

$$\mathrm{d}h = \left(\frac{\partial h}{\partial \eta}\right)_{p}\mathrm{d}\eta + \left(\frac{\partial h}{\partial p}\right)_{\eta}\mathrm{d}p. \qquad (1.79)$$

Comparing the last two equations we have

$$T = \left(\frac{\partial h}{\partial \eta}\right)_{p} \qquad \text{and} \qquad \alpha = \left(\frac{\partial h}{\partial p}\right)_{\eta}. \qquad (1.80)$$

Noting that

$$\frac{\partial^2 h}{\partial \eta \partial p} = \frac{\partial^2 h}{\partial p \partial \eta} \tag{1.81}$$

we evidently must have

$$\left(\frac{\partial T}{\partial p}\right)_\eta = \left(\frac{\partial \alpha}{\partial \eta}\right)_p, \tag{1.82}$$

and this is our second Maxwell relation.

To obtain the third, we write

$$\mathrm{d}I = T\,\mathrm{d}\eta - p\,\mathrm{d}\alpha = \mathrm{d}(T\eta) - \eta\,\mathrm{d}T - \mathrm{d}(p\alpha) + \alpha\,\mathrm{d}p, \tag{1.83}$$

or

$$\mathrm{d}G = -\eta\,\mathrm{d}T + \alpha\,\mathrm{d}p, \tag{1.84}$$

where $G \equiv I - T\eta + p\alpha$ is called the 'Gibbs free energy'. Now, formally, we have

$$\mathrm{d}G = \left(\frac{\partial G}{\partial T}\right)_p \mathrm{d}T + \left(\frac{\partial G}{\partial p}\right)_T \mathrm{d}p. \tag{1.85}$$

Comparing the last two equations we see that $\eta = -(\partial G/\partial T)_p$ and $\alpha = (\partial G/\partial p)_T$. Furthermore, because

$$\frac{\partial^2 G}{\partial p \partial T} = \frac{\partial^2 G}{\partial T \partial p} \tag{1.86}$$

we have our third Maxwell equation,

$$\left(\frac{\partial \eta}{\partial p}\right)_T = -\left(\frac{\partial \alpha}{\partial T}\right)_p. \tag{1.87}$$

The fourth Maxwell equation, whose derivation is left to the reader, is

$$\left(\frac{\partial \eta}{\partial \alpha}\right)_T = \left(\frac{\partial p}{\partial T}\right)_\alpha, \tag{1.88}$$

and all four Maxwell equations are summarized in the box at the top of the next page. All of them follow from the fundamental thermodynamic relation, (1.71), which is the real silver hammer of thermodynamics.

* Equation of state revisited

The fundamental equation of state (1.65) gives complete information about a fluid in thermodynamic equilibrium, and given this we can obtain expressions for the temperature, pressure and chemical potential using (1.72). These are also equations of state; however, each of them contains less information than the fundamental equation because a derivative has been taken, although all three together provide the same information. Equivalent to the fundamental equation of state are, using (1.78), an expression for the enthalpy as a function of pressure, entropy and composition, or, using (1.84) the Gibbs function as a function of pressure, temperature and composition. The conventional equation of state, (1.58), is obtained by eliminating entropy between (1.72a) and

Maxwell's Relations

The four Maxwell equations are:

$$\left(\frac{\partial T}{\partial \alpha}\right)_\eta = -\left(\frac{\partial p}{\partial \eta}\right)_\alpha, \qquad \left(\frac{\partial T}{\partial p}\right)_\eta = \left(\frac{\partial \alpha}{\partial \eta}\right)_p,$$
$$\left(\frac{\partial \eta}{\partial p}\right)_T = -\left(\frac{\partial \alpha}{\partial T}\right)_p, \qquad \left(\frac{\partial \eta}{\partial \alpha}\right)_T = \left(\frac{\partial p}{\partial T}\right)_\alpha. \tag{M.1}$$

These imply:

$$\frac{\partial(T, \eta)}{\partial(p, \alpha)} \equiv \left(\frac{\partial T}{\partial p}\right)\left(\frac{\partial \eta}{\partial \alpha}\right) - \left(\frac{\partial T}{\partial \alpha}\right)\left(\frac{\partial \eta}{\partial p}\right) = 0. \tag{M.2}$$

(1.72b). Given the fundamental equation of state, the thermodynamic state of a body is fully specified by a knowledge of any two of p, ρ, T, η and I, plus its composition.

One simple fundamental equation of state is to take the internal energy to be a function of density and not entropy; that is, $I = I(\alpha)$. Bodies with such a property are called *homentropic*. Using (1.72) temperature and chemical potential have no role and the density is a function of pressure alone — the defining property of a barotropic fluid. Neither water nor air are, in general, homentropic but under some circumstances the flow may be adiabatic and $p = p(\rho)$ (e.g., problem 1.10).

In an ideal gas the molecules do not interact except by elastic collisions, and the volume of the molecules is negligible compared to the total volume they occupy. The internal energy then depends only on temperature, and not on the density. A *simple* ideal gas is an ideal gas for which the heat capacity is constant, so that

$$I = cT, \tag{1.89}$$

where c is a constant. Using this and the conventional ideal gas equation, $p = \rho RT$, where R is also constant, we can infer the fundamental equation of state; however, we will defer that until we discuss potential temperature in section 1.5.4. A *general* ideal gas also obeys $p = \rho RT$, but it has heat capacities that may be a function of temperature (but only of temperature — see problem 1.12).

Internal energy and specific heats

We can obtain some useful relations between the internal energy and specific heat capacities, and some useful estimates of their values, by some simple manipulations of the fundamental thermodynamic relation. Assuming that the composition of the fluid is constant (1.71) is

$$T \, d\eta = dI + p \, d\alpha, \tag{1.90}$$

so that

$$T \, \mathrm{d}\eta = \left(\frac{\partial I}{\partial T}\right)_\alpha \mathrm{d}T + \left[\left(\frac{\partial I}{\partial \alpha}\right)_T + p\right]\mathrm{d}\alpha. \tag{1.91}$$

From this, we see that the heat capacity at constant volume (or constant α) c_v is given by

$$c_v \equiv T\left(\frac{\partial \eta}{\partial T}\right)_\alpha = \left(\frac{\partial I}{\partial T}\right)_\alpha. \tag{1.92}$$

Thus, c in (1.89) is equal to c_v.

Similarly, using (1.78) we have

$$\begin{aligned} T \, \mathrm{d}\eta &= \mathrm{d}h - \alpha \, \mathrm{d}p \\ &= \left(\frac{\partial h}{\partial T}\right)_p \mathrm{d}T + \left[\left(\frac{\partial h}{\partial p}\right) - \alpha\right]\mathrm{d}p. \end{aligned} \tag{1.93}$$

The heat capacity at constant pressure, c_p, is then given by

$$c_p \equiv T\left(\frac{\partial \eta}{\partial T}\right)_p = \left(\frac{\partial h}{\partial T}\right)_p. \tag{1.94}$$

For later use, we define the ratios $\gamma \equiv c_p/c_v$ and $\kappa \equiv R/c_p$.

For an ideal gas $h = I + RT = T(c_v + R)$. But $c_p = (\partial h/\partial t)_p$, and hence $c_p = c_v + R$, and $(\gamma - 1)/\gamma = \kappa$. Statistical mechanics tells us that for a simple ideal gas the internal energy is equal to $kT/2$ per molecule, or $RT/2$ per unit mass, for each excited degree of freedom, where k is the Boltzmann constant and R the gas constant. The diatomic molecules N_2 and O_2 that comprise most of our atmosphere have two rotational and three translational degrees of freedom, so that $I \approx 5RT/2$, and so $c_v \approx 5R/2$ and $c_p \approx 7R/2$, both being constants. These are in fact very good approximations to the measured values for the earth's atmosphere, and give $c_p \approx 10^3 \, \mathrm{J\,kg^{-1}K^{-1}}$. The internal energy is simply $c_v T$ and the enthalpy is $c_p T$. For a liquid, especially one containing dissolved salts such as seawater, no such simple relations are possible: the heat capacities are functions of the state of the fluid, and the internal energy is a function of pressure (or density) as well as temperature.

1.5.3 Thermodynamic equations for fluids

The thermodynamic relations — for example (1.71) — apply to identifiable bodies or systems; thus, the heat input affects the fluid parcel to which it is applied, and we can apply the material derivative to the above thermodynamic relations to obtain equations of motion for a moving fluid. But in doing so we make two assumptions:

(i) That locally the fluid is in thermodynamic equilibrium. This means that, although the thermodynamic quantities like temperature, pressure and density vary in space and time, locally they are related by the thermodynamic relations such as the equation of state and Maxwell's relations.

(ii) That macroscopic fluid motions are reversible and so not entropy producing. Thus, the diabatic term $\mathrm{d}Q$ represents the entropy sources — such effects as viscous dissipation of energy, radiation, and conduction — whereas the macroscopic fluid motion itself is adiabatic.

The first point requires that the temperature variation on the macroscopic scales must be slow enough that there can exist a volume that is small compared to the scale of macroscopic variations, so that temperature is effectively constant within it, but that is also sufficiently large to contain enough molecules so that macroscopic variables such as temperature have a proper meaning. Accepting these assumptions, the expression

$$T \, \mathrm{d}\eta = \mathrm{d}Q \tag{1.95}$$

implies that we may write

$$T \frac{\mathrm{D}\eta}{\mathrm{D}t} = \dot{Q}, \tag{1.96}$$

where $\dot{Q}$ is the total rate of heat input per unit mass. This is a thermodynamic equation of motion of the fluid.

For seawater a full specification of its thermodynamic state requires a knowledge of the salinity S, and this is determined by the conservation equation

$$\frac{\mathrm{D}S}{\mathrm{D}t} = \dot{S}, \tag{1.97}$$

where $\dot{S}$ represents effects of evaporation and precipitation at the ocean surface, and molecular diffusion. Somewhat analogously, for atmosphere the thermodynamics involve water vapour whose evolution is given by the conservation of water vapour mixing ratio

$$\frac{\mathrm{D}w}{\mathrm{D}t} = \dot{w} \tag{1.98}$$

where $\dot{w}$ represents the effects of condensation and evaporation. Salt has an important effect on the density of seawater, whereas the effect of water vapour on the density of air is slight.

Equation (1.96) is not a *useful* equation unless the entropy can be related to the other fluid variables, temperature, pressure and density. This can be done using the equation of state and the thermodynamic relations we have derived, and is the subject of the following sections. An ideal gas is the simplest case with which to start.

1.5.4 Thermodynamic equation for an ideal gas

For a fluid parcel of constant composition the fundamental thermodynamic relation is

$$\mathrm{d}Q = \mathrm{d}I + p \, \mathrm{d}\alpha \tag{1.99}$$

For an ideal gas the internal energy is a function of temperature only and $\mathrm{d}I = c_v \, \mathrm{d}T$ (also see problems 1.12 and 1.14), so that

$$\mathrm{d}Q = c_v \, \mathrm{d}T + p \, \mathrm{d}\alpha \qquad \text{or} \qquad \mathrm{d}Q = c_p \, \mathrm{d}T - \alpha \, \mathrm{d}p, \tag{1.100a,b}$$

where the second expression is derived using $\alpha = RT/p$ and and $c_p - c_v = R$. Forming the material derivative of (1.99) gives the general thermodynamic equation

$$\frac{DI}{Dt} + p\frac{D\alpha}{Dt} = \dot{Q}. \tag{1.101}$$

Similarly, for an ideal gas (1.100a,b) respectively give

$$c_v\frac{DT}{Dt} + p\frac{D\alpha}{Dt} = \dot{Q}, \qquad \text{or} \qquad c_p\frac{DT}{Dt} - \frac{RT}{p}\frac{Dp}{Dt} = \dot{Q}. \tag{1.102a,b}$$

Although (1.102) are equations in the state variables p, T and/or α, time derivatives act on two variables and this is not convenient for many purposes. Using the mass continuity equation, (1.102a) may be written

$$c_v\frac{DT}{Dt} + p\alpha\nabla\cdot v = \dot{Q}. \tag{1.103}$$

Alternatively, using the ideal gas equation we may eliminate T in favor of p and α, giving the equivalent equation

$$\frac{Dp}{Dt} + \gamma p\nabla\cdot v = \dot{Q}\frac{\rho R}{c_v}. \tag{1.104}$$

Potential temperature and potential density

When a fluid parcel changes pressure adiabatically, it will expand or contract and, using (1.100b), its temperature change is determined by

$$c_p\,dT = \alpha\,dp. \tag{1.105}$$

As this temperature change occurs is not caused by heating, it is useful to define a temperature-like quantity that changes *only* if diabatic effects are present. To this end, we define the *potential temperature, θ*, to be the temperature that a fluid would have if moved adiabatically to some reference pressure (often taken to be the 1000 hPa, which is close to the pressure at the earth's surface). Thus, in adiabatic flow the potential temperature of a fluid parcel is conserved, essentially by definition, and

$$\frac{D\theta}{Dt} = 0. \tag{1.106}$$

Such an evolution equation holds, for adiabatic flow at constant composition, for the potential temperature of any fluid, but to be useful we must be able to relate θ to the other thermodynamic variables. For an ideal gas we use (1.100b) and the equation of state to write the thermodynamic equation as

$$d\eta = c_p\,d\ln T - R\,d\ln p. \tag{1.107}$$

The definition of potential temperature then implies that

$$c_p\,d\ln\theta = c_p\,d\ln T - R\,d\ln p, \tag{1.108}$$

and this is satisfied by

$$\theta = T \left(\frac{p_R}{p} \right)^{\kappa} \tag{1.109}$$

where p_R is a reference pressure and $\kappa = R/c_p$.

Note that

$$d\eta = c_p \frac{d\theta}{\theta} \tag{1.110}$$

and, if c_p is constant,

$$\eta = c_p \ln \theta. \tag{1.111}$$

Equation (1.110) is in fact a general expression for potential temperature of a fluid parcel of constant composition (see section 1.8.1), but (1.111) applies only if c_p is constant, as in, to a very good approximation, the earth's atmosphere.

Using (1.108), the thermodynamic equation in the presence of heating is simply

$$\boxed{c_p \frac{D\theta}{Dt} = \frac{\theta}{T} \dot{Q}}, \tag{1.112}$$

with θ given by (1.109). Equations (1.103), (1.104) and (1.112) are all equivalent forms of the thermodynamic equation for an ideal gas.

The *potential density*, ρ_θ, is the density that a fluid parcel would have if moved adiabatically and at constant composition to a reference pressure, p_R. If the equation of state is written as $\rho = f(p, T)$ then the potential density is just

$$\rho_\theta = f(p_R, \theta). \tag{1.113}$$

For an ideal gas we therefore have

$$\rho_\theta = \frac{p_R}{R\theta}; \tag{1.114}$$

that is, potential density is proportional to the inverse of potential temperature. We may also write (1.114) as

$$\rho_\theta = \rho \left(\frac{p_R}{p} \right)^{1/\gamma}. \tag{1.115}$$

Finally, for later use we note that for small variations around a reference state manipulation of the ideal gas equation gives

$$\frac{\delta\theta}{\theta} = \frac{\delta T}{T} - \kappa \frac{\delta p}{p} = \frac{1}{\gamma} \frac{\delta p}{p} - \frac{\delta\rho}{\rho}. \tag{1.116}$$

* Potential temperature and the fundamental equation of state

Eq. (1.111) is closely related to the fundamental equation of state: using $I = c_v T$, (1.109), and the equation of state $p = \rho R T$, we can express the entropy explicitly in terms of the density and the internal energy, to wit

$$\boxed{\eta = c_v \ln I - R \ln \rho + \text{constant}}.$$ (1.117)

This is the fundamental equation of state for a simple ideal gas. If we were to *begin* with this, we could straightforwardly derive all the thermodynamic quantities of interest for a simple ideal gas: for example, using (1.74a) we immediately recover $P = \rho R T$, and from (1.74b) we obtain $I = c_v T$. Indeed, (1.117) could be used to define a simple ideal gas, but such an *a priori* definition seems a little unmotivated. Of course the heat capacities must still be determined by experiment or by a kinetic theory — they are not given by the thermodynamics, and (1.117) holds only if they are constant.

1.5.5 * Thermodynamic equation for liquids

For a liquid such as seawater no simple exact equation of state exists. Thus, although (1.112) holds at constant salinity for a liquid by virtue of the definition of potential temperature, an accurate expression relating potential temperature to the other thermodynamic variables is nonlinear, complicated and, to most eyes, uninformative. Yet for both theoretical and modelling work a thermodynamic equation is needed to represent energy conservation, and an equation of state needed to close the system, and one of two approaches is thus generally taken: For most theoretical work and for idealized models a simple analytic but approximate equation of state is used, but in situations where more accuracy is called for, such as quantitative modelling or observational work, an accurate but complex semi-empirical equation of state is used. This section outlines how relatively simple thermodynamic equations may be derived that are adequate in many circumstances, and which illustrate the principles used in deriving more complicated equations.

Thermodynamic equation using pressure and density

If we regard η as a function of pressure and density (and salinity if appropriate) we obtain

$$T \, d\eta = T \left(\frac{\partial \eta}{\partial \rho} \right)_{p,S} d\rho + T \left(\frac{\partial \eta}{\partial p} \right)_{\rho,S} dp + T \left(\frac{\partial \eta}{\partial S} \right)_{\rho,p} dS$$

$$= T \left(\frac{\partial \eta}{\partial \rho} \right)_{p,S} d\rho - T \left(\frac{\partial \eta}{\partial \rho} \right)_{p,S} \left(\frac{\partial \rho}{\partial p} \right)_{\eta,S} dp + T \left(\frac{\partial \eta}{\partial S} \right)_{\rho,p} dS.$$ (1.118)

From this, and using (1.96) and (1.97), we obtain for a moving fluid

$$T \left(\frac{\partial \eta}{\partial \rho} \right)_{p,S} \frac{D\rho}{Dt} - T \left(\frac{\partial \eta}{\partial \rho} \right)_{p,S} \left(\frac{\partial \rho}{\partial p} \right)_{\eta,S} \frac{Dp}{Dt} = \dot{Q} - T \left(\frac{\partial \eta}{\partial S} \right)_{\rho,p} \dot{S}$$ (1.119)

But $(\partial p/\partial \rho)_{\eta,S} = c_s^2$ where c_s is the speed of sound (see section 1.6). This is a measurable quantity in a fluid, and often nearly constant, and so useful to keep in an equation. Then the thermodynamic equation may be written in the form

$$
\boxed{\frac{\mathrm{D}\rho}{\mathrm{D}t} - \frac{1}{c_s^2}\frac{\mathrm{D}p}{\mathrm{D}t} = Q[\rho]}
\tag{1.120}
$$

where $Q[\rho] = (\partial \rho/\partial \eta)_{p,S}\,\dot{Q}/T - (\partial \rho/\partial S)_{\rho,p}\dot{S}$ appropriately represents the effects of all diabatic and salinity source terms. This form of the thermodynamic equation is valid for both liquids and gases.

Approximations: The speed of sound in a fluid is related to its compressibility — the less compressible the fluid, the greater the sound speed. In a fluid it is often sufficiently high that the second term in (1.120) can be neglected, and the thermodynamic equation takes the simple form:

$$
\frac{\mathrm{D}\rho}{\mathrm{D}t} = Q[\rho].
\tag{1.121}
$$

This equation is a very good approximation for many laboratory fluids. Note that this equation is a thermodynamic equation, arising from the principle of conservation of energy for a liquid. It is a very different equation from the mass conservation equation, which for compressible fluids is also an evolution equation for density.

In the ocean the enormous pressures resulting from columns of seawater kilometers deep mean that although the the second term in (1.120) may be small, it is not negligible, and a better approximation results if we suppose that the pressure is given by the weight of the fluid above it — the hydrostatic approximation. In this case $\mathrm{d}p = -\rho g\,\mathrm{d}z$ and (1.120) becomes

$$
\frac{\mathrm{D}\rho}{\mathrm{D}t} + \frac{\rho g}{c_s^2}\frac{\mathrm{D}z}{\mathrm{D}t} = Q[\rho].
\tag{1.122}
$$

In the second term the height field varies much more than the density field, so a good approximation is to replace ρ by a constant, ρ_0, in this term only. Taking the speed of sound also to be constant gives

$$
\frac{\mathrm{D}}{\mathrm{D}t}\left[\rho + \frac{\rho_0 z}{H_\rho}\right] = Q[\rho]
\tag{1.123}
$$

where

$$
H_\rho = c_s^2/g
\tag{1.124}
$$

is the *density scale height* of the ocean. In water, $c_s \approx 1500\,\mathrm{m\,s^{-1}}$ so that $H_\rho \approx 200\,\mathrm{km}$. The quantity in square brackets in (1.123) is (in this approximation) the *potential density,* this being the density that a parcel would have if moved adiabatically and with constant composition to the reference height

$z = 0$. The density scale height as defined here is due to the mean compressibility (i.e., the change in density with pressure) of seawater and, because sound speed varies only slightly in the ocean, this is nearly a constant. The adiabatic lapse rate of density is the rate at which the density of a parcel changes when undergoing an adiabatic displacement. From (1.123) it is approximately

$$-\left(\frac{\partial\rho}{\partial z}\right)_\eta \approx \frac{\rho_0 g}{c_s^2} \approx 5\,(\mathrm{kg\,m^{-3}})/\mathrm{km} \tag{1.125}$$

so that if a parcel is moved adiabatically from the surface to the deep ocean (5 km depth, say) its density its density will increase by about $25\,\mathrm{kg\,m^{-3}}$, a fractional density increase of about 1/40 or 2.5%.

Thermodynamic equation using pressure and temperature

Taking entropy to be a function of pressure and temperature (and salinity if appropriate) we have

$$\begin{aligned} T\,\mathrm{d}\eta &= T\left(\frac{\partial\eta}{\partial T}\right)_{p,S}\mathrm{d}T + T\left(\frac{\partial\eta}{\partial p}\right)_{T,S}\mathrm{d}p + T\left(\frac{\partial\eta}{\partial S}\right)_{T,p}\mathrm{d}S \\ &= c_p\mathrm{d}T + T\left(\frac{\partial\eta}{\partial p}\right)_{T,S}\mathrm{d}p + T\left(\frac{\partial\eta}{\partial S}\right)_{T,p}\mathrm{d}S. \end{aligned} \tag{1.126}$$

For a moving fluid, and using (1.96) and (1.97), this implies,

$$\frac{\mathrm{D}T}{\mathrm{D}t} + \frac{T}{c_p}\left(\frac{\partial\eta}{\partial p}\right)_{T,S}\frac{\mathrm{D}p}{\mathrm{D}t} = Q[T]. \tag{1.127}$$

where $Q[T] = \dot{Q}/c_p - Tc_p^{-1}\dot{S}(\partial\eta/\partial S)$ includes the effects of the entropy and saline source terms. Now substitute the Maxwell relation (1.87) in the form

$$\left(\frac{\partial\eta}{\partial p}\right)_T = \frac{1}{\rho^2}\left(\frac{\partial\rho}{\partial T}\right)_p \tag{1.128}$$

to give

$$\frac{\mathrm{D}T}{\mathrm{D}t} + \frac{T}{c_p\rho^2}\left(\frac{\partial\rho}{\partial T}\right)_p\frac{\mathrm{D}p}{\mathrm{D}t} = Q[T], \tag{1.129a}$$

or, equivalently,

$$\frac{\mathrm{D}T}{\mathrm{D}t} - \frac{T}{c_p}\left(\frac{\partial\alpha}{\partial T}\right)_p\frac{\mathrm{D}p}{\mathrm{D}t} = Q[T]. \tag{1.129b}$$

The density and temperature are related through a measurable coefficient of thermal expansion β_T where

$$\left(\frac{\partial\rho}{\partial T}\right)_p = -\beta_T\rho \tag{1.130}$$

Equation (1.129) then becomes

$$\boxed{\frac{\mathrm{D}T}{\mathrm{D}t} - \frac{\beta_T T}{c_p \rho}\frac{\mathrm{D}p}{\mathrm{D}t} = Q[T]}.$$

(1.131)

This is form of the thermodynamic equation is valid for both liquids and gases, and in an ideal gas $\beta_T = 1/T$.

> *Approximations:* Liquids are characterized by a small coefficient of thermal expansion, and it is sometimes acceptable in laboratory fluids to neglect the second term on the left-hand side of (1.131). We then obtain an equation analogous to (1.121), namely
>
> $$\frac{\mathrm{D}T}{\mathrm{D}t} = Q[T].$$
>
> (1.132)
>
> This approximation relies on the smallness of the coefficient of thermal expansion. A better approximation is to again suppose that the pressure in (1.131) varies according only to the weight of the fluid above it. Then $\mathrm{d}p = -\rho g \mathrm{d}z$ and (1.131) becomes
>
> $$\frac{1}{T}\frac{\mathrm{D}T}{\mathrm{D}t} + \frac{\beta_T g}{c_p}\frac{\mathrm{D}z}{\mathrm{D}t} = \frac{Q[T]}{T}.$$
>
> (1.133)
>
> For small variations of T, and if β_T is nearly constant, this simplifies to
>
> $$\frac{\mathrm{D}}{\mathrm{D}t}\left(T + \frac{T_0 z}{H_T}\right) = Q[T]$$
>
> (1.134)
>
> where
>
> $$H_T = c_p/(\beta_T g)$$
>
> (1.135)
>
> is the *temperature scale height* of the fluid. The quantity $T + T_0 z/H_T$ is (in this approximation) the *potential temperature, θ,* so called because it is the temperature that a fluid at a depth z would have if moved adiabatically to a reference depth, here taken as $z = 0$ — the temperature changing because of the work done by or on the fluid parcel as it expands or is compressed. That is,
>
> $$\theta \approx T + \frac{\beta_T g T_0}{c_p}z$$
>
> (1.136)
>
> In seawater, however, the expansion coefficient β_T and c_p are functions of pressure and (1.136) is not good enough for quantitative calculations. With the approximate values for the ocean of $\beta_T \approx 2 \times 10^{-4}\,\mathrm{K}^{-1}$ and $c_p \approx 4 \times 10^3\,\mathrm{J\,kg^{-1}\,K^{-1}}$ we obtain $H_T \approx 2000\,\mathrm{km}$.
>
> The adiabatic lapse rate is rate at which the temperature of a parcel changes in the vertical when undergoing an adiabatic displacement. From (1.133) it is
>
> $$\Gamma_{\mathrm{ad}} = -\left(\frac{\partial T}{\partial z}\right)_\eta = \frac{T g \beta_T}{c_p}.$$
>
> (1.137)

Forms of the Thermodynamic Equation

General form

For a parcel of constant composition the thermodynamic equation is

$$T\frac{D\eta}{Dt} = \dot{Q} \qquad \text{or} \qquad c_p\frac{D\ln\theta}{Dt} = \frac{1}{T}\dot{Q} \tag{T.1}$$

where η is the entropy, θ is the potential temperature, $c_p\ln\theta = \eta$ and $\dot{Q}$ is the heating rate. Apppplying the first law of thermodynamics $T\,d\eta = dI + p\,d\alpha$ gives:

$$\frac{DI}{Dt} + p\frac{D\alpha}{Dt} = \dot{Q} \qquad \text{or} \qquad \frac{DI}{Dt} + RT\nabla\cdot\boldsymbol{v} = \dot{Q} \tag{T.2}$$

where I is the internal energy.

Ideal gas

For an ideal gas $dI = c_v\,dT$, and the (adiabatic) thermodynamic equation may be written in the following equivalent, exact, forms:

$$
\begin{aligned}
c_p\frac{DT}{Dt} - \alpha\frac{Dp}{Dt} &= 0, & \frac{Dp}{Dt} + \gamma p\nabla\cdot\boldsymbol{v} &= 0, \\
c_v\frac{DT}{Dt} + p\alpha\nabla\cdot\boldsymbol{v} &= 0, & \frac{D\theta}{Dt} &= 0,
\end{aligned}
\tag{T.3}
$$

where $\theta = T(p_R/p)^\kappa$. The two expressions on the second line are usually the most useful in modelling and theoretical work.

Liquids

For liquids we may usefully write the (adiabatic) thermodynamic equation as a conservation equation for potential temperature θ or potential density ρ_{pot} and represent these in terms of other variables. For example:

$$\frac{D\theta}{Dt} = 0, \qquad \theta \approx \begin{cases} T & \text{(approximately)} \\ T + (\beta_T gz/c_p) & \text{(with some thermal expansion),} \end{cases} \tag{T.4a}$$

$$\frac{D\rho_{\text{pot}}}{Dt} = 0, \quad \rho_{\text{pot}} \approx \begin{cases} \rho & \text{(very approximately)} \\ \rho + (\rho_0 gz/c_s^2) & \text{(with some compression).} \end{cases} \tag{T.4b}$$

Unlike (T.3) these are not equivalent forms. More accurate semi-empirical expressions that may also include saline effects are often used for quantitative applications.

In general it is a function of temperature, salinity and pressure, but it is a

calculable quantity if β_T is known. With the oceanic values above, it is approximately $0.15\,\mathrm{K\,km^{-1}}$. Again this is not accurate enough for quantitative oceanography because the expansion coefficient is a function of pressure. Nor is it a good measure of stability, because of the effects of salt.

It is interesting that the scale heights given by (1.124) and (1.135) differ so much. As mentioned, the first is due to the compressibility of seawater [and so related to c_s^2, or β_p in (1.63)] whereas the second is due to the change of density with temperature [β_T in (1.63)], and is the distance over which the the difference between temperature and potential temperature changes by an amount equal to the temperature itself (i.e., by about 273 K). The two heights differ so much because the value of thermal expansion coefficient is not directly tied to the compressibility — for example, fresh water at $4°\,\mathrm{C}$ has a zero thermal expansion, and so would have an infinite temperature scale height, but its compressibility differs little from water at $20°\,\mathrm{C}$. (See also problem 1.20.)

In the atmosphere the ideal gas relationship gives $\beta_T = 1/T$ and so

$$\Gamma_{\mathrm{ad}} = \frac{g}{c_p} \tag{1.138}$$

which is approximately $10\,\mathrm{K\,km^{-1}}$. The only approximation involved in deriving this is the use of the hydrostatic relationship.

Thermodynamic equation using density and temperature

Taking entropy to be a function of density and temperature (and salinity if appropriate) we have

$$
\begin{aligned}
T\mathrm{d}\eta &= T\left(\frac{\partial\eta}{\partial T}\right)_{\alpha,S}\mathrm{d}T + T\left(\frac{\partial\eta}{\partial\alpha}\right)_{T,S}\mathrm{d}p + T\left(\frac{\partial\eta}{\partial S}\right)_{T,\alpha}\mathrm{d}S \\
&= c_v\mathrm{d}T + T\left(\frac{\partial\eta}{\partial\alpha}\right)_{T,S}\mathrm{d}\alpha + T\left(\frac{\partial\eta}{\partial S}\right)_{T,\alpha}\mathrm{d}S.
\end{aligned}
\tag{1.139}
$$

For a moving fluid this implies,

$$\frac{\mathrm{D}T}{\mathrm{D}t} + \frac{T}{c_v}\left(\frac{\partial\eta}{\partial\alpha}\right)_{T,S}\frac{\mathrm{D}\alpha}{\mathrm{D}t} = \frac{\dot{Q}}{c_v}. \tag{1.140}$$

If density is nearly constant, as in many liquids, then the second term in (1.140) is small, and also $c_p \approx c_v$.

The thermodynamic equations for a fluid are summarized on page 30, and the complete equations of motion for a fluid are summarized on page 32. Also, note that for ideal gas (1.120) and (1.131) are exactly equivalent to (1.103) or (1.104) (problem 1.11).

The Equations of Motion of a Fluid

For dry air, or for a salt-free liquid, the complete set of equations of motion may be written as follows:

The *mass continuity equation:*

$$\frac{\partial \rho}{\partial t} + \nabla \cdot (\rho \boldsymbol{v}) = 0. \tag{EOM.1}$$

If density is constant this reduces to $\nabla \cdot \boldsymbol{v} = 0$.

The *momentum equation:*

$$\frac{\mathrm{D}\boldsymbol{v}}{\mathrm{D}t} = -\frac{\nabla p}{\rho} + \nu \nabla^2 \boldsymbol{v} + \boldsymbol{F}, \tag{EOM.2}$$

where $\boldsymbol{F}$ represents the effects of body forces such as gravity and ν is the kinematic viscosity. If density is constant, or pressure is given as a function of density alone (e.g., $p = C\rho^\gamma$), then (EOM.1) and (EOM.2) form a complete system.

The *thermodynamic equation:*

$$\frac{\mathrm{D}\theta}{\mathrm{D}t} = \frac{1}{c_p}\left(\frac{\theta}{T}\right)\dot{Q}. \tag{EOM.3}$$

where $\dot{Q}$ represents external heating and diffusion, the latter being $\kappa \nabla^2 \theta$ where κ is the diffusivity.

The *equation of state:*

$$\rho = g(\theta, p) \tag{EOM.4}$$

where g is a given function. For example, for an ideal gas, $\rho = p_{\mathrm{R}}^\kappa/(R\theta p^{\kappa-1})$.

The equations describing fluid motion are called the *Euler equations* if the viscous term is omitted, and the *Navier-Stokes equations* if viscosity is included.[7] Sometimes the Euler equations are taken to mean the momentum and mass conservation equations for an inviscid fluid of constant density.

1.6 SOUND WAVES

> *Full of sound and fury, signifying nothing.*
> William Shakespeare, *Macbeth,* c. 1606.

We now consider, rather briefly, one of the most common phenomena in fluid dynamics yet one which is relatively unimportant for geophysical fluid dynamics — sound waves. Sound itself is not a meteorologically or oceanographically important phenomenon, except in a few special cases, for the pressure disturbance produced by sound waves

is a tiny fraction of the ambient pressure and too small to be of importance for the circulation. For example, the ambient surface pressure in the atmosphere is about 10^5 Pa and variations due to large-scale weather phenomena are about 10^3 Pa, often larger, whereas sound waves of 60 dB produce pressure variations of about 10 Pa.

The smallness of the disturbance produced by sound waves justifies a linearization of the equations of motion about a spatially uniform basic state (denoted by a subscript 0) that is a time-independent solution to the equations of motion. Thus, we write $v = v_0 + v'$, $\rho = \rho_0 + \rho'$ and so on, substitute in the equations of motion, and neglect terms involving products of primed quantities, as these are assumed small. By choice of our reference frame we will simplify matters further by setting $v_0 = 0$. The linearized momentum and mass conservation equations are then

$$\rho_0 \frac{\partial v'}{\partial t} = -\nabla p' \tag{1.141}$$

$$\rho_0 \frac{\partial \rho'}{\partial t} = -\rho_0 \nabla \cdot v' \tag{1.142}$$

These linear equations do not in themselves determine the magnitude of the disturbance, and the linear approximation must be checked *a posteriori* (problem 1.5). Now, sound waves are largely adiabatic. Thus,

$$\frac{dp}{dt} = \left(\frac{\partial p}{\partial \rho}\right)_\eta \frac{d\rho}{dt}, \tag{1.143}$$

where $(\partial p/\partial \rho)_\eta$ is the derivative at constant entropy, whose particular form is given by the equation of state for the fluid at hand. Then, from (1.141) – (1.143) we obtain a single equation for pressure,

$$\frac{\partial^2 p'}{\partial t^2} = c_s^2 \nabla^2 p', \tag{1.144}$$

where $c_s^2 = (\partial p/\partial \rho)_\eta$. Eq. (1.144) is the classical wave equation; solutions propagate at a speed c_s which thus may be identified as the speed of sound. In an ideal gas manipulation of the equation of state leads to $p = C\rho^\gamma$ for adiabatic compressions, whence $c_s^2 = \gamma p/\rho = \gamma RT$ where $\gamma = c_p/c_v$. Values of γ typically range from 5/3 for a monatomic gas to 7/5 for a diatomic gas. For air, which is almost entirely diatomic, this leads to $c_s \approx 350 \, \text{m s}^{-1}$ at 300 K. In seawater no such theoretical approximation is easily available but measurements show that $c_s \approx 1500 \, \text{m s}^{-1}$.

1.7 COMPRESSIBLE AND INCOMPRESSIBLE FLOW

There are many important circumstances in fluid dynamics when the dynamics are completely specified by the momentum equation and a form of the mass conservation equation. This arises in general when the equation of state does not introduce temperature, and the simplest such equation of state would be that density be constant. Although there are probably no fluids of exactly constant density, in many cases the density of a fluid will vary so little that it is a very good approximation to consider the density

effectively constant in the mass conservation equation. The motion is then said to be incompressible. For example, in the earth's oceans the density varies by less that 5%, even though the pressure at the ocean bottom, a few kilometers below the surface, is several hundred times the atmospheric pressure at the surface.

Let us first note how the mass conservation equation simplifies when density is strictly constant, and then consider under what conditions this is a good approximation.

1.7.1 Constant density fluids

If a fluid is strictly of constant density, the mass continuity equation (1.38) simplifies easily by neglecting all derivatives of density yielding

$$\boxed{\nabla \cdot \boldsymbol{v} = 0} \ . \tag{1.145}$$

The *prognostic* equation (1.38) has become a *diagnostic* equation (1.145), or a constraint to be satisfied by the velocity at each instant of the fluid motion. A consequence of this equation is that the volume of each material fluid element remains constant. To see this recall the expression for the conservation of mass in the form

$$\frac{\mathrm{D}}{\mathrm{D}t}(\rho \Delta V) = 0. \tag{1.146}$$

If ρ is constant this reduces to an expression for volume conservation, namely $\mathrm{D}\Delta V/\mathrm{D}t = 0$, whence (1.145) is recovered because $\mathrm{D}\Delta V/\mathrm{D}t = \Delta V \nabla \cdot \boldsymbol{v}$. The absolute constancy of density is an idealization which is rarely, if ever, realized in the natural world. However, there are many cases in which it is a very good approximation to use (1.145) in place of the full continuity equation. These depend not only on the physical nature of the fluid but also on the flow itself, as we shall now discuss.

1.7.2 Incompressible flows

An incompressible fluid is one in which the density of a given fluid element does not change.[8] Thus, in the mass continuity equation

$$\frac{\mathrm{D}\rho}{\mathrm{D}t} + \rho \nabla \cdot \boldsymbol{v} = 0, \tag{1.147}$$

the material derivative of density is neglected and we obtain,

$$\nabla \cdot \boldsymbol{v} = 0. \tag{1.148}$$

In reality no fluid is truly incompressible and for (1.148) to approximately hold we just require that that

$$|D\rho/Dt| \ll |\rho \nabla \cdot \boldsymbol{v}|. \tag{1.149}$$

Our working definition of incompressibility, then, is that *in an incompressible fluid density changes (from whatever cause) are so small that they have a negligible affect on*

the mass balance, and (1.147) may be replaced by (1.148). We do not need to assume that the densities of differing fluid elements are similar to each other, just that the density of any particular fluid element is nearly constant, but in the ocean (and in most liquids) it is in fact the case that variations in density are everywhere small compared to the mean density, and it this is condition that we generally apply. The atmosphere is not incompressible and (1.148) does not in general hold there. Note also that the fact that $\nabla \cdot \boldsymbol{v} = 0$ does *not* imply that we may independently use $D\rho/Dt = 0$. Indeed for a liquid with equation of state $\rho = \rho_0(1 - \beta_T(T - T_0))$ and thermodynamic equation $c_p DT/Dt = \dot{Q}$ we obtain

$$\frac{D\rho}{Dt} = -\frac{\beta_T \rho_0}{c_p} \dot{Q}. \tag{1.150}$$

Note too that incompressibility does not necessarily imply the neglect of density variations in the momentum equation — it is only in the mass continuity equation that density variations are neglected.

Some conditions for incompressibility

The condition that density is largely unaffected by pressure gives one necessary condition for the legitimate use of (1.148), as follows. First assume adiabatic flow, and omit the gravitational term. Then

$$\frac{dp}{dt} = \left(\frac{\partial p}{\partial \rho}\right)_\eta \frac{d\rho}{dt} = c_s^2 \frac{d\rho}{dt} \tag{1.151}$$

so that the density and pressure variations of a fluid parcel are related by

$$\delta p \sim c_s^2 \delta\rho. \tag{1.152}$$

From the momentum equation we estimate

$$\frac{U^2}{L} \sim \frac{1}{L}\frac{\delta p}{\rho_0}, \tag{1.153}$$

where U and L are typical velocities and lengths and where ρ_0 is a representative value of the density. Using (1.152) and (1.153) gives $U^2 \sim c_s^2 \delta\rho/\rho_0$. The incompressibility condition $\delta\rho/\rho_0 << 1$ then becomes

$$\frac{U^2}{c_s^2} << 1. \tag{1.154}$$

That is, for a flow to be incompressible the fluid velocities must be less than the speed of sound, or the Mach number, $M \equiv U/c_s$, must be small.

In the earth's atmosphere it is apparent that density changes significantly with height. Assuming hydrostatic balance and an ideal gas, then

$$\frac{1}{\rho}\frac{\partial p}{\partial z} = -g, \tag{1.155}$$
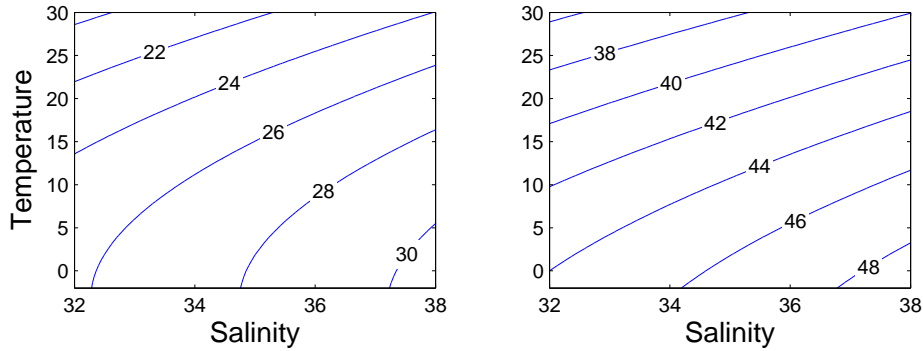
Fig. 1.3 A temperature-salinity diagram for seawater, calculated using an empirical equation of state. Contours are (density - 1000) kg m^{-3}, and the temperature is potential temperature, which in the deep ocean may be less than *in situ* temperature a degree or so (see Fig. 1.4). Left panel: at sea-level ($p = 10^5$ Pa = 1000 mb). Right panel: at $p = 4 \times 10^7$ Pa, a depth of about 4 km. Note that in both cases the contours are slightly convex.

and if (for simplicity) we assume that atmosphere is isothermal then

$$\frac{\partial p}{\partial z} = \left(\frac{\partial p}{\partial \rho}\right)_T \frac{\partial \rho}{\partial z} = RT_0 \frac{\partial \rho}{\partial z}. \tag{1.156}$$

Using (1.155) and (1.156) gives

$$\rho = \rho_0 \exp(-z/H_\rho), \tag{1.157}$$

where $H_\rho = RT_0/g$ is the (density) *scale height* of the atmosphere. It is easy to see that density changes are negligible only if we concern ourselves with motion less than the scale height, so this is another necessary condition for incompressibility.

In the atmosphere, although the Mach number is small for most flows, vertical displacements often exceed the scale height and in those cases the flow cannot be considered incompressible. In the ocean density changes from all causes are small and in most circumstances the ocean may be considered to contain an incompressible fluid. We return to this in the next chapter when we consider the Boussinesq equations.

1.8 * MORE THERMODYNAMICS OF LIQUIDS

1.8.1 Potential temperature, potential density and entropy

For an ideal gas we were able to derive a single prognostic equation for a single variable, potential temperature. As potential temperature is in turn simply related to the temperature and pressure, this is a useful prognostic equation. Can we achieve something similar with a more general equation of state, with non-constant coefficients of expansion?

Potential temperature

The potential temperature is defined as the temperature that a parcel would have if moved adiabatically to a given reference pressure p_R, often taken as 10^5 Pa (or 1000 hPa, or 1000 mb, approximately the pressure at the sea-surface). Thus it may be calculated, at least in principle, through an integral of the form

$$\theta(S, T, p; p_R) = T + \int_p^{p_R} \Gamma'_{\mathrm{ad}}(S, T, p) \, \mathrm{d}p \qquad (1.158)$$

where $\Gamma'_{\mathrm{ad}} = (\partial T/\partial p)_\eta$. The potential temperature of a fluid parcel is directly related to its entropy, provided its composition does not change. We already demonstrated this for an ideal gas, and to see it explicitly in the general case let us first write the equation of state in the form

$$\eta = \eta(S, T, p). \qquad (1.159)$$

Now, by definition of potential temperature we have

$$\eta = \eta(S, \theta; p_R) \quad \text{and} \quad \theta = \theta(\eta, S; p_R). \qquad (1.160)$$

For a parcel of constant salinity, changes in entropy are caused only by changes in potential temperature so that

$$\mathrm{d}\eta = \frac{\partial \eta(S, \theta; p_R)}{\partial \theta} \, \mathrm{d}\theta. \qquad (1.161)$$

Now, if we express entropy as a function of temperature and pressure then

$$\begin{aligned}
T\mathrm{d}\eta &= T\left(\frac{\partial \eta}{\partial T}\right)_p \mathrm{d}T + T\left(\frac{\partial \eta}{\partial p}\right)_T \mathrm{d}p \\
&= c_p \, \mathrm{d}T - T\left(\frac{\partial \alpha}{\partial T}\right)_p \mathrm{d}p.
\end{aligned} \qquad (1.162)$$

using one of the Maxwell relations. Suppose a fluid parcel moves adiabatically, then $\mathrm{d}\eta = 0$ and, by (1.161), $\mathrm{d}\theta = 0$. That is, the potential temperature at each point along its trajectory is constant and $\theta = \theta(\eta)$. How do we evaluate this function? Simply note that the temperature at the reference pressure p_R *is* the potential temperature, so that directly from (1.162)

$$\boxed{\mathrm{d}\eta = c_p(p_R, \theta)\frac{\mathrm{d}\theta}{\theta}}, \qquad (1.163)$$

and $\mathrm{d}\eta/\mathrm{d}\theta = c_p(p_R, \theta)/\theta$. If c_p is constant this integrates to

$$\eta = c_p \ln \theta + \text{constant} \qquad (1.164)$$

as for a simple ideal gas (1.111).

Since potential temperature is conserved in adiabatic motion, the thermodynamic equation can be written

$$c_p\frac{\mathrm{D}\theta}{\mathrm{D}t} = \frac{\theta}{T}\dot{Q}. \qquad (1.165)$$

where the right-hand-side represents heating. (If salinity is changing, then the right-hand side should also include any saline source terms and saline diffusion. However, such terms usually have a very small effect.) This equation is equivalent to (1.120) or (1.131), although it is only useful if θ can be simply related to the other state variables. In principle this can be done using (1.158), and in practice empirical relationships have been derived that express potential temperature in terms of the local temperature, pressure and salinity, and density in terms of potential temperature, salinity and pressure (see section 1.8.2 for more discussion).

Potential density

Potential density, ρ_θ, is defined as the density that a parcel would have if moved adiabatically and with fixed composition to a given reference pressure p_R often, but not always, taken as 10^5 Pa, or 1 bar. If the equation of state is of the form $\rho = \rho(S, T, p)$ then by definition we have

$$\rho_\theta = \rho(S, \theta; p_R). \tag{1.166}$$

For a parcel moving adiabatically (i.e., fixed salinity and entropy or potential temperature) its potential density is therefore conserved. For an ideal gas (1.166) gives $\rho_\theta = p_R/(R\theta)$ [as in (1.114)] and potential density provides no more information than potential temperature. However, in the oceans potential density accounts for the effect of salinity on density and so is a much better measure of the static stability of a column of water than density itself.

From (1.123) an approximate expression for the potential density in the ocean is

$$\rho_\theta = \left(\rho + \frac{\rho_0 g z}{c_s^2}\right). \tag{1.167}$$

Although this may suffice for theoretical or some modelling work, the vertical gradient of potential temperature in the ocean is often close to zero and a still more accurate, generally semi-empirical, expression is needed to determine stability properties.

Because density is so nearly constant in the ocean, it is common to subtract the amount $1000 \, \text{kg} \, \text{m}^{-3}$ before quoting its value, and depending on whether this value refers to *in situ* density or the potential density the results are called σ_t ('sigma-tee') or σ_θ ('sigma-theta') respectively. Thus,

$$\sigma_t = \rho(p, T, S) - 1000, \qquad \sigma_\theta = \rho(p_R, \theta, S) - 1000. \tag{1.168a,b}$$

If the potential density is referenced to a particular level, this is denoted by a subscript on the σ. Thus, σ_2 is the potential density referenced to 200 bars of pressure, or about 2 kilometers depth.

1.8.2 * More About Seawater

We now consider, rather didactically, some of the properties of the equation of state for seawater, noting in particular those nonlinearities that, although small, give it somewhat peculiar properties. We use a prototypical equation of state, (1.64) that, although not

Parameter	Description	Value
ρ_0	Reference Density	$1.027 \times 10^3 \, \text{kg m}^{-3}$
α_0	Reference Specific Volume	$9.738 \times 10^{-4} \, \text{m}^3 \, \text{kg}^{-1}$
T_0	Reference temperature	$283 \, \text{K}$
S_0	Reference salinity	$35 \, \text{psu} \approx 35\%o$
c_0	Reference sound speed	$1490 \, \text{m s}^{-1}$
β_T	First thermal expansion coefficient	$1.67 \times 10^{-4} \, \text{K}^{-1}$
β_T^*	Second thermal expansion coefficient	$1.00 \times 10^{-5} \, \text{K}^{-2}$
β_S	Haline contraction coefficient	$0.78 \times 10^{-3} \, \text{psu}^{-1}$
β_p	Inverse bulk modulus ($\approx \alpha_0/c_0^2$)	$4.39 \times 10^{-10} \, \text{m s}^2 \, \text{kg}^{-1}$
γ^*	Thermobaric parameter ($\approx \gamma'^*$)	$1.1 \times 10^{-8} \, \text{Pa}^{-1}$
c_{p0}	Specific heat capacity at constant pressure	$3986 \, \text{J kg}^{-1} \, \text{K}^{-1}$

Table 1.2 Various thermodynamic and equation-of-state parameters for seawater. Specifically, these parameters may be used in the approximate equations of state (1.64) and (1.178).

highly accurate except for small variations around a reference state, does capture the essential nonlinearities.[9] That equation of state may be written as:

$$\alpha = \alpha_0 \left[1 + \beta_T(1 + \gamma^* p)(T - T_0) + \frac{\beta_T^*}{2}(T - T_0)^2 - \beta_S(S - S_0) - \beta_p(p - p_0) \right],$$
(1.169)

where we may take $p_0 = 0$ and $\beta_p = \alpha_0/c_0'^2$, where c_0' is a reference sound speed. The starred parameters are associated with the nonlinear terms: β_T^* is the second expansion coefficient and γ^* is the 'thermobaric parameter', which determines the extent to which the thermal expansion of water depends on temperature. An equation of this form is useful because its coefficients can, in principle, be measured in the field or in the laboratory, and approximate values are given in table 1.2. However, it may not be the most useful form for modelling or observational work, because T is not materially conserved. Let us use this equation to deduce various thermodynamic quantities of interest, and also transform it to a more useful form for modelling.

Potential temperature of seawater

It would be useful to express (1.169) in terms of materially conserved variables, and so in terms of potential temperature rather than temperature. Now, by definition the potential temperature is obtained by integrating the adiabatic lapse rate from the in situ pressure to the reference pressure (zero); that is

$$\theta - T = \int_z^{z(p=0)} \left(\frac{\partial T}{\partial z} \right)_\eta \, dz = \int_p^0 \left(\frac{\partial T}{\partial p} \right)_\eta \, dp \qquad (1.170)$$
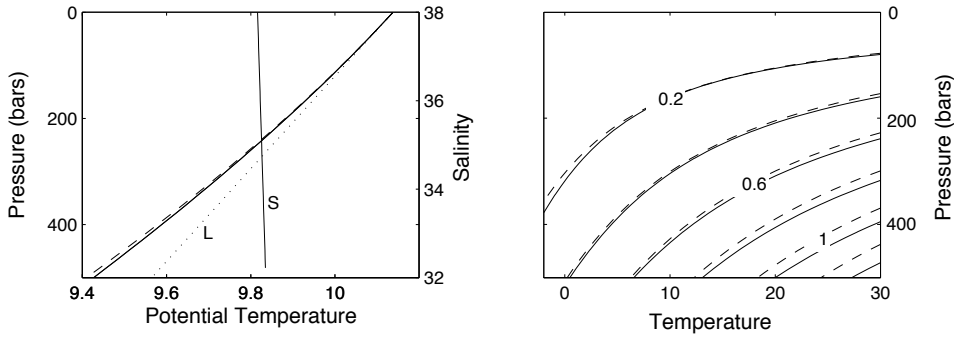
Fig. 1.4 Examples of variation of potential temperature of seawater with pressure, temperature and salinity. Left panel: the sloping lines show potential temperature as a function of pressure at fixed salinity ($S = 35$ psu) and temperature (13.36°C, the value of potential temperature at the surface). The solid line is computed using an accurate, empirical equation of state, the almost-coincident dashed line uses the simpler expression (1.177a) and the dotted line (labelled L) uses the even simpler linear expression (1.177c). The near vertical solid line, labelled S, shows the variation of potential temperature with salinity at fixed temperature and pressure. Right panel: Contours of the difference between temperature and potential temperature, ($T - \theta$) in the pressure-temperature plane, again for $S = 35$ psu. The solid lines use very accurate empirical formula, and the dashed lines use (1.177). The simpler equation can be improved locally, but not globally, by tuning the coefficients. (100 bars of pressure (10^7 Pa or 10 MPa) is approximately 1 km depth.)

Using (1.162), the adiabatic lapse rate is

$$\left(\frac{\partial T}{\partial p}\right)_\eta = \frac{T}{c_p}\left(\frac{\partial \alpha}{\partial T}\right)_{p,S} = \frac{T}{c_p}\alpha_0[\beta_T(1 + \gamma^* p) + \beta_T^*(T - T_0)]. \qquad (1.171)$$

Now, c_p satisfies $c_p = T(\partial \eta/\partial T)_p$, so that, using the Maxwell relation (1.87),

$$\left(\frac{\partial c_p}{\partial p}\right)_{T,S} = T\left(\frac{\partial}{\partial T}\left(\frac{\partial \eta}{\partial p}\right)_T\right)_p = T\frac{\partial^2 \alpha}{\partial T^2}. \qquad (1.172)$$

Thus, for our equation of state, we have

$$\left(\frac{\partial c_p}{\partial p}\right)_{T,S} = -T\alpha_0\beta_T^*, \qquad (1.173)$$

and therefore

$$c_p = c_{p0}(T, S) - pT\alpha_0\beta_T^*. \qquad (1.174)$$

The first term cannot be determined solely from the conventional equation of state; in fact for seawater specific heat varies very little with temperature (of order one part in

a thousand for a 10 K temperature variation). It varies more with salinity, changing by about $-5\,\mathrm{J\,kg^{-1}\,K^{-1}}$ per part-per-thousand change in salinity. Thus we take

$$c_{p0}(T, S) = c_{p1} + c_{p2}(S - S_0), \tag{1.175}$$

where c_{p1} and c_{p2} are constants that may be experimentally determined.

Using (1.174) and (1.171) in (1.170) gives,

$$\theta = T \exp\left\{-\frac{\alpha_0 \beta_T p}{c_{p0}}\left[1 + \frac{1}{2}\gamma^* p + \frac{\beta_T^*}{\beta_T}(T - T_0)\right]\right\}. \tag{1.176}$$

This equation is a relationship between T, θ and p analogous to (1.109) for an ideal gas. The exponent itself is small, the second and third terms in square brackets are small compared to unity, and the deviations of both T and θ from T_0 are also presumed small. Taking advantage of all of this enables the expression to be rewritten, with increasing levels of approximation, as

$$T' \approx \frac{T_0 \alpha_0 \beta_T}{c_{p0}} p\left(1 + \frac{1}{2}\gamma^* p + T_0\frac{\alpha_0 \beta_T^*}{c_{p0}}p\right) + \theta'\left(1 + T_0\frac{\alpha_0 \beta_T^*}{c_{p0}}p\right), \tag{1.177a}$$

$$\approx \frac{T_0 \alpha_0 \beta_T}{c_{p0}} p\left(1 + \frac{1}{2}\gamma^* p\right) + \theta'\left(1 + T_0\frac{\alpha_0 \beta_T^*}{c_{p0}}p\right), \tag{1.177b}$$

$$\approx \frac{T_0 \alpha_0 \beta_T}{c_{p0}} p + \theta', \tag{1.177c}$$

where $T' = T - T_0$ and $\theta' = \theta - T_0$. The last of the three, (1.177c), holds for a linear equation of state, and is useful for calculating approximate differences between temperature and potential temperature; making use of the hydrostatic approximation reveals that it is essentially the same as (1.136). Note that the potential temperature is related to temperature via the thermal expansion coefficient and not, as one might naïvely have expected, the compressibility coefficient. Plots of the difference between temperature and potential temperature, that also give both a sense of of the accuracy of these simpler formula, is given in Fig. 1.4.

Using (1.177b) in the equation of state (1.169) we find that, approximately,

$$\alpha = \alpha_0\left[1 - \frac{\alpha_0 p}{c_0^2} + \beta_T(1 + \gamma'^* p)\theta' + \frac{1}{2}\beta_T^*\theta'^2 - \beta_S(S - S_0)\right], \tag{1.178}$$

where $\gamma'^* = \gamma^* + T_0\beta_T^*\alpha_0/c_{p0} \approx \gamma^*$ and $c_0^{-2} = c_0'^{-2} - \beta_T^2 T_0/c_p \approx c_0'^{-2}$ is a reference value of the speed of sound (γ^* and γ'^* differ by a few percent, and c_0^2 and $c_0'^2$ differ by only a few parts in a thousand). Given (1.178), it is in principle straightforward, although in practice rather tedious, to compute various thermodynamic quantities of interest; a calculation of the buoyancy frequency is given in problem 2.19. We may approximate (1.178) further by using the hydrostatic pressure instead of the actual pressure; thus, letting $p = -g(z - z_0)/\alpha_0$ where z_0 is the nominal value of z at which $p = 0$, we obtain

$$\alpha = \alpha_0\left[1 + \frac{g(z - z_0)}{c_0^2} + \beta_T\left(1 - \gamma'^*\frac{g(z - z_0)}{\alpha_0}\right)\theta' + \frac{\beta_T^*}{2}\theta'^2 - \beta_S(S - S_0)\right]. \tag{1.179}$$

(a) Density vs temperature, with legend: S=35, $p = 5 \times 10^7$ (solid); S=35, $p = 10^5$ (dash-dot).

(b) Density vs salt, with legend: $\theta=5$, $p = 5 \times 10^7$ (solid); $\theta=13$, $p = 10^5$ (dash-dot).

(c) Density vs pressure ($\times 10^7$), with legend: S=35, $\theta=13$ (solid); S=35, $\theta=30$ (dash-dot).

(d) $\beta_T \times 10^3$ vs temperature, with legend: S=35, $p = 5 \times 10^7$ (solid); S=35, $p = 10^5$ (dash-dot).
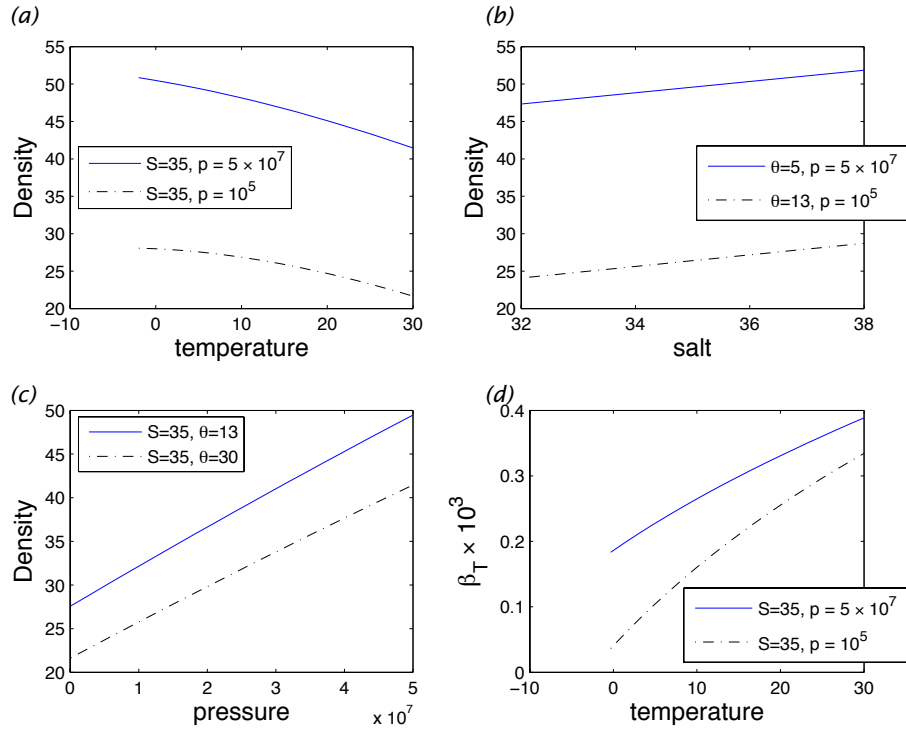
Fig. 1.5 Examples of the variation of density of seawater (minus $1000\,\mathrm{kg\,m^{-3}}$) with (a) potential temperature (K); (b) salt (psu); and (c) pressure (Pa), for seawater. Panel (d), shows the thermal expansion coefficient, $\beta_T = -\rho_0^{-1}(\partial\rho/\partial T)_{p,S}\,\mathrm{K^{-1}}$, for each of the two curves in panel (a).

Using z instead of p in the equation of state entails a slight loss of accuracy, but it turns out to be necessary to ensure that the Boussinesq equations conserve energy and potential vorticity, as discussed in later chapters.

The variation of density with potential temperature and salinity and pressure is illustrated in Fig. 1.3.

1.9 THE ENERGY BUDGET

The total energy of a fluid includes the kinetic, potential and internal energies. Both fluid flow and pressure forces will in general move energy from place to place, but we nevertheless expect energy to be conserved in an enclosed volume. Let us now consider what form energy conservation takes in a fluid.

1.9.1 Constant density fluid

For a constant density fluid the momentum equation and the mass continuity equation $\nabla\cdot$ $\boldsymbol{v} = 0$, are sufficient to completely determine the evolution of a system. The momentum

equation is

$$\frac{\mathrm{D}\boldsymbol{v}}{\mathrm{D}t} = -\nabla\left(\phi + \Phi\right) + \nu\nabla^2\boldsymbol{v}, \tag{1.180}$$

where $\phi = p/\rho_0$ and Φ is the potential for any conservative force (e.g., gz for a uniform gravitational field). We can rewrite the advective term on the left-hand-side using the identity,

$$(\boldsymbol{v}\cdot\nabla)\boldsymbol{v} = -\boldsymbol{v}\times\boldsymbol{\omega} + \nabla(\boldsymbol{v}^2/2), \tag{1.181}$$

where $\boldsymbol{\omega} \equiv \nabla\times\boldsymbol{v}$ is the *vorticity,* discussed more in later chapters. Then, omitting viscosity, we have

$$\frac{\partial\boldsymbol{v}}{\partial t} + \boldsymbol{\omega}\times\boldsymbol{v} = -\nabla B, \tag{1.182}$$

where $B = (\phi + \Phi + \boldsymbol{v}^2/2)$ is the *Bernoulli function* for constant density flow. Consider for a moment steady flows ($\partial\boldsymbol{v}/\partial t = 0$). Streamlines are, by definition, parallel to $\boldsymbol{v}$ everywhere, and the vector $\boldsymbol{v}\times\boldsymbol{\omega}$ is everywhere orthogonal to the streamlines, so that taking the dot product of the steady version of (1.182) with $\boldsymbol{v}$ gives $\boldsymbol{v}\cdot\nabla B = 0$. That is, for steady flows the Bernoulli function is constant along a streamline, and $\mathrm{D}B/\mathrm{D}t = 0$.

Reverting back to the time-varying case, take the dot product with $\boldsymbol{v}$ and include the density to yield

$$\frac{1}{2}\frac{\partial\rho_0\boldsymbol{v}^2}{\partial t} + \rho_0\boldsymbol{v}\cdot(\boldsymbol{\omega}\times\boldsymbol{v}) = -\rho_0\boldsymbol{v}\cdot\nabla B \tag{1.183}$$

The second term on the left-hand-side vanishes identically. Defining the kinetic energy density K, or energy per unit volume, by $K = \rho_0\boldsymbol{v}^2/2$, (1.183) becomes an expression for the rate of change of K,

$$\frac{\partial K}{\partial t} + \nabla\cdot(\rho_0\boldsymbol{v}B) = 0. \tag{1.184}$$

Because Φ is time-independent this may be written

$$\frac{\partial}{\partial t}\left[\rho_0(\frac{1}{2}\boldsymbol{v}^2 + \Phi)\right] + \nabla\cdot\left[\rho_0\boldsymbol{v}\left(\frac{1}{2}\boldsymbol{v}^2 + \Phi + \phi\right)\right] = 0. \tag{1.185}$$

or

$$\frac{\partial E}{\partial t} + \nabla\cdot[\boldsymbol{v}(E + p)] = 0. \tag{1.186}$$

where $E = K + \rho_0\Phi$ is the total energy density (i.e, the total energy per unit volume). This has the form of a general conservation equation in which a local change in a quantity is balanced by the divergence of its flux. However, the energy flux, $\boldsymbol{v}(\rho_0\boldsymbol{v}^2/2 + \rho_0\Phi + \rho_0\phi)$, is *not* simply the velocity times the energy density $\rho_0(\boldsymbol{v}^2/2 + \Phi)$; there is an additional term, $\boldsymbol{v}\,p$, that represents the energy transfer occurring when work is done by the fluid against the pressure force.

Now consider a volume through which there is no mass flux, for example a domain bounded by rigid walls. The rate of change of energy within that volume is then given by the integral of (1.183)

$$\frac{\mathrm{d}\widehat{K}}{\mathrm{d}t} \equiv \frac{\mathrm{d}}{\mathrm{d}t}\int_V K\,\mathrm{d}V = -\int_V \nabla\cdot(\rho_0\boldsymbol{v}B)\,\mathrm{d}V = -\int_S \rho_0 B\boldsymbol{v}\cdot\mathrm{d}\boldsymbol{S} = 0, \tag{1.187}$$

using the divergence theorem, and where $\widehat{K}$ is the total kinetic energy. Thus, the total kinetic energy within the volume is conserved. Note that for a constant density fluid the gravitational potential energy, $\widehat{P}$, is given by

$$\widehat{P} = \int_V \rho_0 g z \, \mathrm{d}V, \tag{1.188}$$

which is a constant, not affected by a re-arrangement of the fluid. Thus, in a constant density fluid there is no exchange between kinetic energy and potential energy and the kinetic energy itself is conserved.

1.9.2 Variable density fluids

We start with the momentum equation

$$\rho \frac{\mathrm{D}\boldsymbol{v}}{\mathrm{D}t} = -\nabla p - \rho \nabla \Phi, \tag{1.189}$$

and take its dot product with $\boldsymbol{v}$ to obtain an equation for the evolution of kinetic energy,

$$\begin{aligned} \frac{1}{2}\rho \frac{\mathrm{D}\boldsymbol{v}^2}{\mathrm{D}t} &= -\boldsymbol{v} \cdot \nabla p - \rho \boldsymbol{v} \cdot \nabla \Phi \\ &= -\nabla \cdot (p\boldsymbol{v}) + p\nabla \cdot \boldsymbol{v} - \rho \boldsymbol{v} \cdot \nabla \Phi. \end{aligned} \tag{1.190}$$

From (1.90) the internal energy equation for adiabatic flow is

$$\rho \frac{\mathrm{D}I}{\mathrm{D}t} = -\rho p \frac{\mathrm{D}\alpha}{\mathrm{D}t} = -p\nabla \cdot \boldsymbol{v} \tag{1.191}$$

where the second equality follows by use of the continuity equation. Finally, and somewhat trivially, the potential energy density obeys

$$\rho \frac{\mathrm{D}\Phi}{\mathrm{D}t} = \rho \boldsymbol{v} \cdot \nabla \Phi. \tag{1.192}$$

Adding (1.190), (1.191) and (1.192) we obtain

$$\rho \frac{\mathrm{D}}{\mathrm{D}t}\left(\frac{1}{2}\boldsymbol{v}^2 + I + \Phi\right) = -\nabla \cdot (p\boldsymbol{v}), \tag{1.193}$$

which, on expanding the material derivative and using the mass conservation equation, becomes

$$\frac{\partial}{\partial t}\left[\rho\left(\frac{1}{2}\boldsymbol{v}^2 + I + \Phi\right)\right] + \nabla \cdot \left[\rho \boldsymbol{v}\left(\frac{1}{2}\boldsymbol{v}^2 + I + \Phi + p/\rho\right)\right] = 0. \tag{1.194}$$

This may be written

$$\boxed{\frac{\partial E}{\partial t} + \nabla \cdot [\boldsymbol{v}(E + p)] = 0}, \tag{1.195}$$

where $E = \rho(\boldsymbol{v}^2/2 + I + \Phi)$ is the total energy per unit volume, or the total energy density, of the fluid. This is the energy equation for an unforced, inviscid and adiabatic, compressible fluid. Just as for the constant density case, the energy flux contains the term $p\boldsymbol{v}$ that represents the work done against pressure and, again, the second term vanishes when integrated over a closed domain with rigid boundaries, implying that the total energy is conserved. However, now there can now be an exchange of energy between kinetic, potential and internal components. The quantity $\sigma = I + p\alpha + \Phi = h + \Phi$ is sometimes referred to as the static energy, or the dry static energy. However, it is not a component of the globally conserved total energy; the conserved energy contains only the quantity $I + \Phi$ plus the kinetic energy, and it is it is only the *flux* of static energy that affects the energetics. For an ideal gas we have $\sigma = c_v T + RT + \Phi = c_p T + \Phi$, and if the potential is caused by a uniform gravitational field then $\sigma = c_p T + gz$.

Bernoullis' theorem

For steady flow $\partial/\partial t = 0$ and $\nabla \cdot \rho\boldsymbol{v} = 0$ so that (1.194) may be written $\boldsymbol{v} \cdot \nabla B = 0$ where B is the Bernoulli function given by

$$B = \left(\frac{1}{2}\boldsymbol{v}^2 + I + \Phi + p/\rho\right) = \left(\frac{1}{2}\boldsymbol{v}^2 + h + \Phi\right). \tag{1.196}$$

This means that, for steady flow,

$$\frac{\mathrm{D}B}{\mathrm{D}t} = 0, \tag{1.197}$$

and the Bernoulli function is a constant along streamline. For an ideal gas in a constant gravitation field $B = \boldsymbol{v}^2/2 + c_p T + gz$.

For adiabatic flow we also have $\mathrm{D}\theta/\mathrm{D}t = 0$. Thus, steady flow is both along surfaces of constant θ and along surfaces of constant B, and the vector

$$\boldsymbol{l} = \nabla\theta \times \nabla B \tag{1.198}$$

is parallel to streamlines.[10] A related result for unsteady flow is given in section 4.8.

1.9.3 Viscous Effects

We might expect that viscosity will always act to reduce the kinetic energy of a flow, and we will demonstrate this for a constant density fluid. Retaining the viscous term in (1.180), the energy equation becomes

$$\frac{\mathrm{d}\widehat{E}}{\mathrm{d}t} \equiv \frac{\mathrm{d}}{\mathrm{d}t}\int_V E\,\mathrm{d}V = \mu\int_V \boldsymbol{v}\cdot\nabla^2\boldsymbol{v}\,\mathrm{d}V. \tag{1.199}$$

The right hand side is negative definite. To see this we use the vector identity

$$\nabla \times (\nabla \times \boldsymbol{v}) = \nabla(\nabla \cdot \boldsymbol{v}) - \nabla^2\boldsymbol{v}, \tag{1.200}$$

and because $\nabla \cdot \boldsymbol{v} = 0$ we have $\nabla^2\boldsymbol{v} = -\nabla \times \boldsymbol{\omega}$, where $\boldsymbol{\omega} \equiv \nabla \times \boldsymbol{v}$. Thus,

$$\frac{\mathrm{d}\widehat{E}}{\mathrm{d}t} = -\mu\int_V \boldsymbol{v}\cdot(\nabla\times\boldsymbol{\omega})\,\mathrm{d}V = -\mu\int_V \boldsymbol{\omega}\cdot(\nabla\times\boldsymbol{v})\,\mathrm{d}V = -\mu\int_V \boldsymbol{\omega}^2\,\mathrm{d}V, \tag{1.201}$$

after integrating by parts, providing $\boldsymbol{v} \times \boldsymbol{\omega}$ vanishes at the boundary. Thus, viscosity acts to extract kinetic energy from the flow. The loss of kinetic energy reappears as an irreversible warming of the fluid ('Joule heating'), and the total energy of the fluid is conserved, but this effect plays no role in a constant density fluid. The effect is normally locally small, at least in the earth's ocean and atmosphere, although it is sometimes included in comprehensive General Circulation Models.

1.10 AN INTRODUCTION TO NON-DIMENSIONALIZATION AND SCALING

The units we use to measure length, velocity and so on are irrelevant to the dynamics, and not necessarily the most appropriate units for a given problem. Rather, it is convenient to express the equations of motion, so far as is possible, in so-called 'nondimensional' variables, by which we mean expressing every variable (such as velocity) as the ratio of its value to some reference value. For velocity the reference could, for example, be the speed of of light — but this would not be very helpful for fluid dynamical problems in the earth's atmosphere or ocean! Rather, we should choose the reference value as a natural one for a given flow, in order that, so far as possible, the nondimensional variables are order-unity quantities, and doing this is called *scaling the equations*. Evidently, there is no reference velocity that is universally appropriate, and much of the art of fluid dynamics lies in choosing sensible scaling factors for the problem at hand. Non-dimensionalization plays an important role in fluid dynamics, and we introduce it here with a simple example.

1.10.1 The Reynolds number

Consider the constant-density momentum equation in Cartesian coordinates. If a typical velocity is U, a typical length is L, a typical timescale is T, and a typical value of the pressure deviation is Φ, then the approximate sizes of the various terms in the momentum equation are given by

$$\frac{\partial \boldsymbol{v}}{\partial t} + (\boldsymbol{v} \cdot \nabla)\boldsymbol{v} = -\nabla \phi + \nu \nabla^2 \boldsymbol{v} \tag{1.202a}$$

$$\frac{U}{T} \qquad \frac{U^2}{L} \quad \sim \quad \frac{\Phi}{L} \quad \nu \frac{U}{L^2}. \tag{1.202b}$$

The ratio of the inertial terms to the viscous terms is $\left(U^2/L\right)\big/\left(\nu U/L^2\right) = UL/\nu$, and this is the *Reynolds number*.[11] More formally, we can nondimensionalize the momentum equation by writing

$$\widehat{\boldsymbol{v}} = \frac{\boldsymbol{v}}{U}, \qquad \widehat{\boldsymbol{x}} = \frac{\boldsymbol{x}}{L}, \qquad \widehat{t} = \frac{t}{T}, \qquad \widehat{\phi} = \frac{\phi}{\Phi}, \tag{1.203}$$

where the terms with hats on are *nondimensional* values of the variables and the capitalized quantities are known as *scaling values*, and these are the approximate magnitudes of the variables. We choose the nondimensionalization so that the nondimensional variables are of order unity. Thus, for example, we choose U so that $u = \mathcal{O}(U)$ where this

should be taken to mean that the magnitude of the variable u is approximately U, or that $u \sim U$, and we say that 'u scales like U'. [This $\mathcal{O}()$ notation differs somewhat from the conventional mathematical meaning of 'order', in which $a = O(\epsilon^\alpha)$ represents a limit in which $a/\epsilon^\alpha \to$ constant as $\epsilon \to 0$.] Thus, if there are well-defined length and velocity scales in the problem, and we choose these scales to perform the nondimensionalization, then the nondimensional variables are of order unity. That is, $\hat{u} = \mathcal{O}(1)$, and similarly for the other variables.

Because there are no external forces in this problem, appropriate scaling values for time and pressure are

$$T = \frac{L}{U}, \qquad \Phi = U^2. \tag{1.204}$$

Substituting (1.203) and (1.204) into the momentum equation we obtain

$$\frac{U^2}{L}\left[\frac{\partial \hat{\boldsymbol{v}}}{\partial \hat{t}} + (\hat{\boldsymbol{v}} \cdot \hat{\nabla})\hat{\boldsymbol{v}}\right] = -\frac{U^2}{L}\hat{\nabla}\hat{\phi} + \frac{\nu U}{L^2}\hat{\nabla}^2 \boldsymbol{v}, \tag{1.205}$$

where $\hat{\nabla}$ is the nondimensional gradient operator. Eq. (1.205) simplifies to

$$\frac{\partial \hat{\boldsymbol{v}}}{\partial \hat{t}} + (\hat{\boldsymbol{v}} \cdot \hat{\nabla})\hat{\boldsymbol{v}} = -\hat{\nabla}\hat{\phi} + \frac{1}{Re}\hat{\nabla}^2\hat{\boldsymbol{v}}, \tag{1.206}$$

where

$$Re \equiv \frac{UL}{\nu} \tag{1.207}$$

is, again, the Reynolds number. If we have chosen our length and velocity scales sensibly — that is, if we have scaled them properly — each variable in (1.206) is order unity, with the viscous term being multiplied by $1/Re$. There are two important conclusions:

(i) The ratio of the importance of the inertial terms to the viscous terms is given by the *Reynolds number,* defined by (1.207). In the absence of other forces, such as those due to gravity and rotation, the Reynolds number is the only non-dimensional parameter explicitly appearing in the momentum equation. Hence its value, along with the boundary conditions, controls the behaviour of the system.

(ii) More generally, by scaling the equations of motion appropriately the parameters determining the behaviour of the system become explicit. *Scaling the equations is intelligent nondimensionalization.*

Notes

1 Parts of the first few chapters, and many of the problems, draw on notes prepared over the years for a graduate class at Princeton University, originally written by Steve Garner, Isaac Held and Yoshio Kurihara and also taught by Paul Kushner and myself.

2 Joseph-Louis Lagrange (1736–1813) was a Franco-Italian, born and raised in Turin who then lived and worked mainly in Germany and France. He made notable contributions in analysis, number theory and mechanics and was recognized as one

of the greatest mathematicians of the 18th century. He laid the foundations of the calculus of variations (to wit, the 'Lagrange multiplier') and first formulated the principle of least action, and his monumental treatise *Mécanique Analytique* (1788) provides a unified analytic framework (it contains no diagrams, a feature virtually emulated in Whitaker's *Analytical Dynamics,* 1927) for all Newtonian mechanics.

Leonard Euler (1707–1783), a Swiss mathematician who lived and worked for extended periods in Berlin and St. Petersburg, made important contributions in many areas of mathematics and mechanics, including the analytical treatment of algebra, the theory of equations, calculus, number theory and classical mechanics. He was the first to establish the form of the equations of motion of fluid mechanics, writing down both the field description of fluids *and* what we now call the material or advective derivative.

Truesdell (1954) points out that 'Eulerian' and 'Lagrangian' coordinates, especially the latter, are inappropriate eponyms. The so-called Eulerian description was introduced by d'Alembert in 1749 and generalized by Euler in 1752, and the so-called Lagrangian description was introduced by Euler in 1759. The modern confusion evidently stems from a monograph by Dirichlet in 1860 that credits Euler in 1757 and Lagrange in 1788 for the respective methods. One perhaps should therefore refer to the two points of view as the 'field' or 'spatial' view, and the 'material' view; we will also use 'Eulerian' because it implies a special rules for taking derivatives, but will eschew 'Lagrangian'.

3   For example Batchelor (1967).

4   R_d and R_v are related by the molecular weights of water and dry air, M_v and M_d, so that $\alpha \equiv R_d/R_v = M_v/M_d = 0.62$. Rather than allow the gas constant to vary, meteorologists sometimes incorporate the variation of humidity into the definition of temperature, so that instead of $p = \rho R_{\text{eff}} T$ we use $p = \rho R_d T_v$, so defining the 'virtual temperature', T_v. It is easy to show that $T_v \approx [1 + w(\alpha^{-1} - 1)]T$. Atmospheric GCMs often use a virtual temperature.

5   The form of (1.64) was suggested by de Szoeke (2003). More accurately, and with more complication, the international equation of state of seawater (Unesco 1981) is an empirical equation that fits measurements to an accuracy of order 10^{-5} (see Fofonoff 1985). Somewhat simpler, more easily computable and generally accurate formulae are also available from Mellor (1991), Wright (1997), and (with particular attention to high accuracy) McDougall et al. (2002). The formulae of Wright and McDougall *et al* are of the form:

$$\rho = \frac{p + p_0}{\lambda + \alpha_0 (p + p_0)}$$

where α_0, p_0 and λ are expressed as polynomials in potential temperature and salinity, using the Gibbs function of Feistel and Hagen (1995), which is as or more accurate than the UNESCO formula. Wright's formula used are used for Fig. 1.5 and Fig. 1.3. Bryden (1973) provides polynomial formulae for potential temperature of seawater in terms of temperature, salinity and pressure and this is used for Fig. 1.4. In most numerical ocean models potential temperature and salinity are the prognostic thermodynamic variables and an empirical equation of state is used to compute density and potential density.

6 This section does not develop thermodynamics from its fundamentals; for that see, e.g., Callen (1985).

7 Claude-Louis-Marie-Henri Navier (1785–1836) was a French civil engineer, professor at the École Polytechnique and later at the École des Ponts et Chaussée. He was a expert in road and bridge building (he developed the theory of suspension bridges) and, relatedly, made lasting theoretical contributions to the theory of elasticity, being the first to publish a set of general equations for the dynamics of an elastic solid. In fluid mechanics, he laid down the now-called *Navier-Stokes equations,* including the viscous terms, in 1822.

George Gabriel Stokes (1819–1903). Irish born (in Skreen, County Sligo), he held the Lucasian chair of Mathematics at Cambridge from 1849 until his retirement. As well as having a role in the development of fluid mechanics, especially through his considerations of viscous effects, Stokes worked on the dynamics of elasticitiy, fluorescence, the wave theory of light, and was (rather ill-advisedly in hindsight) a proponent of the idea of an ether permeating all space.

8 Some sources take incompressibility to mean that density is unaffected by pressure, but this alone is insufficient to guarantee that the mass conservation equation can be approximated by $\nabla \cdot \boldsymbol{v} = 0$.

9 Following de Szoeke (2003), where a more complete discussion is to be found.

10 These results, usually known as Bernoulli's theorem, were developed by Daniel and Johannes Bernoulli and so should be known as the Bernoullis' theorem.

11 Osborne Reynolds (1842-1912) was an Irish born (Belfast) physicist who was professor of engineering at Manchester University from 1868–1905. His early work was in electricity and magnetism, but he is now most famous for his work in hydrodynamics. The 'Reynolds number,' which determines the ratio of inertial to viscous forces, and the 'Reynolds stress,' which is the stress on the mean flow due to the fluctuating components, are both named after him. He was also one of the first scientists to think about the concept of group velocity.

Further Reading

There are numerous books on hydrodynamics; some of them are:

Lamb, H. 1932. *Hydrodynamics,* 6th edn.
    This is a classic text in the subject, although its notation is now too dated to make it really useful as an introduction. Another very well-known text is:

Batchelor, G. K. 1967. *An Introduction to Fluid Dynamics.*
    This mainly treats incompressible flow. It is rather heavy going for the true beginner, but nevertheless is a very useful reference for the fundamentals. Two other useful references are:

Tritton, D. J. 1988. *Physical Fluid Dynamics,* 2nd edn.

Kundu, P. and I. M. Cohen 1990. *Fluid Mechanics.*
    Both are introductions written at the advanced undergraduate/beginning graduate level, and are easier-going than Batchelor. Kundu and Cohen's book has more material on geophysical fluid dynamics.

There are also numerous books on thermodynamics, two clear and useful ones being:

Reif, F., 1965. *Fundamentals of Statistical and Thermal Physics,*

Callen, E. B. 1985 *Thermodynamics and an Introduction to Thermostatistics.*
    Reif's book has become something of a classic, and Callen provides a rather more
    axiomatic approach.

An introduction to thermodynamic effects in fluids, with an emphasis on fundamental
properties, is provided by:

Salmon, R, 1998, *Lectures on Geophysical Fluid Dynamics.*

Problems

> *It is by the solution of problems that the investigator tests the temper of his*
> *steel; he finds new methods and new outlooks, and gains a wider and freer*
> *horizon.*
> David Hilbert (1862–1943).

1.1 For an infinitesimal volume, informally show that

$$\frac{\mathrm{D}}{\mathrm{D}t}(\rho\phi\Delta V) = \rho\Delta V \frac{\mathrm{D}\phi}{\mathrm{D}t}, \tag{P1.1}$$

and hence informally deduce that

$$\frac{\mathrm{D}}{\mathrm{D}t}\int_V \rho\phi\,\mathrm{d}V = \int_V \rho\frac{\mathrm{D}\phi}{\mathrm{D}t}\,\mathrm{d}V. \tag{P1.2}$$

where ϕ is an arbitrary, differentiable, property of the fluid.

1.2 Show that the derivative of an integral is given by

$$\frac{\mathrm{d}}{\mathrm{d}t}\int_{x_1(t)}^{x_2(t)} \phi(x,t)\,\mathrm{d}x = \int_{x_1}^{x_2} \frac{\partial\phi}{\partial t}\,\mathrm{d}x + \frac{\mathrm{d}x_2}{\mathrm{d}t}\phi(x_2,t) - \frac{\mathrm{d}x_1}{\mathrm{d}t}\phi(x_1,t). \tag{P1.3}$$

By generalizing to three-dimensions show that the material derivative of an integral
of a fluid property is given by

$$\frac{\mathrm{D}}{\mathrm{D}t}\int_V \phi(\boldsymbol{x},t)\,\mathrm{d}V = \int_V \frac{\partial\phi}{\partial t}\,\mathrm{d}V + \int_S \phi\boldsymbol{v}\cdot\mathrm{d}\boldsymbol{S} = \int_V \left[\frac{\partial\phi}{\partial t} + \nabla\cdot(\boldsymbol{v}\phi)\right]\mathrm{d}V, \tag{P1.4}$$

where the surface integral ($\int_S$) is over the surface bounding the volume V. Hence
deduce that

$$\frac{\mathrm{D}}{\mathrm{D}t}\int_V \rho\phi\,\mathrm{d}V = \int_V \rho\frac{\mathrm{D}\phi}{\mathrm{D}t}\,\mathrm{d}V. \tag{P1.5}$$

1.3 Why is there no diffusion term in the mass continuity equation?

1.4 By invoking Galilean invariance we can often choose, without loss of generality, the
    basic state for problems in sound waves to be such that $u_0 \equiv 0$. The perturbation
    velocity is then certainly larger than the basic state velocity. How can we then justify
    ignoring the nonlinear term in the perturbation equation, as the term $u'\partial u'/\partial x$ is
    certainly no smaller than the linear term $u_0\partial u'/\partial x$?

1.5 For sound waves in air of amplitude 60 dB, show that the linear approximation to
    the equations of motion is a good one. For example, in a one-dimensional problem,
    show that the term $u'\partial u'/\partial x$ is much smaller than $\partial u'/\partial t$. What amplitude of sound
    wave is required for the nonlinear terms to become important? Is this achieved at a
    rock concert?

1.6 Using the observed value of molecular diffusion of heat in water, estimate how long it would take for a temperature anomaly to mix from the top of the ocean to the bottom, assuming that molecular diffusion alone is responsible. Comment on whether you think the real ocean has reached equilibrium after the last ice age (which ended about 12,000 years ago).

1.7 Consider the following flow:

$$u = \Gamma z$$
$$v = V \sin[k(x - ct)]$$

where Γ, V, k and c are positive constants. (This is similar to the flow in the mid-latitude troposphere — an eastward flow increasing with height, with a transverse wave superimposed.) Suppose that $\Gamma z > c$ for the region of interest. Consider particles located along the $y = 0$ axis at $t = 0$, and compute their position at some later time t. Compare this with the *streamfunction* for the flow at the same time. (*Hint:* Show that the meridional particle displacement is $\eta = \psi/(u - c)$, where ψ is the streamfunction and u and c are parameters.)

1.8 Consider the two-dimensional flow

$$u = A(y) \sin \omega t, \qquad v = A(y) \cos \omega t. \tag{P1.6}$$

The time-mean of this at a fixed point flow is zero. If A is independent of y, then fluid parcels move clockwise in a circle. What is its radius? If A does depend on y, find an *approximate* expression for the average drift of a particle,

$$\lim_{t \to \infty} \frac{x(a, t)}{t}$$

where a is a particle label and A is suitably 'small'. Be precise about what small means.
Partial solution: Write $A(y) = A_0 + ay$ and solve

$$\frac{dy}{dt} = (A_0 + ay) \cos \omega t \tag{P1.7}$$

as a polynomial function of $\sin \omega t$. Then solve

$$\frac{dx}{dt} = (A_0 + ay) \sin \omega t$$

using the solution for y. The rectification of the standing oscillation by the oscillating trajectory now appears, because $\langle \sin \omega t \sin \omega t \rangle \neq 0$. The small parameter is the relative variation of A across a particle displacement, namely

$$\frac{\delta A}{A} = \frac{(a A_0/b)}{A_0} = \frac{a}{b}.$$

That is, the shear is small compared to the frequency.

1.9 Suppose that a sealed, insulated container consists of two compartments, and that one of them is filled with an ideal gas and the other is a vacuum. The partition separating the compartments is removed. How does the temperature of the gas change? (Answer: It stays the same.) Reconcile this answer with the first law of thermodynamics for an ideal gas:

$$dQ = T \, d\eta = dI + dW = c_v \, dT + p \, d\alpha, \tag{P1.8}$$

as well as with the notion that a parcel that is ascending adiabatically through the atmosphere will generally cool.

1.10 Show that adiabatic flow in an ideal gas satisfies $p\rho^{-\gamma}$ where $\gamma = c_p/cv$.

1.11 *(a)* Show that for an ideal gas (1.120) is equivalent to (1.104). You may use the Maxwell relation $(\partial\alpha/\partial\eta)_p = (\partial T/\partial p)_\eta$.
   (b) Show that for an ideal gas (1.131) is equivalent to (1.103). You may use the results of part (a).

1.12 Show that it follows directly from the equation of state, $P = RT/\alpha$, that the internal energy of an ideal gas is a function of temperature only.
   Solution: From (1.91) and $p = RT/\alpha$ we have

$$\mathrm{d}\eta = \frac{1}{T}\left(\frac{\partial I}{\partial T}\right)_\alpha \mathrm{d}T + \left[\frac{1}{T}\left(\frac{\partial I}{\partial \alpha}\right)_T + \frac{R}{\alpha}\right]\mathrm{d}\alpha. \qquad (P1.9)$$

But, mathematically,

$$\mathrm{d}\eta = \left(\frac{\partial\eta}{\partial T}\right)_\alpha \mathrm{d}T + \left(\frac{\partial\eta}{\partial\alpha}\right)_T \mathrm{d}\alpha. \qquad (P1.10)$$

Equating the coefficient of $\mathrm{d}T$ and $\mathrm{d}\alpha$ in these two expressions gives

$$\left(\frac{\partial\eta}{\partial T}\right)_\alpha = \frac{1}{T}\left(\frac{\partial I}{\partial T}\right)_\alpha \quad \text{and} \quad \left(\frac{\partial\eta}{\partial\alpha}\right)_T = \frac{1}{T}\left(\frac{\partial I}{\partial\alpha}\right)_T + \frac{R}{\alpha}. \qquad (P1.11)$$

Noting that $\partial^2\eta/(\partial\alpha\partial T) = \partial^2\eta/(\partial T\partial\alpha)$ we obtain

$$\frac{\partial^2 I}{\partial\alpha\partial T} = \frac{\partial^2 I}{\partial T\partial\alpha} - \left(\frac{\partial I}{\partial\alpha}\right)_T. \qquad (P1.12)$$

Thus, $(\partial I/\partial\alpha)_T = 0$. Because, in general, the internal energy may be considered either a function of temperature and density or temperature and pressure, this proves that for an ideal gas the internal energy is a function *only* of temperature.

1.13 Show that it follows directly from the equation of state $P = RT/\alpha$, that for an ideal gas the heat capacity at constant volume, c_v, is, at most, a function of temperature.

1.14 Show that for an ideal gas
$$T\mathrm{d}\eta = c_v\mathrm{d}T + p\mathrm{d}\alpha. \qquad (P1.13)$$

and that its internal energy is given by $I = \int c_v\mathrm{d}T$.
Solution: Let us regard η as a function of T and α, where α is the specific volume $1/\rho$. Then

$$T\mathrm{d}\eta = T\left(\frac{\partial\eta}{\partial T}\right)_\alpha \mathrm{d}T + T\left(\frac{\partial\eta}{\partial\alpha}\right)_T \mathrm{d}\alpha$$
$$= c_v\,\mathrm{d}T + T\left(\frac{\partial\eta}{\partial\alpha}\right)_T \mathrm{d}\alpha \qquad (P1.14)$$

by definition of c_v. For an ideal gas the internal energy is a function of temperature alone (problem 1.12), so that using (1.74) the pressure of a fluid $p = T\left(\partial\eta/\partial\alpha\right)_I = T\left(\partial\eta/\partial\alpha\right)_T$ and (P1.14) becomes

$$T\mathrm{d}\eta = c_v\,\mathrm{d}T + p\,\mathrm{d}\alpha \qquad (P1.15)$$

But, *in general*, the fundamental thermodynamic relation is

$$T \mathrm{d}\eta = \mathrm{d}I + p\,\mathrm{d}\alpha. \tag{P1.16}$$

The terms on the right hand side of (P1.15) are identifiable as the change in the internal energy and the work done on a fluid, and so $\mathrm{d}I = c_v\,\mathrm{d}T$. The heat capacity need not necessarily be constant, although for air it very nearly is, but it must be a function of temperature only.

1.15 *(a)* Beginning with the expression for potential temperature for an ideal gas, $\theta = T(p_{\mathrm{R}}/p)^{\kappa}$, where $\kappa = R/c_p$, show that

$$\mathrm{d}\theta = \frac{\theta}{T}(\mathrm{d}T - \alpha \mathrm{d}p), \tag{P1.17}$$

and therefore that the first law of thermodynamics may be written as

$$\mathrm{d}Q = T\mathrm{d}\eta = c_p\frac{T}{\theta}\mathrm{d}\theta. \tag{P1.18}$$

(b) Show that (P1.18) is generally true, without making the ideal gas approximation.

1.16 Obtain an expression for the Gibbs function for an ideal gas in terms of pressure and temperature.

1.17 From (1.117) derive the conventional equation of state for an ideal gas, and obtain expressions for the heat capacities.

1.18 Consider an ocean at rest with known vertical profiles of potential temperature and salinity, $\theta(z)$ and $S(z)$. Suppose we also know the equation of state in the form $\rho = \rho(\theta, S, p)$. Obtain an expression for the buoyancy frequency. Check your expression by substituting the equation of state for an ideal gas and recovering a known expression for the buoyancy frequency.

1.19 ♦ Obtain an expression, in terms of temperature and pressure, for the potential temperature of a van der Waals gas, with equation of state $(p + a/\alpha^2)(\alpha - b) = RT$, where a and b are constants. Show that it reduces to the expression for an ideal gas in the limit $a \to 0$, $b \to 0$.

1.20 ♦ In seawater, why does potential temperature differ from in situ temperature? Is is because of the compressibility (with pressure) or the thermal expansion of water? A good answer will include, *inter alia,* a physical explanation of the difference in scale heights of (1.124) and (1.135) and a discussion of the lapse rate and scale heights of water that is between 0° and 4°C.

If a body is moving in any direction, there is a force, arising from the earth's rotation, which always deflects it to the right in the northern hemisphere, and to the left in the southern.

William Ferrel, *The influence of the Earth's rotation upon the relative motion of bodies near its surface*, 1858.

CHAPTER 2

Effects of Rotation and Stratification

THE ATMOSPHERE AND OCEAN are shallow layers of fluid on a sphere in that their thickness or depth is much less than their horizontal extent. Furthermore, their motion is strongly influenced by two effects: rotation and stratification, the latter meaning that there is a mean vertical gradient of (potential) density that is often large compared with its horizontal gradient. Here we consider how the equations of motion are affected by these effects. First, we consider some elementary effects of rotation on a fluid and derive the Coriolis and centrifugal forces, and then we write down the equations of motion appropriate for motion on a sphere. Then we discuss some approximations to the equations of motion that are appropriate for large-scale flow in the ocean and atmosphere, in particular the hydrostatic approximation, and how the presence of strong stratification can be used to further simplify the governing equations.

2.1 THE EQUATIONS OF MOTION IN A ROTATING FRAME OF REFERENCE

Newton's second law of motion, that the acceleration on a body is proportional to the imposed force divided by the body's mass, applies in so-called inertial frames of reference. The earth rotates with a period of about almost 24 hours (23h 56m) relative to the distant stars, and the surface of the earth manifestly is not, in that sense, an inertial frame. Nevertheless, because the surface of the earth is moving (in fact at speeds of up to a few hundreds of meters per second) it is very convenient to describe the flow relative to the earth's surface, rather than in some inertial frame. This necessitates recasting the equations into a form that is appropriate for a rotating frame of reference, and that is the subject of this section.

55

Figure 2.1 A vector C rotating at an angular velocity Ω. It appears to be a constant vector in the rotating frame, whereas in the inertial frame it evolves according to $(\mathrm{d}C/\mathrm{d}t)_I = \Omega \times C$.
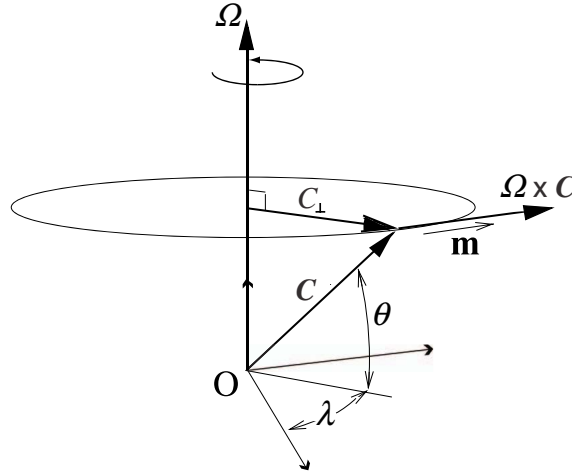
2.1.1 Rate of change of a vector

Consider first a vector C of constant length rotating relative to an inertial frame at a constant angular velocity Ω. Then, in a frame rotating with that same angular velocity it appears stationary and constant. If in small interval of time δt it the vector C rotates through a small angle $\delta\lambda$ then the change in C, as perceived in the inertial frame, is given by (see Fig. 2.1)

$$\delta C = |C| \cos\theta \, \delta\lambda \, m, \tag{2.1}$$

where the vector m is the unit vector in the direction of change of C, which is perpendicular to both C and Ω. But the rate of change of the angle λ is just, by definition, the angular velocity so that $\delta\lambda = |\Omega|\delta t$ and

$$\delta C = |C||\Omega| \sin\widehat{\theta} \, m \, \delta t = \Omega \times C \, \delta t. \tag{2.2}$$

using the definition of the vector cross product, where $\widehat{\theta} = (\pi/2 - \theta)$ is the angle between Ω and C. Thus

$$\left(\frac{\mathrm{d}C}{\mathrm{d}t}\right)_I = \Omega \times C \tag{2.3}$$

where the left hand side is the rate of change of C as perceived in the inertial frame.

Now consider a vector B that changes in the inertial frame. In a small time δt the change in B as seen in the rotating frame is related to the change seen in the inertial frame by

$$(\delta B)_I = (\delta B)_R + (\delta B)_{\mathrm{rot}} \tag{2.4}$$

where the terms are, respectively, the change seen in the inertial frame, the change due to the vector itself changing as measured in the rotating frame, and the change due to the rotation. Using (2.2) $(\delta B)_{\mathrm{rot}} = \Omega \times B \, \delta t$, and so the rates of change of the vector B in the inertial and rotating frames are related by

$$\boxed{\left(\frac{\mathrm{d}B}{\mathrm{d}t}\right)_I = \left(\frac{\mathrm{d}B}{\mathrm{d}t}\right)_R + \Omega \times B} . \tag{2.5}$$

This relation applies to a vector $\boldsymbol{B}$ that, as measured at any one time, is the same in both inertial and rotating frames.

2.1.2 Velocity and acceleration in a rotating frame

The velocity of a body is not measured to be the same in the inertial and rotating frames, so care must be taken when applying (2.5) to velocity. First apply (2.5) to $\boldsymbol{r}$, the position of a particle to obtain

$$\left(\frac{\mathrm{d}\boldsymbol{r}}{\mathrm{d}t}\right)_I = \left(\frac{\mathrm{d}\boldsymbol{r}}{\mathrm{d}t}\right)_R + \boldsymbol{\Omega} \times \boldsymbol{r} \tag{2.6}$$

or

$$\boldsymbol{v}_I = \boldsymbol{v}_R + \boldsymbol{\Omega} \times \boldsymbol{r}. \tag{2.7}$$

We refer to $\boldsymbol{v}_R$ and $\boldsymbol{v}_I$ as the relative and inertial velocity, respectively, and (2.7) relates the two. Apply (2.5) again, this time to the velocity $\boldsymbol{v}_R$ to give

$$\left(\frac{\mathrm{d}\boldsymbol{v}_R}{\mathrm{d}t}\right)_I = \left(\frac{\mathrm{d}\boldsymbol{v}_R}{\mathrm{d}t}\right)_R + \boldsymbol{\Omega} \times \boldsymbol{v}_R, \tag{2.8}$$

or, using (2.7)

$$\left(\frac{\mathrm{d}}{\mathrm{d}t}(\boldsymbol{v}_I - \boldsymbol{\Omega} \times \boldsymbol{r})\right)_I = \left(\frac{\mathrm{d}\boldsymbol{v}_R}{\mathrm{d}t}\right)_R + \boldsymbol{\Omega} \times \boldsymbol{v}_R, \tag{2.9}$$

or

$$\left(\frac{\mathrm{d}\boldsymbol{v}_I}{\mathrm{d}t}\right)_I = \left(\frac{\mathrm{d}\boldsymbol{v}_R}{\mathrm{d}t}\right)_R + \boldsymbol{\Omega} \times \boldsymbol{v}_R + \frac{\mathrm{d}\boldsymbol{\Omega}}{\mathrm{d}t} \times \boldsymbol{r} + \boldsymbol{\Omega} \times \left(\frac{\mathrm{d}\boldsymbol{r}}{\mathrm{d}t}\right)_I. \tag{2.10}$$

Then, noting that

$$\left(\frac{\mathrm{d}\boldsymbol{r}}{\mathrm{d}t}\right)_I = \left(\frac{\mathrm{d}\boldsymbol{r}}{\mathrm{d}t}\right)_R + \boldsymbol{\Omega} \times \boldsymbol{r} = (\boldsymbol{v}_R + \boldsymbol{\Omega} \times \boldsymbol{r}), \tag{2.11}$$

and assuming that the rate of rotation is constant, (2.10) becomes

$$\left(\frac{\mathrm{d}\boldsymbol{v}_R}{\mathrm{d}t}\right)_R = \left(\frac{\mathrm{d}\boldsymbol{v}_I}{\mathrm{d}t}\right)_I - 2\boldsymbol{\Omega} \times \boldsymbol{v}_R - \boldsymbol{\Omega} \times (\boldsymbol{\Omega} \times \boldsymbol{r}). \tag{2.12}$$

This equation may be interpreted as follows. The term on the left-hand side is the rate of change of the relative velocity as measure in the rotating frame. The first term on the right-hand side is the rate of change of the inertial velocity as measured in the inertial frame (or, loosely, the inertial acceleration). Thus, by Newton's second law, it is equal to force on a fluid parcel divided by its mass. The second and third terms on the right-hand side (including the minus signs) are the 'Coriolis force' and the 'centrifugal force' per unit mass. Neither of these are true forces — they may be thought of as quasi-forces (i.e., 'as if' forces); that is, when a body is observed from a rotating frame it seems to behave as if unseen forces are present that affect its motion. If (2.12) is written, as is common, with the terms $+2\boldsymbol{\Omega} \times \boldsymbol{v}_r$ and $+\boldsymbol{\Omega} \times (\boldsymbol{\Omega} \times \boldsymbol{r})$ on the left-hand side then these terms should be referred to as the Coriolis and centrifugal *accelerations*.[1]

Centrifugal force

If $r_\perp$ is the perpendicular distance from the axis of rotation (see Fig. 2.1 and substitute r for C), then, because $\boldsymbol{\Omega}$ is perpendicular to $r_\perp$, $\boldsymbol{\Omega} \times r = \boldsymbol{\Omega} \times r_\perp$. Then, using the vector identity $\boldsymbol{\Omega} \times (\boldsymbol{\Omega} \times r_\perp) = (\boldsymbol{\Omega} \cdot r_\perp)\boldsymbol{\Omega} - (\boldsymbol{\Omega} \cdot \boldsymbol{\Omega})r_\perp$ and noting that the first term is zero, we see that the centrifugal force per unit mass is just given by

$$F_{\mathrm{ce}} = -\boldsymbol{\Omega} \times (\boldsymbol{\Omega} \times r) = \Omega^2 r_\perp. \tag{2.13}$$

This may usefully be written as the gradient of a scalar potential,

$$F_{\mathrm{ce}} = -\nabla \Phi_{\mathrm{ce}}. \tag{2.14}$$

where $\Phi_{\mathrm{ce}} = -(\Omega^2 r_\perp^2)/2 = -(\boldsymbol{\Omega} \times r_\perp)^2/2$.

Coriolis force

The Coriolis force per unit mass is:

$$F_{\mathrm{Co}} = -2\boldsymbol{\Omega} \times v_R. \tag{2.15}$$

It plays a central role in much of geophysical fluid dynamics and will be considered extensively later on. For now, we just note three basic properties:

(i) There is no Coriolis force on bodies that are stationary in the rotating frame.

(ii) The Coriolis force acts to deflect moving bodies at right angles to their direction of travel.

(iii) The Coriolis force does no work on a body, a consequence of the fact that $v_R \cdot (\boldsymbol{\Omega} \times v_R) = 0$.

2.1.3 Momentum equation in a rotating frame

Since (2.12) simply relates the accelerations of a particle in the inertial and rotating frames, then in the rotating frame of reference the momentum equation may be written

$$\frac{\mathrm{D}v}{\mathrm{D}t} + 2\boldsymbol{\Omega} \times v = -\frac{1}{\rho}\nabla p - \nabla \Phi. \tag{2.16}$$

We have dropped the subscript R; henceforth, unless ambiguity is present, all velocities without a subscript will be considered to be relative to the rotating frame.

2.1.4 Mass and tracer conservation in a rotating frame

Let ϕ be a scalar field that, in the inertial frame, obeys

$$\frac{\mathrm{D}\phi}{\mathrm{D}t} + \phi \nabla \cdot v_I = 0. \tag{2.17}$$

Now, observers in both the rotating and inertial frame measure the same value of ϕ. Further, $\mathrm{D}\phi/\mathrm{D}t$ is simply the rate of change of ϕ associated with a material parcel, and therefore is reference frame invariant. Thus,

$$\left(\frac{\mathrm{D}\phi}{\mathrm{D}t}\right)_R = \left(\frac{\mathrm{D}\phi}{\mathrm{D}t}\right)_I \tag{2.18}$$

where $(D\phi/Dt)_R = (\partial\phi/\partial t)_R + \boldsymbol{v}_R \cdot \nabla\phi$ and $(D\phi/Dt)_I = (\partial\phi/\partial t)_I + \boldsymbol{v}_I \cdot \nabla\phi$ and the local temporal derivatives $(\partial\phi/\partial t)_R$ and $(\partial\phi/\partial t)_I$ are evaluated at fixed locations in the rotating and inertial frames, respectively.

Further, since $\boldsymbol{v} = \boldsymbol{v}_I - \boldsymbol{\Omega} \times \boldsymbol{r}$, we have that

$$\nabla \cdot \boldsymbol{v}_I = \nabla \cdot (\boldsymbol{v}_I - \boldsymbol{\Omega} \times \boldsymbol{r}) = \nabla \cdot \boldsymbol{v}_R \tag{2.19}$$

since $\nabla \cdot (\boldsymbol{\Omega} \times \boldsymbol{r}) = 0$. Thus, using (2.18) and (2.19), (2.17) is equivalent to

$$\frac{D\phi}{Dt} + \phi\nabla \cdot \boldsymbol{v} = 0 \tag{2.20}$$

where all observables are measured in the *rotating* frame. Thus, the equation for the evolution of a scalar whose measured value is the same in rotating and inertial frames is unaltered by the presence of rotation. In particular, the mass conservation equation is unaltered by the presence of rotation.

Although we have taken (2.18) as true *a priori*, the individual components of the material derivative differ in the rotating and inertial frames. In particular

$$\left(\frac{\partial\phi}{\partial t}\right)_I = \left(\frac{\partial\phi}{\partial t}\right)_R - (\boldsymbol{\Omega} \times \boldsymbol{r}) \cdot \nabla\phi \tag{2.21}$$

because $\boldsymbol{\Omega} \times \boldsymbol{r}$ is the velocity, in the inertial frame, of a uniformly rotating body. Similarly,

$$\boldsymbol{v}_I \cdot \nabla\phi = (\boldsymbol{v}_R + \boldsymbol{\Omega} \times \boldsymbol{r}) \cdot \nabla\phi. \tag{2.22}$$

Adding the last two equations reprises and confirms (2.18).

2.2 EQUATIONS OF MOTION IN SPHERICAL COORDINATES

The earth is very nearly spherical and it might appear obvious that we must cast our equations in spherical coordinates. Although this does turn out to be true, the presence of a centrifugal force causes some complications which we must first discuss. The reader who is willing *ab initio* to treat the earth as a perfect sphere and to neglect the horizontal component of the centrifugal force may skip the next section.

2.2.1 * The centrifugal force and spherical coordinates

The centrifugal force is a potential force, like gravity, and so we may therefore define an 'effective gravity' equal to the sum of the true gravity and the centrifugal force. The true gravitational force is directed toward the center of the earth, except possibly for tiny effects due to the earth's lack of sphericity and inhomogeneity, but the line of action of the effective gravity will in general differ slightly from this, and therefore have a component in the 'horizontal' plane, that is the plane perpendicular to the radial direction. The magnitude of the centrifugal force is $\Omega^2 r_\perp$, and so the effective gravity is given by

$$\boldsymbol{g} \equiv \boldsymbol{g}_{\text{eff}} = \boldsymbol{g}_{\text{grav}} + \Omega^2 \boldsymbol{r}_\perp \tag{2.23}$$
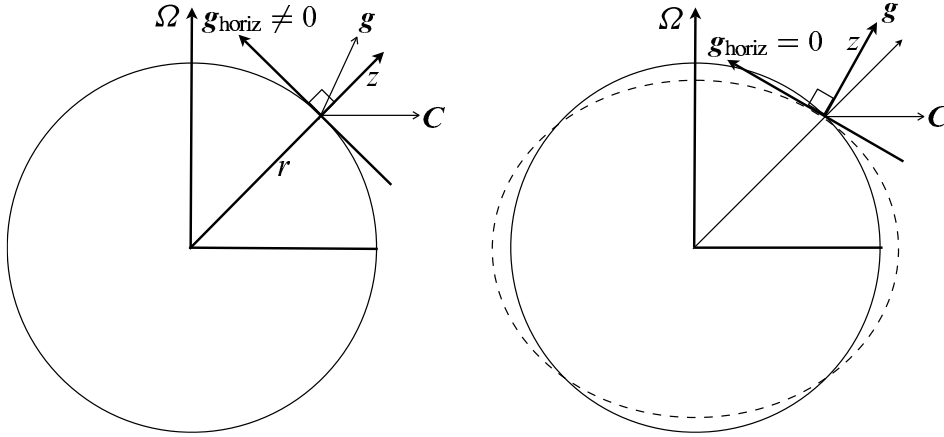
Fig. 2.2 Left: Directions of forces and coordinates in true spherical geometry. g is the apparent gravity (including the centrifugal force, C) and its horizontal component is evidently non-zero. Right: a modified coordinate system, in which the vertical direction is defined by the direction of g, and so the horizontal component of g is identically zero. The dashed line schematically indicates a surface of constant geopotential. The differences between the direction of g and the direction of the radial coordinate, and between the sphere and the geopotential surface, are much exaggerated and in reality are similar to the thickness of the lines themselves.

where g_{grav} is the gravitational force due to the gravitational attraction of the earth and $r_\perp = r \cos \vartheta$. Both gravity and centrifugal force are potential forces and therefore we may define the *geopotential, Φ*, such that

$$g = -\nabla \Phi \tag{2.24}$$

Surfaces of constant Φ are not quite spherical because $r_\perp$, and hence the centrifugal force, vary with latitude (Fig. 2.2).

The components of the centrifugal force parallel and perpendicular to the radial direction are $\Omega^2 r \cos^2 \vartheta$ and $\Omega^2 r \cos \vartheta \sin \vartheta$. Newtonian gravity is much larger than either of these, and at the earth's surface the ratio of centrifugal to gravitational terms is approximately, and no more than,

$$\alpha \approx \frac{\Omega^2 a}{g} \approx \frac{(7.27 \times 10^{-5})^2 \times 6.4 \times 10^6}{10} \approx 3 \times 10^{-3} \tag{2.25}$$

(Note that at the equator and pole the horizontal component of the centrifugal force is zero and the effective gravity does point toward the center of the earth.) The angle between g and the line to the center of the earth is given by a similar expression and so is also small, typically around 3×10^{-3} radians. However, the horizontal component of the centrifugal force is still large compared to the Coriolis force, their ratio in mid-latitudes being given by

$$\frac{\text{Horizontal centrifugal force}}{\text{Coriolis force}} \approx \frac{\Omega^2 a \cos \vartheta \sin \vartheta}{2 \Omega u} \approx \frac{\Omega a}{4|u|} \approx 10, \tag{2.26}$$

using $u = 10\,\mathrm{m\,s^{-1}}$. The centrifugal term therefore dominates over the Coriolis term, and is largely balanced by a pressure gradient force. Thus, if we adhered to true spherical coordinates, both the horizontal and radial components of the momentum equation would be dominated by a static balance between a pressure gradient and gravity or centrifugal terms. Although in principle there is nothing wrong with writing the equations this way, it obscures the dynamical balances involving the Coriolis force and pressure that determine the large-scale horizontal flow.

A way around this problem is to use the direction of the geopotential force to *define* the vertical direction, and then to regard the surfaces of constant Φ as being true spheres.[2] The horizontal component of apparent gravity is then identically zero, and we have traded a potentially large dynamical error for a very small geometric error. The geopotential Φ is then a function of the vertical coordinate alone, and for many purposes we can just take $\Phi = gz$. In fact, over time, the earth has developed an equatorial bulge to compensate for and neutralize the centrifugal force, so that the effective gravity does in fact act in a direction virtually normal to the earth's surface; that is, the surface of the earth is an oblate spheroid of nearly constant geopotential and, because the oblateness is very small (the polar diameter is about 12,714 km, whereas the equatorial diameter is about 12,756 km) using spherical coordinates is a very accurate way to map the spheroid. The direction normal to geopotential surfaces, the local vertical, is, in this approximation, taken to be the direction of increasing r in spherical coordinates. If the angle between apparent gravity and a natural direction of the coordinate system were not small then more heroic measures would be called for. Note, though, that the equatorial bulge is not a sine qua non of this approximation: if the solid earth were a true sphere the dynamics of the atmosphere would be virtually unaltered, and we would use the same equations to describe that motion, with a similar small geometric error in the coordinates.

2.2.2 Some identities in spherical coordinates

The location of a point is given by the coordinates (λ, ϑ, r) where λ is the angular distance eastward (i.e., longitude), ϑ is angular distance poleward (i.e., latitude) and r is the radial distance from the center of the earth. (See Fig. 2.3. In many fields co-latitude is used as a spherical coordinate, but meteorology and oceanography use latitude.) If a is the radius of the earth, then we also define $z = r - a$. At a given location we may also define the Cartesian increments $(\delta x, \delta y, \delta z) = (r \cos\vartheta\, \delta\lambda, r\delta\vartheta, \delta r)$.

For a scalar quantity ϕ the material derivative in spherical coordinates is

$$\frac{\mathrm{D}\phi}{\mathrm{D}t} = \frac{\partial\phi}{\partial t} + \frac{u}{r\cos\vartheta}\frac{\partial\phi}{\partial\lambda} + \frac{v}{r}\frac{\partial\phi}{\partial\vartheta} + w\frac{\partial\phi}{\partial r}, \tag{2.27}$$

where the velocity components corresponding to the coordinates λ, ϑ, r) are

$$(u, v, w) \equiv \left(r\cos\vartheta\frac{\mathrm{D}\lambda}{\mathrm{D}t}, r\frac{\mathrm{D}\vartheta}{\mathrm{D}t}, \frac{\mathrm{D}r}{\mathrm{D}t} \right). \tag{2.28}$$

That is, u is the zonal velocity, v is the meridional velocity and w the vertical velocity.

Figure 2.3 The spherical co-ordinate system. The orthogonal unit vectors **i**, **j** and **k** point in the direction of increasing longitude λ, latitude ϑ, and altitude z. Locally, one may apply a Cartesian system with variables x, y and z measuring distances along **i**, **j** and **k**.
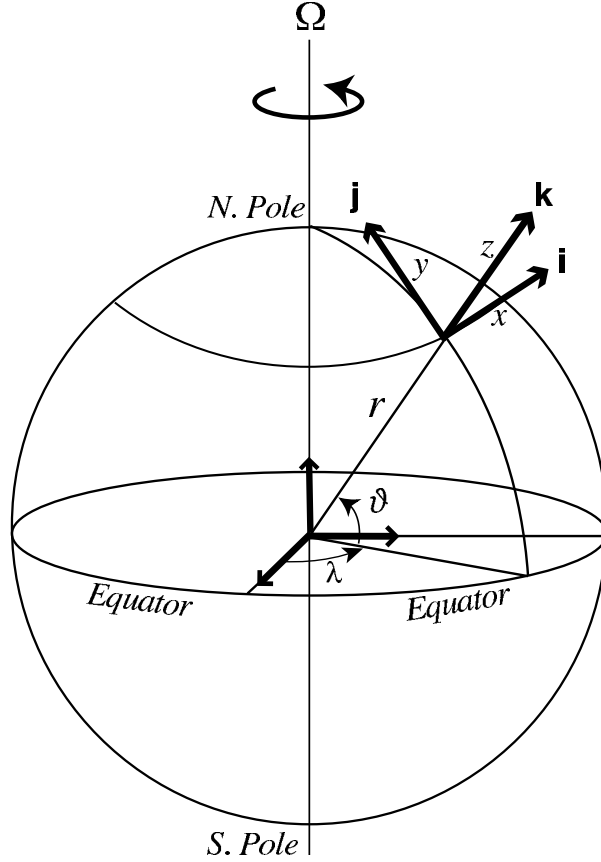
If we define $(\mathbf{i}, \mathbf{j}, \mathbf{k})$ to be the unit vectors in the direction of increasing (λ, ϑ, r) then

$$\boldsymbol{v} = \mathbf{i}u + \mathbf{j}v + \mathbf{k}w. \tag{2.29}$$

Note also that $\mathrm{D}r/\mathrm{D}t = \mathrm{D}z/\mathrm{D}t$.

The divergence of a vector $\boldsymbol{B} = \mathbf{i}B_\lambda + \mathbf{j}B_\vartheta + \mathbf{k}B_z$ is

$$\nabla \cdot \boldsymbol{B} = \frac{1}{\cos\vartheta} \left[\frac{1}{r} \frac{\partial B_\lambda}{\partial \lambda} + \frac{1}{r} \frac{\partial}{\partial \vartheta} (B_\vartheta \cos\vartheta) + \frac{\cos\vartheta}{r^2} \frac{\partial}{\partial r} (r^2 B_r) \right]. \tag{2.30}$$

The vector gradient of a scalar is:

$$\nabla\phi = \mathbf{i}\frac{1}{r\cos\vartheta} \frac{\partial\phi}{\partial\lambda} + \mathbf{j}\frac{1}{r}\frac{\partial\phi}{\partial\vartheta} + \mathbf{k}\frac{\partial\phi}{\partial r} \tag{2.31}$$

The Laplacian of a scalar is:

$$\nabla^2\phi \equiv \nabla \cdot \nabla\phi = \frac{1}{r^2\cos\vartheta} \left[\frac{1}{\cos\vartheta} \frac{\partial^2\phi}{\partial\lambda^2} + \frac{\partial}{\partial\vartheta}\left(\cos\vartheta\frac{\partial\phi}{\partial\vartheta}\right) + \cos\vartheta\frac{\partial}{\partial r}\left(r^2\frac{\partial\phi}{\partial r}\right) \right]. \tag{2.32}$$

The curl of a vector is:

$$\text{curl } \boldsymbol{B} = \nabla \times \boldsymbol{B} = \frac{1}{r^2 \cos \vartheta} \begin{vmatrix} \mathbf{i}\, r \cos \vartheta & \mathbf{j}\, r & \mathbf{k} \\ \partial/\partial \lambda & \partial/\partial \vartheta & \partial/\partial r \\ B_\lambda r \cos \vartheta & B_\vartheta r & B_r \end{vmatrix} \qquad (2.33)$$

The vector Laplacian $\nabla^2 \boldsymbol{B}$ (used for example when calculating viscous terms in the momentum equation) may be obtained from the vector identity:

$$\nabla^2 \boldsymbol{B} = \nabla(\nabla \cdot \boldsymbol{B}) - \nabla \times (\nabla \times \boldsymbol{B}) \qquad (2.34)$$

Only in Cartesian coordinates does this take the simple form,

$$\nabla^2 \boldsymbol{B} = \frac{\partial^2 \boldsymbol{B}}{\partial x^2} + \frac{\partial^2 \boldsymbol{B}}{\partial y^2} + \frac{\partial^2 \boldsymbol{B}}{\partial z^2}. \qquad (2.35)$$

The expansion in spherical coordinates is rather uninformative and rarely needed.

Rate of change of unit vectors

In spherical coordinates the defining unit vectors are $\mathbf{i}$, the unit vector pointing eastward, parallel to a line of latitude; $\mathbf{j}$ is the unit vector pointing polewards, parallel to a meridian; and $\mathbf{k}$, the unit vector pointing radially outward. The directions of these vectors change with location, and in fact this is the case in nearly all coordinate systems, with the notable exception of the Cartesian one, and thus their material derivative is not zero. One way to evaluate this is to consider geometrically how the coordinate axes change with position (2.5). We will approach the problem a little differently, by first obtaining the effective rotation rate $\boldsymbol{\Omega}_{\text{flow}}$, relative to the earth, of a unit vector as it moves with the flow, and then applying (2.3). Specifically, let the fluid velocity be $\boldsymbol{v} = (u, v, w)$. The meridional component, v, produces a displacement $r \delta \vartheta = v \delta t$, and this give rise a local effective vector rotation rate around the local zonal axis of $-(v/r)\mathbf{i}$, the minus sign arising because a displacement in the direction of the north pole is produced by negative rotational displacement around the $\mathbf{i}$ axis. Similarly, the zonal component, u, produces a displacement $\delta \lambda r \cos \vartheta = u \delta t$ and so an effective rotation rate, but now about the earth's rotation axis, of $u/(r \cos \vartheta)$. Now, a rotation around the earth's rotation axis may be written as (see Fig. 2.4)

$$\boldsymbol{\Omega} = \Omega(\mathbf{j} \cos \vartheta + \mathbf{k} \sin \vartheta). \qquad (2.36)$$

If the scalar rotation rate is not Ω but is $u/(r \cos \vartheta)$, then the vector rotation rate is

$$\frac{u}{r \cos \vartheta}(\mathbf{j} \cos \vartheta + \mathbf{k} \sin \vartheta) = \mathbf{j}\frac{u}{r} + \mathbf{k}\frac{u \tan \vartheta}{r}. \qquad (2.37)$$

Thus, the total rotation rate of a vector that moves with the flow is

$$\boldsymbol{\Omega}_{\text{flow}} = -\mathbf{i}\frac{v}{r} + \mathbf{j}\frac{u}{r} + \mathbf{k}\frac{u \tan \vartheta}{r}. \qquad (2.38)$$

Applying (2.3) to (2.38), we find

$$\frac{D\mathbf{i}}{Dt} = \boldsymbol{\Omega}_{\text{flow}} \times \mathbf{i} = \frac{u}{r\cos\vartheta}(\mathbf{j}\sin\vartheta - \mathbf{k}\cos\vartheta), \tag{2.39a}$$

$$\frac{D\mathbf{j}}{Dt} = \boldsymbol{\Omega}_{\text{flow}} \times \mathbf{j} = -\mathbf{i}\frac{u}{r}\tan\vartheta - \mathbf{k}\frac{v}{r}, \tag{2.39b}$$

$$\frac{D\mathbf{k}}{Dt} = \boldsymbol{\Omega}_{\text{flow}} \times \mathbf{k} = \mathbf{i}\frac{u}{r} + \mathbf{j}\frac{v}{r}. \tag{2.39c}$$

2.2.3 Equations of motion

Mass Conservation and Thermodynamic Equation

The mass conservation equation, (1.38a), expanded in spherical co-odinates, is

$$\frac{\partial\rho}{\partial t} + \frac{u}{r\cos\vartheta}\frac{\partial\rho}{\partial\lambda} + \frac{v}{r}\frac{\partial\rho}{\partial\vartheta} + w\frac{\partial\rho}{\partial r}$$
$$+ \frac{\rho}{r\cos\vartheta}\left[\frac{\partial u}{\partial\lambda} + \frac{\partial}{\partial\vartheta}(v\cos\vartheta) + \frac{1}{r}\frac{\partial}{\partial r}(wr^2\cos\vartheta)\right] = 0 \tag{2.40}$$

Equivalently, using the form (1.38b), this is

$$\frac{\partial\rho}{\partial t} + \frac{1}{r\cos\vartheta}\frac{\partial(u\rho)}{\partial\lambda} + \frac{1}{r\cos\vartheta}\frac{\partial}{\partial\vartheta}(v\rho\cos\vartheta) + \frac{1}{r^2}\frac{\partial}{\partial r}(r^2 w\rho) = 0. \tag{2.41}$$

The thermodynamic equation, (1.112), is a tracer advection equation. Thus, using (2.27), its (adiabatic) spherical coordinate form is

$$\frac{D\theta}{Dt} = \frac{\partial\theta}{\partial t} + \frac{u}{r\cos\vartheta}\frac{\partial\theta}{\partial\lambda} + \frac{v}{r}\frac{\partial\theta}{\partial\vartheta} + w\frac{\partial\theta}{\partial r} = 0, \tag{2.42}$$

and similarly for tracers such as water vapour or salt.

Momentum Equation

Recall that inviscid momentum equation is:

$$\frac{D\boldsymbol{v}}{Dt} + 2\boldsymbol{\Omega} \times \boldsymbol{v} = -\frac{1}{\rho}\nabla p - \nabla\Phi. \tag{2.43}$$

where Φ is the geopotential. In spherical coordinates the directions of the coordinate axes change with position and so the component expansion of (2.43) is

$$\frac{D\boldsymbol{v}}{Dt} = \frac{Du}{Dt}\mathbf{i} + \frac{Dv}{Dt}\mathbf{j} + \frac{Dw}{Dt}\mathbf{k} + u\frac{D\mathbf{i}}{Dt} + v\frac{D\mathbf{j}}{Dt} + w\frac{D\mathbf{k}}{Dt} \tag{2.44a}$$

$$= \frac{Du}{Dt}\mathbf{i} + \frac{Dv}{Dt}\mathbf{j} + \frac{Dw}{Dt}\mathbf{k} + \boldsymbol{\Omega}_{\text{flow}} \times \boldsymbol{v} \tag{2.44b}$$
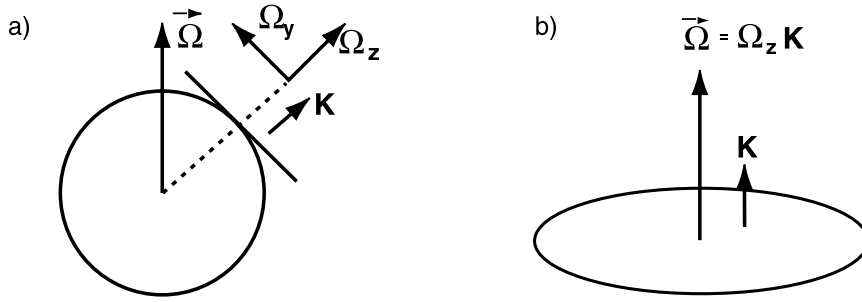
Fig. 2.4 a) On the sphere the rotation vector $\boldsymbol{\Omega}$ can be decomposed into two components, one in the local vertical and one in the local horizontal, pointing toward the pole. That is, $\boldsymbol{\Omega} = \Omega_y \mathbf{j} + \Omega_z \mathbf{k}$ where $\Omega_y = \Omega \cos \vartheta$ and $\Omega_z = \Omega \sin \vartheta$. In geophysical fluid dynamics, the rotation vector in the local vertical is often the more important component in the horizontal momentum equations. On a rotating disk, (b), the rotation vector $\boldsymbol{\Omega}$ is parallel to the local vertical $\mathbf{k}$.

using (2.39). Using either (2.44a) and the expressions for the rates of change of the unit vectors given in (2.39), or (2.44b) and the expression for $\boldsymbol{\Omega}_{\text{flow}}$ given in (2.38), this becomes

$$
\begin{aligned}
\frac{D\boldsymbol{v}}{Dt} = {}& \mathbf{i} \left(\frac{Du}{Dt} - \frac{uv \tan \vartheta}{r} + \frac{uw}{r} \right) + \mathbf{j} \left(\frac{Dv}{Dt} + \frac{u^2 \tan \vartheta}{r} + \frac{vw}{r} \right) \\
& + \mathbf{k} \left(\frac{Dw}{Dt} - \frac{u^2 + v^2}{r} \right).
\end{aligned}
\tag{2.45}
$$

Using the definition of a vector cross product the Coriolis term is:

$$
\begin{aligned}
2\boldsymbol{\Omega} \times \boldsymbol{v} = {}& \begin{vmatrix} \mathbf{i} & \mathbf{j} & \mathbf{k} \\ 0 & 2\Omega \cos \vartheta & 2\Omega \sin \vartheta \\ u & v & w \end{vmatrix} \\
= {}& \mathbf{i} \left(2\Omega w \cos \vartheta - 2\Omega v \sin \vartheta \right) + \mathbf{j}\, 2\Omega u \sin \vartheta - \mathbf{k}\, 2\Omega u \cos \vartheta.
\end{aligned}
\tag{2.46}
$$

Using (2.45) and (2.46), and the gradient operator given by (2.31), the momentum equation (2.43) becomes:

$$
\frac{Du}{Dt} - \left(2\Omega + \frac{u}{r \cos \vartheta} \right) (v \sin \vartheta - w \cos \vartheta) = -\frac{1}{\rho r \cos \vartheta} \frac{\partial p}{\partial \lambda},
\tag{2.47a}
$$

$$
\frac{Dv}{Dt} + \frac{wv}{r} + \left(2\Omega + \frac{u}{r \cos \vartheta} \right) u \sin \vartheta = -\frac{1}{\rho r} \frac{\partial p}{\partial \vartheta},
\tag{2.47b}
$$

$$
\frac{Dw}{Dt} - \frac{u^2 + v^2}{r} - 2\Omega u \cos \vartheta = -\frac{1}{\rho} \frac{\partial p}{\partial r} - g.
\tag{2.47c}
$$

The terms involving Ω are called Coriolis terms, and the quadratic terms on the left-hand sides involving $1/r$ are often called metric terms.

2.2.4 The primitive equations

The so-called *primitive equations* of motion are simplifications of the above equations frequently used in atmospheric and oceanic modelling.[3] Three related approximations are involved; these are:

(i) *The hydrostatic approximation.* In the vertical momentum equation the gravitational term is assumed to be balanced by the pressure gradient term, so that

$$\frac{\partial p}{\partial z} = -\rho g. \tag{2.48}$$

The advection of vertical velocity, the Coriolis terms, and the metric term $(u^2 + v^2)/r$ are all neglected.

(ii) *The shallow-fluid approximation.* We write $r = a + z$ where the constant a is the radius of the earth and z increases in the radial direction. The coordinate r is then replaced by a except where it used as the differentiating argument. Thus, for example,

$$\frac{1}{r^2}\frac{\partial(r^2 w)}{\partial r} \rightarrow \frac{\partial w}{\partial z}. \tag{2.49}$$

(iii) *The traditional approximation.* Coriolis terms in the horizontal momentum equations involving the vertical velocity, and the still smaller metric terms uw/r and vw/r, are neglected.

The second and third of these approximations should be taken, or not, together, the underlying reason being that they both relate to the presumed small aspect ratio of the motion, so the approximations succeed or fail together. If we make one approximation but not the other then we are being asymptotically inconsistent, and angular momentum and energy conservation are not assured [see section 2.2.7]. The hydrostatic approximation also depends on the small aspect ratio of the flow but in a slightly different way. For large-scale flow in the terrestrial atmosphere and ocean all three approximations are in fact all very accurate approximations. We defer a more complete treatment until section 2.7, in part because a treatment of the hydrostatic approximation is done most easily in the context of the Boussinesq equations, derived in section 2.4.

Making these approximations, the momentum equations become

$$\frac{\mathrm{D}u}{\mathrm{D}t} - 2\Omega\sin\vartheta\, v - \frac{uv}{a}\tan\vartheta = -\frac{1}{a\rho\cos\vartheta}\frac{\partial p}{\partial\lambda}, \tag{2.50a}$$

$$\frac{\mathrm{D}v}{\mathrm{D}t} + 2\Omega\sin\vartheta\, u + \frac{u^2\tan\vartheta}{a} = -\frac{1}{\rho a}\frac{\partial p}{\partial\vartheta}, \tag{2.50b}$$

$$0 = -\frac{1}{\rho}\frac{\partial p}{\partial z} - g. \tag{2.50c}$$

where

$$\frac{\mathrm{D}}{\mathrm{D}t} = \left(\frac{\partial}{\partial t} + \frac{u}{a\cos\vartheta}\frac{\partial}{\partial\lambda} + \frac{v}{a}\frac{\partial}{\partial\vartheta} + w\frac{\partial}{\partial z}\right). \tag{2.51}$$

We note the ubiquity of the factor $2\Omega \sin \vartheta$, and take the opportunity to define the *Coriolis parameter*, $f \equiv 2\Omega \sin \vartheta$.

The corresponding mass conservation equation for a shallow fluid layer is:

$$\frac{\partial \rho}{\partial t} + \frac{u}{a \cos \vartheta} \frac{\partial \rho}{\partial \lambda} + \frac{v}{a} \frac{\partial \rho}{\partial \vartheta} + w \frac{\partial \rho}{\partial z}$$
$$+ \rho \left[\frac{1}{a \cos \vartheta} \frac{\partial u}{\partial \lambda} + \frac{1}{a \cos \vartheta} \frac{\partial}{\partial \vartheta} (v \cos \vartheta) + \frac{\partial w}{\partial z} \right] = 0, \tag{2.52}$$

or equivalently,

$$\frac{\partial \rho}{\partial t} + \frac{1}{a \cos \vartheta} \frac{\partial (u\rho)}{\partial \lambda} + \frac{1}{a \cos \vartheta} \frac{\partial}{\partial \vartheta} (v\rho \cos \vartheta) + \frac{\partial (w\rho)}{\partial z} = 0. \tag{2.53}$$

2.2.5 Primitive equations in vector form

The primitive equations may be written in a compact vector form provided we make a slight reinterpretation of the material derivative of the coordinate axes. Let $\boldsymbol{u} = u\mathbf{i} + v\mathbf{j} + 0\,\mathbf{k}$ be the horizontal velocity. The primitive equations (2.50a) and (2.50b) may be written as

$$\frac{\mathrm{D}\boldsymbol{u}}{\mathrm{D}t} + \boldsymbol{f} \times \boldsymbol{u} = -\frac{1}{\rho} \nabla_z p \tag{2.54}$$

where $\boldsymbol{f} = f\mathbf{k} = 2\Omega \sin \vartheta \mathbf{k}$ and $\nabla_z p = [(a \cos \vartheta)^{-1} \partial p / \partial \lambda, a^{-1} \partial p / \partial \vartheta]$, the gradient operator at constant z. In (2.54) the material derivative of the horizontal velocity is given by

$$\frac{\mathrm{D}\boldsymbol{u}}{\mathrm{D}t} = \mathbf{i}\frac{\mathrm{D}u}{\mathrm{D}t} + \mathbf{j}\frac{\mathrm{D}v}{\mathrm{D}t} + u\frac{\mathrm{D}\mathbf{i}}{\mathrm{D}t} + v\frac{\mathrm{D}\mathbf{j}}{\mathrm{D}t}, \tag{2.55}$$

where instead of (2.39) we have

$$\frac{\mathrm{D}\mathbf{i}}{\mathrm{D}t} = \widetilde{\boldsymbol{\Omega}}_{\text{flow}} \times \mathbf{i} = \mathbf{j}\frac{u \tan \vartheta}{a}, \tag{2.56a}$$

$$\frac{\mathrm{D}\mathbf{j}}{\mathrm{D}t} = \widetilde{\boldsymbol{\Omega}}_{\text{flow}} \times \mathbf{j} = -\mathbf{i}\frac{u \tan \vartheta}{a}, \tag{2.56b}$$

where $\widetilde{\boldsymbol{\Omega}}_{\text{flow}} = \mathbf{k}u \tan \vartheta / a$ [which is the vertical component of (2.38), with r replaced by a.]. The advection of the horizontal wind $\boldsymbol{u}$ is still by the three-dimensional velocity $\boldsymbol{v}$. The vertical momentum equation is the hydrostatic equation, (2.50c), and the mass conservation equation is

$$\frac{\mathrm{D}\rho}{\mathrm{D}t} + \rho \nabla \cdot \boldsymbol{v} = 0 \quad \text{or} \quad \frac{\partial \rho}{\partial t} + \nabla \cdot (\rho \boldsymbol{v}) = 0. \tag{2.57}$$

where $\mathrm{D}/\mathrm{D}t$ on a scalar is given by (2.51), and the second expression is written out in full in (2.53).

2.2.6 The vector invariant form of the momentum equation

The 'vector invariant' form of the momentum equation is so-called because it appears to take the same form in all coordinate systems — there is no advective derivative of the coordinate system to worry about. Restricting attention to the incompressible case, with the aid of the identity $(v \cdot \nabla)v = -v \times \omega + \nabla(v^2/2)$ the three dimensional momentum equation may be written:

$$\frac{\partial v}{\partial t} + (2\boldsymbol{\Omega} + \boldsymbol{\omega}) \times v = -\nabla B. \tag{2.58}$$

where $B = \phi + v^2/2 + \Phi$ is the Bernoulli function and $\boldsymbol{\omega}$ is the relative vorticity, $\boldsymbol{\omega} = \nabla \times v$. In spherical coordinates this is:

$$\boldsymbol{\omega} = \nabla \times v = \frac{1}{r^2 \cos \vartheta} \begin{vmatrix} \mathbf{i}\, r \cos \vartheta & \mathbf{j}\, r & \mathbf{k} \\ \partial/\partial \lambda & \partial/\partial \vartheta & \partial/\partial r \\ u r \cos \vartheta & r v & w \end{vmatrix} \tag{2.59}$$

$$= \mathbf{i} \frac{1}{r} \left(\frac{\partial w}{\partial \vartheta} - \frac{\partial (rv)}{\partial r} \right) - \mathbf{j} \frac{1}{r \cos \vartheta} \left(\frac{\partial w}{\partial \lambda} - \frac{\partial}{\partial r} (u r \cos \vartheta) \right)$$

$$+ \mathbf{k} \frac{1}{r \cos \vartheta} \left(\frac{\partial v}{\partial \lambda} - \frac{\partial}{\partial \vartheta} (u \cos \vartheta) \right). \tag{2.60}$$

Making the traditional approximation, and considering the horizontal and vertical components of the momentum equation separately, gives

$$\frac{\partial u}{\partial t} + (2\boldsymbol{\Omega} + \mathbf{k}\zeta) \times u + w \frac{\partial u}{\partial z} = -\nabla_z B_h \tag{2.61}$$

where $u = (u, v, 0)$, $\boldsymbol{\Omega} = \mathbf{k}\, \Omega \sin \vartheta$, $B_h = \phi + u^2/2$, ∇_z is the horizontal gradient operator (the gradient at a constant value of z), and using (2.60), ζ is given by

$$\zeta = \frac{1}{a \cos \vartheta} \frac{\partial v}{\partial \lambda} - \frac{1}{a \cos \vartheta} \frac{\partial}{\partial \vartheta} (u \cos \vartheta) = \frac{1}{a \cos \vartheta} \frac{\partial v}{\partial \lambda} - \frac{1}{a} \frac{\partial u}{\partial \vartheta} + \frac{u}{a} \tan \vartheta. \tag{2.62}$$

The separate components of the momentum equation are then found to be:

$$\frac{\partial u}{\partial t} - (f + \zeta)v + w \frac{\partial u}{\partial z} = -\frac{1}{a \cos \vartheta} \frac{\partial B_h}{\partial \lambda}, \tag{2.63}$$

and

$$\frac{\partial v}{\partial t} + (f + \zeta)u + w \frac{\partial v}{\partial z} = -\frac{1}{a} \frac{\partial B_h}{\partial \vartheta}. \tag{2.64}$$

Similar expressions arise in a compressible fluid, with a different form for the right-hand side (problem 2.2).

2.2.7 Angular Momentum

The zonal momentum equation can be usefully expressed as a statement about axial angular momentum; that is, angular momentum about the rotation axis. The zonal angular

momentum per unit mass is the component of angular momentum in the direction of the axis of rotation and it is given by, without making any shallow atmosphere approximation,

$$m = (u + \Omega r \cos \vartheta) r \cos \vartheta. \tag{2.65}$$

The evolution equation for this quantity follows from the zonal momentum equation and has the simple form

$$\frac{Dm}{Dt} = -\frac{1}{\rho} \frac{\partial p}{\partial \lambda} \tag{2.66}$$

where the material derivative is

$$\frac{D}{Dt} = \frac{\partial}{\partial t} + \frac{u}{r \cos \vartheta} \frac{\partial}{\partial \lambda} + \frac{v}{r} \frac{\partial}{\partial \vartheta} + w \frac{\partial}{\partial r}. \tag{2.67}$$

Using the mass continuity equation, this can be written as

$$\frac{D\rho m}{Dt} + \rho m \nabla \cdot \boldsymbol{v} = -\frac{\partial p}{\partial \lambda} \tag{2.68}$$

or

$$\frac{\partial \rho m}{\partial t} + \frac{1}{r \cos \vartheta} \frac{\partial (\rho u m)}{\partial \lambda} + \frac{1}{r \cos \vartheta} \frac{\partial}{\partial \vartheta} (\rho v m \cos \vartheta) + \frac{\partial}{\partial z} (\rho m w) = -\frac{\partial p}{\partial \lambda}. \tag{2.69}$$

This is an angular momentum conservation equation.

If the fluid is confined to a shallow layer near the surface of a sphere, then we may replace r, the radial coordinate, by a, the radius of the sphere, in the definition of m, and we define $\tilde{m} \equiv (u + \Omega a \cos \vartheta) a \cos \vartheta$. Then (2.66) is replaced by

$$\frac{D\tilde{m}}{Dt} = -\frac{1}{\rho} \frac{\partial p}{\partial \lambda} \tag{2.70}$$

where now

$$\frac{D}{Dt} = \frac{\partial}{\partial t} + \frac{u}{a \cos \vartheta} \frac{\partial}{\partial \lambda} + \frac{v}{a} \frac{\partial}{\partial \vartheta} + w \frac{\partial}{\partial z}. \tag{2.71}$$

Using mass continuity this may be written as

$$\frac{\partial \rho \tilde{m}}{\partial t} + \frac{u}{a \cos \vartheta} \frac{\partial \tilde{m}}{\partial \lambda} + \frac{v}{a} \frac{\partial \tilde{m}}{\partial \vartheta} + w \frac{\partial \tilde{m}}{\partial z} = -\frac{1}{\rho} \frac{\partial p}{\partial \lambda}. \tag{2.72}$$

which is the appropriate angular momentum conservation equation for a shallow atmosphere.

* From angular momentum to the spherical component equations

A somewhat indirect way to derive the three components of the momentum equation in spherical polar coordinates is to *begin* with (2.66) and the principle of conservation of energy. That is, we take the equations for conservation of angular momentum and energy as true *a priori* and demand that the forms of the momentum equation be constructed to satisfy these. Expanding the material derivative in (2.66), noting that

$\mathrm{D}r/\mathrm{D}t = w$ and $\mathrm{D}\cos\vartheta/\mathrm{D}t = -(v/r)\sin\vartheta$, immediately gives (2.47a). Multiplication by u then yields

$$u\frac{\mathrm{D}u}{\mathrm{D}t} - 2\Omega uv\sin\vartheta + 2\Omega uw\cos\vartheta - \frac{u^2 v\tan\vartheta}{r} + \frac{u^2 w}{r} = -\frac{u}{\rho r\cos\vartheta}\frac{\partial p}{\partial\lambda}. \quad (2.73)$$

Now suppose that the meridional and vertical momentum equations are of the form

$$\frac{\mathrm{D}v}{\mathrm{D}t} + \text{Coriolis and metric terms} = -\frac{1}{\rho r}\frac{\partial p}{\partial\vartheta} \qquad (2.74a)$$

$$\frac{\mathrm{D}w}{\mathrm{D}t} + \text{Coriolis and metric terms} = -\frac{1}{\rho}\frac{\partial p}{\partial r}, \qquad (2.74b)$$

but that we do not know what form the Coriolis and metric terms take. To determine that form, construct the kinetic energy equation by multiplying these equations by v and w. Now, the metric terms must vanish when we sum the resulting equations, so that (2.74a) must contain the Coriolis term $2\Omega u\sin\vartheta$ as well as the metric term $u^2\tan\vartheta/r$, and (2.74b) must contain a $-2\Omega u\cos\phi$ as well as the metric term u^2/r. But if (2.74b) contains the term u^2/r it must also contain the term v^2/r by isotropy, and therefore (2.74a) must also contain the term vw/r. In this way, (2.47) is precisely reproduced, although the skeptic might argue that the uniqueness of the form has not been proven.

A particular advantage of this approach arises in determining the appropriate momentum equations that conserve angular momentum and energy in the shallow-fluid approximation. We begin with (2.70) and expand to obtain (2.50a). Multiplying by u gives

$$u\frac{\mathrm{D}u}{\mathrm{D}t} - 2\Omega uv\sin\vartheta - \frac{u^2 v\tan\vartheta}{a} = -\frac{u}{\rho a\cos\vartheta}\frac{\partial p}{\partial\lambda}. \qquad (2.75)$$

Evidently, the meridional momentum equation must contain the Coriolis term $2\Omega u\sin\vartheta$ and the metric term $u^2\tan\vartheta/a$, but the vertical momentum equation must have neither of the metric terms appearing in (2.47c). Thus we deduce the following equations:

$$\frac{\mathrm{D}u}{\mathrm{D}t} - \left(2\Omega\sin\vartheta + \frac{u\tan\vartheta}{a}\right)v = -\frac{1}{\rho a\cos\vartheta}\frac{\partial p}{\partial\lambda} \qquad (2.76a)$$

$$\frac{\mathrm{D}v}{\mathrm{D}t} + \left(2\Omega\sin\vartheta + \frac{u\tan\vartheta}{a}\right)v = -\frac{1}{\rho a}\frac{\partial p}{\partial\vartheta} \qquad (2.76b)$$

$$\frac{\mathrm{D}w}{\mathrm{D}t} = -\frac{1}{\rho}\frac{\partial\rho}{\partial r} - g. \qquad (2.76c)$$

This equation set, when used in conjunction with the thermodynamic and mass continuity equations, conserves appropriate forms of angular momentum and energy. In the hydrostatic approximation the material derivative of w in (2.76c) is *additionally* neglected. Thus, the hydrostatic approximation is mathematically and physically consistent with the shallow-fluid approximation, but it is an additional approximation with slightly different requirements that one may choose, rather than being required, to make.

From an asymptotic perspective, the difference lies in the small parameter necessary for either approximation to hold, namely

$$\text{Shallow fluid and traditional approximations:} \quad \gamma \equiv \frac{H}{a} \ll 1 \qquad \text{(2.77a)}$$

$$\text{Small aspect ratio for hydrostatic approximation:} \quad \alpha \equiv \frac{H}{L} \ll 1. \qquad \text{(2.77b)}$$

where L is the horizontal scale of the motion and a is the radius of the earth. For hemispheric or global scale phenomena $L \sim a$ and the two approximations coincide. (Requirement (2.77b) for the hydrostatic approximation is derived in section 2.7.)

2.3 CARTESIAN APPROXIMATIONS: THE TANGENT PLANE

2.3.1 The f-plane

Although the rotation of the earth is central for many dynamical phenomena, the sphericity of the earth is not always so. This is especially true for phenomena on a scale somewhat smaller than global where the use of spherical coordinates becomes awkward, and it is more convenient to use a locally Cartesian representation of the equations. Referring to Fig. 2.4 we will define a plane tangent to the surface of the earth at a latitude ϑ_0, and then use a Cartesian coordinate system (x, y, z) to describe motion on that plane. For small excursions on the plane, $(x, y, z) \approx (a\lambda \cos \vartheta_0, a(\vartheta - \vartheta_0), z)$. Consistently, the velocity is $\boldsymbol{v} = (u, v, w)$, so that u, v and w are the components of the velocity *in the tangent plane*. These are approximately in the east-west, north-south and vertical directions, respectively.

The momentum equations for flow in this plane are then

$$\frac{\partial u}{\partial t} + (\boldsymbol{v} \cdot \nabla)u + 2\Omega_y w - 2\Omega_z v = -\frac{1}{\rho}\frac{\partial p}{\partial x}, \qquad \text{(2.78a)}$$

$$\frac{\partial v}{\partial t} + (\boldsymbol{v} \cdot \nabla)v + 2\Omega_z u = -\frac{1}{\rho}\frac{\partial p}{\partial y}, \qquad \text{(2.78b)}$$

$$\frac{\partial w}{\partial t} + (\boldsymbol{v} \cdot \nabla)w + 2(\Omega_x v - \Omega_y u) = -\frac{1}{\rho}\frac{\partial p}{\partial z} - g, \qquad \text{(2.78c)}$$

where the rotation vector $\boldsymbol{\Omega} = \Omega_x \mathbf{i} + \Omega_y \mathbf{j} + \Omega_z \mathbf{k}$ and $\Omega_x = 0$, $\Omega_y = \Omega \cos \vartheta_0$ and $\Omega_z = \Omega \sin \vartheta_0$. If we make the traditional approximation, and so ignore the components of $\boldsymbol{\Omega}$ not in the direction of the local vertical, then

$$\frac{\mathrm{D}u}{\mathrm{D}t} - f_0 v = -\frac{1}{\rho}\frac{\partial p}{\partial x}, \qquad \text{(2.79a)}$$

$$\frac{\mathrm{D}v}{\mathrm{D}t} + f_0 u = -\frac{1}{\rho}\frac{\partial p}{\partial y}, \qquad \text{(2.79b)}$$

$$\frac{\mathrm{D}w}{\mathrm{D}t} = -\frac{1}{\rho}\frac{\partial p}{\partial z} - \rho g. \qquad \text{(2.79c)}$$

where $f_0 = 2\Omega_z \sin\vartheta_0$. Defining the horizontal velocity vector $\boldsymbol{u} = (u, v, 0)$, the first two equations may also be written as

$$\frac{\mathrm{D}\boldsymbol{u}}{\mathrm{D}t} + \boldsymbol{f}_0 \times \boldsymbol{u} = -\frac{1}{\rho}\nabla_z p, \tag{2.80}$$

where $\mathrm{D}\boldsymbol{u}/\mathrm{D}t = \partial\boldsymbol{u}/\partial t + \boldsymbol{v}\cdot\nabla\boldsymbol{u}$, $\boldsymbol{f}_0 = 2\Omega\sin\vartheta_0\mathbf{k} = f_0\mathbf{k}$, and $\mathbf{k}$ is the direction perpendicular to the plane (it does not change its orientation with latitude). These equations are, evidently, exactly the same as the momentum equations in a system in which the rotation vector is aligned with the local vertical, as illustrated in the right panel in Fig. 2.4. They will describe flow on the surface of a rotating sphere to a good approximation provided the flow is of limited latitudinal extent so that the effects of sphericity are unimportant. This is known as the *f-plane* approximation since the Coriolis parameter is a constant. We may in addition make the hydrostatic approximation, in which case (2.79c) becomes the familiar $\partial p/\partial z = -\rho g$.

2.3.2 The beta-plane approximation

The magnitude of the vertical component of rotation varies with latitude, and this has important dynamical consequences. We can approximate this effect by allowing the effective rotation vector to vary. Thus, noting that, for small variations in latitude,

$$f = 2\Omega\sin\vartheta \approx 2\Omega\sin\vartheta_0 + 2\Omega\cos\vartheta_0(\vartheta - \vartheta_0), \tag{2.81}$$

then on the tangent plane we may mimic this by allowing the Coriolis parameter to vary as

$$\boxed{f = f_0 + \beta y}, \tag{2.82}$$

where $f_0 = 2\Omega\sin\vartheta_0$ and $\beta = \partial f/\partial y = (2\Omega\cos\vartheta_0)/a$. This important approximation is known as the *beta-plane*, or *β-plane,* approximation. It captures the the most important *dynamical* effects of sphericity, without the complicating *geometric* effects, which are not essential to describe many phenomena. The momentum equations (2.79a), (2.79b) and (2.79c) (or its hydrostatic counterpart) are unaltered, save that f_0 is replaced by $f_0 + \beta y$ to represent a varying Coriolis parameter. Thus, sphericity combined with rotation is dynamically equivalent to a *differentially rotating* system. For future reference, we write down the β-plane horizontal momentum equations:

$$\frac{\mathrm{D}\boldsymbol{u}}{\mathrm{D}t} + \boldsymbol{f} \times \boldsymbol{u} = -\frac{1}{\rho}\nabla_z p, \tag{2.83}$$

where $\boldsymbol{f} = (f_0 + \beta y)\hat{\mathbf{k}}$. In component form this equation becomes

$$\frac{\mathrm{D}u}{\mathrm{D}t} - fv = -\frac{1}{\rho}\frac{\partial p}{\partial x}, \qquad \frac{\mathrm{D}v}{\mathrm{D}t} + fu = -\frac{1}{\rho}\frac{\partial p}{\partial y}, \tag{2.84a,b}$$

The mass conservation, thermodynamic and hydrostatic equations in the β-plane approximation are the same as the usual Cartesian (f-plane) forms of those equations.

2.4 EQUATIONS FOR A STRATIFIED OCEAN: THE BOUSSINESQ APPROXIMATION

The density variations in the ocean are quite small compared to the mean density, and we may exploit this to derive somewhat simpler but still quite accurate equations of motion. Let us first examine how much density does vary in the ocean.

2.4.1 Variation of density in the ocean

The variations of density in the ocean are due to three effects: the compression of water by pressure (which we denote as $\Delta_p \rho$), the thermal expansion of water if its temperature changes ($\Delta_T \rho$), and the haline contraction if its salinity changes ($\Delta_S \rho$). How big are these? An appropriate equation of state to approximately evaluate these effects is the linear one

$$\rho = \rho_0 \left[1 - \beta_T (T - T_0) + \beta_S (S - S_0) + \frac{p}{\rho_0 c_s^2} \right], \qquad (2.85)$$

where $\beta_T \approx 2 \times 10^{-4} \, \mathrm{K}^{-1}$, $\beta_S \approx 10^{-3} \, \mathrm{psu}^{-1}$ and $c_s \approx 1500 \, \mathrm{m \, s}^{-1}$ (see the table on page 39). The three effects are then:

Pressure compressibility: We have $\Delta_p \rho \approx \Delta p / c^2 \approx \rho_0 g H / c^2$ where H is the depth and the pressure change is quite accurately evaluated using the hydrostatic approximation. Thus,

$$\frac{|\Delta_p \rho|}{\rho_0} \ll 1 \qquad \text{if} \qquad \frac{gH}{c^2} \ll 1, \qquad (2.86)$$

or if $H \ll c^2/g$. The quantity $c^2/g \approx 200 \, \mathrm{km}$ is the density scale height of the ocean. Thus, the pressure at the bottom of the ocean (say $H = 10 \, \mathrm{km}$ in the deep trenches), enormous as it is, is insufficient to compress the water enough to make a significant change in its density. Changes in density due to dynamical variations of pressure are small if the Mach number is small, and this is also the case.

Thermal expansion: We have $\Delta_T \rho \approx -\beta_T \rho_0 \Delta T$ and therefore

$$\frac{|\Delta_T \rho|}{\rho_0} \ll 1 \qquad \text{if} \qquad \beta_T \Delta T \ll 1. \qquad (2.87)$$

For $\Delta T = 20 \, \mathrm{K}$, $\beta_T \Delta T \approx 4 \times 10^{-3}$, and evidently we would require temperature differences of order β_T^{-1}, or 5000 K to obtain order one variations in density.

Saline contraction: We have $\Delta_S \rho \approx \beta_S \rho_0 \Delta S$ and therefore

$$\frac{|\Delta_S \rho|}{\rho_0} \ll 1 \qquad \text{if} \qquad \beta_S \Delta S \ll 1. \qquad (2.88)$$

As changes is salinity in the ocean rarely exceed 5 psu, for which $\beta_S \Delta S = 5 \times 10^{-3}$, the fractional change in the density of seawater is correspondingly very small.

Evidently, fractional density changes in the ocean are very small.

2.4.2 The Boussinesq equations

The *Boussinesq equations* are a set of equations that exploit the smallness of density variations in many liquids.[4] To set notation we write

$$\rho = \rho_0 + \delta\rho(x, y, z, t) \tag{2.89a}$$

$$= \rho_0 + \widehat{\rho}(z) + \rho'(x, y, z, t) \tag{2.89b}$$

$$= \widetilde{\rho}(z) + \rho'(x, y, z, t) \tag{2.89c}$$

where ρ_0 is a constant and we assume that

$$|\widehat{\rho}|, |\rho'|, |\delta\rho| \ll \rho_0. \tag{2.90}$$

We need not assume that $|\rho'| \ll |\widehat{\rho}|$, but this is often the case in the ocean. To obtain the Boussinesq equations we will just use (2.89a), but (2.89c) will be useful for the anelastic equations considered later.

Associated with the reference density is a reference pressure that is defined to be in hydrostatic balance with it. That is,

$$p = p_0(z) + \delta p(x, y, z, t) \tag{2.91a}$$

$$= \widetilde{p}(z) + p'(x, y, z, t), \tag{2.91b}$$

where $|\delta p| \ll p_0$, $|p'| \ll \widetilde{p}$ and

$$\frac{\mathrm{d} p_0}{\mathrm{d} z} \equiv -g\rho_0, \qquad \frac{\mathrm{d}\widetilde{p}}{\mathrm{d} z} \equiv -g\widetilde{\rho}. \tag{2.92a,b}$$

Note that $\nabla_z p = \nabla_z p' = \nabla_z \delta p$ and that $p_0 \approx \widetilde{p}$ if $|\widehat{\rho}| \ll \rho_0$.

Momentum equations

To obtain the Boussinesq equations we use $\rho = \rho_0 + \delta\rho$, and assume $\delta\rho/\rho_0$ is small. Without approximation, the momentum equation can be written as

$$(\rho_0 + \delta\rho)\left(\frac{\mathrm{D}\boldsymbol{v}}{\mathrm{D}t} + 2\Omega \times \boldsymbol{v}\right) = -\nabla\delta p - \frac{\partial p_0}{\partial z}\mathbf{k} - g(\rho_0 + \delta\rho)\mathbf{k}, \tag{2.93}$$

and using (2.92a) this becomes, again without approximation,

$$(\rho_0 + \delta\rho)\left(\frac{\mathrm{D}\boldsymbol{v}}{\mathrm{D}t} + 2\Omega \times \boldsymbol{v}\right) = -\nabla\delta p - g\delta\rho\mathbf{k}. \tag{2.94}$$

If density variations are small this becomes

$$\boxed{\left(\frac{\mathrm{D}\boldsymbol{v}}{\mathrm{D}t} + 2\Omega \times \boldsymbol{v}\right) = -\nabla\phi + b\mathbf{k}}, \tag{2.95}$$

where $\phi = \delta p/\rho_0$ and $b = -g\delta\rho/\rho_0$ is the *buoyancy*. Note that we should not and do not neglect the term $g\delta\rho$, for there is no reason to believe it to be small ($\delta\rho$ may be small, but g is big). Eq. (2.95) is the momentum equation in the Boussinesq approximation, and it is common to say that the Boussinesq approximation ignores all variations of density of a fluid in the momentum equation, except when associated with the gravitational term.

For most large-scale motions in the ocean the *deviation* pressure and density fields are also approximately in hydrostatic balance, and in that case the vertical component of (2.95) becomes

$$\frac{\partial \phi}{\partial z} = b. \tag{2.96}$$

A condition for (2.96) to hold is that vertical accelerations are small *compared to* $g\delta\rho/\rho_0$, *and not compared to the acceleration due to gravity itself.* For more discussion of this point, see section 2.7.

Mass Conservation

The unapproximated mass conservation equation is

$$\frac{\mathrm{D}\delta\rho}{\mathrm{D}t} + (\rho_0 + \delta\rho)\nabla \cdot \boldsymbol{v} = 0. \tag{2.97}$$

Provided that time scales advectively — that is to say that $\mathrm{D}/\mathrm{D}t$ scales in the same way as $\boldsymbol{v} \cdot \nabla$ — then we may approximate this equation by

$$\boxed{\nabla \cdot \boldsymbol{v} = 0}, \tag{2.98}$$

which is the same as that for a constant density fluid. This *absolutely does not* allow one to go back and use (2.97) to say that $D\delta\rho/Dt = 0$; the evolution of density is given by the thermodynamic equation in conjunction with an equation of state, and this should not be confused with the mass conservation equation. Note that in eliminating the time-derivative of density we eliminate the possibility of sound waves.

Thermodynamic equation and equation of state

The Boussinesq equations are closed by the addition of an equation of state, a thermodynamic equation and, as appropriate, a salinity equation. Neglecting salinity for the moment, a useful starting point is to write the thermodynamic equation, (1.120), as

$$\frac{\mathrm{D}\rho}{\mathrm{D}t} - \frac{1}{c^2}\frac{\mathrm{D}p}{\mathrm{D}t} = \frac{\dot{Q}}{(\partial\eta/\partial\rho)_p T} \approx -\dot{Q}\left(\frac{\rho_0 \beta_T}{c_p}\right) \tag{2.99}$$

using $(\partial\eta/\partial\rho)_p = (\partial\eta/\partial T)_p(\partial T/\partial\rho)_p \approx c_p/(T\rho_0\beta_T)$.

Given the expansions (2.89a) and (2.91a) this can be written as

$$\frac{\mathrm{D}\delta\rho}{\mathrm{D}t} - \frac{1}{c^2}\frac{\mathrm{D}p_0}{\mathrm{D}t} = -\dot{Q}\left(\frac{\rho_0 \beta_T}{c_p}\right), \tag{2.100}$$

or, using (2.92a),

$$\frac{\mathrm{D}}{\mathrm{D}t}\left(\delta\rho + \frac{\rho_0 g}{c^2}z\right) = -\dot{Q}\left(\frac{\rho_0\beta_T}{c_p}\right),$$ (2.101)

as in (1.123). The severest approximation to this is to neglect the second term in brackets, and noting that $b = -g\delta\rho/\rho_0$ we obtain

$$\boxed{\frac{\mathrm{D}b}{\mathrm{D}t} = \dot{b}},$$ (2.102)

where $\dot{b} = g\beta_T\dot{Q}/c_p$. The momentum equation (2.95), mass continuity equation (2.98) and thermodynamic equation (2.102) then form a closed set, called the *simple Boussinesq equations*.

A somewhat more accurate approach is to include the compressibility of the fluid that is due to the hydrostatic pressure. Eq. (2.101) suggests that we define the potential density as $\delta\rho_{\mathrm{pot}} = \delta\rho + \rho_0 gz/c_s^2$ the *potential buoyancy,* the buoyancy based on potential density, as

$$b_\sigma \equiv -g\frac{\delta\rho_{\mathrm{pot}}}{\rho_0} = -\frac{g}{\rho_0}\left(\delta\rho + \frac{\rho_0 gz}{c_s^2}\right) = b - g\frac{z}{H_\rho},$$ (2.103)

where $H_\rho = c_s^2/g$. The thermodynamic equation, (2.101), may be written

$$\frac{\mathrm{D}b_\sigma}{\mathrm{D}t} = \dot{b}_\sigma,$$ (2.104)

where $\dot{b}_\sigma = \dot{b}$. Buoyancy itself is obtained from b_σ by the 'equation of state', $b = b_\sigma + gz/H_\rho$.

In many applications we may need to use a still more accurate equation of state. In that case (see section 1.5.5) we replace (2.102) by the thermodynamic equations

$$\boxed{\frac{\mathrm{D}\theta}{\mathrm{D}t} = \dot{\theta}, \qquad \frac{\mathrm{D}S}{\mathrm{D}t} = \dot{S}},$$ (2.105a,b)

where θ is the potential temperature and S is salinity, along with an equation of state. This has the the general form $b = b(\theta, S, p)$, but to be consistent with the level of approximation in the other Boussinesq equations we should replace p by the hydrostatic pressure calculated with the reference density, that is by $-\rho gz$, and the equation of state takes the form

$$\boxed{b = b(\theta, S, z)}.$$ (2.106)

An example of (2.106) is (1.179) taken with the definition of buoyancy $b = -g\delta\rho/\rho_0$. The closed set of equations (2.95), (2.98), (2.105) and (2.106) are the *general Boussinesq equations*. (If we were to use the equation of state $b = b(\theta, S, p)$, we might call the resulting equations the 'pseudo-Boussinesq' set.) Using an accurate equation of state and the Boussinesq approximation is the procedure used in many comprehensive ocean general circulation models. The Boussinesq equations, which with the hydrostatic and traditional approximations are often considered to be the oceanic primitive equations, are summarized in the shaded box.

Summary of Boussinesq Equations

The simple Boussinesq equations are, for an inviscid fluid:

$$\text{Momentum equations:} \qquad \frac{D\boldsymbol{v}}{Dt} + \boldsymbol{f} \times \boldsymbol{v} = -\nabla\phi + b\mathbf{k} \qquad (\text{B.1})$$

$$\text{Mass conservation:} \qquad \nabla \cdot \boldsymbol{v} = 0 \qquad (\text{B.2})$$

$$\text{Buoyancy equation:} \qquad \frac{Db}{Dt} = \dot{b} \qquad (\text{B.3})$$

A more general form replaces the buoyancy equation by:

$$\text{Thermodynamic equation:} \qquad \frac{D\theta}{Dt} = \dot{\theta} \qquad (\text{B.4})$$

$$\text{Salinity equation:} \qquad \frac{DS}{Dt} = \dot{S} \qquad (\text{B.5})$$

$$\text{Equation of state:} \qquad b = b(\theta, S, z) \qquad (\text{B.6})$$

*** Mean stratification and the buoyancy frequency*

The processes that cause density to vary in the vertical often differ from those that cause it to vary in the horizontal. For this reason it is sometimes useful to write $\rho = \rho_0 + \widehat{\rho}(z) + \rho'(x, y, z, t)$ and define $\widetilde{b}(z) \equiv -g\widehat{\rho}/\rho_0$ and $b' \equiv -g\rho'/\rho_0$. Using the hydrostatic equation to evaluate pressure, the thermodynamic equation (2.99) becomes, to a good approximation,

$$\frac{Db'}{Dt} + N^2 w = 0, \qquad (2.107)$$

where

$$N^2(z) = \left(\frac{d\widetilde{b}}{dz} - \frac{g^2}{c_s^2}\right) = \frac{d\widetilde{b}_\sigma}{dz}. \qquad (2.108)$$

where $\widetilde{b}_\sigma = \widetilde{b} - gz/H_\rho$. The quantity N^2 is a measure of the mean stratification of the fluid, and is equal to the vertical gradient of the mean potential buoyancy. N is known as the buoyancy frequency, something we return to in section 2.9. Equations (2.107) and (2.108) also hold in the simple Boussinesq equations, but with $c_s^2 = \infty$.

2.4.3 Energetics of the Boussinesq system

In a uniform gravitational field but with no other forcing or dissipation, we write the simple Boussinesq equations as

$$\frac{Dv}{Dt} + 2\boldsymbol{\Omega} \times \boldsymbol{v} = b\mathbf{k} - \nabla\phi, \qquad \nabla \cdot \boldsymbol{v} = 0, \qquad \frac{Db}{Dt} = 0. \qquad \text{(2.109a,b,c)}$$

From (2.109a) and (2.109b) the kinetic energy density evolution (c.f., section 1.9) is given by

$$\frac{1}{2}\frac{Dv^2}{Dt} = bw - \nabla \cdot (\phi \boldsymbol{v}) \qquad \text{(2.110)}$$

where the constant reference density ρ_0 is omitted. Let us now define the potential Φ such that $\nabla\Phi = -\mathbf{k}$ (so $\Phi = -z$) and so

$$\frac{D\Phi}{Dt} = \nabla \cdot (\boldsymbol{v}\Phi) = -w. \qquad \text{(2.111)}$$

Using this and (2.109c) gives

$$\frac{D}{Dt}(b\Phi) = -wb. \qquad \text{(2.112)}$$

Adding this to (2.110) and expanding the material derivative gives

$$\frac{\partial}{\partial t}\left(\frac{1}{2}\boldsymbol{v}^2 + b\Phi\right) + \nabla \cdot \left[\boldsymbol{v}\left(\frac{1}{2}\boldsymbol{v}^2 + b\Phi + \phi\right)\right] = 0. \qquad \text{(2.113)}$$

This constitutes an energy equation for the Boussinesq system, and may be compared to (1.194). (See also problem 2.12.) The energy density (divided by ρ_0) is just $\boldsymbol{v}^2/2 + b\Phi$. What does the second term represent? Its integral, multiplied by ρ_0, is the potential energy of the flow minus that of the basic state, or $\int g(\rho - \rho_0)z\,dz$. If there were a heating term on the right-hand side of (2.109c) this would directly provide a source of potential energy, rather than internal energy as in the compressible system. Because the fluid is incompressible, there is no conversion from kinetic and potential energy into internal energy.

* Energetics with a general equation of state

Now consider the energetics of the general, adiabatic, Boussinesq equations. Suppose first that we allow the equation of state to be a function of pressure; the equations are motion are then (2.109) except that (2.109c) is replaced by

$$\frac{D\theta}{Dt} = 0, \qquad \frac{DS}{Dt} = 0, \qquad b = b(\theta, S, \phi). \qquad \text{(2.114a,b,c)}$$

A little algebraic experimentation will reveal that no energy conservation law of the form (2.113) generally exists for this system! The problem arises because, by requiring that the fluid be incompressible, we eliminate the proper conversion of internal energy to kinetic energy. However, if we use the consistent approximation $b = b(\theta, S, z)$, the system conserves an energy, as we now show.[5]

Define the potential, Π, by the integral of b at constant potential temperature and salinity

$$\Pi(\theta, S, z) \equiv -\int b\,dz. \qquad \text{(2.115)}$$

Taking its material derivative gives

$$\frac{\mathrm{D}\Pi}{\mathrm{D}t} = \left(\frac{\partial \Pi}{\partial \theta}\right)_{S,z} \frac{\mathrm{D}\theta}{\mathrm{D}t} + \left(\frac{\partial \Pi}{\partial S}\right)_{\theta,z} \frac{\mathrm{D}S}{\mathrm{D}t} + \left(\frac{\partial \Pi}{\partial z}\right)_{\theta,S} \frac{\mathrm{D}z}{\mathrm{D}t} = -bw, \qquad (2.116)$$

using (2.114a,b). Combining (2.116) and (2.110) gives

$$\frac{\partial}{\partial t}\left(\frac{1}{2}\boldsymbol{v}^2 + \Pi\right) + \nabla \cdot \left[\boldsymbol{v}\left(\frac{1}{2}\boldsymbol{v}^2 + \Pi + \phi\right)\right] = 0. \qquad (2.117)$$

Thus, energetic consistency is maintained with an arbitrary equation of state, provided the pressure is replaced by a function of z. If b is not an explicit function of z in this equation of state, the conservation law is identical to (2.113).

2.5 EQUATIONS FOR A STRATIFIED ATMOSPHERE: THE ANELASTIC APPROXIMATION

2.5.1 Preliminaries

In the atmosphere the density varies significantly, especially in the vertical. However deviations of both ρ and p from a statically balanced state are often quite small, and the relative vertical variation of potential temperature is also small. We can usefully exploit these observations to give a somewhat simplified set of equations, useful both for theoretical and numerical analysis because sound waves are eliminated by way of an 'anelastic' approximation.[6] To begin we set

$$\rho = \widetilde{\rho}(z) + \delta\rho(x, y, z, t), \qquad p = \widetilde{p}(z) + \delta p(x, y, z, t) \qquad (2.118)$$

where we assume that $|\delta\rho| \ll |\widetilde{\rho}|$ and we define $\widetilde{p}$ such that

$$\frac{\partial \widetilde{p}}{\partial z} \equiv -g\widetilde{\rho}(z). \qquad (2.119)$$

The notation is similar to that for the Boussinesq case except that, importantly, the density basic state is now a (given) function of vertical coordinate. As with the Boussinesq case, the idea is to ignore dynamic variations of density (i.e., of $\delta\rho$) except where associated with gravity. First recall a couple of ideal gas relationships involving potential temperature, θ, and entropy s (divided by c_p, so $s \equiv \log \theta$), namely

$$s \equiv \log \theta = \log T - \frac{R}{c_p}\log p = \frac{1}{\gamma}\log p - \log \rho, \qquad (2.120)$$

where $\gamma = c_p/c_v$, implying

$$\delta s = \frac{1}{\gamma}\frac{\delta p}{p} - \frac{\delta\rho}{\rho} \approx \frac{1}{\gamma}\frac{\delta p}{\widetilde{p}} - \frac{\delta\rho}{\widetilde{\rho}} \qquad (2.121)$$

Further, if $\widetilde{s} \equiv \gamma^{-1}\log \widetilde{p} - \log \widetilde{\rho}$ then

$$\frac{\mathrm{d}\widetilde{s}}{\mathrm{d}z} = \frac{1}{\gamma\widetilde{p}}\frac{\mathrm{d}\widetilde{p}}{\mathrm{d}z} - \frac{1}{\widetilde{\rho}}\frac{\mathrm{d}\widetilde{\rho}}{\mathrm{d}z} = -\frac{g\widetilde{\rho}}{\gamma\widetilde{p}} - \frac{1}{\widetilde{\rho}}\frac{\mathrm{d}\widetilde{\rho}}{\mathrm{d}z}. \qquad (2.122)$$

In the atmosphere, the left-hand side is, typically, much smaller than either of the two terms on the right-hand side.

2.5.2 The Momentum equation

The exact inviscid horizontal momentum equation is

$$(\widetilde{\rho} + \rho')\frac{\mathrm{D}\boldsymbol{u}}{\mathrm{D}t} + \boldsymbol{f} \times \boldsymbol{u} = -\nabla_z \delta p. \tag{2.123}$$

Neglecting ρ' where it appears with $\widetilde{\rho}$ leads to

$$\frac{\mathrm{D}\boldsymbol{u}}{\mathrm{D}t} + \boldsymbol{f} \times \boldsymbol{u} = -\nabla_z \phi, \tag{2.124}$$

where $\phi = \delta p/\widetilde{\rho}$, and this is similar to the corresponding equation in the Boussinesq approximation.

The vertical component of the inviscid momentum equation is, without approximation,

$$(\widetilde{\rho} + \delta\rho)\frac{\mathrm{D}w}{\mathrm{D}t} = -\frac{\partial \widetilde{p}}{\partial z} - \frac{\partial \delta p}{\partial z} - g\widetilde{\rho} - g\delta\rho = -\frac{\partial \delta p}{\partial z} - g\delta\rho. \tag{2.125}$$

using (2.118). Neglecting $\delta\rho$ on the left-hand-side we obtain

$$\frac{\mathrm{D}w}{\mathrm{D}t} = -\frac{1}{\widetilde{\rho}}\frac{\partial \delta p}{\partial z} - g\frac{\delta\rho}{\widetilde{\rho}} = -\frac{\partial}{\partial z}\left(\frac{\delta p}{\widetilde{\rho}}\right) - \frac{\delta p}{\widetilde{\rho}^2}\frac{\partial \widetilde{\rho}}{\partial z} - g\frac{\delta\rho}{\widetilde{\rho}}. \tag{2.126}$$

This is not a useful form for a gaseous atmosphere, since the variation of the mean density cannot be ignored. However, we may eliminate $\delta\rho$ in favour of δs using (2.121) to give

$$\frac{\mathrm{D}w}{\mathrm{D}t} = g\delta s - \frac{\partial}{\partial z}\left(\frac{\delta p}{\widetilde{\rho}}\right) - \frac{g}{\gamma}\frac{\delta p}{\widetilde{p}} - \frac{\delta p}{\widetilde{\rho}^2}\frac{\partial \widetilde{\rho}}{\partial z}, \tag{2.127}$$

and using (2.122) gives

$$\frac{\mathrm{D}w}{\mathrm{D}t} = g\delta s - \frac{\partial}{\partial z}\left(\frac{\delta p}{\widetilde{\rho}}\right) + \frac{\mathrm{d}\widetilde{s}}{\mathrm{d}z}\frac{\delta p}{\widetilde{\rho}}. \tag{2.128}$$

What have these manipulations gained us? Two things:

(i) The gravitational term now involves δs rather than $\delta\rho$ which enables a more direct connection with the thermodynamic equation.

(ii) The potential temperature scale height ($\sim 100\,\mathrm{km}$) in the atmosphere is much larger than the density scale height ($\sim 10\,\mathrm{km}$), and so the last term in (2.128) is small.

The second item thus suggests that we choose our reference state to be one of constant potential temperature (see also problem 2.17). The term $\mathrm{d}\widetilde{s}/\mathrm{d}z$ then vanishes and the vertical momentum equation becomes

$$\boxed{\frac{\mathrm{D}w}{\mathrm{D}t} = g\delta s - \frac{\partial \phi}{\partial z}}, \tag{2.129}$$

where $\phi = \delta p/\widetilde{\rho}$, $\delta s = \delta\theta/\widetilde{\theta}$ and $\widetilde{\theta} = \theta_0$, a constant. If we define a buoyancy by $b_a \equiv g\delta s = g\delta\theta/\widetilde{\theta}$, then (2.124) and (2.129) have the same form as the Boussinesq momentum equations, but with different definitions of b and ϕ.

2.5.3 Mass conservation

Using (2.118a) the mass conservation equation may be written, without approximation, as

$$\frac{\partial \delta\rho}{\partial t} + \nabla \cdot [(\widetilde{\rho} + \delta\rho)\boldsymbol{v}] = 0. \tag{2.130}$$

We neglect $\delta\rho$ where it appears with $\widetilde{\rho}$ in the divergence term. Further, the local time derivative will be small if time itself is scaled advectively (i.e., $T \sim L/U$ and sound waves do not dominate), giving

$$\nabla \cdot \boldsymbol{u} + \frac{1}{\widetilde{\rho}}\frac{\partial}{\partial z}(\widetilde{\rho}w) = 0 \tag{2.131}$$

It is here that the eponymous 'anelastic approximation' arises: the elastic compressibility of the fluid is neglected, and this serves to eliminate sound waves. For reference, in spherical coordinates the equation is

$$\frac{1}{a\cos\vartheta}\frac{\partial u}{\partial \lambda} + \frac{1}{a\cos\vartheta}\frac{\partial}{\partial \vartheta}(v\cos\vartheta) + \frac{1}{\widetilde{\rho}}\frac{\partial(w\widetilde{\rho})}{\partial z} = 0. \tag{2.132}$$

In an ideal gas, the choice of constant potential temperature determines how the reference density $\widetilde{\rho}$ varies with height. In some circumstances it is convenient to let $\widetilde{\rho}$ be a constant, ρ_0 (effectively choosing a different equation of state), in which case the anelastic equations become identical with the Boussinesq equations, although we may continue to interpret the buoyancy in terms of potential temperature.

2.5.4 Thermodynamic equation

The thermodynamic equation for an ideal gas may be written

$$\frac{\mathrm{D}\ln\theta}{\mathrm{D}t} = \frac{\dot{Q}}{Tc_p}. \tag{2.133}$$

In the anelastic equations, $\theta = \widetilde{\theta} + \delta\theta$ where $\widetilde{\theta}$ is constant, and the thermodynamic equation is

$$\frac{\mathrm{D}\delta s}{\mathrm{D}t} = \frac{\widetilde{\theta}}{Tc_p}\dot{Q}. \tag{2.134}$$

Summarizing, the complete set of anelastic equations, with rotation but with no dissipation or diabatic terms, is

$$\boxed{\begin{aligned} \frac{\mathrm{D}\boldsymbol{v}}{\mathrm{D}t} + 2\boldsymbol{\Omega} \times \boldsymbol{v} &= \mathbf{k}b_a - \nabla\phi \\ \frac{\mathrm{D}b_a}{\mathrm{D}t} &= 0 \\ \nabla \cdot (\widetilde{\rho}\boldsymbol{v}) &= 0 \end{aligned}} \, , \tag{2.135}$$

where $b_a = g\delta s = g\delta\theta/\widetilde{\theta}$. The main difference between the anelastic and Boussinesq sets of equations is in the mass continuity equation, and when $\widetilde{\rho} = \rho_0 = $ constant the two equation sets are formally identical. However, whereas the Boussinesq approximation is a very good one for ocean dynamics, the anelastic approximation is much less so for large-scale atmosphere flow: the constancy of the reference potential temperature state is then not a particularly good approximation and so the deviations in density from its reference profile are not especially small, leading to inaccuracies in the momentum equation. Nevertheless, the anelastic equations have been used very productively in limited area 'large-eddy-simulations' where one does not wish to make the hydrostatic approximation but where sound waves are unimportant.[7] The equations also provide a good jumping-off point for theoretical studies and the still simpler models that will be considered in the chapter 5.

2.5.5 * Energetics of the anelastic equations

Conservation of energy follows in much the same way as for the Boussinesq equations, except that $\widetilde{\rho}$ enters. Take the dot product of (2.135a) with $\widetilde{\rho}\boldsymbol{v}$ to obtain

$$\widetilde{\rho}\frac{\mathrm{D}}{\mathrm{D}t}\left(\frac{1}{2}\boldsymbol{v}^2\right) = -\nabla\cdot(\phi\widetilde{\rho}\boldsymbol{v}) + b_a\widetilde{\rho}w \tag{2.136}$$

Now, define a potential $\Phi(z)$ such that $\nabla\Phi = -\mathbf{k}$, and so

$$\widetilde{\rho}\frac{\mathrm{D}\Phi}{\mathrm{D}t} = -w\widetilde{\rho}. \tag{2.137}$$

Combining this with the thermodynamic equation (2.135b) gives

$$\widetilde{\rho}\frac{\mathrm{D}(b_a\Phi)}{\mathrm{D}t} = -wb_a\widetilde{\rho}. \tag{2.138}$$

Adding this to (2.136) gives

$$\widetilde{\rho}\frac{\mathrm{D}}{\mathrm{D}t}\left(\frac{1}{2}\boldsymbol{v}^2 + b_a\Phi\right) = -\nabla\cdot(\phi\widetilde{\rho}\boldsymbol{v}), \tag{2.139}$$

or, expanding the material derivative,

$$\frac{\partial}{\partial t}\left[\widetilde{\rho}\left(\frac{1}{2}\boldsymbol{v}^2 + b_a\Phi\right)\right] + \nabla\cdot\left[\widetilde{\rho}\boldsymbol{v}\left(\frac{1}{2}\boldsymbol{v}^2 + b_a\Phi + \phi\right)\right] = 0. \tag{2.140}$$

This equation has the form

$$\frac{\partial E}{\partial t} + \nabla\cdot[\boldsymbol{v}(E + \widetilde{\rho}\phi)] = 0 \tag{2.141}$$

where $E = \widetilde{\rho}(\boldsymbol{v}^2/2 + b_a\Phi)$ is the energy density of the flow. This is a consistent energetic equation for the system, and when integrated over a closed domain the total energy is evidently conserved. The total energy density comprises the kinetic energy and a term $\widetilde{\rho}b_a\Phi$, which is analogous to the potential energy of a Boussinesq system. However, it is not exactly equal to that because b_a is the bouyancy based on potential temperature, not density; rather, the term combines contributions from both the internal energy and the potential energy.

2.6 CHANGING VERTICAL COORDINATE

Although using z as a vertical coordinate is a natural choice given our Cartesian world-view, it is not the only option, nor is it always the most useful one. Any variable that has a one-to-one correspondence with z in the vertical, so any variable that varies monotonically with z, could be used; pressure and, perhaps surprisingly, entropy, are common choices. In the atmosphere pressure almost always falls monotonically with height, and using it instead of z provides a useful simplification of the mass conservation and geostrophic relations, as well as a more direct connection with observations, which are often taken at fixed values of pressure. (In the ocean pressure is almost the same as height, because density is almost constant.) Entropy seems an exotic vertical coordinate, but it is very useful in adiabatic flow, and we consider that in chapter 3.

2.6.1 Pressure coordinates

The primitive equations of motion for an ideal gas can be written,

$$\frac{D\boldsymbol{u}}{Dt} + \boldsymbol{f} \times \boldsymbol{u} = -\frac{1}{\rho}\nabla p, \tag{2.142a}$$

$$\frac{\partial p}{\partial z} = -\rho g, \tag{2.142b}$$

$$\frac{D\theta}{Dt} = 0, \tag{2.142c}$$

$$\frac{D\rho}{Dt} + \rho \nabla \cdot \boldsymbol{v} = 0, \tag{2.142d}$$

where $p = \rho R T$ and $\theta = T\,(p_R/p)^{R/c_p}$, and p_R is the reference pressure. These equations can be put into a form similar to the Boussinesq equations by transforming from Cartesian [i.e., (x, y, z)] to *pressure coordinates*, (x, y, p). The analog of the vertical velocity is $\omega \equiv Dp/Dt$, and the advective derivative itself is given by

$$\frac{D}{Dt} = \frac{\partial}{\partial t} + \boldsymbol{u} \cdot \nabla_p + \omega \frac{\partial}{\partial p}. \tag{2.143}$$

The horizontal and time derivatives are taken at constant pressure. However, x and y are still purely horizontal coordinates, and $\boldsymbol{u} = u\mathbf{i} + v\mathbf{j}$ is still a strictly horizontal velocity, perpendicular to the vertical (z) axis. The operator D/Dt is of course the same in pressure or height coordinates because is simply the total derivative of some property of a fluid parcel. However, the individual terms comprising it in general differ between height and pressure coordinates.

To obtain an expression for the pressure force, first consider a general vertical coordinate, ξ. Then the chain rule gives

$$\left(\frac{\partial}{\partial x}\right)_\xi = \left(\frac{\partial}{\partial x}\right)_z + \left(\frac{\partial z}{\partial x}\right)_\xi \frac{\partial}{\partial z}. \tag{2.144}$$

Now let $\xi = p$ and apply the relationship to p itself to give

$$0 = \left(\frac{\partial p}{\partial x}\right)_z + \left(\frac{\partial z}{\partial x}\right)_p \frac{\partial p}{\partial z}, \tag{2.145}$$

which, using the hydrostatic relationship, gives

$$\left(\frac{\partial p}{\partial x}\right)_z = \rho\left(\frac{\partial \Phi}{\partial x}\right)_p,\tag{2.146}$$

where $\Phi = gz$ is the *geopotential*. Thus, the horizontal pressure force in the momentum equations is

$$\frac{1}{\rho}\nabla_z p = \nabla_p \Phi,\tag{2.147}$$

where the subscripts on the gradient operator indicate that the horizontal derivatives are taken at constant z or constant p. Also, from (2.142b), the hydrostatic equation is just

$$\frac{\partial \Phi}{\partial p} = -\alpha.\tag{2.148}$$

Mass continuity

The mass conservation equation simplifies attractively in pressure coordinates, if the hydrostatic approximation is used. Recall that the mass conservation equation can be derived from the Lagrangian form

$$\frac{D}{Dt}\rho\,\delta V = 0,\tag{2.149}$$

where $\delta V = \delta x \delta y \delta z$ is a volume element. But by the hydrostatic relationship $\rho\,\delta z = (1/g)\delta p$ and thus

$$\frac{D}{Dt}(\delta x \delta y \delta p) = 0.\tag{2.150}$$

This is completely analogous to the expression for the Lagrangian conservation of volume in an incompressible fluid, (1.15). Thus, without further ado, we write the mass conservation in pressure coordinates as

$$\nabla_p \cdot \boldsymbol{u} + \frac{\partial \omega}{\partial p} = 0,\tag{2.151}$$

where the horizontal derivative is taken at constant pressure. (See also problem 2.20.) The primitive equations in pressure coordinates are thus:

$$\boxed{\begin{aligned} \frac{D\boldsymbol{u}}{Dt} + \boldsymbol{f} \times \boldsymbol{u} &= -\nabla_p \Phi \\ \frac{\partial \Phi}{\partial p} &= -\alpha \\ \frac{D\theta}{Dt} &= 0 \\ \nabla_p \cdot \boldsymbol{u} + \frac{\partial \omega}{\partial p} &= 0 \end{aligned}}\tag{2.152}$$

where D/Dt is given by (2.143). The equation set is completed with the addition of the ideal gas equation and the definition of potential temperature. These are not quite isomorphic to the Boussinesq equations, because the hydrostatic equation is $\partial \Phi / \partial p = -\alpha = -(\theta R / p_R)(p_R / p)^{1/\gamma}$ and not, as we would require, $\partial \Phi / \partial p = -\theta$.

The main practical difficulty with these equations is the lower boundary condition. Using

$$w \equiv \frac{Dz}{Dt} = \frac{\partial z}{\partial t} + \boldsymbol{u} \cdot \nabla_p z + \omega \frac{\partial z}{\partial p}, \qquad (2.153)$$

and (2.148), the boundary condition of $w = 0$ at $z = z_s$ becomes

$$\frac{\partial \Phi}{\partial t} + \boldsymbol{u} \cdot \nabla_p \Phi - \alpha \omega = 0 \qquad (2.154)$$

at $p(x, y, z_s, t)$. In theoretical studies, it is common to assume that the lower boundary is in fact a constant pressure surface and simply assume that $\omega = 0$, or sometimes the condition $\omega = -\alpha^{-1} \partial \Phi / \partial t$ is used. For realistic studies (with general circulation models, say) the fact that the level $z = 0$ is not a coordinate surface must be properly accounted for. For this reason, and especially if the lower boundary is uneven because of the presence of topography, so-called *sigma coordinates* are sometimes used, in which the vertical coordinate is chosen so that the lower boundary is a coordinate surface. Sigma coordinates may use height itself as a measure of displacement (typical in oceanic applications) or use pressure (typical in atmospheric applications). In the latter case the vertical coordinate is $\sigma = p/p_s$ where $p_s(x, y, t)$ is the surface pressure. The difficulty of applying (2.154) is replaced by a prognostic equation for the surface pressure, which is derived from the mass conservation equation (problem 2.21).

Log-pressure coordinates

A variant of pressure coordinates is *log-pressure* coordinates, in which the vertical coordinate is $Z = -H \ln(p/p_R)$ where p_R is a reference pressure (say 1000 mb) and H a constant (for example the scale height RT_s/g) so that Z has units of length. The 'vertical velocity' for the system is now

$$W \equiv \frac{DZ}{Dt} \qquad (2.155)$$

and the advective derivative is now

$$\frac{D}{Dt} \equiv \frac{\partial}{\partial t} + \boldsymbol{u} \cdot \nabla_p + W \frac{\partial}{\partial Z}, \qquad (2.156)$$

(Capital letters are conventionally used for some variables in log-pressure coordinates, and these are not to be confused with scaling parameters.) It is straightforward to show (problem 2.22) that the primitive equations of motion in these coordinates are:

$$\frac{D\boldsymbol{u}}{Dt} + \boldsymbol{f} \times \boldsymbol{u} = -\nabla_Z \Phi \qquad (2.157a)$$

$$\frac{\partial \Phi}{\partial Z} = \frac{RT}{H} \qquad (2.157b)$$

$$\frac{\mathrm{D}\theta}{\mathrm{D}t} = 0 \tag{2.157c}$$

$$\frac{\partial u}{\partial x} + \frac{\partial v}{\partial y} + \frac{\partial W}{\partial Z} - \frac{W}{H} = 0. \tag{2.157d}$$

The last equation may be written $\nabla_Z \cdot \boldsymbol{u} + \rho_*^{-1} \partial (\rho_* W)/\partial z = 0$, where $\rho_* = \exp(-z/H)$, a form similar to the mass conservation equation in the anelastic equations.

2.7 HYDROSTATIC BALANCE

In this section and the next we consider two of the most fundamental balances in geophysical fluid dynamics — hydrostatic balance and geostrophic balance. Neither are exact, but their approximate satisfaction has profound consequences on the behaviour of the atmosphere and ocean.

2.7.1 Preliminaries

Consider the relative sizes of terms in (2.78c),

$$\frac{W}{T} + \frac{UW}{L} + \frac{W^2}{H} + \Omega U \sim \frac{1}{\rho}\frac{\partial p}{\partial z} - g \tag{2.158}$$

For most large-scale motion in the atmosphere and ocean the terms on the right-hand side are orders of magnitude larger than those on the left, and therefore must be approximately equal. Explicitly, suppose $W \sim 1\,\mathrm{cm\,s^{-1}}$, $L \sim 10^5\,\mathrm{m}$, $H \sim 10^3\,\mathrm{m}$, $U \sim 10\,\mathrm{m\,s^{-1}}$, $T = L/U$. Then by substituting into (2.158) it seems that the pressure term is the only one which could balance the gravitational term, and we are led to the following vertical momentum equation,

$$\frac{\partial p}{\partial z} = -\rho g, \tag{2.159}$$

otherwise known as *hydrostatic balance*.

However, (2.159) is not necessarily a useful equation! Let us suppose that the density is a constant, ρ_0 ; we can then write the pressure as

$$p(x, y, z, t) = p_0(z) + p'(x, y, z, t), \tag{2.160}$$

where

$$\frac{\partial p_0}{\partial z} \equiv -\rho_0 g. \tag{2.161}$$

That is, p_0 and ρ_0 are in hydrostatic balance. The vertical momentum equation becomes, without approximation,

$$\frac{\mathrm{D}w}{\mathrm{D}t} = -\frac{1}{\rho_0}\frac{\partial p'}{\partial z} + \nu\nabla^2 w. \tag{2.162}$$

Thus, for constant density fluids, the gravitational term has no dynamical effect: there

is no buoyancy force, and the pressure term in the horizontal momentum equations can be replaced by p'. Hydrostatic balance, and in particular (2.161), is certainly not an appropriate vertical momentum equation in this case. If the fluid is stratified, we should therefore subtract off the hydrostatic pressure associated with the mean density before we can determine whether hydrostasy is a useful *dynamical* approximation, accurate enough to determine the horizontal pressure gradients. This is automatic in the Boussinesq equations, where the vertical momentum equation is

$$\frac{\mathrm{D}w}{\mathrm{D}t} = -\frac{\partial \phi}{\partial z} + b. \tag{2.163}$$

and the hydrostatic balance of the basic state is already subtracted out. In the more general equation,

$$\frac{\mathrm{D}w}{\mathrm{D}t} = -\frac{1}{\rho}\frac{\partial p}{\partial z} - g, \tag{2.164}$$

we need to compare the advective term on the left-hand side with the pressure variations arising from horizontal flow in order to determine whether hydrostasy is an appropriate vertical momentum equation. Of course, if we simply need to determine the pressure for use in an equation of state then we simply need to compare the sizes of the dynamical terms in (2.78c) with g itself in order to determine whether a hydrostatic approximation will suffice.

2.7.2 Scaling and the aspect ratio

In a non-rotating Boussinesq fluid the horizontal momentum equation $\mathrm{D}\boldsymbol{u}/\mathrm{D}t = -\nabla\phi$ implies the scaling

$$\phi \sim U^2 \tag{2.165}$$

If we now use mass conservation to scale vertical velocity, so that

$$\frac{W}{H} \sim \frac{U}{L} \tag{2.166}$$

then the advective terms in the vertical momentum equation all scale as

$$\frac{\mathrm{D}w}{\mathrm{D}t} \sim \frac{UW}{L} = \frac{U^2 H}{L^2} \tag{2.167}$$

Using (2.165) and (2.167) the ratio of the advective term to the pressure gradient term in the vertical momentum equations then scales as

$$\frac{|\mathrm{D}w/\mathrm{D}t|}{|(1/\rho)\partial\phi/\partial z|} \sim \frac{U^2 H/L^2}{U^2/H} \sim \left(\frac{H}{L}\right)^2. \tag{2.168}$$

Thus, the condition for hydrostasy is:

$$\boxed{\alpha^2 \equiv \left(\frac{H}{L}\right)^2 \ll 1}, \tag{2.169}$$

in which case the advective term in the vertical momentum is small. Thus, hydrostasy is an *aspect ratio approximation;* it holds when the aspect ratio $\alpha \equiv H/L$ is small.

Effects of rotation

In the presence of rapid rotation geostrophic-balance suggests the pressure scaling $\phi \sim fUL$ holds and we obtain

$$\frac{|Dw/Dt|}{|(1/\rho)\partial p/\partial z|} \sim \frac{WH}{fL^2} = Ro\frac{WH}{UL}. \tag{2.170}$$

Furthermore, in geostrophic balance the horizontal flow may be nearl non-divergent (as we see in the next section), so that $W \sim UH/L$ is an overestimate of the magnitude of the vertical velocity. Let us thus write $W \sim \epsilon UH/L$ where $\epsilon \ll 1$. (Later on we'll see that ϵ is in fact related to the Rossby number.) Using this in (2.170) gives

$$\frac{|Dw/Dt|}{|(1/\rho)\partial p/\partial z|} \sim \epsilon Ro\left(\frac{H}{L}\right)^2, \tag{2.171}$$

which is evidently very small for the large-scale flow. In particular, because $\epsilon Ro \ll 1$, rotation tends to weaken further the conditions needed for hydrostasy; that is, a rapidly rotating fluid is more likely to be in hydrostatic balance than a non-rotating fluid, other conditions being equal.

* Effects of stratification

The above results say little about the dynamics that might give rise to hydrostatic or non-hydrostatic flow. Our intuition suggests that hydrostatic balance might be questionable in small-scale convective activity where the vertical velocity is high, and most applicable in highly stratified flow for then vertical velocity is diminished. But in highly stratified flow the estimate of W from (2.167) may be too restrictive. Furthermore, the vertical scale H is not always known *a priori,* for it need not be the domain scale. In a laboaratory rotating tank, for example, the aspect ratio of the fluid is $\mathcal{O}(1)$, but the vertical scale of the motion is much smaller. We thus give another estimate of the vertical velocity that takes explicit account of known stratification and use it to derive a slightly weaker condition for hydrostasy.

To obtain an estimate of the vertical velocity, we use the Boussinesq approximation with a vertical momentum equation:

$$\frac{Dw}{Dt} = -\frac{\partial\phi}{\partial z} + b. \tag{2.172}$$

For hydrostatic balance we demand

$$\frac{UW}{L} \ll \Delta b, \tag{2.173}$$

where Δb is the scaling magnitude for b. It is only the horizontal variations of b that matter, so let us assume that the magnitude for w is given by the thermodynamic equation written in the form

$$\frac{Db'}{Dt} + N^2 w = 0, \tag{2.174}$$

where the mean stratification (N^2) is given — determined, for example, by the larger scale circulation. Then,

$$W \sim \frac{U\Delta b}{LN^2} \tag{2.175}$$

This implies that $W/H = (U/L)\,\Delta b/(HN^2)$, and, assuming that $\Delta b/H \ll N^2$, that $W/H \ll U/L$ and horizontal advection dominates vertical advection of the buoyancy anomaly. Using (2.175), the condition for hydrostatic balance, (2.173), becomes

$$\boxed{\frac{U^2}{L^2 N^2} \ll 1} \, . \tag{2.176}$$

Since the buoyancy frequency N is a measure of stratification (the higher the frequency, the more stratified the fluid), (2.176) formalizes our intuitive expectation that the more stratified a fluid the more vertical motion is suppressed and the more likely hydrostatic balance is to hold.

The *Froude number* may be defined by

$$F \equiv \frac{U}{NH}. \tag{2.177}$$

Then

$$\frac{U^2}{L^2 N^2} = F^2 \frac{H^2}{L^2}, \tag{2.178}$$

and using (2.176) the hydrostatic condition is

$$\boxed{F^2 \alpha^2 \ll 1} \, , \tag{2.179}$$

where $\alpha = H/L$ is the aspect ratio of the motion. Thus, for a given Froude number a small aspect ratio will favor hydrostasy. This derivation differs from that leading to (2.169) in its use of the thermodynamic equation, rather than the mass conservation equation, to give an estimate of the vertical velocity.

Why bother with any of this scaling? Why not just say that hydrostatic balance holds when $|Dw/Dt| \ll |b|$? One reason is that don't really have a good idea of the value of W from direct measurements, and it may change significantly in different oceanic and atmospheric parameter regimes. On the other hand the Froude number and the aspect ratio are familiar nondimensional parameters with a wide applicability in other contexts, and which we can control in a laboratory setting or estimate more easily in the ocean or atmosphere. Still, as in most scaling theory, deciding which parameters are given and which should be derived is often a *choice*, rather than being set *a priori*.

Hydrostatic balance in waves

If the motion is predominantly wavelike, rather than advective, then the advective derivative scales like a frequency: $D/Dt \sim \omega$. Using the vertical momentum equation we then require

$$\omega w \ll b, \tag{2.180}$$

and the thermodynamic equation has the scaling

$$\omega b \sim N^2 w. \tag{2.181}$$

These together demand that

$$\omega^2 \ll N^2 \tag{2.182}$$

for hydrostatic balance to hold. Buoyancy oscillations have $\omega \approx N$ and are essentially non-hydrostatic.

Oceanic applicability

For the large scale ocean circulation, let $N \sim 10^{-2}\,\mathrm{s}^{-1}$, $U \sim 0.1\,\mathrm{m\,s}^{-1}$ and $H \sim 1\,\mathrm{km}$. Then

$$F = \frac{U}{NH} \sim 10^{-2} \ll 1 \tag{2.183}$$

Thus, $F^2\gamma^2 \ll 1$ even for unit aspect-ratio motion. For gyre scale flow $L \sim 10^6\,\mathrm{m}$ and $F^2\gamma^2 \sim 10^{-10}$ and hydrostatic balance is a very good approximation indeed.

For intense convection, for example in the Labrador Sea, the hydrostatic approximation may be less appropriate. The intense descending plumes may have an aspect ratio (H/L) of one or greater and the stratification is very weak: the hydrostatic condition is then simply a requirement that stratification is sufficiently strong that the Froude number is small. Representative orders of magnitude are $U \sim W \sim 0.1\,\mathrm{m\,s}^{-1}$, $H \sim 1\,\mathrm{km}$ and $N \sim 10^{-3}\,\mathrm{s}^{-1}$–$10^{-4}\,\mathrm{s}^{-1}$. For these values F ranges between 0.1 and 1, and at the upper end of this range hydrostatic balance is violated.

Atmospheric applicability

Similar considerations apply to the atmosphere, although the details differ. Over much of the lower atmosphere $N \sim 10^{-2}\,\mathrm{s}^{-1}$ so that with $U = 10\,\mathrm{m\,s}^{-1}$ and $H = 1\,\mathrm{km}$ for large-scale flow $F \sim 1$. Hydrostasy is then maintained because the aspect ratio H/L is much less than unity. For smaller scale atmospheric motion associated with fronts and, especially, convection, there can be little expectation that hydrostatic balance will be a good approximation.

2.8 GEOSTROPHIC AND THERMAL WIND BALANCE

We now consider the dominant dynamical balance in the horizontal components of the momentum equation. In the horizontal plane (meaning along geopotential surfaces) we find that the Coriolis term is much larger than the advective terms and the dominant balance is between it and the horizontal pressure force. This balance is called *geostrophic balance,* and it occurs when the Rossby number is small, as we now investigate.

2.8.1 The Rossby Number

The *Rossby number* characterizes the importance of rotation in a fluid.[8] It is, essentially, the ratio of the magnitude of the relative acceleration to the Coriolis acceleration, and

Variable	Scaling Symbol	Meaning	Atmos. value	Ocean value
(x, y)	L	Horizontal length	10^6 m	10^5 m
t	T	Timescale	1 day (10^5 s)	10 days (10^6 s)
(u, v)	U	Horizontal velocity	$10\,\mathrm{m\,s^{-1}}$	$0.1\,\mathrm{m\,s^{-1}}$
	Ro	Rossby number, U/fL	0.1	0.01

Table 2.1 Scales of large-scale flow in atmosphere and ocean. The choices given are representative of large-scale eddying motion in both systems.

it is of fundamental importance in geophysical fluid dynamics. It arises from a simple scaling of horizontal momentum equation, namely

$$\frac{\partial \boldsymbol{u}}{\partial t} + (\boldsymbol{v} \cdot \nabla)\boldsymbol{u} + \boldsymbol{f} \times \boldsymbol{u} = -\frac{1}{\rho}\nabla_z p, \qquad (2.184a)$$

$$U^2/L \qquad fU \qquad\qquad\qquad (2.184b)$$

where U is the approximate magnitude of the horizontal velocity and L is a typical lengthscale over which that velocity varies. (We assume that $W/H \lesssim U/L$, so that vertical advection does not dominate the advection.) The ratio of the sizes of the advective and Coriolis terms is defined to be the Rossby number,

$$\boxed{Ro \equiv \frac{U}{fL}}. \qquad (2.185)$$

If the Rossby number is small then rotation effects are important, and as the values in table 2.1 indicate this is the case for large-scale flow in both ocean and atmosphere.

Another intuitive way to think about the Rossby number is in terms of timescales. The Rossby number based on a timescale is

$$Ro_t \equiv \frac{1}{fT} \qquad (2.186)$$

where T is a timescale associated with the dynamics at hand. If the timescale is an advective one, meaning that $T \sim L/U$, then this definition is equivalent to (2.185). Now, $f = 2\Omega \sin \vartheta$, where Ω is the angular velocity of the rotating frame and equal to $2\pi \sin \vartheta / T_p$ where T_p is the period of rotation (24 hours). Thus,

$$Ro_t = \frac{T_p}{4\pi T \sin \vartheta} = \frac{T_i}{T} \qquad (2.187)$$

where $T_i = 1/f$ is the 'inertial timescale', about three hours in midlatitudes. Thus, for phenomena with timescales much longer than this, such as the motion of the Gulf

Stream or a mid-latitude atmospheric weather system, the effects of the earth's rotation can be expected to be important, whereas a short-lived phenomena, such as a cumulus cloud or tornado, may be oblivious to such rotation. The expressions (2.185) and (2.186) of course, just approximate measures of the importance of rotation.

2.8.2 Geostrophic Balance

If the Rossby number is sufficiently small in (2.184a) then the rotation term will dominate the nonlinear advection term, and if the time period of the motion scales advectively then the rotation term also dominates the local time derivative. The only term which can then balance the rotation termis the pressure term, and therefore we must have

$$\boldsymbol{f} \times \boldsymbol{u} \approx -\frac{1}{\rho}\nabla_z p, \tag{2.188}$$

or, in Cartesian component form

$$fu \approx -\frac{1}{\rho}\frac{\partial p}{\partial y}, \qquad fv \approx \frac{1}{\rho}\frac{\partial p}{\partial x}. \tag{2.189}$$

This balance is known as *geostrophic balance,* and its consequences are profound, giving geophysical fluid dynamics a special place in the broader field of fluid dynamics. We *define* the geostrophic velocity by

$$\boxed{fu_g \equiv -\frac{1}{\rho}\frac{\partial p}{\partial y}, \qquad fv_g \equiv \frac{1}{\rho}\frac{\partial p}{\partial x}}, \tag{2.190}$$

and for low Rossby number flow $u \approx u_g$ and $v \approx v_g$. In spherical coordinates the geostrophic velocity is

$$fu_g = -\frac{1}{\rho a}\frac{\partial p}{\partial \vartheta}, \qquad fv_g = \frac{1}{a\rho\cos\vartheta}\frac{\partial p}{\partial \lambda}, \tag{2.191}$$

where $f = 2\Omega\sin\vartheta$. Geostrophic balance has a number of immmediate ramifications:

* ⋆ Geostrophic flow is parallel to lines of constant pressure (isobars). If $f > 0$ the flow is anti-clockwise round a region of low pressure and clokwise around a region of high pressure (see Fig. 2.5).

* ⋆ If the Coriolis force is constant and if the density does not vary in the horizontal the geostrophic flow is horizontally non-divergent and

$$\boxed{\nabla_z \cdot \boldsymbol{u}_g = \frac{\partial u_g}{\partial x} + \frac{\partial v_g}{\partial y} = 0}. \tag{2.192}$$
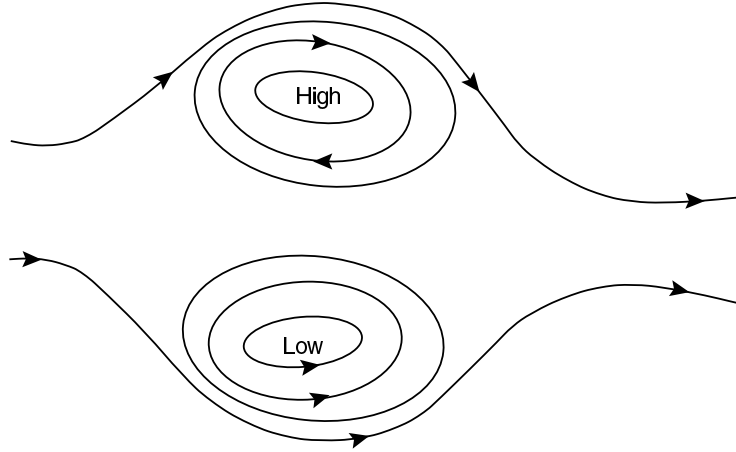
Fig. 2.5 Schematic of geostrophic flow with a positive value of the Coriolis parameter f. Flow is parallel to the lines of constant pressure (isobars). Cyclonic flow is anticlockwise around a low pressure region and anticyclonic flow is clockwise around a high. If f were negative, as in the Southern hemisphere, (anti-)cyclonic flow would be (anti-)clockwise.

We may define the *streamfunction, ψ,* by

$$\psi \equiv \frac{p}{f_0 \rho_0},\tag{2.193}$$

whence

$$u_g = -\frac{\partial \psi}{\partial y}, \qquad v_g = \frac{\partial \psi}{\partial x}.\tag{2.194}$$

The vertical component of vorticity, ζ, is then given by

$$\zeta = \mathbf{k} \cdot \nabla \times \boldsymbol{v} = \frac{\partial v}{\partial x} - \frac{\partial u}{\partial y} = \nabla_z^2 \psi.\tag{2.195}$$

⋆ If the Coriolis parameter is not constant, then cross-differentiating (2.190) gives, for constant density geostrophic flow,

$$v_g \frac{\partial f}{\partial y} + f \nabla_z \cdot \boldsymbol{u}_g = 0,\tag{2.196}$$

which implies, using mass continuity,

$$\beta v_g = f \frac{\partial w}{\partial z}.\tag{2.197}$$

where $\beta \equiv \partial f / \partial y = 2\Omega \cos \vartheta / a$. This geostrophic vorticity balance is sometimes known as Sverdrup balance, although that expression is better restricted to the case when the vertical velocity results from external agents, and specifically a wind stress, as considered in chapter 14.

2.8.3 Taylor-Proudman effect

If $\beta = 0$, then (2.197) implies that the vertical velocity is not a function of height. In fact, in that case none of the components of velocity vary with height if density is also constant. To show this, in the limit of zero Rossby number we first write the three-dimensional momentum equation as

$$\boldsymbol{f}_0 \times \boldsymbol{v} = -\nabla\phi - \nabla\chi, \tag{2.198}$$

where $\boldsymbol{f}_0 = 2\boldsymbol{\Omega} = 2\Omega\mathbf{k}$, $\phi = p/\rho_0$, and $\nabla\chi$ represents other potential forces. If $\chi = gz$ then the vertical component of this equation represents hydrostatic balance, and the horizontal components represent hydrostatic balance. On taking the curl of this equation, the terms on the right-hand side vanish and the left-hand side becomes

$$(\boldsymbol{f}_0 \cdot \nabla)\boldsymbol{v} - \boldsymbol{f}_0 \nabla \cdot \boldsymbol{v} - (\boldsymbol{v} \cdot \nabla)\boldsymbol{f}_0 + \boldsymbol{v}\nabla \cdot \boldsymbol{f}_0 = 0. \tag{2.199}$$

But $\nabla \cdot \boldsymbol{v} = 0$ by mass conservation, and because $\boldsymbol{f}_0$ is constant both $\nabla \cdot \boldsymbol{f}_0$ and $(\boldsymbol{v} \cdot \nabla)\boldsymbol{f}_0$ vanish. Thus

$$(\boldsymbol{f}_0 \cdot \nabla)\boldsymbol{v} = 0, \tag{2.200}$$

which, since $\boldsymbol{f}_0 = f_0\mathbf{k}$, implies $f_0 \partial\boldsymbol{v}/\partial z = 0$, and in particular we have

$$\frac{\partial u}{\partial z} = 0, \quad \frac{\partial v}{\partial z} = 0, \quad \frac{\partial w}{\partial z} = 0. \tag{2.201}$$

A different presentation of this argument proceeds as follows. If the flow is exactly in geostrophic and hydrostatic balance then

$$v = \frac{1}{f_0}\frac{\partial\phi}{\partial x}, \qquad u = -\frac{1}{f_0}\frac{\partial\phi}{\partial y}, \qquad \frac{\partial\phi}{\partial z} = -g \tag{2.202a,b,c}$$

Differentiating (2.202a,b) with respect to z, and using (2.202c) yields

$$\frac{\partial v}{\partial z} = \frac{-1}{f_0}\frac{\partial g}{\partial x} = 0, \quad \frac{\partial u}{\partial z} = \frac{1}{f_0}\frac{\partial g}{\partial y} = 0, \tag{2.203}$$

Noting that the geostrophic veclocities are horizontally non-divergent ($\nabla_z \cdot \boldsymbol{u} = 0$), and using mass continuity then gives $\partial w/\partial z = 0$, as before.

If there is a solid horizontal boundary anywhere in the fluid, for example at the surface, then $w = 0$ at that surface and thus $w = 0$ everywhere. Hence the motion occurs in planes that lie perpendicular to the axis of rotation, and the flow is 'two-dimensional.' This result is known as the *Taylor-Proudman effect,* namely that for constant density flow in geostrophic and hydrostatic balance the vertical derivatives of the horizontal and the vertical velocities are zero.[9] At zero Rossby number, if the vertical velocity is zero somewhere in the flow, it is zero everywhere in that vertical column; furthermore, the horizontal flow has no vertical shear, and the fluid moves like a slab. The effects of rotation have provided a *stiffening* of the fluid in the vertical.

In neither the atmosphere nor the ocean do we observe precisely such vertically coherent flow, mainly because of the effects of stratification. However, it is typical of

geophysical fluid dynamics that the assumptions underlying a derivation are not fully satisfied, yet there are manifestations of it in real flow. Thus, one might have naïvely expected, because $\partial w / \partial z = -\nabla_z \cdot \boldsymbol{u}$, that the scales of the various variables would be related by $W/H \sim U/L$. However, if the flow is rapidly rotating we expect that the horizontal flow will be in near geostrophic balance and therefore nearly divergence free; thus $\nabla_z \cdot \boldsymbol{u} \ll U/L$, and $W \ll HU/L$.

2.8.4 Thermal wind balance

Thermal wind balance arises by combining the geostrophic and hydrostatic approximations, and this is most easily done in the context of the anelastic (or Boussinesq) equations, or in pressure coordinates. For the anelastic equations, in spherical coordinates geostrophic balance may be written

$$-f v_g = -\frac{\partial \phi}{\partial x} = -\frac{1}{a \cos \vartheta} \frac{\partial \phi}{\partial \lambda} \tag{2.204a}$$

$$f u_g = -\frac{\partial \phi}{\partial y} = -\frac{1}{a} \frac{\partial \phi}{\partial \vartheta} \tag{2.204b}$$

Combining these with hydrostatic balance, $\partial \phi / \partial z = b$, gives

$$\boxed{\begin{aligned} -f \frac{\partial v_g}{\partial z} &= -\frac{\partial b}{\partial x} = -\frac{1}{a \cos \lambda} \frac{\partial b}{\partial \lambda} \\ f \frac{\partial u_g}{\partial z} &= -\frac{\partial b}{\partial y} = -\frac{1}{a} \frac{\partial b}{\partial \vartheta} \end{aligned}} \ . \tag{2.205a,b}$$

These equations are known as *thermal wind balance,* and the vertical derivative of the geostrophic wind is the thermal wind. In terms of the zonal angular momentum, the second of these equations may be written

$$\frac{\partial m_g}{\partial z} = -\frac{a}{2\Omega \tan \vartheta} \frac{\partial b}{\partial y}, \tag{2.206}$$

where $m_g = (u_g + \Omega a \cos \vartheta) a \cos \vartheta$. Potentially more accurate than geostrophic balance is the so-called cyclostrophic or gradient-wind balance

$$2u\Omega \sin \vartheta + \frac{u^2}{a} \tan \vartheta \approx -\frac{\partial \phi}{\partial y} = -\frac{1}{a} \frac{\partial \phi}{\partial \vartheta}. \tag{2.207}$$

For large-scale flow this differs significantly from geostrophic balance only very close to the equator. Combining cyclostrophic and hydrostatic balance gives a modified thermal wind relation, and this takes a simple form when expressed in terms of angular momentum, namely

$$\frac{\partial m^2}{\partial z} \approx -\frac{a^3 \cos^3 \vartheta}{\sin \vartheta} \frac{\partial b}{\partial y}. \tag{2.208}$$

If the density or buoyancy is constant then there is no shear and (2.205) or (2.208)

reduce to the Taylor-Proudman result. But suppose that the temperature falls in the polewards direction. Then thermal wind balance implies that the (eastwards) wind will increase with height — just as is observed in the atmosphere! In general a vertical shear of the horizontal wind is associated with a horizontal temperature gradient, and this is one of the most simple and far-reaching effects in geophysical fluid dynamics.

Pressure coordinates

In pressure coordinates geostrophic balance is just

$$\boldsymbol{f} \times \boldsymbol{u}_g = -\nabla_p \Phi \tag{2.209}$$

where Φ is the geopotential and ∇_p is the gradient operator taken at constant pressure. If f if constant, it follows from (2.209) that the geostrophic wind is non-divergent on pressure surfaces. Taking the vertical derivative of (2.209) (that is, its derivative with respect to p) and using the hydrostatic equation, $\partial \Phi / \partial p = -\alpha$, gives the thermal wind equation

$$\boldsymbol{f} \times \frac{\partial \boldsymbol{u}_g}{\partial p} = \nabla_p \alpha = \frac{R}{p} \nabla_p T, \tag{2.210}$$

where the last equality follows using the ideal gas equation and because the horizontal derivative is at constant pressure. In component form this is

$$-f \frac{\partial v_g}{\partial p} = -\frac{R}{p} \frac{\partial T}{\partial x}, \qquad f \frac{\partial u_g}{\partial p} = -\frac{R}{p} \frac{\partial T}{\partial y}. \tag{2.211}$$

In log-pressure coordinates, with $Z = -H \ln(p/p_{\mathrm{R}})$, thermal wind is simply:

$$\boldsymbol{f} \times \frac{\partial \boldsymbol{u}_g}{\partial Z} = -\frac{R}{H} \nabla_Z T, \tag{2.212}$$

2.9 STATIC INSTABILITY AND THE PARCEL METHOD

In this and the next couple of sections we consider how a fluid might oscillate if it were perturbed away from a resting state. Our focus is on vertical displacements, and the restoring force is gravity, and we will neglect the effects of rotation, and indeed initially we will neglect horizontal motion entirely. Given that, the simplest and most direct way to approach the problem is to consider from first principles the pressure and gravitational forces on a dispaced parcel. To this end, consider a fluid at rest in a constant gravitational field, and therefore in hydrostatic balance. Suppose that a small parcel of the fluid is adiabatically displaced upwards by the small distance δz, without altering the overall pressure field — that is, the fluid parcel instantly assumes the pressure of its environment. If after the displacement the parcel is lighter than its environment, it will accelerate upwards, because the upward pressure gradient force is now greater downwards gravity force on the parcel — that is, the parcel is *buoyant* (a manifestation of Archimedes' principle) and the fluid is *statically unstable*. If on the other hand the fluid parcel finds itself heavier than its surroundings, the downward gravitational force

will be greater than the upward pressure force and the fluid will sink back towards its original position and an oscillatory motion will develop. Such an equilibrium is *statically stable*. Using such simple 'parcel' arguments we will now develop criteria for the stability of the environmental profile.

2.9.1 A simple special case: a density-conserving fluid

Consider first the simple case of an incompressible fluid in which the density of the displaced parcel is conserved, that is $D\rho/Dt = 0$ (and refer to Fig. 2.6 setting $\rho_\theta = \rho$). If the environmental profile is $\widetilde{\rho}(z)$ and the density of the parcel is ρ then a parcel displaced from a level z [where its density is $\widetilde{\rho}(z)$] to a level $z + \delta z$ [where the parcel's density is still $\widetilde{\rho}(z)$] will find that its density then differs from its surroundings by the amount

$$\delta\rho = \rho(z + \delta z) - \widetilde{\rho}(z + \delta z) = \widetilde{\rho}(z) - \widetilde{\rho}(z + \delta z) = -\frac{\partial\widetilde{\rho}}{\partial z}\delta z. \qquad (2.213)$$

The parcel will be heavier than its surroundings, and therefore the parcel displacement will be stable, if $\partial\widetilde{\rho}/\partial z < 0$. Similarly, it will be unstable if $\partial\widetilde{\rho}/\partial z > 0$. The upward force (per unit volume) on the displaced parcel is given by

$$F = -g\delta\rho = g\frac{\partial\widetilde{\rho}}{\partial z}\delta z, \qquad (2.214)$$

and thus Newton's second law implies that the motion of the parcel is determined by

$$\rho(z)\frac{\partial^2\delta z}{\partial t^2} = g\frac{\partial\widetilde{\rho}}{\partial z}\delta z, \qquad (2.215)$$

or

$$\frac{\partial^2\delta z}{\partial t^2} = \frac{g}{\widetilde{\rho}}\frac{\partial\widetilde{\rho}}{\partial z}\delta z = -N^2\delta z, \qquad (2.216)$$
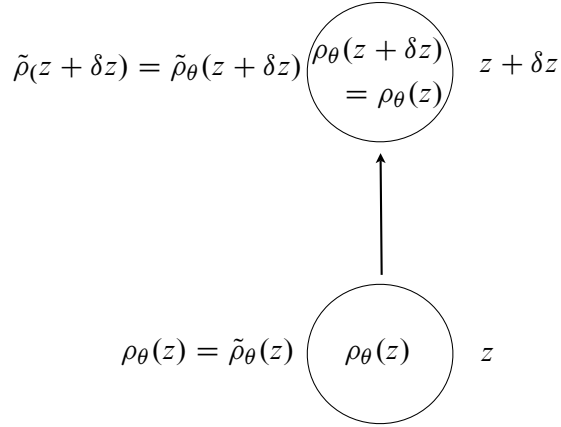
where

$$N^2 = -\frac{g}{\widetilde{\rho}}\frac{\partial\widetilde{\rho}}{\partial z} \qquad (2.217)$$

is the *buoyancy frequency*, or the *Brunt-Väisälä frequency,* for this problem. If $N^2 > 0$ then a parcel displaced upward is heavier than its surroundings, and thus experiences a restoring force; the density profile is said to be stable and N is the frequency at which the fluid parcel oscillates. If $N^2 < 0$, the density profile is unstable and the parcel continues to ascend and convection ensues. In liquids it is often a good approximation to replace $\widetilde{\rho}$ by ρ_0 in the demoninator of (2.217).

2.9.2 The general case: using potential density

More generally, in an adiabatic displacement it is *potential density, ρ_θ*, and not density itself that is materially conserved. Consider a parcel that is displaced adiabatically a vertical distance from z to $z + \delta z$; the parcel preserves its potential density, and let us

Figure 2.6 A parcel is adiabatically displaced upward from level z to $z + \delta z$. If the resulting density difference, $\delta\rho$, between the parcel and its new surroundings is positive the displacement is stable, and conversely. If $\widetilde{\rho}$ is the environmental values, and ρ_θ is potential density, we see that $\delta\rho = \widetilde{\rho}_\theta(z) - \widetilde{\rho}_\theta(z + \delta z)$

$$\widetilde{\rho}(z + \delta z) = \widetilde{\rho}_\theta(z + \delta z) \underset{= \rho_\theta(z)}{\overset{\rho_\theta(z + \delta z)}{\bigcirc}} \quad z + \delta z$$

$$\rho_\theta(z) = \widetilde{\rho}_\theta(z) \bigcirc \rho_\theta(z) \quad z$$

use the pressure at level $z + \delta z$ as the reference level. The *in situ* density of the parcel at $z + \delta z$, namely $\rho(z + \delta z)$, is then equal to its potential density $\rho_\theta(z + \delta z)$ and, because ρ_θ is conserved, this is equal to the potential density of the environment at z, $\widetilde{\rho}_\theta(z)$. The difference in *in situ* density between the parcel and the environment at $z + \delta z$, $\delta\rho$, is thus equal to the difference between the potential density of the environment at z and at $z + \delta z$. Putting this together (and see Fig. 2.6) we have

$$\delta\rho = \rho(z + \delta z) - \widetilde{\rho}(z + \delta z) = \rho_\theta(z + \delta z) - \widetilde{\rho}_\theta(z + \delta z)$$
$$= \rho_\theta(z) - \widetilde{\rho}_\theta(z + \delta z) = \widetilde{\rho}_\theta(z) - \widetilde{\rho}_\theta(z + \delta z), \tag{2.218}$$

and therefore

$$\delta\rho = -\frac{\partial \widetilde{\rho}_\theta}{\partial z}\delta z. \tag{2.219}$$

where the right-hand side is the environmental gradient of potential density. If the right-hand-side is positive, the parcel is heavier than its surroundings and the displacement is stable. Thus, the conditiona for stability are:

$$\text{Stability}: \qquad\qquad \frac{\partial \widetilde{\rho}_\theta}{\partial z} < 0 \tag{2.220a}$$

$$\text{Instability}: \qquad\qquad \frac{\partial \widetilde{\rho}_\theta}{\partial z} > 0 \tag{2.220b}$$

The equation of motion of the fluid parcel is

$$\frac{\partial^2 \delta z}{\partial t^2} = \frac{g}{\rho}\left(\frac{\partial \widetilde{\rho}_\theta}{\partial z}\right)\delta z = -N^2 \delta z \tag{2.221}$$

where, noting that $\rho(z) = \widetilde{\rho}_\theta(z)$ to within $O(\delta z)$,

$$\boxed{N^2 = -\frac{g}{\widetilde{\rho}_\theta}\left(\frac{\partial \widetilde{\rho}_\theta}{\partial z}\right)}. \tag{2.222}$$

This is a general expression for the buoyancy frequency, true in both liquids and gases. It is important to realize that the quantity $\widetilde{\rho}_\theta$ is the *locally-referenced* potential density of the environment, as will become more clear below.

An ideal gas

In the atmosphere potential density is related to potential temperature by $\rho_\theta = p_R/(\theta R)$. Using this in (2.222) gives

$$N^2 = \frac{g}{\widetilde{\theta}} \left(\frac{\partial \widetilde{\theta}}{\partial z} \right),$$

(2.223)

where $\widetilde{\theta}$ refers to the environmental profile of potential temperature. The reference value p_R does not appear, and we are free to choose this value arbitrarily — the surface pressure is a common choice. In the troposphere (the lowest several kilometers of the atmosphere) N is about $0.01\,\mathrm{s}^{-1}$, with a corresponding period, $(2\pi/N)$, of about 10 minutes. In the stratosphere (which lies above the troposphere) N^2 is a few times higher than this.

A liquid ocean

No simple, accurate, analytic expression is available for computing static stability in the ocean. If the ocean had no salt, then the potential density referenced to the surface would generally be a measure of the sign of stability of a fluid column, if not of the buoyancy frequency. However, in the presence of salinity, the surface-referenced potential density is not necessarily even a measure of the sign of stability, because the coefficients of compressibility β_T and β_S vary in different ways with pressure. To see this, suppose two neighbouring fluid elements at the surface have the same potential density, but different salinities and temperatures. Displace them both adiabatically to the deep ocean. Although their potential densities (referenced to the surface) are still equal, we can say little about their actual densities, and hence their stability relative to each other, without doing a detailed calculation because they will each have been compressed by different amounts. It is the profile of the *locally-referenced* potential density that determines the stability.

A sometimes-useful expression for stability arises by noting that in an adiabatic displacement

$$\delta\rho_\theta = \delta\rho - \frac{1}{c_s^2}\delta p = 0.$$

(2.224)

If the fluid is hydrostatic $\delta p = -\rho g \delta z$ so that if a parcel is displaced adiabatically its density changes according to

$$\left(\frac{\partial \rho}{\partial z} \right)_{\rho_\theta} = -\frac{\rho g}{c_s^2}.$$

(2.225)

If a parcel is displaced a distance δz upwards then the density difference between it and its new surroundings is

$$\delta\rho = -\left[\left(\frac{\partial \rho}{\partial z} \right)_{\rho_\theta} - \left(\frac{\partial \widetilde{\rho}}{\partial z} \right) \right]\delta z = \left[\frac{\rho g}{c_s^2} + \left(\frac{\partial \widetilde{\rho}}{\partial z} \right) \right]\delta z,$$

(2.226)

where the tilde again denotes the environmental field. It follows that the stratification is

given by

$$N^2 = -g \left[\frac{g}{c_s^2} + \frac{1}{\tilde{\rho}} \left(\frac{\partial \tilde{\rho}}{\partial z} \right) \right].$$

(2.227)

This expression holds for both liquids and gases, and for ideal gases it is precisely the same as (2.223) (problem 2.8). In liquids, a good approximation is to use a reference value ρ_0 for the undifferentiated density in the denominator, whence it becomes equal to the Boussinesq expression (2.108). Typical values of N in the upper ocean where the density is changing most rapidly (i.e., in the pycnocline — 'pycno' for density, 'cline' for changing) are about 0.01 s^{-1}, falling to 0.001 s^{-1} in the more homogeneous abyssal ocean. These correspond to periods of about 10 and 100 minutes, respectively.

* Cabbeling

Cabbeling is an instability that arises because of the nonlinear equation of state of seawater. From Fig. 1.3 we see that the contours are slightly convex, bowing upward, especially in the plot at sea level. Suppose we mix two parcels of water, each with the same density ($\sigma_\theta = 28$, say), but with different initial values of temperature and salinity. Then the resulting parcel of water will have a temperature and a salinity equal to the average of the two parcels, but its density will be *higher* than either of the two original parcels. In the appropriate circumstances such mixing may thus lead to a convective instability; this may, for example, be an important source of 'bottom water' formation in the Weddell Sea, off Antarctica.[10]

2.9.3 Lapse rates in dry and moist atmospheres

A dry ideal gas

The negative of the rate of change of the temperature in the vertical is known as the *temperature lapse rate*, or often just the lapse rate, and the rate corresponding to $\partial \theta / \partial z = 0$ is called the *dry adiabatic lapse rate*. Using $\theta = T(p_0/p)^{R/c_p}$ and $\partial p / \partial z = -\rho g$ we find that the lapse rate and the potential temperature lapse rate are related by

$$\frac{\partial \tilde{T}}{\partial z} = \frac{\tilde{T}}{\tilde{\theta}} \frac{\partial \tilde{\theta}}{\partial z} - \frac{g}{c_p},$$

(2.228)

so that the dry adiabatic lapse rate is given by

$$\Gamma_d = \frac{g}{c_p},$$

(2.229)

as in (1.138). (We use the subscript d, for dry, to differentiate it from the moist lapse rate considered below.) The conditions for static stability of the environmental profiles are thus:

$$\text{Stability} : \qquad \frac{\partial \tilde{\theta}}{\partial z} > 0; \qquad -\frac{\partial \tilde{T}}{\partial z} < \Gamma_d \equiv \frac{g}{c_p},$$

(2.230a)

$$\text{Instability}: \qquad \frac{\partial \widetilde{\theta}}{\partial z} < 0; \qquad -\frac{\partial \widetilde{T}}{\partial z} > \Gamma_d \equiv \frac{g}{c_p}. \qquad (2.230\text{b})$$

The atmosphere is in fact generally stable by this criterion: the observed lapse rate, corresponding to an observed buoyancy frequency of about $10^{-2}\,\text{s}^{-1}$, is often about $7\,\text{K\,km}^{-1}$, compared to a dry adiabatic lapse rate of about $10\,\text{K\,km}^{-1}$. Why the discrepancy? One reason, particularly important in the tropics, is that the atmosphere contains water vapour.

* Effects of water vapour on the lapse rate of an ideal gas

The amount of water vapour that can be contained in a given volume is an increasing function of temperature, with the presence or otherwise of dry air in that volume being largely irrelevant. Thus, if a parcel of water vapour is cooled, it will eventually become saturated and water vapour will condense into liquid water. A measure of the amount of water vapour in a unit volume is its partial pressure, and the partial pressure of water vapour at saturation, e_s, is given by the Clausius-Clapeyron equation,

$$\frac{\mathrm{d}e_s}{\mathrm{d}T} = \frac{L_c e_s}{R_v T^2}, \qquad (2.231)$$

where L_c is the latent heat of condensation or vapourization (per unit mass) and R_v is the gas constant for water vapour. If a parcel rises adiabatically it will cool, and at some height (known as the 'lifting condensation level', a function of its initial temperature and humidity only) the parcel will become saturated and any further ascent will cause the water vapour to condense. The ensuing condensational heating causes the parcel's temperature, and buoyancy, to increase; the parcel thus rises further, causing more water vapour to condense, and so on, and the consequence of this is that an environmental profile that is stable if it is dry may be unstable if it is saturated. Let us now derive an expression for the lapse rate of a saturated parcel that is ascending adiabatically apart from the affects of condensation.

Let w denote the mass of water vapour per unit mass of dry air, the mixing ratio, and let w_s be the saturation mixing ratio. ($w_s = \alpha e_s/(p - e_s) \approx \alpha_w e_s/p$ where $\alpha_w = 0.62$, the ratio of the mass of a water molecule to one of dry air.) The diabatic heating associated with condensation is then given by

$$Q_{\text{cond}} = -L_c \frac{\mathrm{D}w_s}{\mathrm{D}t}, \qquad (2.232)$$

so that the thermodynamic equation is

$$c_p \frac{\mathrm{D}\ln\theta}{\mathrm{D}t} = -\frac{L_c}{T}\frac{\mathrm{D}w_s}{\mathrm{D}t}, \qquad (2.233)$$

or, in terms of p and and T

$$c_p \frac{\mathrm{D}\ln T}{\mathrm{D}t} - R\frac{\mathrm{D}\ln P}{\mathrm{D}t} = -\frac{L_c}{T}\frac{\mathrm{D}w_s}{\mathrm{D}t}. \qquad (2.234)$$

If these material derivatives are due to the parcel ascent then

$$\frac{\mathrm{d}\ln T}{\mathrm{d}z} - \frac{R}{c_p}\frac{\mathrm{d}\ln p}{\mathrm{d}z} = -\frac{L_c}{Tc_p}\frac{\mathrm{d}w_s}{\mathrm{d}z}, \qquad (2.235)$$

and using the hydrostatic relationship and the fact that w_s is a function of T and p we obtain

$$\frac{\mathrm{d}T}{\mathrm{d}z} + \frac{g}{c_p} = -\frac{L_c}{c_p}\left[\left(\frac{\partial w_s}{\partial T}\right)_p \frac{\mathrm{d}T}{\mathrm{d}z} - \left(\frac{\partial w_s}{\partial p}\right)_T \rho g\right]. \qquad (2.236)$$

Solving for $\mathrm{d}T/\mathrm{d}z$, the lapse rate, Γ_s, of an ascending saturated parcel is given by

$$\Gamma_s = -\frac{\mathrm{d}T}{\mathrm{d}z} = \frac{g}{c_p}\frac{1 - \rho L_c(\partial w_s/\partial p)_T}{1 + (L_c/c_p)(\partial w_s/\partial T)_p} \approx \frac{g}{c_p}\frac{1 + L_c w_s/(RT)}{1 + L_c^2 w_s/(c_p RT^2)}. \qquad (2.237)$$

where the last near-equality follows with use of the Clausius-Clapeyron relation. This (Γ_s) is variously called the *pseudoadiabatic* or *moist adiabatic* or *saturated adiabatic* lapse rate. Because g/c_p is the dry adiabatic lapse rate Γ_d, $\Gamma_s < \Gamma_d$, and values of Γ_s are typically around $6\,\mathrm{K\,km^{-1}}$ in the lower atmosphere, and because $\mathrm{d}w_s/\mathrm{d}T$ is an increasing function of T, Γ_s decreases with increasing temperature and can be as low as $3.5\,\mathrm{K\,km^{-1}}$. For a saturated parcel, the stability conditions analogous to (2.230) are

$$\text{Stability}: \qquad -\frac{\partial\widetilde{T}}{\partial z} < \Gamma_s, \qquad (2.238a)$$

$$\text{Instability}: \qquad -\frac{\partial\widetilde{T}}{\partial z} > \Gamma_s. \qquad (2.238b)$$

where $\widetilde{T}$ is the environmental temperature. The observed environmental profile in convecting situations is often a combination of the dry adiabatic and moist adiabatic profiles: an unsaturated parcel that is is unstable by the dry criterion will rise and cool following a dry adiabat, Γ_d, until it becomes saturated at the 'lifting condensation level', above which it will rise following a saturation adiabat, Γ_s. Such convection will proceed until the atmospheric column is stable and, especially in low latitudes, the lapse rate of the atmosphere is largely determined by such convective processes.

* Equivalent potential temperature

Suppose that all the moisture in a parcel of air condenses, and that all the heat released goes into heating the parcel. The *equivalent potential temperature*, θ_{eq} is the potential temperature that the parcel then achieves. We may obtain an approximate analytic expression for it by noting that the first law of thermodynamics, $\mathrm{d}Q = T\,\mathrm{d}\eta$, then implies, by definition of potential temperature,

$$-L_c\mathrm{d}w = c_p T\,\mathrm{d}\ln\theta \qquad (2.239)$$

where $\mathrm{d}w$ is the change in water vapour mixing ratio, so that a reduction of w via condensation leads to heating. Integrating gives, by definition of equivalent potential temperature,

$$-\int_w^0 \frac{L_c w}{c_p T}\,\mathrm{d}w = \int_\theta^{\theta_{\mathrm{eq}}}\mathrm{d}\ln\theta, \qquad (2.240)$$

and so, if T and L_c are assumed constant,

$$\theta_{\text{eq}} = \theta \exp\left(\frac{L_c w}{c_p T}\right).$$ (2.241)

The equivalent potential temperature so defined is approximately conserved during condensation, the approximation arising going from (2.240) to (2.241). It is a useful expression for diagnostic purposes, and in constructing theories of convection, but it is not accurate enough to use as a prognostic variable in a putatively realistic numerical model. The 'equivalent temperature' may be defined in terms of the equivalent potential temperature by

$$T_{\text{eq}} = \theta_{\text{eq}}\left(\frac{p}{p_{\text{R}}}\right)^{\kappa}.$$ (2.242)

2.10 GRAVITY WAVES

The parcel approach to oscillations and stability, while simple and direct, is divorced from the fluid-dynamical equations of motion, making it hard to include other effects such as rotation, or to explore the effects of possible differences between the hydrostatic and non-hydrostatic cases. To remedy this, we now use the equations of motion to analyze the motion resulting from a small disturbance.

2.10.1 Gravity waves and convection in a Boussinesq fluid

Let us consider a Boussineq fluid, at rest, in which the buoyancy varies linearly with height and the bouyancy frequency, N, is a constant. Linearizing the equations of motion about this basic state we obtain

$$\frac{\partial u'}{\partial t} = -\frac{\partial \phi'}{\partial x},$$ (2.243a)

$$\frac{\partial w'}{\partial t} = -\frac{\partial \phi'}{\partial z} + b',$$ (2.243b)

$$\frac{\partial u'}{\partial x} + \frac{\partial w'}{\partial z} = 0,$$ (2.243c)

$$\frac{\partial b'}{\partial t} + w'N^2 = 0,$$ (2.243d)

where for simplicity we assume that the flow is a function only of x and z. A little algebra gives a single equation for w',

$$\left[\left(\frac{\partial^2}{\partial x^2} + \frac{\partial^2}{\partial z^2}\right)\frac{\partial^2}{\partial t^2} + N^2\frac{\partial^2}{\partial x^2}\right]w' = 0.$$ (2.244)

Seeking solutions of the form $w' = \text{Re}\,W\exp[i(kx + mz - \omega t)]$ (where Re denotes the real part) yields the important dispersion relationship for gravity waves:

$$\boxed{\omega^2 = \frac{k^2 N^2}{k^2 + m^2}}.$$ (2.245)

Figure 2.7 Scaled frequency, ω/N, plotted as a function of scaled horizontal wavenumber, k/m, using the full dispersion relation of (2.245) (solid line, asymptoting to unit value for large k/m) and with the hydrostatic dispersion relation (2.249) (dashed line, tending to ∞ for large k/m).
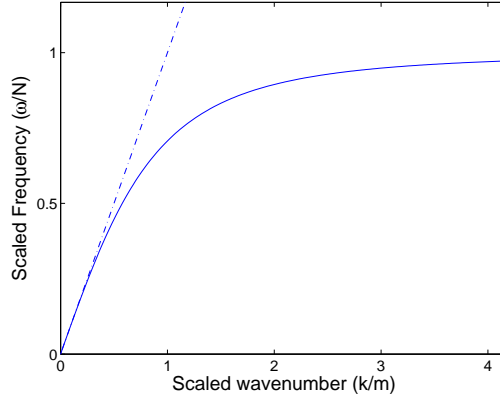
The frequency (see Fig. 2.7) is thus always less than N, approaching N for small horizontal scales, $k \gg m$. If we explicitly neglect pressure perturbations, as in the parcel argument, then the two equations,

$$\frac{\partial w'}{\partial t} = b', \qquad \frac{\partial b'}{\partial t} + w'N^2 = 0, \tag{2.246}$$

form a closed set, and give $\omega^2 = N^2$.

If the basic state density increases with height then $N^2 < 0$ and we expect this state to be unstable. Indeed, (2.245) then gives

$$\sigma = \frac{\pm k\widetilde{N}}{(k^2 + m^2)^{1/2}}, \tag{2.247}$$

where $\widetilde{N}^2 = -N^2$, and the disturbance grows exponentially according to $\exp(\sigma t)$. Most convective activity in the ocean and atmosphere is, ultimately, related to an instability of this form, although of course there are many complicating issues — water vapour in the atmosphere, salt in the ocean, the effects of rotation and so forth.

Hydrostatic gravity waves and convection

Let us now suppose that the fluid satisfies the hydrostatic Boussinesq equations. The linearized two-dimensional equations of motion become

$$\frac{\partial u'}{\partial t} = -\frac{\partial \phi'}{\partial x}, \qquad 0 = -\frac{\partial \phi'}{\partial z} + b', \tag{2.248a}$$

$$\frac{\partial u'}{\partial x} + \frac{\partial w'}{\partial z} = 0, \tag{2.248b}$$

$$\frac{\partial b'}{\partial t} + w'N^2 = 0, \tag{2.248c}$$

being the horizontal and vertical momentum equations, mass continuity, and the thermodynamic equation respectively. Then a little algebra gives the dispersion relation,

$$\omega^2 = \frac{k^2 N^2}{m^2}. \tag{2.249}$$

The frequency and, if N^2 is negative the growth rate, is unbounded for as $k/m \rightarrow \infty$, and the hydrostatic approximation thus has quite unphysical behaviour for small horizontal scales (see also problem 2.10).[11]

2.11 * ACOUSTIC-GRAVITY WAVES IN AN IDEAL GAS

We now consider wave motion in a stratified, compressible fluid such as the earth's atmosphere. The complete problem is complicated and uninformative; we will specialize to the case of an isothermal, stationary atmosphere and ignore the effects of rotation and sphericity, but otherwise we will make few approximations. In this section we will denote the unperturbed state with a subscript 0 and the perturbed state with a prime ($'$). Because it is at rest, the basic state is in hydrostatic balance,

$$\frac{\partial p_0}{\partial z} = -\rho_0(z)g \tag{2.250}$$

Ignoring variations in the y-direction for algebraic simplicity, the linearized equations of motion are:

u-momentum: $$\rho_0 \frac{\partial u'}{\partial t} = -\frac{\partial p'}{\partial x} \tag{2.251a}$$

w-momentum: $$\rho_0 \frac{\partial w'}{\partial t} = -\frac{\partial p'}{\partial z} - \rho' g \tag{2.251b}$$

mass conservation: $$\frac{\partial \rho'}{\partial t} + w' \frac{\partial \rho_0}{\partial z} = -\rho_0 \left(\frac{\partial u'}{\partial x} + \frac{\partial w'}{\partial z} \right) \tag{2.251c}$$

thermodynamic: $$\frac{\partial \theta'}{\partial t} + w' \frac{\partial \theta_0}{\partial z} = 0 \tag{2.251d}$$

equation of state: $$\frac{\theta'}{\theta_0} + \frac{\rho'}{\rho_0} = \frac{1}{\gamma} \frac{p'}{p_0}. \tag{2.251e}$$

For an isothermal basic state we have $p_0 = \rho_0 R T_0$ where T_0 is a constant, so that $\rho_0 = \rho_s e^{-z/H}$ and $p_0 = p_s e^{-z/H}$ where $H = RT_0/g$. Further, using $\theta = T(p_s/p)^\kappa$ where $\kappa = R/c_p$, we have that $\theta_0 = T_0 e^{\kappa z/H}$ and so $N^2 = \kappa g/H$. Using these then, after a little algebra, the set of equations (2.251) becomes

$$\left(\frac{\partial^2}{\partial t^2} - c^2 \frac{\partial^2}{\partial x^2} \right) u' = c^2 \left(\frac{\partial}{\partial z} - \frac{1}{\gamma H} \right) \frac{\partial}{\partial z} w' \tag{2.252a}$$

and

$$\left(\frac{\partial^2}{\partial t^2} - c^2 \left[\frac{\partial^2}{\partial x^2} - \frac{1}{H} \frac{\partial}{\partial z} \right] \right) w' = c^2 \left(\frac{\partial}{\partial z} - \frac{\kappa}{H} \right) \frac{\partial u'}{\partial x}, \tag{2.252b}$$

where $c^2 = \partial(/\partial p/\rho)_\eta = \gamma R T_0$ is the square of the speed of sound. These two equations in turn combine to give

$$\frac{\partial^4 w'}{\partial t^4} - c^2 \frac{\partial^2}{\partial t^2} \left(\frac{\partial^2}{\partial x^2} + \frac{\partial^2}{\partial z^2} - \frac{1}{H} \frac{\partial}{\partial z} \right) w' - c^2 \frac{\kappa g}{H} \frac{\partial^2 w'}{\partial x^2} = 0. \tag{2.253}$$

If we set $w' = W(x, z, t)e^{z/(2H)}$ (so that $W = (\rho_0/\rho_s)^{1/2}w$) then the term with the single z-derivative is eliminated, giving

$$\frac{\partial^4 W}{\partial t^4} - c^2 \frac{\partial^2}{\partial t^2}\left(\frac{\partial^2}{\partial x^2} + \frac{\partial^2}{\partial z^2} - \frac{1}{4H^2}\right)W - c^2\frac{\kappa g}{H}\frac{\partial^2 w'}{\partial x^2} = 0. \qquad (2.254)$$

Although superficially complicated, this equation has constant coefficients and we may seek wavelike solutions of the form

$$W = \mathrm{Re}\, \widetilde{W} e^{i(kx+mz-\omega t)}, \qquad (2.255)$$

where $\widetilde{W}$ is the complex amplitude, and this leads to the dispersion relation for acoustic-gravity waves, namely

$$\omega^4 - c^2\omega^2\left(k^2 + m^2 + \frac{1}{4H^2}\right) + c^2 N^2 k^2 = 0, \qquad (2.256)$$

with solution

$$\boxed{\omega^2 = \frac{1}{2}c^2 K^2\left[1 \pm \left(1 - \frac{4N^2 k^2}{c^2 K^4}\right)^{1/2}\right],} \qquad (2.257)$$

where $K^2 = k^2 + m^2 + 1/(4H^2)$. (The factor $[1 - 4N^2 k^2/(c^2 K^4)]$ is always positive — see problem 2.23.) For an isothermal, ideal-gas, atmosphere $4N^2 H^2/c^2 \approx 0.8$ and so this may be written

$$\frac{\omega^2}{N^2} \approx 2.5\widehat{K}^2\left[1 \pm \left(1 - \frac{0.8\widehat{k}^2}{\widehat{K}^4}\right)^{1/2}\right], \qquad (2.258)$$

where $\widehat{K}^2 = \widehat{k}^2 + \widehat{m}^2 + 1/4$, and $(\widehat{k}, \widehat{m}) = (kH, mH)$.

2.11.1 Interpretation

Acoustic and gravity waves

There are two branches of roots in (2.257), corresponding to acoustic waves (using the plus sign in the dispersion relation) and internal gravity waves (using the minus sign). These (and the Lamb wave, described below) are plotted in Fig. 2.8. If $4N^2 k^2/c^2 K^4 \ll 1$ then the two sets of waves are well separated. From (2.257) this is satisfied when

$$\frac{4\kappa}{\gamma}(kH)^2 \approx 0.8(kH)^2 \ll \left[(kH)^2 + (mH)^2 + \tfrac{1}{4}\right]^2; \qquad (2.259)$$

that is, when *either* $mH \gg 1$ or $kH \gg 1$. The two roots of the dispersion relation are then

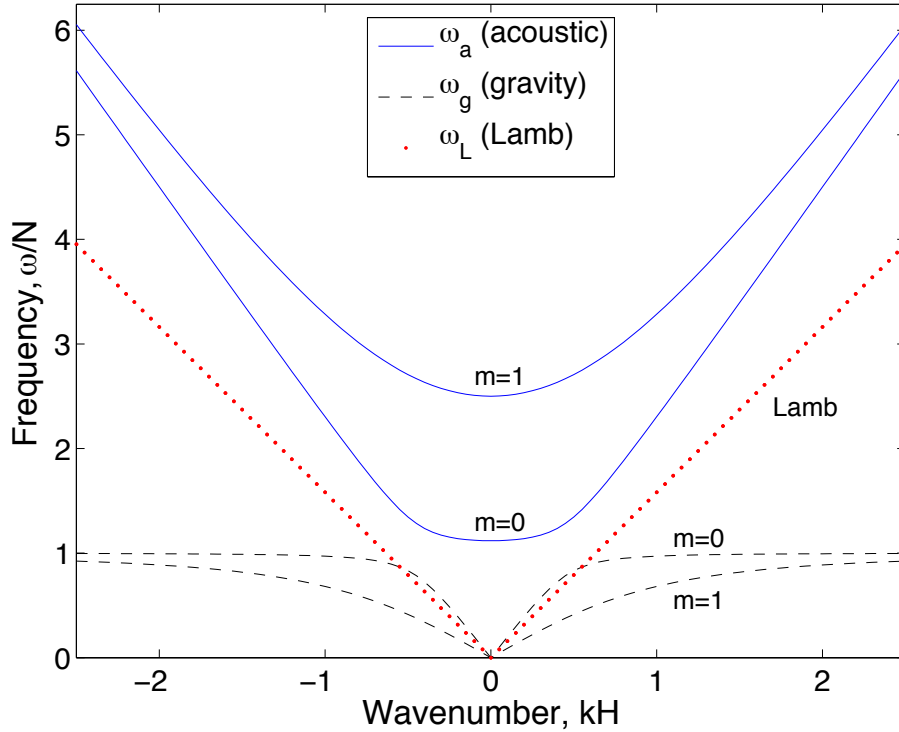$$\omega_a^2 \approx c^2 K^2 = c^2\left(k^2 + m^2 + \frac{1}{4H^2}\right) \qquad (2.260)$$

Fig. 2.8 Dispersion diagram for acoustic gravity waves in an isothermal atmosphere, calculated using (2.258). The frequency is given in units of the the buoyancy frequency N, and the wavenumbers are non-dimensionalized by the inverse of the scale height, H. The solid curves indicate acoustic waves, whose frequency is always higher than that of the corresponding Lamb wave at the same wavenumber (i.e. ck), and of the base acoustic frequency $\approx 1.12N$. The dashed curves indicate internal gravity waves, whose frequency asymptotes to N at small horizontal scales.

and

$$\omega_g^2 \approx \frac{N^2 k^2}{k^2 + m^2 + 1/(4H^2)}. \tag{2.261}$$

corresponding to acoustic and gravity waves, respectively. The acoustic waves owe their existence to the presence of compressibility in the fluid, and they have no counterpart in the Boussinesq system. On the other hand, the internal gravity waves are just modified forms of those found in the Boussinesq system, and if we take the limit $(kH, mH) \to \infty$ then the gravity wave branch reduces to $\omega_g^2 = N^2 k^2/(k^2 + m^2)$, which is the dispersion relationship for gravity waves in the Boussinesq approximation. We may consider this to be the limit of infinite scale height or (equivalently) the case in which wavelengths of the internal waves are sufficiently small that the fluid is essentially incompressible.

Vertical structure

Recall that $w' = W(x, z, t)e^{z/(2H)}$ and, by inspection of (2.252), u' has the same vertical structure. That is,

$$w' \propto e^{z/(2H)}, \qquad u' \propto e^{z/(2H)}, \qquad (2.262)$$

the amplitude of the velocity field internal waves increasing with height. The pressure and density perturbation amplitudes fall off with height, varying like

$$p' \propto e^{-z/(2H)}, \qquad \rho' \propto e^{-z/(2H)}. \qquad (2.263)$$

The kinetic energy of the perturbation, $\rho_0(u'^2 + w'^2)$ is *constant* with height, because $\rho_0 = \rho_s e^{-z/H}$.

Hydrostatic approximation and Lamb waves

Equations (2.252) also admit to a solution with $w' = 0$. We then have

$$\left(\frac{\partial^2}{\partial t^2} - c^2 \frac{\partial^2}{\partial x^2} \right) u' = 0 \qquad \text{and} \qquad \left(\frac{\partial}{\partial z} - \frac{\kappa}{H} \right) \frac{\partial u'}{\partial x} = 0 \qquad (2.264)$$

and these have solutions of the form

$$u' = \text{Re}\, \tilde{U} e^{\kappa z/H} e^{i(kx - \omega t)}, \qquad \omega = ck, \qquad (2.265)$$

where $\tilde{U}$ is a constant, complex, amplitude. These are horizontally propagating sound waves, known as *Lamb waves* after the hydrodynamicist Horace Lamb. Their velocity perturbation amplitude increases with height, but the pressure perturbation falls with height; that is

$$u' \propto e^{\kappa z/H} \approx e^{2z/(7H)}, \qquad p' \propto e^{(\kappa-1)z/H} \approx e^{-5z/(7H)}. \qquad (2.266)$$

Their kinetic energy density $\rho_0 u'^2$ varies as

$$K.E. \propto e^{-z/H + 2\kappa z/H} = e^{(2R - c_p)z/(c_p H)]} = e^{(R - c_v)z/(c_p H)} \approx e^{-3z/(7H)} \qquad (2.267)$$

for an ideal gas. (In a simple ideal gas, $c_v = nR/2$ where n is the number of excited degrees of freedom, 5 for a diatomic molecule.) In this sense Lamb waves are trapped at the surface and are an example of edge waves or surface waves.

   Consider now the slightly more general case, in which we make the hydrostatic approximation *ab initio,* but do not restrict the perturbation to have $w' = 0$. The linearized equations are identical to (2.251), except that (2.251b) is replaced by

$$\frac{\partial p'}{\partial z} = -\rho' g \qquad (2.268)$$

It is left as a problem for the reader to show that the dispersion relation is now

$$\omega^2 = \frac{N^2 k^2}{m^2 + 1/(4H^2)}. \qquad (2.269)$$

This may be compared with the corresponding Boussinesq result (2.249). Again, the frequency increases without bound as the horizontal wavelength diminishes.
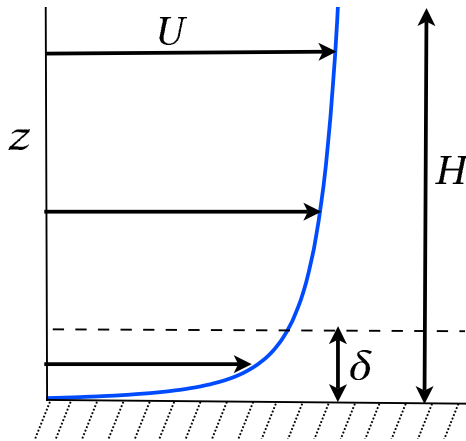
Figure 2.9 A schematic of a boundary layer. The values of a field, such as velocity, U, may vary rapidly in a boundary in order to satisfy the boundary conditions at a rigid surface. The parameter δ is a measure of the boundary layer thickness, and H is a typical scale of variation away from the boundary.

2.12 THE EKMAN LAYER

In the final topic of this chapter, we return to geostrophic flow and consider the effects of friction. The fluid fields in the interior of a domain are often set by different physical processes than those occuring at a boundary, and consequently often change rapidly in a thin *boundary layer,* as in Fig. 2.9. Such boundary layers nearly always involve one or both of viscosity and diffusion, because these appear in the terms of highest differential order in the equations of motion, and so are responsible for the number and type of boundary conditions that the equations must satisfy — for example, the presence of molecular viscosity leads to the condition that the tangential flow (as well as the normal flow) must vanish at a rigid surface.

In many boundary layers in non-rotating flow the dominant balance in the momentum equation is between the advective and viscous terms. In some contrast, in large-scale atmospheric and oceanic flow the effects of rotation are large, and this results in a boundary layer, known as the *Ekman layer,* in which the dominant balance is between Coriolis and frictional terms.[12] Now, the direct effects of molecular viscosity and diffusion are nearly always negligible at distances more than a few millimeters away from a solid boundary, but it is inconceivable that the entire boundary layer between the free atmosphere (or ocean) and the surface is only a few millimeters thick. Rather, in practice a balance occurs between the Coriolis terms and the stress due to small-scale turbulent motion, and this gives rise to a boundary layer that has a typical depth of tens to hundreds of meters. Because the stress arises from the turbulence we cannot with confidence determine its precise form; thus, we should try to determine what general properties Ekman layers may have that are *independent* of the precise form of the friction.

The atmospheric Ekman layer occurs near the ground, and the stress at the ground itself is due to the surface wind (and its vertical variation). In the ocean the main Ekman layer is near the surface, and the stress at ocean surface is largely due to the presence of the overlying wind. There is also a weak Ekman layer at the bottom of the ocean, analogous to the atmospheric Ekman layer. To analyze all these layers, let us assume that:

⋆ The Ekman layer is Boussinesq. This is a very good assumption for the ocean, and a reasonable one for the atmosphere if the boundary layer is not too deep.

⋆ The Ekman layer has a finite depth that is less than the total depth of the fluid, this depth being given by the level at which the frictional stresses essentially vanish. Within the Ekman layer, frictional terms are important, whereas geostrophic balance holds beyond it.

⋆ The nonlinear and time dependent terms in the equations of motion are negligible, hydrostatic balance holds in the vertical, and buoyancy is constant, not varying in the horizontal.

⋆ As needed, we shall assume that friction can be parameterized by a viscous term of the form $\rho_0^{-1} \partial \boldsymbol{\tau} / \partial z = A \partial^2 \boldsymbol{u} / \partial z^2$, where A is constant and $\boldsymbol{\tau}$ is the stress. In laboratory settings A may be the molecular viscosity, whereas in the atmosphere and ocean it is a so-called *eddy viscosity*. (In turbulent flows momentum is transferred by the near-random motion of small parcels of fluid and, by analogy with the motion of molecules that produces a molecular viscosity, the associated stress is approximately represented, or parameterized, using a turbulent or eddy viscosity that may be orders of magnitude larger than the molecular one.) In all cases it is the vertical derivative of the stress that dominates.

2.12.1 Equations of motion and scaling

Frictional-geostrophic balance in the horizontal momentum equation is:

$$\boldsymbol{f} \times \boldsymbol{u} = -\nabla_z \phi + \frac{\partial \widetilde{\boldsymbol{\tau}}}{\partial z}. \tag{2.270}$$

where $\widetilde{\boldsymbol{\tau}} \equiv \boldsymbol{\tau} / \rho_0$ is the kinematic stress (and $\boldsymbol{\tau}$ is the stress itself), and f is allowed to vary with latitude. If we model the stress with an eddy viscosity (2.270) becomes

$$\boldsymbol{f} \times \boldsymbol{u} = -\nabla_z \phi + A \frac{\partial^2 \boldsymbol{u}}{\partial z^2}. \tag{2.271}$$

The vertical momentum equation is hydrostatic balance, $\partial \phi / \partial z = b$, and, because buoyancy is constant, we may without loss of generality write this as

$$\frac{\partial \phi}{\partial z} = 0. \tag{2.272}$$

The equation set is completed by the mass continuity equation $\nabla \cdot \boldsymbol{v} = 0$.

The Ekman number

We non-dimensionalize the equations by setting

$$(u, v) = U(\widehat{u}, \widehat{v}), \quad (x, y) = L(\widehat{x}, \widehat{y}), \quad f = f_0 \widehat{f}, \quad z = H\widehat{z}, \quad \phi = \Phi \widehat{\phi}, \tag{2.273}$$

where hatted variables are non-dimensional. H is a scaling for the height, and at this stage we will suppose it to be some height scale in the free atmosphere or ocean, not

the height of the Ekman layer itself. Geostrophic balance suggests that $\Phi = f_0 U L$. Substituting (2.273) into (2.271) we obtain

$$\widehat{\boldsymbol{f}} \times \widehat{\boldsymbol{u}} = -\widehat{\nabla}\widehat{\phi} + Ek\frac{\partial^2 \widehat{\boldsymbol{u}}}{\partial \widehat{z}^2}, \tag{2.274}$$

where the parameter

$$\boxed{Ek \equiv \left(\frac{A}{f_0 H^2}\right)}, \tag{2.275}$$

is the *Ekman number*, and it determines the importance of frictional terms in the horizontal momentum equation. If $Ek \ll 1$ then the friction is small in the flow interior where $\widehat{z} = \mathcal{O}(1)$. However, the friction term cannot necessarily be neglected in the boundary layer because it is of the highest differential order in the equation, and so determines the boundary conditions; if Ek is small the vertical scales become small and the second term on the right-hand side of (2.274) remains finite. The case when this term is simply omitted from the equation is therefore a *singular limit,* meaning that it differs from the case with $Ek \rightarrow 0$. If $Ek \geq 1$ friction is important everywhere, but it is usually the case that Ek is small for atmospheric and oceanic large-scale flow, and the interior flow is very nearly geostrophic. (In part this is because A itself is only large near a rigid surface where the presence of a shear creates turbulence and a significant eddy viscosity.)

Momentum balance in the Ekman layer

For definiteness, suppose the fluid lies above a rigid surface at $z = 0$. Sufficiently far away from the boundary the velocity field is known, and we suppose this flow to be in geostrophic balance. We then write the velocity field and the pressure field as the sum of the interior geostrophic part, plus a boundary layer correction:

$$\widehat{\boldsymbol{u}} = \widehat{\boldsymbol{u}}_g + \widehat{\boldsymbol{u}}_E, \qquad \widehat{\phi} = \widehat{\phi}_g + \widehat{\phi}_E, \tag{2.276}$$

where the Ekman layer corrections, denoted with a subscript E, are negligible away from the boundary layer. Now, in the fluid interior we have, by hydrostatic balance, $\partial\widehat{\phi}_g/\partial\widehat{z} = 0$. In the boundary layer we have still $\partial\widehat{\phi}_g/\partial\widehat{z} = 0$ so that, to satisfy hydrostasy, $\partial\widehat{\phi}_E/\partial\widehat{z} = 0$. But because $\widehat{\phi}_E$ vanishes away from the boundary we have $\widehat{\phi}_E = 0$ everywhere. This is an important result: *there is no boundary layer in the pressure field.* Note that this is a much stronger result than saying that pressure is continuous, which is nearly always true in fluids; rather, it is a special result about Ekman layers. (See also problem 2.25.)

Using (2.276) with $\widehat{\phi}_E = 0$, the dimensional horizontal momentum equation (2.270) becomes, in the Ekman layer,

$$\boldsymbol{f} \times \boldsymbol{u}_E = \frac{\partial \widetilde{\boldsymbol{\tau}}}{\partial z}. \tag{2.277}$$

The dominant force balance in the Ekman layer is thus between the Coriolis force and

the friction. We can determine the thickness of the Ekman layer if we model the stress with an eddy viscosity so that

$$\boldsymbol{f} \times \boldsymbol{u}_E = A \frac{\partial^2 \boldsymbol{u}_E}{\partial z^2} \tag{2.278}$$

or, non-dimensionally,

$$\widehat{\boldsymbol{f}} \times \widehat{\boldsymbol{u}}_E = Ek \frac{\partial^2 \widehat{\boldsymbol{u}}_E}{\partial \widehat{z}^2} \tag{2.279}$$

It is evident this equation can only be satisfied if $\widehat{z} \neq \mathcal{O}(1)$, implying that H is not a proper scaling for z in the boundary layer. Rather, if the vertical scale in the Ekman layer is $\widehat{\delta}$ (meaning $\widehat{z} \sim \widehat{\delta}$) we must have $\widehat{\delta} \sim Ek^{1/2}$. In dimensional terms this means the thickness of the Ekman layer is

$$\delta = H\widehat{\delta} = H Ek^{1/2} \tag{2.280}$$

or

$$\boxed{\delta = \left(\frac{A}{f_0} \right)^{1/2}}. \tag{2.281}$$

[This estimate also emerges directly from (2.278).] Note that (2.280) can be written as

$$Ek = \left(\frac{\delta}{H} \right)^2. \tag{2.282}$$

That is, the Ekman number is equal to the square of the ratio of the depth of the Ekman layer to an interior depth scale of the fluid motion. In laboratory flows where A is the molecular viscosity we can thus estimate the Ekman layer thickness, and if we know the eddy viscosity of the ocean or atmosphere we can estimate the thickness of their respective Ekman layers. We can invert this argument and obtain an estimate of A if we know the Ekman layer depth. In the atmosphere, deviations from geostrophic balance are very small in the atmosphere above 1 km, and using this gives $A \approx 10^2 \, \mathrm{m^2 \, s^{-1}}$. In the ocean Ekman depths are about 50 m or less, and eddy viscosities about $0.1 \, \mathrm{m^2 \, s^{-1}}$.

2.12.2 Integral properties of the Ekman layer

What can we deduce about the Ekman layer without specifying the detailed form of the frictional term? Reverting to dimensional notation, we recall frictional-geostrophic balance,

$$\boldsymbol{f} \times \boldsymbol{u} = -\nabla \phi + \frac{\partial \widetilde{\boldsymbol{\tau}}}{\partial z} \tag{2.283}$$

where $\widetilde{\boldsymbol{\tau}}$ is zero at the edge of the Ekman layer. In the Ekman layer itself we have

$$\boldsymbol{f} \times \boldsymbol{u}_E = \frac{\partial \widetilde{\boldsymbol{\tau}}}{\partial z}. \tag{2.284}$$

Consider either a top or bottom Ekman layer, and integrate over its thickness. From (2.284) we obtain

$$\boldsymbol{f} \times \boldsymbol{M}_E = \widetilde{\boldsymbol{\tau}}_t - \widetilde{\boldsymbol{\tau}}_b \tag{2.285}$$

where

$$\boldsymbol{M}_E = \int_{\mathrm{Ek}} \boldsymbol{u}_E \, \mathrm{d}z \tag{2.286}$$

is the ageostrophic transport in the Ekman layer, and where $\widetilde{\boldsymbol{\tau}}_t$ and $\widetilde{\boldsymbol{\tau}}_b$ is the stress at the top and the bottom of the layer. The former (latter) will be zero in a bottom (top) Ekman layer. We can rewrite (2.285) as:

Top Ekman Layer:
$$\boxed{\boldsymbol{M}_E = -\frac{1}{f}\mathbf{k} \times \widetilde{\boldsymbol{\tau}}_t} \tag{2.287}$$

Bottom Ekman Layer:
$$\boxed{\boldsymbol{M}_E = \frac{1}{f}\mathbf{k} \times \widetilde{\boldsymbol{\tau}}_b} \tag{2.288}$$

The transport in the Ekman layer is thus at right-angles to the stress at the surface. This has a simple physical explanation: integrated over the depth of the Ekman layer the surface stress must be balanced by the Coriolis force, which in turn acts at right angles to the mass transport. This result is particularly useful in the ocean, where the stress at the upper surface is primarily due to the wind, and can be regarded as *independent* of the interior flow. If f is positive, as in the Northern hemisphere, then an Ekman transport is induced 90° to the right of the direction of the wind stress. This has innumerable important consequences — for example, in inducing coastal upwelling when, as is not uncommon, the wind blows parallel to the coast. Upwelling off the coast of California is one example. In the atmosphere, however, the stress arises as a consequence of the interior flow, and we need to parameterize the stress in terms of the flow in order to calculate the surface stress.

Finally, we obtain an expression for the vertical velocity induced by an Ekman layer. The mass conservation equation is

$$\frac{\partial u}{\partial x} + \frac{\partial v}{\partial y} + \frac{\partial w}{\partial z} = 0. \tag{2.289}$$

Integrating this over an Ekman layer gives

$$\nabla \cdot \boldsymbol{M}_t = -(w_t - w_b) \tag{2.290}$$

where $\boldsymbol{M}_t$ is the total (Ekman plus geostrophic) transport in the Ekman layer,

$$\boldsymbol{M}_t = \int_{\mathrm{Ek}} \boldsymbol{u} \, \mathrm{d}z = \int_{\mathrm{Ek}} (\boldsymbol{u}_g + \boldsymbol{u}_E) \, \mathrm{d}z \equiv \boldsymbol{M}_g + \boldsymbol{M}_E, \tag{2.291}$$

and w_t and w_b are the vertical velocities at the top and bottom of the Ekman layer; the former (latter) is zero in a top (bottom) Ekman layer. From (2.285)

$$\mathbf{k} \times (\boldsymbol{M}_t - \boldsymbol{M}_g) = \frac{1}{f}(\widetilde{\boldsymbol{\tau}}_t - \widetilde{\boldsymbol{\tau}}_b). \tag{2.292}$$

Taking the curl of this (i.e., cross-differentiating) gives

$$\nabla \cdot (\boldsymbol{M}_t - \boldsymbol{M}_g) = \operatorname{curl}_z[(\widetilde{\boldsymbol{\tau}}_t - \widetilde{\boldsymbol{\tau}}_b)/f] \tag{2.293}$$

where the curl_z operator on a vector $\boldsymbol{A}$ is defined by $\operatorname{curl}_z \boldsymbol{A} \equiv \partial_x A_y - \partial_y A_x$. Using (2.290) we obtain, for bottom and top Ekman layers respectively,

$$\boxed{w_b = \operatorname{curl}_z \frac{\widetilde{\boldsymbol{\tau}}_t}{f} + \nabla \cdot \boldsymbol{M}_g, \qquad w_t = \operatorname{curl}_z \frac{\widetilde{\boldsymbol{\tau}}_b}{f} - \nabla \cdot \boldsymbol{M}_g}, \tag{2.294a,b}$$

where $\nabla \cdot \boldsymbol{M}_g = -\beta \boldsymbol{M}_g / f$ is the divergence of the geostrophic transport in the Ekman layer, which is often small compared to the other terms in these equations. Thus, friction induces a vertical velocity at the edge of the Ekman layer, proportional to the curl of the stress at the surface, and this is perhaps the most used result in Ekman layer theory. Numerical models sometimes do not have the vertical resolution to explicitly resolve an Ekman layer, and (2.294) provides a means of *parameterizing* the Ekman layer in terms of resolved or known fields. It is particularly useful for the top Ekman layer in the ocean, where the stress can be regarded as a given function of the overlying wind.

2.12.3 Explicit solutions. I: A bottom boundary layer

We now assume that the frictional terms can be parameterized as an eddy viscosity and calculate the explicit form of the solution in the boundary layer. The frictional-geostrophic balance may be written as

$$\boldsymbol{f} \times (\boldsymbol{u} - \boldsymbol{u}_g) = A \frac{\partial^2 \boldsymbol{u}}{\partial z^2} \tag{2.295a}$$

where

$$f(u_g, v_g) = \left(-\frac{\partial \phi}{\partial y}, \frac{\partial \phi}{\partial x} \right). \tag{2.295b}$$

We continue to assume there are no horizontal gradients of temperature, so that, via thermal wind, $\partial u_g / \partial z = \partial v_g / \partial z = 0$.

Boundary conditions and solution

Appropriate boundary conditions for a bottom Ekman layer are:

At $z = 0$: $u = 0, \quad v = 0$ (the no slip condition)   (2.296a)

As $z \to \infty$: $u = u_g, \quad v = v_g$ (a geostrophic interior).   (2.296b)

Let us seek solutions to (2.295a) of the form

$$u = u_g + A_0 e^{\alpha z}, \qquad v = v_g + B_0 e^{\alpha z} \tag{2.297}$$

where A_0 and B_0 are constants. Substituting into (2.295a) gives two homogeneous algebraic equations

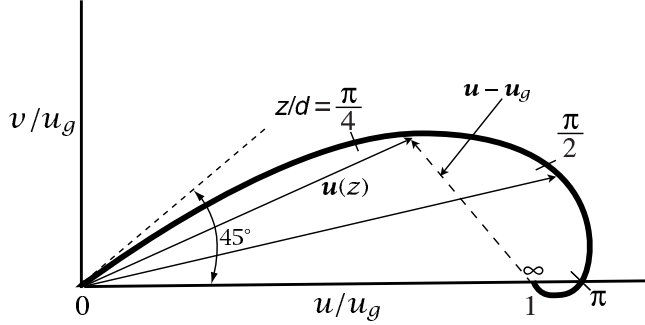$$A_0 f - B_0 A \alpha^2 = 0 \tag{2.298a}$$

Figure 2.10 The idealised Ekman layer solution in the lower atmosphere, plotted as a hodograph of the wind components: the arrows show the velocity vectors at a particular heights, and the curve traces out the continuous variation of the velocity. The values on the curve are of the nondimensional variable z/d, where $d = (2A/f)^{1/2}$, and v_g is chosen to be zero.

$$-A_0 A \alpha^2 - B_0 f = 0 \tag{2.298b}$$

and thus the solvability condition $\alpha^4 = -f^2/A^2$, from which we find $\alpha = \pm(1 \pm i)\sqrt{f/2A}$. Using the boundary conditions we then obtain the solution

$$u = u_g - e^{-z/d}\left[u_g \cos(z/d) + v_g \sin(z/d)\right] \tag{2.299a}$$

$$v = v_g + e^{-z/d}\left[u_g \sin(z/d) - v_g \cos(z/d)\right] \tag{2.299b}$$

where $d = \sqrt{2A/f}$; this is, within a constant factor, the depth of the Ekman layer obtained from scaling considerations. The solution decays exponentially from the surface with this e-folding scale, so that d is a good measure of the Ekman layer thickness. Note that the boundary layer correction depends on the interior flow, since the boundary layer serves to bring the flow to zero at the surface.

To illustrate the solution, suppose that the pressure force is directed in the y-direction (northward), so that the geostrophic current is eastward. Then the solution, the now-famous *Ekman spiral*, is plotted in Fig. 2.10 and Fig. 2.11). The wind falls to zero at the surface, and its direction just above the surface is northeastward; that is, it is rotated by 45° to the left of its direction in the free atmosphere. Although this result is independent of the value of the frictional coefficients, it is dependent on the form of the friction chosen. The force balance in the Ekman layer is between the Coriolis force, the stress, and the pressure force. At the surface the Coriolis force is zero, and the balance is entirely between the northward pressure force and the southwards stress force.

Mass transport, force balance and vertical velocity

The cross-isobaric flow is given by (for $v_g = 0$)

$$V = \int_0^\infty v\,\mathrm{d}z = \int_0^\infty u_g e^{-z/d} \sin(z/d)\,\mathrm{d}z = \frac{u_g d}{2} \tag{2.300}$$

Figure 2.11
Solutions for a bottom Ekman layer with a given flow in the fluid interior (left), and for a top Ekman layer with a given surface stress (right), both with $d = 1$. On the left we have $u_g = 1$, $v_g = 0$. On the right we have $u_g = v_g = 0$, $\widetilde{\tau}_y = 0$ and $\sqrt{2}\widetilde{\tau}_x/(fd) = 1$.
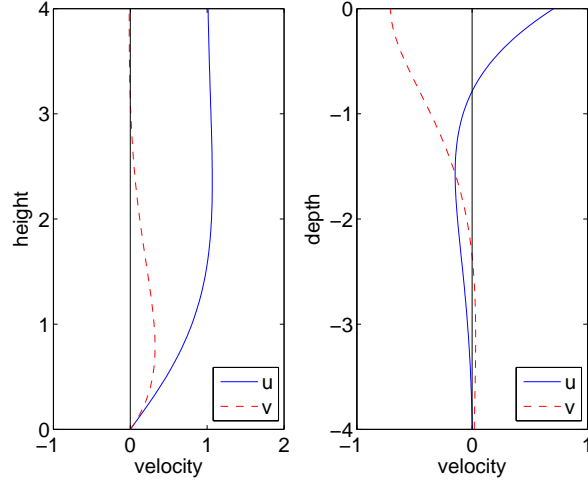
For positive f, this is to the left of the geostrophic flow — that is, down the pressure gradient. In the general case ($v_g \neq 0$) we obtain

$$V = \int_0^\infty (v - v_g)\,\mathrm{d}z = \frac{d}{2}(u_g - v_g) \tag{2.301}$$

Similarly, the additional zonal transport produced by frictional effects are, for $v_g = 0$,

$$U = \int_0^\infty (u - u_g)\,\mathrm{d}z = -\int_0^\infty e^{-z/d}\sin(z/d)\,\mathrm{d}z = -\frac{u_g d}{2} \tag{2.302}$$

and in the general case

$$U = \int_0^\infty (u - u_g)\,\mathrm{d}z = -\frac{d}{2}(u_g + v_g) \tag{2.303}$$

So the total transport caused by frictional forces is

$$\boldsymbol{M}_E = \frac{d}{2}\left[-\mathbf{i}(u_g + v_g) + \mathbf{j}(u_g - v_g)\right]. \tag{2.304}$$

The total stress at the bottom surface $z = 0$ induced by frictional forces is

$$\widetilde{\boldsymbol{\tau}}_b = A\frac{\partial \boldsymbol{u}}{\partial z}\bigg|_{z=0} = \frac{A}{d}\left[\mathbf{i}(u_g - v_g) + \mathbf{j}(u_g + v_g)\right], \tag{2.305}$$

using the solution (2.299). Thus, using (2.304), (2.305) and $d^2 = 2A/f$, we see that the total frictionally induced transport in the Ekman layer is related to the stress at the surface by $\boldsymbol{M}_E = (\mathbf{k} \times \widetilde{\boldsymbol{\tau}}_b)/f$, reprising the result of the more general analysis, (2.288). From (2.305), the stress is at an angle of 45° to the left of the velocity at the surface. (However, this result is not generally true for all forms of stress.) These properties are illustrated in Fig. 2.12.
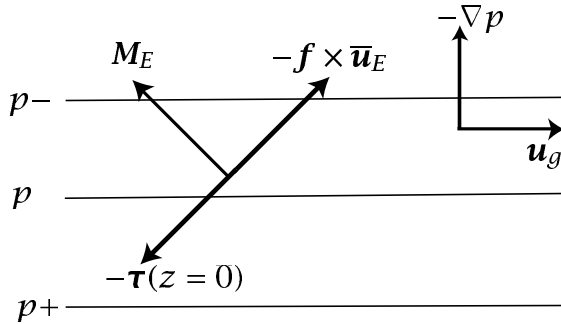
Figure 2.12 A bottom Ekman layer, generated from an eastwards geostrophic flow above. An overbar denotes a vertical integral over the Ekman layer, so that $-f \times \overline{u}_E$ is the Coriolis force on the vertically integrated Ekman velocity. M_E is the frictionally induced boundary layer transport, and τ is the stress.

The vertical velocity at the top of the Ekman layer, w_E, is obtained using (2.304) and (2.305). If f if constant we obtain

$$w_E = -\nabla \cdot M_E = \frac{1}{f_0} \text{curl}_z \tilde{\tau}_b = V_x - U_y = \frac{d}{2}\zeta_g \qquad (2.306)$$

where ζ_g is the vorticity of the geostrophic flow. Thus, the vertical velocity at the top of the Ekman layer, which arises because of the frictionally-induced divergence of the cross-isobaric flow in the Ekman layer, is proportional to the geostrophic vorticity in the free fluid and is proportional to the Ekman layer height $\sqrt{2A/f_0}$.

Another bottom boundary condition

In the analysis above we assumed a *no slip* condition at the surface, namely that the velocity tangential to the surface vanishes. This is certainly appropriate if A is a molecular velocity, but in a turbulent flow, where A is interpreted as an eddy viscosity, the flow very close to the surface may be far from zero. Then, unless we wish to explicitly calculate the flow in an additional very thin viscous boundary layer the no-slip condition may be inappropriate. A slightly more general boundary condition is to suppose that the stress at the surface is given by

$$\tau = \rho_0 C u \qquad (2.307)$$

where C is a constant. The surface boundary condition is then

$$A\frac{\partial u}{\partial z} = C u. \qquad (2.308)$$

If C is infinite we recover the no-slip condition. If $C = 0$, we have instead a condition of no stress at the surface, also known as a *free slip* condition. For intermediate values of C the boundary condition is known as a 'mixed condition'. Evaluating the solution in these cases is left as an exercise for the reader (problem 2.27).

2.12.4 Explicit solutions. II: The upper ocean

Boundary conditions and solution

Figure 2.13 An idealized Ekman spiral in a Southern Hemisphere ocean, driven by an imposed wind-stress. A Northern Hemisphere spiral would be the reflection of this about the vertical axis. Such a clean spiral is rarely observed in the real ocean. The net transport is at right angles to the wind, independent of the detailed form of the friction. The angle of the surface flow is 45° to the wind only for a Newtonian viscosity.
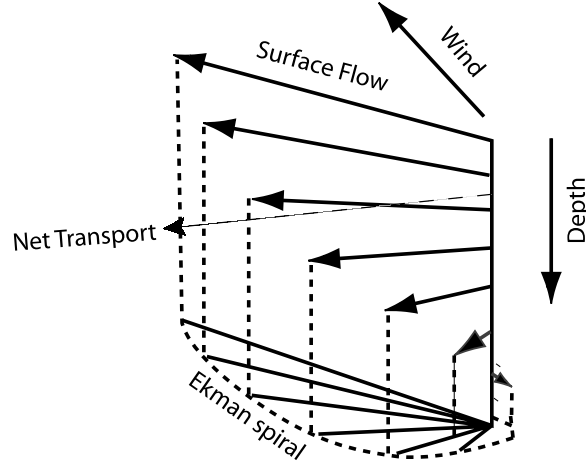
The wind provides a stress on the upper ocean, and the Ekman layer serves to communicate this to the oceanic interior. Appropriate boundary conditions are thus:

$$\text{At } z = 0: \qquad A\frac{\partial u}{\partial z} = \tilde{\tau}^x, \quad A\frac{\partial v}{\partial z} = \tilde{\tau}^y \quad \text{(a given surface stress)} \qquad (2.309a)$$

$$\text{As } z \to -\infty: \quad u = u_g, \quad v = v_g \qquad \text{(a geostrophic interior)} \qquad (2.309b)$$

where $\tilde{\tau}$ is the given (kinematic) wind stress at the surface. Solutions to (2.295a) with (2.309) are found by the same methods as before, and are

$$u = u_g + \frac{\sqrt{2}}{fd}e^{z/d}\left[\tilde{\tau}^x \cos(z/d - \pi/4) - \tilde{\tau}^y \sin(z/d - \pi/4)\right], \qquad (2.310)$$

and

$$v = v_g + \frac{\sqrt{2}}{fd}e^{z/d}\left[\tilde{\tau}^x \sin(z/d - \pi/4) + \tilde{\tau}^y \cos(z/d - \pi/4)\right]. \qquad (2.311)$$

Note that the boundary layer correction depends only on the imposed surface stress, and not the interior flow itself. This is a consequence of the type of boundary conditions chosen, for in the absence of an imposed stress the boundary layer correction is zero — the interior flow already satisfies the gradient boundary condition at the top surface. Similar to the bottom boundary layer the velocity vectors of the solution trace a diminishing spiral as they descend into the interior (Fig. 2.13, which is drawn for the Southern Hemisphere).

Mass flux, surface flow and vertical velocity

The mass flux induced by the surface stress is obtained by integrating (2.310) and (2.311) from the surface to $-\infty$. We explicitly find

$$U = \int_{-\infty}^{0}(u - u_g)\,dz = \frac{\tilde{\tau}^y}{f}, \qquad V = \int_{-\infty}^{0}(v - v_g)\,dz = -\frac{\tilde{\tau}^x}{f} \qquad (2.312)$$
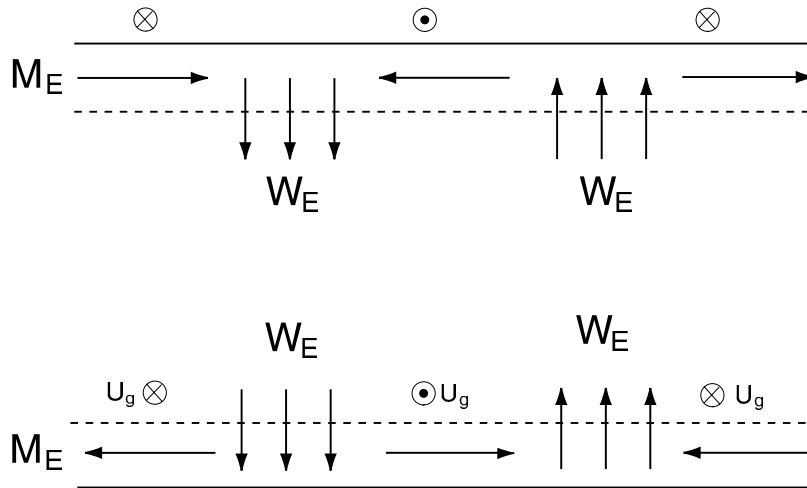
Fig. 2.14 Upper and lower Ekman layers. The upper Ekman layer in the ocean is primarily driven by an imposed wind stress, whereas the lower Ekman layer in the atmosphere or ocean largely results from the interaction of interior geostrophic velocity and a rigid lower surface. The upper part of figure shows the vertical Ekman 'pumping' velocities that result from the given wind stress, and the lower part of the figure shows the Ekman pumping velocities given the interior geostrophic flow.

which indicates that the ageostrophic mass transport is perpendicular to the wind-stress, as noted previously from more general considerations.

Suppose that the surface wind is eastward. Then $\widetilde{\tau}^y = 0$ and the solutions immediately give

$$u(0) - u_g = (\widetilde{\tau}^x/fd)\cos(\pi/4), \qquad v(0) - v_g = (\widetilde{\tau}^x/fd)\sin(\pi/4). \qquad (2.313)$$

Therefore the magnitudes of the frictional flow in the x and y directions are equal to each other, and the flow is 45° to the right (for $f > 0$) of the wind. This result is dependent on the form of the frictional parameterization chosen, but not on the size of the viscosity.

At the edge of the Ekman layer the vertical velocity is given by (2.294), and so is proportional to the curl of the wind-stress. (The second term on the right-hand side of (2.294) is the vertical velocity due to the divergence of the geostrophic flow, and is usually much smaller than the first term.) The production of a vertical velocity at the edge of the Ekman layer is one of most important effects of the layer, especially with regard to the large-scale circulation, for it provides an efficient means whereby surface fluxes are communicated to the interior flow (see Fig. 2.14).

2.12.5 Observations

Ekman layers are quite hard to observe, in either ocean or atmosphere, largely because of a signal-to-noise problem — the noise largely coming from inertial and grav-

ity waves (section 2.10) and, especially in the atmosphere, the effects of stratification and buoyancy-driven turbulence. As regards oceanography, from about 1980 onwards improved instruments have made it possible to observe the vector current with depth, and to average that current and correlate it with the overlying wind, and a number of observations consistent with Ekman dynamics have emerged.[13] The main differences between observations and theory can be ascribed to the effects of stratification (which causes a shallowing and flattening of the spiral), and the interaction of the Ekman spiral with turbulence (and the inadequacy of the eddy-diffusivity parameterization). In spite of these differences of detail, Ekman layer theory remains a remarkable and enduring foundation of geophysical fluid dynamics.

2.12.6 Frictional parameterization

[Some readers will be reading these sections on Ekman layers after having been introduced to quasi-geostrophic theory; this section is for them. Other readers may return to this section after reading chapter 5, or take (2.314) on faith.]

Suppose that the free atmosphere is described by the quasi-geostrophic vorticity equation,

$$\frac{D\zeta_g}{Dt} = f_0 \frac{\partial w}{\partial z} \qquad (2.314)$$

where ζ_g is the geostrophic relative vorticity. Let us further model the atmosphere as a single homogeneous layer of thickness H lying above an Ekman layer of thickness $d \ll H$. If the vertical velocity is negligible at the top of the layer (at $z = H + d$) the equation of motion becomes

$$\frac{D\zeta_g}{Dt} = \frac{f_0[w(H+d) - w(d)]}{H} = -\frac{f_0 d}{2H}\zeta_g \qquad (2.315)$$

using (2.306). This equation shows that the Ekman layer acts as a *linear drag* on the interior flow, with a drag coefficient r equal to $f_0 d/2H$ and with associated timescale T_{Ek} given by

$$T_{\text{Ek}} = \frac{2H}{f_0 d} = \frac{2H}{\sqrt{2 f_0 A}} \qquad (2.316)$$

In the oceanic case the corresponding vorticity equation for the interior flow is

$$\frac{D\zeta_g}{Dt} = \frac{1}{H}\text{curl}_z \tau_s \qquad (2.317)$$

where τ_s is the surface stress. The surface stress thus acts as if it were a body force on the interior flow, and neither the Coriolis parameter nor the depth of the Ekman layer explicitly appear in this formula.

The Ekman layer is actually a very efficient way of communicating surface stresses to the interior. To see this, suppose that eddy mixing were the sole mechanism of transferring stress from the surface to the fluid interior, and there were no Ekman layer. Then the timescale of spindown of the fluid would be given by using

$$\frac{d\zeta}{dt} = A\frac{\partial^2 \zeta}{\partial z^2} \qquad (2.318)$$

implying a turbulent spindown time, T_{turb} of

$$T_{turb} \sim \frac{H^2}{A} \qquad (2.319)$$

where H is the depth over which we require a spin-down. This is much longer than the spin-down of a fluid that has an Ekman layer, for we have

$$\frac{T_{turb}}{T_{Ek}} = \frac{(H^2/A)}{(2H/f_0 d)} = \frac{H}{d} \gg 1, \qquad (2.320)$$

using $d = \sqrt{2A/f_0}$. The effects of friction are evidently enhanced because of the presence of a secondary circulation confined to the Ekman layers (as in Fig. 2.14) in which the vertical scales are much smaller than those in the fluid interior and so where viscous effects become significant, and these frictional stresses are then communicated to the fluid interior via the induced vertical velocities at the edge of the Ekman layers.

Notes

1 The distinction between Coriolis force and acceleration has not always been made in the literature. For a fluid in geostrophic balance, one might either say that there is a balance between the pressure force and the Coriolis force, with no net acceleration, or that the pressure force produces a Coriolis acceleration. The descriptions are equivalent, because of Newton's second law, but should not be conflated.

The Coriolis forces is named after Gaspard Gustave de Coriolis (1792-1843), who introduced the force in the context of rotating mechanical systems (Coriolis 1832, 1835). See Persson (1998) for a historical account as well as a physical interpretation of the Coriolis force.

2 Phillips (1973). See also Stommel and Moore (1989) and Gill (1982). (There are typographic errors in the second term of each of Gill's equations (4.12.11) and (4.12.12).)

3 Phillips (1966). See White (2003) for a review. In the early days of numerical modelling these equations were the most primitive — i.e., the least filtered — equations that could practically be integrated numerically. Associated with increasing computer power there is a tendency for comprehensive numerical models to use non-hydrostatic equations of motion that do not make the shallow-fluid or traditional approximations, and it is conceivable that the meaning of the word 'primitive' may evolve to accomodate them.

4 The Boussinesq approximation is named after Boussinesq (1903), although similar approximations were used earlier by Oberbeck (1879, 1888). Spiegel and Veronis (1960) give a physically based derivation, and Mihaljan (1962) provides a systematic asymptotic derivation of the equations, expanding the Navier-Stokes equations in two small parameters, proportional to the coefficient of volume expansion and the square of the thermal diffusivity. Mahrt (1986) discusses its applicability in the atmosphere.

5 I thank W. R. Young for this derivation.

6 Various versions of anelastic equations exist — see Batchelor (1953), Ogura and

Phillips (1962), Gough (1969), Lipps and Hemler (1982) and Durran (1989), although not all have potential vorticity and energy conservation laws (Bannon 1995, 1996), Scinocca and Shepherd (1992). The system we derive is most similar to that of Ogura and Phillips (1962) and unpublished notes by J. S. A. Green.

7   A numerical model that includes sound waves must take very small timesteps in order to maintain numerical stability, in particular to satisfy the CFL criterion. An alternative is to use an implicit time-stepping scheme that effectively lets the numerics do the filtering of the sound waves, and this approach is favoured by many numerical modellers. If we make the hydrostatic approximation then all sound waves except those that propagate horizontally are eliminated, and there is little need to also make the anelastic approximation.

8   It is named for C.-G. Rossby (see endnote on page 250) but seems to have been first used by Kibel (1940) and is sometimes called the Kibel or Rossby-Kibel number. The notion of geostrophic balance and so, implicitly, that of a small Rossby number, predates either Rossby or Kibel.

9   After Taylor (1921b) and Proudman (1916). The Taylor-Proudman effect is sometimes called the Taylor-Proudman 'theorem', but it is more usefully thought of as a physical effect, with manifestations even when the conditions for the satisfaction of the theorem are not met.

10 Foster (1972).

11 Many numerical models of the large-scale circulation in the atmosphere and ocean do make the hydrostatic approximation. In these models convection must be *parameterized;* otherwise, it would simply occur at the smallest scale available, namely the size of the numerical grid, and this type of unphysical behaviour should be avoided. Of course in non-hydrostatic models convection must also be parameterized if the horizontal resolution of the model is too coarse to properly resolve the convective scales. See also problem 2.10.

12 After Ekman (1905). The problem was posed to Ekman, a student of Vilhelm Bjerknes, by Fridtjof Nansen, the polar explorer and statesman, who wanted to understand the motion of icebergs.

13 Davis et al. (1981), Price et al. (1987), Rudnick and Weller (1993).

Further Reading

Cushman-Roisin, B., 1994. *An Introduction to Geophysical Fluid Dynamics.*
    This compact book provides a nice introduction to a variety of topics in GFD.

Gill, A. E. 1982. *Atmosphere-Ocean Dynamics.*
    A rich and book, especially strong on equatorial dynamics and gravity wave motion.

Holton, J. R. 1992. *An Introduction to Dynamical Meteorology.*
    A deservedly well-known textbook at the upper-division undergraduate/beginning graduate level.

Pedlosky, J., 1987. *Geophysical Fluid Dynamics.*
    A primary reference, especially for flow at low Rossby number. Although the book requires some effort, there is a handsome pay-off for those who study it closely.

White (2002) provides a clear and thorough summary of the equations of motion for meteorology, including the non-hydrostatic and primitive equations.

Zdunkowski, W. and Bott, A. 2003. *Dynamics of the Atmosphere: A Course in Theoretical Meteorology.*
Emphasizes the fundamental aspects and the equations describing them.

Problems

2.1 For an ideal gas in hydrostatic balance, show that:

(a) The integral of the potential plus internal energy from the surface to the top is is equal to its enthalpy;

(b) $d\sigma/dz = c_p(T/\theta)d\theta/dz$, where $\sigma = I + p\alpha + \Phi$ is the dry static energy;

(c) The following expressions for the pressure gradient force are all equal (even without hydrostatic balance):

$$-\frac{1}{\rho}\nabla p = -\theta\,\nabla\Pi = -\frac{c_s^2}{\rho\theta}\nabla(\rho\theta). \tag{P2.1}$$

where $\Pi = c_p T/\theta$ is the Exner function.

2.2 Show that, without approximation, the unforced, inviscid momentum equation may be written in the forms

$$\frac{D\boldsymbol{v}}{Dt} = T\nabla\eta - \nabla(p\alpha + I) \tag{P2.2}$$

and

$$\frac{\partial\boldsymbol{v}}{\partial t} + \boldsymbol{\omega}\times\boldsymbol{v} = T\nabla\eta - \nabla B \tag{P2.3}$$

where $\boldsymbol{\omega} = \nabla\times\boldsymbol{v}$, η is the specific entropy ($d\eta = c_p\,d\ln\theta$) and $B = I + \boldsymbol{v}^2/2 + p\alpha$ where I is the internal energy per unit mass.
Hint: First show that $T\nabla\eta = \nabla I + p\nabla\alpha$, and note also the vector identity $\boldsymbol{v}\times(\nabla\times\boldsymbol{v}) = \frac{1}{2}\nabla(\boldsymbol{v}\cdot\boldsymbol{v}) - (\boldsymbol{v}\cdot\nabla)\boldsymbol{v}$.

2.3 Consider two-dimensional fluid flow in a rotating frame of reference on the f−plane. Linearize the equations about a state of rest.

(a) Ignore the pressure term and determine the general solution to the resulting equations. Show that the speed of fluid parcels is constant. Show that the trajectory of the fluid parcels is a circle with radius $|U|/f$, where $|U|$ is the fluid speed.

(b) What is the period of oscillation of a fluid parcel? Why is this not the same as the period of rotation of the frame of reference?

2.4 A fluid at rest evidently satisfies the hydrostatic relation, which says that the pressure at the surface is given by the weight of the fluid above it. Now consider a *deep* atmosphere on a spherical planet. A unit cross-sectional area at the planet's surface supports a column of fluid whose cross-section increases with height, because the total area of the atmosphere increases with distance away from the center of the planet. Is the pressure at the surface still given by the hydrostatic relation, or is it greater than this because of the increased mass of fluid in the column? If it is still given by the hydrostatic relation, then the pressure at the surface, integrated over the entire area of the planet, is less than the total weight of the fluid; resolve this paradox. But if the pressure at the surface is greater than that implied by hydrostatic balance, explain how the hydrostatic relation fails.

2.5 By considering how the direction of the coordinate axes change with position, show geometrically that in spherical coordinates:

$D\mathbf{i}/Dt = u\partial\mathbf{i}/\partial x = (u/r\cos\vartheta)(\mathbf{j}\sin\vartheta - \mathbf{k}\cos\vartheta);$

$D\mathbf{j}/Dt = u\partial\mathbf{j}/\partial x + v\partial\mathbf{j}/\partial y = -\mathbf{i}(u/r)\tan\vartheta - \mathbf{k}v/a;$

$D\mathbf{k}/Dt = u\partial\mathbf{k}/\partial x + v\partial\mathbf{k}/\partial y = \mathbf{i}(u/r) + \mathbf{j}(v/r).$

Then, using

$$\frac{D\boldsymbol{v}}{Dt} = \mathbf{i}\frac{Du}{Dt} + \mathbf{j}\frac{Dv}{Dt} + \mathbf{k}\frac{Dw}{Dt} + u\frac{D\mathbf{i}}{Dt} + v\frac{D\mathbf{j}}{Dt} + w\frac{D\mathbf{k}}{Dt}, \tag{P2.4}$$

show that

$$\frac{D\boldsymbol{v}}{Dt} = \mathbf{i}\left(\frac{Du}{Dt} - \frac{uv\tan\vartheta}{r} + \frac{uw}{r}\right) + \mathbf{j}\left(\frac{Dv}{Dt} + \frac{u^2\tan\vartheta}{r} + \frac{vw}{r}\right)$$
$$+ \mathbf{k}\left(\frac{Dw}{Dt} - \frac{u^2 + v^2}{r}\right). \tag{P2.5}$$

2.6 At what latitude is the angle between the direction of Newtonian gravity (due solely to the mass of the earth) and that of apparent gravity (Newtonian gravity plus centrifugal terms) the largest? At what latitudes, if any, is this angle zero?

2.7 ◆ Write the momentum equations in true spherical coordinates, including the centrifugal and gravitational terms. Show that for reasonable values of the wind, the dominant balance in the meridional component of this equation involve a balance between centrifugal and pressure gradient terms. Can this balance be subtracted out of the equations in a sensible way, so leaving a useful horizontal momentum equation that involves the Coriolis and acceleration terms? If so, obtain a closed set of equations for the flow this way. Discuss the pros and cons of this approach versus the geometric approximation discussed in section 2.2.1.

2.8 For an ideal gas show that the expressions (2.223) and (2.227) are equivalent.

2.9 Consider an ocean at rest with known vertical profiles of potential temperature and salinity, $\theta(z)$ and $S(z)$. Suppose we also know the equation of state in the form $\rho = \rho(\theta, S, p)$. Obtain an expression for the buoyancy frequency. Check your expression by substituting the equation of state for an ideal gas and recovering a known expression for the buoyancy frequency.

2.10 Convection and its parameterization.

(a) Consider a Boussinesq system in which the vertical momentum equation is modified by the parameter α to read

$$\alpha^2\frac{Dw}{Dt} = -\frac{\partial\phi}{\partial z} + b, \tag{P2.6}$$

and the other equations are unchanged. (If $\alpha = 0$ the system is hydrostatic, and if $\alpha = 1$ the system is the original one.) Linearise these equations about a state of rest and of constant stratification (as in section 2.10.1) and obtain the dispersion relation for the system, and plot it for various values of α, including 0 and 1. Show that, for $\alpha > 1$ the system approaches the limiting frequency of N more rapidly than with $\alpha = 1$.

(b) ◆ Argue that if $N^2 < 0$, convection in a system with $\alpha > 1$ generally occurs at a larger scale than with $\alpha = 1$. Show this explicitly by adding some diffusion or friction to the right-hand sides of the equations of motion and obtaining the dispersion relation. You may do this approximately.

2.11 *(a)* The *geopotential height* is the height of a given pressure level. Show that in an atmosphere with a uniform lapse rate (i.e., $\mathrm{d}T/\mathrm{d}z = \Gamma = $ constant) the geopotential height at a pressure p is given by

$$z = \frac{T_0}{\Gamma}\left[1 - \left(\frac{p_0}{p}\right)^{-R\Gamma/g}\right] \qquad (\text{P2.7})$$

where T_0 is the temperature at $z = 0$.

(b) In an isothermal atmosphere, obtain an expression for the geopotential height as function of pressure, and show that this is consistent with the expression (P2.7) in the appropriate limit.

2.12 Consider the simple Boussinesq equations, $\mathrm{D}\boldsymbol{v}/\mathrm{D}t = \mathbf{k}b + \nu\nabla^2\boldsymbol{v}$, $\nabla \cdot \boldsymbol{v} = 0$, $\mathrm{D}b/\mathrm{D}t = Q + \kappa\nabla^2 b$. Obtain an energy equation similar to (2.113) but now with the terms on the right-hand side that represent viscous and diabatic effects. Over a closed volume, show that the dissipation of kinetic energy is balanced by a buoyancy source. Show also that, in a statistically steady state, the heating must occur at a lower level than the cooling if a kinetic-energy dissipating circulation is to be maintained.

2.13 ◆ Suppose a fluid is contained in a closed container, with insulating sidewalls, and heated from below and cooled from above. The heating and cooling are adjusted so that there is no net energy flux into the fluid. Let us also suppose that any viscous dissipation of kinetic energy is returned as heating, so the total energy of the fluid is exactly constant. Suppose the fluid starts out at rest and at a uniform temperature, and the heating and cooling are then turned on. A very short time afterwards, the fluid is lighter at the bottom and heavier at the top; that is, its potential energy has increased. Where has this energy come from? Discuss this paradox for both a compressible fluid (e.g., an ideal gas) and for a simple Boussinesq fluid.

2.14 Consider a rapidly rotating (i.e., in near geostrophic balance) Boussinesq fluid on the f-plane.

(a) Show that the pressure divided by the density scales as $\phi \sim fUL$.

(b) Show that the horizontal divergence of the geostrophic wind vanishes. Thus, argue that the scaling $W \sim UH/L$ is an *overestimate* for the magnitude of the vertical velocity. (Optional extra: obtain a scaling estimate for the magnitude of vertical velocity in rapidly rotating flow.)

(c) Using these results, or otherwise, discuss whether hydrostatic balance is more or less likely to hold in a rotating flow that in non-rotating flow.

2.15 Using either the anelastic equations in height coordinates, or the equations of motion in pressure coordinates, show that for rapidly rotating flow the vertical shear of horizontal velocity is proportional to the horizontal temperature gradient. Estimate the size of the zonal wind 5 km above the surface in the midlatitude atmosphere in summer and winter using (approximate) values for the meridional temperature gradient in the atmosphere. What is the shear corresponding to the pole-equator temperature gradient in the ocean?

2.16 Using approximate but realistic values for the observed stratification, what is the buoyancy period for (a) the mid-latitude troposphere, (b) the stratosphere, (c) the oceanic thermocline, (d) the oceanic abyss?

2.17 Consider a dry, hydrostatic, ideal-gas atmosphere whose lapse rate is one of constant potential temperature. What is its vertical extent? That is, at what height does

the density vanish? Is this a problem for the anelastic approximation discussed in the text?

2.18 Show that for an ideal gas, the expressions (2.227), (2.222), (2.223) are all equivalent, and express N^2 terms of the temperature lapse rate, $\partial T / \partial z$.

2.19 ◆ Calculate a reasonably accurate, albeit approximate, expression for the buoyancy equation for seawater. (Derived from notes by R. deSzoeke)
   Solution (i): The buoyancy frequency is given by

$$N^2 = -\frac{g}{\rho} \left(\frac{\partial \rho_{\text{pot}}}{\partial z} \right)_{\text{env}} = \frac{g}{\alpha} \left(\frac{\partial \alpha_{\text{pot}}}{\partial z} \right)_{\text{env}} = -\frac{g^2}{\alpha^2} \left(\frac{\partial \alpha_{\text{pot}}}{\partial p} \right)_{\text{env}} \qquad \text{(P2.8)}$$

where $\alpha_{\text{pot}} = \alpha(\theta, S, p_{\text{R}})$ is the potential density, and p_{R} a reference pressure. From (1.178)

$$\alpha_{\text{pot}} = \alpha_0 \left[1 - \frac{\alpha_0}{c_0^2} p_{\text{R}} + \beta_T (1 + \gamma^* p_{\text{R}}) \theta' + \frac{1}{2} \beta_T^* \theta'^2 - \beta_S (S - S_0) \right] \qquad \text{(P2.9)}$$

Using this and (P2.8) we obtain the buoyancy frequency,

$$N^2 = -\frac{g^2}{\alpha^2} \alpha_0 \left[\beta_T \left(1 + \gamma p_{\text{R}} + \frac{\beta_T^*}{\beta_T} \theta \right) \left(\frac{\partial \theta}{\partial p} \right)_{\text{env}} - \beta_S \left(\frac{\partial S}{\partial p} \right)_{\text{env}} \right], \qquad \text{(P2.10)}$$

although we must substitute local pressure for the reference pressure p_{R}. (Why?)
   Solution (ii): The sound speed is given by

$$c^{-2} = -\frac{1}{\alpha^2} \left(\frac{\partial \alpha}{\partial p} \right)_{\theta, S} = \frac{1}{\alpha^2} \left(\frac{\alpha_0^2}{c_0^2} - \gamma \alpha_1 \theta \right) \qquad \text{(P2.11)}$$

and, using (P2.8) and (2.227) the square of the buoyancy frequency may be written

$$N^2 = \frac{g}{\alpha} \left(\frac{\partial \alpha}{\partial z} \right)_{\text{env}} - \frac{g^2}{c^2} = -\frac{g^2}{\alpha^2} \left[\left(\frac{\partial \alpha}{\partial p} \right)_{\text{env}} + \frac{\alpha^2}{c^2} \right] \qquad \text{(P2.12)}$$

Using (1.178), (P2.11) and (P2.12) we recover (P2.10), although now with p explicitly in place of p_{R}.

2.20 Begin with the mass conservation in the height-coordinates, namely $D\rho/Dt + \rho \nabla \cdot \boldsymbol{v} = 0$. Transform this into pressure coordinates using the chain rule (or otherwise) and derive the mass conservation equation in the form $\nabla_p \cdot \boldsymbol{u} + \partial \omega / \partial p = 0$.

2.21 Starting with the primitive equations in pressure coordinates, derive the form of the primitive equations of motion in sigma-pressure coordinates. In particular, show that the prognostic equation for surface pressure is,

$$\frac{\partial p_s}{\partial t} + \nabla \cdot (p_s \boldsymbol{u}) + p_s \frac{\partial \dot{\sigma}}{\partial \sigma} = 0 \qquad \text{(P2.13)}$$

and that hydrostatic balance may be written $\partial \Phi / \partial \sigma = -RT/\sigma$.

2.22 Starting with the primitive equations in pressure coordinates, derive the form of the primitive equations of motion in log-pressure coordinates in which $Z = -H \ln(p/p_r)$ is the vertical coordinate. Here, H is a reference height (e.g., a scale height RT_r/g where T_r is a typical or an average temperature) and p_r is a reference pressure

(e.g., 1000 mb). In particular, show that if the 'vertical velocity' is $W = DZ/Dt$ then $W = -H\omega/p$ and that

$$\frac{\partial \omega}{\partial p} = -\frac{\partial}{\partial p}\left(\frac{pW}{H}\right) = \frac{\partial W}{\partial Z} - \frac{W}{H}. \tag{P2.14}$$

and obtain the mass conservation equation (2.157d). Show that this can be written in the form

$$\frac{\partial u}{\partial x} + \frac{\partial v}{\partial y} + \frac{1}{\rho_s}\frac{\partial}{\partial Z}(\rho_s W) = 0 \tag{P2.15}$$

where $\rho_s = \rho_r \exp(-Z/H)$.

2.23 (a) Prove that the argument of the square root in (2.257) is always positive.
    Solution: The largest value or the argument occurs when $m = 0$ and $k^2 = 1/(4H^2)$. The argument is then $1 - 4H^2N^2/c^2$. But $c^2 = \gamma R T_0 = \gamma g H$ and $N^2 = g\kappa/H$ so that $4N^2H^2/c^2 = 4\kappa/\gamma \approx 0.8$.
    (b) ◆ This argument seems to depend on the parameters in the ideal gas equation of state. Is it more general than this? Is a natural system possible for which the argument is negative, and if so what physical interpretation could one ascribe to the situation?

2.24 Consider a ideal-gas isothermal atmosphere that obeys the hydrostatic equations of motion. Show that small deviations around a resting state, as described by (2.251), but with (2.251b) is replaced by (2.268), give rise to internal gravity waves with a dispersion relation given by (2.269). Show also that the Lamb wave is present in this system.

2.25 Suppose that we allow for the possibility of friction in the vertical momentum equation, and write this as

$$\frac{\partial \phi}{\partial z} = A\frac{\partial^2 w}{\partial z^2}. \tag{P2.16}$$

Show that if $Ek \ll 1$ the term on the right-hand side is negligible if $L \geq H$, and that there is no boundary layer in the pressure field, as in the inviscid case.

2.26 Consider a wind stress imposed by a mesoscale cyclonic storm (in the atmosphere) given by

$$\boldsymbol{\tau} = -Ae^{-(r/\lambda)^2}(y\,\mathbf{i} + x\,\mathbf{j}) \tag{P2.17}$$

where $r^2 = x^2 + y^2$, and A and λ are constants. Also assume constant Coriolis gradient $\beta = \partial f/\partial y$ and constant ocean depth H. Find (a) the Ekman transport, (b) the vertical velocity $w_E(x, y, z)$ below the Ekman layer, (c) the northward velocity $v(x, y, z)$ below the Ekman layer and (d) indicate how you would find the westward velocity $u(x, y, z)$ below the Ekman layer.

2.27 In an atmospheric Ekman layer on the f-plane for a fluid with $\rho = \rho_a = 1$ let us write the momentum equation as

$$\boldsymbol{f} \times \boldsymbol{u} = -\nabla\phi + \frac{\partial \boldsymbol{\tau}}{\partial z} \tag{P2.18}$$

where $\boldsymbol{\tau} = K\partial\boldsymbol{u}/\partial z$ and K is a constant coefficient of viscosity. An *independent* formula for the stress at the ground is $\boldsymbol{\tau} = C\boldsymbol{u}$, where C is a constant. Assume that in the free atmosphere the wind is geostrophic and zonal, with $\boldsymbol{u}_g = U\mathbf{i}$.

(a) Find an expression for the wind vector at the ground. Discuss the limits $C = 0$ and $C = \infty$. Show that when $C = 0$ the frictionally-induced vertical velocity at the top of the Ekman layer is zero.

(b) Find the vertically integrated horizontal mass flux caused by the boundary layer.

(c) When the stress on the atmosphere is $\boldsymbol{\tau}$, the stress on the ocean beneath is $-\boldsymbol{\tau}$. Determine the direction and strength of the surface current in terms of the surface wind, the oceanic Ekman depth and the ratio ρ_a/ρ_o, where ρ_o is the density of the seawater. How does the boundary-layer mass flux in the ocean compare to that in the atmosphere?

Partial solution: A useful trick in Ekman layer problems is to write the velocity as a complex number, $\tilde{u} = u + \mathrm{i}v$. The Ekman layer equation, (2.295a), may then be written as

$$A\frac{\partial^2 \tilde{U}}{\partial z^2} = \mathrm{i}f\tilde{U} \qquad\qquad (P2.19)$$

where $\tilde{U} = \tilde{u} - \tilde{u}_g$. The solution to this is

$$\tilde{u} - \tilde{u}_g = (\tilde{u}(0) - \tilde{u}_g)\exp\left[-\frac{(1+\mathrm{i})z}{d}\right]. \qquad\qquad (P2.20)$$

where the boundary condition of finiteness at infinity eliminates the exponentially growing solution. The boundary condition at $z = 0$ is $\partial \boldsymbol{u}_g/\partial z = (C/K)\boldsymbol{u}_g$ which gives $(\tilde{u}(0) - \tilde{u}_g)\exp(\mathrm{i}\pi/4) = -Cd/(\sqrt{2}K)\tilde{u}(0)$, and the rest of the solution follows.

2.28 *The logarithmic boundary layer*

Close to ground rotational effects are unimportant and small-scale turbulence generates a *mixed layer.* In this layer, assume that the stress is constant and that it can be parameterized by an eddy diffusivity the size of which is proportional to the distance from the surface. Show that the velocity then varies logarithmically with height.

Solution: Write the stress as $\tau = \rho_0 u^{*2}$ where the constant u^* is called the frictional velocity. Using the eddy diffusivity hypothesis this stress is given by

$$\tau = \rho_0 u^{*2} = \rho_0 A\frac{\partial u}{\partial z} \quad \text{where} \quad A = u^* k z \qquad\qquad (P2.21)$$

where k is von Karman's ('universal') constant (approximately equal to 0.4). From (P2.21) we have $\partial u/\partial z = u^*/(Az)$ which integrates to give $u = (u^*/k)\ln(z/z_0)$. The parameter z_0 is known as the roughness length, and is typically of order centimeters or a little larger, depending on the surface.

Another advantage of a mathematical statement is that it is so definite that it might be definitely wrong... Some verbal statements have not this merit.

L. F. Richardson (1881–1953).

Shallow Water Systems and Isentropic Coordinates

C ONVENTIONALLY, 'THE' SHALLOW WATER EQUATIONS describe a thin layer of constant density fluid in hydrostatic balance, rotating or not, bounded from below by a rigid surface and from above by a free surface, above which we suppose is another fluid of negligible inertia. Such a configuration can be generalized to multiple layers of immiscible fluids lying one on top of each other, forming a 'stacked shallow water' system, and this class of systems is the main subject of this chapter.

The single-layer model is one of the simplest useful models in geophysical fluid dynamics, because it allows for a consideration of the effects of rotation in a simple framework without with the complicating effects of stratification. By adding layers we can then study the effects of stratification, and indeed the model with just two layers is not only a simple model of a stratified fluid, it is a surprisingly good model of many phenomena in the ocean and atmosphere. Indeed, the models are more than just pedagogical tools — we will find that there is a close physical and mathematical analogy between the shallow water equations and a description of the continuously stratified ocean or atmosphere written in isopycnal or isentropic coordinates, with a meaning beyond a coincidental similarity in the equations. We begin with the single-layer case.

3.1 DYNAMICS OF A SINGLE, SHALLOW LAYER

Shallow water dynamics apply, by definition, to a fluid layer of constant density in which the horizontal scale of the flow is much greater than the depth of the water. The fluid motion is then fully determined by the momentum and mass continuity equations, and because of the assumed small aspect ratio the the hydrostatic approximation is well
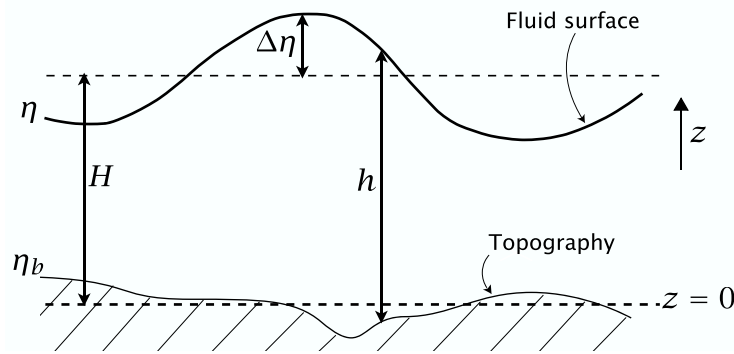
Fig. 3.1   A shallow water system. $h(x, y)$ is the thickness of a water column, H its mean thickness, $\eta(x, y)$ the height of the free surface and η_b is the height of the lower, rigid, surface, above some arbitrary origin, typically chosen such that the average of η_b is zero. $\Delta\eta$ is the deviation free surface height, so we have $\eta = \eta_b + h = H + \Delta\eta$.

satisfied, and we invoke this from the outset. Consider, then, fluid in a container above which is another fluid of negligible density (and therefore negligible inertia) relative to the fluid of interest, as illustrated in Fig. 3.1. As usual, our notation is that $\boldsymbol{v} = u\mathbf{i} + v\mathbf{j} + w\mathbf{k}$ is the three dimensional velocity and $\boldsymbol{u} = u\mathbf{i} + v\mathbf{j}$ is the horizontal velocity. $h(x, y)$ is thickness of the liquid column, H is its mean height, and η is the height of the free surface. In a flat-bottomed container $\eta = h$, whereas in general $h = \eta - \eta_b$, where η_b is the height of the floor of the container.

3.1.1 Momentum equations

The vertical momentum equation is just the hydrostatic equation,

$$\frac{\partial p}{\partial z} = -\rho g, \tag{3.1}$$

and, because density is assumed constant, we may integrate this to

$$p(x, y, z) = -\rho g z + p_o \tag{3.2}$$

At the top of the fluid, $z = \eta$, the pressure is determined by the weight of the overlying fluid and this is assumed negligible. Thus, $p = 0$ at $z = \eta$ giving

$$p(x, y, z) = \rho g(h(x, y) - z) \tag{3.3}$$

The consequence of this is that the horizontal gradient of pressure is independent of height. That is

$$\nabla_z p = \rho g \nabla_z \eta \tag{3.4}$$

where

$$\nabla_z = \mathbf{i}\frac{\partial}{\partial x} + \mathbf{j}\frac{\partial}{\partial y} \tag{3.5}$$

is the gradient operator at constant z. (In the rest of this chapter we will drop the subscript z unless that causes ambiguity. The three-dimensional gradient operator will be denoted ∇_3. We will also mostly use Cartesian coordinates, but the shallow water equations may certainly be applied over a spherical planet — indeed, 'Laplace's tidal equations' are essentially the shallow water equations on a sphere.) The horizontal momentum equations therefore become

$$\frac{D\boldsymbol{u}}{Dt} = -\frac{1}{\rho}\nabla p = -g\nabla\eta \tag{3.6}$$

The right-hand side of this equation is independent of the vertical coordinate z. Thus, if the flow is initially independent of z, it must stay so. (This z-independence is unrelated to that arising from the rapid rotation necessary for the Taylor-Proudman effect.) The velocities u and v are functions only of x, y and t and the horizontal momentum equation is therefore

$$\frac{D\boldsymbol{u}}{Dt} = \frac{\partial\boldsymbol{u}}{\partial t} + u\frac{\partial\boldsymbol{u}}{\partial x} + v\frac{\partial\boldsymbol{u}}{\partial y} = -g\nabla\eta. \tag{3.7}$$

That the horizontal velocity is independent of z is a consequence of the hydrostatic equation, which ensures that the horizontal pressure gradient is independent of height. (Another starting point would be to take this independence of the horizontal motion with height as the *definition* of shallow water flow. In real physical situations such independence does not hold exactly — for example, friction at the bottom may induce a vertical dependence of the flow in a boundary layer.) In the presence of rotation (3.7) easily generalizes to

$$\boxed{\frac{D\boldsymbol{u}}{Dt} + \boldsymbol{f} \times \boldsymbol{u} = -g\nabla\eta}\,, \tag{3.8}$$

where $\boldsymbol{f} = f\mathbf{k}$. Just as with the primitive equations, f may be constant or may vary with latitude, so that on a spherical planet $f = 2\Omega\sin\vartheta$ and on the β-plane $f = f_0 + \beta y$.

3.1.2 Mass conservation equation

From first principles

The mass contained in a fluid column of height h and cross-sectional area A is given by $\int_A \rho h \, dA$ (Fig. 3.2). If there is a net flux of fluid across the column boundary (by advection) then this must be balanced by a net increase in the mass in A, and therefore a net increase in the height of the water column. The mass convergence into the column is given by

$$F_m = \text{Mass flux in} = -\int_S \rho\boldsymbol{u} \cdot d\boldsymbol{S} \tag{3.9}$$

where S is the area of the vertical boundary of the column. The surface area of the column is comprised of elements of area $h\boldsymbol{n}\delta l$, where δl is a line element circumscribing

Figure 3.2 The mass budget for a column of area A in a shallow water system. The fluid leaving the column is $\oint \rho h \boldsymbol{u} \cdot \boldsymbol{n}\,\mathrm{d}l$ where $\boldsymbol{n}$ is the unit vector normal to the boundary of the fluid column. There is a non-zero vertical velocity at the top of the column if the mass convergence into the column is non-zero.
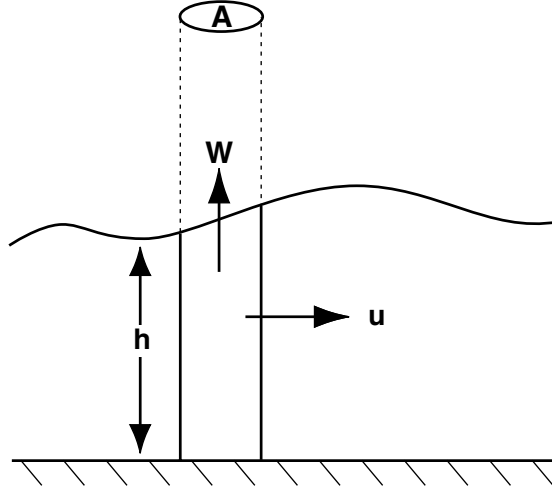
the column and $\boldsymbol{n}$ is a unit vector perpendicular to the boundary, pointing outwards. Thus (3.9) becomes

$$F_m = -\oint \rho h \boldsymbol{u} \cdot \boldsymbol{n}\,\mathrm{d}l \tag{3.10}$$

Using the divergence theorem in two-dimensions, (3.10) simplifies to

$$F_m = -\int_A \nabla \cdot (\rho \boldsymbol{u} h)\,\mathrm{d}A. \tag{3.11}$$

where the integral is over the cross-sectional area of the fluid column (looking down from above). This is balanced by the local increase in height of the water column, given by

$$F_m = \frac{\mathrm{d}}{\mathrm{d}t}\int \rho\,\mathrm{d}V = \frac{\mathrm{d}}{\mathrm{d}t}\int_A \rho h\,\mathrm{d}A = \int_A \rho\frac{\partial h}{\partial t}\,\mathrm{d}A \tag{3.12}$$

The balance between (3.11) and (3.12) thus leads to

$$\int_A \left[\frac{\partial}{\partial t}h + \nabla \cdot (\boldsymbol{u}h) \right]\mathrm{d}A = 0 \tag{3.13}$$

Because the area is arbitrary the integrand itself must vanish, whence,

$$\boxed{\frac{\partial h}{\partial t} + \nabla \cdot (\boldsymbol{u}h) = 0}, \tag{3.14}$$

or equivalently

$$\boxed{\frac{\mathrm{D}h}{\mathrm{D}t} + h\nabla \cdot \boldsymbol{u} = 0}. \tag{3.15}$$

This derivation holds whether or not the lower surface is flat. If it is, then $h = \eta$, and if not $h = \eta - \eta_b$. Eqs. (3.8) and (3.14) or (3.15) form a complete set, summarized in the shaded box on page 134.

From the 3D mass conservation equation

Since the fluid is incompressible, the three-dimensional mass continuity equation is just $\nabla \cdot \boldsymbol{v} = 0$. Writing this out in component form

$$\frac{\partial w}{\partial z} = -\left(\frac{\partial u}{\partial x} + \frac{\partial v}{\partial y}\right) = -\nabla \cdot \boldsymbol{u} \tag{3.16}$$

Integrate this from the bottom of the fluid ($z = \eta_b$) to the top ($z = \eta$), noting that the right-hand side is independent of z, to give

$$w(\eta) - w(\eta_b) = -h\nabla \cdot \boldsymbol{u}. \tag{3.17}$$

At the top the vertical velocity is the matarial derivative of the position of a particular fluid element. But the position of the fluid at the top is just η, and therefore (see Fig. 3.2)

$$w(\eta) = \frac{\mathrm{D}\eta}{\mathrm{D}t}. \tag{3.18}$$

At the bottom of the fluid we have similarly

$$w(\eta_b) = \frac{\mathrm{D}\eta_b}{\mathrm{D}t}, \tag{3.19}$$

where, absent earthquakes and the like, $\partial \eta_b / \partial t = 0$. Using the last two equations, (3.17) becomes

$$\frac{\mathrm{D}}{\mathrm{D}t}(\eta - \eta_b) + h\nabla \cdot \boldsymbol{u} = 0 \tag{3.20}$$

or

$$\frac{\mathrm{D}h}{\mathrm{D}t} + h\nabla \cdot \boldsymbol{u} = 0. \tag{3.21}$$

as in (3.15).

3.1.3 A rigid lid

The case where the *upper* surface is held flat by the imposition of a rigid lid is sometimes of interest. The ocean suggests one such example, for here the bathymetry at the bottom of the ocean provides much larger variations in fluid thickness than do the small variations in the height of the ocean surface. Suppose then the upper surface is at a contant height H then, from (3.14) with $\partial h/\partial t = 0$ the mass conservation equation becomes

$$\nabla_h \cdot (\boldsymbol{u}h_b) = 0. \tag{3.22}$$

where $h_b = H - \eta_b$ Note that this allows us to define an incompressible *mass-transport velocity*, $\boldsymbol{U} \equiv h_b\boldsymbol{u}$.

Although the upper surface is flat, the pressure there is no longer constant because a force must be provided by the rigid lid to keep the surface flat. The horizontal momentum equation is

$$\frac{\mathrm{D}\boldsymbol{u}}{\mathrm{D}t} = -\frac{1}{\rho_0}\nabla p_{\mathrm{lid}} \tag{3.23}$$

The Shallow Water Equations

For a single-layer fluid, and including the Coriolis term, the inviscid shallow water equations are:
Momentum:
$$\frac{D\boldsymbol{u}}{Dt} + \boldsymbol{f} \times \boldsymbol{u} = -g\nabla\eta. \tag{SW.1}$$

Mass Conservation:
$$\frac{Dh}{Dt} + h\nabla \cdot \boldsymbol{u} = 0 \qquad \text{or} \qquad \frac{\partial h}{\partial t} + \nabla \cdot (h\boldsymbol{u}) = 0. \tag{SW.2}$$

where $\boldsymbol{u}$ is the horizontal velocity, h is the total fluid thickness, η is the height of the upper free surface and η_b is the height of the lower surface (the bottom topography). Thus, $h(x, y, t) = \eta(x, y, t) - \eta_b(x, y)$. The material derivative is

$$\frac{D}{Dt} = \frac{\partial}{\partial t} + \boldsymbol{u} \cdot \nabla = \frac{\partial}{\partial t} + u\frac{\partial}{\partial x} + v\frac{\partial}{\partial y}, \tag{SW.3}$$

with the rightmost expresion holding in Cartesian coordinates.

where p_{lid} is the pressure at the lid, and the complete equations of motion are then (3.22) and (3.23).[1] If the lower surface is flat, the two-dimensional flow itself is divergence-free, and the equations reduce to the two-dimensional incompressible Euler equations.

3.1.4 Stretching and the vertical velocity

Because the horizontal velocity is depth independent, the vertical velocity plays no role in advection. However, w is certainly not zero for then the free surface would be unable to move up or down, but because of the vertical independence of the horizontal flow w does have a simple vertical structure; to determine this we write the mass conservation equation as
$$\frac{\partial w}{\partial z} = -\nabla \cdot \boldsymbol{u} \tag{3.24}$$
and integrate upwards from the bottom to give
$$w = w_b - (\nabla \cdot \boldsymbol{u})(z - \eta_b). \tag{3.25}$$
Thus, the vertical velocity is a linear function of height. Eq. (3.25) can be written
$$\frac{Dz}{Dt} = \frac{D\eta_b}{Dt} - (\nabla \cdot \boldsymbol{u})(z - \eta_b), \tag{3.26}$$
and at the upper surface $w = D\eta/Dt$ so that here we have
$$\frac{D\eta}{Dt} = \frac{D\eta_b}{Dt} - (\nabla \cdot \boldsymbol{u})(\eta - \eta_b), \tag{3.27}$$

Eliminating the divergence term from the last two equations gives

$$\frac{D}{Dt}(z - \eta_b) = \frac{z - \eta_b}{\eta - \eta_b}\frac{D}{Dt}(\eta - \eta_b), \tag{3.28}$$

which in turn gives

$$\frac{D}{Dt}\left(\frac{z - \eta_b}{\eta - \eta_b}\right) = \frac{D}{Dt}\left(\frac{z - \eta_b}{h}\right) = 0. \tag{3.29}$$

This means that the ratio of the height of a fluid parcel above the floor to the total depth of the column is fixed; that is, the fluid stretches uniformly in a column, and this is kinematic property of the shallow water system.

3.1.5 Analogy with Compressible Flow

The shallow water equations (3.8) and (3.14) are analogous to the compressible gas dynamic equations in two dimensions, namely

$$\frac{D\boldsymbol{u}}{Dt} = -\frac{1}{\rho}\nabla p \tag{3.30}$$

and

$$\frac{\partial \rho}{\partial t} + \nabla \cdot (\boldsymbol{u}\rho) = 0, \tag{3.31}$$

along with an equation of state which we take to be $p = f(\rho)$. The mass conservation equations (3.14) and (3.31) are identical, with the replacement $\rho \leftrightarrow h$. If $p = C\rho^\gamma$, then (3.30) becomes

$$\frac{D\boldsymbol{u}}{Dt} = -\frac{1}{\rho}\frac{dp}{d\rho}\nabla \rho = -C\gamma\rho^{\gamma-2}\nabla\rho \tag{3.32}$$

If $\gamma = 2$ then the momentum equations (3.8) and (3.32) become equivalent, with $\rho \leftrightarrow h$ and $C\gamma \leftrightarrow g$. In an ideal gas $\gamma = c_p/c_v$ and values typically are in fact less than two (in air $\gamma \approx 7/5$); however, if the equations are linearized, then the analogy is exact for all values of γ, for then (3.32) becomes $\partial \boldsymbol{v}'/\partial t = -\rho_0^{-1}c_s^2\nabla\rho'$ where $c_s^2 = dp/d\rho$, and the linearized shallow water momentum equation is $\partial \boldsymbol{u}'/\partial t = -H^{-1}(gH)\nabla h'$, so that $\rho_0 \leftrightarrow H$ and $c_s^2 \leftrightarrow gH$. The sound waves of a compressible fluid are then analogous to shallow water waves, considered in section 3.7.

3.2 REDUCED GRAVITY EQUATIONS

Consider now a single shallow moving layer of fluid on top a deep, quiescent fluid layer (Fig. 3.3), and beneath a fluid of negligible inertia. This configuration is often used a model of the upper ocean: the upper layer represents flow in perhaps the upper few hundred meters of the ocean, the lower layer the near-stagnant abyss. If we turn the model upside-down we have a model, perhaps slightly less realistic, of the atmosphere: the lower layer represents motion in the troposphere above which lies an inactive stratosphere. The equations of motion are virtually the same in both cases.
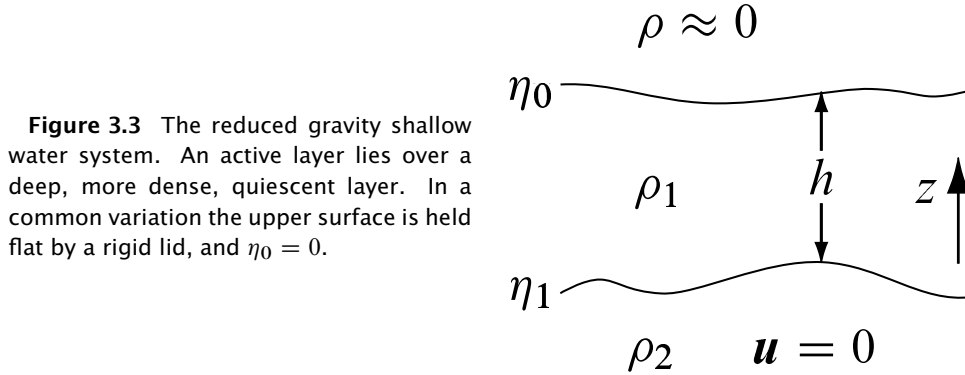
$$\rho \approx 0$$

η_0

ρ_1 h z

η_1

ρ_2 $\boldsymbol{u} = 0$

Figure 3.3 The reduced gravity shallow water system. An active layer lies over a deep, more dense, quiescent layer. In a common variation the upper surface is held flat by a rigid lid, and $\eta_0 = 0$.

3.2.1 Pressure gradient in the active layer

We'll derive the equations for the oceanic case (active layer on top) in two cases, which differ slightly in the assumption made about the upper surface.

I Free upper surface

The pressure in the upper layer is given by integrating the hydrostatic equation down from the upper surface. Thus, at a height z in the upper layer

$$p_1(z) = g\rho_1(\eta_0 - z), \tag{3.33}$$

where η_0 is the height of the upper surface. Hence, everywhere in the upper layer,

$$\frac{1}{\rho_1}\nabla p_1 = -g\nabla\eta_0, \tag{3.34}$$

and the momentum equation is

$$\frac{\mathrm{D}\boldsymbol{u}}{\mathrm{D}t} + \boldsymbol{f} \times \boldsymbol{u} = -g\nabla\eta_0. \tag{3.35}$$

In the lower layer the the pressure is also given by the weight of the fluid above it. Thus, at some level z in the lower layer,

$$p_2(z) = \rho_1 g(\eta_0 - \eta_1) + \rho_2 g(\eta_1 - z). \tag{3.36}$$

But if this layer is motionless the horizontal pressure gradient in it is zero and therefore

$$\rho_1 g\eta_0 = -\rho_1 g'\eta_1 + \text{constant}, \tag{3.37}$$

where $g' = g(\rho_2 - \rho_1)/\rho_1$ is the *reduced gravity*. The momentum equation becomes

$$\frac{\mathrm{D}\boldsymbol{u}}{\mathrm{D}t} + \boldsymbol{f} \times \boldsymbol{u} = g'\nabla\eta_1. \tag{3.38}$$

The equations are completed by the usual mass conservation equation,

$$\frac{\mathrm{D}h}{\mathrm{D}t} + h\nabla \cdot \boldsymbol{u} = 0, \tag{3.39}$$

where $h = \eta_0 - \eta_1$. Because $g \gg g'$, (3.37) shows that surface displacements are *much smaller* than the displacements at the interior interface. We see this in the real ocean where the mean interior isopycnal displacements may be several tens of meters but variations in the mean height of ocean surface are of order centimeters.

II *The rigid lid approximation*

The smallness of the upper surface displacement suggests that we will make little error is we impose a *rigid lid* at the top of the fluid. Displacements are no longer allowed, but the lid will in general impart a pressure force to the fluid. Suppose that this is $P(x, y, t)$, then the horizontal pressure gradient in the upper layer is simply

$$\nabla p_1 = \nabla P. \tag{3.40}$$

The pressure in the lower layer is again given by hydrostasy, and is

$$\begin{aligned} p_2 &= -\rho_1 g \eta_1 + \rho_2 g (\eta_1 - z) + P \\ &= \rho_1 g h - \rho_2 g (h + z) + P, \end{aligned} \tag{3.41}$$

so that

$$\nabla p_2 = -g(\rho_2 - \rho_1)\nabla h + \nabla P, \tag{3.42}$$

Then if $\nabla p_2 = 0$ we have

$$g(\rho_2 - \rho_1)\nabla h = \nabla P \tag{3.43}$$

and the momentum equation for the upper layer is just

$$\frac{D\boldsymbol{u}}{Dt} + \boldsymbol{f} \times \boldsymbol{u} = -g_1' \nabla h. \tag{3.44}$$

where $g' = g(\rho_2 - \rho_1)/\rho_1$. These equations differ from the usual shallow water equations only in the use of a reduced gravity g' in place of g itself. It is the *density difference* between the two layers that is important. Similarly, if we take a shallow water system, with the moving layer on the bottom, and we suppose that overlying it is a stationary fluid of finite density, then we would easily find that the fluid equations for the moving layer are the same as if the fluid on top had zero inertia, except that g would be replaced by an appropriate reduced gravity (problem 3.1).

3.3 MULTI-LAYER SHALLOW WATER EQUATIONS

We now consider the dynamics of multiple layers of fluid stacked on top of each other. This is a crude representation of continuous stratification, but it turns out to be a powerful model of many geophysically interesting phenomena as well as being physically realizable in the laboratory. The pressure is continuous across the interface, but the density jumps discontinuously and this allows the horizontal velocity to have a corresponding discontinuity. The set up is illustrated in Fig. 3.4.

In each layer pressure is given by the hydrostatic approximation, and so anywhere in the interior we can find the pressure by integrating down from the top. Thus, at a height z in the first layer we have

$$p_1 = \rho_1 g (\eta_0 - z), \tag{3.45}$$

and in the second layer,

$$p_2 = \rho_1 g (\eta_0 - \eta_1) + \rho_2 g (\eta_1 - z) = \rho_1 g \eta_0 + \rho_0 g_1' \eta_1 - \rho_2 g z, \tag{3.46}$$

Figure 3.4 The multi-layer shallow water system. The layers are numbered from the top down. The coordinates of the interfaces are denoted η, and the layer thicknesses h, so that $h_i = \eta_i - \eta_{i-1}$.
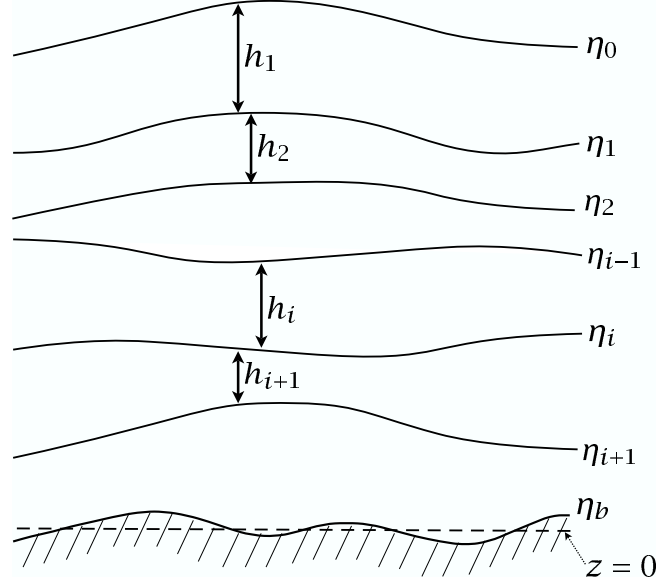
where $g_1' = g(\rho_2 - \rho_1)/\rho_1$, and so on. The term involving z is irrelevant for the dynamics, because only the horizontal derivative enters the equation of motion. Omitting this term, for the n'th layer the dynamical pressure is given by the sum from the top down:

$$p_n = \rho_1 \sum_{i=0}^{n-1} g_i' \eta_i, \tag{3.47}$$

where $g_i' = g(\rho_{i+1} - \rho_i)/\rho_1$ (taking $\rho_0 = 0$). This may be expressed in terms of the layer thicknesses by summing from the bottom up:

$$\eta_n = \eta_b + \sum_{i=n+1}^{i=N} h_i. \tag{3.48}$$

The momentum equation for each layer may then be written, in general,

$$\frac{D\boldsymbol{u}_n}{Dt} + \boldsymbol{f} \times \boldsymbol{u}_n = -\frac{1}{\rho_n} \nabla p_n, \tag{3.49}$$

where the pressure is given by (3.47) and in terms of the layer depths using (3.49). If we make the Boussinesq approximation then ρ_n on the right-hand side of (3.49) is replaced by ρ_1.

Finally, the mass conservation equation for each layer has the same form as the single-layer case, and is

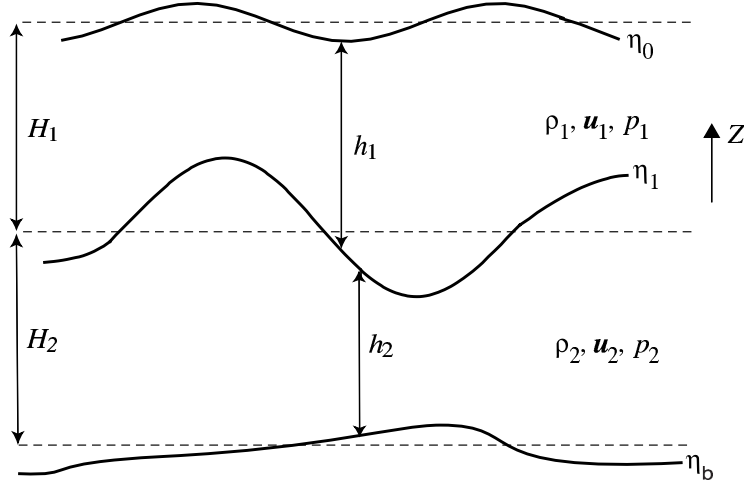$$\frac{Dh_n}{Dt} + h_n \nabla \cdot \boldsymbol{u}_n = 0. \tag{3.50}$$

Fig. 3.5 The two layer shallow water system. A fluid of density ρ_1 lies over a denser fluid of density ρ_2. In the reduced gravity case the lower layer may be arbitrarily thick and is assumed stationary and so has no horizontal pressure gradient. In the 'rigid-lid' approximation the top surface displacement is neglected, but there is then a non-zero pressure gradient induced by the lid.

The two- and three-layer cases

The two-layer model is the simplest model to capture the effects of stratification. Evaluating the pressures using (3.47) and (3.48) we find:

$$p_1 = \rho_1 g \eta_0 = \rho_1 g (h_1 + h_2 + \eta_b) \tag{3.51a}$$

$$p_2 = \rho_1 [g \eta_0 + g_1' \eta_1] = \rho_1 \left[g(h_1 + h_2 + \eta_b) + g_1'(h_2 + \eta_b) \right]. \tag{3.51b}$$

The momentum equations for the two layers are then

$$\frac{D\boldsymbol{u}_1}{Dt} + \boldsymbol{f} \times \boldsymbol{u}_1 = -g\nabla\eta_0 = -g\nabla(h_1 + h_2 + \eta_b). \tag{3.52a}$$

and in the bottom layer

$$\begin{aligned}
\frac{D\boldsymbol{u}_2}{Dt} + \boldsymbol{f} \times \boldsymbol{u}_2 &= -\frac{\rho_1}{\rho_2} \left(g\nabla\eta_0 + g_1'\nabla\eta_1 \right) \\
&= -\frac{\rho_1}{\rho_2} \left[g\nabla(\eta_b + h_1 + h_2) + g_1'\nabla(h_2 + \eta_b) \right]
\end{aligned} \tag{3.52b}$$

In the Boussinesq approximation ρ_1/ρ_2 is replaced by unity.

In a three layer model the dynamical pressures are found to be

$$p_1 = \rho_1 g h \tag{3.53a}$$

$$p_2 = \rho_1 \left[gh + g_1'(h_2 + h_3 + \eta_b) \right] \tag{3.53b}$$

$$p_3 = \rho_1 \left[gh + g_1'(h_2 + h_3 + \eta_b) + g_2'(h_3 + \eta_b) \right], \tag{3.53c}$$

where $h = \eta_0 = \eta_b + h_1 + h_2 + h_3$ and $g_2' = g(\rho_3 - \rho_2)/\rho_1$. More layers can obviously be added in a systematic fashion.

3.3.1 Reduced-gravity multi-layer equation

As with a single active layer, we may envision multiple layers of fluid overlying a deeper stationary layer. This is a useful model of the stratified upper ocean overlying a nearly stationary and nearly unstratified abyss. Indeed we use such a model to study the 'ventilated thermocline' in chapter 16 and a detailed treatment may be found there. If we suppose there is a lid at the top, then the model is almost the same as that of the previous section. However, now the horizontal pressure gradient in the lowest model layer is zero, and so we may obtain the pressures in all the active layers by integrating the hydrostatic equation upwards from this layer. Suppose we have N moving layers, then the reader may verify that the dynamic pressure in the n'th layer is given by

$$p_n = -\sum_{i=n}^{i=N} \rho_1 g_i' \eta_i \qquad (3.54)$$

where as before $g_i' = g(\rho_{i+1} - \rho_i)/\rho_1$. If we have a lid at the top, so that $\eta_0 = 0$, then the interface displacements are related to the layer thicknesses by

$$\eta_n = -\sum_{i=1}^{i=n} h_i. \qquad (3.55)$$

From these expressions the momentum equation in each layer is easily constructed.

3.4 GEOSTROPHIC BALANCE AND THERMAL WIND

Geostrophic balance occurs in the shallow water equations, just as in the continuously stratifed equations, when the Rossby number U/fL is small and the Coriolis term dominates the advective terms. In the single-layer shallow water equations the geostrophic flow is:

$$\boldsymbol{f} \times \boldsymbol{u}_g = -\nabla \eta \qquad (3.56)$$

Thus, the geostrophic velocity is proportional to the slope of the surface, as sketched in Fig. 3.6. (For the rest of this section, we will drop the subscript g, and take all velocites to be geostrophic.)

In both the single-layer and multi-layer case, the slope of an interfacial surface is directly related to the difference in pressure gradient on either side and so, by geostrophic balance, to the shear of the flow. This is the shallow water analog of the thermal wind relation. To obtain an expression for this, consider the interface, η, between two layers labelled 1 and 2. The pressure in two layers is given by the hydrostatic relation and so,

$$p_1 = A(x, y) - \rho_1 g z \qquad \text{(at some z in layer 1)} \qquad (3.57a)$$
$$\begin{aligned} p_2 &= A(x, y) - \rho_1 g \eta + \rho_2 g(\eta - z) \\ &= A(x, y) + \rho_1 g_1' \eta - \rho_2 g z \end{aligned} \qquad \text{(at some z in layer 2)} \qquad (3.57b)$$

where $A(x, y)$ is the pressure where $z = 0$, but we don't need to specifiy where this is. Thus we find

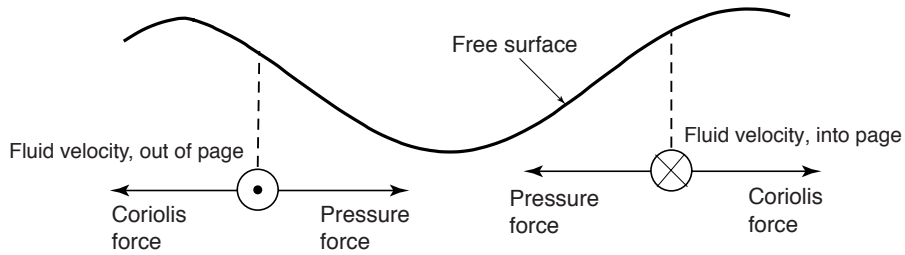$$\frac{1}{\rho_1} \nabla(p_1 - p_2) = -g_1' \nabla \eta. \qquad (3.58)$$

Fig. 3.6 Geostrophic flow in a shallow water system, with a positive value of the Coriolis parameter f, as in the Northern hemisphere. The pressure force is directed down the gradient of the height field, and this can be balanced by the Coriolis force if the fluid velocity is at right angles to it. If f were negative, the geostrophic flow would be reversed.

If the flow is geostrophically balanced and Boussinesq then, in each layer, the velocity obeys

$$f \boldsymbol{u}_i = \frac{1}{\rho_1} \mathbf{k} \times \nabla p_i. \tag{3.59}$$

Using (3.58) then gives

$$f(\boldsymbol{u}_1 - \boldsymbol{u}_2) = -\mathbf{k} \times g_1' \nabla \eta, \tag{3.60}$$

or in general

$$f(\boldsymbol{u}_n - \boldsymbol{u}_{n+1}) = \mathbf{k} \times g_n' \nabla \eta. \tag{3.61}$$

This is the thermal wind equation for the shallow water system. It applies at any interface, and it implies *the shear is proportional to the interface slope,* a result sometimes know as the 'Margules relation'.

Suppose that we represent the atmosphere by two layers of fluid then a meridionally decreasing temperature may be represented by an interface that slopes upward toward the pole, and in the Northern hemisphere $\partial \eta / \partial y > 0$. Then, in the northern hemisphere where f is positive we have

$$u_1 - u_2 = \frac{g_1}{f} \frac{\partial \eta}{\partial y} > 0, \tag{3.62}$$

and the temperature gradient is associated with a positive shear. (See problem 3.2.)

3.5 FORM DRAG

When the interface between two layers varies with position — that is, when it is wavy — the layers exert a pressure force on each other. Similarly, if the bottom is not flat then the topography and the bottom layer can exert forces on each other. This is known as *form drag,* and it is an important means whereby momentum can be added to or extracted from a flow.[2] Consider a layer confined between two interfaces, $\eta_1(x, y)$ and

$\eta_2(x, y)$. Then over some zonal interval L the average zonal pressure force on that fluid layer is given by

$$F_p = -\frac{1}{L} \int_{x_1}^{x_2} \int_{\eta_2}^{\eta_1} \frac{\partial p}{\partial x} \, \mathrm{d}x \, \mathrm{d}z. \qquad (3.63)$$

Integrating by parts first in z and then in x, and noting that by hydrostasy $\partial p/\partial z$ does not depend on horizontal position within the layer, we obtain

$$\begin{aligned}
F_p &= -\frac{1}{L} \int_{x_1}^{x_2} \left[\frac{\partial p}{\partial x} z \right]_{\eta_2}^{\eta_1} \mathrm{d}x \\
&= -\overline{\eta_1 \frac{\partial p_1}{\partial x}} + \overline{\eta_2 \frac{\partial p_2}{\partial x}} = +\overline{p_1 \frac{\partial \eta_1}{\partial x}} - \overline{p_2 \frac{\partial \eta_2}{\partial x}},
\end{aligned} \qquad (3.64)$$

where p_1 is the pressure at η_1, and similarly for p_2, and to obtain the second line we suppose that the integral is around a closed path, such as a circle of latitude, and the average is denoted with an overbar. These terms represent the transfer of momentum from one layer to the next, and at a particular interface, i, we may define the form drag, τ_i, by

$$\tau_i \equiv \overline{p_i \frac{\partial \eta_i}{\partial x}} = -\overline{\eta_i \frac{\partial p_i}{\partial x}}. \qquad (3.65)$$

The form drag is a stress, and as the layer depth shrinks to zero its vertical derivative, $\partial \tau/\partial z$, is the force on the fluid. It is a particularly important mechanism for the vertical transfer of momentum and its ultimate removal in an eddying fluid, and it one of the the main mechanisms wherby the wind stress at the top of the ocean is communicated to the ocean bottom. At the fluid bottom the form drag is $\overline{p\eta_{bx}}$, where η_b is the bottom topography, and this is proportional to the momentum exchange with the solid earth. This is a significant mechanism for the ultimate removal of momentum in the ocean, especially in the Antarctic Circumpolar Current where it is likely to be much larger than bottom (Ekman) drag arising from small scale turbulence and friction. In the two layer, flat-bottomed case the only form drag occurring as that at the interface, and the momentum transfer between the layers is just $\overline{p_1 \partial \eta_1/\partial x}$ or $-\overline{\eta_1 \partial p/\partial x}$; then, the force on each layer due to the other is equal and opposite, as we would expect from momentum conservation.

For flows in geostrophic balance, the form drag is closely related to the meridional heat flux. The pressure gradient and velocity are related by $\rho f v' = \partial p'/\partial x$ and the interfacial displacement is proportional to the temperature perturbation, b' (in fact one may show that $\eta' \approx -b'/(\partial \overline{b}/\partial z)$). Thus $-\overline{\eta' \partial p'_\eta/\partial x} \propto \overline{v'b'}$, a correspondence that will re-occur when we consider the *Eliassen-Palm flux* in chapter 7.

3.6 CONSERVATION PROPERTIES OF SHALLOW WATER SYSTEMS

There are two common types of conservation property in fluids: (i) material invariants, and (ii) integral invariants. Material invariance occurs when a property (ϕ say) is conserved on each fluid element, and so obeys the equation $\mathrm{D}\phi/\mathrm{D}t = 0$. An integral invariant is one that is conserved when integrated over some volume, usually closed; energy is an example.

3.6.1 A material invariant: potential vorticity

The vorticity of a fluid (considered at greater length in chapter 4), denoted $\boldsymbol{\omega}$, is defined to be the curl of the velocity field, so that

$$\boldsymbol{\omega} \equiv \nabla \times \boldsymbol{v} \tag{3.66}$$

Let us also define the shallow water vorticity, $\boldsymbol{\omega}^*$, as the curl of the horizontal velocity, so that

$$\boldsymbol{\omega}^* \equiv \nabla \times \boldsymbol{u} \tag{3.67}$$

and, because $\partial u/\partial z = \partial v/\partial z = 0$, only its vertical component is non-zero and

$$\boldsymbol{\omega}^* = \mathbf{k}\left(\frac{\partial v}{\partial x} - \frac{\partial u}{\partial y}\right) \equiv \mathbf{k}\,\zeta. \tag{3.68}$$

Using the vector identity

$$(\boldsymbol{u} \cdot \nabla)\boldsymbol{u} = \frac{1}{2}\nabla(\boldsymbol{u} \cdot \boldsymbol{u}) - \boldsymbol{u} \times (\nabla \times \boldsymbol{u}), \tag{3.69}$$

we write the momentum equation (3.8) as

$$\frac{\partial \boldsymbol{u}}{\partial t} + \boldsymbol{\omega}^* \times \boldsymbol{u} = -\nabla(gh + \frac{1}{2}\boldsymbol{u}^2). \tag{3.70}$$

To obtain an evolution equation for the vorticity we take the curl of (3.70), and make use of the vector identity

$$\nabla \times (\boldsymbol{\omega}^* \times \boldsymbol{u}) = (\boldsymbol{u} \cdot \nabla)\boldsymbol{\omega}^* - (\boldsymbol{\omega}^* \cdot \nabla)\boldsymbol{u} + \boldsymbol{\omega}^* \nabla \cdot \boldsymbol{u} - \boldsymbol{u}\nabla \cdot \boldsymbol{\omega}^*$$
$$= (\boldsymbol{u} \cdot \nabla)\boldsymbol{\omega}^* + \boldsymbol{\omega}^* \nabla \cdot \boldsymbol{u}, \tag{3.71}$$

where $\nabla \cdot \boldsymbol{\omega}^*$ is the divergence of a curl and therefore zero, and $(\boldsymbol{\omega}^* \cdot \nabla)\boldsymbol{u} = 0$ because $\boldsymbol{\omega}^*$ is perpendicular to any direction in which $\boldsymbol{u}$ varies. The curl of (3.70) is then

$$\frac{\partial \boldsymbol{\omega}^*}{\partial t} + (\boldsymbol{u} \cdot \nabla)\boldsymbol{\omega} = -\boldsymbol{\omega}^* \nabla \cdot \boldsymbol{u}, \tag{3.72}$$

or

$$\frac{\partial \zeta}{\partial t} + (\boldsymbol{u} \cdot \nabla)\zeta = -\zeta\nabla \cdot \boldsymbol{u}. \tag{3.73}$$

where $\zeta = \mathbf{k} \cdot \boldsymbol{\omega}^*$. However, the mass conservation equation may be written as

$$-\zeta\nabla \cdot \boldsymbol{u} = \frac{\zeta}{h}\frac{Dh}{Dt}. \tag{3.74}$$

Thus, (3.73) becomes

$$\frac{D\zeta}{Dt} = \frac{\zeta}{h}\frac{Dh}{Dt}, \tag{3.75}$$

which simplifies to

$$\frac{D}{Dt}\left(\frac{\zeta}{h}\right) = 0. \tag{3.76}$$

The important quantity ζ/h, often denoted Q, is known as the *potential vorticity*, and (3.76) is known as the potential vorticity equation. We re-derive this conservation law in a more general way in section 4.6

Because Q is conserved on parcels, then so is any function of Q; that is, $F(Q)$ is a material invariant, where F is any function. To see this algebraically, multiply (3.76) by $F'(Q)$, the derivative of F with respect to Q, giving

$$F'(Q)\frac{\mathrm{D}Q}{\mathrm{D}t} = \frac{\mathrm{D}}{\mathrm{D}t}F(Q) = 0. \tag{3.77}$$

Since F is arbitrary there are an infinite number of Lagrangian invariants corresponding to different choices of F.

Effects of rotation

In a rotating frame of reference, the shallow water momentum equation is

$$\frac{\mathrm{D}\boldsymbol{u}}{\mathrm{D}t} + \boldsymbol{f} \times \boldsymbol{u} = -g\nabla h, \tag{3.78}$$

where (as before) $\boldsymbol{f} = f\mathbf{k}$. This may be written in vector invariant form as

$$\frac{\partial \boldsymbol{u}}{\partial t} + (\boldsymbol{\omega}^* + \boldsymbol{f}) \times \boldsymbol{u} = -\nabla(gh + \frac{1}{2}\boldsymbol{u}^2), \tag{3.79}$$

and taking the curl of this gives the vorticity equation

$$\frac{\partial \zeta}{\partial t} + (\boldsymbol{u} \cdot \nabla)(\zeta + f) = -(f + \zeta)\nabla \cdot \boldsymbol{u}. \tag{3.80}$$

This is the same as the shallow water vorticity equation in a non-rotating frame, save that ζ is replaced by $\zeta + f$, the reason for this being that f is the vorticity that the fluid has by virtue of the background rotation. Thus, (3.80) is simply the equation of motion for the total or absolute vorticity, $\boldsymbol{\omega}_a = \boldsymbol{\omega}^* + \boldsymbol{f} = (\zeta + f)\mathbf{k}$.

The potential vorticity equation in the rotating case follows, much as in non-rotating case, by combining (3.80) with the mass conservation equation, giving

$$\boxed{\frac{\mathrm{D}}{\mathrm{D}t}\left(\frac{\zeta + f}{h}\right) = 0}. \tag{3.81}$$

That is, $Q \equiv (\zeta + f)/h$, the potential vorticity in a rotating shallow system, is a material invariant. (We use the same symbol for potential vorticity in both rotating and non-rotating cases).

Vorticity and circulation

Although vorticity itself is not a material invariant, its integral over a horizontal material area is. To demonstrate this in the non-rotating case, consider the integral

$$C = \int_A \zeta\, \mathrm{d}A = \int_A Qh\, \mathrm{d}A, \tag{3.82}$$

over a surface 'A', the cross-sectional area of a column of height h (as in Fig. 3.2). Taking the material derivative of this gives

$$\frac{\mathrm{D}C}{\mathrm{D}t} = \int_A \frac{\mathrm{D}Q}{\mathrm{D}t} h \, \mathrm{d}A + \int_A Q \frac{\mathrm{D}}{\mathrm{D}t}(h \, \mathrm{d}A). \tag{3.83}$$

The first term is zero, by (3.75); the second term is just the derivative of the volume of a column of fluid and it too is zero, by mass conservation. Thus,

$$\frac{\mathrm{D}C}{\mathrm{D}t} = \frac{\mathrm{D}}{\mathrm{D}t} \int_A \zeta \, \mathrm{d}A = 0 \tag{3.84}$$

Thus, the integral of the vorticity over a some cross-sectional area of the fluid is unchanging, although both the vorticity and area of the fluid may individually change. Using Stokes' theorem, it may be written

$$\frac{\mathrm{D}C}{\mathrm{D}t} = \frac{\mathrm{D}}{\mathrm{D}t} \oint \boldsymbol{u} \cdot \mathrm{d}\boldsymbol{l} \tag{3.85}$$

where the line integral is around the boundary of 'A'. This is an example of Kelvin's circulation theorem, which we shall meet again in more general form in chapter 4, where we also consider the rotating case.

A slight generalization of (3.84) is possible. Consider the integral $I = \int F(Q) h \, \mathrm{d}A$ where again F is any differentiable function of its argument. It is clear that

$$\frac{\mathrm{D}}{\mathrm{D}t} \int_A F(Q) h \, \mathrm{d}A = 0. \tag{3.86}$$

If the area of integration in (3.70) or (3.86) is the whole domain (enclosed by frictionless walls, for example) then it is clear that the integral of $h F(Q)$ is a constant, including as a special case the integral of ζ.

3.6.2 Energy conservation — an integral invariant

Since we have made various simplifications in deriving the shallow water system, it is not self-evident that energy should be conserved, or indeed what form the energy takes. The kinetic energy density, that is the kinetic energy per unit area, is $\rho h \boldsymbol{u}^2 / 2$. The potential energy density of the fluid is

$$PE = \int_0^h \rho_0 g z \, \mathrm{d}z = \frac{1}{2} \rho_0 g h^2 \tag{3.87}$$

The factor ρ_0 appears in both kinetic and potential energies and, because it is a constant, we will omit it.

Using the mass conservation equation (3.15) we obtain an equation for the evolution of potential energy density:

$$\frac{\mathrm{D}}{\mathrm{D}t} \frac{g h^2}{2} + g h^2 \nabla \cdot \boldsymbol{u} = 0 \tag{3.88a}$$

or

$$\frac{\partial}{\partial t}\frac{gh^2}{2} + \nabla \cdot \left(\boldsymbol{u}\frac{gh^2}{2}\right) + \frac{gh^2}{2}\nabla \cdot \boldsymbol{u} = 0. \tag{3.88b}$$

From the momentum and mass continuity equations we obtain an equation for the evolution of kinetic energy density, namely

$$\frac{\mathrm{D}}{\mathrm{D}t}\frac{h\boldsymbol{u}^2}{2} + \frac{\boldsymbol{u}^2 h}{2}\nabla \cdot \boldsymbol{u} = -g\boldsymbol{u} \cdot \nabla\frac{h^2}{2} \tag{3.89a}$$

or

$$\frac{\partial}{\partial t}\frac{h\boldsymbol{u}^2}{2} + \nabla \cdot \left(\boldsymbol{u}\frac{h\boldsymbol{u}^2}{2}\right) + g\boldsymbol{u} \cdot \nabla\frac{h^2}{2} = 0. \tag{3.89b}$$

Adding (3.88b) and (3.89b) we obtain

$$\frac{\partial}{\partial t}\frac{1}{2}\left(h\boldsymbol{u}^2 + gh^2\right) + \nabla \cdot \left[\frac{1}{2}\boldsymbol{u}\left(gh^2 + h\boldsymbol{u}^2 + gh^2\right)\right] = 0 \tag{3.90}$$

or

$$\frac{\partial E}{\partial t} + \nabla \cdot \boldsymbol{F} = 0 \tag{3.91}$$

where $E = KE + PE = (h\boldsymbol{u}^2 + gh^2)/2$ is the density of the total energy and $\boldsymbol{F} = \boldsymbol{u}(h\boldsymbol{u}^2 + gh^2 + gh^2)/2$ is the energy flux. If the fluid is confined to a domain bounded by rigid walls, on which the normal component of velocity vanishes, then on integrating (3.90) over that area and using Gauss's theorem, the total energy is seen to be conserved; that is

$$\frac{\mathrm{d}\widehat{E}}{\mathrm{d}t} = \frac{1}{2}\frac{\mathrm{d}}{\mathrm{d}t}\int_A (h\boldsymbol{u}^2 + gh^2)\,\mathrm{d}A = 0. \tag{3.92}$$

Such an energy principle also holds in the case with bottom topography. Note that, as we found in the case for a compressible fluid in chapter 2, the energy flux in (3.91) is not just the energy density multiplied by the velocity but it contains an additional term $g\boldsymbol{u}h^2/2$, and this represents the energy transfer occurring when the fluid does work against the pressure force (see problem 3.3).

3.7 SHALLOW WATER WAVES

3.7.1 Non-rotating

To first understand the basic properties of wave motion in shallow water, we linearize the equations around a mean height H, and a state of rest. Thus let

$$h(x, y, t) = H + h'(x, y, t), \tag{3.93a}$$
$$\boldsymbol{u}(x, y, t) = \boldsymbol{u}'(x, y, t). \tag{3.93b}$$

The mass conservation equation becomes

$$\frac{\partial h'}{\partial t} + (H + h')\nabla \cdot \boldsymbol{u} + \boldsymbol{u}' \cdot \nabla h' = 0, \tag{3.94}$$

and neglecting squares of small quantities this becomes

$$\frac{\partial h'}{\partial t} + H\nabla \cdot \boldsymbol{u}' = 0. \tag{3.95}$$

The advective terms drop out of the momentum equation, since we are linearizing around a state of rest, yielding

$$\frac{\partial \boldsymbol{u}'}{\partial t} = -g\nabla h'. \tag{3.96}$$

For the remainder of the section we will drop the primes on the linearized fields.

Eliminating velocity by differentiating (3.95) with respect to time and taking the divergence of (3.96) leads to

$$\frac{\partial^2 h}{\partial t^2} - gH\nabla^2 h = 0 \tag{3.97}$$

which may be recognized as a wave equation. We can find the dispersion relationship for this by substituting the trial solution

$$h = \operatorname{Re} h_0 e^{i(\boldsymbol{k}\cdot\boldsymbol{x}-\omega t)} \tag{3.98}$$

where h_0 is a complex constant, $\boldsymbol{k} = \mathbf{i}k + \mathbf{j}l$ is the horizontal wavenumber, and Re indicates that the real part of the solution should be taken. If for simplicity we restrict attention for the moment to the one-dimensional problem, with no variation in the y-direction, then substituting into (3.97) leads to the dispersion relationship

$$\omega = \pm ck, \tag{3.99}$$

where $c = \sqrt{gH}$. That is, the wave speed is proportional to the square root of the mean fluid depth and is independent of the wavenumber — that is, the waves are dispersionless. The general solution is a superposition of all such waves, with the amplitudes of each wave (or Fourier component) being determined by the Fourier decomposition of the initial conditions.

Because the waves are dispersionless, the general solution can be written

$$h(x,t) = \frac{1}{2}\left[F(x-ct) + F(x+ct)\right] \tag{3.100}$$

where $F(x)$ is the height field at $t = 0$. From this, it is easy to see that the shape of an initial disturbance is preserved as it propagates both to the right and to the left at speed c. (See also problem 3.7.)

3.7.2 Rotating, constant Coriolis parameter

Linearizing the rotating, flat-bottomed shallow water equations about a state of rest we obtain

$$\frac{\partial u}{\partial t} - f_0 v = -g\frac{\partial h}{\partial x}, \tag{3.101a}$$

$$\frac{\partial v}{\partial t} + f_0 u = -g\frac{\partial h}{\partial x}, \tag{3.101b}$$

$$\frac{\partial h}{\partial t} + H(u_x + v_y) = 0. \tag{3.101c}$$

We nondimensionalize these equations with length- and time-scales L and T respectively, so that $U = L/T$, and nondimensionalize the surface height deviation by the depth of the fluid, H. The equations become

$$\frac{\partial \widehat{u}}{\partial \widehat{t}} - \widehat{f}_0 \widehat{v} = -\widehat{c}^2 \frac{\partial \widehat{h}}{\partial \widehat{x}}, \tag{3.102a}$$

$$\frac{\partial \widehat{v}}{\partial \widehat{t}} + \widehat{f}_0 \widehat{u} = -\widehat{c}^2 \frac{\partial \widehat{h}}{\partial \widehat{y}}, \tag{3.102b}$$

$$\frac{\partial \widehat{h}}{\partial \widehat{t}} + (\widehat{u}_{\widehat{x}} + \widehat{v}_{\widehat{y}}) = 0. \tag{3.102c}$$

All the variables with hats on are nondimensional, and $\widehat{f}_0 = f_0 T$ and $\widehat{c} = \sqrt{gH}/U$ is the nondimensional speed of nonrotating shallow-water waves. (It is also the inverse of the Froude number $U/\sqrt{gH}$.) To obtain a dispersion relationship we let

$$(\widehat{u}, \widehat{v}, \widehat{h}) = (u_0, v_0, h_0)e^{i(\widehat{\boldsymbol{k}}\cdot\widehat{\boldsymbol{x}} - \widehat{\omega}\widehat{t})}, \tag{3.103}$$

where $\widehat{\boldsymbol{k}} = \widehat{k}\mathbf{i} + \widehat{l}\mathbf{j}$ and $\widehat{\omega}$ is the nondimensional frequency, and substitute into (3.102), giving

$$\begin{pmatrix} i\widehat{\omega} & -\widehat{f}_0 & i\widehat{c}^2\widehat{k} \\ \widehat{f}_0 & i\widehat{\omega} & i\widehat{c}^2\widehat{l} \\ i\widehat{k} & i\widehat{l} & i\widehat{\omega} \end{pmatrix} \begin{pmatrix} u_0 \\ v_0 \\ h_0 \end{pmatrix} = 0. \tag{3.104}$$

This homogeneous equation has nontrivial solutions only if the determinant of the matrix vanishes. This gives

$$\widehat{\omega}(\widehat{\omega}^2 - \widehat{f}_0^2 - \widehat{c}^2\widehat{K}^2) = 0. \tag{3.105}$$

where $\widehat{K}^2 = \widehat{k}^2 + \widehat{l}^2$. There are two classes of solution to (3.105). The first is simply $\widehat{\omega} = 0$, time-independent flow corresponding to geostrophic balance in (3.101). (Because geostrophic balance gives a divergence-free velocity field for constant Coriolis parameter the equations are satisfied by a time-independent solution.) The second set of solutions is given by

$$\widehat{\omega}^2 = \widehat{f}_0^2 + \widehat{c}^2(\widehat{k}^2 + \widehat{l}^2). \tag{3.106}$$

In dimensional form this equation is

$$\boxed{\omega^2 = f_0^2 + gH(k^2 + l^2)} \tag{3.107}$$

The corresponding waves are known as *Poincaré* waves, and the dispersion relationship is illustrated in Fig. 3.7.[3] Note that the frequency is always greater than the Coriolis frequency f_0. There are two interesting limits:
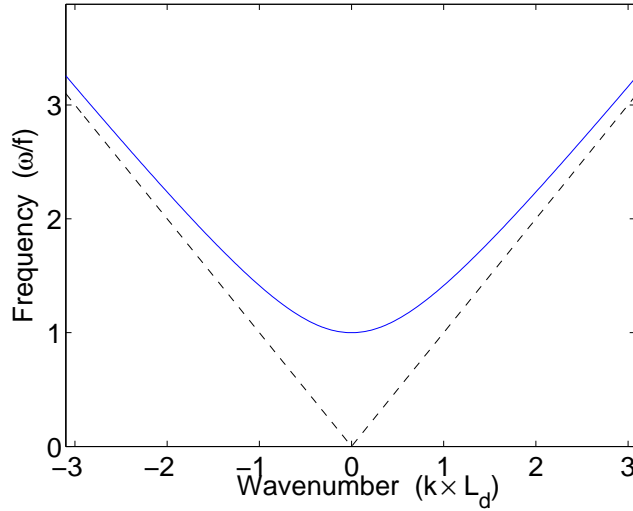
Fig. 3.7 Dispersion relation for Poincaré waves (solid line) and nonrotating shallow water waves (dashed line). The frequency is normalized by the Coriolis frequency f and the wavenumber by the (inverse) deformation radius $\sqrt{gH}/f$. The frequency is always greater than f. For long waves (small wavenumbers) the frequency is approximately f, as for inertial oscillations. For short waves (high wavenumbers) the frequency asymptotes to that of nonrotating shallow water waves, namely (in dimensional form) $\sqrt{gH}k$.

(i) The short waves limit: If

$$K^2 \gg \frac{f_0^2}{gH} \tag{3.108}$$

where $K^2 = k^2 + l^2$, then the dispersion relationship reduces to that of the nonrotating case (3.99). This condition is equivalent to requiring that the wavelength be much shorter than the deformation radius, L_d. Specifically, if $l = 0$ and $\lambda = 2\pi/k$ is the wavelength, the condition is

$$\lambda^2 \ll L_d^2(2\pi)^2 \tag{3.109}$$

The numerical factor of $(2\pi)^2$ is more than an order of magnitude, so care must be taken when deciding if the condition is satisfied in particular cases. Furthermore, the wavelength must still be longer than the depth of the fluid, else the shallow water condition is not met.

(ii) The long wave limit: If

$$K^2 \ll \frac{f_0^2}{gH}, \tag{3.110}$$

that is if the wavelength is much longer than the deformation radius L_d, then the

dispersion relationship is

$$\omega = f_0. \tag{3.111}$$

These are known as *inertial oscillations.* The equations of motion giving rise to them are

$$\frac{\partial u}{\partial t} - f_0 v = 0, \qquad \frac{\partial v}{\partial t} + f_0 u = 0, \tag{3.112}$$

which are equivalent to Lagrangian equations for free particles in a rotating frame, namely

$$\frac{\mathrm{d}^2 x}{\mathrm{d}t^2} - f_0 v = 0, \qquad \frac{\mathrm{d}^2 y}{\mathrm{d}t^2} + f_0 u = 0. \tag{3.113}$$

In this limit fluid parcels are thus undergoing free, inertial, oscillations in the rotating coordinate system, unrestrained by pressure forces (see problem 3.9).

3.7.3 Kelvin waves

The Kelvin wave is a particular type of gravity wave that exists in the presence of both rotation and a lateral boundary. Suppose there is a solid boundary at $y = 0$; clearly harmonic solutions in the y-direction are not allowable, as these would not satisfy the condition of no-normal flow at the boundary. Do any wavelike solutions exist? The affirmative answer to this question was provided by Kelvin and the associated waves are now eponymously known as *Kelvin waves.*[4]

We begin with the linearized shallow water equations

$$\frac{\partial u}{\partial t} - f_0 v = -g\frac{\partial \eta}{\partial x}, \qquad \frac{\partial v}{\partial t} + f_0 u = -g\frac{\partial \eta}{\partial y}, \tag{3.114a,b}$$

$$\frac{\partial \eta}{\partial t} + H\left(\frac{\partial u}{\partial x} + \frac{\partial v}{\partial y}\right) = 0. \tag{3.115}$$

The fact that $v = 0$ at $x = 0$ suggests that we look for a solution with $v = 0$ everywhere, whence the equations become

$$\frac{\partial u}{\partial t} = -g\frac{\partial \eta}{\partial x}, \quad f_0 u = -g\frac{\partial \eta}{\partial y}, \tag{3.116a,b}$$

$$\frac{\partial \eta}{\partial t} + H\frac{\partial u}{\partial x} = 0. \tag{3.117}$$

Equations (3.116a) and (3.117) lead to the standard wave equation

$$\frac{\partial^2 u}{\partial t^2} = c^2 \frac{\partial^2 u}{\partial x^2}, \tag{3.118}$$

where $c = \sqrt{gH}$, the usual wave speed of shallow water waves. The solution of (3.118) is

$$u = F_1(x + ct, y) + F_2(x - ct, y), \tag{3.119}$$

with corresponding surface displacement

$$\eta = \sqrt{H/g}\,[-F_1(x+ct,y) + F_2(x-ct,y)]. \tag{3.120}$$

The solution represents the superposition of two waves, one (F_1) travelling in the negative x-direction, and the other in the positive x-direction. To obtain the y-dependence of these functions we use (3.116b) which gives

$$\frac{\partial F_1}{\partial y} = \frac{f_0}{\sqrt{gH}} F_1, \qquad \frac{\partial F_2}{\partial y} = -\frac{f_0}{\sqrt{gH}} F_2, \tag{3.121}$$

with solutions

$$F_1 = F(x+ct)e^{y/L_d} \qquad F_2 = G(x-ct)e^{-y/L_d}, \tag{3.122}$$

where $L_d = \sqrt{gH}/f_0$ is the radius of deformation. The solution F_1 grows exponentially away from the wall, and so fails to satisfy the condition of boundedness at infinity. It must be thus eliminated, leaving the general solution

$$u = e^{-yu/L_d}G(x-ct), \quad v = 0, \tag{3.123a}$$

$$\eta = \sqrt{H/g}e^{-yu/L_d}G(x-ct). \tag{3.123b}$$

The solution thus decays exponentially away from the boundary. If f_0 is positive, as in the Northern hemisphere, the boundary is to the right of an observer moving with the wave. Given a constant Coriolis parameter, we could equally well have obtained a solution on a meridional wall, in which case we would find that the wave again moves such that the wall is to the right of the wave direction. (This is obvious once it is realized that f-plane dynamics are isotropic in x and y.). Thus, in the Northern Hemisphere the wave moves anticlockwise round a basin, and conversely in the Southern Hemisphere, and in both hemispheres the direction is cyclonic.

3.8 GEOSTROPHIC ADJUSTMENT

We noted in chapter 2 that the large-scale, extra-tropical circulation of the atmosphere is in near-geostrophic balance. Why is this? Why should the Rossby number be small? Arguably, the magnitude of the velocity in the atmosphere and ocean is ultimately given by the strength of the forcing, and so ultimately by the differential heating between pole and equator (although even this argument is not satisfactory, since the forcing mainly determines the energy throughput, not directly the energy itself, and the forcing is itself dependent on the atmosphere's response). But even supposing that the velocity magnitudes are given, there is no *a priori* guarantee that the forcing or the dynamics will produce length-scales that are such that the Rossby number is small. In fact, there is a powerful and ubiquitious process whereby a fluid in an initially unbalanced state naturally evolves toward a state of geostrophic balance, namely *geostrophic adjustment*. This process occurs quite generally in rotating fluids, stratified or not. To pose the problem in a simple form we will consider the free evolution of a single shallow layer

of fluid whose initial state is manifestly unbalanced, and we will suppose that surface displacements are small so that the evolution of the system is described by the linearized shallow equations of motion. These are

$$\frac{\partial \boldsymbol{u}}{\partial t} + \boldsymbol{f} \times \boldsymbol{u} = -g\nabla\eta, \qquad \frac{\partial \eta}{\partial t} + H\nabla \cdot \boldsymbol{u} = 0, \qquad (3.124)$$

where η is the free surface displacement and H is the mean fluid depth, and we omit the primes on the linearized variables.

3.8.1 Non-rotating flow

We consider first the non-rotating problem set, with little loss of generality, in one dimension. We suppose that initially the fluid is at rest but with a simple discontinuity in the height field so that

$$\eta(x, t = 0) = \begin{cases} +\eta_0 & x < 0 \\ -\eta_0 & x > 0 \end{cases} \qquad (3.125)$$

and $u(x, t = 0) = 0$ everywhere. We can physically realize these initial conditions by separating two fluid masses of different depths by a thin dividing wall, and then quickly removing the wall. What is the subsequent evolution of the fluid? The general solution to the linear problem is given by (3.100) where the functional form is determined by the initial conditions so that here

$$F(x) = \eta(x, t = 0) = -\eta_0 \text{sgn}(x). \qquad (3.126)$$

Equation (3.100) states that this initial pattern is propagated to the right and to the left. That is, two discontinuities in fluid height simply propagate to the right and left at a speed $c = \sqrt{gH}$. Specifically, the solution is

$$\eta(x, t) = -\frac{1}{2}\eta_0[\text{sgn}(x + ct) + \text{sgn}(x - ct)] \qquad (3.127)$$

The initial conditions may be much more complex than a simple front, but, because the waves are dispersionless, the solution is still simply a sum of the translation of those initial conditions to the right and to the left at speed c. The velocity field in this class of problem is obtained from

$$\frac{\partial u}{\partial t} = -g\frac{\partial \eta}{\partial x} \qquad (3.128)$$

giving

$$u = \frac{g}{2c}[F(x + ct) - F(x - ct)] \qquad (3.129)$$

Thus, at a given location, away from the initial disturbance, the fluid remains at rest and undisturbed until the fronts arrive. After the fronts have passed, the fluid is again at rest. Ultimately, then, all the kinetic energy of the fluid is propagated away to infinity.

3.8.2 Rotating flow — the Rossby-Gill problem

Rotation makes a profound difference to the adjustment problem of the shallow water system, because a steady, adjusted, solution can exist with nonzero gradients in the height field, because the pressure field can be balanced by the Coriolis force. We will find also find that potential vorticity conservation provides powerful constraint on the fluid evolution. In a rotating shallow fluid that conservation is represented by

$$\frac{\partial Q}{\partial t} + \boldsymbol{u} \cdot \nabla Q = 0, \tag{3.130}$$

where $Q = (\zeta + f)/h$. In the linear case with constant Coriolis parameter (3.130) becomes

$$\frac{\partial q}{\partial t} = 0, \qquad q = \left(\zeta - f_0 \frac{\eta}{H}\right). \tag{3.131}$$

This equation may be obtained either from the linearized velocity and mass conservation equations, (3.124), or from the (3.130) directly. In the latter case, we write

$$Q = \frac{\zeta + f_0}{H + \eta} \approx \frac{1}{H}(\zeta + f_0)\left(1 - \frac{\eta}{H}\right) \approx \frac{1}{H}\left(f_0 + \zeta - f_0\frac{\eta}{H}\right) = \frac{f_0}{H} + \frac{q}{H} \tag{3.132}$$

having used $f_0 \gg |\zeta|$ and $H \gg |\eta|$. The term f_0/H is a constant and so dynamically unimportant, as is the H^{-1} factor multiplying q. Further, the advective term $\boldsymbol{u} \cdot \nabla Q$ becomes $\boldsymbol{u} \cdot \nabla q$, and this is second order in perturbed quantities and so is neglected. Thus, making these approximations, (3.130) reduces to (3.131). The potential vorticity field is therefore fixed in space! Of course, this was also true in the nonrotating case where the fluid is initially at rest. Then $\zeta = 0$ and the fluid remains irrotational throughout the subsequent evolution of the flow. However, this is rather a weak constraint on the subsequent evolution of the fluid; it does nothing, for example, to prevent all the kinetic energy of the fluid being radiated to infinity. However, in the rotating case the potential vorticity is non-zero, and potential vorticity conservation and geostrophic balance are all we need to infer the final steady state, assuming it exists, without solving for the details of the flow evolution, as we now see.

   With an initial condition for the height field given by (3.125), the initial potential vorticity is given by

$$q(x, y) = \begin{cases} -f_0\eta_0/H & x < 0 \\ f_0\eta_0/H & x > 0, \end{cases} \tag{3.133}$$

and this remains unchanged throughout the adjustment process. The final steady state is then the solution of the equations

$$\zeta - f_0\frac{\eta}{H} = q(x, y), \qquad f_0 u = -g\frac{\partial \eta}{\partial y}, \qquad f_0 v = g\frac{\partial \eta}{\partial x}, \tag{3.134a,b,c}$$

where $\zeta = \partial v/\partial x - \partial u/\partial y$. Because the Coriolis parameter is constant, the velocity
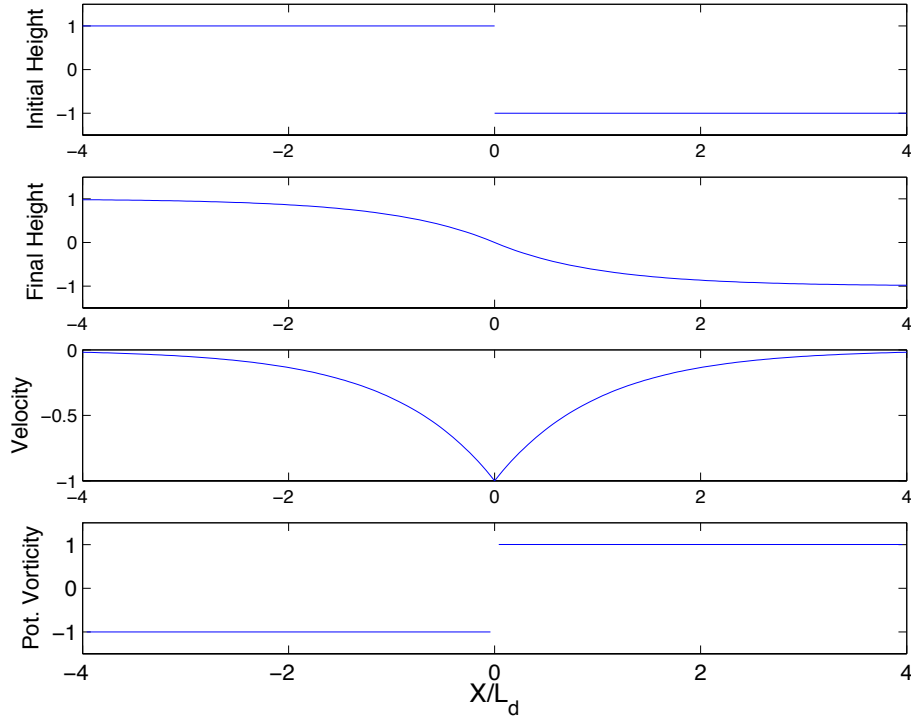
Fig. 3.8 Solutions of a linear geostrophic adjustment problem. Top panel: the initial height field, given by (3.125) with $\eta_0 = 1$. Second panel: equilibrium height field, η given by (3.137) and $\eta = f_0\psi/g$. Third panel: equilibrium geostrophic velocity (normal to the gradient of height field), given by (3.138). Bottom panel: potential vorticity, given by (3.133), and this does note evolve. The distance, x is non-dimensionalized by the deformation radius $L_d = \sqrt{gH}/f_0$, and the velocity by $\eta_0(g/f_0L_d)$. Changes to the initial state occur only within $\mathcal{O}(L_d)$ of the initial discontinuity; and as $x \to \pm\infty$ the initial state is unaltered.

field is horizontally non-divergent and we may define a streamfunction $\psi = g\eta/f_0$. Equations (3.134) then reduce to

$$\left(\nabla^2 - \frac{1}{L_d^2}\right)\psi = q(x, y), \tag{3.135}$$

where $L_d = \sqrt{gH}/f_0$ is known as the *Rossby radius of deformation* or often just the 'deformation radius' or the 'Rossby radius'. It is a naturally occurring length-scale in problems involving both rotation and gravity, and arises in slightly different form in stratified fluids.

The initial conditions (3.133) admit of a nice analytic solution, for the flow will

remain uniform in y, and (3.135) reduces to

$$\frac{\partial^2 \psi}{\partial x^2} - \frac{1}{L_d^2}\psi = -\frac{f_0 \eta_0}{H}\operatorname{sgn}(x). \tag{3.136}$$

We solve this separately for $x > 0$ and $x < 0$ and then match the solutions and their first derivatives at $x = 0$, imposing also the condition that the streamfunction decay to zero as $x \to \pm\infty$. The solution is

$$\psi = \begin{cases} -(g\eta_0/f_0)(1 - e^{-x/L_d}) & x > 0 \\ +(g\eta_0/f_0)(1 - e^{x/L_d}) & x < 0. \end{cases} \tag{3.137}$$

The velocity field associated with this is obtained from (3.134b,c), and is

$$u = 0, \qquad v = -\frac{g\eta_0}{fL_d}e^{-|x|/L_d}. \tag{3.138}$$

The velocity is perpendicular to the slope of the free surface, and a jet forms along the initial discontinuity, as illustrated in Fig. 3.8.

The important point of this problem is that the variations in the height and field are not radiated away to infinity, as in the non-rotating problem. Rather, potential vorticity conservation constrains the influence of the adjustment to within a deformation radius (we see now why this name is appropriate) of the initial disturbance. This property is a general one in geostrophic adjustment — it also arises if the initial condition consists of a velocity jump, as considered in problem 3.11.

3.8.3 Energetics of adjustment

How much of the initial potential energy of the flow is lost to infinity by gravity wave radiation, and how much is converted to kinetic energy? The linear equations (3.124) satisfy

$$\frac{1}{2}\frac{\partial}{\partial t}(H\boldsymbol{u}^2 + g\eta^2) + gH\nabla \cdot (\boldsymbol{u}\eta) = 0, \tag{3.139}$$

so that energy conservation holds in the form

$$E = \frac{1}{2}\int (H\boldsymbol{u}^2 + g\eta^2)\,\mathrm{d}\boldsymbol{x}, \qquad \frac{\mathrm{d}E}{\mathrm{d}t} = 0. \tag{3.140}$$

The fluid has a non-zero potential energy, $(1/2)\int_{-\infty}^{\infty} g\eta^2\,\mathrm{d}x$, if there are variations in fluid height. The initial potential energy is

$$PE_I = \int_0^{\infty} g\eta_0^2\,\mathrm{d}x, \tag{3.141}$$

which is nominally infinite if the fluid has no boundaries. In the non-rotating case the final state has no variations in free-surface height, and its potential energy is zero. That is, *all* of its initial potential energy is converted to kinetic energy which is 'radiated away

to infinity'. However, in the rotating case the final potential energy, after adjustment, is, using 3.137,

$$PE_F = \frac{1}{2}g\eta_0^2 \left[\int_0^\infty \left(1 - e^{-x/L_d}\right)^2 dx + \int_{-\infty}^0 \left(1 - e^{x/L_d}\right)^2 dx \right] \qquad (3.142)$$

This is also nominally infinite, but the change in potential energy is finite and is given by

$$PE_I - PE_F = g\eta_0^2 \int_0^\infty (2e^{-x/L_d} - e^{-2x/L_d}) \, dx = \frac{3}{2}g\eta_0^2 L_d. \qquad (3.143)$$

The initial kinetic energy is zero, because the fluid is at rest, and its final value is, using (3.138),

$$KE_F = \frac{1}{2}H \int u^2 \, dx = H \left(\frac{g\eta_0}{fL_d}\right)^2 \int_0^\infty e^{-2x/L_d} \, dx = \frac{g\eta_0^2 L_d}{2}. \qquad (3.144)$$

Thus, in this problem, one-third of the difference between the initial and final potential energies is converted to kinetic energy that is trapped within a distance of order a deformation radius, and the remainder, an amount $gL_d\eta_0^2$ is lost to infinity. In any finite region surrounding the initial discontinuity the final energy is less than the initial energy, but the conservation of potential vorticity prevents the complete loss of energy. In other adjustment problems the ratios will differ but the qualitative effect will remain (problem 3.10).

3.8.4 * General initial conditions

Because of the linearity of the (linear) adjustment problem a spectral viewpoint is useful, in which the fields are represented as the sum or integral of *non-interacting* Fourier modes. For example, suppose that the height field of the initial disturbance is a two-dimensional field given by

$$\eta = \iint \tilde{\eta}_{0k,l} e^{i(kx+ly)} \, dk \, dl \qquad (3.145)$$

where the Fourier coefficients $\tilde{\eta}_{k,l}$ are given, and the initial velocity field is zero. Then the initial (and final) potential vorticity field is given by

$$q = -\frac{f_0}{H} \iint \tilde{\eta}_{0k,l} e^{i(kx+ly)} \, dk \, dl. \qquad (3.146)$$

To obtain an expression for the final height and velocity fields, we express the potential vorticity field as

$$q = \int \tilde{q}_{k,l} \, dk \, dl \qquad (3.147)$$

where in the final, geostrophically balanced, state,

$$q = \frac{g}{f_0}\nabla^2\eta - \frac{f_0}{H}\eta, \qquad (3.148)$$

so that

$$\widetilde{q}_{k,l} = \left(-\frac{g}{f_0}K^2 - \frac{f_0}{H}\right)\widetilde{\eta}_{k,l}, \tag{3.149}$$

where $K^2 = k^2 + l^2$. Using (3.146) and (3.149), the Fourier components of the final height field satisfy

$$\left(-\frac{g}{f_0}K^2 - \frac{f_0}{H}\right)\widetilde{\eta}_{k,l} = -\frac{f_0}{H}\widetilde{\eta}_{k,l}^{(0)} \tag{3.150}$$

or

$$\widetilde{\eta}_{k,l} = \frac{\widetilde{\eta}_{0k,l}}{K^2 L_d^2 + 1}. \tag{3.151}$$

In physical space the final height field is just the spectral integral of this, namely

$$\eta = \iint \widetilde{\eta}_{k,l}\,\mathrm{d}k\,\mathrm{d}l = \iint \frac{\widetilde{\eta}_{0k,l}}{K^2 L_d^2 + 1}\,\mathrm{d}k\,\mathrm{d}l. \tag{3.152}$$

We see that at large scales ($K^2 L_d^2 \ll 1$) $\eta_{k,l}$ is almost unchanged from its initial state; the velocity field, which is then determined by geostrophic balance, thus adjusts to the pre-existing height field. At large scales most of the energy in geostrophically balanced flow is potential energy; thus, it is energetically easier for the velocity to change to come into balance with the height field than *vice versa*. At small scales, however, the final height field has much less variability than it did initially.

Conversely, at small scales the height field adjusts to the velocity field. To see this, let us suppose that the initial conditions contain vorticity but have zero height displacement. Specifically, if the initial vorticity is $\nabla^2\psi_0$, where ψ_0 is the initial streamfunction, then it is straightforward to show that the final streamfunction is given by

$$\psi = \iint \widetilde{\psi}_{k,l}\,\mathrm{d}k\,\mathrm{d}l = \iint \frac{K^2 L_d^2 \widehat{\psi}_{0k,l}}{K^2 L_d^2 + 1}\,\mathrm{d}k\,\mathrm{d}l. \tag{3.153}$$

The final height field then obtained from this, via geostrophic balance, by $\eta = (f_0/g)\psi$. Evidently, for *small* scales ($K^2 L_d^2 \gg 1$) the streamfunction, and hence the vortical component of the velocity field, are almost unaltered from their initial values. On the other hand, at large scales the final streamfunction has much less variability than it does initially, and so the height field will be largely governed by whatever variation it (and not the velocity field) had initially. In general, the final state is a superposition of the states given by (3.152) and (3.153). The divergent component of the initial velocity field does not affect the final state because it has no potential vorticity, and so all of the associated energy is lost to infinity.

Finally, we remark that just as in the problem with a discontinuous initial height profile the change in total energy during adjustment is negative — this can be seen from the form of the integrals above, although we leave the specifics as a problem to the reader. That is, some of the initial potential and kinetic energy is lost to infinity, but some is trapped by the potential vorticity constraint.

3.8.5 A variational perspective

In the non-rotating problem, all of the initial potential energy is converted to kinetic energy. This energy is in turn radiated to infinity. In the rotating problem, the final state contains both potential and kinetic energy. Why is the energy not all radiated away to infinity? It is because potential vorticity conservation on parcels prevents all of the energy being dispersed. This suggests that it may be informative to think of the geostrophic adjustment problem as a *variational problem:* we seek to minimize the energy consistent with the conservation of potential vorticity. We stay in the linear approximation in which, because the advection of potential vorticity is neglected, potential vorticity remains constant at each point.

The energy of the flow is given by the sum of potential and kinetic energies, namely

$$\text{Energy} = \int H(\boldsymbol{u}^2 + g\eta^2)\,\mathrm{d}\boldsymbol{x}, \tag{3.154}$$

(where $\mathrm{d}\boldsymbol{x} \equiv \mathrm{d}x\,\mathrm{d}y$) and the potential vorticity field is

$$q = \zeta - f\frac{\eta}{H}. \tag{3.155}$$

The problem is then to extremize the energy subject to potential vorticity conservation. This is a constrained problem in the calculus of variations, sometimes called an *isoperimetric* problem because of its origins in maximizing the area of a surface for a given perimeter.[5] The mathematical problem is to extremize the integral

$$I = \int \left\{ H(u^2 + v^2) + g\eta^2 + \lambda(x, y)\big[(v_x - u_y) - f_0\eta/H\big] \right\} \mathrm{d}\boldsymbol{x}. \tag{3.156}$$

where $\lambda(x, y)$ is a Lagrange multiplier, undetermined at this stage. It is a function of space: if it were a constant, the integral would merely extremize energy subject to a given integral of potential vorticity, and rearrangements of potential vorticity (which here we wish to disallow) would leave the integral unaltered.

As there are three independent variables there are three Euler-Lagrange equations obtained by minimizing I. These are

$$\frac{\partial L}{\partial h} - \frac{\partial}{\partial x}\frac{\partial L}{\partial h_x} - \frac{\partial}{\partial y}\frac{\partial L}{\partial h_y} = 0,$$

$$\frac{\partial L}{\partial u} - \frac{\partial}{\partial x}\frac{\partial L}{\partial u_x} - \frac{\partial}{\partial y}\frac{\partial L}{\partial u_y} = 0, \qquad \frac{\partial L}{\partial v} - \frac{\partial}{\partial x}\frac{\partial L}{\partial v_x} - \frac{\partial}{\partial y}\frac{\partial L}{\partial v_y} = 0, \tag{3.157}$$

where L is the integrand appearing in (3.156). After a little algebra these equations yield

$$2g\eta - \lambda f_0 = 0, \qquad 2u + \frac{\partial\lambda}{\partial y} = 0, \qquad 2v - \frac{\partial\lambda}{\partial x} = 0, \tag{3.158}$$

and eliminating λ gives the simple relationships

$$u = -\frac{g}{f_0}\frac{\partial\eta}{\partial y}, \qquad v = \frac{g}{f_0}\frac{\partial\eta}{\partial x}, \tag{3.159}$$

which are the equations of geostrophic balance. Thus, in the linear approximation, *geostrophic balance is a minimum energy state for a given field of potential vorticity.*

3.9 ISENTROPIC COORDINATES

We now return to the continuously stratified primitive equations, and consider the use of potential density as a vertical coordinate. In practice this means using potential temperature in the atmosphere or buoyancy (density) in the ocean; such coordinate systems are generically called *isentropic coordinates,* and sometimes *isopycnal coordinates* if density is used. Although a seemingly odd thing to do, for adiabatic flow in particular the resulting equations of motion have an attractive form that aids the interpretation of large-scale flow. The thermodynamic equation then becomes a statement for the conservation of the mass of fluid with a given value of potential density and, because the the flow of both the atmosphere and ocean is largely along isentropic surfaces, the momentum and vorticity equations have quasi-two-dimensional form.

The particular choice of vertical coordinate is determined by the form of the thermodynamic equation in the equation-set at hand; thus, if the thermodynamic equation is $D\theta/Dt = \dot{\theta}$, we transform the equations from (x, y, z) coordinates to (x, y, θ) coordinates. The material derivative in this coordinate system is

$$
\begin{aligned}
\frac{D}{Dt} &= \frac{\partial}{\partial t} + u \left(\frac{\partial}{\partial x} \right)_\theta + v \left(\frac{\partial}{\partial y} \right)_\theta + \frac{D\theta}{Dt} \frac{\partial}{\partial \theta} \\
&= \frac{\partial}{\partial t} + \boldsymbol{u} \cdot \nabla_\theta + \dot{\theta} \frac{\partial}{\partial \theta}
\end{aligned}
\tag{3.160}
$$

where the last term is zero for adiabatic flow, and the two-dimensional velocity $\boldsymbol{u} \equiv (u, v)$ is parallel to the isentropes.

3.9.1 A hydrostatic Boussinesq fluid

In the simple Boussinesq equations (see the table on page 77) the buoyancy is the relevant thermodynamic variable. With hydrostatic balance the horizontal and vertical momentum equations are, in height coordinates,

$$
\frac{D\boldsymbol{u}}{Dt} + \boldsymbol{f} \times \boldsymbol{u} = -\nabla\phi, \qquad b = \phi_z
\tag{3.161}
$$

where b is the buoyancy, the variable analogous to the potential temperature θ of an ideal gas. The adiabatic thermodynamic equation is

$$
\frac{Db}{Dt} = 0,
\tag{3.162}
$$

and because $b = -g\delta\rho/\rho_0$, isentropic coordinates are the same as isopycnal coordinates.

Using (2.144) the horizontal pressure gradient may be transformed to isentropic coordinates

$$
\left(\frac{\partial \phi}{\partial x} \right)_z = \left(\frac{\partial \phi}{\partial x} \right)_b - \left(\frac{\partial z}{\partial x} \right)_b \frac{\partial \phi}{\partial z} = \left(\frac{\partial \phi}{\partial x} \right)_b - b \left(\frac{\partial z}{\partial x} \right)_b = \left(\frac{\partial M}{\partial x} \right)_b
\tag{3.163}
$$

where

$$
M \equiv \phi - zb.
\tag{3.164}
$$

Thus, the horizontal momentum equation becomes

$$\frac{\mathrm{D}\boldsymbol{u}}{\mathrm{D}t} + \boldsymbol{f} \times \boldsymbol{u} = -\nabla_b M. \tag{3.165}$$

where the material derivative is given by (3.160). Using (3.164) the hydrostatic equation becomes

$$\frac{\partial M}{\partial b} = -z. \tag{3.166}$$

The mass continuity equation may be derived by noting that the mass element may be written as

$$\delta m = \frac{\partial z}{\partial b} \delta b \delta x \delta y. \tag{3.167}$$

The mass continuity equation, $\mathrm{D}m/\mathrm{D}t = 0$, becomes

$$\frac{\mathrm{D}}{\mathrm{D}t}\frac{\partial z}{\partial b} + \frac{\partial z}{\partial b}\nabla_3 \cdot \boldsymbol{v} = 0 \tag{3.168}$$

where $\nabla_3 \cdot \boldsymbol{v}$ is the three dimensional derivative of the velocity in isentropic coordinates. Thus,

$$\frac{\mathrm{D}\sigma}{\mathrm{D}t} + \sigma\nabla_b \cdot \boldsymbol{u} = -\sigma\frac{\partial \dot{b}}{\partial b} \tag{3.169}$$

where $\sigma \equiv \partial z/\partial b$ is a measure of the thickness between two isentropic surfaces. Equations (3.165), (3.166) and (3.169) comprise a closed set, with dependent variables $\boldsymbol{u}$, M and z in the space of independent variables x, y and b.

3.9.2 A hydrostatic ideal gas

Deriving the equations of motion for this system requires a little more work than in the Boussinesq case but the idea is the same. For an ideal gas in hydrostatic balance we have, using (1.116),

$$\frac{\delta\theta}{\theta} = \frac{\delta T}{T} - \kappa\frac{\delta p}{p} = \frac{\delta T}{T} + \frac{\delta\Phi}{c_p T} = \frac{1}{c_p T}\delta M \tag{3.170}$$

where $M \equiv c_p T + \Phi$ is the 'Montgomery potential', equal to the dry static energy. (We use some of the same symbols as in the Boussinesq case to facilitate comparison, but their meanings are slightly different.) From this

$$\frac{\partial M}{\partial \theta} = \Pi \tag{3.171}$$

where $\Pi \equiv c_p T/\theta = c_p(p/p_{\mathrm{R}})^{R/c_p}$ is the 'Exner function'. Equation (3.171) represents the hydrostatic relation in isentropic coordinates. Note also that $M = \theta\Pi + \Phi$.

To obtain the an appropriate form for the horizontal pressure gradient first note that, in the usual height coordinates, it is given by

$$\frac{1}{\rho}\nabla_z p = \theta\nabla_z \Pi \tag{3.172}$$

where $\Pi = c_p T / \theta$. Using (2.144) gives

$$\theta \nabla_z \Pi = \theta \nabla_\theta \Pi - \frac{\theta}{g} \frac{\partial \Pi}{\partial z} \nabla_\theta \Phi. \tag{3.173}$$

Then, using the definition of Π and the hydrostatic approximation to help evaluate the vertical derivative, we obtain

$$\frac{1}{\rho} \nabla_z p = c_p \nabla_\theta T + \nabla_\theta \Phi = \nabla_\theta M. \tag{3.174}$$

Thus, the horizontal momentum equation is

$$\frac{\mathrm{D} \boldsymbol{v}}{\mathrm{D} t} + \boldsymbol{f} \times \boldsymbol{u} = -\nabla_\theta M. \tag{3.175}$$

As in the Boussinesq case the mass continuity equation may be derived by noting that the mass element may be written as

$$\delta m = \frac{\partial p}{\partial \theta} \delta \theta \delta x \delta y. \tag{3.176}$$

The mass continuity equation, $\mathrm{D} m / \mathrm{D} t = 0$, becomes

$$\frac{\mathrm{D}}{\mathrm{D} t} \frac{\partial p}{\partial \theta} + \frac{\partial p}{\partial \theta} \nabla_3 \cdot \boldsymbol{v} = 0 \tag{3.177}$$

or

$$\frac{\mathrm{D} \sigma}{\mathrm{D} t} + \sigma \nabla_\theta \cdot \boldsymbol{u} = -\sigma \frac{\partial \dot{\theta}}{\partial \theta} \tag{3.178}$$

where now $\sigma \equiv \partial p / \partial \theta$ is a measure of the (pressure) thickness between two isentropic surfaces. Equations (3.171), (3.175) and (3.178) form a closed set, analogous to (3.166), (3.165) and (3.169).

Analogy to shallow water equations

The equations of motion in isentropic coordinates have an obvious analogy with the shallow water equations, and we may think of the shallow water equations to be a finite-difference representation of the primitive equations written in isentropic coordinates, or think of the latter as the continuous limit of the shallow water equations as the number of layers increases. For example, consider a two-isentropic-level representation of (3.171), (3.175) and (3.178), in which the lower boundary is an isentrope. A natural finite differencing gives

$$-M_1 = -z_0 \Delta \theta_0 \tag{3.179a}$$
$$M_1 - M_2 = -z_1 \Delta \theta_1 \tag{3.179b}$$

and the momentum equations for each layer become

$$\frac{\mathrm{D} \boldsymbol{u}_1}{\mathrm{D} t} + \boldsymbol{f} \times \boldsymbol{u}_1 = -\Delta \theta_0 \nabla z_0 \tag{3.180a}$$

$$\frac{D\boldsymbol{u}_2}{Dt} + \boldsymbol{f} \times \boldsymbol{u}_2 = -\Delta\theta_0 \nabla z_0 - \Delta\theta_1 \nabla z_1 \qquad (3.180b)$$

which, together with the mass continuity equation for each level, are just like the two-layer shallow water equations (3.52). This means that results that one might easily derive for the shallow water equations will often have a continuous analog that may be derived by straightforward extension.

3.10 AVAILABLE POTENTIAL ENERGY

In this the final section of this chapter we revisit the issue of the internal and potential energy in stratified flow, motivated by the following remarks. In adiabatic, inviscid flow the total amount of energy is conserved, and there are conversions between internal energy, potential energy and kinetic energy. In an ideal gas the potential energy and the internal energy of a column extending throughout the atmosphere are in a constant ratio to each other, and their sum is called the *total potential energy*. In a simple Boussinesq fluid, energetic conversions involve only the potential and kinetic energy, and not the internal energy, and the total potential energy is just the potential energy. Yet, plainly, in neither a Boussinesq fluid nor an ideal gas can *all* the total potential energy in a fluid be converted to kinetic energy, for then all of the fluid would be adjacent to the ground and the fluid would have no thickness, which intuitively seems impossible. Given a state of the atmosphere or ocean, how much of its total potential energy is available for conversion to kinetic energy? In particular, because total energy is conserved only in adiabatic flow, we may usefully ask: how much potential energy is available for conversion to kinetic energy under an adiabatic re-arrangement of fluid parcels?

Suppose that at any given time the flow is stably stratified, but that the isentropes (or more generally the surfaces of constant potential density) are sloping, as sketched in Fig. 3.9. Evidently, the potential energy of the system would be reduced if the isentropes were flattened, for then heavier fluid would be moved to lower altitudes, with lighter fluid replacing it at higher altitudes. In an adiabatic re-arrangement the amount of fluid between the isentropes would remain constant, and a state with flat isentropes (meaning parallel to the geopotential surfaces) evidently constitutes a state of minimum total potential energy. The difference between the total potential energy of the fluid and the total potential energy after an adiabatic re-arrangement to a state in which the isentropic surfaces are flat is called the *available potential energy,* or *APE*.[6]

3.10.1 A Boussinesq fluid

The potential energy of a column of Boussinesq fluid of unit area is given by

$$P = \int_0^H bz\, dz = \int_0^H \frac{b}{2}\, dz^2. \qquad (3.181)$$

and the potential energy of the entire fluid is given by the horizontal integral of this. The minimum potential energy of the fluid arises after an adiabatic re-arrangement in which the isopycnals are flattened, and the resulting buoyancy is only a function of z.
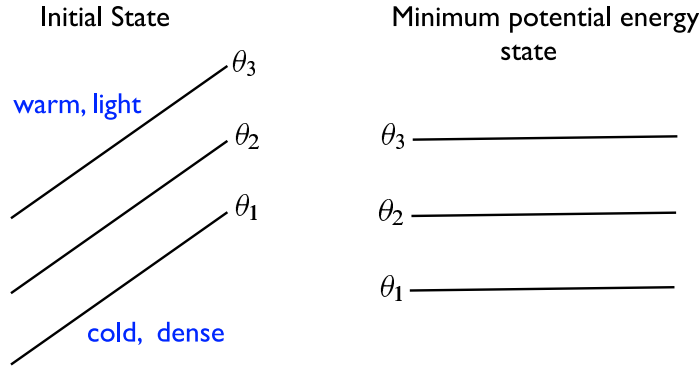
Initial State   Minimum potential energy
                                                        state

warm, light θ_3

                                    θ_2 θ_3 ————————

                                    θ_1 θ_2 ————————

                                                        θ_1 ————————

cold, dense

Fig. 3.9 If a stably stratified initial state with sloping isentropes (left) is adiabatically re-arranged then the state of minimum potential energy has flat isentropes, as on the right, but the amount of fluid contained between each isentropic surface is unchanged. The difference between the potential energies of the two states is the *available potential energy*.

The available potential energy is then the difference between the energy of the initial state and of this minimum state, and to obtain an approximate expression for this we first integrate (3.181) by parts to give

$$P = -\int_0^{b_m} z^2 \, \mathrm{d}b, \qquad (3.182)$$

where b_m is the maximum value of b in the column. (We omit a constant of integration that cancels when the state of minimum potential energy is subtracted. Alternatively, take the upper limit of the z-integral to be $z = 0$ and at the lower limit, at $z = -H$ say, take $b = 0$.) The minimum potential energy state arises when z is a function only of b, $z = Z(b)$ say. Because mass is conserved in the re-arrangement, Z is equal to the horizontally averaged value of z on a given isopycnal surface, $\overline{z}$, and the surfaces $\overline{z}$ and $\overline{b}$ thus define each other completely. The average available potential energy, per unit area, is then given by

$$APE = \int_0^{b_m} (\overline{z^2} - \overline{z}^2) \, \mathrm{d}b = \int_0^{b_m} \overline{z'^2} \, \mathrm{d}b, \qquad (3.183)$$

where $z = \overline{z} + z'$; that is z' is the height variation of an isopycnal surface. The available potential energy is thus proportional to the integral of the variance of the altitude of such a surface, and it is a positive-definite quantity. To obtain an expression in z-coordinates, we express the height variations on an isopycnal surface in terms of buoyancy variations on a constant-height surface by Taylor-expanding the height about its value on the isopycnal surface. Referring to Fig. 3.10 this gives

$$z(\overline{b}) = \overline{z} + \left.\frac{\partial z}{\partial b}\right|_{b=\overline{b}} [\overline{b} - b(\overline{z})] = \overline{z} - \left.\frac{\partial z}{\partial b}\right|_{b=\overline{b}} b' \qquad (3.184)$$

$$b = \overline{b}$$

$$z \approx \overline{z} + \frac{\partial z}{\partial b}\Big|_{b=\overline{b}}[\overline{b} - b(\overline{z})]$$

$$\approx \overline{z} - \frac{b'}{\partial \overline{b}/\partial z}$$

$$z'$$

$$z = \overline{z}$$

$$b \approx \overline{b} + \frac{\partial b}{\partial z}\Big|_{z=\overline{z}}[\overline{z} - z(\overline{b})]$$

$$\approx \overline{b} - \left(\frac{\partial \overline{b}}{\partial z}\right)z'$$
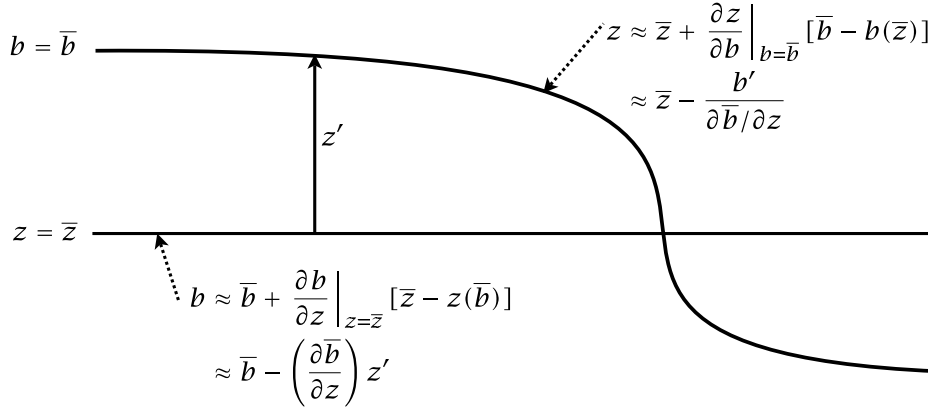
Fig. 3.10 An isopycnal surface, $b = \overline{b}$, and the constant height surface, $z = \overline{z}$. $\overline{z}$ is the height of the isopycnal surface after a re-arrangement to a minimum potential energy state, equal to the average height of the isopycnal surface. The values of z on the isopycnal surface, and of b on the constant height surface, can be obtained by the Taylor expansions shown. For an ideal gas in pressure coordinates, replace z by p and b by θ.

where $b' = b(\overline{z}) - \overline{b}$ is corresponding buoyancy perturbation on the $\overline{z}$ surface and $\overline{b}$ is the average value of b on the $\overline{z}$ surface. Furthermore, $\partial z/\partial b|_{z=\overline{b}} \approx \partial \overline{z}/\partial b \approx (\partial \overline{b}/\partial z)^{-1}$, and (3.184) thus becomes

$$z' = z(\overline{b}) - \overline{z} \approx -b'\left(\frac{\partial \overline{z}}{\partial b}\right) \approx -\frac{b'}{(\partial \overline{b}/\partial z)}. \tag{3.185}$$

where $z' = z(b) - \overline{z}$ is the height perturbation of the isopycnal surface, from its average value. Using (3.185) in (3.183) we obtain an expression for the *APE* per unit area, to wit

$$APE \approx \int_0^H \frac{\overline{b'^2}}{\partial \overline{b}/\partial z}\,\mathrm{d}z\,. \tag{3.186}$$

The total *APE* of the fluid is the horizontal integral of this, and is thus proportional to the variance of the buoyancy on a height surface. We emphasize that *APE* is not defined for single column of fluid, for it depends on the variations of buoyancy over a horizontal surface. Note too that this derivation neglects the effects of topography. This, and the use of a basic state stratification, effectively restrict the use of (3.186) to at most a single ocean basin, and even for that the approximations used limit the accuracy of the expressions.

3.10.2 An ideal gas

The expression for the *APE* for an ideal gas is obtained in the same way, *mutatis mutandis,* as it was for a Boussinesq fluid and the trusting reader may skip directly to (3.194).

The internal energy of an ideal gas column of unit area is given by

$$I = \int_0^\infty c_v T \rho \, \mathrm{d}z = \int_0^{p_s} \frac{c_v}{g} T \, \mathrm{d}p, \tag{3.187}$$

where p_s is the surface pressure, and the corresponding potential energy is given by

$$P = \int_0^\infty \rho g z \, \mathrm{d}z = \int_0^{p_s} z \, \mathrm{d}p = \int_0^\infty p \, \mathrm{d}z = \int_0^{p_s} \frac{R}{g} T \, \mathrm{d}p. \tag{3.188}$$

In (3.187) we use hydrostasy, and in (3.188) the equalities make successive use of hydrostasy, an integration by parts, and hydrostasy and the ideal gas relation. Thus, the total potential energy is given by

$$TPE \equiv I + P = \frac{c_p}{g} \int_0^{p_s} T \, \mathrm{d}p. \tag{3.189}$$

Using the ideal gas equation of state we can write this as

$$TPE = \frac{c_p}{g} \int_0^{p_s} \left(\frac{p}{p_s} \right)^\kappa \theta \, \mathrm{d}p = \frac{c_p p_s}{g(1+\kappa)} \int_0^\infty \left(\frac{p}{p_s} \right)^{\kappa+1} \mathrm{d}\theta, \tag{3.190}$$

after an integration by parts. (We omit a term proportional to $p_s^{\kappa+1} \theta_s$ that arises in the integration by parts, because it plays no role in what follows.) The total potential energy of the entire fluid is equal to a horizontal integral of (3.190). The minimum total potential energy arises when the pressure in (3.190) a function only of θ, $p = P(\theta)$, where by conservation of mass P is the average value of the original pressure on the isentropic surface, $P = \overline{p}$. The average available potential energy per unit area is then given by the difference between the initial state and this minimum, namely

$$APE = \frac{c_p p_s}{g(1+\kappa)} \int_0^\infty \left[\overline{\left(\frac{p}{p_s} \right)^{\kappa+1}} - \left(\frac{\overline{p}}{p_s} \right)^{\kappa+1} \right] \mathrm{d}\theta, \tag{3.191}$$

which is a positive definite quantity. A useful approximation to this expression is obtained by expressing it in terms of the variance of the potential temperature on a pressure surface. We first use the binomial expansion to expand $p^{\kappa+1} = (\overline{p} + p')^{\kappa+1}$. Neglecting third and higher order terms (3.191) becomes

$$APE = \frac{R\overline{p}_s}{2g} \int_0^\infty \left(\frac{\overline{p}}{p_s} \right)^{\kappa+1} \overline{\left(\frac{p'}{\overline{p}} \right)^2} \mathrm{d}\theta. \tag{3.192}$$

The variable $p' = p(\theta) - \overline{p}$ is a pressure perturbation on an isentropic surface, and is related to the potential temperature perturbation on an isobaric surface by [c.f., (3.185)]

$$p' \approx -\theta' \frac{\partial \overline{p}}{\partial \theta} \approx -\frac{\theta'}{\partial \overline{\theta} / \partial p}. \tag{3.193}$$

where $\theta' = \theta(p) - \theta(\overline{p})$ is the potential temperature perturbation on the $\overline{p}$ surface. Using (3.193) in (3.192) we finally obtain

$$APE = \frac{R\overline{p_s}^{-\kappa}}{2} \int_0^{p_s} p^{\kappa-1} \left(-g\frac{\partial\overline{\theta}}{\partial p}\right)^{-1} \overline{\theta'^2}\, \mathrm{d}p .   \tag{3.194}$$

The *APE* is thus proportional to the variance of the potential temperature on the pressure surface or, from (3.192), proportional to the variance of the pressure on an isentropic surface.

3.10.3 Use, interpretation, and the atmosphere and ocean

The potential energy of a fluid is reduced when the dynamics act to flatten the isentropes. Consider, for example, the earth's atmosphere, with isentropes sloping upward toward the pole (Fig. 3.9 with the pole on the right). Flattening these isentropes amounts to a sinking of dense air and a rising of light air, and this reduction of potential energy leads to a corresponding production of kinetic energy. Thus, if the dynamics is such as to try reduce the temperature gradient between equator and pole, then *APE* is continually being converted to *KE*. A stastistically steady state is achieved because the heating from the sun continually acts to restore the horizontal temperature gradient between equator and pole, so replenishing the pool of *APE*, and to this extent the large-scale atmospheric circulation acts like a heat engine. The weighting of the expression (3.194) with stratification may be understood by noting that the more stable the stratification (i.e., the greater the value of $-\partial\overline{\theta}/\partial p$) then, in a given mass of fluid, the greater is the volume of lighter fluid and the less the amount of potential energy that can be converted to kinetic energy. (Note also that a change in *APE* corresponds to a change in the total potential energy of the fluid by the same amount.)

It is a useful exercise to calculate the total potential energy of the atmosphere and ocean, the available potential energy and the kinetic energy (problem 3.15). One finds

$$TPE \gg APE > KE   \tag{3.195}$$

with, very approximately, $TPE \sim 100\,APE$ and $APE \sim 10\,KE$. The first inequality should not surprise us (for it was this that lead us to define *APE* in the first instance), but the second is not obvious (and in fact the ratio is larger in the ocean). It is related to the fact that the instabilities of the atmosphere and ocean occur at a scale smaller than the size of the domain, and are unable to release all the potential energy that might be available. Understanding this more fully is the topic of chapters 6 and 9.

Notes

1 The algorithm to numerically solve these equations differs from that of the free-surface shallow water equations because the mass conservation equation can no

longer be stepped forward in time. Rather, an elliptic equation for p_{lid} must be derived by eliminating time derivatives from from (3.23) using (3.22), and this then solved at each timestep.

2 This expression 'form drag' is also commonly used in aerodynamics, and the two usages are related. In aerodynamics, form drag is the force due to pressure difference between the front and rear of an object, or any other 'form', moving through a fluid. Aerodynamic form drag may include frictional effects between the wind and the surface itself, but this effect is absent in most geophysical uses.

3 (Jules-)Henri Poincaré (1854–1912) was a prodigious French mathematician, physicist and philosopher, regarded as one the greatest mathematicians living at the turn of the 20th century. He is probably most remembered now for his original work in analysis (e.g., solvability of algebraic equations), dynamical systems and celestial mechanics, obtaining many results in what would be called non-linear dynamics and chaos when these fields re-emerged some 60 years later. He also independently obtained a number of the results of special relativity, as well as working on the theory of rotating fluids — hence the Poincaré waves of this chapter [also discussed by Kelvin (1879)]. He also wrote extensively and successfully for the general public on the meaning, importance and philosophy of science. Among other things he discussed whether scientific knowledge was a mere convention, a notion that remains discussed and controversial to this day. (His answer: 'convention', in part, yes; 'mere', no.) He was a proponent of the role of intuition in mathematical and scientific progress, and did not believe that mathematics could ever be wholly reduced to pure logic. One of the last polymaths.

4 Thomson, W. (Lord Kelvin) (1879). See Gill (1982) or Philander (1990) for more detailed discussions.

5 An introduction to variational problems may be found in Weinstock (1952) and a number of other textbooks. Applications to many traditional problems in mechanics are discussed by Lanczos (1970).

6 Margules (1903) introduced the concept of potential energy that is available for conversion to kinetic energy, Lorenz (1955) clarified its meaning and derived useful, approximate formulae for its computation. Shepherd (1993) showed that the *APE* is just the non-kinetic part of the pseudo-energy, an interpretation that naturally leads to a number of extensions of the concept. There are a host of other papers on the subject, including that of Huang (1998) who looked at some of the limitations of the approximate expressions in an oceanic context.

Further Reading

Gill, A. E. 1982. *Atmosphere-Ocean Dynamics.*
This remains a classic reference for geostrophic adjustment and gravity waves. The time-dependent geostrophic adjustment problem is discussed in section 7.3.

Problems

3.1 Derive the appropriate shallow water equations for a single moving layer of fluid of density ρ_1 above a rigid floor, and where above the moving fluid is a stationary fluid of density ρ_0, where $\rho_0 < \rho_1$. Show that as $(\rho_0/\rho_1) \to 0$ the usual shallow water equations emerge.

3.2 *(a)* Model the atmosphere as two immiscible, 'shallow water' fluids of different density stacked one above the other. Using reasonable values for the values of any needed physical parameters such as the density of the two layers, estimate the displacement of the interfacial surface associated with a pole–equator temperature gradient of 60 K.

(b) Similarly estimate an interfacial displacement in the ocean associated with a temperature gradient of 20 K over a distance of 4000 km. (This is a crude representation of the main oceanic thermocline.)

3.3 ♦ For a shallow water fluid the energy equation, (3.91), has the form $\partial E / \partial t + \nabla \cdot (v(E + gh^2/2) = 0$. But for a compressible fluid, the corresponding energy equation, (1.195), has the form $\partial E / \partial t + \nabla \cdot (v(E + p) = 0$. In a shallow water fluid, $p \neq gh^2/2$ at a point so these equations are superficially different. Explain this and reconcile the two forms. (Hint: The shallow water equations are in hydrostatic balance. What is the average pressure in a fluid column?)

3.4 ♦ Can the shallow water equations for an incompressible fluid be derived by way of an asymptotic expansion in the aspect ratio? If so, do it. That is, without assuming hydrostasy ab initio, expand the Euler equations with a free surface in small paramter equal to the ratio of the depth of the fluid to the horizontal scale of the motion, and so obtain the shallow water equations.

3.5 ♦ The inviscid shallow water equations, rotating or not, can support gravity waves of arbitrarily short wavelengths. For sufficiently high wavenumber, the wavelength will be shorter than the depth of the fluid. Is this consistent with an asymptotic nature of the shallow water equations? Discuss.

3.6 Show that the vertical velocity within a shallow-water system is given by

$$w = \frac{z - \eta_b}{h} \frac{\mathrm{D}h}{\mathrm{D}t} + \frac{\mathrm{D}\eta_b}{\mathrm{D}t}. \tag{P3.1}$$

Interpret this result, showing that it gives sensible answers at the top and bottom of the fluid layer.

3.7 What is the appropriate generalization of (3.100) to two-dimensions? Suppose that at time $t = 0$ the height field is given by a Gaussian distribution $h' = Ae^{-r^2/\sigma^2}$ where $r^2 = x^2 + y^2$. What is the subsequent evolution of this, in the linear approximation? Show that the distribution remains Gaussian, and that its width increases at speed $\sqrt{gH}$, where H is the mean depth of the fluid.

3.8 In an adiabatic shallow water fluid in a rotating reference frame show that the potential vorticity conservation law is

$$\frac{\mathrm{D}}{\mathrm{D}t} \frac{\zeta + f}{\eta - h_b} = 0 \tag{P3.2}$$

where η is the height of the free surface and h_b is the height of the bottom topography, both referenced to the same flat surface.

(a) A cylindrical column of air at 30° latitude with radius 100 km expands horizontally to twice its original radius. If the air is initially at rest, what is the mean tangential velocity at the perimeter after the expansion.

(b) An air column at 60°N with zero relative vorticity ($\zeta = 0$) stretches from the surface to the tropopause, which we assume is a rigid lid, at 10 km. The air column moves zonally onto a plateau 2.5 km high. What is its relative vorticity?

Suppose it then moves southward to 30° N. What is its vorticity? (Assume density is constant.)

3.9 ◆ In the long-wave limit of Poincaré waves, fluid parcels behave as free-agents; that is, like free solid particles moving in a rotating frame unencumbered by pressure forces. Why then, is their frequency given by $\omega = f = 2\Omega$ where Ω is the rotation rate of the coordinate system, and not by Ω itself? Do particles that are stationary or move in a straight line in the inertial frame of reference satisfy the dispersion relationship for Poincaré waves in this limit? Explain.

3.10 Linearize the f-plane shallow-water system about a state of rest. Suppose that there is an initial disturbance that is given in the general form

$$\eta = \iint \widetilde{\eta}_{k,l} e^{i(kx+ly)} \, dk \, dl \qquad (P3.3)$$

where η is the deviation surface height and the Fourier coefficients $\widetilde{\eta}_{k,l}$ are given, and that the initial velocity is zero.

(a) Obtain the geopotential field at the completion of geostrophic adjustment, and show that the deformation scale is a natural length scale in the problem.

(b) Show that the change in total energy during the adjustment is always less than or equal to zero. Neglect any initial divergence.
N.B. Because the problem is linear, the Fourier modes do not interact.

3.11 *Geostrophic adjustment of a velocity jump*
Consider the evolution of the linearized f-plane shallow water equations in an infinite domain. Suppose that initially the fluid surface is flat, the zonal velocity is zero and the meridional velocity is given by

$$v(x) = v_0 \text{sgn}(x) \qquad (P3.4)$$

(a) Find the equilibrium height and velocity fields at $t = \infty$.

(b) What are the initial and final kinetic and potential energies?

Partial Solution:
The potential vorticty is $q = \zeta - f_0\eta/H$, so that the initial and final state is

$$q = 2v_0\delta(x). \qquad (P3.5)$$

(Why?) The final state streamfunction is thus given by $\left(\partial^2/\partial x^2 - L_d^{-2}\right)\psi = q$, with solution $\psi = \psi_0 \exp(x/L_d)$ and $\psi = \psi_0 \exp(-x/L_d)$ for $x < 0$ and $x > 0$, where $\psi_0 = L_d v_0$ (why?), and $\eta = f_0\psi/g$. The energy is $E = \int (Hv^2 + g\eta^2)/2 \, dx$. The initial KE is infinite, the initial PE is zero, and the final state has $PE = KE = gL_d\eta_0^2/4$ — that is, the energy is equipartitioned between kinetic and potential.

3.12 In the shallow water equations show that, if the flow is approximately geostrophically balanced, the energy at large scales is predominantly potential energy and that energy at small scales is predominantly kinetic energy. Define precisely what 'large scale' and 'small scale' mean in this context.

3.13 In the shallow-water geostrophic adjustment problem, show that at large scales the velocity adjusts to the height field, and that at small scales the height field adjusts to the velocity field.

3.14 ♦ Consider the problem of minimizing the full energy [i.e., $\int (h\boldsymbol{u}^2 + g\eta^2)\, \mathrm{d}\boldsymbol{x}$], given the potential vorticity field $q(x, y) = (\zeta + f)/h$. Show that the balance relations analogous to (3.8.5) are $uh = -\partial(Bq^{-1})/\partial y$ and $vh = \partial(Bq^{-1})/\partial x$ where B is the Bernoulli function $B = g\eta + \boldsymbol{u}^2/2$. Show that steady flow does not necessarily satisfy these equations. Discuss.

3.15 Using realistic values for temperature, velocity etc., calculate *approximate* values for the total potential energy, the available potential energy, and the kinetic energy, of either a hemisphere in the atmosphere or an ocean basin.

All real fluid motions are rotational.
Clifford Truesdell, *The Kinematics of Vorticity*, 1954.

CHAPTER 4

Vorticity and Potential Vorticity

VORTICITY AND POTENTIAL VORTICITY both play a central role in geophysical fluid dynamics — indeed, we shall find that the large scale circulation of the ocean and atmosphere is in large-part governed by the evolution of the latter. In this chapter we define these quantities and deduce some of their dynamical properties. Along the way we will come across *Kelvin's circulation theorem,* one of the most fundamental conservation laws in all of fluid mechanics, and we will find that the conservation of potential vorticity is intimately tied to this.

4.1 VORTICITY AND CIRCULATION

4.1.1 Preliminaries

Vorticity is defined to be the curl of velocity, and is normally denoted by the symbol $\boldsymbol{\omega}$. Thus

$$\boldsymbol{\omega} \equiv \nabla \times \boldsymbol{v}. \tag{4.1}$$

Circulation is defined to be the integral of velocity around a closed fluid loop. That is,

$$C \equiv \oint \boldsymbol{v} \cdot \mathrm{d}\boldsymbol{l}, \tag{4.2}$$

which by Stokes' theorem can be written as

$$C = \int_S \boldsymbol{\omega} \cdot \mathrm{d}\boldsymbol{S}. \tag{4.3}$$

where S is any surface bounded by the loop. That is, the circulation around some path is equal to the integral of the normal component of vorticity over *any* surface bounded by that path. The circulation is not a field like vorticity and velocity. Rather, we think of the

circulation around a particular material line of finite length, and so its value generally depends on the path chosen. If δS is an infinitesimal surface element whose normal points in the direction of the unit vector $\hat{\boldsymbol{n}}$, then

$$\hat{\boldsymbol{n}} \cdot (\nabla \times \boldsymbol{v}) = \frac{1}{\delta S} \oint_{\delta l} \boldsymbol{v} \cdot \mathrm{d}\boldsymbol{l} \tag{4.4}$$

where the line integral is around the infinitesimal area. Thus at a point the component of vorticity in the direction of $\boldsymbol{n}$ is proportional to the circulation around the surrounding infinitesimal fluid element, divided by the elemental area bounded by the path of the integral. A heuristic test for the presence of vorticity is then to imagine a small paddle-wheel in the flow: the paddle wheel acts as a 'circulation-meter' and so rotates if the vorticity is non-zero.

4.1.2 Simple axi-symmetric examples

Consider axi-symmetric motion in two dimensions, so that the flow is confined to a plane. We use cylindrical coordinates (r, ϕ, z) where z is the direction perpendicular to the plane. Then

$$u_z = u_r = 0, \qquad u_\phi \neq 0. \tag{4.5}$$

Rigid Body Motion

The velocity distribution is given by

$$u_\phi = \Omega r \tag{4.6}$$

where Ω is the angular velocity of the fluid. Associated with this is the vorticity

$$\boldsymbol{\omega} = \nabla \times \boldsymbol{v} = \omega_z \mathbf{k}, \tag{4.7}$$

where

$$\omega_z = \frac{1}{r} \frac{\partial}{\partial r}(r u_\phi) = \frac{1}{r} \frac{\partial}{\partial r}(r^2 \Omega) = 2\Omega. \tag{4.8}$$

The vorticity of a fluid in solid body rotation is thus twice the angular velocity of the fluid, and is pointed in a direction orthogonal to the plane of rotation.

The 'vr' vortex

This vortex is so-called because the tangential velocity (i.e., 'v') is such that the product vr is constant. In our notation we therefore have

$$u_\phi = \frac{K}{r}, \tag{4.9}$$

where K is a constant determining the vortex strength. Evaluating the z-component of vorticity gives

$$\omega_z = \frac{1}{r} \frac{\partial}{\partial r}(r u_\phi) = \frac{1}{r} \frac{\partial}{\partial r}\left(r \frac{K}{r}\right) = 0, \tag{4.10}$$
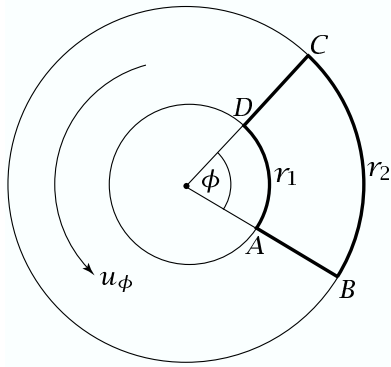
Figure 4.1 Evaluation of circulation in the axi-symmetric vr vortex. The circulation around path A-B-C-D is zero. This result does not depend on the radii r_1 or r_2 or the angle ϕ, and the circulation around any infinitesimal path not enclosing the origin is zero. Thus the vorticity is zero everywhere except at the origin.

except where $r = 0$, at which the expression is singular and the vorticity is infinite. Obviously the paddle wheel rotates when placed at the vortex center, but, less obviously, does not if placed elsewhere.

We can also obtain the result by calculating the circulation $\oint \boldsymbol{u} \cdot \mathrm{d}l$ around an appropriate contour. If the contour is a circle that encloses the origin, the circulation is given by

$$C_\circ = \oint \frac{K}{r} r \, \mathrm{d}\phi = 2\pi K \tag{4.11}$$

This does not depend on the radius, and so it is true if the radius is infinitesimal, provided the contour encloses the origin. Since the vorticity is the circulation divided by the area, the vorticity at the origin must be infinite. Consider now a contour that does not enclose the origin, for example the contour a–b–c–d–a in Fig. 4.1. Over the segments a–b and c–d the velocity is orthogonal to the contour, and so the contribution is zero. Over b-c and d–a we have

$$C_{\mathrm{bc}} = \frac{K}{r_2} \theta r_2 = K\phi, \qquad C_{\mathrm{da}} = -\frac{K}{r_1} \theta r_1 = -K\phi \tag{4.12}$$

The net circulation around the contour C_{abcda} is zero. If we shrink this contour to an infinitesimal size then within this contour, by Stokes' theorem, the vorticity is zero. Thus the vorticity is everywhere zero, except at the origin.

4.2 THE VORTICITY EQUATION

Using the vector identity $\boldsymbol{v} \times (\nabla \times \boldsymbol{v}) = \nabla(\boldsymbol{v} \cdot \boldsymbol{v})/2 - (\boldsymbol{v} \cdot \nabla)\boldsymbol{v}$, we can write the momentum equation as

$$\frac{\partial \boldsymbol{v}}{\partial t} + \boldsymbol{\omega} \times \boldsymbol{v} = -\frac{1}{\rho}\nabla p - \frac{1}{2}\nabla v^2 + \nu \nabla^2 \boldsymbol{v}. \tag{4.13}$$

Taking the curl of this gives the vorticity equation

$$\frac{\partial \boldsymbol{\omega}}{\partial t} + \nabla \times (\boldsymbol{\omega} \times \boldsymbol{v}) = \frac{1}{\rho^2}(\nabla \rho \times \nabla p), \tag{4.14}$$

where here, and in most of the rest of this chapter, we ignore viscosity.

Now, the vector identity

$$\nabla \times (\boldsymbol{a} \times \boldsymbol{b}) = (\boldsymbol{b} \cdot \nabla)\boldsymbol{a} - (\boldsymbol{a} \cdot \nabla)\boldsymbol{b} + \boldsymbol{a}\nabla \cdot \boldsymbol{b} - \boldsymbol{b}\nabla \cdot \boldsymbol{a}, \tag{4.15}$$

implies that the second term on the left hand side of (4.14) may be written

$$\nabla \times (\boldsymbol{\omega} \times \boldsymbol{v}) = (\boldsymbol{v} \cdot \nabla)\boldsymbol{\omega} - (\boldsymbol{\omega} \cdot \nabla)\boldsymbol{v} + \boldsymbol{\omega}\nabla \cdot \boldsymbol{v} - \boldsymbol{v}\nabla \cdot \boldsymbol{\omega}. \tag{4.16}$$

Because vorticity is the curl of velocity, its divergence vanishes, whence we obtain

$$\frac{\partial \boldsymbol{\omega}}{\partial t} + (\boldsymbol{v} \cdot \nabla)\boldsymbol{\omega} = (\boldsymbol{\omega} \cdot \nabla)\boldsymbol{v} - \boldsymbol{\omega}\nabla \cdot \boldsymbol{v} + \frac{1}{\rho^2}(\nabla\rho \times \nabla p). \tag{4.17}$$

The divergence term may be eliminated with the aid of the mass-conservation equation to give

$$\boxed{\frac{\mathrm{D}\widetilde{\boldsymbol{\omega}}}{\mathrm{D}t} = (\widetilde{\boldsymbol{\omega}} \cdot \nabla)\boldsymbol{v} + \frac{1}{\rho^3}(\nabla\rho \times \nabla p)}. \tag{4.18}$$

where $\widetilde{\boldsymbol{\omega}} = \boldsymbol{\omega}/\rho$.

The last term on the right-hand side of (4.17), as well as the term on the right-hand side of (4.18), is called the *baroclinic* term, the *non-homentropic* term, or the *solenoidal* term. The solenoidal vector is defined by

$$\boldsymbol{S} = \frac{1}{\rho^2}\nabla\rho \times \nabla p = -\nabla\alpha \times \nabla p \tag{4.19}$$

A solenoid is a tube directed perpendicular to both $\nabla\alpha$ and ∇p, with elements of length proportional to $\nabla p \times \nabla\alpha$. If the isolines of p and α are parallel to each other, then solenoids do not exist. This occurs when the density is a function only of pressure for then

$$\nabla\rho \times \nabla p = \nabla\rho \times \nabla p \frac{\mathrm{d}p}{\mathrm{d}\rho} = 0. \tag{4.20}$$

The solenoidal vector may also be written

$$\boldsymbol{S} = -\nabla\eta \times \nabla T. \tag{4.21}$$

(This follows most easily by first writing the momentum equation in the form $\partial\boldsymbol{v}/\partial t + \boldsymbol{\omega} \times \boldsymbol{v} = T\nabla\eta - \nabla B$, and taking its curl; see problem 2.2.) Evidently, then, the solenoidal term vanishes if: (i) isolines of pressure and density are parallel; (ii) isolines of temperature and entropy are parallel; (ii) density or entropy or temperature or pressure are constant. A *barotropic* fluid has by definition $p = p(\rho)$ and therefore no solenoids. A *baroclinic* fluid is one for which ∇p is not parallel to $\nabla\rho$. An important result immediately follows from (4.18): the baroclinic term must be balanced by either the nonlinear terms or the vorticity tendency and therefore, in general, *a baroclinic fluid is a moving fluid,* and a stationary baroclinic fluid has a tendency to produce motion. This result holds even in the presence of viscosity.

For a barotropic fluid the vorticity equation takes the simple form,

$$\frac{D\widetilde{\boldsymbol{\omega}}}{Dt} = (\widetilde{\boldsymbol{\omega}} \cdot \nabla)\boldsymbol{v}. \tag{4.22}$$

If the fluid is also incompressible, meaning that $\nabla \cdot \boldsymbol{v} = 0$, then we have the even simpler form,

$$\frac{D\boldsymbol{\omega}}{Dt} = (\boldsymbol{\omega} \cdot \nabla)\boldsymbol{v}. \tag{4.23}$$

The terms on the right-hand side of (4.22) or (4.23) are conventionally divided into 'stretching' and 'tipping' (or 'tilting') terms, and we return to these in section 4.3.1.

An integral conservation property

Consider a single Cartesian component in (4.17). Then

$$\begin{aligned}
\frac{\partial \omega_x}{\partial t} &= -\boldsymbol{v} \cdot \nabla \omega_x - \omega_x \nabla \cdot \boldsymbol{v} + (\boldsymbol{\omega} \cdot \nabla)v_x + S_x \\
&= -\nabla \cdot (\boldsymbol{v}\omega_x) + \nabla \cdot (\boldsymbol{\omega} v_x) + S_x
\end{aligned} \tag{4.24}$$

where S_x is the (x-component of) the solenoidal term. This may be written as

$$\frac{\partial \omega_x}{\partial t} + \nabla \cdot (\boldsymbol{v}\omega_x - \boldsymbol{\omega} v_x) = S_x, \tag{4.25}$$

and this implies the Cartesian tensor form of the vorticity equation, namely

$$\frac{\partial \omega_i}{\partial t} + \frac{\partial}{\partial x_j}(v_j \omega_i - v_i \omega_j) = S_i \tag{4.26}$$

with summation over repeated indices. The tendency of vorticity is given by the solenidal term plus the divergence of a vector field, and thus if the former vanishes the volume integrated vorticity can only be altered by boundary effects. In both atmosphere and ocean the solenoidal term *is* important, but we will see in section 4.5 that a useful conservation law for a scalar quantity can still be obtained.

4.2.1 Two-dimensional flow

In two-dimensional flow the fluid is confined to a surface, and independent of the third dimension normal to that surface. Let us initially stay in a Cartesian geometry, and then two-dimensional flow is flow on a plane, and the velocity normal to the plane, and the rate of change of any quantity normal to that plane, are zero. Let the normal direction be the z-direction and then the velocity in the plane, denoted by $\boldsymbol{u}$, is

$$\boldsymbol{v} = \boldsymbol{u} = u\mathbf{i} + v\mathbf{j}, \qquad w = 0. \tag{4.27}$$

Only one component of vorticity non-zero and this is given by

$$\boldsymbol{\omega} = \mathbf{k}\left(\frac{\partial v}{\partial x} - \frac{\partial u}{\partial y}\right). \tag{4.28}$$

That is, in two-dimensional flow the vorticity is perpendicular to the velocity. We let $\zeta \equiv \omega_z = \boldsymbol{\omega} \cdot \mathbf{k}$. Both the stretching and tilting terms vanish in two-dimensional flow, and the two-dimensional vorticity equation becomes, for incompressible flow,

$$\frac{\mathrm{D}\zeta}{\mathrm{D}t} = 0, \tag{4.29}$$

where $D\zeta/Dt = \partial\zeta/\partial t + \boldsymbol{u}\cdot\nabla\zeta$. That is, in two-dimensional flow vorticity is conserved following the fluid elements; each material parcel of fluid keeps its value of vorticity even as it is being advected around. Furthermore, specification of the vorticity completely determines the flow field. To see this, we use the incompressibility condition to define a streamfunction ψ such that

$$u = -\frac{\partial\psi}{\partial y}, \qquad v = \frac{\partial\psi}{\partial x}, \tag{4.30}$$

and

$$\zeta = \nabla^2 \psi. \tag{4.31}$$

Given the vorticity, the Poisson equation (4.31) can be solved for the streamfunction and the velocity fields obtained through (4.30), and this process is called 'inverting the vorticity'.

Numerical integration of (4.29) is then a process of time-stepping plus inversion. The vorticity equation may then be written as an advection equation for vorticity,

$$\frac{\partial\zeta}{\partial t} + \boldsymbol{u} \cdot \nabla\zeta = 0 \tag{4.32}$$

in conjunction with (4.30) and (4.31). The vorticity is stepped forward one time-step using a finite-difference representation of (4.32), and the vorticity inverted to obtain a velocity using (4.31) and (4.30). (The notion that complete or nearly complete information about the flow may be obtained by inverting one field plays an important role in geophysical fluid dynamics, as we will see later on.)

In the presence of rotation the two-dimensional vorticity equation becomes

$$\frac{\partial\zeta}{\partial t} + \boldsymbol{u} \cdot \nabla(\zeta + f) = 0 \tag{4.33}$$

where $f = 2\boldsymbol{\Omega} \cdot \mathbf{k}$. This may be written

$$\frac{\mathrm{D}}{\mathrm{D}t}(\zeta + f) = 0, \tag{4.34}$$

implying that the absolute vorticity, $\zeta_a \equiv \zeta + f$, is materially conserved. If f is a constant, then (4.33) reduces to (4.32), and background rotation plays no role. If f varies linearly with y, so that $f = f_0 + \beta y$, then (4.33) becomes

$$\frac{\partial\zeta}{\partial t} + \boldsymbol{u} \cdot \nabla\zeta + \beta v = 0 \tag{4.35}$$

which is known as the β-plane vorticity equation.
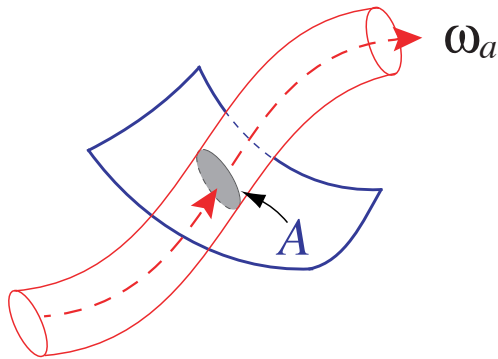
Figure 4.2 A vortex tube passing through a material sheet. The circulation is the integral of the velocity around the boundary of A, and is equal to the integral of the normal component of vorticity over A.

Finally, we note that two-dimensional flow is not restricted to a single, Cartesian plane, and we may certainly envision two-dimensional flow on the surface of a sphere. In this case, the velocity normal to the spherical surface (the 'vertical velocity') vanishes. However, aside from their expression in spherical coordinates the equations of motion are largely unchanged, and in particular vorticity (absolute vorticity if the sphere is rotating) is conserved on parcels as they move over the spherical surface.

4.3 VORTICITY AND CIRCULATION THEOREMS

4.3.1 The 'frozen-in' property of vorticity

Let us first consider some simple topological properties of the vorticity field and its evolution. We define a *vortex-line* to be a line drawn through the fluid which is everywhere in the direction of the local vorticity. This definition is analogous to that of a streamline, which is everywhere in the direction of the local velocity. A *vortex-tube* is formed by the collection of vortex lines passing through a closed curve (Fig. 4.2. A *material-line* is just a line that connects material fluid elements. Suppose we draw a vortex line through the fluid; such a line obviously connects fluid elements and therefore defines a co-incident material line. As the fluid moves the material line deforms, and the vortex line also evolves in a manner determined by the equations of motion. A remarkable property of vorticity is that, for an unforced and inviscid barotropic fluid, the flow evolution is such that a vortex line remains co-incident with the same material line with which it was initially associated. Put another way, a vortex line always contains the same material elements — the vorticity is 'frozen' or 'glued' to the material fluid.

To prove this we consider how an infinitesimal material line element $\delta \boldsymbol{l}$ evolves, $\delta \boldsymbol{l}$ being the infinitesimal material element connecting $\boldsymbol{l}$ with $\boldsymbol{l} + \delta \boldsymbol{l}$. The rate of change of $\delta \boldsymbol{l}$ following the flow is given by

$$\frac{\mathrm{D}\delta \boldsymbol{l}}{\mathrm{D}t} = \frac{1}{\delta t}\big(\delta \boldsymbol{l}(t + \delta t) - \delta \boldsymbol{l}(t)\big), \tag{4.36}$$

which follows from the definition of the material derivative in the limit $\delta t \rightarrow 0$. From
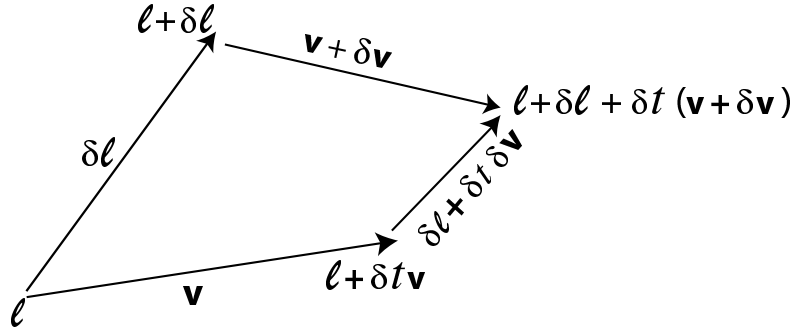
Fig. 4.3 Evolution of an infinitesimal material line δl from time t to time $t + \delta t$. It can be seen from the diagram that $D\,\delta l/Dt = \delta \boldsymbol{v}$.

the Taylor expansion of $\delta l(t)$ and the definition of velocity it is also apparent that

$$
\begin{aligned}
\delta l(t + \delta t) &= l(t) + \delta l(t) + (\boldsymbol{v} + \delta \boldsymbol{v})\delta t - (l(t) + \boldsymbol{v}\delta t) \\
&= \delta l + \delta \boldsymbol{v}\delta t,
\end{aligned}
\tag{4.37}
$$

as illustrated in Fig. 4.3. Substituting into (4.36) gives

$$
\frac{D\delta l}{Dt} = \delta \boldsymbol{v}
\tag{4.38}
$$

But since $\delta \boldsymbol{v} = (\delta l \cdot \nabla)\boldsymbol{v}$ we have that

$$
\frac{D\delta l}{Dt} = (\delta l \cdot \nabla)\boldsymbol{v}
\tag{4.39}
$$

Comparing this with (4.18), we see that vorticity evolves in the same way as a line element. To see what this means, at some initial time we can define an infinitesimal material line element parallel to the vorticity at that location, that is,

$$
\delta l(\boldsymbol{x}, t) = A\boldsymbol{\omega}(\boldsymbol{x}, t)
\tag{4.40}
$$

where A is a (dimensional) constant. Then, for all subsequent times, the magnitude of the vorticity of that fluid element (wherever that particular element may be in the fluid) remains proportional to the length of the fluid element and points in the same direction — that is:

$$
\boldsymbol{\omega}(\boldsymbol{x}', t') = A^{-1}\delta l(\boldsymbol{x}', t').
\tag{4.41}
$$

To see the same result in a slightly different way note that a vortex line element is determined by the condition $\delta l = A\boldsymbol{\omega}$ or, because A is just an arbitrary scaling factor, $\boldsymbol{\omega} \times \delta l = 0$. Now, for any line element we have that

$$
\frac{D}{Dt}(\boldsymbol{\omega} \times \delta l) = \frac{D\boldsymbol{\omega}}{Dt} \times \delta l - \frac{D\delta l}{Dt} \times \boldsymbol{\omega}.
\tag{4.42}
$$

We also have that

$$\frac{\mathrm{D}\delta l}{\mathrm{D}t} = \delta v = \delta l \cdot \nabla v \tag{4.43a}$$

and

$$\frac{\mathrm{D}\omega}{\mathrm{D}t} = \omega \cdot \nabla v. \tag{4.43b}$$

If the line element is initially a vortex line element then, at $t = 0$, $\delta l = A\omega$ and, using (4.43), the right hand side of (4.42) vanishes. Thus, the *tendency* of $\omega \times \delta l$ is zero, and the vortex line continues to be a material line.

Stretching and tilting

The frozen-in property of vorticity allows us to intepret the terms on the right-hand side of (4.22) or (4.23) in terms of 'stretching' and 'tipping' (or 'tilting'). Consider a single Cartesian component of (4.23),

$$\frac{\mathrm{D}\omega_x}{\mathrm{D}t} = \omega_x \frac{\partial u}{\partial x} + \omega_y \frac{\partial u}{\partial y} + \omega_z \frac{\partial u}{\partial z}. \tag{4.44}$$

The second and third terms of this are the tilting or tipping terms because they involve changes in the orientation of the vorticity vector. They tell us that vorticity in x-direction may be generated from vorticity in the y- and z-directions if the advection acts to tilt the material lines. Because vorticity is tied to these lines, vorticity oriented in one direction becomes oriented in another, and in Fig. 4.4 we see how vorticity in the z-direction may be created by the tilting of vortex lines that initially have a purely horizontal orientation.

The first term on the right-hand side of (4.44) is the stretching term, and it acts to intensify the x-component of vorticity if the velocity is increasing in the x-direction — that is, if the material lines are being stretched (Fig. 4.5). This effect again arises because a vortex line is tied to a material line, and therefore vorticity is amplified if the material line aligned with it is stretched, and in proportion to that stretching. This effect leads to the amplification of vorticity in tornadoes, to give one example. If the fluid is incompressible the the volume of a mass of material fluid remains fixed, so that stretching in one direction is accompanied by convergence in another, and this leads to the conservation of circulation, as we now discuss.

4.3.2 Kelvin's Circulation Theorem

Kelvin's circulation theorem states that under certain circumstances the circulation around a material fluid parcel is conserved; that is, the circulation is conserved 'following the flow'. The primary restrictions are that body forces are conservative (i.e., they are representable as potential forces, and therefore that the flow be inviscid), and that the fluid is baroropic [i.e., $p = p(\rho)$]. Of these, the latter is the more restrictive for geophysical fluids.

The circulation in the theorem is defined with respect to an inertial frame of reference; specifically, the velocity in (4.48) is the velocity relative to an inertial frame. We
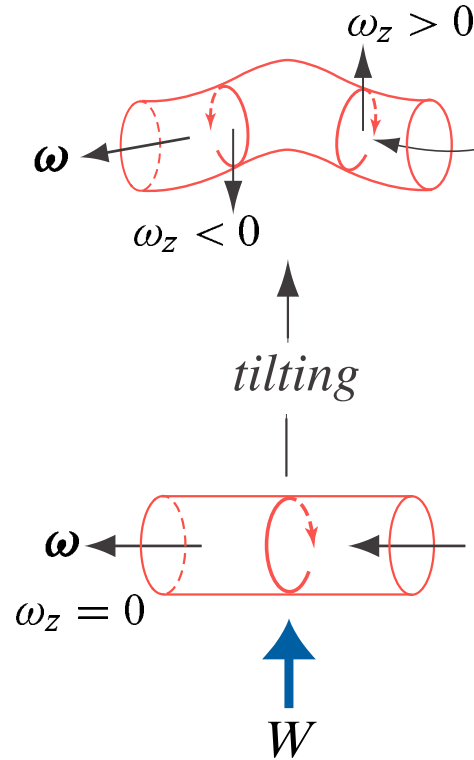
Figure 4.4 The tilting of vorticity. Suppose that vorticity, $\boldsymbol{\omega}$ is initially directed horizontally, as in the lower figure, so that ω_z, its vertical component, is zero. The material lines, and therefore the vortex lines also, are tilted by the postive vertical velocity W, so creating a vertically oriented vorticity. This mechanism is important in creating vertical vorticity in the atmospheric boundary layer (and, one may show, the β-effect in large-scale flow).

will give a straightforward proof, beginning with the inviscid momentum equation,

$$\frac{\mathrm{D}\boldsymbol{v}}{\mathrm{D}t} = -\frac{1}{\rho}\nabla p - \nabla\Phi, \tag{4.45}$$

where $\nabla\Phi$ represents the conservative body forces on the system. Applying the material derivative to the circulation, (4.2), gives

$$\begin{aligned}
\frac{\mathrm{D}C}{\mathrm{D}t} = \frac{\mathrm{D}}{\mathrm{D}t}\oint \boldsymbol{v}\cdot\mathrm{d}\boldsymbol{r} &= \oint\left(\frac{\mathrm{D}\boldsymbol{v}}{\mathrm{D}t}\cdot\mathrm{d}\boldsymbol{r} + \boldsymbol{v}\cdot\mathrm{d}\boldsymbol{v}\right) \\
&= \oint\left[\left(-\frac{1}{\rho}\nabla p - \nabla\Phi\right)\cdot\mathrm{d}\boldsymbol{r} + \boldsymbol{v}\cdot\mathrm{d}\boldsymbol{v}\right] \\
&= \oint -\frac{1}{\rho}\nabla p\cdot\mathrm{d}\boldsymbol{r}
\end{aligned} \tag{4.46}$$

using (4.45) and $D(\delta\boldsymbol{l})/Dt = \delta\boldsymbol{v}$. The line integration is over a closed, material, circuit. The second and third terms on the second line vanish separately, because they are exact differentials integrated around a closed loop. The term on the last line vanishes if density is constant or, more generally, if pressure is a function of density alone in which case ∇p is parallel to $\nabla\rho$. To see this, note that

$$\oint\frac{1}{\rho}\nabla p\cdot\mathrm{d}\boldsymbol{r} = \int_S \nabla\times\left(\frac{\nabla p}{\rho}\right)\cdot\mathrm{d}\boldsymbol{A} = \int_A \frac{-\nabla\rho\times\nabla p}{\rho^2}\cdot\mathrm{d}\boldsymbol{A}, \tag{4.47}$$
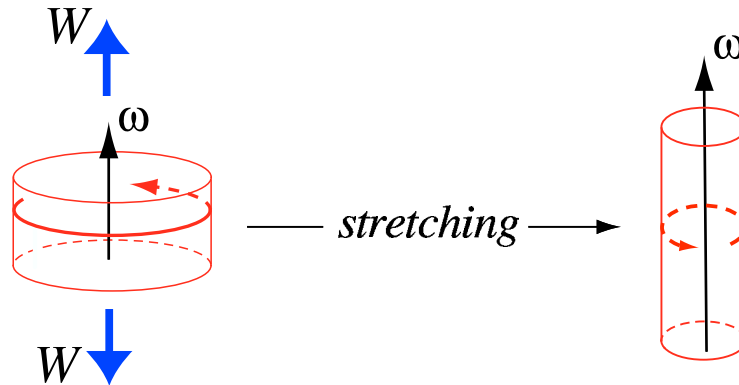
Fig. 4.5 Stretching of material lines distorts the cylinder of fluid as shown. Vorticity is tied to material lines, and so is amplified in the direction of the stretching. However, because the volume of fluid is conserved, the end surfaces shrink, the material lines through the cylinder ends converge, and the integral of vorticity over a material surface (the circulation) remains constant, as discussed in section 4.3.2.

using Stokes's theorem where A is any surface bounded by the path of the line integral, and this evidently vanishes identically if p is a function of ρ alone. The last term is the integral of the solenoidal vector, and if it is zero (4.46) becomes

$$\boxed{\frac{\mathrm{D}}{\mathrm{D}t} \oint \boldsymbol{v} \cdot \mathrm{d}\boldsymbol{r} = 0} . \tag{4.48}$$

This is Kelvin's circulation theorem. In words, *the circulation around a material loop is invariant for a barotropic fluid that is subject only to conservative forces.* Using Stokes' theorem, the circulation theorem may also be written

$$\boxed{\frac{\mathrm{D}}{\mathrm{D}t} \int \boldsymbol{\omega} \cdot \mathrm{d}\boldsymbol{S} = 0} . \tag{4.49}$$

That is, the area-integral of the normal component of vorticity across any material surface is constant, under the same conditions. This form is both natural and useful, and it arises because of the way vorticity is tied to material fluid elements, as we now see.

Stretching and circulation

We now informally consider how vortex stretching and mass conservation work together to give the circulation theorem. Let the fluid be incompressible so that the volume of a fluid mass is constant, and consider a surface normal to a vortex tube, that is he plane of the surface perpendicular to the direction of the vorticity, as in Fig. 4.5). Let the volume of a small material box around the surface be δV, the length of the material lines be δl and the surface area be δA. Then

$$\delta V = \delta l \, \delta A . \tag{4.50}$$

Because of the frozen-in property, vorticity passing through the surface is proportional to the length of the material lines. That is $\omega \propto \delta l$, and

$$\delta V \propto \omega \, \delta A. \tag{4.51}$$

The right-hand side is just the circulation around the surface. Now, if the corresponding material tube is stretched δl increases, but the volume, δV, remains constant by mass conservation. Thus, the circulation given by the right-hand side of (4.51) also remains constant. In other words, because of the frozen-in property vorticity itself is amplified by the stretching, but the vortex lines get closer together in such a way that the product $\omega \, \delta S$ remains constant and circulation is conserved.

Baroclinic flow and the solenoidal term

In baroclinic flow, the circulation is not generally conserved. and we have

$$\frac{DC}{Dt} = -\oint \frac{\nabla p}{\rho} \cdot dl = -\oint \frac{dp}{\rho} \tag{4.52}$$

and this is sometimes called Bjerknes's circulation theorem.[1] Noting the fundamental thermodynamic relation $T \, d\eta = dI + p \, d\alpha$ we have

$$\alpha \, dp = d(p\alpha) - T \, d\eta + dI \tag{4.53}$$

so that the solenoidal term on the right-hand side of (4.52) may be written as

$$S_o \equiv -\oint \alpha \, dp = \oint T \, d\eta = -\oint \eta \, dT = -R \oint T \, d\log p \tag{4.54}$$

where the last equality holds only for an ideal gas. Using Stokes's theorem S_o can also be written as

$$S_o = -\int_A \nabla \alpha \times \nabla p \cdot dA = -\int_A \left(\frac{\partial \alpha}{\partial T} \right)_p \nabla \alpha \times \nabla p \cdot dA = \int_A \nabla T \times \nabla \eta \cdot dA. \tag{4.55}$$

The rate of change of the circulation across a surface depends on the existence of this solenoidal term (Fig. 4.6 and, for an example, problem 4.6).

However, even if the solenoidal vector is in general non-zero, circulation *is* conserved if the material path is in a surface of constant entropy, η, *and if* $D\eta/Dt = 0$. In this case the solenoidal term vanishes and, because $D\eta/Dt = 0$, entropy remains constant on that same material loop as it evolves. This result gives rise to the conservation of potential vorticity, discussed in section 4.5

Circulation in a rotating frame

In a rotating frame of reference, the appropriate form of the circulation theorem is obtained by using

$$\frac{D}{Dt} \oint (v_r + \boldsymbol{\Omega} \times r) \cdot dr = \oint \left[\left(\frac{Dv_r}{Dt} + \boldsymbol{\Omega} \times v_r \right) \cdot dr + (v_r + \boldsymbol{\Omega} \times r) \cdot dv_r \right], \tag{4.56}$$
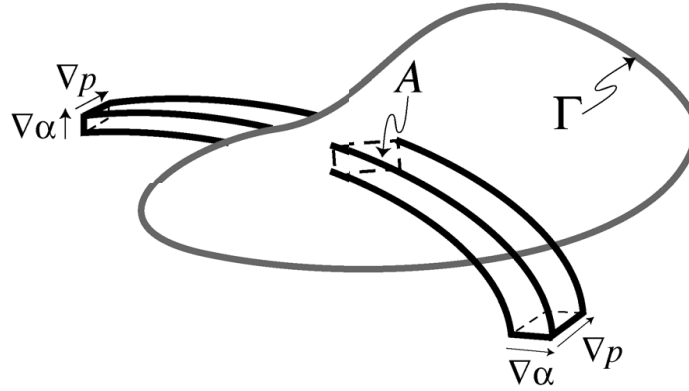
Fig. 4.6 A schematic of the solenoids and the circulation theorem. The circulation over a surface is the integral of the vortex lines passing through it. Solenoids are tubes perpendicular to both $\nabla\alpha$ and ∇p, and they have a non-zero cross-sectional area if isolines of α and p do not coincide. The rate of change of circulation over a material surface is given by the sum of all the solenoidal areas crossing the surface. If $\nabla\alpha \times \nabla p = 0$ there are no solenoids.

where for emphasis we explicitly use the subscript r to denote the rotating frame. But $\oint \boldsymbol{v}_r \cdot \mathrm{d}\boldsymbol{v}_r = 0$ and, integrating by parts,

$$
\oint (\boldsymbol{\Omega} \times r) \cdot \mathrm{d}\boldsymbol{v}_r = \oint \left\{ \mathrm{d}[(\boldsymbol{\Omega} \times r) \cdot \boldsymbol{v}_r] - (\boldsymbol{\Omega} \times \mathrm{d}r) \cdot \boldsymbol{v}_r \right\}
$$
$$
= \oint \left\{ \mathrm{d}[(\boldsymbol{\Omega} \times r) \cdot \boldsymbol{v}_r] + (\boldsymbol{\Omega} \times \boldsymbol{v}_r) \cdot \mathrm{d}r \right\}.
$$
(4.57)

The first term is on the right-hand side is zero and so (4.56) becomes

$$
\frac{\mathrm{D}}{\mathrm{D}t} \oint (\boldsymbol{v}_r + \boldsymbol{\Omega} \times r) \cdot \mathrm{d}r = \oint \left(\frac{\mathrm{D}\boldsymbol{v}_r}{\mathrm{D}t} + 2\boldsymbol{\Omega} \times \boldsymbol{v}_r \right) \cdot \mathrm{d}r = -\oint \frac{\mathrm{d}p}{\rho},
$$
(4.58)

where the second equality uses the momentum equation. The term on the last line vanishes if the fluid is barotropic, and if so the circulation theorem is

$$
\frac{\mathrm{D}}{\mathrm{D}t} \oint (\boldsymbol{v}_r + \boldsymbol{\Omega} \times r) \cdot \mathrm{d}r = 0.
$$
(4.59)

Using Stokes's theorem this may be written,

$$
\frac{\mathrm{D}}{\mathrm{D}t} \int (\boldsymbol{\omega}_r + 2\boldsymbol{\Omega}) \cdot \mathrm{d}\boldsymbol{S} = 0.
$$
(4.60)

having used $\nabla \times (\boldsymbol{\Omega} \times r) = 2\boldsymbol{\Omega}$, and where $\boldsymbol{\omega}_r$ is the relative vorticity, or the vorticity of a fluid parcel as measured in the rotating frame.[2]

4.3.3 The circulation theorem for hydrostatic flow

A version of Kelvin's circulation theorem holds for hydrostatic flow. For simplicity we restrict attention to the f-plane, and start with the hydrostatic momentum equations,

$$\frac{D\boldsymbol{u}_r}{Dt} + 2\boldsymbol{\Omega} \times \boldsymbol{u}_r = -\frac{1}{\rho}\nabla_z p, \qquad (4.61a)$$

$$0 = -\frac{1}{\rho}\frac{\partial p}{\partial z} - \nabla\Phi, \qquad (4.61b)$$

where now $\Phi = gz$ is the gravitational potential and $\boldsymbol{\Omega} = \Omega\mathbf{k}$. The advecting field is three-dimensional, and in particular we still have $D\delta r/Dt = \delta\boldsymbol{v} = (\delta\boldsymbol{r}\cdot\nabla)\boldsymbol{v}$. Thus, using (4.61) we have

$$\frac{D}{Dt}\oint(\boldsymbol{u}_r + \boldsymbol{\Omega}\times\boldsymbol{r})\cdot d\boldsymbol{r} = \oint\left[\left(\frac{D\boldsymbol{u}_r}{Dt} + \boldsymbol{\Omega}\times\boldsymbol{v}_r\right)\cdot d\boldsymbol{r} + (\boldsymbol{u}_r + \boldsymbol{\Omega}\times\boldsymbol{r})\cdot d\boldsymbol{v}_r\right]$$

$$= \oint\left(\frac{D\boldsymbol{u}_r}{Dt} + 2\boldsymbol{\Omega}\times\boldsymbol{u}_r\right)\cdot d\boldsymbol{r}$$

$$= \oint\left(-\frac{1}{\rho}\nabla p - \nabla\Phi\right)\cdot d\boldsymbol{r}, \qquad (4.62)$$

as with (4.58), having used $\boldsymbol{\Omega}\times\boldsymbol{v}_r = \boldsymbol{\Omega}\times\boldsymbol{u}_r$, and where the gradient operator ∇ is three-dimensional. The last term on the right-hand side vanishes because it is the integral of the gradient of a potential around a closed path. The first term vanishes if the fluid is barotropic, so that the circulation theorem is

$$\frac{D}{Dt}\oint(\boldsymbol{u}_r + \boldsymbol{\Omega}\times\boldsymbol{r})\cdot d\boldsymbol{r} = 0. \qquad (4.63)$$

Using Stokes's theorem we have the equivalent form

$$\frac{D}{Dt}\int(\boldsymbol{\omega}_{\text{hy}} + 2\boldsymbol{\Omega})\cdot d\boldsymbol{S} = 0, \qquad (4.64)$$

where the subscript 'hy' denotes hydrostatic and, in Cartesian coordinates,

$$\boldsymbol{\omega}_{\text{hy}} = \nabla\times\boldsymbol{u} = -\mathbf{i}\frac{\partial v}{\partial z} + \mathbf{j}\frac{\partial u}{\partial z} + \mathbf{k}\left(\frac{\partial v}{\partial x} - \frac{\partial u}{\partial y}\right). \qquad (4.65)$$

4.4 VORTICITY EQUATION IN A ROTATING FRAME

Perhaps easiest way to derive the vorticity equation appropriate for a rotating reference frame is to begin with the momentum equation in the form

$$\frac{\partial\boldsymbol{v}_r}{\partial t} + (2\boldsymbol{\Omega} + \boldsymbol{\omega}_r)\times\boldsymbol{v}_r = -\frac{1}{\rho}\nabla p + \nabla\left(\Phi - \frac{1}{2}v_r^2\right), \qquad (4.66)$$

$$\int_A (\boldsymbol{\omega} + 2\boldsymbol{\Omega}) \cdot \mathrm{d}A = 2\Omega A_\perp$$
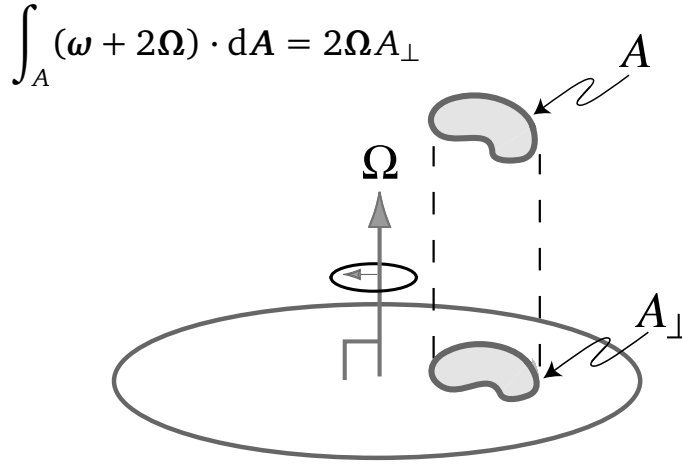
Fig. 4.7 The projection of a material circuit on to the equatorial plane. If a fluid element moves poleward, keeping its orientation to the local vertical fixed (e.g., it stays horizontal) then the area of its projection on to the equatorial plane increases. If its total (absolute) circulation is to be maintained, then the vertical component of the relative vorticity must diminish. That is, $\int_A (\boldsymbol{\omega} + 2\boldsymbol{\Omega}) \cdot \mathrm{d}A = \int_A (\zeta + f)\mathrm{d}A = $ constant. Thus, the β term in $\mathrm{D}(\zeta + f)/\mathrm{D}t = \mathrm{D}\zeta/\mathrm{D}t + \beta v = 0$ ultimately arises from the *tilting* of a parcel relative to the axis of rotation as it moves meridionally.

where the potential Φ contains the gravitational and centrifugal forces. Take the curl of this and use the identity (4.15), which here implies

$$\nabla \times [(2\boldsymbol{\Omega} + \boldsymbol{\omega}_r) \times \boldsymbol{v}_r] = (2\boldsymbol{\Omega} + \boldsymbol{\omega}_r)\nabla \cdot \boldsymbol{v}_r + (\boldsymbol{v}_r \cdot \nabla)(2\boldsymbol{\Omega} + \boldsymbol{\omega}_r) - [(2\boldsymbol{\Omega} + \boldsymbol{\omega}_r) \cdot \nabla]\boldsymbol{v}_r, \quad (4.67)$$

(noting that $\nabla \cdot (2\boldsymbol{\Omega} + \boldsymbol{\omega}) = 0$), to give the vorticity equation

$$\frac{\mathrm{D}\boldsymbol{\omega}_r}{\mathrm{D}t} = [(2\boldsymbol{\Omega} + \boldsymbol{\omega}_r) \cdot \nabla]\boldsymbol{v} - (2\boldsymbol{\Omega} + \boldsymbol{\omega}_r)\nabla \cdot \boldsymbol{v}_r + \frac{1}{\rho^2}(\nabla\rho \times \nabla p). \quad (4.68)$$

Note that because $\boldsymbol{\Omega}$ is a constant, $\mathrm{D}\boldsymbol{\omega}_r/\mathrm{D}t = \mathrm{D}\boldsymbol{\omega}_a/\mathrm{D}t$ where $\boldsymbol{\omega}_a = \boldsymbol{\Omega} + \boldsymbol{\omega}_r$ is the absolute vorticity. The only difference between the vorticity equation in the rotating and inertial frames of reference is in the presence of the solid-body vorticity $2\boldsymbol{\Omega}$ on the right-hand side. The second term on the right-hand side may be folded in to the material derivative using mass continuity, and after a little manipulation (4.68) becomes

$$\frac{\mathrm{D}}{\mathrm{D}t}\left(\frac{\boldsymbol{\omega}_a}{\rho}\right) = \frac{1}{\rho}(2\boldsymbol{\Omega} + \boldsymbol{\omega}_r) \cdot \nabla \boldsymbol{v}_r + \frac{1}{\rho^3}(\nabla\rho \times \nabla p). \quad (4.69)$$

However, note that it is the absolute voricity, $\boldsymbol{\omega}_a$, that now appears on the left-hand side. If ρ is constant, $\boldsymbol{\omega}_a$ may be replaced by $\boldsymbol{\omega}_r$.

4.4.1 The circulation theorem and vortex tilting

What are the implications of the circulation theorem on a rotating, spherical planet? Let us define relative circulation over some material loop as

$$C_r \equiv \oint \boldsymbol{v}_r \cdot \mathrm{d}\boldsymbol{l}, \tag{4.70}$$

and because $\boldsymbol{v}_r = \boldsymbol{v}_a - 2\boldsymbol{\Omega} \times \boldsymbol{r}$ we have

$$C_r = C_a - \int 2\boldsymbol{\Omega} \cdot \mathrm{d}\boldsymbol{S} = C_a - 2\boldsymbol{\Omega}\, A_\perp \tag{4.71}$$

where C_a is the total or absolute circulation and $A_\perp$ is the area enclosed by the projection of the material circuit onto the plane normal to the rotation vector; that is, onto the equatorial plane (see Fig. 4.7). If the solenoidal term is zero then the circulation theorem, (4.60), may be written as

$$\frac{\mathrm{D}}{\mathrm{D}t}(C_r + 2\Omega A_\perp) = 0 \tag{4.72}$$

This equation tells us that the relative circulation around a circuit will change if the orientation of the plane changes; that it, if the area of its projection on to the equatorial plane changes. In large scale dynamics the most common cause of this is when a fluid parcel changes its latitude. For example, consider the two-dimensional flow of an infinitesimal, horizontal, homentropic fluid surface at a latitude ϑ with area δS, so that the projection of its area on the equatorial plane is $\delta S \sin \vartheta$. If the fluid surface moves, but remains horizontal, then directly from (4.72) the relative vorticity changes as

$$\frac{\mathrm{D}\zeta_r}{\mathrm{D}t} = -2\Omega \frac{\mathrm{D}}{\mathrm{D}t} \sin \vartheta = -v_r \frac{2\Omega \cos \vartheta}{a}. \tag{4.73}$$

The means by which the relative vorticity of a parcel changes by virtue of its latitudinal displacement is known as the *beta effect,* or the β *effect.* It is a manifestation of the tilting term in the vorticity equation, and it is often the most important means by which relative vorticity does change in large-scale flow. We define

$$\beta \equiv \frac{\mathrm{d}f}{\mathrm{d}y} = \frac{2\Omega}{a} \cos \vartheta, \tag{4.74}$$

so that in this instance $\mathrm{D}\zeta_r/\mathrm{D}t = -\beta v_r$. The β term directly arises in the full vorticity equation, as we now see.

4.4.2 The vertical vorticity equation

For many applications, especially in large-scale dynamics, the most important, although not the largest, component of the vorticity is the vertical one, because this contains much of the information about the horizontal flow. We can obtain an explicit expression for it by taking the vertical component of (4.68), although care must be taken because the unit vectors ($\mathbf{i}$, $\mathbf{j}$, $\mathbf{k}$) are functions of position (see problem 2.5.) An alternative derivation

that results in a useful form begins with the horizontal momentum equations in the form

$$\frac{\partial u}{\partial t} - v(\zeta + f) + w\frac{\partial u}{\partial z} = -\frac{1}{\rho}\frac{\partial p}{\partial x} - \frac{1}{2}\frac{\partial}{\partial x}(u^2 + v^2) + F_x \tag{4.75a}$$

$$\frac{\partial v}{\partial t} + u(\zeta + f) + w\frac{\partial v}{\partial z} = -\frac{1}{\rho}\frac{\partial p}{\partial y} - \frac{1}{2}\frac{\partial}{\partial y}(u^2 + v^2) + F_y. \tag{4.75b}$$

$$\tag{4.75c}$$

where in this section we again drop the subscript r on variables measured in the rotating frame. Cross-differentiating gives, after a little algebra,

$$\begin{aligned}\frac{\mathrm{D}}{\mathrm{D}t}(\zeta + f) = &- (\zeta + f)\left(\frac{\partial u}{\partial x} + \frac{\partial v}{\partial y}\right) + \left(\frac{\partial u}{\partial z}\frac{\partial w}{\partial y} - \frac{\partial v}{\partial z}\frac{\partial w}{\partial x}\right)\\ &+ \frac{1}{\rho^2}\left(\frac{\partial \rho}{\partial x}\frac{\partial p}{\partial y} - \frac{\partial \rho}{\partial y}\frac{\partial p}{\partial x}\right) + \left(\frac{\partial F_y}{\partial x} - \frac{\partial F_x}{\partial y}\right).\end{aligned} \tag{4.76}$$

The brave reader may verify that this equation holds in spherical coordinates, with $\partial/\partial x = (r\cos\vartheta)^{-1}\partial/\partial\lambda$ and $\partial/\partial y = r^{-1}\partial/\partial\vartheta$. We interpret the various terms as follows:

$\mathrm{D}\zeta/\mathrm{D}t = \partial\zeta/\partial t + \boldsymbol{v}\cdot\nabla\zeta$: The material derivative of the vertical component of the vorticity.

$\mathrm{D}f/\mathrm{D}t = v\partial f/\partial y = v\beta$: The β-effect. The vorticity is affected by the meridional motion of the fluid, so that, apart from the terms on the right-hand side, $(\zeta + f)$ is conserved on parcels. Because the Coriolis parameter changes with latitude this is like saying that the system has differential rotation. This effect is precisely that due to the change in orientation of fluid surfaces with latitude, as given above in section 4.4.1 and Fig. 4.7.

$-(\zeta + f)(\partial u/\partial x + \partial v/\partial y)$: The divergence term, which gives rise to vortex stretching. In an incompressible fluid this may be written $(\zeta + f)\partial w/\partial z$, so that vorticity is amplified if the vertical velocity increases with height, so stretching the material lines and the vorticity.

$(\partial u/\partial z)(\partial w/\partial y) - (\partial v/\partial z)(\partial w/\partial x)$: The tilting term, whereby a vertical component of vorticity may be generated by a vertical velocity acting on a horizontal vorticity. See Fig. 4.4.

$\rho^{-2}\left[(\partial\rho/\partial x)(\partial p/\partial y) - (\partial\rho/\partial y)(\partial p/\partial x)\right] = \rho^{-2}J(\rho, p)$: The solenoidal term, also called the non-homentropic or baroclinic term, arising when isosurfaces of pressure and density are not parallel.

$(\partial F_y/\partial x - \partial F_x/\partial y)$: The forcing and friction term. If the only contribution to this is from molecular viscosity then this term is $\nu\nabla^2\zeta$.

In inviscid two-dimensional incompressible flow, all of the terms on the right-hand side vanish and we have the simple equation

$$\frac{\mathrm{D}(\zeta + f)}{\mathrm{D}t} = 0. \tag{4.77}$$

For inviscid shallow water flow, we can show that (see chapter 3)

$$\frac{\mathrm{D}(\zeta + f)}{\mathrm{D}t} = -(\zeta + f)\left(\frac{\partial u}{\partial x} + \frac{\partial v}{\partial y}\right). \tag{4.78}$$

In this equation the vanishing of the tilting term is perhaps the only aspect which is perhaps not immediately apparent, but this too gives way with a little thought.

4.5 POTENTIAL VORTICITY CONSERVATION

Although Kelvin's circulation theorem is a general statement about vorticity conservation, in its original form it is not always a very *useful* statement for two reasons. First, it is a not a statement about a *field*, such as vorticity itself. Second, it is not satisfied for baroclinic flow, such as is found in the atmosphere and ocean. (Of course non-conservative forces such as viscosity also lead to circulation non-conservation, but this applies to virtually all conservation laws and does not diminish them.) It turns out that it is possible to derive a beautiful conservation law that overcomes both of these failings and one, furthermore, that is extraordinarily useful in geophysical fluid dynamics. This is the conservation of *potential vorticity* introduced first by Rossby and then in a more general form by Ertel.[3] The idea is that we can use a scalar field that is being advected by the flow to keep track of, or to take care of, the evolution of fluid elements. For a baroclinic fluid this scalar field must be chosen in a special way (it must be a function of the density and pressure alone), but the restriction to barotropic fluid can then be avoided. Then using the scalar evolution equation in conjunction with the vorticity equation gives us a scalar conservation equation. In the next few subsections we derive the equation for potential vorticity conservation in several superficially different ways. We do not treat rotation explicitly until section 4.5.5, and so the vorticity in what follows should be regarded as the absolute vorticity.

4.5.1 PV conservation from the circulation theorem

Barotropic fluids

Let us begin with the simple case of a barotropic fluid. For an infinitesimal volume we write Kelvin's theorem as:

$$\frac{\mathrm{D}}{\mathrm{D}t}[(\boldsymbol{\omega}_a \cdot \boldsymbol{n})\delta A] = 0 \tag{4.79}$$

where $\boldsymbol{n}$ is a unit vector normal to an infinitesimal surface δA. Now consider a volume bounded by two isosurfaces of values χ and $\chi + \delta\chi$, where χ is any materially conserved tracer, so satisfying $\mathrm{D}\chi/\mathrm{D}t = 0$, so that δA initially lies in an isosurface of χ (see Fig. 4.8). Since $\boldsymbol{n} = \nabla\chi/|\nabla\chi|$ and the infinitesimal volume $\delta V = \delta h \delta A$, where δh is the
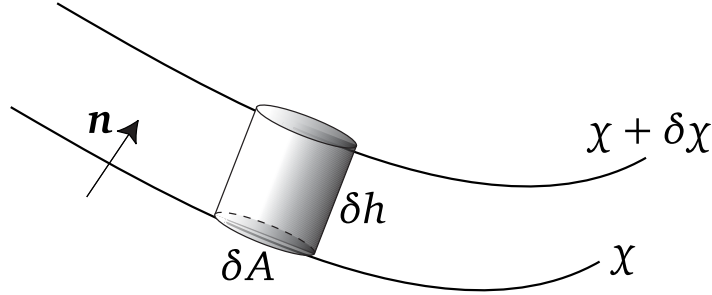
Fig. 4.8 An infinitesimal fluid element, bounded by two isosurfaces of the conserved tracer χ. As $D\chi/Dt = 0$, then $D\delta\chi/Dt = 0$.

separation between the two surfaces, we have

$$\boldsymbol{\omega}_a \cdot \boldsymbol{n}\,\delta A = \boldsymbol{\omega}_a \cdot \frac{\nabla\chi}{|\nabla\chi|}\frac{\delta V}{\delta h}. \tag{4.80}$$

Now, the separation between the two surfaces, δh may be obtained from

$$\delta\chi = \delta\boldsymbol{x} \cdot \nabla\chi = \delta h|\nabla\chi|, \tag{4.81}$$

and using this in (4.79) we obtain

$$\frac{D}{Dt}\left[\frac{(\boldsymbol{\omega}_a \cdot \nabla\chi)\delta V}{\delta\chi}\right] = 0. \tag{4.82}$$

Now, as χ is conserved on material elements, then so is $\delta\chi$, and it may be taken out of the differentiation. The mass of the volume element $\rho\,\delta V$ is also conserved, so that (4.82) becomes

$$\frac{\rho\delta V}{\delta\chi}\frac{D}{Dt}\left(\frac{\boldsymbol{\omega}_a}{\rho} \cdot \nabla\chi\right) = 0 \tag{4.83}$$

or

$$\frac{D}{Dt}(\widetilde{\boldsymbol{\omega}}_a \cdot \nabla\chi) = 0 \tag{4.84}$$

where $\widetilde{\boldsymbol{\omega}}_a = \boldsymbol{\omega}_a/\rho$. Eq. (4.84) is a statement of potential vorticity conservation for a barotropic fluid. The field χ may be chosen arbitrarily, provided that it be materially conserved.

The general case

For a baroclinic fluid the above derivation fails simply because the statement of the conservation of circulation, (4.79) is not, in general, true: there are solenoidal terms on the right-hand side and from (4.52) and (4.54) we have

$$\frac{D}{Dt}[(\boldsymbol{\omega}_a \cdot \boldsymbol{n})\delta A] = \boldsymbol{S} \cdot \boldsymbol{n}\delta A, \qquad \boldsymbol{S} = -\nabla\alpha \times \nabla p = -\nabla\eta \times \nabla T. \tag{4.85}$$
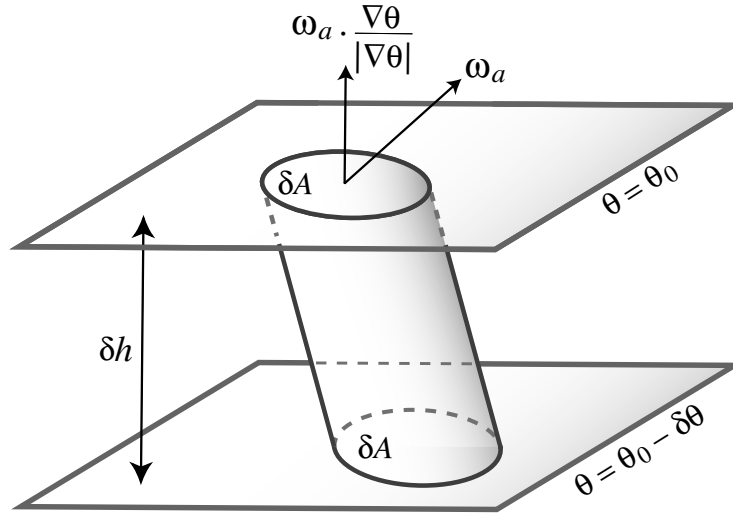
Mass: $\rho \, \delta A \, \delta h = \text{constant}$

Entropy: $|\nabla \theta| \, \delta h = \text{constant}$

Fig. 4.9 Geometry of potential vorticity conservation. The circulation equation is $D[(\omega_a \cdot \boldsymbol{n})\delta A]/Dt = \boldsymbol{S} \cdot \boldsymbol{n} \, \delta A$ where $\boldsymbol{S} \propto \nabla\theta \times \nabla T$. We choose $\boldsymbol{n} = \nabla\theta/|\nabla\theta|$, where θ is materially conserved, to annihilate the solenoidal term on the right-hand side, and we note that $\delta A = \delta V/\delta h$, where δV is the volume of the cylinder, and that $\delta h = \delta\theta/|\nabla\theta|$. The circulation is $C \equiv \omega_a \cdot \boldsymbol{n}\delta A = \omega_a \cdot (\nabla\theta/|\nabla\theta|)(\delta V/\delta h) = [\rho^{-1}\omega_a \cdot \nabla\theta](\delta M/\delta\theta)$ where $\delta M = \rho\delta V$ is the mass of the cylinder. As δM and $\delta\theta$ are materially conserved, so is the potential vorticity $\rho^{-1}\omega_a \cdot \nabla\theta$.

However, the right-hand side may be annihilated by choosing the circuit around which we evaluate the circulation be such that the solenoidal term is identically zero. Given the form of $\boldsymbol{S}$, this occurs if the values of any of p, ρ, η, T are constant on that circuit; that is, if $\chi = p, \rho, \eta$ or T. But the derivation also demands that χ be a materially conserved quantity, which usually restricts its choice to η (or potential temperature), or to ρ itself if the thermodynamic equation is $D\rho/Dt = 0$. Thus, the conservation of potential vorticity for inviscid, adiabatic flow is

$$\frac{D}{Dt}(\widetilde{\boldsymbol{\omega}}_a \cdot \nabla\theta) = 0 \qquad (4.86)$$

where $D\theta/Dt = 0$. For diabatic flow source terms appear on the right-hand side, and we derive these later on. A summary of this derivation provided Fig. 4.9.

4.5.2 PV conservation from the frozen-in property

In this section we show that potential vorticity conservation is a consequence of the frozen-in property of vorticity. This is not surprising, because the circulation theorem itself has a similar origin. Thus, this derivation is not independent of the derivation in the previous section, just a minor re-expression of it. We first consider the case in which the solenoidal term vanishes from the outset.

Barotropic fluids

If χ is a materially conserved tracer then the difference in χ between two infinitesimally close fluid elements is also conserved and

$$\frac{D}{Dt}(\chi_1 - \chi_2) = \frac{D\delta\chi}{Dt} = 0. \tag{4.87}$$

But $\delta\chi = \nabla\chi \cdot \delta\boldsymbol{l}$ where $\delta\boldsymbol{l}$ is the infinitesimal vector connecting the two fluid elements. Thus

$$\frac{D}{Dt}(\nabla\chi \cdot \delta\boldsymbol{l}) = 0 \tag{4.88}$$

But since the line element and the vorticity (divided by density) obey the same equation, we can replace the line element by vorticity (divided by density) in (4.88) to obtain again

$$\frac{D}{Dt}\left(\frac{\nabla\chi \cdot \boldsymbol{\omega}_a}{\rho}\right) = 0. \tag{4.89}$$

That is, the potential vorticity, $Q = (\widetilde{\boldsymbol{\omega}}_a \cdot \nabla\chi)$ is a material invariant, where χ is any scalar quantity that satisfies $D\chi/Dt = 0$.

Baroclinic fluids

In baroclinic fluids we cannot casually substitute the vorticity for that of a line element in (4.88) because of the presence of the solenoidal term, and in any case a little more care would not be amiss. From (4.88) we obtain

$$\delta\boldsymbol{l} \cdot \frac{D\nabla\chi}{Dt} + \nabla\chi \cdot \frac{D\delta\boldsymbol{l}}{Dt} = 0 \tag{4.90}$$

or, using (4.39),

$$\delta\boldsymbol{l} \cdot \frac{D\nabla\chi}{Dt} + \nabla\chi \cdot [(\delta\boldsymbol{l} \cdot \nabla)\boldsymbol{v}] = 0. \tag{4.91}$$

Now, let us choose $\delta\boldsymbol{l}$ to correspond to a vortex line, so that at the initial time $\delta\boldsymbol{l} = \epsilon\widetilde{\boldsymbol{\omega}}_a$. (Note that in this case the association of $\delta\boldsymbol{l}$ with a vortex line can only be made instantaneously, and we cannot set $D\delta\boldsymbol{l}/Dt \propto D\boldsymbol{\omega}_a/Dt$.) Then,

$$\widetilde{\boldsymbol{\omega}}_a \cdot \frac{D\nabla\chi}{Dt} + \nabla\chi \cdot [(\boldsymbol{\omega}_a \cdot \nabla)\boldsymbol{v}] = 0, \tag{4.92}$$

or, using the vorticity equation (4.18),

$$\widetilde{\boldsymbol{\omega}}_a \cdot \frac{D\nabla\chi}{Dt} + \nabla\chi \cdot \left[\frac{D\widetilde{\boldsymbol{\omega}}_a}{Dt} - \frac{1}{\rho^3}\nabla\rho \times \nabla p\right] = 0. \tag{4.93}$$

This may be written

$$\frac{D}{Dt}\widetilde{\boldsymbol{\omega}}_a \cdot \nabla\chi = \frac{1}{\rho^3}\nabla\chi \cdot (\nabla\rho \times \nabla p). \tag{4.94}$$

The term on the right hand side is in general non-zero for an arbitrary choice of scalar, but it will evidently vanish if ∇p, $\nabla\rho$ and $\nabla\chi$ are coplanar. If χ is any function of p and ρ this will be satisfied, but χ must also be a materially conserved scalar. If, as for an ideal gas, $\rho = \rho(\eta, p)$ (or $\eta = \eta(p, \rho)$) where η is the entropy (which is materially conserved), and if χ is a function of entropy η alone, then χ satisfies both conditions. Explicitly, the solenoidal term vanishes because

$$\nabla\chi \cdot (\nabla\rho \times \nabla p) = \frac{d\chi}{d\eta}\nabla\eta \cdot \left[\left(\frac{\partial\rho}{\partial p}\nabla p + \frac{\partial\rho}{\partial\eta}\nabla\eta\right) \times \nabla p\right] = 0. \tag{4.95}$$

Thus, provided χ satisfies the two conditions

$$\frac{D\chi}{Dt} = 0 \quad \text{and} \quad \chi = \chi(p, \rho), \tag{4.96}$$

then (4.94) becomes

$$\frac{D}{Dt}\left(\frac{\boldsymbol{\omega}_a \cdot \nabla\chi}{\rho}\right) = 0. \tag{4.97}$$

The natural choice for χ is potential temperature, whence

$$\boxed{\frac{D}{Dt}\left(\frac{\boldsymbol{\omega}_a \cdot \nabla\theta}{\rho}\right) = 0}. \tag{4.98}$$

The presence of a density term in the denominator is not necessary for incompressible flows (i.e., if $\nabla \cdot \boldsymbol{v} = 0$).

4.5.3 * An algebraic derivation

Finally, we give a straightforward algebraic derivation of potential vorticity conservation. We will take the opportunity to include frictional and diabatic processes, although these may also be included in the derivations above.[4] We begin with the frictional vorticity equation in the form

$$\frac{D\widetilde{\boldsymbol{\omega}}_a}{Dt} = (\widetilde{\boldsymbol{\omega}}_a \cdot \nabla)\boldsymbol{v} + \frac{1}{\rho^3}(\nabla\rho \times \nabla p) + \frac{1}{\rho}(\nabla \times \boldsymbol{F}). \tag{4.99}$$

where $\boldsymbol{F}$ represents any nonconservative force term on the right-hand side of the momentum equation (i.e., $D\boldsymbol{v}/Dt = -\rho^{-1}\nabla p + \boldsymbol{F}$). We have also the equation for our materially conserved scalar χ,

$$\frac{D\chi}{Dt} = \dot{\chi} \tag{4.100}$$

where $\dot{\chi}$ represents any sources and sinks of χ. Now

$$(\widetilde{\boldsymbol{\omega}}_a \cdot \nabla)\frac{D\chi}{Dt} = \widetilde{\boldsymbol{\omega}}_a \cdot \frac{D\nabla\chi}{Dt} + [(\widetilde{\boldsymbol{\omega}}_a \cdot \nabla)\boldsymbol{v}] \cdot \nabla\chi. \tag{4.101}$$

which may be obtained just by expanding the left-hand side. Thus, using (4.100),

$$\widetilde{\boldsymbol{\omega}}_a \cdot \frac{D\nabla\chi}{Dt} = (\widetilde{\boldsymbol{\omega}}_a \cdot \nabla)\,\dot{\chi} - [(\widetilde{\boldsymbol{\omega}}_a \cdot \nabla)\boldsymbol{v}] \cdot \nabla\chi. \qquad (4.102)$$

Now take the dot product of (4.99) with $\nabla\chi$:

$$\nabla\chi \cdot \frac{D\widetilde{\boldsymbol{\omega}}_a}{Dt} = \nabla\chi \cdot [(\widetilde{\boldsymbol{\omega}}_a \cdot \nabla)\boldsymbol{v}] + \nabla\chi \cdot \left[\frac{1}{\rho^3}(\nabla\rho \times \nabla p)\right] + \nabla\chi \cdot \left[\frac{1}{\rho}(\nabla \times \boldsymbol{F})\right]. \quad (4.103)$$

The sum of the last two equations yields

$$\frac{D}{Dt}(\widetilde{\boldsymbol{\omega}}_a \cdot \nabla\chi) = \widetilde{\boldsymbol{\omega}}_a \cdot \nabla\dot{\chi} + \nabla\chi \cdot \left[\frac{1}{\rho^3}(\nabla\rho \times \nabla p)\right] + \frac{\nabla\chi}{\rho} \cdot (\nabla \times \boldsymbol{F}). \qquad (4.104)$$

This equation reprises (4.94), but with the addition of frictional and diabatic terms. As before, the solenoidal term is annihilated if we choose $\chi = \theta(p, \rho)$, so giving the evolution equation for potential vorticity in the presence of forcing and diabatic terms, namely:

$$\boxed{\frac{D}{Dt}(\widetilde{\boldsymbol{\omega}}_a \cdot \nabla\theta) = \widetilde{\boldsymbol{\omega}}_a \cdot \nabla\dot{\theta} + \frac{\nabla\theta}{\rho} \cdot (\nabla \times \boldsymbol{F})}. \qquad (4.105)$$

4.5.4 Effects of salinity and moisture

For seawater the equation of state may be written as

$$\theta = \theta(\rho, p, S) \qquad (4.106)$$

where θ is potential temperature and S is salinity. In the absence of diabatic terms (which include saline diffusion) potential temperature is a materially conserved quantity. However, because of the presence of salinity, θ cannot be used to annihilate the solenoidal term; that is

$$\nabla\theta \cdot (\nabla\rho \times \nabla p) = \left(\frac{\partial\theta}{\partial S}\right)_{p,\rho} \nabla S \cdot (\nabla\rho \times \nabla p) \neq 0. \qquad (4.107)$$

Strictly speaking then, *there is no potential vorticity conservation principle for seawater.* However, such a blunt statement rather overemphasizes the importance of salinity in the ocean, and the nonconservation of potential vorticity because of this effect is rather small.

In a moist atmosphere in which condensational heating occurs there is no 'moist potential vorticity' that is generally conserved. We may choose to define a moist PV (Q_e say) based on moist equivalent potential temperature but it does not always obey $DQ_e/Dt = 0$.[5]
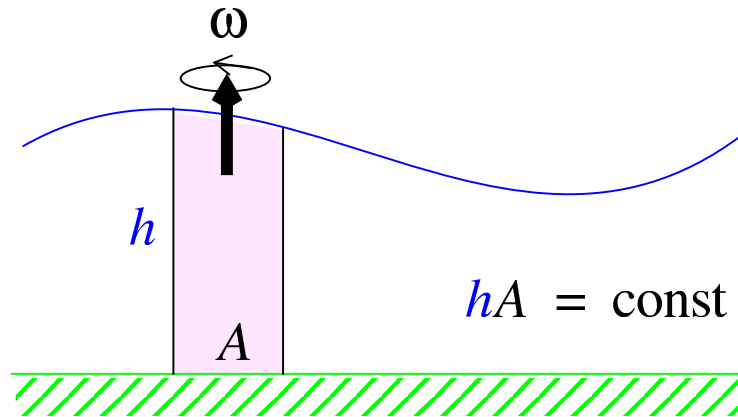
Fig. 4.10 The mass of a column of fluid, hA, is conserved in the shallow water system. Furthermore, the vorticity is tied to material lines so that ζA is also a material invariant, where $\zeta = \boldsymbol{\omega} \cdot \mathbf{k}$ is the vertical component of the vorticity. From this, ζ/h must be materially conserved; that is $D(\zeta/h)/Dt = 0$, which is the conservation of potential vorticity in a shallow water system. In a rotating system this readily generalizes to $D[(\zeta + f)/h]/Dt = 0$.

4.5.5 Effects of rotation, and summary remarks

In a rotating frame the potential vorticity conservation equation is obtained simply by replacing $\boldsymbol{\omega}_a$ by $\boldsymbol{\omega} + 2\boldsymbol{\Omega}$, where $\boldsymbol{\Omega}$ is the rotation rate of the rotating frame. The operator D/Dt is reference-frame invariant, and so may be evaluated using the usual formulae with velocities measured in the rotating frame.

The conservation of potential vorticity has profound consequences in fluid dynamics, especially in a rotating, stratified fluid. The nonconservative terms are often small, and large-scale flow in both the ocean and atmosphere is characterized by conservation of potential vorticity. Such conservation is a very powerful constraint on the flow, and indeed it turns out that potential vorticity is a much more useful quantity for baroclinic, or nonhomentropic fluids than for barotropic fluids, because the required use of a special conserved scalar imparts additional information. A large fraction of the remainder of this book explores, in one way or another, the consequences of potential vorticity conservation.

4.6 * POTENTIAL VORTICITY IN THE SHALLOW WATER SYSTEM

In chapter 3 we derived potential vorticity conservation by direct manipulation of the shallow water equations. We now show that here too, potential vorticity is related to the conservation of circulation. Specifically, we will begin with the the three-dimensional form of Kelvin's theorem, and then make the small aspect ratio assumption (which is the key assumption underlying shallow water dynamics), and thereby recover shallow water potential vorticity conservation. In the following two subsections we give two variants of such derivation (see also Fig. 4.10).

4.6.1 Using Kelvin's theorem

We begin with

$$\frac{D}{Dt}(\boldsymbol{\omega}_3 \cdot \delta \boldsymbol{S}) = 0, \tag{4.108}$$

where $\boldsymbol{\omega}_3$ is the curl of the three-dimensional velocity and $\delta \boldsymbol{S} = \hat{\boldsymbol{n}} \delta S$ is an arbitrary infinitesimal vector surface element, with $\boldsymbol{n}$ pointing in the direction normal to the surface. If we separate the vorticity and surface element into vertical and horizontal components we can write (4.108) as

$$\frac{D}{Dt}[(\zeta + f)\delta A + \boldsymbol{\omega}_h \cdot \delta \boldsymbol{S}_h] = 0 \tag{4.109}$$

where $\boldsymbol{\omega}_h$ and $\delta \boldsymbol{S}_h$ are the horizontally-directed components of the vorticity and the surface element, and $\delta A = \boldsymbol{k} \delta \boldsymbol{S}$ is the area of a horizontal cross-section of a fluid column. In Cartesian form the horizontal component of the vorticity is

$$\boldsymbol{\omega}_h = \boldsymbol{i} \left(\frac{\partial w}{\partial y} - \frac{\partial v}{\partial z} \right) - \boldsymbol{j} \left(\frac{\partial w}{\partial x} - \frac{\partial v}{\partial z} \right) = \boldsymbol{i} \frac{\partial w}{\partial y} - \boldsymbol{j} \frac{\partial w}{\partial x}, \tag{4.110}$$

where vertical derivatives of the horizontal velocity are zero by virtue of the nature of the shallow water system. Now, the vertical velocity in the shallow water system is smaller than the horizontal velocity by the order of the apect ratio — the ratio of the fluid depth to the horizontal scale of motion. Furthermore, the size of the horizontally-directed surface element is also an aspect-ratio smaller than the vertically-directed component. That is,

$$|\boldsymbol{\omega}_h| \sim \alpha |\zeta| \qquad \text{and} \qquad |\delta \boldsymbol{S}_h| \sim \alpha |\delta A|, \tag{4.111}$$

where $\alpha = H/L$ is the aspect ratio. Thus $\boldsymbol{\omega}_h \cdot \delta \boldsymbol{S}_h$ is an aspect-number squared smaller than the term $\zeta \delta A$ and in the small aspect ratio approximation should be neglected. Kelvin's circulation theorem, (4.109) becomes

$$\frac{D}{Dt}[(\zeta + f)\delta A] = 0 \qquad \text{or} \qquad \frac{D}{Dt}\left[\frac{(\zeta + f)}{h} h \delta A \right] = 0, \tag{4.112}$$

where h is the depth of the fluid column. But $h \delta A$ is the volume of the fluid column, and this is constant. Thus, as in (3.81), we have

$$\frac{D}{Dt}\left(\frac{\zeta + f}{h} \right) = 0, \tag{4.113}$$

where, because horizontal velocities are independent of the vertical coordinate, the advection is purely horizontal.

4.6.2 Using an appropriate scalar field

In a constant density fluid we can write potential vorticity conservation as

$$\frac{D}{Dt}(\boldsymbol{\omega}_3 \cdot \nabla \chi) = 0, \tag{4.114}$$

where χ is any materially-conserved scalar [c.f. (4.84) or (4.89)]. In the flat-bottomed shallow water system, a useful choice of scalar is the ratio z/h, where h is the local thickness of the fluid column because, from (3.29),

$$\frac{\mathrm{D}}{\mathrm{D}t}\left(\frac{z}{h}\right) = 0, \tag{4.115}$$

the fluid is flat-bottomed (for simplicity). With this choice of scalar, potential vorticity conservation becomes

$$\frac{\mathrm{D}}{\mathrm{D}t}\left[\boldsymbol{\omega} \cdot \nabla\left(\frac{z}{h}\right)\right] = 0, \tag{4.116}$$

where $\boldsymbol{\omega}$ and $\mathrm{D}/\mathrm{D}t$ are fully three dimensional. Expanding the dot product gives

$$\frac{\mathrm{D}}{\mathrm{D}t}\left[\frac{\zeta + f}{h} - \frac{z}{h^2}\boldsymbol{\omega}_h \cdot \nabla_z h\right] = 0. \tag{4.117}$$

For an order-unity Rossby number, the ratio of the size of the two terms in this equation is

$$\frac{|\zeta|}{|(z/h)\boldsymbol{\omega}_h \cdot \nabla_h h|} \sim \frac{[U/L]}{\left[WH/L^2\right]} = \frac{UL}{WH} = \alpha^2 \ll 1. \tag{4.118}$$

Thus, the second term in (4.117) is an aspect-ratio squared smaller than the first and, upon its neglect, (4.113) is recovered.

4.7 POTENTIAL VORTICITY IN APPROXIMATE, STRATIFIED MODELS

If approximate models of stratified flow — Boussinesq, hydrostatic and so on — are to be useful then they should conserve an appropriate form potential vorticity, and we consider a few such cases here.

4.7.1 The Boussinesq equations

The Boussinesq equations are incompressible (that is, the volume of a fluid element is conserved) and the equation for vorticity itself is isomorphic to that for a line element. However the Boussinesq equations are not barotropic — $\nabla\rho$ is not parallel to ∇p — and although the pressure gradient term $\nabla\phi$ disappears on taking its curl (or equivalently disappears on integration around a closed path) the buoyancy term $\mathbf{k}b$ does not, and it is this that prevents Kelvin's circulation theorem from holding. Specifically, the evolution of circulation in the Boussinesq equations obeys

$$\frac{\mathrm{D}}{\mathrm{D}t}[(\boldsymbol{\omega}_a \cdot \boldsymbol{n})\delta A] = (\nabla \times b\mathbf{k}) \cdot \boldsymbol{n}\delta A \tag{4.119}$$

The right-hand side is annihilated if we choose $\boldsymbol{n}$ to be parallel to ∇b, because $\nabla b \cdot \nabla \times (b\mathbf{k}) = 0$. In the simple Boussinesq equations the thermodynamic equation is

$$\frac{\mathrm{D}b}{\mathrm{D}t} = 0, \tag{4.120}$$

and potential vorticity conservation is therefore (with $\boldsymbol{\omega}_a = \boldsymbol{\omega} + \boldsymbol{\Omega}$)

$$\frac{\mathrm{D}Q}{\mathrm{D}t} = 0, \qquad Q = (\boldsymbol{\omega} + 2\boldsymbol{\Omega}) \cdot \nabla b. \qquad (4.121\text{a,b})$$

Expanding (4.121b) in Cartesian coordinates with $\boldsymbol{\Omega} = f\mathbf{k}$ we obtain:

$$Q = (v_x - u_y)b_z + (w_y - v_z)b_x + (u_z - w_x)b_y + fb_z. \qquad (4.122)$$

In the general Boussinesq equations b itself is not materially conserved. We cannot expect to obtain a conservation law if salinity is present, but if the equation of state and thermodynamic equation are:

$$b = b(\theta, z), \qquad \frac{\mathrm{D}\theta}{\mathrm{D}t} = 0, \qquad (4.123)$$

then potential vorticity conservation follows, because taking the dot-product with $\nabla\theta$ will annihilate the right-hand side of (4.119). That is,

$$\nabla\theta \cdot \nabla \times (b\mathbf{k}) = \left(\frac{\partial\theta}{\partial z}\nabla z + \frac{\partial\theta}{\partial b}\nabla b\right) \cdot \nabla \times (b\mathbf{k}) = 0. \qquad (4.124)$$

The materially conserved potential vorticity is then just $Q = \boldsymbol{\omega}_a \cdot \nabla\theta$. Note that if the equation of state is $b = b(\theta, \phi)$, where ϕ is the pressure, then potential vorticity is not conserved because $\nabla p \cdot \nabla \times (b\mathbf{k}) \neq 0$.

4.7.2 The hydrostatic equations

Making the hydrostatic approximation has no effect on the satisfaction of Kelvin's circulation theorem or, in a baroclinic fluid, Bjerknes's theorem. Thus, in a baroclinic hydrostatic fluid we have

$$\frac{\mathrm{D}}{\mathrm{D}t}\int (\boldsymbol{\omega}_{\text{hy}} + 2\boldsymbol{\Omega}) \cdot \mathrm{d}\boldsymbol{S} = -\int \nabla\alpha \times \nabla p \cdot \mathrm{d}\boldsymbol{S} \qquad (4.125)$$

where, from (4.65) $\boldsymbol{\omega}_{\text{hy}} = \nabla \times \boldsymbol{u} = -\mathbf{i}v_z + \mathbf{j}u_z + \mathbf{k}(v_x - u_y)$, but the gradient operator and material derivative are fully three-dimensional. Derivation of potential vorticity conservation then proceeds, as in section 4.5.1, by choosing the circuit over which the circulation is calculated to be such that the right-hand side vanishes; that is, to be such that the solenoidal term is annihilated. Precisely as before, this occurs if the circuit is barotropic and without further ado we write

$$\frac{\mathrm{D}Q_{\text{hy}}}{\mathrm{D}t} = \frac{\mathrm{D}}{\mathrm{D}t}\left(\frac{(\boldsymbol{\omega}_h + 2\boldsymbol{\Omega}) \cdot \nabla\theta}{\rho}\right) = 0. \qquad (4.126)$$

Expanding this gives in Cartesian coordinates

$$Q_{\text{hy}} = \frac{1}{\rho}\left[(v_x - u_y)\theta_z - v_z\theta_x + u_z\theta_y + 2\Omega\theta_z\right]. \qquad (4.127)$$

In spherical coordinates the hydrostatic approximation is usually accompanied by the traditional approximation and the expanded expression for a conserved potential vorticity is more complicated. It can still be derived from Kelvin's theorem, but this is left as an exercise for the reader (problem 4.4).

4.7.3 Potential Vorticity on Isentropic Surfaces

If we begin with the primitive equations in isentropic coordinates then potential vorticity conservation follows quite simply. Cross differentiating the horizontal momentum equations (3.165) gives the vorticity equation [c.f. (3.73)]

$$\frac{D}{Dt}(\zeta + f) + (\zeta + f)\nabla_\theta \cdot \boldsymbol{u} = 0. \tag{4.128}$$

where $D/Dt = \partial/\partial t + \boldsymbol{u} \cdot \nabla_\theta$. The thermodynamic equation is

$$\frac{D\sigma}{Dt} + \sigma \nabla \cdot \boldsymbol{u} = 0, \tag{4.129}$$

where $\sigma = \partial z/\partial b$ (Boussinesq) or $\partial p/\partial \theta$ (ideal gas) is the thickness of an isopycnal layer. Eliminating the divergence between (4.128) and (4.129) gives

$$\frac{D}{Dt}\left(\frac{\zeta + f}{\sigma}\right) = 0. \tag{4.130}$$

The derivation, and the result, are precisely the same as with the shallow water equations (sections 3.6.1 and 4.6).

A connection between isentropic and height coordinates

The hydrostatic potential vorticity written in height coordinates may be transformed into a form that reveals its intimate connection with isentropic surfaces. Let us make the Boussinesq approximation for which the potential vorticity is

$$Q_{\text{hy}} = (v_x - u_y)b_z - v_z b_x + u_z b_y, \tag{4.131}$$

where b is the buoyancy. We can write this as

$$Q_{\text{hy}} = b_z\left[\left(v_x - v_z\frac{b_x}{b_z}\right) - \left(u_y - u_z\frac{b_y}{b_z}\right)\right]. \tag{4.132}$$

But the terms in the inner brackets are just the horizontal velocity derivatives at constant b. To see this, note that

$$\left(\frac{\partial v}{\partial x}\right)_b = \left(\frac{\partial v}{\partial x}\right)_z + \frac{\partial v}{\partial z}\left(\frac{\partial z}{\partial x}\right)_b = \left(\frac{\partial v}{\partial x}\right)_z - \frac{\partial v}{\partial z}\left(\frac{\partial b}{\partial x}\right)_z \bigg/ \frac{\partial b}{\partial z}, \tag{4.133}$$

with a similar expression for $(\partial u/\partial y)_b$. (These relationships follow from standard rules of partial differentiation. Derivatives with respect to z are taken at constant x and y.) Thus, we obtain

$$Q_{\text{hy}} = \frac{\partial b}{\partial z}\left[\left(\frac{\partial v}{\partial x}\right)_b - \left(\frac{\partial u}{\partial y}\right)_b\right] = \frac{\partial b}{\partial z}\zeta_b \tag{4.134}$$

Thus, potential vorticity is simply the horizontal vorticity evaluated on a surface of constant buoyancy, multiplied by the vertical derivative of buoyancy, a measure of static stability. An analogous derivation, with a similar result, proceeds for the ideal gas equations, with potential temperature replacing buoyancy.

4.8 THE IMPERMEABILITY OF ISENTROPES TO POTENTIAL VORTICITY

A kinematical result is a result valid forever.
Clifford Truesdell, *The Kinematics of Vorticity,* 1954.

An interesting property of isentropic surfaces is that they are 'impermeable' to potential vorticity, meaning that the mass integral of potential vorticity ($\int Q\rho \, dV$) over a volume bounded by an isentropic surface remains constant, even in the presence of diabatic sources, provided the surfaces do not intersect a non-isentropic surface like the ground.[6] This may seem surprising, especially because unlike most conservation laws the result does not require adiabatic flow, and for that reason it leads to interesting interpretations of a number of phenomena. However, at the same time impermeability is a consequence of the definition of potential vorticity rather than the equations of motion, and in that sense is a kinematic property.

To derive the result we define $s \equiv \rho Q = \nabla \cdot (\theta \boldsymbol{\omega})$ and integrate over some volume V to give

$$I = \int_V s \, dV = \int_V \nabla \cdot (\theta \boldsymbol{\omega}) \, dV = \int_S \theta \boldsymbol{\omega} \cdot d\boldsymbol{S}, \qquad (4.135)$$

using the divergence theorem, where S is the surface surrounding the volume V. If this is an isentropic surface then we have

$$I = \theta \int_S \boldsymbol{\omega} \cdot d\boldsymbol{S} = \theta \int_V \nabla \cdot \boldsymbol{\omega} \, dV = 0, \qquad (4.136)$$

again using the divergence theorem. That is, over a volume wholly enclosed by a single isentropic surface the integral of s vanishes. If the volume is bounded by more than one isentropic surface neither of which intersect the surface, for example by concentric spheres of different radii as in Fig. 4.11a, the result still holds. The quantity s is called 'potential vorticity concentration', or 'PV concentration'. The integral of s over a volume is akin to the total amount of a conserved material property, like salt content, and so may be called 'PV substance'. That is, the PV concentration is the amount of potential vorticity substance per unit volume and

$$\text{PV substance} = \int s \, dV = \int \rho Q \, dV, \qquad (4.137)$$

which follows the sstandard chemical meaning for concentration.

Suppose now that fluid volume is enclosed by an isentrope that intersects the ground, as in Fig. 4.11b. Let A denote the isentropic surface, B denote the ground, θ_A the constant value of θ on the isentrope, and $\theta_B(x, y, t)$ the non-constant value of θ on the ground. The integral of s over the volume is then

$$\begin{aligned} I = \int_V \nabla \cdot (\theta \boldsymbol{\omega}) \, dV &= \theta_A \int_A \boldsymbol{\omega} \cdot d\boldsymbol{S} + \int_B \theta_B \boldsymbol{\omega} \cdot d\boldsymbol{S} \\ &= \theta_A \int_{A+B} \boldsymbol{\omega} \, d\boldsymbol{S} + \int_B (\theta_B - \theta_A) \boldsymbol{\omega} \cdot d\boldsymbol{S} \qquad (4.138) \\ &= \int_B (\theta_B - \theta_A) \boldsymbol{\omega} \cdot d\boldsymbol{S}. \end{aligned}$$
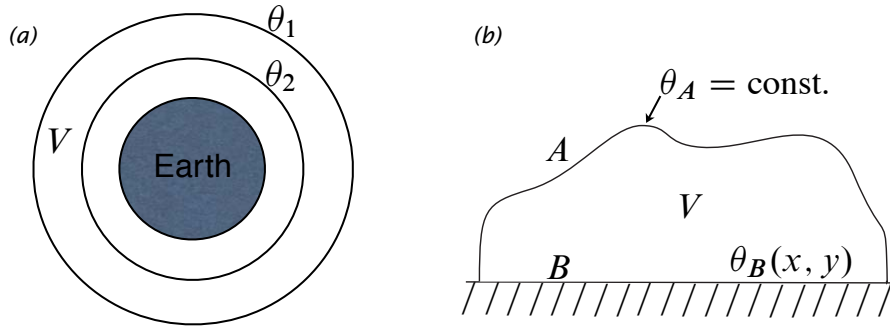
Fig. 4.11 (a) Two isentropic surfaces that do not intersect the ground. The integral of PV concentration over the volume between then, V, is zero, even if there is heating and the contours move. (b) An isentropic surface, A, intersects the ground, B, so enclosing a volume V. The rate of change of PV concentration over the volume is given by an integral over B.

The first term on the second line vanishes after using the divergence theorem. Thus, the value of I, and so its rate of change, is a function *only of an integral over the surface B,* and the PV flux there must be calculated using the full equations of motion. However, we do not need to be concerned with a flux of PV concentration through the isentropic surface. Put another way, the PV substance in a volume can change only when isentropes enclosing the volume intersect a boundary such as the earth's surface.

4.8.1 Interpretation and application

Motion of the isentropic surface

How can the above results hold in the presence of heating? The isentropic surfaces must move in such a way that the total amount of PV concentration contained between them nevertheless stays fixed, and we now demonstrate this explicitly. The potential vorticity equation may be written

$$\frac{\partial Q}{\partial t} + \boldsymbol{v} \cdot \nabla Q = S_Q, \tag{4.139}$$

where, from (4.105), $S_Q = (\boldsymbol{\omega}/\rho) \cdot \nabla\dot\theta + \nabla\theta \cdot (\nabla \times \boldsymbol{F})/\rho$. Using mass continuity this may be written as

$$\frac{\partial s}{\partial t} + \nabla \cdot \boldsymbol{J} = 0, \tag{4.140}$$

where $\boldsymbol{J} \equiv \rho\boldsymbol{v}Q + \boldsymbol{N}$ and $\nabla \cdot \boldsymbol{N} = -\rho S_Q$. Written this way, the quantity $\boldsymbol{J}/(\rho Q)$ is a notional velocity, $\boldsymbol{v}_Q$ say, and s satisfies

$$\frac{\partial s}{\partial t} + \nabla \cdot (\boldsymbol{v}_Q s) = 0. \tag{4.141}$$

That is, s evolves as if it were being fluxed by the velocity $\boldsymbol{v}_Q$. A chemical tracer χ, where χ is the amount of tracer per unit volume, obeys a similar equation, to wit

$$\frac{\partial \chi}{\partial t} + \nabla \cdot (\boldsymbol{v}\chi) = 0, \tag{4.142}$$

However, whereas (4.142) implies that $D(\chi/\rho)/Dt = 0$, (4.141) does not imply that $\partial Q/\partial t + \boldsymbol{v}_Q \cdot \nabla Q = 0$ because $\partial \rho/\partial t + \nabla \cdot (\rho \boldsymbol{v}_Q) \neq 0$.

Now, the impermeability result tells us that there can be no notional velocity across an isentropic surface. How can this be satisfied by the equations of motion? We write the right-hand side of (4.139) as

$$\rho S_q = \nabla \cdot (\dot{\theta}\boldsymbol{\omega} + \theta \nabla \times \boldsymbol{F}) = \nabla \cdot (\dot{\theta}\boldsymbol{\omega} + \boldsymbol{F} \times \nabla \theta). \qquad (4.143)$$

Thus, the $\boldsymbol{J}$ vector is

$$\boldsymbol{J} = \rho \boldsymbol{v} Q - \dot{\theta}\boldsymbol{\omega} - \boldsymbol{F} \times \nabla \theta \qquad (4.144a)$$

$$= \rho Q(\boldsymbol{v}_\perp + \boldsymbol{v}_\parallel) - \dot{\theta}\boldsymbol{\omega}_\parallel - \boldsymbol{F} \times \nabla \theta, \qquad (4.144b)$$

where

$$\boldsymbol{v}_\parallel = \boldsymbol{v} - \frac{\boldsymbol{v} \cdot \nabla \theta}{|\nabla \theta|^2}\nabla \theta, \qquad \boldsymbol{v}_\perp = -\frac{\partial \theta/\partial t}{|\nabla \theta|^2}\nabla \theta, \qquad (4.145a)$$

$$\boldsymbol{\omega}_\parallel = \boldsymbol{\omega} - \frac{\boldsymbol{\omega} \cdot \nabla \theta}{|\nabla \theta|^2}\nabla \theta = \boldsymbol{\omega} - \frac{Q}{|\nabla \theta|^2}\nabla \theta. \qquad (4.145b)$$

The subscripts '$\perp$' and '$\parallel$' denote components perpendicular and parallel to the local isentropic surface, and $\boldsymbol{v}_\perp$ is the velocity of the isentropic surface normal to itself. Equation (4.144) may be verified by using (4.145) and $D\theta/Dt = \dot{\theta}$.

The 'parallel' terms in (4.144) are all vectors parallel to the local isentropic surface, and therefore do not lead to any flux of PV concentration across that surface. Furthermore, the term $\rho Q\boldsymbol{v}_\perp$ is ρQ multiplied by the normal velocity of the surface. That is to say, the notional velocity associated with the flux normal to the isentropic surface is equal to the normal velocity of the isentropic surface itself, and so it too provides no flux of PV concentration across that surface (even through there may well be a mass flux across the surface). Put simply, the isentropic surface always moves in such a way as to ensure that there is no flux of PV concentration across it. In our proof of the impermeability result in the previous section we used the fact that the potential vorticity multiplied by density is the divergence of something. In the demonstration above we used the fact that the terms *forcing* this are the divergence of something.

* Dynamical choices of PV flux and a connection to Bernoullis' theorem

If we add a non-divergent vector to the flux, $\boldsymbol{J}$, then it has no effect on the evolution of s. This gauge invariance means that the notional velocity, $v_Q = \boldsymbol{J}/(\rho Q)$ is similarly non-unique, although it does not mean that there are not dynamical choices for it that are more approropriate in given circumstances. To explore this, let us obtain a general expression for $\boldsymbol{J}$ by starting with the definition of s, so that

$$\frac{\partial s}{\partial t} = \nabla \theta \cdot \frac{\partial \boldsymbol{\omega}}{\partial t} + \boldsymbol{\omega} \cdot \nabla \frac{\partial \theta}{\partial t}$$

$$= \nabla \theta \cdot \nabla \times \frac{\partial \boldsymbol{v}}{\partial t} + \nabla \cdot \left(\boldsymbol{\omega} \frac{\partial \theta}{\partial t}\right) = -\nabla \cdot \boldsymbol{J}' \qquad (4.146)$$

where

$$\boldsymbol{J}' = \nabla\theta \times \frac{\partial \boldsymbol{v}}{\partial t} - \frac{\partial \theta}{\partial t}\boldsymbol{\omega} + \nabla\phi \times \nabla\chi. \tag{4.147}$$

The last term in this expression is an arbitrary divergence-free vector. If we choose $\phi = \theta$ and $\chi = B$, where B is the Bernoulli function given by $B = I + \boldsymbol{v}^2/2 + p/\rho$ where I is the internal energy per unit mass, then

$$\boldsymbol{J}' = \nabla\theta \times \left(\nabla B + \frac{\partial \boldsymbol{v}}{\partial t}\right) - \boldsymbol{\omega}(\dot{\theta} - \boldsymbol{v} \cdot \nabla\theta), \tag{4.148}$$

having used the thermodynamic equation $\mathrm{D}\theta/\mathrm{D}t = \dot{\theta}$. Now, the momentum equation may be written, without approximation, in the form (see problems 2.1 and 2.2)

$$\frac{\partial \boldsymbol{v}}{\partial t} = -\boldsymbol{\omega} \times \boldsymbol{v} + T\nabla\eta + \boldsymbol{F} - \nabla B \tag{4.149}$$

where η is the specific entropy ($\mathrm{d}\eta = c_p\,\mathrm{d}\ln\theta$). Using (4.148) and (4.149) gives

$$\boldsymbol{J}' = \rho Q\boldsymbol{v} - \dot{\theta}\boldsymbol{\omega} + \nabla\theta \times \boldsymbol{F}. \tag{4.150}$$

which is the same as (4.144a). Furthermore, using (4.147) for steady flow,

$$\boldsymbol{J} = \nabla\theta \times \nabla B. \tag{4.151}$$

That is, the flux of potential vorticity (in this gauge) is aligned with the intersection of θ- and B-surfaces. For steady *inviscid and adiabatic* flow the Bernoulli function is constant along streamlines; that is, surfaces of constant Bernoulli function are aligned with streamlines, and, because θ is materially conserved, streamlines are formed at intersecting θ- and B-surfaces, as in (1.198). In the presence of forcing, this property is replaced by (4.151), that the flux of PV concentration is along such intersections.

   This choice of gauge leading to (4.150) is physical in that it reduces to the true advective flux $\boldsymbol{v}\rho Q$ for unforced, adiabatic flow, but it is not a unique choice, nor mandated by the dynamics. Choosing $\chi = 0$ leads to

$$\boldsymbol{J}_1 = \rho Q\boldsymbol{v} - \dot{\theta}\boldsymbol{\omega} + \nabla\theta \times (\boldsymbol{F} - \nabla B) \tag{4.152}$$

and using (4.147) this vanishes for steady flow, a potentially useful property.

4.8.2 Summary Remarks

The impermeability result has a number of consequences, some obvious with hindsight, and it also provides an interesting point of view and diagnostic tool.[7] Here, we will just remark:

   ★ There can be no net transport of potential vorticity across an isentropic surface, and the total amount of potential vorticity in a volume wholly enclosed by isentropic surfaces is zero.

★ Thus, and trivially, the amount of potential vorticity contained between two isen-tropes isolated from the earth's surface in the northern hemisphere is the negative of the corresponding amount in the southern hemisphere.

★ Potential vorticity flux lines (i.e., lines everwhere parallel to J) can either close in on themselves or begin and end at boundaries (e.g., the ground, the ocean surface). However, J may change its character. Thus, for example, at the base of the oceanic mixed layer J may change from from being a diabatic flux above to an adiabatic advective flux below. There may be a similar change in character at the atmospheric tropopause.

★ The flux vector J is defined only to within the curl of a vector. Thus the vector $J' = J + \nabla \times A$, where A is an arbitrary vector, is as valid as is J in the above derivations and diagnostics.

Notes

1 The theorem was first obtained by Silberstein (1896), but it was Bjerknes (1898) who applied it to meteorological and oceanographic problems and realized its importance (Thorpe et al. 2003). 'Bjerknes' theorem' is sometimes stated to be that the evolution of circulation around a circuit is determined by the number of solenoids passing through any surface bounded by that circuit, but the meaning is that of (4.52).

Vilhelm Bjerknes (1862–1951) was a physicist and hydrodynamicist who in 1917 moved to the University of Bergen as founding head of the Bergen Geophysical Institute. Here, late in his career, he did what is probably his most influential work in meteorology, setting up and contributing to the 'Bergen School of Meteorology'. Among other things he and his colleagues were the first to consider, as a practical proposition, the use of numerical methods — initial data in conjunction with the fluid equations of motion — to forecast the state of the atmosphere, based on earlier work describing how that task might be done (Bjerknes 1904). Innaccurate initial velocity fields compounded with the shear complexity of the effort ultimately defeated them, but the effort was continued (also unsuccessfully) by L. F. Richardson (Richardson 1922), before J. Charney, R. Fjortoft and J. Von Neumann eventually made what may be regarded as the first successful numerical forecast (Charney et al. 1950). Their success can be attributed to the used of a simplified, filtered, set of equations and the use of an electronic computer.

Vilhelm's son, Jacob Bjerknes (1897-1975) was a leading player in the Bergen school. He was responsible for the now-famous frontal model of cyclones (Bjerknes 1919), and was one of the first to seriously discuss the role of cyclones in the general circulation of the atmosphere. In collaboration with Halvor Solberg and Tor Bergeron the frontal model lead to a prescient picture of the life-cycle of extra-tropical cyclones (see chapter 9), in which a wave grows initially on the polar front (akin to baroclinic instability with the meridional temperature gradient compressed to a front, but baroclinic instability theory was not yet developed), develops into a mature cyclone, occludes and decays. In 1939 Bjerknes

moved to the U.S. and, largely because of WWII, stayed, joining UCLA and heading its Dept. of Meteorology after its formation in 1945. He developed an interest in air-sea interactions, and notably proposed the essential mechanism governing El Niño, a feedback between sea-surface temperatures and the strength of the trade winds (Bjerknes 1969). [See also Friedman (1989), Cressman (1996), articles in Shapiro and Grønas (1999), and a memoir by Arnt Eliassen available from http://www.nap.edu/readingroom/books/biomems/jbjerknes.html.]

2   The result (4.60) is sometimes attributed to Bjerknes (1902), although it was evidently known to Poincaré (1893).

3   The first derivation of the PV conservation law was given for the shallow water equations Rossby (1936), with a generalization to multiple layers in Rossby (1938). In the 1936 paper Rossby notes [his eq. (75)] that a fluid column satisfies $f + \zeta = cD$ where c is a constant and D is the thickness of a fluid column; equivently, $(f + \zeta)/D$ is a material invariant. In Rossby (1940) this was generalized slightly to an isentropic layer, in which ζ is computed using horizontal derivates taken at constant density or potential temperature. In this paper Rossby also introduces the expression 'potential vorticity', as follows: *'This quantity, which may be called the potential vorticity, represents the vorticity the air column would have it it were brought, isopycnally or isentropically, to a standard latitude (f_0) and stretched or shrunk vertically to a standard depth D_0 or weight $\triangle_0$.'* (Rossby's italics.) That is,

$$\text{Potential Vorticity} = \zeta_0 = \left(\frac{\zeta + f}{D}\right) D_0 - f_0, \qquad (4.153)$$

which follows from his eq. (11), and this is the sense he uses it in that paper. However, potential vorticity has come to mean the quantity $(\zeta + f)/D$, which of course does not have the dimensions of vorticity. We use it in this latter, now conventional, sense throughout this book. Ironically, quasi-geostrophic potential vorticity as usually defined does have the dimensions of vorticity.

The expression for potential vorticity in a continuously stratified fluid was given by Ertel (1942a), and its relationship to circulation was given by Ertel (1942b). It is now commonly known as the *Ertel potential vorticity.* Interestingly, in Rossby (1940) we find the Fermat-like comment 'It is possible to derive corresponding results for an atmosphere in which the potential temperature varies continuously with elevation. . . . The generalized treatment will be presented in another place.'(!) Opinions differ as to whether Rossby's and Ertel's derivations were independent: Charney (in Lindzen et al. 1990) suggests they were, and Cressman (1996) remarks that the origin of the concept of potential vorticity is a 'delicate one that has aroused some passion in private correspondences'. In fact, Ertel visited MIT in autumn 1937 and presumably talked to Rossby and became aware of his work. The likeliest scenario is that Ertel did know of Rossby's shallow water theorems, and that he subsequently provided an independent and significant generalization. Rossby and Ertel apparently remained on good terms, but further collaboration was stymied by WWII. They did later publish a short joint paper, with both German and English versions, describing their conservation theorems (Ertel and Rossby 1949) . (I thank A. Persson and R. Samelson for some historical details.)

4   Truesdell (1951, 1954) and Obukhov (1962) were early explorers of the consequences of heating and friction on potential vorticity.

5   Schubert et al. (2001) provide more discussion of this topic. They derive a 'moist

PV' that, although not materially conserved, is an extension of the dry Ertel PV to moist atmospheres and has an impermeability result.

6 Haynes and McIntyre (1987, 1990). See also Danielsen (1990), Schär (1993) [who obtained the result in (4.151)], Bretherton and Schär (1993) and Davies-Jones (2003).

7 See for example McIntyre and Norton (1990) and Marshall and Nurser (1992). The latter use *J* vectors to study the creation and transport of potential vorticity in the oceanic thermocline.

Further Reading

Truesdell, C. 1954. *The Kinematics of Vorticity.*
A unique book, written in Truesdell's inimitable style, on many aspects of vorticity and with many historical references (and with a generous definition of what constitutes a 'kinematic' result).

Batchelor, G. K. 1967. *An Introduction to Fluid Dynamics.*
This contains an extensive discussion of vorticity and vortices.

Salmon, R. S. 1998. *Geophysical Fluid Dynamics.*
Chapter 4 contains a brief discussion of potential vorticity, and chapter 7 a longer discussion of Hamiltonian fluid dynamics, in which the particle relabeling symmetry that gives rise to potential vorticity conservation is discussed.

Problems

4.1 For the vr vortex, choose a contour of arbitrary shape (e.g., a square) with segments neither parallel nor perpendicular to the radius, and not enclosing the origin. Show explicitly that the circulation around the contour is zero. (This problem is a little perverse.)

4.2 ♦ *Vortex stretching and viscosity.*
Suppose there is an incompressible swirling flow given in cylindrical coordinates (r, ϕ, z):

$$\boldsymbol{v} = (v_r, v_\phi, v_z) = (-\frac{1}{2}\alpha r, v_\phi, \alpha z) \qquad (\text{P4.1})$$

Show that this satisfies the mass conservation equation. Show too that vorticity is only non-zero in the vertical direction. Show that the vertical component of the vorticity equation contains only the stretching term and that in steady state it is

$$-\frac{1}{2}\alpha r \frac{\partial \zeta}{\partial r} = \zeta \alpha + v \frac{1}{r} \frac{\partial}{\partial r} \left(r \frac{\partial \zeta}{\partial r} \right). \qquad (\text{P4.2})$$

Show that this may be integrated to $\zeta = \zeta_0 \exp(-\alpha r^2/4v)$. Thus deduce that there is a rotational core of thickness $r_o = 2 (v/\alpha)^{1/2}$, and that the radial velocity field is given by

$$v_\phi(r) = -\frac{1}{r} \frac{2v}{\alpha} \zeta_0 \exp \left[-\frac{\alpha r^2}{4v} \right] + \frac{A}{r} \qquad (\text{P4.3})$$

where $A = 2v\zeta_0/\alpha$. What is the swirling velocity field? (Batchelor 1967)

4.3 (a) Beginning with the three-dimensional vorticity equation in a rotating frame of

reference [either (4.68) or (4.69)] show that in Cartesian coordinates the evolution of the vertical component of vorticity is given by

$$
\begin{aligned}
\frac{\mathrm{D}\zeta}{\mathrm{D}t} = & -(\zeta + f)\left(\frac{\partial u}{\partial x} + \frac{\partial v}{\partial y}\right) \\
& + \left(\frac{\partial v}{\partial z}\frac{\partial w}{\partial x} - \frac{\partial u}{\partial z}\frac{\partial w}{\partial y}\right) + \left(\frac{\partial \rho}{\partial x}\frac{\partial p}{\partial y} - \frac{\partial \rho}{\partial y}\frac{\partial p}{\partial x}\right)
\end{aligned}
\tag{P4.4}
$$

where 'vertical' means the direction parallel to the rotation vector.

(b) ♦ Repeat this derivation, but in now spherical coordinates where vertical means the radial direction, and discuss the differences (if any) between the resulting equation and (P4.4). Show carefully how the β-term arises, and in particular that it may be interpreted as arising from tilting term in the vorticity equation.

4.4 ♦ Making use of Kelvin's circulation theorem obtain an expression for the potential vorticity that is conserved following the flow (for an adiabatic and unforced fluid) and that is appropriate for the hydrostatic primitive equations on a spherical planet. Express this in terms of the components of the spherical coordinate system.

4.5 ♦ In pressure coordinates for hydrostatic flow on the f-plane, the horizontal momentum equation takes the form

$$
\frac{\mathrm{D}\boldsymbol{u}}{\mathrm{D}t} + \boldsymbol{f} \times \boldsymbol{u} = -\nabla\phi
\tag{P4.5}
$$

On taking the curl of this, there appears to be no baroclinic term. Show that Kelvin's circulation theorem is nevertheless not in general satisfied, even for unforced, adiabatic flow. By appropriately choosing a path on which to evaluate the circulation obtain an expression for potential vorticity, in this coordinate system, that is conserved following the flow. *Hint:* look at the hydrostatic equation.

4.6 *Solenoids and sea-breezes.*
A land-sea temperature contrast of 20 K forces a sea breeze in the surface "mixed layer" (potential temperature nearly uniform with height), as illustrated schematically. The layer extends through the lowest 10% of the mass of the atmosphere.
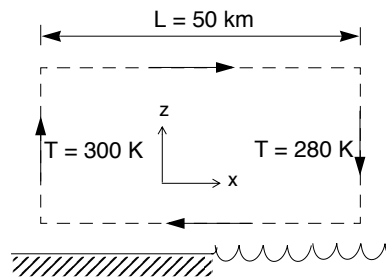
(a) In the absence of dissipation and diffusion, at what rate does the circulation change on a material circuit indicated? You may assume the horizonal flow is isobaric, and express your answer in m/s per hour.

(b) Suppose the sea breeze is equilibrated by a nonlinear surface drag of the form

$$
\frac{\mathrm{d}V}{\mathrm{d}t} = -\frac{V^2}{L_F}
\tag{P4.6}
$$

with $L_F = (3\,\mathrm{m\,s^{-1}})(3600\,\mathrm{s})$. What is the steady speed of the horizontal wind in the case L = 50 km?

(c) Suppose that the width of the circulation is determined by a horizontal thermal diffusion of the form

$$\frac{\mathrm{D}\theta}{\mathrm{D}t} = \kappa_H \frac{\partial^2 \theta}{\partial x^2} \tag{P4.7}$$

Provide an estimate of κ_H that is consistent with $L = 50\,\mathrm{km}$. Comment on whether you think the extent of real sea breezes is really determined this way.

CHAPTER 5

Simplified Equations for the Ocean and Atmosphere

LARGE-SCALE FLOW IN THE OCEAN AND ATMOSPHERE is characterized by an approximate balance in the vertical between the pressure gradient and gravity (hydrostatic balance), and in the horizontal between the pressure gradient and the Coriolis force (geostrophic balance). In this chapter we exploit these balances to simplify the Navier-Stokes equations and thereby obtain various sets of simplified 'geostrophic equations'. Depending on the precise nature of the assumptions we make, we are led to the *quasi-geostrophic* system for horizontal scales similar to that on which most synoptic activity takes place and, for very large-scale motion, to the *planetary-geostrophic* set of equations. By eliminating unwanted or unimportant modes of motion, in particular sound waves and gravity waves, and by building in the important balances between flow fields, these filtered equation sets allow the investigator to better focus on a particular class of phenomenon and to potentially achieve a deeper understanding than might otherwise be possible.[1]

Simplifying the equations in this way relies first on scaling the equations. The idea is that we *choose* the scales we wish to describe, typically either on some *a priori* basis or by using observations as a guide. We then attempt to derive a set of equations that is simpler than the original set but that consistently describes motion of the chosen scale. An asymptotic method is one approach to this, for it systematically tells us which terms we can drop and which we should keep. The combined approach — scaling plus asymptotics — has proven enormously useful, but it is useful to always remember two things: (i) that scaling is a choice; (ii) that the approach does not explain the existence of particular scales of motion, it just describes the motion that might occur on such scales.

5.1 GEOSTROPHIC SCALING

I have no satisfaction in formulas unless I feel their numerical magnitude.
William Thomson, Lord Kelvin (1824–1907).

5.1.1 Scaling in the Shallow Water Equations

Postponing the complications that come with stratification, we begin with the shallow water equations. With the odd exception, we will denote the scales of variables by capital letters; thus, if L is a typical length scale of the motion we wish to describe, and U a typical velocity scale, and assuming the scales are horizontally isotropic, we write

$$(x, y) \sim L \qquad \text{or} \qquad (x, y) = \mathcal{O}(L)$$
$$(u, v) \sim L \qquad \text{or} \qquad (u, v) = \mathcal{O}(U). \tag{5.1}$$

and similarly for other variables. We may then nondimensionalize the variables by writing

$$(x, y) = L(\hat{x}, \hat{y}), \qquad (u, v) = U(\hat{u}, \hat{v}) \tag{5.2}$$

where the hatted variables are nondimensional and, by supposition, are $\mathcal{O}(1)$. The various terms in the momentum equation then scale as:

$$\frac{\partial \boldsymbol{u}}{\partial t} + \boldsymbol{u} \cdot \nabla \boldsymbol{u} - \boldsymbol{f} \times \boldsymbol{u} = -g \nabla \eta \tag{5.3a}$$

$$\frac{U}{T} \qquad \frac{U^2}{L} \qquad fU \qquad g\frac{\mathcal{H}}{L} \tag{5.3b}$$

where the ∇ operator acts in the x, y plane and $\mathcal{H}$ is the amplitude of the variations in the surface displacement. (We use η to denote the height of the free surface above some arbitrary reference level, as in Fig. 3.1. Thus, $\eta = H + \Delta\eta$, where $\Delta\eta$ denotes the variation of η about its mean position.)

The ratio of the advective term to the rotational term in the momentum equation (5.3) is $(U^2/L)\big/(fU) = U/fL$; this is the Rossby number, first encountered in chapter 2.[2] Using values typical of the large-scale circulation (e.g., from table 2.1) we find that $Ro \approx 0.1$ for the atmosphere and $Ro \approx 0.01$ for the ocean, small in both cases. If we are interested in motion that has the advective timescale $T = L/U$ then we scale time by L/U so that

$$t = \frac{L}{U}\hat{t}, \tag{5.4}$$

and the local time derivative and the advective term then both scale as U^2/L, and both are order Rossby number smaller than the rotation term. Then, either the Coriolis term is the dominant term in the equation, in which case we have a state of no motion with $-fv = 0$, or else the Coriolis force is balanced by the pressure force, and the dominant balance is

$$-fv = -g\frac{\partial \eta}{\partial x}, \tag{5.5}$$

namely *geostrophic balance*, as encountered in chapter 2. If we make this nontrivial choice, then the equation informs us that variations in η scale according to

$$\Delta\eta \sim \mathcal{H} = \frac{fUL}{g} \tag{5.6}$$

We can also write $\mathcal{H}$ as

$$\mathcal{H} = Ro\frac{f^2L^2}{g} = RoH\frac{L^2}{L_d^2}. \tag{5.7}$$

where $L_d = \sqrt{gH}/f$ is the deformation radius, and H is the mean depth of the fluid. The variations in fluid height thus scale as

$$\frac{\Delta\eta}{H} \sim Ro\frac{L^2}{L_d^2}, \tag{5.8}$$

and the height of the fluid may be written as

$$\eta = H\left(1 + Ro\frac{L^2}{L_d^2}\widehat{\eta}\right) \quad \text{and} \quad \Delta\eta = Ro\frac{L^2}{L_d^2}H\widehat{\eta}, \tag{5.9}$$

where $\widehat{\eta}$ is the $\mathcal{O}(1)$ nondimensional value of the surface height deviation.

Nondimensional momentum equation

If we use (5.9) to scale height variations, (5.2) to scale lengths and velocities, and (5.4) to scale time, then the momentum equation (5.3) becomes

$$\boxed{Ro\left[\frac{\partial\widehat{\boldsymbol{u}}}{\partial\widehat{t}} + (\widehat{\boldsymbol{u}}\cdot\nabla)\widehat{\boldsymbol{u}}\right] + \widehat{\boldsymbol{f}}\times\widehat{\boldsymbol{u}} = -\nabla\widehat{\eta}}, \tag{5.10}$$

where $\widehat{\boldsymbol{f}} = \mathbf{k}\widehat{f} = \mathbf{k}f/f_0$, where f_0 is a representative value of the Coriolis parameter. (If f is a constant, then $\widehat{f} = 1$, but it is useful to to keep it in the equations to indicate the presence of Coriolis parameter. Also, where the operator ∇ operates on a nondimensional variable then the differentials are taken with respect to the nondimensional variables $\widehat{x}$, $\widehat{y}$.) All the variables in (5.10) will be supposed to be of order unity, and the Rossby number multiplying the local time derivative and the advective terms indicates the smallness of those terms. By construction, the dominant balance in this equation is the geostrophic balance between the last two terms.

Nondimensional mass continuity (height) equation

The (dimensional) mass continuity equation can be written

$$\frac{1}{H}\frac{D\eta}{Dt} + \left(1 + \frac{\Delta\eta}{H}\right)\nabla\cdot\boldsymbol{u} = 0 \tag{5.11}$$

Using (5.2), (5.4) and (5.9) this equation may be written

$$\boxed{Ro \left(\frac{L}{L_{\mathrm{d}}}\right)^2 \frac{D\hat{\eta}}{D\hat{t}} + \left(1 + Ro \left(\frac{L}{L_{\mathrm{d}}}\right)^2 \hat{\eta}\right) \nabla \cdot \hat{\boldsymbol{u}} = 0} \, . \tag{5.12}$$

Equations (5.10) and (5.12) are the nondimensional versions of the full shallow water equations of motion. Evidently, some terms in the equations of motion are small and may be eliminated with little loss of accuracy, and the way this done will depend on the size of the second nondimensional parameter, $(L/L_{\mathrm{d}})^2$. We explore this in sections 5.2 and 5.3.

Froude and Burger numbers

The Froude number may be generally defined as the ratio of a fluid particle speed to a wave speed. In a shallow-water system this gives

$$Fr \equiv \frac{U}{\sqrt{gH}} = \frac{U}{f_0 L_{\mathrm{d}}} = Ro \frac{L}{L_{\mathrm{d}}}. \tag{5.13}$$

The Burger number[3] is a useful measure of scale of motion of the fluid, relative to the deformation radius, and may be defined by

$$Bu \equiv \left(\frac{L_{\mathrm{d}}}{L}\right)^2 = \frac{gH}{f_0^2 L^2} = \left(\frac{Ro}{Fr}\right)^2. \tag{5.14}$$

It is also useful to define the parameter $F \equiv Bu^{-1}$, which is like the square of a Froude number but uses the rotational speed fL instead of U in the numerator.

5.1.2 Geostrophic scaling in the stratified equations

We now apply the same scaling ideas, *mutatis mutandis,* to the stratified primitive equations. We use the hydrostatic anelastic equations, which we write as:

$$\frac{D\boldsymbol{u}}{Dt} + \boldsymbol{f} \times \boldsymbol{u} = -\nabla_z \phi, \tag{5.15a}$$

$$\frac{\partial \phi}{\partial z} = b, \tag{5.15b}$$

$$\frac{Db}{Dt} = 0, \tag{5.15c}$$

$$\nabla \cdot (\tilde{\rho} \boldsymbol{v}) = 0. \tag{5.15d}$$

where b is the buoyancy and $\tilde{\rho}$ is a reference density profile. Anticipating that the average stratification may not scale in the same way as the deviation from it, let us separate out the contribution of the advection of a reference stratification in (5.15c) by writing

$$b = \tilde{b}(z) + b'(x, y, z, t). \tag{5.16}$$

Then the thermodynamic equation becomes

$$\frac{\mathrm{D}b'}{\mathrm{D}t} + N^2 w = 0 \tag{5.17}$$

where $N^2 \equiv \partial \widetilde{b}/\partial z$. We then let $\phi = \widetilde{\phi}(z) + \phi'$ where $\widetilde{\phi}$ is hydrostatically balanced by $\widetilde{b}$, and the hydrostatic equation becomes

$$\frac{\partial \phi'}{\partial z} = b'. \tag{5.18}$$

Equations (5.17) and (5.18) replace (5.15c) and (5.15b).

Non-dimensional equations

We nondimensionalize the basic variables by supposing that

$$(x, y) \sim L, \quad (u, v) \sim U, \quad t \sim \frac{L}{U}, \quad z \sim H, \quad f \sim f_0, \tag{5.19}$$

where the scaling variables (capitalized, except for f_0) are chosen such that the nondimensional values have values of order unity. We presume that the scales chosen are such that the Rossby number is small, and $Ro = U/(f_o L) \ll 1$. In the momentum equation the pressure term then balances the Coriolis force,

$$|\boldsymbol{f} \times \boldsymbol{u}| \sim |\nabla \phi'| \tag{5.20}$$

and so the pressure scales as

$$\phi' \sim \Phi = f_o U L. \tag{5.21}$$

Using the hydrostatic relation, (5.21) implies that the buoyancy scales as

$$b' \sim B = \frac{f_0 U L}{H}, \tag{5.22}$$

and from this we obtain

$$\frac{(\partial b'/\partial z)}{N^2} \sim Ro \frac{L^2}{L_{\mathrm{d}}^2}, \tag{5.23}$$

where $L_{\mathrm{d}} \equiv NH/f_0$ is the deformation radius in the continuosly stratified fluid, analogous to the quantity $\sqrt{gH}/f_0$ the shallow water system, and we use the same symbol for both. In the continuously stratified system, *if the scale of motion is the same as or smaller than the deformation radius, and the Rossby number is small, then the variations in stratification are small.* The choice of scale is the key difference between the planetary geostrophic and quasi-geostrophic equations.

Finally, we will initially assume that the appropriate scale of vertical motion is given by the mass conservation equation,

$$\frac{1}{\widetilde{\rho}} \frac{\partial \widetilde{\rho} w}{\partial z} = - \left(\frac{\partial u}{\partial x} + \frac{\partial v}{\partial y} \right), \tag{5.24}$$

and that this implies

$$w \sim W = \frac{UH}{L}. \tag{5.25}$$

This scaling may not always hold: if the Coriolis parameter is nearly constant the geostrophic velocity is nearly horizontally non-divergent and the right-hand side of (5.24) is small, and $W \ll UH/L$. We then estimate w by cross-differentiating geostrophic balance to obtain the linear geostrophic vorticity equation,

$$\beta v \approx f \frac{\partial w}{\partial z}, \tag{5.26}$$

which leads to the estimate

$$w \sim W = \frac{\beta UH}{f_0}. \tag{5.27}$$

If variations in the Coriolis parameter are large and $\beta \sim f_0/L$, then (5.27) is the same as (5.25).

Given the scaling above [and using (5.25)] we nondimensionalize our variables by setting

$$(\hat{x}, \hat{y}) = L^{-1}(x, y), \qquad \hat{z} = H^{-1}z, \quad (\hat{u}, \hat{v}) = U^{-1}(u, v), \quad \hat{t} = \frac{U}{L}t,$$
$$\hat{w} = \frac{L}{UH}w, \quad \hat{f} = f_0^{-1}f, \quad \hat{\phi} = \frac{\phi'}{f_0 UL}, \quad \hat{b} = \frac{H}{f_0 UL}b'. \tag{5.28}$$

The horizontal momentum and hydrostatic equations then become

$$Ro\frac{D\hat{u}}{D\hat{t}} + \hat{f} \times \hat{u} = -\nabla\hat{\phi}, \tag{5.29}$$

and

$$\frac{\partial \hat{\phi}}{\partial \hat{z}} = \hat{b}. \tag{5.30}$$

The non-dimensional mass conservation equation is simply

$$\frac{1}{\tilde{\rho}}\nabla \cdot (\tilde{\rho}\hat{\boldsymbol{v}}) = \left(\frac{\partial \hat{u}}{\partial \hat{x}} + \frac{\partial \hat{v}}{\partial \hat{y}} + \frac{1}{\tilde{\rho}}\frac{\partial \tilde{\rho}\hat{w}}{\partial \hat{z}}\right) = 0. \tag{5.31}$$

and the nondimensional thermodynamic equation is

$$\frac{f_0 UL}{H}\frac{U}{L}\frac{D\hat{b}}{D\hat{t}} + N^2\frac{HU}{L}\hat{w} = 0, \tag{5.32}$$

or

$$Ro\frac{D\hat{b}}{D\hat{t}} + \left(\frac{L_{\mathrm{d}}}{L}\right)^2 \hat{w} = 0. \tag{5.33}$$

The nondimensional primitive equations are summarized in the box on the facing page.

Nondimensional Primitive Equations

Horizontal momentum:
$$Ro\frac{\mathrm{D}\widehat{\boldsymbol{u}}}{\mathrm{D}\widehat{t}} + \widehat{\boldsymbol{f}} \times \widehat{\boldsymbol{u}} = -\nabla\widehat{\phi} \qquad \text{(NDPE.1)}$$

Hydrostatic:
$$\frac{\partial\widehat{\phi}}{\partial\widehat{z}} = \widehat{b} \qquad \text{(NDPE.2)}$$

Mass continuity:
$$\left(\frac{\partial\widehat{u}}{\partial\widehat{x}} + \frac{\partial\widehat{v}}{\partial\widehat{y}} + \frac{1}{\widetilde{\rho}}\frac{\partial\widetilde{\rho}\widehat{w}}{\partial\widehat{z}}\right) = 0 \qquad \text{(NDPE.3)}$$

Thermodynamic:
$$Ro\frac{\mathrm{D}\widehat{b}}{\mathrm{D}\widehat{t}} + \left(\frac{L_{\mathrm{d}}}{L}\right)^{2}\widehat{w} = 0 \qquad \text{(NDPE.4)}$$

These equations are written for the anelastic equations. The Boussinesq equations result if we take $\widetilde{\rho} = 1$. The equations in pressure coordinates have a very similar form to the Boussinesq equations, but with a slight difference in hydrostatic equation.

5.2 THE PLANETARY GEOSTROPHIC EQUATIONS

We now use the low Rossby number scalings above to derive equation sets that are simpler than the original, 'primitive', ones. The planetary geostrophic equations are probably the simplest such set of equations, and we derive these equations first for the shallow water equations, and then for the stratified primitive equations.

5.2.1 Using the shallow water equations

Informal derivation

The advection and time derivative terms in the momentum equation (5.10) are order Rossby number smaller than the Coriolis and pressure terms (the term in square brackets is multiplied by Ro), and therefore let us neglect them. The momentum equation straightforwardly becomes
$$\widehat{\boldsymbol{f}} \times \widehat{\boldsymbol{u}} = -\nabla\widehat{\eta}. \qquad (5.34)$$

The mass conservation equation (5.12), contains two nondimensional parameters, Ro and F and we must make a choice as to the relationship of these two numbers. We will choose
$$FRo = \mathcal{O}(1), \qquad (5.35)$$

which implies
$$L^{2} \gg L_{\mathrm{d}}^{2} \qquad \text{or equivalently} \qquad Bu \ll 1. \qquad (5.36)$$

That is to say, we suppose that the scales of motion are much larger than the deformation scale. Given this choice, all the terms in the mass conservation equation, (5.12),

are of roughly the same size, and we retain them all. Thus, the shallow water planetary geostrophic equations are the full mass continuity equation along with geosrophic balance and a geometric relationship between the height field and fluid thickness, and in dimensional form these are:

$$
\frac{\mathrm{D}h}{\mathrm{D}t} + h\nabla \cdot \boldsymbol{u} = 0
$$
$$
\boldsymbol{f} \times \boldsymbol{u} = -g\nabla\eta, \qquad \eta = h + \eta_b
$$

. $\qquad$ (5.37a,b)

We emphasize that *the planetary geostrophic equations are only valid for scales of motion much larger than the deformation radius.* The height variations are then as large as the mean height field itself; that is, using (5.8), $\Delta\eta/H = \mathcal{O}(1)$.

Formal derivation

We assume that:

 (i) The Rossby number is small. $Ro = U/f_0 L \ll 1$.

 (ii) The scale of the motion is significantly larger than the deformation scale. That is, (5.35) holds or

$$
F = Bu^{-1} = \left(\frac{L}{L_\mathrm{d}}\right)^2 \gg 1 \qquad (5.38)
$$

   and in particular

$$
FRo = \mathcal{O}(1). \qquad (5.39)
$$

 (iii) Time scales advectively, so that $T = L/U$.

The idea is now to expand the nondimensional variables velocity and height fields in an asymptotic series with Rossby number as the small parameter, substitute into the equations of motion, and derive a simpler set of equations. It is a nearly trivial exercise in this instance, and so it illustrates well the methodology. The expansions are

$$
\hat{\boldsymbol{u}} = \hat{\boldsymbol{u}}_0 + Ro\hat{\boldsymbol{u}}_1 + Ro^2\hat{\boldsymbol{u}}_1 + \cdots \qquad (5.40a)
$$

and

$$
\hat{\eta} = \hat{\eta}_0 + Ro\hat{\eta}_1 + Ro^2\hat{\eta}_1 + \cdots \qquad (5.40b)
$$

Then substituting (5.40a) and (5.40b) into the momentum equation gives

$$
Ro\left[\frac{\partial\hat{\boldsymbol{u}}_0}{\partial\hat{t}} + \hat{\boldsymbol{u}}_0 \cdot \nabla\hat{\boldsymbol{u}}_0 + \hat{\boldsymbol{f}} \times \hat{\boldsymbol{u}}_1\right] + \hat{\boldsymbol{f}} \times \hat{\boldsymbol{u}}_0 = -\nabla\hat{\eta}_0 - Ro\left[\nabla_0\hat{\eta}_1\right] + \mathcal{O}(Ro^2) \quad (5.41)
$$

The Rossby number is now an asymptotic ordering parameter; thus, the sum of all the terms at any particular order in Rossby number must vanish. At lowest order we obtain the simple expression

$$
\hat{\boldsymbol{f}} \times \hat{\boldsymbol{u}}_0 = -\nabla\hat{\eta}_0. \qquad (5.42)
$$

Note that although f_0 is a representative value of f, we have made no assumptions about the constancy of f. In particular, f is allowed to vary by an order one amount, provided that it does not become so small that the Rossby number $(U/f_0 L)$ is not small.

The appropriate height (mass conservation) equation is similarly obtained by substituting (5.40a) and (5.40b) into the shallow water mass conservation equation. Because $FRo = \mathcal{O}(1)$ at lowest order we simply retain all the terms in the equation to give

$$FRo \left[\frac{\partial \widehat{\eta}_0}{\partial t} + \widehat{\boldsymbol{u}}_0 \cdot \nabla \widehat{\eta}_0 \right] + [1 + FRo\widehat{\eta}] \nabla \cdot \widehat{\boldsymbol{u}}_0 = 0. \tag{5.43}$$

Equations (5.42) and (5.43) are a closed set, and constitute the nondimensional planetary geostrophic equations. The dimensional forms of these equations are just (5.37).

Variation of the Coriolis parameter

Suppose then that f is a constant (f_0), or nearly so. Then, from the curl of (5.42), $\nabla \cdot \boldsymbol{u}_0 = 0$. This means that we can define a streamfunction for the flow and, from geostrophic balance, the height field is just that streamfunction. That is, in dimensional form,

$$\psi = \frac{g}{f_0} \eta, \qquad \boldsymbol{u} = -\mathbf{k} \times \nabla \psi, \tag{5.44}$$

and (5.43) becomes

$$\frac{\partial \eta}{\partial t} + \boldsymbol{u} \cdot \nabla \eta = 0, \qquad \text{or} \qquad \frac{\partial \eta}{\partial t} + J(\psi, \eta) = 0. \tag{5.45}$$

where $J(a,b) \equiv a_x b_y - a_y b_x$. But since $\eta \propto \psi$ the advective term is proportional to $J(\psi, \psi)$, which is zero. Thus, the flow does not evolve at this order. The planetary geostrophic equations are *uninteresting* if the scale of the motion is such that the Coriolis parameter is not variable. On earth, the scale of motion on which this parameter regime exists is rather limited, since the planetary geostrophic equations require that the scale of motion is also larger than the deformation radius. In the earth's atmosphere, any scale that is larger than the deformation radius will be such that the Coriolis parameter varies significantly over it, and we do not encounter this parameter regime. On the other hand, in the earth's ocean the deformation radius is relatively small and there exists a small parameter regime that has scales larger than the deformation radius but smaller than that on which the Coriolis parameter varies.[4]

Potential vorticity

The shallow water PG equations may be written as an evolution equation for an approximated potential vorticity. A little manipulation reveals that (5.37) are equivalent to:

$$\boxed{\begin{aligned} \frac{\mathrm{D}Q}{\mathrm{D}t} &= 0 \\[2mm] Q = \frac{f}{h}, \quad \boldsymbol{f} \times \boldsymbol{u} &= -g\nabla\eta, \quad \eta = h + \eta_b \end{aligned}} \tag{5.46}$$

Thus, potential vorticity is a material invariant in the approximate equation set, just as it is in the full equations. The other variables — the free surface height and the velocity — are diagnosed from it, a process known as inverting potential vorticity. In the planetary geostrophic approxmation, the inversion proceeds using the approximate form

f/h rather than the full potential vorticity, $(f + \zeta)/h$. (We do not, strictly speaking, approximate potential vorticity, because this is the evolving variable. Rather, we approximate the inversion relations from which we derive the height and velocity fields.) The simplest way of all to derive the shallow water PG equations is to *begin* with the conservation of potential vorticity, and to note that at small Rossby number the expression $(\zeta + f)/h$ may be approximated by f/h. Then, noting in addition that the flow is geostrophic, (5.46) immediately emerges. We will find that *every* approximate set of equations that we derive in this chapter may be expressed as the evolution of potential vorticity, with the other fields being obtained diagnotically from it.

5.2.2 The Planetary Geostrophic Equations for Stratified Flow

To explore the stratified system we will use the (inviscid and adiabatic) Boussinesq equations of motion with the hydrostatic approximation. The derivation carries through easily enought using the anelastic or pressure-coordinate equations, but as the PG equations have more oceanographic importance than atmospheric using the incompressible equations is quite appropriate.

Simplifying the equations

The nondimensional equations we begin with are (5.29)–(5.33). As in the shallow water case we expand these in a series in Rossby number, so that:

$$\hat{u} = \hat{u}_0 + \epsilon\hat{u}_1 + \epsilon^2\hat{u}_2 + \cdots, \qquad \hat{b} = \hat{b}_0 + \epsilon\hat{b}_1 + \epsilon^2\hat{b}_2 + \cdots, \qquad (5.47)$$

and similarly for $\hat{v}$, $\hat{w}$ and $\hat{\phi}$, where $\epsilon = Ro$, the Rossby number. Substituting into the nondimensional equations of motion (on page 215) and equating powers of ϵ gives the lowest order momentum, hydrostatic, and mass conservation equations:

$$\hat{\boldsymbol{f}} \times \hat{\boldsymbol{u}}_0 = -\nabla\hat{\phi}_0, \qquad (5.48a)$$

$$\frac{\partial\hat{\phi}_0}{\partial\hat{z}} = \hat{b}_0, \qquad (5.48b)$$

$$\nabla \cdot \hat{\boldsymbol{v}}_0 = 0. \qquad (5.48c)$$

If we also assume that $L_{\mathrm{d}}/L = \mathcal{O}(1)$, then the thermodynamic equation (5.33) becomes

$$\left(\frac{L_{\mathrm{d}}}{L}\right)^2 \hat{w}_0 = 0. \qquad (5.49)$$

Of course we have neglected any diabatic terms in this equation, which would in general provide a non-zero right-hand side. Nevertheless, this is not a useful equation, because the set of the equations we have derived, (5.48)–(5.48c), can no longer evolve: all the time derivatives have been scaled away! Thus, although instructive, these equations are not very useful. If instead we assume that the scale of motion is much larger than the deformation scale then the other terms in the thermodynamic equation will become equally important. Thus, we suppose that $L_{\mathrm{d}} \ll L^2$ or, more formally, that $L^2 = \mathcal{O}(Ro^{-1})L_{\mathrm{d}}^2$, and then all the terms in the thermodynamic equation are retained. A closed set of equations is then given by (5.48) and the thermodynamic equation (5.33).

Dimensional equations

Restoring the dimensions, dropping the asymptotic subscripts, and allowing for the possibility of a source term, denoted $S[b']$, in the thermodynamic equation, the *planetary-geostrophic* equations of motion are:

$$
\begin{aligned}
\frac{Db'}{Dt} + wN^2 &= S[b'] \\
\boldsymbol{f} \times \boldsymbol{u} &= -\nabla\phi' \\
\frac{\partial\phi'}{\partial z} &= b' \\
\nabla \cdot \boldsymbol{v} &= 0
\end{aligned}
\tag{5.50}
$$

The thermodynamic equation may also be written simply as

$$
\frac{Db}{Dt} = \dot{b}
\tag{5.51}
$$

where b now represents the total stratification. The relevant pressure, ϕ, is then the pressure that is in hydrostatic balance with b, so that geostrophic and hydrostatic balance are most usefully written as

$$
\boldsymbol{f} \times \boldsymbol{u} = -\nabla\phi, \qquad \frac{\partial\phi}{\partial z} = b.
\tag{5.52a,b}
$$

Potential vorticity

Manipulation of (5.50) reveals that we can equivalently write the equations as an evolution equation for potential vorticity. Thus, the evolution equations may be written

$$
\begin{aligned}
\frac{DQ}{Dt} &= \dot{Q} \\
Q &= f\frac{\partial b}{\partial z}
\end{aligned}
\tag{5.53}
$$

where $\dot{Q} = f\partial\dot{b}/\partial z$, and the inversion — i.e., the diagnosis of velocity, pressure and buoyancy — is carried out using the hydrostatic, geostrophic and mass conservation equations.

Applicability to the ocean and atmosphere

In the atmosphere a typical deformation radius NH/f is about 1,000 km. The constraint that the scale of motion be much larger than the deformation radius is thus quite hard to satisfy, since one quickly runs out of room on a planet whose equator-to-pole distance is 10,000 km. Thus, only the largest planetary waves can satisfy the planetary-geostrophic scaling in the atmosphere and we should then also write the equations in spherical coordinates.

In the ocean the deformation radius is about 100 km, so there is lots of room for the planetary-geostrophic equations to hold, and indeed much of the theory of the large-scale structure of the ocean involves the planetary-geostrophic equations.

5.3 THE SHALLOW WATER QUASI-GEOSTROPHIC EQUATIONS

We now derive a set of geostrophic equations that is valid (unlike the PG equations) when the horizontal scale of motion is similar to that of the deformation radius. These equations are called the *quasi-geostrophic* equations, and are perhaps the most widely used set of equations for theoretical studies of the atmosphere and ocean. The specific assumptions we make are:

 (i) The Rossby number is small, so that the flow is in near-geostrophic balance.

 (ii) The scale of the motion is not significantly larger than the deformation scale. Specifically, we shall require that

$$Ro \left(\frac{L}{L_{\mathrm{d}}} \right)^2 = \mathcal{O}(Ro). \tag{5.54}$$

For the shallow water equations, this assumption implies, using (5.9), that the variations in fluid depth are small compared to its total depth. For the continuously stratified system it implies, using (5.23), that the variations in stratification are small compared to the background stratification.

 (iii) Variations in the Coriolis parameter are small. That is, $|\beta L| \ll |f_0|$ where L is the length-scale of the motion.

 (iv) Time scales advectively; that is, the scaling for time is given by $T = L/U$.

The second and third of these differ from the planetary geostrophic counterparts: we make the second assumption because we wish to explore a different parameter regime, and we then find that the third assumption is necessary to avoid a rather trivial state (i.e., a leading order balance of $\beta v = 0$, see the discussion surrounding (5.78)). All of the assumptions are the same whether we consider the shallow water equations or a continuously stratified flow, and in this section we consider the former.

5.3.1 Single-layer shallow water quasi-geostrophic equations

The algorithm is, again, to expand the variables $\widehat{u}, \widehat{v}, \widehat{\eta}$ in an asymptotic series with Rossby number as the small parameter, substitute into the equations of motion, and derive a simpler set of equations. Thus we let

$$\widehat{u} = \widehat{u}_o + Ro\widehat{u}_1 + Ro^2\widehat{u}_2 + \cdots, \qquad \widehat{v} = \widehat{v}_o + Ro\widehat{v}_1 + Ro^2\widehat{v}_2 + \cdots \tag{5.55a}$$

$$\widehat{\eta} = \widehat{\eta}_0 + Ro\widehat{\eta}_1 + Ro^2\widehat{\eta}_2 \cdots. \tag{5.55b}$$

We will recognize the smallness of β compared to f_0/L by letting $\beta = \widehat{\beta}U/L^2$, where $\widehat{\beta}$ is assumed to be a parameter of order unity. Then the expression $f = f_0 + \beta y$ becomes

$$\widehat{f} = f/f_0 = \widehat{f}_0 + Ro\widehat{\beta}\widehat{y}. \tag{5.56}$$

where $\widehat{f_0}$ is the nondimensional value of f_0; its value is unity, but it is helpful to denote it explicitly. Substitute (5.55) into the nondimensional momentum equation (5.10), and equate powers of Ro. At lowest order we obtain

$$\widehat{f_0}\widehat{u}_0 = -\frac{\partial \widehat{\eta}_0}{\partial \widehat{y}}, \qquad \widehat{f_0}\widehat{v}_0 = \frac{\partial \widehat{\eta}_0}{\partial \widehat{x}}. \qquad (5.57)$$

Cross-differentiating gives

$$\nabla \cdot \widehat{\boldsymbol{u}}_0 = 0, \qquad (5.58)$$

where, when ∇ operates on a nondimensional variable, the derivatives are taken with respect to the nondimensional variables $\widehat{x}$ and $\widehat{y}$. From (5.58) we see that the velocity field is divergence-free, and that this arises from the momentum equation rather than the mass conservation equation.

The mass conservation equation is also, at lowest order, $\nabla \cdot \widehat{\boldsymbol{u}}_0 = 0$, and at next order we have

$$F\frac{\partial \widehat{\eta}_0}{\partial \widehat{t}} + F\widehat{\boldsymbol{u}}_0 \cdot \nabla\widehat{\eta}_0 + \nabla \cdot \widehat{\boldsymbol{u}}_1 = 0 \qquad (5.59)$$

This equation is not closed, because the evolution of the zeroth order term involves evaluation of a first order quantity. For closure, we go to next order in the momentum equation:

$$\frac{\partial \widehat{\boldsymbol{u}}_0}{\partial \widehat{t}} + (\widehat{\boldsymbol{u}}_0 \cdot \nabla)\widehat{\boldsymbol{u}}_0 + \widehat{\beta}\widehat{y}\mathbf{k} \times \widehat{\boldsymbol{u}}_0 - \widehat{f_0}\mathbf{k} \times \widehat{\boldsymbol{u}}_1 = -\nabla\widehat{\eta}_1 \qquad (5.60)$$

We obtain the vorticity equation by taking the curl of this to give

$$\frac{\partial \widehat{\zeta}_0}{\partial \widehat{t}} + (\widehat{\boldsymbol{u}}_0 \cdot \nabla)(\widehat{\zeta}_0 + \widehat{\beta}\widehat{y}) = -\widehat{f_0}\nabla \cdot \widehat{\boldsymbol{u}}_1. \qquad (5.61)$$

The term on the right hand side is the *vortex stretching* term. Only vortex stretching by the background or planetary vorticity is present, because the vortex stretching by the relative vorticity is a factor Rossby number smaller. This equation is also not closed. However, we may use (5.59) to eliminate the divergence term in (5.61) to give

$$\frac{\partial \widehat{\zeta}_0}{\partial \widehat{t}} + (\widehat{\boldsymbol{u}}_0 \cdot \nabla)(\widehat{\zeta}_0 + \widehat{\beta}\widehat{y}) = \widehat{f_0}\left(F\frac{\partial \widehat{\eta}_0}{\partial t} + F\widehat{\boldsymbol{u}} \cdot \nabla\widehat{\eta}_0\right), \qquad (5.62)$$

or

$$\frac{\partial}{\partial \widehat{t}}(\widehat{\zeta}_0 - \widehat{f_0}F\widehat{\eta}_0) + (\widehat{\boldsymbol{u}}_0 \cdot \nabla)(\widehat{\zeta}_0 + \widehat{\beta}y - F\widehat{\eta}_0) = 0. \qquad (5.63)$$

The final step is to note that the lowest order vorticity and height fields are related through geostrophic balance, so that using (5.57) we can write

$$\widehat{u}_0 = -\frac{\partial \widehat{\psi}_0}{\partial \widehat{y}}, \qquad \widehat{v}_0 = \frac{\partial \widehat{\psi}_0}{\partial \widehat{x}}, \qquad \widehat{\zeta}_0 = \nabla^2\widehat{\psi}_0, \qquad (5.64)$$

where $\widehat{\psi}_0 = \widehat{\eta}_0/\widehat{f_0}$ is the streamfunction. Eq. (5.63) can thus be written,

$$\frac{\partial}{\partial \widehat{t}}(\nabla^2\widehat{\psi}_0 - \widehat{f_0}^2 F\widehat{\psi}_0) + (\widehat{\boldsymbol{u}}_0 \cdot \nabla)(\widehat{\zeta}_0 + \widehat{\beta}\widehat{y} - \widehat{f_0}^2 F\widehat{\psi}_0) = 0, \qquad (5.65)$$

or

$$\frac{D_0}{\widehat{Dt}}(\nabla^2\widehat{\psi}_0 + \widehat{\beta}\widehat{y} - \widehat{f}_0^2 F\widehat{\psi}_0) = 0, \tag{5.66}$$

where the subscript '0' on the material derivative indicates that the lowest order velocity, the geostrophic velocity, is the advecting velocity. Restoring the dimensions, (5.66) becomes

$$\boxed{\frac{D}{Dt}(\nabla^2\psi + \beta y - \frac{1}{L_d^2}\psi) = 0}, \tag{5.67}$$

where $\psi = (g/f_0)\eta$ and the advective derivative is

$$\frac{D}{Dt} = \frac{\partial}{\partial t} + u_g\frac{\partial}{\partial x} + v_g\frac{\partial}{\partial y} = \frac{\partial}{\partial t} - \frac{\partial\psi}{\partial y}\frac{\partial}{\partial x} + \frac{\partial\psi}{\partial x}\frac{\partial}{\partial y} = \frac{\partial}{\partial t} + J(\psi, \cdot). \tag{5.68}$$

Noting that $L_d^2 = gH/f_0^2$, another form of (5.67) is

$$\frac{D}{Dt}(\zeta + \beta y - \frac{f_0}{H}\eta) = 0, \tag{5.69}$$

with $\zeta = (g/f_0)\nabla^2\eta$. Equations (5.67) and (5.69) are both known as the shallow-water quasi-geostrophic potential vorticity equation. The quantity

$$\boxed{q \equiv \zeta + \beta y - \frac{f_0}{H}\eta = \nabla^2\psi + \beta y - \frac{1}{L_d^2}\psi} \tag{5.70}$$

is the *shallow water quasi-geostrophic potential vorticity.*

Connection to shallow water potential vorticity

The quantity q given by (5.70) is an approximation (except for dynamically unimportant constant additive and multiplicative factors) to the shallow water potential vorticity. To see the truth of this statement, begin with the expression for the shallow water potential vorticity,

$$Q = \frac{f + \zeta}{h}. \tag{5.71}$$

Now let $h = H(1 + \eta'/H)$, where η' is the perturbation of the free-surface height, and assume that η'/H is small to obtain

$$Q \approx \frac{1}{H}(f + \zeta)\left(1 - \frac{\eta'}{H}\right) \approx \frac{1}{H}\left(f_0 + \beta y + \zeta - f_0\frac{\eta}{/H}\right). \tag{5.72}$$

Because f_0/H is a constant it has no effect in the evolution equation, and the quantity given by

$$q = \beta y + \zeta - f_0\frac{\eta'}{H} \tag{5.73}$$

is materially conserved. Using geostrophic balance we have $\zeta = \nabla^2\psi$ and $\eta' = f_0\psi/g$ so that (5.73) is identical to (5.70). [Note that only the variation in η are important in (5.69) or (5.70).]

The approximations needed to go from (5.71) to (5.70) are the same as those used in our earlier, more long-winded, derivation of the quasi-geostrophic equations. That is, we assumed that f itself were nearly constant, and that f_0 were much larger than ζ, equivalent to a low Rossby number assumption. It was also necessary to assume that $H \gg \eta'$ to enable the expansion of the height field which, using assumption *(ii)* on page 220, is equivalent to requiring that scale of motion not be significantly larger than the deformation scale. This derivation of the quasi-geostrophic system is completed by noting that the advection of the potential vorticity should be by the geostrophic velocity alone, and we recover (5.67) or (5.69).

Two interesting limits

There are two interesting limits to the quasi-geostrophic potential vorticity equation:

(i) *Motion on scales much smaller than the deformation radius.*
   That is, $L \ll L_d$ and thus $Bu \gg 1$ or $F \ll 1$. Then (5.66) becomes

$$\frac{\partial \zeta}{\partial t} + \boldsymbol{u}_\psi \cdot \nabla \zeta = 0 \qquad \text{or} \qquad \frac{\partial \zeta}{\partial t} + J(\psi, \zeta) = 0, \qquad (5.74)$$

   where $\zeta = \nabla^2 \psi$ and $J(\psi, \zeta) = \psi_x \zeta_y - \psi_y \zeta_x$. Thus, the motion obeys the two-dimensional vorticity equation. Physically, on small length scales the deviations in the height field are very small and may be neglected.

(ii) *Motion on scales much larger than the deformation radius.*
   Although scales are not allowed to become so large that $Ro(L/L_d)^2$ is of order unity, we may, *a posteriori,* still have $L \gg L_d$, whence the potential vorticity equation becomes

$$\frac{\partial \eta}{\partial t} + \boldsymbol{u}_\psi \cdot \nabla \eta = 0 \qquad \text{or} \qquad \frac{\partial \eta}{\partial t} + J(\psi, \eta) = 0. \qquad (5.75)$$

   However, because $\psi = g\eta/f_0$, the Jacobian term vanishes. Thus, one is left with a trivial equation that implies there is no advective evolution of the height field. There is nothing wrong with our reasoning; the mathematics have indeed pointed out a limit interesting in its uninterestingness. From a physical point of view, however, such (lack of) motion is likely to be rare, because on such large scales the Coriolis parameter varies considerably, and we are led to the planetary geostrophic equations.

In practice, often the most severe restriction of quasi-geostrophy is that variations in layer thickness are small: what does this have to do with geostrophy? If we scale η assuming geostrophic balance then $\eta \sim fUL/g$ and $\eta/H \sim Ro(L/L_d)^2$. Thus, if Ro is to remain small, η/H can only be order one if $(L/L_d)^2 \gg 1$. That is, the height variations must occur on a large scale, or we are led to a scaling inconsistency. Put another way, *if there are order-one height variations over a length-scale less than or order of the deformation scale, the Rossby number will not be small.* Large height variations are allowed if the scale of motion is large, but this contingency is described by the planetary geostrophic equations.

Another flow regime

Although perhaps of little terrestrial interest, we can imagine a regime in which the Coriolis parameter varies fully, but the scale of motion remains no larger than the deformation radius. This parameter regime is not quasigeostrophic, but it gives an interesting result. Because $\eta'/H \sim Ro(L/L_d)^2$ deviations of the height field are at least order Rossby number smaller than the reference height and $|\eta'| \ll H$. The dominant balance in height equation is then

$$H\nabla \cdot \boldsymbol{u} = 0, \tag{5.76}$$

presuming that time still scales advectively. This zero horizontal divergence must remain consistent with geostrophic balance

$$\boldsymbol{f} \times \boldsymbol{u} = -g\nabla\eta, \tag{5.77}$$

where now f is a fully variable Coriolis parameter. Taking the curl of (i.e., cross-differentiating) (5.77) gives

$$\beta v + f\nabla \cdot \boldsymbol{u} = 0, \tag{5.78}$$

whence, using (5.76), $v = 0$, and the flow is purely zonal. Although not at all useful as an evolution equation, this illustrates the constraining effect that differential rotation has on meridional velocity. This effect may be the cause of the banded, highly zonal flow on some the the giant planets, and we will revisit this issue in our discussion of geostrophic turbulence.

5.3.2 The Two-layer and Multi-layer Quasi-Geostrophic Systems

Just as for the one-layer case, the multi-layer shallow water equations simplify to a corresponding quasi-geostrophic system in appropriate circumstances. The assumptions are virtually same as before, although we assume that the variation in the thickness of *each* layer is small compared to its mean thickness. The basic fluid system for a two-layer case is sketched in Fig. 5.1 (and see also Fig. 3.5).

Let us proceed directly from the potential vorticity equation for each layer. We will also stay in dimensional variables, foregoing a more systematic approach for the sake of informality and perhaps insight. For each layer the potential vorticity equation is just

$$\frac{DQ_i}{Dt} = 0, \qquad Q_i = \frac{\zeta_i + f}{h_i}. \tag{5.79}$$

Let $h_i = H_i + h_i'$ where $|h_i'| << H_i$. The potential vorticity then becomes

$$Q_i \approx \frac{1}{H_i}(\zeta_i + f)\left(1 - \frac{h_i'}{H_i}\right) \qquad \text{— variations in layer thickness are small} \tag{5.80a}$$

$$\approx \frac{1}{H_i}\left(f + \zeta_i - f\frac{h_i'}{H_i}\right) \qquad \text{— the Rossby number is small} \tag{5.80b}$$
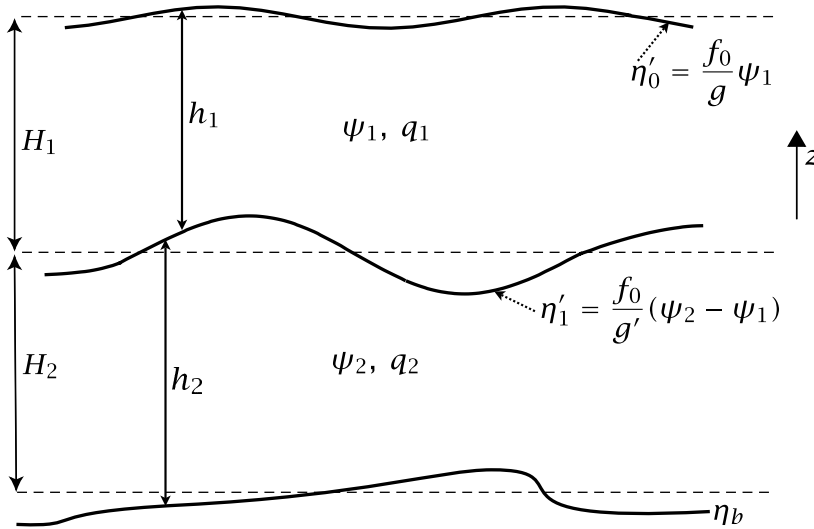
Fig. 5.1 A quasi-geostrophic fluid system consisting of two immiscible fluids of different density. The quantities η' are the interface displacemens from the resting basic state, denoted with dashed lines.

$$\approx \frac{1}{H_i}\left(f + \zeta_i - f_0\frac{h'_i}{H_i}\right) \qquad \text{— variations in Coriolis parameter are small}$$

$$(5.80c)$$

Now, because Q appears in the equations only as an advected quantity, it is only the *variations* in Coriolis parameter that are important in the the first term on the right-hand side of (5.80c), and with this all three terms are of the same asymptotic order. Then, because mean layer thicknesses are constant, we can define the quasi-geostrophic potential vorticity in each layer by

$$q_i = \left(\beta y + \zeta_i - f_0\frac{h'_i}{H_i}\right), \qquad (5.81)$$

and this will evolve according to $Dq_i/Dt = 0$, where the advective derivative is by the geostrophic wind. As in the one-layer case, quasi-geostrophic potential vorticity has different dimensions from the full shallow water potential vorticity.

To obtain a closed set of equations we must obtain an advecting field from the potential vorticity, and for simplicity we begin with the two-layer case in the Boussinesq approximation. Because the flow is geostrophically balanced we have, neglecting the advective derivative in (3.52) on page 139,

$$f_0 \times \boldsymbol{u}_1 = -g\nabla(h'_1 + h'_2 + \eta_b) \qquad (5.82a)$$

$$f_0 \times \boldsymbol{u}_2 = -g\nabla(h'_1 + h'_2 + \eta_b) - g'\nabla(h_2 + \eta_b) \qquad (5.82b)$$

where $g' = (\rho_2 - \rho_1)/\rho_1$ and η_b is the height of any bottom topography, and, because

variations in the Coriolis parameter are presumptively small, we use a constant value of f (i.e., f_0) on the left-hand side. We thus define the streamfunction for each layer by

$$\psi_1 = \frac{g}{f_0}(h_1' + h_2' + \eta_b), \qquad \psi_2 = \frac{g}{f_0}(h_1' + h_2' + \eta_b) + \frac{g'}{f_0}(h_2' + \eta_b), \quad \text{(5.83a,b)}$$

and these two equations may be manipulated to give

$$h_1' = \frac{f_0}{g'}(\psi_1 - \psi_2) + \frac{f_0}{g}\psi_1, \qquad h_2' = \frac{f_0}{g'}(\psi_2 - \psi_1) - \eta_b. \qquad \text{(5.84a,b)}$$

We note as an aside that the interface displacements are given by

$$\eta_0' = \frac{f_0}{g}\psi_1, \qquad \eta_1' = \frac{f_0}{g'}(\psi_2 - \psi_1). \qquad \text{(5.85a,b)}$$

Using (5.81) and (5.84) the quasi-geostrophic potential vorticity for each layer becomes

$$\boxed{\begin{aligned} q_1 &= \beta y + \nabla^2 \psi_1 + \frac{f_0^2}{g'H_1}(\psi_2 - \psi_1) + \frac{f_0^2}{gH_1}\psi_1 \\ q_2 &= \beta y + \nabla^2 \psi_2 + \frac{f_0^2}{g'H_2}(\psi_1 - \psi_2) + f_0\frac{\eta_b}{H_2} \end{aligned}} \qquad \text{(5.86a,b)}$$

In the rigid-lid approximation the last term in (5.86a) is neglected. The potential vorticity in each layer is just advected by the geostrophic velocity, so that the evolution equation for each layer is just

$$\frac{\partial q_i}{\partial t} + J(\psi_i, q_i) = 0, \qquad\qquad i = 1, 2. \qquad \text{(5.87)}$$

* Multi-layer model

A multi-layer quasi-geostrophic model may be constructed by a straightforward extension of the above two-layer procedure (see Fig. 5.2). The quasi-geostrophic potential vorticity for each layer is still given by (5.81). The pressure field in each layer can be expressed in terms of the thickness of each layer using (3.47) and (3.48) on page 138, and by geostrophic balance the pressure is proportional to the streamfunction, ψ_i, for each layer. Carrying out these steps we obtain (after some algebra, but the general form is revealed by the three-layer equations) the following expression for the quasi-geostrophic potential vorticity of an interior layer, in the Boussinesq approximation:

$$\boxed{q_i = \beta y + \nabla^2 \psi_i + \frac{f_0^2}{H_i}\left(\frac{\psi_{i-1} - \psi_i}{g_{i-1}'} - \frac{\psi_i - \psi_{i+1}}{g_i'}\right)}, \qquad \text{(5.88)}$$

and for the top and bottom layers,

$$q_1 = \beta y + \nabla^2 \psi_1 + \frac{f_0^2}{H_1}\left(\frac{\psi_2 - \psi_1}{g_1'}\right) + \frac{f_0^2}{gH_2}\psi_1, \qquad \text{(5.89a)}$$
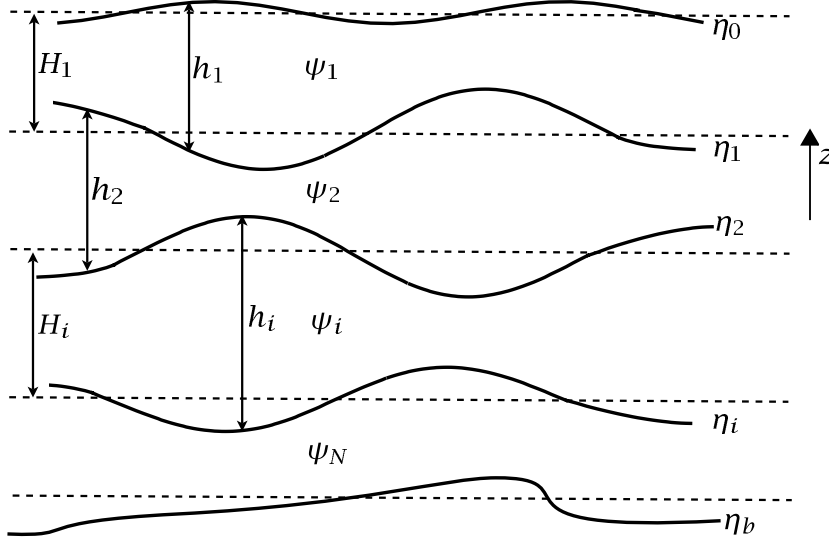
Fig. 5.2 A multi-layer quasi-geostrophic fluid system. Layers are numbered from the top down, i denotes a general interior layer and N denotes the bottom layer.

$$q_N = \beta y + \nabla^2 \psi_N + \frac{f_0^2}{H_N}\left(\frac{\psi_{N-1} - \psi_N}{g'_{N-1}}\right) + \frac{f_0}{H_N}\eta_b. \qquad (5.89b)$$

In these equations H_i is the basic-state thickness of the i'th layer, and $g'_i = g(\rho_{i+1} - \rho_i)/\rho_1$. In each layer the evolution equation is (5.87), now for $i = 1 \cdots N$. The displacements of each interface are given, similarly to (5.85), by

$$\eta'_0 = \frac{f_0}{g}\psi_1, \qquad \eta'_i = \frac{f_0}{g'_i}(\psi_{i+1} - \psi_i). \qquad (5.90a,b)$$

5.3.3 * Non-asymptotic and intermediate models

The form of the derivation of the previous section suggests that we might be able to improve on the accuracy and range of applicability of the quasi-geostrophic equations, whilst still filtering gravity waves. For example, a seemingly improved set of geostrophic evolution equations might be

$$\frac{\partial q_i}{\partial t} + \boldsymbol{u}_i \cdot \nabla q_i = 0, \qquad (5.91)$$

with

$$q_i = \frac{f + \zeta_i}{h_i}, \qquad \zeta_i = \frac{\partial v_i}{\partial x} - \frac{\partial u_i}{\partial y}, \qquad (5.92a,b)$$

and with the velocities given by geostrophic balance. In this set of equations, potential vorticity is not linearized about a resting state [compare (5.92a) with (5.81)], and

we might also choose to keep the full variation of the Coriolis parameter in (5.82). Thus, the equation set contains both the planetary geostrophic and quasi-geostrophic equations. However, the informality of the derivation hides the fact that this is not an asymptotically consistent set of equations: it mixes asymptotic orders in the same equation, and good conservation properties are not assured. The set above does not, in fact, exactly conserve energy. Models that are either more accurate or more general than the quasi-geostrophic or planetary geostrophic equations yet that still filter gravity waves are called 'intermediate models', and they can be useful and insightful.[5]

A model that is derived asymptotically will, in general, maintain the conservation properties of the original set. To see this in a abstract way, suppose that the original equations (e.g., the primitive equations) may be written, symbolically and in non-dimensional form, as

$$\frac{\partial \phi}{\partial t} = F(\phi, \epsilon) \tag{5.93}$$

where ϕ is a set of variables, F is some operator, and ϵ is a small parameter, like the Rossby number. Suppose also that this set of equations has various invariants (such as energy and potential vorticity) that hold for any value of ϵ. The asymptotically-derived lowest order model (such as quasi-geostrophy) is simply a version of this equation set valid in the limit $\epsilon = 0$, and therefore it will preserve the invariants of the original set. These invariants may seem to have a different form in the simplified set: for example, in deriving the hydrostatic primitive equations from the Navier-Stokes equations the small parameter is the aspect ratio, and this multiplies the vertical velocity. Thus, in the limit of zero aspect ratio, and therefore in the primitive equations, the conserved kinetic energy has contributions only from the horizontal velocity. Indeed, in some cases some conservation properties may be reduced to trivialities in the simplified set. Also, and on the other hand, there is nothing to preclude new invariants emerging that hold only in the limit $\epsilon = 0$, and enstrophy (considered later in this chapter) is one example.[6]

5.4 THE CONTINUOUSLY STRATIFIED QUASI-GEOSTROPHIC SYSTEM

We now consider the quasi-geostrophic equations for the continuously stratified hydrostatic system. The primitive equations of motion are given by (5.15), and we extract the mean stratification so that the thermodynamic equation is given by (5.17). We also stay on the β-plane for simplicity. Readers who wish for a briefer, more informal derivation may peruse the box on page 235; however, it is important to realize that there is a systematic asymptotic derivation of the quasi-geostrophic equations, for it is this that ensures that the resulting equations have good conservation properties, as explained in section 5.3.3.

5.4.1 Scaling and assumptions

The scaling assumptions we make are just those we made for the shallow water system on page 220, with a deformation radius now given by $L_{\rm d} = NH/f_0$. The nondimensionalization and scaling is initially precisely that of section 5.1.2, and so we obtain the

following non-dimensional equations:

Horizontal momentum:
$$Ro\frac{D\widehat{\boldsymbol{u}}}{D\widehat{t}} + \widehat{\boldsymbol{f}} \times \widehat{\boldsymbol{u}} = -\widehat{\nabla}_z\widehat{\phi}, \tag{5.94}$$

Hydrostatic:
$$\frac{\partial\widehat{\phi}}{\partial\widehat{z}} = \widehat{b}, \tag{5.95}$$

Mass continuity:
$$\left(\frac{\partial\widehat{u}}{\partial\widehat{x}} + \frac{\partial\widehat{v}}{\partial\widehat{y}} + \frac{1}{\widetilde{\rho}}\frac{\partial\widetilde{\rho}\widehat{w}}{\partial\widehat{z}}\right) = 0, \tag{5.96}$$

Thermodynamic:
$$Ro\frac{D\widehat{b}}{D\widehat{t}} + \left(\frac{L_{\mathrm{d}}}{L}\right)^2 \widehat{w} = 0. \tag{5.97}$$

In Cartesian coordinates we may express the Coriolis parameter as

$$\boldsymbol{f} = \boldsymbol{f}_0 + \beta y\, \mathbf{k} \tag{5.98}$$

where $\boldsymbol{f}_0 = f_0\mathbf{k}$. The variation of the Coriolis parameter is assumed small (this is a key difference between the quasi-geostrophic system and the planetary geostrophic system), and in particular we shall assume that βy is approximately the size of the relative vorticity, and so much smaller than f_0 itself.[7] Thus,

$$\beta y \sim \frac{U}{L}, \qquad \beta \sim \frac{U}{L^2}, \tag{5.99}$$

and so we define an $\mathcal{O}(1)$ non-dimensional beta parameter by

$$\widehat{\beta} = \frac{\beta L^2}{U} = \frac{\beta L}{Ro\, f_0}. \tag{5.100}$$

From this it follows that if $f = f_0 + \beta y$, the corresponding nondimensional version is

$$\widehat{f} = \widehat{f}_0 + Ro\widehat{\beta}\widehat{y}. \tag{5.101}$$

where $\widehat{f} = f/f_0$ and $\widehat{f}_0 = f_0/f_0 = 1$.

5.4.2 Asymptotics

We now expand the nondimensional dependent variables in an asymptotic series in Rossby number, and write

$$\widehat{\boldsymbol{u}} = \widehat{\boldsymbol{u}}_0 + Ro\widehat{\boldsymbol{u}}_1 + \cdots, \qquad \widehat{\phi} = \widehat{\phi}_0 + Ro\widehat{\phi}_1 + \cdots, \qquad \widehat{b} = \widehat{b}_0 + Ro\widehat{b}_1 + \cdots. \tag{5.102}$$

Substituting these into the equations of motion, the lowest order momentum equation is simply geostrophic balance,

$$\widehat{\boldsymbol{f}}_0 \times \widehat{\boldsymbol{u}}_0 = -\nabla\widehat{\phi}_0 \tag{5.103}$$

with a *constant* value of the Coriolis parameter. (For the rest of this chapter we drop the subscript z from the ∇ operator.) From (5.103) it is evident that

$$\nabla \cdot \widehat{\boldsymbol{u}}_0 = 0. \tag{5.104}$$

Thus, the horizontal flow is, to leading order, non-divergent; this is a consequence of geostrophic balance, and is *not* a mass conservation equation. (We henceforth drop the subscript from the ∇ operator). Using (5.104) in the mass conservation equation, (5.96), gives

$$\frac{\partial}{\partial \widehat{z}}(\widetilde{\rho}\widehat{w}_0) = 0, \tag{5.105}$$

which implies that if w_0 is zero somewhere (e.g., at a solid surface) then w_0 is zero everywhere (essentially the Taylor-Proudman effect). Thus, a nontrivial result of the scaling is that the lowest order vertical velocity is zero. A physical way of saying this is that the scaling estimate $W = UH/L$ is an overestimate of the size of the vertical velocity, because even though $\partial w/\partial z \approx -\nabla \cdot \boldsymbol{u}$, the horizontal divergence of the geostrophic flow is small if f is nearly constant and $|\nabla \cdot \boldsymbol{u}| \ll U/L$. We might have anticipated this from the outset, and scaled w differently, perhaps using the geostrophic vorticity balance estimate, $w \sim \beta UH/f_0 = RoUH/L$ as the scaling factor for w, and the end result would be the same.

At next order the momentum equation is

$$\frac{\mathrm{D}_0 \widehat{\boldsymbol{u}}_0}{\mathrm{D}\widehat{t}} + \widehat{\beta}\widehat{y}\mathbf{k} \times \widehat{\boldsymbol{u}}_0 + \widehat{\boldsymbol{f}} \times \widehat{\boldsymbol{u}}_1 = -\nabla\widehat{\phi}_1, \tag{5.106}$$

where $D_0/Dt = \partial/\partial\widehat{t} + (\widehat{\boldsymbol{u}}_0 \cdot \nabla)$, and the next order mass conservation equation is

$$\nabla_z \cdot (\widetilde{\rho}\widehat{\boldsymbol{u}}_1) + \frac{\partial}{\partial z}(\widetilde{\rho}\widehat{w}_1) = 0. \tag{5.107}$$

From (5.97), the lowest order thermodynamic equation is just

$$\left(\frac{L_{\mathrm{d}}}{L}\right)^2 \widehat{w}_0 = 0 \tag{5.108}$$

provided that, as we have assumed, the scales of motion are not sufficiently large that $Ro(L/L_{\mathrm{d}})^2 = \mathcal{O}(1)$. (This is a key difference between quasi-geostrophy and planetary geostrophy.) At next order we obain an evolution equation for the buoyancy, and this is

$$\frac{\mathrm{D}_0 \widehat{b}_0}{\mathrm{D}\widehat{t}} + \widehat{w}_1 \left(\frac{L_{\mathrm{d}}}{L}\right)^2 = 0. \tag{5.109}$$

The potential vorticity equation

To obtain a single evolution equation for lowest order quantities we eliminate w_1 between the thermodynamic and momentum equations. Cross differentiating the first order momentum equation (5.106) gives the vorticity equation,

$$\frac{\partial\widehat{\zeta}_0}{\partial\widehat{t}} + (\widehat{\boldsymbol{u}}_0 \cdot \nabla)\widehat{\zeta}_0 + \widehat{v}_0\widehat{\beta} = -\widehat{f}_0\nabla_z \cdot \widehat{\boldsymbol{u}}_1. \tag{5.110}$$

(In dimensional terms, the divergence on the right-hand side is small, but is multiplied by the large term f_0, and their product is the same order as the terms on the left-hand side.) Using the mass conservation equation (5.107), (5.110) becomes

$$\frac{D_0}{D\hat{t}}(\zeta_0 + \hat{f}) = \frac{\hat{f}_0}{\tilde{\rho}} \frac{\partial}{\partial z}(w_1 \tilde{\rho}) \tag{5.111}$$

Combining (5.111) and (5.109) gives

$$\frac{D_0}{D\hat{t}}(\zeta_0 + \hat{f}) = -\frac{\hat{f}_0}{\tilde{\rho}} \frac{\partial}{\partial \hat{z}}\left(\frac{D_0}{D\hat{t}}(F\tilde{\rho}b_0)\right) \tag{5.112}$$

where $F \equiv (L/L_d)^2$. The right-hand side of this equation is

$$\frac{\partial}{\partial \hat{z}}\left(\frac{D_0 \hat{b}}{D\hat{t}}\right) = \frac{D_0}{D\hat{t}}\left(\frac{\partial \hat{b}}{\partial \hat{z}}\right) + \frac{\partial \hat{\boldsymbol{u}}_0}{\partial \hat{z}} \cdot \nabla \hat{b}. \tag{5.113}$$

The second term on the right-hand side vanishes identically using the thermal wind equation

$$\mathbf{k} \times \frac{\partial \hat{\boldsymbol{u}}_0}{\partial \hat{z}} = -\frac{1}{\hat{f}_0}\nabla b_0, \tag{5.114}$$

and so (5.112) becomes

$$\frac{D_0}{D\hat{t}}\left[\zeta_o + \hat{f} + \frac{\hat{f}_0}{\tilde{\rho}} \frac{\partial}{\partial z}(\tilde{\rho}Fb_0)\right] = 0, \tag{5.115}$$

or, using the hydrostatic equation,

$$\frac{D_0}{D\hat{t}}\left[\zeta_0 + \hat{f} + \frac{\hat{f}_0}{\tilde{\rho}} \frac{\partial}{\partial z}\left(\tilde{\rho}F\frac{\partial \phi_0}{\partial z}\right)\right] = 0. \tag{5.116}$$

Since the lowest-order horizontal velocity is divergence-free, we can define a stream-function ψ such that

$$\hat{u}_0 = -\frac{\partial \hat{\psi}}{\partial y}, \qquad \hat{v}_0 = \frac{\partial \hat{\psi}}{\partial x} \tag{5.117}$$

where also, using (5.103), $\phi_0 = \hat{f}_0 \hat{\psi}$. The vorticity is then given by $\hat{\zeta}_0 = \nabla^2 \hat{\psi}$ and (5.116) becomes a single equation in a single unknown, to wit

$$\boxed{\frac{D_0}{D\hat{t}}\left[\nabla^2 \hat{\psi} + \hat{\beta}\hat{y} + \frac{\hat{f}_0^2}{\tilde{\rho}} \frac{\partial}{\partial \hat{z}}\left(\tilde{\rho}F\frac{\partial \hat{\psi}}{\partial \hat{z}}\right)\right] = 0}, \tag{5.118}$$

where the material derivative is evaluated using $\hat{\boldsymbol{u}}_0 = \mathbf{k} \times \nabla \hat{\psi}$. This is the nondimensional form of the quasi-geostrophic potential vorticity equation, one of the most important equations in dynamical meteorology and oceanography. In deriving it we have reduced the Navier Stokes equations, which are six coupled nonlinear partial differential equations in six unknowns (u, v, w, T, p, ρ) to a single (albeit nonlinear) first-order partial differential equation in a single unknown.[8]

Dimensional equations

The dimensional version of the equation may be written,

$$
\frac{Dq}{Dt} = 0,
$$
$$
q = \nabla^2 \psi + f + \frac{f_0^2}{\tilde{\rho}} \frac{\partial}{\partial z} \left(\frac{\tilde{\rho}}{N^2} \frac{\partial \psi}{\partial z} \right)
$$

(5.119a,b)

where only the variable part of f (e.g., βy) is relevant in the second term on the right-hand side of the expression for q. The quantity q is known as the *quasi-geostrophic potential vorticity*. It is analogous to the exact (Ertel) potential vorticity (see section 5.5 for more about this), and it is conserved when advected by the *horizontal* geostrophic flow. All the other dynamical variables may be obtained from potential vorticity as follows:

(i) Streamfunction [2nd line of (5.119)]

(ii) Velocity: $\boldsymbol{u} = \mathbf{k} \times \nabla \psi \; [\equiv \nabla^\perp \psi = -\nabla \times (\mathbf{k}\psi)]$.

(iii) Relative vorticity: $\zeta = \nabla^2 \psi$.

(iv) Perturbation pressure: $\phi = f_0 \psi$.

(v) Perturbation buoyancy: $b' = f_0 \partial \psi / \partial z$.

The length-scale $L_d = NH/f_0$, emerges naturally from the QG dynamics. It is the scale at which buoyancy and relative vorticity effects contribute equally to the potential vorticity, and is called the *deformation radius;* it is analogous to the quantity $\sqrt{gH}/f_0$ arising in shallow water theory. In the upper ocean, with $N \approx 10^{-2}\,\mathrm{s}^{-1}$, $H \approx 10^3\,\mathrm{m}$, and $f_0 \approx 10^{-4}\,\mathrm{s}^{-1}$, then $L_d \approx 100\,\mathrm{km}$. At high latitudes the ocean is much less stratified and $N^2 \sim 10^{-3}\,\mathrm{s}^{-1}$, and f is somewhat larger, and the deformation radius is correspondingly smaller. In the atmosphere, with $N \approx 10^{-2}\,\mathrm{s}^{-1}$, $H \approx 10^4\,\mathrm{m}$, then $L_d \approx 1000\,\mathrm{km}$. It is this order of magnitude difference in the deformation scales that accounts for a great deal of the quantitative difference in the dynamics of the ocean and atmosphere. If we take the limit $L_d \to \infty$ then the stratified quasi-geostrophic equations reduce to

$$
\frac{Dq}{Dt}t = 0, \qquad q = \nabla^2 + f
$$

(5.120)

This is the two-dimensional vorticity equation, identical to (4.77). The high stratification of this limit has suppressed all vertical motion, and variations in the flow become confined to the horizontal plane. Finally, we note that it is typical in quasi-geostrophic applications to omit the prime on the buoyancy perturbations, and write $b = f_0 \partial \psi / \partial z$; however, we will keep the prime in this chapter.

5.4.3 Buoyancy advection at the surface

The solution of the elliptic equation in (5.119) requires vertical boundary conditions on ψ at the ground and at the top of the atmosphere, and these are given by use of the

thermodynamic equation. For a flat, slippery, rigid surface the vertical velocity is zero so that the thermodynamic equation may be written

$$\frac{\mathrm{D}b'}{\mathrm{D}t} = 0, \qquad b' = f_0 \frac{\partial \psi}{\partial z}. \tag{5.121}$$

We apply this at the ground and at the tropopause, treating the latter as a lid on the lower atmosphere. In the presence of friction and topography the vertical velocity is not zero, but is given by

$$w = r\nabla^2 \psi + \boldsymbol{u} \cdot \nabla \eta_b \tag{5.122}$$

where the first term represents Ekman friction (with the constant r proportional to the thickness of the Ekman layer) and the second term represents topographic forcing. The boundary condition becomes

$$\frac{\partial}{\partial t}\left(\frac{\partial \psi}{\partial z}\right) + \boldsymbol{u} \cdot \nabla \left(\frac{\partial \psi}{\partial z} + N^2 \eta_b\right) + N^2 r \nabla^2 \psi = 0, \tag{5.123}$$

where all the fields are evaluated at $z = 0$ and $z = H$, the height of the lid. Thus, the quasi-geostrophic system is characterized by the horizontal advection of potential vorticity in the interior and the advection of buoyancy at the boundary. Instead of a lid at the top, then in a compressible fluid like the atmosphere we may suppose that all disturbances tend to zero as $z \to \infty$.

* A potential vorticity sheet at the boundary

Rather than regarding buoyancy advection as providing the boundary condition, it is sometimes useful to think of there being a very thin sheet of potential vorticity just above the ground and another just below the lid, specifically with a vertical distribution proportional to $\delta(z - \epsilon)$ or $\delta(z - H + \epsilon)$. The boundary condition (5.121) or (5.123) can be replaced by this, along with the condition that there are no variations of buoyancy at the boundary and $\partial \psi / \partial z = 0$ at $z = 0$ and $z = H$.[9]

To see this, we first note that the differential of a step function is a delta function. Thus, a discontinuity in $\partial \psi / \partial z$ at a level $z = z_1$ is equivalent to a delta function in potential vorticity there:

$$q(z_1) = \left[\frac{f_0^2}{N^2}\frac{\partial \psi}{\partial z}\right]_{z_1-}^{z_1+} \delta(z - z_1). \tag{5.124}$$

Now, suppose that the lower boundary condition, given by (5.121), has some arbitrary distribution of buoyancy on it. We can replace this condition by the simpler condition $\partial \psi / \partial z = 0$ at $z = 0$, provided we also add to our definition of potential vorticity a term given by (5.124) with $z_1 = \epsilon$. This term is then advected by the horizontal flow, as are the other contributions. A buoyancy source at the boundary must similarly be treated as a sheet of potential vorticity source in the interior. Any flow with buoyancy variations over a horizontal boundary is thus equivalent to a flow with uniform buoyancy at the boundary, but with a spike in potential vorticity adjacent to the boundary. The conceptual advantage is that now everything is expressed in terms of potential vorticity and its advection. However, in practice there may be little to be gained, because the boundary terms must still be included in any particular calculation that is to be performed.

5.4.4 Quasi-geostrophy in pressure coordinates

The derivation of the quasi-geostrophic system in pressure coordinates is very similar to that in height coordinates, with the main difference coming at the boundaries, and we give only the results. The starting point is the primitive equations in pressure coordinates, (2.152). In pressure coordinates quasi-geostrophic potential vorticity is found to be

$$q = f + \nabla^2 \psi + \frac{\partial}{\partial p} \left(\frac{f_0^2}{S^2} \frac{\partial \psi}{\partial p} \right), \tag{5.125}$$

where ψ is the streamfunction and

$$S^2 \equiv -\frac{R}{p} \left(\frac{p}{p_R} \right)^\kappa \frac{\mathrm{d}\tilde{\theta}}{\mathrm{d}p} = -\frac{1}{\rho\theta} \frac{\mathrm{d}\tilde{\theta}}{\mathrm{d}p} \tag{5.126}$$

where $\tilde{\theta}$ is a reference profile, a function of pressure only. In log-pressure coordinates, with $Z = -H \ln p$, this may be written

$$q = f + \nabla^2 \psi + \frac{1}{\rho_*} \frac{\partial}{\partial Z} \left(\frac{\rho_* f_0^2}{N_Z^2} \frac{\partial \psi}{\partial Z} \right), \tag{5.127}$$

where

$$N_Z^2 = S^2 \left(\frac{p}{H} \right)^2 = -\left(\frac{R}{H} \right) \left(\frac{p}{p_R} \right)^\kappa \frac{\mathrm{d}\tilde{\theta}}{\mathrm{d}Z} \tag{5.128}$$

is the buoyancy frequency and $\rho_* = \exp(-z/H)$. Temperature and potential temperature are related to the streamfunction by

$$T = -\frac{f_0 p}{R} \frac{\partial \psi}{\partial p} = \frac{H f_0}{R} \frac{\partial \psi}{\partial Z}, \tag{5.129a}$$

$$\theta = -\left(\frac{p_R}{p} \right)^\kappa \left(\frac{f_0 p}{R} \right) \frac{\partial \psi}{\partial p} = \left(\frac{p_R}{p} \right)^\kappa \left(\frac{H f_0}{R} \right) \frac{\partial \psi}{\partial Z}. \tag{5.129b}$$

The surface boundary condition again is derived from the thermodynamic equation. This is, in log-pressure coordinates,

$$\frac{\mathrm{D}}{\mathrm{D}t} \left(\frac{\partial \psi}{\partial Z} \right) + \frac{N_Z^2}{f_0} W = 0. \tag{5.130}$$

where $W = \mathrm{D}Z/\mathrm{D}t$. This is not the real vertical velocity, w, but it is related to it by

$$w = \frac{f_0}{g} \frac{\partial \psi}{\partial t} + \frac{RT}{gH} W. \tag{5.131}$$

Thus, choosing $H = RT(0)/g$, we have, at $Z = 0$,

$$\frac{\partial}{\partial t} \left(\frac{\partial \psi}{\partial Z} - \frac{N_Z^2}{g} \psi \right) + \boldsymbol{u} \cdot \nabla \psi = -\frac{N^2}{f_0} w, \tag{5.132}$$

where

$$w = \boldsymbol{u} \cdot \nabla \eta_b + r \nabla^2 \psi. \tag{5.133}$$

This differs from the expression in height coordinates only by the second term in the local time derivative. In applications where accuracy is not the main issue the simpler boundary condition $\mathrm{D}(\partial_Z \psi)/\mathrm{D}t = 0$ is sometimes used.

Informal Derivation of Stratified QG Equations

For simplicity we use the Boussinesq equations, but similar derivations could be given for the anelastic equations or in pressure coordinates. The first ingredient is the vertical component of the vorticity equation, (4.76); in the Boussinesq version (or the pressure coordinate or anelastic versions) there is no baroclinic term and:

$$\frac{D_3}{Dt}(\zeta + f) = -(\zeta + f)\left(\frac{\partial u}{\partial x} + \frac{\partial v}{\partial y}\right) + \left(\frac{\partial u}{\partial z}\frac{\partial w}{\partial y} - \frac{\partial v}{\partial z}\frac{\partial w}{\partial x}\right). \qquad \text{(QG.1)}$$

We now apply the assumptions on page 220. The advection and the vorticity on the left-hand side become geostrophic, but we keep the horizontal divergence (which is purely ageostrophic, and therefore small) on the right-hand side where it is multiplied by the big term f. Furthermore, because f is nearly constant we replace it with f_0 except where it is differentiated. The tilting term is smaller than the advection terms by the ratio $[UW/(HL)]/[U^2/L^2] = [W/H]/[U/L] \ll 1$, because w is small ($\partial w/\partial z$ being equal to the divergence of the ageostrophic velocity). We therefore neglect it, and given all this (QG.1) becomes

$$\frac{D_g}{Dt}(\zeta_g + f) = -f_0\left(\frac{\partial u}{\partial x} + \frac{\partial v}{\partial y}\right) = f_0\frac{\partial w}{\partial z}, \qquad \text{(QG.2)}$$

where the second equality uses mass continuity and $D_g/Dt = \partial/\partial t + \boldsymbol{u}_g \cdot \nabla$.

The second major ingredient is the thermodynamic equation,

$$D_3 b/Dt = 0. \qquad \text{(QG.3)}$$

The stratification is assumed nearly constant, so we write $b = \widetilde{b}(z) + b'(x, y, z, t)$ where $\widetilde{b}$ is the basic state buoyancy. Furthermore, because w is small it only advects the basic state, and with $N^2 = \partial\widetilde{b}/\partial z$ (QG.3) becomes

$$D_g b'/Dt + wN^2 = 0. \qquad \text{(QG.4)}$$

Hydrostatic and geostrophic wind balance enable us to write the geostrophic velocity, vorticity, and buoyancy in terms of streamfunction ψ $[= p/(f_0\rho_0)]$:

$$\boldsymbol{u}_g = \mathbf{k} \times \nabla\psi, \qquad \zeta_g = \nabla^2\psi, \qquad b' = f_0\partial\psi/\partial z. \qquad \text{(QG.5)}$$

The quasi-geostrophic potential vorticity equation is obtained by eliminating w between (QG.2) and (QG.4), and this gives

$$\boxed{\frac{D_g q}{Dt} = 0, \qquad q = \zeta_g + f + \frac{\partial}{\partial z}\left(\frac{f_0 b'}{N^2}\right)}. \qquad \text{(QG.6)}$$

This equation is the Boussinesq version of (5.119), and using (QG.5) it may be expressed entirely in terms of the streamfunction, with $D_g \cdot/Dt = \partial/\partial t + J(\psi, \cdot)$. The vertical boundary conditions, at $z = 0$ and $z = H$ say, are given by (QG.4) with $w = 0$, with straightforward generalizations if topography or friction are present.

Fig. 5.3 The two-level quasi-geostrophic system with a flat bottom and rigid lid at which $w = 0$.

5.4.5 The Two-Level Quasi-Geostrophic System

The quasi-geostrophic system derived above has continuous variation in the vertical (and horizontal, of course). By finite-differencing the continuous equations we can obtain a *multi-level* model, and a crude but important special case of this is the *two-level* model, which allows only two-degrees of freedom in the vertical. To obtain the equations of motion one way to proceed is to take a crude finite difference of the continuous relation between potential vorticity and streamfunction given in (5.119b), but here as a variation we will apply the quasi-geostrophic vorticity equation to levels 1 and 2, and the thermodynamic equation in the center. In the Boussinesq case (or in pressure coordinates, with a slight reinterpretation of the meaning of the symbols) we have

$$q = \zeta + f + \frac{\partial}{\partial z}\left(\frac{f_0 b'}{N^2}\right) \tag{5.134}$$

where $b' = f_0 \partial b'/\partial z$. In the case with a flat bottom and rigid lid at the top (and incorporating topography is an easy extension) the boundary condition of $w = 0$ is satisfied by $\mathrm{D}\partial_z \psi /\mathrm{D}t = 0$ at the top and bottom, and then an obvious finite differencing of (5.134) in the vertical (see Fig. 5.3) gives

$$q_1 = \zeta_1 + f + \frac{2f_0^2}{N^2 H_1 H}(\psi_2 - \psi_1), \qquad q_2 = \zeta_2 + f + \frac{2f_0^2}{N^2 H_2 H}(\psi_1 - \psi_2). \tag{5.135}$$

In atmospheric problems it is common to choose $H_1 = H_2$, whereas in oceanic problems we might choose to have a thinner upper layer, representing the flow above the main thermocline. Note that the boundary conditions of $w = 0$ at the top and bottom are already taken care of (5.135): they are incorporated into the definition of the potential vorticity — a finite-difference analog of the delta-function construction of section 5.4.3. At each level the potential vorticity is advected by the streamfunction so that the

evolution equation for each level is:

$$\frac{Dq_i}{Dt} = \frac{\partial q_i}{\partial t} + \boldsymbol{u}_i \cdot q_i = \frac{\partial q_i}{\partial t} + J(\psi_i, q_i) = 0, \qquad i = 1, 2. \qquad (5.136)$$

Models with more than two levels can be easily constructed by extending the finite-differencing procedure.

Connection to the layered system

The two-level expressions, (5.135), have an obvious similarity with the *two-layer* expressions, (5.86). Noting that $N^2 = \partial \widehat{b}/\partial z$ and that $b = -g\delta\rho/\rho_0$ it is natural to let

$$N^2 = -\frac{g}{\rho_0} \frac{\rho_1 - \rho_2}{H/2} = \frac{g'}{H/2}. \qquad (5.137)$$

With this identification we find that (5.135) becomes

$$q_1 = \zeta_1 + f + \frac{f_0^2}{g'H_1}(\psi_2 - \psi_1), \qquad q_2 = \zeta_2 + f + \frac{f_0^2}{g'H_2}(\psi_1 - \psi_2). \qquad (5.138)$$

These expressions are identical with (5.86) in the flat-bottomed, rigid lid case. This is an example of the similarity between layered models and the finite difference representation of the continuous representation, and indeed a multi-layered system with n layers, is equivalent to a finite-difference representation with n levels. However, in the pantheon of quasi-geostrophic models the two-level and two-layer models hold preeminent places.

5.5 * QUASI-GEOSTROPHY AND ERTEL POTENTIAL VORTICITY

When using the shallow water equations, quasi-geostrophic theory could be naturally developed beginning with the expression for potential vorticity. Is such an approach possible for the stratified primitive equations? The answer is yes, but the approach is more complicated, as we see.

5.5.1 Using height coordinates

We begin with the expression for potential vorticity in the Boussinesq hydrostatic equations [c.f., (4.127)]

$$Q = \left[(v_x - u_y)b_z - v_z\theta_x + u_z\theta_y + f\theta_z\right], \qquad (5.139)$$

where the x, y, z subscripts denote derivatives. Without approximation, we write the stratification as $b = \widetilde{b}(z) + b'(x, y, z, t)$, and the potential vorticity becomes

$$Q = [f_0 N^2] + [(\beta y + \zeta)N^2 + f_0 b_z'] + [(\beta y + \zeta)b_z' - (v_z b_x' - u_z b_y')], \qquad (5.140)$$

where, under quasi-geostrophic scaling, the terms in square brackets are in decreasing order of size. Neglecting the third term, and taking the velocity and buoyancy fields

to be in geostrophic and thermal wind balance, we can write the potential vorticity as $Q \approx \widetilde{Q} + Q'$, where $\widetilde{Q} = f_0 N^2$ and

$$Q' = (\beta y + \zeta)N^2 + f_0 b'_z = (\beta y + \nabla^2 \psi)N^2 + f_0^2 \frac{\partial \psi}{\partial z}. \tag{5.141}$$

The potential vorticity evolution equation is then

$$\frac{\mathrm{D}Q'}{\mathrm{D}t} + w \frac{\partial \widetilde{Q}}{\partial z} = 0. \tag{5.142}$$

The vertical advection is important only in advecting the basic state potential vorticity $\widetilde{Q}$. Thus, after dividing by N^2, (5.142) becomes

$$\frac{\partial q_*}{\partial t} + \boldsymbol{u}_g \cdot \nabla q_* + \frac{w}{N^2} \frac{\partial \widehat{q}}{\partial z} = 0, \tag{5.143}$$

where

$$q_* = (\beta y + \zeta) + \frac{f_0}{N^2} b'_z. \tag{5.144}$$

This is the approximation to the (perturbation) Ertel potential vorticity in the quasi-geostrophic limit. However, it is not the same as the expression for the quasi-geostrophic potential vorticity, (5.119) and, furthermore, (5.143) involves a vertical advection. (Thus, we might refer to the expression in (5.119) as the 'quasi-geostrophic pseudo-potential vorticity', but the prefix 'quasi-geostrophic' alone normally suffices.) We can derive (5.119) (taking $\widetilde{\rho} = 1$ for simplicity) by eliminating w between (5.143) and the quasi-geostrophic thermodynamic equation $\partial b'/\partial t + \boldsymbol{u}_g \cdot \nabla b' + w \partial \widetilde{b}/\partial z = 0$.

5.5.2 Using isentropic coordinates

An illuminating path from Ertel potential vorticity to the quasi-geostrophic equations goes by way of isentropic coordinates.[10] We begin with the isentropic expression for Ertel potential vorticity for an ideal gas,

$$Q = \frac{f + \zeta}{\sigma} \tag{5.145}$$

where $\sigma = -\partial p/\partial \theta$ is the thickness density (which we will just call the thickness), and in adiabatic flow potential vorticity is advected along isopycnals. We now employ quasi-geostrophic scaling to derive an approximate equation set from this. First assume that variations in thickness are small compared to the reference state, so that

$$\sigma = \widetilde{\sigma}(\theta) + \sigma', \qquad |\sigma'| \ll |\sigma|. \tag{5.146}$$

and similarly for pressure and density. Assuming also that the variations in Coriolis parameter are small, (5.145) becomes

$$Q \approx \left[\frac{f_0}{\widetilde{\sigma}} \right] + \left[\frac{1}{\widetilde{\sigma}}(\zeta + \beta y) - \frac{f_0}{\widetilde{\sigma}} \frac{\sigma'}{\widetilde{\sigma}} \right]. \tag{5.147}$$

We now use geostrophic and hydrostatic balance to express the terms on the right-hand side in terms of a single variable, noting that the first term does not vary along isentropic surfaces. Hydrostatic balance is

$$\frac{\partial M}{\partial \theta} = \Pi \tag{5.148}$$

where $M = c_p T + gz$ and $\Pi = c_p(p/p_R)^\kappa$. Writing $M = \widetilde{M}(\theta) + M'$ and $\Pi = \widetilde{\Pi}(\theta) + \Pi'$, where $\widetilde{M}$ and $\widetilde{\Pi}$ are hydrostatically balanced reference profiles, we obtain

$$\frac{\partial M'}{\partial \theta} = \Pi' \approx \frac{d\widetilde{\Pi}}{dp} p' = \frac{1}{\theta \widetilde{\rho}} p' \tag{5.149}$$

where the last equality follows using the equation of state for an ideal gas and $\widetilde{\rho}$ is a reference profile. The perturbation thickness field may then be written as

$$\sigma' = -\frac{\partial}{\partial \theta}\left(\widetilde{\rho}\theta \frac{\partial M'}{\partial \theta}\right). \tag{5.150}$$

Geostrophic balance is $\boldsymbol{f}_0 \times \boldsymbol{u} = -\nabla_\theta M'$ where the velocity, and the horizontal derivatives, are along isentropic surfaces. This enables us to define a flow streamfunction by

$$\psi \equiv \frac{M'}{f_0}. \tag{5.151}$$

and we can then write all the variables in terms of ψ:

$$u = -\left(\frac{\partial \psi}{\partial y}\right)_\theta, \qquad v = \left(\frac{\partial \psi}{\partial x}\right)_\theta,$$

$$\zeta = \nabla_\theta^2 \psi, \qquad \sigma' = f_0 \frac{\partial}{\partial \theta}\left(\widetilde{\rho}\theta \frac{\partial M'}{\partial \theta}\right). \tag{5.152}$$

Using (5.147) (5.151) and (5.152), the quasi-geostrophic system in isentropic coordinates may be written

$$\boxed{\begin{array}{c}\dfrac{Dq}{Dt} = 0 \\[2mm] q = f + \nabla_\theta^2 \psi + \dfrac{f_0^2}{\widetilde{\sigma}}\dfrac{\partial}{\partial \theta}\left(\widetilde{\rho}\theta \dfrac{\partial \psi}{\partial \theta}\right)\end{array}} . \tag{5.153a,b}$$

where the advection of potential vorticity is by the geostrophically balanced flow, along isentropes. The variable q is an approximation to the second term in square brackets in (5.147), multiplied by $\widetilde{\sigma}$,

Projection back to height coordinates

We can recover the height or pressure coordinate quasi-geostrophic systems by projecting (5.153) onto height coordinates. This is straightforward because, by assumption,

the isentropes in a quasi-geostrophic system are nearly flat. Recall that [c.f., (2.144)] a transformation between vertical coordinates may be effected by

$$\left.\frac{\partial}{\partial x}\right|_{\theta} = \left.\frac{\partial}{\partial x}\right|_{z} + \left.\frac{\partial z}{\partial x}\right|_{\theta}\frac{\partial}{\partial z},$$

(5.154)

but the second term is $\mathcal{O}(Ro)$ smaller than the first because, under quasi-geostrophic scaling, isentropic slopes are small. Thus $\nabla_\theta^2\psi$ in (5.153b) may be replaced by $\nabla_p^2\psi$ or $\nabla_z^2\psi$. The vortex stretching term in (5.153) becomes

$$\frac{f_0^2}{\widetilde{\sigma}}\frac{\partial}{\partial\theta}\left(\widetilde{\rho}\theta\frac{\partial\psi}{\partial\theta}\right) \approx \frac{f_0^2}{\widetilde{\sigma}}\frac{\mathrm{d}\widetilde{p}}{\mathrm{d}\theta}\frac{\partial}{\partial p}\left(\widetilde{\rho}\theta\frac{\mathrm{d}\widetilde{p}}{\mathrm{d}\theta}\frac{\partial\psi}{\partial p}\right) = \frac{\partial}{\partial p}\left(\frac{f_0^2}{S^2}\frac{\partial\psi}{\partial p}\right)$$

(5.155)

where S^2 is given by (5.126). The expression for the quasi-geostrophic potential vorticity in isentropic coordinates is thus approximately equal to the quasi-geostrophic potential vorticity in pressure coordinates. This near-equality holds because the isentropic expression, (5.153b), does not contain a component proportional to the mean stratification: the second term on the right-hand side (5.147) is the only dynmcally relevant one, and its evolution along isentropes is mirrored by the evolution along isobaric surfaces of quasi-geostrophic potential vorticity in pressure coordinates.

5.6 * ENERGETICS OF QUASI-GEOSTROPHY

If the quasi-geostrophic set of equations is to represent a real fluid system in a physically meaningful way, then it should have a consistent set of energetics. In particular, total energy should be conserved, and there should be analogs of kinetic and potential energy and conversion between the two. We now show that this is indeed the case, using the Boussinesq set as an example.

Let us write the governing equations as a potential vorticity equation in the interior,

$$\frac{\mathrm{D}}{\mathrm{D}t}\left[\nabla^2\psi + \frac{\partial}{\partial z}\left(\frac{f_0^2}{N^2}\frac{\partial\psi}{\partial z}\right)\right] + \beta\frac{\partial\psi}{\partial x} = 0, \qquad 0 < z < 1,$$

(5.156)

and buoyancy advection at the boundary,

$$\frac{\mathrm{D}}{\mathrm{D}t}\left(\frac{\partial\psi}{\partial z}\right) = 0, \qquad z = 0, 1.$$

(5.157)

For lateral boundary conditions we may assume that $\psi = $ constant, or impose periodic conditions. If we multiply (5.156) by $-\psi$ and integrate over the domain, using the boundary conditions, we easily find

$$\frac{\mathrm{d}\widehat{E}}{\mathrm{d}t} = 0, \qquad \widehat{E} = \frac{1}{2}\int_V\left[(\nabla\psi)^2 + \frac{f_0^2}{N^2}\left(\frac{\partial\psi}{\partial z}\right)^2\right]\mathrm{d}V.$$

(5.158a,b)

The term involving β makes no direct contribution to the energy budget. Eq. (5.158)

is the fundamental energy equation for quasi-geostrophic motion, and it states that in the absence of viscous or diabatic terms the total energy is conserved. The two terms in (5.158b) can be identified as the kinetic and available potential energy of the flow, where

$$KE = \frac{1}{2} \int_V (\nabla \psi)^2 \, \mathrm{d}V, \qquad APE = \frac{1}{2} \int_V \frac{f_0^2}{N^2} \left(\frac{\partial \psi}{\partial z}\right)^2 \, \mathrm{d}V. \qquad (5.159a,b)$$

The available potential energy may also be written as

$$APE = \frac{1}{2} \int_V \frac{H}{L_d^2} \left(\frac{\partial \psi}{\partial z}\right)^2 \, \mathrm{d}V, \qquad (5.160)$$

where L_d is the deformation radius NH/f_0 and we may choose H such that $z \sim H$. At some scale L the ratio of the kinetic energy to the potential energy is thus, roughly,

$$\frac{KE}{APE} \sim \frac{L_d^2}{L^2}. \qquad (5.161)$$

For scales much larger than L_d the potential energy dominates the kinetic energy, and contrariwise.

5.6.1 Conversion between APE and KE

Let us return to the vorticity and thermodynamic equations,

$$\frac{\mathrm{D}\zeta}{\mathrm{D}t} = f \frac{\partial w}{\partial z} \qquad (5.162)$$

where $\zeta = \nabla^2 \psi$, and

$$\frac{\mathrm{D}b'}{\mathrm{D}t} + N^2 w = 0 \qquad (5.163)$$

where $b' = f_0 \partial \psi / \partial z$. From (5.162) we form a kinetic energy equation namely

$$\frac{1}{2} \frac{\mathrm{d}}{\mathrm{d}t} \int_V (\nabla \psi)^2 \, \mathrm{d}V = -\int_V f_0 \frac{\partial w}{\partial z} \psi \, \mathrm{d}V = \int_V f_0 w \frac{\partial \psi}{\partial z} \, \mathrm{d}V. \qquad (5.164)$$

From (5.163) we form a potential energy equation, namely

$$\frac{\mathrm{d}}{\mathrm{d}t} \frac{1}{2} \int_V \frac{f_0^2}{N^2} \left(\frac{\partial \psi}{\partial z}\right)^2 \, \mathrm{d}V = -\int_V f_0 w \frac{\partial \psi}{\partial z} \, \mathrm{d}V. \qquad (5.165)$$

Thus, the *conversion* from APE to KE is represented by

$$\frac{\mathrm{d}}{\mathrm{d}t} KE = -\frac{\mathrm{d}}{\mathrm{d}t} APE = \int_v f_0 w \frac{\partial \psi}{\partial z} \, \mathrm{d}V. \qquad (5.166)$$

Because the buoyancy is proportional to $\partial \psi / \partial z$, when warm fluid rises there is a correlation between w and $\partial \psi / \partial z$ and available potential energy is converted to kinetic energy. Whether such a phenomenon occurs depends of course on the dynamics of the flow; however, such a conversion *is* in fact a common feature of geophysical flows, and in particular of baroclinic instability, as we see in chapter 6.

5.6.2 Energetics of two-layer flows

Two-layer or two-level flows are an important special case. For layers of equal thickness let us write the evolution equations as

$$\frac{\mathrm{D}}{\mathrm{D}t}\left(\nabla^2\psi_1 - \frac{1}{2}k_d^2(\psi_1 - \psi_2)\right) + \beta\frac{\partial\psi_1}{\partial x} = 0 \qquad (5.167a)$$

$$\frac{\mathrm{D}}{\mathrm{D}t}\left(\nabla^2\psi_2 + \frac{1}{2}k_d^2(\psi_1 - \psi_2)\right) + \beta\frac{\partial\psi_2}{\partial x} = 0 \qquad (5.167b)$$

where $k_d^2/2 = (2f_0/NH)^2$. On multiplying these two equations by $-\psi_1$ and $-\psi_2$ respectively and integrating over the horizontal domain, the advective term in the material derivatives and the beta term all vanish, and we obtain

$$\frac{\mathrm{d}}{\mathrm{d}t}\int_A\left[\frac{1}{2}(\nabla\psi_1)^2 + \frac{1}{2}k_d^2\psi_1(\psi_1 - \psi_2)\right]\mathrm{d}A = 0, \qquad (5.168a)$$

$$\frac{\mathrm{d}}{\mathrm{d}t}\int_A\left[\frac{1}{2}(\nabla\psi_2)^2 - \frac{1}{2}k_d^2\psi_2(\psi_1 - \psi_2)\right]\mathrm{d}A = 0. \qquad (5.168b)$$

Adding these gives

$$\frac{\mathrm{d}}{\mathrm{d}t}\int_A\left[\frac{1}{2}(\nabla\psi_1)^2 + \frac{1}{2}(\nabla\psi_2)^2 + k_d^2\widehat{\psi}^2\right]\mathrm{d}A = 0. \qquad (5.169)$$

This is the energy conservation statement for the two layer model. The first two terms represent the kinetic energy and the last term the available potential energy.

Energy in the baroclinic and barotropic modes

A useful partitioning of the energy is between the energy in the barotropic and baroclinic modes. The barotropic streamfunction, $\overline{\psi}$ is the vertically averaged streamfunction and the baroclinic mode is the difference between the streamfunctions in the two layers. That is, for equal layer thicknesses,

$$\overline{\psi} \equiv \frac{1}{2}(\psi_1 + \psi_2), \qquad \tau \equiv \frac{1}{2}(\psi_1 - \psi_2) \qquad (5.170)$$

Substituting (5.170) into (5.169) reveals that

$$\frac{\mathrm{d}}{\mathrm{d}t}\int_A\left[(\nabla\overline{\psi})^2 + (\nabla\tau)^2 + k_d^2\tau^2\right]\mathrm{d}\boldsymbol{x} = 0 \qquad (5.171)$$

The energy density in the barotropic mode is thus just $(\nabla\overline{\psi})^2$, and that in the baroclinic mode is $(\nabla\tau)^2 + k_d^2\tau^2$. This partitioning will prove particularly useful when we consider baroclinic turbulence in chapter 9.

5.6.3 Enstrophy conservation

Potential vorticity is advected only by the horizontal flow, and thus it is materially conserved on the horizontal surface at every height and

$$\frac{Dq}{Dt} = \frac{\partial q}{\partial t} + \boldsymbol{u} \cdot \nabla q = 0. \tag{5.172}$$

Furthermore, the advecting flow is divergence-free so that $\boldsymbol{u} \cdot \nabla q = \nabla \cdot (\boldsymbol{u} q)$. Thus, on multiplying (5.172) by q and integrating over a horizontal domain, A, using either no-normal flow or periodic boundary conditions, we straightforwardly obtain

$$\frac{d\widehat{Z}}{dt} = 0, \qquad \widehat{Z} = \frac{1}{2} \int_A q^2 \, dA. \tag{5.173}$$

The quantity $\widehat{Z}$ is known as the enstrophy, and this is conserved at each height as well as, naturally, over the entire volume.

The enstrophy is just one of an infinity of invariants in quasi-geostrophic flow. Because the potential vorticity of a fluid element is conserved, *any* function of the potential vorticity must be a material invariant and we can immediately write

$$\frac{D}{Dt} F(q) = 0. \tag{5.174}$$

To verify that this is true, simply note that (5.174) implies that $(d F/dq)Dq/Dt = 0$, which is true by virtue of (5.172). (However, by virtue of the material advection, the function $F(q)$ need not be differentiable function in order for (5.174) to hold.) Each of the material invariant corresponding to different choices of $F(q)$ has a corresponding integral invariant; that is

$$\frac{d}{dt} \int_A F(q) \, dA = 0. \tag{5.175}$$

The enstrophy invariant corresponds to choosing $F(q) = q^2$; it plays a particularly important role because, like energy, it is a quadratic invariant, and its presence profoundly alters the behaviour of two-dimensional and quasi-geostrophic flow compared to three-dimensional flow (see section 8.3).

5.7 ROSSBY WAVES

Consider now what wave motion is possible in the quasi-geostrophic shallow water system. We will consider a flat-bottomed β-plane system, for which the unforced, inviscid quasi-geostrophic equation of motion is

$$\frac{D}{Dt}(\zeta + f - \psi/L_d^2) = 0, \tag{5.176}$$

where $\zeta = \nabla^2 \psi$ is the vorticity and ψ the streamfunction.

Infinite deformation radius

Consider first the simple case in which the scale of motion is much less than the deformation scale. For flow on the β-plane the equation of motion is then

$$\frac{D}{Dt}(\zeta + \beta y) = 0. \tag{5.177}$$

Expanding the material derivative gives

$$\frac{\partial \zeta}{\partial t} + \boldsymbol{u} \cdot \nabla \zeta + \beta v = 0 \qquad \text{or} \qquad \frac{\partial \zeta}{\partial t} + J(\psi, \zeta) + \beta \frac{\partial \psi}{\partial x} = 0. \tag{5.178}$$

The idea now is to *linearize* this equation — that is, to suppose that the flow consists of a time-independent component (the 'basic state') plus a perturbation, with the perturbation being small compared to the mean flow. Such a mean flow must satisfy the time independent equation of motion, and purely zonal flow will do this, and for simplicity we choose a flow with no meridional dependence. To achieve all this we let

$$\psi = \Psi + \psi'(x, y, t) \tag{5.179}$$

where $\Psi = -Uy$ and $|\psi'| \ll |\Psi|$. (The symbol U now represents the mean zonal flow, not a magnitude for scaling purposes.) Substitute (5.179) into (5.178) and neglect the nonlinear terms involving products of ψ' to give

$$\frac{\partial \zeta'}{\partial t} + J(\Psi, \zeta') + \beta \frac{\partial \psi'}{\partial x} = 0, \tag{5.180}$$

or

$$\frac{\partial}{\partial t} \nabla^2 \psi' + U \frac{\partial \nabla^2 \zeta'}{\partial x} + \beta \frac{\partial \psi'}{\partial x} = 0. \tag{5.181}$$

Solutions to this equation may be found in the form of a plane-wave,

$$\psi' = \text{Re}\, \widetilde{\psi} e^{i(kx + ly - \omega t)}, \tag{5.182}$$

where Re indicates the real part of the function (and this will sometimes be omitted if no ambiguity is so-caused). The amplitude of the oscillation is given by $\widetilde{\psi}$ and the phase by $kx + ly - \omega t$, where k and l are the x- and y-wavenumbers and ω is the frequency of the oscillation.

Substituting (5.182) into (5.181) yields

$$[(-\omega + Uk)(K^2) + \beta k]\widetilde{\psi} = 0, \tag{5.183}$$

where $K^2 = k^2 + l^2$. For nontrivial solutions this implies

$$\boxed{\omega = Uk - \frac{\beta k}{K^2}}. \tag{5.184}$$

This is the *dispersion relation* for Rossby waves. For reference, the phase speed and group velocity in the x-direction are[11]

$$c_p^x \equiv \frac{\omega}{k} = U - \frac{\beta}{K^2}, \qquad c_g^x \equiv \frac{\partial \omega}{\partial k} = U + \frac{\beta(k^2 - l^2)}{(k^2 + l^2)^2}. \tag{5.185a,b}$$

The velocity U provides a uniform translation, and doppler shifts the frequency. Note that current speed required to hold the waves of a particular wavenumber stationary (i.e., $c_p^x = 0$) is $U = \beta/K^2$.

Finite deformation radius

For finite deformation radius the basic state $\Psi = -Uy$ is still a solution of the original equations of motion, but the potential vorticity corresponding to this state is $Q = Uy/L_d^2 + \beta y$ and its gradient is $\nabla Q = (\beta + U/L_d^2)\mathbf{j}$. The linearized equation of motion is thus,

$$\left(\frac{\partial}{\partial t} + U\frac{\partial}{\partial x}\right)(\nabla^2\psi' - \psi'/L_d^2) + (\beta + U/L_d^2)\frac{\partial\psi'}{\partial x} = 0. \qquad (5.186)$$

Substituting $\psi' = \widetilde{\psi}e^{i(kx+ly-\omega t)}$ we obtain the dispersion relation,

$$\boxed{\omega = \frac{k(UK^2 - \beta)}{K^2 + 1/L_d^2} = Uk - k\frac{\beta + U/L_d^2}{K^2 + 1/L_d^2}}. \qquad (5.187)$$

The corresponding phase speed and group velocity in the x-direction are

$$c_p^x = U - \frac{\beta + Uk_d^2}{K^2 + k_d^2} = \frac{UK^2 - \beta}{K^2 + k_d^2}, \qquad c_g^x = U + \frac{(\beta + Uk_d^2)(k^2 - l^2 - k_d^2)}{(k^2 + l^2 + k_d^2)^2},$$
$$(5.188\text{a,b})$$

where $k_d = 1/L_d$. The uniform velocity field now no longer provides just a simple Doppler shift of the frequency. From (5.188a) the waves are stationary when $K^2 = K_s^2 \equiv \beta/U$; that is, the current speed required to hold waves of a particular wavenumber stationary is $U = \beta/K^2$. However, this is *not* simply the magnitude of the phase speed of waves of that wavenumber in the absence of a current — this is given by

$$c_p^x = -\frac{\beta}{K_s^2 + k_d^2} = -\frac{U}{1 + k_d^2/K_s^2}. \qquad (5.189)$$

Why is there a difference? It is because the current does not just provide a uniform translation, but, for finite L_d, also modifies the basic potential vorticity gradient. The basic state height field η_0 is sloping, that is $\eta_0 = -(f_0/g)\Psi y$, and the ambient potential vorticity field increases with y, that is $Q = (\beta + U/L_d^2)y$. Thus, the basic state defines a preferred frame of reference, and the problem is not Galilean invariant.[12]

5.7.1 Rossby waves in two layers

Now consider the dynamics of the two-layer model, linearized about a state of rest. The two (coupled) linear equations describing the motion in each layer are

$$\frac{\partial}{\partial t}\left[\nabla^2\psi_1 + F_1(\psi_2 - \psi_1)\right] + \beta\frac{\partial\psi_1}{\partial x} = 0, \qquad (5.190\text{a})$$

$$\frac{\partial}{\partial t}\left[\nabla^2\psi_2 + F_2(\psi_1 - \psi_2)\right] + \beta\frac{\partial\psi_2}{\partial x} = 0, \qquad (5.190\text{b})$$

where $F_1 = f_0^2/g'H_1$ and $F_2 = f_0^2/g'H_2$. By inspection these may be transformed into two uncoupled equations: one equation is obtained by multiplying the first by F_2

and the second by F_1 and adding, and the other is obtained by subtracting the two. Then, defining

$$\overline{\psi} = \frac{F_1\psi_2 + F_2\psi_1}{F_1 + F_2}, \qquad \tau = \frac{1}{2}(\psi_1 - \psi_2), \qquad (5.191\text{a,b})$$

(think 'τ for temperature'), (5.190) become

$$\frac{\partial}{\partial t}\nabla^2\overline{\psi} + \beta\frac{\partial\overline{\psi}}{\partial x} = 0, \qquad (5.192\text{a})$$

$$\frac{\partial}{\partial t}\left[(\nabla^2 - k_d^2)\tau\right] + \beta\frac{\partial\tau}{\partial x} = 0. \qquad (5.192\text{b})$$

where now we define $k_d = (F_1 + F_2)^{1/2}$. The internal radius of deformation for this problem is the inverse of this, namely

$$L_d = k_d^{-1} = \frac{1}{f_0}\left(\frac{g' H_1 H_2}{H_1 + H_2}\right)^{1/2}. \qquad (5.193)$$

The variables $\overline{\psi}$ and τ are the vertical normal coordinates for the two layer model; they oscillate independently of each other, and the solution in physical space is just their superposition. [For the continuous equations the analogous eigenfunctions are given by solutions of $\partial_z[(f_0^2/N^2)\partial_z\phi] = \lambda^2\phi$, where eigenvalue, λ, is inversely proportional tos the deformation radius.] The equation for $\overline{\psi}$ is identical to that of the single-layer, rigid-lid model, namely (5.181) with $U = 0$, and its dispersion relation is just

$$\omega = -\frac{\beta k}{K^2}. \qquad (5.194)$$

The barotropic mode corresponds to synchronous, depth-independent, motion in the two layers with a flat interface — the interface slope is given by $2f_0\tau/g'$, proportional to the amplitude of the baroclinic mode. The dispersion relation for the baroclinic mode is

$$\omega = -\frac{\beta k}{K^2 + k_d^2}. \qquad (5.195)$$

The mass transport associated with this mode is identically zero, since from (5.191) we have

$$\psi_1 = \overline{\psi} + \frac{2F_1\tau}{F_1 + F_2}, \qquad \psi_2 = \overline{\psi} - \frac{2F_2\tau}{F_1 + F_2}, \qquad (5.196\text{a,b})$$

and this implies

$$H_1\psi_1 + H_2\psi_2 = (H_1 + H_2)\overline{\psi}. \qquad (5.197)$$

The left-hand side is proportional to the total mass transport, which is evidently associated with the barotropic mode.

The deformation radius only affects the baroclinic mode. For scales much smaller than the deformation radius, $k_x^2, k_y^2 \gg k_d^2$, the baroclinic mode obeys the same equation as the barotropic mode so that

$$\frac{\partial}{\partial t}\nabla^2\tau + \beta\frac{\partial\tau}{\partial x} = 0. \qquad (5.198)$$
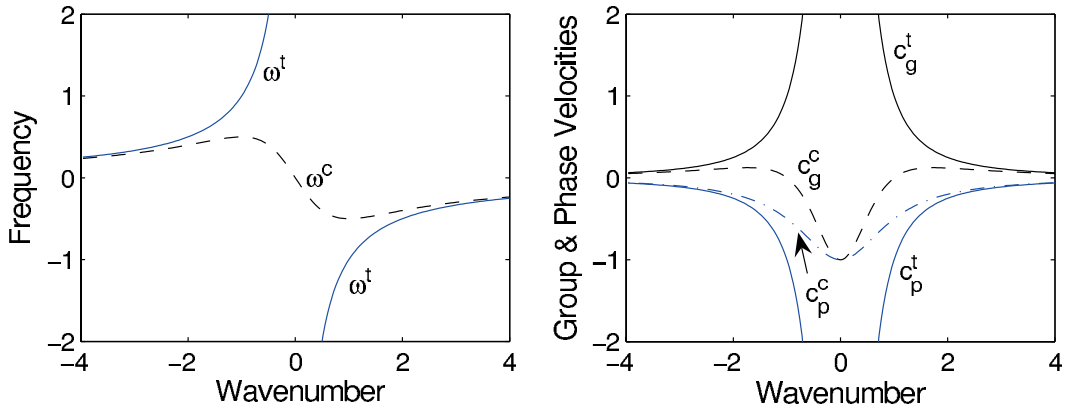
Fig. 5.4 Left: The dispersion relation for barotropic (ω^t, solid line) and baroclinic (ω^c, dashed line) Rossby waves in the two-layer model, calculated using (5.194) and (5.195) with $k_y = 0$, plotted for both positive and negative zonal wavenumbers and, consequently, frequencies. The x-wavenumber is nondimensionalised by k_d, and the frequency is non-dimensionalized by β/k_d. Right: the corresponding zonal group and phase velocities, $c_g = \partial\omega/\partial k_x$ and $c_p = \omega/k_x$, with superscript 't' or 'c' for the barotropic or baroclinic mode. The velocities are non-dimensionalized by β/k_d^2. The phase velocities are always negative, or westward. The group velocity of these barotropic waves is always eastward, but long baroclinic waves have a westward group velocity. For very short waves, $k^2 \gg k_d^2$, the baroclinic and barotropic velocities coincide and their phase and group velocities are equal and opposite.

For a purely baroclinic mode $F_2\psi_1 + F_1\psi_2 = 0$ and using this in (5.198) gives

$$\frac{\partial}{\partial t}\nabla^2\psi_i + \beta\frac{\partial\psi_i}{\partial x} = 0, \qquad i = 1, 2. \qquad (5.199)$$

That is to say, the two layers are uncoupled from each other. At the other extreme, for very long baroclinic waves the relative vorticity is unimportant. The phase speed is negative, westward, for both baroclinic and barotropic Rossby waves but the group velocity may be positive for sufficiently long waves — see Fig. 5.4. In the figure the frequencies, velocities and wavenumbers are all non-dimensional. With a deformation radius of 50 km, typical for the mid-laititude ocean, then a nondimensional frequency of unity corresponds to a dimensional frequency of $5 \times 10^{-7}\,\mathrm{s}^{-1}$ or a period of about 100 days. In an atmosphere with a deformation radius of 1000 km a non-dimensional frequency of unity corresponds to $1 \times 10^{-5}\,\mathrm{s}^{-1}$ or a period of about 7 days. Nondimensional velocities of unity correspond to respective dimensional velocities of about $0.25\,\mathrm{m\,s}^{-1}$ (ocean) and $10\,\mathrm{m\,s}^{-1}$ (atmosphere).

5.8 ROSSBY WAVES IN STRATIFIED QUASI-GEOSTROPHIC FLOW

5.8.1 Preliminaries

Let us now consider the dynamics of linear waves in stratified quasi-geostophic flow, with a resting basic state. Our emphasis will be on the basic dynamics; in chapter **??** we explore the role of Rossby waves in a more realistic setting.

The quasi-geostrophic equations, linearized about a state of rest, are: (i) the potential vorticity equation,

$$\frac{\partial}{\partial t}\left[\nabla^2\psi + \frac{1}{\widetilde{\rho}(z)}\frac{\partial}{\partial z}\left(\widetilde{\rho}(z)F(z)\frac{\partial\psi}{\partial z}\right)\right] + \beta\frac{\partial\psi}{\partial x} = 0, \qquad (5.200)$$

which describes flow in the interior; and (ii) the thermodynamic equation with $w = 0$,

$$\frac{\partial}{\partial t}\left(\frac{\partial\psi}{\partial z}\right) = 0, \qquad (5.201)$$

which describes flow at a flat, rigid surface such as the ground and, with somewhat less justification, at the tropopause where the higher static stability of the stratosphere inhibits vertical motion. An alternative upper boundary condition is to require that perturbations decay to zero as $z \to \infty$. If the ground is not flat or if friction provides a vertical velocity by way of an Ekman layer the boundary condition must be correspondingly modified, but we will stay with the simplest case here and apply (5.201) at $z = 0$ and $z = H$. The variable $\widetilde{\rho}$ is the density profile of the basic state, and $F(z) = f_0^2/N^2$, the square of the inverse Prandtl ratio, N/f_0. In the Boussinesq approximation $\widetilde{\rho} = \rho_0$, a constant.

5.8.2 Wave motion

For simplicity we will consider motion on a horizontally doubly-periodic Cartesian β-plane. We seek solutions of the form

$$\psi = \mathrm{Re}\,\widetilde{\psi}(z)e^{i(kx+ly-\omega t)} \qquad (5.202)$$

where $\widetilde{\psi}(z)$ will determine the vertical structure of the waves. The case of a zonal channel is an easy step from this — assume a horizontal variation proportional of the form $\sin ly$. The case of a sphere is more complicated but introduces no truly new physical phenomena.

Substituting (5.202) into (5.200) gives

$$\omega\left[-K^2\widetilde{\psi}(z) + \frac{1}{\widetilde{\rho}}\frac{\partial}{\partial z}\left(\widetilde{\rho}F(z)\frac{\partial\widetilde{\psi}}{\partial z}\right)\right] - \beta k\widetilde{\psi}(z) = 0. \qquad (5.203)$$

Now, if $\widetilde{\psi}$ satisfies

$$\frac{1}{\widetilde{\rho}}\frac{\partial}{\partial z}\left(\widetilde{\rho}F(z)\frac{\partial\widetilde{\psi}}{\partial z}\right) = -\Gamma\widetilde{\psi} \qquad (5.204)$$

then the equation of motion becomes

$$-\omega \left[K^2 + \Gamma \right] \widetilde{\psi} - \beta k \widetilde{\psi} = 0, \tag{5.205}$$

and the dispersion relation follows, namely

$$\boxed{\omega = -\frac{\beta k}{K^2 + \Gamma}}. \tag{5.206}$$

Equation (5.204), which is to be solved with boundary conditions at the vertical limits of the domain, constitues an eigenvalue problem for the vertical structure. The resulting eigenvalues, Γ are proportional to the inverse of the squares of the deformation radii for the problem and the eigenfunctions are the vertical structure functions.

A simple example

Consider the case in which $F(z)$ and $\widetilde{\rho}$ are constant, and in which the domain is confined between two rigid surfaces at $z = 0$ and $z = H$. Then the eigenvalue problem for the vertical structure is

$$F \frac{\partial^2 \widetilde{\psi}}{\partial z^2} = -\Gamma \widetilde{\psi} \tag{5.207a}$$

with boundary conditions of

$$\frac{\partial \widehat{\psi}}{\partial z} = 0, \qquad \text{at } z = 0, 1. \tag{5.207b}$$

There is a sequence of solutions to this, namely

$$\widetilde{\psi}_n(z) = \cos(n\pi z/H), \qquad n = 1, 2 \dots \tag{5.208}$$

with corresponding eigenvalues

$$\Gamma_n = n^2 \frac{F\pi^2}{H^2} = (n\pi)^2 \left(\frac{f_0}{NH} \right)^2, \qquad n = 1, 2 \dots . \tag{5.209}$$

This last expression may be used to define the deformation radii for this problem, the successive radii being given by

$$\lambda_n \equiv \frac{NH}{n\pi f_0}. \tag{5.210}$$

The first deformation radius is the same as the expression obtained by dimensional analysis NH/f, except for a factor of π. Definitions of the deformation radii both with and without the factor of π are common in the literature, and neither is obviously more correct. In this book we shall, unless noted, use a definition of deformation radius that does not include the factor of π, so that the first deformation radius in a problem with uniform stratification is given by NH/f, equal to $\pi/\sqrt{\Gamma_1}$.

   In addition to these baroclinic modes, it is clear that the case with $n = 0$, that is

with $\widetilde{\psi} = 1$, is also a solution of (5.207) for any $F(z)$. Using (5.206) and (5.209) the dispersion relation becomes

$$\omega = -\frac{\beta k}{K^2 + (n\pi)^2 (f_0/NH)^2}, \qquad n = 0, 1, 2 \dots \qquad (5.211)$$

and, of course, the horizontal wavenumbers k and l are also quantized in a finite domain. The dynamics of the barotropic mode are independent of height and independent of the stratification of the basic state, and so these Rossby waves are *identical* with the Rossby waves in a homogeneous fluid contained between two flat rigid surfaces. The structure of the baroclinic modes, which in general depends on the structure of the stratification, becomes increasingly complex as the vertical wavenumber n increases. This increasing complexity naturally leads to a certain delicacy, making it rare that they can be unambiguosly identified in nature.

5.8.3 More general stratification

In the more general case, for example with profiles of $N(z)$ taken from observations in the atmosphere or ocean, it is not possible to analytically calculate the vertical normal modes, but they may be calculated numerically. The results of one such calculation are given in Fig. 5.5. The case with uniform stratification reproduces cosine modes, whereas in the more realistic case the modes tend to have highest amplitude in the upper ocean, where the stratification is strongest — a result is typical of oceanic profiles.[13]

The eigenproblem for a realistic atmospheric profile is more complex because of the lack of a rigid lid at the top of the atmosphere.[14] Nevertheless, the problem again succumbs to a numerical approach.

Notes

1 The phrase 'quasi-geostrophic' seems to have been introduced by Durst and Sutcliffe (1938) and the ideas used in Sutcliffe's development theory of baroclinic systems (Sutcliffe 1939, 1947). The first systematic derivation of the quasi-geostrophic equations based on scaling theory was given by Charney (1948). The planetary geostrophic equations were used by Robinson and Stommel (1959) and Welander (1959) in studies of the thermocline (and were first known as the 'thermocline equations'), and were put in the context of other approximate equation sets by Phillips (1963).

2   Carl-Gustav Rossby (1898-1957) played a dominant role in the development of dynamical meteorology in the early and middle parts of the 20th century, and his work permeates all aspects of dynamical meteorology today. Perhaps the most fundamental non-dimensional number in rotating fluid dynamics, the Rossby number, is named for him, as is the perhaps the most fundamental wave, the Rossby wave. He also discovered the conservation of potential vorticity (later generalised by Ertel) and contributed important ideas to atmospheric turbulence and the theory of air masses. Swedish born, he studied first with V. Bjerknes before taking
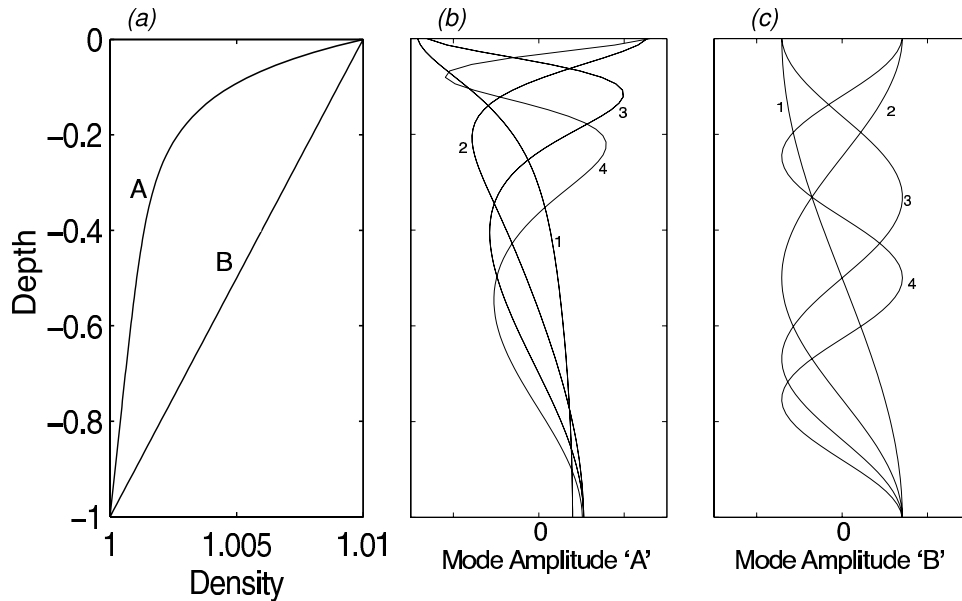
Fig. 5.5 (a): two density profiles $[1 + (\rho_0 - \rho)/\rho_0]$, a fairly realistic oceanic case with enhanced stratification in the upper ocean (profile A), and uniform stratification (profile B). (b) and (c): the corresponding four baroclinic modes [eigenfunctions of $(\partial/\partial z)[N^2(z)\partial\phi/\partial z] = \lambda^2\phi$ using N^2 calculated from the profiles and with boundary conditions of $\partial\phi/\partial z = 0$ at top and bottom]. With profile B the eigenmodes are cosines, whereas in the whereas in profile A they have largest amplitude in the upper ocean. The number of zero crossings is equal to the mode number.

a position in Stockholm in 1922 with the Swedish Meteorological Hydrologic Service and receiving a 'Licentiat' from the University of Stockholm in 1925. Shortly thereafter he moved to the United States, joining the Government Weather Bureau, a precursor of NOAA's National Weather Service. In 1928 he moved to MIT, playing an important role in developing the meteorology department there, while still maintaining connections with the Weather Bureau. In 1940 he moved to the University of Chicago, where he similarly helped develop meteorology there. In 1947 he became director of the newly-formed Institute of Meteorology in Stockholm, and subsequently divided his time between there and the United States. Thus, as well as his scientific contributions, he played a very influential role in the institutional development of the field.

3 Burger (1958)

4 This is the so-called 'frontal geostrophic' regime (Cushman-Roisin 1994).

5 Numerical integrations of the potential vorticity equation using (5.92), and performing the inversion without linearizing potential vorticity, do in fact indicate improved accuracy over either the quasi-geostrophic or planetary geostrophic equations (Mundt et al. 1997). In a similar vein, McIntyre and Norton (2000) show how useful potential vorticity inversion can be, and Allen et al. (1990a,b) demonstrate

the high accuracy of certain intermediate models. Certainly, asymptotic correctness should not be the only criterion used in constructing a filtered model, because the parameter range in which the model is useful may be too limited. (Note the difference between extending the parameter range in which a filtered model is useful, and going to higher asymptotic order accuracy in a given parameter regime, as in Allen (1993) and Warn et al. (1995).) Using Hamiltonian mechanics it is possible to derive equations that span different asymptotic regimes, and that also have good conservation properties (Salmon 1983, Allen et al. 2002).

6 I thank T. Warn for a conversation on this matter.

7 There is a difference between the *dynamical* demands of the quasi-geostrophic system in requiring β to be small, and the *geometric* demands of the Cartesian geometry. On earth the two demands are similar in practice. But without dynamical inconsistency we may imagine a Cartesian system in which $\beta y \sim f$, and indeed this is common in idealized, planetary geostrophic, models of the large-scale ocean circulation.

8 Atmospheric and oceanic sciences are sometimes thought of as not being 'beautiful' in the same way as are some branches of theoretical physics. Yet surely quasi-geostrophic theory, and the quasi-geostrophic potential vorticity equation, are quite beautiful, both for their austerity of description and richness of behaviour.

9 Bretherton (1966). Schneider et al. (2003) look at the non QG extension. The equivalence between boundary conditions and delta-function sources is a common feature of elliptic problems, and is analogous to the generation of electromagnetic fields by point charges. It is sometimes exploited in the numerical solution of elliptic equations, both as a simple way to include non-homogeneous boundary conditions and, using the so-called capacitance matrix method, to solve problems in irregular domains (e.g., Hockney 1970, Pares-Sierra and Vallis 1989).

10 Charney and Stern (1962). See also Vallis (1996).

11 We won't make use of group velocity until chapter 12. Treatments of group velocity are given by, in order of increasing generality, Pedlosky (1987), Lighthill (1978) and Whitham (1974), among others.

12 This non-Doppler effect also arises quite generally, even in models in height coordinates. See White (1977) and problem 5.9.

13 For example Kundu et al. (1975).

14 Chapman and Lindzen (1970) have argued that for a realistic atmospheric stratification profiles no baroclinic modes of a resting atmosphere exist. For our purposes, the importance of such a Rossby wave analysis is not that any particular form of waves do or do not exist, but that it provides a foundation for more complete analyses with non-resting basic states, leading into the theory of baroclinic instability discussed in chapter 6, as well as an understanding of the propagation of Rossby waves.

Further Reading

Majda, A. 2003. *Introduction to PDEs and waves for the atmosphere and ocean.*

Provides a compact, mathematical introduction to various equation sets and their properties, including quasi-geostrophy.

Problems

5.1 In the derivation of the quasi-geostrophic equations, geostrophic balance leads to the lowest order velocity being divergence-free — that is, $\nabla_z \cdot \boldsymbol{u}_0 = 0$. It seems that this can also be obtained from the mass conservation equation at lowest order. Is this a coincidence? Suppose that the Coriolis parameter varied, and that the momentum equation yielded $\nabla_2 \cdot \boldsymbol{u}_0 \neq 0$. Would there be an inconsistency?

5.2 ♦ In the planetary geostrophic approximation, obtain an evolution equation and corresponding inversion conditions that conserves potential vorticity and that is accurate to one higher order in Rossby number than the usual shallow water planetary geostrophic equations.

5.3 Consider the flat-bottomed shallow water potential vorticity equation in the form

$$\frac{\mathrm{D}}{\mathrm{D}t} \frac{\zeta + f}{h} = 0 \qquad (\text{P5.1})$$

(a) Suppose that deviations of the height field are small compared to the mean height field, and that the Rossby number is small (so $|\zeta| \ll f$). Further consider flow on a β-plane such that $f = f_0 + \beta y$ where $|\beta y| \ll f_0$. Show that the evolution equation becomes

$$\frac{\mathrm{D}}{\mathrm{D}t} \left(\zeta + \beta y - \frac{f_0 \eta}{H} \right) = 0 \qquad (\text{P5.2})$$

where $h = H + \eta$ and $|\eta| \ll H$. Using geostrophic balance in the form $f_0 u = -g \partial \eta / \partial y$, $f_0 v = g \partial \eta / \partial x$, obtain an expression for ζ in terms of η.

(b) Linearize (P5.2) about a state of rest, and show that the resulting system supports two-dimensional Rossby waves that are similar to those of the usual two-dimensional barotropic system. Discuss the limits in which the wavelength is much shorter or much longer than the deformation radius.

(c) Linearize (P5.2) about a *geostrophically balanced state* that is translating uniformly eastwards. Note that this means that:

$$u = U + u' \qquad \eta = \eta(y) + \eta' \qquad (\text{P5.3})$$

where $\eta(y)$ is in geostrophic balance with U. Obtain an expression for the form of $\eta(y)$.

(d) Obtain the dispersion relation for Rossby waves in this system. Show that their speed is different from that obtained by adding a constant U to the speed of Rossby waves in part (b), and discuss why this should be so. (That is, why is the problem not *Galilean invariant?*)

5.4 Obtain solutions to the two-layer Rossby wave problem by seeking solutions of the form

$$\psi_1 = \mathrm{Re}\, \widetilde{\psi}_1 e^{i(k_x x + k_y y - \omega t)},$$
$$\psi_1 = \mathrm{Re}\, \widetilde{\psi}_2 e^{i(k_x x + k_y y - \omega t)}. \qquad (\text{P5.4})$$

Substitute (P5.4) directly into (5.190) to obtain the dispersion relation, and show that the ensuing two roots correspond to the baroclinic and barotropic modes. Show that the baroclinic mode has no net (vertically integrated) transport associated with it, and that the motion of the barotropic is independent of depth.

5.5 ♦ (Not difficult, but messy.) Obtain the vertical normal modes and the dispersion relationship of the two-layer quasi-geostrophic problem with a free surface, for which the equations of motion linearized about a state of rest are

$$\frac{\partial}{\partial t}\left[\nabla^2\psi_1 + F_1(\psi_2 - \psi_1)\right] + \beta\frac{\partial\psi_1}{\partial x} = 0 \qquad \text{(P5.5a)}$$

$$\frac{\partial}{\partial t}\left[\nabla^2\psi_2 + F_2(\psi_1 - \psi_2) - F_{\text{ext}}\psi_1\right] + \beta\frac{\partial\psi_2}{\partial x} = 0. \qquad \text{(P5.5b)}$$

where $F_{\text{ext}} = f_0/(gH_2)$.

5.6 Given the baroclinic dispersion relation

$$\omega = -\frac{\beta k_x}{k_x^2 + k_d^2}, \qquad \text{(P5.6)}$$

for what value of k_x is the x-component of group velocity the largest (i.e., the most positive), and what is the corresponding value of the group velocity?

5.7 Beginning with the vorticity and thermodynamic equations for a two layer model, obtain an expression for the conversion between available potential energy and kinetic energy in the two-layer model. Show that these expressions are consistent with the conservation of total energy as expressed by (5.169). Show also that the expression might be considered to be a simple finite-difference approximation to (5.166).

5.8 ♦ The vertical normal modes are the eigenfunctions of

$$\frac{1}{\widetilde{\rho}}\frac{\partial}{\partial z}\left(\frac{\widetilde{\rho}}{N^2}\frac{\partial\Psi}{\partial z}\right) = -\Gamma\Psi \qquad \text{(P5.7)}$$

along with boundary conditions on $\Psi(z)$. Numerically obtain the vertical normal modes for some or all of the following profiles, or others of your choice.

(a) $\widetilde{\rho} = 1$, $N^2(z) = 1$, $\Psi_z = 0$ at $z = 0, 1$. (This is profile 'b' of Fig. 5.5. An analytic solution is possible.)

(b) $\widetilde{\rho} = 1$ and an $N^2(z)$ profile corresponding to a density profile similar to profile 'a' of Fig. 5.5 (e.g., an exponential), and $\Psi_z = 0$ at $z = 0, 1$.

(c) An isothermal atmosphere, with $\Psi_z = 0$ at $z = 0, 1$. (Similar to (i), except that $\widetilde{\rho}$ varies with height.)

(d) An isothermal atmosphere, now assuming that $\psi \to 0$ as $z \to \infty$.

(e) An fluid with $N^2 = 1$ for $0 < z < 0.5$ and $N^2 = 4$ for $0.5 < z < 1$, with continuous b, and with $\Psi_z = 0$ at $z = 0, 1$.

In the atmospheric cases it is easiest to do the problem first with $\widetilde{\rho} = 1$ (the Boussinesq case) and then extend the problem (and the code) to the compressible case. Then remove the upper boundary to larger and larger values of z.

5.9 ♦ The non-Doppler effect arises relatively straightforwardly in the layered formulation of the quasi-geostrophic equations. Show that it also arises when the problem is formulated using geometric height as the vertical coordinates, using the modified quasi-geostrophic set of White (1977). In particular, obtain the dispersion relation for stratified quasi-geostrophic flow with a resting basic state. Then obtain the dispersion relation for the equations linearized about a uniformly translating state, paying attention to the lower boundary condition, and note the conditions under which the waves are stationary. Discuss.

5.10 Using log-pressure as a vertical coordinate, show that the linearized lower boundary condition equivalent to (**??**) is

$$\frac{\partial}{\partial t}\left(\frac{\partial \psi'}{\partial Z} - \frac{N^2}{g}\psi'\right) + \overline{u}\frac{\partial}{\partial x}\frac{\partial \psi'}{\partial Z} - v'\frac{\partial \overline{u}}{\partial Z} = -\frac{N^2}{f_0}\left(\overline{u}\frac{\partial h_b}{\partial x} + \alpha\nabla^2\psi'\right). \quad \text{(P5.8)}$$

In particular, show how first term on left-hand side arises.

Optional (◆): Show that essentially the same lower boundary condition arises using the geometric-height as a vertical coordinate in the modified quasi-geostrophic system of White (1977).

5.11 Derive the quasi-geostrophic potential vorticity equation in isopycnal coordinates for a Boussinesq fluid. Show that the isopycnal expression for potential vorticity is approximately equal to the corresponding expression in height coordinates, carefully stating any assumptions that may be necessary to show this.

5.12 *(a)* Obtain the dispersion relationship for free Rossby waves for the single-layer quasi-geostrophic potential vorticity equation with linear drag [i.e., for (13.10) with $\widehat{h} = 0$].

(b) Obtain the dispersion relation for free Rossby waves in the linearized two-layer potential vorticity equation with linear drag in the lowest layer.

(c) ◆ Obtain the dispersion relation for free waves in the continuously stratified quasi-geostrophic equations, with the effects of linear drag appearing in the thermodynamic equation for the lower boundary condition. That is, the boundary condition at $z = 0$ is $\partial_t(\partial_z\psi) + N^2 w = 0$ where $w = \alpha\zeta$ where α is a constant. You may make the Boussinesq approximation and assume N^2 is constant if you like.

Part II

INSTABILITIES AND TURBULENCE

Ceci n'est pas une pipe.
René Magritte (1898–1967), title of painting.

Barotropic and Baroclinic Instability

WHAT HYDRODYNAMIC STATES ACTUALLY OCCUR IN NATURE? Any flow must clearly be a solution of the equations of motion, and there are, in fact, many steady solutions to the equations of motion — a purely zonal flow, for example. However, steady solutions do not abound in nature because, in order to persist, they must be stable to those small perturbations that inevitably arise. Indeed, all the steady solutions that are known for the large-scale flow in the earth's atmosphere and ocean have been found to be unstable.

There are a myriad forms of hydrodynamic instability, but our focus in this chapter is on barotropic and baroclinic instability. The latter is at the heart of the large- and mesoscale motion in the atmosphere and ocean — it gives rise to atmospheric weather systems, for example. Barotropic instability is important to us for two reasons. First, it is important in its own right as an instability mechanisms for jets and vortices, and is a driving mechanism in both two- and three-dimensional turbulence. Second, many problems in barotropic and baroclinic instability are formally and dynamically similar, so that the solutions and insight we obtain in the often simpler problems in barotropic instability are often useful in the baroclinic problem.

6.1 KELVIN-HELMHOLTZ INSTABILITY

To introduce the issue, we will first consider, rather informally, perhaps the simplest physically interesting instance of a fluid-dynamical instability — that of a constant-density flow with a shear perpendicular to the fluid's mean velocity, this being an example of a *Kelvin-Helmholtz instability.*[1] Let us consider two fluid masses of equal density, with a common surface at $y = 0$, moving with velocities $-U$ and $+U$ in the x-direction respectively (Fig. 6.1). There is no variation in the basic flow in the z-direction (into the page), and we will assume this is also true for the instability (these restrictions are

Figure 6.1 A simple basic state giving rise to shear-flow instability. The velocity profile is discontinuous, the density uniform.
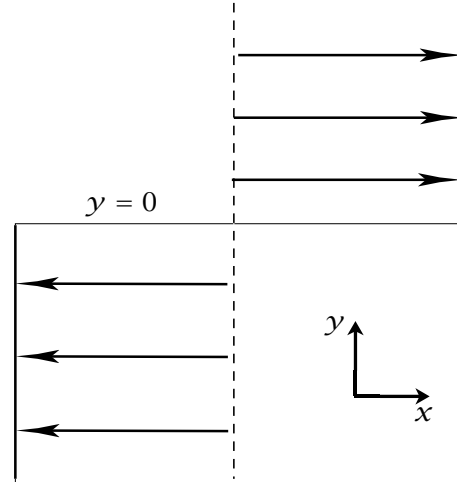
not essential). This flow is clearly a solution of the the Euler equations. What happens if the flow is perturbed slightly? If the perturbation is initially small then even if it grows we can, for small times after the onset of instability, neglect the nonlinear interactions in the governing equations because these are the squares of small quantities. The equations determining the evolution of the initial perturbation are then the Euler equations linearized about the steady solution. Thus, denoting perturbation quantities with a prime and basic state variables with capital letters, for $y > 0$ the perturbation satisfies

$$\frac{\partial \boldsymbol{u}'}{\partial t} + U \frac{\partial \boldsymbol{u}'}{\partial x} = -\nabla p', \qquad \nabla \cdot \boldsymbol{u}' = 0 \tag{6.1a,b}$$

and a similar equation hold for $y < 0$, but with U replaced by $-U$. Given periodic boundary conditions in the x-direction, we can represent the perturbations by a Fourier expansion of the form

$$\phi'(x, y, t) = \text{Re} \sum_k \widetilde{\phi}_k(y, t) \exp(ikx), \tag{6.2}$$

where ϕ is any field variable (e.g., pressure or velocity), and Re denotes that only the real part should be taken. (Typically we use tildes over variables to denote Fourier-like modes, and we will often omit the marker 'Re'.) Because (6.1a) is linear, the Fourier modes do not interact and we may confine attention to just one. Taking the divergence of (6.1a), the left-hand side vanishes and the pressure satisfies Laplace's equation

$$\nabla^2 p' = 0 \tag{6.3}$$

For $y > 0$, this has solutions in the form

$$p' = \text{Re} \, \widetilde{p}_1 e^{ikx - ky} e^{\sigma t}. \tag{6.4}$$

where we assume that the time dependence has the form $e^{\sigma t}$. In general the growth-rate σ is complex: if it has a positive real component, the amplitude of the perturbation

will grow and there is an instability; if σ has a non-zero imaginary component, then there will be oscillatory motion, and there may of course be both oscillatory motion *and* an instability. To obtain the dispersion relationship, we consider the y-component of (6.1a), namely (for $y > 0$)

$$\frac{\partial v_1'}{\partial t} + U\frac{\partial v_1'}{\partial x} = -\frac{\partial p_1'}{\partial y} \tag{6.5}$$

Substituting a solution of the form $v_1' = \tilde{v}_1 \exp(ikx + \sigma t)$ yields, with (6.4),

$$(\sigma + ikU)\tilde{v}_1 = k\tilde{p}_1 \tag{6.6}$$

But the velocity normal to the discontinuity is, at the discontinuity, nothing but the rate of change of the discontinuity itself. That is, at the interface $y = +0$

$$v_1 = \frac{\partial \eta}{\partial t} + U\frac{\partial \eta}{\partial x}, \tag{6.7}$$

or

$$\tilde{v}_1 = (\sigma + ikU)\tilde{\eta}. \tag{6.8}$$

where η is the displacement of the interface from its equilibrium state. Using this in (6.6) gives

$$(\sigma + ikU)^2\tilde{\eta} = k\tilde{p}_1. \tag{6.9}$$

The above few equations pertain to motion on the $y > 0$ side of the interface. Similar reasoning on the other side gives (at $y = -0$)

$$(\sigma - ikU)^2\tilde{\eta} = -k\tilde{p}_2. \tag{6.10}$$

But at the interface $p_1 = p_2$ (because pressure must be continuous). The dispersion relationship then emerges from (6.9) and (6.10), giving

$$\sigma^2 = k^2U^2. \tag{6.11}$$

This equation has two roots, one of which is positive. Thus, the amplitude of the perturbation grows exponentially, like $e^{\sigma t}$, and the flow is *unstable*. The instability itself can be seen in the natural world when billow clouds appear wrapped up into spirals: the clouds are acting as tracers of fluid flow, indicating a shear in the atmosphere.

6.2 INSTABILITY OF PARALLEL SHEAR FLOW

We now consider a little more systematically the instability of *parallel shear flows,* such as are illustrated in Fig. 6.2.[2] This is a classic problem in hydrodynamic stability theory, and there are two particular reasons for our own interest:

(i) The instability is an example of *barotropic instability,* which abounds in the ocean and atmosphere. Loosely, barotropic instability arises when a flow is unstable by virtue of its *shear,* with gravitational and buoyancy effects being secondary.

(ii) The instability is in many ways analogous to *baroclinic instability,* which is the main instability giving rise to weather systems in the atmosphere and similar phenomena in the ocean.

We will define these instabilities more precisely later on. For now, we will restrict attention to two dimensional, incompressible flow. This illustrates the physical mechanisms in the most transparent way, in part because it allows for the introduction of a streamfunction and the automatic satisfaction of the mass conservation equation. In fact, for parallel two-dimensional shear flows the most unstable disturbances are two-dimensional ones.[3]

The vorticity equation for incompressible two-dimensional flow is just

$$\frac{D\zeta}{Dt} = 0. \tag{6.12}$$

We suppose the basic state to be a parallel flow in the x-direction that may vary in y-direction. That is

$$\overline{u} = U(y)\mathbf{i}. \tag{6.13}$$

The linearized vorticity equation is then

$$\frac{\partial \zeta'}{\partial t} + U\frac{\partial \zeta'}{\partial x} + v'\frac{\partial \mathcal{Z}}{\partial y} = 0 \tag{6.14}$$

where $\mathcal{Z} = -U_y$. Because the mass conservation equation has the simple form

$$\frac{\partial u'}{\partial x} + \frac{\partial v'}{\partial y} = 0, \tag{6.15}$$

we may introduce a streamfunction ψ such that $u' = -\partial\psi'/\partial y$, $v' = \partial\psi'/\partial x$ and $\zeta' = \nabla^2\psi'$. The linear vorticity equation is then

$$\frac{\partial \nabla^2\psi'}{\partial t} + U\frac{\partial \nabla^2\psi'}{\partial x} + \frac{\partial \mathcal{Z}}{\partial y}\frac{\partial \psi'}{\partial x} = 0. \tag{6.16}$$

The coefficients of the x-derivatives are not themselves functions of x. Thus we may seek solutions that are harmonic functions (sines and cosines) in the x-direction, but the y-dependence must remain arbitrary at this point. Thus, anticipating our interest in wavelike or exponentially growing solutions, we seek solutions of the form,

$$\psi' = \text{Re}\,\widetilde{\psi}(y)e^{ik(x-ct)}. \tag{6.17}$$

We envision that the solution will be a superposition of all wavenumbers, but since the problem is linear the waves do not interact and it suffices to consider them separately. The variable c determines the stability, or otherwise, of the solution. If c is purely real then c is the phase speed of the wave; if c has a positive imaginary component then the wave will grow exponentially, and any disturbance that has a projection onto wavenumber k is thus *unstable*.
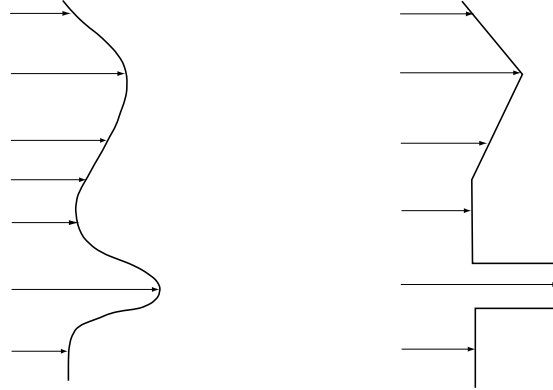
Fig. 6.2 Left: example of smooth velocity profile — both the velocity and vorticity are continuous. Right: example piecewise continuous profile — the velocity and vorticity may have finite discontinuities. In general, it is impossible to analytically solve the linear eigenvalue problem (6.19) that determines stability for a continuous profile. However, solving the problem for a piecewise linear profile is often possible, for then the solution of the eigenvalue problem is effected by solving a finite number of jump conditions at the discontinuities.

From (6.17) we have

$$u' = \widetilde{u}(y)e^{ik(x-ct)} = -\widetilde{\psi}_y e^{ik(x-ct)},$$ (6.18a)

$$v' = \widetilde{v}(y)e^{ik(x-ct)} = ik\widetilde{\psi}e^{ik(x-ct)},$$ (6.18b)

$$\zeta' = \widetilde{\zeta}(y)e^{ik(x-ct)} = (-k^2\widetilde{\psi} + \widetilde{\psi}_{yy})e^{ik(x-ct)},$$ (6.18c)

where the y subscript denotes a derivative. Using (6.18) and (6.17) in (6.14) gives

$$\boxed{(U - c)(\widetilde{\psi}_{yy} - k^2\widetilde{\psi}) - U_{yy}\widetilde{\psi} = 0},$$ (6.19)

sometimes known as *Rayleigh's equation*. It is the linear vorticity equation for disturbances to parallel shear flow, and in the presence of a β-effect it generalizes slightly to

$$\boxed{(U - c)(\widetilde{\psi}_{yy} - k^2\widetilde{\psi}) + (\beta - U_{yy})\widetilde{\psi} = 0}.$$ (6.20)

6.2.1 Piecewise linear flows

Although Rayleigh's equation is linear and has a simple form, it is nevertheless quite difficult to analytically solve for an arbitrary smoothly varying profile. It is simpler to consider *piecewise linear* flows, in which U_y is a constant over some interval, with U or U_y changing abruptly to another value at a line of discontinuity, as illustrated in Fig. 6.2. The curvature is accounted for through the satisfaction of matching conditions, analogous to boundary conditions, at the lines of discontinuity, and solutions in each interval are then exponential functions.

Matching conditions

The idea, then, is to solve the linearized vorticity equation separately in the continuous intervals in which vorticity is constant, matching the solution with that in the adjacent regions. The matching conditions arise from two physical conditions:

 (i) That normal stress should be continuous across the interface. For an inviscid fluid this implies that pressure be continuous.

(ii) That the normal velocity of the fluid on either side of the interface should be consistent with the motion of the interface itself.

Let us consider the implications of these two conditions.

 (i) Continuity of pressure:

   The linearized momentum equation in the direction along the interface is:

$$\frac{\partial u'}{\partial t} + U \frac{\partial u'}{\partial x} + v' \frac{\partial U}{\partial y} = -\frac{\partial p'}{\partial x}. \tag{6.21}$$

   For normal modes, $u' = -\widetilde{\psi}_y e^{ik(x-ct)}$ and $v' = ik\widetilde{\psi} e^{ik(x-ct)}$ and (6.21) becomes

$$ik(U-c)\widetilde{\psi}_y - ik\widetilde{\psi}U_y = -ik\widehat{p}. \tag{6.22}$$

   Because pressure is continuous across the interface we have the first *matching* or *jump condition,*

$$\boxed{\Delta[(U-c)\widetilde{\psi}_y - \widetilde{\psi}U_y] = 0} \tag{6.23}$$

   where the operator Δ denotes the difference in the values of the argument (in square brackets) across the interface. That is, the quantity $(U-c)\widetilde{\psi}_y - \widetilde{\psi}U_y$ is continuous.

   We can obtain this condition directly from Rayleigh's equation, (6.20), written in the form

$$[(U-c)\widetilde{\psi}_y - U_y\widetilde{\psi}]_y + [\beta - k^2(U-c)]\widetilde{\psi} = 0. \tag{6.24}$$

   Integrating across the interface gives (6.23).

(ii) Material interface condition:

   At the interface, the normal velocity v is given by the kinematic condition

$$v = \frac{D\eta}{Dt} \tag{6.25}$$

   where η is the interface displacement. The linear version of (6.25) is

$$\frac{\partial \eta}{\partial t} + U \frac{\partial \eta}{\partial x} = \frac{\partial \psi'}{\partial x}. \tag{6.26}$$

   If the fluid itself is continuous (no cavitation, for instance) then this equation must

hold at either side of the interface, giving two equations and their normal mode counterparts, namely,

$$\frac{\partial \eta}{\partial t} + U_1 \frac{\partial \eta}{\partial x} = \frac{\partial \psi_1'}{\partial x} \qquad \longrightarrow \qquad (U_1 - c)\eta = \tilde{\psi}_1, \qquad (6.27)$$

$$\frac{\partial \eta}{\partial t} + U_2 \frac{\partial \eta}{\partial x} = \frac{\partial \psi_2'}{\partial x} \qquad \longrightarrow \qquad (U_2 - c)\eta = \tilde{\psi}_2. \qquad (6.28)$$

Material continuity at the interface thus gives the second jump condition

$$\boxed{\Delta \left[\frac{\tilde{\psi}}{U - c} \right] = 0} \qquad (6.29)$$

That is, $\tilde{\psi}/(U - c)$ is continuous at the interface. Note that if U is continuous across the interface the condition becomes one of continuity of the normal velocity.

6.2.2 Kevin-Helmholtz instability, revisited

We now use Rayleigh's equation and the jump conditions to consider the situation illustrated in Fig. 6.1; that is, vorticity is everywhere zero except in a thin sheet at $y = 0$. On either side of the interface, Rayleigh's equation is simply

$$(U - c)(\partial_{yy}\tilde{\psi}_i - K^2\tilde{\psi}_i) = 0 \qquad i = 1, 2 \qquad (6.30)$$

or, assuming that $U \neq c$, $\tilde{\psi}_{yy} - K^2\tilde{\psi} = 0$. (This is just Laplace's equation, coming from $\nabla^2 \psi' = \zeta'$, with $\zeta' = 0$ everywhere except at the interface.) Solutions of this that decay away on either side of the interface are

$$y > 0 : \qquad \tilde{\psi}_1 = \Psi_1 e^{-ky}, \qquad (6.31a)$$

$$y < 0 : \qquad \tilde{\psi}_2 = \Psi_2 e^{ky}, \qquad (6.31b)$$

where Ψ_1 and Ψ_2 are constants. The boundary condition (6.23) gives

$$(U_1 - c)(-k)\Psi_1 = (U_2 - c)(k)\Psi_2, \qquad (6.32)$$

and (6.29) gives

$$\frac{\Psi_1}{(U_1 - c)} = \frac{\Psi_2}{(U_2 - c)}. \qquad (6.33)$$

The last two equations combine to give $(U_1 - c)^2 = -(U_2 - c)^2$, which, supposing that $U = U_1 = -U_2$ gives $c^2 = -U^2$. Thus, since U is purely real, $c = \pm iU$, and the disturbance grows exponentially as $\exp(kU_1 t)$, just as we obtained in section 6.1. All wavelengths are unstable, and indeed the shorter the wavelength the greater the instability. In reality, viscosity will damp the smallest waves, but at the same time the presence of viscosity would mean that initial profile is also not an exact, steady solution of the equations of motion.

Figure 6.3 Velocity profile of a stable jet. Although the vorticity is discontinuous, a small perturbation gives rise only to *edge waves* centered at $y = 0$.
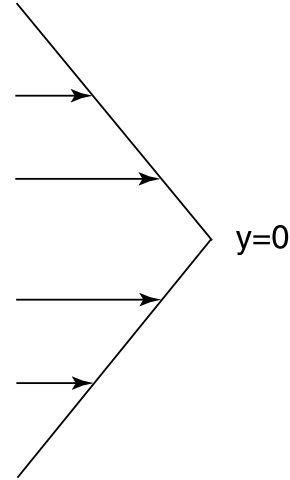
6.2.3 Edge Waves

We now consider a case sketched in Fig. 6.3 in which the velocity is continuous, but the vorticity is discontinuous. Since on either side of the interface $U_{yy} = 0$, Rayleigh's equation is just

$$(U - c)(\widetilde{\psi}_{yy} - K^2 \widetilde{\psi}) = 0. \tag{6.34}$$

Provided $c \neq U$ this has solutions,

$$\widetilde{\psi} = \begin{cases} \Phi_1 e^{-ky} & y > 0 \\ \Phi_2 e^{ky} & y < 0. \end{cases} \tag{6.35}$$

The value of c is found by applying the jump conditions (6.23) and (6.29) at $y = 0$. Using (6.35) these give

$$-k(U_0 - c)\Phi_1 - \Phi_1 U_{1y} = k(U_0 - c)\Phi_2 - \Phi_2 U_{2y} \tag{6.36a}$$

$$\Phi_1 = \Phi_2 \tag{6.36b}$$

where U_1 and U_2 are the values of U at either side of the interface, and both are equal to U_0 at the interface. After a line of algebra these equations give

$$c = U_0 + \frac{\partial_y U_1 - \partial_y U_2}{2k}. \tag{6.37}$$

This is the dispersion relationship for *edge waves* that propagate along the interface a speed equal to the sum of the fluid speed and a factor proportional to the difference in the vorticity between the two layers. No matter what the shear is on either side of the interface, the phase speed is purely real and there is no instability. Eq. (6.37) is imperfectly analogous to the Rossby wave dispersion relation $c = U_0 - \beta/K^2$, and reflects a similarity in the physics — β is a planetary vorticity gradient, which in (6.37) is collapsed to a front and represented by the difference $U_{1y} - U_{2y} = -(\mathcal{Z}_1 - \mathcal{Z}_2)$, where $\mathcal{Z}_1$ and $\mathcal{Z}_2$ are the basic-state vorticities on either side of the interface.
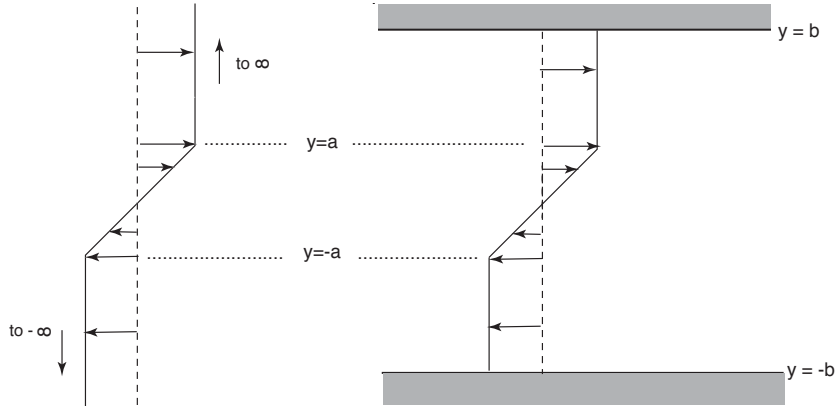
Fig. 6.4 Barotropically unstable velocity profiles. In the simplest case, on the left, a region of shear is sandwiched between two infinite regions of constant velocity. The edge waves at $y = \pm a$ interact to produce an instability. If $a = 0$, then the situation corresponds to that of Fig. 6.1, giving Kelvin-Helmholtz instability. In the case on the right, the flow is bounded at $y = \pm b$. It may be shown that the flow is still unstable, provided that b is sufficiently larger than a. If $b = a$ (plane Couette flow) the flow is stable to infinitesimal disturbances.

6.2.4 Interacting edge waves producing instability

Now we consider a slightly more complicated case in which edge waves may interact giving rise, as we shall see, to an instability. The physical situation is illustrated in Fig. 6.4. We consider the simplest case, that of a shear layer (which we denote region 2) sandwiched between two semi-infinite layers, regions 1 and 3, as in the left panel of the figure. Thus, the basic state is:

$$y > a: \qquad U = U_1 = U_0 \ \text{(a constant)}, \tag{6.38a}$$

$$-a < y < a: \qquad U = U_2 = \frac{U_0}{a}y, \tag{6.38b}$$

$$y < -a: \qquad U = U_3 = -U_0. \tag{6.38c}$$

We assume a solution of Rayleigh's equation of the form:

$$y > a: \qquad \widetilde{\psi}_1 = Ae^{-k(y-a)}, \tag{6.39a}$$

$$-a < y < a: \qquad \widetilde{\psi}_2 = Be^{-k(y-a)} + Ce^{k(y+a)}, \tag{6.39b}$$

$$y < -a: \qquad \widetilde{\psi}_3 = De^{k(y+a)}. \tag{6.39c}$$

Applying the jump conditions (6.23) and (6.29) at the interfaces at $y = a$ and $y = -a$ gives the following relations between the coefficients:

$$A[(U - c)k] = B\left[(U - c)k + \frac{U}{a}\right] + Ce^{2ka}\left[\frac{U}{a} - (U - c)k\right], \tag{6.40a}$$
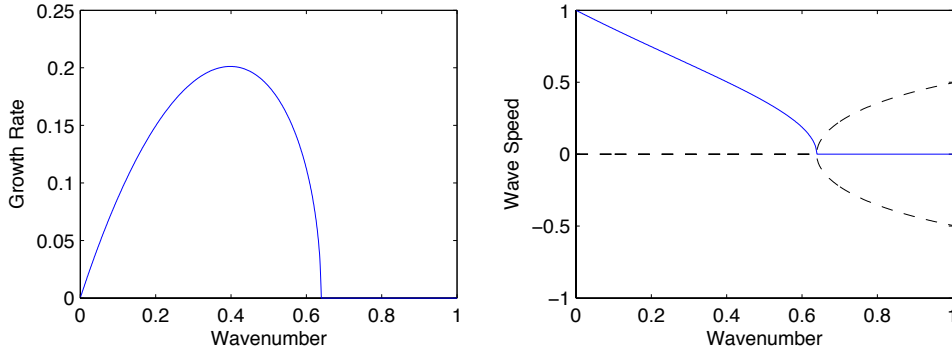
Fig. 6.5 Left: growth rate ($\sigma = kc_i$) calculated from (6.42) with c nondi-mensionalized by U and k nondimensionalized by $1/a$ (equivalent to setting $a = U = 1$). Right: Real (c_r, dashed) and imaginary (c_i, solid) wave speeds. The flow is unstable for $k < 0.63$, with the maximum instability occurring at $k = 0.39$.

$$A = B + Ce^{2ka}, \tag{6.40b}$$

$$D[(U + c)k] = Be^{2ka}\left[-(U + c)k + \frac{U}{a}\right] + C\left[\frac{U}{a} + (U + c)k\right], \tag{6.40c}$$

$$D = Be^{2ka} + C. \tag{6.40d}$$

These are a set of four homogeneous equations, with the unknown parameters A, B, C and D, which may be written in the form of a matrix equation,

$$\begin{pmatrix} k(U - c) & -k(U - c) - U/a & e^{2ka}[k(U - c) - (U/a)] & 0 \\ 1 & -1 & -e^{2ka} & 0 \\ 0 & e^{2ka}[k(U + c) - (U/a)] & -k(U + c) - (U/a) & k(U + c) \\ 0 & e^{2ka} & 1 & -1 \end{pmatrix} \begin{pmatrix} A \\ B \\ C \\ D \end{pmatrix}$$
$$= 0. \tag{6.41}$$

For non-trivial solutions the determinant of the matrix must be zero, and solving the ensuing equation gives the dispersion relationship, first obtained by Rayleigh,

$$c^2 = \left(\frac{U}{2ka}\right)^2 \left[(1 - 2ka)^2 - e^{-4ka}\right], \tag{6.42}$$

and this is plotted in Fig. 6.5. The flow is unstable for sufficiently long wavelengths, for then the right-hand side of (6.42) is negative. The critical wavenumber below which instability occurs is found by solving $(1 - 2ka)^2 = e^{-4ka}$, which gives instability for $ka < 0.63293$. A numerical solution of the initial value problem is illustrated in Fig. 6.6 and Fig. 6.7.[4] Here, the initial perturbation is small and random, containing components at all wavenumbers. All the modes in the unstable range grow exponentially, and the pattern is soon dominated by the mode that grows fastest — a horizontal wavenumber
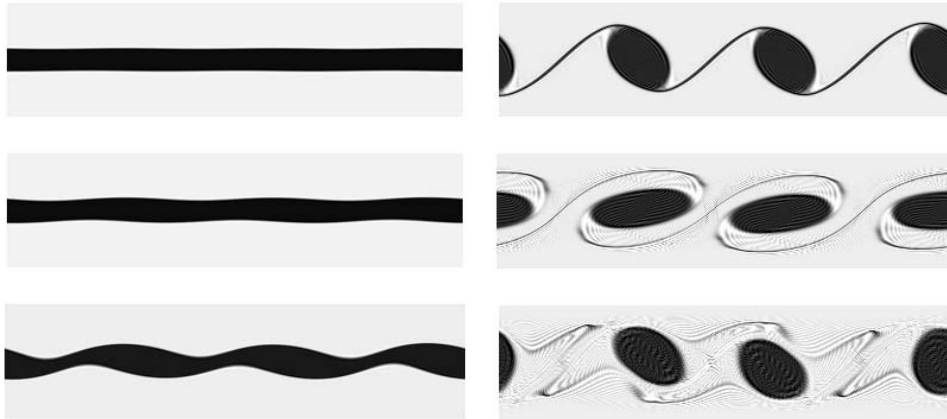
Fig. 6.6 A sequence of plots of the vorticity, at equal time intervals, from a numerical solution of the nonlinear vorticity equation (6.12), with initial conditions as in Fig. 6.4, plus a very small random perturbation. Time increases first down the left column, then down the right column. The solution is obtained in a rectangular (4×1) domain, with periodic conditions in the x-direction and slippery walls at $y = (0, 1)$. The initial shear is confined to a region $0.4 < y < 0.6$ so that $a = 0.1$, and the maximum instability thus occurs for a wavelength of 1.57. For a domain of length 4, this corresponds to a nondimensional wavenumber of 2.55. Since the periodic domain quantizes the allowable wavenumbers, the maximum instability is at wavenumber 3, and this is what emerges. Only in the first two or three frames is the linear approximation valid.

three in this problem. Eventually, the perturbation grows sufficiently that the linear equations are no longer valid and, as is seen in the lower three panels of Fig. 6.6, vortices form and pinch off. Eventually, the vortices interact and the flow develops into two-dimensional turbulence, considered in chapter 8.

The mechanism of the instability — an informal view

[A similar mechanism is discussed in section 6.8, and the reader may wish to read the two descriptions in tandem.] An edge wave in isolation is stable, the instability arising when two edge waves have sufficient cross-stream extent that they can interact with each other. This occurs for sufficiently long wavelengths because the cross-stream decay scale is proportional to the along-stream wavelength — hence the high-wavenumber cut-off. To see the mechanism of the instability, let us first suppose that the interfaces are, in fact, sufficiently far away that the edge waves at each interface do not interact. Using (6.37) the edge waves at $y = -a$ and $y = +a$ have dispersion relationships

$$ c_{+a} = U_0 - \frac{U_0/a}{2k}, \qquad c_{-a} = -U_0 + \frac{U_0/a}{2k} \qquad \text{(6.43a,b)} $$

If the two waves are to interact these phase speeds must be equal, giving the condition

$$ c = 0, \qquad k = 1/(2a). \qquad \text{(6.44a,b)} $$
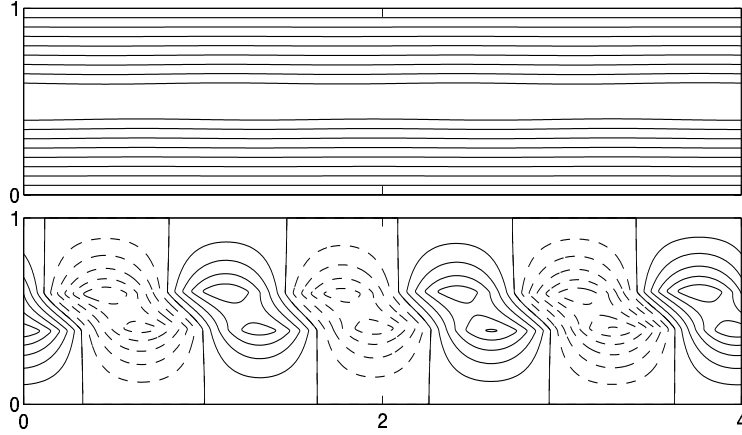
Fig. 6.7 Total streamfunction (top panel) and perturbation streamfunction from the same numerical calculation as in Fig. 6.6, at a time corresponding to the second frame. Positive values (a clockwise circulation) are solid lines, and negative values are dashed. The perturbation pattern grows exponentially, but is locked in place.

That is, the waves are stationary, and their wavelength is proportional to the separation of the two edges. In fact, (6.44) approximately characterizes the conditions at the critical wavenumber $k = 0.63/a$ (see Fig. 6.5). In the region of the shear the two waves have the form

$$\psi_{+a} = \text{Re}\,\widetilde{\psi}_{+a}(t)e^{k(y-a)}e^{i\phi}e^{ikx}, \qquad \psi_{+a} = \text{Re}\,\widetilde{\psi}_{-a}(t)e^{-k(y+a)}e^{ikx} \quad \text{(6.45a,b)}$$

where ϕ is the phase shift between the waves; in the case of pure edge waves we have $\widetilde{\psi}_{\pm a} = A_{\pm a}e^{-ikct}$ where we may take $A_{\pm a}$ to be real.

Now consider how the wave generated at $y = -a$ might affect the wave at $y = +a$ and vice versa. The contribution of ψ_{-a} to acceleration of ψ_{+a} is given by applying the x-momentum equation, (6.21), at either side of the interface at $y = +a$, and similarly for the acceleration at $y = -a$. We obtain

$$\frac{\partial u'_{+a}}{\partial t} \sim -v'_{-a}\frac{\partial U}{\partial y}, \qquad\qquad \frac{\partial u'_{-a}}{\partial t} \sim -v'_{+a}\frac{\partial U}{\partial y}, \qquad\qquad \text{(6.46a,b)}$$

at $y = +a$ and $y = -a$ respectively, omitting the terms that give the neutral edge waves. If the spatial dependence of the waves (6.45) this gives, at $y = \pm a$,

$$-ke^{i\phi}\frac{\partial \widetilde{\psi}_{+a}}{\partial t} \sim -ik\widetilde{\psi}_{-a}\frac{\partial U}{\partial y}, \qquad k\frac{\partial \widetilde{\psi}_{-a}}{\partial t} \sim -ike^{i\phi}\widetilde{\psi}_{+a}\frac{\partial U}{\partial y}, \qquad \text{(6.47a,b)}$$

If ψ_{+a} and ψ_{-a} have the right phase with respect to each other, then the two edge waves can feed back on each other. In particular, from (6.47) we see that the system is unstable when $\phi = \pi/2$, and the wave at $y = +a$ lags the wave at $y = -a$. That is, *the perturbation is unstable when it tilts into the shear,* and this is seen in the full solution, Fig. 6.7.

6.3 NECESSARY CONDITIONS FOR INSTABILITY

6.3.1 Rayleigh's criterion

For simple profiles it may be possible to calculate, or even intuit, the instability properties, but for continuous profiles of $U(y)$ this is often impossible and it would be nice to have some general guidelines as to when a profile might be unstable. To this end, we will derive a *necessary* condition for instability, or a *sufficient* criterion for stability that will at least tell us if a flow *might* be unstable. We first write Rayleigh's equation, with a β-effect, as

$$\widetilde{\psi}_{yy} - k^2\widetilde{\psi} + \frac{\beta - U_{yy}}{U - c}\widetilde{\psi} = 0 \qquad (6.48)$$

Multiply by $\widetilde{\psi}*$ (the complex conjugate of $\widetilde{\psi}$) and integrate over the domain of interest. After integrating the first term by parts, this gives

$$\int_{y_1}^{y_2} \left[\left|\frac{\partial \widetilde{\psi}}{\partial y}\right|^2 + k^2|\widetilde{\psi}|^2 \right] dy - \int_{y_1}^{y_2} \frac{\beta - U_{yy}}{U - c}|\widetilde{\psi}|^2 \, dy = 0. \qquad (6.49)$$

assuming that $\widetilde{\psi}$ vanishes at the boundaries. (The limits to the integral may be infinite, in which case it is assumed that $\widetilde{\psi}$ decays to zero as $|y|$ approaches ∞.) The only variable in this expression that is complex is c, and thus the first integral is real. The imaginary component of the second integral is

$$c_i \int \frac{\beta - U_{yy}}{|U - c|^2}|\widetilde{\psi}|^2 \, dy = 0. \qquad (6.50)$$

Thus, *either* c_i vanishes or the integral does. For there to be an instability, c_i must be nonzero and because the eigenvalues of Rayleigh's equation come in pairs (because it is a second order ODE), for each decaying mode (negative c_i) there is a corresponding growing mode (positive c_i). Therefore:

> *A necessary condition for instability is that the expression*
>
> $$\beta - U_{yy}$$
>
> *change sign somewhere in the domain.*

Equivalently, a sufficient criterion for stability is that $\beta - U_{yy}$ not vanish in the domain interior; it may vanish at the boundaries, or tend to zero for large $|y|$. This condition is known as Rayleigh's inflexion point criterion.[5]

An alternate, more general, derivation

Consider again the vorticity equation, linearized about a parallel shear flow,

$$\frac{\partial \zeta}{\partial t} + U\frac{\partial \zeta}{\partial x} + v\left(\frac{\partial Z}{\partial y} + \beta\right) = 0. \qquad (6.51)$$

(dropping the primes on the perturbation quantities). Multiply by ζ and divide by $\beta + \mathcal{Z}_y$ to obtain

$$\frac{\partial}{\partial t}\left(\frac{\zeta^2}{\beta + \mathcal{Z}_y}\right) + \frac{U}{\beta + \mathcal{Z}_y}\frac{\partial \zeta^2}{\partial x} + v\zeta = 0, \tag{6.52}$$

and then integrate with respect to x to give

$$\frac{\mathrm{d}}{\mathrm{d}t}\int\left(\frac{\zeta^2}{\beta + \mathcal{Z}_y}\right)\mathrm{d}x = -\int v\zeta\,\mathrm{d}x. \tag{6.53}$$

Now,

$$v\zeta = -\frac{\partial}{\partial y}(uv) + \frac{1}{2}\frac{\partial}{\partial x}(u^2 + v^2). \tag{6.54}$$

That is, *the flux of vorticity is the divergence of some quantity.* Its integral therefore vanishes provided there are no contributions from the boundary, and integrating (6.53) with respect to y gives

$$\frac{\mathrm{d}}{\mathrm{d}t}\int\left(\frac{\zeta^2}{\beta + \mathcal{Z}_y}\right)\mathrm{d}x\,\mathrm{d}y = 0. \tag{6.55}$$

If there is to be an instability ζ must grow, but the integral is identically zero. These two conditions can only be simultaneously satisfied if $\beta + \mathcal{Z}_y$, or equivalently $\beta - U_{yy}$, is zero somewhere in the domain.

   This derivation shows that the Rayleigh-Kuo criterion applies even if disturbances are not of normal-mode form. The quantity $\zeta^2/(\beta + \mathcal{Z}_y)$ is an example of a *wave-activity density* — a wave activity being a conserved quantity, quadratic in the amplitude of the wave. Such quantities play an important role in instabilities, and we consider then further in chapter 7.

6.3.2 Fjørtoft's criterion

Another necessary condition for instability was obtained by Fjørtoft.[6] From the real part of (6.49) we find

$$\int_{y_1}^{y_2}(\beta - U_{yy})\frac{(U - c_r)}{|U - c|^2}|\widetilde{\psi}|^2\,\mathrm{d}y = \int_{y_1}^{y_2}\left|\frac{\partial\widetilde{\psi}}{\partial y}\right|^2 + k^2|\widetilde{\psi}|^2\,\mathrm{d}y > 0. \tag{6.56}$$

Now, for an instability we also know that

$$\int_{y_1}^{y_2}\frac{\beta - U_{yy}}{|U - c|^2}|\widetilde{\psi}|^2\,\mathrm{d}y = 0. \tag{6.57}$$

Using this and (6.56) it is clear that, for an instability,

$$\int_{y_1}^{y_2}(\beta - U_{yy})\frac{(U - U_s)}{|U - c|^2}|\widetilde{\psi}|^2\,\mathrm{d}y > 0 \tag{6.58}$$

where U_s is *any* real constant. It is most useful to choose this constant to be the value of $U(y)$ at which $\beta - U_{yy}$ vanishes. This leads directly to the criterion:

> *A necessary condition for instability is that the expression*
>
> $$(\beta - U_{yy})(U - U_s)$$
>
> *where U_s is the value of $U(y)$ at which $\beta - U_{yy}$ vanishes, be positive somewhere in the domain.*

This is equivalent to saying that the magnitude of the vorticity must have a maximum inside the domain, and not at the boundary or at infinity, as can be seen by perusing Fig. 6.8. Why choose U_s in the manner we did? Suppose we chose U_s to have a very large negative or large positive value, so that $U - U_s$ is of one sign everywhere. Then (6.58) just implies that $\beta - U_{yy}$ must be negative somewhere and must be positive somewhere, which is already known from Rayleigh's criterion. The most stringent criterion is obtained by choosing U_s to be the value of $U(y)$ at which $\beta - U_{yy}$ vanishes. Again it should be noted that both Fjørtoft's and Rayleigh's criteria are necessary conditions for instability, and examples may be constructed which do satisfy their criterion, yet which are stable to infinitesimal perturbations. Note that the β-effect can stabilize the middle two profiles of Fig. 6.8, because if it is large enough $\beta - U_{yy}$ will be one-signed. However, the β-effect can destabilize a westward point jet, $U(y) = -(1 - |y|)$ (the negative of the jet in Fig. 6.3), because $\beta - U_{yy}$ is negative at $y = 0$ and positive elsewhere. An eastward point jet is stable, with or without β.

6.4 BAROCLINIC INSTABILITY

Baroclinic instability is a hydrodynamic instability that occurs in stably stratified, rotating fluids, and it is ubiquitous in the planetary atmospheres and oceans. It gives rise to weather, and thus is the form of hydrodynamic instability that most affects the human condition.

6.4.1 A physical picture

We will first draw a picture of baroclinic instability as a form of 'sloping convection' in which the fluid, although statically stable, is able to release available potential energy when parcels move along a sloping path. To this end, let us ask: what is the basic state that is baroclinically unstable? In a stably stratified fluid potential density decreases with height; we can also easily imagine a state in which the basic state temperature decreases, and so the potential density increases, polewards. (We will couch most of our discussion in terms of the Boussinesq equations, and henceforth drop the qualifier 'potential' from density.) Can we construct a steady solution from these two conditions? The answer is yes, provided the fluid is also rotating; rotation is necessary because the meridional temperature gradient generally implies a meridional pressure gradient; there is nothing to balance this in the absence of rotation, and a fluid parcel would therefore accelerate. In a rotating fluid this pressure gradient can be balanced by the Coriolis force and a steady solution maintained even in the absence of viscosity. Consider a stably-stratified Boussinesq fluid in geostrophic and hydrostatic balance on an f-plane,
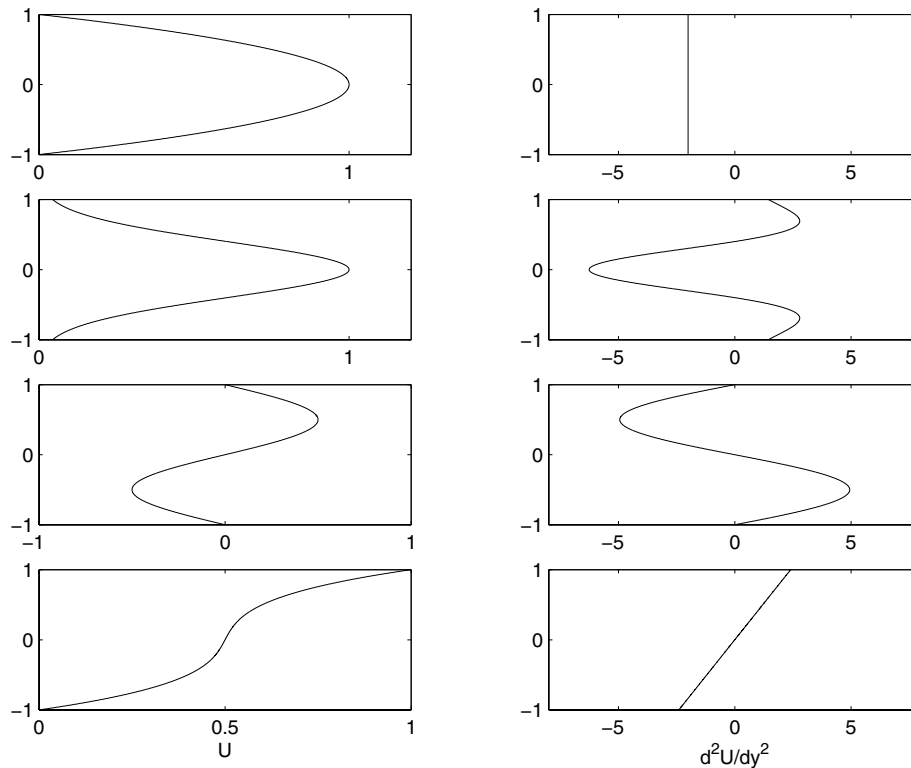
Fig. 6.8 Example parallel velocity profiles (left column) and their second derivatives (right column). From the top: Poiseuille flow ($u = 1 - y^2$); a Gaussian jet; a sinusoidal profile; a polynomial profile. By Rayleigh's criterion, the top profile is stable, whereas the lower three are potentially unstable. However, the bottom profile is stable by Fjørtoft's criterion (and note that the vorticity maxima are at the boundaries). If the β-effect were present and large enough it would stabilize the middle two profiles.

with buoyancy decreasing uniformly polewards. Then $fu = -\partial\phi/\partial y$ and $\partial\phi/\partial z = b$, where $b = -g\rho'/\rho_0$ is the buoyancy. These together give the thermal wind relation, $\partial u/\partial z = \partial b/\partial y$. If there is no variation of these fields in the zonal direction, then, for *any* variation of b with y, this is a steady solution to the primitive equations of motion, with $v = w = 0$.

The density structure corresponding to a uniform increase of density in the meridional direction is illustrated in Fig. 6.9. Is this structure stable to perturbations? The answer is no, although the perturbations must be a little special. Suppose the particle at 'A' is displaced upwards; then, since the fluid is (by assumption) stably stratified it will be denser than its surroundings and hence experience a restoring force, and similarly if displaced downwards. Suppose, however, we interchange the two parcels at positions 'A' and 'B'. Parcel 'A' finds itself surrounded by parcels of higher density that itself, and it is therefore buoyant; it is also higher than where it started. Parcel 'B' is negatively
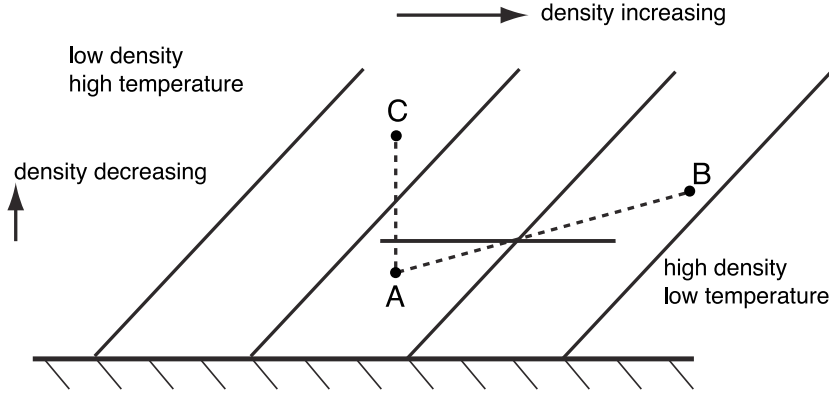
Fig. 6.9 A steady basic state giving rise to baroclinic instability. Potential density decreasing upwards and equatorwards, and the associated horizontal pressure gradient is balanced by the Coriolis force. Parcel 'A' is heavier than 'C', and so statically stable, but it is lighter than 'B'. Hence, if 'A' and 'B' are interchanged there is a release of potential energy.

buoyant, and at a lower altitude than where is started. Thus, overall, the centre of gravity of the fluid has been lowered, and so its overall potential energy lowered. This loss in potential energy of the basic state must be accompanied by a gain in kinetic energy of the perturbation. Thus, the perturbation amplifies and converts potential energy to kinetic energy.

The loss of potential energy is easily calculated. Since

$$PE = \int \rho g \, dz \qquad (6.59)$$

the change in potential energy due to the interchange is

$$\Delta PE = g(\rho_A z_A + \rho_B z_B - \rho_A z_B - \rho_B z_B)$$
$$= g(z_A - z_B)(\rho_A - \rho_B) = g\Delta\rho\Delta z \qquad (6.60)$$

If both $\rho_B > \rho_A$ and $z_B > z_A$ then the initial potential energy is larger than the final, energy is released and the state is unstable. If the slope of the isopycnals is ϕ [so that $\phi = -(\partial_y \rho)/(\partial_z \rho)$] and the slope of the displacements is α, then for a displacement of horizontal distance L the change in potential energy is given by

$$\Delta PE = g\Delta\rho\Delta z = g\left(L\frac{\partial\rho}{\partial y} + L\alpha\frac{\partial\rho}{\partial z}\right)\alpha L = gL^2\alpha\frac{\partial\rho}{\partial y}\left(1 - \frac{\alpha}{\phi}\right), \qquad (6.61)$$

if α and ϕ are small. If $0 < \alpha < \phi$ then energy is released by the perturbation, and it is maximized when $\alpha = \phi/2$. For the atmosphere the actual slope of the isotherms is about 10^{-3}, so that the slope and potential parcel trajectories are indeed shallow.

Although intuitively appealing, the thermodynamic arguments presented in this section pay no attention to satisfying the dynamical constraints of the equations of motion, and we now turn our attention to that,

6.5 LINEARIZED QUASI-GEOSTROPHIC EQUATIONS

To explore the dynamics of baroclinic instability we use the quasi-geostrophic equations, specifically a potential vorticity equation for the fluid interior and a buoyancy or temperature equation at two vertical boundaries, one representing the ground and the other the tropopause, the boundary between the troposphere and stratosphere at about 10 km. (The tropopause is not a true rigid surface, but the higher static stability of the stratosphere does inhibit vertical motion. We return to this in section 6.10.) For a Boussinesq fluid the equations are

$$\frac{\partial q}{\partial t} + \boldsymbol{u} \cdot \nabla q = 0, \qquad 0 < z < H,$$
$$q = \nabla^2 \psi + \beta y + \frac{\partial}{\partial z}\left(F\frac{\partial \psi}{\partial z}\right), \tag{6.62}$$

where $F = f_0^2/N^2$, and the buoyancy equation with $w = 0$,

$$\frac{\partial b}{\partial t} + \boldsymbol{u} \cdot \nabla b = 0, \qquad z = 0, H,$$
$$b = f_0 \frac{\partial \psi}{\partial z}. \tag{6.63}$$

A solution of these equations is a purely zonal flow, $\boldsymbol{u} = U(y, z)\mathbf{i}$ with a corresponding temperature field given by thermal wind balance. The potential vorticity of this basic state is

$$Q = \beta y - U_y + \frac{\partial}{\partial z}F\frac{\partial \Psi}{\partial z} = \beta y + \Psi_{yy} + \frac{\partial}{\partial z}F\frac{\partial \Psi}{\partial z} \tag{6.64}$$

where Ψ is the streamfunction of the basic state, related to U by $U = -\partial \Psi/\partial y$. Linearizing (6.62) about this zonal flow gives the potential vorticity equation for the interior,

$$\frac{\partial q'}{\partial t} + U\frac{\partial q'}{\partial x} + v'\frac{\partial Q}{\partial y} = 0, \qquad 0 < z < H \tag{6.65}$$

where $q' = \nabla^2 \psi' + \partial_z\left(F\partial_z\psi'\right)$ and $v' = \partial\psi'/\partial x$. Similarly, the linearized buoyancy equation is

$$\frac{\partial b'}{\partial t} + U\frac{\partial b'}{\partial x} + v'\frac{\partial B}{\partial y} = 0, \qquad z = 0, H, \tag{6.66}$$

where $b' = f_0\partial\psi'/\partial z$ and $\partial B/\partial y = \partial_y(f_0\partial_z\Psi) = -f_0\partial U/\partial z$.

Just as for the barotropic problem, a standard way to of proceeding is to seek normal-mode solutions of these equations. Since the coefficients of the equations are functions of y and z, but not of x, we seek solutions of the form

$$\psi'(x, y, z, t) = \operatorname{Re} \widetilde{\psi}(y, z)e^{ik(x-ct)}, \tag{6.67}$$

and similarly for the derived quantities u', v' and q'. In particular

$$\widehat{q} = \widetilde{\psi}_{yy} + \frac{\partial}{\partial z}F\frac{\partial \widetilde{\psi}}{\partial z} - k^2\widetilde{\psi}. \tag{6.68}$$

Substituting (6.67) and (6.68) into (6.65) into (6.66) gives

$$\boxed{(U - c)\left(\widetilde{\psi}_{yy} + (F\widetilde{\psi}_z)_z - k^2\widetilde{\psi}\right) + Q_y\widetilde{\psi} = 0} \qquad 0 < z < H, \qquad (6.69a)$$

$$\boxed{(U - c)\widetilde{\psi}_z - U_z\widetilde{\psi} = 0} \qquad\qquad z = 0, H. \qquad (6.69b)$$

These equations are analogous to Rayleigh's equations for parallel shear flow, and emphasize the similarity between baroclinic instability and that of a parallel shear flow.

6.5.1 Necessary conditions for baroclinic instability

Necessary conditions for instability may be obtained following a procedure analogous to that used for parallel shear flows. First, integrating by parts, we note that

$$\int_{y_1}^{y_2} \widetilde{\psi}^* \widetilde{\psi}_{yy}\, dy = \left[\widetilde{\psi}^*\widetilde{\psi}_y\right]_{y_1}^{y_2} - \int_{y_1}^{y_2} |\widetilde{\psi}_y|^2\, dy. \qquad (6.70)$$

If the integral is performed between two quiescent latitudes, or the domain is a channel with $\psi = 0$ at the boundaries, then the first term on the right-hand-side vanishes. Similarly,

$$\int_0^H \widetilde{\psi}^*(F\widetilde{\psi}_z)_z\, dz = \left[F\widetilde{\psi}^*\widetilde{\psi}_z\right]_0^H - \int_0^H F|\widetilde{\psi}_z|^2\, dz$$

$$= \left[\frac{FU_z|\widetilde{\psi}|^2}{(U - c)}\right]_0^H - \int_0^H F|\widetilde{\psi}_z|^2\, dz, \qquad (6.71)$$

using (6.69b). Now, multiply (6.69a) by $\widetilde{\psi}^*$ and integrate over y and z, and use (6.70) and (6.71) to obtain

$$\int_0^H \int_{y_1}^{y_2} |\psi_y|^2 + F|\widetilde{\psi}_z|^2 + k^2|\widetilde{\psi}|^2]\, dy\, dz$$

$$- \int_{y_1}^{y_2}\left\{\int_0^H \frac{Q_y}{U - c}|\widetilde{\psi}|^2\, dz + \left[\frac{FU_z|\widetilde{\psi}|^2}{U - c}\right]_0^H\right\} dy = 0. \qquad (6.72)$$

The term on the first line is purely real. The term on the second line is complex, and its imaginary component is given by

$$- c_i \int_{y_1}^{y_2}\left\{\int_0^H \frac{Q_y}{|U - c|^2}|\widetilde{\psi}|^2\, dz + \left[\frac{FU_z|\widetilde{\psi}|^2}{|U - c|^2}\right]_0^H\right\} dy = 0. \qquad (6.73)$$

If there is to be instability c_i must be non-zero, and the integrand must therefore vanish. This gives the *Charney-Stern-Pedlosky* (CSP) necessary condition for instability, namely that one of the following criteria be satisfied:[7]

(i) Q_y changes sign in the interior.

(ii) Q_y is the opposite sign to U_z at the upper boundary, $z = H$.

(iii) Q_y is the same sign as U_z at the lower boundary, $z = 0$.

(iv) U_z is the same sign at the upper and lower boundaries, a condition which differs from (ii) or (iii) if $Q_y = 0$.

In the earth's atmosphere, Q_y is often dominated by β, and is positive everywhere, as, frequently, is the shear. The instability criterion is then normally satisfied through (iii): that is, both Q_y and $U_z(0)$ are positive.

6.6 THE EADY PROBLEM

We now proceed to explicitly calculate the stability properties of a particular configuration that has become to be known as the *Eady problem*. This was one of the first two mathematical descriptions of baroclinic instability, the other being the *Charney problem*.[8] The two were formulated independently, each being the (largely unsupervised) Ph.D. thesis of its respective author, and although the Charney problem is in some respects more complete (for example in allowing a β-effect) the Eady problem displays the instability in a more transparent form. The Charney problem in its entirety is also quite mathematically opaque,[9] and for these reasons we will first consider the Eady problem. The β-effect can be incorporated relatively simply in the two-layer model (the 'Phillips problem') considered in the next section, and in section 6.10.1 we look at some aspects of the Charney problem approximately. These models were all initially envisioned as models for instabilities in the atmosphere, but the process of baroclinic instability is also ubiquitous in the ocean. To begin, let us make the following simplifying assumptions:

(i) The motion is on the f-plane ($\beta = 0$). This assumption, although not particularly realistic, greatly simplifies the analysis.

(ii) The fluid is uniformly stratified. That is, N^2 is a constant. This is a reasonable approximation for the atmosphere below the tropopause, but less so for the ocean where the stratification is quite non-uniform, being much larger in the upper ocean.

(iii) The basic state has uniform shear; that is, $U_0(z) = \Lambda z = Uz/H$ where Λ is the (constant) shear and U is the zonal velocity at $z = H$ where H the domain depth. Again, this profile is more appropriate for the atmosphere than the ocean — below the thermocline the ocean is relatively quiescent and the shear small.

(iv) The motion is contained between two rigid, flat horizontal surfaces. In the atmosphere this corresponds to the ground and a 'lid' at a constant-height tropopause.

Assumptions (ii)–(iv) are rather inappropriate for the ocean, and will preclude us from drawing any quantitative conclusions about that system from our analysis. The most restrictive assumption vis-a-vis the atmosphere is (i), and we explore the role of the β-effect in baroclinic instability later on.

6.6.1 The linearized problem

With a basic state streamfunction of $\Psi = -\Lambda z y$, the basic state potential vorticity, Q, is

$$Q = \nabla^2 \Psi + \frac{H^2}{L_d^2} \frac{\partial}{\partial z} \left(\frac{\partial \Psi}{\partial z} \right) = 0. \tag{6.74}$$

The fact that $Q = 0$ makes the Eady problem a special case, albeit an illuminating one. The linearized potential vorticity equation is

$$\left(\frac{\partial}{\partial t} + \Lambda z \frac{\partial}{\partial x} \right) \left(\nabla^2 \psi' + \frac{H^2}{L_d^2} \frac{\partial^2 \psi'}{\partial z^2} \right) = 0 \tag{6.75}$$

This equation has no x-dependent coefficients and in a periodic channel we may seek solutions in the form (6.67), namely $\psi'(x, y, z, t) = \mathrm{Re}\, \widetilde{\psi}(y, z) e^{ik(x-ct)}$. Substituting this into (6.75) yields

$$(\Lambda z - c) \left(\frac{\partial^2 \widetilde{\psi}}{\partial y^2} + \frac{H^2}{L_d^2} \frac{\partial^2 \widetilde{\psi}}{\partial z^2} - k^2 \widetilde{\psi} \right) = 0, \tag{6.76}$$

which is (6.69a) applied to the Eady problem.

Boundary Conditions

There are two sets of boundary conditions to satisfy, the vertical boundary conditions at $z = 0$ and $z = 1$ and the lateral boundary conditions. In the horizontal plane we may either consider the flow to be confined to a channel, periodic in x and confined between two meridional walls, or, with a slightly greater degree of idealization but with little change to the essential dynamics, suppose that domain is doubly-periodic. Either case is dealt with easily enough by the choice of geometric basis function; we will choose a channel of width L and impose $\psi = 0$ at $y = +L/2$ and $y = -L/2$ and, to satisfy this, seek solutions of the form $\Psi = \Phi(z) \sin ly$ or, using (6.67)

$$\psi'(x, y, z, t) = \mathrm{Re}\, \Phi(z) \sin ly\, e^{ik(x-ct)}. \tag{6.77}$$

where $l = n\pi/L$ where n is a positive integer.

The vertical boundary conditions are that $w = 0$ at $z = 0$ and $z = H$. We follow the procedure of section 6.5 and from (6.66) we obtain

$$\left(\frac{\partial}{\partial t} + \Lambda z \frac{\partial}{\partial x} \right) \frac{\partial \psi'}{\partial z} - \Lambda \frac{\partial \psi'}{\partial x} = 0, \qquad \text{at } z = 0, H. \tag{6.78}$$

Solutions

Substituting (6.77) into (6.76) gives the interior potential vorticity equation

$$(\Lambda z - c) \left[\frac{H^2}{L_d^2} \frac{\partial^2 \Phi}{\partial z^2} - (k^2 + l^2) \Phi \right] = 0, \tag{6.79}$$

and substituting (6.77) into (6.78) gives, at $z = 0$ and $z = H$,

$$c\frac{d\Phi}{dz} + \Lambda\Phi = 0 \qquad \text{and} \qquad (c - \Lambda H)\frac{d\Phi}{dz} + \Lambda\Phi = 0. \qquad \text{(6.80a,b)}$$

These are equivalent to (6.69b) applied to the Eady problem. If $\Lambda z \neq c$ then (6.79) becomes[10]

$$H^2\frac{d^2\Phi}{dz^2} - \mu^2\Phi = 0, \qquad \text{(6.81)}$$

where $\mu^2 = L_d^2(k^2 + l^2)$. The nondimensional parameter μ is a horizontal wavenumber, scaled by the inverse of the Rossby radius of deformation. Solutions of (6.81) are

$$\Phi(z) = A\cosh\mu\hat{z} + B\sinh\mu\hat{z}, \qquad \text{(6.82)}$$

where $\hat{z} = z/H$; thus, μ determines the vertical structure of the solution. The boundary conditions (6.80) are satisfied if

$$A \times [\Lambda H] + B \times [\mu c] = 0,$$
$$A \times [(c - \Lambda H)\mu\sinh\mu + \Lambda H\cosh\mu] + B \times [(c - \Lambda H)\mu\cosh\mu + \Lambda H\sinh\mu] = 0.$$
$$\text{(6.83)}$$

Equations (6.83) are two coupled homogeneous equations in the two unknowns A and B. Non-trivial solutions will only exist if the determinant of their coefficients (the terms in square brackets) vanishes, and this leads to

$$c^2 - Uc + U^2(\mu^{-1}\coth\mu - \mu^{-2}) = 0, \qquad \text{(6.84)}$$

where $U \equiv \Lambda H$ and $\coth\mu = \cosh\mu/\sinh\mu$. The solution of (6.84) is

$$c = \frac{U}{2} \pm \frac{U}{\mu}\left[\left(\frac{\mu}{2} - \coth\frac{\mu}{2}\right)\left(\frac{\mu}{2} - \tanh\frac{\mu}{2}\right)\right]^{1/2}. \qquad \text{(6.85)}$$

The waves, being proportional to $\exp(-ikct)$, will grow exponentially if c has an imaginary part. Since $\mu/2 > \tanh(\mu/2)$ for all μ, for an instability we require that

$$\frac{\mu}{2} < \coth\frac{\mu}{2}, \qquad \text{(6.86)}$$

which is satisfied when $\mu < \mu_c$ where $\mu_c = 2.399$. The growth rates of the instabilities themselves are given by the imaginary part of (6.85), multiplied by the x-wavenumber. That is

$$\sigma = kc_i = k\frac{U}{\mu}\left[\left(\coth\frac{\mu}{2} - \frac{\mu}{2}\right)\left(\frac{\mu}{2} - \tanh\frac{\mu}{2}\right)\right]^{1/2}. \qquad \text{(6.87)}$$

These solutions suggest a natural nondimensionalization: scale length by L_d, height by H and time by L_d/U. The *Eady growth rate* is the inverse of the time scaling, and is defined by

$$\sigma_E \equiv \frac{\Lambda H}{L_d} = \frac{U}{L_d} \qquad \text{(6.88)}$$

Its inverse, the Eady timescale, may also be written as

$$T_{\rm E} = \frac{L_{\rm d}}{U} = \frac{NH}{f_0 U} = \frac{1}{Fr f_0} = \frac{\sqrt{Ri}}{f_0}, \tag{6.89}$$

where $Fr = U/(NH)$ and $Ri = N^2/\Lambda^2$ are the Froude and Richardson numbers for this problem.

From (6.87) we may determine that the maximum growth rate occurs when $\mu = \mu_m = 1.61$, with associated (nondimensional) growth rate of $kc_i/\sigma_E = 0.31$, and phase speed $c_r/U = 0.5$. Note that for any given x-wavenumber, the most unstable wavenumber has $l = 0$, so that $L_{\rm d}k = \mu$. The unstable x-wavenumbers and corresponding wavelengths occur for

$$k < k_c = \frac{\mu_c}{L_{\rm d}} = \frac{2.4}{L_{\rm d}}, \qquad \lambda > \lambda_c = \frac{2\pi L_{\rm d}}{\mu_c} = 2.6 L_{\rm d}. \tag{6.90a,b}$$

The wavenumber and wavelength at which the instability is greatest are:

$$k_m = \frac{1.6}{L_{\rm d}}, \qquad \lambda_m = \frac{2\pi L_{\rm d}}{\mu_m} = 3.9 L_{\rm d}. \tag{6.91a,b}$$

These properties are illustrated in the left panels of Fig. 6.10 and in Fig. 6.11.

Given c, we may use (6.83) to determine the vertical structure of the Eady wave and this is, to within an arbitrary constant factor,

$$\Phi(z) = \cosh \mu \hat{z} - \frac{U}{\mu c} \sinh \mu \hat{z} = \left[\cosh \mu \hat{z} - \frac{U c_r \sinh \mu \hat{z}}{\mu |c^2|} + \frac{i U c_i \sinh \mu \hat{z}}{\mu |c^2|} \right]. \tag{6.92}$$

The wave therefore has a phase, $\theta(z)$, given by

$$\theta(z) = \tan^{-1} \left(\frac{U c_i \sinh \mu z}{\mu |c^2| \cosh \mu \hat{z} - U c_r \sinh \mu \hat{z}} \right). \tag{6.93}$$

These are plotted in the right panels of Fig. 6.10,

6.6.2 Atmospheric and oceanic parameters

To get a qualitative sense of the nature of the instability we may choose some typical parameters, as follows.

For the atmosphere

Let us choose

$$H \sim 10\,{\rm km}, \qquad U \sim 10\,{\rm m\,s}^{-1}, \qquad N \sim 10^{-2}\,{\rm s}^{-1}. \tag{6.94}$$

We then obtain:

$$\text{Deformation Radius:} \quad L_{\rm d} = \frac{NH}{f} \approx \frac{10^{-2} 10^4}{10^{-4}} \approx 1000\,{\rm km}, \tag{6.95}$$
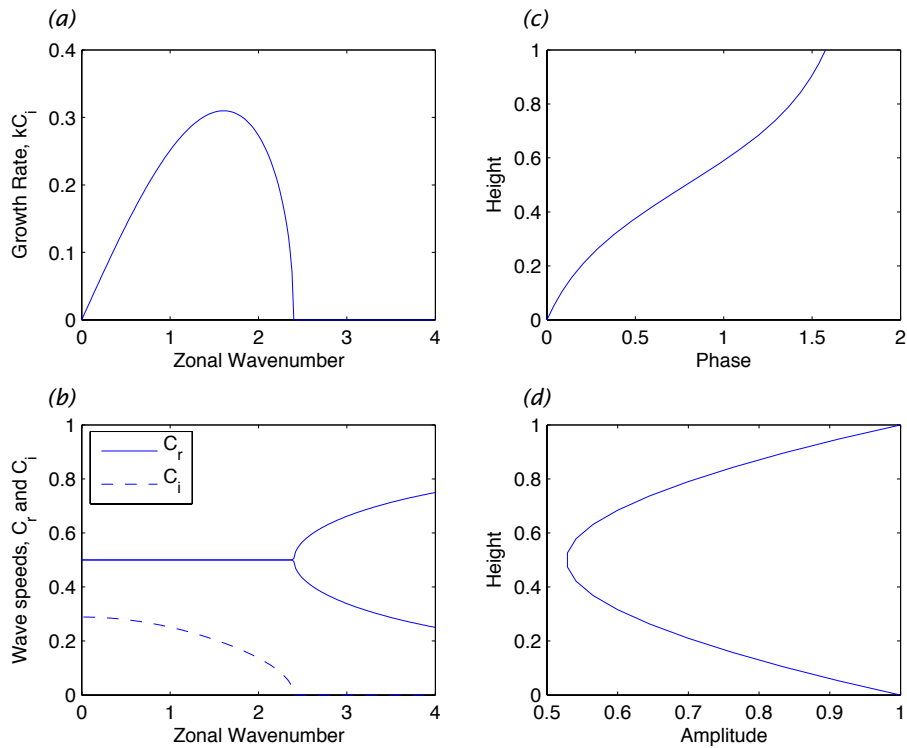
Fig. 6.10 Solution of the Eady problem, in non-dimensional units. (a) Growth rate, kc_i, of the most unstable Eady modes (i.e., those with the gravest meridional scale) as a function of scaled wavenumber μ, from (6.87) with $\Lambda = H = 1$. The scaled x-wavenumber k. (b) The real (solid) and imaginary (dashed) wave speeds of those modes, as a function of horizontal wavenumber. (c) The phase of the single most unstable mode as a function of height. (d) The amplitude of that mode as a function of height. To obtain dimensional values, multiply the growth rate by $\Lambda H/L_d$ and the wavenumber by $1/L_d$.

Figure 6.11 Contours of growth rate, σ, in the Eady problem, in the k–l plane using (6.87), nondimensionalized as in Fig. 6.10. The growth rate peaks near the deformation scale, and for any given zonal wavenumber the most unstable wavenumber is that with the gravest meridional scale.
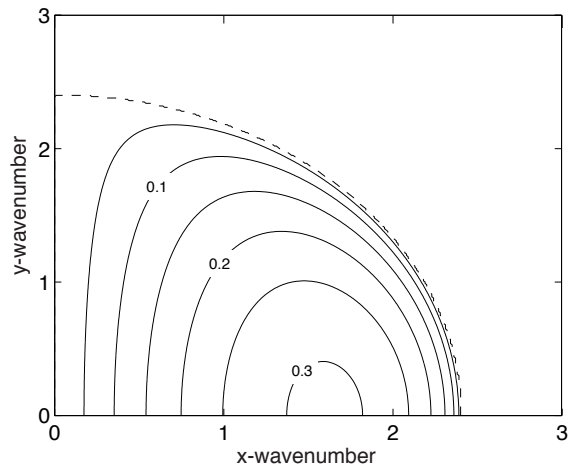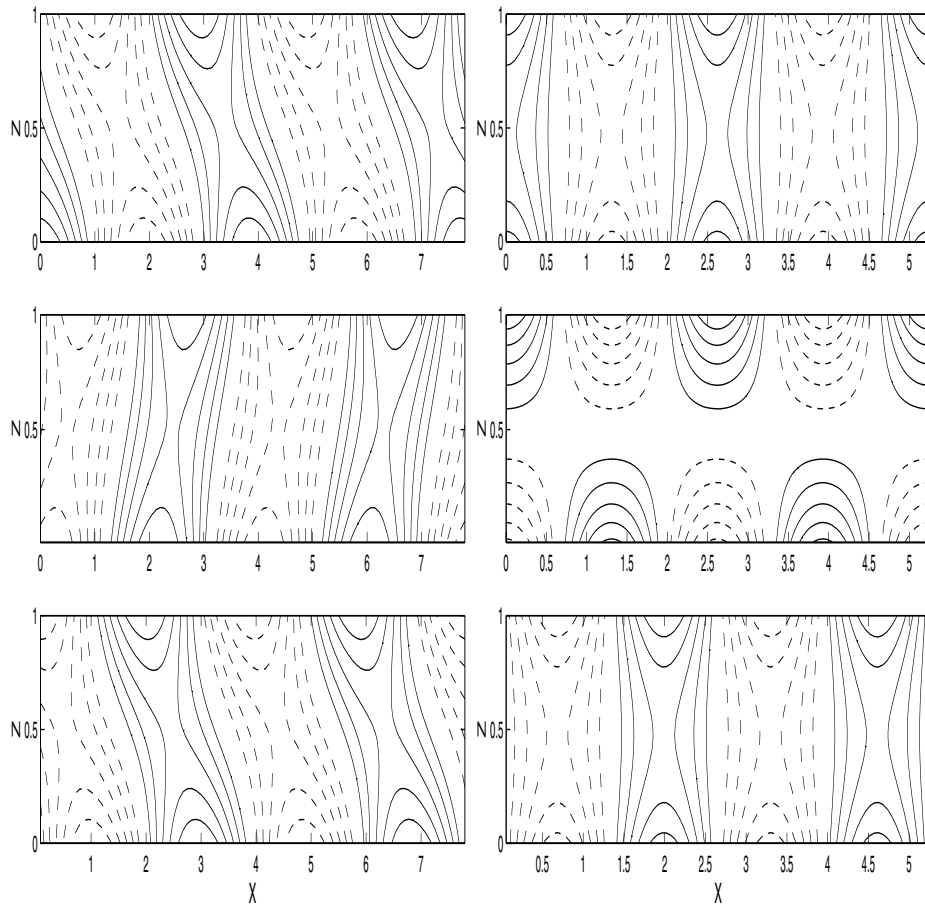
Fig. 6.12 Left column: Vertical structure of the most unstable Eady mode. Top: contours of streamfunction. Middle: temperature, proportional to $\partial\psi/\partial z$. Bottom: meridional velocity, proportional to $\partial\psi/\partial y$. Negative contours are dashed, and two complete wavelengths are present in the horizontal. Poleward flowing (positive v) air is generally warmer than equatorward flowing air. Right column: Same, but now for a wave just beyond the short-wave cut-off. There is no phase-tilt in the vertical, and the temperature perturbations at the upper and lower boundaries are no longer able to interact.

$$\text{Scale of maximum instability:} \qquad L_{max} \approx 3.9 L_d \approx 4000\,\text{km}, \qquad (6.96)$$

$$\text{Growth Rate:} \qquad \sigma \approx 0.3\frac{U}{L_d} \approx \frac{0.3 \times 10}{10^6}\,\text{s}^{-1} \approx 0.26\,\text{day}^{-1}. \qquad (6.97)$$

For the ocean

For the main thermocline in the ocean let us choose

$$H \sim 1\,\text{km} \qquad U \approx 0.1\,\text{m s}^{-1} \qquad N \sim 10^{-2}\,\text{s}^{-1}. \qquad (6.98)$$

Summary of Results from the Eady Problem

⋆ The length-scales of the instability are characterized by the deformation scale. The most unstable scale has a wavelength about four times the deformation radius L_d, where $L_d = NH/f_0$.

⋆ The growth rate of the instability is approximately

$$\sigma \sim \frac{U}{L_d} = \Lambda \frac{f_0}{N}. \tag{1}$$

That is, it is proportional to the shear, and scaled by the Prandtl ratio f_0/N. The value σ is known as the *Eady growth rate*.

⋆ The most unstable waves for a given zonal scale are those with the gravest meridional scale.

⋆ There is a *short-wave cutoff* beyond which (i.e., at higher wavenumber than) there is no instability. This occurs near the deformation radius.

⋆ The instability relies on an interaction between waves at the upper and lower boundaries. If either boundary is removed, the instability dies. This point is be considered further in section 6.8.

We then obtain:

$$\text{Deformation Radius:} \quad L_d = \frac{NH}{f} \approx \frac{10^{-2}\,1000}{10^{-4}} = 100\,\text{km}, \tag{6.99}$$

$$\text{Scale of maximum instability:} \quad L_{max} \approx 3.9 L_d \approx 400\,\text{km}, \tag{6.100}$$

$$\text{Growth Rate:} \quad \sigma \approx 0.3 \frac{U}{L_d} \approx \frac{0.3 \times 0.1}{10^5}\,\text{s}^{-1} \approx 0.026\,\text{day}^{-1}. \tag{6.101}$$

In the ocean, the Eady problem is not quantitatively applicable because of the non-unifomity of the stratification and non-zonality of the flow. Nevertheless, the above estimates give a qualitative sense of the scale and growth rate of the instability relative to the corresponding values in the atmosphere. A summary of the main points of the Eady problem is given in the shaded box above.

6.7 TWO-LAYER BAROCLINIC INSTABILITY

The eigenfunctions displaying the largest growth rates in the Eady problem have a relatively simple vertical structure. This suggests that an even simpler mathematical model

of baroclinic instability might be constructed in which the vertical structure is *a priori* restricted to a very simple form, namely the two-layer QG model. One notable advantage over the Eady model is that it is possible to include the β–effect in a simple way.

6.7.1 Posing the problem

We begin with the two-layer potential vorticity equations, which we write in the dimensional form,

$$\frac{D}{Dt}\left[\zeta_i + \beta y + \frac{k_d^2}{2}(\psi_j - \psi_i)\right] = 0, \qquad i = 1, 2, \quad j = 3 - i, \qquad (6.102)$$

where

$$\frac{k_d^2}{2} = \left(\frac{2f_0}{NH}\right)^2 \quad \rightarrow \quad k_d = \frac{\sqrt{8}}{L_d}, \qquad (6.103)$$

where H is the total depth of the domain, as in the Eady problem. The basic state we choose is:

$$\Psi_1 = -U_1 y, \qquad \Psi_2 = -U_2 y = +U_1 y. \qquad (6.104)$$

There is no topography and so the system is Galilean invariant, and without loss of generality we choose $U_2 = -U_1$. The basic basic state potential vorticity gradient is then given by

$$Q_1 = \beta y + k_d^2 U y, \qquad Q_2 = \beta y - k_d^2 U y \qquad (6.105)$$

where $U = U_1$. (Note that this differs by a constant factor from the U in the Eady problem.) Even in the absence of β there is a non-zero potential vorticity gradient. Why should this be different from the Eady problem? — after all, the shear is uniform in both problems. The difference arises from the vertical boundary conditions. In the standard layered formulation the temperature gradient at the boundary conditions is absorbed into the definition of the potential vorticity in the interior. This results in a nonzero interior potential vorticity gradient at the two levels adjacent to the boundary (the only layers in the two-layer problem), but isothermal boundary conditions $D/Dt(\partial\psi/\partial z) = 0$. In the Eady problem we have a zero interior gradient of potential vorticity but a temperature gradient at the boundary. The two formulations are physically equivalent — a finite-difference example of the Bretherton boundary layer.

The linearized potential vorticity equation is, for each layer,

$$\frac{\partial q_i'}{\partial t} + U_i \frac{\partial q_i'}{\partial x} + v_i' \frac{\partial Q_i}{\partial y} = 0, \qquad i = 1, 2 \qquad (6.106)$$

or, more explicitly,

$$\left[\frac{\partial}{\partial t} + U \frac{\partial}{\partial x}\right]\left[\nabla^2 \psi_1' + \frac{k_d^2}{2}(\psi_2' - \psi_1')\right] + \frac{\partial \psi_1'}{\partial x}(\beta + k_d^2 U) = 0, \qquad (6.107a)$$

$$\left[\frac{\partial}{\partial t} - U\frac{\partial}{\partial x}\right]\left[\nabla^2\psi_2' + \frac{k_d^2}{2}(\psi_1' - \psi_2')\right] + \frac{\partial\psi_2'}{\partial x}(\beta - k_d^2 U) = 0. \qquad \text{(6.107b)}$$

For simplicity we will set the problem in a square, doubly-periodic domain, and so seek solutions in the form,

$$\psi_i' = \operatorname{Re}\Psi_i e^{i(kx+ly-\omega t)} = \operatorname{Re}\Psi_i e^{ik(x-ct)}e^{ily}, \qquad\qquad i = 1, 2. \qquad \text{(6.108)}$$

Here, k and l are the x- and y-wavenumbers, and $(k, l) = (2\pi/L)(m, n)$ where L is the size of the domain and m and n are integers. The constant Ψ_i is the complex amplitude.

6.7.2 The solution

Substituting (6.108) into (6.107) we obtain

$$[ik(U - c)]\left[-K^2\Psi_1 + k_d{}^2(\Psi_2 - \Psi_1)/2\right] + ik\Psi_1(\beta + k_d^2 U) = 0, \quad \text{(6.109a)}$$

$$[-ik(U + c)]\left[-K^2\Psi_2 + k_d{}^2(\Psi_1 - \Psi_2)/2\right] + ik\Psi_1(\beta - k_d{}^2 U) = 0, \quad \text{(6.109b)}$$

where $K^2 = k^2 + l^2$. Adding and subtracting these two equations gives

$$\left[(U - c)(k_d{}^2/2 + K^2) - (\beta + k_d^2 U)\right]\Psi_1 - \left[k_d^2(U - c)/2\right]\Psi_2 = 0, \quad \text{(6.110a)}$$

$$-\left[k_d^2(U + c)/\right]\Psi_1 + \left[(U + c)(k_d{}^2/2 + K^2) + (\beta - k_d{}^2 U)\right]\Psi_2 = 0. \quad \text{(6.110b)}$$

These equations are of the form

$$[A]\Psi_1 + [B]\Psi_2 = 0, \qquad [C]\Psi_1 + [D]\Psi_2 = 0, \qquad\qquad \text{(6.111)}$$

and for nontrivial solutions the determinant of coefficients must be zero; that is $AD - BC = 0$. This gives a quadratic equation in c and solving this we obtain

$$\boxed{c = -\frac{\beta}{K^2 + k_d^2}\left\{1 + \frac{k_d{}^2}{2K^2} \pm \frac{k_d^2}{2K^2}\left[1 + \frac{4K^4(K^4 - k_d{}^4)}{k_\beta^4 k_d^4}\right]^{1/2}\right\}}, \qquad \text{(6.112)}$$

where $K^4 = (k^2 + l^2)^2$ and $k_\beta = \sqrt{\beta/U}$ (its inverse is known as the Kuo scale). We may nondimensionalize this equation using the deformation radius L_d as the length scale and the shear velocity U as the velocity scale.[11] Then, denoting non-dimensional parameters with hats, we have

$$k = \frac{\widehat{k}}{L_d}, \qquad c = \widehat{c}\,U, \qquad t = \frac{L_d}{U}\widehat{t} \qquad\qquad \text{(6.113)}$$

and the nondimensional form of (6.112) is just

$$\hat{c} = -\frac{\hat{k}_\beta^2}{\hat{K}^2 + \hat{k}_d^2} \left\{ 1 + \frac{\hat{k}_d^2}{2\hat{K}^2} \pm \frac{\hat{k}_d^2}{2\hat{K}^2} \left[1 + \frac{4\hat{K}^4(\hat{K}^4 - \hat{k}_d^4)}{\hat{k}_\beta^4 \hat{k}_d^4} \right]^{1/2} \right\}, \tag{6.114}$$

where $\hat{k}_\beta = k_\beta L_d$ and $\hat{k}_d = \sqrt{8}$, as in (6.103). The nondimensional parameter

$$\gamma = \frac{1}{4}\hat{k}_\beta^2 = \frac{\beta L_d^2}{4U}, \tag{6.115}$$

is often useful as a measure of the importance of β; it is proportional to the square of the ratio of the deformation radius to the Kuo scale $\sqrt{U/\beta}$. (It is also the two layer version of the 'Charney-Green number' considered more in section 6.10.1.) Let us look at two special cases first, before considering the general solution to these equations.

I. Zero Shear

If there is no shear (i.e., $U = 0$) then (6.110a) and (6.110b) are identical and two roots of the equation give the purely real phase speeds c

$$c = -\frac{\beta}{K^2}, \qquad c = -\frac{\beta}{K^2 + k_d^2} \tag{6.116}$$

The first of these is the dispersion relationship for Rossby waves in a purely barotropic flow, and corresponds to the eigenfunction $\Psi_1 = \Psi_2$. The second solution corresponds to the baroclinic eigenfunction $\Psi_1 + \Psi_2 = 0$.

II. Zero β

If $\beta = 0$, then (6.110) yields, after a little algebra,

$$c = \pm U \left[\frac{K^2 - k_d^2}{K^2 + k_d^2} \right]^{1/2} \tag{6.117}$$

or, defining the growth rate σ by $\sigma = -i\omega$,

$$\sigma = Uk \left[\frac{k_d^2 - K^2}{K^2 + k_d^2} \right]^{1/2} \tag{6.118}$$

These expressions are very similar to those in the Eady problem. Indeed, as we increase the number of layers (using a numerical method to perform the calculation) the growth rate converges to that of the Eady problem, as illustrated in Fig. 6.13. We note that:

★ There is an instability for *all* values of U.

★ There is a high-wavenumber cut-off, at a scale proportional to the radius of deformation. For the two-layer model, if $K > k_d = 2.82/L_d$ there is no growth. For the Eady problem, the high wavenumber cut-off occurs at $2.4/L_d$.

Figure 6.13 Growth rates for models with varying numbers of vertical layers, all with $\beta = 0$ and the same uniform stratification and shear. The dashed line is the solution to the continuous (Eady) problem, and the solid lines are results obtained using two, four and eight layers. The two and four layer results are labelled, and the eight layer result is almost coincident with the dashed line. Results with 16 layers (not shown) are indistinguishable from the Eady result.
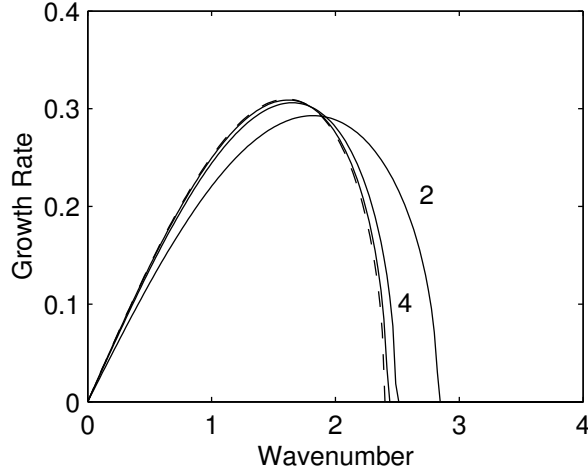
- ★ There is no low wavenumber cut-off.

- ★ For any given k, the highest growth rate occurs for $l = 0$. In the two-layer model, from (6.118), for $l = 0$ the maximum growth rate occurs when $k = 0.634k_d = 1.79/L_d$. For the Eady problem, the maximum growth rate occurs at $1.61/L_d$.

The solution in the case with non-zero β

Using (6.114), the growth rate and wave speeds as function of wavenumber are plotted in Fig. 6.14. We observe that there still appears to be a high wavenumber cut-off and, for $\beta = 0$, there is a low-wavenumber cut-off. A little analysis elucidates these features.

The neutral curve:

For instability, there must be an imaginary component to the phase speed in (6.114). That is, we require

$$k_\beta^4 k_d^4 + 4K^4(K^4 - k_d^4) < 0. \tag{6.119}$$

This is a quadratic equation in K^4 for the value of K, K_c say, at which the growth rate is zero. Solving, we find

$$K_c^4 = \frac{1}{2}k_d^4 \left(1 \pm \sqrt{1 - k_\beta^4/k_d^4}\right), \tag{6.120}$$

and this is plotted in Fig. 6.15. From (6.119) useful approximate expressions can be obtained for the critical shear as a function of wavenumber in the limits of small K and $K \approx k_d$, and these are left as exercises for the reader.
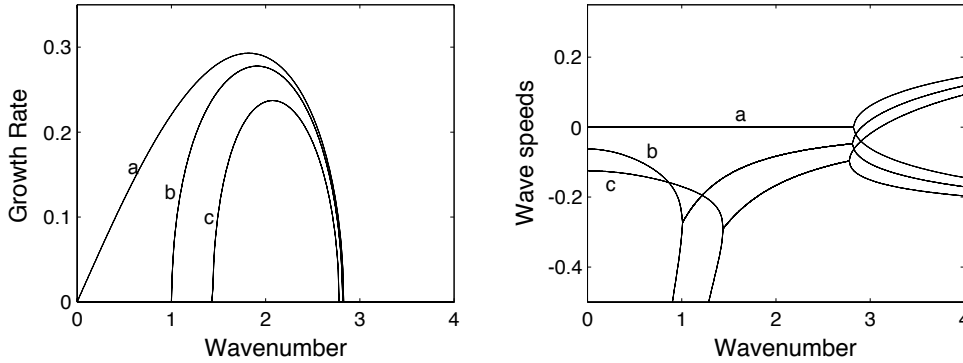
Fig. 6.14 Growth rates and wave speeds for the two-layer baroclinic instability problem, from (6.114), with three (nondimensional) values of β: a, $\gamma = 0$ ($\hat{k}_\beta = 0$); b, $\gamma = 0.5$ ($\hat{k}_\beta = \sqrt{2}$); c, $\gamma = 1$ ($\hat{k}_\beta = 2$). As β increases, so does the low-wavenumber cut-off to instability, but the high-wavenumber cut-off is little changed. (The solutions are obtained from (6.114), with $\hat{k}_d = \sqrt{8}$ and $U_1 = -U_2 = 1/4$.)

Minimum shear for instability:

From (6.119), instability arises when $\beta^2 \hat{k}_d^4 / U^2 < 4K^4(\hat{k}_d^4 - K^4) < 0$ The maximum value of the right-hand-side of this expression arises when $K^4 = \hat{k}_d^4/2$; thus, instability arises only when

$$\frac{\beta^2 k_d^4}{U^2} < 4\frac{k_d^4}{2}\frac{k_d^4}{2} \tag{6.121}$$

or

$$\boxed{U_s > \frac{2\beta}{k_d^2}} \tag{6.122}$$

where $U_s = U_1 - U_2 = 2U$. In terms of the deformation radius itself the minimum shear for instability is

$$U_s > \frac{1}{4}\beta L_d^2. \tag{6.123}$$

Fig. 6.16 sketches how this might vary with latitude in the atmosphere and ocean. (In (6.123), the shear is the difference in the velocity between level 1 and level 2, whereas the deformation radius, NH/f_0, is based on the total height of the fluid. If we were to use half the depth of the fluid in the definition of the deformation radius, the factor of 4 would disappear.) If the shear is just this critical value, the instability occurs at $k = 2^{-1/4}k_d = 0.84k_d = 2.37/L_d$. As the shear increases, the wavenumber at which the growth rate is maximum decreases slightly (see Fig. 6.15), and for a sufficiently large shear the β-effect is negligible and the wavenumber of maximum instability is, as we saw earlier, $0.634\,k_d$ or $1.79/L_d$.
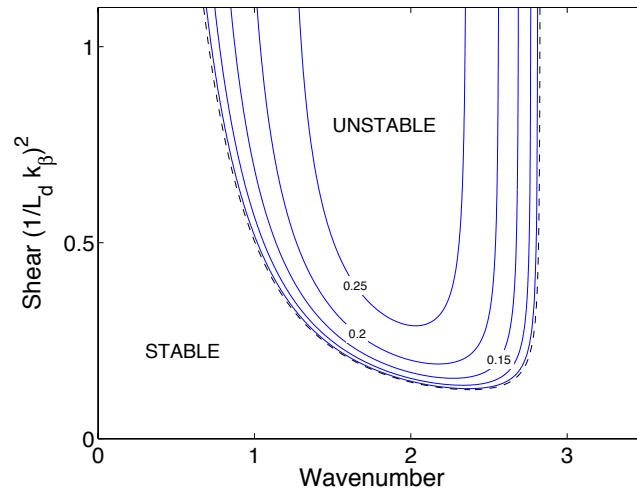
Fig. 6.15 Contours of growth rate in the two-layer baroclinic instability problem. The dashed line is the neutral stability curve obtained from (6.120), and the other curves are contours of growth rates obtained from (6.114). Outside of the dashed line, the flow is stable. The wavenumber is scaled by $1/L_d$ (i.e., by $k_d/\sqrt{8}$) and growth rates are scaled by the inverse of the Eady timescale (i.e., by U/L_d). Thus, for $L_d = 1000\,\text{km}$ and $U = 10\,\text{m s}^{-1}$, a nondimensional growth rate of 0.25 corresponds to a dimensional growth rate of $0.25 \times 10^{-5}\,\text{s}^{-1} = 0.216\,\text{day}^{-1}$.
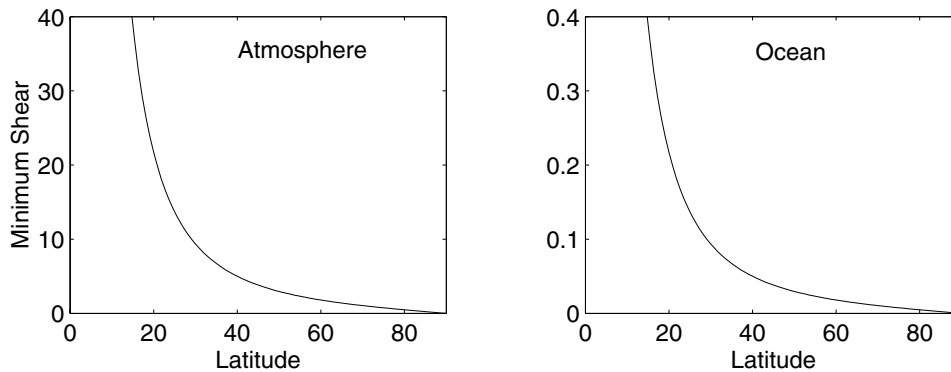
Fig. 6.16 The minimimum shear ($U_s = U_1 - U_2$, in m/s) required for baroclinic instability in a two-layer model, calculated using (6.123), i.e. $U_s = \beta L_d^2/4$ where $\beta = 2\Omega a^{-1}\cos\vartheta$ and $L_d = NH/f$, were $f = 2\Omega\sin\vartheta$. The left panel uses atmospheric parameters of $H = 10\,\text{km}$ and $N = 10^{-2}\,\text{s}^{-1}$, the right panel uses oceanic parameters representative of the main thermocline, $H = 1\,\text{km}$ and $N = 10^{-2}\,\text{s}^{-1}$. Because of the nonuniform stratification and nonzonal flow in the ocean, these values are likely to be even less quantitatively accurate than those of the atmosphere. However, the implications that the minimum shear is much less for the ocean and that in both atmosphere and ocean it increases rapidly at low latitudes, are quite robust.

Note the relationship of the minimum shear to the basic state potential vorticity gradient in the respective layers. In the upper and lower layers the potential vorticity gradients are given by, respectively,

$$\frac{\partial Q_1}{\partial y} = \beta + k_d{}^2 U, \qquad \frac{\partial Q_2}{\partial y} = \beta - k_d{}^2 U \qquad \text{(6.124a,b)}$$

Thus, the requirement for instability is exactly that which causes the potential vorticity gradient to change sign somewhere the domain, in this case in the lower layer. This is an example of the general rule that potential vorticity (suitably generalized to include the surface boundary conditions) must change sign somewhere in the domain in order for there to be an instability.

High-wavenumber cut-off:
Instability can only arise when, from (6.119),

$$4K^4(k_d^4 - K^4) > k_\beta^4 k_d^4, \qquad \text{(6.125)}$$

so that a necessary condition for instability is

$$k_d^2 > K^2. \qquad \text{(6.126)}$$

Thus, waves shorter than the deformation radius are always stable, no matter the value of β. We also see from Fig. 6.14 and Fig. 6.15 that the high wavenumber cut-off in fact varies little with β if $k_d \gg k_\beta$. Note that the critical shear required for instability approaches infinity as k approaches k_d.

Low-wavenumber cut-off:
Suppose that $k \ll k_d$. Then (6.119) simplifies to $k_\beta^4 < 4K^4$. That is, for instability we require

$$K^2 > \frac{1}{2} k_\beta^2 = \frac{\beta}{2U}. \qquad \text{(6.127)}$$

Thus, using (6.126) and (6.127) the unstable waves lie approximately in the interval $\beta/(\sqrt{2}U) < k < k_d$.

6.8 AN INFORMAL VIEW OF THE MECHANISM OF BAROCLINIC INSTABILITY

In this section we take a more intuitive look at baroclinic instability, trying to understand the mechanism without treating the problem in full generality or exactness. We will do this by way of semi-kinematic argument that shows how the waves in each layer of a two-layer model, or the waves on the top and bottom boundaries in the Eady model, can constructively interact to produce a growing instability. It is kinematic in the sense that we initially treat the waves independently, and only subsequently allow them to interact — but it is this dynamical interaction that gives the instability. We first revisit the two-layer model and simplify it to its bare essentials.

6.8.1 The two-layer model

A simple dynamical model

We first re-derive the instability *ab initio* from the equations of motion written in terms of the baroclinic streamfunction τ and the barotropic streamfunction ψ where

$$\tau \equiv \frac{1}{2}(\psi_1 - \psi_2), \qquad \psi \equiv \frac{1}{2}(\psi_1 + \psi_2). \qquad (6.128)$$

We linearize about a sheared basic state of with zero barotropic velocity and with $\beta = 0$. Thus, with $psi = 0 + \psi'$ and $\tau = -Uy + \tau'$ the linearized equations of motion, equivalent to (6.107) with $\beta = 0$, are

$$\frac{\partial}{\partial t}\nabla^2\psi = -U\frac{\partial}{\partial x}\nabla^2\tau, \qquad (6.129a)$$

$$\frac{\partial}{\partial t}(\nabla^2 - k_d^2)\tau = -U\frac{\partial}{\partial x}(\nabla^2 + k_d^2)\psi. \qquad (6.129b)$$

Seeking solutions of the form $(\psi, \tau) = \mathrm{Re}\,(\widetilde{\psi}, \widetilde{\tau})\exp[ik(x - ct)]$ gives

$$c\widetilde{\psi} - U\widetilde{\tau} = 0, \qquad (6.130a)$$

$$c(K^2 + k_d^2)\widetilde{\tau} - U(K^2 - k_d^2)\widetilde{\psi} = 0. \qquad (6.130b)$$

These equations have nontrivial solutions if the determinant of the matrix of coefficients is zero, giving the quadratic equation $c^2(K^2 + k_d^2) - U^2(K^2 - k_d^2) = 0$. Solving this gives

$$c = \pm U\left(\frac{K^2 - k_d^2}{K^2 + k_d^2}\right)^{1/2}. \qquad (6.131)$$

Instabilities occur for $K^2 < k_d^2$, for which $c = ic_i$; that is, it is purely imaginary. From (6.130) unstable modes have

$$\widetilde{\tau} = i\frac{c_i}{U}\widetilde{\psi} = e^{i\pi/2}\frac{c_i}{U}\widetilde{\psi}. \qquad (6.132)$$

That is, τ *lags* ψ by 90° for a growing wave ($c_i > 0$). Similarly, τ *leads* ψ by 90° for a decaying wave. Now, the temperature is proportional to τ, and it is advected by the vertically averaged perturbation meridional velocity, V (with Fourier mode $\widetilde{V}$) where $V = \partial\psi/\partial x$. Thus, for growing or decaying waves,

$$\widetilde{V} = \widetilde{\tau}\frac{kU}{c_i} \qquad (6.133)$$

and the meridional velocity is exactly *in phase* with the temperature for growing modes, and is *out of phase* with the temperature for decaying modes. That is, for unstable modes, polewards flow is correlated with high temperatures, and for decaying modes polewards flow is correlated with low temperatures. For neutral waves, $\widetilde{\tau} = c_r\widetilde{\psi}/U$ and so $\widetilde{V} = ik\tau U/c_r$ and the meridional velocity and temperature are $\pi/2$ out of phase. Thus, to summarize:

- ★ Growing waves transport heat (or buoyancy) polewards.
- ★ Decaying waves transport heat equatorward.
- ★ Neutral waves do not transport heat.

Further simplifications to the two-layer model

First consider (6.129) for waves much larger than the deformation radius; we obtain

$$\frac{\partial}{\partial t}\nabla^2\psi = -U\frac{\partial}{\partial x}\nabla^2\tau, \qquad \frac{\partial}{\partial t}\tau = U\frac{\partial}{\partial x}\psi. \qquad (6.134\text{a,b})$$

for which we obtain $c = \pm iU$; that is, the flow is unstable. To see the mechanism, suppose that the initial perturbation is barotropic and sinusoidal in x, with no y variation. Polowards flowing fluid (with $\partial\psi/\partial x > 0$ will, by (6.134b), generate a positive τ, and the baroclinic flow will be out of phase with the barotropic flow. Then, by (6.134a), the advection of τ by the mean shear produces growth of ψ that is in phase with the original disturbance. Contrast this case with that for very small disturbances, for which $K^2 \gg k_d^2$ and (6.129) becomes

$$\frac{\partial}{\partial t}\nabla^2\psi = -U\frac{\partial}{\partial x}\nabla^2\tau, \qquad \frac{\partial}{\partial t}\nabla^2\tau = -U\frac{\partial}{\partial x}\nabla^2\psi. \qquad (6.135\text{a,b})$$

or, in terms of the equations for each layer,

$$\frac{\partial}{\partial t}\nabla^2\psi_1 = -U\frac{\partial}{\partial x}\nabla^2\psi_1, \qquad \frac{\partial}{\partial t}\nabla^2\psi_2 = +U\frac{\partial}{\partial x}\nabla^2\psi_2. \qquad (6.136\text{a,b})$$

That is, the layers are completely decoupled and no instability can arise. Motivated by this, consider waves that propagate independently in each layer on the potential vorticity gradient caused by β (if non-zero) and shear. Thus in (6.107) we keep the potential vorticity gradients but neglect k_d^2 where it appears alongside ∇^2 and find

$$\left[\frac{\partial}{\partial t} + U\frac{\partial}{\partial x}\right]\nabla^2\psi_1' + \frac{\partial\psi_1'}{\partial x}\frac{\partial Q_1}{\partial y} = 0, \qquad (6.137\text{a})$$

$$\left[\frac{\partial}{\partial t} - U\frac{\partial}{\partial x}\right]\nabla^2\psi_2' + \frac{\partial\psi_2'}{\partial x}\frac{\partial Q_2}{\partial y} = 0. \qquad (6.137\text{b})$$

where $\partial Q_1/\partial y = \beta + k_d^2 U$ and $\partial Q_1/\partial y = \beta - k_d^2 U$. The phase speeds of the associated waves are

$$c_1 = U - \frac{\partial_y Q_1}{K^2}, \qquad c_2 = -U - \frac{\partial_y Q_2}{K^2}, \qquad (6.138\text{a,b})$$

In the upper layer the phase speed is a combination of an eastward advection and a fast westward wave propagation due to a strong potential vorticity gradient. In the lower layer the phase speed is a combination of a westward advection and a slow eastward wave propagation due to the weak potential vorticity gradient. The two phase speeds are, in general, not equal, but they would need to be so if they are to combine to cause an instability. From (6.138) this occurs when $K^2 = k_d^2$ and $c_1 = c_2 = -\beta/k_d^2$. These conditions are just those occuring at the high-wavenumber cut-off to instability in the two-level model. For higher wavenumbers, the waves are unable to synchronize, whereas lower wavenumbers they may become inextricably coupled.

Let us suppose that the phase of the wave in the upper layer lags that (i.e., is westward of) that in the lower layer, as illustrated in the top panel Fig. 6.17. The lower

Figure 6.17 Baroclinically unstable waves in a two layer model. The streamfunction is shown in the top panel, ψ_1 for the top layer and ψ_2 for the bottom layer. Given the westward tilt shown, the temperature, τ, and meridional velocity, V, (bottom panel) are in phase, and the instability grows.
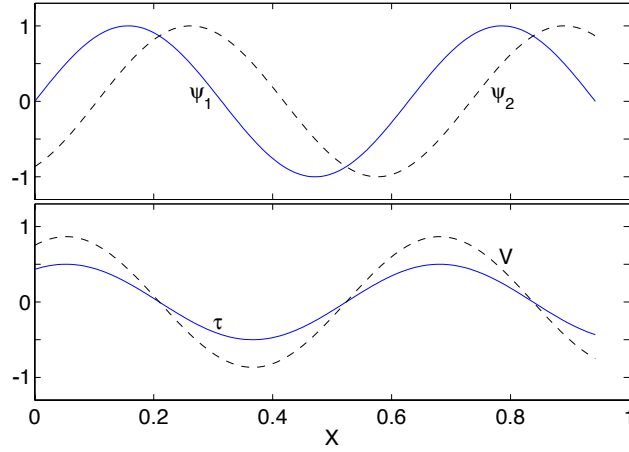
panel shows the temperature field, $\tau = (\psi_1 - \psi_2)/2$, and the average meridional velocity, $V = \partial_x(\psi_1 + \psi_2)/2$. In this configuration, the temperature field is *in phase* with the meridional velocity, meaning that warm fluid is advected polewards. Now, let us allow the waves in the two layers to interact by adding one dynamical equation, the thermodynamic equation, which in its simplest form is

$$\frac{\partial \tau}{\partial t} = -v \frac{\partial \overline{\tau}}{\partial y} = f_0 v \frac{\partial \overline{u}}{\partial z}, \tag{6.139}$$

where $\overline{\tau}$ is the basic state temperature field. The temperature field grows in proportion to v, which is proportional to τ if the waves tilt westward with height, and an instability results. This dynamical mechanism is just that which is compactly described by (6.134). It is a straightforward matter to show that if the streamfunction tilts eastward with height, v is out of phase with τ and the waves decay.

6.8.2 Interacting edge waves in the Eady problem

A very similar description applies to the Eady problem. As in the two-layer case, first consider the case in which the bottom and top surfaces are essentially uncoupled. Instead of solutions of (6.81) that have the structure (6.82) (which satisfies both boundary conditions) consider solutions that *separately* satisfy the bottom and top boundary conditions and that decay into the interior. These are, including the x-dependence,

$$\psi_B = \text{Re } A_B \, e^{ik(x-c_1 t)} e^{-\mu z/H}, \qquad \psi_T = \text{Re } A_T \, e^{i\phi} e^{ik(x-c_2 t)} e^{\mu(z-H)/H}. \tag{6.140a,b}$$

for the bottom and top surfaces respectively, and ϕ is the phase shift, with A_B and A_T being real constants. The boundary conditions (6.80) then determine the phase speeds of the two systems and we find

$$c_B = \frac{\Lambda H}{\mu}, \qquad c_T = \Lambda H \left(1 - \frac{1}{\mu}\right). \tag{6.141a,b}$$

These are the phase speeds of *edge waves* in the Eady problem; they are real and in general they are unequal. It must therefore be the *interaction* of the waves on the upper and lower boundaries that is necessary for instability; this can occur when their phase speeds are equal and from (6.141) this is when $\mu = 2$, giving

$$k = \frac{2}{L_\mathrm{d}} \qquad \text{and} \qquad c = \frac{\Lambda H}{2} \qquad\qquad (6.142\text{a,b})$$

This phase speed is just that of the flow at mid-level, and at the critical wavenumber in the full Eady problem [$k_c = 2.4/L_\mathrm{d}$, from (6.90)] the phase speed is purely real and equal to that of (6.142b) — see Fig. 6.10. Thus, (6.142) approximately characterizes the critical wavenumber in the full problem.

   To turn this kinematic description into a dynamical instability, suppose that the two rigid surfaces are close enough so that the waves can interact, but still far enough so that their structure is approximately given by (6.140). (Note that if μ is too large, the waves decay rapidly away from the edges and will not interect.) Specifically, let the temperature perturbation at a given boundary be advected by the total meridional velocity perturbation, including that arising from the perturbation at the other boundary, so that at the top boundary

$$\frac{\partial b'_\mathrm{T}}{\partial t} = -(v'_\mathrm{B} + v'_\mathrm{T})\frac{\partial \overline{b}_\mathrm{T}}{\partial y} \qquad\qquad (6.143)$$

and similarly for the lower. The waves will reinforce each other if v'_T is in phase with b'_B at the lower boundary, and if v'_B is in phase with b'_B at the upper boundary. Now, the velocity and buoyancy associated with (6.140) are given by, omitting the harmonic x-dependence,

$$b_\mathrm{B} = -\mathrm{Re}\, kNA_\mathrm{B}\, e^{-\mu z/H}, \qquad b_\mathrm{T} = \mathrm{Re}\, kNA_\mathrm{T}\, e^{i\phi}e^{\mu(z-H)/H}, \qquad (6.144\text{a})$$

$$v_\mathrm{B} = \mathrm{Re}\, ikA_\mathrm{B}\, e^{-\mu z/H}, \qquad v_\mathrm{T} = \mathrm{Re}\, ikA_\mathrm{T}\, e^{i\phi}e^{\mu(z-H)/H}. \qquad (6.144\text{b})$$

The fields b_T and v_T, and b_B and v_T, will will be positively correlated if $0 < \phi < \pi$, and will be exactly in in phase if $\phi = \pi/2$, and this case is illustrated in Fig. 6.18. Just as in the two-layer case, this phase corresponds to a westward tilt with height, and it is this, in conjunction with geostrophic and hydrostatic balance, that allows warm fluid to move poleward and available potential energy to be released. From (6.143), the perturbation will grow and an instability will result. The analogy between baroclinic instability and barotropic instability should be evident from the similarity of this description and that of section 6.2.4, with z in the baroclinic problem playing the role of y in the barotropic problem, and b the role of v. However, the analogy is not perfect, on two grounds. First, the boundary condition that $w = 0$ does have an exact correspondence in the barotropic problem; second, the nonlinear development of the baroclinic problem, discussed in chapterch:geoturb, is generally three-dimensional whereas barotropic development can remain two-dimensional.

Figure 6.18 Interacting edge waves in the Eady model. The upper panel shows waves on the top surface, and the lower panel waves on the bottom. If the streamfunction tilts westward with height, then the temperature on the top (bottom) is correlated with the meridional velocity on the bottom (top), the waves can reinforce each other. See also Fig. 6.12.
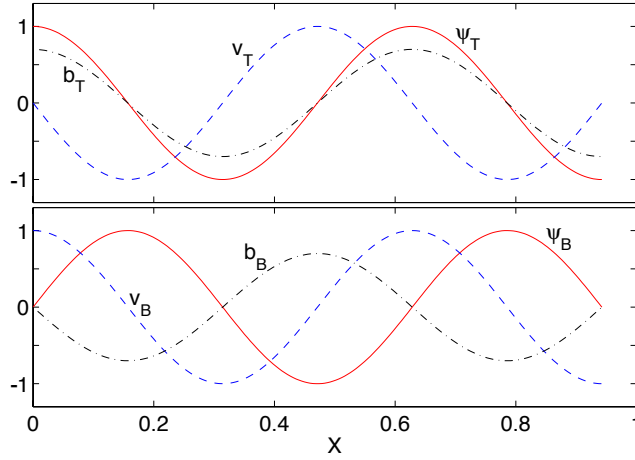
6.9 * THE ENERGETICS OF LINEAR BAROCLINIC INSTABILITY

In baroclinic instability, warm parcels move poleward and cold parcels move equatorward. This motion draws on the available potential energy of the mean state, because warm light parcels move upward, and cold dense parcels downward and the height of the mean center of gravity of the fluid falls, and the loss of potential energy is converted to kinetic energy of the perturbation. However, because the instability is growing, the energy of the perturbation is of course not conserved, and both the kinetic energy and the available potential energy of the perturbation will grow. However, we still expect a conversion of potential energy to kinetic, and the purpose of this section is to demonstrate that explicitly. For simplicity, we restrict attention to the two-layer model with $\beta = 0$.

As in section 5.6, the energy may be partitioned into kinetic energy and available potential energy. In a three-dimensional quasi-geostrophic flow the kinetic energy is given by, in general,

$$KE = \frac{1}{2} \int (\nabla \psi)^2 \, dV \tag{6.145}$$

which, in the case of the two-layer model becomes

$$KE = \frac{1}{2} \int (\nabla \psi_1)^2 + (\nabla \psi_2)^2 \, dA = \int (\nabla \psi)^2 + (\nabla \tau)^2 \, dA. \tag{6.146}$$

Restricting attention to a single Fourier mode this becomes

$$KE = k^2 \widetilde{\psi}^2 + k^2 \widetilde{\tau}^2. \tag{6.147}$$

The available potential energy in the continuous case is given by

$$APE = \frac{1}{2} \int \left(\frac{f_0}{N} \right)^2 \left(\frac{\partial \psi}{\partial z} \right)^2 \, dV. \tag{6.148}$$

For a single Fourier mode in a two layer model this becomes

$$APE = k_d^2 \widetilde{\tau}^2. \tag{6.149}$$

Now, the nonlinear vorticity equations for each level is

$$\frac{\partial}{\partial t} \nabla^2 \psi_1 + J(\psi_1, \nabla^2 \psi_1) = -2 \frac{f_0 w}{H} \qquad (6.150a)$$

$$\frac{\partial}{\partial t} \nabla^2 \psi_2 + J(\psi_2, \nabla^2 \psi_2) = 2 \frac{f_0 w}{H} \qquad (6.150b)$$

where w is the vertical velocity between the levels. Multiplying these equation by $-\psi_1$ and $-\psi_2$ and adding we find

$$\frac{\mathrm{d}}{\mathrm{d}t} KE = \frac{4 f_0}{H} \int w\tau \, \mathrm{d}A \qquad (6.151a)$$

For a single Fourier mode this becomes

$$\frac{\mathrm{d}}{\mathrm{d}t} KE = \mathrm{Re} \, \frac{4 f_0}{H} \widehat{w} \widetilde{\tau}^* \qquad (6.151b)$$

where $w = \widehat{w} \exp[i(kx - ct)] + \text{c.c.}$, and the asterisk denotes complex conjugacy.

The continuous thermodynamic equation is

$$\frac{\mathrm{D}b}{\mathrm{D}t} + wN^2 = 0 \qquad (6.152)$$

which, using $b = f_0 \partial \psi / \partial z$ and finite-differencing, becomes in the two-level model

$$\frac{\partial \tau}{\partial t} + J(\psi, \tau) + \frac{wN^2 H}{4 f_0} = 0. \qquad (6.153)$$

The change of available potential energy is obtained from this by multiplying by $k_d^2 \tau$ and integrating, giving

$$\int \left(\frac{1}{2} \frac{\mathrm{d}}{\mathrm{d}t} k_d^2 \tau^2 + \tau w \frac{2 f_0}{H} \right) \mathrm{d}A = 0 \qquad (6.154)$$

or

$$\frac{\mathrm{d}}{\mathrm{d}t} APE = -\frac{4 f_0}{H} \int w\tau \, \mathrm{d}A \qquad (6.155a)$$

or, for a single Fourier mode,

$$\frac{\mathrm{d}}{\mathrm{d}t} APE = -\mathrm{Re} \, \frac{4 f_0}{H} \widetilde{w} \, \widetilde{\tau}^*. \qquad (6.155b)$$

From (6.151) and (6.155) it is clear that in the nonlinear equations the sum of the kinetic energy and the available potential energy is conserved.

We now specialize by obtaining w from the linear baroclinic instability problem. Using this in (6.151) and (6.155) will give us the conversion between kinetic energy and potential energy in the growing baroclinic wave. It is important to realize that the total energy of the disturbance is not conserved — both the potential and kinetic energy are growing, exponentially in this problem, because they are extracting energy from

the mean state. To calculate w we use the linearized thermodynamic equation. From (6.153) this is

$$\frac{\partial \tau}{\partial t} - U \frac{\partial \psi}{\partial x} + \frac{HwN^2}{4f_0} = 0, \qquad (6.156)$$

omitting the primes on perturbation quantities. For a single Fourier mode, this gives

$$\frac{HN^2}{4f_0} \widetilde{w} = ik(c\widetilde{\tau} + U\widetilde{\psi}). \qquad (6.157)$$

But, from (6.130), $c\widetilde{\psi} = U\widetilde{\tau}$ in two-layer f-plane baroclinic instability and so

$$\frac{HN^2}{4f_0} \widetilde{w} = ikc\widetilde{\tau}\left(1 + \frac{U^2}{c^2}\right) = ikc\widetilde{\tau}\left(\frac{2k^2}{k^2 - k_d^2}\right). \qquad (6.158)$$

using (6.131). For stable waves, $k^2 > k_d^2$ and $c = c_r$ and in that case the vertical velocity is $\pi/2$ out of phase with the temperature, and there is no conversion of APE to KE. For unstable waves $c = ic_i$ and $k^2 < k_d^2$, and the vertical velocity is in phase with the temperature. That is, warm air is rising and so there is a conversion of APE to KE To see this more formally, recall that the conversion from APE to KE is given by $4W\widetilde{\tau}^* f_0/H$. Thus, using (6.158),

$$\frac{\mathrm{d}}{\mathrm{d}t}(APE \rightarrow KE) = \mathrm{Re}\, 2ikck_d^2 \left(\frac{2k^2}{k^2 - k_d^2}\right)\widetilde{\tau}^2. \qquad (6.159)$$

If the wave is growing, then $k^2 < k_d^2$ and $c = ic_i$ and the right-hand side is real and positive. For neutral waves, If $c = c_r$ the right-hand side of (6.159) is pure imaginary, and so the conversion is zero. This completes our demonstration that baroclinic instability converts potential energy into kinetic energy.

6.10 * BETA, SHEAR AND STRATIFICATION IN A CONTINUOUS MODEL

The two-layer model illustrates many of the qualitative effects of β on baroclinic instability. Do these carry over to the continuously stratified case? The answer by-and-large is yes, but with some important qualifications that generally concern weak or shallow instabilities. In particular, we will find that there is no short-wave cut-off in the continuous model with non-zero beta, and that the instability determines its own depth scale. We will illustrate these properties first by way of scaling arguments, and then by way of numerical calculations.[12]

6.10.1 Scaling arguments for growth rates, scales and depth

With finite density scale height and non-zero β, the potential vorticity equation, linearized about a mean zonal velocity $U(z)$, is

$$\left(\frac{\partial}{\partial t} + U\frac{\partial u}{\partial x}\right)q' + \frac{\partial \psi'}{\partial x}\frac{\partial Q}{\partial y} = 0, \qquad (6.160)$$

where

$$q' = \nabla^2 \psi' + \frac{f_0^2}{\rho} \frac{\partial}{\partial z} \left(\frac{\rho}{N^2} \frac{\partial \psi'}{\partial z} \right), \tag{6.161}$$

$$\frac{\partial Q}{\partial y} = \beta - \frac{f_0^2}{\rho} \frac{\partial}{\partial z} \left(\frac{\rho}{N^2} \frac{\partial U}{\partial z} \right), \tag{6.162}$$

and ρ is a specified density profile. If we assume that $U = \Lambda z$ where Λ is constant and that N is constant, and let $H_\rho^{-1} = -\rho^{-1} \partial \rho / \partial z$, then

$$\frac{\partial Q}{\partial y} = \beta + \frac{f_0^2 \Lambda}{N^2 H_\rho} = \beta(1 + \alpha) \tag{6.163}$$

where

$$\alpha = \left(\frac{f_0^2 \partial U / \partial z}{\beta N^2 H_\rho} \right), \tag{6.164}$$

The boundary conditions on (6.160) are

$$\left(\frac{\partial}{\partial t} + U \frac{\partial}{\partial x} \right) \frac{\partial \psi'}{\partial z} - \frac{\partial \psi'}{\partial x} \frac{\partial U}{\partial z} = 0, \qquad \text{at } z = 0 \tag{6.165}$$

and that $\psi \to 0$ as $z \to \infty$. The problem we have defined essentially constitutes the Charney problem. We can reduce this to the Eady problem by setting $\beta = 0$ and $H_\rho = \infty$, and providing a lid some finite height above the ground.

As in the Eady problem, we seek solutions of the form

$$\psi = \text{Re } \widetilde{\psi}(z) e^{i(kx + ly - kct)} \tag{6.166}$$

and substituting into (6.160) gives

$$\left(\frac{f_0^2}{H_\rho^2 N^2} \right) \left(H_\rho^2 \frac{d^2 \widetilde{\psi}}{dz^2} - H_\rho \frac{d\widetilde{\psi}}{dz} \right) - \left(K^2 - \frac{\beta + \Lambda f_0^2 / (N^2 H_\rho)}{\Lambda z - c} \right) \widetilde{\psi} = 0 \quad (6.167)$$

The Boussinesq version of this expression for a fluid contained between two horizontal surfaces is just

$$\left(\frac{f_0^2}{N^2} \right) \frac{d^2 \widetilde{\psi}}{dz^2} - \left(K^2 - \frac{\beta}{\Lambda z - c} \right) \widetilde{\psi} = 0 \tag{6.168}$$

It seems natural to nondimensionalize (6.167) using:

$$z = H_\rho \hat{z}, \qquad c = \Lambda H_\rho \hat{c}, \qquad K = \left(\frac{f_0}{N H_\rho} \right) \hat{K}, \tag{6.169}$$

whence it becomes

$$\frac{d^2 \widetilde{\psi}}{d\hat{z}^2} - \frac{d\widetilde{\psi}}{d\hat{z}} - \left(\hat{K}^2 - \frac{\gamma + 1}{\hat{z} - \hat{c}} \right) \widetilde{\psi} = 0 \tag{6.170}$$

where

$$\gamma = \alpha^{-1} = \frac{\beta N^2 H_\rho}{f_0^2 \Lambda} = \frac{\beta L_d^2}{H_\rho \Lambda} = \frac{H_\rho}{h}. \tag{6.171}$$

where $h \equiv \Lambda f_0^2/(\beta N^2)$. The non-dimensional parameter γ is known as the Charney-Green number.[13] The Boussinesq version, (6.168), may be non-dimensionalized using H_D in place of H_ρ, where H_D is the depth of the fluid between two rigid surfaces. In that case

$$\frac{\mathrm{d}^2 \widetilde{\psi}}{\mathrm{d}\widehat{z}^2} - \left(\widehat{K}^2 - \frac{\gamma}{\widehat{z} - \widehat{c}} \right) \widetilde{\psi} = 0, \tag{6.172}$$

where here the non-dimensional variables are scaled with H_D.

Now, suppose that γ is large, for example if β or the static stability are large or the shear is weak. Eq. (6.170) admits of no non-trivial balance, suggesting that we rescale the variables using h instead of H_ρ as the vertical scale in (6.169). The rescaled version of (6.170) is then

$$\frac{\mathrm{d}^2 \widetilde{\psi}}{\mathrm{d}\widehat{z}^2} - \frac{1}{\gamma} \frac{\mathrm{d}\widetilde{\psi}}{\mathrm{d}\widehat{z}} - \left(\widehat{K}^2 - \frac{1 + \gamma^{-1}}{\widehat{z} - \widehat{c}} \right) \widetilde{\psi} = 0, \tag{6.173}$$

or, approximately,

$$\frac{\mathrm{d}^2 \widetilde{\psi}}{\mathrm{d}\widehat{z}^2} - \left(\widehat{K}^2 - \frac{1}{\widehat{z} - \widehat{c}} \right) \widetilde{\psi} = 0. \tag{6.174}$$

This is exactly the same equation as results from a similar rescaling of the Boussinesq system, (6.172), as we might have expected because now the dynamical vertical scale, h, is much smaller than the scale height H_ρ (or H_D) and the system is essentially Boussinesq. Thus, noting that (6.174) has the same nondimesional form as (6.172) save that γ is replaced by unity, and that (6.174) with $\gamma = 1$ must produce the same scales and growth rates as in the Eady problem, we may deduce that:

 (i) The wavelength of the instability is $\mathcal{O}(Nh/f_0)$.
 (ii) The growth rate of the instability is $\mathcal{O}(Kc) = \mathcal{O}(f_0 \Lambda/N)$.
 (iii) The vertical scale of the instability is $\mathcal{O}(h) = \mathcal{O}(f_0^2 \Lambda/(\beta N^2))$.

These are the same as for the Eady problem, except with the dynamical height h replacing the geometric or scale height H_D. Effectively, the dynamics has determined its own vertical scale, h, that is much less than the scale height or geometric height, producing 'shallow modes'.

In the limit $\gamma \ll 1$ (strong shear, weak β), the Boussinesq and compressible problems differ. The Boussinesq problem reduces to the Eady problem, considered previously, whereas (6.170) becomes, approximately,

$$\frac{\mathrm{d}^2 \widetilde{\psi}}{\mathrm{d}\widehat{z}^2} - \frac{\mathrm{d}\widetilde{\psi}}{\mathrm{d}\widehat{z}} - \left(\widehat{K}^2 - \frac{1}{\widehat{z} - \widehat{c}} \right) \widetilde{\psi} = 0, \tag{6.175}$$

and in this limit the appropriate vertical scale is the density scale height H_ρ. Because $H_\rho \gg h$ these are 'deep modes', occupying the entire vertical extent of the domain.

The scale h does not arise in the two-level model, but there is a connection between it and the critical shear for instability in the two-level model. The condition $\gamma \ll 1$, or $h \gg H$, may be written as

$$H\Lambda \gg \beta \left(\frac{NH}{f_0} \right)^2. \tag{6.176}$$

Compare this with the necessary condition for instability in a two-level model, (6.123), namely

$$(U_1 - U_2) > \beta \left(\frac{N H_\Delta}{f_0} \right)^2 \tag{6.177}$$

where H_Δ is the vertical distance between the two levels. Thus, essentially the same condition governs the onset of instability in the two-level model as governs the production of deep modes in the continuous model. This correspondence is a natural one, because the two-level model *all* modes are 'deep', and the model fails (as it should) to capture the shallow modes of the continuous system. For similar reasons, there is a high-wavenumber cut-off in the two-level model: in the continuous model these modes are shallow and so cannot be captured by two-level dynamics. Somewhat counter-intuitively, for these modes the β-effect must be important, even though the modes have small horizontal scale: when $\beta = 0$ the instability arises via an interaction between edge waves at the top and bottom of the domain, whereas the shallow instability arises via an interaction of the edge waves at the surface with Rossby waves just above the surface.

6.10.2 Some numerical calculations

Adding β to the Eady model

Our first step add the β-effect to the Eady problem.[14] That is, we suppose a Boussinesq fluid with uniform stratification, that the shear is zonal and constant, and that the entire problem is sandwiched between two rigid surfaces. Growth rates and phase speeds of such an instability calculation are illustrated in Fig. 6.19 and the vertical structure is shown in Fig. 6.20. As in the two-layer problem, there is a low-wavenumber cut-off to the main instability, although there is now an additional weak instability at very large-scales. These so-called *Green modes* have no counterpart in the two-layer model — they are deep, slowly growing modes that will be dominated by faster growing modes in most real situations. Also, the fact that the Green modes have a scale much larger than the deformation scale suggests a degree of caution in the accuracy of the quasi-geostrophic calculation is warranted. At high wavenumbers is no cut-off to the instability in the continuous problem in the case of non-zero beta; the high-wavenumber modes are shallow and unstable via an interaction between edge waves at the lower boundary and Rossby waves in the lower atmosphere, and so have no counterpart in either the the two-layer problem (where the modes are deep) or the Eady problem (which has no Rossby waves).

Effects of nonuniform shear and stratification

If the shear or stratification is non-uniform an analytic treatment is, even in problems without β, usually impossible and the resulting equations must be solved numerically. However, if we restrict attention to a *discontinuity* in the shear or the stratification, then resulting problem is very similar to the problem with rigid boundaries, and this property provides much of the justification for using the Eady problem to model instabilities in the earth's atmosphere: in the troposphere the stratification is (approximately) constant,
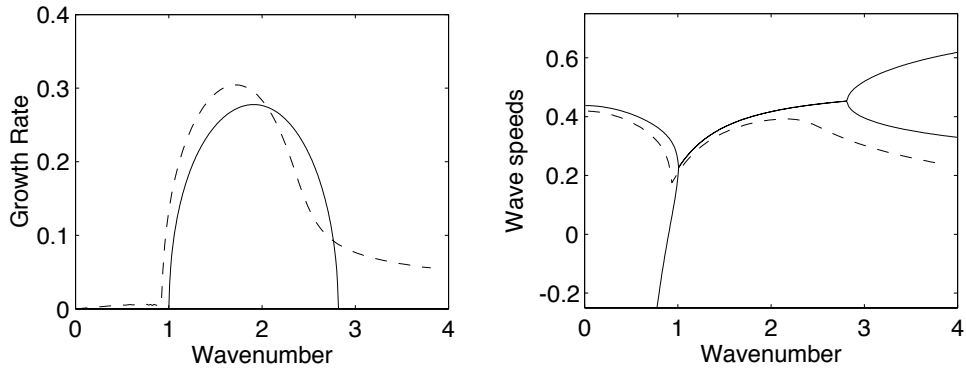
Fig. 6.19 Growth rates and wave speeds for the two-layer (solid) and continuous (dashed) models, with the same values of the Charney-Green number, γ, and uniform shear and stratification. (In the two-layer case $\gamma = \beta L_d^2/[2(U_1-U_2)] = 0.5$, and in the continuous case $\gamma = \beta L_d^2/(H\Lambda) = 0.5$.) In the continuous case only the wave speed associated with the unstable mode is shown. In the two-layer case there are two real wave speeds which coalesce in the unstable region. The two-layer model has an abrupt short-wave and long-wave cut-off, whereas the growth rate of the continuous model tails off gradually at small wavelengths, and has a weak instability (the 'Green modes') at large wavelengths.

and the rapid increase in stratification in the stratosphere can be approximated by a lid at tropopause. Heuristically, we can see this from the form of the thermodynamic equation, namely

$$\frac{\mathrm{D}b}{\mathrm{D}t} + N^2 w = 0. \tag{6.178}$$
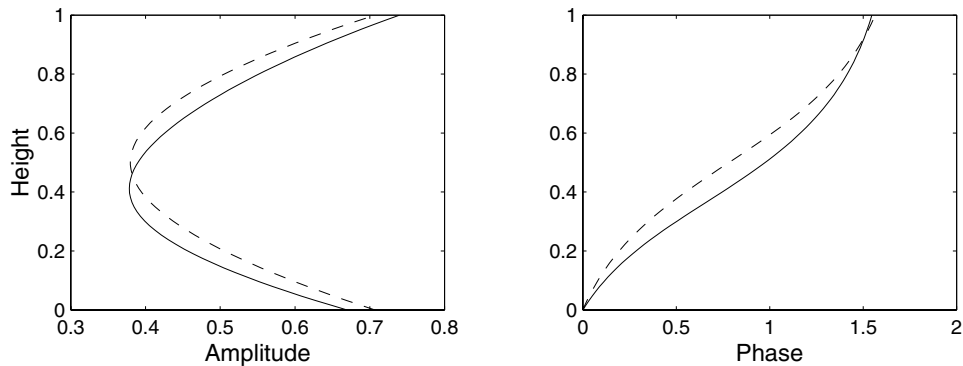
Fig. 6.20 Vertical structure of the most unstable modes in a continuously stratified instability calculation with $\beta = 0$ (dashed lines, the Eady problem) and $\beta \neq 0$ (solid lines), as in Fig. 6.19. The effect of beta is to depress the height of maximum amplitude of the instability.

If N^2 is high this suggests w will be small, and a lid is the limiting case of this. The oceanic problem is rather more involved, because although both the stratification and shear are concentrated in the upper ocean, they vary relatively smoothly; furthermore, the shear is high where the stratification is high, and the two have opposing effects.

To go one step further, consider Boussinesq potential vorticity equation, linearized about a zonally uniform state $\Psi(y, z)$, with a rigid surface at $z = 0$. The normal-mode evolution equations are similar to (6.69), namely

$$(U - c)\left[\frac{\partial^2}{\partial y^2} - k^2 + \frac{\partial}{\partial z}\left(F\frac{\partial}{\partial z}\right)\right]\tilde{\psi} + \frac{\partial Q}{\partial y}\tilde{\psi} = 0, \qquad\qquad z > 0, \quad (6.179\text{a})$$

$$(U - c)\frac{\partial \tilde{\psi}}{\partial z} - \frac{\partial U}{\partial z}\tilde{\psi} = 0, \qquad\qquad \text{at } z = 0. \quad (6.179\text{b})$$

where $\partial_y Q = \beta - \partial_{yy}U - \partial_z(F\partial_z U)$. Now suppose that there is a discontinuity in the shear and/or the stratification in the interior of the fluid, at some level $z = z_c$.

Integrating (6.179a) across the discontinuity, noting that $\tilde{\psi}$ is continuous in z, gives

$$(U - c)\left[F\frac{\partial \tilde{\psi}}{\partial z}\right]_{z_c-}^{z_c+} - \tilde{\psi}(y, z_c)\left[F\frac{\partial U}{\partial z}\right]_{z_c-}^{z_c+} = 0. \qquad\qquad (6.180)$$

which has similar form to (6.179b). This construction is evocative of the equivalence of a delta-function sheet of potential vorticity at a rigid boundary, except that now a discontinuity in the potential vorticity in the *interior* has a similarity with a rigid boundary.

We can illustrate the effects of an interior discontinuity that crudely represents the tropopause by numerically solving the linear eigenvalue problem. For simplicity, we pose the problem on the f-plane, in a horizontally doubly-periodic domain, with no horizontal variation of shear, and between two horizontal rigid lids. The eigenvalue problem is defined by (6.69), and the numerical procedure then solves for the complex eigenvalue c and eigenfunction $\tilde{\psi}(z)$; various results are illustrated in Fig. 6.21. To parse this rather complex figure, first look at the solid curves in all the panels. These arise when the problem is solved with a uniform shear and a uniform stratification, with a lid at $z = 0$ and $z = 1$, so simply giving the Eady problem. The familiar growth rates and vertical structure of the solution are given by the solid curves in panels (b), (c) and (d), and these are just the same as in Fig. 6.10. The various dotted and dashed curves show the results when the lid at $z = 1$ is replaced by stratosphere stretching from $1 < z < 2$ either with high stratification, zero shear, or both, an in all of these cases the stratosphere acts in the same qualitative way as a rigid lid. The vertical structure of the solution in the troposphere in all cases is quite similar, and the amplitude decays rapidly above the idealized tropopause, consistent with the almost uniform phase of the disturbance illustrated in (panel (d); recall that a tilting of the disturbance with height is necessary for instability). It is these properties that make the Eady problem, or more generally any baroclinic instability problem that is posed between two rigid lids, of more general applicability to the earth's atmosphere than might be first thought: the high stratification above the tropopause and consequent decay of the instability is mimicked by the imposition of a rigid lid. (Of course, the β effect is still absent in the Eady problem.)
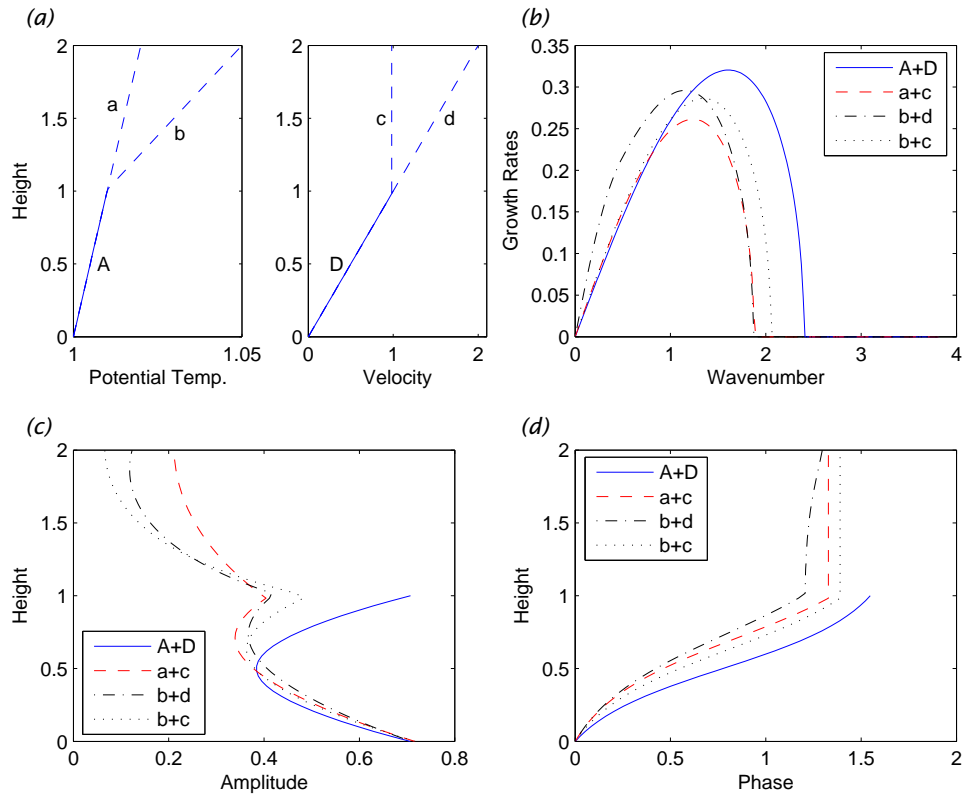
Fig. 6.21 The effect of a stratosphere on baroclinic instability. (a) the given profiles of shear and stratification; (b) The growth rate of the instabilities; (c) amplitude of the most unstable mode as a function of height; (d) phase of the most unstable mode. The instability problem is numerically solved with various profiles of stratification and shear. In each profile, in the idealized troposphere ($z < 1$) the shear and stratification are uniform and the same in each case. We consider four idealized stratospheres ($z \geq 1$): 1, A lid at $z = 1$, i.e., no stratosphere, so Eady problem itself (profiles A+D, solid lines); 2, Stratospheric stratification same as the troposphere, but zero shear (profiles a+c, dashed); 3, Stratospheric shear same as troposphere, but stratification (N^2) four times the tropospheric value (b+d, dot-dashed); 4, Zero shear and high stratification in the stratosphere (b+c, dotted). In the troposphere the amplitude and structure of the instability is similar in all cases, illustrating the similarity of a rigid-lid and abrupt changes in shear or stratification. Either a high stratification or a low shear (or both) will result in weak stratospheric instability.

In the ocean, the stratification is highest in the upper ocean where the shear is also strongest, and numerical calculations of the structure and growth rate of idealized profiles illustrated in Fig. 6.22. The solid currve shows the Eady problem, and the various dashed curves show the phase speeds, growth rates and phase with combinations of the profiles illustrated in panel (a). Much of the ocean is characterized by having both a higher shear and a higher stratification in the upper 1 km or so, and this case is the one with the dotted line in Fig. 6.22. In this case the amplitude of the instability is
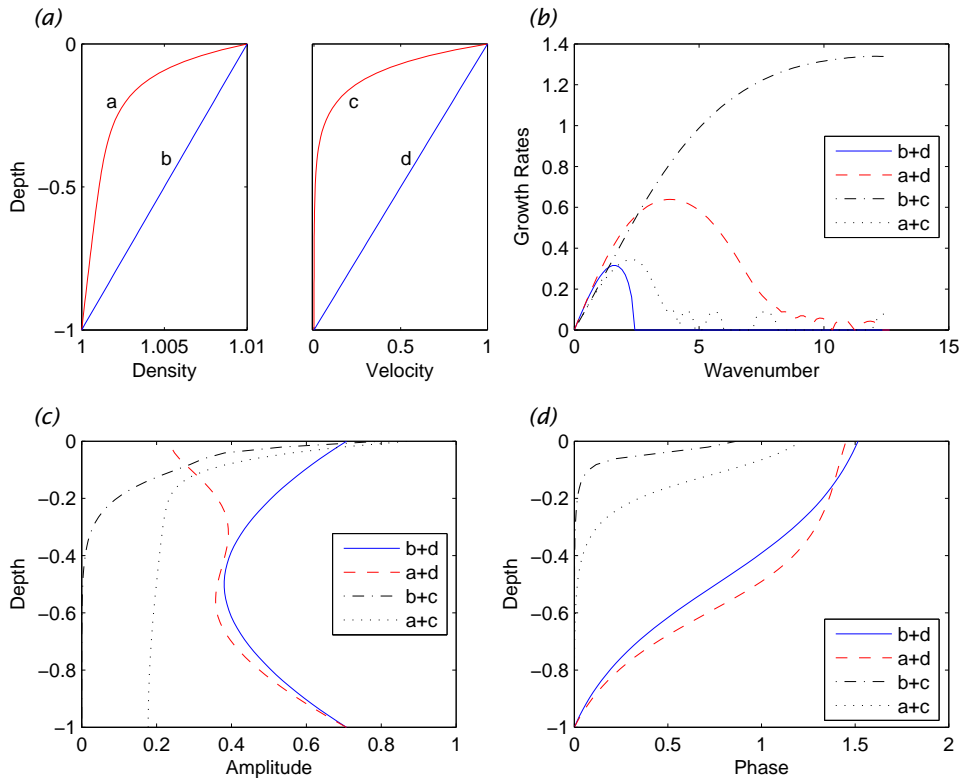
Fig. 6.22 The baroclinic instability in an idealized ocean, with four different profiles of shear or stratification. The panels are: (a) The profiles of velocity and density (and so N^2) used; (b) the growth rates of the various cases; (c) The vertical structure of the amplitude of the most unstable models; (d) the phase in the vertical of the most unstable modes. The instability is numerically calculated with four combinations of shear and stratification: 1, Uniform stratification and shear i.e. the Eady problem, (profiles b+d, solid lines). 2, Uniform shear, upper-ocean enhanced stratification (a+d, dashed); 3, Uniform stratification, upper ocean enhanced shear (b+c, dot-dashed); 4, Both stratification and shear enhanced in upper ocean (a+c, dotted). Case 2 is really more like to an atmosphere with a stratosphere (see Fig. 6.21), and the amplitude of the disturbance falls off, rather unrealistically, in the upper ocean. Case 4 (a+c, dotted) is the most oceanically relevant.

also largely confined to the upper ocean, and unlike the Eady problem it does not arise through the interaction of edge waves at the top and bottom: the potential vorticity changes sign because of the interior variations due to the nonuniform shear, mainly in the upper ocean. Consistently, the phase of the baroclinic waves is nearly constant in the lower ocean in the two cases in which the shear is confined to the upper ocean. The ocean itself is still more complicated, because the most unstable regions near intense western boundary currents are often also barotropically unstable, and the mean flow itself may be meridionally directed. Nevertheless, the result that linear baroclinic instability is primarily an *upper ocean* phenomonom is quite robust.[15] However, we

will find in chaper 9 that the nonlinear evolution of baroclinic instability leads to eddies throughout the water column.

Notes

1 Thomson, W. (Lord Kelvin) (1871), Helmholtz (1868). The more general case, considered by Lord Kelvin (a.k.a. W. Thomson), allows the fluid's density to vary.

2 See Drazin and Reid (1981) and Chandrasekhar (1961) for more detail.

3 This is Squire's theorem, which states that for every three-dimensional disturbance to a plane-parallel flow there corresponds a more unstable two-dimensional one. This means that the most unstable disturbances are two-dimensional, and there is no need to consider three dimensional effects to determine whether such a flow is unstable. See Drazin and Reid (1981).

4 The solution of Fig. 6.6 is obtained with a gridpoint code with 400×400 equally spaced gridpoints. This kind of problem is also well suited to contour dynamics approach, as in Dritschel (1989).

5 Rayleigh himself did not consider the case with β; this was added by Kuo in 1949.

6 Fjørtoft (1950).

7 Charney and Stern (1962), Pedlosky (1964).

8 Eady (1949), Charney (1947). Eric Eady (1915–1966) is best remembered today as the author of the iconic 'Eady model' of baroclinic instability, which describes the fundamental hydrodynamic instability mechanism that gives rise to weather systems. After an undergraduate education in mathematics he joined the U. K. Meteorological Office in 1937, becoming a forecaster and upper air analyst, in which capacity he served throughout the war. In 1946 he joined the Department of Mathematics at Imperial College, presenting his Ph.D. thesis in 1948 on 'The theory of development in dynamical meteorology', subsequently summarized in Tellus (Eady 1949). This work, masterly in its combination of austerity and relevance, provides a mathematical description of the essential aspects of cyclone development that stands to this day as a canonical model in the field. It also includes, rather obliquely, a derivation of the stratified quasi-geostrophic equations, albeit in a special form. The impact of the work was immediate and it led to visits to Bergen (in 1947 with J. Bjerknes), Stockholm (in 1952 with C.-G. Rossby) and Princeton (in 1953 with J. von Neumann and Charney). Eady followed his baroclinic instability work with prescient discussions of the general circulation of the atmosphere (Eady 1950, Eady and Sawyer 1951, Eady 1954). A perfectionist who sought to understand it all, Eady's subsequent published output was small and he later turned his attention to fundamental problems in other areas of fluid mechanics, the dynamics of the sun and the earth's interior, and biochemistry. He finally took his own life. There is little published about him, save for the obituary by Charnock et al. (1966).

Jule Charney (1917–1981) played a defining role in dynamical meteorology in the second half of the 20th century. He made seminal contributions in many areas including: the theory of baroclinic instability (Charney 1947); a systematic scaling theory for large-scale atmospheric motions and the derivation of the quasi-

geostrophic equations (Charney 1948); a theory of stationary waves in the atmosphere (Charney and Eliassen 1949); the demonstration of the feasibility of numerical weather forecasts (Charney et al. 1950); planetary wave propagation into the stratosphere (Charney and Drazin 1961); a criterion for baroclinic instability (Charney and Stern 1962); a theory for hurricane growth (Charney and Eliassen 1964); the concept of geostrophic turbulence (Charney 1971). His Ph.D. is from UCLA in 1946 and this, entitled 'Dynamics of long waves in a baroclinic westerly current', became his well-known 1947 paper. After this he spent a year at Chicago and another at Oslo, and in 1948 joined the Institute of Advanced Study in Princeton where he stayed until 1956 (and where Eady visited for a while). He spent most of his subsequent career at MIT, interspersed with many visits to Europe, especially Norway. For a more complete picture of Charney, see Lindzen et al. (1990) and a brief biography by N. Phillips available at http://www.nap.edu/readingroom/books/biomems/jcharney.html

9   At least I find it so. My treatment of the Eady problem draws from unpublished notes by J. S. A. Green.

10 If c is purely real (and so the waves are neutral), then there exists the possibility that $\Lambda z - c = 0$, and the equation for Φ is

$$\frac{\mathrm{d}^2\Phi}{\mathrm{d}z^2} - \mu^2\Phi = C\delta(z - z_c), \qquad z_c = c/\Lambda. \tag{6.181}$$

where C is a constant. Because z_c is continuous in the interval $[0, 1]$ so is c, and these solutions have a *continuous spectrum* of eigenvalues. The associated eigenfunctions provide formal completeness to the normal modes, enabling any function to be represented as their superposition.

11 Our nondimensionalization of the two-layer system is such as to be in correpondence with that for the continuous system. Thus we choose H to be the total depth of the domain. This choice produces growth rates and wavenumbers that are equivalent to those in the Eady problem.

12 Green (1960) and Branscome (1983). Lindzen and Farrell (1980) also provide an approximate calculation of growth rates in the Charney problem.

13 After Charney (1947), in whose problem it appears, and Green (1960), who appreciated its importance.

14 Our numerical procedure is to assume a wavelike solution in the horizontal of the form $\tilde{\psi} \exp[i(kx + ly - \omega t)]$, and to finite difference the equations in the vertical. The resulting eigenvalue equations are solved by standard matrix methods, for each horizontal wavenumber. See Smith and Vallis (1998).

15 Gill et al. (1974) and Robinson and McWilliams (1974) were among the first to look at baroclinic instability in the ocean.

Further Reading

Drazin P. and W. H. Reid 1981. *Hydrodynamic Stability*.
  A standard text on hydrodynamic instability theory. It discusses nearly all the classic cases in a straightforward and clear fashion. It includes a more extensive discussion of the linear instability of parallel shear flow than is contained here, although the treatment of baroclinic instability is rather brief.

Chandrasekhar, S. 1961. *Hydrodynamic and Hydromagnetic Stability*.

A classic text discussing many forms of instability but not, alas, baroclinic instability.

Pierrehumbert and Swanson (1995) review many aspects of baroclinic instability from fairly modern point of view.

Problems

6.1 Derive the jump condition (6.29) without directly considering the motion of the interface. In particular, from the momentum equation along the interface show that

$$\frac{\partial}{\partial y}\left(\frac{\tilde{\psi}}{U-c}\right) = -\frac{\tilde{\psi}}{(U-c)^2} \qquad \text{(P6.1)}$$

and show that (6.29) follows. Be explicit about the conditions under which the right-hand-side vanishes when integrated across the interface. (For help see Drazin and Reid 1981).

6.2 By applying the matching conditions (6.23) and (6.29) at $y = \pm a$ to Rayleigh's equation, explicitly derive the dispersion relationship (6.42).

6.3 Show that for very long waves, or as the shear layer becomes thinner, the growth rate given by (6.42) reduces to that of Kelvin-Helmholtz instability of a vortex sheet.

6.4 Obtain the stability properties of the triangular jet, with a basic state velocity given by

$$U(y) = \begin{cases} 0 & \text{for } z \geq 1 \\ 1 - |y| & \text{for } -1 \leq y \leq 1 \\ 0 & \text{for } z \leq -1 \end{cases} \qquad \text{(P6.2)}$$

In particular, obtain the eigenfunctions and eigenvalues of the problem, and show that each eigenfunction is either even or odd. Perturbations with even ψ' are known as 'sinuous modes' and those with odd ψ' are 'varicose modes'. Show that sinuous waves are unstable for sufficiently long wavelengths in the z-direction, but that all varicose modes are stable.

6.5 Consider the incompressible piecewise linear shear flow below:
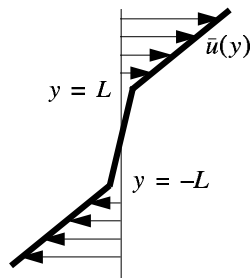
$$u = \begin{cases} AL + b(y - L), & y \geq L \\ Ay, & -L \leq y \leq L \\ -AL + B(y + L), & y \leq -L, \end{cases} \qquad \text{(P6.3)}$$

The flow is two-dimensional, and A and B are constants with $B > 0$.

(a) Find the two normal mode frequencies as a function of zonal wavenumber k.

(b) Find the stability boundaries in terms of k and A and provide a physical interpretation. If $A = B$ is the flow stable or unstable? Why?

(If the algebra defeats you, explain carefully the method for doing the problem.)

6.6 Show numerically or analytically that, in the Eady problem:

(a) Instability occurs for $\mu < 2.399$.

(b) The wavenumber at which the instability is greatest is $\mu = 1.61$.

(c) The nondimensional growth rate at that wavenumber is 0.31.

6.7 ♦ Consider the vertical modes of continuously stratified problems:

(a) When solving the continuous form of the eigenvalue stability problem (as in the Eady problem, for example) the differential equation typically seems to have just one pair of eigenvalues. However, if the equation is solved on a vertical grid with N levels, the resulting difference equation has N roots. Does this mean that $N - 2$ roots are spurious, and if so how might the 'correct' eigenvalues be identified? Alternatively, are there corresponding additional roots in the continuously stratified problem?

(b) The N-level problem is equivalent to a physically realizable N-*layer* system, in which there are presumably N physically meaningful eigenvalues. As N becomes large, with the density differences and thicknesses of each layer chosen to become smaller in a consistent way, the equations describing the layered system presumably converge to those describing the continuous system, yet there are still N eigenvalues in the former. How may this paradox be resolved? What is the physical nature of the extra eigenvalues in the layered system?

6.8 Show, using the two-layer model (or otherwise) that the presence of β reduces the efficiency of baroclinic instability. For example, show that it makes the meridional velocity slightly out of phase with the temperature.

6.9 ♦ Consider the baroclinic instability problem with a discontinuity in the stratification, but a uniform shear. For example, suppose the shear is uniform for $z \in (0, 1)$ with an abrupt change in stratification at $z = 0.5$. How does the amplitude of the instability vary on either side of the discontinuity? Your answer may be an analytical or a numerical calculation, or both.

A simpler explanation is always useful.
Chinese fortune cookie.

Wave–Mean Flow Interaction

Wave-mean flow interaction is concerned with how some mean flow, perhaps a time or zonal average, interacts with a departure from that mean, and this chapter provides an elementary introduction to a number of topics in this area. It is 'elementary' because our derivations and discussion are obtained by direct and straightforward manipulations of the equations of motion, often in the simplest case that will illustrate the relevant principle. It is implicit in what we do that it is a sensible thing to decompose the fields into a mean plus some departure, and one case when this is so is when the departure is of small amplitude. Departures from the mean — generically called *eddies* — are of course not always small; for example, in the midlatitude troposphere the eddies are often of similar amplitude to the mean flow, and chapter 9 and 10 explore this from the standpoint of turbulence. However, here we will generally assume that eddies are indeed of small amplitude.

A *wave* is a special case of an eddy that is assumed to satisfy, at least approximately, a dispersion relation. It is the presence of such a dispersion relation that enables a number of results to be obtained that would otherwise be out of our reach, and that gives rise to the appellation '*wave*–mean flow'. In midlatitudes the relevent waves are usually Rossby waves, as introduced in chapter 5, although gravity waves also interact with the mean flow. It is implicit in defining waves this way that they are generally of small amplitude, for it is this that allows the equations of motion to be sensibly linearized and a disperion relation to be obtained (although an isolated wave may have finite amplitude and still satisfy a dispersion relation). However, this does not mean that the waves do not interact with each other and with the mean flow; we may expect, or at least hope, that the qualitative nature of such interactions, as calculated by wave–mean flow interaction theory, will carry over and provide insights into the finite-amplitude problem. Thus, one goal of this chapter is to provide a way of qualitatively understanding more realistic

situations, and to suggest diagnostics that might be used to analyze both observations and numerical solutions of the fully nonlinear problem. We will almost exclusively concern ourselves with a *zonal* mean, for this is the simplest and often most useful case because of the presence of periodic boundary conditions. (With care some of our results can be extended to the case of a temporal mean.) We will also be mainly concerned with quasi-geostrophic dynamics on a β-plane.

7.1 QUASI-GEOSTROPHIC PRELIMINARIES

To fix our dynamical system and our notation, we write down the quasi-geostrophic potential vorticity equation

$$\frac{\partial q}{\partial t} + J(\psi, q) = D \tag{7.1}$$

where D represents any nonconservative terms and the potential vorticity in a Boussinesq system is

$$q = \beta y + \zeta + \frac{\partial}{\partial z}\left(\frac{f_0}{N^2} b\right), \tag{7.2}$$

where ζ is the relative vorticity and b is the buoyancy perturbation from the background state characterized by N^2, where $N^2 = \mathrm{d}\tilde{b}/\mathrm{d}z$ where $\tilde{b}$ is a reference profile. [In an ideal gas we have very similar equations, but with $q = \beta y + \zeta + (f_0/\rho_s)\partial/\partial z\,(\rho_s b/N^2)$.] We will refer to lines of constant b as isentropes (and also sometimes loosely refer to b as the temperature). In terms of streamfunction, the variables are

$$\zeta = \nabla^2 \psi, \qquad b = f_0 \frac{\partial \psi}{\partial z}, \qquad q = \beta y + \left[\nabla^2 + \frac{\partial}{\partial z}\left(\frac{f_0^2}{N^2}\frac{\partial}{\partial z}\right)\right]\psi. \tag{7.3}$$

where $\nabla^2 \equiv (\partial_x^2 + \partial_y^2)$. The potential vorticity equation holds in the fluid interior; the boundary conditions on (7.3) are provided by the thermodynamic equation

$$\frac{\partial b}{\partial t} + J(\psi, b) + wN^2 = J, \tag{7.4}$$

where J represents heating terms. The vertical velocity at the boundary, w, is zero in the absence of topography and Ekman friction, and if J is also zero the boundary condition is just:

$$\frac{\partial b}{\partial t} + J(\psi, b) = 0. \tag{7.5}$$

Equations (7.1) and (7.5) are the evolution equations for the sytem and if both D and J are zero they conserve both the total energy and the total enstrophy:

$$\frac{\mathrm{d}\widehat{E}}{\mathrm{d}t} = 0, \qquad \widehat{E} = \int_V (\nabla \psi)^2 + \frac{f_0^2}{N^2}\left(\frac{\partial \psi}{\partial z}\right)^2 \mathrm{d}V,$$

$$\frac{\mathrm{d}\widehat{Z}}{\mathrm{d}t} = 0, \qquad \widehat{Z} = \int_V q^2 \, \mathrm{d}V. \tag{7.6}$$

where V is a volume bounded by surfaces at which the normal velocity is zero, or that has periodic boundary conditions. The enstrophy is also conserved layerwise — that is, the horizontal integral of q^2 is conserved at every level.

7.1.1 Potential vorticity and buoyancy fluxes in the linear equations

Let us decompose the fields into a mean (to be denoted with an overbar) plus a perturbation (denoted with a prime), and let us suppose the perturbation fields are of small amplitude. The linearised quasi-geostrophic potential vorticity equation is

$$\frac{\partial q'}{\partial t} + \overline{u}\frac{\partial q'}{\partial x} + u'\frac{\partial \overline{q}}{\partial x} + \overline{v}\frac{\partial q'}{\partial y} + v'\frac{\partial \overline{q}}{\partial y} = D'. \tag{7.7}$$

If the mean is a zonal mean, or just if the basic state is not a function of x, then $\overline{v} = 0$ and this simplifies to

$$\frac{\partial q'}{\partial t} + \overline{u}\frac{\partial q'}{\partial x} + v'\frac{\partial \overline{q}}{\partial y} = D', \tag{7.8}$$

where

$$\frac{\partial \overline{q}}{\partial y} = \beta - \frac{\partial^2 \overline{u}}{\partial y^2} - \frac{\partial}{\partial z}\left(\frac{f_0^2}{N^2}\frac{\partial \overline{u}}{\partial z}\right). \tag{7.9}$$

Multiplying by q' and zonally averaging gives the enstrophy equation:

$$\frac{1}{2}\frac{\partial}{\partial t}\overline{q'^2} = -\overline{v'q'}\frac{\partial \overline{q}}{\partial y} + \overline{D'q'}. \tag{7.10}$$

The quantity $\overline{v'q'}$ is the meridional flux of potential vorticity; this is downgradient when first term on the right-hand side is positive, and it then acts to increase the variance of the perturbation. (This occurs, for example, when the flux is diffusive so that $\overline{v'q'} = -\kappa \partial \overline{q}/\partial y$ where κ may vary but is everywhere positive.) This argument may be inverted: for inviscid flow, if the waves are growing, as for example in the canonical models of baroclinic instability discussed in chapter 6, then *the potential vorticity flux is downgradient*. If the second term on the right-hand side is negative, as it will be if D is a dissipative process (for example if $D = \kappa'\nabla^2 q$ or if $D = -rq$, where κ' and r are positive) then a statistical balance can be achieved between enstrophy production via downgradient transport, and dissipation. If the waves are steady (by which we mean statistically steady, neither growing nor decaying in amplitude) and conservative (i.e., $D' = 0$) then we must have:

$$\overline{v'q'} = 0. \tag{7.11}$$

Similar results follow for the buoyancy at the boundary. We start by linearizing the thermodynamic equation (7.5) to give

$$\frac{\partial b'}{\partial t} + \overline{u}\frac{\partial b'}{\partial x} + v'\frac{\partial \overline{b}}{\partial y} = J', \tag{7.12}$$

and multiplying by b' and averaging gives

$$\frac{1}{2}\frac{\partial}{\partial t}\overline{b'^2} = -\overline{v'b'}\frac{\partial \overline{b}}{\partial y} + \overline{J'b'}. \tag{7.13}$$

Thus growing adiabatic waves have a downgradient flux of buoyancy at the boundary.

In the Eady problem there is no interior gradient of basic-state potential vorticity and all the terms in (7.10) are zero, but the perturbation grows at the boundary. If the waves are steady and adiabatic then, analogously to (7.11),

$$\overline{v'b'} = 0. \tag{7.14}$$

The boundary conditions and fluxes may be absorbed into the interior definition of potential vorticity and its fluxes by way of Bretherton's boundary layer construction, described in chapter 5. This can provide notational and conceptual advantages over dealing with boundary fluxes explicitly, but if an actual calculation is to be performed there is often little to be gained, for the boundary terms have to be dealt with one way or the other.

7.2 THE ELIASSEN-PALM FLUX

In terms of the flux of vorticty and buoyancy the eddy flux of potential vorticity is

$$\overline{v'q'} = \overline{v'\zeta'} + f_0 \overline{v' \frac{\partial}{\partial z} \left(\frac{b'}{N^2} \right)} \tag{7.15}$$

The second term on the right-hand side can be written

$$
\begin{aligned}
f_0 \overline{v' \frac{\partial}{\partial z} \left(\frac{b'}{N^2} \right)} &= f_0 \frac{\partial}{\partial z} \left(\frac{\overline{v'b'}}{N^2} \right) - f_0 \overline{\frac{\partial v'}{\partial z} \frac{b'}{N^2}} \\
&= f_0 \frac{\partial}{\partial z} \left(\frac{\overline{v'b'}}{N^2} \right) - f_0 \overline{\frac{\partial}{\partial x} \left(\frac{\partial \psi'}{\partial z} \right) \frac{b'}{N^2}} \\
&= f_0 \frac{\partial}{\partial z} \left(\frac{\overline{v'b'}}{N^2} \right) - \frac{f_0^2}{N^2} \frac{\partial}{\partial x} \overline{\left(\frac{1}{2} \frac{\partial \psi'}{\partial z} \right)^2}
\end{aligned}
\tag{7.16}
$$

using $b' = f_0 \partial \psi' / \partial z$.

Similarly, the flux of relative vorticity can be written

$$\overline{v'\zeta'} = -\frac{\partial}{\partial y} \overline{u'v'} + \frac{1}{2} \frac{\partial}{\partial x} (\overline{v'^2} - \overline{u'^2}) \tag{7.17}$$

Using (7.16) and (7.17), (7.15) becomes

$$\boxed{\overline{v'q'} = -\frac{\partial}{\partial y} (\overline{u'v'}) + \frac{\partial}{\partial z} \left(\frac{f_0}{N^2} \overline{v'b'} \right) + \frac{\partial}{\partial x} \left(\frac{1}{2} (\overline{v'^2} - \overline{u'^2}) - \frac{\overline{b'^2}}{N^2} \right)} \tag{7.18}$$

Thus the potential vorticity flux, in the quasi-geostrophic approximation, can be written as the divergence of a vector: $\overline{v'q'} = \nabla \cdot \boldsymbol{\mathcal{E}}$ where

$$\boldsymbol{\mathcal{E}} \equiv \left(\frac{1}{2} (\overline{v'^2} - \overline{u'^2}) - \frac{\overline{b'^2}}{N^2} \right) \mathbf{i} - (\overline{u'v'}) \mathbf{j} + \left(\frac{f_0}{N^2} \overline{v'b'} \right) \mathbf{k}. \tag{7.19}$$

A particularly useful form of this arises after zonally averaging, after which (7.18) becomes

$$\boxed{\overline{v'q'} = -\frac{\partial}{\partial y}\overline{u'v'} + \frac{\partial}{\partial z}\left(\frac{f_0}{N^2}\overline{v'b'}\right)}.\tag{7.20}$$

The vector defined by

$$\mathcal{F} \equiv -\overline{u'v'}\,\mathbf{j} + \frac{f_0}{N^2}\overline{v'b'}\,\mathbf{k}\tag{7.21}$$

is called the *Eliassen-Palm flux*,[1] and its divergence, given by (7.20), gives the polewards flux of potential vorticity:

$$\overline{v'q'} = \nabla_x \cdot \mathcal{F},\tag{7.22}$$

where $\nabla_x \cdot \equiv (\partial/\partial y, \partial/\partial z)$ is the divergence in the meridional plane. Unless the meaning is unclear, the subscript x on the meridional divergence will be dropped.

For reference, in spherical coordinates and for an ideal gas the EP flux is (see also the appendix to chapter 12 on page 559):

$$\mathcal{F} = -\cos\vartheta\,\overline{u'v'}\,\mathbf{j} + \cos\vartheta\,\frac{f_0}{\partial_z\overline{\theta}}\overline{v'\theta'}\,\mathbf{k},\tag{7.23}$$

and multiplying by ρ_R and taking the divergence gives

$$\nabla\cdot\rho_R\mathcal{F} = \frac{-\rho_R}{a\cos\vartheta}\frac{\partial}{\partial\vartheta}(\overline{u'v'}\cos^2\vartheta) + \frac{\partial}{\partial z}\left(\frac{\rho_R f_0}{\partial_z\overline{\theta}}\overline{v'\theta'}\cos\vartheta\right) = \rho_R\cos\vartheta\,\overline{v'q'}.\tag{7.24}$$

where ρ_R is a reference profile of density,

7.2.1 The Eliassen-Palm relation

On dividing by $\partial\overline{q}/\partial y$ and using (7.22), the enstrophy equation (7.10) becomes

$$\boxed{\frac{\partial\mathcal{A}}{\partial t} + \nabla\cdot\mathcal{F} = \mathcal{D}},\tag{7.25a}$$

where

$$\mathcal{A} = \frac{\overline{q'^2}}{2\partial\overline{q}/\partial y}, \qquad \mathcal{D} = \frac{\overline{D'q'}}{\partial\overline{q}/\partial y}\tag{7.25b}$$

Eq. (7.25a) is known as the *Eliassen-Palm relation,* and it is a conservation law for the the *wave activity density* $\mathcal{A}$, for if we integrate this expression over a meridional area A bounded by walls where the eddy activity vanishes, and if $\mathcal{D} = 0$, we obtain

$$\frac{\mathrm{d}}{\mathrm{d}t}\int_A \mathcal{A}\,\mathrm{d}A = 0.\tag{7.26}$$

In general, a wave activity is a quantity that is quadratic in the amplitude of the perturbation and that is conserved in the absence of forcing and dissipation. More specifically,

$\mathcal{A}$ is the negative of the *pseudomomentum,* for reasons we will encounter later. Note that neither perturbation energy nor perturbation enstrophy are wave activities of the linearized equations, because there can be an exchange of energy or enstrophy between mean and perturbation — indeed, this is how a perturbation grows in baroclinic or barotropic instability! This is already evident from (7.10), or in general take (7.7) with $D' = 0$ and multiply by q' to give the enstrophy equation

$$\frac{1}{2}\frac{\partial q'^2}{\partial t} + \frac{1}{2}\overline{\boldsymbol{u}} \cdot \nabla q'^2 + \boldsymbol{u}'q' \cdot \nabla\overline{q} = 0 \tag{7.27}$$

where here the overbar is an average (although it need not be a zonal average). Integrating this over a volume V gives

$$\frac{\mathrm{d}\hat{Z}'}{\mathrm{d}t} \equiv \frac{\mathrm{d}}{\mathrm{d}t}\int_V \frac{1}{2}q'^2 \,\mathrm{d}V = -\int_V \boldsymbol{u}'q' \cdot \nabla\overline{q}\,\mathrm{d}V. \tag{7.28}$$

The right-hand side does not in general vanish and so $\hat{Z}'$ is not in general conserved. The ave activity $\mathcal{A}$ is thus both a measure of the amplitude of a wave and a conserved quantity, in the sense of (7.25a).

7.2.2 The group velocity property and Rossby waves

The vector $\mathcal{F}$ describes how the wave activity propagates. In general, we cannot express it simply in terms of $\mathcal{A}$, but in the case in which the disturbance is composed of plane or almost plane waves that permit a group velocity to be defined, then $\mathcal{F} = \boldsymbol{c}_g\mathcal{A}$, where $\boldsymbol{c}_g$ is the group velocity and (7.25a) becomes

$$\frac{\partial \mathcal{A}}{\partial t} + \nabla \cdot (\mathcal{A}\boldsymbol{c}_g) = 0. \tag{7.29}$$

We shall now demonstrate this when the waves in question are plane Rossby waves, although the property holds for waves of other types when a group velocity can be defined.[2]

The Boussinesq quasi-geostrophic equation on the β-plane, linearized around a uniform zonal flow and with constant static stability, is

$$\frac{\partial q'}{\partial t} + \overline{u}\frac{\partial q'}{\partial x} + v'\frac{\partial \overline{q}}{\partial y} = 0 \tag{7.30}$$

where $q' = [\nabla^2 + (f_0^2/N^2)\partial^2/\partial z^2]\psi'$ and, if $\overline{u}$ is constant, $\partial\overline{q}/\partial y = \beta$. Thus we have

$$\left(\frac{\partial}{\partial t} + \overline{u}\frac{\partial}{\partial x}\right)\left[\nabla^2\psi' + \frac{\partial}{\partial z}\left(\frac{f_0^2}{N^2}\frac{\partial \psi'}{\partial z}\right)\right] + \beta\frac{\partial \psi'}{\partial x} = 0. \tag{7.31}$$

Seeking solutions of the form

$$\psi' = \mathrm{Re}\,\Psi e^{i(kx+ly+mz-\omega t)}, \tag{7.32}$$

we find the dispersion relation,

$$\omega = \overline{u}k - \frac{\beta k}{\kappa^2}. \tag{7.33}$$

with group velocities,

$$c_g^y = \frac{2\beta kl}{\kappa^2}, \qquad c_g^z = \frac{2\beta km f_0^2/N^2}{\kappa^2}, \tag{7.34}$$

where $\kappa^2 = (k^2 + l^2 + m^2 f_0^2/N^2)$. Also, if $u' = \mathrm{Re}\, \widehat{u} \exp[i(kx + ly + mz - \omega t)]$, and similarly for the other fields, then

$$\begin{aligned}
\widehat{u} &= -\mathrm{Re}\, ik\Psi, & \widehat{v} &= \mathrm{Re}\, il\Psi, \\
\widehat{b} &= \mathrm{Re}\, im f_0 \Psi, & \widehat{q} &= -\mathrm{Re}\, \kappa^2 \Psi.
\end{aligned} \tag{7.35}$$

The wave activity is then

$$\mathcal{A} = \frac{1}{2}\frac{\overline{q'^2}}{\beta} = \frac{\kappa^4}{4\beta}|\Psi^2| \tag{7.36}$$

where the additional factor of 2 in the denominator arises from the averaging. Using (7.35) the EP flux, (7.21), is

$$\begin{aligned}
\mathcal{F}^y &= -\overline{u'v'} = \frac{1}{2}kl|\Psi^2| \\
\mathcal{F}^z &= \frac{f_0}{N^2}\overline{v'b'} = \frac{f_0^2}{2N^2}km|\Psi^2|.
\end{aligned} \tag{7.37}$$

Using this (7.34) and (7.36) gives

$$\boxed{\mathcal{F} = (\mathcal{F}^y, \mathcal{F}^z) = \boldsymbol{c}_g \mathcal{A}} \tag{7.38}$$

If the properties of the medium are varying, but only on scales larger than the scale of the waves and we can still define a group velocity, then this is a useful expression to estimate how the wave activity propagates in the atmosphere and in numerical simulations.

7.2.3 The orthogonality of modes

It is a direct consequence of the conservation of wave activity that disturbance modes are orthogonal in the wave activity norm, and thus are a useful measure of the amplitude of a particular mode. To show this, we start with the linearized potential vorticity equation,

$$\frac{\partial q'}{\partial t} + \overline{u}\frac{\partial q'}{\partial x} + v'\frac{\partial \overline{q}}{\partial y} = 0. \tag{7.39}$$

Let us seek solutions of the form $\psi' = \mathrm{Re}\, \Psi \exp(ikx)$ where Ψ is the sum of *modes*

$$\Psi = \sum_n \psi_n(y, z)e^{-ikc_n t}. \tag{7.40}$$

that satisfy

$$(\overline{u}\Delta_k^2 + \overline{q}_y)\psi_n = c_n\Delta_k^2\psi_n, \tag{7.41}$$

where

$$\Delta_k^2 = \frac{\partial^2}{\partial y^2} + \frac{\partial}{\partial z}\left(\frac{f_0^2}{N^2}\frac{\partial}{\partial z}\right) - k^2. \tag{7.42}$$

The upper and lower boundary conditions (at $z = 0, -H$) are given by the thermodynamic equation

$$\frac{\partial b'}{\partial t} + \overline{u}\frac{\partial b'}{\partial x} + v'\frac{\partial \overline{b}}{\partial y} = 0, \tag{7.43}$$

and if we simplify further by supposing $\partial\overline{u}/\partial z = 0$ then the boundary condition becomes

$$\frac{\partial \psi_z'}{\partial t} + \overline{u}\frac{\partial \psi_z'}{\partial x} = 0. \tag{7.44}$$

There are no meridional buoyancy fluxes at the boundary. If N^2 is a constant then we can let $\psi_n(y,z) = \psi_n(y)\cos mz$, with $m = j\pi/H$ where j is an integer, so that $q_n = \Delta_{k,m}^2\psi_n$ where

$$\Delta_{k,m}^2 = \frac{\partial^2}{\partial y^2} - (f_0^2/N^2)m^2 - k^2, \tag{7.45}$$

and the boundary conditions are then built-in to any solution we construct from (7.41) and (7.45).[3] We may then consider a single zonal and a single vertical wavenumber, with the mode n characterizing the meridional variation. (Of course if there is no horizontal variation of the shear, then these too are harmonic functions, with $\psi_n \propto \sin(n\pi y/L)$ for a channel of width L.)

For a given basic state we may imagine solving (7.41), numerically or analytically, and determining the modes. However, these modes are not orthogonal in the sense of either energy or enstrophy. That is, denoting the inner product by

$$\langle a, b\rangle \equiv L^{-1}\int_L ab\,\mathrm{d}y, \tag{7.46}$$

then, in general,

$$\begin{aligned} I_E &= \langle\psi_n, q_m\rangle \neq 0, \\ I_Z &= \langle q_n, q_m\rangle \neq 0, \end{aligned} \tag{7.47}$$

for $n \neq m$, where $q_n = \Delta_{k,m}^2\psi_n$. Perturbation energy and enstrophy are thus not wave activities of the linearized equations, and it is not meaningful to talk about the energy or enstrophy of a particular mode. However, by the same token we may expect orthogonality in the wave activity norm. To prove this and understand what it means, suppose that at $t = 0$ the disturbance consists of two modes, n and m, so that at a later time $q = (q_n e^{-ikc_n t} + q_m e^{-ikc_m t} + \text{c.c.})$, where $c_m \neq c_n$ and we assume that both are real. The wave activity is

$$P \equiv \int \mathcal{A}\,\mathrm{d}y\,\mathrm{d}z = \langle q_n, q_m^*/\overline{q}_y\rangle e^{ik(c_n-c_m)t} + \langle q_m, q_m^*/\overline{q}_y\rangle + \langle q_n, q_n^*/\overline{q}_y\rangle + \text{c.c.} \tag{7.48}$$

The second and third terms of this are the wave activities of each mode, and these are constants (to see this, consider the case when the disturbance is just a single mode). Now, because $dP/dt = 0$ the first term must vanish if $c_n \neq c_m$, implying the modes are orthogonal and in particular

$$\text{Re} \int \frac{1}{\overline{q}_y} q_n q_m^* \, dy = 0, \qquad (7.49)$$

for $n \neq m$. Readers who would prefer a more direct derivation of the orthogonality condition directly from the eigenvalue equation (7.41) should see problem 7.6. Orthogonality is a useful result, for it means that the wave activity is a proper measure of the amplitude of a given mode unlike, for example, energy. The conservation of wave activity will lead to a more general derivation of the necessary conditions for stability, in section 7.6.

7.3 THE TRANSFORMED EULERIAN MEAN

The so-called *transformed Eulerian mean,* or TEM, provides a useful framework for discussing eddy effects under a wide range of conditions.[4] It is useful because, as we shall see, it is equivalent to a very natural form of averaging the equations that serves to eliminate eddy fluxes in the thermodynamic equation and collect them together, in a simple form, in the momentum equation, highlighting the role of potential vorticity fluxes. It also provides a natural separation between diabatic and adiabatic effects or between advective and diffusive fluxes and, in the case in which the flow is adiabatic, a nice simplification of the equations. In later chapters we will use the TEM to better understand the mid-latitude troposphere and the dynamics of the Antarctic Circumpolar current, and as a framework for the parameterization of eddy fluxes. Of course, there being no free lunch, the TEM brings with it its own difficulties, and in particular the implementation of boundary conditions can cause difficulties, especially in the actual numerical integration of the TEM equations.

7.3.1 Quasi-geostrophic form

Recall the conventional zonally averaged Eulerian mean equations for the zonally averaged zonal velocity and the buoyancy on the beta-plane:

$$\frac{\partial \overline{u}}{\partial t} - (f + \overline{\zeta})\overline{v} = -\frac{\partial}{\partial y}\overline{u'v'} - \frac{\partial}{\partial z}\overline{u'w'} + \overline{F} \qquad (7.50a)$$

$$\frac{\partial \overline{b}}{\partial t} + w\frac{\partial \overline{b}}{\partial z} = -\frac{\partial}{\partial y}\overline{v'b'} - \frac{\partial}{\partial z}\overline{w'b'} + \overline{J} \qquad (7.50b)$$

where $\overline{F}$ and $\overline{J}$ represent frictional and heating terms. Note that the only contribution to $\overline{v}$ is from the ageostrophic meridional velocity. Using quasi-geostrophic scaling we neglect the vertical eddy flux divergences and all ageostrophic velocities except when

multiplied by f_0 or N^2. The equations then become

$$\frac{\partial \overline{u}}{\partial t} = f_0 \overline{v} - \frac{\partial}{\partial y} \overline{u'v'} + \overline{F}, \tag{7.51a}$$

$$\frac{\partial \overline{b}}{\partial t} = -N^2 w - \frac{\partial}{\partial y} \overline{v'b'} + \overline{J}, \tag{7.51b}$$

where $\overline{b}$ is in thermal wind balance with $\overline{u}$, $f_0 \partial \overline{u}/\partial z = -\partial \overline{b}/\partial y$ (in the Boussinesq approximation). One less-than-ideal aspect of these equations is that in the extratropics the dominant balance is usually between the first two terms on the right-hand sides of each equation, even in time-dependent cases. Thus, the Coriolis force closely balances the divergence of the eddy momentum fluxes, and the advection of the mean stratification ($N^2 w$, or 'adiabatic cooling') often balances the convergence of eddy heat flux, with heating being a small residual. This may lead to an underestimation of the importance of diabatic heating, for this is ultimately responsible for the mean meridional circulation. Thus, in the thermodynamic equation we might seek to combine the terms $N^2 w$ and the eddy flux into a single total (or 'residual') heat transport term that in a steady state is balanced by the diabatic term $\overline{J}$. The TEM provides this reformulation, and in doing so the eddy terms in the momentum equation also take a different form.

To begin, note that because $\overline{v}$ and $\overline{w}$ are related by mass conservation, we can define a mean meridional streamfunction ψ_m such that

$$(\overline{v}, \overline{w}) = \left(-\frac{\partial \psi_m}{\partial z}, \frac{\partial \psi_m}{\partial y} \right). \tag{7.52}$$

Then, if we define a 'residual' streamfunction by

$$\psi^* \equiv \psi_m + \frac{1}{N^2} \overline{v'b'} \tag{7.53}$$

the components of the *residual mean meridional circulation* are given by

$$(\overline{v}^*, \overline{w}^*) = \left(-\frac{\partial \psi^*}{\partial z}, \frac{\partial \psi^*}{\partial y} \right), \tag{7.54}$$

and

$$\overline{v}^* = \overline{v} - \frac{\partial}{\partial z} \left(\frac{1}{N^2} \overline{v'b'} \right), \qquad \overline{w}^* = \overline{w} + \frac{\partial}{\partial y} \left(\frac{1}{N^2} \overline{v'b'} \right). \tag{7.55}$$

Note that by construction, the residual overturning circulation satisfies

$$\frac{\partial \overline{v}^*}{\partial y} + \frac{\partial \overline{w}^*}{\partial z} = 0. \tag{7.56}$$

Substituting (7.55) into (7.51a) and (7.51b) the zonal momentum and buoyancy equations then take the simple forms

$$\boxed{\begin{aligned} \frac{\partial \overline{u}}{\partial t} &= f_0 \overline{v}^* + \overline{v'q'} + \overline{F} \\ \frac{\partial \overline{b}}{\partial t} &= -N^2 \overline{w}^* + \overline{J} \end{aligned}}, \tag{7.57}$$

which are known as the (quasi-geostrophic) *transformed Eulerian mean equations.* The potential vorticity flux is given in terms of the heat and vorticity fluxes by (7.15) or (7.20). For reference, for an ideal gas in spherical coordinates we have:

$$\rho_R \cos\vartheta\,(\overline{v}^*, \overline{w}^*) = \left(-\frac{\partial \psi^*}{\partial z}, \frac{1}{a}\frac{\partial \psi^*}{\partial \vartheta}\right), \qquad \psi^* = \overline{\psi} + \rho_R \cos\vartheta\,\frac{\overline{v'\theta'}}{\partial_z\overline{\theta}}, \qquad (7.58a)$$

so that

$$\overline{v}^* = \overline{v} - \frac{1}{\rho_R}\frac{\partial}{\partial z}\left(\rho_R\frac{\overline{v'\theta'}}{\partial_z\overline{\theta}}\right), \qquad \overline{w}^* = \overline{w} + \frac{1}{a\cos\vartheta}\frac{\partial}{\partial\vartheta}\left(\cos\vartheta\,\frac{\overline{v'\theta'}}{\partial_z\overline{\theta}}\right). \qquad (7.58b)$$

The TEM equations make it apparent that we may consider the potential vorticity fluxes, rather than the separate contributions of the vorticity and heat fluxes, to force the circulation. If we know the potential vorticity flux as well as $\overline{F}$ and $\overline{J}$, then (7.56) and (7.57), along with thermal wind balance

$$f_0\frac{\partial \overline{u}}{\partial z} = -\frac{\partial \overline{b}}{\partial y} \qquad (7.59)$$

form a complete set. The meridional overturning circulation is obtained by eliminating time derivatives from (7.57) using (7.59) to give

$$f_0^2\frac{\partial^2 \psi^*}{\partial z^2} + N^2\frac{\partial^2 \psi^*}{\partial y^2} = f_0\frac{\partial}{\partial z}\overline{v'q'} + f_0\frac{\partial \overline{F}}{\partial z} + \frac{\partial \overline{J}}{\partial y}. \qquad (7.60)$$

Thus, the residual or net overturning circulation is 'driven' by the (vertical derivative of the) potential vorticity fluxes and the diabatic terms — driven in the sense that if we know those terms we can calculate the overturning circulation. Note that this equation applies at every instant, even if the equations are not in a steady state.

7.3.2 The TEM in isentropic coordinates

The residual circulation has an illuminating interpretion if we think of the fluid as comprising multiple layers of shallow water, or equivalently if we cast the problem in isentropic coordinates (section 3.9). The momentum and mass conservation equation can then be written as

$$\frac{\partial u}{\partial t} + \boldsymbol{u}\cdot\nabla u - fv = F \qquad (7.61a)$$

$$\frac{\partial h}{\partial t} + \nabla\cdot(h\boldsymbol{u}) = J \qquad (7.61b)$$

In isentropic coordinates h is the thickness between two isentropic surfaces and $H = H(b)$ is its mean thickness, and the layer thickness is a measure of the temperature of the layer. With quasi-geostrophic scaling (so that β and variations in layer thickness are small) zonally averaging in a conventional way gives

$$\frac{\partial \overline{u}}{\partial t} - f_0\overline{v} = \overline{v'\zeta'} + \overline{F} \qquad (7.62a)$$

$$\frac{\partial \overline{h}}{\partial t} + H \frac{\partial \overline{v}}{\partial y} = -\frac{\partial}{\partial y} \overline{v'h'} + \overline{J}[h] \tag{7.62b}$$

The overbars in these equations denote averages taken along isentropes, but are otherwise conventional, and the meridional velocity is purely ageostrophic. We now choose to define the residual circulation by

$$\overline{v}^* = \overline{v} + \frac{1}{H} \overline{v'h'} \tag{7.63}$$

which is analogous to (7.55). Using (7.63) in (7.62) gives

$$\frac{\partial \overline{u}}{\partial t} - f_0 \overline{v}^* = \overline{v'q'} + \overline{F} \tag{7.64a}$$

$$\frac{\partial \overline{h}}{\partial t} + H \frac{\partial \overline{v}^*}{\partial y} = \overline{J}[h]. \tag{7.64b}$$

where

$$\overline{v'q'} = \overline{v'\zeta'} + \frac{f_0}{H} \overline{v'h'}. \tag{7.65}$$

From (7.63) we see that the residual velocity is a measure of the *total meridional mass flux*, eddy plus mean, in an isentropic layer. This is often a more useful quantity than the Eulerian velocity $\overline{v}$ because it is generally the former, not the latter, that is constrained by the external forcing. What we have done, of course, is to effectively use a mass-weighted mean in (7.61b); that is, if we define the mass-weighted mean by

$$\overline{v}_* \equiv \frac{\overline{hv}}{\overline{h}} \tag{7.66}$$

so that

$$\overline{v}_* = \overline{v} + \frac{1}{\overline{h}} \overline{v'h'}, \tag{7.67}$$

then the zonal average of (7.61b) is just

$$\frac{\partial \overline{h}}{\partial t} + \frac{\partial}{\partial y} (\overline{h} \overline{v}_*) = \overline{J}[h], \tag{7.68}$$

which is the same as (7.64b) if $\overline{h} = H$. Similarly, if we use the mass weighted velocity (7.67) in the momentum equation (7.62a) we obtain (7.64a).

Evidently, if the mass-weighted meridional velocity is used in the momentum and thickness equations then the eddy mass flux does not enter the equations explicitly — the only eddy flux in (7.64) is that of potential vorticity. That is, in isentropic coordinates the equations in TEM form are equivalent to the equations that arise from a particular form of averaging — mass weighted averaging — rather that the conventional Eulerian averaging. Does a similar relationship hold in height coordinates? The answer is yes, as we now see.
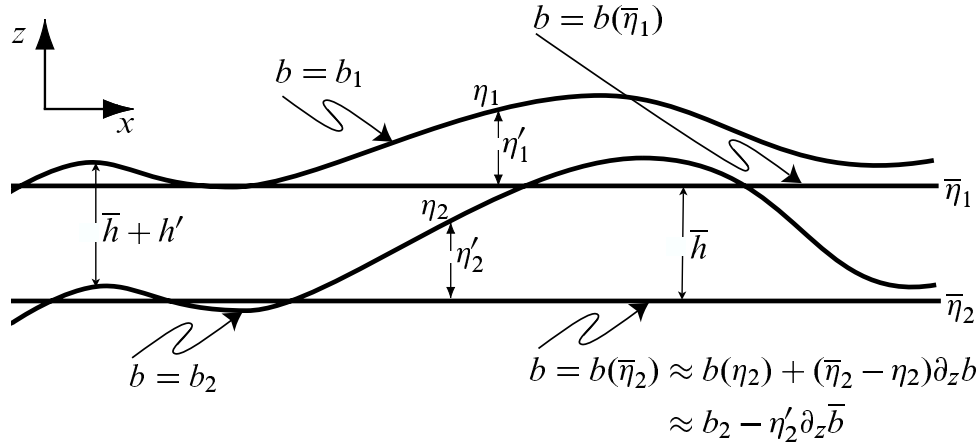
Fig. 7.1 Two isentropic surfaces, η_1 and η_2, and their mean positions, $\overline{\eta}_1$ and $\overline{\eta}_2$. The departure of an isentrope from its mean position is proportional to the temperature perturbation at the isentrope's mean position, and the variations in thickness (h') of the isentropic layer are proportional to the vertical derivative of this.

7.3.3 Connection between the residual and mass-weighted circulation

We now show that averaging the total transport in isentropic layers is equivalent to the mass transport evaluated by the TEM formalism in height coordinates.[5]

Consider two isentropic surfaces, η_1 and η_2 with mean positions $\overline{\eta}_1$ and $\overline{\eta}_2$, as in Fig. 7.1. (We use z to denote the vertical coordinate, and η to denote the location of isentropic surfaces.) The meridional transport between these surfaces is given by

$$T = \int_{\eta_2}^{\eta_1} v \, \mathrm{d}z. \tag{7.69}$$

If the velocity does not vary with height within the layer (and in the limit of layer thickness going to zero this is the case) then $T = vh$ where $h = \eta_1 - \eta_2$ is the thickness of the isentropic layer. The zonally-averaged transport is then given by

$$\overline{T} = \frac{1}{L}\int_L T \, \mathrm{d}x = \frac{1}{L}\int_L \left(\int_{\eta_2}^{\eta_1} v \, \mathrm{d}z \right) \mathrm{d}x = \overline{\int_{\eta_2}^{\eta_1} v \, \mathrm{d}z} = \overline{vh} = \overline{v}\,\overline{h} + \overline{v'h'} \tag{7.70}$$

with obvious notation, and an overbar denoting a zonal average. Letting the distance between isentropes shrink to zero this result allows us to write

$$\overline{v}_* = \frac{\overline{T}}{\overline{h}} = \overline{v}^b + \overline{v'h'}^b / \overline{h} \tag{7.71}$$

where now $\overline{h} = \partial z / \partial b$ is the thickness density, a measure of the thickness between two isentropes, and this result is equivalent to (7.67).

The averaged quantity $\overline{v}_*$ is not proportional to the average of the velocity at constant height, or even to the average along an isentrope; rather, it is the *thickness-weighted* zonal average of the velocity *between* two isentropic surfaces of mean separation $\overline{h}$. Our goal is to express this transport in terms of Eulerian-averaged quantities, at a constant height z.

Let us first connect an average along an isentrope of some variable χ to its average at constant height by writing, for small isentropic displacements,

$$\overline{\chi}^b = \overline{\chi(z + \eta')}^z \approx \overline{\chi(z) + \eta' \partial\chi/\partial z}^z \tag{7.72}$$

where the superscript explicitly denotes how the zonal average is taken, and η' is the displacement of the isotherm from its mean position. This can be expressed in terms of the temperature perturbation at the location of the mean isentrope by Taylor expanding b around its value on that mean isentrope. That is,

$$b(\eta) = b(\overline{\eta}) + \left(\frac{\partial b}{\partial z}\right)_{z=\overline{\eta}} (\eta - \overline{\eta}) + \cdots, \tag{7.73}$$

giving

$$\eta' \approx \frac{-b'}{\partial_z b(\overline{\eta})} \approx -\frac{b'}{\partial_z \overline{b}^z}, \tag{7.74}$$

where $\eta' = \eta - \overline{\eta}$ and $b' = b(\overline{\eta}) - b(\eta)$. Using (7.74) in (7.72) (and omitting the superscript z on $\partial_z \overline{b}$) we obtain, with $\chi = v$,

$$\overline{v}^b = \overline{v}^z - \frac{\overline{b' \partial_z v'}^z}{\partial_z \overline{b}}. \tag{7.75}$$

Note that if v is in thermal wind balance with b then the second term vanishes identically, but we will not invoke this.

We now transform the second term on the right-hand side (7.71) to an average at constant z. The variations in thickness of an isothermal layer are given by

$$h' \approx \overline{h}\frac{\partial \eta'}{\partial z} = -\overline{h}\frac{\partial}{\partial z}\left(\frac{b'}{\partial_z \overline{b}}\right), \tag{7.76}$$

using (7.74). Thus, neglecting terms that are third-order in amplitude,

$$\overline{v'h'}^b = -\overline{h}\overline{v'\frac{\partial}{\partial z}\left(\frac{b'}{\partial_z \overline{b}}\right)}^z \tag{7.77}$$

Using both (7.75) and (7.77), (7.71) becomes

$$\begin{aligned}
\overline{v}_* &= \overline{v}^z - \frac{\overline{b' \partial_z v'}^z}{\partial_z \overline{b}} - \overline{v'\frac{\partial}{\partial z}\left(\frac{b'}{\partial_z \overline{b}}\right)}^z \\
&= \overline{v}^z - \frac{\partial}{\partial z}\overline{\left(\frac{v'b'}{\partial_z \overline{b}}\right)}^z .
\end{aligned} \tag{7.78}$$

Aspects of the TEM formulation

Properties and features

★ The residual mean circulation is equivalent to the total mass-weighted (eddy plus Eulerian mean) circulation, and it is this circulation that is driven by the diabatic forcing.

★ There are no explicit eddy fluxes in the buoyancy budget; the only eddy term is the flux of potential vorticity, and this is divergence of the Eliassen-Palm flux; that is $\overline{v'q'} = \nabla_x \cdot \boldsymbol{E}$.

★ The residual circulation, $\overline{v}^*$, becomes part of the solution, just as $\overline{v}$ is part of the solution in an Eulerian mean formulation.

But note

★ The TEM formulation does not solve the parameterization problem, and eddy fluxes are still present in the equations.

★ The theory and practice are well developed for a zonal average, less so for three-dimensional, non-zonal flow.[6]

★ The boundary conditions on the residual circulation are neither necessarily simple nor easily determined; for example, at a horizontal boundary $\overline{w}^*$ is not zero if there are horizontal buoyancy fluxes.

Examples of the use of the TEM in the general circulation of the atmosphere and ocean arise in sections 12.2, 12.5 and 16.6.

The right-hand side of this is just the TEM form of the residual velocity. Thus, we have shown that:

$$\overline{v}_* \equiv \frac{\overline{vh}}{\overline{h}} = \overline{v}^b + \frac{\overline{v'h'}^b}{\overline{h}} \approx \overline{v}^z - \frac{\partial}{\partial z}\left(\frac{\overline{v'b'}^z}{\partial_z \overline{b}}\right) \equiv \overline{v}^* . \tag{7.79}$$

We see the equivalence of the thickness weighted mean velocity on the left-hand side and the residual velocity on the right-hand side. In the quasi-geostrophic limit $N^2 = \partial_z \overline{b}$ and $H = \overline{h}$.

7.3.4 * The TEM in the primitive equations

We now look at the TEM equations in a slightly more general way, although we will largely restrict our attention to the thermodynamic budget. The basic idea, as before, is that we seek to replace the advecting velocity in the equations of motion by the residual velocity $\overline{v}^*$ where

$$\overline{v}^* = v - \nabla \times \psi \tag{7.80}$$

where we choose the vector streamfunction ψ to simplify the resulting equations as far as possible, and in particular we will now try to distinguish clearly between diffusive and advective eddy fluxes, in a given coordinate system. The meaning of this last statement will become clearer below, and at this stage the transformation (7.80) is purely formal. (See section 10.6 and the ones following for possible applications of this approach.)

We begin with the standard, incompressible, Boussinesq primitive equations. If we decompose these into Eulerian mean and eddy terms, denoted with an overbar and a prime, then the momentum and thermodynamic equations may be written

$$\frac{\partial \overline{u}}{\partial t} + \overline{v} \cdot \nabla \overline{u} + f \times \overline{u} = -\nabla \overline{\varphi} + R, \tag{7.81a}$$

$$\frac{\partial \overline{b}}{\partial t} + \overline{u} \cdot \nabla \overline{b} = J[b] - \nabla \cdot F[b], \tag{7.81b}$$

and a tracer, φ, obeys

$$\frac{\partial \overline{\varphi}}{\partial t} + \overline{u} \cdot \nabla \overline{\varphi} = J[\varphi] - \nabla \cdot F[\varphi]. \tag{7.81c}$$

The equations are completed with the hydrostatic ($\partial \phi / \partial z = \overline{b}$) and mass conservation ($\nabla \cdot \overline{v} = 0$) equations. The term R represents the various Reynolds stress terms, the J terms are sources such as diffusion and heating, and the $\nabla \cdot F$ terms are eddy fluxes of the tracer indicated in the square brackets. Thus,

$$\nabla \cdot F[\varphi] = \frac{\partial \overline{u'\varphi'}}{\partial x} + \frac{\partial \overline{v'\varphi'}}{\partial y} + \frac{\partial \overline{w'\varphi'}}{\partial z} = \nabla \cdot \overline{v'\varphi'}. \tag{7.82}$$

and similarly for $\nabla \cdot F[b]$. (We will omit the identifying label in quare brackets if there is no ambiguity. Also, in this section, the divergence and related operators are three dimensional unless noted.) The fluxes may be divided into components along and across the tracer gradient,

$$F = F_\perp + F_\parallel = (n \cdot F)n + (n \times F) \times n \tag{7.83}$$

where $n = \nabla \overline{\varphi} / |\nabla \overline{\varphi}|$. Thus,

$$F_\perp = \frac{F \cdot \nabla \overline{\varphi}}{|\nabla \overline{\varphi}|^2} \nabla \overline{\varphi}, \qquad F_\parallel = \frac{\nabla \overline{\varphi} \times F}{|\nabla \overline{\varphi}|^2} \times \nabla \overline{\varphi} \tag{7.84}$$

so that $F_\perp$ ($F_\parallel$) is perpendicular to (along) iso-surfaces of tracer. Such a decomposition

is possible for any vector, of course. The component $\boldsymbol{F}_{\|}$ is known as a *skew flux*, and this may be written as if it were an advection by some divergence-free velocity $\tilde{\boldsymbol{v}}$. That is,

$$\nabla \cdot \boldsymbol{F}_{\|} = \nabla \cdot \left(\frac{\nabla \phi \times \boldsymbol{F}}{|\nabla \overline{\varphi}|^2} \times \nabla \overline{\varphi} \right) = \left(\nabla \times \frac{\nabla \overline{\varphi} \times \boldsymbol{F}}{|\nabla \overline{\varphi}|^2} \right) \cdot \nabla \overline{\varphi} \equiv \tilde{\boldsymbol{v}} \cdot \nabla \overline{\varphi}, \qquad (7.85)$$

using the vector identity $\nabla \cdot (\boldsymbol{A} \times \nabla \phi) = \nabla \phi \cdot \nabla \times \boldsymbol{A}$. Furthermore, $\tilde{\boldsymbol{v}} \cdot \nabla \overline{\varphi} = \nabla \cdot (\tilde{\boldsymbol{v}} \overline{\varphi})$ so that the skew flux is adiabatic: that is, it serves to redistribute ϕ, but, just like advection by a true incompressible velocity, it does not of itself change the distribution, or the census, of φ. (It may create a situation in which true dissipation is more effective, by the production of small scales and enhanced tracer gradients.)

If we use (7.80) in (7.81c) then we obtain

$$\frac{\partial \overline{\varphi}}{\partial t} + \overline{\boldsymbol{v}}^* \cdot \nabla \overline{\varphi} = J[\varphi] - \nabla \cdot \boldsymbol{F}^*[\varphi]. \qquad (7.86)$$

where

$$\nabla \cdot \boldsymbol{F}^*[\varphi] = \nabla \cdot (\boldsymbol{F}[\varphi] + \overline{\varphi} \nabla \times \boldsymbol{\psi}) = \nabla \cdot (\boldsymbol{F}[\varphi] - \nabla \overline{\varphi} \times \boldsymbol{\psi}), \qquad (7.87)$$

using the vector identity $\nabla \cdot (\overline{\varphi} \nabla \times \boldsymbol{\psi}) = \nabla \cdot (\boldsymbol{\psi} \times \nabla \overline{\varphi})$. Thus, we may define the *residual flux* with respect to φ by

$$\boldsymbol{F}^*[\varphi] \equiv \boldsymbol{F}[\varphi] - \nabla \overline{\varphi} \times \boldsymbol{\psi}, \qquad (7.88)$$

remembering that the flux is only relevant up to a non-divergent additive factor. From (7.88) we see that, no matter how we choose $\boldsymbol{\psi}$, the components of the residual and raw flux along the mean tracer gradient, or across isosurfaces of tracer, are the same:

$$\boldsymbol{F}^*[\varphi] \cdot \nabla \overline{\varphi} = \boldsymbol{F}[\varphi] \cdot \nabla \overline{\varphi}. \qquad (7.89)$$

However, the two fluxes along the tracer contours — that is, the skew fluxes — differ and we may choose $\boldsymbol{\psi}$ in such a way that this is zero for the residual flux. Why is this a useful choice? It is because a skew flux is already present in the advective term, $\overline{\boldsymbol{v}}^* \cdot \nabla \varphi$ on the left-hand side and so it is useful for the right-hand side to contain only diagradient fluxes.

To remove the residual skew flux, we simply make the choice

$$\boldsymbol{\psi} = \frac{\boldsymbol{F}[\varphi] \times \nabla \overline{\varphi}}{|\nabla \overline{\varphi}|^2}. \qquad (7.90)$$

The flux associated with this is just the negative of the raw skew flux, because from (7.88) this is

$$-\nabla \overline{\varphi} \times \boldsymbol{\psi} = \frac{\nabla \overline{\varphi} \times \boldsymbol{F}[\varphi]}{|\nabla \overline{\varphi}|^2} \times \nabla \overline{\varphi} = -\boldsymbol{F}_{\|}. \qquad (7.91)$$

Making this choice, the tracer evolution equation may be written

$$\frac{\partial \overline{\varphi}}{\partial t} + \overline{\boldsymbol{v}}^* \cdot \nabla \overline{\varphi} = -\nabla \cdot \boldsymbol{F}^*[\varphi] \qquad (7.92a)$$

where

$$\overline{\boldsymbol{v}}^* = \overline{\boldsymbol{v}} - \nabla \times \boldsymbol{\psi} = \overline{\boldsymbol{v}} - \nabla \times \frac{\boldsymbol{F}[\varphi] \times \nabla\overline{\varphi}}{|\nabla\overline{\varphi}|^2} \tag{7.92b}$$

and

$$\boldsymbol{F}^*[\varphi] = \frac{\boldsymbol{F}[\varphi] \cdot \nabla\overline{\varphi}}{|\nabla\overline{\varphi}|^2}\nabla\overline{\varphi}. \tag{7.92c}$$

Evidently there is a different residual flux and a TEM formulation for any advected tracer, be it a passive tracer or an active one like potential temperature or potential vorticity. We must choose just one, and in doing so the skew flux of the other tracers will not be removed. The one most commonly chosen, for both oceanographic and atmospheric applications, is potential temperature. For diagnostic purposes the choice of scalar may not in fact be critical: the various eddy fluxes are in reality caused by advection by small-scale turbulent motion, and such motion acts similarly on all conserved tracers. Thus, removing the skew flux in potential temperature is likely to nearly remove it for all nearly-conserved tracers. Potential vorticity might be another suitable choice in some circumstances.

Suppose that the eddying flow is adiabatic, which is a particularly good approximation in the ocean interior and, if not to quite the same extent, in the stratosphere. This means that there is no eddy buoyancy flux across isopycnals (or heat flux across isotherms) and the diagradient residual flux with respect to bouyancy is zero. The thermodynamic equation is then

$$\frac{\partial b}{\partial t} + \overline{\boldsymbol{v}}^* \cdot \nabla b = J[b]. \tag{7.93}$$

Thus, in much the same way as arose in the quasi-geostrophic equations, the transformed thermodynamic equation appears devoid of explicit eddy terms. However, the (usually numerical) solution of the transformed equations is not necessarily straightforward, because the residual velocity does not vanish at the boundary. Thus, for example, in $\overline{w}^* \neq 0$ at a surface where there are nonzero heat fluxes.

A zonal average

Let the averages in the above expression (as denoted by the overbar) be a zonal average; the residual streamfunction is then a scalar, ψ, where $\boldsymbol{\psi} = \mathbf{i}\psi$ and

$$\overline{v}^* = -\frac{\partial\psi}{\partial z}, \qquad \overline{w}^* = \frac{\partial\psi}{\partial y}. \tag{7.94}$$

The residual streamfunction of (7.90) becomes

$$\psi = \frac{\overline{v'b'}\,\overline{b}_z - \overline{w'b'}\,\overline{b}_y}{|\nabla_m b|^2} \tag{7.95}$$

and the residual flux is

$$\boldsymbol{F}^*[b] = \frac{\overline{v'b'}\,\overline{b}_y + \overline{w'b'}\,\overline{b}_z}{|\nabla_m b|^2}\nabla b \tag{7.96}$$

where $\nabla_m b = \mathbf{j}\,\partial b/\partial y + \mathbf{k}\,\partial b/\partial z$. Given a residual streamfunction, the zonally averaged zonal momentum equation can then be cast in TEM form, and a form of the EP flux naturally appears on the right-hand side.[7]

Relation to quasi-geostrophy

If the isotherms are nearly flat then the above forms reduce to the quasi-geostrophic TEM equations. Specifically, (i) $|\nabla \overline{b}|$ is approximated by $\overline{b}_z = b_{0z}$, and (ii) vertical eddy thermal fluxes are neglected. The streamfunction (7.95) then reduces to

$$\psi = \frac{\overline{v'b'}}{|\overline{b}_z|} \tag{7.97}$$

which is the same as the eddy part of (7.53).

* More general forms

Transformations more general than that of (7.90) are possible that still lead to a transformed thermodynamic budget with the same general form, and in particular still partition the flux into a skew component and a diagradient component, and that may be particularly useful as boundaries are approached.[8] In particular, we may choose

$$\boldsymbol{\psi} = \frac{\boldsymbol{F}[\overline{\varphi}] \times \nabla \overline{\varphi}}{|\nabla \overline{\varphi}|^2} + \frac{\boldsymbol{F}[\varphi] \cdot \nabla \overline{\varphi}}{|\nabla \overline{\varphi}|^2}\boldsymbol{\alpha}. \tag{7.98}$$

where $\boldsymbol{\alpha}$ is an arbitrary vector. The transformed evolution equation for $\overline{\varphi}$ is then

$$\frac{\partial \overline{\varphi}}{\partial t} + \overline{\boldsymbol{v}}^* \cdot \nabla \overline{\varphi} = -\nabla \cdot \boldsymbol{F}^*[\varphi]. \tag{7.99}$$

where

$$\boldsymbol{F}^*[\varphi] = \frac{\boldsymbol{F}[\varphi] \cdot \nabla \overline{\varphi}}{|\nabla \overline{\varphi}|^2}(\nabla \overline{\varphi} + \boldsymbol{\alpha} \times \nabla \overline{\varphi}) \tag{7.100}$$

and $\overline{\boldsymbol{v}}^* = \boldsymbol{v} - \nabla \times \boldsymbol{\psi}$. The residual flux is still proportional to the diagradient flux, and will be zero if the eddies are adiabatic. However, unlike (7.92c) the flux is not directed parallel to to the gradient.

   A particularly common choice is to choose $\boldsymbol{\alpha}$ to be proportional to the isothermal slope. Then, with $\varphi = b$, we have

$$\boldsymbol{\alpha} = -\frac{\mathbf{k} \times \nabla \overline{b}}{\overline{b}_z} \tag{7.101}$$

or, in the zonally averaged case $\boldsymbol{\alpha} = \mathbf{i}\alpha = -\mathbf{i}\overline{b}_y/\overline{b}_z$. After some algebra, we then find

$$\boldsymbol{\psi} = \frac{\boldsymbol{F}[b] \times \mathbf{k}}{\overline{b}_z} = \frac{1}{\overline{b}_z}\left(\mathbf{i}\,\overline{v'b'} - \mathbf{j}\,\overline{u'b'},\right) \tag{7.102}$$

and

$$\boldsymbol{F}^*[b] = \frac{\boldsymbol{F}[b] \cdot \nabla \overline{b}}{\overline{b}_z}\mathbf{k}. \tag{7.103}$$

In full, the averaged thermodynamic equation may be written as

$$\frac{\partial \overline{b}}{\partial t} + (\overline{\boldsymbol{u}} + \tilde{\boldsymbol{u}}) \cdot \nabla \overline{b} + (\overline{w} + \tilde{w})\frac{\partial \overline{b}}{\partial z} = \frac{\partial G}{\partial z}. \tag{7.104}$$

where

$$G = \frac{\overline{v'b'} \cdot \nabla \overline{b}}{\partial_z \overline{b}} = \frac{1}{\partial_z \overline{b}} \left(\overline{u'b'} \cdot \nabla_z \overline{b} + \overline{w'b'} \frac{\partial \overline{b}}{\partial z} \right). \tag{7.105}$$

It may also be readily verified by direct manipulation that this is exactly equivalent to the usual, Eulerian averaged, thermodynamic equation. The eddy induced velocities $\tilde{u}$ and $\tilde{w}$ may also be conveniently written in terms of a streamfunction as

$$\tilde{\boldsymbol{u}} = -\frac{\partial \tilde{\boldsymbol{\psi}}}{\partial z}, \qquad \tilde{w} = \nabla \cdot \tilde{\boldsymbol{\psi}} \tag{7.106a}$$

where

$$\tilde{\boldsymbol{\psi}} = \frac{\boldsymbol{F}[b]}{\partial_z \overline{b}} = \frac{\overline{u'b'}}{\partial_z \overline{b}}. \tag{7.106b}$$

[Note $\tilde{\boldsymbol{\psi}}$ is different from the $\boldsymbol{\psi}$ of (7.102).] The quasi-geostrophic form follows particularly easily from this by setting $G = 0$ and $\overline{b} = b_0$ in (7.106).

This can be a particularly useful form in the diagnosis of numerical experiments and observations in the interior of the ocean or atmosphere where isopycnal slopes are small, and here it differs little from (7.92) but is easier to calculate and interpret. It is also useful for eddy flux parameterization schemes, considered in chapter 10. The various forms of TEM do differ when isopycnals are steeply sloping and, relatedly, near boundaries. Note, for example, that the vertical residual velocity does not vanish at a horizontal boundary if there is a non-zero horizontal buoyancy flux.[9]

7.4 THE NONACCELERATION RESULT

For the rest of this chapter we return to quasi-geostrophic dynamics, and consider further the interpretation and application of potential vorticity fluxes and its relatives. We first consider a particularly important result in wave–mean flow dynamics, the nonacceleration result.[10]

7.4.1 A derivation directly from the potential vorticity equation

Consider how the potential vorticity fluxes affect the mean fields. If the waves are steady and conservative then, from (7.11) or (7.25a), the EP flux is non-divergent and the meridional potential vorticity flux, $\overline{v'q'}$, is zero. Now, the zonally-averaged potential vorticity equation is

$$\frac{\partial \overline{q}}{\partial t} + \frac{\partial \overline{v'q'}}{\partial y} = \overline{D}. \tag{7.107}$$

Thus, if the above conditions are satisfied we have $\partial \overline{q}/\partial t = 0$. Now, in quasi-geostrophic theory the buoyancy and geostrophically balanced velocity can be determined from the potential vorticity via an elliptic equation, and in particular

$$\overline{q} - \beta y = \frac{\partial^2 \overline{\psi}}{\partial y^2} + \frac{\partial}{\partial z} \left(\frac{f_0^2}{N^2} \frac{\partial \overline{\psi}}{\partial z} \right). \tag{7.108}$$

and so differentiating (7.107) with respect to y and using (7.22) we obtain

$$\left[\frac{\partial^2}{\partial y^2} + \frac{\partial}{\partial z}\left(\frac{f_0^2}{N^2}\frac{\partial}{\partial z}\right)\right]\frac{\partial \overline{u}}{\partial t} = (\nabla \cdot \mathcal{F})_{yy} - \overline{D}_y. \tag{7.109}$$

Thus, if the terms on the right-hand side are zero then a solution is

$$\frac{\partial \overline{u}}{\partial t} = 0, \tag{7.110}$$

and this is the unique solution if there is no acceleration at the boundaries. This is a *nonacceleration result*. That is to say, under the non-acceleration conditions the tendency of the mean fields, and in particular the zonally-averaged zonal flow, are independent of the waves and, in the absence of other terms, are zero. Explicitly, the nonacceleration conditions are that:

 (i) The waves are steady (so that, using (7.25a), $\mathcal{A}$ does not vary).

 (ii) The waves and mean flow are conservative (i.e., $\mathcal{D} = 0$ and $\overline{D} = 0$), so that it is not the presence of dissipative terms that allow there to be a non-zero potential vorticty flux. Given this and the first condition, (7.25a) implies that $\nabla \cdot \mathcal{F} = 0$.

 (iii) The waves are of small amplitude (all of our analysis has neglected terms that are cubic in perturbation amplitude).

 (iv) The waves do not affect the boundary conditions (so there are no boundary contributions to the acceleration).

The result applies to the buoyancy and velocity fields that are directly invertible from potential vorticity, and not to the ageostrophic velocities. Given the way we have derived it, it does not seem a surprising result; however, it can be powerful and counter-intuitive, for it means that steady waves (i.e., whose amplitude does not vary) do not affect the zonal flow. However, they do affect the meridional overturning circulation, and the relative vorticity flux also may be nonzero. In fact, the nonacceleration theorem is telling us that the changes in the vorticity flux are exactly compensated for by changes in the meridional circulation, and there is no net effect on the zonally-averaged zonal flow. It is *irreversibility*, often manifested by the breaking of waves, that leads to permanent changes in the mean flow.

The derivation of this result by way of the momentum equation, which one might expect to be more natural, is rather awkward because one must consider momentum and buoyancy fluxes separately. Furthermore, the zonally averaged meridional circulation comes into play: for example, meridional velocity, $\overline{v}$, is, although small because it is purely ageostrophic, not zero and we cannot neglect it because it is multiplied by Coriolis parameter, which is large. Thus, the eddy vorticity fluxes can affect both the meridional circulation and the acceleration of the zonal mean flow, and it might seem impossible to disentangle the two effects without completely solving the equations of motion. Fortunately, the situation is simplified and clarified via the use of the TEM, as we now see.

7.4.2 Use of TEM to given the nonacceleration result

A two-dimensional case

Consider two-dimensional incompressible flow on the β-plane, for which there is no buoyancy flux. The linearized vorticity equation is

$$\frac{\partial \zeta'}{\partial t} + \overline{u}\frac{\partial \zeta'}{\partial x} + v'\frac{\partial \overline{\zeta}}{\partial y} = D \tag{7.111}$$

from which we derive, analogously to (7.25a), the Eliassen-Palm relation

$$\frac{\partial \mathcal{A}}{\partial t} + \frac{\partial \mathcal{F}}{\partial y} = \mathcal{D} \tag{7.112}$$

where $\mathcal{F} = -\overline{u'v'}$, $\mathcal{D}$ represents nonconservative forces, and

$$\mathcal{A} = \frac{\overline{\zeta'^2}}{2\partial_y \overline{\zeta}} = \frac{1}{2}\overline{\eta'^2}\frac{\partial \overline{\zeta}}{\partial y} \tag{7.113}$$

The quantity $\eta' \equiv -\zeta'/\partial_y \overline{\zeta}$ is proportional to the meridional particle displacement in a disturbance. Now consider the x-momentum equation

$$\frac{\partial u}{\partial t} = -\frac{\partial u^2}{\partial x} - \frac{\partial uv}{\partial y} - \frac{\partial \phi}{\partial x} + fv \tag{7.114}$$

Zonally averaging, noting that $\overline{v} = 0$, gives

$$\frac{\partial \overline{u}}{\partial t} = -\frac{\partial \overline{uv}}{\partial y} = \overline{v'\zeta'} = \frac{\partial \mathcal{F}}{\partial y}. \tag{7.115}$$

Finally, combining (7.112) and (7.115) gives

$$\frac{\partial}{\partial t}(\overline{u} + \mathcal{A}) = \mathcal{D} \tag{7.116}$$

In the absence of nonconservative terms (i.e., if $\mathcal{D} = 0$) the quantity $\overline{u}+\mathcal{A}$ is constant.[11] Further, if the waves are steady and conservative then $\mathcal{A}$ is constant and, therefore, so is $\overline{u}$.

The stratified case

In the stratified case we can use the TEM form of the momentum equation to derive a similar result. The unforced zonally averaged zonal momentum equation can be written

$$\frac{\partial \overline{u}}{\partial t} - f_0 \overline{v}^* = \nabla \cdot \boldsymbol{\mathcal{F}}, \tag{7.117}$$

and using the Eliassen-Palm relation this may be written,

$$\frac{\partial}{\partial t}(\overline{u} + \mathcal{A}) - f_0 \overline{v}^* = \mathcal{D} \tag{7.118}$$

and so again $\mathcal{A}$ is related to the momentum of the flow. If, furthermore, the waves are steady ($\partial \mathcal{A}/\partial t = 0$) and conservative ($\mathcal{D} = 0$), then then $\partial \overline{u}/\partial t - f_0 \overline{v}^* = 0$. However, under these same conditions the residual circulation will also be zero. This is because the residual meridional circulation ($\overline{v}^*, \overline{w}^*$) arises via the necessity to keep the temperature and velocity fields in thermal wind balance, and is thus determined by an elliptic equation, namely (7.60). If the waves are steady and adiabatic then the right-hand side of this equation is zero and

$$f_0^2 \frac{\partial^2 \psi^*}{\partial z^2} + N^2 \frac{\partial^2 \psi^*}{\partial y^2} = 0. \tag{7.119}$$

If $\psi^* = 0$ at the boundaries, then the unique solution of this is $\psi^* = 0$ everwhere. At the meridional boundaries we may certainly suppose that ψ^* vanishes if these are quiescent latitudes, and at the horizontal boundaries the buoyancy flux will vanish if the waves there are steady, because from (7.10)

$$\overline{v'b'}\frac{\partial \overline{b}}{\partial y} = -\frac{1}{2}\frac{\partial}{\partial t}\overline{b'^2} = 0. \tag{7.120}$$

Under these circumstances, then, the residual meridional circulation vanishes in the interior, and from (7.117), the mean flow is steady.

Compare (7.117) with the momentum equation in conventional Eulerian form, namely

$$\frac{\partial \overline{u}}{\partial t} - f_0 \overline{v} = \overline{v'\zeta'} \tag{7.121}$$

There is no reason that the vorticity flux should vanish when waves are present, even if they are steady. However, such a flux is (under nonacceleration conditions) precisely compensated by the meridional circulation $f_0\overline{v}$, something that is almost impossible to infer or intuit directly from (7.121). Even when nonacceleration conditions do not apply there will be a significant cancellation between the two terms, and any acceleration of the mean flow will largely be a result of additional terms in the equation. Unlike the proof of the nonacceleration result given in section 7.4.1 the above argument does not use the invertibility property of potential vorticty so directly, suggesting an extension to the primitive equations, but we do not pursue that here.[12] Various results regarding the TEM and nonacceleration are summarized in the shaded box on the next page.

7.4.3 The EP flux and form drag

It may seem a little magical that the zonal flow is driven by the Eliassen-Palm flux via (7.117). The polewards vorticity flux is clearly related to the momentum flux convergence, but why should a polewards buoyancy flux affect the momentum? The TEM form of the momentum equation is

$$\frac{\partial \overline{u}}{\partial t} = \frac{\partial}{\partial z}\left(\frac{f_0}{N^2}\overline{v'b'}\right) + F_m. \tag{7.122}$$

TEM, Residual Velocities, Nonacceleration, and All That

For a Boussinesq quasi-geostrophic system, the TEM form of the momentum and thermodynamic equations are:

$$\frac{\partial \overline{u}}{\partial t} - f_0 \overline{v}^* = \nabla \cdot \boldsymbol{\mathcal{F}}, \qquad \frac{\partial \overline{b}}{\partial t} + \overline{w}^* \frac{\partial}{\partial z} \overline{b}_0 = \overline{J} \qquad (\text{T.1})$$

where $\partial \overline{b}_0/\partial z = N^2$, $\overline{J}$ represents diabatic effects, $\boldsymbol{\mathcal{F}}$ is the Eliassen-Palm (EP) flux (and $\nabla_x \cdot \boldsymbol{\mathcal{F}} = \overline{v'q'}$) and the residual velocities are

$$\overline{v}^* = \overline{v} - \frac{\partial}{\partial z}\left(\frac{1}{N^2}\overline{v'b'}\right), \qquad \overline{w}^* = \overline{w} + \frac{\partial}{\partial y}\left(\frac{1}{N^2}\overline{v'b'}\right). \qquad (\text{T.2})$$

Spherical coordinate and ideal gas versions of these take a similar form. We may define a meridional overturning streamfunction such that $(\overline{v}^*, \overline{w}^*) = (-\partial \psi^*/\partial z, \partial \psi^*/\partial y)$, and using thermal wind to eliminate time-derivatives in (T.1) we obtain

$$f_0^2 \frac{\partial^2 \psi^*}{\partial z^2} + N^2 \frac{\partial^2 \psi^*}{\partial y^2} = f_0 \frac{\partial}{\partial z} \overline{v'q'} + \frac{\partial \overline{J}}{\partial y}. \qquad (\text{T.3})$$

The above manipulations may seem formal, in that they simply transform the momentum and thermodynamic equation from one form to another. However, the resulting equations have two potential advantages over the untransfomed ones:

(i) The residual meridional velocity is approximately equal to the average thickness-weighted velocity between two neighbouring isentropic surfaces, and so is a measure of the total (Eulerian mean plus eddy) meridional transport.

(ii) The EP flux has certain attractive features, directly related to the physical properties of waves. The divergence of the EP flux is the meridional flux of potential vorticity:

$$\boldsymbol{\mathcal{F}} = -(\overline{u'v'})\mathbf{j} + \left(\frac{f_0}{N^2}\overline{v'b'}\right)\mathbf{k}, \qquad \nabla \cdot \boldsymbol{\mathcal{F}} = \overline{v'q'}. \qquad (\text{T.4})$$

Furthermore, the EP flux satisfies, to second order in wave amplitude,

$$\frac{\partial \mathcal{A}}{\partial t} + \nabla \cdot \boldsymbol{\mathcal{F}} = \mathcal{D}, \qquad \text{where} \quad \mathcal{A} = \frac{\overline{q'^2}}{2\partial\overline{q}/\partial y}, \quad \mathcal{D} = \frac{\overline{D'q'}}{\partial\overline{q}/\partial y}. \qquad (\text{T.5})$$

The quantity $\mathcal{A}$ is a *wave activity density,* and $\mathcal{D}$ is its dissipation. For nearly plane waves, $\mathcal{A}$ and $\boldsymbol{\mathcal{F}}$ are connected by the *group velocity property,*

$$\boldsymbol{\mathcal{F}} = (\mathcal{F}^y, \mathcal{F}^z) = \boldsymbol{c}_g \mathcal{A}. \qquad (\text{T.6})$$

where $\boldsymbol{c}_g$ is the group velocity of the waves. If the waves are steady ($\partial \mathcal{A}/\partial t = 0$) and dissipationless ($\mathcal{D} = 0$) then $\nabla \cdot \boldsymbol{\mathcal{F}} = 0$ and, using (T.1) and (T.3) there is no wave-induced acceleration of the mean flow. More commonly there is enstrophy dissipation, or wave-breaking, and $\nabla \cdot \boldsymbol{\mathcal{F}} < 0$; such *wave drag* leads to flow deceleration and/or a polewards residual meridional velocity.

where $F_m = \overline{v'\zeta'} + f_0\overline{v}^*$ represents forces from the momentum flux and Coriolis force. The first term on the right-hand side certainly does not look like a force; however, it turns out to be directly proportional to the *form drag* between isentropic layers. Recall from section 3.5 that the form drag, τ_d, at an interface between two layers of shallow water is

$$\tau_d = -\overline{\eta'\frac{\partial p'}{\partial x}} \tag{7.123}$$

where η is the interfacial displacement. But from (7.74) $\eta = -b'/N^2$ and with this and geostrophic balance we have

$$\tau_d = \frac{f_0}{N^2}\overline{v'b'} \tag{7.124}$$

Thus, the vertical component of the EP flux (i.e., the meridional buoyancy flux) is in fact a real stress acting on a fluid layer and equal to the momentum flux caused by the wavy interface. The net momentum convergence into an infinitesimal layer of mean thickness $\overline{h}$ is then [c.f., (3.64)],

$$F_d = \overline{h}\frac{\partial \tau_d}{\partial z} = \overline{h}\frac{\partial}{\partial z}\left(\frac{\overline{v'b'}}{N^2}\right). \tag{7.125}$$

and a layer of mean thickness $\overline{h}$ is accelerated according to

$$\frac{\partial \overline{u}}{\partial t} = f_0 \frac{\partial}{\partial z}\left(\frac{\overline{v'b'}}{\partial_z \overline{b}}\right) + F_m. \tag{7.126}$$

The appearance of the bouyancy flux is really a consequence of the way we have chosen to average the equations: obtaining (7.126) involved averaging the forces over an isentropic layer, and given this it can only be the residual circulation that contributes to the Coriolis force. One might say that the vertical component of the EP flux is a force in drag, masquerading as a bouyancy flux.

7.5 INFLUENCE OF EDDIES ON THE MEAN FLOW IN THE EADY PROBLEM

We now consider the eddy fluxes in the Eady problem, and in particular how these might feed back onto the mean flow. Because of the simplicity of the setting the problem can be fully solved in both the Eulerian or residual frameworks, and it is therefore an instructive example of the TEM methodology.

7.5.1 Formulation

Let us first distinguish between the basic flow, the zonal mean fields, and the perturbation. The basic flow is the flow around which the equations of motion are linearized; this flow is unstable, and the perturbations, assumed small, grow exponentially with time. Because they are (formally) always small they do not affect the basic flow, but

they do produce changes in the zonal mean velocity and buoyancy fields. In Eulerian form this is represented by,

$$\frac{\partial \overline{u}}{\partial t} = f_0 \overline{v} - \frac{\partial \overline{u'v'}}{\partial y}, \qquad \frac{\partial \overline{b}}{\partial t} = -N^2 \overline{w} - \frac{\partial \overline{b'v'}}{\partial y}, \qquad (7.127)$$

and the TEM version of these equation is

$$\frac{\partial \overline{u}}{\partial t} = f_0 \overline{v}^* + \overline{v'q'}, \qquad \frac{\partial \overline{b}}{\partial t} = -N^2 \overline{w}^*, \qquad (7.128)$$

where in the Eady problem $\partial_y (\overline{u'v'})$ and $\overline{v'q'}$ are both zero. We can calculate the perturbation quantities from the solution to Eady problem (e.g., calculate $\overline{v'b'}$) and thus infer the structure of the mean flow tendencies $\partial \overline{u}/\partial t$ and $\partial \overline{b}/\partial t$ and the meridional circulation, $(\overline{v}, \overline{w})$ or $(\overline{v}^*, \overline{w}^*)$. All of these fields are perturbation quantities and all are exponentially growing, and so in reality they will eventually have a finite effect on the pre-existing zonal flow, but in the Eady problem, or any similar linear problem, such rectification is assumed small and neglected.

Using the thermal wind relation, $f_0 \partial_z \overline{u} = -\partial_y \overline{b}$ to eliminate time derivatives in (7.127) gives an equation for the meriodional streamfunction ψ_E, namely,

$$\frac{L^2}{L_d^2} \frac{\partial^2 \psi_E}{\partial z^2} + \frac{\partial^2 \psi_E}{\partial y^2} = -\frac{1}{N^2} \frac{\partial^2 \overline{b'v'}}{\partial y^2} \qquad (7.129)$$

where $(\overline{v}, \overline{w}) = (-\partial \psi_E / \partial z, \partial \psi_E / \partial y)$ and we have nondimensionalized z with D and y with L. The boundary conditions are that $\psi_E = 0$ at $y = 0, L$ and $z = 0, D$. Similarly, and analogously to to (7.60), we obtain an equation for the residual streamfunction, ψ^*, namely

$$\frac{L^2}{L_d^2} \frac{\partial^2 \psi^*}{\partial z^2} + \frac{\partial^2 \psi^*}{\partial y^2} = 0 \qquad (7.130)$$

where now the boundary conditions are that $N^2 \overline{w}^* = \partial \overline{v'b'}/\partial y$ at the upper and lower boundaries, and $v = 0$ at the lateral boundaries. In terms of the residual streamfunction this is

$$\psi^* = \frac{1}{N^2} \overline{v'b'}, \text{ at } z = 0, 1, \qquad \psi^* = 0, \text{ at } y = 0, 1. \qquad (7.131)$$

The residual and overturning circulations are related by (7.53), and (7.130) and (7.131) are, at one level, simply different representations of the same problem, connected by a simple mathematical transformation. However, the residual streamfunction better represents the total transport of the fluid. Eq. (7.130) is particularly simple, because of the absence of potential vorticity fluxes in the interior, and it is apparent that the residual circulation is driven by boundary sources. We care only about the spatial structure of the right-hand sides of (7.130) and the boundary conditions of (7.131). The former is given by

$$-\frac{\partial^2 \overline{b'v'}}{\partial y^2} \propto -\frac{\partial^2}{\partial y^2} \sin^2 ly = -2l^2 \cos 2ly. \qquad (7.132)$$
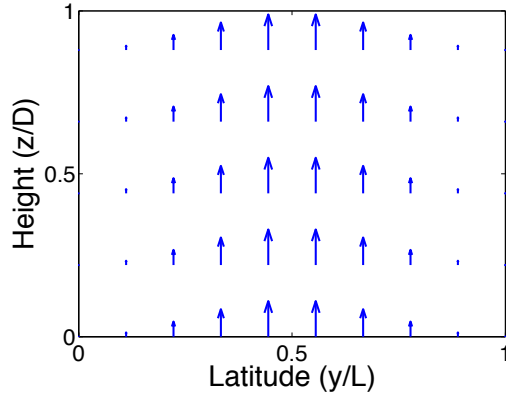
Figure 7.2 The Eliassen-Palm vector in the Eady problem.

The eddy heat fluxes in the Eady problem are independent of height, as noted in chapter 6. This follows without detailed calculation, by first noting that the eddy potential vorticity flux is zero because the basic state has zero potential vorticity and therefore none may be generated. Further, because the basic state does not vary in y the there can be no momentum flux convergence in the y-direction, and so the momentum flux itself is zero if it is zero on the boundary. This, the eddy heat flux is independent of height and using (7.21) the EP vectors are directed purely vertically (Fig. 7.2).

The boundary conditions for the residual circulation are

$$\psi^*(y,0) = \psi^*(y,1) \propto \sin^2 ly. \tag{7.133}$$

7.5.2 Solution

The solutions to (7.129) and (7.130) may be obtained either analytically or numerically. In a domain $0 < y < 1$ and $0 < z < 1$ the residual streamfunction for $l = \pi$ is given by:

$$\psi^* = \sum_{n=1}^{\infty} A_n \sin[(2n-1)ly]\frac{\cosh[L_d\pi(2n-1)(z-0.5)/L]}{\cosh[L_d\pi(2n-1)/2L]},$$

$$A_n = \frac{2}{\pi(2n-1)} - \frac{1}{\pi(2n-1)-2l} - \frac{1}{\pi(2n-1)+2l}. \tag{7.134}$$

The solution is obtained by first projecting the boundary conditions [proportional to $\sin^2 ly$, or $(1 - \cos 2ly)/2$] onto the eigenfunctions of the horizontal part of the Laplacian (i.e., sine functions), and this gives the coefficients of A_n. The vertical structure is then obtained by solving $(L/L_d)^2\partial_z^2\psi^* = -\partial_y^2\psi^*$, which gives the cosh functions. The series converges very quickly, and the first term in the series captures the dominant structure of the solution, essentially because, for $l = \pi$, $\sin ly$ is not unlike $\sin^2 ly$ on the interval $[0, 1]$.

The Eulerian circulation is obtained from the residual circulation using (7.53) and

$$\psi_E \text{ (Eulerian)}$$
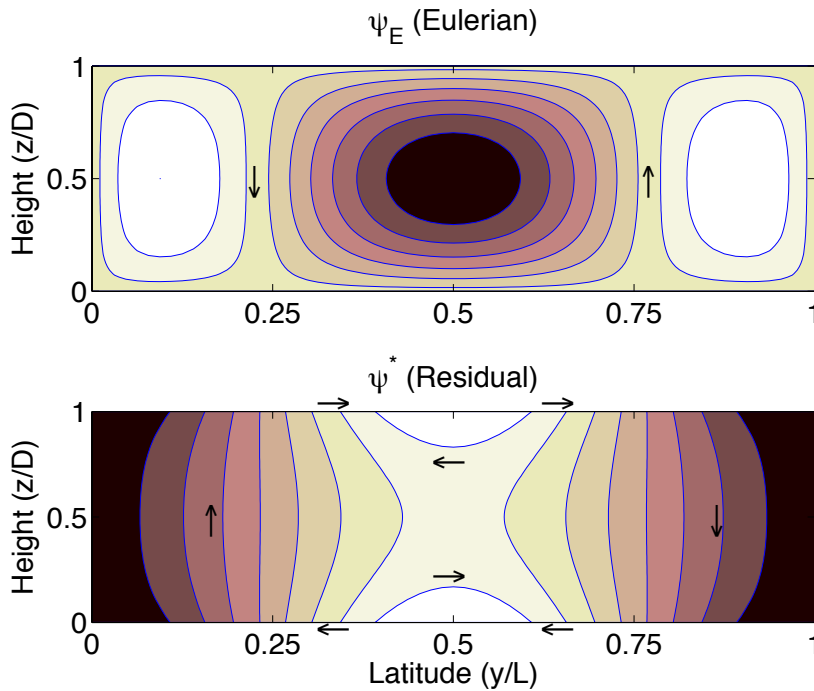
$$\psi^* \text{ (Residual)}$$

Fig. 7.3 The Eulerian streamfunction (top) and the residual streamfunction for the Eady problem, calculated using (7.129) and (7.130), with $L^2/L_d^2 = 9$.

so by the addition of a field independent of z and proportional to $\sin^2 ly$. The resulting structure is dominated by this and the first term of (7.134) (proportional to $\sin ly$) and, noting that the circulation is symmetric about $z = 1/2$, we obtain a circulation dominated by a single cell, with equatorwards motion aloft and polewards motion near the surface (Fig. 7.3). This suggests that heat flux convergence in high latitudes is leading to mean rising motion, with the precise shape of the streamfunction determined by the need to satisfy the boundary conditions. Although this is true, the heat flux arises *because* of the motion of fluid parcels, so it may be a little misleading to infer, as one might from the Eulerian streamfunction, that the heat flux *causes* the individual parcels to rise or sink in this fashion. The residual streamfunction is a better indicator of the total mass transport and, perhaps as one might intuitively expect, these show parcels rising in the low latitudes and sinking in high latitudes, providing a tendency to flatten the isopycnals and reduce the meridional temperature gradient.

The residual circulation also shows fluid entering of leaving the domain at the boundary — what does this represent? Suppose that instead of solving the continuous problem we had posed the problem in a finite number of layers (and we explicitly consider the two-layer problem below). As the number of layers increases the solutions to the linear baroclinic instability problem approach that of the Eady problem (e.g., Fig. 6.13); however, as we saw in section 7.3 the residual circulation is closed in the layered model, and the sum over all the layers of the meridional transport vanishes. Now, in
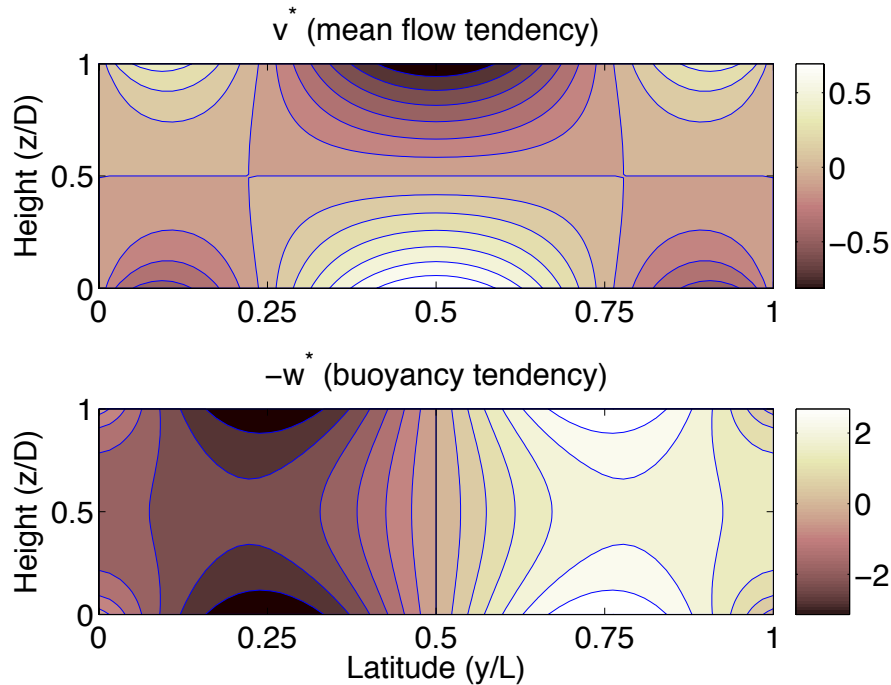
Fig. 7.4 The tendency of the zonal mean flow ($\partial \overline{u}/\partial t$) and the buoyancy ($\partial \overline{b}/\partial t$) for the Eady problem. Lighter (darker) shading means a positive (negative) tendency, but the units themselves are arbitrary.

the layered model the vertical boundary conditions are built in to the representation by way of a redefinition of potential vorticity of the top and bottom layer, so that, in the layered version of Eady problem there appears to be a potential vorticity gradient in these two layers, instead of a buoyancy gradient at the boundary. The residual circulation is then closed by a return flow that occurs only in the top and bottom layers, and as the number of layers increases this flow is confined to a thinner and thinner layer, and to a delta-function in the continuous limit. To indicate this we have placed arrows just above and below the domain in Fig. 7.3. (This equivalence between boundary conditions and delta-function sources is the same as that giving rise to the delta-function boundary layer of section 5.4.3.)

The effect on the mean flow is inferred directly from the residual circulation: the mean flow acceleration is proportional to $\overline{v}^*$ and the buoyancy tendency is proportional to $-\overline{w}^*$, and these are plotted in Fig. 7.4 and Fig. 7.5. Because there is no momentum flux convergence in the problem the zonal flow tendency is entirely baroclinic — its vertical integral is zero — and over most of the domain is such as to reduce the mean shear. Consistently (using thermal wind) the buoyancy tendency is such as to reduce the meridional temperature gradient; that is, the instabilities act to transport heat polewards and reduce the instability of the mean flow.
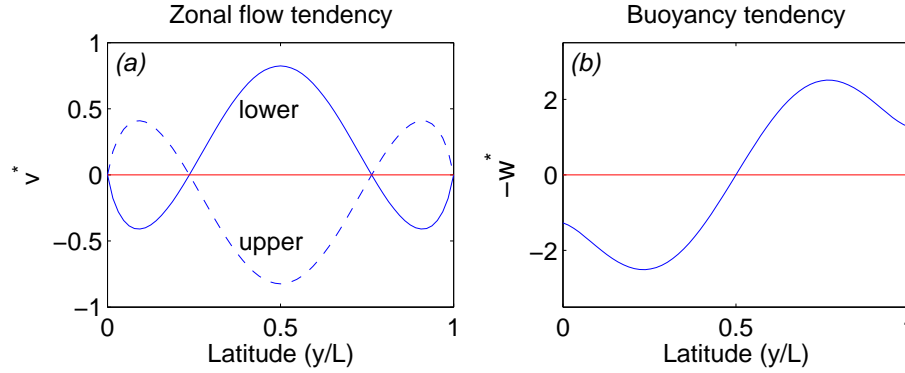
Fig. 7.5 (a) The tendency of the zonal mean flow ($\partial \overline{u}/\partial t$) just below the upper lid (dashed) and just above the surface (solid) in the Eady problem. The vertically integrated tendency is zero. (b) The vertically averaged buoyancy tendency.

7.5.3 The two-level problem

The residual circulation and mean-flow tendencies can also be calculated for the two-level (Phillips) problem, and now the β-effect can be included. The potential vorticity fluxes in each layer are non-zero and the mean flow equations are, for $i = 1, 2$,

$$\frac{\partial \overline{u}_i}{\partial t} = f_0 \overline{v}_i^* + \overline{v_1' q_1'}, \qquad \frac{\partial \overline{b}}{\partial t} = -N^2 \overline{w}^* \tag{7.135}$$

The vertical velocity and buoyancy are evaluated at mid-depth, and the thermal wind equation is $\overline{u}_1 - \overline{u}_2 = -(D/2)\partial_y \overline{b}$ and, by mass conservation, $\overline{v}_1^* = -\overline{v}_2^*$. The vertical velocity and buoyancy are evaluated at the layer interface. If we define a residual streamfunction ψ^* such that

$$\overline{v}_1^* = -\overline{v}_2^* = \psi^*, \qquad \overline{w}^* = \frac{\partial \psi^*}{\partial y}, \tag{7.136}$$

then eliminating time derivatives in (7.135) gives an equation for the residual streamfunction,

$$\frac{\partial^2 \psi^*}{\partial y^2} - \frac{k_d^2}{2}\psi^* = \frac{2 f_0 L^2}{N^2 D}(\overline{v_1' q_1'} - \overline{v_2' q_2'}), \tag{7.137}$$

where $k_d^2/2 = [2f_0/(NH)]^2$ where D is the total depth of the fluid, and we have nondimensionalized vertical scales by D and horizontal scales by L. As in the Eady problem it is only the spatial structure of the terms on the right-hand side that are relevant, and these may be calculated from the solutions to the two-level instability problem in a channel. The main difference from the Eady problem is that the potential vorticity fluxes are non-zero, even in the case with $\beta = 0$: effectively, the boundary fluxes of the Eady problem are absorbed into the potential vorticity fluxes of the two layers. Solving for the residual circulation and interpreting the mean-flow tendencies, is left as an instructive exercise for the reader.[13]

7.6 * NECESSARY CONDITIONS FOR INSTABILITY

Let's take a taxi to the finish line.

Chris Garrett, Ocean Science Meeting, Hawaii 2002.

In the remainder of this chapter we use the ideas of wave-activity conservation to derive necessary conditions for instability. In sections 6.3 and 6.5.1 we derived such conditions assuming that the instability to be of normal-mode form. Here we show that such an assumption is often not necessary, and give a derivations that are both more general and, in some ways, simpler. The derivations rely on the fact that the potential vorticity flux may be written as a divergence of a vector — and therefore vanishes when integrated over a domain, apart from boundary contributions.

7.6.1 Stability conditions from wave activity conservation

Consider again the perturbation enstrophy equation

$$\frac{1}{2}\frac{\partial}{\partial t}\overline{q'^2} = -\frac{\partial \overline{q}}{\partial y}\nabla_x \cdot \boldsymbol{\mathcal{F}}. \tag{7.138}$$

where $\boldsymbol{\mathcal{F}}$ is the Eliassen-Palm flux given by (7.21)

Dividing by $\partial q/\partial y$ and integrating over a domain $\mathcal{D}$ which is such that the Eliassen-Palm flux vanishes at the boundaries (assuming for now that this is possible) gives

$$\int_{\mathcal{D}} \frac{\partial_t \overline{q'^2}}{\partial_y \overline{q}}\,\mathrm{d}x\,\mathrm{d}y = 0 \tag{7.139}$$

The quantity $q'^2/\partial_y \overline{q}$ is the pseudomomentum for this problem. Eq. (7.139) implies that, in the *norm* $\left[q'^2/\partial_y \overline{q}\right]$, the perturbation cannot grow unless $\partial \overline{q}/\partial y$ changes sign somewhere in the domain, or at the boundaries. This result does not depend on there being a normal mode instability. The simplest result of all occurs in a barotropic problem with no vertical variation. Then $\partial \overline{q}/\partial y = \partial \overline{\zeta}_a/\partial y = \beta - \partial^2 \overline{u}/\partial y^2$, and demanding that this must change sign for an instability is the Rayleigh condition for instability, or the Rayleigh-Kuo condition if β is present. In the more general case, if $\partial \overline{q}/\partial y$ changes sign along a vertical line then the instability is called a baroclinic instability, and if it changes sign along a horizontal the instability is barotropic — these may be taken as the definitions of those terms. A mixed instability has a change of sign along both a horizontal and vertical.

7.6.2 Inclusion of boundary terms

Suppose now the flow is contained between two flat boundaries, at $z = 0$ and $z = H$, and the relevant equations of motion are now the potential vorticity evolution in the interior, supplemented by the thermodynamic equation at the boundary. These give, in the usual way, [c.f. (7.10) and (7.13)]

$$\frac{\partial}{\partial t}\left(\frac{1}{2}\frac{\overline{q'^2}}{\partial_y \overline{q}}\right) = -\overline{v'q'}, \qquad 0 < z < H, \tag{7.140}$$

and

$$\frac{\partial}{\partial t}\left(\frac{1}{2}\frac{\overline{b'^2}}{\partial_y\overline{b}}\right) = -\overline{v'b'}, \qquad z = 0, H. \qquad (7.141)$$

Now, the polewards flux of potential vorticity is

$$\overline{v'q'} = -\frac{\partial}{\partial y}\overline{u'v'} + \frac{\partial}{\partial z}\left(\frac{f_0}{N^2}\overline{v'b'}\right), \qquad (7.142)$$

and integrating this expression with respect to both y and z gives

$$\int_D \overline{v'q'}\,\mathrm{d}y\,\mathrm{d}z = \left[\frac{f_0}{N^2}\overline{v'b'}\right]_0^H, \qquad (7.143)$$

assuming that the meridional boundaries are at quiescent latitudes. Integrating (7.140) over y and z, and using (7.143) gives

$$\frac{\partial}{\partial t}\iint\frac{1}{2}\frac{\overline{q'^2}}{\partial_y\overline{q}}\,\mathrm{d}y\,\mathrm{d}z = -\left[\frac{f_0}{N^2}\overline{v'b'}\right]_0^H. \qquad (7.144)$$

Using (7.141) to eliminate $\overline{v'b'}$ finally gives

$$\frac{\partial}{\partial t}\left\{\iint\frac{1}{2}\frac{\overline{q'^2}}{\partial_y\overline{q}}\,\mathrm{d}y\,\mathrm{d}z - \int\left[\frac{1}{2}\frac{f_0}{N^2}\frac{\overline{b'^2}}{\partial_y\overline{b}}\right]_0^H\,\mathrm{d}y\right\} = 0. \qquad (7.145)$$

If this expression is positive or negative definite the perturbation cannot grow and therefore the basic state is stable. Stability thus depends on the meridional gradient of potential vorticity in the interior, and the meridional gradient of buoyancy at the boundary. If $\partial\overline{q}/\partial y$ changes sign in the interior, or $\partial\overline{b}/\partial y$ changes sign at the boundary, we have the potential for instability. If these are both one signed, then various possibilities exist, for example (with $f_0 > 0$):

I. A stable case:

$$\frac{\partial\overline{q}}{\partial y} > 0 \ \ \text{and} \ \ \left.\frac{\partial\overline{b}}{\partial y}\right|_{z=0} > 0 \ \ \text{and} \ \ \left.\frac{\partial\overline{b}}{\partial y}\right|_{z=H} < 0 \implies \text{stability.} \qquad (7.146)$$

Using the thermal wind relationship, $f_0\partial\overline{u}/\partial z - -\partial\overline{b}/\partial y$ this is equivalent to:

$$\frac{\partial\overline{q}}{\partial y} > 0 \ \ \text{and} \ \ \left.\frac{\partial u}{\partial z}\right|_{z=0} < 0 \ \ \text{or} \ \ \left.\frac{\partial u}{\partial z}\right|_{z=H} > 0 \implies \text{stability.} \qquad (7.147)$$

Stability also ensues if all inequalities are switched.

II. Instability via interior-surface interactions:

$$\frac{\partial\overline{q}}{\partial y} > 0 \ \ \text{and} \ \ \left.\frac{\partial\overline{b}}{\partial y}\right|_{z=0} < 0 \ \ \text{or} \ \ \left.\frac{\partial\overline{b}}{\partial y}\right|_{z=H} > 0 \implies \text{potential instability.}$$

$$(7.148)$$

Using thermal wind this may be written:

$$\frac{\partial \overline{q}}{\partial y} > 0 \quad \text{and} \quad \frac{\partial u}{\partial z}\bigg|_{z=0} > 0 \quad \text{or} \quad \frac{\partial u}{\partial z}\bigg|_{z=H} < 0 \implies \text{potential instability.}$$

(7.149)

The condition $\partial q/\partial y > 0$ and $(\partial u/\partial z)_{z=0} > 0$ is the most common criterion for instability that is met in the atmosphere. In the troposphere we can sometimes ignore contributions of the buoyancy fluxes at the tropopause ($z = H$), and stability is then determined by the interior potential vorticity gradient and the surface buoyancy gradient. Similarly, in the ocean contributions from the ocean floor are normally very small.

III. *Instability via edge wave interaction:*

$$\frac{\partial \overline{b}}{\partial y}\bigg|_{z=0} < 0 \quad \text{and} \quad \frac{\partial \overline{b}}{\partial y}\bigg|_{z=H} < 0 \implies \text{potential instability.}$$

(7.150)

And similarly, with both inequalities switched. Using thermal wind this may be written:

$$\frac{\partial u}{\partial z}\bigg|_{z=0} > 0 \quad \text{or} \quad \frac{\partial u}{\partial z}\bigg|_{z=H} > 0 \implies \text{stability.}$$

(7.151)

This occurs in the Eady problem, and in effect in the real atmosphere, where the troposphere acts to some degree like a lid in the linear problem.

Typically, in the atmosphere, the zonally averaged potential vorticity gradient in the interior is positive almost everywhere, and baroclinic instability arises because of temperature gradient at the lower boundary. Consider, for example, the Eady problem in which the basic state is $\overline{u} = \Gamma z$, N^2 is a constant and $\beta = 0$. Then the basic state has $\overline{q} = 0$ in the interior and the instability arises because $\partial \overline{b}/\partial y$ has the same sign at the upper and lower boundaries, as in case III above. If there is no lid at $z = H$, then the instability in the Eady problem disappears. However, instability may arise if there is a positive shear at the lower boundary and a positive potential vorticity gradient in the interior and this occurs in the Charney problem.

One consequence of the upper boundary condition is that it provides a condition on depth of the disturbance. In the Eady problem the evolution of the system is determined by temperature evolution at the surface,

$$\frac{\mathrm{D}b}{\mathrm{D}t} = 0 \quad \text{at} \quad z = 0, \; H,$$

(7.152)

(where $b = f_0 \partial \psi/\partial z$) and zero potential vorticity in the interior, which implies that

$$\nabla^2 \psi + k_d^2 H^2 \frac{\partial^2 \psi}{\partial z^2} = 0 \quad 0 < z < H,$$

(7.153)

where $k_d = f_0/(HN)$. Assuming a solution of the form $b \sim \sin kx$ then the Poisson equation (7.153) becomes

$$H^2 k_d^2 \frac{\partial^2 \psi}{\partial z^2} = -k^2 \psi$$

(7.154)

with solutions $\psi = A\exp(-\alpha z) + B\exp(\alpha z)$ where $\alpha^2 = k^2 N^2 / f_0^2$. The scale height of the disturbance is thus

$$h \sim \frac{f_0 L}{2\pi N} \tag{7.155}$$

where $L \sim 2\pi/k$ is the horizontal scale of the disturbance. If the upper boundary is higher than this, it cannot interact strongly with the surface, because the disturbances at either boundary decay before reaching the other. Put another way, if the structure of the disturbance is such that it is shallower than H, the presence of the upper boundary is not felt. In the Eady problem, we know that the upper boundary must be important, because it is only by its presence that the flow can be unstable. Thus, all unstable modes in the Eady problem must be 'deep' in this sense, which can be verified by direct calculation. This condition gives rise to a physical interpretation of the high-wavenumber cut-off: if L is too small, the modes are too shallow to span the full depth of the fluid, and from (7.155) the condition for this is

$$L_c = 2\pi \frac{NH}{f_0} \tag{7.156}$$

or

$$K_c = \frac{f_0}{NH} = L_{\mathrm{d}}. \tag{7.157}$$

Wavenumbers larger than the deformation radius are stable in the Eady problem. If β is non-zero, this condition does not apply, because the necessary condition for instability can be satisfied by a combination of a surface temperature gradient and an interior gradient of potential vorticity provided by β, as in condition (II) in section 7.6.2. Thus, we may expect that, if $\beta \neq 0$, higher wavenumbers ($k > k_d$) may be unstable but if so they will be shallow, and this may be confirmed by explicit calculation (see figures 6.12, 6.19 and **??**.) In the two-level model shallow modes are, by construction, not allowed so that high wavenumbers will be stable, with or without beta.

7.7 * NECESSARY CONDITIONS FOR INSTABILITY: PSEUDOENERGY

In this section we derive another necessary condition for instability, based on the conservation properties of energy and enstrophy.[14]

7.7.1 Two-dimensional flow

First consider inviscid, incompressible two-dimensional flow governed by the equation of motion

$$\frac{\partial q}{\partial t} + J(\psi, q) = 0 \tag{7.158}$$

where $q = \zeta + f = \nabla^2 \psi + f$ is the absolute vorticity and ψ is the streamfunction. In a steady state, the streamfunction and the potential vorticity are functions of each other so that

$$q = Q(\Psi), \qquad \text{and} \qquad \psi = \Psi(Q) \tag{7.159}$$

where Q is a differentiable but otherwise arbitrary function of its argument, and Ψ its functional inverse. Eq. (7.158) is then

$$\frac{\partial q}{\partial t} = -\frac{\mathrm{d}Q}{\mathrm{d}\psi} J(\Psi, \Psi) = 0, \tag{7.160}$$

and all steady solutions are of the form (7.159). We shall prove that if $\mathrm{d}\Psi/\mathrm{d}Q > 0$ then the flow is stable, in a sense to be made explicit below. Consider the evolution of perturbations about such a steady state, so that

$$q = Q + q', \qquad \psi = \Psi + \psi', \tag{7.161}$$

and we suppose that the perturbation vanishes at the domain boundary or that the boundary conditions are periodic. The linearized perturbation satisfies

$$\frac{\partial q'}{\partial t} + J(\psi', Q) + J(\Psi, q') = 0. \tag{7.162}$$

Now, because potential vorticity is conserved on parcels any function of potential vorticity is also materially conserved, and in particular

$$\frac{\mathrm{D}\Psi(q)}{\mathrm{D}t} = 0. \tag{7.163}$$

Linearizing this about $q = Q$ gives

$$\frac{\mathrm{d}\Psi}{\mathrm{d}Q}\frac{\partial q'}{\partial t} + J(\psi', \Psi) + J(\Psi, \frac{\mathrm{d}\Psi}{\mathrm{d}Q}q') = 0. \tag{7.164}$$

Form an energy equation from (7.162) by mulitplying by $-\psi'$ and integrating over the domain. Integrating the first term by parts we find

$$\frac{\mathrm{d}}{\mathrm{d}t}\int \frac{1}{2}(\nabla\psi')^2 \,\mathrm{d}A = \int \psi' J(\Psi, q') \,\mathrm{d}A. \tag{7.165}$$

Similarly, from (7.164) we obtain

$$\frac{\mathrm{d}}{\mathrm{d}t}\int \frac{1}{2}\frac{\mathrm{d}\Psi}{\mathrm{d}Q}q'^2 \,\mathrm{d}A = -\int \left[q' J(\psi', \Psi) + q' J(\Psi, \frac{\mathrm{d}\Psi}{\mathrm{d}Q}q')\right] \mathrm{d}A. \tag{7.166}$$

The second term in square brackets vanishes. This follows using the property of Jacobians, obtained by integrating by parts, that

$$\langle a J(b, c)\rangle = \langle b J(c, a)\rangle = \langle c J(a, b)\rangle = -\langle c J(b, a)\rangle, \tag{7.167}$$

where the angle brackets denote horizontal integration. Using this we have

$$\left\langle q' J(\Psi, \frac{\mathrm{d}\Psi}{\mathrm{d}Q}q')\right\rangle = -\left\langle \frac{\mathrm{d}\Psi}{\mathrm{d}Q}q' J(\Psi, q')\right\rangle = -\frac{1}{2}\left\langle \frac{\mathrm{d}\Psi}{\mathrm{d}Q} J(\Psi, q'^2)\right\rangle = -\frac{1}{4}\left\langle J(\frac{\mathrm{d}\Psi^2}{\mathrm{d}Q}, q'^2)\right\rangle = 0. \tag{7.168}$$

Adding (7.165) and (7.166) then gives us the conservation law,

$$
\boxed{
\begin{aligned}
\widehat{H} &= \frac{1}{2} \int \left[(\nabla \psi')^2 + \frac{\mathrm{d}\Psi}{\mathrm{d}Q} q'^2 \right] \mathrm{d}A \\
\frac{\mathrm{d}\widehat{H}}{\mathrm{d}t} &= 0
\end{aligned}
}
\tag{7.169}
$$

The quantity $\widehat{H}$ is known as the *pseudoenergy* of the disturbance and because it is a conserved quantity, quadratic in the wave amplitude, it is (like pseudomomentum) a wave-activity. Its conservation holds whether the disturbance is growing, decaying, or neutral.

If $\mathrm{d}\Psi/\mathrm{d}Q$ is positive everywhere the pseudoenergy is a positive-definite quantity, and the growth of the disurbance is then strictly limited, and the basic state is *stable in the sense of Liapunov*. This means that the magnitude of the perturbation, as measured by some norm, is bounded by its initial magnitude. In this case we define the norm

$$
||\psi||^2 \equiv \int \left[(\nabla \psi)^2 + \frac{\mathrm{d}\Psi}{\mathrm{d}Q} (\nabla^2 \psi)^2 \right] \mathrm{d}A,
\tag{7.170}
$$

so that

$$
||\psi'(t)||^2 = ||\psi'(0)||^2.
\tag{7.171}
$$

If $\mathrm{d}\Psi/\mathrm{d}Q > 0$ then, although the energy of the disturbance can grow, its final amplitude is bounded by the initial value of the pseudoenergy, because if perturbation energy is to grow perturbation enstrophy must shrink but it cannot shrink past zero. Normal mode instability, in which modes grow exponentially, is completely precluded.

If the pseudoenergy is *negative definite* then stability is also assured, but this is a less common situation for it demands that $\mathrm{d}\Psi/\mathrm{d}Q$ is sufficiently negative so that the (negative of the) enstrophy contribution is always larger than the energy contribution, and this can usually only be satisfied in a sufficiently small domain. To see this, suppose that $q' = \nabla^2 \psi'$, and that in the domain under consideration the Lapacian operator has eigenvalues k^2 where

$$
\nabla^2 \psi' = -k^2 \psi'
\tag{7.172}
$$

and the smallest eigenvalue is k_0^2. Then by Poincaré's inequality,

$$
\int (\nabla^2 \psi')^2 \, \mathrm{d}A \geq k_0^2 \int (\nabla \psi')^2 \, \mathrm{d}A,
\tag{7.173}
$$

a sufficient condition to make $\widehat{H}$ negative definite is that

$$
\frac{\mathrm{d}\Psi}{\mathrm{d}Q} < -\frac{1}{k_0^2}.
\tag{7.174}
$$

As the domain gets bigger, k_0 diminishes and this condition becomes harder to satisfy.[15]

Parallel shear flow and Fjørtoft's condition

Consider the stability of a zonal flow (i.e., a flow in the x-direction), that varies only with y. The flow stability condition is then

$$\frac{\mathrm{d}\Psi}{\mathrm{d}Q} = \frac{\mathrm{d}\Psi/\mathrm{d}y}{\mathrm{d}Q/\mathrm{d}y} = -\frac{U - U_s}{\beta - U_{yy}} > 0, \qquad (7.175)$$

where the last equality follows because the problem is Galilean invariant, and we are therefore at liberty to add an arbitrary constant zonal flow, U_s to the problem. (It is typical in applications of the pseudoenergy argument that we choose a zonal flow appropriately to obtain a useful stability condition.) To connect this with Fjørtoft's condition (chapter 6) multiply top and bottom by $(\beta - U_{yy})$, whence we see that a sufficient condition for stability is that $(U - U_s)(\beta - U_{yy})$ is everywhere negative. The derivation here, unlike our earlier one, makes it clear that the condition does not only apply to normal mode instabilities.

7.7.2 * Stratified quasi-geostrophic flow

The extension of the pseudoenergy arguments to quasi-geostrophic flow is mostly straightforward, but with a complication from the vertical boundary conditions at the surface and at an upper boundary, and the reader may wish to skip straight to the results, (7.180)–(7.182).[16] For definiteness, we consider Boussinesq, β-plane quasi-geostrophic flow confined between flat rigid surfaces at $z = 0$ and $z = H$. The interior flow is governed by the familiar potential vorticity equation $\mathrm{D}q/\mathrm{D}t = 0$ and the buoyancy equation $\mathrm{D}b/\mathrm{D}t = 0$ at the two boundaries, where

$$q = \nabla^2 \psi + \beta y + \frac{\partial}{\partial z}\left(S(z)\frac{\partial \psi}{\partial z}\right), \qquad b = f_0 \frac{\partial \psi}{\partial z}, \qquad (7.176)$$

and $S(z) = f_0^2/N^2$ is positive. The basic state ($\psi = \Psi, q = Q, b = B_1, B_2$) satisfies

$$\psi = \Psi(Q), \quad 0 < z < H,$$
$$\psi = \Psi_1(B_1), \quad z = 0 \quad \text{and} \quad \psi = \Psi_2(B_2), \quad z = H. \qquad (7.177)$$

Analogous to the barotropic case, we obtain the equations of motion for the interior perturbation

$$\frac{\partial q'}{\partial t} + J(\psi', Q) + J(\Psi, q') = 0, \qquad (7.178a)$$

$$\frac{\mathrm{d}\Psi}{\mathrm{d}Q}\frac{\partial q'}{\partial t} + J(\psi', \Psi) + J\left(\Psi, \frac{\mathrm{d}\Psi}{\mathrm{d}Q}q'\right) = 0, \qquad (7.178b)$$

and at the two boundaries

$$\frac{\partial b'}{\partial t} + J(\psi', B_i) + J(\Psi_i, b') = 0, \qquad (7.179a)$$

$$\frac{\mathrm{d}\Psi_i}{\mathrm{d}B_i}\frac{\partial b'}{\partial t} + J(\psi', \Psi_i) + J\left(\Psi_i, \frac{\mathrm{d}\Psi_i}{\mathrm{d}B_i}b'\right) = 0, \qquad (7.179b)$$

for $i = 1, 2$. (By $\mathrm{d}\Psi_1/\mathrm{d}B_1$ we mean the derivative of Ψ_1 with respect to its argument, evaluated at B_1.) From these equations, we form the pseudoenergy by multiplying (7.178a) by $-\psi'$, (7.178b) by q', and (7.179a) by ψ', (7.179b) by b'. After some manipulation we obtain the pseudoenergy conservation law:

$$\boxed{\begin{aligned} \widehat{H} &= \mathcal{E} + \mathcal{Z} + \mathcal{B}_1 + \mathcal{B}_2 \\ \frac{\mathrm{d}\widehat{H}}{\mathrm{d}t} &= 0 \end{aligned}}, \qquad (7.180)$$

where

$$\mathcal{E} = \frac{1}{2}\left\{ (\nabla\psi')^2 + S\left(\frac{\partial\psi'}{\partial z}\right)^2 \right\}, \qquad \mathcal{Z} = \frac{1}{2}\left\{ \frac{\mathrm{d}\Psi}{\mathrm{d}Q}q'^2 \right\},$$
$$\mathcal{B}_1 = \frac{1}{2}\left\langle \frac{S(0)}{f_0}\frac{\mathrm{d}\Psi_1}{\mathrm{d}B_1}b'(0)^2 \right\rangle, \qquad \mathcal{B}_2 = -\frac{1}{2}\left\langle \frac{S(H)}{f_0}\frac{\mathrm{d}\Psi_2}{\mathrm{d}B_2}b'(H)^2 \right\rangle. \qquad (7.181)$$

where the curly brackets denote a three-dimensional integration over the fluid interior, and the angle brackets denote a horizontal integration over the boundary surfaces at 0 and H. The pseudoenergy $\widehat{H}$ is positive-definite, and therefore stability is assured in that norm, if all of the following conditions are satisfied:

$$\frac{\mathrm{d}\Psi}{\mathrm{d}Q} > 0, \qquad \frac{1}{f_0}\frac{\mathrm{d}\Psi_1}{\mathrm{d}B_1} > 0, \qquad \frac{1}{f_0}\frac{\mathrm{d}\Psi_2}{\mathrm{d}B_2} < 0. \qquad (7.182)$$

If the flow is compressible then potential vorticity is $q = \nabla^2\psi + \beta y + \rho^{-1}\partial_z(\rho S\partial_z\psi)$, where $\rho = \rho(z)$, but the final stability conditions are unaltered. If the upper boundary is then removed to infinity where $\rho(z) = 0$ then only the lower boundary condition contributes to (7.182). In the layered form of the quasi-geostrophic equations the vertical boundary conditions are built-in to the definitions of potential vorticity in the top and bottom layers. In this case, a sufficient condition for stability is that $\mathrm{d}\Psi/\mathrm{d}Q > 0$ in each layer. Indeed, an alternate derivation of (7.180)–(7.182) would be to incorporate the boundary conditions on buoyancy into the definition of potential vorticity by the delta-function construction of section 5.4.3.

Zonal shear flow

Consider now zonally uniform zonal flows, such as might give rise to baroclinic instability in a channel. The fields are then functions of y and z only, and the sufficient conditions for stability are:

$$\begin{aligned} \frac{\mathrm{d}\Psi}{\mathrm{d}Q} &= \frac{\partial\Psi/\partial y}{\partial Q/\partial y} = -\frac{U}{\mathrm{d}Q/\mathrm{d}y} > 0, \\ \frac{\mathrm{d}\Psi_1}{\mathrm{d}B_1} &= \frac{\mathrm{d}\Psi_1/\mathrm{d}y}{\mathrm{d}B_1/\mathrm{d}y} = \frac{U(0)}{\mathrm{d}U(0)/\mathrm{d}z} > 0, \\ \frac{\mathrm{d}\Psi_2}{\mathrm{d}B_2} &= \frac{\mathrm{d}\Psi_2/\mathrm{d}y}{\mathrm{d}B_2/\mathrm{d}y} = \frac{U(H)}{\mathrm{d}U(H)/\mathrm{d}z} < 0. \end{aligned} \qquad (7.183)$$

using the thermal wind relation, and setting $f_0 = 1$ (its value is irrelevant). These results generalize Fjørtoft's condition to the stratified case,[17] and as in that case we are at liberty to add a uniform zonal flow to all the velocities.

7.8 * NECESSARY CONDITIONS FOR BAROCLINIC INSTABILITY

The conditions derived in the previous section can be used to provide useful necessary conditions for baroclinic instability.

7.8.1 Minimum shear in two-layer flow

A pseudoenergy argument

We consider two-layers of equal depth, on a flat-bottomed β-plane with basic state

$$\Psi_1 = -U_1 y, \qquad\qquad \Psi_2 = -U_2 y \qquad\qquad (7.184a)$$

$$Q_1 = \beta y - \frac{k_d^2}{2}(U_2 - U_1)y, \qquad Q_2 = \beta y - \frac{k_d^2}{2}(U_1 - U_2)y \qquad (7.184b)$$

This state is characterized by $Q_i = \gamma_i \Psi_i$ where

$$\gamma_1 = -\frac{(\beta + k_d^2 \widehat{U})}{(\overline{U} + \widehat{U})}, \qquad \gamma_2 = -\frac{(\beta - k_d^2 \widehat{U})}{(\overline{U} - \widehat{U})} \qquad (7.185)$$

where $\overline{U} = (U_1 + U_2)/2$ and $\widehat{U} = (U_1 - U_2)/2$. The barotropic flow does not affect the stability properties, so without loss of generality we may *choose* $\overline{U} < -\widehat{U}$, and this makes $\gamma_1 > 0$. Then γ_2 is also positive if $\beta > k_d^2 \widehat{U}/2$. Thus, a sufficient condition for stability is that

$$\widehat{U} < \frac{\beta}{k_d^2}, \qquad\qquad (7.186)$$

as obtained in chapter 6. The derivation here shows that the condition is not restricted to normal mode instabilities.[18]

Pseudomomentum

The flow will also be stable if in both layers $\partial Q/\partial y > 0$, for then the conserved pseudomomentum will be positive definite. From (7.184) $dQ_1/dy > 0$ and dQ_2/dy will both be positive (for $U_1 > U_2$), and the flow will therefore be stable, if

$$\widehat{U} = \frac{1}{2}(U_1 - U_2) < \frac{\beta}{k_d^2} \qquad\qquad (7.187)$$

as in (7.186).

7.8.2 The high wavenumber cut-off in two-layer baroclinic instability

We can use a pseudoenergy argument to show that there is a high-wavenumber cut-off to two layer baroclinic instability, with the basic state (7.184). The conserved pseudoenergy analogous to (7.180) and (7.181) is readily found to be

$$\widehat{H} = \left\langle (\nabla\psi'_1)^2 + (\nabla\psi'_2)^2 + \frac{1}{2}k_d^2(\psi'_1 - \psi'_2)^2 + \frac{q_1'^2}{\gamma_1} + \frac{q_2'^2}{\gamma_2} \right\rangle = 0. \qquad (7.188)$$

Let us choose (without loss of generality) the barotropic flow to be $\overline{U} = \beta/k_d^2$. We then have $\gamma_1 = \gamma_2 = -1/k_d^2$, and the pseudoenergy then just the actual energy minus k_d^{-2} times the total enstrophy. If we define $\psi = (\psi'_1 + \psi'_2)/2$ and $\tau = (\psi'_1 - \psi'_2)/2$ then, using (9.30a) and (9.33), (7.188) may be expressed as

$$\widehat{H} = \left\langle (\nabla\psi)^2 + (\nabla\tau)^2 + k_d^2\tau^2 - k_d^{-2}\left\{ (\nabla^2\psi)^2 + \left[(\nabla^2 - k_d^2)\tau \right]^2 \right\} \right\rangle \qquad (7.189)$$

Now, let us express the fields as Fourier sums,

$$(\tau, \psi) = \sum_{k,l} (\widetilde{\tau}_{k,l}, \widetilde{\psi}_{k,l})e^{i(kx+ly)}. \qquad (7.190)$$

(This expression assumes a doubly-periodic domain; essentially the same end-result is obtained in a channel.) The pseudoenergy may then be written as

$$\widehat{H} = \sum_{k,l} \left[K^2\widetilde{\psi}_{k,l}^2(k_d^2 - K^2) + K'^2\widetilde{\tau}_{k,l}^2(k_d^2 - K'^2) \right] \qquad (7.191)$$

where $K^2 = k^2 + l^2$ and $K'^2 = K^2 + k_d^2$. If the deformation radius is sufficiently large (or the domain sufficiently small) that $K^2 > k_d^2$, then the pseudoenergy is *negative-definite,* so the flow is stable, no matter what the shear may be. Such a situation might arise on a planet whose circumference were less than the deformation radius, or in a small ocean basin. In the linear problem, in which perturbation modes do not interact, horizontal wavenumbers with $k^2 > k_d^2$ are stable and there is thus a high-wavenumber cut-off to instability, as was found in chapter 6 by direct calculation.

Notes

1 After Eliassen and Palm (1961).

2 A more general derivation of the group velocity property follows directly from (7.25a). See Hayes (1977).

3 These restrictions on the basic state are not necessary to prove orthogonality, but they make the algebra simpler. Also, we don't pay attention here to the nature of the eigenvalues of (7.41), which in general consist of both a discrete and continuous spectrum. See Farrell (1984) and McIntyre and Shepherd (1987).

4 Andrews and McIntyre (1976, 1978) and Boyd (1976).

5 Original derivation by McIntosh and McDougall (1996). I'm grateful to A. Plumb for a discussion about the derivation given here, which differs slightly from theirs. See also deSzoeke and Bennett (1993) for related earlier work, and Juckes (2001) and Nurser and Lee (2004) for generalizations.

6 This problem can be worked around in some cases; see e.g., Plumb (1990) and Greatbatch (1998).

7 Andrews and McIntyre (1978).

8 Plumb and Ferrari (2005). Also see Held and Schneider (1999).

9 The issues involved are not settled and progress is being made apace, so it is hard to say more without soon being out of date.

10 Nonacceleration arguments have a long history, including contributions from Charney and Drazin (1961), Eliassen and Palm (1961), Holton (1974) and Boyd (1976), and the final result may be called the 'Charney-Drazin-Boyd nonacceleration theorem'. Andrews and McIntyre (1978) put these results in the context of the EP flux and the TEM formalism, and Dunkerton (1980) reviews and provides examples.

11 Conservation laws of this ilk, their connection to the underlying symmetries of the basic state and (relatedly) their finite amplitude extension, are discussed by McIntyre and Shepherd (1987) and Shepherd (1990). Conservation of momentum is related to the translational invariance of the medium; conservation of $\mathcal{A}$ is related to the translational invariance of the mean flow, and hence the appellation 'pseudomomentum'.

12 See Andrews and McIntyre (1978).

13 See Shepherd (1983).

14 This is an example of a so-called Arnold condition. Such conditions can be derived more generally by variational methods, but our derivation will be elementary and direct. The original papers are Arnold (1965, 1966), and a number of results were developed by Holm et al. (1985). See Shepherd (1990) for a review.

15 More discussion, especially with regard to boundary conditions, is given in McIntyre and Shepherd (1987). This stability criterion is sometimes referred to as 'Arnold's second condition'.

16 Blumen (1968), but the method we use is more direct.

17 Pedlosky (1964) derived these conditions by a normal mode approach.

18 Pierini and Vulpiani (1981) and Vallis (1985) show that the condition is not even restricted to small amplitude perturbations.

Further Reading

Andrews, D. G., Holton, J. R. and Leovy, C.B., 1987. *Middle Atmosphere Dynamics.*
    Provides a discussion of a number of topics in wave dynamics and wave–mean flow interaction, including the TEM, mainly in the context of stratospheric dynamics.

Problems

7.1 Prove that
$$\langle a J(b,c) \rangle = \langle b J(c,a) \rangle = \langle c J(a,b) \rangle = -\langle c J(b,a) \rangle \qquad \text{(P7.1)}$$

where the angle brackets denote a horizontal integration, and the boundary conditions are either no-normal-flow or periodic.

7.2 Consider an axi-symmetric barotropic shear flow given by

$$\zeta = \begin{cases} 2\Omega & r \le R \\ 0 & r > R \end{cases} \tag{P7.2}$$

where Ω and R are constants. Thus, the inner region is in solid body rotation and the outer region is irrotational, and we suppose that the velocity is continuous. (Is this implied by (P7.2) or is it an extra condition?) Suppose that the boundary between the two regions is perturbed. Find the phase speed of this disturbance in terms of its azimuthal wavenumber. Show that for large wavenumbers this reduces to the dispersion relation for a point jet [i.e., , or $c = U_0 + (\zeta_1 - \zeta_2)/2k$ — see (6.37)], and define what 'large' means in this context.

7.3 Demonstrate the group velocity property for the Eliassen-Palm flux for barotropic Rossby waves on the β-plane when the basic state is horizontally sheared.

7.4 Show that on the sphere and in a compressible, ideal gas atmosphere the EP flux is given by
$$\boldsymbol{F} = [F_\vartheta, F_z] = [-\rho_s \cos\vartheta \overline{u'v'}, \rho_s f \cos\vartheta \overline{v'\theta'}/(\partial\overline{\theta}/\partial z)]. \tag{P7.3}$$
where ϑ is latitude, θ is potential temperature and ρ_s is a reference profile. You may use either height coordinates with the anelastic approximation, or log-pressure coordinates. In this expression, should f vary or should it be equal to a constant, f_0?

7.5 Show that on the sphere and in a compressible, ideal gas atmosphere the residual streamfunction corresponding to (7.53) is given by

$$\psi^* = \psi + a\rho_s \cos\vartheta \frac{\overline{v'\theta'}}{\partial_z\overline{\theta}}. \tag{P7.4}$$

where θ is potential temperature and ϑ is latitude.

7.6 ♦ Show that perturbations to a horizontally sheared flow are orthogonal with respect to the wave activity norm. You may restrict attention to two-dimensional (barotropic) flow on the β-plane.
Partial solution: The eigenvalue value equation is
$$(\overline{u}\nabla_k^2 + \partial_y\overline{q})\psi = c\nabla_k^2\psi \tag{P7.5}$$
where $\nabla_k^2 = \partial_{yy} - k^2$. If $q = \nabla_k^2\psi$ then the eigenvalue equation may be written
$$Mq \equiv (\overline{u} + \partial_y\overline{q}\,\nabla_k^{-2})q = cq \tag{P7.6}$$
or
$$Nq \equiv \left(\frac{\overline{u}}{\partial_y\overline{q}} + \nabla_k^{-2}\right)q = c\frac{q}{\partial_y\overline{q}} \tag{P7.7}$$
The operator N on the left-hand side of (P7.7) is self-adjoint (show this) so that the eigenfunctions associated with two different eigenvalues are orthogonal with respect to $\partial_y\overline{q}$; that is, for $n \ne m$,
$$\int\int \frac{q_n q_m}{\partial_y\overline{q}}\,\mathrm{d}y = 0. \tag{P7.8}$$

If this derivation holds, why is not simply the case that, from (P7.6), that

$$\int q_n q_m \, \mathrm{d}y = 0. \qquad \text{(P7.9)}$$

for $n \neq m$? (Is M self-adjoint?)

7.7 Obtain an expression for the EP flux due to equatorial Kelvin waves. What is the sign of the wave drag in a region of Kelvin wave generation?

7.8 ♦ Can the high-wavenumber cut-off to instability in the Eady problem be obtained by wave-activity arguments (e.g., by proving the pseudo-energy is negative definite, as in the two-layer problem). If so, do so. (I do not know if there is a solution.)

7.9 ♦ Stability conditions in the continuously stratified QG model.
Consider the modified Eady problem (Boussinesq, uniform stratification, flow contained between two flat horizontal surfaces at 0 and H), but instead of a uniform shear suppose that the basic state is given by

$$U = -U_0 \cos(\pi p z / H) \qquad \text{(P7.10)}$$

where $U_0 > 0$, and allow β to be non-zero.

(a) Show there is a critical shear, that and that this diminishes as p increases.
(b) Show there is a high-wavenumber cut-off to instability.

Compare the results to those of the two-layer model.
Sketch of solution:

(a) The basic state has no temperature gradient at the boundary, and so stability is assured if $\partial Q / \partial y$ is positive everywhere. The basic state potential vorticity is $Q = \nabla^2 \Psi + (f_0^2 / N^2) \partial^2 \Psi / \partial z^2 + \beta y$, so that

$$\frac{\mathrm{d}Q}{\mathrm{d}y} = \beta - k_d^2 \pi^2 p^2 U_0 \cos(\pi p z / H) \qquad \text{(P7.11)}$$

where $k_d^2 = f_0^2 H^2 / N^2$ and $U = -\partial \Psi / \partial y$. Thus, stability is assured if $U_0 < (\beta / k_d^2 \pi^2 p^2)$.

(b) Choose a barotropic flow equal to $-\beta / (k_d^2 \pi^2 p^2)$ so that the mean flow is $U = U_0 \cos(\pi p z / H) - \beta / (k_d^2 p^2)$. Then $\gamma(z) \equiv Q / \Psi = -k_d^2 \pi^2 p^2$. Expand the perturbation streamfunction as $\psi = \sum_{\mathbf{k}, \alpha} \psi_{\mathbf{k}, \alpha} e^{i\mathbf{k} \cdot \mathbf{x}} \cos \alpha z$ and obtain an expression for the pseudoenergy analogous to (7.191), and find the conditions under which it is sign-definite.

7.10 Obtain, or at least verify, the solution (7.134). Plot it for various values of deformation radii (using appropriate computer software).

7.11 ♦ Obtain and plot the residual circulation in the linear two-level (Phillips) baroclinic instability problem, both for $\beta = 0$ and $\beta \neq 0$. Also obtain and plot the corresponding tendencies of the zonally-averaged zonal wind and buoyancy fields, and interpret your results. A good answer will include a comparison of the solutions with and without beta, and a comparison of the solutions with those of the Eady problem.

7.12 ♦ *Balance of terms in the mean flow equations.*

(a) In the Eady problem the mean flow evolves according to (7.127). To what degree is there an instantaneous balance between the terms on the right-hand side? That is, is the mean-flow evolution a residual between two-larger terms? (The answer is trivial for the zonal flow evolution, less so for buoyancy.)

(b) Repeat this problem for the two-layer problem, in both Eulerian and TEM forms. For the latter, calculate the balance between the potential vorticity flux, the residual meridional flow and the zonal flow tendency.

I shall not today attempt further to define the kinds of material...embraced within that shorthand definition.... But I know it when I see it.
Potter Stewart, Supreme Court Associate Justice, *Jacobellis vs. Ohio,* 1964.

CHAPTER 8

Basic Theory of Incompressible Turbulence

T URBULENCE IS HIGH REYNOLDS NUMBER FLUID FLOW, dominated by nonlinearity, with both spatial and temporal disorder. No definition is perfect, and it is hard to be disentangle a definition from a property, but this statement captures the essential aspects. A turbulent flow has eddies with a spectrum of sizes between some upper and lower bounds, the former usually determined by the forcing scale or the domain scale, and the latter usually by viscosity. The individual eddies come and go, and are inherently unpredictable.

The circulation of the atmosphere and ocean is, *inter alia,* the motion of a forced-dissipative fluid subject to various constraints such as rotation and stratification. The larger scales are orders of magnitude larger than the dissipation scale (the scale at which molecular viscosity becomes important) and at many if not all scales the motion is highly nonlinear and quite unpredictable. Thus, we can justifiably say that the atmosphere and ocean are turbulent fluids. Note that we are not primarily talking about the small scale flows traditionally regarded as turbulent; our main focus will be the large-scale flows associated with baroclinic instability and greatly influenced by rotation and stratification, a kind of turbulence known as geostrophic turbulence (and sometimes called macro-turbulence). However, before discussing turbulence in the atmosphere and ocean, in this chapter we consider from a fairly elementary standpoint the basic theory of two- and three-dimensional turbulence, and in particular the theory of inertial ranges. We do not provide a comprehensive introduction to turbulence; rather, we provide an introduction to those aspects of most interest or relevance to the dynamical oceanographer or meteorologist. In the next chapter we consider the effects of rotation and stratification and the problem of geostrophic turbulence.

8.1 THE FUNDAMENTAL PROBLEM OF TURBULENCE

Turbulence is a difficult subject because it is nonlinear, and because (and relatedly) there are interactions between scales of motion. Let us first see what difficulties these bring.

8.1.1 The Closure Problem

Although in a turbulent flow it may be virtually impossible to predict the detailed motion of each eddy, the statistical properties — time averages for example — might not be changing and we might like to predict such averages. Thus, we might accept we can't predict the weather but we can try to predict the climate. Even though we know which equations determine the system, this task proves to be very difficult because the equations are nonlinear, and we come up against the *closure problem*. To see what this is, let us decompose the velocity field into mean and fluctuating components,

$$\boldsymbol{v} = \overline{\boldsymbol{v}} + \boldsymbol{v}'. \tag{8.1}$$

Here $\overline{\boldsymbol{v}}$ is the mean velocity field, and $\boldsymbol{v}'$ is the deviation from that mean. The mean might be a time average, in which case $\overline{\boldsymbol{v}}$ is a function only of space and not time, or it might be a time mean over a finite period (e.g., a season if we are dealing with the weather), or it might be some form of ensemble mean. The average of the deviation is, by definition, zero; that is $\overline{\boldsymbol{v}'} = 0$. The idea is to substitute (8.1) into the momentum equation and try to obtain a closed equation for the mean quantity $\overline{\boldsymbol{v}}$. Rather than dealing with the full Navier-Stokes equations, let us carry out this program for a model nonlinear system which obeys

$$\frac{\mathrm{d}u}{\mathrm{d}t} + uu + ru = 0 \tag{8.2}$$

where r is a constant. The average of this equation is:

$$\frac{\mathrm{d}\overline{u}}{\mathrm{d}t} + \overline{uu} + r\overline{u} = 0 \tag{8.3}$$

The value of the term $\overline{uu}$ is not deducible simply by knowing $\overline{u}$, since it involves correlations between eddy quantities $\overline{u'u'}$. That is, $\overline{uu} = \overline{u}\,\overline{u} + \overline{u'u'} \neq \overline{u}\,\overline{u}$. We can go to next order to try (vainly!) to obtain an equation for $\overline{uu}$. First multiply (8.2) by u to obtain an equation for u^2, and then average it to yield:

$$\frac{1}{2}\frac{\mathrm{d}\overline{u^2}}{\mathrm{d}t} + \overline{uuu} + r\overline{u^2} = 0 \tag{8.4}$$

This equation contains the undetermined cubic term $\overline{uuu}$. An equation determining this would contain a quartic term, and so on in an unclosed hierarchy. Many methods of 'closing the hierarchy' make assumptions about the relationship of $(n + 1)$'th order terms to n'th order terms, for example by supposing that:

$$\overline{uuuu} = \alpha\overline{uu}\,\overline{uu} + \beta\overline{uuu} \tag{8.5}$$

where α and β are some parameters, and closures set in physical space or in spectral space (i.e., acting on the Fourier transformed variables) both exist. If we know that the variables are distributed normally then such closures can be made exact, but this is not generally the case in fluid turbulence.

This same closure problem arises in the Navier-Stokes equations. If density is constant (say $\rho = 1$) the x-momentum equation for an averaged flow is

$$\frac{\partial \overline{u}}{\partial t} + (\overline{\boldsymbol{v}} \cdot \nabla)\overline{u} = -\frac{\partial \overline{p}}{\partial x} - \nabla \cdot \overline{\boldsymbol{v}'u'}. \tag{8.6}$$

Written out in full in Cartesian coordinates, the last term is

$$\nabla \cdot \overline{\boldsymbol{v}'u'} = \frac{\partial}{\partial x}\overline{u'u'} + \frac{\partial}{\partial y}\overline{u'v'} + \frac{\partial}{\partial z}\overline{u'w'} \tag{8.7}$$

These terms, and the similar ones in the y- and z- momentum equations, represent the effects of eddies on the mean flow and are known as *Reynolds stress* terms. One way of expressing the 'problem of turbulence' is to find a representation of such Reynolds stress terms in terms of mean flow quantities. Nobody has been able to close the system, in any useful way, without introducing physical assumptions not directly deducible from the equations of motion themselves. Indeed, not only has the problem not been solved, it is not clear that a useful closed-form solution generally exists.

8.1.2 Triad Interactions in turbulence

The nonlinear term in the equations of motion not only leads to difficulties in closing the equations, but it leads to interactions among different length scales, and in this section we write the equations of motion in a form that makes this explicit. Purely for algebraic simplicity we will restrict attention two-dimensional flows, but very similar considerations also apply in three-dimensions, and the details of the algebra following are not of themselves important to subsequent sections.[1]

The equation of motion for an incompressible fluid in two-dimensions [see for example (4.77) or (5.120)] may be written as

$$\frac{\partial \zeta}{\partial t} + J(\psi, \zeta) = F + \nu \nabla^2 \psi, \qquad \zeta = \nabla^2 \psi. \tag{8.8}$$

where we include a forcing and viscous term but no Coriolis term. Let us suppose that the fluid is contained in a square, doubly-periodic domain of side L, and let us expand the streamfunction and vorticity in Fourier series so that, with a tilde denoting a Fourier coefficient,

$$\psi(x, y, t) = \sum_{\boldsymbol{k}} \widetilde{\psi}(\boldsymbol{k}, t)\mathrm{e}^{i\boldsymbol{k}\cdot\boldsymbol{x}}, \qquad \zeta(x, y, t) = \sum_{\boldsymbol{k}} \widetilde{\zeta}(\boldsymbol{k}, t)\mathrm{e}^{i\boldsymbol{k}\cdot\boldsymbol{x}}, \tag{8.9}$$

where $\boldsymbol{k} = \mathbf{i}k^x + \mathbf{j}k^y$, $\widetilde{\zeta} = -k^2\widetilde{\psi}$ where $k^2 = k^{x2} + k^{y2}$ and, to ensure that ψ is real, $\widetilde{\psi}(k^x, k^y, t) = \widetilde{\psi}^*(-k^x, -k^y, t)$, a property known as conjugate symmetry. The summations are over all positive and negative x- and y-wavenumbers, and $\widetilde{\psi}(\boldsymbol{k}, t)$ is

shorthand for $\widetilde{\psi}(k^x, k^y, t)$. Substituting (8.9) in (8.8) gives, with (for the moment) F and ν both zero,

$$
\frac{\partial}{\partial t} \sum_{k} \widetilde{\zeta}(\boldsymbol{k}, t) \mathrm{e}^{i \boldsymbol{k} \cdot \boldsymbol{x}} = -\sum_{p} p^x \widetilde{\psi}(\boldsymbol{p}, t) \mathrm{e}^{i \boldsymbol{p} \cdot \boldsymbol{x}} \times \sum_{q} q^y \widetilde{\zeta}(\boldsymbol{q}, t) \mathrm{e}^{i \boldsymbol{q} \cdot \boldsymbol{x}}
$$
$$
+ \sum_{p} p^y \widetilde{\psi}(\boldsymbol{p}, t) \mathrm{e}^{i \boldsymbol{p} \cdot \boldsymbol{x}} \times \sum_{q} q^x \widetilde{\zeta}(\boldsymbol{q}, t) \mathrm{e}^{i \boldsymbol{q} \cdot \boldsymbol{x}}.
$$

(8.10)

where $\boldsymbol{p}$ and $\boldsymbol{q}$ are, like $\boldsymbol{k}$, horizontal wave vectors. We may obtain an evolution equation for the wavevector $\boldsymbol{k}$ by multiplying (8.10) by $\exp(-i\boldsymbol{k} \cdot \boldsymbol{x})$ and integrating over the domain, and using the fact that the Fourier modes are orthogonal; that is

$$
\int \mathrm{e}^{i \boldsymbol{p} \cdot \boldsymbol{x}} \mathrm{e}^{i \boldsymbol{q} \cdot \boldsymbol{x}} \, \mathrm{d}A = \frac{1}{L^2} \delta(\boldsymbol{p} + \boldsymbol{q}).
$$

(8.11)

where $\delta(\boldsymbol{p} + \boldsymbol{q})$ equals unity if $\boldsymbol{p} = -\boldsymbol{q}$ and is zero otherwise. Using this, (8.10) becomes, restoring the forcing and dissipation terms,

$$
\frac{\partial}{\partial t} \widetilde{\psi}(\boldsymbol{k}, t) = \sum_{\boldsymbol{p}, \boldsymbol{q}} A(\boldsymbol{k}, \boldsymbol{p}, \boldsymbol{q}) \widetilde{\psi}(\boldsymbol{p}, t) \widetilde{\psi}(\boldsymbol{q}, t) + \widetilde{F}(\boldsymbol{k}) - \nu k^4 \widetilde{\psi}(\mathbf{k}, t),
$$

(8.12)

where $A(\boldsymbol{k}, \boldsymbol{p}, \boldsymbol{q}) = (q^2 / k^2)(p^x q^y - p^y q^x) \delta(\boldsymbol{p} + \boldsymbol{q} - \mathbf{k})$ is an 'interaction coefficient', and the summation is over all $\boldsymbol{p}$ and $\boldsymbol{q}$; however, note that only those wavevector triads with $\boldsymbol{p} + \boldsymbol{q} = \mathbf{k}$ make a nonzero contribution, because of presence of the delta function.

Consider, then, a fluid a fluid in which just two Fourier modes are initially excited, with wavevectors $\boldsymbol{p}$ and $\boldsymbol{q}$ say (along with their conjugate-symmetric partners at $-\boldsymbol{p}$ and $-\boldsymbol{q}$). These modes interact [obeying (8.12)] to generate third and fourth wavenumbers, $\boldsymbol{k} = \boldsymbol{p} + \boldsymbol{q}$ and $\boldsymbol{m} = \boldsymbol{p} - \boldsymbol{q}$ (again along with their conjugate-symmetric partners). These four wavenumbers can interact among themselves to generate several additional wavenumbers, $\boldsymbol{k} + \boldsymbol{p}, \boldsymbol{k} + \boldsymbol{m}$ etc, and these in turn lead to still more interactions so potentially filling out the entire spectrum of wavenumbers. The individual interactions are called *triad interactions,* and it is by way of such interactions that energy is transferred between scales in turbulent flows, in both two and three dimensions. The dissipation term does not lead to interactions between modes with different wavevectors; rather, it acts like a drag on each Fourier mode, with a coefficient that increases with wavenumber and therefore that preferentially affects small scales.

The selection rule for triad interactions — that $\boldsymbol{k} = \boldsymbol{p} + \boldsymbol{q}$ — does not restrict the scales of these interacting wavevectors, and the types of triad interactions fall between two extremes:

 (i) Local interactions, in which $k \sim p \sim q$;

 (ii) Nonlocal interactions, in which $k \sim p \gg q$.

These two kinds of triads are schematically illustrated in Fig. 8.1. Without very detailed analysis of the solutions of the equations of motion — an analysis that is impossible for fully-developed turbulence — it is impossible to say whether one particular kind of triad interaction dominates. The theory of Kolmogorov considered below, and its
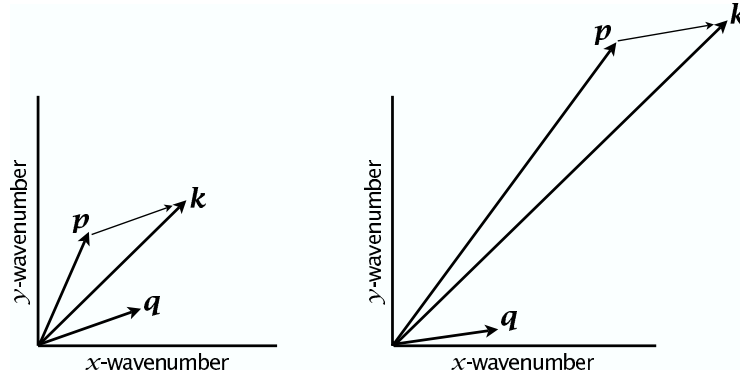
Fig. 8.1 Two interacting triads, each with $\boldsymbol{k} = \boldsymbol{p} + \boldsymbol{q}$. On the left, a local triad with $k \sim p \sim q$. On the right, a nonlocal triad with $k \sim p \gg q$.

two-dimensional analog, assume that it is the *local* triads that are most important in transferring energy; this is a reasonable assumption because from the perspective of a small edddy, large eddies appear as a nearly-uniform flow, and so simply translate the small eddies around without distorting them and thus without transferring energy between scales.

8.2 THE KOLMOGOROV THEORY

The foundation of many theories of turbulence is the spectral theory of Kolmogorov.[2] This theory does not close the equations in quite as explicit a manner as (8.5), but it does provide a prediction for the energy spectrum of a turbulent flow (loosely speaking, how much energy is present at a particular spatial scale) and it does this by suggesting a relationship between the energy spectrum (a second order quantity in velocity) and the spectral energy flux (a third order quantity).

8.2.1 The physical picture

Consider high Reynolds number (*Re*) incompressible flow that is being maintained by some external force. Then the evolution of the system is governed by

$$\frac{\partial \boldsymbol{v}}{\partial t} + (\boldsymbol{v} \cdot \nabla)\boldsymbol{v} = -\nabla p + \boldsymbol{F} + \nu \nabla^2 \boldsymbol{v} \tag{8.13}$$

and

$$\nabla \cdot \boldsymbol{v} = 0 \tag{8.14}$$

Here, $\boldsymbol{F}$ is some force we apply to maintain fluid motion — for example, we stir the fluid with a spoon. (A pedant might argue that such stirring is not a force like gravity but a continuous changing of the boundary conditions. Having noted this, we treat it as a force.) A simple scale analysis of these equations seems to indicate that the relative sizes of the inertial terms on the left-hand-side to the viscous term is the Reynolds number

VL/ν. To be explicit let us consider the ocean, and take $V = 0.1 \, \mathrm{m \, s^{-1}}$, $L = 1000 \, \mathrm{km}$ and $\nu = 10^{-6} \, \mathrm{m^2 \, s^{-1}}$. Then $Re = VL/\nu \approx 10^{11}$, and it seems that we can neglect the viscous term on the right hand side of (8.13). But this can lead to a paradox. The fluid is being forced, and this forcing is likely to put energy into the fluid. We obtain the energy budget for (8.13) by multiplying by $\boldsymbol{v}$ and integrating over a domain. If there is no flow into or out of our domain, the inertial terms in the momentum equation conserve energy and, recalling the results of section 1.9, the energy equation is

$$\frac{\mathrm{d}\widehat{E}}{\mathrm{d}t} = \frac{\mathrm{d}}{\mathrm{d}t} \int \frac{1}{2} \boldsymbol{v}^2 \, \mathrm{d}V = \int \left(\boldsymbol{F} \cdot \boldsymbol{v} + \nu \boldsymbol{v} \cdot \nabla^2 \boldsymbol{v} \right) \mathrm{d}V = \int \left(\boldsymbol{F} \cdot \boldsymbol{v} - \nu \boldsymbol{\omega}^2 \right) \mathrm{d}V$$

(8.15)

where $\widehat{E}$ is the total energy. If we neglect the viscous term we are led to an inconsistency, since the forcing term is a source of energy: $\overline{\boldsymbol{F} \cdot \boldsymbol{v}} > 0$, because a force will normally, on average, produce a velocity that is correlated with the force itself. Without viscosity, energy keeps on increasing.

What is amiss? It is true that for motion with a 1000 km length scale and a velocity of a few centimetres per second we can neglect viscosity when considering the balance of forces in the momentum equation. But this does not mean that there is no motion at much smaller length scales — indeed we seem to be led to the inescapable conclusion that there must be some motion at smaller scales in order to remove energy. Scale analysis of the momentum equation suggests that viscous terms will be comparable with the inertial terms at a scale L_ν where the Reynolds number based on that scale is of order unity, giving

$$L_\nu \sim \frac{\nu}{V}.$$

(8.16)

This is a very small scale for geophysical flows, of order millimetres or less. Where and how are such small scales generated? Boundaries are one important region. If there is high Reynolds number flow above a solid boundary, for example the wind above the ground, then viscosity *must* become important in bringing the velocity to zero in order that it can satisfy the no-slip condition at the surface, as illustrated in Fig. 2.9.

Motion on very small scales may also be generated in the fluid interior. How might this happen? Suppose the forcing acts only at large scales, and its direct action is to set up some correspondingly large scale flow, composed of eddies and shear flows and such-like. Then typically there will be an instability in the flow, and a smaller eddy will grow: initially, the large scale flow may be treated as an unchanging shear flow, and the disturbance while small will obey linear equations of motion similar to those applicable in idealized Kelvin-Helmholtz instability. This instability clearly must draw from the large scale quasi-stationary flow, and it will eventually saturate at some finite amplitude. Although it has grown in intensity, it is still typically smaller than the large scale flow which fostered it (remember how the growth rate of the shear instability gets larger as wavelength of the perturbation decreased). As it reaches finite amplitude, the perturbation itself may become unstable, and smaller eddies will feed off its energy and grow, and so on.[3] The picture that emerges is of a large scale flow that is unstable to eddies somewhat smaller in scale. These eddies grow, and develop still smaller eddies. Energy is transferred to smaller and smaller scales in a cascade-like process, sketched
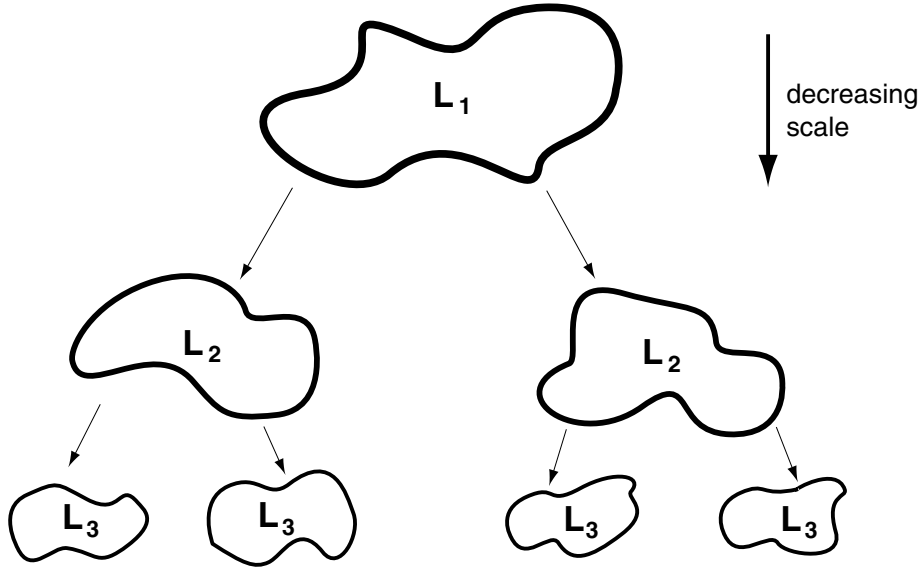
Fig. 8.2 Schema of a 'cascade' of energy to smaller scales: eddies at a large scale break up into smaller scale eddies, thereby transferring energy to smaller scales. If the transfer occurs between eddies of similar sizes (i.e., if it is spectrally local) the transfer is said to be a cascade. The eddies in reality are embedded within each other.

in Fig. 8.2. Finally, eddies are generated which are sufficiently small that they feel the effects of viscosity, and energy is drained away. Thus, there is a flux of energy from the large scales to the small scales, where it becomes dissipated.

8.2.2 Inertial range theory

Given the above picture it becomes possible to predict what the energy spectrum is. Let us suppose that the flow is statistically isotropic (i.e., the same in all directions) and homogeneous (i.e., the same everywhere; note that all isotropic flows are homogeneous, but not vice versa). Homogeneity precludes the presence of solid boundaries but can be achieved in a periodic domain. This puts an upper limit, sometimes called the outer scale, on the size of eddies.

If we decompose the velocity field into Fourier components, then in a finite domain we may write

$$u(x, y, z, t) = \sum_{k^x, k^y, k^z} \widetilde{u}(k^x, k^y, k^z, t) e^{i(k^x x + k^y y + k^z z)} \tag{8.17}$$

where $\widetilde{u}$ is the Fourier transformed field of u, with similar identities for v and w. The sum is over all wavenumbers and in finite domain the wavenumbers are quantized, so that, for example, $k^x = 2\pi n/L$, where n is an integer and L the domain size. Finally, to ensure that u is real we require that $\widetilde{u}(-k^x, -k^y, -k^z) = \widetilde{u}^*(k^x, k^y, k^z)$, where the

asterisk denotes the complex conjugate. The energy in the fluid is given by (assuming density is unity)

$$
\widehat{E} = \int E \, dV = \frac{1}{2} \int (u^2 + v^2 + w^2) \, dV
$$

$$
= \frac{1}{2} \sum (|\widetilde{u}|^2 + |\widetilde{v}|^2 + |\widetilde{w}|^2) \, d\boldsymbol{k} \qquad (8.18)
$$

using Parseval's theorem, where $\widehat{E}$ is the total energy and E is the energy per unit volume. We will now suppose that the turbulence is homogeneous and isotropic, and furthermore we will suppose that the domain is sufficiently large that the sums in the above equations may be replaced by integrals. We then write (8.18) as

$$
\widehat{E} \equiv \int \mathcal{E}(k) \, dk \qquad (8.19)
$$

where $\mathcal{E}(k)$ is the energy spectral density, or the energy spectrum, (so that $\mathcal{E}(k)\delta k$ is the energy in the small wavenumber interval δk) and because of the assumed isotropy, the energy is a function only of the scalar wavenumber k, where $k^2 = k^{x2} + k^{y2} + k^{z2}$.

We now suppose that the fluid is stirred at large scales and, via the nonlinear terms in the momentum equation, that this energy is transferred to small scales where it is dissipated by viscosity. The key assumption is to suppose that, if forcing scale is sufficiently larger than the dissipation scale, there exists a range of scales intermediate between the large scale and the dissipation scale where neither forcing nor dissipation are explicitly important to the dynamics. This assumption, known as the *locality hypothesis,* depends on the nonlinear transfer of energy being sufficiently local (in spectral space). This intermediate range is known as the *inertial range,* because the inertial terms and not forcing or dissipation must dominate in the momentum balance. If the rate of energy input per unit volume by stirring is equal to ε, then if we are in a steady state there must be a flux of energy from large scales to small also equal to ε, and an energy dissipation rate, also ε.

Now, we have no general theory for the energy spectrum of a turbulent fluid but we we might write it in the general form general form

$$
\mathcal{E}(k) = g(\varepsilon, k, k_0, k_\nu) \qquad (8.20)
$$

where the right-hand side denotes a function of the energy flux ε, the wavenumber k, the forcing wavenumber k_0 and the wavenumber at which dissipation acts, k_ν (and $k_\nu \sim L_\nu^{-1}$). The function f will of course depend on the particular nature of the forcing. Now, the locality hypothesis essentially says that at some scale within the inertial range the flux of energy to smaller scales depends only on processes occurring at or near that scale. That is to say, the energy flux is only a function of $\mathcal{E}$ and k, or equivalently that the energy spectrum can be a function *only* of the energy flux ε and the wavenumber itself. From a physical point of view, as energy cascades to smaller scales the details of the forcing are forgotten but the effects of viscosity are not yet apparent, and the energy spectrum takes the form,

$$
\mathcal{E}(k) = g(\varepsilon, k). \qquad (8.21)
$$

Dimensions and the Kolmogorov Spectrum

Quantity	Dimension
Wavenumber, k	$1/L$
Energy per unit mass, E	$U^2 = L^2/T^2$
Energy spectrum, $\mathcal{E}(k)$	$EL = L^3/T^2$
Energy Flux, ε	$E/T = L^2/T^3$

If $\mathcal{E} = f(\varepsilon, k)$ then the only dimensionally consistent relation for the energy spectrum is

$$\mathcal{E} = \mathcal{K}\varepsilon^{2/3}k^{-5/3}$$

where $\mathcal{K}$ is a dimensionless constant.

The function g is, within this theory, *universal,* the same for every turbulent flow.

Let us now use dimensional analysis to gives us the form of the function $f(\varepsilon, k)$ (see the shaded box). In (8.21), the left hand side has dimensionality L^3/T^2; the dimension T^{-2} on the left-hand side can only be balanced by $\varepsilon^{2/3}$ because k has no time dependence; that is,

$$\mathcal{E}(k) \sim \varepsilon^{2/3} g(k)$$

$$\frac{L^3}{T^2} \sim \frac{L^{4/3}}{T^2} g(k). \tag{8.22}$$

where $g(k)$ is some function; this function $g(k)$ must have dimensions $L^{5/3}$ and the functional relationship we must have, if the physical assumptions are right, is

$$\boxed{\mathcal{E}(k) = \mathcal{K}\varepsilon^{2/3}k^{-5/3}}. \tag{8.23}$$

This is the famous 'Kolmogorov -5/3 spectrum', enshrined as one of the cornerstones of turbulence theory, and sketched in Fig. 8.3, and some experimental results are shown in Fig. 8.4. The parameter $\mathcal{K}$ is a dimensionless constant, undetermined by the theory. It is known as Kolmogorov's constant and experimentally it is found to be approximately 1.5.[4]

An equivalent, perhaps slightly more intuitive, way to derive this is to first define an eddy turnover time τ_k, which is the time taken for a parcel with velocity v_k to move a distance $1/k$, v_k being the velocity associated with the (inverse) scale k. On dimensional considerations $v_k = (\mathcal{E}(k)k)^{1/2}$ so that

$$\tau_k = (k^3 \mathcal{E}(k))^{-1/2}. \tag{8.24}$$

Kolmogorov's assumptions are then equivalent to setting

$$\varepsilon \sim \frac{v_k^2}{\tau_k} = \frac{k\mathcal{E}(k)}{\tau_k}. \tag{8.25}$$

Figure 8.3 Schema of energy spectrum in three-dimensional turbulence, in the theory of Kolmogorov. Energy is supplied at some rate ε; it is transferred ('cascaded') to small scales, where it is ultimately dissipated by viscosity. There is no systematic energy transfer to scales larger than the forcing scale, so here the energy falls off.
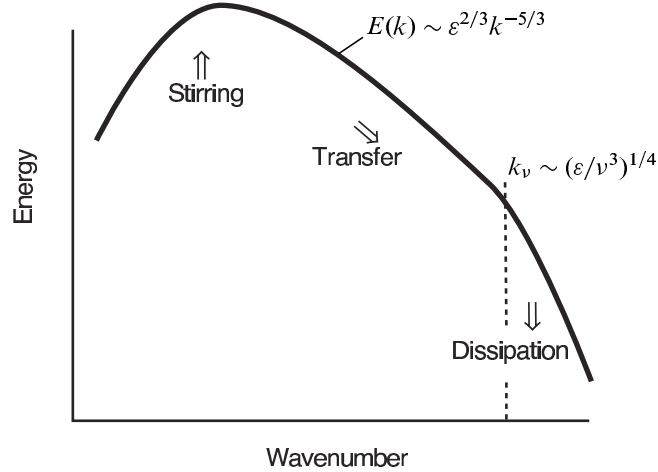
If we demand that ε be constant then (8.24) and (8.25) yield (8.23).

The viscous scale and energy dissipation

At some small length-scale we should expect viscosity to become important and the scaling theory we have just set up will fail. What is that scale? In the inertial range friction is unimportant because the timescales on which it acts are too long for it be important and dynamical effects dominate. In the momentum equation the viscous term is $\nu\nabla^2 u$ so that a viscous or dissipation timescale at a scale k^{-1}, τ_k^ν, is

$$\tau_k^\nu \sim \frac{1}{k^2\nu}, \tag{8.26}$$

so that the viscous timescale decreases with scale. The eddy turnover time, τ_k — that is, the inertial timescale — in the Kolmogorov spectrum is

$$\tau_k = \varepsilon^{-1/3}k^{-2/3}. \tag{8.27}$$

The wavenumber at which dissipation becomes important is then given by equating these two timescales, yielding the dissipation wavenumber, k_ν and the associated length-scale, L_ν,

$$k_\nu \sim \left(\frac{\varepsilon}{\nu^3}\right)^{1/4}, \qquad L_\nu \sim \left(\frac{\nu^3}{\varepsilon}\right)^{1/4}. \tag{8.28a,b}$$

L_ν is called the *Kolmogorov scale*. It is the *only* quantity which can be created from the quantities ν and ε that has the dimensions of length. (It is the same as the scale given by provided that in that expression V is the velocity magnitude at the Kolmogorov scale.) Thus, for $L \gg L_\nu$, $\tau_k \ll \tau_k^\nu$ and inertial effects dominate. For $L \ll L_\nu$, $\tau_k^\nu \ll \tau_k$ and frictional effects dominate. In fact for length-scales smaller than the dissipation scale, (8.27) is inaccurate; the energy spectrum falls off more rapidly than $k^{-5/3}$ and the inertial timescale falls off less rapidly than (8.27) implies, and dissipation dominates even more.
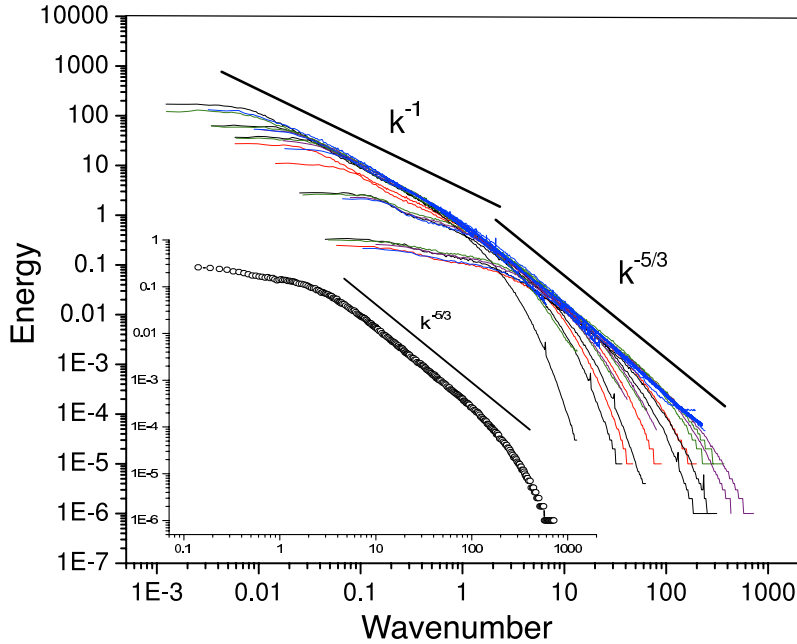
Fig. 8.4 The energy spectrum of 3D turbulence measured in some experiments at the Princeton Superpipe facility.[5] The outer plot shows the spectra from a large-number of experiments at different Reynolds numbers, with the magnitude of their spectra appropriately rescaled. Smaller scales show a good -5/3 spectrum, whereas at larger scales the eddies feel the effects of the pipe wall and the spectra are a little shallower. The inner plot shows the spectrum in the centre of the pipe in a single experiment at $Re \approx 10^6$.

Given the dissipation scale, let us estimate the energy dissipation rate. This is given by (section 1.9)

$$\dot{\hat{E}} = \int \nu \boldsymbol{v} \cdot \nabla^2 \boldsymbol{v} \, dV. \qquad (8.29)$$

The length at which dissipation acts is the Kolmogorov scale and, noting that $v_k^2 \sim \varepsilon^{2/3} k^{-2/3}$ and using (8.28a), the energy dissipation rate scales as (for a box of unit size)

$$\dot{\hat{E}} \sim \nu k_\nu^2 v_{k_\nu}^2 \sim \nu k_\nu^2 \frac{\varepsilon^{2/3}}{k_\nu^{2/3}} \sim \varepsilon. \qquad (8.30)$$

That is, the energy dissipation rate is equal to the energy cascade rate. On the one hand this seems sensible, but on the other hand it is *independent of the viscosity.* In particular, in the limit of viscosity tending to zero, L_ν tends to zero, but the energy dissipation does not! Surely the energy dissipation rate must go to zero if viscosity goes to zero? To see that this is not the case, consider that energy is input at some large scales, and the magnitude of the stirring largely determines the energy input and cascade rate. The scale at which viscous effects then become important is determined by the viscous scale, L_ν, given by (8.28b). *As viscosity tends to zero L_ν^{-1} becomes smaller in just such*

a way as to preserve the constancy of the energy dissipation. This is one of the most important results in three-dimensional turbulence. Now, we established in section 1.9 that the Euler equations (i.e., the fluid equations with the viscous term omitted from the outset) do conserve energy. This means that the Euler equations are a *singular limit* of the Navier-Stokes equations: the behaviour of the Navier-Stokes equations as viscosity tends to zero is different from the behaviour resulting from' simply omitting the viscous term from the equations *ab initio*.

How big is L_ν in the atmosphere? A crude estimate, perhaps wrong by an order of magnitude, comes from noting that ε has units of U^3/L, and that at length-scales of order $100\,\mathrm{m}$ in the atmospheric boundary layer (where there might be a three-dimensional energy cascade to small scales) velocity fluctuations are of order $1\,\mathrm{cm\,s^{-1}}$, giving $\varepsilon \approx 10^{-8}\,\mathrm{m^2\,s^{-3}}$. Using (8.28b) we then find the dissipation scale to be of order a millimetre or so. In ocean the dissipation scale is also of order millimetres.

Degrees of freedom

How many degrees of freedom does a turbulent fluid like the atmosphere potentially have? We might estimate this number, N say, by the expression

$$ N \sim \left(\frac{L}{L_\nu}\right)^3, \tag{8.31} $$

where L is the length scale of the energy-containing eddies at the large scale. If we take $L = 1000\,\mathrm{km}$ and $L_\nu = 1\,\mathrm{mm}$ this gives about 10^{27}! On a rather more general basis, we can obtain an expression for N using (8.28b), to give

$$ N \sim L^3 \left(\frac{\varepsilon}{\nu^3}\right)^{3/4}, \tag{8.32} $$

or, using $\varepsilon \sim U^3/L$,

$$ N \sim \left(\frac{UL}{\nu}\right)^{9/4} = Re^{9/4}, \tag{8.33} $$

where Re is the Reynolds number based on the large-scale flow. For typical large-scale atmospheric flows with $U \sim 10\,\mathrm{m\,s^{-1}}$, $L \sim 10^6\,\mathrm{m}$ and $\nu = 10^5\,\mathrm{m^2\,s^{-1}}$, $Re \sim 10^{12}$ and again $N \sim 10^{27}$. Obviously, this number is very approximate, but nevertheless the number of potential degrees of freedom in the atmosphere is truly enormous, greater than Avogadro's number. Thus trying to explicitly model the turbulent atmosphere explicitly is akin to trying to model the gas in a room by following the motion of each individual molecule, and it seems unnecessary. How *should* we model it? That, in a nutshell, is the (unsolved) problem of turbulence.

8.2.3 * An alternative scaling argument for inertial ranges

Kolmogorov's spectrum, as well as some other useful scaling relationships, can be obtained in a slightly different way as follows. If we for the moment ignore viscosity, the Euler equations are invariant under the following scaling transformation:

$$ x \to x\lambda \qquad v \to v\lambda^r \qquad t \to t\lambda^{1-r}, \tag{8.34} $$

where r is an arbitrary scaling exponent. So far there is minimal physics. Now make the following *physical* assumptions about the behaviour of a turbulent fluid, *with viscosity:*

(i) That the flux of energy from large to small scales (i.e., ε) is finite and constant.

(ii) That the scale invariance (8.34) holds, on a time-average, in the intermediate scales between the forcing scales and dissipation scales.

The second assumption plays the role of the locality hypothesis. Dimensional analysis then tells us that the energy flux at some wavenumber k scales as

$$\varepsilon_k \sim \frac{v_k^3}{l_k} \sim \lambda^{3r-1}. \tag{8.35}$$

where v_k and l_k are the velocity and length scales at wavenumber k. Invoking assumption (i), that ε is independent of scale, gives $r = 1/3$. The velocity then scales as

$$v_k \sim \varepsilon^{1/3} k^{-1/3}, \tag{8.36}$$

and the velocity gradient (and so vorticity) scales as $k v_k \sim \varepsilon^{1/3} k^{2/3}$. (This becomes infinite at very small scales, but this behaviour is avoided in any real physical situation by the presence of viscosity.) We can now recover (8.23) because, on dimensional grounds,

$$\mathcal{E}(k) \sim v_k^2 k^{-1} \sim \varepsilon^{2/3} k^{-2/3} k^{-1} \sim \varepsilon^{2/3} k^{-5/3}. \tag{8.37}$$

In general, the slope of the energy spectrum, k^n, is related to the scaling exponent by $n = -(2r + 1)$. The 'structure functions' S_m, which are the average of the m'th power of the velocity difference over distances $l \sim 1/k$, scale as $S_m \sim (v_k)^m \sim \varepsilon^{m/3} k^{-m/3}$. In particular the second-order structure function, which is the Fourier transform of the energy spectra, scales as $S_2 \sim \varepsilon^{2/3} k^{-2/3}$. Other results of the Kolmogorov theory follow similarly.

8.2.4 A final note on our assumptions

The assumptions of homogeneity and isotropy that are made in the Kolmogorov theory are ansatzes, in that we make them because we want to have a tractable model of turbulence (and certainly we can conceive of an experiment in which turbulence *is* for most practical purposes homogeneous and isotropic). The essential *physical* assumptions are: (i) that there exists an inertial range in which the energy flux is constant, and (ii) that the energy is cascaded from large to small scales in a series of small steps, for then the energy spectra will be determined by spectrally local quantities. The second assumption is the locality assumption and without it we could have

$$\mathcal{E}(k) = C \varepsilon^{2/3} k^{-5/3} g(k/k_0) h(k/k_v), \tag{8.38}$$

where g and h are unknown functions; this is just as dimensionally consistent as (8.23). Kolmogorov essentially postulated that there exists a range of intermediate wavenumbers over which the energy spectrum has no functional dependence of the energy spectra on the forcing or dissipation scale, and $g(k/k_0) = h(k/k_v) = 1$.

The first, and less obvious, assumption might be called the *non-intermittency* assumption, and it demands that rare events (in time or space) with large amplitudes do not dominate the energy flux or the dissipation rate. If they were to do so, then the flux would fluctuate strongly, the turbulent statistics would not be completely characterized by ε and Kolmogorov's theory would not be exactly right. (Note that in the theory ε is the mean energy cascade rate.) In fact, in high Reynolds turbulence the $-5/3$ spectra is often observed to a fairly high degree of accuracy (e.g., as in Fig. 8.4), although the higher-order statistics (e.g., higher-order structure functions) predicted by the theory are often found to be in error, and it is generally believed that Kolmogorov's theory is not exact.[6]

8.3 TWO-DIMENSIONAL TURBULENCE

Two-dimensional turbulence behaves in a profoundly different way from three-dimensional turbulence, largely because of the presence of another quadratic invariant, the enstrophy (see also section 5.6.3). In two dimensions, the vorticity equation for incompressible flow is:

$$\frac{\partial \zeta}{\partial t} + \boldsymbol{u} \cdot \nabla \zeta = F + \nu \nabla^2 \zeta \tag{8.39}$$

where $\boldsymbol{u} = u\mathbf{i} + v\mathbf{j}$ and $\zeta = \mathbf{k} \cdot \nabla \times \boldsymbol{u}$ and F is a stirring term. In terms of a streamfunction, $u = -\partial \psi / \partial y$, $v = \partial \psi / \partial x$, and $\zeta = \nabla^2 \psi$, and (8.39) may be written:

$$\frac{\partial \nabla^2 \psi}{\partial t} + J(\psi, \nabla^2 \psi) = F + \nu \nabla^4 \psi. \tag{8.40}$$

We obtain an energy equation by multiplying by $-\psi$ and integrating over the domain, and an enstrophy equation by multiplying by ζ and integrating. When $F = \nu = 0$ we find:

$$\widehat{E} = \frac{1}{2} \int_A (u^2 + v^2)\, \mathrm{d}A = \frac{1}{2} \int_A (\nabla \psi)^2\, \mathrm{d}A, \qquad \frac{\mathrm{d}\widehat{E}}{\mathrm{d}t} = 0, \tag{8.41a}$$

$$\widehat{Z} = \frac{1}{2} \int_A \zeta^2\, \mathrm{d}A = \frac{1}{2} \int_A (\nabla^2 \psi)^2\, \mathrm{d}A, \qquad \frac{\mathrm{d}\widehat{Z}}{\mathrm{d}t} = 0. \tag{8.41b}$$

where the integral is over a finite area with either no-normal flow or periodic boundary conditions. The quantity $\widehat{E}$ is the energy, and $\widehat{Z}$ is known as the *enstrophy*. This enstrophy invariant arises because the vortex stretching term, so important in three-dimensional turbulence, vanishes identically in two dimensions. In fact, because vorticity is conserved on parcels it is clear that the integral of *any* function of vorticity is zero when integrated over A; that is, from (8.39)

$$\frac{\mathrm{D}g(\zeta)}{\mathrm{D}t} = 0 \qquad \text{and} \qquad \frac{\mathrm{d}}{\mathrm{d}t} \int_A g(\zeta)\, \mathrm{d}A = 0. \tag{8.42}$$

where $g(\zeta)$ is an arbitrary function. Of this infinity of conservation properties, enstrophy conservation (with $g(\zeta) = \zeta^2$) in particular has been found to have enormous consequences to the flow of energy between scales, as we soon discover.[7]

Initial   Later
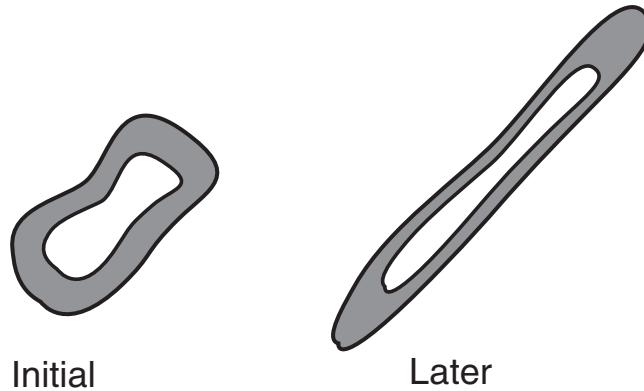
Fig. 8.5 In incompressible two-dimensional flow, a band of fluid will generally be elongated, but its area will be preserved. Since vorticity is tied to fluid parcels, the values of the vorticity in the hatched area (and in the hole in the middle) are maintained; thus, vorticity gradients will increase and the enstrophy is thereby, on average, moved to smaller scales.

8.3.1 Energy and Enstrophy Transfer in Two-Dimensional Turbulence

In three dimensional turbulence we posited that energy is cascaded to small scales via vortex stretching. In two dimensions that mechanism is absent, and it turns out that it is more reasonably to expect energy to be transferred to *larger scales*. This counter-intuitive behaviour arises from the twin integral constraints of energy and enstrophy conservation, and the following three arguments illustrate why this should be so.

I Vorticity elongation

Consider a band or a patch of vorticity, as in Fig. 8.5, in a nearly inviscid fluid. The vorticity of each element of fluid is conserved as the fluid moves. Now, we should expect that quasi-random motion of the fluid will act to elongate the band but, as its area must be preserved, the band narrows and so vorticity gradients will increase. This is equivalent to the enstrophy moving to smaller scales. Now, the energy in the fluid is

$$\widehat{E} = -\frac{1}{2} \int \psi \zeta \, dA, \tag{8.43}$$

where the streamfunction is obtained by solving the Poisson equation $\nabla^2 \psi = \zeta$. If the vorticity is locally elongated primarily only in one direction (as it must be to preserve area), the integration involved in solving the Poisson equation will lead to the scale of the streamfunction becoming larger in the direction of stretching, but virtually no smaller in the perpendicular direction. Because stretching occurs, on average, in all directions, the overall scale of the streamfunction will increase in all directions, and the cascade of enstrophy to small scales will be accompanied by a transfer of energy to large scales.

II An energy-enstrophy conservation argument

A moments thought will reveal that the distribution of energy and enstrophy in wavenumber space are respectively analogous to the distribution of mass and moment of inertia of a lever, with wavenumber playing the role of distance from the fulcrum. Any rearrangement of mass such that its distribution also becomes wider must be such that the centre of mass moves toward the fulcrum. Thus, analogously, any rearrangement of a flow that preserves both energy and enstrophy, and that causes the distribution to spread out in wavenumber space, will tend to move energy to small wavenumbers and enstrophy to large. To prove this we begin with expressions for the total energy and enstrophy:

$$\widehat{E} = \int \mathcal{E}(k)\,\mathrm{d}k, \qquad \widehat{Z} = \int \mathcal{Z}(k)\,\mathrm{d}k = \int k^2 \mathcal{E}(k)\,\mathrm{d}k, \qquad (8.44)$$

where $\mathcal{E}(k)$ and $\mathcal{Z}(k)$ are the energy and enstrophy spectra. A wavenumber characterizing the spectral location of the energy is the centroid,

$$k_{\mathrm{e}} = \frac{\int k\mathcal{E}(k)\,dk}{\int \mathcal{E}(k)\,\mathrm{d}k} \qquad (8.45)$$

and, for simplicity, we normalize units so that the denominator is unity. The spreading out of the energy distribution is formalized by setting

$$I \equiv \int (k - k_{\mathrm{e}})^2 \mathcal{E}(k)\,\mathrm{d}k, \qquad \frac{\mathrm{d}I}{\mathrm{d}t} > 0. \qquad (8.46)$$

Here, I measures the width of the energy distribution, and this is assumed to increase. Expanding out the integral gives

$$I = \int k^2 \mathcal{E}(k)\,dk - 2k_{\mathrm{e}} \int k\mathcal{E}(k)\,\mathrm{d}k + k_{\mathrm{e}}^2 \int \mathcal{E}(k)\,\mathrm{d}k$$

$$= \int k^2 \mathcal{E}(k)\,dk - k_{\mathrm{e}}^2 \int \mathcal{E}(k)\,\mathrm{d}k, \qquad (8.47)$$

where the last equation follows because $k_e = \int k\mathcal{E}(k)\,\mathrm{d}k$ is, from (8.45), the energy-weighted centroid. Because both energy and enstrophy are conserved, (8.47) gives

$$\frac{\mathrm{d}k_{\mathrm{e}}^2}{\mathrm{d}t} = -\frac{1}{\widehat{E}}\frac{\mathrm{d}I}{\mathrm{d}t} < 0. \qquad (8.48)$$

Thus, the centroid of the distribution moves to smaller wavenumber and to larger scale (see Fig. 8.6).

An appropriately defined measure of the centre of the enstrophy distribution, on the other hand, moves to higher wavenumber. The demonstration follows easily if we work with the inverse wavenumber, which is a direct measure of length. Let $q = 1/k$ and assume that the enstrophy distribution spreads out by nonlinear interactions, so that, analogously to (8.46),

$$J = \int (q - q_{\mathrm{e}})^2 \mathcal{Z}(q)\,\mathrm{d}q, \qquad \frac{\mathrm{d}J}{\mathrm{d}t} > 0, \qquad (8.49)$$
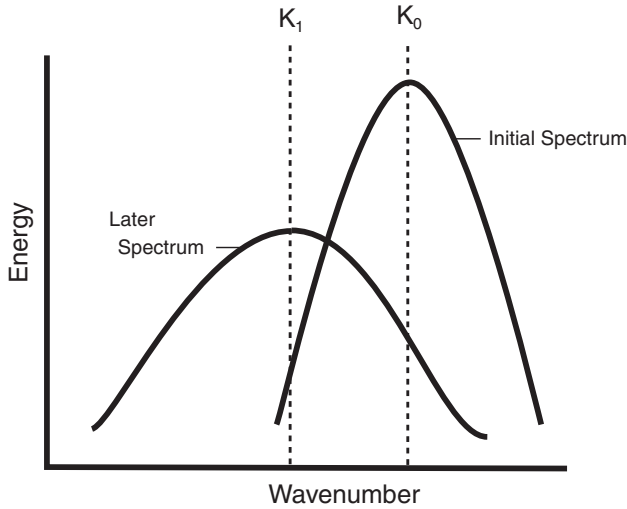
Figure 8.6 In two-dimensional flow, the centroid of the energy spectrum will move to large scales (smaller wavenumber) provided that the width of the distribution increases, which can be expected in a nonlinear, eddying flow

where

$$q_e = \frac{\int q\,Z(q)\,dq}{\int Z(q)\,dq}. \tag{8.50}$$

Expanding the integrand in (8.49) and using (8.50) gives

$$J = \int q^2 Z(q)\,dq - q_e^2 \int Z(q)\,dq, \tag{8.51}$$

But $\int q^2 Z(q)\,dq$ is conserved, because this is the energy. Thus,

$$\frac{dJ}{dt} = -\frac{d}{dt} q_e^2 \int Z(q)\,dq \tag{8.52}$$

whence

$$\frac{dq_e^2}{dt} = -\frac{1}{\hat{Z}}\frac{dJ}{dt} < 0 \tag{8.53}$$

Thus, the length scale characterizing the enstrophy distribution gets smaller, and the corresponding wavenumber gets larger.

III A similarity argument

Consider an initial value problem, in which a fluid with some initial distribution of energy is allowed to freely evolve, unencumbered by boundaries. We note two aspects of the problem:

  (i) There is no externally imposed length-scale (because of the way the problem is posed).
  (ii) The energy is conserved (this being an assumption).

It is the second condition that limits the argument to two dimensions, for in three dimensions energy is quickly cascaded to small scales and dissipated, but let us here posit that this does not occur. These two assumptions are then sufficient to infer the general

direction of transfer of energy, using a rather general similarity argument. To begin, write the total energy (per unit mass) of the fluid as

$$\widehat{E} = U^2 = \int \mathcal{E}(k,t)\,\mathrm{d}k, \qquad (8.54)$$

where $\mathcal{E}(k,t)$ is the energy spectrum and U is measure of the total energy, with units of velocity. Now, solely on dimensional considerations we can write

$$\mathcal{E}(k,t) = U^2 L\widehat{\mathcal{E}}(\widehat{k},\widehat{t}), \qquad (8.55)$$

where $\widehat{\mathcal{E}}$, and its arguments, are nondimensional quantities, and L is some length-scale. However, on physical considerations, the only parameters available to determine the energy spectrum are U, t and k, the wavenumber. A little thought reveals that the most general form for the energy spectrum with no L dependence is

$$\mathcal{E}(k,t) = U^3 t\widehat{\mathcal{E}} = U^3 t g(Ukt), \qquad (8.56)$$

where g is an arbitrary function of its arguments. The argument of g is the only non-dimensional grouping of U, t and k, and $U^3 t$ provides the proper dimensions for $\mathcal{E}$. Conservation of energy now implies that the integral

$$I = \int_0^\infty t g(Ukt)\,\mathrm{d}k \qquad (8.57)$$

not be a function of time. Defining $\vartheta = Ukt$, this requirement is met if

$$\int_0^\infty g(\vartheta)\,\mathrm{d}\vartheta = \text{constant.} \qquad (8.58)$$

Now, the spectrum is a function of k only through the combination $\vartheta = Ukt$. Thus, as time proceeds features in the spectrum move to smaller k. Suppose, for example, that the energy is initially peaked at some wavenumber k_p; the product tk_p is preserved, so k_p must diminish with time and the energy must move to larger scales. Similarly, the energy weighted mean wavenumber, k_e, moves to smaller wavenumber, or larger scale. To see this explicitly, we have

$$k_e = \frac{\int k\mathcal{E}\,\mathrm{d}k}{\int \mathcal{E}\,\mathrm{d}k} = \frac{\int k\mathcal{E}\,\mathrm{d}k}{U^2} = \int kUt\,g(Ukt)\,\mathrm{d}k = \int \frac{\vartheta g(\vartheta)}{Ut}\,\mathrm{d}\vartheta = \frac{C}{Ut} \qquad (8.59)$$

where all the integrals are over the interval $(0,\infty)$ and $C = \int \vartheta g(\vartheta)\,d\vartheta$ is a constant. Thus, the wavenumber centroid of the energy distribution decreases with time, and the characteristic scale of the flow, $1/k_e$, increases with time. Interestingly, the enstrophy does not explicitly enter this argument, and in general it is not conserved; rather, it is the requirement that energy be conserved that limits the argument to two dimensions, If we accept *ab initio* that energy *is* conserved, it must be transferred to larger scales.[8]

8.3.2 Inertial ranges in 2D turbulence

If, unlike the case in three dimensions, energy is transferred to larger scales in inviscid, nonlinear, two-dimensional flow then we might expect two-dimensional turbulence, and any associated inertial ranges, to be quite different from their three-dimensional counterparts. Before looking in detail at the inertial ranges themselves, we establish a couple of general properties of forced-dissipative flow in two dimensions.

Some properties forced-dissipative flow

We will first show that, unlike the case in three dimensions, energy dissipation goes to zero as Reynolds number rises. In the absence of forcing terms, the total dissipation of energy is, from (8.39)),

$$\frac{\mathrm{d}\widehat{E}}{\mathrm{d}t} = -\nu \int \zeta^2 \, \mathrm{d}A \tag{8.60}$$

Energy dissipation can only remain finite as $\nu \to 0$ if vorticity becomes infinite. However, this cannot happen because vorticity is conserved on parcels except for the action of viscosity, meaning that $\mathrm{D}\zeta/\mathrm{D}t = \nu\nabla^2\zeta$. However, the viscous term can only *reduce* the value of vorticity on a parcel, and so vorticity can never become infinite if it is not so initially, and therefore using (8.60) energy dissipation goes to zero with ν. (In three dimensions vorticity becomes infinite as viscosity goes to zero because of the effect of vortex stretching.) This conservation of energy is related to the fact that energy is trapped at large scales, even in forced-dissipative flow. On the other hand, enstrophy is transferred to small scales and therefore we expect it to be dissipated at large wavenumbers, even as the Reynolds number becomes very large.

We can show that energy is trapped at large scales in forced-dissipative two-dimensional flow (in a sense that will be made explicit) by the following argument.[9] Suppose that the forcing of the fluid is confined to a particular scale, characterized by the wavenumber k_f, and that dissipation is effected by a linear drag and a small viscosity. The equation of motion is

$$\frac{\partial \zeta}{\partial t} + J(\psi, \zeta) = F - r\zeta + \nu\nabla^2\zeta. \tag{8.61}$$

where F is the stirring and r and ν are positive constants. This leads to the following energy and enstrophy equations:

$$\frac{\mathrm{d}\widehat{E}}{\mathrm{d}t} = -2r\widehat{E} - \int \psi F \, \mathrm{d}x + \int \nu\zeta^2 \, \mathrm{d}A \approx -2r\widehat{E} - \int \psi F \, \mathrm{d}A, \tag{8.62a}$$

$$\frac{\mathrm{d}\widehat{Z}}{\mathrm{d}t} = -2r\widehat{Z} + \int \zeta F \, \mathrm{d}A + D_Z \approx -2r\widehat{Z} - k_\mathrm{f}^2 \int \psi F \, \mathrm{d}A + D_Z, \tag{8.62b}$$

where $D_Z = \int \nu(\nabla\zeta)^2 \, \mathrm{d}A$ is the enstrophy dissipation. To obtain the right-most expressions, in (8.62a) we assume there is no dissipation of energy by the viscous term, and in (8.62b) we assume that the forcing is confined to wavenumbers near k_f. In a statistically steady state, and writing $\widehat{E} = \int E(k) \, \mathrm{d}k$ and $\widehat{Z} = \int k^2 E(k) \mathrm{d}k$, these

expressions combine to give

$$\int k^2 E(k)\, \mathrm{d}k + \frac{D_Z}{2r} = \int k_\mathrm{f}^2 E(k)\, \mathrm{d}k, \tag{8.63}$$

integrating over all wavenumbers. Now, from the inequality $\int (k - k_\mathrm{e})^2 E(k)\, \mathrm{d}k \geq 0$, where k_e is the energy centroid defined in (8.45), we obtain

$$\int \left(k^2 - k_\mathrm{e}^2 \right) E(k)\, \mathrm{d}k \geq 0. \tag{8.64}$$

Combining (8.63) and (8.64) gives

$$\int \left(k_\mathrm{f}^2 - k_\mathrm{e}^2 \right) E(k)\, \mathrm{d}k \geq \frac{D_Z}{2R} > 0. \tag{8.65}$$

Thus, the energy containing scale, as characterized by k_e^{-1}, is larger than the forcing scale k_f^{-1}. This demonstration (rather like argument II in section 8.3.1) relies both on the conservation of energy and enstrophy by the nonlinear terms and on the particular relationship between the energy and enstrophy spectra.

   This result, and (especially) the arguments of section 8.3.1, suggest that in a forced-dissipative two-dimensional fluid, energy is transferred to larger scales and enstrophy is transferred to small scales. To obtain a statstically steady state friction (such as the Rayleigh drag of (8.61)) is necessary to remove energy at large scales, and enstrophy must be removed at small scales, but if the forcing scale is sufficiently well separated in spectral space from such frictional effects then two inertial ranges may form — an *energy inertial range* carrying energy to larger scales, and an *enstrophy inertial range* carrying enstrophy to small scales (Fig. 8.7). These ranges are analogous to the three-dimensional inertial range of of section 8.2, and similar conditions must apply if the ranges are to be truly inertial — in particular we must assume spectral locality of the energy or enstrophy transfer. But given that, we can calculate their properties, as follows.

The enstrophy inertial range

In the enstrophy inertial range the enstrophy cascade rate η, equal to the rate at whicn enstrophy is supplied by stirring, is assumed constant. By analogy with (8.25) we may assume that this rate is given by

$$\eta \sim \frac{k^3 \mathcal{E}(k)}{\tau_k}. \tag{8.66}$$

With τ_k (still) given by (8.24) we obtain

$$\boxed{\mathcal{E}(k) = \mathcal{K}_\eta \eta^{2/3} k^{-3}}, \tag{8.67}$$

where $\mathcal{K}_\eta$ is, we presume, a universal constant, analogous to the Kolmogorov constant of (8.23).
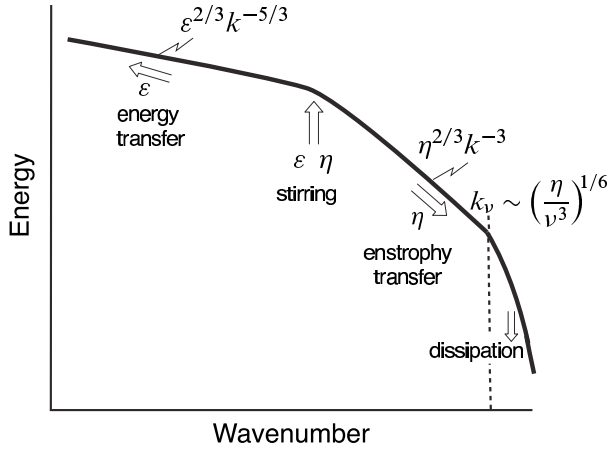
Figure 8.7 The energy spectrum of two-dimensional turbulence. (Compare with Fig. 8.3.) Energy supplied at some rate ε is transferred to large scales, whereas enstrophy supplied at some rate η is transferred to small scales, where it may be dissipated by viscosity. If the forcing is localized at a scale k_f^{-1} then $\eta \approx k_f^2 \varepsilon$.

It is also possible to obtain (8.67) from scaling arguments similar to those in section 8.2.3. The scaling transformation (8.34) still holds, but now instead of (8.35) we assume that the enstrophy flux is constant with wavenumber. Dimensionally, and analogously to (8.35), we have

$$\eta \sim \frac{v_k^3}{l_k^3} \sim \lambda^{3r-3}, \tag{8.68}$$

and the constancy of η gives $r = 1$ for the scaling exponent. The exponent n determining the slope of the inertial range is given, as before, by $n = -(2r + 1)$ yielding the -3 spectra of (8.67). The velocity at a particular wavenumber then scales as

$$v_k \sim \eta^{1/3} k^{-1}, \tag{8.69}$$

and the time scales as

$$t_k \sim l_k/v_k \sim \eta^{-1/3}. \tag{8.70}$$

We may also obtain (8.70) by substituting (8.67) into (8.24). Thus, *the eddy turnover time in the enstrophy range of two-dimensional turbulence is length-scale invariant.* The appropriate viscous scale is given by equating the inertial and viscous terms in (8.39). Using (8.69) we obtain, analogously to (8.28a),

$$k_v \sim \left(\frac{\eta^{1/3}}{\nu}\right)^{1/2}. \tag{8.71}$$

The enstrophy dissipation, analogously to (8.30) goes to a finite limit given by

$$\dot{\hat{Z}} = \nu \int_A \zeta \nabla^2 \zeta \, \mathrm{d}A \sim \nu k_v^4 v_{k_v}^2 \sim \eta, \tag{8.72}$$

using (8.69) and (8.71). Thus, the enstrophy dissipation in two-dimensional turbulence is (at least according to this theory) independent of the viscosity.

Energy inertial range

The energy inertial range of two-dimensional turbulence is quite similar to that of three-dimensional turbulence, except in one major respect: the energy flows from smaller to larger scales! Because the atmosphere and ocean both behave in some ways as two-dimensional fluids, this has profound consequences on their behaviour, and is something we return to in the next chapter. The upscale energy flow is known as the *inverse cascade,* and the associated energy spectrum is, as in the three-dimensional case,

$$\boxed{\mathcal{E}(k) = \mathcal{K}_\varepsilon \varepsilon^{2/3} k^{-5/3}} \,, \tag{8.73}$$

where $\mathcal{K}_\varepsilon$ is a nondimensional constant [not necessarily equal to $\mathcal{K}$ in (8.23)], and ε is the rate of energy transfer to larger scales. Of course we now need a mechanism to remove energy at large scales, else it will pile up at the scale of the domain and a statistical steady state will not be achieved. Introducing a linear drag, $-r\zeta$, into the vorticity equation, as in (8.61), is one means to achieve this, and such a term may be physically justified by appeal to Ekman layer theory (section 2.12). Although such a term appears to be scale invariant, its effects will be felt only at large scales because at smaller scales the timescale of the turbulence is much shorter than that of the friction. We may estimate the scale at which the drag becomes important by equating the drag timescale to the inertial timescale. The latter is given by (8.27), and equating this to the frictional timescale r^{-1} gives

$$r^{-1} = \varepsilon^{-1/3} k_r^{-2/3} \quad \longrightarrow \quad k_r = \left(\frac{r^3}{\varepsilon}\right)^{1/2} \,, \tag{8.74}$$

where k_r is the frictional wavenumber. Frictional effects are important at scales *larger* than k_r^{-1}.

8.3.3 † More about the phenomenology

The phenomenology of two-dimensional turbulence is not quite as straightforward as the above arguments imply. Note, for example, that timescale (8.70) is independent of length scale, whereas in three dimensional turbulence the timescale decreases with length scale, which seems more physical and more conducive to spectrally local interactions. A useful measure of this locality is given by estimating the contributions to the straining rate, $S(k)$, from motions at all scales.[10] The strain rate scales like the shear, so that an estimate of the total strain rate is given by

$$S(k) = \left[\int_{k_0}^{k} \mathcal{E}(p) p^2 \, \mathrm{d}p\right]^{1/2} \,, \tag{8.75}$$

where k_0 is the wavenumber of the largest scale present. The contributions to the integrand from a given wavenumber octave are given by

$$\int_{p}^{2p} \mathcal{E}(p') p'^3 \, d \log p' \sim \mathcal{E}(p) p^3 \,. \tag{8.76}$$

In three dimensions, use of the $-5/3$ spectrum indicates that the contributions from each octave below a given wavenumber k increase with wavenumber, being a maximum close to k, and this is *a posteriori* consistent with the locality hypothesis. However, in two-dimensional turbulence with a -3 spectrum each octave makes the same contribution. That is to say, the contributions to the strain rate at a given wavenumber, as defined by (8.75), are not spectrally local. This does not prove that the enstrophy transfer is spectrally non-local, but nor does it build confidence in the theory.

Dimensionally the strain rate is the inverse of a time, and if this is a spectrally nonlocal quantity then, instead of (8.24), we might use the inverse of the strain rate as an eddy turnover time giving

$$\tau_k = \left[\int_{k_0}^{k} p^2 \mathcal{E}(p) \, \mathrm{d}p \right]^{-1/2}. \tag{8.77}$$

This has the advantage over (8.24) in that it is a non-increasing function of wavenumber, whereas if the spectrum is steeper than k^{-3} (8.24) implies a timescale increasing with wavenumber. Using this in (8.66) gives a prediction for the enstrophy inertial range, namely

$$\mathcal{E}(k) = \mathcal{K}_\eta \eta^{2/3} \left[\log(k/k_0) \right]^{-1/3}, k^{-3}, \tag{8.78}$$

which is similar to (8.67) except for a logarithmic correction. This expression is, of course, spectrally non-local, in contradiction to our original assumption: this new prediction has arisen by noting the spectral locality inherent in (8.75), and proposing a reasonable, although *ad hoc*, solution.

The discussion above suggests that phenomenology of the forward enstrophy cascade is on the verge of being internally inconsistent, and that the -3 spectral slope might be the shallowest limit that is likely to be actually achieved in nature or in any particular computer simulation rather than a robust, universal slope. To see this argument, suppose the detailed fluid dynamics attempt in some way to produce a shallower slope; then, using (8.76), the strain is local and the shallow slope is forbidden by the Kolmogorovian scaling results. However, if the dynamics organizes itself into structures with a slope steeper than k^{-3} the strain is quite nonlocal. The fundamental assumption of Kolmogorov scaling is not satisfied, and there is no internal inconsistency — the theory simply doesn't apply.

There are two other potential problems with the theory of two-dimensional turbulence described above. One is that enstrophy is only one of an infinity of invariants of inviscid two-dimensional flow, and the theory takes no account of the presence of others. The second is that, as in three-dimensional turbulence, if there is strong intermittency the flow cannot be fully characterized by single enstrophy and energy cascade rates. In spite of all this, the notions of a forward transfer of enstrophy and an inverse transfer of energy are quite robust, and have considerable numerical support.[11]

8.3.4 Numerical illustrations

Numerical simulations nicely illustrate both the classical phenomenology and its shortcomings. In the simulations shown in Fig. 8.8 and Fig. 8.9 the vorticity field is initial-

ized 'randomly', meaning that there is no structure in the initial field, but with only a few non-zero Fourier components, and the flow is allowed to freely evolve, save for the effects of a weak viscosity. Vortices soon form, and between them enstrophy is cascaded to small scales where it is dissipated, producing a flat and nearly featureless landscape. The energy cascade to larger scales is reflected in the streamfunction field, the length-scale of which slowly grows larger with time. The vortices themselves form through a roll-up mechanism, similar to that illustrated in Fig. 6.6, and their presence provides problems to the phenomenology. Because circular vortices are nearly exact, stable solutions of the inviscid equations they can 'store' enstrophy, disrupting the relationship between enstrophy flux and enstrophy itself that is assumed in the Kolmogorov-Kraichnan phenomenology and providing a form of intermittency.

Nevertheless, some forced-dissipative numerical simulations suggest that the presence of vortices may be confined to scales close to that of the forcing, and if the resolution is sufficiently high then the $-5/3$ inverse cascade and -3 forward enstrophy cascade may appear. Certainly, if the forcing is spectrally localized, then a well-defined $-5/3$ spectrum robustly forms, as illustrated in Fig. 8.10. Typically, however, the foward k^{-3} spectrum is more delicate, being influenced by the presence of coherent vortices.[13]

8.4 † PREDICTABILITY OF TURBULENCE

> *Small differences in the initial conditions may produce very great ones in the final phenomenon... Prediction becomes impossible... A tenth of a degree more or less at any given point, and the cyclone will burst here and not there, and extend its ravages over districts it might otherwise have spared.*
> Henri Poincaré, *Science and Method,* 1908.

It is a truth universally acknowledged that weather is unpredictable. That this is so stems from the fact that the atmosphere is chaotic, and chaotic systems are unpredictable virtually by definition. However, the atmosphere, and turbulence in general, is certainly not, in general, a *low-dimensional* system (meaning a system with only a few degrees of freedom), and the connection between atmospheric unpredictability and the 'sensitive dependance on initial conditions' of low-dimensional systems is not as straightforward as it might seem. In this section we expand and clarify these issues, beginning with an informal discussion of a few aspects of low-dimensional dynamical systems.

8.4.1 Low dimensional chaos and unpredictability

Chaos, or temporal disorder leading to effective indeterminism, is a ubiquitous property of nonlinear dynamical systems. Much of this was known to Poincaré, but in its modern reincarnation it stems in part from the 'Lorenz equations'.[14] These are a set of three coupled nonlinear ordinary differential equations, originally derived by way of a rather *ad hoc* truncation of the fluid equations governing a two-dimensional convective system: The streamfunction of a convective role is written as $\psi(\hat{x}, \hat{z}, t) = x(t) \sin k\hat{x} \sin \pi\hat{z}$, and the temperature perturbation as $\theta(\hat{x}, \hat{z}, t) = y(t) \cos k\hat{x} \sin \pi\hat{z} + z(t) \sin 2\pi\hat{z}$,
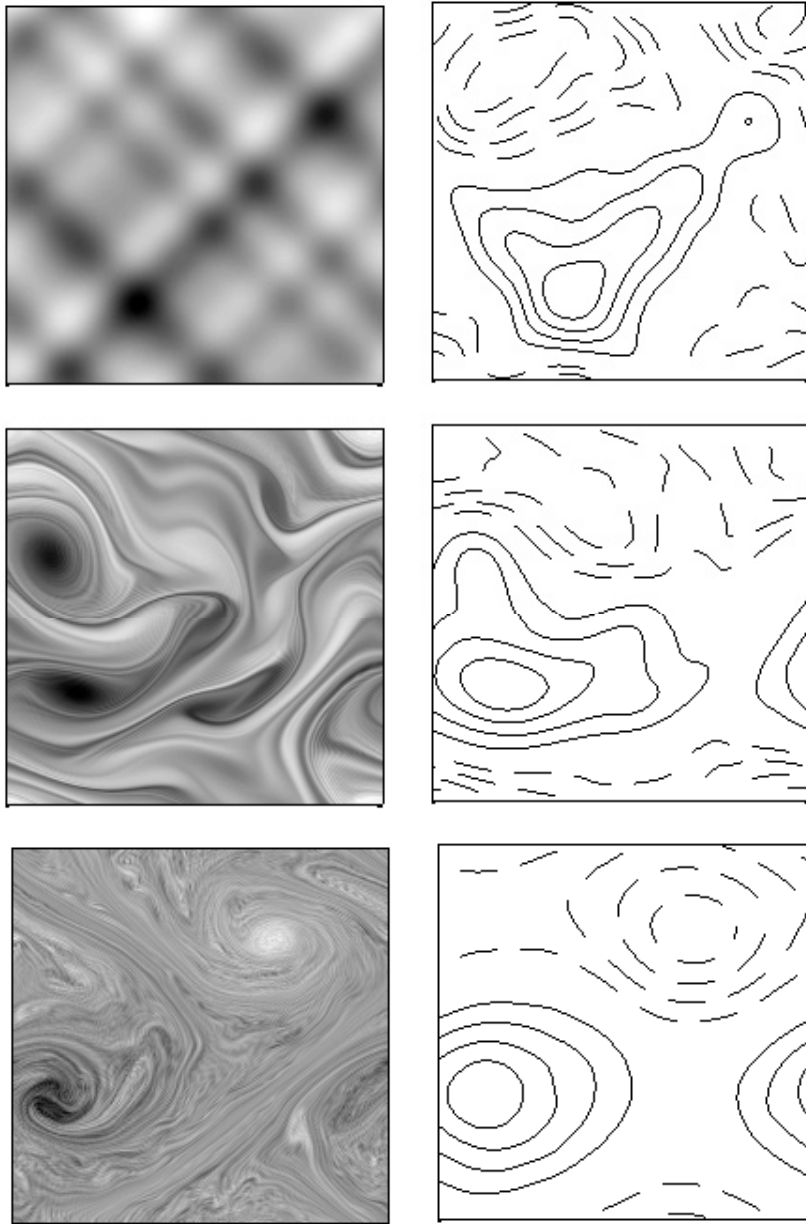
Fig. 8.8 Nearly-free evolution of vorticity (left column) and streamfunction (right column) in a doubly-periodic square domain (of length 2π) at times (from the top, and in units of inverse vorticity) $t = 0$, $t = 50$ and $t = 260$, obeying the two-dimensional vorticity equation with no forcing but with a weak viscous term. The initial conditions have just a few non-zero Fourier modes with randomly generated phases, producing a maximum value of vorticity of about 3. Kelvin-Helmholtz instability leads to vortex formation and roll-up (as in Fig. 6.6), and like-signed vortices merge, ultimately leading to a state of just two oppositely-signed vortices. Between the vortices enstrophy cascades to smaller scales. The scale of the stream function grows larger, reflecting the transfer of energy to larger scales.
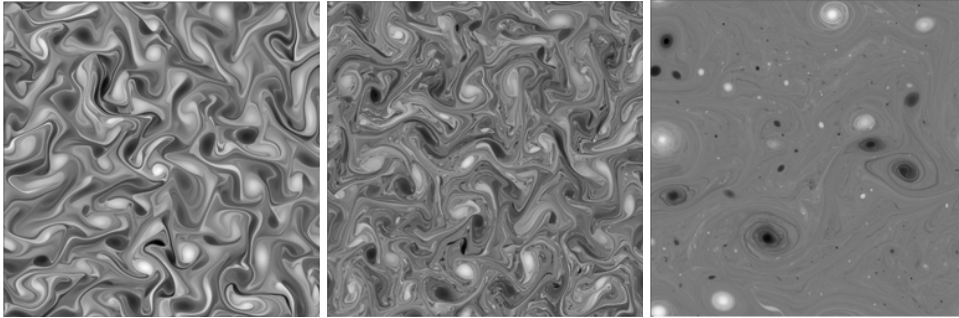
Fig. 8.9 Snapshots of the vorticity field in decaying two-dimensional turbulence, similar to Fig. 8.8, with time increasing left to right. The flow ultimately consists of a small number of vortices whose trajectories are similar to that of interacting point vortices, with occasional close encounters leading to vortex merger.

where $\hat{x}$ and $\hat{z}$ are the horizontal and vertical coordinates in physical space, k is a wavenumber, and x, y, z are amplitudes. Thus, x represents the rotational speed of the convection roll, y the temperature difference horizontally across the roll, and z the deviation temperature from a background vertical stratification. The resulting equations are, in notation standard for them,

$$\frac{\mathrm{d}x}{\mathrm{d}t} = \sigma(y - x), \qquad \frac{\mathrm{d}y}{\mathrm{d}t} = rx - y - xz, \qquad \frac{\mathrm{d}z}{\mathrm{d}t} = xy - bz, \qquad (8.79\text{a,b,c})$$

where the parameters are σ, the Prandtl number; r, proportional to the Rayleigh number; and b, a wavenumber dependent dissipation coefficient. The behaviour of the system varies with the parameters, and a well studied set uses $\sigma = 10$, $r = 28$ and $b = 8/3$. A typical solution of the system, a 'flow', is given in Fig. 8.11, and evidently

Figure 8.10 The energy spectrum in a numerical simulation of forced-dissipative two-dimensional turbulence. The fluid is stirred at wavenumber k_f and dissipated at large scales with a linear drag, and there is an $k^{-5/3}$ spectrum at intermediate scales. The arrows schematically indicate the direction of the energy flow.[12]
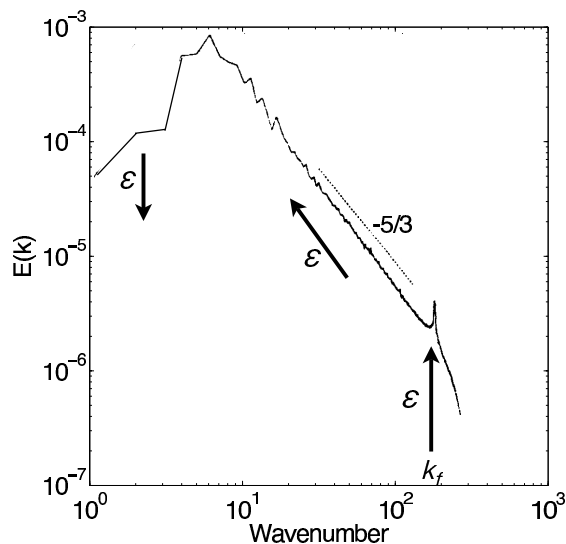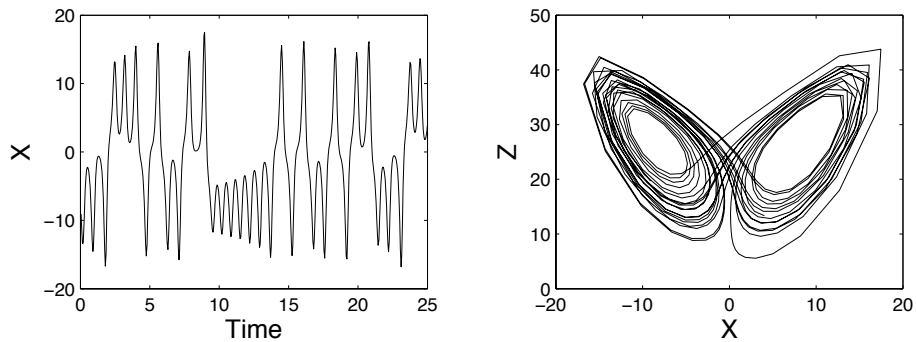
Fig. 8.11 A solution of the Lorenz equations, with $\sigma = 10$, $r = 28$ and $b = 8/3$. The left panel plots x as a function of time. The right panel plots x against z.

the behaviour is quite complex. It is aperiodic, and the frequency spectrum (not shown) is quite broad.

Now, suppose that at any given instant the flow is perturbed slightly. Or to put it another way, suppose that we are trying to predict the future behaviour of the system by integrating the equations of motion but that we only have inaccurate knowledge about the sytem at some particular time. We find that the evolution of the original flow and that of the perturbed flow diverge from each other, and after a little while the two systems are completely different (Fig. 8.12). Because we can never expect to have completely accurate information about the state of the system, the system is thus unpredictable. Three points are apparent:

  (i) The time taken for the trajectories to diverge depends on the magnitude of the initial perturbation. Small perturbations grow exponentially at first, and at any given point in the trajectory, the smaller the perturbation the longer the predictability.

 (ii) Once the perturbation has reached finite amplitude, the predictability time — the time for the error to become as large as the solution itself — will typically be of order the characteristic advective time of the system, the time for a convective roll to overturn.

(iii) The predictability time depends on the location of the system in (x, y, z) space: in the examples of Fig. 8.12 the perturbed system follows the original quite closely for a while, then quickly diverges.

8.4.2 * Predictability of a turbulent flow

The atmosphere is a nonlinear dynamical system, but one enormously more complex than the Lorenz system. It is is not only chaotic, it is turbulent — it has both spatial and temporal disorder — so we should certainly expect its evolution also to be very sensitive to its initial conditions.[15]

However, turbulence is richer than low-order chaos because a turbulent flow con-
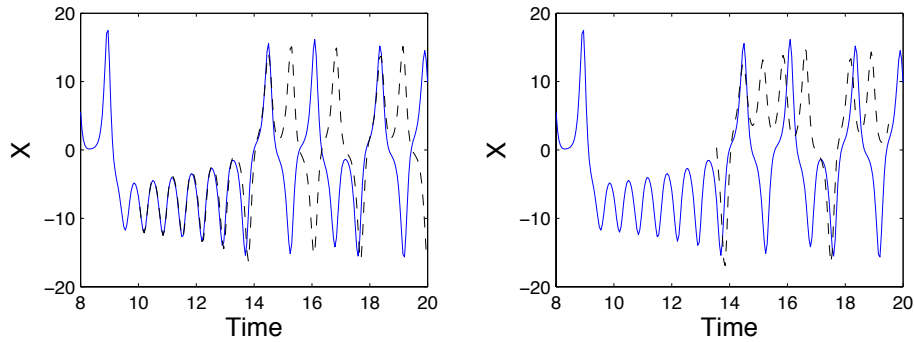
Fig. 8.12 Examples of the evolution of the Lorenz model subject to a small perturbation at time 10 (left panel) and time 13.5 (right panel). The original and perturbed systems are the solid and dashed lines, respectively.

tains multiple scales of motion; the error is typically initially largely confined to small scales, but the 'predictability time' of the atmosphere may be taken as the time taken to contaminate all scales of motion. There are two possible routes that the error may take in affecting the larger scales. In the first we suppose, following classical turbulence phenomenology, that errors on a small scale will mostly contaminate the motion on the next larger scale (in a logarithmic sense), at that this contamination occurs on the local eddy turnover time. Eddies on this larger scale then grow and affect the next larger scale, and the error field is so cascaded upscale via local local triad interactions finally reaching the largest scales of the fluid. Note that this mechanism does not rely on there being an inverse cascade of energy — it is only the error, or the contamination, that is cascaded upscale. In the second route we suppose that errors occurring on the small scale immediately contaminate the largest scales, with an initial error equal to the amplitude of the small scale, and that the large-scale error then grows exponentially.

I. Error growth via a local cascade

Let us suppose that the error is initially confined to some small scale characterized by the (inverse of) the wavenumber k_1, as determined by the resolution of our observing network. For modes at that scale the error may be considered finite rather than infinitesimal, and it will saturate and contaminate the next largest scale in a timescale comparable to the eddy turnover time at that scale. Thus, in general, errors initially confined to a scale k will contaminate the scale $2k$ after a time τ_k, with τ_k given by (8.24). The total time taken for errors to propagate from the small scale k_1 to the largest scale k_0 is then given by

$$T = \int_{k_0}^{k_1} \tau_k \, \mathrm{d}(\ln k) = \int_{k_0}^{k_1} [k^3 \mathcal{E}(k)]^{-1/2} \, \mathrm{d}(\ln k), \qquad (8.80)$$

treating the wavenumber spectrum as continuous. The logarithmic integral arises because the cascade proceeds logarithmically — error cascades from k to $2k$ in a time τ_k.

For an energy spectrum of the form $E = Ak^{-n}$ this becomes

$$T = \frac{2}{A^{1/2}(n-3)} \Big[k^{(n-3)/2} \Big]_{k_0}^{k_1}. \tag{8.81}$$

for $n \neq 3$, and $T = A^{-1/2} \ln(k_1/k_0)$ for $n = 3$. If in two dimensional turbulence we have $n = 3$ and $A = \eta^{2/3}$, and if in three-dimensional turbulence we have $n = 5/3$ and $A = \varepsilon^{2/3}$, then the respective predictability times are given by:

$$\boxed{\begin{aligned} T_{2d} &\sim \eta^{-1/3} \ln(k_1/k_0), \\ T_{3d} &\sim \varepsilon^{-1/3} k_0^{-2/3} \end{aligned}} \tag{8.82a,b}$$

As $k_1 \to \infty$, that is as the initial error is confined to smaller and smaller scales, predictability time grows larger for two dimensional turbulence (and for $n \geq 3$ in general), but remains finite for three dimensional turbulence.

II. Error growth via a direct interaction

Let us now assume that the small scale error directly affects the large scales, where the error then grows exponentially until it saturates. That is, if ϕ is a measure of the amplitude of the large-scale error then

$$\phi \sim \phi_0 \exp(\sigma t), \tag{8.83}$$

where σ is the inverse of the eddy turnover time at the large scale, and ϕ_0 is the amplitude of its initial error and this, we assume, is equal to the amplitude of the motion at the poorly-observed small scales at wavenumber k_1. In two dimensional turbulence the eddy turnover time is given by $\tau_k \sim \eta^{-1/3}$ and $A \sim \eta^{2/3}$, and so we take

$$\sigma = \eta^{1/3} = A^{1/2}, \qquad \phi_0 = Ak_1^{-n}. \tag{8.84}$$

where $n = 3$. The time, T'_{2d}, needed for the error to saturate is then approximately given by the solution of

$$Ak_0^{-n} = Ak_1^{-n} \exp(A^{1/2} T'_{2d}), \tag{8.85}$$

giving

$$T'_{2d} \sim \eta^{-1/3} \ln(k_1/k_0). \tag{8.86}$$

In three-dimensional turbulence the eddy turnover time is given by $\tau_k \sim \varepsilon^{-1/3} k^{-2/3}$ and $A \sim \varepsilon^{2/3}$, and so we take

$$\sigma = k_0^{2/3} A^{1/2}, \qquad \phi_0 = Ak_1^{-n} \tag{8.87}$$

where $n = 5/3$. The time, T'_{3d}, needed for an error to saturate on large scale is then approximately given by the solution of

$$Ak_0^{-n} = Ak_1^{-n} \exp(k_0^{2/3} A^{1/2} T'_{3d}), \tag{8.88}$$

giving

$$T'_{3d} \sim k_0^{-2/3} \varepsilon^{-1/3} \ln(k_1/k_0). \tag{8.89}$$

The estimates (8.86) and (8.89) are to be compared with (8.82). For two dimensional turbulence, the estimates are equal (reflecting the scale independence of the eddy turnover time), whereas for three-dimensional turbulence the estimate from (8.82) is much shorter than that from (8.89) if $k_1 \gg k_0$, meaning that the local cascade mechanism of error growth will dominate.

8.4.3 Implications and weather predictability

In two-dimensional flow the predictability time, (8.82a) increases without bound as the scale of the initial error decreases. This is consistent with what has been rigorously proven about the two-dimensional Navier-Stokes equations, namely that, provided the initial conditions are sufficiently smooth, the solutions have a continuous dependence on the initial conditions, and a change in solution at some later time is bounded by the magnitude of the change in the initial conditions. This does not mean that two-dimensional flow is in practice necessarily predictable: a small error or small amount of noise in the system will still render a flow truly unpredictable sometime in the future, but we can put off that time indefinitely if we know the initial conditions well enough.

In three dimensions, with a spectrum of $k^{-5/3}$, the predictability-time estimate from (8.82b) is not dependent on the scale of the initial error. Thus, even if the initial error is confined to smaller and smaller scales, the predictability time is bounded. The time it takes for such errors to spread to the largest scales is simply a few large eddy turnover times, essentially because the eddy turnover times of the small scales are so small. For such a fluid, there is no unique error doubling time, because the error growth rate is a function of scale.

In the troposphere the large scale flow behaves more like a two-dimensional fluid than a three-dimensional fluid and from scales from a few hundred to a few thousand kilometers it has, roughly, a k^{-3} spectrum (look ahead to Fig. 9.7). If this spectrum extended indefinitely to small scales the predictability time would be correspondingly large, but at scales smaller than about 100 km or so, the atmosphere starts to behave more three-dimensionally and the predictability time cannot be significantly extended by making observations at still finer scales. That is, the effective limit to predictability is governed by the horizontal scale at which the atmosphere turns three-dimensional. (Hypothetically, we might be able to again increase the predictability time if we could observe scales well into the viscous regime where the specrum again steepens, but this would entail other problems.) Putting in the numbers gives a predictability limit of about 12 days (but there is at least a factor of two uncertainty in such a calculation), and small perturbations that are impossible to observe will change the course of the large-scale weather systems on this timescale. The 'butterfly effect' has its origins in this argument: a butterfly flapping its wings is, so it goes, able to change the course of the weather a week or so later.[16]

Thus, as regards our attempts to predict weather, as the atmosphere becomes observed more and more accurately, the initial error will become concentrated at smaller

and smaller scale, eventually reaching the scale at which the atmosphere ceases to behave as a quasi-two-dimensional fluid and where its spectrum flattens. The initial error growth rate will then increase, indicating the unavoidable onset of diminishing returns in adding better observing systems. Note that, unlike the situation in a low-order chaotic system, the growth rate of errors in a turbulent flow is not in general exponential (except for a pure -3 spectrum) even for a small initial error. This is because the initial error will never be properly infinitesimal, in that a given error will nearly always project onto some scale at finite amplitude.[17]

8.5 * SPECTRUM OF A PASSIVE TRACER

Let us now consider, heuristically, the spectrum of a passive tracer that obeys

$$\frac{\mathrm{D}\phi}{\mathrm{D}t} = F[\phi] + \kappa \nabla^2 \phi, \qquad (8.90)$$

where $F[\phi]$ is the stirring of the dye, and κ is its diffusivity, which in general differs from the kinematic molecular viscosity ν. If ϕ is temperature, the ratio of viscosity to diffusivity is called the *Prandtl number* and denoted σ, so that $\sigma \equiv \nu/\kappa$. If ϕ is a passive tracer, the ratio is sometimes called the *Schmidt number,* but we shall call it the Prandtl number in all cases. We assume that the tracer variance is created at some well-defined scale k_0, and that κ is sufficiently small that dissipation only occurs at very small scales. (Note that dissipation only reduces the tracer *variance,* not the amount of tracer itself.) The turbulent flow will generically tend to stretch patches of dye into elongated filaments, in much the same way as vorticity in two-dimensional turbulence is filamented — note that Fig. 8.5 applies just as well to a passive tracer in either two or three dimensions as it does to vorticity in two dimensions. Thus we expect a transfer of tracer variance from large-scales to small. If the dye is stirred at a rate χ then, by analogy with our treatment of the cascade of energy, we posit that

$$\mathcal{K}_\chi \chi \propto \frac{\mathcal{P}(k)k}{\tau_k}, \qquad (8.91)$$

where $\mathcal{P}(k)$ is the spectrum of the tracer, k is the wavenumber, τ_k is an eddy timescale and $\mathcal{K}_\chi$ is a constant, not necessarily the same constant in all cases. (In the rest of the section, Kolmogorov-like constants will be denoted $\mathcal{K}$, differentiated with miscellaneous superscripts or subscripts.) Let us first assume that τ_k is given by

$$\tau_k = [k^3 \mathcal{E}(k)]^{-1/2}. \qquad (8.92)$$

Suppose that the turbulent spectrum is given by $\mathcal{E}(k) = Ak^{-n}$, then using (8.92), (8.91) becomes

$$\mathcal{K}_\chi \chi = \frac{\mathcal{P}(k)k}{[Ak^{3-n}]^{-1/2}}, \qquad (8.93)$$

and

$$\boxed{\mathcal{P}(k) = \mathcal{K}_\chi A^{-1/2} \chi k^{(n-5)/2}.} \qquad (8.94)$$

Note that the steeper the energy spectrum the shallower the tracer spectrum. If the energy spectrum is steeper than -3 then (8.92) may not be a good estimate of the eddy turnover time, and we use instead

$$\tau_k = \left[\int_{k_0}^{k} p^2 \mathcal{E}(p) dp \right]^{-1/2}, \tag{8.95}$$

where k_0 is the low-wavenumber limit of the spectrum. If the energy spectrum is shallower than -3, then the integrand is dominated by the contributions from high wavenumbers and (8.95) effectively reduces to (8.92). If the energy spectrum is steeper than -3, then the integrand is dominated by contributions from low wavenumbers. For $k \gg k_0$ we can approximate the integral by $[k_0^3 E(k_0)]^{-1/2}$, that is the eddy-turnover time at large scales, τ_{k_0}, given by (8.92). The tracer spectrum then becomes

$$\boxed{\mathcal{P}(k) = \mathcal{K}'_\chi \chi \tau_{k_0} k^{-1}}, \tag{8.96}$$

where $\mathcal{K}'_\chi$ is a constant. In all these cases the tracer cascade is to smaller scales even if, as may happen in two-dimensional turbulence, energy is cascading to larger scales.

The scale at which diffusion becomes important is given by equating the turbulent time-scale τ_k to the diffusive time-scale $(\kappa k^2)^{-1}$. This is independent of the flux of tracer, χ, essentially because the equation for the tracer is linear. Determination of expressions for these scales in two and three dimensions are left as problems for the reader.

8.5.1 Examples of tracer spectra

Energy inertial range flow in three dimensions

Consider a range of wavenumbers over which neither viscosity nor diffusivity directly influence the turbulent motion and the tracer. Then in (8.94) $A = \mathcal{K} \varepsilon^{2/3}$ where ε is the rate of energy transfer to small scales , $\mathcal{K}$ is the Kolmogorov constant, and $n = 5/3$. The tracer spectrum becomes[18]

$$\mathcal{P}(k) = \mathcal{K}_\chi^{3d} \varepsilon^{-1/3} \chi k^{-5/3}. \tag{8.97}$$

where $\mathcal{K}_\chi^{3d}$ is a (putatively universal) constant. It is interesting that the $-5/3$ exponent appears in both the energy spectrum and the passive tracer spectrum. Using (8.92), this is the only spectral slope for which this occurs. Experiments show that this range does, at least approximately, exist with a value of $\mathcal{K}_\chi^{3d}$ of about 0.5–0.6 in three dimensions.

Inverse energy-cascade range in two-dimensional turbulence

Suppose that the energy injection occurs at a smaller scale than the tracer injection, so that there exists a range of wavenumbers over which energy is cascading to larger scales while tracer variance is simultaneously cascading to smaller scales. The tracer spectrum is then

$$\mathcal{P}(k) = \mathcal{K}_\chi^{2d} \varepsilon^{-1/3} \chi k^{-5/3}, \tag{8.98}$$

the same as (8.97), although ε is now the energy cascade rate to larger scales and the constant $\mathcal{K}_\chi^{2d}$ does not necessarily equal $\mathcal{K}_\chi^{3d}$.

Enstrophy inertial range in two-dimensional turbulence

In the forward enstrophy inertial range the eddy timescale is $\tau_k = \eta^{-1/3}$ (assuming of course that the classical phenomenology holds). Directly from (8.91) the corresponding tracer spectrum is then

$$\mathcal{P}(k) = \mathcal{K}_\chi^{2d*}\eta^{-1/3}\chi k^{-1}. \tag{8.99}$$

The passive tracer spectrum now has the same slope as the spectrum of vorticity variance (i.e., the enstrophy spectrum), which is perhaps comforting since the tracer and vorticity obey similar equations in two dimensions.

The viscous-advective range of large Prandtl number flow

If $\sigma = \nu/\kappa \gg 1$ (and in seawater $\sigma \approx 7$) then there may exist a range of wavenumbers in which viscosity is important but not tracer diffusion. The energy spectrum is then very steep, and (8.96) will apply. The straining then comes from wavenumbers near the viscous scale, so that for three dimensional flow the appropriate k_0 to use in (8.96) is the viscous wavenumber, and $k_0 = k_\nu = (\varepsilon/\nu^3)^{1/4}$. The dynamical timescale at this wavenumber is given by

$$\tau_{k_\nu} = \left(\frac{\nu}{\varepsilon}\right)^{1/2}, \tag{8.100}$$

and using this and (8.96) the tracer spectrum in this viscous-advective range becomes

$$\mathcal{P}(k) = \mathcal{K}'_B\left(\frac{\nu}{\varepsilon}\right)^{1/2}\chi k^{-1}. \tag{8.101}$$

This spectral form applies for $k_\nu < k < k_\kappa$, where k_κ is the wavenumber at which diffusion becomes important, found by equating the eddy turnover time given by (8.100) with the diffusive timescale $(\kappa k^2)^{-1}$. This gives

$$k_\kappa = \left(\frac{\varepsilon}{\nu\kappa^2}\right)^{1/4}, \tag{8.102}$$

and k_κ is known as the Batchelor wavenumber (and its inverse is the Batchelor scale). Beyond k_κ, the diffusive flux is not constant and the tracer spectrum can be expected to decay as wavenumber increases. A heuristic way to calculate the spectrum in this range is to first note that in the diffusive range the flux of the tracer is no longer constant but diminishes according to

$$\frac{d\chi'(k)}{dk} = -2\kappa k^2 \mathcal{P}(k). \tag{8.103}$$

where χ' is the wavenumber-dependent rate of tracer transfer. Let us nevertheless assume that χ' and $\mathcal{P}(k)$ are related by (8.91), except that now we take the eddy turnover time to be a constant, given by (8.100). Thus,

$$\mathcal{K}_B\chi' = \frac{\mathcal{P}(k)k}{\tau_{k_\kappa}} = \frac{\mathcal{P}(k)k}{(\nu/\varepsilon)^{1/2}} \tag{8.104}$$

Figure 8.13 The energy spectra, $\mathcal{E}(k)$ and passive tracer spectra $\mathcal{P}(k)$ in large Prandtl number three-dimensional turbulence (top) and two-dimensional turbulence (bottom). In three dimensions $\mathcal{P}(k)$ is given by (8.97) for $k < k_\nu$ and by (8.106) for $k > k_\nu$. In two dimensions, if k_{tr} marks the transition between a $k^{-5/3}$ inverse energy cascade and a k^{-1} forward enstrophy cascade, then $\mathcal{P}(k)$ is given by (8.98) for $k < k_{\mathrm{tr}}$ and by (8.107) for $k > k_{\mathrm{tr}}$. In both two and three dimensions the tracer spectra falls off rapidly for $k > k_\kappa$.
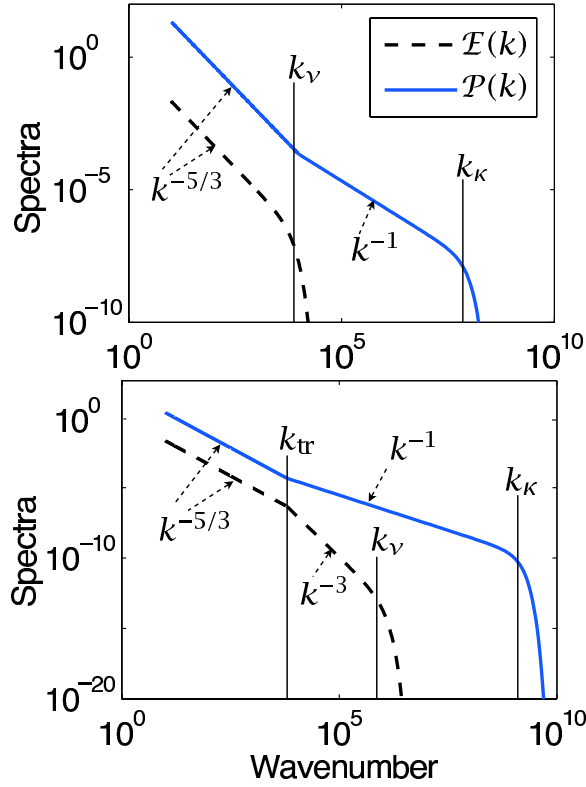
where $\mathcal{K}_B$ is a constant. Using (8.103) and (8.104) we obtain

$$\frac{\mathrm{d}\chi'}{\mathrm{d}k} = -2\mathcal{K}_B \kappa k \left(\frac{\nu}{\varepsilon}\right)^{1/2} \chi. \tag{8.105}$$

Solving this, using $\chi' = \chi$ for small k, gives

$$\mathcal{P}(k) = \mathcal{K}_B \left(\frac{\nu}{\varepsilon}\right)^{1/2} \chi k^{-1} \exp[-\mathcal{K}_B(k/k_\kappa)^2]. \tag{8.106}$$

This reduces to (8.101) if $k \ll k_\kappa$, and is known as the Batchelor spectrum.[19] Its high-wavenumber part $k > k_\kappa$ is known as the viscous-diffusive subrange. The spectrum, and its two-dimensional analog, is illustrated in Fig. 8.13

In two dimensions the the viscous-advective range occurs for wavenumbers greater than $k_\nu = (\eta/\nu^3)^{1/6}$. The appropriate timescale within this subrange by $\eta^{-1/3}$, and therefore gives a spectrum with the precisely the same form as (8.99). At sufficiently high wavenumbers tracer diffusion becomes important, with the diffusive scale now given by equating the eddy turnover time $\eta^{-1/3}$ with the viscous timescale $(\kappa k^2)^{-1}$. This gives the diffusive wavenumber, analogous to (8.102), of $k_\kappa = (\eta/\kappa^3)^{1/6}$. Using (8.105) and the procedure above we then obtain an expression for the spectrum in the region $k > k_\nu$, that is a two-dimensional analog of (8.106), namely

$$\mathcal{P}(k) = \mathcal{K}'_B \eta^{-1/3} \chi k^{-1} \exp[-\mathcal{K}'_B(k/k_\kappa)^2]. \tag{8.107}$$

For $k \ll k_\kappa$ this reduces to (8.99), possibly with a different value of the Kolmogorov-like constant.

† The inertial-diffusive range of small Prandtl number flow

For small Prandtl number ($\nu/\kappa \ll 1$) the energy inertial range may co-exist with a range over which tracer variance is being dissipated, giving us the so-called inertial-diffusive range. The tracer will begin to be dissipated at a wavenumber obtained by equating a dynamical eddy turnover time with a diffusive time, and this gives a diffusive wavenumber

$$k'_\kappa = \begin{cases} (\varepsilon/\kappa^3)^{1/4} & \text{in three dimensions,} \\ (\eta/\kappa^3)^{1/6} & \text{in two dimensions.} \end{cases} \tag{8.108}$$

Beyond the diffusive wavenumber the flux of the tracer is no longer constant but diminishes according to (8.103).

Given a non-constant flux and an eddy-turnover time that varies with wavenumber there is no self-evidently correct way to proceed. One way is to assume that χ and $\mathcal{P}(k)$ are related by $\mathcal{K}''_\chi \chi = \mathcal{P}(k)k/\tau_k$, as in (8.104) but with a potentially different proportionality constant and with τ_k given by (8.92); that is, $\tau_k = \varepsilon^{-1/3}k^{-2/3}$ in three dimensional turbulence. Using this in (8.103) leads to

$$\mathcal{P}(k) = \mathcal{K}''_\chi \chi \varepsilon^{-1/3}k^{-5/3}\exp[-(\mathcal{K}''_\chi 3/2)(k/k'_\kappa)^{4/3}]. \tag{8.109}$$

where χ is the tracer flux at the beginning of the tracer dissipation range. (A similar expression emerges in two dimensional turbulence.) However, given such a steep spectrum an argument based on spectral locality is sometimes thought to be suspect. Another argument posits a particular relationship between the tracer spectrum and energy spectrum in the inertial-diffusive range, and this leads to

$$\mathcal{P}(k) = \frac{\mathcal{K}''_B}{3}\chi_0\varepsilon^{2/3}\kappa^{-3}k^{-17/3} = \mathcal{K}''_B\chi_0\varepsilon^{-1/3}k^{-5/3}g(k/k_\kappa), \tag{8.110}$$

where $g(\alpha) = \alpha^{-4}/3$ and $\mathcal{K}''_B$ is a constant.[20]

Notes

1 The algebra of the three-dimensional case is more complicated because of the pressure term and because the momentum equation is a vector equation. In incompressible flow we can take the diveregence of the momentum equation to obtain an elliptic equation for pressure of the form $\nabla^2 p = \mathcal{L}(v)$ where the right-hand side is a quadratic function of velocity and its derivatives, and then Fourier transform this and proceed in much the same way.

2 A. N. Kolmogorov (1903–1987) was a Russian mathematician and theoretical physicist, who made seminal contributions to turbulence (in two famous papers in 1941 and another in 1962), to probability and statistics, and to classical mechanics (e.g, the Kolmogorov-Arnold-Moser theorem). Yaglom (1994) provides more details on both the man and his scientific contributions.

3 The process has been encapsulated in the following ditty by Lewis Fry (L.F.) Richardson (1881–1953), his own summary of Richardson (1920):

   Big whorls have little whorls, that feed on their velocity;
   And little whorls have lesser whorls, and so on to viscosity.

   The verse follows a well-known one by the mathematician Augustus de Morgan (in *A Budget of Paradoxes* 1872), *'Great fleas have little fleas upon their backs to bite 'em. . . '*, which in turn is a parody on a poem by Jonathan Swift. Richardson himself was a British scientist best known as the person who (following earlier work by V. Bjerknes) envisioned weather forecasting in its current form — that is, numerical weather prediction. However, as described in his 1922 book, instead of an electronic computer performing the calculations, he imagined, perhaps fancifully, a hall full of people performing calculations in unison all directed by a conductor at the front. His first numerical forecast, calculated by hand, was wildly inaccurate both because he failed to 'initialize' his atmosphere properly and because his timestep was too long and did not satisfy the CFL condition, and unrealistic gravity waves dominated the solution. However, it was a prescient and important effort. He also worked on turbulence, and seems to have envisioned the turbulent cascade prior to Kolomgorov (to wit the verse above); the 'Richardson number', a measure of fluid stratification, is also named for him. He also made contributions to the theory of war and was known as a pacifist — he was a conscientious objector and drove ambulances in the first World War, and resigned from the U. K. Meteorological Office because it became part of the Air Ministry.

4 Kolmogorov (1941) obtained the result in a slightly different way, using distances in real space rather than wavenumber and deriving the equivalent result for the longitudinal structure function, $D(r) \equiv \langle [u_l(x + r) - u_l(x)]^2 \rangle \sim r^{2/3}$. It was Obukhov (1941) who gave an argument in spectral space and first wrote down that $E(k) \sim k^{-5/3}$, but Kolmogorov's argument is regarded as more general and hence the $5/3$ spectrum is usually named for him. Sometimes it is called the 'Kolmogorov-Obukhov' $5/3$ spectrum.

5 Experiments carried out and data kindly provided by R. Zhao.

6 The first observations confirming the -5/3 predictions were from a tidal channel (Grant et al. 1962). These results were initially presented at a turbulence conference in Marseille in 1961, ironically at the same time as Kolmogorov presented a modification of his original theory that incorporated a local mean dissipation rate, to try to take intermittency into account, recognizing that his first theory was incomplete (Kolmogorov 1962). It is said to have been L. D. Landau who pointed out the consequences of intermittency to Kolmogorov, soon after the K41 theory first appeared.

7 Two-dimensional turbulence was first considered by Lee (1951) and Fjørtoft (1953), the latter recognizing the two-dimensional nature of large-scale atmospheric motion. The theory was developed by Kraichnan (1967) (who predicted the spectral shapes of the two-dimensional cascades), Leith (1968) and Batchelor (1969). Lilly (1969) performed some early numerical integrations. For extensive reviews of two-dimensional turbulence see Kraichnan and Montgomery (1980) and Danilov and Gurarie (2001).

8 This similarity argument is due to Batchelor (1969), and its validity was explored by Bartello and Warn (1996) using direct numerical simulations of decaying two-dimensional turbulence. They found that the similarity hypothesis is not quantita-

tively accurate, and in particular that higher-order moments of the vorticity do not obey the predictions of the theory. This failure may be ascribed to the fact that in two-dimensional flow vorticity is conserved on parcels, and in the presence of coherent vortices this is an effective constraint that is not included in the theory. In flow with a finite deformation radius coherent vortices are found to be less important and an analogous similarity hypothesis appears to work better (Iwayama et al. 2002).

9 Colin De Verdiere (1980), Arbic et al. (2005).

10 To read more about strain, see Lesieur (1997).

11 The idea that in two-dimensional turbulence energy is transferred to larger scales was arguably one of the most important developments in fluid mechanics in the second half of the 20th century. One might characterize the upscale cascade in two-dimensional turbulence by:

    Small whorls beget bigger whorls, that feed upon their energy;
    And bigger whorls beget larger whorls, and so on, using synergy.

12 From Maltrud and Vallis (1991).

13 For numerical simulations illustrating these and other properties of two-dimensional turbulence see, among others, McWilliams (1984), Maltrud and Vallis (1991), Oetzel and Vallis (1997), Lindborg and Alvelius (2000), Smith et al. (2002). Also look at Jupiter through a telescope!

14 The Lorenz equations were written down by Lorenz (1963), based in part on some earlier work of (Saltzman 1962), and inspired a veritable industry of study. The field of chaos, or more generally nonlinear dynamics, has grown enormously since then, prompted also by work in mathematics occurring at about the same time, and its development is sometimes regarded as one of the true revolutions of science in the 20'th century. Aubin and Dahan Dalmedico (2002) write an interesting history of it. The correspondence of the Lorenz equations to a real fluid system is tenuous, but the importance of the properties they demonstrate transcends this; we regard the equations simply as an example of a chaotic system with some fluid relevance. The equations and variations about them have re-appeared in studies of, among other things, lasers, dynamos, chemical reactions, mechanical waterwheels and El Niño.

15 That a turbulent flow is unpredictable follows from two suppositions: that chaotic systems are unpredictable, and that turbulent flow is (among other things) a chaotic system. The former is almost definitionally true, and the latter result follows from the work of Lorenz (1963), Ruelle and Takens (1971) and others who showed that fluid turbulence was generically a consequence of a small number of bifurcations as some controlling parameter (like Reynolds number) is changed. Prior to this turbulence was sometimes thought, following Landau (1944), to be a large collection of periodic motions with incommensurate frequencies that would have complex and non-repeating but presumably predictable behaviour. Notwithstanding that, it seems to have been known, well before the development of nonlinear dynamical systems theory in the 1960's and 1970's, that the weather was unpredictable. Poincaré was probably the first to properly recognize this at the turn of the 20th century, and weather forecasters seem to have intuited that the atmosphere was intrinsically, and not just practically, difficult to forecast: in the 1941 novel *Storm* by G. R. Stewart (1895–1980, a professor of English at UC Berkeley) we find a

forecaster musing that 'A Chinaman sneezing in Shen-si may set men to shovel-ing snow in New York City'. (*Storm* is also notable because it used female names for intense storms, a practice that became common among forecasters in WWII and that was used by the US Weather Service from 1953–1978, after which gender equity pertained.) In a more academic setting, the predictability problem is men-tioned in the book by Godske et al. (1957) (much of which written in the 1930s and 40s), and Thompson (1957) and Novikov (1959) studied the unpredictability of atmospheric flows from the perspective of turbulence, evidently unaware of, or at least uninfluenced by, either Poincaré or Landau. Phil Thompson himself was in the Joint Numerical Weather Prediction Unit of the U.S. government in the 1950s, whose task was to numerically produce weather forecasts, and this practical expe-rience undoubtedly confronted and guided his theoretical thinking. These various strands came together and were clarified by the dynamical systems viewpoint cou-pled with the view of the atmosphere as a geostrophically turbulent fluid, and this has led to the viewpoint we describe here, and to estimates of the limit to pred-icability time of the atmospheric weather of about two weeks. However, at any particular time the predictability may be much shorter or longer than this depend-ing on the synoptic state of the atmosphere — it may be in a particularly persistent blocking regime, for example — but 'predicting the predictability' is difficult. It may also be possible to predict the average weather for much longer if the more slowly varying parts of the climate system such as the ocean have a systematic effect on the atmosphere.

16 The more technical phrase 'sensitive dependence on initial conditions' is a para-phrase of one of Poincaré, but the catchier one 'butterfly effect' seems to have more recent origins. Its precise origins are obscure, but the phrase certainly be-come more common among meteorologists following a lecture by Lorenz to the AAAS in 1979 entitled 'Predictability: does the flap of a butterfly's wings in Brazil set off a tornado in Texas?'. The shape of the Lorenz attractor in phase space also resembles a butterfly, and the two (not unrelated) phenomena are sometimes conflated.

17 My thanks to Tim Palmer for an email conversation on this topic. A related point is that the predictability of a turbulent system is not well characterized by its spec-trum of Lyapunov exponents: in a turbulent system in three dimensions the largest Lyapunov exponent is likely be associated with very small scales of motion, and the error growth associated with this effectively saturates at small scales.

18 First derived by Obukhov (1949) and Corrsin (1951).

19 Batchelor (1959), who also suggests that the constant $\mathcal{K}_B$ in (8.106) should have the value 2. There is some observational support for the k^{-1} viscous-advective range in the temperature spectra of the ocean, one of the first measurements being that of Grant et al. (1968). Aside from their intrinsic interest, the viscous and diffusive scales are used in microstructure theory and measurements that lead to estimates of the ocean's energy dissipation rate. See, for example, Gregg (1998) and Stips (2005).

20 Batchelor et al. (1959). There is some numerical support for the $-17/3$ spectrum using a Large-Eddy Simulation (LES) model (Chasnov 1991). See also O'Gorman and Pullin (2005).

Other Reading

There are a number of books on turbulence, including:

Tennekes H. and J. Lumley 1972. *A First Course in Turbulence.*
  This remains a classic introduction to the subject.

McComb, W. D. 1990. *The Physics of Fluid Turbulence.*

Lesieur, M. 1997. *Turbulence in Fluids.*
  The above two books deal with both the statistical and phenomenological aspects of turbulence, with somewhat different emphases and styles.

Frisch, U. 1995. *Turbulence: The Legacy of A. N. Kolmogorov.*
  A modern account of turbulence written in a slightly personal but readable style and concentrating, as its title might suggest, on the statistical aspects of the subject.

A set of articles covering a very wide range of topics related to turbulence in marine systems, on both large and small scales, is collected in:

Baumert, H. Z, Simpson, J. H., and Sünderman, J., Eds., 2003. *Marine Turbulence: Theories, Observations and Models.*
  Given its price, check it out from your library.

The more applied side of numerical weather prediction and predictability is discussed by:

Kalnay, E. 2003. *Atmospheric Modeling, Data Assimilation and Predictability.*

Problems

8.1 Different averaging processes (time, space, or ensemble means, projection operators, etc.) may lead to different rules for the products of averages. Let $a = \overline{a} + a'$, where $\overline{a}$ is some kind of average, and similarly for the variable b. Thus

$$\overline{ab} = \overline{\overline{a}\overline{b}} + \overline{\overline{a}b'} + \overline{a'\overline{b}} + \overline{a'b'} \qquad (P8.1)$$

Is this expression always equal to $\overline{a}\overline{b} + \overline{a'b'}$? Give an example of an averaging operator for which this is true, and, if possible, another for which it is not true. Similarly, is it always true that $\overline{a\overline{b}} = \overline{a}\overline{b}$?

8.2 Consider the upscale energy transfer of two-dimensional turbulence, obeying the equation of motion, $D\zeta/Dt = -r\zeta + F$, where F is a stirring that is non-zero only at large wavenumbers and that produces an upscale energy transfer at the rate ε_0, and r is a constant drag coefficient.

(a) Show that drag is important only for wavenumbers smaller than $k_r = (r^3/\varepsilon_0)^{1/2}$.

(b) ♦ Suppose that, at all wavenumbers, the energy spectrum $\mathcal{E}(k)$ and the cascade rate ε are related by $\varepsilon = \mathcal{E}(k)k/\tau_k$ where $\tau_k = (\mathcal{E}(k)k^3)^{-1/2}$. However, at wavenumbers smaller than k_r, the energy cascade rate diminishes with wavenumber because of frictional effects. Obtain an expression for the energy spectrum in this frictional range.

8.3 ♦ Two-dimensional flow with a finite deformation radius obeys

$$\frac{\partial q}{\partial t} + J(\psi, q) = 0, \qquad q = (\nabla^2 - k_d^2)\psi. \qquad (8.2a,b)$$

Consider the asymptotic case with $k_d \to \infty$.

394 Chapter 8. Turbulence, Basic Theory

(a) Show that the equation may be written in the form $\partial \hat{q}/\partial \hat{t} + J(\hat{\psi}, \hat{q}) = 0$ where $\hat{t} = t/k_{\mathrm{d}}^2$, $\hat{q} = \psi$ and $\hat{\psi} = \nabla^2 \hat{q}$.

(b) What are the inviscid invariants of such a model?

(c) Consider the forced-dissipative case, with forcing confined to a small range of wavenumbers. Argue that we may expect forward and inverse cascades of appropriate inviscid invariants, and obtain expressions for the associated specta.

(d) In the unforced but viscous case, assume (as in Batchelor 1969), that energy is conserved and that the energy spectrum evolves in a self-similar way. Show that the energy spectrum then obeys

$$\mathcal{E}(k) = k_{\mathrm{d}}^{-3/4} E^{9/8} t^{1/4} F(k k d^{-3/4} E^{1/8} t^{1/4}), \tag{P8.3}$$

where F is a function of universal form and E is the total energy.

[See Watanabe et al. (1998) and Smith et al. (2002).]

8.4 Assuming that a small error cascades upscale:

(a) Using the observed spectrum of the atmosphere as a guide, estimate the predictability time of the atmosphere.

(b) Suppose that the large-scales of the atmosphere behave two dimensionally and the small scales three dimensionally. Estimate the predictability time as a function of the cross-over scale, and plot this.

(c) Estimate the error doubling time as a function of scale (of the error) in a the atmosphere, and plot it.

8.5 ♦ Consider predictability in an isotropic fluid that has a -4 energy spectrum, and a largest scale at wavenumber k_0.

(a) Suppose that a small error projects entirely onto a small scale characterized by a wavenumber k_1 ($k_1 \gg k_0$), such that scales $1/k_1$ and smaller are effectively unobserved scales larger than this are perfectly observed. Supposing error cascades via specrally local interactions to larges scales, estimate the predictability time.

(b) Now suppose that the initial error projects almost entirely onto the largest scale, so that it is a small perturbation on the scale k_0, but that its amplitude (the rms difference between the perturbed and unperturbed streamfunction) is the same as in the first case. Estimate the predictability time by supposing that the error growth is exponential, and compare it to the solution of the first part.

8.6 In the limit of zero viscosity (8.72) implies that enstrophy dissipation remains constant, and therefore that palinstrophy (mean square curl of the vorticity) is infinite somewhere. However, it has been shown rigorously that the two-dimensional Euler equations have *no* singularities in finite time if the initial conditions are sufficiently smooth, and also that their enstrophy dissipation is zero. Resolve this paradox.
Qualitative solution: We are concerned with the zero viscosity *limit* in (8.72). But in this limit it takes the fluid an infinite time to come to equilibrium with an infinitely long inertial range, and only then is the enstrophy dissipation non-zero. However, the rigorous results only prohibit singularities forming in finite time, and so there is no contradiction.

Oh brave new world, That has such people in't!
William Shakespeare, *The Tempest,* c. 1611.

Geostrophic Turbulence and Baroclinic Eddies

GEOSTROPHIC TURBULENCE may be defined as turbulence in stably-stratified flow that is in near-geostrophic balance. Perhaps ironically, it is sometimes easier to say something interesting about this form of turbulence than about incompressible isotropic two- or three-dimensional turbulence. In the latter class of problems there is nothing else to understand other than the problem of turbulence itself; on the other hand, rotation and stratification give one something else to grasp, and it becomes possible to address geophysically interesting phenomena without having to solve the whole turbulence problem. Furthermore, in inhomogeneous geostrophic turbulence asking questions about the the *mean fields* is meaningful and useful, whereas this is trivial in homogeneous turbulence. The constraining effects of rotation and stratification that are so important are captured in a simple and direct way by the quasi-geostophic equations and these will be our main tool. Let us consider the effects of rotation first, then stratification.

9.1 EFFECTS OF DIFFERENTIAL ROTATION IN TWO-DIMENSIONAL TURBULENCE

One of the effects of rapid rotation on a fluid is its two-dimensionalization, as manifested by the Taylor-Proudman effect for example. In the limit of motion of a scale much shorter than the deformation radius, and with no topography, the quasi-geostrophic potential vorticity equation reduces to the two-dimensional equation,

$$\frac{\mathrm{D}q}{\mathrm{D}t} = 0 \tag{9.1}$$

where $q = \zeta + f$. This is the perhaps the simplest equation with which to study the effects of rotation on turbulence. The effects of rotation are of course already playing a role in enabling us to reduce a complex three-dimensional flow to two-dimensional flow. Further, suppose that the Coriolis parameter is constant. Then (9.1) becomes simply the two-dimensional vorticity equation

$$\frac{\mathrm{D}\zeta}{\mathrm{D}t} = 0. \tag{9.2}$$

Thus constant rotation has *no* effect on purely two-dimensional motion. Flow that is already two-dimensional — flow on a soap film, for example — is unaffected by rotation.

Suppose, though, that the Coriolis parameter is variable, as in $f = f_0 + \beta y$. Then we have

$$\frac{\mathrm{D}}{\mathrm{D}t}(\zeta + \beta y) = 0 \qquad \text{or} \qquad \frac{\mathrm{D}\zeta}{\mathrm{D}t} + \beta v = 0. \tag{9.3a,b}$$

If the dominant term in these equations is the one involving β, then we obtain $\beta v = 0$. That is, there is no flow in the meridional direction and any flow is purely *zonal*. [*An aside:* From the point of view of the quasi-geostrophic asymptotics used in deriving (9.3), one assumes that variations in Coriolis parameter are small, i.e., that $\beta y = O(Ro)f$. However, this does *not* preclude the β term being the dominant one in any subsequent equation, so long as it is not supposed to be $1/O(Ro)$ bigger than the other terms. Alternatively, one might have posited two-dimensionality, and (9.1), *ab initio* so that there is no asymptotic restriction on the size of f.] This constraint may be interpreted as a consequence of angular momentum and energy conservation. A ring of fluid encircling the earth at a velocity u has an angular momentum per unit mass $a\cos\theta(u + \Omega a\cos\theta)$ where θ is the latitude and a is the radius of the earth. Moving this ring of air polewards (i.e., giving it a meridional velocity) while conserving its angular momentum requires its velocity and hence energy to increase. Unless there is a source for that energy the flow is constrained to remain zonal.

9.1.1 Organization of turbulence into zonal flow

Scaling

Let us now consider how flow can become organized into zonal bands, from the perspective of two-dimensional turbulence. Re-write (9.1) in full as

$$\frac{\partial \zeta}{\partial t} + \boldsymbol{u} \cdot \nabla \zeta + \beta v = 0. \tag{9.4}$$

If $\zeta \sim U/L$ and if $t \sim T$ then the respective terms in this equation scale as

$$\frac{U}{LT} \qquad \frac{U^2}{L^2} \qquad \beta U \tag{9.5}$$

How time scales (i.e., advectively or with a Rossby wave frequency scaling) is determined by which of the other two terms dominates, and this in turn is scale dependent.

For large scales the β-term will be dominant, and at smaller scales the advective term is dominant. The cross-over scale, or the 'β-scale' or 'Rhines scale' L_β, is given by[1]

$$L_\beta \sim \sqrt{\frac{U}{\beta}}. \tag{9.6}$$

This is not a unique definition of the cross-over scale, since we have chosen the same length scale that connects vorticity to velocity and to be the β-scale, and it is by no means *a priori* clear that this should be so. If the scale is different, the three terms in (9.4) scale as

$$\frac{Z}{T} \quad : \quad \frac{UZ}{L} \quad : \quad \beta U \tag{9.7}$$

where Z is the scaling for vorticity (i.e., $\zeta = \mathcal{O}Z$). Equating the second and third terms gives the scale

$$L_{\beta Z} = \frac{Z}{\beta}. \tag{9.8}$$

In any case, (9.6) and (9.8) both indicate that at some *large* scale Rossby waves are likely to dominate whereas at small scales advection, and turbulence, dominates.

Another heuristic way to derive (9.6) is by a direct consideration of timescales. The Rossby wave frequency is β/k and an inverse advective timescale is Uk, where k is the wavenumber. Equating these two gives an equation for the β-wavenumber

$$\boxed{k_\beta \sim \sqrt{\frac{\beta}{U}}}. \tag{9.9}$$

This equation is the inverse of (9.6), but note that factors of order unity cannot be revealed by simple scaling arguments such as these. The cross-over between waves and turbulence is reasonably sharp, as indicated in Fig. 9.1.

Phenomenology

Can we be more precise about the scaling, using the phenomenology of turbulence? Let us suppose that the fluid is stirred at some well-defined scale k_f, producing an energy input ε. Then (assuming no energy is lost to smaller scales) energy cascades to large scales at that same rate. At some scale, the β term in the vorticity equation will start to make its presence felt. By analogy with the procedure for finding the dissipation scale in turbulence, we can find the scale at which linear Rossby waves dominate by equating the inverse of the turbulent eddy turnover time to the Rossby wave frequency. The eddy-turnover time is

$$\tau_k = \varepsilon^{-1/3} k^{-2/3}, \tag{9.10}$$

and equating this to the inverse Rossby wave frequency k/β gives the β-scale

$$\boxed{k_\beta \sim \left(\frac{\beta^3}{\varepsilon}\right)^{1/5}}. \tag{9.11}$$
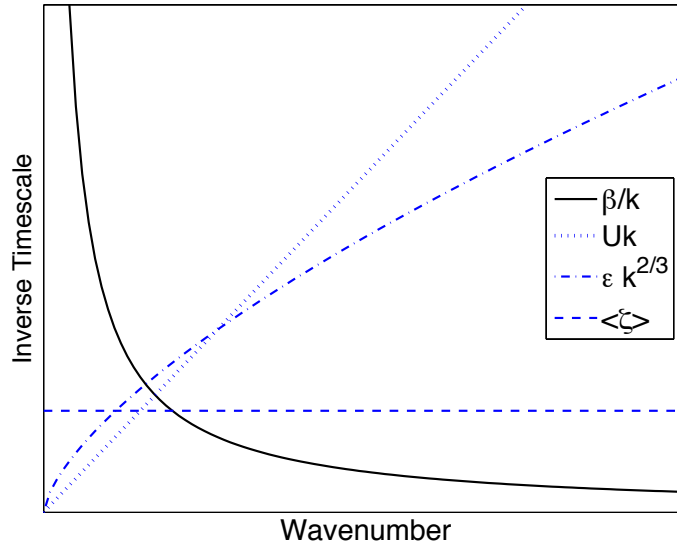
Fig. 9.1 Three estimates of the wave-turbulence cross-over, in wavenumber space. The solid curve is the frequency of Rossby waves, proportional to β/k. The other three curves are various estimates of the inverse turbulence timescale, or 'turbulence frequency.' These are the turbulent eddy transfer rate, proportional to $\varepsilon k^{2/3}$ in a $k^{-5/3}$ spectrum; the simple estimate Uk where U is an rms velocity; and the mean vorticity, which is constant. Where the Rossby wave frequency is larger (smaller) than the turbulent frequency, i.e., at large (small) scales, Rossby waves (turbulence) dominate the dynamics.

From a practical perspective this is less useful than (9.9), since it is generally much easier to measure velocities than energy transfer rates, or even vorticity. Nonetheless, it is a little more fundamental from the point of view of turbulence since one can often imagine that ε is determined by processes largely independent of β, whereas the magnitude of the eddies (i.e. U) at the energy containing scales is likely to be a function of β.

Generation of anisotropy

None of the measures discussed so far take into account the anisotropy inherent in Rossby waves, nor do they suggest how the flow might organize itself into zonal structures. To understand that, let us note that energy transfer will be relatively inefficient at those scales where linear Rossby waves dominate. But the wave-turbulence boundary is not isotropic; the Rossby wave frequency is quite anisotropic, being given by

$$\omega_\beta = -\frac{\beta k^x}{k^{x2} + k^{y2}}.$$

(9.12)
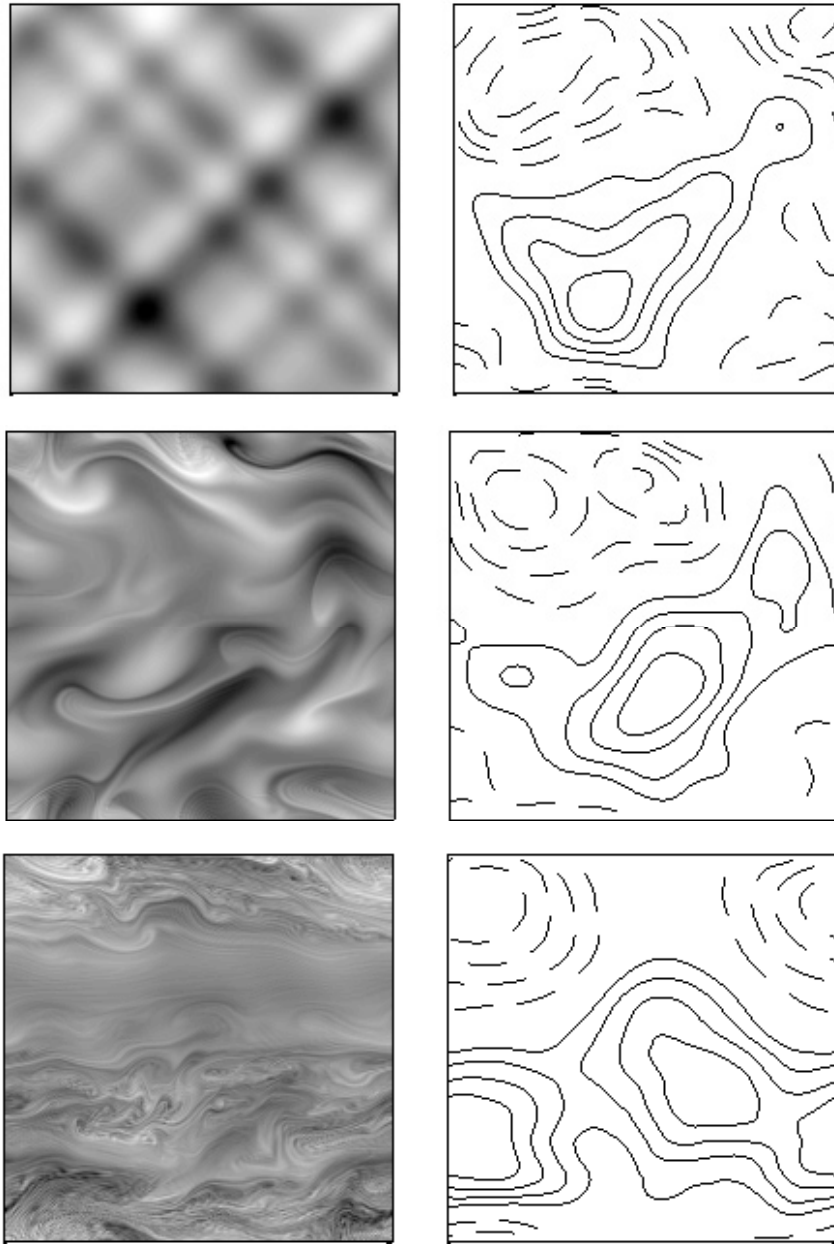
Fig. 9.2 Evolution of vorticity (greyscale, left column) and streamfunction (contour plots, right column) in a doubly-periodic square domain (of length 2π) at times $t = 0$, $t = 50$ and $t = 260$ (in units of inverse vorticity), obeying (9.4) with the addition of a weak viscous term on the right-hand-side. The initial conditions are the same as for Fig. 8.8, with maximum value of vorticity about 3. As $\beta = 3$, the β-Rossby number, $|\zeta|/\beta L$ is about unity. Compared to Fig. 8.8, vortex formation is inhibited and there is tendency toward zonal flow.

Figure 9.3 The anisotropic wave-turbulence boundary k_β, in wave-vector space calculated by equating the turbulent eddy transfer rate, proportional to $k^{2/3}$ in a $k^{-5/3}$ spectrum, to the Rossby wave frequency $\beta k^x/k^2$, as in (9.14). Within the dumbbell Rossby waves dominate and energy transfer is inhibited. The inverse cascade plus Rossby waves thus leads to a generation of zonal flow.
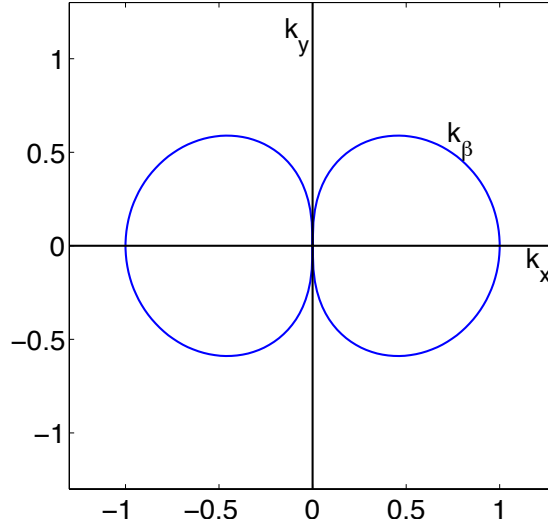
If, as a first approximation, we suppose that the turbulent part of the flow remains isotropic, the wave turbulence boundary is then given from the solution of

$$\varepsilon^{1/3} k^{2/3} = \frac{\beta k^x}{k^2} \tag{9.13}$$

where k is the isotropic wavenumber. Solving this gives expressions for the x- and y-wavenumber components of the wave-turbulence boundary, namely

$$k_\beta^x = \left(\frac{\beta^3}{\varepsilon}\right)^{1/5} \cos^{8/5}\theta, \qquad k_\beta^y = \left(\frac{\beta^3}{\varepsilon}\right)^{1/5} \sin\theta \cos^{3/5}\theta, \tag{9.14}$$

where the polar coordinate is parameterized by the angle $\theta = \tan^{-1}(k^y/k^x)$. This rather uninformative-looking formula is illustrated in Fig. 9.3.

The region inside the dumbbell shapes in Fig. 9.3 is dominated by Rossby waves, where the natural frequency of the oscillation is *higher* than the turbulent frequency. If the flow is stirred at a wavenumber higher than this the energy will cascade to larger scales, but because of the frequency mismatch the turbulent flow will be unable to efficiently excite modes within the dumbbell. Nevertheless, there is still a natural tendency of the energy to seek the gravest mode, and it may do this by cascading toward the $k^x = 0$ axis — that is, toward zonal flow. In this way zonally elongated structures are produced.

Slight variations on this temes are produced by using different expressions for the 'turbulence frequency'. For example, if we use the simple expression Uk then the wave turbulence boundary is given from

$$Uk = \frac{\beta k^x}{k^2}, \tag{9.15}$$

which has solutions that may be written as

$$k_\beta^x = \left(\frac{\beta}{U}\right)^{1/2} \cos^{3/2}\theta, \qquad k_\beta^y = \left(\frac{\beta}{U}\right)^{1/2} \sin\theta \cos^{1/2}\theta. \tag{9.16a,b}$$
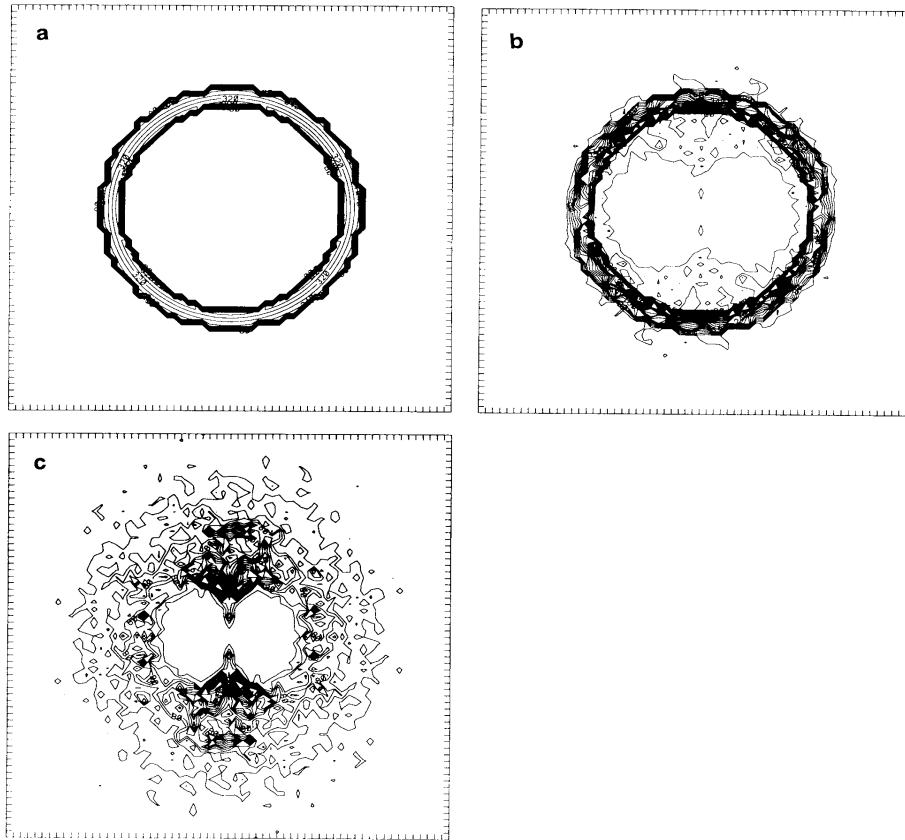
Fig. 9.4 Evolution of the energy spectrum in a freely-evolving two-dimensional simulation on the β-plane. The panels show contours of energy in wavenumber (k, l) space. The initial spectrum (a) is isotropic. The energy 'implodes', but its passage to large scales is impeded by the β-effect, and panels (b) and (c) show the spectrum at later times, illustrating the dumbbell predicted by (9.14) and Fig. 9.3.[2]

A plot of this is very similar to Fig. 9.3.

Does this putative mechanism actually work? Fig. 9.4 shows the freely evolving (unforced, inviscid) energy spectrum in a simulation on a β–plane, with an initially isotropic spectrum. The energy implodes, cascading to larger scales but avoiding the region inside the dumbbell and piling up at $k^x = 0$. A similar picture emerges in a forced-dissipative simulations, and with zonally-periodic boundary conditions these show a robust tendency to produce zonally-elongated structures and jets (Fig. 9.5). In closed domains, such as occur in the earth's ocean, the production of such jets is interrupted by the meridional boundaries.
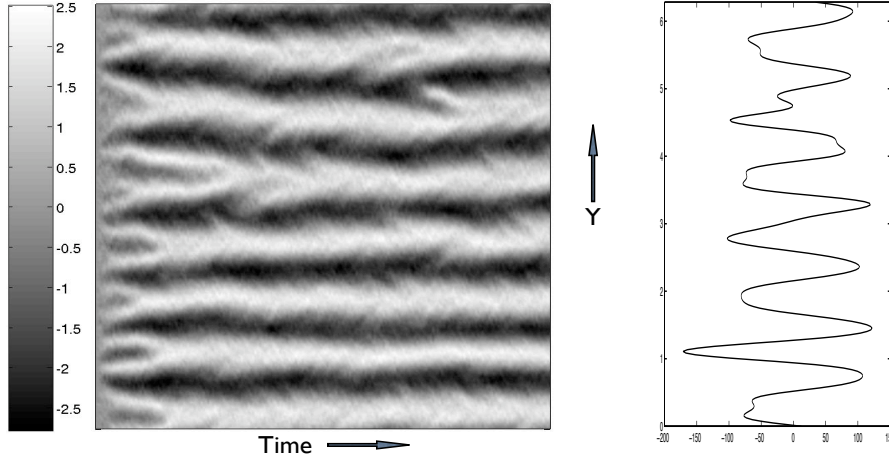
Fig. 9.5 Left: Gray-scale image of zonally average zonal velocity ($\overline{u}$) as a function of time and latitude (Y), produced in a simulation forced around wavenumber 80 and with $k_\beta = \sqrt{\beta/U} \approx 10$ (in a domain of size 2π). Right: Values of $\partial^2 \overline{u}/\partial y^2$ as a function of latitude, late in the integration. Jets form very quickly from the random initial conditions, and are subsequently quite steady.[3]

9.2 STRATIFIED GEOSTROPHIC TURBULENCE

9.2.1 Quasi-geostrophic flow as an analogue to two-dimensional flow

Now let us consider stratified effects in a simple setting, namely the quasi-geostrophic equations with constant Coriolis parameter and constant stratification.[4] The (dimensional) unforced and inviscid governing equation may then be written

$$\frac{\mathrm{D}q}{\mathrm{D}t} = 0, \qquad q = \nabla^2 \psi + Pr^2 \frac{\partial^2 \psi}{\partial z^2}, \tag{9.17a}$$

where $Pr = f_0/N$ is the *Prandtl ratio* (and Pr/H is the inverse of the deformation radius) and $D/Dt = \partial/\partial t + \boldsymbol{u} \cdot \nabla$ is the two-dimensional material derivative. The vertical boundary conditions are

$$\frac{\mathrm{D}}{\mathrm{D}t} \left(\frac{\partial \psi}{\partial z} \right) = 0, \qquad \text{at } z = 0, H. \tag{9.17b}$$

These equations are analogous to the equations of motion for purely two-dimensional flow. In particular, with periodic lateral boundary conditions, or conditions of no-normal flow, there are two quadratic invariants of the motion, the energy and the enstrophy, which are obtained by multiplying (9.17a) by ψ and q and integrating over the domain, as in chapter 5. The conserved energy is

$$\frac{\mathrm{d}\widehat{E}}{\mathrm{d}t} = 0, \qquad \widehat{E} = \int_V \left[(\nabla\psi)^2 + Pr^2 \left(\frac{\partial \psi}{\partial z} \right)^2 \right] \mathrm{d}V, \tag{9.18}$$

where the integral is over a *three-dimensional* domain. The enstrophy is conserved at each vertical level, and of course the volume integral is also conserved, namely

$$\frac{\mathrm{d}\widehat{Z}}{\mathrm{d}t} = 0, \qquad \widehat{Z} = \int_V q^2 \, \mathrm{d}V = \int_V \left[\nabla^2 \psi + Pr^2 \left(\frac{\partial^2 \psi}{\partial z^2} \right) \right]^2 \mathrm{d}V. \qquad (9.19)$$

The analogy with two-dimensional flow is even more transparent if we further rescale the vertical coordinate by $1/Pr$, and so let $z' = z/Pr$. Then the energy and enstrophy invariants are:

$$\widehat{E} = \int (\nabla_3 \psi)^2 \, \mathrm{d}V, \qquad \widehat{Z} = \int q^2 dV = \int (\nabla_3^2 \psi)^2 \, \mathrm{d}V \qquad (9.20)$$

where $\nabla_3 = \mathbf{i} \, \partial/\partial x + \mathbf{j} \, \partial/\partial y + \mathbf{k} \, \partial/\partial z'$. The invariants then have almost same form as the two-dimensional invariants, but with a three-dimensional Laplacian operator instead of a two-dimensional one.

Given these invariants, we should expect that any dynamical behaviour that occurs in the two-dimensional equations *that depends solely on the energy/enstrophy constraints* should have an analogy in quasi-geostrophic flow. In particular, the transfer of energy to large-scales and enstrophy to small scales will also occur in quasi-geostrophic flow with, in so far as these transfers are effected by a local cascade, corresponding spectra of $k^{-5/3}$ and a k^{-3}. However, the wavenumber is the now *three-dimensional* wavenumber, appropriately scaled by the Prandtl ratio in the vertical. Interestingly, then, the energy cascade to larger horizontal scales is accompanied by a cascade to larger vertical scales — a *barotropization* of the flow. This is an important and robust process in geostrophic turbulence and we come back to it later. However, the analogy should not be taken too far, because in quasi-geostrophic flow the potential vorticity is advected only by the horizontal flow. Thus, the dynamics of quasi-geostrophic turbulence will *not* in general be isotropic in three-dimensional wavenumber. To examine the detailed dynamical behaviour of quasi-geostrophic turbulence, we turn to a simpler model, that of two-layer flow

9.2.2 Two-layer geostrophic turbulence

Let us now consider flow in two layers of equal depth, governed by the quasi-geostrophic equations with (for now) $\beta = 0$, namely

$$\frac{\partial q_i}{\partial t} + J(\psi_i, q_i) = 0, \qquad\qquad i = 1, 2, \qquad (9.21)$$

where

$$q_1 = \nabla^2 \psi_1 + \frac{1}{2} k_\mathrm{d}^2 (\psi_2 - \psi_1), \qquad q_2 = \nabla^2 \psi_2 + \frac{1}{2} k_\mathrm{d}^2 (\psi_1 - \psi_2), \qquad (9.22a)$$

$$J(a, b) = \frac{\partial a}{\partial x} \frac{\partial b}{\partial y} - \frac{\partial b}{\partial y} \frac{\partial a}{\partial x}, \qquad \frac{1}{2} k_\mathrm{d}^2 = \frac{2 f_0^2}{g' H} \equiv \frac{4 f_0^2}{N^2 H^2}. \qquad (9.22b)$$

The wavenumber k_d is inversely proportional to the baroclinic radius of deformation, and the two equivalent expressions given are appropriate in a layered model and a level model, respectively. The equations conserve the total energy,

$$\frac{d\widehat{E}}{dt} = 0, \qquad \widehat{E} = \frac{1}{2} \int \left[(\nabla \psi_1)^2 + (\nabla \psi_2)^2 + \frac{1}{2} k_d^2 (\psi_1 - \psi_2)^2 \right] dA, \qquad (9.23)$$

and the enstrophy in each layer

$$\frac{d\widehat{Z}_1}{dt} = 0, \qquad \widehat{Z}_1 = \int_A q_1^2 \, dA, \qquad (9.24)$$

$$\frac{d\widehat{Z}_2}{dt} = 0, \qquad \widehat{Z}_2 = \int_A q_2^2 \, dA. \qquad (9.25)$$

The first two terms in the energy expression represent the kinetic energy, and the last term is the available potential energy, proportional to the variance of temperature.

Baroclinic and barotropic decomposition

Define the barotropic and barotropic streamfunctions by

$$\psi \equiv \frac{1}{2}(\psi_1 + \psi_2), \qquad \tau \equiv \frac{1}{2}(\psi_1 - \psi_2). \qquad (9.26)$$

Then the potential vorticities for each layer may be written:

$$q_1 = \nabla^2 \psi + (\nabla^2 - k_d^2)\tau \qquad (9.27a)$$

$$q_2 = \nabla^2 \psi - (\nabla^2 - k_d^2)\tau \qquad (9.27b)$$

and the equations of motion may be rewritten as evolution equations for ψ and τ as follows:

$$\frac{\partial}{\partial t} \nabla^2 \psi + J(\psi, \nabla^2 \psi) + J(\tau, (\nabla^2 - k_d^2)\tau) = 0 \qquad (9.28a)$$

$$\frac{\partial}{\partial t} (\nabla^2 - k_d^2)\tau + J(\tau, \nabla^2 \psi) + J(\psi, (\nabla^2 - k_d^2)\tau) = 0 \qquad (9.28b)$$

We note the following:

(i) ψ and τ are like vertical modes. That is, ψ is the barotropic mode with a 'vertical wavenumber', k^z, of zero, and τ is a baroclinic mode with a vertical wavenumber of one.

(ii) Just as purely two dimensional turbulence can be considered to be a plethora of interacting triads, whose two-dimensional vector wavenumbers sum to zero, it is clear from (9.28b) geostrophic turbulence may be considered to be similarly comprised of a sum of interacting triads. The types of triad interaction are:

$$(\psi, \psi) \to \psi, \quad (\tau, \tau) \to \psi, \quad (\psi, \tau) \to \tau. \qquad (9.29)$$

The first kind is a *barotropic triad,* for it involves only the barotropic mode. The other two are examples of a *baroclinic triad.* If a barotropic mode has a vertical wavenumber of zero, and a baroclinic mode has a vertical wavenumber of plus or minus one, then the vertical wavenumbers of the triad interactions must sum to zero. There is no triad that involves only the baroclinic mode, as we may see from the form of (9.28). (If the layers are of unequal depths, then purely baroclinic triads do exist.)

(iii) Wherever the Laplacian operator acts on τ, it is accompanied by $-k_d^2$. That is, it is *as if* the effective horizontal wavenumber (squared) of τ is shifted, so that $k^2 \rightarrow k^2 + k_d^2$.

Conservation properties

Multiplying (9.28a) by ψ and (9.28b) by τ and horizontally integrating over the domain, assuming once again that the domain is either periodic or has solid walls, gives

$$\widehat{T} = \int_A (\nabla \psi)^2 \, dA, \qquad \frac{d\widehat{T}}{dt} = \int_A \psi J(\tau, (\nabla^2 - k_d^2)\tau) \, dA \qquad (9.30a)$$

$$\widehat{C} = \int_A [(\nabla \tau)^2 + k_d^2 \tau^2] \, dA, \qquad \frac{d\widehat{C}}{dt} = \int_A \tau J(\psi, (\nabla^2 - k_d^2)\tau) \, dA. \qquad (9.30b)$$

Here, $\widehat{T}$ is the energy associated with the barotropic flow and $\widehat{C}$ is the energy of the baroclinic flow. An integration by parts shows that

$$\int_A \psi J(\tau, (\nabla^2 - k_d^2)\tau) \, dA = - \int_A \tau J(\psi, (\nabla^2 - k_d^2)\tau) \, dA, \qquad (9.31)$$

and therefore

$$\frac{d\widehat{E}}{dt} = \frac{d}{dt}(\widehat{T} + \widehat{C}) = 0. \qquad (9.32)$$

That is, total energy is conserved.

An enstrophy invariant is obtained by multiplying (9.28a) by $\nabla^2 \psi$ and (9.28b) by $(\nabla^2 - k_d^2)\tau$ and integrating over the domain and adding the two expressions. The result is

$$\frac{d\widehat{Z}}{dt} = 0, \qquad \widehat{Z} = \int_A (\nabla^2 \psi)^2 + \left[(\nabla^2 - k_d^2)\tau\right]^2 dA. \qquad (9.33)$$

This also follows from (9.24).

Just as for two-dimensional turbulence, we may define the spectra of the energy and enstrophy. Then, with obvious notation, for the energy we have

$$\widehat{T} = \int T(k) \, dk \quad \text{and} \quad \widehat{C} = \int C(k) \, dk, \qquad (9.34)$$

and the enstrophy spectrum $Z(k)$ is related to the energy spectra by

$$\widehat{Z} = \int Z(k) \, dk = \int \left[k^2 T(k) + (k^2 + k_d^2)C(k)\right] dk. \qquad (9.35)$$

which is analogous to the relationship between energy and enstrophy in two-dimensional flow. We thus begin to suspect that the phenomenology to two-layer turbulence is closely related to, but perhaps richer than, that of two-dimensional turbulence.

9.2.3 Triad interactions

Two types of triad interactions are possible:

Barotropic triads: An interaction that is purely barotropic (i.e., as if $\tau = 0$) conserves $\hat{T}$, the barotropic energy, and the associated enstrophy $\int k^2 \mathcal{T}(k) dk$, and a barotropic triad behaves as purely two-dimensional flow. Explicitly, the conserved quantities are

$$\text{Energy:} \qquad \frac{d}{dt}\Big(\mathcal{T}(k) + \mathcal{T}(p) + \mathcal{T}(q) \Big) = 0, \qquad (9.36)$$

$$\text{Enstrophy:} \qquad \frac{d}{dt}\Big(k^2 \mathcal{T}(k) + p^2 \mathcal{T}(p) + q^2 \mathcal{T}(q) \Big) = 0. \qquad (9.37)$$

Baroclinic triads: Baroclinic triads involve two baroclinic wavenumbers (say p, q) interacting with a barotropic wavenumber (say k). The energy and enstrophy conservation laws for this triad are

$$\text{Energy:} \qquad \frac{d}{dt}\left(\mathcal{T}(k) + C(p) + C(q) \right) = 0, \qquad (9.38a)$$

$$\text{Enstrophy:} \qquad \frac{d}{dt}\left(k^2 \mathcal{T}(k) + (p^2 + k_d^2)C(p) + (q^2 + k_d^2)C(q) \right) = 0. \qquad (9.38b)$$

Consider the following four cases of baroclinic triad:

I. $(p, q) \gg k_d$. Then neglect k_d^2 in (9.38a) and (9.38b), and a baroclinic triad behaves like a barotropic triad, for (9.38b) is similar to (9.37). Alternatively, but equivalently, reconsider the layer form of the equations,

$$\frac{\partial q_i}{\partial t} + J(\psi_i, q_i) = 0 \qquad (9.39)$$

where

$$q_i = \nabla^2 \psi_i + k_d^2(\psi_j - \psi_i) \approx \nabla^2 \psi_i \qquad i = 1, 2, \ j = 3 - i \qquad (9.40)$$

In this case, each layer is decoupled from the other. Enstrophy is cascaded to small scales and, were there to be an energy source at small scales, energy would be transferred upscales until it reached a scale comparable with the deformation scale. Note that the transfer of enstrophy to small scales in a purely two-dimensional fashion depends on the two-layer nature of the flow. In reality, the small scales

of a continuously stratified flow may not be representable by a two-layer model: remember that in a continuously stratified quasi-geostrophic model the enstrophy cascade occurs in *three-dimensional* wavenumber. Thus, as the horizontal scales become smaller, so does the vertical scale and higher deformation radii will start to play a role.

II. $(p, q, k) \ll k_d$. The energy and enstrophy conservation laws collapse to:

$$\frac{d}{dt} (C(p) + C(q)) = 0. \tag{9.41}$$

That is to say, energy is conserved among the baroclinic modes alone, with the barotropic mode k mediating the interaction. There is no constraint preventing the transfer of baroclinic energy to smaller scales, and no production of barotropic energy at $k \ll k_d$.

III. $(p, q, k) \sim k_d$. In this case both baroclinic and barotropic modes are important. Suppose that we define the pseudo-wavenumber k' by $k'^2 \equiv k^2 + k_d^2$ for a baroclinic mode and $k'^2 = k^2$ for a barotropic mode, and similarly for p' and q'. Then energy and enstrophy conservation can be written

$$\frac{d}{dt} (\mathcal{E}(k) + \mathcal{E}(p) + \mathcal{E}(q)) = 0, \tag{9.42a}$$

$$\frac{d}{dt} \left(k'^2 \mathcal{E}(k) + p'^2 \mathcal{E}(p) + q'^2 \mathcal{E}(q) \right) = 0 \tag{9.42b}$$

where $\mathcal{E}(k)$ is the total energy (barotropic plus baroclinic) of the particular mode. These are formally identical with the conservation laws for purely two-dimensional flow and so we expect energy to seek the gravest (smallest pseudo-wavenumber) mode. Since the gravest mode has $k_d = 0$ this implies a *barotropization* of the flow.

IV. *Baroclinic Instability.* Baroclinic instability in the classic two-layer problem concerns the instability of a flow with vertical but no horizontal shear. This is like a triad interaction for which $p \ll (k, q, k_d)$. The conservation laws are,

$$\frac{d}{dt} (\mathcal{T}(k) + C(p) + C(q)) = 0,$$

$$\frac{d}{dt} \left(k^2 \mathcal{T}(k) + k_d^2 C(p) + (q^2 + k_d^2) C(q) \right) = 0. \tag{9.43}$$

From these, and with $k^2 \approx q^2$, we derive

$$k^2 \dot{C}(q) = (k_d^2 - k^2) \dot{\mathcal{T}}(k). \tag{9.44}$$

Baroclinic instability requires that both $\dot{C}(q)$ and $\dot{\mathcal{T}}(k)$ be positive. This can only occur if

$$k^2 < k_d^2. \tag{9.45}$$

wind or solar
net input

baroclinic energy

scattering
into 3-d
turbulence

barotropic energy

K_0 K_R K_D

Net loss to boundary
layer friction
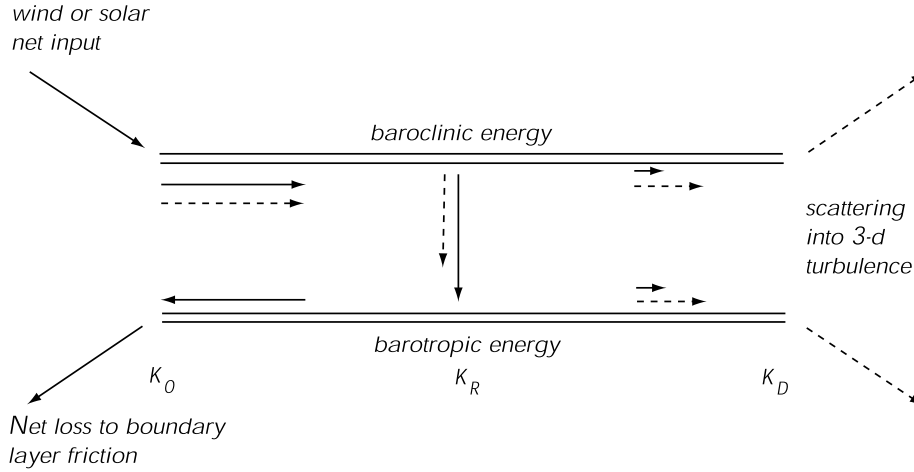
Fig. 9.6 Schema of idealized two-layer baroclinic turbulence. The horizontal axis represents horizontal wavenumber, and the vertical variation is decomposed into two vertical modes — the barotropic and first baroclinic. Large-scale forcing maintains the available potential energy, and so provides energy to the baroclinic mode at very large scales. At these large scales, the equation for the baroclinic streamfunction is approximately that of a passive tracer, and so energy is transferred to smaller scales. It is also transferred to barotropic energy, at horizontal scales comparable to and larger than the deformation radius (this is baroclinic instability) and thence to larger barotropic scales. The entire process of energy transfer may be thought of as a generalized inverse cascade in which the energy passes to smaller pseudo-wavenumber $k'^2 \equiv k^2 + k_d^2$. At scales smaller than the first deformation radius the layers are decoupled and enstrophy in each layer cascades to smaller scales. The two-layer model may become less accurate for such small scales, because of the influence of higher baroclinic modes not present in a two-layer model.[5].

Thus, there is a *high-wavenumber cut-off* for baroclinic instability. This cut-off arises solely from considerations of energy and enstrophy conservation, and is not dependent on linearizing the equations and looking for exponentially growing normal mode instabilities.

For small scales, i.e., $k^2 \gg k_d^2$, the potential vorticity in each layer is, with $\beta = 0$,

$$q_1 = \nabla^2 \psi_1 + \frac{1}{2}k_d^2(\psi_2 - \psi_1) \approx \nabla^2 \psi_1, \qquad (9.46a)$$

$$q_2 = \nabla^2 \psi_2 + \frac{1}{2}k_d^2(\psi_1 - \psi_2) \approx \nabla^2 \psi_2. \qquad (9.46b)$$

Thus, each layer is decoupled from the other. Thus, enstrophy will cascade to smaller scales and, should there be an energy source at scales smaller than the deformation scale it will cascade to larger scales. However, baroclinic instability (of the mean flow) occurs at scales *larger* than the deformation radius. Thus, energy extracted from the mean flow is essentially trapped at scales larger than the deformation scale.

Summary of phenomenology
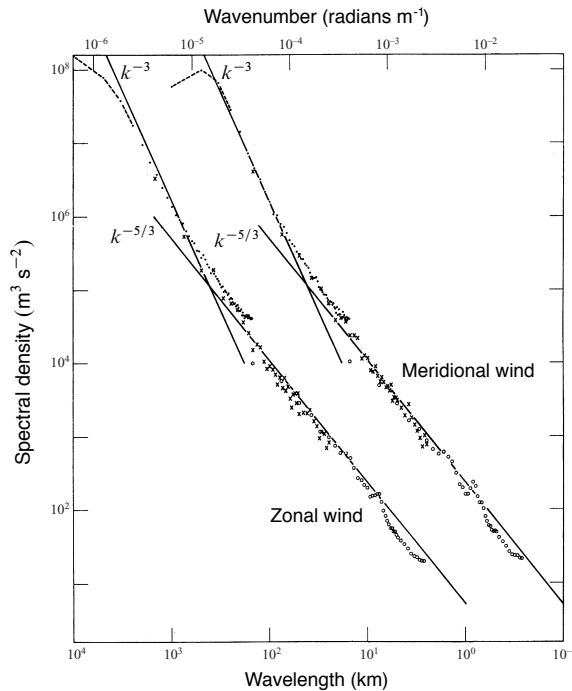
Figure 9.7 Energy spectra of the zonal and meridional wind near the tropopause, from thousands of commercial aircraft measurements between 1975 and 1979. The meridional spectrum is shifted one decade to the right. (Adapted from Gage and Nastrom 1986)

Putting together the considerations above leads to the following picture of geostrophic turbulence in a two-layer system (and see Fig. 9.6). At large horizontal scales we imagine some source of baroclinic energy, which in the atmosphere might be the differential heating between pole and equator, or in the ocean might be the wind and surface heat fluxes. Baroclinic instability effects a nonlocal transfer of energy to the deformation scale, where both baroclinic and barotropic modes are excited. From here there is an enstrophy cascade in each layer to smaller and smaller scales, until eventually the scale is small enough so that non-geostrophic effects become important and enstrophy is scattered by three-dimensional effects. At scales larger than the deformation radius, there is an inverse barotropic cascade of energy to larger scales. The energy of the large-scale barotropic modes is eventually dissipated by boundary layer effects such as Ekman drag. These ideas do not precisely apply to either atmosphere or ocean. In the latter, the turbulence is quite inhomogeneous except perhaps in the Antarctic Circumpolar Current. In the atmosphere, the deformation radius is almost as large as the Rhines scale, leaving little room for an inverse cascade. However, the atmosphere does display k^{-3} spectra at scales similar to and somewhat smaller than the deformation radius, as in Fig. 9.7, and analysis of this indicates that it may indeed be associated with a forward cascade of enstrophy.[6]

9.3 † A SCALING THEORY FOR GEOSTROPHIC TURBULENCE

We now construct a phenomenological, but quantitative, theory of two-layer forced-dissipative geostrophic turbulence.[7] We will consider a system in which the basic state

is a purely zonal flow with constant vertical shear and no horizontal variation, and our goal is to construct a theory for the amplitude and the scale of the eddies that result from the baroclinic instability of this flow. The assumption that the mean flow and the stratification are constants is quite severe. One might extend the model by adding an evolution equation for the mean flow, but allowing the stratification to vary spatially or temporally is not allowed within quasi-geostrophic theory. In reality, eddies may modify the stratification as well as the mean flow, so the model, even if correct within its own terms of reference, cannot be a complete theory of mid-latitude flow.

9.3.1 Preliminaries

The system we seek to quantify is that illustrated in Fig. 9.6. Baroclinic instability at large scales leads to a transfer of energy to the barotropic mode at a scale comparable to the deformation radius, followed by an inverse cascade of energy within the barotropic mode, and the energy is finally dissipated in the Ekman layer. At scales smaller than the deformation radius the layers are largely uncoupled, and in each layer there is an enstrophy cascade to small scales. The equations of motion describing all of this are (9.28), but we will explicitly recognize the effect of a shear flow by replacing τ by $\tau - Uy$, where U is constant, this being equivalent to supposing there is a constant shear in the flow. The equations become

$$\frac{\partial}{\partial t}\nabla^2\psi + J(\psi, \nabla^2\psi) + J(\tau, (\nabla^2 - k_d^2)\tau) + U\frac{\partial}{\partial x}\nabla^2\tau = D[\psi], \tag{9.47a}$$

$$\frac{\partial}{\partial t}(\nabla^2 - k_d^2)\tau + J(\tau, \nabla^2\psi) + J(\psi, (\nabla^2 - k_d^2)\tau) + U\frac{\partial}{\partial x}(\nabla^2\psi + k_d^2\psi) = D[\tau]. \tag{9.47b}$$

These are similar to the equations used for studying two-layer baroclinic instability in chapter 6, but we now retain the nonlinear terms and include dissipation, represented by $D[]$.

Large Scales

Let us focus on scales larger than the deformation radius. We therefore take $\nabla^2 \sim k^2 \ll k_d^2$, and eliminate terms in (9.47) involving ∇^2 if they appear along with terms involving k_d^2. Noting also that $J(\tau, k_d^2\tau) = 0$ we find

$$\frac{\partial}{\partial t}\nabla^2\psi + J(\psi, \nabla^2\psi) = -J(\tau, \nabla^2\tau) - U\frac{\partial}{\partial x}\nabla^2\tau + D[\psi], \tag{9.48}$$

$$\frac{\partial\tau}{\partial t} + J(\psi, \tau) = U\frac{\partial\psi}{\partial x} + D[\tau]. \tag{9.49}$$

We remark on two aspects to these equations:

 (i) The equation for ψ is just the barotropic vorticity equation, 'forced' via its interaction with the baroclinic mode, namely the terms on the right-hand side of (9.48)

 (ii) The equation for the baroclinic streamfunction is the same as the equation for a passive scalar, except for the forcing term $U\partial\psi/\partial x$.

In the barotropic equation, we may argue that in the energy containing scales, $k^2 \ll k_d^2$, the magnitude of the barotropic stream function is much larger than that of the baroclinic streamfunction; that is, $|\psi| \gg |\tau|$, as follows. We may reasonably suppose that the forcing of the barotropic vorticity equation occurs at wavenumbers close to k_d, as in baroclinic instability. At larger scales the barotropic streamfunction obeys the two-dimensional vorticity equation, and we may expect an energy cascade to large scales with energy spectrum given by

$$\mathcal{E}_\psi(k) = \mathcal{K}_1 \varepsilon^{2/3} k^{-5/3}, \tag{9.50}$$

where $\mathcal{K}$ is the Kolmogorov-Kraichnan constant for the inverse cascade and ε is the as yet undetermined energy flux through the system. We may suppose that this cascade holds for wavenumbers $k_0 < k \ll k_d$, where the wavenumber k_0 is the halting scale of the inverse cascade, determined by one or more of friction, the β–effect, and the domain size. Now, in this same wavenumber regime the baroclinic streamfunction is being advected as a passive tracer — it is being stirred by ψ. Thus, any baroclinic energy that is put in at large scales by the interaction with the mean flow (via the term proportional to $U\psi_x$) will be cascaded to smaller scales. Thus, we expect the baroclinic energy spectrum to be that of a passive tracer whose variance is cascading to smaller scales in a forward cascade, with a spectrum given by [c.f., (8.98)]

$$\mathcal{E}_\tau(k) = \mathcal{K}_2 \varepsilon_\tau \varepsilon^{-1/3} k^{-5/3}, \tag{9.51}$$

where $\mathcal{K}_2$ is a constant, ε_τ is the transfer rate of baroclinic energy and ε is the same quantity appearing in (9.50). Now, because energy is not lost to small scales we must have that $\varepsilon_\tau = \varepsilon$, both being equal to the energy flux in the system. Thus, using (9.50) and (9.51), the energy in the barotropic and baroclinic modes are comparable at sufficiently large scales. Since the energy density in the former is $(\nabla \psi)^2$ and in the latter $(\nabla \tau)^2 + k_d^2 \tau^2 \sim k_d^2 \tau^2$ the magnitude of ψ must then be much larger than that of τ, and specifically

$$|\psi| \sim \frac{k_d |\tau|}{k_0} \gg |\tau|. \tag{9.52}$$

9.3.2 Scaling properties

Let us write the baroclinic equation (9.49) in the form

$$\frac{\partial \tau}{\partial t} + J(\psi, \tau - Uy) = 0, \tag{9.53}$$

which is the equation for a passive tracer (τ) in a mean gradient (U), stirred by the flow (ψ), and we omit dissipation. Because there is a large scale separation (in fact, an infinite one) between the scale of the mean gradient of τ (i.e., the scale of variations of U) and the scale of its fluctuations we can write

$$\tau \sim l' \frac{\partial \overline{\tau}}{\partial y} = -l' U \tag{9.54}$$

where l' is the scale of the fluctuation. Thus, at the scale k_0^{-1} the magnitude of τ, and the associated baroclinic velocity v_τ, are given by

$$\tau \sim \frac{U}{k_0}, \qquad v_\tau \sim U. \tag{9.55}$$

At this scale, and using (9.52), the magnitude of the barotropic streamfunction and its associated velocity are given by

$$\psi \sim \frac{k_{\mathrm{d}} U}{k_0^2}, \qquad v_\psi \sim \frac{k_{\mathrm{d}} U}{k_0}. \tag{9.56}$$

How much energy flows through the system? The mean shear is the ultimate source of energy here, and for simplicity this shear is kept constant in time, analogous to an infinite heat bath supplying energy to a smaller system without its own temperature changing. The conversion of energy from the mean shear to the eddy flow is given by multiplying (9.49) by $k_{\mathrm{d}}^2 \tau$ and integrating over the domain. This gives an expression for the rate of increase of the available potential energy of the system, namely

$$\frac{\mathrm{d}}{\mathrm{d}t} APE = \frac{1}{2} \frac{\mathrm{d}}{\mathrm{d}t} \int_A k_{\mathrm{d}}^2 \tau^2 \, \mathrm{d}A = \int_A U k_{\mathrm{d}}^2 \tau \frac{\partial \psi}{\partial x} \, \mathrm{d}A \tag{9.57}$$

(Note that the energy input to the system equals the polewards heat flux.) From this we estimate the average energy flux as

$$\varepsilon = U k_{\mathrm{d}}^2 \overline{\psi_x \tau} \sim \frac{U^3 k_{\mathrm{d}}^3}{k_0^2}. \tag{9.58}$$

The correlation between ψ_x and τ cannot be determined by this argument. This aside, we have produced a physically based 'closure' for the flux of energy through the system in terms only of the mean shear, the halting scale k_0 (discussed below) and the deformation scale k_{d}.

Finally, we calculate the eddy diffusivity defined by

$$\kappa \equiv -\frac{\overline{v_\psi \tau}}{\partial_y \overline{\tau}} \tag{9.59}$$

Using (9.55) and (9.56) gives

$$\kappa \sim \frac{k_{\mathrm{d}} U}{k_0^2} \tag{9.60}$$

which, if the mixing velocity is the barotropic stirring velocity, implies a mixing length of k_0^{-1}. (Note also that the eddy diffusivity is just the magnitude of the barotropic streamfunction at the energy containing scales.)

9.3.3 The halting scale and the β–effect

Let us suppose that, as discussed in section 9.1, the β–effect provides a barrier for the inverse cascade at the scale (9.11), namely $k_\beta \sim (\beta^3/\varepsilon)^{1/5}$. Using (9.58) this becomes

$$k_\beta = \frac{\beta}{Uk_{\mathrm{d}}}, \tag{9.61}$$

and using (9.60) and (9.61) we obtain for the energy flux and the eddy diffusivity,

$$\varepsilon \sim \frac{U^5 k_{\mathrm{d}}^5}{\beta^2}, \qquad \kappa \sim \frac{U^3 k_{\mathrm{d}}^3}{\beta^2} \tag{9.62}$$

The magnitudes of the eddies themselves are easily given using (9.56) and (9.55), whence

$$\tau \sim \frac{U^2 k_{\mathrm{d}}}{\beta}, \quad v_\tau \sim U, \qquad \psi \sim \frac{U^3 k_{\mathrm{d}}^3}{\beta^2}, \quad v_\psi \sim \frac{U^2 k_{\mathrm{d}}^2}{\beta}. \tag{9.63}$$

Clearly, in this model (in which the mean shear and deformation radius are fixed), the eddies become *less* energetic with increasing β, and the eddy amplitudes and poleward heat flux increase very rapidly with the mean shear, more so than in a model in which the energy containing scale is fixed. This is because as β decreases, the inverse cascade can extend to larger scales, thereby increasing the overall energy of the flow. Similarly, as U increases not only does the eddy amplitude increase as a direct consequence [as is (9.55) and (9.56)] but also k_β falls [see (9.61)], and these effects combine to give a rapid increase of the eddy magnitudes with U.

Frictional effects

Whether β is present or not, friction is necessary to ultimately remove the energy flowing through the system, as well as to remove enstrophy at small scales. Friction provides another mechanism for halting the inverse cascade, and the simplest case is that of a linear drag representing Ekman friction, in which case we write

$$D[\psi] = -r\nabla^2\psi. \tag{9.64}$$

and the stopping scale for a given ε is given, as in (8.74), by $k_r = (r^3/\varepsilon)^{1/2}$. However, the use of this in (9.58) fails to give result for ε. From a physical perspective, a linear drag that is weak enough to allow an inverse cascade forming is, *ipso facto,* too weak equilibrate the flow. A friction that becomes larger at larger scales, for example an 'inverse Laplacian', has no such problems. More physically, a nonlinear drag, proportional to the square of the amplitude of the flow, also leads to a well-posed problem with the cascade halting at a well-defined scale. Finally, we should point out that in neither the atmosphere or ocean is there an extended inverse cascade, because the deformation scale and the Rhines scale are not asymptotically well separated (although the β effect does not prevent an inverse cascade to large zonal scales).

9.4 † PHENOMENOLOGY OF BAROCLINIC EDDIES IN THE ATMOSPHERE AND OCEAN

In the remaining sections of this chapter we take a phenomenological approach, illustrated by numerical experiments and observations, to the problem of baroclinic eddies in the atmosphere and ocean. We draw from our treatment of geostrophic turbulence but by being a little less precise we are able to travel farther, for we spend less time looking at the map (but with a concomitant danger that we lose our way).

9.4.1 The Magnitude and Scale of Baroclinic Eddies

How big, in both amplitude and scale, do baroclinic eddies become? Suppose that the time-mean flow is given, and that it is baroclinically unstable. Eddies will grow, initially according to the linear theory of chapter 6, but they cannot and do not continue to amplify: they ultimately equilibrate, and this by way of nonlinear mechanisms. The eddies will extract energy from the mean flow, but at the same time the available energy of the mean flow is being replenished by external forcing (i.e., the maintenance of an equator–pole temperature gradient by radiative forcing in the atmosphere, and wind and buoyancy forcing at the surface in the ocean). Thus, we cannot a priori determine the amplitude of baroclinic eddies by simply assuming that all of the available potential energy in the mean flow is converted to eddying motion. To close the problem we find we need to make three, not necessarily independent, assumptions:

 (i) An assumption about the magnitude of the baroclinic eddies;

 (ii) An assumption relating eddy kinetic energy to eddy available potential energy;

 (iii) An assumption about the horizontal scale of the eddies.

Baroclinic eddies extract available potential energy (APE) from the mean flow, and it is reasonable to suppose that an eddy of horizontal scale L_e can extract, as an upper bound, the APE of the mean flow contained within that scale. The APE is proportional to the variation of the buoyancy field so that

$$(\Delta b')^2 \sim |\Delta\overline{b}|^2 \sim L_{\rm e}^2|\nabla\overline{b}|^2 \tag{9.65}$$

where $\Delta\overline{b}$ is the variation in the buoyancy over the horizontal scale $L_{\rm e}$. (For simplicity we stay with the Boussinesq equations, and $b = -g\delta\rho/\rho_0$. However, we might easily apply this to an ideal-gas atmosphere with $b = g\delta\theta/\theta_0$.) Equivalently, we might simply write

$$\boxed{b' \sim L_{\rm e}|\nabla\overline{b}|} , \tag{9.66}$$

which arises from a mixing-length approach. Supposing that the temperature gradient is mainly in the y-direction then, using thermal wind, we have

$$b' \sim L_{\rm e}f\frac{\partial\overline{u}}{\partial z} \qquad\text{and}\qquad v'_{\tau} \sim \overline{u}, \tag{9.67a,b}$$

where v'_{τ} is an estimate of the shear (multiplied by the depth scale) of the eddying flow. [These estimates are the same as (9.55), with $\overline{u}$ replacing U.]

Our second assumption is to relate the barotropic eddy kinetic energy to the eddy available potential energy, and the most straightforward one to make is that there is a rough equipartition between the two. This assumption is reasonable because in the baroclinic lifecycle (or baroclinic inverse cascade) energy is continuously transferred from eddy available potential energy to eddy kinetic energy, and the assumption is then equivalent to supposing that the relevant eddy magnitude is always proportional to this rate of transfer. Thus we assume $v_\psi^2 \sim (b'/N)^2$ or

$$\boxed{v_\psi' \sim \frac{b'}{N}}. \tag{9.68}$$

Finally, the scale of the eddies is determined by the extent to which the eddies might grow through nonlinear interactions. As we discussed earlier, possibilities for this scale include the deformation radius itself (if the inverse cascade is weak) or the Rhines scale (if the inverse cascade is slowed by the beta effect), or even the domain scale if neither of these apply.

Some consequences

These simple manipulations have some very interesting consequences. Using (9.67) and (9.68) we find

$$v_\psi' \sim \frac{f L_e}{N H} \overline{u} \approx \frac{L_e}{L_d} \overline{u} \tag{9.69}$$

where $L_d = N H / f_0$ is the deformation radius and $\overline{u}$ is the amplitude of the mean baroclinic velocity, that is the mean shear multiplied by the height scale. This important relationship relates the magnitude of the eddy kinetic energy to that of the mean. In the atmosphere the scale of the motion not much larger than the deformation radius (which is about 1000 km) the eddy and mean ksinetic energies are, consistently, comparable to each other. In the ocean the deformation radius (about 50 km over large areas) is significantly smaller than the scale of mesoscale eddies (which typically might be more like 200 km), and observations consistently reveal that the eddy kinetic energy is an order of magnitude larger than the mean kinetic energy.[8]

One other important and somewhat counter-intuitive result concerns the timescale of eddies. From (9.69) we have

$$T_E \sim \frac{L_e}{v_\psi'} \sim \frac{L_d}{\overline{u}}, \tag{9.70}$$

and this is simply the Eady timescale. That it, the eddy timescale (at the scale of the largest eddies) is independent of the process that ultimately determines the spatial scale of those eddies; if the eddy length scale increases somehow, perhaps because friction or β are decreased, the velocity scale increases in proportion.

Let us now consider various aspects of baroclinic eddies in the atmosphere and the ocean.

9.4.2 Baroclinic Eddies in the Atmosphere

Amplitude and Scale

We saw in section 6.10.2 that baroclinic instability in the atmosphere occurs predominantly in the troposphere, i.e., in the lowest 10 km or so of the atmosphere, with the higher stratification of the eponymous stratosphere inhibiting instability. In the mid-latitude troposphere the vertical shear and the stratification are also relatively uniform which is why fairly simple models, such as the two-layer model or the Eady model (with the addition of the β-effect) are reasonable first-order models.

The mean pole-equator temperature gradient is about 40 K and the deformation radius NH/f is about 1000 km. The Rhines scale, $\sqrt{u_{rms}/\beta}$ is a little larger than this, perhaps 2000 km, and is similar to the width of the main mid-latitude baroclinic zone which lies between about 40° and 65°, in either hemisphere. Given these, and especially given that the maximum wavelength for instability occurs at scales somewhat larger than the deformation radius, there is little prospect of an extended upscale cascade, and for this reason the earth's atmosphere has comparable eddy kinetic and mean kinetic energies.[9]

The baroclinic lifecycle

The baroclinic lifecycle of geostrophic turbulence, sketched schematically in Fig. 9.6, can be nicely illustrated by way of numerical initial value problems, and we describe two such. The first is very idealized: take a doubly-period quasi-geostrophic model on the f-plane, initialize it with baroclinic energy at large horizontal scales, and then let the flow freely evolve. Fig. 9.8 shows the results. The flow, initially concentrated in high vertical wavenumbers to best illustrate the energy transfer, is baroclinically unstable, and energy is transferred to barotropic flow at wavenumbers close to the first radius of deformation, here at about wavenumber 15. Energy then slowly cascades back to large scales in a predominantly barotropic inverse cascade, piling up at the largest scales much as in decaying, two-dimensional turbulence. Nearly all of the initial baroclinic energy is converted to barotropic, eddy kinetic energy and, even without any surface friction, the flow evolves to a baroclinically stable state. Couched in these terms, it is easy to see the baroclinic lifecyle as a form of baroclinic inverse cascade, with an energy transfer to large total wavenumber, K_{tot}, that is made up of contributions from both horizontal and vertical wavenumbers:

$$K_{tot}^2 = K_h^2 + k_d^2 m^2 \qquad (9.71)$$

where m is the vertical and K_h the horizontal wavenumber. As we noted earlier, the twin constraints of energy and enstrophy consevation prevent the excitation of horizontal scales with very large horizontal wavenumbers, and so the lifecyle proceeds through wavenumbers at the deformation scale.

The results of second, and more realistic, initial value problem are illustrated in Fig. 9.9. Here, the atmospheric primitive equations on a sphere are integrated forward, beginning from a baroclinically unstable zonal flow, plus a small-amplitude disturbance at zonal wavenumber six. The disturbance grows rapidly through baroclinic instability, accompanined by a conversion of energy initial from the zonal mean potential energy
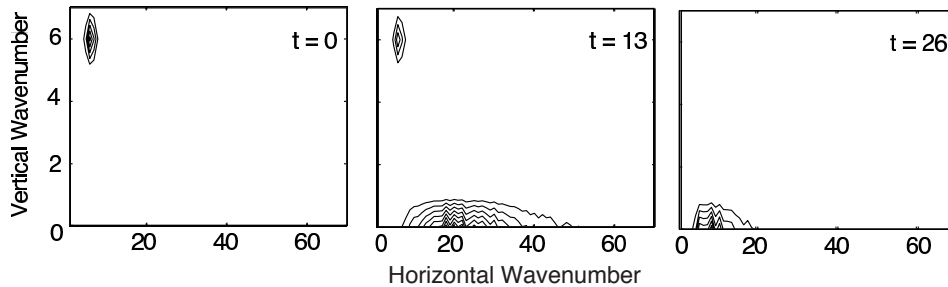
Fig. 9.8 A numerical simulation of a very idealized baroclinic lifecyle, showing contours of energy in spectral space at successive times. Initially, there is baroclinic energy at low horizontal wavenumber, as in a large-scale shear. Baroclinic instability transfers this energy to barotropic flow at the scale of the deformation radius, and this is followed by a barotropic inverse cascade to large scales. Most of the transfer to the barotropic mode in fact occurs quite quickly, between times 11 and 14, but the ensuing barotropic inverse cascade is slower. The entire process may be thought of as a generalized inverse cascade. The stratification (N^2) is uniform, and the first deformation radius is at about wavenumber 15. There is no friction in the simulation, except for a small hyperviscosity to remove small scale noise. Times are in units of eddy turnover time.[10]

to eddy available potential energy (EAPE), and then from EAPE to eddy kinetic energy (EKE), and finally from EKE to zonal kinetic energy (ZKE). The last stage of this corresponds to the barotropic inverse cascade of quasi-geostrophic theory, and because of the presence of a β-effect the flow becomes organized into a zonal jet. The parameters in the earth's atmosphere are such that there is only one such jet, and in the lower panel of Fig. 9.9 we see its amplitude increase quickly from days 10 though 12, associated with the conversion of EKE to ZKE.

Of course, the atmosphere is never in a zonally uniform state as used in our baroclinic instability studies or the liefecycle study. At any given time, finite amplitude eddies exist and these provide a finite amplitude perturbation to the baroclinically unstable zonal flow, and thus we will rarely, if ever, see an exponentially growing normal mode. Furthermore, given any instantaneous atmospheric state, zonally symmetric or otherwise, the fastest growing (linear) instability is not necessarily exponential but may be 'non-modal', with a secular or linear growth that, over some finite time period and in some given norm, is much more rapid than exponential.[12] A baroclinically turbulent atmosphere is of course maintained because of the underlying presence of baroclinic instability, and the classic baroclinic instability problems and nonlinear lifecyles illustrate, in an idealized way, the continuous growth, maturation and decay of eddies embedded in that flow.

9.4.3 Baroclinic Eddies in the Ocean

There are more things in Heaven and Earth, Horatio, Than are dreamt of in

Figure 9.9 Top: Energy conver-
sion and dissipation processes in
a numerical simulation of an ide-
alized atmospheric baroclinic life-
cycle, simulated with a GCM Bot-
tom: Evolution of the maximum
zonal-mean velocity. A_Z and A_E are
zonal and eddy available potential
energies, and K_Z and K_E the cor-
responding kinetic energies. Ini-
tially baroclinic processes domi-
nate, with conversions from zonal
to eddy kinetic energy and then
eddy kinetic to eddy available po-
tential energy, followed by the
barotropic conversion of eddy ki-
netic to zonal kinetic energy. The
latter process is reflected in the
increase of the maximum zonal-
mean velocity at about day 10.[11]
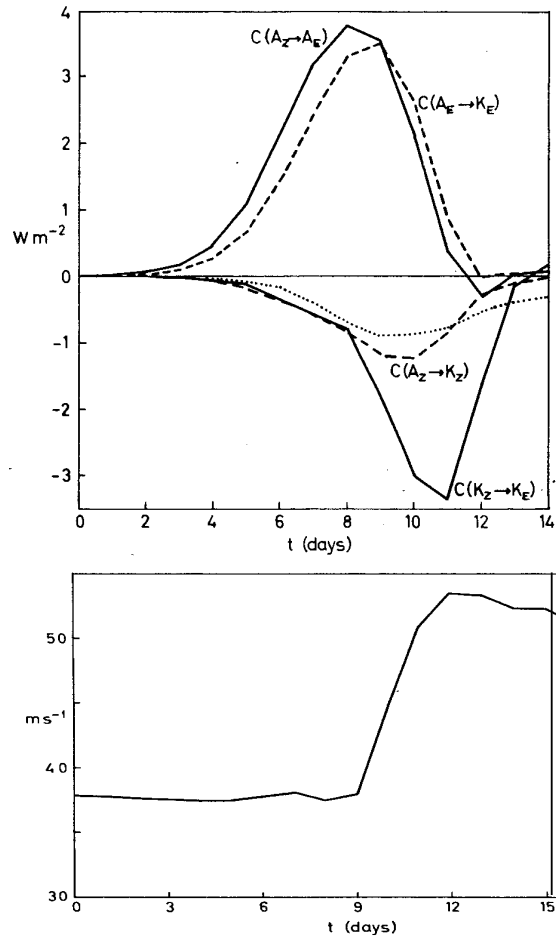
thy philosophy.
William Shakespeare, *Hamlet,* c. 1602.

Basic ideas

Baroclinic instability was first developed as a theory for midlatitude synoptic-scale instabilities in the atmosphere and the original, now classic, problems are accordingly set in a zonally re-entrant channel. The ocean, apart from the Antarctic Circumpolar Current (ACC), is not zonally re-entrant. However, the ocean is driven by buoyancy and wind-forcing at the surface, and these combine to produce a region of enhanced stratification and associated shear in the ocean in the upper 500–1000 m or so, in the 'thermocline', as discussed more fully in chapter 16 (e.g., Fig. 15.2). The sloping isopycnals indicate that there is a pool of available potential energy that might be converted to kinetic energy, and so that the ocean is potentially baroclinically unstable. Satellite observations indicated that baroclinic eddies are almost ubiquitous in the mid- and high-latitude oceans, two particularly eddy-rich regions being the areas in and surrounding intense western boundary currents, such as the Gulf Stream, and in the ACC.[13] In addition to the geometry, the main differences between the oceanic and atmospheric problems are:

(i) In the ocean, the shear and the stratification are not uniform between two rigid lids, nor even uniform between one rigid lid and a structure like the tropopause. Instead, both stratification and shear are largest in the upper ocean, decaying into a quiescent and nearly unstratified abyss.

(ii) The first radius of deformation is much smaller than the scale of the large-scale flow — that is, of the gyres or the large-scale overturning circulation.

A consequence of the first item is that the amplitude of the growing waves is also largely concentrated in the upper ocean, as we saw in Fig. 6.22. Regarding item (ii), we can estimate the oceanic deformation radius as

$$
L_{\mathrm{d}} = \frac{NH}{f} \approx \frac{10^{-2} \times 500}{10^{-4}} \approx 50 \, \text{km}. \tag{9.72}
$$

More precisely, in quasi-geostrophic theory we may define the deformation radii by solution of the eigenvalue problem

$$
\frac{\partial}{\partial z} \frac{f_0^2}{N^2} \frac{\partial \phi_n}{\partial z} + E_n \phi_n = 0. \tag{9.73}
$$

The successive eigenvalues, E_n, are related to the successive deformation radii by $L_{dn}^2 = 1/E_n$, and the results of a similar calculation are given in Fig. 9.10. Note that in uniform stratification the deformation radius as defined by (9.73) and displayed in Fig. 9.10 is a factor of π smaller than the simple estimate NH/f, so that the most baroclinically unstable waves have a wavelength several times L_{d1}. Nevertheless, we may expect baroclinic instability to occur on a scale much smaller than that in the atmosphere, and much smaller than the scale of the domain.
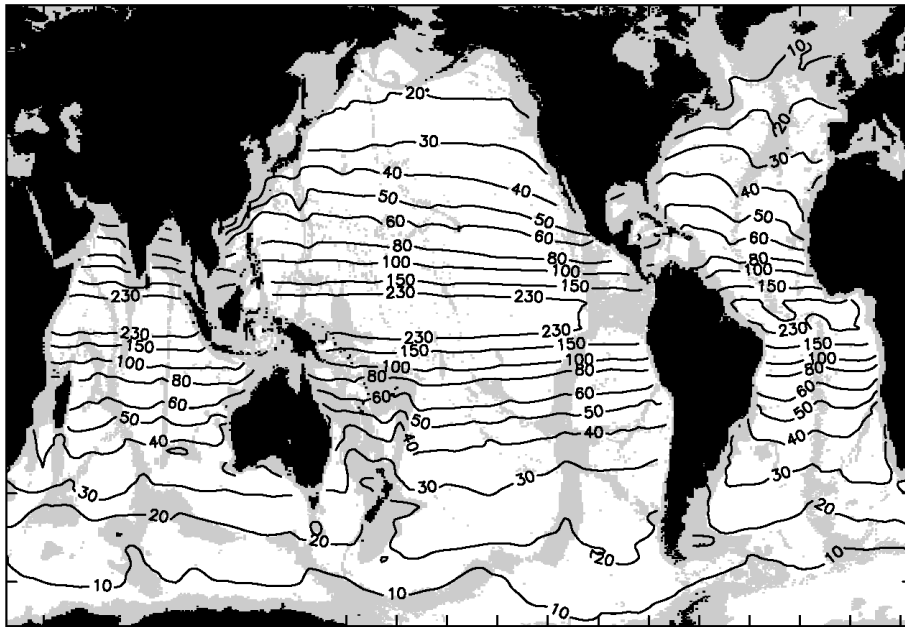
Fig. 9.10 The oceanic first deformation radius L_d, calculated by using the observed stratification from the eigenproblem:
$\partial^2\phi/\partial z^2 + (N^2(z)/c^2)\phi = 0$ with $\phi = 0$ at $z = 0$ and $z = -H$, where H is the ocean depth and N is the observed buoyancy frequency. The deformation radius is given by $L_d = c/f$ where c is the first eigenvalue and f is the latitudinally varying Coriolis parameter. Near equatorial regions are excluded, and regions of ocean shallower than 3500 m are shaded. Variations in Coriolis parameter are responsible for much of large-scale variability, although weak stratification also reduces the deformation radius at high latitudes.[14]

Amplitude and Scale

The consequences of this small deformation radius on the lifecycle and finite-amplitude equilibration of oceanic baroclinic eddies are potentially far-reaching, the most important of which is that there is more scope for an inverse cascade than in the atmosphere, and indeed observations indicate that the horizontal scale of the eddies is typically a few to several times larger than the local deformation radius itself. The situation is not clear cut, however: the eddy scale does seem to be somewhat larger than the deformation scale, but some observations[15] indicate that the eddy size nevertheless scales with the local deformation radius, suggesting that the eddy scale may be set by the instability scale and not an inverse cascade. In any case, suppose then that an ocean eddy is of horizontal scale 200 km, and that it sits in the subtropical gyre where the mean temperature gradient is 10^{-5} K m^{-1}, that the mean shear and ensuing baroclinic activity is mainly confined to the upper 1000 m of the ocean, and that the deformation radius is 50 km. The temperature gradient corresponds to a temperature difference of about 20 K
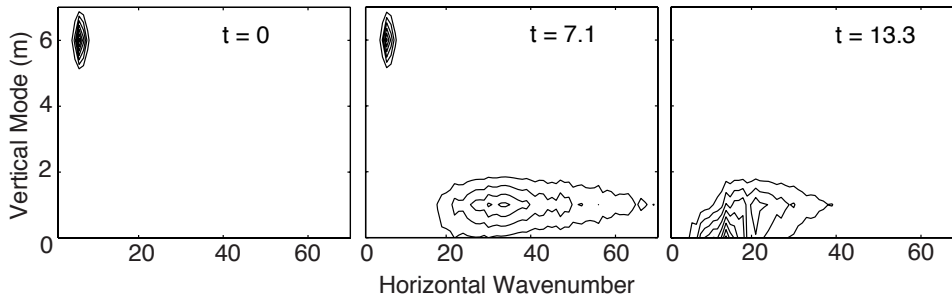
Fig. 9.11 Idealized baroclinic lifecyle, similar to that in Fig. 9.8, but with enhanced stratification of the basic state in the upper domain, representing the oceanic thermocline.

across 2000 km, a horizontal buoyancy gradient of about 2×10^{-9} s^{-2} (using the simple equation of state $\rho = \rho(1 - \beta_T \Delta T)$ where $\beta_T = 2 \times 10^{-4}$ K^{-1}) and a shear of about 2 cm s^{-1} over the upper 1 km of ocean. Then, using (9.69), we can estimate a typical eddy velocity scale as

$$v'_\psi \sim \frac{L_\mathrm{e}}{L_\mathrm{d}} \overline{u} \approx 4\overline{u} \approx 8 \, \mathrm{cm \, s^{-1}}, \tag{9.74}$$

implying, as we noted earlier, an EKE that is an order of magnitude larger than the mean kinetic energy. Associated with this are typical temperature perturbations whose magnitude we can estimate using (9.66) or (9.67) as being about 2 K. These estimates are comparable to those observed in mid ocean, with more energetic eddies forming near intense western boundary currents where gradients are large and barotropic instability also provides a source of energy for the eddies. There is least a factor of a few uncertainty, but it is noteworthy that they are roughly comparable to the values observed.

Lifecycles

The lifecyle of a mid-oceanic baroclinic eddy will differ from its atmospheric counterpart in two main respects:

  (i) Baroclinic eddies may be advected by the mean flow into regions with quite different properties from where they initially formed.

 (ii) The nonuniformity of the stratification affects the passage to barotropic flow.

Both of these can properly only be studied by numerical means. Regarding the first, eddies will often form in or near intense western boundary currents, but then will be advected by that current into the potentially less unstable open ocean before completing their lifecyle. Regarding the second, an oceanic analog of the lifecyle illustrated in Fig. 9.8 is shown in Fig. 9.11. The main difference between this and the atmospheric case is that baroclinic instability initially leads to the transfer of energy to vertical mode one, followed by a transfer to larger horizontal scales in the barotropic mode, as illustrated schematically in Fig. 9.12.[16] If the energy is initially solely in the first baroclinic mode the cycle is more similar to the atmospheric one, but higher baroclinic modes may be more readily excited in the ocean than the atmosphere.

Figure 9.12 Energy transfer paths as a function of vertical mode and horizontal wavenumber, in a fluid with an oceanic stratification — i.e., with a thermocline. BT is the barotropic mode, and BC refer to the baroclinic modes.
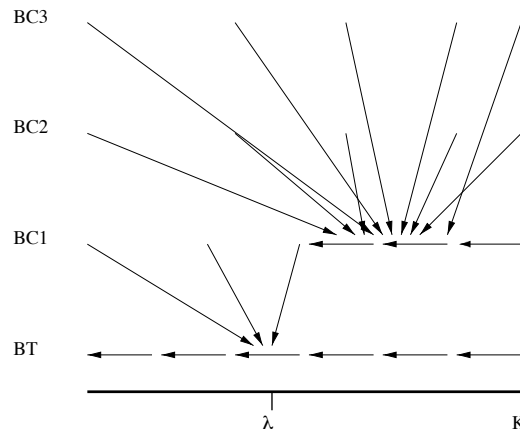
Notes

1 Rhines (1975). See also Holloway and Hendershott (1986) and Vallis and Maltrud (1993).

2 Adapted from Vallis and Maltrud (1993).

3 Simulation kindly performed by K. S. Smith.

4 Quasi-geostrophic turbulence was introduced by Charney (1971). Salmon (1980) and Rhines (1977) provided much of the two-level phenomenology discussed here. Some laboratory experiments are reviewed by Read (2001).

5 Adapted from Salmon (1980)

6 Lindborg (1999) concluded that the data was consistent with a forward cascade of enstrophy between wavelengths of a few thousand kilometers and a few hundred kilometers. Boer and Shepherd (1983) also found a k^{-3} spectrum at similar scales. At scales smaller than than 100 km or so the spectrum is shallower. This may be due to nongeostrophic effects, for example a forward cascade of energy associated with gravity wave breaking or perhaps a two-dimensional inverse cascade of energy with a energy source at very small scales due to convection.

7 Larichev and Held (1995) and Held and Larichev (1996). See Spall (2000) for an oceanic extension.

8 Atmospheric energetics, and atmospheric observations in general, are described by Peixoto and Oort (1992). For the oceanic case, see Wyrtki et al. (1976), Richardson (1983) and Stammer (1997). Related arguments concerning eddy magnitudes were given by Gill et al. (1974).

9 This does not address the issue as to *why* the Rhines scale and deformation radius are similar. See chapter 12.

10 Modified from Smith and Vallis (2001).

11 Adapted from Simmons and Hoskins (1978).

12 The theory of this has been developed by Farrell and Ioannou (1996), and ref-

erences therein. These authors have emphasized that exponential growth is the exception, not the rule, in the real world.

13 The realization that the ocean is, literally, a sea of eddies came to fruition as a result of the bilateral US-USSR POLYMODE project in the 1970s. See Robinson (1984).

14 From Chelton et al. (1998).

15 Stammer (1997).

16 Fu and Flierl (1980) and Smith and Vallis (2001) examined this issue in more detail, both analytically and numerically. Fig. 9.12 is adatpted from these papers. Barnier et al. (1991) and Hua and Haidvogel (1986) looked at the role of high baroclinic modes in oceanic eddies and geostrophic turbulence.

CHAPTER 10

Turbulent Diffusion and Eddy Transport

THE TRANSPORT OF FLUID PROPERTIES BY UNSTEADY MOTION, that is, the way in which the properties of a fluid may be carried from one location to another by waves and turbulence, is one of the most important topics in geophysical fluid dynamics. It may be the dominant transport in a fluid, greatly exceeding that of the mean flow — in the atmosphere, for example, heat is transferred polewards primarily by the action of unsteady weather systems, not by the much weaker time-mean flow. Thus, we might seek to *parameterize* such transport in terms of the mean flow; unfortunately, no general theory exists for such transport, for indeed such a theory would amount to a theory of turbulence. In the absence of this, we focus our attention in this chapter on the theory (such as it is) and practice of *turbulent diffusion*. In such models, the turbulent transport is often simply related to the gradient of the mean flow, and it is the simplicity of the resulting expressions that has led to their wide adoption in areas as different as turbulent pipe flow, atmospheric boundary layer transport and large-scale ocean modelling. These models are, by and large, rational, simple and tractable — a blend of heuristic reasoning and elementary mathematics, the latter needed to ensure that certain basic requirements (conservation laws, for example) of a physical process are captured by a parameterization. However, just like other turbulent closures, they rely on rather physical assumptions that cannot be rigorously justified. In the first part of the chapter we consider turbulent diffusion from a general standpoint, and then specialize our discussion to geofluids, and in particular to large-scale transport by baroclinic eddies. Those readers with some background in the former may choose to skip ahead to section 10.6.

10.1 DIFFUSIVE TRANSPORT

We begin with a brief discussion of the diffusion equation itself, to wit

$$\frac{\partial \phi}{\partial t} = \kappa \nabla^2 \phi, \tag{10.1}$$

where κ is a constant, positive, scalar diffusivity and the tracer ϕ is a scalar field. We expect that an initially concentrated blob of tracer would spread out — it would diffuse — and thus small parcels of tracer are transported. How quickly does this occur, or, put another way, is there an effective diffusive transport velocity?

If the rate of spreading becomes independent of the initial conditions then, purely from dimensional considerations, the spreading can depend only on the diffusivity and time itself and we can write

$$\overline{X^2} = \alpha \kappa t \tag{10.2}$$

where $\overline{X^2}$ is the mean square displacement, t is time and α is a nondimensional constant. Let us quantify this with an explicit calculation. If ϕ is interpreted as the density of markers of fluid parcels, then the mean square displacement of the markers is given by (in three dimensions)

$$\overline{X^2} = \frac{\int_0^\infty r^2 \phi r^2 \, dr}{\int_0^\infty \phi r^2 \, dr} \tag{10.3}$$

where the denominator, the total amount of tracer present, is a constant and we have assumed a spherically symmetric distribution of tracer. Using (10.1) we find

$$\frac{d}{dt} \int_0^\infty r^2 \phi r^2 \, dr = \kappa \int_0^\infty r^2 \frac{1}{r^2} \frac{\partial}{\partial r} \left(r^2 \frac{\partial \phi}{\partial r} \right) r^2 \, dr = 6\kappa \int_0^\infty \phi r^2 \, dr \tag{10.4}$$

after a couple of integrations by parts. Thus

$$\frac{d}{dt} \overline{X^2} = 6\kappa \tag{10.5}$$

and because κ is a constant we have the important result that

$$\boxed{\overline{X^2} = 6\kappa t}. \tag{10.6}$$

In two dimensions the equivalent calculation begins with

$$\overline{X^2} = \frac{\int_0^\infty r^2 \phi r \, dr}{\int_0^\infty \phi r \, dr} \tag{10.7}$$

and using the diffusion equation we find

$$\frac{d}{dt} \int_0^\infty r^2 \phi r \, dr = \kappa \int_0^\infty r^2 \frac{1}{r} \frac{\partial}{\partial r} \left(r \frac{\partial \phi}{\partial r} \right) r \, dr = 4\kappa \int_0^\infty \phi r \, dr. \tag{10.8}$$

Thus we obtain

$$\overline{X^2} = 4\kappa t. \tag{10.9}$$

Finally, in one dimension (i.e. spreading along a line) it is easy to show that

$$\overline{X^2} = 2\kappa t. \tag{10.10}$$

10.1.1 An explicit example

We gain gain a little more intuition about what the above calculations mean by considering the case in which the initial tracer distribution is a delta function at the origin. If the total amount of tracer is unity, then in three dimensions at subsequent times the tracer is given by the distribution

$$\phi(r,t) = \frac{1}{8(\pi\kappa t)^{3/2}} \exp(-r^2/4\kappa t), \tag{10.11}$$

as may be checked by substitution back into the equation of motion. (See problem 10.1.) The distribution clearly broadens with time, and the mean square distance from the origin is given by

$$\overline{X^2} = \int_0^\infty \frac{4\pi r^2}{8(\pi\kappa t)^{3/2}} \exp(-r^2/4\kappa t)\, dr = 6\kappa t, \tag{10.12}$$

as in (10.6). The important point is that the mean distance travelled by a particle during a time interval t is proportional to the square root of that time interval. This is, of course, redolent of a random walk, which brings us to the subject of turbulent diffusion.

10.2 TURBULENT DIFFUSION

Fluids differ from solids in that they can transport properties by advection — thus, heat is transferred polewards in the atmosphere by air motion, warm parcels of air moving polewards and cool parcels of air moving equatorwards. Turbulent fluid motion differs from laminar fluid motion in that such advective transport may be greatly enhanced by the seemingly random motion of the fluid, the net transport being much larger than that which would be effected by the time-mean fluid motion alone. Indeed, to continue the atmospheric example, away from the tropics the polewards transport of heat in the atmosphere is largely effected by way of the (large-scale) turbulent transfer of heat in mid-latitude weather systems. Of course, such transfer *is* simply by advection, and if we could explicitly calculate the motion of the fluid parcels we could explicitly calculate the transport. However, turbulent transport is both very complicated and sensitive to the initial conditions, so that any hope of performing such a calculation in a real situation is often forlorn one.

Turbulent transport is most important in *inhomogeneous* situations, because it is the divergence of the transport that is important and the mean divergence is non-zero only if there is inhomogeneity. The theories of chapters 8 and 9 do not lend lend themselves to an easy extension to inhomogeneous flow, and we turn to a slightly more empirical approach.[1]

10.2.1 Simple theory

Let us consider how fluid markers are transported in a statistically steady, homogeneous, turbulent flow. The markers are introduced at the origin $x = y = z = 0$ at $t = 0$; we may create an ensemble of such markers by performing many such tracer release

A Random Walk

Here we give an elementary derivation of the most basic result in random walk theory, the relationship of the mean-square displacement to the number of steps taken.[2] A loose analogy is that of drunkards staggering randomly from here to there, with no correlation between their successive steps. After any number of steps, the *mean* displacement the drunkards is zero, but we expect their *root-mean-square* displacement to increase: this is because drunkards independently thrown out of the same bar will generally wander off in different directions (which is why the mean displacement is zero), but after some time most of them will indeed end up some distance away.

For simplicity consider steps, s_n, each with random orientation but equal magnitude, s. The displacement after n steps is related to the displacement after $n-1$ steps by

$$D_n = D_{n-1} + s_n. \tag{R.1}$$

so that the amplitude of D_n, namely D_n, is given by

$$
\begin{aligned}
D_n^2 &= (D_{n-1} + s_n) \cdot (D_{n-1} + s_n) \\
&= D_{n-1}^2 + s^2 + 2 D_{n-1} \cdot s_n
\end{aligned}
\tag{R.2}
$$

Taking an ensemble average over many realizations gives

$$\overline{D_n^2} = \overline{D_{n-1}^2} + s^2 \tag{R.3}$$

having used $\overline{D_{n-1} \cdot s_n} = 0$, because each step is random.

Now, $D_0 = 0$, so that $\overline{D_1^2} = s^2$, $\overline{D_2^2} = 2s^2$ and so on. Thus, using (R.3) to proceed inductively, we have

$$\overline{D_n^2} = ns^2, \tag{R.4}$$

or

$$\boxed{\overline{D_n^2}^{1/2} = \sqrt{n}s}. \tag{R.5}$$

Thus, in a random walk the *root mean square displacement increases with the half-power of the number of steps taken.* More work is required to calculate the distribution of the random walkers, but it may be shown that in the limit of infinitesimally small steps the random walk becomes a Wiener process and the distribution becomes Gaussian, as in (10.11) (but with the exact form depending on the dimensionality of the problem), indicating a diffusive process.

experiments on different realizations of the turbulent flow, but with each flow having the same statistical properties. The question is, what is the average rate of dispersion of a single particle of fluid?

The displacement of a marker at a time t is given by

$$X(t) = \int_0^t V(t') \, dt' \tag{10.13}$$

where V is the velocity of the fluid parcel — a material velocity. [We will use upper case variables to denote material ('Lagrangian') quantities.] The mean square displacement is

$$\overline{X^2(t)} = \int_0^t dt_1 \int_0^t \overline{V(t_1) \cdot V(t_2)} \, dt_2 \tag{10.14}$$

where the overbar denotes an ensemble average, and thus $\overline{V(t_1) \cdot V(t_2)}$ is a measure of the velocity correlation between the velocities of the fluid parcels at times t_1 and t_2. That is,

$$\overline{V(t_1) \cdot V(t_2)} = \overline{v^2} R(t_2 - t_1) = \overline{v^2} R(\tau) \tag{10.15}$$

where $R(t_2 - t_1)$ is the velocity correlation function and, because the turbulence is statistically steady, this depends only on the time difference $\tau = t_2 - t_1$. Furthermore, $R(-\tau) = R(\tau)$. Thus,

$$\overline{X^2(t)} = \int_0^t dt_1 \, \overline{v^2} \int_0^t R(t_2 - t_1) \, dt_2 \tag{10.16a}$$

$$= \int_0^t d\hat{t} \, \overline{v^2} \int_{-\hat{t}}^{t - \hat{t}} R(\tau) \, d\tau \tag{10.16b}$$

changing variables to τ and $\hat{t} = t_1$ (see Fig. 10.1). We expect the velocity correlation function to fall monotonically from its initial value of unity to a value approaching zero as $\tau \to \infty$, as in Fig. 10.2, and typically, there will be some characteristic time τ_{corr} that parameterizes the behaviour of the function. In general, we cannot obtain explicit general solutions without detailed knowledge of this correlation function, but there are two interesting limits:

(i) *The short-time limit:* For small times, i.e., for $t \ll \tau_{\text{corr}}$ (and so $t_1, t_2 \ll \tau_{\text{corr}}$) the correlation function will be approximately unity and so (10.16) becomes

$$\overline{X^2(t)} \approx \int_0^t d\hat{t} \, \overline{v^2} \int_0^t d\hat{t}$$

$$= \overline{v^2} t^2 \tag{10.17}$$

Thus, the root mean square displacement increases linearly with time, and linearly with the root mean square velocity of the flow. For small times, the fluid parcel's behaviour is well correlated with that at the initial time, and so the displacement increases linearly in the direction it was initially going. Indeed, directly from (10.13) we have, for small times, $X(t) \approx V t$, which directly leads to (10.17).
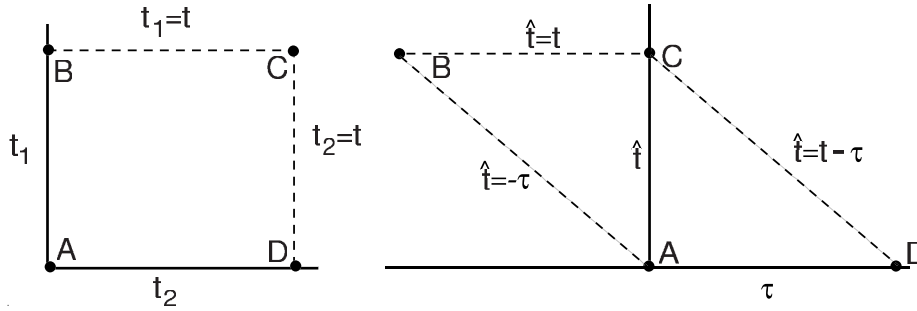
Fig. 10.1 Changes of time variables involved in (10.16) and (10.32). The original two dimensional integral is over the rectangle $ABCD$. Defining $\tau = t_2 - t_1$ and $\hat{t} = t_1$, then the area is spanned by $[\hat{t} = (0, t),\ \tau = (t - \hat{t}, -\hat{t})]$ as in (10.16), or by $[\tau = (0, t),\ \hat{t} = (0, t - \tau)]$ (i.e. ACD) plus $[\tau = (-t, 0),\ \hat{t} = (-\tau, t)]$ (i.e. ABC) in (10.32).

(ii) The long-time limit: We are now concerned with the case $t \gg \tau_{\text{corr}}$. Because the correlation function falls with time, most of the contributions to the second integrand (involving $R(\tau)$) in (10.16b) are from $\tau \leq \tau_{\text{corr}}$. Thus, without much loss in accuracy, we can replace the limits of integration by $-\infty$ and $+\infty$; that is

$$\overline{X^2(t)} \approx \int_0^t \mathrm{d}\hat{t}\, \overline{v^2} \int_{-\infty}^{\infty} R(\tau)\, \mathrm{d}\tau \tag{10.18}$$

Assuming the second integral converges, it is just a number; in fact, noting that $R(\tau) = R(-\tau)$, we may use it to *define* the correlation time τ_{corr} by:

$$\tau_{\text{corr}} \equiv \int_0^{\infty} R(\tau)\, \mathrm{d}\tau. \tag{10.19}$$

We then have the important result that

$$\boxed{\overline{X^2(t)} \approx 2\overline{v^2} t \int_0^{\infty} R(\tau)\, \mathrm{d}\tau = 2\overline{v^2}\tau_{\text{corr}} t} \;. \tag{10.20}$$

That is, for times long compared to the turbulence correlation time, the distance travelled by a fluid parcel in some time interval is proportional to the square-root of that time interval, just as for a diffusive process; this is because the fluid parcels too are largely undergoing random walks. The expression connects two quite different fluid properties: the left-hand side tells us how tracers are dispersed in a turbulent flow, a material property, whereas the right-hand side can be evaluated from the Eulerian velocity field at different times. Both the left- and right-hand sides can be directly measured, by looking at the dispersion of a dye and by measuring the velocity at successive times.

We may define a *coefficient of turbulent diffusivity* by

$$\boxed{K_{\text{turb}} = \tfrac{1}{3}\overline{v^2}\tau_{\text{corr}}} \;, \tag{10.21}$$

and then we have the result that

$$\overline{X^2(t)} = 6K_{\text{turb}}t. \tag{10.22}$$

Comparison of (10.22) with (10.6) indicates that the transport of turbulent flow, under these conditions, is like a diffusive transport, with a coefficient of diffusivity given by (10.21). [Sometimes, the numerical factors are neglected, and a diffusivity is defined by the expressions

$$K_{\text{turb}} \equiv \frac{\mathrm{d}\overline{X^2(t)}}{\mathrm{d}t} \qquad \text{or} \qquad K_{\text{turb}} \equiv \frac{1}{2}\frac{\mathrm{d}\overline{X^2(t)}}{\mathrm{d}t}. \tag{10.23}$$

These lose the exact connection with a true diffusion coefficient, but usually the turbulent diffusivity can only be estimated, anyway.]

We may define a correlation length scale equal to the approximate distance that a parcel moves, on average, in a Lagrangian correlation time. Thus

$$l_{\text{corr}} \equiv v_{\text{rms}}\tau_{\text{corr}} \tag{10.24}$$

where $v_{\text{rms}} = (\overline{v^2})^{1/2}$, whence

$$\boxed{K_{\text{turb}} = \tfrac{1}{3}v_{\text{rms}}l_{\text{corr}}}. \tag{10.25}$$

In most situations, the numerical coefficient (1/3 here) cannot be trusted because a real turbulent flow is unlikely to satisfy the restrictions of stationarity and homogeneity that we have imposed. Nevertheless, a relationship similar to (10.25) — that a turbulent diffusivity is proportional to an r.m.s. turbulent velocity and a decorrelation length-scale, is the foundation for semi-empirical *mixing length* theories that we discuss in section 10.4.

The simple relationships between the mean-square displacement, the Lagrangian time-scale, the mean square velocity and the eddy diffusivity allows the diffusivity to be computed from the statistics of particle trajectories. Thus, suppose that a cluster of floats is released into the ocean, or some balloons are released in the atmosphere. If neutrally buoyant, these instruments then essentially become labeled fluid particles, and one may compute K_{turb} directly from the dispersion of the cluster using (10.22). If it is possible to measure their root-mean-square velocity, then one may use (10.21) to estimate the diffusivity from this and the Lagrangian correlation timescale.

10.2.2 * A slight generalization

We now consider the correlation between the different components of the displacement in anisotropic, but still homogeneous, flow.[3] The displacement of a fluid particle is

Figure 10.2 Schematic of a velocity correlation function in turbulent flow with correlation time $\tau_{\text{corr}} = \mathcal{O}(1)$. For small times, $\tau \ll \tau_{\text{corr}}$, $R(\tau) \approx 1$. For large times, $\tau \gg \tau_{\text{corr}}$, $R(\tau) \ll 1$. We may define the correlation time by $\tau_{\text{corr}} = \int_0^\infty R(\tau)\,d\tau$.
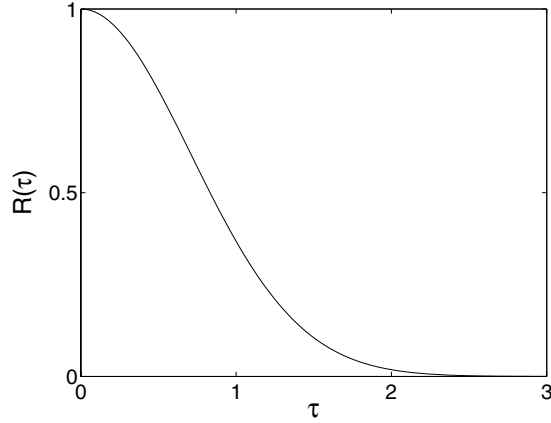
given by (10.13), and this is a random vector. Thus, generalizing (10.14), we may define the fluid particle displacement covariance tensor by

$$D_{ij}(t) = \overline{X_i(t)X_j(t)} = \int_0^t \int_0^t \overline{V_i(t_1)V_j(t_2)}\,dt_1\,dt_2. \tag{10.26}$$

where the velocity denoted by V_i is the i'th component of the velocity of a fluid element. For small times, $X_i(t) \approx v_i(\boldsymbol{a},0)t$, where $v_i(\boldsymbol{a},0)$ is the fluid velocity at the parcel's initial position, $\boldsymbol{a}$, and we obtain

$$D_{ij}(t) \approx \overline{v_i(\boldsymbol{a},0)v_j(\boldsymbol{a},0)}t^2. \tag{10.27}$$

If the flow is statistically steady and homogeneous the average of any quantity has no spatial or temporal dependence and so

$$D_{ij}(t) = A_{ij}t^2, \tag{10.28}$$

where the tensor $A_{ij} = \overline{v_i v_j}$ has constant entries, and this is a slight generalization of (10.17).

The velocity covariance of a fluid parcel at times t_1 and t_2 is, as before, function only of the time difference $t_1 - t_2$ and so it must have the form

$$\overline{V_i(t_1)V_j(t_2)} = \left(\overline{v_i^2}\,\overline{v_j^2}\right)^{1/2} R_{ij}(t_2 - t_1), \tag{10.29}$$

Except in the case of isotropic flow $R_{ij}(\tau) \neq R_{ij}(-\tau)$, but we do have

$$R_{ij}(\tau) = R_{ji}(-\tau). \tag{10.30}$$

Now, to obtain a generalization of (10.20), we first use (10.29) in (10.26) to obtain

$$D_{ij}(t) = \left(\overline{v_i^2}\,\overline{v_j^2}\right)^{1/2} \int_0^t \int_0^t R_{ij}(t_2 - t_1)\,dt_1\,dt_2. \tag{10.31}$$

If we change variables to $\tau = t_2 - t_1$ and $\hat{t} = t_1$ we obtain[4]

$$D_{ij}(t) = \left(\overline{v_i^2}\,\overline{v_j^2}\right)^{1/2} \left(\int_0^t \mathrm{d}\tau \int_0^{t-\tau} \mathrm{d}\hat{t}\, R_{ij}(\tau) + \int_{-t}^0 \mathrm{d}\tau \int_{-\tau}^t \mathrm{d}\hat{t}\, R_{ij}(\tau)\right), \quad (10.32)$$

(see Fig. 10.1) and using (10.30) this becomes

$$D_{ij}(t) = 2\left(\overline{v_i^2}\,\overline{v_j^2}\right)^{1/2} \int_0^t \mathrm{d}\tau \int_0^{t-\tau} \mathrm{d}\hat{t}\, \widehat{R}_{ij}(\tau), \qquad (10.33)$$

where $\widehat{R}_{ij} = (R_{ij} + R_{ji})/2$. This order of integration enables us to perform the integration over $\hat{t}$, giving

$$D_{ij}(t) = 2\left(\overline{v_i^2}\,\overline{v_j^2}\right)^{1/2} \int_0^t (t - \tau)\widehat{R}_{ij}(\tau)\,\mathrm{d}\tau. \qquad (10.34)$$

For long times, i.e., for $t \gg \tau_{\mathrm{corr}}$, the upper limit of the integration may be taken to be infinity, again because the contributions to the integrand from $\widehat{R}_{ij}(\tau)$ all come from small τ. Furthermore, we expect that for large t

$$\int_0^\infty t\,\widehat{R}_{ij}(\tau)\,\mathrm{d}\tau \gg \int_0^\infty \tau\,\widehat{R}_{ij}(\tau)\,\mathrm{d}\tau. \qquad (10.35)$$

because $R_{ij}(\tau)$ is only non-negligible for small τ, and $t \gg \tau$ in this range. Thus we finally obtain a generalization of (10.20) for the displacement covariance of two components of the displacement, namely

$$D_{ij} = 2\left(\overline{v_i^2}\,\overline{v_j^2}\right)^{1/2} t \int_0^\infty \widehat{R}_{ij}(\tau)\,\mathrm{d}\tau. \qquad (10.36)$$

The integral is a tensor with constant entries, analogous to the turbulent decorrelation timescale of (10.19). Then, with $\tau_{ij} \equiv \int_0^\infty \widehat{R}_{ij}(\tau)\,\mathrm{d}\tau$, the corresponding turbulent diffusivity is

$$K_{ij} = \tfrac{1}{3}\left(\overline{v_i^2}\,\overline{v_j^2}\right)^{1/2} \tau_{ij}. \qquad (10.37)$$

10.2.3 Discussion

We have shown that, for sufficiently long times, the distance travelled by a fluid parcel in some time is proportional to the square root of that time, just as for a diffusive process and just as for a random walk. The motion of our fluid parcel is analogous to that of a dust particle undergoing Brownian motion — both are continually buffeted and undergo random walks as a result. Still, it may appear that the usefulness of our results is limited by the assumptions of stationarity and homogeneity — it is well-nigh impossible in nature to produce a statistically stationary, homogeneous turbulent flow, because statistical stationarity implies there must be an energy source and this, as well as the presence of boundaries, militate against homogeneity. However, we should not be so pessimistic, on two counts:

(i) The above results may be directly applied to flows that are homogeneous in one direction.[5]

(ii) Often, a flow will *not* be homogeneous in any direction. However, if the *statistics* of the eddy motion vary on a space scale that is longer than $v_{rms}\tau_{corr}$, then the eddy transport properties may be determined by a local theory. For example, the size of the eddy diffusivity is then determined by $D_t \sim v_{rms}l_{corr}$ where the parameters, and so the diffusion coefficient, vary, but only on a scale longer than the energy-containing scale.

The essential results of this section then lie in equations (10.20), (10.21) and (10.25): that the dispersion of a fluid particle in a turbulent flow is *diffusive* in nature, and that the turbulent diffusivity is proportional to the product of the root-mean-square velocity and the correlation length.

10.3 TWO-PARTICLE DIFFUSIVITY

Now consider the problem of determining the mutual separation of two fluid parcels. The problem differs from the one-particle problem, because the separation of the particles itself will affect the rate of increase of the separation. In the one-particle problem in homogeneous flow, the position of the particular tagged fluid particle plays no direct role in determining its rate of spreading from its initial condition — any one position is the same as any other. But if two particles are close together, they may be swept away together by some large eddy, without affecting their mutual separation whereas two particles that are widely separated will undergo largely uncorrelated motion. Thus, we identify two regimes:

(i) A regime in which the separation of the particles is greater than the scale of the largest eddies. In this case, each particle is undergoing a random walk that is effectively uncorrelated with that of the other particle.

(ii) A regime in which the separation of the particles is less than the energy-containing scale of the motion. In this case, the eddies that most contribute to the two-particle separation are those that are comparable in scale to the separation itself.

If we attempt to apply the Taylor analysis *ab initio* we evidently have, by analogy to (10.13)

$$Y(t) = X_1(0) - X_2(0) + \int_0^t [V_1(t') - V_2(t')]\,dt' \tag{10.38}$$

and a mean square separation of

$$\overline{Y^2(t)} = \overline{(X_1(0) - X_2(0))^2} + \int_0^t dt_1 \int_0^t [W_1(t_1) \cdot W_2(t_2)]\,dt_2 \tag{10.39}$$

where $W(t) = V_1(t) - V_2(t)$. However, it is now difficult to proceed much further. The problem is that we cannot write

$$\overline{W(t_1) \cdot W(t_2)} = \overline{w^2}\,R(t_2 - t_1) \tag{10.40}$$

because the correlation will depend on the initial separation of the particles as well as the time since then. Thus, the diffusivity will depend on both time and the initial particle separation, and the results analogous to those of the single-particle diffusivity cannot easily be recovered. However, we can make some progress by separately considering the two above-mentioned regimes.

10.3.1 Large particle separation

This case is analogous to the single-particle case. The particle separation is given by

$$Y(t) = X_1(t) - X_2(t) \tag{10.41}$$

so the mean square separation is

$$\overline{Y^2(t)} = \overline{X_1(t)^2} + \overline{X_2(t)^2} - \tag{10.42}$$

For long times, the last term is zero because the motion of the two particles is uncorrelated. Furthermore, each of the first two terms is given by (10.20) or (10.22), so that the mean separation varies as

$$\overline{Y^2(t)} = 4\overline{v^2}\tau_{\text{corr}}t \tag{10.43}$$

and the rate of separation, for large t, is given by

$$\frac{d\overline{Y^2(t)}}{dt} = 4\overline{v^2}\tau_{\text{corr}} = 12K_{\text{turb}}. \tag{10.44}$$

Thus, the relative diffusion is twice that of the single-particle process, in the limit that the particles are separated by an amount larger than the largest eddies.

10.3.2 Separation within the inertial range

How do fluid parcels whose separation is at inertial scales behave relative to each other?[6] Suppose that two particles are tagged, and that their separation is greater than the viscous scale but smaller than the scales of the largest eddies — that is, the separation lies within the inertial range of the flow. Then, the rate of separation of the two particles can depend only on two quantities, the separation itself and properties of the inertial range, meaning (in three dimensions) the energy flux, ε, through the system. It cannot depend on the time itself, because this would imply that the subsequent rate of particle separation depends on the history of how the particles came to their current positions. Thus we can write

$$\frac{d\overline{L}^2}{dt} = g(\overline{L}, \varepsilon) \tag{10.45}$$

where $\overline{L} \equiv \overline{Y(t)^2}^{1/2}$. Dimensional analysis then gives

$$\frac{d\overline{L}^2}{dt} = \varepsilon^{1/3}\overline{L}^{4/3}. \tag{10.46}$$

where A is a nondimensional constant, and this is known as 'Richardson's four-thirds law'. We can also integrate this to give

$$\overline{L}^2 \sim \varepsilon t^3. \tag{10.47}$$

Another way of deriving (10.46) is to suppose that the separation obeys the diffusive law

$$\frac{\mathrm{d}\overline{L}^2}{\mathrm{d}t} = K_{\text{turb}} \tag{10.48}$$

where K_{turb} is a turbulent diffusivity that is *a function of the separation itself*. This is because the farther apart the eddies are, the larger the scale of the eddies that can move the two particles independently, rather than just sweeping them along together. An estimate of the diffusivity is then

$$\mathscr{K}_{\text{turb}} \sim vl \tag{10.49}$$

where v is the characteristic velocity of an eddy of scale l, and $l \sim \overline{L} = \overline{Y^2}^{1/2}$. Using the inertial range scaling $v \sim (l\varepsilon)^{1/3}$ this is

$$\mathscr{K}_{\text{turb}} \sim \varepsilon^{1/3}\overline{L}^{4/3}, \tag{10.50}$$

and so (10.48) becomes

$$\frac{\mathrm{d}\overline{L}^2}{\mathrm{d}t} \sim \varepsilon^{1/3}\overline{L}^{4/3}, \tag{10.51}$$

as before. Of course, dimensional consistency demands that we obtain the same result, but the derivation is intuitive and the estimate of the two-particle diffusivity, (10.50), is useful — that the eddy diffusivity governing the separation of two fluid parcels goes as the 4/3 power of their root mean square separation. If the particle separation is greater than the scale of the largest eddies in the system, l_{max}, then

$$K_{\text{turb}} \sim v(l_{\text{max}})l_{\text{max}} \sim \varepsilon^{1/3}l_{\text{max}}^{4/3} = \text{constant}. \tag{10.52}$$

The two-particle separation then proceeds as a conventional random walk or diffusive process, with the mean square separation increasing linearly with time.

Diffusion in two-dimensional flow

In two dimensions the turbulent diffusivity will differ depending on whether the two-particle separation is in the energy inertial range or in the enstrophy inertial range. In the energy inertial range the scaling is the same as in the three-dimensional case, but in the enstrophy inertial range the rate of separation will depend on the enstrophy cascade rate, η, and the separation itself. Dimensional analysis then leads to

$$\frac{\mathrm{d}\overline{L}^2}{\mathrm{d}t} = B\eta^{1/3}\overline{L}^2, \tag{10.53}$$
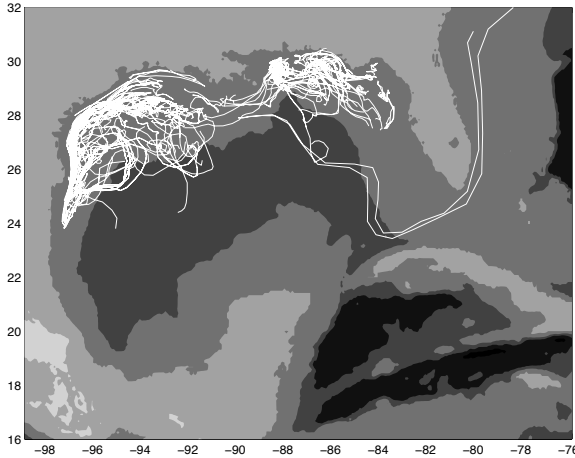
Figure 10.3 Trajectories of surface drifters in the Gulf of Mexico, each truncated to produce paths of just 25 days. The drifters were released as part of 'SCULP' — the Surface CUrrent and Lagrangian drift Program.[7]

where B is a nondimensional constant. This integrates to

$$\overline{L}^2 = \overline{L(0)}^2 \exp(B\eta^{1/3}t), \tag{10.54}$$

or $\overline{Y^2(t)} = \overline{Y^2(0)}\exp(B\eta^{1/3}t)$. Thus, the rate of separation is *exponential* in the enstrophy inertial range, a result unique to two-dimensional turbulence. Similarly, using $v \sim \eta^{1/3}l$, the turbulent diffusivity is given by

$$K_{\text{turb}} \sim \eta^{1/3}\overline{L}^2. \tag{10.55}$$

A geophysical example

These ideas are well illustrated by analysing the trajectories of surface drifters in the Gulf of Mexico. The drifters are free-moving buoys which float about a half meter below the surface and which thus act as imperfect fluid markers — imperfect because they cannot follow the full three-dimensional motion of water parcels. Nevertheless, the motion at these scales can be expected to be quasi-geostrophic and nearly horizontal, so the associated error will be small. The drifters are tracked by satellite and their trajectories, proxies for the motion of fluid parcels, are shown in Fig. 10.3. The two-particle, or two-drifter, separation is illustrated in Fig. 10.4 and two regimes may be discerned. In the first, the pair separations grow approximately exponentially in time, with an e-folding time of 2 days, consistent with motion within an enstrophy inertial range using (10.54). The second regime is charaterized by a power law growth, proportional to $t^{2.2}$, somewhat slower than the t^3 separation expected for an energy inverse cascade using (10.47). The boundary for the two regimes occurs at about 75 km, which is similar to the first deformation radius. Note that no late-time diffusive regime (where the dispersion goes like $t^{1/2}$) is observed, suggesting that there exist long-time drifter correlations; these correlations arise because the separation of the drifters is never significantly larger than the energy-containing scale of the eddies themselves.

   In the atmosphere similar exponential separation of pairs of drifting balloons in the

Figure 10.4 Relative dispersion (the mean square separation) for 140 drifter pairs as a function of time. The analysis utilizes all drifter pairs which come within 1 km of each other during their lifetimes.
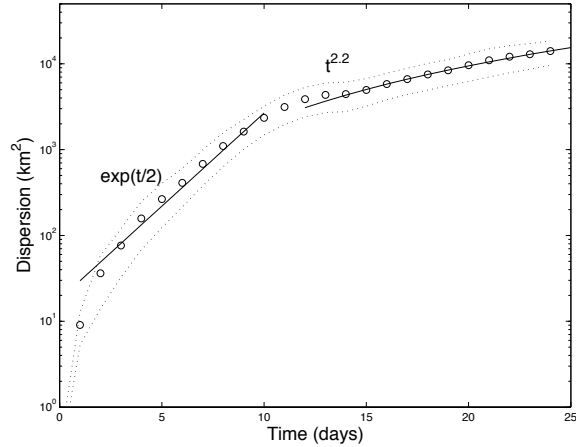
stratosphere at scales of less than 1000 km has been seen, consistent with an enstrophy inertial range. Evidence of a t^3 separation at larger scales, consistent with an energy inverse cascade, has been less forthcoming.[8]

10.4 MIXING LENGTH THEORY

The above discussion of the previous two sections deals with the dispersion of marked fluid parcels. For practical reasons, we would like to be able to represent the turbulent transport of a fluid property in an Eulerian form. For definiteness, consider the equation for a conserved quantity ϕ in an incompressible turbulent flow

$$\frac{D\overline{\phi}}{Dt} = -\nabla \cdot (\overline{v'\phi'}) + \kappa \nabla^2 \overline{\phi} \tag{10.56}$$

where κ is the molecular diffusivity and the overbar denotes some kind of averaging, perhaps a time average. We also adopt the convention that, unless noted, whenever the material derivative written as D/Dt is applied to an averaged field, the advection is by the averaged velocity only. We expect the transport of ϕ to be enhanced by the turbulent flow and, as we saw in the previous sections, in some circumstances this transport will have a diffusive nature, completely overwhelming the molecular diffusivity. Let us consider this from an Eulerian angle, and by analogy with molecular mixing.

Given the mean distribution $\overline{\phi}(x, y, z)$, let a fluid parcel be displaced from its mean position by a turbulent fluctuation. Suppose that the displaced parcel of fluid is able to carry its initial properties a distance l' before mixing with its surroundings. Then just prior to mixing with the environment the fluctuation of ϕ is given by, in the one-dimensional case,

$$\phi' = -l'\frac{\partial \overline{\phi}}{\partial x} - \frac{1}{2}l'^2\frac{\partial^2 \overline{\phi}}{\partial x^2} + \mathcal{O}(l'^3) \tag{10.57}$$

If the mean gradient if varying on a space-scale that is larger than the mixing length l',

that is if

$$\frac{|\partial\overline{\phi}/\partial x|}{|\partial^2\overline{\phi}/\partial x^2|} \gg l' \tag{10.58}$$

then we can neglect terms in l'^2 and higher. The turbulent flux of ϕ-stuff is then given by

$$F = \overline{u'\phi'} = -\overline{v'l'}\frac{\partial\overline{\phi}}{\partial x}. \tag{10.59}$$

In more than one dimension, we have

$$\boldsymbol{F} = F_i = -\overline{v'_i l'_j}\partial_j\overline{\phi} = -K_{ij}\partial_j\overline{\phi} \tag{10.60}$$

with summation over repeated indices, where $K_{ij} \equiv \overline{v'_i l'_j}$. Thus, in a two-dimensional flow,

$$F_x = -\overline{u'l'_x}\frac{\partial\overline{\phi}}{\partial x} - \overline{u'l'_y}\frac{\partial\overline{\phi}}{\partial y}. \tag{10.61}$$

The quantity K_{ij} (which we shall also write as $\boldsymbol{K}$) is known as the eddy (or turbulent) diffusivity tensor. At high Reynolds number it is a property of the flow rather than the fluid itself but, supposing that it can somehow be determined the equation for the mean value of ϕ becomes

$$\frac{\mathrm{D}\overline{\phi}}{\mathrm{D}t} = \nabla\cdot(\boldsymbol{K}\nabla\overline{\phi}) = \partial_i(K_{ij}\partial_j\overline{\phi}), \tag{10.62}$$

neglecting molecular diffusion.

Suppose that there exists a coordinate system in which the displacements in one direction (say the $\hat{x}$-direction) are not correlated with the fluctuating velocity in another, orthogonal, direction (the $\hat{y}$-direction) and for simplicity we restrict ourselves to two dimensions. Then, in that coordinate system $\boldsymbol{K}$ is symmetric and

$$\boldsymbol{K} = \begin{pmatrix} \overline{u'l'_{\hat{x}}} & \overline{u'l'_{\hat{y}}} \\ \overline{v'l'_{\hat{x}}} & \overline{v'l'_{\hat{y}}} \end{pmatrix} = \begin{pmatrix} \overline{u'l'_{\hat{x}}} & 0 \\ 0 & \overline{v'l'_{\hat{y}}} \end{pmatrix} \tag{10.63}$$

The tensor may then, if needs be, be rotated to a conventional Cartesian coordinate system, but it will remain a symmetric tensor. In isotropic flow the two diagononal entries are equal and the equation of motion is,

$$\frac{\mathrm{D}\overline{\phi}}{\mathrm{D}t} = \nabla\cdot(K\nabla\overline{\phi}), \tag{10.64}$$

which is identical to the equation with molecular diffusion, save that the eddy diffusivity, K, is different from the molecular diffusivity. To the extent, then, that K_{ij} is a symmetric tensor with constant entries, then the turbulence acts like an enhanced diffusion. If the flow is homogeneous, then K does not spatially vary.

10.4.1 Requirements for turbulent diffusion

Turbulent diffusion evidently seems to be a tractable and rational approach for param-eterizing the effects of turbulent transport.[9] However, the underlying assumptions are not always satisfied and the derivation itself is rather heuristic, and turbulent diffusion is in no way a fundamental solution to the turbulence closure problem. Nonetheless, it can be an extremely useful parameterization in the appropriate circumstances, these being that, ideally,

(i) There should be a scale separation between the mean gradient and the maximum mixing length, and the mixing length and decorrelation time-scale should be well-defined;

(ii) The diffused property ϕ should be a semi-materially conserved variable; that is, materially conserved except for the effects of item (iii);

(iii) The diffused property ϕ should be able to *mix* with its environment.

These are all largely self-evident from the derivation, but items (ii) and (iii) deserve more discussion.

Conservation of tracer

We assumed that a parcel of fluid carries its value of ϕ a distance, on average, equal to its mixing length before irreversibly mixing with its environment; this assumption is necessary in order that one may write $\phi' = -l' \partial\phi/\partial x$. If ϕ is not materially-conserved over this scale other terms enter this formula. In particular, momentum is affected by the pressure force, and so is not normally a good candidate for turbulent diffusion al-though it was, in fact, momentum to which Ludwig Prandtl originally applied such a theory, and in some boundary layer applications this may be appropriate. Using mo-mentum is also complicated because it is a vector and so its eddy diffusivity tensor is fourth order, although if the flow is isotropic many of its entries can be simplified by symmetry considerations. Potential vorticity is better candidate, because it is a true ma-terial invariant, save for dissipative terms, and in large-scale geophysical flows potential vorticity also contains most of the information about the flow. Note that there is no *ab initio* requirement that the tracer be passive, and if it is not then its turbulent transport will of course affect the flow itself.

Mixing and turbulent cascades

If a parcel cannot mix with its surroundings, then turbulent mixing cannot take place at all. Instead, we then have what might be called turbulent stirring and if ϕ were, say, a dye then it would merely become threaded through the environment, producing streaks and swirls of colour rather than a truly mixed fluid. As another example, let ϕ be temperature and suppose that it has mean gradient, so that temperature falls in the direction of increasing y. Now, we intuitively expect that turbulence can be a much more efficient transporter of heat than molecular diffusion. However, if a displaced parcel of fluid does not mix with or assume the value of its new environment at some stage, then there will be no correlation between the velocity producing the displacement

and the value of the fluctuating quantity ϕ'. To see this, suppose that an eddy causes parcels to be displaced from their mean positions, as in Fig. **??**. If a displaced parcel mixes with its surroundings, then a correlation will develop between v' and ϕ', and in the situation illustrated, we would have $\overline{v'\phi'} > 0$. However, if no mixing occurs, then the eddy simply recirculates with eddies retaining their initial values, and $\overline{v'\phi'}$ is zero because of a lack of correlation between the two quantities. Thus, it is essential that there be a degree of *irreversibility* to the flow in order that turbulent diffusion be appropriate.

Molecular diffusion is not the only process that enables an eddy to assume the value of its surroundings — a Newtonian or other relaxation back to a specified temperature may have much the same effect. Indeed, in the atmosphere a displaced parcel will be subject to a radiation field that acts in qualitatively this way. That is to say, suppose that the temperature equation is

$$\frac{\mathrm{D}T}{\mathrm{D}t} = -\lambda(T - T^*(y, z)). \qquad (10.65)$$

where the right-hand-side crudely represents radiative effects via a relaxation back to a specified profile. Then a displaced parcel will be subject to a radiative damping that is different from that at its initial position, and this will allow the the parcel to take on the value of its surroundings, and so enable turbulent diffusion to potentially occur.

For molecular diffusion to be the mechanism whereby a parcel mixes with its surroundings, the turbulence must create scales that are small enough for it to act. This means that turbulence must create a cascade of ϕ-stuff to small scales. This is entirely consistent with the notion that ϕ is a Lagrangian conserved quantity, because a scalar field satisfying

$$\frac{\mathrm{D}\phi}{\mathrm{D}t} = F[\phi] + \kappa\nabla^2\phi, \qquad (10.66)$$

(where F might represent a source of variance of ϕ) is certainly cascaded to smaller scales. The presence of a molecular diffusion does not substantially affect the requirement that ϕ be conserved on parcels, because on scales comparable to the eddy mixing length the effect of molecular diffusion is negligible. (And if it were not, perhaps because κ were extremely large or because the turbulence were anæmic, we would not be particularly interested in the turbulent transport.)

10.4.2 A macroscopic perspective

Consider turbulent diffusion from more macroscopic point of view, an in particular consider the transport of a nearly materially conserved tracer obeying

$$\frac{\mathrm{D}\phi}{\mathrm{D}t} = D \qquad (10.67)$$

where the advecting flow is incompressible and D is a dissipative process such that $\overline{D\phi} \leq 0$, and A conventional harmonic diffusision has this property, for example. By

decomposing the fields into mean and eddy components in the usual way an equation for the evolution of the tracer variance can be straightforwardly derived, namely

$$\frac{1}{2}\frac{\partial}{\partial t}\overline{\phi'^2} + \overline{\boldsymbol{v}'\phi'}\cdot\nabla\overline{\phi} + \frac{1}{2}\overline{\boldsymbol{v}}\cdot\nabla\overline{\phi'^2} + \frac{1}{2}\nabla\cdot\overline{\boldsymbol{v}'\phi'^2} = \overline{D'\phi'},\qquad(10.68)$$

and where we may assume $\overline{D'\phi'} < 0$. If the mean flow is small and if the third-order term may be neglected then in a statistically steady state we have

$$\overline{\boldsymbol{v}'\phi'}\cdot\nabla\overline{\phi} \approx \overline{D'\phi'} < 0 \qquad(10.69)$$

Therefore, on average, the flux of ϕ is downgradient in regions of dissipation, implying a positive eddy diffusivity, and a balance is maintained between the downgradient flux of ϕ (which increases the variance) and dissipation. However, it should also be clear from (10.68) that if the turbulence is not statistically stationary, or if there is a mean flow, then downgradient diffusion cannot necessarily be expected. Indeed, the transport may be upgradient in regions where the eddy variance is falling, for then we may have the balance

$$\overline{\boldsymbol{v}'\phi'}\cdot\nabla\overline{\phi} \approx -\frac{1}{2}\frac{\partial}{\partial t}\overline{\phi'^2} > 0. \qquad(10.70)$$

10.5 HOMOGENIZATION OF A SCALAR THAT IS ADVECTED AND DIFFUSED

Let us now assume that the effects of turbulence on a tracer are indeed diffusive. An important consequence of this is that, in the absence of additional forcing, there can be no extreme values of the tracer in the interior of the fluid and, in some circumstances, the diffusion will *homogenize* values of the tracer in broad regions. In this section we demonstrate and explore these properties.

10.5.1 Non-existence of extrema

Consider a tracer that obeys the equation

$$\frac{\mathrm{D}\phi}{\mathrm{D}t} = \nabla\cdot(\kappa\nabla\phi) + S \qquad(10.71)$$

where $\kappa > 0$ and the advecting velocity is divergence-free. We now show that in regions where the source term, S, is zero there can be no interior extrema of ϕ if the flow is steady.

The proof is in the form of a *reductio ad absurdum* — we first suppose there *is* an extrema of ϕ in the fluid. There will then be a surrounding surface (in three dimensions), or a surrounding contour (in two), connecting constant values of ϕ. For simplicity we consider the two-dimensional problem for which the steady flow satisfies

$$\nabla\cdot(\boldsymbol{u}\phi) = \nabla\cdot(\kappa\nabla\phi). \qquad(10.72)$$

Integrating the left-hand-side over the area enclosed by the above-mentioned contour, and applying the divergence theorem, gives

$$\iint \nabla \cdot (\boldsymbol{u}\phi) \, \mathrm{d}A = \oint (\boldsymbol{u}\phi) \cdot \boldsymbol{n} \, \mathrm{d}l = \phi \oint \boldsymbol{u} \cdot \boldsymbol{n} \, \mathrm{d}l = \phi \iint \nabla \cdot \boldsymbol{u} \, \mathrm{d}A = 0. \quad (10.73)$$

But the integral of right-hand side of (10.72) over the same area is nonzero. That is

$$\oint \kappa \nabla \phi \cdot \boldsymbol{n} \, \mathrm{d}l \neq 0. \quad (10.74)$$

if the integral surrounds an isolated extremum. This is a contradiction for steady flow. Hence, there can be no isolated extrema of a conserved quantity in the interior of a fluid, if there is any diffusion at all. The result (which applies in two or three dimensions) is kinematic, in that ϕ can be any tracer at all, active or passive. The physical essence of the result is the intergrated effects of diffusion are non-zero surrounding an extremum, and they cannot be balanced by advection.

10.5.2 Homogenization in two-dimensional flow

The non-existence of an isolated extremum in a steady fluid is quite a rigorous result, requiring minimal assumptions. However, it tells us little else about the circulation. We can obtain a more informative result if we allow ourselves to make more assumptions about the strength and nature of the diffusion, and restrict ourselves to two-dimensional advection. The steady distribution of a scalar quantity being advected by an incompressible flow is governed by

$$J(\psi, \phi) = \nabla \cdot (\kappa \nabla \phi) + S. \quad (10.75)$$

where the terms on the right-hand-side represent diffusion and source terms. Suppose that these terms are small, in the sense that the individual terms on the left-hand-side nearly balance, so that

$$|J(\psi, \phi)| \ll \frac{U\Phi}{L}. \quad (10.76)$$

This means we are in the high Peclet number limit:

$$P = \frac{UL}{\kappa} \gg 1. \quad (10.77)$$

It also suggests that the solution to (10.75) is of the form

$$\phi = G(\psi) + \mathcal{O}(P^{-1}) \quad (10.78)$$

where G is (at the moment) any function of its argument. Thus, isolines of ϕ are nearly coincident with streamlines, and

$$\nabla \phi \approx \nabla \psi \frac{\mathrm{d}\phi}{\mathrm{d}\psi}. \quad (10.79)$$

Integrating (10.72) around a mean streamline, $\psi = \psi_0$, gives

$$0 = \iint S \, dA + \oint_{\psi_0} \kappa \nabla \phi \cdot \boldsymbol{n} \, dl \qquad (10.80)$$

and using (10.79) gives

$$\iint S \, dA = -\oint_{\psi_0} \kappa \frac{d\phi}{d\psi} \nabla \psi \cdot \boldsymbol{n} \, dl \qquad (10.81)$$

Since $d\phi/d\psi$ is constant along streamlines we have

$$\frac{d\phi}{d\psi} = -\frac{\iint S \, dA}{\oint_{\psi_0} \kappa \boldsymbol{u} \cdot d\boldsymbol{l}}. \qquad (10.82)$$

This relationship determines ϕ as a function of ψ in terms of the forcing and dissipation acting on the fluid. If the fluid is both unforced and inviscid, then a steady solution pertains when ϕ is an *arbitrary* function of ψ. If the source term S is zero, but dissipation is non-zero then the denominator of (10.82) is nonzero and therefore the ϕ is uniform: ϕ has been *homogenized*.

The homogenization result also follows we choose to integrate over an area surrounded by an isoline of ϕ, ϕ_0 say. Then the advective term again vanishes and

$$0 = \iint S \, dA + \oint_{\phi_0} \kappa \nabla \phi \cdot \boldsymbol{n} \, dl. \qquad (10.83)$$

In this case the direction normal to the contour is given by $\boldsymbol{n} = (\nabla \phi / |\nabla \phi|)$ so that

$$\iint S \, dA = -\oint_{\phi_0} \frac{\nabla \phi \cdot \nabla \phi}{|\nabla \phi|} \, dl \qquad (10.84)$$

Again, if the source term is zero, ϕ must be uniform.

Interpretation

The homogenization result applies to a statisically steady flow in which the eddy transport of ϕ-stuff by the eddying motion may be parameterized diffusively, and in which there is an approximate functional relationship between mean ϕ and mean ψ. The first of these assumptions we have discussed at length in previous sections. The second requires that the diffusion must not be too strong, so that locally the tracer is conserved on fluid parcels. In the steady state the tracer is then a function of streamfunction, the same function everywhere within the closed region.

Given these assumptions, the dynamics giving rise to homogenization is transparent: integrating round a contour of ψ or ϕ the effect of the advective terms vanish; the source (S) and the diffusion must balance each other, and if there is no source term there can be no tracer gradient. Put another way, the flow will circulate endlessly and steadily around the contours of ψ, which nearly coincide with contours of ϕ. Advection cannot alter the mean value of ϕ, so diffusion smooths out gradients within the closed contours, effectively *expelling* gradients of ϕ to the boundaries and forming a plateau of

ϕ-values. Because extrema of ϕ are forbidden, the value of ϕ on the plateau cannot be a maximum or minimum: at the edge of the plateau the values of ϕ must fall somewhere, and rise somewhere else. The plateau can be a flat region etched out of a hillside, but a plateau on top of a butte is forbidden, for in that case diffusion would erode the butte down to the level of the surrounding land.

Our derivation makes no distinction between a passive scalar like a dye and an active scalar, like potential vorticity. In the latter case, dynamics will further constrain the flow because the scalar distribution must be consistent with the velocity field that advects it, and this is particularly important in the dynamics of ocean gyres.

10.6 † TRANSPORT BY BAROCLINIC EDDIES

In the next few sections we discuss the transport of fluid properties by large-scale eddies typically generated by baroclinic instability — mesoscale eddies in the ocean, and weather systems in the atmosphere. Our motivation is twofold:

(i) Mesoscale eddies in the ocean cannot be easily resolved in numerical models of its large-scale circulation, especially those used for climate simulations involving integrations of the global ocean over decades and centuries. In such models, the effects of eddies must be *parameterized* in terms of properties of the mean flow.

(ii) An understanding of this eddy-mean flow interaction is simply an essential part of the dynamics of the atmosphere and ocean.

The first of these will, ultimately, be 'solved' for us by the increasing power of computers, and indeed in the atmosphere numerical models of the general circulation already resolve most of the effects of baroclinic eddies, although for paleo-climate studies involving timescales of millions of years such eddy-resolving atmospheric models are still too slow and inefficient. We may also feel we *should* be able to predict the statistics of the climate of the ocean and atmosphere without resolving the smaller-scale eddies, since it is only the cumulative effects of such eddies that really matter. In any case, as computer power increases and we resolve mesoscale eddies, item (i) is replaced with the no less difficult problem of understanding those massive, turbulent, numerical integrations.

10.6.1 Diffusion: basic properties

A tracer evolving freely save for the effects of molecular diffusivity obeys the equation

$$\frac{\mathrm{D}\phi}{\mathrm{D}t} = \nabla \cdot (\kappa_m \nabla \phi) \tag{10.85}$$

where κ_m is the molecular diffusivity, a positive scalar quantity. Let us now consider the dynamics of the more general case

$$\frac{\mathrm{D}\phi}{\mathrm{D}t} = -\nabla \cdot \boldsymbol{F}[\phi] = \nabla \cdot \boldsymbol{K}\nabla \phi \tag{10.86}$$

where K is, in general, a second-rank tensor and $F[\phi] = -K\nabla\phi$ is the diffusive flux of ϕ. (We will omit the identifying field in square brackets if no ambiguity is so caused.) The flux has a component across the gradient of ϕ, which we will call the diagradient flux, and a component along the gradient, called a skew flux [c.f., (7.83) and (7.84)]. We will see below that these fluxes are associated with the symmetric and antisymmetric components of the diffusivity tensor, respectively, where

$$K = S + A \qquad (10.87)$$

and, using component notation,

$$S_{mn} = \frac{1}{2}(K_{mn} + K_{nm}), \qquad A_{mn} = \frac{1}{2}(K_{mn} - K_{nm}). \qquad (10.88)$$

The diagonal elements of antisymmetric tensor are zero. The transport that is effected by these two tensors has different physical characteristics, as we now discuss.

10.6.2 Diffusion with the symmetric tensor

In the simplest case of all, with an isotropic medium, K is diagonal with equal entries,

$$K = S = \begin{pmatrix} \kappa & 0 & 0 \\ 0 & \kappa & 0 \\ 0 & 0 & \kappa \end{pmatrix}, \qquad (10.89)$$

and we have the familiar

$$F = -\kappa\nabla\phi. \qquad (10.90)$$

and (10.86) has the same form as (10.85). If κ is positive, then the flux is *downgradient*, meaning that

$$F \cdot \nabla\phi < 0, \qquad (10.91)$$

even if κ is spatially nonuniform. Furthermore, such a diffusion is variance-dissipating; to see this, suppose we have the equation of motion

$$\frac{D\phi}{Dt} = \nabla \cdot (\kappa\nabla\phi). \qquad (10.92)$$

Multiplying by ϕ and integrating over the domain V gives

$$\frac{1}{2}\frac{d}{dt}\int_V \phi^2 \, dV = \int_V F \cdot \nabla\phi \, dV = -\int_V \kappa(\nabla\phi)^2 \, dV \leq 0, \qquad (10.93)$$

after an integration by parts and assuming that the normal derivative of ϕ vanishes at the boundaries — i.e. there is no flux of ϕ-stuff through the boundary. However, diffusion does preserve the first moment of the field; that is

$$\frac{d}{dt}\int_V \phi \, dV = \int_V \nabla \cdot (\kappa\nabla\phi) \, dV = 0. \qquad (10.94)$$

again assuming no flux through the boundaries.

The transport that is effected by the symmetric diffusion tensor is the diagradient diffusive flux, $\boldsymbol{F}_d$, where

$$\boldsymbol{F}_{\mathrm{d}} = -\boldsymbol{S}\nabla\phi = -S_{mn}\partial_n\phi \tag{10.95}$$

where we employ the common convention that repeated indices are summed. Suppose, for simplicity, we have the equation of motion

$$\frac{\partial\phi}{\partial t} = -\nabla\cdot\boldsymbol{F}_{\mathrm{d}} = \nabla\cdot(\boldsymbol{S}\nabla\phi). \tag{10.96}$$

This equation preserves the first moment of ϕ, provided there is no flux through the boundary. (The boundary condition that assures this is slightly more complicated than a simple vanishing of the normal derivative; it is left as a problem for the reader.) Tracer variance evolves according to

$$\frac{1}{2}\frac{\partial}{\partial t}\int_V \phi^2\,\mathrm{d}V = \int_V \phi\nabla\cdot(\boldsymbol{S}\nabla\phi) = -\int_V (\boldsymbol{S}\nabla\phi)\cdot\nabla\phi\,\mathrm{d}V \tag{10.97}$$

This can be shown to be negative or zero, provided that $\boldsymbol{S}$ is positive semi-definite, meaning that

$$\nabla\phi\,\boldsymbol{S}\,\nabla\phi = \partial_m\phi\,S_{mn}\partial_n\phi \geq 0. \tag{10.98}$$

The flux effected by such a diffusivity is then downgradient in the sense that

$$\boldsymbol{F}_d\cdot\nabla\phi = -\boldsymbol{S}\nabla\phi\cdot\nabla\phi \leq 0. \tag{10.99}$$

10.6.3 Skew-diffusion

The transport associated with the antisymmetric transport tensor is perpendicular to the gradient of ϕ, and so is neither upgradient nor downgradient. The flux is

$$\boldsymbol{F}_{\mathrm{sk}} = -\boldsymbol{A}\nabla\phi = -A_{mn}\partial_n\phi \tag{10.100}$$

and thus

$$\boldsymbol{F}_{\mathrm{sk}}\cdot\nabla\phi = -\boldsymbol{A}\nabla\phi\cdot\nabla\phi = -A_{mn}\partial_n\phi\partial_m\phi = 0, \tag{10.101}$$

where the final result follows because of the antisymmetry of $\boldsymbol{A}$ — the contraction of a symmetric tensor and an antisymmetric tensor is zero.[10] For this reason, the associated transport is known as a *skew flux* (a term applying in general to fluxes that are along-gradient) or a *skew diffusion* (when those fluxes are parameterized using an antisymmetric diffusivity). It follows from this that if a tracer obeys

$$\frac{\partial\phi}{\partial t} = \nabla\cdot(\boldsymbol{A}\nabla\phi), \tag{10.102}$$

then the tracer variance is conserved. This may be verified by multiplying this equation by ϕ and integrating by parts, assuming that the flux vanishes at the boundaries. That is, *a skew diffusion has no effect on the variance of the skew-diffused variable.* One other

familiar physical process shares these properties, and that is advection by a divergence-free flow. A skew-diffusion is physically equivalent to such an advection in that the divergence of a skew-diffusive flux is the same as the divergence of an appropriately chosen advective flux. We proved this in section 7.3.4, but let us look at it again from the point of view of diffusion.

We define an advective flux of a tracer ϕ to be a flux of the form

$$\boldsymbol{F}_{\text{ad}} = \widetilde{\boldsymbol{v}}\phi \tag{10.103}$$

where $\widetilde{\boldsymbol{v}}$ is a divergence-free vector field. The divergence of the flux is just

$$\nabla \cdot \boldsymbol{F}_{\text{ad}} = \nabla \cdot (\widetilde{\boldsymbol{v}}\phi) = \widetilde{\boldsymbol{v}} \cdot \nabla\phi. \tag{10.104}$$

The field $\widetilde{\boldsymbol{v}}$ is a *pseudo-velocity* or a *quasi-velocity* — it acts like a velocity but is not necessarily the velocity of any fluid particle. Because $\widetilde{\boldsymbol{v}}$ is divergence-free, we may define a vector streamfunction $\boldsymbol{\psi}$ such that

$$\widetilde{\boldsymbol{v}} = \nabla \times \boldsymbol{\psi} \tag{10.105}$$

The field $\boldsymbol{\psi}$ is not unique: the divergence of an arbitrary function may be added to it, this divergence vanishing upon taking the curl, resulting in the same velocity field. That is, if $\boldsymbol{\psi}' = \boldsymbol{\psi} + \nabla\gamma$, then $\widetilde{\boldsymbol{v}} = \nabla \times \boldsymbol{\psi} = \nabla \times \boldsymbol{\psi}'$. The scalar field γ is known as the *gauge,* and the freedom to choose it is the gauge freedom.

The advective flux $\boldsymbol{F}_a$ is related to the skew flux $\boldsymbol{F}_{\text{sk}}$ by

$$\phi\widetilde{\boldsymbol{v}} = \phi\nabla \times \boldsymbol{\psi} = \nabla \times (\phi\boldsymbol{\psi}) - \nabla\phi \times \boldsymbol{\psi} \tag{10.106}$$

or

$$\boldsymbol{F}_{\text{ad}} = \boldsymbol{F}_{\text{r}} + \boldsymbol{F}'_{\text{sk}} \tag{10.107}$$

where $\boldsymbol{F}_{\text{r}} = \nabla \times (\phi\boldsymbol{\psi})$ is a rotational flux with no divergence, and

$$\boldsymbol{F}'_{\text{sk}} = -\nabla\phi \times \boldsymbol{\psi} \tag{10.108}$$

is a skew-flux — 'skewed' because it is manifestly orthogonal to the gradient of ϕ, i.e., $\nabla\phi \cdot \boldsymbol{F}'_{\text{sk}} = 0$. Because $\nabla \cdot \boldsymbol{F}_{\text{r}} = 0$ we have

$$\nabla \cdot \boldsymbol{F}_{\text{ad}} = \nabla \cdot \boldsymbol{F}'_{\text{sk}}. \tag{10.109}$$

However, the skew-flux $-\nabla\phi \times \boldsymbol{\psi}$ and the advective flux $\phi\nabla \times \boldsymbol{\psi}$ may have, and in general do have, different magnitudes and directions; only their divergences are equal. Furthermore, the divergence of the skew-fluxes given by (10.100) and (10.108) are the same, if $\boldsymbol{\psi}$ is properly related to the antisymmetric tensor $\boldsymbol{A}$. We have

$$\begin{aligned}
\nabla \cdot \boldsymbol{F}_{\text{sk}} &= -\partial_m(A_{mn}\partial_n\phi) \\
&= -(\partial_n\phi)(\partial_m A_{mn}) - [A_{mn}\partial_n\partial_m\phi] \\
&= -\partial_n(\phi\partial_m A_{mn}) + [\phi\partial_n\partial_m A_{mn}]
\end{aligned} \tag{10.110}$$

where the quantities in square brackets are zero as a consequence of the antisymmetry of $\boldsymbol{A}$ — a symmetric operator acting on an antisymmetric tensor is zero. But the skew flux divergence is equal to the advective flux divergence

$$\nabla \cdot \boldsymbol{F}_{\mathrm{sk}} = \nabla \cdot \boldsymbol{F}_{\mathrm{ad}} = \partial_n(\phi \widetilde{v}_n), \tag{10.111}$$

so the associated skew velocity is given by

$$\widetilde{v}_n = -\partial_m A_{mn} \tag{10.112}$$

and this is divergence-free because $\partial_n \partial_m A_{mn} = 0$. The streamfunction and the antisymmetric tensor are thus related, because

$$\widetilde{v}_n = \epsilon_{lmn} \partial_l \psi_m \tag{10.113}$$

where the latter expression is equivalent to $\widetilde{\boldsymbol{v}} = \nabla \times \boldsymbol{\psi}$, as can be verified by expanding the expression out in Cartesian coordinates. (The Levi-Civita symbol ϵ_{mnp} is such that $\epsilon_{123} = \epsilon_{231} = \epsilon_{312} = 1$, $\epsilon_{132} = \epsilon_{321} = \epsilon_{213} = -1$, and $\epsilon_{mnp} = 0$ for other combinations.) Using (10.112) and (10.113), and just a little algebra, gives

$$A_{mn} = \epsilon_{mnp} \psi_p = \begin{pmatrix} 0 & \psi_3 & -\psi_2 \\ -\psi_3 & 0 & \psi_1 \\ \psi_2 & -\psi_1 & 0 \end{pmatrix}. \tag{10.114}$$

If the antisymmetric tensor A_{mn} is known, this formula immediately provides the streamfunction for the skew velocity $\widetilde{\boldsymbol{v}}$, to within a gauge.

10.6.4 The story so far

In this chapter we are making a rather large assumption — that we can parameterize turbulent fluxes via some form of diffusive parameterization, but given that let us be reasonably careful how we do it. Thus far, we have established:

★ Any flux can be decomposed into a component across the gradient of a scalar, the diagradient flux, and a component along the gradient, the skew flux.

★ The diagradient flux is effected by a diffusion using a symmetric diffusivity tensor.

★ The skew flux is effected by a diffusion using an antisymmetric diffusivity tensor, and this is equivalent to an advection by some divergence-free velocity.

★ The diagradient diffusive flux reduces tracer variance if the diffusivity is positive, whereas the skew difffusion has no effect on it.

Let us now consider how all this is relevant to the large-scale flow in the atmosphere and ocean.

10.7 † EDDY DIFFUSION IN THE ATMOSPHERE AND OCEAN

10.7.1 Preliminaries

Consider a tracer that obeys the equation

$$\frac{\mathrm{D}\phi}{\mathrm{D}t} = \nabla \cdot (\kappa_m \nabla \phi) \tag{10.115}$$

where κ_m is the molecular diffusivity. If the advecting flow is divergence-free then the ensemble average flow obeys, neglecting the molecular diffusion,

$$\frac{\mathrm{D}\overline{\phi}}{\mathrm{D}t} = -\nabla \cdot \overline{\boldsymbol{v}'\phi'}. \tag{10.116}$$

We can imagine, for example, that we prepare the ensemble by varying the initial conditions; then, if the flow is chaotic, the realizations will differ from each other but the flow statistics will, we will assume, converge such that $\overline{\phi}$ and the other averaged quantities are well-defined. If we parameterize the eddy transport by a diffusion then

$$\boldsymbol{F} = \nabla \cdot \overline{\boldsymbol{v}'\phi'} = -\boldsymbol{K}\nabla \phi \tag{10.117}$$

where $\boldsymbol{K}$ is, in general, a second-rank tensor. If the average is a zonal average then

$$\frac{\mathrm{D}\overline{\phi}}{\mathrm{D}t} = -\frac{\partial \overline{v'\phi'}}{\partial y} - \frac{\partial \overline{w'\phi'}}{\partial z}. \tag{10.118}$$

If we are to employ a diffusive parameterization for the eddy terms these equations, the issues that then arise fall into two general camps:

(i) The overall *magnitude* of the eddy diffusivity, possibly as a function of the mean flow;

(ii) The *structure* of the diffusivity tensor, and in particular the separate structure of its symmetric and anti-symmetric parts.

10.7.2 Magnitude of the eddy diffusivity

If we restrict attention for the moment to the horizontal transfer of tracer properties, then we might write

$$\overline{v'\phi'} = -\kappa^{vy}\frac{\partial \overline{\phi}}{\partial y} - \kappa^{vz}\frac{\partial \overline{\phi}}{\partial z} \tag{10.119}$$

where κ^{vy} and κ^{vz} are components of the eddy diffusivity tensor. These components have the dimensions of a length times a velocity and, to the extent that the diffusion represents the eddying motion we expect that κ^{vy} has an approximate magnitude of

$$\kappa^{vy} \sim v'l' \tag{10.120}$$

where u' is a typical magnitude of the horizontal eddy velocity, and l' is a typical length scale of the eddies, the *mixing length* of the eddies. Larger and more energetic eddies

thus have a larger effect on the mean flow. We can estimate u' and l' in a number of reasonable ways depending on the flow conditions, as the boxed equations below will indicate.[11]

Suppose that the eddies are a consequence of baroclinic instability. Then, we may suppose that a mixing length is given by the first deformation radius, this being the characteristic horizontal scale of the instability. Such linear arguments cannot, however, determine the velocity scale because the equilibration of baroclinic waves, and hence their magnitude, depends on nonlinear processes. It is simplest to suppose that the eddy velocity is of the same approximate magnitude as the mean flow, $\overline{u}$. With these two estimates we have

$$\boxed{\kappa^{vy} \sim L_d\overline{u} = \frac{NH\overline{u}}{f}}.\tag{10.121}$$

Another way of deriving this result is by noting that

$$\kappa \sim l'^2/T \tag{10.122}$$

where T is a characteristic eddy time scale. We may suppose that this is the Eady timescale (the inverse Eady growth rate), namely $L_d/\overline{u}$. With $l' \sim L_d$ we then reproduce (10.121), which may also be written as

$$\kappa^{vy} \sim L_d\overline{u} \sim \frac{L_d^2 f_0}{\sqrt{Ri}} \sim L_d^2 Fr f_0. \tag{10.123}$$

where $Ri \equiv N^2/\Lambda^2 = N^2H^2/\overline{u}^2$ and $Fr \equiv U/(NH)$ are the Richardson and Froude numbers. Writing the estimate in this way may be useful for general scaling purposes or in primitive equation models, but note that f_0 is not a parameter in a quasi-geostrophic model.

Another plausible choice would be to suppose that the mixing length is not the deformation scale, but the overall size of the baroclinically unstable zone. The rationale for this choice is that the ultimate size of the eddies is determined by nonlinear processes, and if there is an inverse cascade then the energy containing scale is determined not by the scale of the initial instability, but it is the size to which eddies ultimately grow, perhaps by way of an inverse cascade. Supposing that the eddy magnitude is still that of the mean flow then gives the simple estimate

$$\boxed{\kappa^{vy} \sim L\overline{u}} \tag{10.124}$$

where L is the size of the baroclinic zone. If this is much larger than the deformation radius, as it might be in the ocean, then we might expect the eddy magnitude, u', also to be larger than that of the mean flow, $\overline{u}$. In that case, rather than explicitly estimating the eddy velocity via some turbulence model, one possibility would be to estimate the diffusivity from the length-scale (the domain scale, L) and a timescale, which one assumes still to be the Eady timescale $L_d/\overline{u}$ — see chapter 9 and section 9.3. This gives

$$\boxed{\kappa^{vy} \sim \frac{L^2}{(L_d/\overline{u})} = \overline{u}L_d\left(\frac{L^2}{L_d^2}\right)}.\tag{10.125}$$

This may differ significantly from (10.121) if the baroclinic zone is much larger than the deformation radius, as for example in the oceanic Antarctic Circumpolar Current. Quantitatively, the two estimates differ less in the atmosphere, where $L \sim L_\mathrm{d}$, but the scaling properties of the two, and so their respective behaviours when parameters change, still differ qualitatively.

The most rational way to choose between all these estimates is to say that our best estimate of the mixing length is that it be the (eddy) energy containing scale. If there is a vigorous inverse cascade then indeed the eddy scale need not be related to the initial instability scale. However, in the atmosphere there is little scale separation between the deformation radius and domain scale, and in the ocean the transfer of energy from deformation scale to larger scales may be rather inefficient,[12] and so eddies may be advected away from each other and away from the unstable zone, or dispersed by Rossby waves, before an inverse cascade can be organized. Thus, in both atmosphere and ocean the energy containing scales may be reasonably close to the deformation scale.

Let us suppose that there *is* an inverse cascade, with an energy cascade rate ε. If this is halted by the β-effect, then the energy containing scale L_e is given by

$$L_\mathrm{e} \sim \left(\frac{\varepsilon}{\beta^3}\right)^{1/5} \tag{10.126}$$

and the velocity at that scale is given by

$$u_\mathrm{e} \sim (\varepsilon L_\mathrm{e})^{1/3} \tag{10.127}$$

Combining these gives an estimate for the diffusivity,

$$\boxed{\kappa^{yy} \sim \left(\frac{\varepsilon^3}{\beta^4}\right)^{1/5}} . \tag{10.128}$$

This estimate may also be obtained directly by dimensional analysis, if it is assumed that the only factors determining κ are ε and β.

If the inverse cascade is halted by friction, say by a linear Ekman drag with coefficient r (such that $\partial\zeta/\partial t + \cdots = -r\zeta$), then the eddy diffusivity is found to be

$$\kappa^{yy} \sim \left(\frac{\varepsilon}{r^2}\right) . \tag{10.129}$$

To summarize: of all the above, the estimates (10.128) and (10.129) are the best justified for fully-developed geostrophic turbulence, and of these if friction is sufficiently small then (10.128) is appropriate. To apply these, we must have an estimate of ε, which might conceivably be supplied by completely independent means (for example, by considering the atmosphere as a heat engine). However, a mixing length based on the deformation radius may be preferred if the inverse cascade is inefficient and the eddies remain at the scale of the deformation radius. The component κ^{yz} may be estimated by arguments concerning the plane of parcel displacements, as we now consider.

10.7.3 Structure: the symmetric transport tensor

Diagradient diffusion is transport by a symmetric transport tensor, as in (10.95). Let us consider transfer in re-entrant channel with zonally homogeneous eddy statistics so that the averaging operator is the zonal average; we are then concerned with both the meridional and upward transport of tracer, and

$$\overline{v'\phi'} = -\kappa^{vy}\frac{\partial\overline{\phi}}{\partial y} - \kappa^{vz}\frac{\partial\overline{\phi}}{\partial z} \tag{10.130}$$

$$\overline{w'\phi'} = -\kappa^{wy}\frac{\partial\overline{\phi}}{\partial y} - \kappa^{wz}\frac{\partial\overline{\phi}}{\partial z} \tag{10.131}$$

where $\kappa^{wy} = \kappa^{vz}$ by the posited symmetry. The relationship between the various transfer coefficients will be affected both by the slope of the isopycnals, or isentropes, and the relationship of the eddy trajectories to those isentropes. In the Cartesian y–z frame the transport tensor is not necessarily diagonal (i.e. κ^{vz} and κ^{wy} may be nonzero) but locally there is always a natural coordinate system in which the diffusivity tensor is diagonal. (This is a *mathematical* result, because a symmetric matrix may always be diagonalized by a suitable rotation of axes.) In the diagonal frame we can write

$$\mathbf{S}' = \kappa_s \begin{pmatrix} 1 & 0 \\ 0 & \alpha \end{pmatrix}, \tag{10.132}$$

where κ_s determines the overall size, and α is the ratio of the transport coefficients in the two orthogonal directions. Now, fluid displacements in large-scale baroclinic eddies are nearly, but not exactly, horizontal — they may be along isopycnals, for example, or at an angle between the horizontal and the isopycnals. We may argue that the coordinate system in which the tensor is diagonal is the coordinate system defined by the plane along which fluid displacements occur. This is sensible because the transfers along and orthogonal to the fluid paths are each a consequence of different physical phenomena, and so we may expect the transfer tensor to be diagonal in this frame.

Because eddy displacements are predominantly horizontal, this coordinate system slopes at a small angle with respect to the horizontal $s = \tan\theta \approx \theta \ll 1$. Furthermore, we expect that the parameter α to be small ($\alpha \ll 1$), because this represents transfer in a direction orthogonal to the eddy fluid motion. We rotate the tensor $\mathbf{S}'$ through an angle θ to move into the usual $y - z$ frame; that is

$$\mathbf{S} = \kappa_s \begin{pmatrix} \cos\theta & -\sin\theta \\ \sin\theta & \cos\theta \end{pmatrix} \begin{pmatrix} 1 & 0 \\ 0 & \alpha \end{pmatrix} \begin{pmatrix} \cos\theta & \sin\theta \\ -\sin\theta & \cos\theta \end{pmatrix} \tag{10.133a}$$

$$\approx \kappa_s \begin{pmatrix} 1 + s^2\alpha & s(1-\alpha) \\ s(1-\alpha) & s^2 + \alpha \end{pmatrix} \quad \text{(for small } s) \tag{10.133b}$$

$$\approx \kappa_s \begin{pmatrix} 1 & s \\ s & s^2 + \alpha \end{pmatrix} \quad \text{(for small } s \text{ and small } \alpha) \tag{10.133c}$$

We can follow the same procedure in three dimensions. Then, if the eddy transport

is isotropic in the plane of eddy displacements, the three-dimensional transport tensor
is

$$
\boldsymbol{S}' = \kappa_s \begin{pmatrix} 1 & 0 & 0 \\ 0 & 1 & 0 \\ 0 & 0 & \alpha \end{pmatrix},
\tag{10.134}
$$

and the slope of the motion is a two-dimensional vector $\boldsymbol{s} = (s_x, s_y)$. (Recall our nota-
tion that a subscript x, y or z denotes a derivative; other subscripts are simply markers.)
If we rotate the transport tensor into physical space then we obtain, analogously to
(10.133), ,

$$
\boldsymbol{S} = \kappa_s \begin{pmatrix} 1 + s_y^2 + \alpha s_x^2 & (\alpha - 1)s_x s_y & (1 - \alpha)s_x \\ (\alpha - 1)s_x s_y & 1 + s_x^2 + \alpha s_y^2 & (1 - \alpha)s_y \\ (1 - \alpha)s_x & (1 - \alpha)s_y & \alpha + s^2 \end{pmatrix}
\tag{10.135a}
$$

$$
\approx \kappa_s \begin{pmatrix} 1 & 0 & s_x \\ 0 & 1 & s_y \\ s_x & s_y & \alpha + s^2 \end{pmatrix},
\tag{10.135b}
$$

for small s and small α, where $s^2 = s_x^2 + s_y^2$.

The plane of eddy displacements

We are now in a position to make heuristic choices about the transfer coefficients, and
we will consider two bases for this:

I *Using linear baroclinic instability theory.*[13]   In a simple model of a growing
   baroclinic (Eady) wave, parcel trajectories that are along half the slope of the mean
   isopycnals are able to release the most potential energy. We thus suppose that $s = s_\rho/2$, where s_ρ is the isopycnal slope, and that $\alpha = 0$ in (10.133c) or (10.135b). In
   two dimensions this gives

$$
\boldsymbol{S} = \kappa_s \begin{pmatrix} 1 & s_\rho/2 \\ s_\rho/2 & s_\rho^2/4 \end{pmatrix}
\tag{10.136}
$$

   and so

$$
\overline{v'\phi'} = -\kappa_s \left(\frac{\partial \overline{\phi}}{\partial y} + \frac{1}{2}s_\rho \frac{\partial \overline{\phi}}{\partial z} \right)
\tag{10.137a}
$$

$$
\overline{w'\phi'} = -\frac{1}{2}\kappa_s s_\rho \left(\frac{\partial \overline{\phi}}{\partial y} + \frac{1}{2}s_\rho \frac{\partial \overline{\phi}}{\partial z} \right).
\tag{10.137b}
$$

   If the tracer ϕ is potential temperature (and not just a passive tracer) then (10.137),
   along with one of the estimates for the size of κ_s given in section 10.7.2, consti-
   tutes a parameterization for the diffusive polewards and upwards heat flux in the
   atmosphere.

II *Flow along neutral surfaces.* If the fluid interior is adiabatic and steady, then fluid trajectories are along neutral surfaces; that is, along surfaces of potential density or potential temperature. One might therefore be inclined to assume that the eddy fluxes are aligned along the mean neutral surfaces and choose $s = s_\rho$. However, even in the adiabatic case, this is not always a good choice. From the adiabatic thermodynamic equation $Db/Dt = 0$ we may derive the equation for the eddy buoyancy variance, namely

$$\frac{1}{2}\frac{\partial \overline{b'^2}}{\partial t} + \frac{1}{2}\overline{u} \cdot \nabla_z \overline{b'^2} + \frac{1}{2}\overline{w}\frac{\partial \overline{b'^2}}{\partial z} + \overline{u'b'} \cdot \nabla_z \overline{b} + \overline{w'b'}\frac{\partial \overline{b}}{\partial z}$$
$$+ \frac{1}{2}\nabla_z \cdot \overline{u'b'^2} + \frac{1}{2}\frac{\partial}{\partial z}\overline{w'b'^2} = 0. \tag{10.138}$$

and specialize to the case of a zonally-uniform, small-ampliude wave. In this case

$$\frac{1}{2}\frac{\partial \overline{b'^2}}{\partial t} = -\overline{u'b'}\frac{\partial \overline{b}}{\partial y} - \overline{w'b'}\frac{\partial \overline{b}}{\partial z}. \tag{10.139}$$

If the wave is statisically steady then the left-hand side is zero and

$$\overline{v'_m b'} \cdot \nabla_m \overline{b} = 0 \tag{10.140}$$

where the subscript m indicates vectors are in the meridional plane. In this case there is indeed no diagradient flux. But if the wave is growing, then

$$\frac{\overline{w'b'}}{\overline{u'b'}} < -\frac{\partial \overline{b}/\partial y}{\partial \overline{b}/\partial z} \tag{10.141}$$

and so the mixing slope is *less* steep than the mean isopycnal slope, even though the flow may be adiabatic. Similarly, if the wave is decaying the, mixing slope is steeper than that of the mean isopycnals. In an inhomogeneous flow, the advection by the mean flow in (10.138) plays a similar role to time-dependence: the advection of eddy variance by the mean flow into a region of larger variance will give rise to a mixing slope that is less steep than the isopycnal slope, and conversely if for flow entering a region of less variance. Only for a statistically steady, adiabatic, linear wave field is the mixing slope guaranteed to be along the isopycnals.

Having said this, let us proceed by assuming that the fluid trajectories are indeed along neutral surfaces. If there is no diffusion orthogonal to this $\alpha = 0$, and the transport tensor is

$$S = \kappa_s \begin{pmatrix} 1 & 0 & s_{\rho x} \\ 0 & 1 & s_{\rho y} \\ s_{\rho x} & s_{\rho y} & |s_\rho|^2 \end{pmatrix}, \tag{10.142}$$

or in two dimensions

$$S = \kappa_s \begin{pmatrix} 1 & s_\rho \\ s_\rho & s_\rho^2 \end{pmatrix}, \tag{10.143}$$

and in this case

$$\overline{v'\phi'} = -\kappa_s \left(\frac{\partial \overline{\phi}}{\partial y} + s_\rho \frac{\partial \overline{\phi}}{\partial z} \right) \tag{10.144}$$

$$\overline{w'\phi'} = -\kappa_s s_\rho \left(\frac{\partial \overline{\phi}}{\partial y} + s_\rho \frac{\partial \overline{\phi}}{\partial z} \right). \tag{10.145}$$

Suppose that ϕ is potential temperature θ, and that surfaces of potential temperature do define neutral surfaces. Then plainly eddy motion along potential temperature surfaces does not transfer potential temperature, and the diffusion defined by (10.144) should have no effect. The equations themselves respect this, for then

$$s_\rho = -\frac{\partial \theta / \partial y}{\partial \theta / \partial z} \tag{10.146}$$

and the eddy transfer of potential temperature is then

$$\overline{v'\theta'} = -\kappa_s \left(\frac{\partial \overline{\theta}}{\partial y} + s_\rho \frac{\partial \overline{\theta}}{\partial z} \right) = 0, \tag{10.147}$$

$$\overline{w'\theta'} = -\kappa_s s_\rho \left(\frac{\partial \overline{\theta}}{\partial y} + s_\rho \frac{\partial \overline{\theta}}{\partial z} \right) = 0. \tag{10.148}$$

In the real ocean the presence of salinity means that the potential temperature, potential density and salinity surfaces are, in general, not parallel and there will be eddy diffusion of θ and S (salinity) along neutral surfaces. However, this does *not* provide a parameterization for the heat flux by baroclinic eddies, because we cannnot expect such transfer to depend for its existence on the presence of a second tracer, salinity. For such a parameterization, we turn to the antisymmetric transport tensor.

10.7.4 Structure: the antisymmetric transport tensor

The antisymmetric transport tensor gives rise to the skew flux, or the pseudo-advection. In two dimensions (one horizontal, one vertical) then we can immediately write down its form, namely,

$$A = \begin{pmatrix} 0 & -\kappa_a' \\ \kappa_a' & 0 \end{pmatrix} \tag{10.149}$$

where κ_a', which may vary space and time depending on the flow itself, determines the overall strength of the transport. In three dimensions then by inspection we can write

$$A = \begin{pmatrix} 0 & 0 & -\kappa_a'^x \\ 0 & 0 & -\kappa_a'^y \\ \kappa_a'^x & \kappa_a'^y & 0 \end{pmatrix}. \tag{10.150}$$

where the superscripts denote components and we have chosen our gauge by convenience and set $A_{21} = -A_{12} = 0$. Note that (10.150) preserves the form of (10.149) if one of the horizontal dimensions is absent — that is, if either row one and column one, or row two and column two, is eliminated. Our remaining choice is to determine the sign and magnitude of the transport coefficients.

An adiabatic, potential-energy diminishing eddy transport scheme

Gent and McWilliams proposed a particular parameterization for the transport of tracers in ocean models by baroclinic eddy fluxes, commonly known as the GM scheme.[14] The maintenance of two properties is the foundation of their scheme:

(i) Moments of the tracer should be preserved; in particular, the amount of fluid between two isopycnal surfaces should be preserved. This suggests the scheme should not diffuse buoyancy across its gradient.

(ii) The amount of available potential energy in the flow should be reduced. In this sense, the parameterization should mimic the effects of baroclinic instability, which transfers available potential energy to kinetic energy.

The first of these is automatically satisfied by using an antisymmetric diffusivity tensor. The second property can be satisfied by choosing the transfer coefficients to be proportional to the slope of the isopycnals, in which case we may write

$$\mathbf{A} = \kappa_a \begin{pmatrix} 0 & 0 & -s_x \\ 0 & 0 & -s_y \\ s_x & s_y & 0 \end{pmatrix}, \tag{10.151}$$

where $\mathbf{s} = (s_x, s_y) = \nabla_\rho z = -\nabla_z \rho / (\partial \rho / \partial z)$ is the isopycnal slope. In an ocean model separately carrying temperature and salinity fields, then (10.151) would be applied to each of these, with the isopycnal slope being determined using the equation of state. To more easily see what properties are implied by the transport, let us specialize to the salt-free case, with buoyancy, b, the only thermodynamic variable. The isopycnal slope is then $\mathbf{s} = -(b_x/b_z, b_y/b_z)$ and the horizontal eddy buoyancy transfer $\mathbf{F}_h = (F_x, F_y)$ is given by

$$\mathbf{F}_h = -\left(-\kappa_a \mathbf{s} \frac{\partial b}{\partial z} \right) = -\kappa_a \left(\frac{\partial b}{\partial x}, \frac{\partial b}{\partial y} \right) = -\kappa_a \nabla_z b. \tag{10.152a}$$

which for positive κ is the same as conventional downgradient diffusion.

The vertical transfer is given by

$$F_z = -\kappa_a \left(s_x \frac{\partial b}{\partial x} + s_y \frac{\partial b}{\partial y} \right) = \kappa_a s^2 \frac{\partial b}{\partial z} \tag{10.152b}$$

where $s^2 = \mathbf{s} \cdot \mathbf{s}$. This flux is *up* the vertical gradient; however, by construction, the total skew flux is neither upgradient nor down gradient.

The combination of the downgradient horizontal flux and the upgradient vertical flux acts to reduce the potential energy of the flow at the same time as preserving the

volume of fluid within each density interval. The upgradient flux in the vertical is a consequence of the need to reduce available potential energy: suppose warm light fluid overlays cold dense fluid in a statically stable configuration, then a downgradient vertical diffusion would raise the centre of gravity of the fluid, increasing its potential energy — just the opposite of the action of baroclinic instability. Thus, the sign on the vertical diffusivity must be negative and this, in combination with the structure of (10.151) (and so a positive horizontal diffusivity) allows both properties (i) and (ii) above to be satisfied. The parameterization does not preserve total energy; the loss of potential energy is not balanced by a corresponding gain of kinetic energy, rather it is supposed lost to dissipation. Finally, to determine the magnitude of the (skew) eddy-diffusivity we may turn again to the phenomenological estimates of section 10.7.2.

The eddy transport velocity

Applying (10.112) to (10.151) gives the eddy transport velocities,

$$
\boxed{
\begin{aligned}
\widetilde{\boldsymbol{u}} &= -\frac{\partial}{\partial z}(\kappa_a \boldsymbol{s}), \\
\widetilde{w} &= \nabla_z \cdot (\kappa_a \boldsymbol{s})
\end{aligned}
}
\tag{10.153}
$$

The streamfunction associated with $\boldsymbol{A}$ is found using (10.114) and (10.151) giving

$$
\boldsymbol{\psi} = (-\kappa_a s_y, \kappa s_x, 0) = \mathbf{k} \times \kappa_a \boldsymbol{s}.
\tag{10.154}
$$

Two equivalent ways of implementing the Gent-McWilliams parameterization are thus as a skew-flux, as in (10.152), or as an advection by the pseudo-velocities (10.153). The vanishing of the normal component of the velocity is equivalent to the vanishing of the normal component of the flux at the boundary, and ensures that the scheme conserves tracer moments. The advective flux of buoyancy is just

$$
\boldsymbol{F}_{\mathrm{ad}} = b\widetilde{\boldsymbol{v}} = b\nabla \times \boldsymbol{\psi} = b\nabla \times (\mathbf{k} \times \kappa_a \boldsymbol{s}),
\tag{10.155}
$$

whereas using (10.108) the skew flux is given by

$$
\boldsymbol{F}_{\mathrm{sk}} = -\nabla b \times \boldsymbol{\psi} = -\nabla b \times (\mathbf{k} \times \kappa_a \boldsymbol{s}).
\tag{10.156}
$$

Vector manipulation easily shows that the divergences of these two fluxes are equal.

10.7.5 Examples

Consider a situation with sloping isotherms (and with density determined solely by temperature) as illustrated in Fig. 10.5. The vertical flux attempts to tighten the temperature distribution, whereas the horizontal flux, being downgradient, attempts to smooth out horizontal inhomogeneities. Taken together, their net is to preserve the amount of fluid between any two isotherms, but at the same time to rotate flatten the isotherms; in this way the available potential energy of the flow is reduced. This is different from a conventional downgradient diffusion. A purely horizontal diffusion would, in principle, act
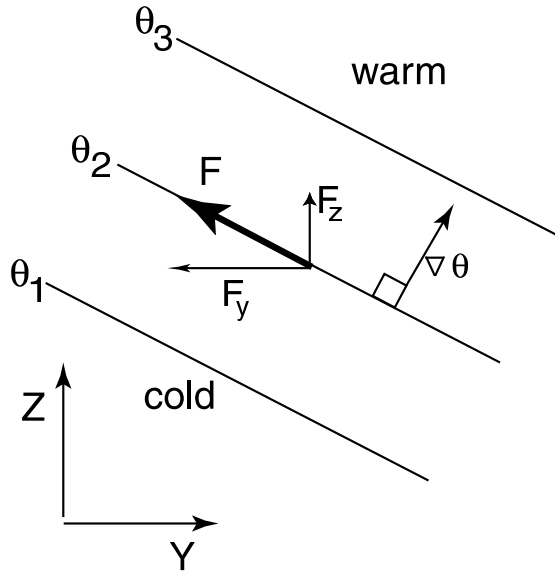
Figure 10.5 The GM skew fluxes arising from sloping isotherms. The flux itself is parallel to the isotherms, with the horizontal flux being directed down the horizontal gradient but the vertical flux being upgradient. The effect of the vertical flux is to lower the centre of gravity of the fluid, and reduce the potential energy. The horizontal flux tries to make the temperature more uniform in the horizontal. The net effect of the skew flux is to *flatten* the isotherms.

to equalize values at each level, and a three-dimensional downgradient diffusion would try to equalise all values. Thus, a skew flux behaves quite differently from the usual downgradient diffusion, which merely acts to reduce gradients without caring much about other fluid properties.

To illustrate this consider a very simple example, that of a two-dimensional (y–z) fluid in which the initial density field is a 3×3 grid, with initial conditions

$$\rho_{\text{init}} = \begin{bmatrix} 2 & 1 & 1 \\ 3 & 2 & 1 \\ 3 & 3 & 2 \end{bmatrix}. \tag{10.157}$$

The isopycnals are sloping, much as in Fig. 10.5, and the flow is statically stable everywhere.

A purely horizontal diffusion would lead to, in the absence of other processes and with zero normal flux at the boundaries, a final state of

$$\rho_{\text{hd}} = \begin{bmatrix} 1.33 & 1.33 & 1.33 \\ 2 & 2 & 2 \\ 2.66 & 2.66 & 2.66 \end{bmatrix}, \tag{10.158}$$

and a full (vertical and horizontal) diffusion would give

$$\rho_{\text{hvd}} = \begin{bmatrix} 2 & 2 & 2 \\ 2 & 2 & 2 \\ 2 & 2 & 2 \end{bmatrix}. \tag{10.159}$$

Neither of the above two final states preserves the density census, and both imply strong diabatic effects — the fluid has been *mixed*, and the density variance has been reduced. This implies that diabatic effects have occurred; since large-scale eddies themselves
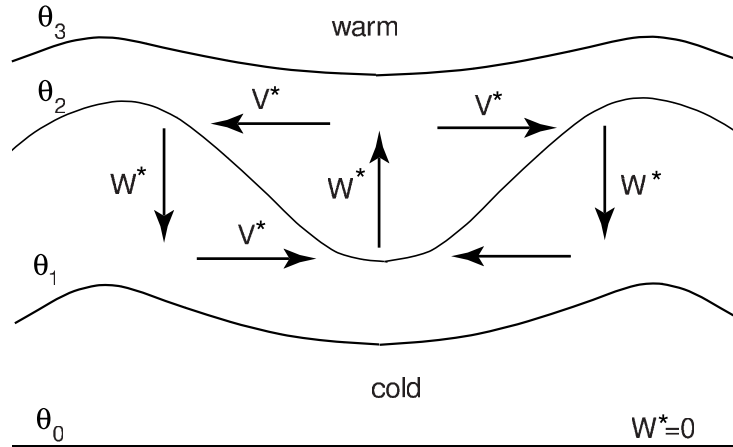
Fig. 10.6 The eddy-induced velocities in the Gent-McWilliams parameterization. The induced circulation attempts to flatten the sloping isopycnals. The induced vertical velocity, W^*, is zero on flat isopycnals.

cannot mix water properties (because the eddies themselves merely advect tracer properties).

In contrast, a skew-diffusion or eddy-transport advection will rotate the density surfaces clockwise until the isopycnal slope is zero, at which point the value of the transfer coefficients becomes zero and the process stops. The final state is then

$$\rho_{\text{GM}} = \begin{bmatrix} 1 & 1 & 1 \\ 2 & 2 & 2 \\ 3 & 3 & 3 \end{bmatrix}. \tag{10.160}$$

This both preserves the density census (and so the density variance) and reduces the available potential energy.

We can equally well interpret these effects in terms of eddy-transport velocities, and this will emphasize that it is not the eddy flux itself that is important; rather, it is the flux divergence. If the slopes of Fig. 10.5 extended uniformly everywhere, then the associated fluxes would have zero divergence, and the eddy-induced velocities, given by (10.153), would be zero. On the other hand, consider the case illustrated in Fig. 10.6, with variously sloping isotherms. For a constant value of the eddy diffusivity κ the slope of the isopycnals, $s = -(\partial\rho/\partial y)/(\partial\rho/\partial z)$, provides the stream function for the eddy-induced velocity:

$$\widetilde{v} = -\frac{\partial\psi}{\partial z} = -\frac{\partial}{\partial z}(\kappa_a s), \qquad \widetilde{w} = \frac{\partial\psi}{\partial y} = \frac{\partial}{\partial y}(\kappa_a s) \tag{10.161}$$

This induces the velocities illustrated in Fig. 10.6, which evidently serve to flatten the isopycnals. (If the isopycnals steepen as they approach the surface, the effects of the scheme may be harder to interpret.)

Finally, we note that diagradient diffusion and skew diffusion would normally be

used together, and the transport tensor will then have both symmetric and antisymmetric components. In ocean models the diagradient (symmetric) diffusion of temperature and salinity is often chosen to mix along isopycnals, because the mixing in the ocean interior is largely adiabatic. On the other hand, in the atmosphere (especially in the troposphere) diabatic effects are quite important and the symmetric tensor should be chosen appropriately.

10.8 † THICKNESS DIFFUSION

In the previous section, we considered the structure of the diffusivity tensor, and then chose the entries by physical reasoning to mimic the effects of baroclinic instability. An alternative approach is to choose, a priori, a quantity to be diffused across its gradient (i.e., not skew-diffused), and to then transform this appropriately to see how that effect should be represented in the equations of motion as commonly used, for example the thermodynamic equation in z-coordinates. The diffusivity need not be isotropic if, for example, the β-effect is important. However, if the diffused quantity is chosen appropriately we would expect there to be a coordinate system in which the diffusion tensor is diagonal; it will then remain symmetric if transformed to a perhaps more convenient coordinate system. In this section we explore the use of thickness as a 'diffusee', from an essentially first-principles perspective, and we see how similar thickness diffusion is to the GM scheme. In the next section we see how these schemes fit into the transformed Eulerian mean (TEM) framework.

Thickness is the vertical distance between two isotherms or isopycnals. It is a candidate for diffusion because a downgradient thickness transfer within an isopycnal layer satisfies two conditions:

(i) The total mass contained between two isopycnals is preserved, provided there is no flux through the lateral boundaries.

(ii) Such a flux serves to flatten isopycnals, and hence reduce the available potential energy of the flow, mimicking baroclinic instability.

However, thickness is *not* a Lagrangian conserved quantity; thus, the arguments of section 10.2 do not apply and so turbulent diffusion of thickness is somewhat *ad hoc*. The following sections explains these issues more fully.

10.8.1 Equations of motion

Thickness and its variance

In a Boussinesq fluid the distance between two surfaces of constant buoyancy is given by

$$\text{Thickness} = \Sigma = \int_{h(b_1)}^{h(b_2)} \mathrm{d}h = \int_{b_1}^{b_2} \frac{\partial h}{\partial b} \, \mathrm{d}b, \qquad (10.162)$$

and thus we may define the thickness field (strictly a 'thickness density' field), $\sigma \equiv \partial h/\partial b$. The volume of fluid between two isopycnal surfaces is proportional to $\sigma \Delta A$,

where ΔA is an infinitesimal area, and in the absence of diabatic processes this is conserved. Thus, we have $\mathrm{D}(\sigma \Delta A)/\mathrm{D}t = 0$ and using $\mathrm{D}\Delta A/\mathrm{D}t = \Delta A \nabla_b \cdot \boldsymbol{u}$ we obtain the the equation of motion for thickness,

$$\frac{\mathrm{D}\sigma}{\mathrm{D}t} + \sigma \nabla_b \cdot \boldsymbol{u} = D_\sigma \qquad \text{or} \qquad \frac{\partial \sigma}{\partial t} + \nabla_b \cdot (\boldsymbol{u}\sigma) = D_\sigma, \qquad (10.163)$$

now including a term D_σ to represents any diabatic terms. From (10.163) we obtain the variance equation

$$\frac{1}{2}\frac{\partial}{\partial t}\overline{\sigma'^2} + \overline{\boldsymbol{u}'\sigma'} \cdot \nabla_b \overline{\sigma} + \frac{1}{2}\overline{\boldsymbol{u}} \cdot \nabla_b \overline{\sigma'^2} + \frac{1}{2}\nabla_b \cdot \overline{\boldsymbol{u}'\sigma'^2} = -\overline{w'\sigma'} + \overline{D_\sigma \sigma'} \qquad (10.164)$$

where we have written $w' = (\sigma \nabla_b \cdot \boldsymbol{u})'$. This equation is to be compared with the corresponding equation for a conserved tracer, (10.68). If the mean flow is small and the the third order correlations may be neglected then

$$\overline{\boldsymbol{u}'\sigma'} \cdot \nabla \overline{\sigma} \approx -\overline{w'\sigma'} + \overline{D_\sigma \sigma'}. \qquad (10.165)$$

Unlike the case for a conserved tracer [c.f., (10.69)], the transport of thickness is not necessarily downgradient in regions of dissipation. However, in regions of baroclinic instability where there may be conversion of available potential energy to kinetic energy $\overline{w'\sigma'}$ is positive and we do then expect thickness to be transferred downgradient, suggesting a diffusive parameterization.

The eddy-induced and residual velocities

Now, let us decompose these variables in the usual manner into a mean component (say an ensemble mean, denoted with an overbar), and an eddy component, denoted with a prime. Then the averaged thickness equation is

$$\frac{\partial \overline{\sigma}}{\partial t} + \nabla_b \cdot \left(\overline{\sigma}\,\overline{\boldsymbol{u}} + \overline{\sigma'\boldsymbol{u}'} \right) = 0. \qquad (10.166)$$

where $\overline{\sigma'\boldsymbol{u}'}$ is the eddy thickness flux. This equation may be written

$$\frac{\partial \overline{\sigma}}{\partial t} + \nabla_b \cdot [(\overline{\boldsymbol{u}} + \widetilde{\boldsymbol{u}})\overline{\sigma}] = 0. \qquad (10.167)$$

where

$$\boxed{\widetilde{\boldsymbol{u}} \equiv \frac{\overline{\sigma'\boldsymbol{u}'}}{\overline{\sigma}}} \qquad (10.168)$$

is the 'eddy-induced velocity', sometimes referred to as the bolus velocity, this appellation arising because the thickness flux is said to be evocative of a peristaltic transfer along a passage bounded by impermeable but elastic walls. The quantity

$$\overline{\boldsymbol{u}}^* = \overline{\boldsymbol{u}} + \widetilde{\boldsymbol{u}} \qquad (10.169)$$

is the residual velocity we encounted in chapter 7, and it accounts for the total transport of thickness, including both eddy and Eulerian mean.

The evolution of a conserved tracer τ, (an amount per unit volume) is given by

$$\frac{D}{Dt}(\tau h \Delta A) = 0 \tag{10.170}$$

whence, because $h \Delta A$ is a constant,

$$\frac{\partial \tau}{\partial t} + \boldsymbol{u} \cdot \nabla_b \tau = 0, \tag{10.171}$$

or equivalently

$$\frac{\partial}{\partial t}(\sigma \tau) + \nabla_b \cdot (\sigma \boldsymbol{u} \tau) = 0. \tag{10.172}$$

The averaged tracer equation (10.172) may be written as

$$\frac{\partial}{\partial t}(\overline{\sigma}\,\overline{\tau} + \overline{\sigma'\tau'}) + \nabla_b \cdot (\overline{\sigma}\,\overline{\boldsymbol{u}}\,\overline{\tau}) + \nabla_b \cdot \overline{\sigma'\boldsymbol{u}'}\overline{\tau} + \nabla_b \cdot [\overline{(\sigma\boldsymbol{u})'\tau'}] = 0, \tag{10.173}$$

or, using (10.166),

$$\frac{\partial \overline{\tau}}{\partial t} + \frac{1}{\overline{\sigma}}\frac{\partial}{\partial t}(\overline{\sigma'\tau'}) + \left[\overline{\boldsymbol{u}} + \frac{\overline{\sigma'\boldsymbol{u}'}}{\overline{\sigma}}\right] \cdot \nabla_b \overline{\tau} = -\frac{1}{\overline{\sigma}}\nabla_b \cdot [\overline{(\sigma\boldsymbol{u})'\tau'}]. \tag{10.174}$$

(To derive these, first let $\overline{\sigma\tau\boldsymbol{u}} = \overline{(\sigma\boldsymbol{u})'\tau'} + \overline{\sigma\boldsymbol{u}}\,\overline{\tau}$.) If we neglect the correlation between σ' and τ', then (10.174) has the form

$$\frac{\partial \overline{\tau}}{\partial t} + (\overline{\boldsymbol{u}} + \widetilde{\boldsymbol{u}}) \cdot \nabla_b \tau = -\frac{1}{\overline{\sigma}}\nabla_b \cdot [\overline{(\sigma\boldsymbol{u})'\tau'}] \tag{10.175}$$

Thus, the averaged tracer evolves as if it were advected by two velocity fields: the large scale field itself, $\overline{\boldsymbol{u}}$, and the eddy-induced velocity $\widetilde{\boldsymbol{u}}$, their sum being the residual velocity. The term on the right-hand-side of (10.175) is the divergence of the transport of tracer along the isopycnals by the eddy-transport $(\sigma\boldsymbol{u})'$.

10.8.2 Diffusive thickness transport

A diagradient diffusion of thickness parameterizes the eddy transport velocity by

$$\widetilde{\boldsymbol{u}} \equiv \frac{\overline{\sigma'\boldsymbol{u}'}}{\overline{\sigma}} = -\frac{1}{\overline{\sigma}}\kappa\nabla_b\overline{\sigma}. \tag{10.176}$$

Similarly, we may parameterize right-hand-side of (10.174) by

$$-\frac{1}{\overline{\sigma}}\nabla_b \cdot [\overline{(\sigma\boldsymbol{u})'\tau'}] = \frac{1}{\overline{\sigma}}\nabla_b \cdot (\kappa'\overline{\sigma}\nabla_b\overline{\tau}), \tag{10.177}$$

that is, as a diffusion of tracer along isopycnals.

Height coordinates

In height coordinates the eddy transport velocity will be a three-dimensional field, obtained by appropriately transforming $\widetilde{\boldsymbol{u}}$. We have

$$
\begin{aligned}
\widetilde{\boldsymbol{u}} &\approx -\frac{1}{\sigma}\kappa\nabla_b\overline{\sigma} = -\kappa\frac{\partial b}{\partial h}\nabla_b\left(\frac{\partial\overline{h}}{\partial b}\right) \\
&= -\kappa\frac{\partial b}{\partial z}\frac{\partial\overline{\boldsymbol{s}}}{\partial b} = -\kappa\frac{\partial\overline{\boldsymbol{s}}}{\partial z}
\end{aligned}
\tag{10.178}
$$

where to go to the second line we use $\nabla_b h = \boldsymbol{s}$, the isopycnal slope. The final result is not quite the same as (10.153), because the diffusivity is now outside the z-derivative. It is a subtle but important distinction, because it means that if κ varies the vertical velocity can no longer be obtained easily as a local function. That is to say, given (10.178), we no longer have $\widetilde{w} = \nabla_z\cdot\kappa\boldsymbol{s}$ as in (10.153). Rather, $\widetilde{w}$ must be evaluated by a nonlocal integration of the mass conservation requirement so that

$$
\widetilde{w} = \int\nabla_z\cdot\left(\kappa\frac{\partial\boldsymbol{s}}{\partial z}\right)\,\mathrm{d}z.
\tag{10.179}
$$

This should not be disconcerting from a physical standpoint, because the baroclinic activity of eddies certainly involves vertical communication — recall for example the tendency toward barotropic flow in baroclinic lifecycles. From a computational standpoint, it is a little less convenient. Nevertheless, the GM scheme is evidently very similar to a thickness diffusion.

10.9 † EDDY TRANSPORT AND THE TRANSFORMED EULERIAN MEAN

A natural framework to discuss how eddy fluxes interact with the mean flow is the transformed Eulerian mean (TEM), discussed in chapter 7. It provides a simplification of the formalism (especially if one is already familiar with TEM theory!) and, more importantly, a means to consider more general cases, such as the flux of potential vorticity and other variables.

From section 7.3.4 the averaged thermodynamic equation may be written as

$$
\frac{\partial\overline{b}}{\partial t} + (\overline{\boldsymbol{u}} + \widetilde{\boldsymbol{u}})\cdot\nabla\overline{b} + (\overline{w} + \widetilde{w})\frac{\partial\overline{b}}{\partial z} = \frac{\partial G}{\partial z}.
\tag{10.180}
$$

where

$$
G = \frac{\overline{\boldsymbol{v}'b'}\cdot\nabla\overline{b}}{\overline{b}_z} = \frac{1}{\overline{b}_z}\left(\overline{\boldsymbol{u}'b'}\cdot\nabla_z\overline{b} + \overline{w'b'}\frac{\partial\overline{b}}{\partial z}\right).
\tag{10.181}
$$

and

$$
\widetilde{\boldsymbol{u}} = -\frac{\partial\widetilde{\boldsymbol{\psi}}}{\partial z}, \qquad \widetilde{w} = \nabla\cdot\widetilde{\boldsymbol{\psi}}
\tag{10.182a}
$$

where

$$
\widetilde{\boldsymbol{\psi}} = \frac{\boldsymbol{F}[b]}{\overline{b}_z} = \frac{\overline{\boldsymbol{u}'b'}}{\overline{b}_z}.
\tag{10.182b}
$$

If the eddy fluxes are parallel to the isopycnals, then $G = 0$ and the sole effect of the eddies on the mean flow is via the eddy induced velocity. Again using the results of section 7.3.4 and diffusing thickness we have

$$\tilde{\boldsymbol{u}} = -\frac{\partial}{\partial z}\left(\frac{\overline{u'b'}}{\overline{b}_z}\right) \approx \left(\frac{\overline{v'\sigma'}}{\overline{\sigma}}\right) \approx -\frac{1}{\overline{\sigma}}\kappa\nabla_b\overline{\sigma} \approx -\kappa_a\frac{\partial\boldsymbol{s}}{\partial z}, \qquad (10.183)$$

recovering, for constant κ_a, the GM scheme. (Strictly, we have only demonstrated the above transformation for a zonal average.) Note that if we write the residual velocity in standard TEM fashion as $\overline{\boldsymbol{v}}^* = \overline{\boldsymbol{v}} - \nabla \times \boldsymbol{\psi}$ then with the GM parameterization the TEM streamfunction may be written as

$$\boldsymbol{\psi} = \kappa_a\frac{\mathbf{k} \times \nabla_z b}{\overline{b}_z}. \qquad (10.184)$$

10.9.1 Potential vorticity diffusion

Preliminaries

From a more fundamental perspective, potential vorticity, Q, is a better candidate for diffusion than thickness because it is a Lagrangian conserved quantity.[15] It is not the only variable that is materially conserved — potential temperature is also. However, potential temperature is advected by the *three-dimensional* velocity field. The vertical advection complicates matters, since any diffusion tensor certainly cannot be isotropic and probably not symmetric. On the other hand, in isentropic coordinates the adiabatic potential vorticity advection occurs the isentropic plane, an in quasi-geostrophic flow advection is purely horizontal. Thus, only the two dimensional diffusion need be considered, and the diffusion tensor will be much simplified. Indeed, if the effects of differential rotation are unimportant, the turbulence may be nearly isotropic and the diffusivity becomes a simple scalar.

However, near the upper and lower boundaries buoyancy may in fact be the appropriate field to diffuse. This is because (for flat boundaries) $w = 0$ and buoyancy is conserved on parcels when advected by the horizontal flow:

$$\frac{\partial b}{\partial t} + \boldsymbol{u} \cdot \nabla_z b = 0. \qquad (10.185)$$

Potential vorticity, on the other hand, becomes singular at boundaries where outcropping occurs: the thickness between two isentropic surfaces goes to zero and $(\zeta + f)/\sigma$ is ill-defined. This has an analog in quasi-geostrophic dynamics, where the equations of motion are horizontal advection of potential vorticity in the fluid interior with horizontal buoyancy advection at the boundaries providing the boundary conditions. Horizontal diffusion of buoyancy is, of course, not an adiabatic parameterization, but diabatic effects do occur at the surface. These considerations suggest that downgradient potential vorticity diffusion on isentropic surfaces in the fluid interior, combined with downgradient buoyancy diffusion at the upper and lower boundaries, is as rational a parameterization of eddy transfer effects as any simple diffusion scheme can be. However, its

implementation may be considerably more difficult than for a thickness diffusion, because of the dynamical and energetic constraints that potential vorticity transport must satisfy, and because when the equations of motion are written in conventional form the potential vorticity flux does not directly appear.

Implementations and approximations

Suppose that the large-scale fields obey planetary-geostrophic scaling, and for simplicity we remain on the β-plane. Then, in isentropic coordinates the potential vorticity is

$$Q = \frac{f + \zeta}{\sigma} \approx \frac{f}{\sigma}, \tag{10.186}$$

which gives

$$\nabla_b Q = \frac{1}{\sigma} \nabla f - \frac{f}{\overline{\sigma}^2} \nabla \overline{\sigma} = \frac{\beta}{\overline{\sigma}} \mathbf{j} - \frac{f}{\overline{\sigma}^2} \nabla_b \overline{\sigma}. \tag{10.187}$$

Potential vorticity diffusion is then just

$$\overline{\boldsymbol{u}'Q'} = -\boldsymbol{K}\nabla_b\overline{Q} = -\boldsymbol{K}\left(\frac{\beta}{\overline{\sigma}}\mathbf{j} - \frac{f}{\overline{\sigma}^2}\nabla_b\overline{\sigma}\right) \tag{10.188}$$

where $\boldsymbol{K}$ is the diffusivity (a two-dimensional symmetric tensor in the isentropic plane, or a scalar). If the eddy flux of potential vorticity also satisfies planetary-geostrophic scaling then

$$\overline{\boldsymbol{u}'Q'} \approx -\frac{f}{\overline{\sigma}^2}\overline{\boldsymbol{u}'\sigma'}. \tag{10.189}$$

Using (10.168) and (10.189) gives

$$\tilde{\boldsymbol{u}} = \frac{1}{\overline{\sigma}}\overline{\boldsymbol{u}'\sigma'} = -\frac{\overline{\sigma}}{f}\overline{\boldsymbol{u}'Q'} \tag{10.190}$$

and using (10.188) yields

$$\tilde{\boldsymbol{u}} = \boldsymbol{K}\left(\frac{\beta}{f}\mathbf{j} - \frac{1}{\overline{\sigma}}\nabla_b\overline{\sigma}\right) \tag{10.191}$$

This differs from (10.176) mainly in the existence of the term involving β on the right-hand-side. It is singular at the equator, a consequence of ignoring the relative vorticity term in the expression for potential vorticity. For use in a z-coordinates, it can be transformed in the same way as (10.176), giving

$$\tilde{\boldsymbol{u}} \approx \boldsymbol{K}\left(\frac{\beta}{f}\mathbf{j} - \frac{\partial \boldsymbol{s}}{\partial z}\right). \tag{10.192}$$

Using the quasi-geostrophic equations

Baroclinic eddies generally obey quasi-geostrophic scaling, and the dynamics of Ertel potential vorticity on isopycnals are mimicked by the dynamics of quasi-geostrophic potential vorticity on height surfaces, thus suggesting the use of quasi-geostrophic scaling. The quasi-geostrophic potential vorticity flux is comprised of a buoyancy flux and a flux of relative vorticity:

$$\overline{\boldsymbol{u}'q'} = \overline{\boldsymbol{u}'\zeta'} + f_0 \overline{\boldsymbol{u}'\frac{\partial}{\partial z}\left(\frac{b'}{N^2}\right)}. \tag{10.193}$$

We also note that:

$$\overline{v'\zeta'} = \frac{1}{2}\frac{\partial}{\partial x}\overline{(v'^2 - u'^2)} - \frac{\partial \overline{u'v'}}{\partial y} \tag{10.194}$$

and

$$\overline{v'\frac{\partial}{\partial z}\left(\frac{b'}{N^2}\right)} = -\frac{1}{2f_0}\frac{\partial}{\partial x}\left(\frac{\overline{b'^2}}{N^2}\right) + \frac{\partial}{\partial z}\left(\frac{\overline{v'b'}}{N^2}\right) \tag{10.195a}$$

and

$$\overline{u'\frac{\partial}{\partial z}\left(\frac{b'}{N^2}\right)} = \frac{1}{2f_0}\frac{\partial}{\partial y}\left(\frac{\overline{b'^2}}{N^2}\right) + \frac{\partial}{\partial z}\left(\frac{\overline{u'b'}}{N^2}\right) \tag{10.195b}$$

having used the thermal wind relation, $f_0 \partial\boldsymbol{v}/\partial z = \mathbf{k} \times \nabla b = \nabla^\perp b$.

Now suppose that two conditions are satisfied:

(i) The magnitude of the eddy available potential energy is about the same as the eddy kinetic energy; that is, $|b'/N| \sim |u'|, |v'|$.

(ii) The eddy *statistics* only vary on scales much larger than the deformation radius NH/f_0 (where H is a typical vertical scale of the eddies). That is, $\partial\overline{\phi}/\partial x \ll \overline{\phi} f_0/(NH)$ where $\overline{\phi}$ is some field of eddy statistics.

If both of these are satisfied, the potential vorticity flux given by (10.193) will be dominated by the thickness flux and so

$$\overline{\boldsymbol{u}'q'} \approx f_0 \overline{\boldsymbol{u}'\frac{\partial}{\partial z}\left(\frac{b'}{N^2}\right)}. \tag{10.196}$$

Furthermore, the second assumption suggests that first terms on the right-hand-side of (10.195) are smaller than the corresponding second ones so that

$$\overline{\boldsymbol{u}'q'} \approx f_0 \frac{\partial}{\partial z}\left(\frac{\overline{\boldsymbol{u}'b'}}{N^2}\right). \tag{10.197}$$

The left-hand side is the potential vorticity flux, which is to be parameterized by a

diffusion. The right-hand side is, again, closely related to a thickness flux and so to the eddy-induced velocity in the TEM. Thus, the eddy transport velocity is

$$\widetilde{\boldsymbol{u}} \approx -\frac{\partial}{\partial z}\left(\frac{\overline{\boldsymbol{u}'b'}}{\partial_z \overline{b}}\right) \approx -\frac{1}{f_0}\overline{\boldsymbol{u}'q'} \qquad (10.198)$$

To close this, we note that at large scales the potential vorticity gradient is dominated by the gradient of planetary vorticity (β) and the buoyancy gradient. Thus,

$$\nabla \overline{q} \approx \beta\,\mathbf{j} + f_0 \nabla_z \frac{\partial}{\partial z}\left(\frac{\overline{b}}{N^2}\right), \qquad (10.199)$$

and a diffusive closure for the quasi-geostrophic potential vorticity flux is effected by setting

$$\overline{\boldsymbol{u}'q'} = -\kappa\nabla\overline{q} = -\kappa\left[\beta\,\mathbf{j} + f_0 \nabla_z \frac{\partial}{\partial z}\left(\frac{\overline{b}}{N^2}\right)\right], \qquad (10.200)$$

with corresponding eddy transport velocity

$$\widetilde{\boldsymbol{u}} = \kappa\left[\frac{\beta}{f_0}\mathbf{j} + \frac{\partial}{\partial z}\left(\frac{\nabla\overline{b}}{N^2}\right)\right]. \qquad (10.201)$$

This is the quasi-geostrophic version of (10.192).

10.9.2 Final Remarks

The above manipulations indicate that it is possible to construct parameterizations for the skew-component of the buoyancy flux based on the assumption that potential vorticity is diffused down gradient on isentropic surfaces, or down the horizontal gradient in quasi-geostrophic theory. Other approaches may be possible, perhaps choosing the transformed Eulerian mean to be with respect to potential vorticity rather than potential temperature. One might also write the entire system of equations in TEM form, whence potential vorticity fluxes appear directly in the momentum equation. However, in all these cases there remain some difficulties, for example:

– Potential vorticity flux is the divergence of a flux (the Eliassen Palm flux). Thus, its integral is determined by the values of the flux at the boundaries, and in particular its vertical integral is determined by the horizontal buoyancy flux. Relatedly, the isopycnal interior diffusion of PV should transition smoothly to a horizontal diffusion of buoyancy or temperature at the boundary.

– To diffuse potential vorticity requires energy, and if the flow is not baroclinically unstable there should be no eddy transport.

– If the Coriolis parameter is allowed to vary, the above closures are singular at the equator, where geostrophic scaling naturally fails.

There seems no unique or self-evidently correct way overcome these, but time will tell![16]

Notes

1 Much of the theory of turbulent diffusion stems from G. I. (Geoffrey Ingram) Taylor (1886–1975), who made important contributions to both fluid and solid mechanics, in the former to meteorology, oceanography, and ærodynamics. In addition to his work in turbulence, Taylor is known for his work on the theory of rotating fluids (the 'Taylor-Proudman' effect, for example) and on hydrodynamic stability (analysis of stability of Couette flow, for example), and for his clear and simple laboratory experiments. The results of this section were first derived by Taylor (1921a). For more details on Taylor, see Batchelor (1986) and other references in that volume.

2 Many textbooks in both fluid dynamics and stochastic processes cover this material, and more. Gardiner (1985) is one.

3 Batchelor (1949).

4 The way variables are changed between (10.31) and (10.32) could also have been used to derive (10.20), but in that case a simpler transformation sufficed.

5 Batchelor and Townsend (1956).

6 This topic was first addressed empirically by Richardson (1926), although it was Obukhov (1941) who first properly obtained the '4/3 power law' describing how the eddy diffusivity varies with separation for parcels in the inertial range. Our treatment takes advantage of Kolmogorov scaling.

7 The figures in this section were kindly provided by Joe LaCasce; see LaCasce and Ohlmann (2003).

8 Morel and Larcheveque (1974) and Er-El and Peskin (1981). Earlier dispersion calculations were made by Richardson (1926) who measured smoke spreading from chimneys, finding results that are consistent with a three-dimensional energy inertial range at small scales.

9 Turbulent diffusion is both widely used and widely criticized. If there is a scale-separation between a well-defined mean flow and the eddies, and if the eddies have a well-defined energy containing scale, then turbulent diffusion can be an extremely useful parameterization in many engineering and geophysical contexts. At the same time, these conditions are often *not* satisfied, because it is unusual in fluid mechanics for the turbulent eddies to be significantly smaller than the mean flow — look at turbulent Rayleigh-Bénard convection, or turbulent Couette flow, for example. Baroclinic turbulence is unusual because there is a natural scale of the turbulence — the deformation radius — that is in general different from the scale of the mean flow, although even this scale separation may be lost if there is an inverse cascade or if the deformation scale is sufficiently large, as in the Earth's atmosphere. Furthermore, properly choosing *what* is to be diffused, and ensuring that various fluid conservation properties remain respected by the diffusion, are difficult problems.

10 If S_{ij} and A_{ij} are symmetric and antisymmetric tensors respectively, then, summing over repeated indices, their contraction is $A_{ij}S_{ij} = -A_{ji}S_{ij} = -A_{ji}S_{ji} = -A_{ij}S_{ij}$, where the last equality follows because the indices are dummy. Thus, the contraction must equal zero.

11 Green (1970) and Stone (1972), in the context of the meridional transport of heat

in the earth's atmosphere, suggested that the magnitude of the turbulent diffusivity coefficients could be obtained by dynamical arguments using such things as baroclinic instability theory and the amount of available potential energy in the atmosphere, although their suggestions differ in such important details as the eddy mixing length. More recent efforts have drawn on geostrophic turbulence theory, for example Held and Larichev (1996) and Smith and Vallis (2002).

12 See Smith and Vallis (2001).

13 Green (1970).

14 What is now called the Gent-McWilliams (GM) scheme originated in Gent and McWilliams (1990) and was clarified by Gent et al. (1995). Previously, Plumb (1979) had noted the connection between symmetric and antisymmetric diffusities and diffusive and advective fluxes, and Griffies (1998) explicitly showed how the GM bolus velocities are related to a skew flux and can be calculated using an antisymmetric diffusivity tensor (see also Griffies 2004). Visbeck et al. (1997) suggested that the values of eddy diffusivities in the GM scheme might be determined by dynamical arguments like those of Green (1970) and Stone (1972).

15 Potential vorticity diffusion was suggested by Green (1970) as a parameterization for large-scale eddies in the atmosphere, and used by Welander (1973), Marshall (1981) and Rhines and Young (1982a) in ocean contexts. Treguier et al. (1997) further explored the use of potential-vorticity based parameterizations for ocean models.
Lee et al. (1997), Marshall et al. (1999), Drijfhout and Hazeleger (2001), and others, have explored numerically whether the eddy transfer of tracers in the ocean is in fact diffusive, and whether potential vorticity or thickness is a better quantity to diffuse. Numerical results can be difficult to interpret because if a property is diffused downgradient then that property tends to become homogeneous, and the resulting diagnostics may be inaccurate.

16 At the time of writing these are active issues in research. See for example Killworth (1997), Smith and Vallis (2002).

Further Reading

Aris, R., 1962, *Vectors, Tensors and the Basic Equations of Fluid Mechanics, 286pp.*
A straightforward introduction to tensors and Cartesian tensors and their application to fluid mechanics.

Monin, A. S. and Yaglom, A. M. 1971, *Statistical Fluid Mechanics: Mechanics of Turbulence.*
This two-volume encyclopaedic reference contains a wealth of information on all aspects of turbulence, and it is particularly strong on turbulent diffusion.

Problems

10.1 *(a)* On the line the Dirac delta function is given (non-uniquely) by
$\delta(x) = \lim_{\epsilon \to 0}(\pi\epsilon)^{-1/2}\exp(-x^2/\epsilon)$. What are the two- and three-dimensional analogs, given circular and spherical symmetry?

(b) In two-dimensions, show that the solution to the diffusion equation

$$\frac{\partial \phi}{\partial t} = D\nabla^2\phi \qquad \qquad (\text{P10.1})$$

with initial conditions $\phi(r, t = 0) = \delta(r)$ is given by

$$\phi(r, t) = \frac{1}{4\pi D t} \exp(-r^2/4Dt). \qquad (P10.2)$$

Show that the mean square distance of a particle that spreads from the origin is given by

$$\overline{r^2} = 4Dt. \qquad (P10.3)$$

You may assume a circularly symmetric solution.

(c) Do this problem in one dimension.

10.2 ♦ Repeat problem 10.1, but in a space of arbitrary dimension m, which if needs be may be integer.

10.3 ♦ Solve the two-dimensional advection-diffusion equation, $\partial\phi/\partial t + \boldsymbol{u} \cdot \nabla\phi = \kappa\nabla^2\phi$, exactly for a passive tracer ϕ in a flow $(u, v) = (\Gamma y, 0)$, with the initial condition $\phi = A\cos kx$. Provide a physical explanation of the long-time behaviour of the solution. *Hint:* Use an integrating factor, and look for a solution like $\phi \sim Ae^{-B[x-u(y)t]}$.

LARGE-SCALE ATMOSPHERIC CIRCULATION

CHAPTER 11

The Overturning Circulation: Hadley and Ferrel Cells

IN THIS CHAPTER AND THE TWO FOLLOWING we discuss the large-scale, circulation, or the *general circulation,* of the atmosphere. In this chapter we focus first on the dynamics of the Hadley Cell and then, rather descriptively, the mid-latitude overturning cell, the Ferrel Cell. This provides a starting point for our second major topic, a discussion of the dynamics of the extra-tropical zonally averaged circulation, and this is presented in chapter 12. Finally, in chapter 13, we explicitly consider the deviations from zonally symmetry — the stationary wave pattern — and the stratosphere. We will use many of the tools developed in the previous chapters, but those readers who already have some acquaintance with GFD may wish to jump directly in here. We preface all of this with a brief observational overview of some of the large-scale features.

11.1 OBSERVED FEATURES

Here we give only a brief overview of the observed circulation, concentrating on the zonally-averaged fields.[1]

11.1.1 The Radiative Equilibrium Distribution

A gross measure characterizing the atmosphere, and the effects that dynamics have on it, is the pole-to-equator temperature distribution. The *radiative equilibrium* temperature distribution is the (three-dimensional) distribution that would obtain if there were no atmospheric or oceanic motion, and given the composition and radiative properties of the atmosphere and surface and this is a function only of the incoming solar radiation at the top of the atmosphere. To evaluate this temperature entails a complicated calculation,
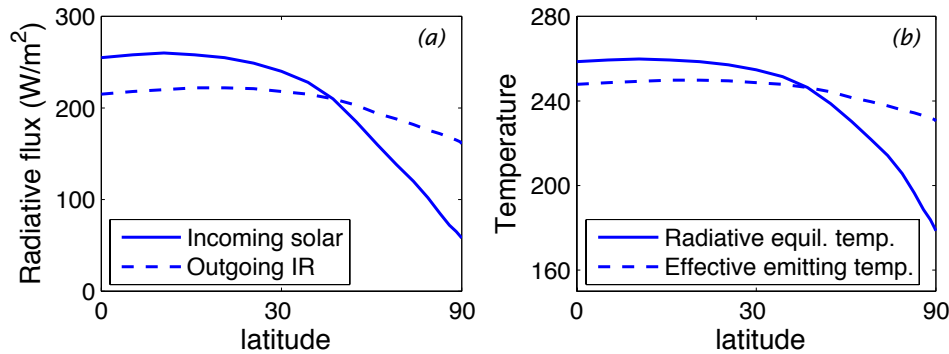
Fig. 11.1 (a) The (approximate) observed net average incoming solar radiation and outgoing infra-red radiation at the top of the atmosphere, as a function of latitude (plotted on a sine scale). (b) The temperatures associated with these fluxes, calculated using $T = (R/\sigma)^{1/4}$, where R is the solar flux for the radiative equilibrium temperature and R is the infrared flux for the effective emitting temperature. Thus, the solid line is an approximate radiative equilibrium temperature

especially as the radiative properties of the atmosphere depend on the amount of water vapour and cloudiness in the atmosphere. A much simpler calculation that illustrates the essence of the situation is to note that at the top of the atmosphere the incoming solar radiation is balanced by the outgoing infra-red radiation, and to parameterize the latter by a single temperature. A black body subject to a net incoming radiation of S (Watts per square meter) has a radiative-equilibrium temperature $T_{\rm rad}$ given by $\sigma T_{\rm rad}^4 = S$, this being Stefan's law with Stefan-Boltzmann constant $\sigma = 5.67 \times 10^{-8} {\rm W\,m^{-2}\,K^{-4}}$. Thus, for the earth, we have

$$\sigma T_{\rm rad}^4 = S(\vartheta)(1 - \alpha), \tag{11.1}$$

where α is the albedo of the earth and $S(\vartheta)$ is the incoming solar radiation at the top of the atmosphere, and its solution is shown in Fig. 11.1. This solution does not quantitatively characterize that temperature at the earth's surface, nor at any single level in the atmosphere, because the atmosphere is not a black body and the outgoing radiation originates from multiple levels. Nevertheless, the qualitative point is evident: the radiative equilibrium temperature has a much stronger pole-to-equator gradient than does the effective emitting temperature, indicating that that there is a polewards transport of heat in the atmosphere-ocean system. More detailed calculations indicate that the atmosphere is further from its radiative equilibrium in winter than summer, indicating a larger heat transport. The transport occurs (in all seasons) because polewards moving air and water tends to be at a higher temperature than the equatorwards moving air and water, and most of this motion is associated with the large-scale circulation. The radiative forcing thus seeks to maintain a pole-to-equator temperature gradient, and the ensuing circulation seeks to reduce this gradient.

11.1.2 Observed wind and temperature fields

The observed zonally-average temperature and zonal wind fields are illustrated in Fig. 11.2. The vertical coordinate is log pressure, multiplied by a constant factor $H = RT_0/g = 7.5$ km, so that the ordinate is similar to height in kilometers. (In an isothermal hydrostatic atmosphere $(RT_0/g)\mathrm{d}\ln p = -\mathrm{d}z$, and the value of H chosen corresponds to $T_0 = 256$ K.) To a good approximation temperature and zonal wind are related by thermal wind balance, which in pressure coordinates is

$$f\frac{\partial u}{\partial p} = \frac{R}{p}\frac{\partial T}{\partial y}. \tag{11.2}$$

In the lowest several kilometers of the atmosphere temperature falls almost monotonically with latitude and height, and this region is called the *troposphere*. The temperature in the lower atmosphere varies more rapidly with latitude than does the effective emitting temperature, T_E, the latter being more characteristic of the temperature in the mid-to-upper troposphere. The meridional temperature gradient is much larger in winter than summer, because in winter high-latitudes receive virtually no direct heating from the sun. It is also strongest at the edge of the subtropics, and here it is associated with a zonal jet, particularly strong in winter. There is no need to 'drive' this thermal wind with convergent momentum fluxes: given the temperature, the flow is a conseqence of thermal wind balance, and to the extent that the upper troposphere is relatively frictionless there is no need to maintain it against dissipation. Of course just as the radiative-equilibrium temperature gradient is much larger than that observed, so the shear associated with it is much larger than that observed. Thus, the overall effect of the atmospheric and oceanic circulation, and in particular of the turbulent circulation of the mid-latitude atmosphere, is to *reduce* the amplitude of the vertical shear of the eastward flow by way of a polewards heat transport. Observations indicate that about two-thirds of this transport is effected by the atmosphere, and about a third by the ocean, more in low latitudes.

Above the troposphere is the *stratosphere,* and here temperature typically increases with height. The boundary between the two regions is called the *tropopause,* and this varies in height from about 16 km in the tropics to about 8 km in polar regions. We consider the maintenance of this stratification in section 12.6.

The surface winds are *not* explained by thermal wind balance. From the equator to the pole these have a typical E-W-E (easterly-westerly-easterly) pattern, although the polar easterlies are weak and barely present in the northern hemisphere. In a given hemisphere, the surface winds are stonger in winter than summer, and they are also consistently stronger in the Southern Hemisphere than in the Northern Hemisphere, because in the former the surface friction is weaker because of the relative lack of continental land masses and topography. The surface winds, unlike upper level winds, must be maintained against the dissipating effects of friction, and this implies a momentum convergence, either from eddies or from the mean flow, into regions of nonzero flow. Typically, the maxima in the eastward surface winds are in midlatitudes and somewhat poleward of the subtropical maxima in the upper-level westerlies and at latitudes where the zonal flow is a little more constant with height.
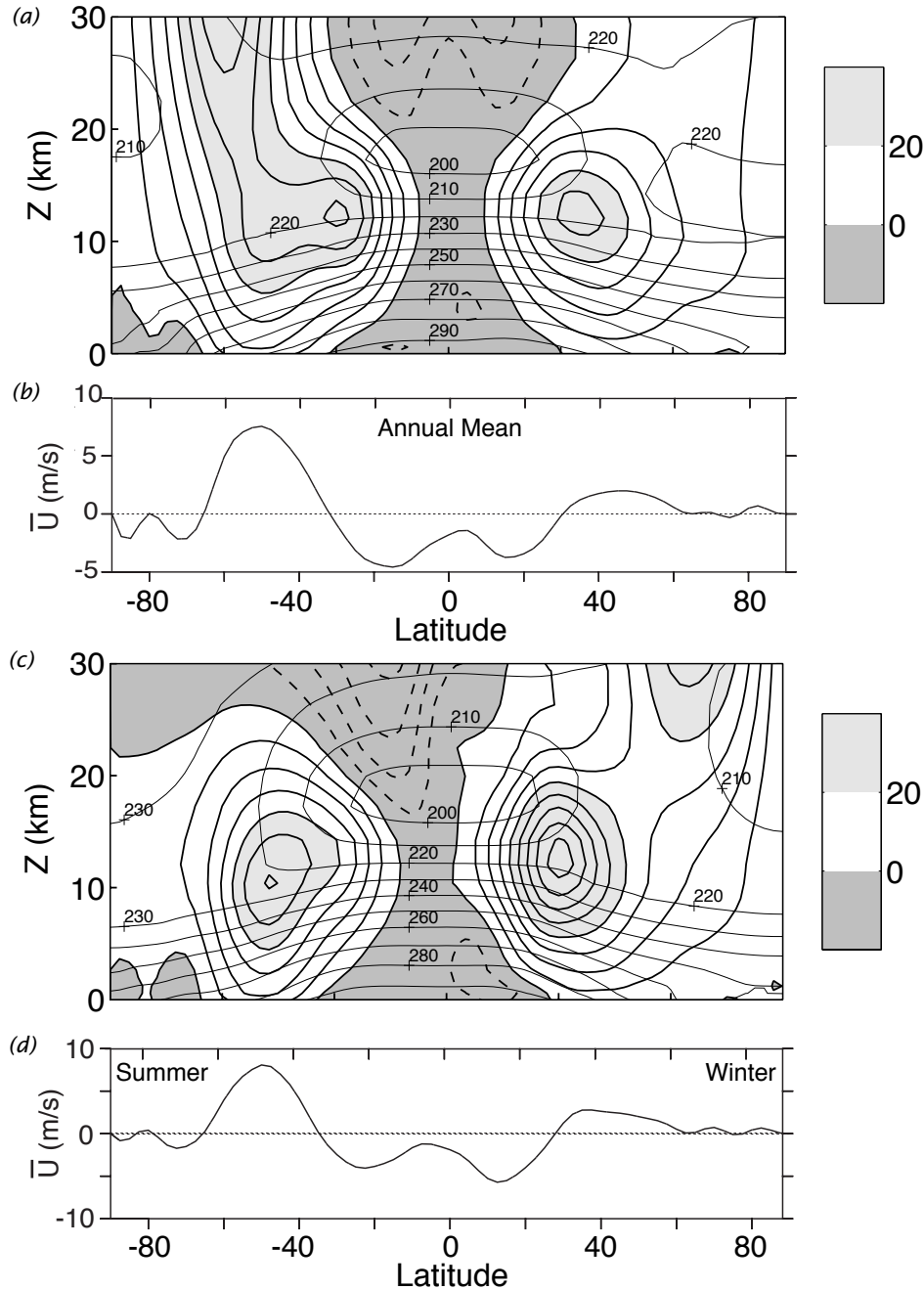
Fig. 11.2 (a) Annual mean, zonally averaged zonal wind (heavy contours and shading) and the zonally averaged temperature (lighter contours). (b) Annual mean, zonally averaged zonal winds at the surface. (c) and (d) Same as (a) and (b), except for northern hemisphere winter (DJF). The wind contours are at intervals of $5\,\mathrm{m\,s^{-1}}$ with shading for eastward winds above $20\,\mathrm{m\,s^{-1}}$ and for all westward winds, and the temperature contours are labelled. The ordinate of (a) and (c) is $Z = -H \log(p/p_{00})$, with scale height $H = 7.5\,\mathrm{km}$.
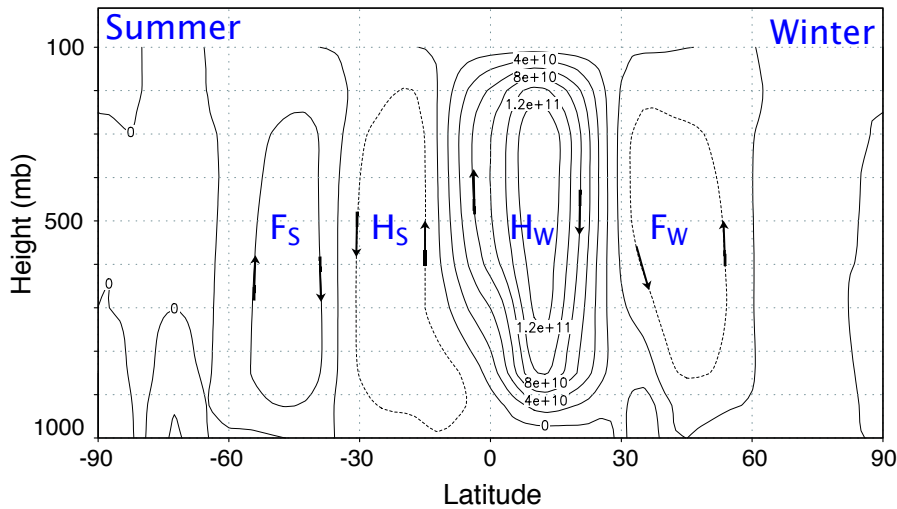
Fig. 11.3 The observed, zonally averaged, meridional overturning circulation of the atmosphere, in units of kg/s, averaged over December-January-February (DJF). In each hemisphere note the presence of a direct *Hadley Cell* (H_W and H_S in winter and summer) with rising motion near the equator, descending motion in subtropics, and an indirect *Ferrel Cell* (F_W and F_S) in midlatitudes. There are also hints of a weak direct cell at high latitudes. The winter Hadley Cell is far stronger than the summer one.

11.1.3 Meridional overturning circulation

The observed (Eulerian) zonally-averaged meridional overturning circulation is illustrated in Fig. 11.3. The figure shows a streamfunction, Ψ for the vertical and meridional velocities such that, in the pressure coordinates used in the figure,

$$\frac{\partial \Psi}{\partial y} = \overline{\omega}, \qquad \frac{\partial \Psi}{\partial p} = -\overline{v}. \tag{11.3}$$

where the overbar indicates a zonal average. In each hemisphere there is rising motion near the equator and sinking in the subtropics, and this circulation is known as the *Hadley Cell*.[2] The Hadley Cell is a thermally direct cell (i.e., the warmer fluid rises, the colder fluid sinks), much stronger in the winter hemisphere, and extending to about 30°. In mid-latitudes the sense of the overturning circulation is apparently reversed, with rising motion in the high-mid-latitudes, at around 60° and sinking in the subtropics, and this is known as the *Ferrel Cell*. However, as with most pictures of averaged streamlines in unsteady flow, this gives a misleading impression as to the actual material flow of parcels of air because of the presence of mid-latitude eddies, and we discuss this in the next chapter. In low latitudes the circulation is more nearly zonally symmetric and the picture does give a qualitatively correct representation of the actual flow. At high latitudes there is again a thermally direct cell, although it is weak and not always present, and thus the atmosphere is often referred to as having a three-celled structure.

Features of the Large-scale Atmospheric Circulation

From Figures 11.1 through 11.3 we see or infer:

★ A pole-equator temperature gradient that is much smaller than the radiative equilibrium gradient.

★ A troposphere, in which temperature generally falls with height, above which lies the stratosphere, in which temperature increases with height. The two regions are separated by a tropopause, which varies in height from about 16 km at the equator to about 6 km at the pole.

★ A monotonically decreasing temperature from equator to pole in the troposphere, but a weakening and sometimes reversal of this above the tropopause.

★ A westerly (i.e., eastward) tropospheric jet. The time- and zonally-averaged jet is a maximum at the edge or just polewards of the subtropics, where it is associated with a strong meridional temperature gradient. In mid-latitudes the jet has a stronger barotropic component.

★ An E-W-E (easterlies-westerlies-easterlies) surface wind distribution. The latitude of the maximum in the surface westerlies is in mid-latitudes, where the zonally-averaged flow is more barotropic.

11.1.4 Summary

Some of the main features of the zonally averaged circulation are summarized in the shaded box above. We emphasize that the zonally-averaged circulation is not synonymous with a zonally symmetric circulation, and the midlatitude circulation is highly asymmetric. On the other hand, the large-scale tropical circulation of the atmosphere is to a large degree zonally symmetric or nearly so, and although monsoonal circulations and the Walker circulation are zonally asymmetric these are relatively weaker than midlaitude weather systems. Indeed the boundary between the tropics and midlatitude may be usefully defined by the latitude at which such zonal asymmetries become dynamically important on the large scale and this boundary, at about 30° on average, is quite sharp. We thus begin our dynamical description with a study of the low latitude zonally symmetric atmospheric circulation.

11.2 A STEADY MODEL OF THE HADLEY CELL

11.2.1 Assumptions

Let us try to construct a zonally symmetric model of the Hadley Cell.[3] Such a model is likely applicable mainly to the tropical atmosphere, this being observed to be more zonally symmetric than the midlatitudes. We will suppose that heating is maximum at the equator, and our intuitive picture, drawing on the observed flow of Fig. 11.3, is of air rising at the equator and moving poleward at some height H, descending at some latitude ϑ_H, and returning equatorwards near the surface. We make three major assumptions about this circulation:

(i) That it is steady.
(ii) That the polewards moving air conserves its axial angular momentum, whereas the zonal flow associated with the near-surface, equatorwards moving flow is frictionally retarded and is weak.
(iii) That it is in thermal wind balance.

We also assume the model is symmetric about the equator (an assumption we relax in section 11.4). These are all reasonable assumptions, but they cannot be rigorously justified — in other words, we are constructing a *model* of the Hadley Cell, schematically illustrated in Fig. 11.4. The model defines a limiting case — steady, invisicid flow — that cannot be expected to quantitatively describe the atmosphere, but that can be analysed fairly completely. Another limiting case is described in section 11.5. The real atmosphere may defy such simple characterizations, but they provide in invaluable benchmark of understanding.

11.2.2 Dynamics

We seek, then, to determine the strength and poleward extent of the Hadley circulation in the steady model. For simplicity we will work with a Boussinesq atmosphere, but this is not an essential aspect. Neglecting friction, the zonally-averaged zonal momentum equation is

$$\frac{\partial \overline{u}}{\partial t} - (f + \overline{\zeta})\overline{v} + \overline{w}\frac{\partial \overline{u}}{\partial z} = -\frac{1}{\cos^2 \vartheta}\frac{\partial}{\partial \vartheta}(\cos^2 \vartheta \overline{u'v'}) - \frac{\partial \overline{u'w'}}{\partial z}. \tag{11.4}$$

where $\overline{\zeta} = -(a\cos\vartheta)^{-1}\partial_y(\overline{u}\cos\vartheta)$. If we neglect the vertical advection and the eddy terms on the right-hand-side, then a steady solution, if it exists, obeys

$$(f + \overline{\zeta})\overline{v} = 0. \tag{11.5}$$

Presuming that the meridional flow $\overline{v}$ is nonzero (an issue we address in section 11.2.6) then $f + \overline{\zeta} = 0$, or equivalently

$$2\Omega \sin\vartheta = \frac{1}{a}\frac{\partial \overline{u}}{\partial \vartheta} - \frac{\overline{u}\tan\vartheta}{a}. \tag{11.6}$$

At the equator we shall assume that $\overline{u} = 0$, because here parcels have risen from the surface where, by assumption, the flow is weak. Eq. (11.6) then has a solution of

$$\boxed{\overline{u} = \Omega a\frac{\sin^2 \vartheta}{\cos\vartheta} \equiv U_M}. \tag{11.7}$$
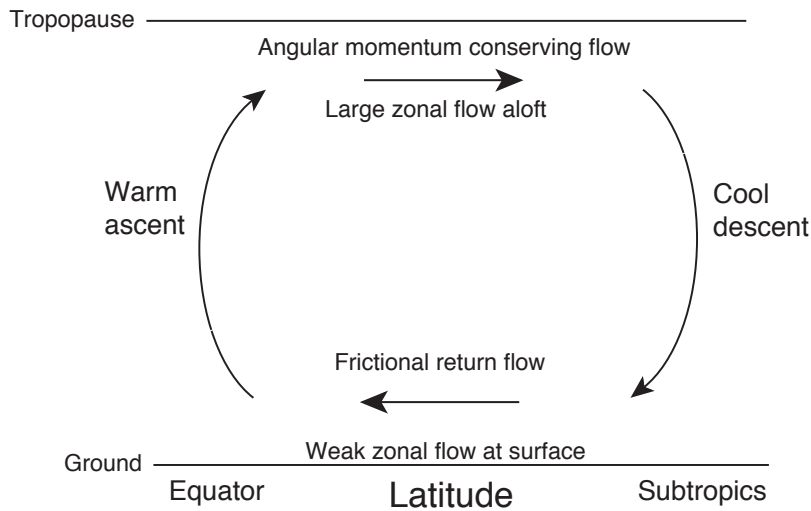
Fig. 11.4 A simple model of the Hadley Cell. Rising air near the equator moves polewards near the tropopause, descending in the subtropics and returning near the surface. The polewards moving air conserves its axial angular momentum, leading to a zonal flow that increases away from the equator. By the thermal wind relation the temperature of the air falls, slowly, as it moves poleward, and to satisfy the thermodynamic budget it sinks in the subtropics, so defining the polewards edge of the cell. The return flow at the surface is frictionally retarded and small.

This gives the zonal velocity of the polewards moving air in the upper branch of the (model) Hadley Cell, above the frictional boundary layer.

We can derive this result directly from the conservation of axial angular mometum, m, of a parcel of air at a latitude ϑ. In the shallow atmosphere approximation we have [c.f., (2.65) and equations following]

$$\overline{m} = (\overline{u} + \Omega a \cos \vartheta)a \cos \vartheta, \tag{11.8}$$

and if $\overline{u} = 0$ at $\vartheta = 0$ and if $\overline{m}$ is conserved on a polewards moving parcel, then (11.8) leads to (11.7). It also may be directly checked that

$$(f + \overline{\zeta}) = -\frac{1}{a^2 \cos \vartheta} \frac{\partial \overline{m}}{\partial \vartheta} \tag{11.9}$$

Thus, if eddy fluxes and frictional effects are negligible, the polewards flow will conserve its angular momentum, and the zonal flow in the earth's rotating frame increases with latitude (see Fig. 11.5). If we do assume this, our model is zonally symmetric and we drop the overbars over the variables.

If (11.7) gives the zonal velocity in the upper branch of the Hadley Cell, and that in the lower branch is close to zero, then the thermal wind equation can be used to infer the vertically averaged temperature. Although the geostrophic wind relation is
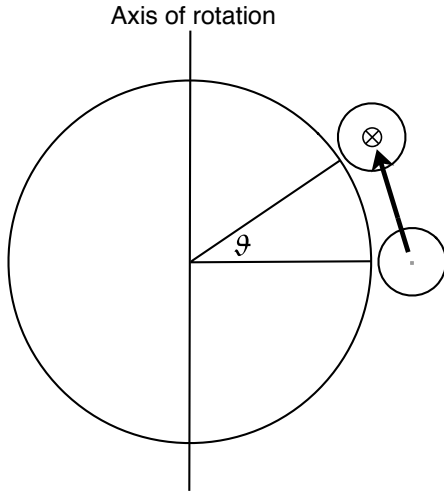
Axis of rotation

Figure 11.5 If a ring of air at the equator moves polewards it moves closer to the axis of rotation. If the parcels in the ring conserve their angular momentum their zonal velocity must increase; thus, if $m = (\overline{u} + \Omega a \cos \vartheta) a \cos \vartheta$ is preserved and $\overline{u} = 0$ at $\vartheta = 0$ we recover (11.7).

not valid at the equator (a more accurate balance is the so-called cyclostrophic balance, $fu + u^2 \tan \vartheta / a = -a^{-1} \partial \phi / \partial \vartheta$) the zonal wind is in fact geostrophically balanced until very close to the equator, and at the equator itself the horizontal temperature gradient in our model vanishes, because of the assumed interhemispheric symmetry. Thus, conventional thermal wind balance suffices for our purposes, and this is

$$2\Omega \sin \vartheta \frac{\partial u}{\partial z} = -\frac{1}{a} \frac{\partial b}{\partial \vartheta} \tag{11.10}$$

where $b = g\delta\theta/\theta_0$ is the buoyancy and $\delta\theta$ is the deviation of potential temperature from a constant reference value θ_0. Vertically integrating from the ground to the height H where the outflow occurs, and substituting (11.7) for u yields

$$\frac{1}{a\theta_0} \frac{\partial \theta}{\partial \vartheta} = \frac{2\Omega^2 a}{H} \frac{\sin^3 \vartheta}{\cos \vartheta}, \tag{11.11}$$

where $\theta = H^{-1} \int_0^H \delta\theta \, dz$ is the vertically averaged potential temperature. If the latitudinal extent of the Hadley Cell is not too great we can make the small-angle approximation, and replace $\sin \vartheta$ by ϑ and $\cos \vartheta$ by one, then integrating (11.11) gives

$$\boxed{\theta = \theta(0) - \frac{\theta_0 \Omega^2 y^4}{2gHa^2}}. \tag{11.12}$$

where $y = a\vartheta$ and $\theta(0)$ is the potential temperature at the equator, as yet unknown. Away from the equator, the zonal velocity given by (11.7) increases rapidly polewards and the temperature correspondingly drops. How far poleward is this solution valid? And what determines the value of the integration constant $\theta(0)$? To answer these questions we turn to thermodynamics.

Thermodynamics

In the above discussion, the temperature field is slaved to the momentum field in that it seems to follow passively from the dynamics of the momentum equation. Nevertheless, the thermodynamic equation must still be satisfied. Let us assume that the thermodynamic forcing can be represented by a Newtonian cooling to some specified radiative equilibrium temperature, θ_E; this is a severe simplification, especially in equatorial regions where the release of heat by condensation is important. The thermodynamic equation is then

$$\frac{D\theta}{Dt} = \frac{\theta_E - \theta}{\tau}, \tag{11.13}$$

where τ is a relaxation timescale, perhaps a few weeks. Let us suppose that θ_E falls monotonically from the equator to the pole, and that it increases linearly with height, and a simple representation of this is

$$\frac{\theta_E(\vartheta, z)}{\theta_0} = 1 - \frac{2}{3}\Delta_H P_2(\sin\vartheta) + \Delta_V \left(\frac{z}{H} - \frac{1}{2}\right), \tag{11.14}$$

where Δ_H and Δ_V are nondimensional constants that determine the fractional temperature difference between equator and pole, and the ground and the top of the fluid, respectively. P_2 is the second Legendre polynomial, and it is usually the leading term in the Taylor expansion of symmetric functions (symmetric around the equator) that decrease from pole to equator; it also integrates to zero over the sphere. $P_2(y) = (3y^2 - 1)/2$, so that in the small angle approximation and at $z = H/2$, or for the vertically averaged field, we have

$$\frac{\theta_E}{\theta_0} = 1 + \frac{1}{3}\Delta_H - \Delta_H \left(\frac{y}{a}\right)^2 \tag{11.15}$$

or

$$\theta_E = \theta_{E0} - \Delta\theta \left(\frac{y}{a}\right)^2, \tag{11.16}$$

where θ_{E0} is the equilibrium temperature at the equator, $\Delta\theta$ determines the equator-pole radiative-equilibrium temperature difference, and

$$\theta_{E0} = \theta_0(1 + \Delta_H/3), \qquad \Delta\theta = \theta_0 \Delta_H. \tag{11.17}$$

Now, let us suppose that the solution (11.12) is valid between the equator and a latitude ϑ_H where $v = 0$, so that within this region the system is essentially closed. Conservation of potential temperature then requires that the solution (11.12) must satisfy

$$\int_0^{Y_H} \theta \, dy = \int_0^{Y_H} \theta_E \, dy, \tag{11.18}$$

where $Y_H = a\vartheta_H$ is as yet undetermined. Poleward of this, the solution is just $\theta = \theta_E$, and

Furthermore, we may demand that the solution be continuous at $y = Y_H$ — without temperature continuity the thermal wind would be infinite — and so

$$\theta(Y_H) = \theta_E(Y_H). \tag{11.19}$$

The constraints (11.18) and (11.19) determine the values of the unknowns $\theta(0)$ and Y_H. A little algebra (excercise 11.1) gives

$$Y_H = \left(\frac{5\Delta\theta g H}{3\Omega^2\theta_0}\right)^{1/2}, \tag{11.20}$$

and

$$\theta(0) = \theta_{E0} - \left(\frac{5\Delta\theta^2 g H}{18a^2\Omega^2\theta_0}\right). \tag{11.21}$$

A useful nondimensional number that parameterizes these solutions is

$$R \equiv \frac{gH\Delta\theta}{\theta_0\Omega^2 a^2} = \frac{gH\Delta_H}{\Omega^2 a^2}, \tag{11.22}$$

which is the the square of the ratio of of the speed of shallow water waves to the rotational velocity of the earth, multiplied by the fractional temperature difference from equator to pole. In terms of this we have

$$Y_H = a\left(\frac{5}{3}R\right)^{1/2}, \tag{11.23}$$

and

$$\theta(0) = \theta_{E0} - \left(\frac{5}{18}R\right)\Delta\theta. \tag{11.24}$$

The solutions are plotted in Fig. 11.6 and Fig. 11.7. Perhaps the single most important aspect of the model is that it predicts that the Hadley Cell has a *finite* meridional extent, *even for an atmosphere that is completely zonally symmetric.* The baroclinic instability that does occur in midlatitudes is not necessary for the Hadley Cell to terminate in the subtropics, although it may be an important factor, or even the determining factor, in the real world. More specifically, the model predicts the the latitudinal extent of the Hadley cell is: (i) proportional to the square root of the meridional temperature gradient; (ii) proportional to the square root of the height of the outward flowing branch; (iii) inversely proportional to the rotation rate Ω.

Zonal wind

The angular momentum conserving zonal wind is given by (11.7), which in the small angle approximation becomes

$$U_M = \Omega\frac{y^2}{a}. \tag{11.25}$$

This holds for $y < Y_H$. The zonal wind corresponding to the radiative-equilibrium solution is given using thermal wind balance and (11.16), which leads to

$$u_E = \Omega a R. \tag{11.26}$$
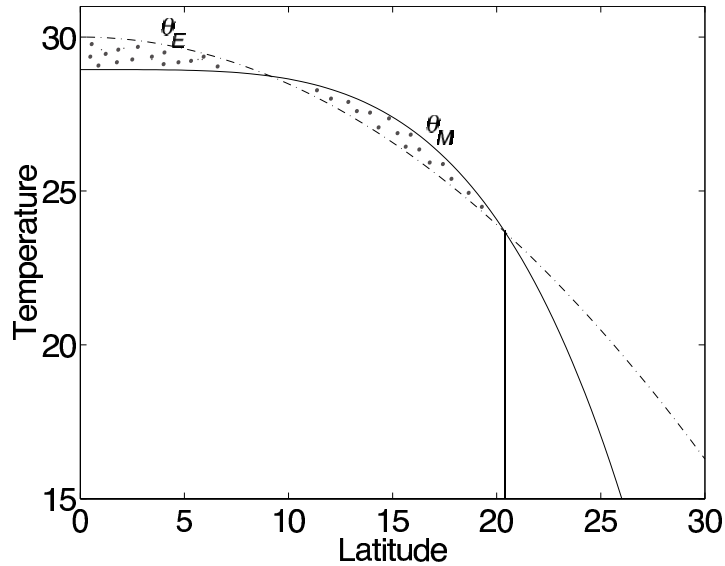
Fig. 11.6 The radiative equilibrium temperature (θ_E, dashed line) and the angular-momentum-conserving solution (θ_M, solid line) as a function of latitude. The two dotted regions have equal areas. The parameters chosen which give the solution here are: $\theta_{EO} = 303\,$K, $\Delta\theta = 50\,$K, $\theta_0 = 300\,$K, $\Omega = 7.272 \times 10^{-5}\,$s^{-1}, $g = 9.81\,$m s^{-2}, $H = 10\,$km. These give values of $R = 0.076$ and $Y_H/a = 0.356$, with a corresponding latitude for the edge of the Hadley Cell of 20.4°.

That the radiative equilibrium zonal wind is a constant follows from our choice of the second Legendre function for the radiative equilibrium temperature and is not a fundamental result; nonetheless, for most reasonable choices of θ_E the corresponding zonal wind will vary much less than the angular momentum conserving wind (11.25). The winds are illustrated in Fig. 11.7. There is a discontinuity in the zonal wind at the edge of the Hadley Cell, and of the meridional temperature gradient, but not of the temperature itself.

11.2.3 Properties of solution

We can see that the model predicts that the latitudinal extent of the Hadley Cell is:

★ Proportional to the square root of the meridional radiative equilibrium temperature gradient — the stronger the gradient, the farther the circulation must extend to achieve thermodynamic balance via the equal area construction in Fig. 11.6;

★ Proportional to the square root of the height of the outward flowing branch — the higher the outward flowing branch, the weaker the ensuing temperature gradient of the solution (via thermal wind balance), and so the further polewards the circulation must go;
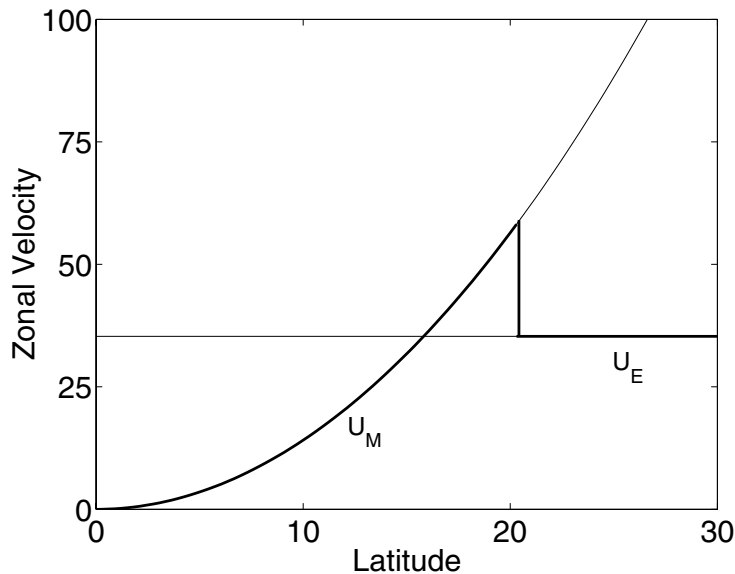
Fig. 11.7 The zonal wind corresponding to the radiative equilibrium temperature (u_E) and the angular-momentum-conserving solution (u_M) as a function of latitude, using (11.25) and (11.26). The parameters are the same as those of Fig. 11.6. The radiative equilibrium wind is a constant, $\Omega a R$, which for these parameters is about $35\,\mathrm{m\,s^{-1}}$. The actual zonal wind (in the model) follows the thick solid line: for $\vartheta < \vartheta_H$ ($y < Y_H$), the angular momentum solution holds, but the radiative equilibrium solution holds for $\vartheta > \vartheta_H$, with a discontinuity at ϑ_H.

* ⋆ Inversely proportional to the rotation rate Ω — the stronger the rotation rate, the stronger the angular momentum conserving wind, the stronger the ensuing temperature gradient and so the more compact the circulation.

These precise dependencies on particular powers of parameters are not especially important, nor robust. For example, had we chosen a meridional distribution of radiative equilibrium temperature different from (11.14) we would find different powers, but nevertheless the qualitative dependencies would remain. With reasonable parameters, the predicted extent of the Hadley Cell is indeed comparable with the observations.

Furthermore, for tropical latitudes (i.e., $y < Y_H$), then $\overline{u} = U_M$, the constant angular momentum solution, whereas for $y > Y_H$, $\overline{u} = U_E$, the radiative equilibrium temperature (discussed below) and $\theta = \theta_E$. There is thus a discontinuity of $\overline{u}$ at $y = Y_H$, because u is related to the meridional gradient of θ which changes discontinuously, but θ itself is continuous. Such a discontinuity is likely to to be barotropically unstable, and so produce eddying motion and a momentum transport that tries to smooth the discontinuity.

11.2.4 Strength of the circulation

We can make an estimate of the strength of the Hadley Cell by consideration of the thermodynamic equation at the equator, namely

$$w \frac{\partial \theta}{\partial z} \approx \frac{\theta_{E0} - \theta}{\tau}, \tag{11.27}$$

a balance between adiabatic cooling and radiative heating. If the static stability is determined largely by the forcing, and not by the meridional circulation itself, then

$$\frac{1}{\theta_0} \frac{\partial \theta}{\partial z} \approx \frac{\Delta_V}{H}. \tag{11.28}$$

and so

$$w \approx \frac{H}{\theta_0 \Delta_V} \frac{\theta_{E0} - \theta}{\tau}. \tag{11.29}$$

Thus, the circulation is proportional to the distance of the solution from the radiative equilibrium temperature. The right-hand side of (11.27) can be evaluated from the solution itself, and from (11.24) we have

$$\frac{\theta_{E0} - \theta}{\tau} = \frac{5R\Delta\theta}{18\tau}. \tag{11.30}$$

The vertical velocity is then given by

$$w \approx \frac{R\Delta\theta H}{\tau \Delta_V \theta_0} = \frac{R\Delta_H H}{\tau \Delta_V}. \tag{11.31}$$

Using mass continuity we can transform this into an estimate for the meridional velocity. Thus, if we let

$$\frac{v}{Y_H} \sim \frac{w}{H} \tag{11.32}$$

and use (11.23), we obtain

$$v \sim \frac{R^{3/2} a \Delta_H}{\tau \Delta_V} \propto \frac{\Delta_H^{5/2}}{\Delta_V}, \tag{11.33}$$

and the mass flux, or the meridional overturning stream function Ψ, of the circulation scales as

$$\Psi \sim vH \sim \frac{R^{3/2} a H \Delta_H}{\tau \Delta_V} \propto (\Delta\theta)^{5/2}. \tag{11.34}$$

This evidently increases fairly rapidly as the gradient of the radiative equilibrium temperature increases. The characteristic overturning time of the circulation, τ_d is then

$$\tau_d = \frac{H}{w} \sim \frac{\tau \Delta_V}{R\Delta_H}. \tag{11.35}$$

We require $\tau_d/\tau \gg 1$ for the effects of the circulation on the static stability to be small and therefore $\Delta_V/\Delta_H \gg 1$, or equivalently, using (11.27).

$$\theta_0 \Delta_V \gg (\theta_E - \theta). \tag{11.36}$$

If the converse were true, and $\tau \gg \tau_d$, then potential temperature would be nearly conserved as a parcel ascended in the rising branch of the Hadley Cell, and the static stability would be nearly neutral.

11.2.5 Effects of moisture

Suppose now that moisture is present, but that the Hadley Cell remains a self-contained system — that is, it neither imports nor exports moisture. We envision that water vapour joins the circulation by way of evaporation from a saturated surface into the equatorward, lower branch of the Hadley cell, and that this water vapour then condenses in and near the upward branch of the cell. The latent heat released by condensation is exactly equal to the heat required to evaporate moisture from the surface, and no heat is lost or gained to the system. However, the heating *distribution* is changed from the dry case, becoming a strong function of the solution itself and likely with a sharp maximum near the equator. Even if we were to try to parameterize this by simply choosing a flow dependent radiative equilibrium temperature, the resulting problem would still be quite nonlinear and a general analytic solution seems out of our reach.[4]

Nevertheless, we may see quite easily the qualitative features of moisture, at least within the context of this model. The meridional distribution of temperature is still given by way of thermal wind balance with an angular momentum conserving zonal wind, and so is still given by (11.12). We may assume that a solution exists with circulation confined to $\vartheta < \vartheta_H$, that is that the extent of the Hadley Cell is unaltered (although it may not be the unique solution). Then, if θ_E^* is the effective radiative equilibrium temperature of the moist solution, we have that $\theta_E^*(Y_H) = \theta_E(Y_H)$ and, in the small angle approximation,

$$\int_0^{Y_H} \theta \, \mathrm{d}y = \int_0^{Y_H} \theta_E^* \, \mathrm{d}y = \int_0^{Y_H} \theta_E \, \mathrm{d}y \tag{11.37}$$

where the first equality holds because it defines the solution, and the second equality holds because moisture provides no net energy source. Because condensation will occur mainly in the upward branch of the Hadley Cell, θ_E^* will be peaked near the equator, as schematically sketched in Fig. 11.8. This construction makes it clear that the main difference between the dry and moist solutions is that the latter has a much more intense overturning circulation, because, from (11.27), this increases with the temperature difference between the solution and the forcing temperature. Concomitantly, the upward branch of the moist Hadley circulation will become much narrower and more intense than the downward branch, and these expectations are confirmed by numerical integrations of the three-dimensional moist equations of motion.

11.2.6 The radiative equilibrium solution

Instead of a solution given by (11.12), could be temperature not be simply be radiative equilibrium temperature everywhere? Such a state would have no meridional overturning circulation and the zonal velocity would be determined by thermal wind balance; that is

$$v = 0, \qquad \theta = \theta_E, \qquad f\frac{u}{H} = -g\frac{\partial}{\partial y}\left(\frac{\theta_E}{\theta_0}\right). \tag{11.38}$$

To answer this question we consider the steady zonally-symmetric zonal angular momentum equation with viscosity; that is, the zonally-averaged, viscous, steady, shallow
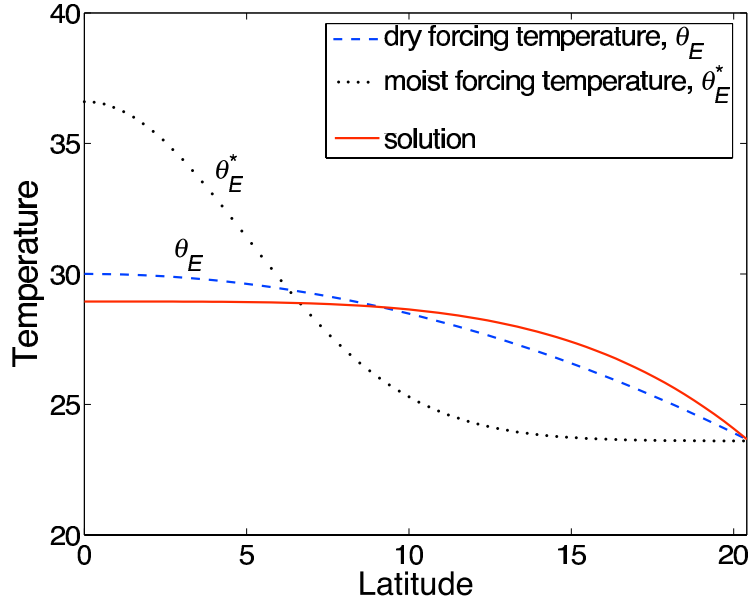
Fig. 11.8 Schematic of the effects of moisture on a model of Hadley cell. The temperature of the solution (solid line) is the same as that of a dry model, because this is determined from the angular momentum conserving wind. The heating distribution (as parameterized by a forcing temperature) is peaked near the equator in the moist case, leading to a more vigorous overturning circulation.

atmosphere version of (2.69), namely

$$\frac{1}{a \cos \vartheta} \frac{\partial}{\partial \vartheta} (vm \cos \vartheta) + \frac{\partial(mw)}{\partial z} = \nu \nabla^2 m, \qquad (11.39)$$

or, in a compact notation,

$$\nabla_x \cdot (\boldsymbol{v} m) = \nu \nabla_x^2 m, \qquad (11.40)$$

where the variables vary only in the ϑ-z, or y-z, plane. Now, in section 10.5.1 we showed that equations of this form can have no extrema of the advected variable within the fluid, m in this case.   Thus, there can be no maximum or minimum of angular momentum in the interior of the fluid.[5] In effect, diffusion always acts to smooth away an isolated extremum, and this cannot be counterbalanced by advection. The result also implies that there cannot be any interior extrema in a statistically steady state if there is any zonally asymmetric eddy motion that transports angular momentum downgradient.

As an aside, we note that maxima of m can, however, occur at the surface. Suppose we add a surface stress to the right-hand side of (11.40), and that this stress acts in the opposite direction to that of the zonal wind. Then, in a region of surface easterlies the surface stress contribution would be positive, acting as a source of postive angular momentum, and there exists the possibility that this will exactly balance the diffusion term away from the surface so that the right-hand side of (11.40) would be zero surrounding

the maximum. However, such a surface stress does not allow this maximum to be a region of surface westerlies at the equator, because the stress would then act in the same way as the diffusion and act to reduce the angular momentum.

Now, returning to the question posed at the head of this section, suppose that the radiative equilibrium solution does hold. Then a radiative equilibrium temperature decreasing away from the equator more rapidly than the angular momentum conserving solution θ_M implies, using thermal wind balance, a maximum of m at the equator and above ther surface, in violation of the no-extremum principle. Of course, we have derived the angular momentum conserving solution in the inviscid limit, in which the principle does not apply. But any small viscosity will make the radiative equilibrium solution completely invalid, but have only a small effect on the angular momentum conserving solution; that is, in the *limit of small viscosity* the angular momentum conserving solution can still approximately hold, whereas the radiative equilibrium solution cannot.

However, if the radiative equilibrium temperature varies more slowly with latitude than the temperature corresponding to the angular momentum conserving solution then a radiative equilibrium solution *can* pertain, without violating Hide's theorem. In particular, this is the case if $\theta_E \propto P_4(\sin \vartheta)$, where P_4 is the fourth Legendre polynomial, and so the possibility exists of two equilibrium solutions for the same forcing. However, P_4 is an unrealistically flat radiative equilibrium temperature for the earth's atmosphere.

11.3 A SHALLOW WATER MODEL OF THE HADLEY CELL

Although expressed in the notation of the primitive equations, the model described above takes no account of any vertical structure in its stratification and is, *de facto,* a shallow water model. Furthermore, the geometric aspects of sphericity play no essential role. Thus, we may transparently express the essence of the model by:

 (i) Explicitly using the shallow water equations instead of the stratified equations;

 (ii) Using the β-plane instead of spherical coordinates.

Let us therefore construct a 'reduced-gravity' model with an active upper layer overlying a stationary lower layer.

11.3.1 Momentum balance

The inviscid zonal momentum equation of the upper layer is

$$\frac{\mathrm{D}u}{\mathrm{D}t} - \beta y v = 0 \tag{11.41}$$

or

$$\frac{\mathrm{D}}{\mathrm{D}t}\left(u - \frac{\beta y^2}{2}\right) = 0. \tag{11.42}$$

which is the β-plane analog of the conservation of axial angular momentum. (In this section, all variables are zonally averaged, but we omit any explicit notation denoting

this.) From (11.42) we obtain the zonal wind as a function of latitude,

$$u = \frac{1}{2}\beta y^2 + A. \tag{11.43}$$

where A is a constant, which is zero if $u = 0$ at the 'equator', $y = 0$. The flow given by (11.43) is then analogous to the angular momentum conserving flow in the spherical model, (11.7). Because the lower layer is stationary, the analog of thermal wind balance in the stratified model is just geostrophic balance, namely

$$fu = -g'\frac{\partial h}{\partial y}, \tag{11.44}$$

where h is the thickness of the active upper layer. Using (11.44) and $f = \beta y$ we obtain

$$g'\frac{\partial h}{\partial y} = -\frac{1}{2}\beta^2 y^3 \tag{11.45}$$

giving

$$h = -\frac{1}{8g'}\beta^2 y^4 + h(0) \tag{11.46}$$

where $h(0)$ is the value of h at $y = 0$.

11.3.2 Thermodynamic Balance

The thermodynamic equation in the shallow water equations is just the mass conservation equation, which we write as

$$\frac{\mathrm{D}h}{\mathrm{D}t} = -\frac{1}{\tau}(h - h^*), \tag{11.47}$$

where the right-hand side represents heating — h^* is the field to which the height relaxes on a timescale τ. For illustrative purposes we will choose

$$h^* = h_0(1 - \alpha|y|). \tag{11.48}$$

(If we chose the more realistic quadratic dependence on y, the model would be more similar to that of the previous section.) To be in thermodynamic equilibrium we require that the right-hand side integrates to zero over the Hadley Cell; that is

$$\int_0^Y (h - h^*)\,\mathrm{d}y = 0 \tag{11.49}$$

where Y is the latitude of the poleward extent of the Hadley Cell, thus far unknown. Poleward of this, the height field is simply in equilibrium with the forcing — there is no meridional motion and $h = h^*$. Since the height field must be continuous, we require that

$$h(Y) = h^*(Y). \tag{11.50}$$

The two constraints (11.49) and (11.50) provide values of the unknowns $h(0)$ and Y, and give

$$Y = \left(\frac{5h_0 \alpha g'}{\beta^2} \right)^{1/3}, \tag{11.51}$$

which is analogous to (11.20), and an expression for $h(0)$ that we leave as a problem for the reader. The qualitative dependence on the parameters is similar to that of the full model, although the latitudinal extent of the Hadley Cell is proportional to the cube root of the meridional thickness gradient α.

11.4 † ASYMMETRY AROUND THE EQUATOR

The sun is overhead at the equator but two days out of the year, and in this section we investigate the effects that asymmetric heating has on the Hadley circulation. Observations indicate except for the brief periods around the equinoxes, the circulation is dominated by single cell with rising motion centered in the summer hemisphere, but extending well into the winter hemisphere. That is, as seen in Fig. 11.3, the 'winter cell' is broader and stronger than the 'summer cell', and it behooves us to try to explain this. We will stay in the framework of the inviscid angular-momentum model of section 11.2, changing only the forcing field to represent the asymmetry and being a little more attentive to the details of spherical geometry.[6]

To represent an asymmetric heating we may choose a radiative equilibrium temperature of the form

$$\begin{aligned}
\frac{\theta_E(\vartheta, z)}{\theta_0} &= 1 - \frac{2}{3} \Delta_H P_2 (\sin \vartheta - \sin \vartheta_0) + \Delta_V \left(\frac{z}{H} - \frac{1}{2} \right) \\
&= 1 + \frac{\Delta_H}{3} \left[1 - 3(\sin \vartheta - \sin \vartheta_0)^2 \right] + \Delta_V \left(\frac{z}{H} - \frac{1}{2} \right).
\end{aligned} \tag{11.52}$$

This is similar to (11.14), but now the forcing temperature falls monotonically from a specfied latitude ϑ_0. If $\vartheta_0 = 0$ the model is identical to the earlier one but if not then w we might then envision a circulation as qualitatively sketched in Fig. 11.9, with rising motion off the equator at some latitude ϑ_1, extending into the winter hemisphere to a latitude ϑ_w, and into the summer hemisphere to ϑ_s. It turns out that, in general, $\vartheta_1 \neq \vartheta_0$ except when $\vartheta_0 = 0$, as we will discover. Following our previous procedure as closely as possible, we then make the following assumptions:

(i) The flow is quasi-steady. That is, for any given time of year the flow adjusts to a steady circulation on a timescale more rapid than that on which the solar zenith angle appreciably changes. Then, even though the forcing is time-dependent, we neglect local time derivatives in the momentum and thermodynamic equations.

(ii) The flows in the upper branches conserve angular momentum, m. Further assuming that $u = 0$ at $\vartheta = \vartheta_1$ so that $m = \Omega a^2 \cos^2 \vartheta_1$ we obtain

$$u(\vartheta) = \frac{\Omega a (\cos^2 \vartheta_1 - \cos^2 \vartheta)}{\cos \vartheta}. \tag{11.53}$$
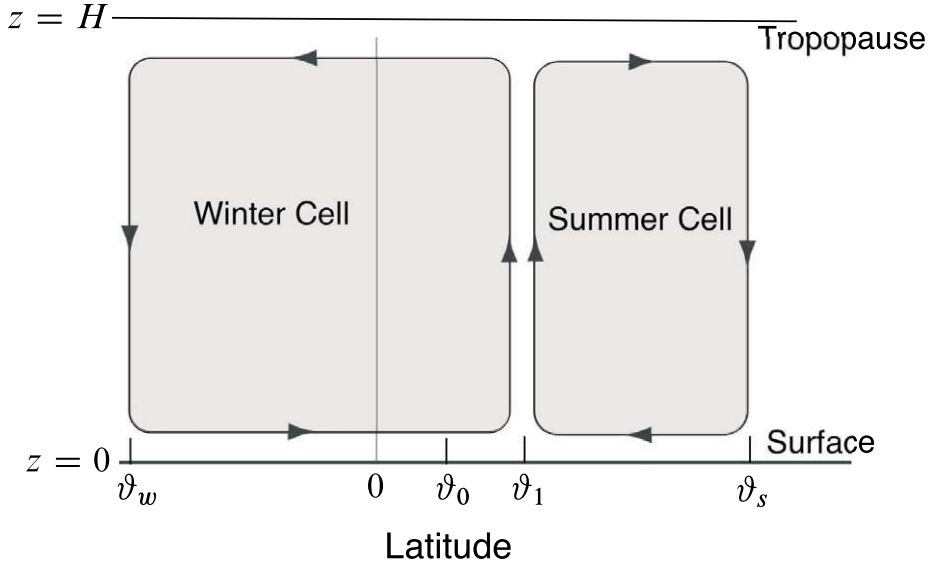
Fig. 11.9 Schematic of a Hadley circulation model when the heating is centered off the equator, at a latitude ϑ_0. The lower level convergence occurs at a latitude ϑ_1 not in general equal to ϑ_0. The resulting winter Hadley Cell is stronger and wider than the summer cell.

Thus, we expect to see westward (negative) winds aloft at the equator. In the lower branches the zonal flow is assumed to be approximately zero, i.e., $u(0) \approx 0$.

(iii) The flow satisfies cyclostrophic and hydrostatic balance. Cyclostrophic balance is

$$ fu + \frac{u^2 \tan \vartheta}{a} = -\frac{1}{a}\frac{\partial \phi}{\partial \vartheta} \tag{11.54} $$

and because the flow crosses the equator we cannot neglect the second term on the left-hand side. Combining this with hydrostatic balance ($\partial \phi / \partial z = g\theta/\theta_0$) leads to a generalized thermal wind balance, which may be written as

$$ m\frac{\partial m}{\partial z} = -\frac{ga^2 \cos^2 \vartheta}{2\theta_0 \tan \vartheta}\frac{\partial \delta \theta}{\partial \vartheta} \tag{11.55} $$

If the undifferentiated m is approximated by $\Omega a^2 \cos^2 \vartheta$, this reduces to conventional thermal wind balance, (11.10). The form of (11.55) is useful because we are assuming that m is conserved, and so from it we can immediately infer the temperature distribution.

(iv) Potential temperature in each cell is conserved when integrated over the extent of the cell. Thus,

$$ \int_{\vartheta_1}^{\vartheta_s} (\theta - \theta_E) \cos \vartheta \, \mathrm{d}\vartheta = 0, \qquad \int_{\vartheta_1}^{\vartheta_w} (\theta - \theta_E) \cos \vartheta \, \mathrm{d}\vartheta = 0, \tag{11.56} $$

for the summer and winter cells, respectively, where θ is the vertically averaged potential temperature.

(v) Potential temperature is continuous at the edge of each cell, so that

$$\theta(\vartheta_s) = \theta_E(\vartheta_s), \qquad \theta(\vartheta_w) = \theta_E(\vartheta_w), \tag{11.57}$$

and is also continuous at ϑ_1. This last condition must be explicitly imposed in the asymmetric model, whereas in the symmetric model it holds by symmetry. Now, recall from the symmetric model that the value of the temperature at the equator was determined by the integral constraint (11.18) and the continuity constraint (11.19). We have analogs of these in each hemisphere [(11.56) and (11.57)] and thus, if ϑ_1 is set equal to ϑ_0 we cannot expect that they each would give the same temperature at ϑ_0. Thus. ϑ_1 must be a free parameter to be determined.

Given these assumptions, the solution may be calculated. Using thermal wind balance, (11.55), with $m(H) = \Omega a^2 \cos^2 \vartheta_1$ and $m(0) = \Omega a^2 \cos^2 \vartheta_1$ we find

$$\frac{\partial \theta}{\partial \vartheta} = \frac{\Omega^2 a^2}{gH} \left(\frac{\sin \vartheta}{\cos^3 \vartheta} \cos^4 \vartheta_1 - \sin \vartheta \cos \vartheta \right) \tag{11.58}$$

which integrates to

$$\theta(\vartheta) - \theta(\vartheta_1) = \frac{\Omega^2 a^2}{2gH} \frac{(\sin^2 \vartheta - \sin^2 \vartheta_1)^2}{\cos^2 \vartheta}. \tag{11.59}$$

The value of ϑ_1, and the value of $\theta(\vartheta_1)$, are determined by the constraints (11.56) and (11.57). It is not in general possible to obtain a solution analytically, but one may be found numerically by an iterative procedure and one such is illustrated in Fig. 11.10. The zonal wind is of the solution is always symmetric around the equator, because it is determined solely by angular momentum conservation, and so, therefore, is temperature — as (11.59) explictly shows. However, the width of the solution in each hemisphere will, in general, be different. Furthermore, because the strength of the circulation increases with difference between the temperature of the solution and the radiative equilibrium temperature, the circulation in the winter hemisphere will also be much stronger than that in the summer (Fig. 11.3), a prediction that is qualitatively consistent with the observations. More detailed calculations show that, because the strength of the model Hadley cell increases nonlinearly with ϑ_0, the time-average strength of the Hadley Cell with seasonal forcing is stronger that that produced by annually-averaged forcing. However, this does not appear to be a feature of either the observations or more complete complete numerical simulations, suggesting that an angular-momentum conserving model has, at least, quantitative deficiences.[8] Possible weaknesses of the model include:

(i) The quasi-steady assumption in the presence of a seasonal cyle. Because the latitude of the upward branch of the Hadley Cell is varying with season, the value of the angular momentum entering the system also varies, and so a homogenized
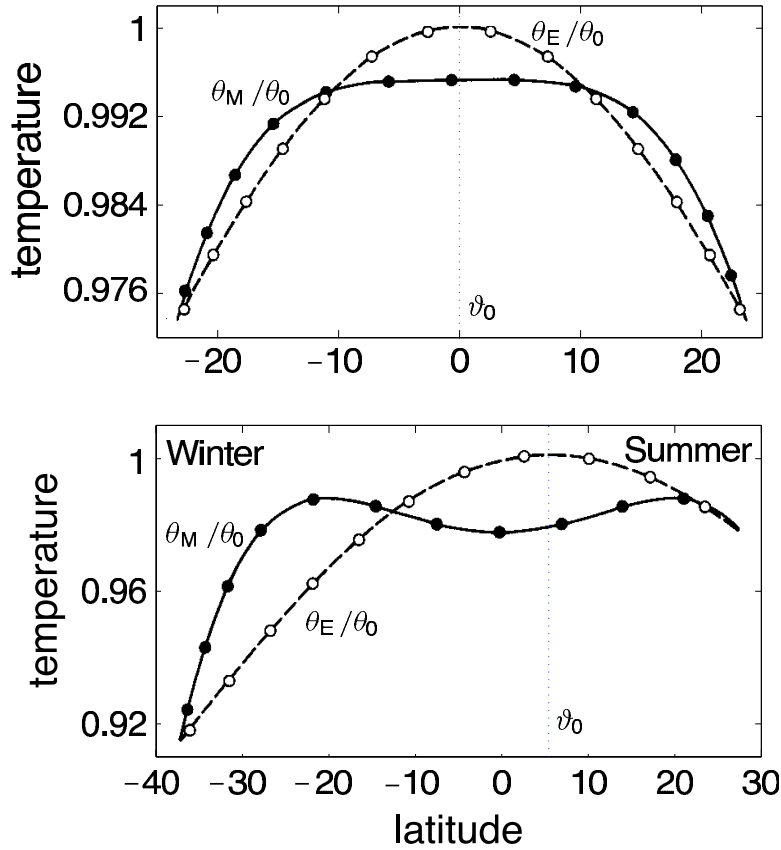
Fig. 11.10 Solutions of the Hadley Cell model with heating centered at the equator ($\vartheta_0 = 0°$, top) and off the equator ($\vartheta_0 = +6°$ N, bottom), with $\Delta_H = 1/6$. Dashed line is the radiative equilibrium temperature, and the solid line the angular-momentum conserving solution. In the lower panel, $\vartheta_1 \approx +18°$, and the circulation is dominated by the cell extending from $+18°$ to $-36°$.[7]

value of angular momentum is hard to achieve. That is, if τ_s is the seasonal timescale we require

$$\tau_s \gg \tau_e, \tag{11.60}$$

where τ_e is some dynamical equilibration timescale, similar to the dynamical timescale $\tau_d = H/w$ (section 11.2.4).

(ii) The lack of consideration of zonal asymmetries, such as monsoonal circulations.

(iii) The lack of angular momentum conservation, even in a steady model with zonally symmetric boundary conditions. Such nonconservation will arise if either diffusion of momentum caused by small-scale turbulence, or the angular momentum transport by baroclinic eddies, are significant.

11.5 EDDIES, VISCOSITY AND THE HADLEY CELL

So far, we have ignored the effects of baroclinic eddies on the Hadley circulation — 'ignored' rather than 'neglected', because we have no *a priori* or observational reason to believe that their effects will be negligible. If their effects are strong, then none of the models we discussed above will be quantitatively valid. With this in mind, in this section we look at the Hadley circulation from a quite different perspective, by supposing that the zonal momentum equation is linear, save for the effects of eddy fluxes on the right-hand side. Our approach is illustrative, not quantitative, and we stay again within the Boussinesq approximation.

We might expect eddy fluxes to be important because the angular momentum conserving solution will develop a large vertical shear and if this extends sufficiently far polewards it will become baroclinically unstable (compare Fig. 11.7 with the mininum shear needed for baroclinic instability sketched in Fig. 6.16). It is a quantitative issue as to whether the Hadley flow becomes strongly unstable before it reaches its polewards extent, and if it does not the angular momentum conserving solution can be expected to be a good one. But let us here assume that the flow is strongly unstable and that the ensuing instability transfers both heat and angular momentum polewards (the mechanisms of this are discussed in the next chapter).

11.5.1 Qualitative considerations

The zonally-averaged zonal momentum equation (11.4) may be written (restoring the overbar on zonally averaged quantities) as an equation for angular momentum, $\overline{m}$,

$$
\frac{\partial \overline{m}}{\partial t} + \frac{1}{\cos \vartheta} \frac{\partial}{\partial y} (\overline{v}\,\overline{m} \cos \vartheta) + \frac{\partial}{\partial z} (\overline{w}\,\overline{m})
$$
$$
= -\frac{1}{\cos \vartheta} \frac{\partial}{\partial y} (\overline{u'v'} a \cos^2 \vartheta) - \frac{\partial}{\partial z} (\overline{u'w'} a \cos \vartheta). \tag{11.61}
$$

where $\overline{m} = (\overline{u} + \Omega a \cos \vartheta) a \cos \vartheta$, $y = a\vartheta$, and the vertical and meridional velocities are related by the mass continuity relation

$$
\frac{1}{\cos \vartheta} \frac{\partial}{\partial y} (\overline{v} \cos \vartheta) + \frac{\partial \overline{w}}{\partial z} = 0. \tag{11.62}
$$

(See section 2.2.) In the angular momentum conserving model the eddy fluxes were neglected and (11.61) was approximated by the simple expression $\partial \overline{m}/\partial y = 0$. The observed values of these eddy terms on the right-hand side are shown in Fig. 11.11. The eddy momentum flux is polewards over most of the midltatitudes in both summer and winter and, although it has a maximum value between 30° and 45°, depending on hemisphere and season, its magnitude, and more particularly its meridional gradient, are not obviously negligible. Neglecting vertical advection and vertical eddy fluxes, (11.61) may be written

$$
\frac{\partial \overline{m}}{\partial t} + \overline{v} \frac{\partial \overline{m}}{\partial y} = -\frac{1}{\cos \vartheta} \frac{\partial}{\partial y} (\overline{u'v'} a \cos^2 \vartheta). \tag{11.63}
$$
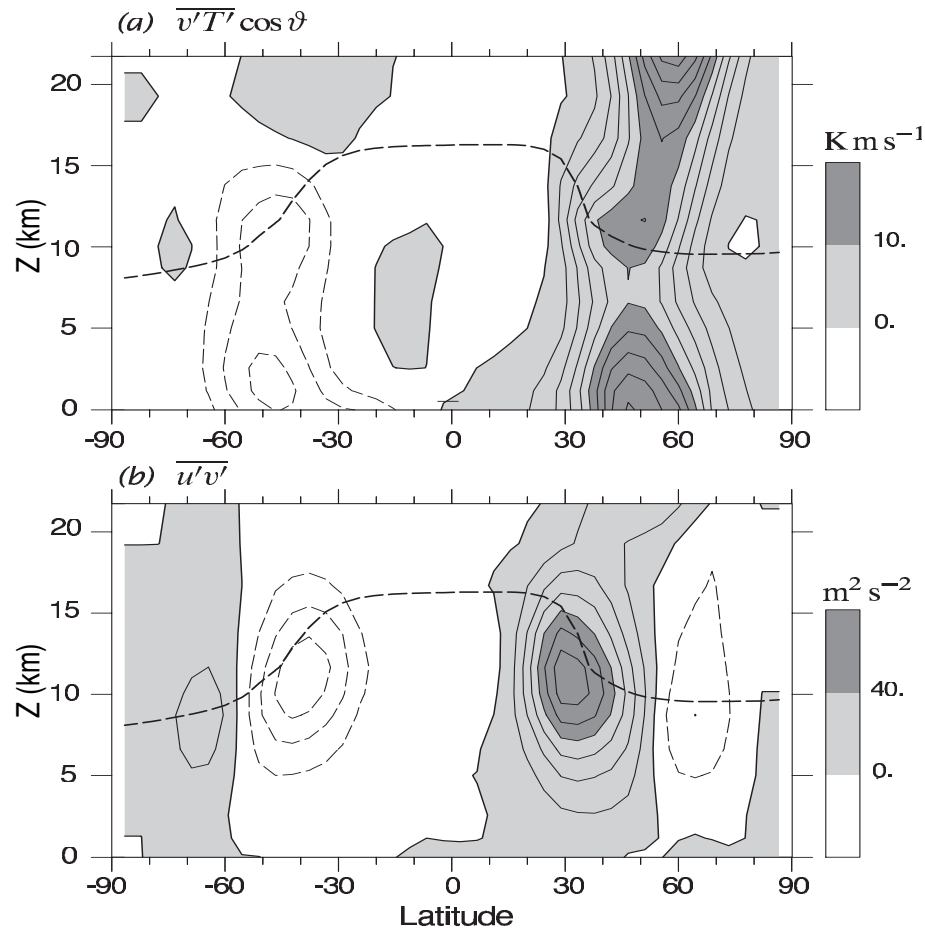
Fig. 11.11 (a) The average meridional eddy heat flux and (b) and the eddy momentum flux in northern hemisphere winter (DJF). The ordinate is $Z = -H \log(p/p_{00})$, with scale height $H = 7.5$ km. Positive (northward) fluxes are shaded in both cases, and the dashed line marks the thermal tropopause. The eddy heat flux (contour interval 2 K m s^{-1}) is largely pole-wards, and down the temperature gradient, in both hemispheres. The eddy momentum flux (contour interval 10 m^2 s^{-2}) *converges* in midlatitudes in the region of the mean jet, and must be upgradient there.[9]

Thus, if $\overline{v} > 0$ (as in the upper branch of the Northern Hemisphere Hadley Cell) and the flow is steady, the eddy fluxes are such as to cause the angular momentum of the zonal flow to decrease as it moves polewards, and the zonal velocity would be lower than it would be in the absence of eddies. (In the Southern Hemisphere the signs of v and the eddy momentum flux are reversed, but the dynamics are equivalent.) Note that we cannot *a priori* determine whether eddies are likely to be important by comparing the magnitudes of the eddy terms with the terms on the left-hand side of (11.63) in the angular momentum conserving solution, because in that solution these terms are

individually zero. Rather, we should compare the eddy fluxes to $\overline{v}\partial m^*/\partial y$, where $m^* = \Omega a^2 \cos \vartheta$ is the angular momentum of the solid earth.

The eddy flux of heat will also affect the Hadley Cell, although in a different fashion. We see from Fig. 11.11 that the eddy flux of temperature is predominantly polewards, and therefore that eddies export heat from the subtropics to higher latitudes. Now, the zonally averaged thermodynamic equation may be written

$$
\frac{\partial \overline{b}}{\partial t} + \frac{1}{\cos \vartheta} \frac{\partial}{\partial y} (\overline{vb} \cos \vartheta) + \frac{\partial}{\partial z} (\overline{wb})
$$
$$
= -\frac{1}{\cos \vartheta} \frac{\partial}{\partial y} (\overline{v'b'} \cos \vartheta) - \frac{\partial}{\partial z} (\overline{w'b'}) + Q[b].
$$
(11.64)

where $Q[b]$ represents the heating. On vertical averaging the vertical advection terms vanish and the resulting equation is the thermodynamic equation implicitly used in the angular momentum conserving model, with the addition of the merfional eddy flux on the right-hand side. If this is taken as given, then a diverging eddy heat flux in the subtropics (as in Fig. 11.11) is equivalent to increasing the meridional gradient of the radiative equilibrium temperature, and therefore will increase the intensity of the overturning circulation.

11.5.2 A simple eddy-driven model

Consider now the extreme case of an 'eddy-driven' Hadley Cell. (The driving for the Hadley Cell, and the atmospheric circulation in general, ultimately comes from the differential heating between equator and pole. Recognizing this, 'eddy driving' is a convenient way to refer to the mediating role of eddies in producing a zonally-averaged circulation.) The model is over-simple, but revealing. The zonally-averaged zonal momentum equation (11.4) may be written as

$$
\frac{\partial \overline{u}}{\partial t} - (f + \overline{\zeta})\overline{v} = -\frac{1}{\cos^2 \vartheta} \frac{\partial}{\partial \vartheta} (\cos^2 \vartheta \overline{u'v'}).
$$
(11.65)

If the Rossby number is sufficiently low this becomes simply

$$
\frac{\partial \overline{u}}{\partial t} - f\overline{v} = M
$$
(11.66)

where M represents the eddy terms. This approximation is not quantitatively accurate (indeed earlier we assumed $f + \overline{\zeta} = 0$!) but it will highlight the role of the eddies. At a similar level of approximation let us write the thermodynamic equation, (11.64), as

$$
\frac{\partial \overline{b}}{\partial t} + N^2 w = J
$$
(11.67)

where $J = Q[b] - (\cos \vartheta)^{-1} \partial_y (\overline{v'b'} \cos \vartheta)$ represents the diabatic terms and eddy forcing. We are assuming, as in quasi-geostrophic theory, that the mean stratification,

N^2 is fixed, and now $\overline{b}$ represents only the (zonally-averaged) deviations from this. If we simplify further by using Cartesian geometry then the mass conservation is

$$\frac{\partial \overline{v}}{\partial y} + \frac{\partial \overline{w}}{\partial z} = 0. \tag{11.68}$$

and we may define a meridional streamfunction Ψ such that

$$\overline{w} = \frac{\partial \Psi}{\partial y}, \qquad \overline{v} = -\frac{\partial \Psi}{\partial z} \tag{11.69}$$

We may then use the thermal wind relation,

$$f\frac{\partial \overline{u}}{\partial z} = -\frac{\partial \overline{b}}{\partial y}. \tag{11.70}$$

to eliminate time-derivatives in (11.66) and (11.67), giving

$$f^2 \frac{\partial^2 \Psi}{\partial z^2} + N^2 \frac{\partial^2 \Psi}{\partial y^2} = f\frac{\partial M}{\partial z} + \frac{\partial J}{\partial y}. \tag{11.71}$$

This is a linear equation for the overturning streamfunction, one that holds even if the flow is not in a steady state, and we see that the overturning circulation is forced by eddy fluxes of heat and momentum, as well as heating and other terms that might appear on the right-hand sides of (11.66) and (11.67). If we rescale the vertical coordinate by the Prandtl ratio (i.e., let $z = z'f/N$) then (11.71) is a Poisson equation for the streamfunction. A few other germane points are:

(i) The horizontal gradient of the thermodynamic forcing partially drives the circulation. In low latitudes, both the heating term and the horiontal eddy flux divergence act in the same sense. An overturning circulation that is forced by diabatic terms, and so with warm fluid rising and cold fluid sinking, is called a 'direct cell'.

(ii) The vertical gradient of the horizontal eddy momentum divergence also partially drives the circulation, and from Fig. 11.11 it is clear these fluxes will intensify the circulation. That is, the same terms that cause angular momentum nonconservation act to strengthen the overturning circulation. This balance is reflected in the momentum equation — the Coriolis term fv is balanced by the eddy momentum flux convergence.

(iii) If M contains frictional terms, such as $\nu \partial^2 u / \partial z^2$, then these may also act to strengthen the meridional circulation.

(iv) If N is small, then the circulation will become stronger if the other terms remain the same. Thus, for example, in a dry atmosphere with a lapse rate close to zero the dry adiabatic lapse rate may have a stronger overturning circulation, because the air can circulate without transporting any heat.

We can generalise (11.71) somewhat by replacing (11.66) by (11.63),

$$\frac{\partial \overline{m}}{\partial t} + \overline{v}\frac{\partial \overline{m}}{\partial y} = M \tag{11.72}$$

Then, using thermal wind equation in the form

$$\frac{f}{a\cos\vartheta}\frac{\partial \overline{m}}{\partial z} = -\frac{\partial \overline{b}}{\partial y}. \tag{11.73}$$

an equation very similar to (11.71) may be derived. However, the coefficients on the left-hand side are functions of the solution, and $f^2\partial^2\Psi/\partial z^2$ is replaced by a term like $f\partial\overline{m}/\partial y\,\partial^2\Psi/\partial z^2$. Then, to the extent that $\partial\overline{m}/\partial y < f$ and the other terms are the same, the overturning will be stronger than that given using (11.71).[10]

11.5.3 Summary

We have presented two models for the Hadley Cell: (i) An angular momentum conserving model and (ii) A largely eddy-driven model. These are the opposite extremes, and both are severe approximations to a more complete representation of the Hadley Cell comprising the zonal momentum equation (11.61), the thermodynamic equation (11.64), and thermal wind balance. In reality, both the conservation of angular momentum and eddy fluxes play a role, and delineating the importance of their respective roles is a task that must be guided by observations and numerical simulations. Illustrative results from two idealized GCM experiments are shown in Fig. 11.12 and Fig. 11.13. The GCM has no explicit representation of moisture, except that the lapse rate is adjusted to a value close to the moist adiabatic lapse rate if exceeds that value. In one experiment the model is constrained to produce an axi-symmetric solution (top panels of the figures), and the zonal wind produced by the model in the Hadley Cell outflow is fairly close to being angular momentum conserving. (The lack of perfect angular momentum conservation may be due to a stress at the upper boundary, which is neglected in the analytic model, and the strength of the Hadley Cell is also more dependent on viscosity than the simple model would suggest.) In a three-dimensional version of the model, in which baroclinic eddies are allowed to form, the zonal wind is significantly reduced from its angular momentum-conserving value, and correspondingly the overturning circulation is much stronger. Indeed, the strength of the Hadley Cell increases roughly linearly with the strength of the eddies in a sequence of numerical integrations similar to those shown, as suggested by (11.71). Qualitatively similar results are found in a model with no convective parameterization. In this case, the lapse rate is closer to neutral, N^2 is small, and the overturning circulation is generally stronger, as also expected from (11.71).

Is the real Hadley circulation 'eddy-driven', as in section 11.5.2, or is it a largely zonally symmetric structure constrained by angular momentum conservation, as in section 11.2 and its hemispherically asymmetric extensions? Observations of the overturning flow in summer and winter provide a guide. Fig. 11.14 shows the thickness
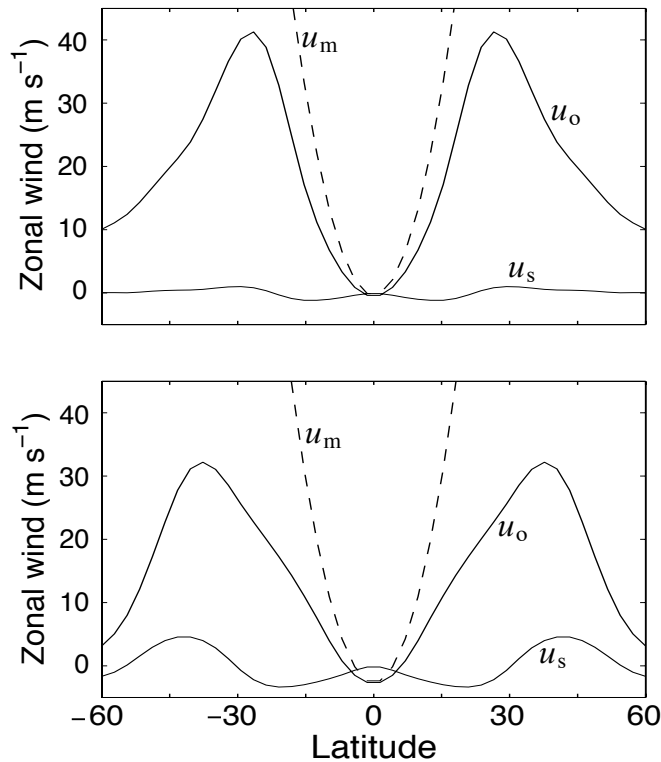
Fig. 11.12 The zonal wind in two numerical simulations. The lower panel is from an idealized dry, three-dimensional atmospheric GCM, and the upper panel is an axi-symmetric version of the same model. Plotted are the zonal wind at the level of the Hadley Cell outflow, u_o; the surface wind, u_s; and the angular momentum conserving value, u_m.[11]

weighted mass transport overturning circulation in isentropic coordinates, and as discussed in chapter 7 this circulation includes both the Eulerian mean transport and the transport due to eddies. In winter there is considerable recirculation within the Hadley Cell, most of it coming from the zonally symmetric flow, and it is a quite distinct structure from the mid-latitude circulation. This suggests that the poleward extent of the winter Hadley Cell is strongly influenced by axisymmetric dynamics, perhaps more than by the baroclinic instability of the subtropical jet, for if the Hadley Cell were primarily a response to eddy fluxes one might expect it to join more smoothly with the mid-latitude Ferrel Cell. It may be that the effects of moisture, and specifically condensation and the concentration of the thermodynamic source, act to give the axisymmetric circulation a significant role. In some contrast, there is virtually no recirculation within the summer Hadley Cell and it does not appear as a self-contained structure, suggestive of eddy effects and strong mid-latitude influence.
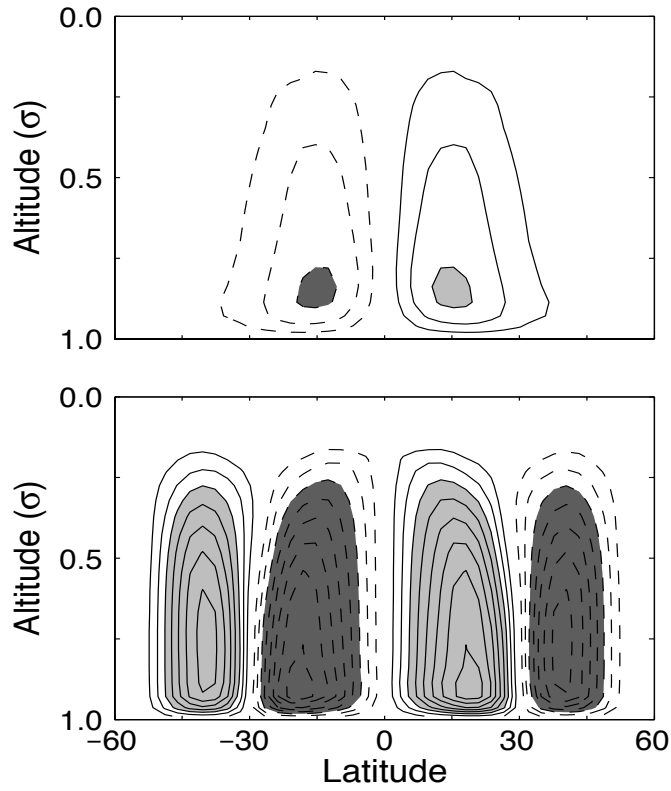
Fig. 11.13 As for Fig. 11.12, but now showing the streamfunction of the overturning circulation. 'Altitude' is $\sigma = p/p_{\text{surface}}$, and contour interval is 5 Sv (i.e., 5×10^9 kg s^{-1}).
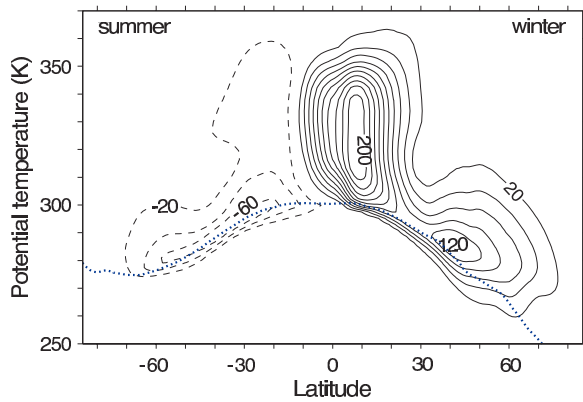
Figure 11.14 The observed mass transport streamfunction in isentropic coordinates in northern hemisphere winter (DJF). The dotted line is the median surface temperature. The return flow is nearly all in a layer near the surface, much of it at a lower temperature than the median surface temperature. Note the more vigorous circulation in the winter hemisphere.[12]

11.6 THE FERREL CELL

In this section we give a brief introduction to the Ferrel Cell, taking the eddy fluxes of heat and momentum to be given and viewing the circulation from a zonally-averaged and Eulerian perspective. We return to the problem from more dynamical perspective in the next chapter.

The Ferrel Cell is an indirect meridional overturning circulation in mid-latitudes (Fig. 11.3) that is apparent in the zonally-averaged v and w fields, or the meridional overturning circulation defined by (11.3) or (11.69). It is 'indirect' because cool air apparently rises in high latitudes, moves equatorwards and sinks in the subtropics. Why should such a circulation exist? The answer, in short, is that it is there to balance the eddy momentum convergence of the mid-latitude eddies and is effectively driven by those eddies. To see this, consider the zonally averaged zonal momentum equation in mid-latitudes; at low Rossby number, and for steady flow this is just

$$- f \overline{v} = -\frac{1}{\cos^2 \vartheta} \frac{\partial}{\partial \vartheta} (\cos^2 \vartheta \overline{u'v'}) + \frac{1}{\rho} \frac{\partial \tau}{\partial z} \qquad (11.74)$$

This is a steady version of (11.66) with the addition of a frictional term $\partial \tau / \partial z$ on the right-hand side. At the surface we may approximate the stress by the simple linear drag $\tau = r \overline{u}_s$, where r is a constant, with the stress falling away with height so that it is important only in the lowest kilometer or so of the atmosphere, in the atmospheric Ekman layer. Above this the eddy momentum flux convergence is balanced by the Coriolis force on the meridional flow. In mid-latitudes (from about 30° to 70°) the eddy momentum flux divergence is negative in both hemispheres (Fig. 11.11) and therefore, from (11.74), the averaged meridional flow must be equatorward.

The flow cannot be equatorward everywhere, simply by mass continuity, and the return flow occurs largely in the Ekman layer, of depth d say. Here the eddy balance is between the Coriolis term and the frictional term, and integrating over this layer gives

$$- f V \approx -r \overline{u}_s. \qquad (11.75)$$

where $V = \int_0^d \rho \overline{v} \, \mathrm{d}z$ is the meridional transport in the boundary layer, above which the stress vanishes. The return flow is polewards (i.e., $V > 0$ in the Northern Hemisphere) producing an eastward Coriolis force that balances the westward frictional force on the eastward flow at the surface. In this picture, then, the zonal flow at the surface is a consequence of the polewards flowing surface branch of the Ferrel Cell, this polewards flow being required by mass continuity given the equatorwards flow in the upper branch of the cell. In this way, the Ferrel Cell is responsible for bringing the mid-latitude eddy momentum flux convergence to the surface where it may be balanced by friction, and this is schematically illustrated in Fig. 11.15.

A more direct way to see that the surface flow must be eastward, given the eddy momentum flux convergence, is to vertically integrate (11.74) from the surface to the top of the atmosphere. By mass conservation, the Coriolis term vanishes (i.e., $\int_0^\infty \rho \overline{v} \, \mathrm{d}z = 0$) and we obtain

$$\int_0^\infty \frac{1}{\cos^2 \vartheta} \frac{\partial}{\partial \vartheta} (\cos^2 \vartheta \overline{u'v'}) \rho \, \mathrm{d}z = \left[\tau \right]_0^\infty = -r \overline{u}_s. \qquad (11.76)$$
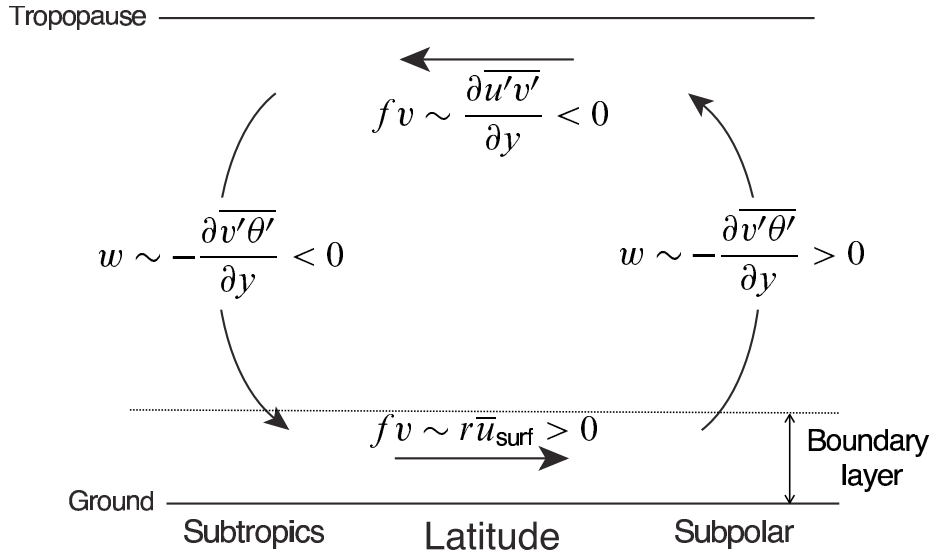
Fig. 11.15 The eddy-driven Ferrel Cell, from an Eulerian point of view. Above the planetary boundary layer the mean flow is largely in balance with the eddy heat and momentum fluxes, as shown. The lower branch of the Ferrel Cell is largely confined to the boundary layer, where is is in a frictional-geostrophic balance.

That is, the surface wind is proportional to the vertically integrated eddy momentum flux convergence. Because there *is* a momentum flux convergence, the left-hand side is negative and the surface winds are eastward.

The eddy heat flux also plays a role in the Ferrel Cell, for in a steady state we have, from (11.67)

$$w = \frac{1}{N^2}\left[Q[b] - \frac{1}{\cos\vartheta}\frac{\partial(\overline{v'b'}\cos\vartheta)}{\partial y} \right] \tag{11.77}$$

and inspection of Fig. 11.11 shows that the observed eddy heat flux produces an overturning circulation in the same sense as the observed Ferrel Cell (again see Fig. 11.15).

Is the circulation produced by the heat fluxes *necessarily* the same as that produced by the momentum fluxes? In a non-steady state the effects of both heat and momentum fluxes on the Ferrel Cell are determined by (11.71) (an equation which applies more accurately in mid-latitudes than in low because of the low-Rossby number assumption), and there is no particular need for the heat and momentum fluxes to act in the same way. But in a steady state they must act to produce a consistent circulation. To show this, for simplicity let us take f and N^2 to be be constant, let us suppose the fluid is incompressible and work in Cartesian coordinates. Take the y-derivative of (11.74) and the z-derivative of (11.77) and use the mass continuity equation. Noting that $\overline{v'\zeta'} = -\partial\overline{u'v'}/\partial y$ we obtain

$$\frac{\partial}{\partial y}\left[\overline{v'\zeta'} + \frac{f_0}{N^2}\frac{\partial\overline{v'b'}}{\partial z}\right] = \frac{\partial}{\partial z}\left(\frac{f_0}{N^2}Q[b]\right) + \frac{\partial}{\partial y}\left(\frac{1}{\rho_0}\frac{\partial\tau}{\partial z}\right). \tag{11.78}$$

The expression on the left-hand side is the divergence of the eddy flux of quasi-geostrophic potential vorticity! That the heat and momentum fluxes act to produce a consistent overturning circulation is therefore equivalent to requiring that the terms in the quasi-geostrophic potential vorticity equation be in a steady-state balance.

Notes

1 Many of the observations presented here are so-called 'reanalyses,' prepared by NCEP and ECMWF (e.g., Kalnay 1996). Unless stated, we use the NCEP re-analysis with data from 1958–2003. Reanalysis products are syntheses of observations and general circulation model results and so are not completely accurate representations of the atmosphere but, especially in data-sparse regions of the globe and for poorly measured fields, they are likely to be more accurate representations of the atmosphere than could be achieved using only the raw data. However, this in turn means they contain biases introduced by the models.

2 George Hadley (1685–1768) was a British meteorologist who formulated the first dynamical theory for the trade winds, presented in a paper (Hadley 1735) entitled 'Concerning the cause of the general trade winds.' He realized that in order to account for the zonal winds the Earth's rotation makes it necessary for there also to be a meridional circulation. His vision was of air heated at low latitudes, cooled at high latitudes, giving rise to a single meridional cell between the equator and each pole. Although he thought of the cell as essentially filling the hemisphere, and he did not account for the instability of such a flow, it was a nevertheless foundational contribution to meteorology. The thermally direct cell in low latitudes is named for him.

A three-celled circulation was proposed by William Ferrel (1817–1891), an American school teacher and meteorologist, and the middle of these cells is now named for him. His explanation of the cell (Ferrel 1856a) was not correct, but this is hardly surprising because the eddy motion producing the angular momentum convergence that drives the Ferrel Cell was not understood for another 100 years or so. Ferrel did however give the first essentially correct description of the role of the Coriolis force and the geostrophic wind in the general circulation (Ferrel 1858), a key development in the history of geophysical fluid dynamics. Ferrel also contributed to tidal theory (in Ferrel (1856b) he noted, for example, that the tidal force due to the moon would slow the earth's rotation) and to ocean dynamics (see http://www.history.noaa.gov/giants/ferrel2.html).

Although Hadley's single-celled picture was superceded by the three-celled one of Ferrel, the modern view of the overturning circulation is, ironically, that of a single cell of 'residual circulation', which, although having distinct tropical and extra-tropical components, in some ways qualitatively resembles Hadley's original picture.

3 Following Held and Hou (1980), who in built on Schneider (1977).

4 However, Fang and Tung (1996) do find some analytic solutions in the presence of moisture and convection.

5 When applied to angular momentum, the requirement that there be no interior extremum of an advected and diffused quantity is often called Hide's theorem, after Hide (1969).

6 Lindzen and Hou (1988).

7 Solutions from Lindzen and Hou (1988).

8 See Dima and Wallace (2003) for an analysis of the relevant observations. They noted that the Hadley cell is also affected by zonally asymmetric monsoonal circulations (which are, of course, not accounted for in the model presented here). Fang and Tung (1999) investigated the effects of time dependence, and essentially noted that (11.60) is not well satisfied, although this alone was unable to limit the nonlinear amplification effect. Walker and Schneider (2005) showed that the effects of vertical momentum diffusion and momentum transport by baroclinic eddies of are both significant in a GCM.

9 Figure courtesy of M. Juckes, using an ECMWF re-analysis.

10 A still more general elliptic equation for the overturning circulation may be derived from the zonally-averaged primitive equations, assuming only that the zonally averaged zonal wind is in cyclostrophic balance with the pressure field (Vallis 1982).

11 Simulations performed and figures kindly provided by C. Walker.

12 Figure courtesy of T. Schneider, using an ECMWF re-analysis.

Further Reading

Lorenz, E. N. 1967. *The General Circulation of the Atmosphere.*
    A classic monograph on the atmospheric general circulation.

Peixoto, J. P. and Oort, A. H., 1992. *Physics of Climate*
    A descriptive but physically based discussion of the climate and the general circulation, with an emphasis on the observations.

Problems

11.1 Explicitly derive equations (11.20) and (11.21).

11.2 Suppose that, in the vertically-integrated Hadley Cell model considered in section 11.2 the radiative equilibrium temperature falls linearly from the equator to the pole. For example, suppose that $\theta_E = \theta_{E0} - \Delta\Theta(|y|/a)$, rather the quadratic fall-off in (11.16). Obtain and discuss the solutions to the Held-Hou problem. Include an expression for the latitudinal extent of the Hadley Cell, and comment on any discontinuities at the edge of the Hadley Cell and at the equator.

11.3 Suppose that the radiative equilibrium temperature falls off with latitude as $P_4(\sin\vartheta)$, where P_4 is the fourth Legendre polynomial. Show that the zonal velocity that is in thermal wind balance with this does not violate Hide's theorem, which states that there can be no interior maximum of angular momentum in the fluid if viscosity is non-zero. Comment on the relevance of this to the issue of whether the radiative equilibrium solution is physically realizable.

11.4 In the angular momentum conserving model of the Hadley Cell, air that starts at rest at the equator develops a large zonal velocity, and hence a large kinetic energy, as it moves polewards. Explain carefully where this energy comes from. (Note that the Coriolis force itself does no work on a fluid parcel.)

11.5 A spinning ice skater with arms outstretched lowers his arms. Show that if the skater's angular momentum is conserved his kinetic energy increases. Where has this energy come from?

11.6 *(a)* Derive and plot the layer thickness as a function of latitude in the shallow-water Hadley Cell model, and the corresponding zonal wind.

(b) Suppose that the equilibrium thickness, h^*, falls quadratically with latitude, rather than linearly as we assume in (11.48). Obtain and plot expressions for the extent of the Hadley Cell, the thickness and the zonal wind.

11.7 The oceanic thermohaline circulation seems similar to Hadley's vision of the the atmospheric circulation, with a large thermally driven cell between pole and equator. Discuss. Is conservation of angular momentum an important factor in the thermohaline circulation? If so, what are its manifestations? If not, why not?

Any theory of the atmospheric circulation must be based on a theory of (large-scale) atmospheric turbulence.

Eric Eady, *The cause of the general circulation of the atmosphere,* 1950.

CHAPTER 12

Zonally-Averaged Mid-latitude Atmospheric Circulation

THE MID-LATITUDE ATMOSPHERIC CIRCULATION differs from the tropical circulation in being essentially zonally asymmetric. It is the zonally asymmetric circulation that provides most of the polewards flux of heat, and that provides the momentum convergence that produces the surface winds. In this chapter our goal is to gain a qualitative understanding of this circulation, and in particular to see how the zonal asymmetries produce the observed zonally averaged circulation.

Because the circulation is so complicated that we cannot expect to understand it fully, or to 'explain' it in terms of a few closed equations that submit to an analytic solution. Unlike the ocean or the low-latitude atmosphere, the large-scale mid-latitude circulation is intrinsically unsteady on the large-scale. And whereas in the ocean, or the low-latitude atmosphere, we could make a great deal of progress by treating the fluid as absolutely steady, this approach fails miserably for the mid-latitude atmosphere. Rather, the eddies *are* the circulation. Put another way, the large-scale midlatitude circulation of the atmosphere is a turbulent flow. Since (alas!) no fully satisfactory theory of turbulence exists we try to make progress by constructing models that are *robust* in their predictions, that don't depend delicately on how we parameterize some particular turbulent process. Indeed, one of our approaches is to use turbulent diffusion to represent the transport due to large-scale eddies in the atmosphere; the subtlety arises in the quantities we choose to parameterize this way, and the constraints that must be imposed to satisfy various dynamical identities.

We will understand the atmosphere when we can describe it in a consistent way on many levels simultaneously. One of these levels will be to predict the flow by numerically solving the governing equations of motion as completely as possible, for example using a comprehensive General Circulation Model (GCM). As successful and impor-

tant as this activity is, it cannot and should not be the whole story, and in this chapter
we concentrate on simpler, more conceptual models (although this includes numerical
approaches). Our emphasis in this chapter is on the *zonally-averaged* circulation, and
in the next chapter we consider the deviations from that average.[1]

The zonal asymmetries that are present in the mid-latitude atmosphere at any given
time are there because of baroclinic instability: even if the boundary conditions and
forcing were perfectly zonally symmetric, the corresponding zonally symmetric solu-
tions of the equations of motion would have a large shear in the zonal wind, and this
would be *unstable* to zonally-asymmetric perturbations, leading to the formation of
time-dependent finite amplitude asymmetries in the circulation, also known as *weather*.
We considered the mechanisms of baroclinic instability in chapter 6, and we considered
one consequence of this, namely geostrophic turbulence, in chapter 9. In the follow-
ing section we explore how these gives rise to some of the observed features in the
midlatitude atmosphere.

12.1 MAINTENANCE OF A BAROTROPIC JET

12.1.1 Motivation

If we look again at the zonally average wind in Fig. 11.2 we see hints of a second jet
somewhat polewards of the subtropical jet. Such a jet is particularly apparent in certain
regions of the globe, when a zonal average is not taken, as in Fig. 12.1. This midlatitude
jet (sometimes called the subpolar jet) is fairly barotropic (it has little vertical structure)
and lies above an eastward surface flow. This flow feels the effect of friction and so
there must be a momentum *convergence* into this region, and we see this clearly in
Fig. 11.11. Although the eddies in which this convergence occurs are a product of
baroclinic instability, the essential mechanism is present in barotropic dynamics, so let
us consider first how an eastward jet can be maintained in a turbulent flow on the surface
of a rotating sphere.[2]

In barotropic turbulence, alternating east-west jets can be maintained if β is non-
zero. However, the case considered in chapter 9 was homogeneous, with no preferred
latitude for a particular direction of jet, whereas in the atmosphere there appears to be
but one mid-latitude jet, and although it meanders it certainly has a preferred average
location. In the subsections that follow we give four explanations as to how this is
achieved. The first of these has a different flavour than the others, but they are all just
different perspectives on the same mechanism.

12.1.2 I. The vorticity budget

Suppose that the absolute vorticity normal to the surface (i.e., $\zeta + 2\Omega \sin \vartheta$) increases
monotonically poleward. (A sufficient condition for this is that the fluid is at rest.) By
Stokes' theorem, the circulation around a line of latitude circumscribing the polar cap
is equal to the integral of the absolute vorticity over the cap. That is,

$$I_1 = \int_{\text{cap}} \boldsymbol{\omega}_{ia} \cdot \mathrm{d}\boldsymbol{A} = \oint_C u_{ia} \, \mathrm{d}l = \oint_C (u_i + 2\Omega a \cos \vartheta) \, \mathrm{d}l \qquad (12.1)$$
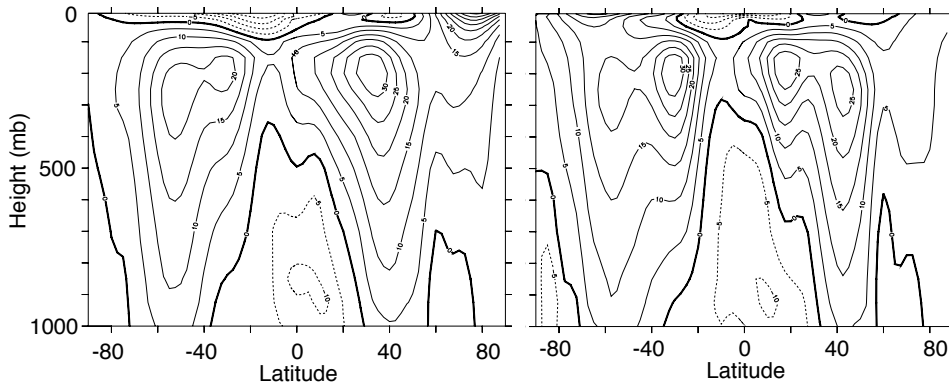
Fig. 12.1 The time-averaged zonal wind at 150°W (in the mid Pacific) in December-January February (DFJ, left), March-April-May (MAM, right). The contour interval is $5\,\mathrm{m\,s^{-1}}$. There is a double jet in each hemisphere, one in the subtropics and one in midlatitudes, especially apparent in the right panel. The subtropical jets are in thermal wind balance with a strong meridional temperature gradient at the subtropical edge of the Hadley Cell, whereas the midlatitude jets have a stronger barotropic component, and are associated with eddy momentum flux convergence and westerly winds at the surface.

where ω_{ia} and u_{ia} are the initial absolute vorticity and velocity, u_i is the initial zonal velocity in the earth's frame of reference, and the line integrals are around the line of latitude. For simplicity let us take $u_i = 0$ and suppose there is a disturbance equatorwards of the polar cap, and that this results in a distortion of the material line around the latitude circle C (Fig. 12.2). Since we are supposing the source of the disturbance is distant from the latitude of interest, then if we neglect viscosity the circulation along
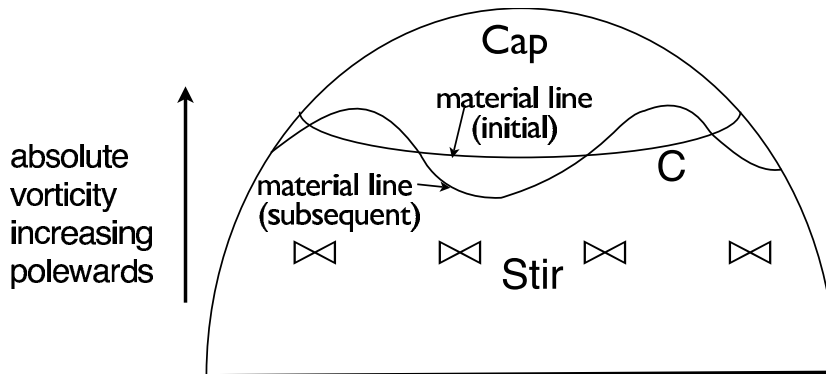
Fig. 12.2 The effects of midlatitude disturbance. If initially the absolute vorticity increases monotonically polewards, then the disturbance will bring fluid with lower absolute vorticity into the cap region. Then, using Stokes theorem, the velocity around the latitude line C will become more westward.

the material line is conserved, by Kelvin's circulation theorem. Thus, vorticity with a lower value is brought into the region of the polar cap, and (using Stokes theorem again) the circulation around the latitude circle C must fall. That is, denoting values after the disturbance with a subscript f,

$$I_f = \int_{\text{cap}} \boldsymbol{\omega}_{fa} \cdot \mathrm{d}A < I_i \tag{12.2}$$

so that

$$\oint_C (u_f + 2\Omega a \cos \vartheta) \, \mathrm{d}l < \oint_C (u_i + 2\Omega a \cos \vartheta) \, \mathrm{d}l \tag{12.3}$$

and

$$\overline{u}_f < \overline{u}_i \tag{12.4}$$

with the overbar indicating a zonal average. Thus, there is a tendency to produce *westward* flow polewards of the disturbance. By a similar argument westward flow is also produced equatorward of the disturbance — to see this apply Kelvin's theorem over all of the globe south of the source of the disturbance (taking care to take the dot-product correctly between the direction of the vorticity vector and the direction of normal to the surface). Finally, note that the overall situation is the same in the Southern Hemisphere. Thus, on the surface of a rotating sphere, external stirring will produce westward flow *away* from the region of the stirring.

Now suppose furthermore that the disturbance imparts no net angular momentum to the fluid. Then the integral of $ua \cos \vartheta$ over the entire hemisphere must be constant. But the fluid is accelerating westward away from the disturbance. Therefore, the fluid in the region of the disturbance must accelerate *eastward*. That, is, angular momentum must converge into the stirred region, producing an eastward flow. This simple mechanism is the essence of the production of eastward eddy-driven jets in the atmosphere, and of the eastward surface winds in mid-latitudes. The stirring that here we have externally imposed comes, of course, from baroclinic instability.

If the stirring subsides then the flow may reversibly go back to its initial condition, with a concomitant reversal of the momentum convergence that caused the zonal flow. Thus, we must have some form of dissipation and irreversibility in order to produce permanent changes, and in particular we need to irreversibly mix vorticity. If the fluid is continuously mixed, then of course we also need a source that restores the absolute vorticity gradient, else we will completely homogenize the vorticity over the hemisphere, and in the next section we set up a simple model that shows how a permanent jet structure can be maintained.

12.1.3 II. The pseudo-momentum budget

The kinematic relation between vorticity flux and momentum flux for non-divergent two-dimensional flow is

$$v\zeta = \frac{1}{2} \frac{\partial}{\partial x} \left(v^2 - u^2 \right) - \frac{\partial}{\partial y} (uv). \tag{12.5}$$

After zonal averaging this gives

$$\overline{v'\zeta'} = -\frac{\partial \overline{u'v'}}{\partial y}. \tag{12.6}$$

noting that $\overline{v} = 0$. In spherical coordinates we have

$$\overline{v'\zeta'}\cos\vartheta = -\frac{1}{a\cos\vartheta}\frac{\partial}{\partial\vartheta}(\cos^2\vartheta\,\overline{u'v'}). \tag{12.7}$$

If (12.6) (or (12.7)) is integrated with respect to y between two quiescent latitudes then the right-hand-side vanishes. That is the zonally-averaged meridional vorticity flux vanishes when integrated over latitude.

Now, the barotropic zonal momentum equation is (for horizontally non-divergent flow)

$$\frac{\partial u}{\partial t} + \frac{\partial u^2}{\partial x} + \frac{\partial uv}{\partial y} - fv = -\frac{\partial\phi}{\partial x} + F_u - D_u \tag{12.8}$$

where F_u and D_u represent the effects of any forcing and dissipation. Zonal averaging, with $\overline{v} = 0$, gives

$$\frac{\partial\overline{u}}{\partial t} = -\frac{\partial\overline{uv}}{\partial y} + \overline{F}_u - \overline{D}_u, \tag{12.9}$$

or, using (12.6),

$$\frac{\partial\overline{u}}{\partial t} = \overline{v'\zeta'} + \overline{F}_u - \overline{D}_u. \tag{12.10}$$

Thus, the zonally averaged wind is maintained by the zonally averaged vorticity flux. There is little direct forcing of the momentum, and most of the dissipation comes from the bottom Ekman layer and if this is parameterized by a linear drag (12.10) becomes

$$\frac{\partial\overline{u}}{\partial t} = \overline{v'\zeta'} - r\overline{u} \tag{12.11}$$

where the constant r is an inverse frictional timescale.

Now consider what maintains this vorticity flux. The barotropic vorticity equation is

$$\frac{\partial\zeta}{\partial t} + \boldsymbol{u}\cdot\nabla\zeta + v\beta = F_\zeta - D_\zeta. \tag{12.12}$$

where F_ζ and D_ζ are forcing and dissipation. Linearize about a mean zonal flow to give

$$\frac{\partial\zeta'}{\partial t} + \overline{u}\frac{\partial\zeta'}{\partial x} + \gamma v' = F' - D' \tag{12.13}$$

where

$$\gamma = \beta - \frac{\partial^2\overline{u}}{\partial y^2} \tag{12.14}$$

is the meridional gradient of absolute vorticity. Multiply (12.13) by ζ'/γ and zonally average to form the pseudo-momentum equation,

$$\frac{\partial P}{\partial t} + \overline{v'\zeta'} = \frac{1}{\gamma}(\overline{\zeta'F'_\zeta} - \overline{\zeta'D'_\zeta}) \tag{12.15}$$

where

$$P = \frac{1}{2\gamma}\overline{\zeta'^2} \tag{12.16}$$

is the pseudomomentum for this problem (see also chapter 7). The parameter γ is positive if the average absolute vorticity increases monotonically northwards, and this is usually the case in both Northern and Southern hemispheres.

In the absence of forcing and dissipation, (12.11) and (12.15) imply an important relationship between the change of the mean flow and the pseudomomentum, namely

$$\frac{\partial \overline{u}}{\partial t} + \frac{\partial P}{\partial t} = 0. \tag{12.17}$$

Now, P is a measure of the wave activity; if for some reason this increases, perhaps because a wave enters an initially quiescent region, then P increases and the mean flow must decrease. However, because the vorticity flux integrates to zero, the zonal flow cannot decrease everywhere. Thus, the zonal flow must increase in the region of the stirring and decrease elsewhere. In the presence of forcing and dissipation this mechanism can lead to the production of a statistically steady jet in the region of the forcing. Equations (12.11) and (12.15) combine to give

$$\frac{\partial \overline{u}}{\partial t} + \frac{\partial P}{\partial t} = -r\overline{u} + \frac{1}{\gamma}(\overline{\zeta' F'_\xi} - \overline{\zeta' D'_\xi}), \tag{12.18}$$

and in a statistically steady state

$$\boxed{r\overline{u} = \frac{1}{\gamma}(\overline{\zeta' F'_\xi} - \overline{\zeta' D'_\xi})} \tag{12.19}$$

The terms on the right-hand-side simply represent the stirring and dissipation of vorticity, and integrated over latitude their sum will vanish, or otherwise the pseudomomentum budget cannot be in a steady state. However, let us suppose that forcing is confined to midlatitudes. In that region, the first term on the right-hand side of (12.19) will be larger than the second, and eastward mean flow will be generated. Away from the direct influence of the forcing, the dissipation term will dominate and westward mean flows will be generated, as sketched in Fig. 12.3 *On a β-plane or on the surface of a rotating sphere an eastward mean zonal flow can be maintained by a vorticity stirring that imparts no net momentum to the fluid.* More generally, stirring in the presence of vorticity gradient gives rise to a mean flow, and on a spherical planet that vorticity gradient is provided by rotation.

In above arguments, the vorticity equation (12.12) was linearized about a mean flow whereas the zonal momentum equation (12.10) was not. Is this consistent? If the eddy amplitude is small, then linearization is certainly appropriate in the vorticity equation. However, even in this case we cannot linearize the zonally averaged zonal momentum equation because there is nothing to linearize it about: there is no large term associated with the mean flow that dominates the other terms if the eddy amplitude is small. The reader may also object that we have not *proven* that the forcing and dissipation terms
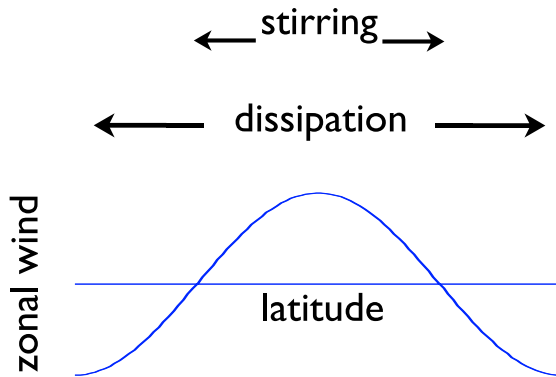
Figure 12.3 Pseudomomentum stirring, which in reality occurs via baroclinic instability, is confined to midlatitudes. Because of Rossyby wave propagation away from the source region, the distribution of pseudomomentum dissipation is broader, and the sum of the two leads to the zonal wind distribution shown, with positive (eastward) values in the region of the stirring. See also Fig. 12.8.

will not locally balance in the region of the forcing, producing no net winds. That can only occur if the dissipation is confined to the region of the forcing, but this is highly unlikely because Rossby waves are generated in the forcing region, and these propagate meridionally before dissipating, as we now discuss.

12.1.4 III. Rossby waves and momentum flux

We have seen that the presence of a mean gradient of vorticity is an essential ingredient in the mechanism whereby a mean flow is generated by stirring. Given such, we expect Rossby waves to be excited, and we now show how Rossby waves are intimately related to the momentum flux maintaining the mean flow.

If a stirring is present in midlatitudes then we expect that Rossby waves will be generated there. To the extent that the waves are quasi-linear and do not interact then
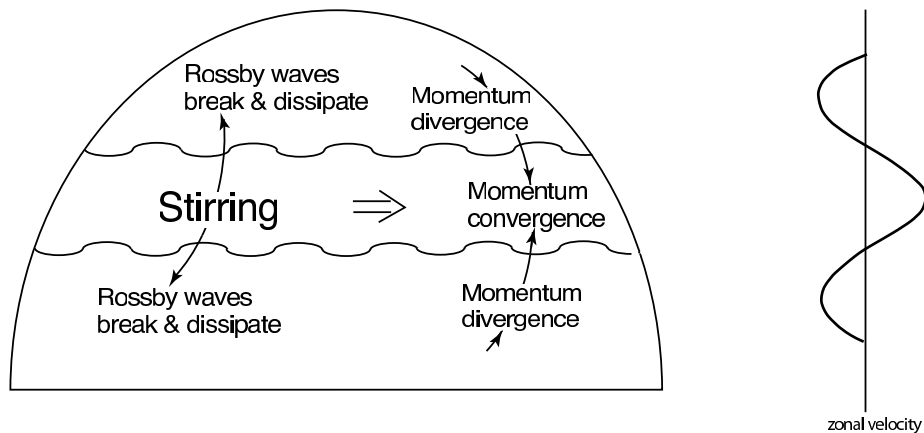
Fig. 12.4 Generation of zonal flow on a β-plane or on a rotating sphere. Stirring in midlatitudes (by baroclinic eddies) generates Rossby waves that propagate away from the disturbance. Momentum converges in the region of stirring, producing eastward flow there and weaker westward flow on its flanks.

away from the immediate source region each wave has the form

$$\psi = \mathrm{Re}\, C e^{i(kx+ly-\omega t)} = \mathrm{Re}\, C e^{i(kx+ly-kct)}, \tag{12.20}$$

where C is a constant, with dispersion relation

$$\omega = ck = \overline{u}k - \frac{\beta k}{k^2 + l^2} \equiv \omega_R, \tag{12.21}$$

provided that there is no meridional shear in the zonal flow. The meridional component of the group velocity is given by

$$c_g^y = \frac{\partial \omega}{\partial l} = \frac{2\beta kl}{(k^2 + l^2)^2}. \tag{12.22}$$

Now, the direction of the group velocity must be *away* from the source region; this is a radiation condition (discussed more in the next subsection), demanded by the requirement that Rossby waves transport energy *away* from the disturbance. Thus, northwards of the source kl is positive and southwards of the source kl is negative. That the product kl can be positive or negative arises because for each k there are two possible values of l that satisfy the dispersion relation (12.21), namely

$$l = \pm \left(\frac{\beta}{\overline{u} - c} - k^2 \right)^{1/2}, \tag{12.23}$$

assuming that the quantity in brackets is positive.

The velocity variations associated with the Rossby waves are

$$u' = -\mathrm{Re}\, C i l e^{i(kx+ly-\omega t)} \tag{12.24a}$$

$$v' = \mathrm{Re}\, C i k e^{i(kx+ly-\omega t)} \tag{12.24b}$$

and the associated momentum flux is

$$\overline{u'v'} = -\frac{1}{2}C^2 kl. \tag{12.25}$$

Thus, given that the sign of kl is determined by the group velocity, northwards of the source the momentum flux associated with the Rossby waves is southward (i.e., $\overline{u'v'}$ is negative), and southwards of the source the momentum flux is northwards (i.e., $\overline{u'v'}$ is positive). That is, the momentum flux associated with the Rossby waves is *toward* the source region. Momentum converges in the region of the stirring, producing net eastward flow there and westward flow to either side.

Another way of seeing this is to note that if kl is positive then lines of constant phase ($kx + ly = $ constant) are tilted north-west/south-east, and the momentum flux associated with such a disturbance is negative ($\overline{u'v'} < 0$). Similarly, if kl is negative then the constant-phase lines are tilted north-east/south-west and the associated momentum flux is positive ($\overline{u'v'} > 0$). The net result is a convergence of momentum flux into the source region. In physical space this is reflected by having eddies that are 'bow-shaped', as in Fig. 12.5.
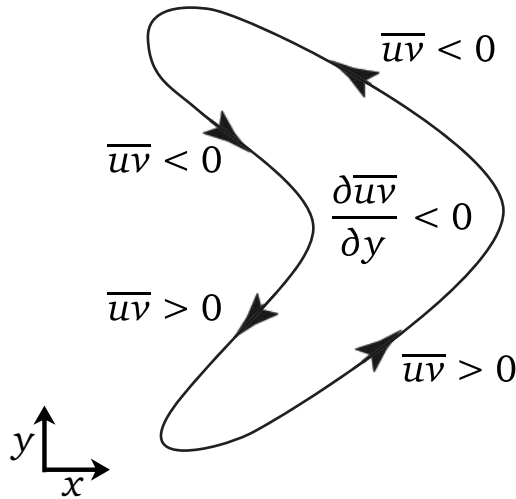
Figure 12.5 The momentum transport in physical space, caused by the propagation of Rossby waves away from a source in midlatitudes. The ensuing bow-shaped eddies are responsible for a convergence of momentum, as indicated in the idealization pictured.

* The radiation condition and Rayleigh friction

A common trick in fluid dynamics, especially in problems of wave propagation, is to add a small amount of friction to the inviscid problem.[3] The solution of the ensuing problem in the limit of small friction will often make clear which solution is physically meaningful in the inviscid problem, and therefore which solution nature chooses. Consider the linear barotropic vorticity equation with linear friction,

$$\frac{\partial \zeta}{\partial t} + \beta \frac{\partial \psi}{\partial x} = -r\zeta \tag{12.26}$$

where r is a small friction coefficient. The dispersion relation is

$$\omega = -\frac{\beta k}{K^2} - ir = \omega_R(k, l) - ir, \tag{12.27}$$

where ω_R is defined by (12.21), and the wave decays with time. Now suppose a wave is generated in some region, and that it propagates meridionally away, decaying as moves away. Then, instead of an imaginary frequency, we may suppose that the frequency is real and the y-wavenumber is imaginary. Specifically, we take $l = l_0 + l'$ where $l_0 = \pm[\beta/(\overline{u} - c) - k^2]^{1/2}$ for some zonal wavenumber k, as in (12.23), and $\omega = \omega_R(k, l_0)$. For small friction, we obtain l' by Taylor-expanding the dispersion relation around its inviscid value, $\omega_R(k, l_0)$, giving

$$\omega + ir = \omega_R(k, l) \approx \omega_R(k, l_0) + \frac{\partial \omega_R(k, l_0)}{\partial l} l', \tag{12.28}$$

and therefore

$$l' = \frac{ir}{c_g^y} \tag{12.29}$$

where $c_g^y = \partial_l \omega_R(k, l_0)$ is the y-component of the group velocity. The wavenumber is imaginary, so that the wave either grows or decays in the y-direction. The wave solution

then obeys

$$\psi \approx C \exp[i(kx - \omega_R t)]\exp(il_0 y - ry/c_g^y). \qquad (12.30)$$

We can now demand that the solution decay away from the source, because any other choice is manifestly unphysical, even as we let r be as small as we please. Thus, with the source at $y = 0$, c_g^y must be positive for positive y and negative for negative y. In other words, the group velocity must be directed *away* from the source region, and therefore momentum flux converges on the source region.

12.1.5 IV. The Eliassen-Palm flux

The Eliassen-Palm (EP) flux provides a useful framework for determining how waves affect the mean flow, and the barotropic case is a particularly simple and instructive example. The zonally averaged momentum equation may be written, for either a stratified or barotropic model, as

$$\frac{\partial \overline{u}}{\partial t} - f_0 \overline{v}^* = \nabla_x \cdot \boldsymbol{\mathcal{F}} - r\overline{u} \qquad (12.31)$$

where $\overline{v}^*$ is the residual meridional velocity and $\boldsymbol{\mathcal{F}}$ is the Eliassen-Palm (EP) flux, and $\nabla_x \cdot$ is the divergence in the meridional plane. In the barotropic case $\overline{v}^* = 0$ and

$$\boldsymbol{\mathcal{F}} = -\mathbf{j}\,\overline{u'v'}. \qquad (12.32)$$

Now, if the momentum flux is primarily the result of interacting nearly-plane Rossby waves, then the EP flux obeys the group velocity property (chapter 7), namely that the flux of wave activity is equal to the group velocity times the wave activity density. Thus,

$$\mathcal{F}_y \equiv \mathbf{j} \cdot \boldsymbol{\mathcal{F}} \approx c_g^y \mathcal{A} \qquad (12.33)$$

where $\mathcal{A}$ is the wave activity density, or pseudomomentum,

$$\mathcal{A} = \frac{\overline{\zeta'^2}}{\overline{q}_y} = \frac{\overline{\zeta'^2}}{\gamma} \approx \frac{\overline{\zeta'^2}}{\beta}, \qquad (12.34)$$

and, if $\gamma > 0$, $\mathcal{A}$ is a positive definite quantity. Now, the group velocity is directed *away* from the region of disturbance, and furthermore if the vorticity gradient is everywhere positive then the EP flux takes the sign of the group velocity (12.22). Thus, as sketched in Fig. 12.5 and Fig. 12.6, momentum converges in the region of the disturbance and an eastward jet is generated. This argument is equivalent to that given in section 12.1.4, and the result of (12.25) essentially illustrates the group velocity property of the EP flux for batoropic Rossby waves in an argument from first principles. (Using (12.22), (12.33) and (12.34) we can explicitly recover (12.25).)

12.1.6 A numerical example

Rossby waves

Stirring

Fluid Acceleration
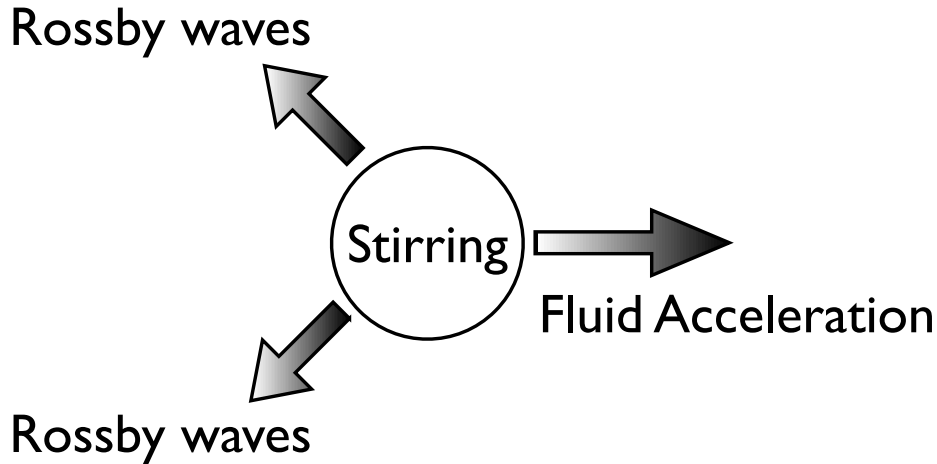
Rossby waves

Fig. 12.6 If a region of fluid on the β-plane or on a rotating sphere is stirred, then Rossby waves will propagate westwards and away from the disturbance, and this is the direction of propagation of wave activity density. Thus, there is positive divergence of wave activity in the stirred region, and using (12.33) and (12.31) this produces a westward acceleration.

We conclude from above arguments that momentum will converge into a rapidly rotating flow that is stirred in a meridionally localized region. To illustrate this, we numerically integrate the barotropic vorticity equation on the sphere, with a meridionally localized stirring term; explicitly, the equation that is integrated is

$$\frac{\partial \zeta}{\partial t} + J(\psi, \zeta) + \beta \frac{\partial \psi}{\partial x} = -r\zeta + \kappa \nabla^4 \zeta + F. \tag{12.35}$$

The first term on the right-hand-side is a linear drag, parameterizing momentum loss in an Ekman layer. The second term removes enstrophy that has cascaded to small scales; it has a negligible impact at large scales. The forcing term F is a 'wavemaker' confined to a zonal strip of about $15°$ meridional extent, centered at about $45°\,\mathrm{N}$, that is statistically zonally uniform and that spatially integrates to zero. Within that region it is a random stirring with a temporal decorrelation scale of a few days and a spatial decorrelation scale corresponding to about wavenumber 8, so mimicking weather scales. Thus, it provides no net source of vorticity or momentum, but it is a source of pseudo-momentum because $\overline{F\zeta} > 0$.

The results of a numerical integration of (12.35) are illustrated in Fig. 12.7 and Fig. 12.8. An eastward jet forms in the vicinity of the forcing, with westward flow on either side. The pseudo-momentum stirring and dissipation that produces this flow is shown in Fig. 12.8. As expected, the dissipation has a broader distribution than the forcing, and their sum (the dot-dashed line in the figure) has the same meridional distribution as the zonal flow itself.
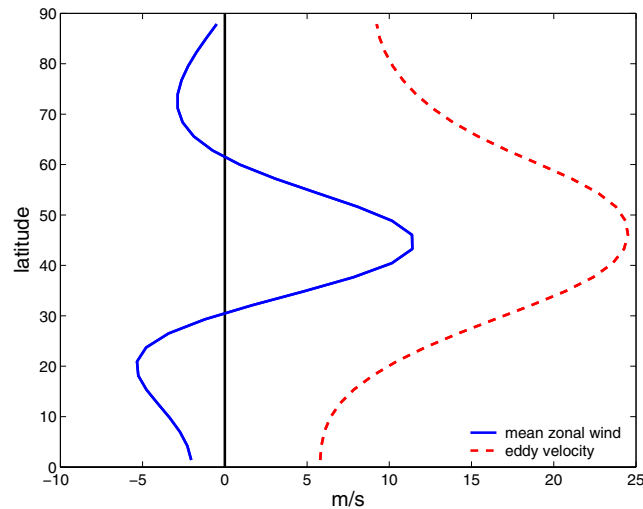
Fig. 12.7 The time- and zonally-averaged wind (solid line) obtained by an integration of the barotropic vorticity equation (12.35) on the sphere. The fluid is stirred in midlatitudes by a random wavemaker that is statistically zonally uniform, acting around zonal wavenumber 8, and that supplies no net momentum. Momentum converges in the stirring region leading to an eastward jet with a westward flow to either side, and zero area-weighted spatially integrated velocity. The dashed line shows the r.m.s. (eddy) velocity created by the stirring.

12.2 LAYERED MODELS OF THE MID-LATITUDE CIRCULATION

Let us now extend our barotropic model in the direction of increasing realism, and we approach this by way of layered models of the circulation, of the type discussed in chapter 3. Our arguments in this section are very phenomenological and, although quite plausible they are not wholly axiomatic. Our approach is similar to the one we use to construct a model of the oceanic ventilated thermocline (section 16.4), in that we simplify a complicated situation by constructing a model with a small number of vertical layers and make use of geostrophic dynamics. However, it differs in that in the oceanic case one can make a small number of reasonable assumptions *ab initio* and the solution follows by direct calculation, whereas in the atmospheric case issues of turbulence immediately arises. In section 12.4 we try turn our model into a systematic calculation; however, here we must make explicit closure assumptions that relate the eddy fluxes to the mean fields and these assumptions are heuristic.

12.2.1 A single layer

We first consider a single layer obeying the shallow water equations. We further restrict the flow by supposing that it is constrained by two rigid surfaces: an upper flat lid and a lower, wavy (but stationary) surface (Fig. 12.9). We may imagine the fluid layer to crudely represent the upper troposphere, with the (given) lower wavy surface
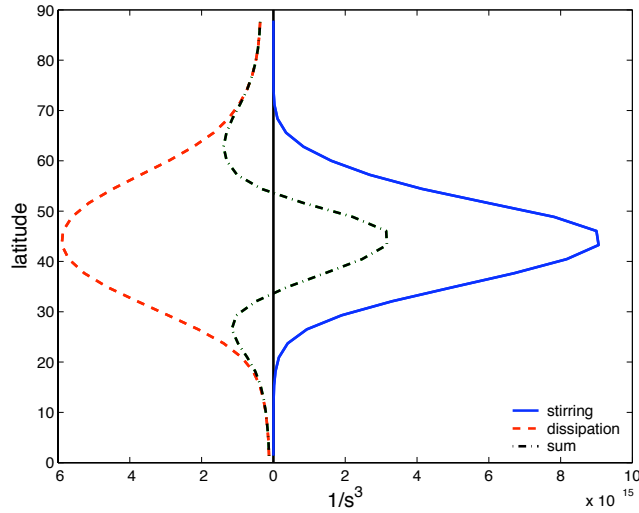
Fig. 12.8 The pseudomentum stirring (solid line, $\overline{F'_\zeta \zeta'}$), dissipation (dashed line, $\overline{D'_\zeta \zeta'}$) and their sum (dot-dashed), for the same integration as Fig. 12.7. Because Rossby waves propagate away from the stirred region before breaking, the distribution of dissipation is broader than the forcing, resulting in an eastward jet where the stirring is centered, with westward flow on either side.

corresponding to the undulating mid-atmosphere interface of a two-layer model. (This section is in some ways an exercise, and too much realism should not be ascribed to the model.) Thus frictional effects are small in the momentum equation, and in particular there is no Ekman layer and no drag on the velocity field. However, there may be some dissipative effects in the vorticity equation, arising from the cascade of enstrophy to small scales. We also suppose the flow satisfies quasi-geostrophic scaling: that is, the Rossby number is small, the variations in layer thickness are small compared to the mean layer thickness, and variations in Coriolis parameter are small. Let the initial flow be a uniform zonal current, passing over the wavy lower boundary. The boundary is waviest in mid-latitudes, creating a disturbance from which Rossby waves emanate. Our questions are: (i) How does this affect the mean zonal flow? (ii) What if any meridional circulation is induced?

Equations of motion

The zonal momentum equation for the layer may be written as as

$$\frac{\partial u}{\partial t} - (f + \zeta)v = -\frac{\partial B}{\partial x} \tag{12.36}$$

where $B = \phi + \boldsymbol{u}^2/2$ is the Bernoulli function and ϕ the pressure in the layer. The zonal average of this is

$$\frac{\partial \overline{u}}{\partial t} - f\overline{v} = \overline{\zeta}\,\overline{v} + \overline{\zeta' v'}. \tag{12.37}$$

Figure 12.9 An atmosphere with a single homogeneous layer of mean thickness H, local thickness h, and a variable lower surface of height η.
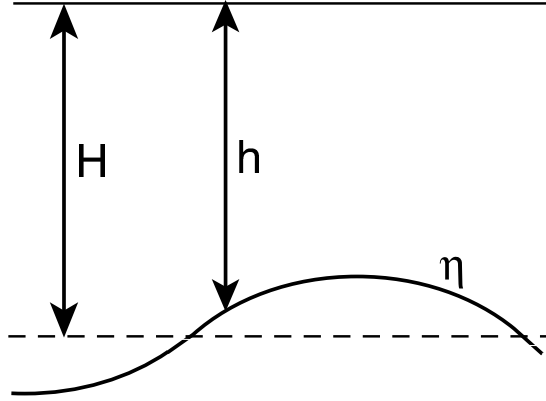
Note that $\overline{v}$ is wholly ageostrophic ($\overline{v}_g = \overline{\partial_x \psi} = 0$). Now, using $\partial u/\partial x + \partial v/\partial y = 0$, the vorticity flux is related to the momentum flux by

$$\overline{v\zeta} = -\frac{\partial \overline{uv}}{\partial y} + \frac{1}{2}\frac{\partial}{\partial x}\overline{(v^2 - u^2)}, \tag{12.38}$$

so that, under quasi-geostrophic scaling, (12.37) simplifies to

$$\boxed{\frac{\partial \overline{u}}{\partial t} - f_0\overline{v} = \overline{\zeta'v'} = -\frac{\partial}{\partial y}\overline{u'v'}}. \tag{12.39}$$

Note that although $\overline{v}$ is small mass conservation does not demand that it be zero, because the thickness of the layer is not constant. Thus, because it is being multiplied by the large term f_0 it should be retained. If the flow is statistically steady and there are no sources or sinks of momentum we have

$$f_0\overline{v} = \frac{\partial}{\partial y}\overline{u'v'}. \tag{12.40}$$

The zonally averaged mass conservation equation is

$$\frac{\partial \overline{h}}{\partial t} + \frac{\partial}{\partial y}\overline{vh} = 0. \tag{12.41}$$

In the situation here $\partial h/\partial t = 0$ because the flow is confined between two rigid surfaces, and so $\partial \overline{vh}/\partial y = 0$. If the mass flux vanishes somewhere, for example at a meridional boundary, it therefore vanishes everywhere and we have

$$\overline{v}\overline{h} + \overline{v'h'} = 0. \tag{12.42}$$

Using (12.40) and (12.42) gives

$$\frac{1}{f_0}\frac{\partial}{\partial y}\overline{u'v'} + \frac{1}{\overline{h}}\overline{v'h'} = 0 \tag{12.43}$$

or

$$\overline{v'\zeta'} - f_0 \frac{1}{h}\overline{v'h'} = 0 \tag{12.44}$$

in a steady state. Because thickness variations are small in quasi-geostrophic flow we can write this as

$$\overline{v'\zeta'} - f_0 \frac{1}{H}\overline{v'h'} = 0 \tag{12.45}$$

where H is the reference thickness of the layer, which may be taken as its mean thickness. [This is just the potential vorticity flux for this problem — look ahead to (12.51).]

The potential vorticity equation for this system is

$$\frac{DQ}{Dt} = \frac{D}{Dt}\left[\frac{\zeta + f}{h}\right] = 0 \tag{12.46}$$

where h is the fluid layer thickness. Under quasi-geostrophic scaling this becomes

$$\frac{Dq}{Dt} = \frac{\partial q}{\partial t} + u\frac{\partial q}{\partial x} + v\frac{\partial q}{\partial y} = 0, \tag{12.47a}$$

$$q = \zeta + \beta y + f_0\frac{\eta}{H}. \tag{12.47b}$$

where $\eta = H - h$ is the height of the lower interface (Fig. 12.9) and this is a function of x and y but not, in this model, time. Using the horizontal non-divergence of the flow, the zonally averaged potential vorticity equation is

$$\frac{\partial \overline{q}}{\partial t} = -\frac{\partial \overline{v}\,\overline{q}}{\partial y} - \frac{\partial \overline{v'q'}}{\partial y}, \tag{12.48}$$

and, using this and (12.47a), the perturbation potential vorticity equation, linearized about a zonally symmetric state, is

$$\frac{\partial q'}{\partial t} + \overline{u}\frac{\partial q'}{\partial x} + \overline{v}\frac{\partial q'}{\partial y} + v'\frac{\partial \overline{q}}{\partial y} = -D[q] \tag{12.49}$$

where we now include a term, $D[q]$, to represent dissipative processes. Multiplying by $q'/(\partial \overline{q}/\partial y)$, zonally averaging and neglecting the term in $\overline{v}$ we obtain the pseudomomentum equation for this system, namely

$$\boxed{\frac{\partial P}{\partial t} = \frac{\partial}{\partial t}\left(\frac{\overline{q'^2}}{2\gamma}\right) = -\overline{v'q'} - \frac{\overline{D'q'}}{\gamma}.} \tag{12.50}$$

where $\gamma = \partial \overline{q}/\partial y$. This equation is the equivalent for the layered system of (12.15). In a turbulent fluid we cannot, in general, demand that $D = 0$, even as the viscosity goes to zero, because of the presence of an enstrophy flux to smaller scales, and a concomitant dissipation. But in regions where it is zero (where there is no wave breaking) then the potential vorticity flux must also be zero in a steady state.

Using (12.47b), the eddy potential vorticity flux is

$$\overline{v'q'} = \overline{v'\zeta'} + \frac{f_0}{H}\overline{v'\eta'} = \overline{v'\zeta'} - \frac{f_0}{H}\overline{v'h'} \tag{12.51}$$

where η' is the topography and h' is the layer thickness perturbation. Using this in the zonal momentum equation (12.39) gives

$$\frac{\partial \overline{u}}{\partial t} = \overline{v'q'} + \frac{f_0}{H}\overline{v'h'} + f_0\overline{v}. \tag{12.52}$$

But the last two terms on the right hand side constitute the total mass flux so we finally write

$$\boxed{\frac{\partial \overline{u}}{\partial t} = \overline{v'q'} + f_0\overline{v}^*}, \tag{12.53}$$

where

$$\overline{v}^* = \overline{v} + \frac{\overline{v'h'}}{\overline{h}} \tag{12.54}$$

is the *residual circulation* for this problem. Now, $\overline{v}^*$ is proportional to the total meridional mass flux and therefore, because the flow is confined between rigid lids then with no sources or sinks of mass, $\overline{v}^* = 0$ everywhere [see (12.42)]. The zonally averaged Eulerian velocity, $\overline{v}$, although small and ageostrophic, is in general nonzero.

Dynamics

When the flow passes over the wavy boundary, Rossby waves will, as in the barotropic case, cause momentum flux to converge in the generation region. If the flow is steady and dissipation-free then from the momentum equation

$$f_0\overline{v} = \frac{\partial \overline{u'v'}}{\partial y}, \tag{12.55}$$

and, in regions of momentum flux convergence (i.e., where $\partial\overline{u'v'}/\partial y < 0$) *the mean meridional velocity is equatorward.* Thus, whereas frictional forces balance the vorticity flux in a constant-thickness barotropic model (because in that case $\overline{v} = 0$) in the free atmosphere a meridional circulation may be generated, and this is basis of the equatorial flow in the upward branch of the Ferrel cell. However, this does not imply that the *total* mass flux is equatorward; in fact, for this single layer model it must be zero and therefore

$$\overline{v'h'} = -\overline{h}\overline{v} > 0 \tag{12.56}$$

That is, *the eddy mass flux is poleward,* balancing the equatorward mean flow.

Another way to arrive at this result is to utilize potential vorticity fluxes directly. For steady, dissipation-free flow the pseudo-momentum equation (12.50) reveals that the potential vorticity flux vanishes. Then using (12.53) and noting that $\overline{v}^* = 0$ we have $\partial\overline{u}/\partial t = 0$ — an example of the non-acceleration theorem that steady non-dissipative waves do not induce a change in the zonal momentum. Then, using (12.51) we find

$$\overline{v'\zeta'} = \frac{f_0}{H}\overline{v'h'} \tag{12.57}$$

and using (12.42) we recover (12.55).

Form drag

We may think of the momentum flux convergence as being balanced by the form drag caused by the flow over the wavy boundary. We write the zonal momentum equation as

$$\frac{\partial \overline{u}}{\partial t} = f_0 \overline{v} + \overline{v'\zeta'} = f_0 \overline{v}^* - \frac{f_0}{H}\overline{v'h'} + \overline{v'\zeta'} \qquad (12.58)$$

where here $\overline{v}^*$ (but not $\overline{v}$) is zero. The term $-(f_0/H)\overline{v'h'}$ is force on the fluid layer coming from the wavy boundary — the interface provides a *form drag,* as described in chapter 3. In particular, the average force per unit area exerted on the layer by the sloping surface is given by

$$F = -f_0 \rho_0 \overline{v'\eta'} = f_0 \rho_o \overline{v'h'}. \qquad (12.59)$$

and dividing by $\rho_0 H$ provides the acceleration on the active fluid layer. The atmosphere also exerts an equal an opposite force on the fluid layer, an effect we consider in the next section. A steady state is achieved, without dissipation, when the form drag is balanced by the eddy momentum flux convergence. From (12.51) or (12.53), this is the same condition that the potential vorticity flux vanishes.

A few remarks

An informal summmary of the single-layer arguments is given in the shaded box on the next page. In the single-layer model, as in the barotropic model, the zonal flow is proximately driven by eddy fluxes of potential vorticity, and in the model the eddy fluxes must be zero if a steady state is to be achieved. As regards the real atmosphere is a little unrealistic, because from the pseudo-momentum equation (12.50) we expect these fluxes to be negative, and there is then nothing to balance them in the momentum equation (12.53), if $\overline{v}^* = 0$. In the real atmosphere, there are effectively sources sinks in the mass conservation equation that arise from the thermodynamics that allow $\overline{v}^*$ to be non-zero. In this case we expect $\overline{v}^* > 0$, but to explore this requires a two-layer model. In such a model the upper level may be thought of as being forced by an undulating interface between the lower and upper layers, a crude representation of stratification, and we now explore this model.

12.2.2 A two-layer model

Now we extend our model to have two active layers, constructing what is probably the simplest model that can capture the dynamics of the mid-latitude tropospheric general circulation without undue approximation. Indeed virtually all of the phenomenology that we associate with the circulation — mid-latitude surface westerly winds, the Ferrel cell, breaking Rossby waves — is present. A three layer model introduces no new physics, although a continuously stratified model does lead to some differences of interpretation.

The physical model we have in mind is one of two isentropic layers of a compressible ideal gas, but as discussed in chapter 3 this is virtually equivalent to a two-layer

Informal Summary of the Single-Layer Arguments

The zonally averaged momentum equation is

$$\frac{\partial \overline{u}}{\partial t} - f_0 \overline{v} = \overline{v'\zeta'} = -\frac{\partial \overline{u'v'}}{\partial y}. \tag{SL.1}$$

A region that is the source of Rossby waves will generally be a region where there is momentum flux convergence, where $\partial \overline{u'v'}/\partial y < 0$. In this region $\overline{v}$ will be directed *equatorward* if $\overline{u}$ is steady, and this flow is the upper branch of the Ferrel Cell. To think about this in terms of potential vorticity, first define the residual meridional velocity by

$$\overline{v}^* = \frac{\overline{v'h'}}{\overline{h}} + \overline{v}. \tag{SL.2}$$

This is proportional to the total meridional mass flux, zero in this one-layer model. The momentum equation is then

$$\frac{\partial \overline{u}}{\partial t} = f_0 \overline{v}^* - \frac{f_0}{\overline{h}}\overline{v'h'} + \overline{v'\zeta'} \tag{SL.3a}$$

$$= \overline{v'q'} + f_0 \overline{v}^*. \tag{SL.3b}$$

using $\overline{v'q'} = \overline{v'\zeta'} - (f_0/\overline{h})\overline{v'h'}$ where q is potential vorticity. The second term on the r.h.s. of (SL.3a) is the *form drag* exerted by the topography on the flow, and in a steady state this balances the momentum flux convergence of the Rossby waves.

We expect the potential vorticity fluxes to be generally negative, smaller in the region of the source. This follows from the pseudomomentum equation

$$\frac{\partial P}{\partial t} = \frac{\partial}{\partial t}\left(\frac{\overline{q'^2}}{2\gamma}\right) = -\overline{v'q'} - \frac{\overline{D'q'}}{\gamma}. \tag{SL.4}$$

If dissipation is identically zero, then the potential vorticity flux is zero if the flow is steady. Then, using (SL.3b), there is no acceleration of the zonal flow — an example of the *non-acceleration theorem*. However, in general, there *will* be some dissipation away from the source region, for example in critical layers ($\overline{u} = c$) where Rossby waves can break, giving (for $\gamma > 0$) a negative potential vorticity flux, $\overline{v'q'} < 0$. In these regions balance in the momentum equation can be achieved either by balancing the PV flux with a friction term, as in the barotropic model, or by a Coriolis force on a polewards residual meridional velocity. That is, $f_0 \overline{v}^* \approx -\overline{v'q'} > 0$, generating a polewards residual flow.

shallow-water model. The notation of the latter is a little simpler and so our presentation will be in those terms. We will continue to assume that quasi-geostrophic scaling holds; that is, the flow is in near geostrophic balance, variations in layer thickness are small compared to their mean thickness, and variations in Coriolis parameter are small. We also assume that the two fluid layers are held between two flat rigid lids — topography is an unnecessary complication at this stage.

Equations of motion

The equations of motion are those of a two-layer Boussinesq shallow water model confined between two rigid flat surfaces, and readers who are comfortable with these dynamics may quickly skip through this section, merely glancing at the boxed equations as they pass. The momentum equations of each layer are

$$\frac{D\boldsymbol{u}_1}{Dt} + \boldsymbol{f} \times \boldsymbol{u}_1 - \nabla\phi_1 \tag{12.60a}$$

$$\frac{D\boldsymbol{u}_2}{Dt} + \boldsymbol{f} \times \boldsymbol{u}_2 - \nabla\phi_2 - r\boldsymbol{u}_2. \tag{12.60b}$$

where $\phi_1 = p_T/\rho_0$ and $\phi_2 = p_T/\rho - g'\nabla\eta$, p_T is the pressure at the lid at the top, and $g' = g(\rho_1 - \rho_2)/\rho_0$ is the reduced gravity. We have also included a simple representation of surface drag, $-r\boldsymbol{u}_2$, in the lowest layer, and r is a constant. Zonally averaging gives

$$\frac{\partial\overline{u}_1}{\partial t} - f_0\overline{v}_1 = \overline{v_1'\zeta_1'} \tag{12.61a}$$

$$\frac{\partial\overline{u}_2}{\partial t} - f_0\overline{v}_2 = \overline{v_2'\zeta_2'} - r\overline{u}_2 \tag{12.61b}$$

Geostrophic balance in each layer implies

$$f_0\boldsymbol{u}_{g1} = \mathbf{k} \times \nabla\phi_T, \tag{12.62a}$$

$$f_0\boldsymbol{u}_{g2} = \mathbf{k} \times \nabla\phi_T - g'\mathbf{k} \times \nabla\eta, \tag{12.62b}$$

where use a constant value of the Coriolis parameter consistent with quasi-geostrophic scaling, and we henceforth we drop the subscript g on geostrophic velocities. We therefore obtain

$$\boxed{f_0(\boldsymbol{u}_1 - \boldsymbol{u}_2) = g'\mathbf{k} \times \nabla\eta} \ . \tag{12.63}$$

and this is thermal wind balance for this system. A temperature gradient thus corresponds to a slope of the interface height (i.e., the isentropic surface), the interface sloping upwards toward lower temperatures.

The quasi-geostrophic potential vorticity for each layer is

$$q_i = \zeta_i + f - f_0\frac{h_i}{H_i} \tag{12.64}$$

where H_i is the reference thickness of each layer, which we take to be its mean thickness. The potential vorticity flux in each layer is then

$$\overline{v_i' q_i'} = \overline{v_i' \zeta_i'} - \frac{f_0}{H_i} \overline{v_i' h_i'}. \tag{12.65}$$

Using this in (12.61) gives

$$\boxed{\begin{aligned} \frac{\partial \overline{u}_1}{\partial t} &= \overline{v_1' q_1'} + f_0 \overline{v}_1^* \\ \frac{\partial \overline{u}_2}{\partial t} &= \overline{v_2' q_2'} + f_0 \overline{v}_2^* - r\overline{u}_2 \end{aligned}} \tag{12.66}$$

where

$$\overline{v}_i^* = \overline{v} + \frac{\overline{v_i' h_i'}}{H_i} \tag{12.67}$$

is the meridional component of the residual velocity in each layer, proportional to the *total* meridional mass flux in each layer.

In the barotropic model of section 12.1 the mean meridional velocity vanished at every latitude, a consequence of mass conservation in a single layer between two rigid flat surfaces. In a single-layer model of section 12.2.1 the mean meridional velocity may be non zero, but the total meridional mass flux (i.e., the meridional component of the residual velocity) is zero if the domain is bounded laterally by soild walls. In the two layer model we will allow a transformation of mass from one layer to another, which is the equivalent of heating: a conversion of mass from the lower layer to the upper layer is heating, and conversely. Thus, heating at low latitudes and cooling at high latitudes leads to the interface sloping upward toward the pole. In the two-layer model the constraint that mass conservation supplies is that, assuming a statistically steady state, the total polewards mass flux summed over both layers must vanish.

The mass conservation equation for each layer is

$$\frac{\partial h_i}{\partial t} + \nabla \cdot (h_i \boldsymbol{u}_i) = S_i \tag{12.68}$$

where S_i is the mass source term and we may suppose that $S_1 + S_2 = 0$ everywhere. A zonal average gives

$$\frac{\partial \overline{h}_i}{\partial t} + \frac{\partial \overline{h_i v_i}}{\partial y} = S_i \tag{12.69}$$

or, setting $\overline{h}_i = H_i$ and using (12.67),

$$\boxed{\frac{\partial h_i}{\partial t} + H_i \frac{\partial \overline{v}_i^*}{\partial y} = S_i}. \tag{12.70}$$

Suppose the diabatic source term is such as to provide heating at low latitudes and cooling in high. This is equivalent to a conversion upper layer mass to lower layer mass
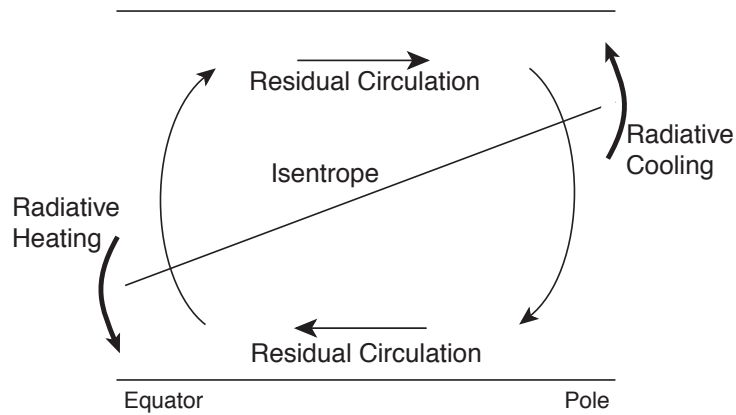
Fig. 12.10 Sketch of the zonally-averaged thermodynamics of a two-layer model. Cooling at high latitudes and heating at low leads steepens the interface (and so the isentropes) upward toward the pole (thicker arrows). Associated with this there is a net mass flux — the residial flow, or the meridional overturning circulation, (lighter arrows). In the tropics this circulation is accounted for by the Hadley Cell, and is nearly all in the mean flow. In midlatitudes the circulation is largely due to baroclinic eddies, and the smaller Eulerian mean flow is actually in the opposite sense.

at high latitudes, and conversely at low latitudes, and this can only be balanced by a poleward mass flux in the upper layer and an equatorward mass flux in the lower layer (Fig. 12.10). That is to say, an earthlike radiative forcing between equator and pole implies that *the total mass flux in the upper layer will be poleward*. This is the opposite of the mean meridional circulation of the Ferrel cell! What's going on?

Manipulating the equations

Because the total depth of the fluid is fixed, the mass conservation equations in each layer (12.69) may each be written as an equation for the interface displacement, namely

$$\frac{\partial \eta}{\partial t} + \nabla \cdot (\eta \boldsymbol{u}_1) = S_1, \qquad \text{or} \qquad \frac{\partial \eta}{\partial t} + \nabla \cdot (\eta \boldsymbol{u}_2) = -S_2 \qquad (12.71)$$

Because of the thermal wind equation (12.63) these equations are identical: $\boldsymbol{u}_1 \cdot \nabla \eta = \boldsymbol{u}_2 \cdot \nabla \eta$ and $S_1 = -S_2$. (If $S_1 \neq -S_2$ the flow would not remain balanced and the thermal wind equation could not be satisfied.) The zonally averaged interface equation may be written as

$$\frac{\partial \overline{\eta}}{\partial t} - H_1 \frac{\partial \overline{v}_1^*}{\partial y} = S, \qquad \text{or} \qquad \frac{\partial \overline{\eta}}{\partial t} + H_2 \frac{\partial \overline{v}_2^*}{\partial y} = S \qquad (12.72)$$

where $S = -S_1 = +S_2$, consistent with the mass conservation statement

$$H_1 \overline{v}_1^* + H_2 \overline{v}_2^* = 0. \qquad (12.73)$$

Now, whereas (12.73) is a kinematic statement about the total mass flux, the dynamics provides a constraint on the *eddy* mass flux in each layer. Using the thermal wind relationship we have

$$\overline{(v_1' - v_2')\eta'} = g'\overline{\frac{\partial \eta'}{\partial x}\eta'} = 0 \tag{12.74}$$

Hence, if the upper and lower surfaces are both flat, we have that

$$\overline{v_1'h_1'} = -\overline{v_2'h_2'} \tag{12.75}$$

and the eddy meridional mass fluxes in each layer are equal and opposite. If the bounding surfaces are not flat, we have

$$\overline{v_1'\eta_T'} - \overline{v_1'h_1'} = \overline{v_1'\eta_B'} + \overline{v_2h_2'} \tag{12.76}$$

instead, where η_T and η_B are the topographies at top and bottom. This is a *dynamical* and not just a kinematic result, for it is equivalent to noting that the form drag on one layer due to the interface displacement is equal and opposite to that on the other, namely

$$\overline{v_1'\eta'} = -[-\overline{v_2'\eta'}] \tag{12.77}$$

where the minus sign inside the square brackets arises because the interface displacement is into layer one but out of layer two.

Using (12.65) (12.76) the eddy potential vorticity fluxes in the two layers are related by

$$H_1\overline{v_1'q_1'} + H_2\overline{v_2'q_2'} = H_1\overline{v_1'\zeta_1'} + H_2\overline{v_2'\zeta_2'} - f_0\overline{v_1'\eta_t'} + f_0\overline{v_1'\eta_b'} \tag{12.78}$$

which is the layered version of the continuous result

$$\int_B^T \overline{v'q'}\,\mathrm{d}z = \int_B^T \overline{v'\zeta'}\,\mathrm{d}z + f_0\left[\overline{v'b'}\right]_B^T \tag{12.79}$$

that arose in chapter 5. For flat upper and lower surfaces we have

$$H_1\overline{v_1'q_1'} + H_2\overline{v_2'q_2'} = H_1\overline{v_1'\zeta_1'} + H_2\overline{v_2'\zeta_2'} \tag{12.80}$$

and, using $\overline{v_i\zeta_i} = -\partial\overline{u_iv_i}/\partial y$ and integrating with respect to y gives

$$\boxed{\int \left[H_1\overline{v_1'q_1'} + H_2\overline{v_2'q_2'} \right]\,\mathrm{d}y = 0} \ . \tag{12.81}$$

That is, the total meridional flux of potential vorticity must vanish. This is a consequence of the fact that the potential vorticity flux is the divergence of a vector field; in the continuous case

$$\overline{v'q'} = \frac{\partial\overline{u'v'}}{\partial y} - f_0\frac{\partial}{\partial z}\frac{\overline{v'T'}}{N^2} \tag{12.82}$$

which similarly vanishes when integrated over a volume if there are no boundary contributions.

12.2.3 Dynamics of the two-layer model

We now consider the climate, or the time-averaged statistics, of our two layer model. The equations of motion are (12.61) or (12.66), and (12.69) or (12.70). These equations are not closed because of the presence of eddy fluxes, and in this section we make some phenomenological and rather general arguments about how these behave in order to get a sense of the general circulation. In the next section we use a specific closure to address the same problem.

The physical situation is simple. The two layers of our model are confined in the vertical between two flat, rigid surfaces, and they are meridionally confined between slippery walls at high and low latitudes (the 'pole' and 'equator'). The circulation is driven thermodynamically, by a heating at low latitudes and cooling at high. In the shallow water model, this translates to a conversion of layer 1 fluid to layer 2 fluid at high latitudes, and the converse at low latitudes (see Fig. 12.10). This sets up a sloping interface (sloping upwards toward the pole) and, by thermal wind, a shear. This situation is baroclinically unstable, and this sets up a field of eddies, most vigorous in mid-latitudes where the temperature gradient (or interface slope) is largest. Three fields encapsulate the dynamics — the surface wind field, the meridional circulation, and the meridional temperature gradient, and our goal is to understand their qualitative structure. We note from the outset that the residual circulation is polewards in the upper layer, equatorwards in the lower layer, and that this is a thermodynamic result, a consequence of heating at low latitudes and cooling at high latitudes.

From (12.66) the steady state surface wind is given by

$$rH_2\bar{u}_2 = H_1\overline{v_1'q_1'} + H_2\overline{v_2'q_2'} = H_1\overline{v_1'\zeta_1'} + H_2\overline{v_2'\zeta_2'} \tag{12.83}$$

using (12.80). That is, the surface wind is determined by the vertical integral of either the vorticity flux or the potential vorticity flux.

Neglecting contributions due to the mean horizontal shear (which are small if the β-Rossby number $U/\beta L^2$ is small) the potential vorticity gradient in each layer is given by

$$\frac{\partial q_1}{\partial y} = \beta - \frac{f_0}{H_1}\frac{\partial \bar{h}_1}{\partial y} > 0 \tag{12.84}$$

and

$$\frac{\partial q_2}{\partial y} = \beta - \frac{f_0}{H_2}\frac{\partial \bar{h}_2}{\partial y} \lesssim 0. \tag{12.85}$$

In upper layer $\partial \bar{h}_1/\partial y$ is negative so that the total potential vorticity gradient is positive and larger than β itself. In the lower layer $\partial \bar{h}_2/\partial y$ is positive and indeed if there is to be baroclinic instability it must be as large as β in order that $\partial q/\partial y$ change sign somewhere. Thus, although negative the potential vorticity gradient is much weaker in the lower layer. Thus, Rossby waves (meaning waves that exist because of a background gradient in potential vorticity) will propagate further in the upper layer, and this asymmetry is the key to the production of surface winds.

Now, the potential vorticity flux must be negative (and downgradient) in the upper

Figure 12.11 Sketch of the potential vorticity fluxes in a two layer model. The surface wind is proportional to their vertical integral. The fluxes are negative (positive) in the upper (lower) layer, but are more uniformly distributed at upper levels, leading to eastward surface winds at midlatitudes.
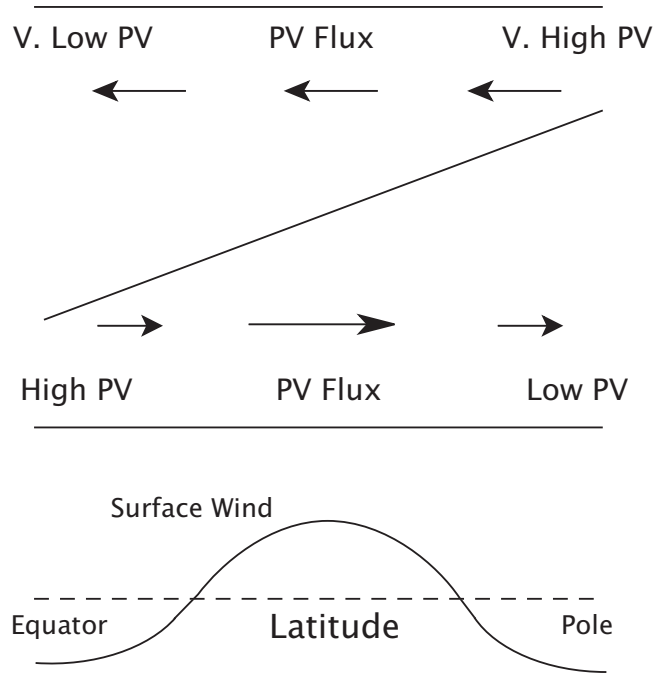
layer, and there are various ways to see this. One is from the upper layer momentum equation (12.66a) which in a steady state gives

$$\overline{v_1' q_1'} = -f_0 \overline{v}_1^*. \tag{12.86}$$

Because $\overline{v}_1^*$ is polewards (positive in the Northern hemisphere), the potential vorticity flux is negative. (The negativity holds in both Northern and Southern Hemispheres.) Equivalently, in the upper layer the radiative forcing is increasing the potential vorticity gradient between equator and pole, so there must be an equatorward potential vorticity flux to compensate. Finally, the perturbation enstrophy or pseudomomentum equations tell us that in a steady state the potential vorticity flux is downgradient (also see section 12.3). This is not an independent argument, since it merely says that the enstrophy budget may be balanced through a balance between production proportional to the potential vorticity gradient and the dissipation. For similar reasons we expect the potential vorticity flux to be positive (poleward) in the lower layer.

If the potential vorticity flux in the lower layer were everywhere equal and opposite to that in the upper layer there would be no surface wind, in contrast to the observations. Thus we must somehow deduce the latitudinal distribution of the potential vorticity flux or the vorticity flux, and we can give a couple of perspectives on what is essentially the same argument.

I. Rossby waves and the vorticity flux

In the upper layer the potential vorticity gradient is stronger and better able to support linear waves than the lower layer. Thus, the vorticity flux in the region

of Rossby wave genesis in midlatitudes will be large and positive in the upper layer, and small and negative in the lower layer. The upshot of this is that the vertical integral of the vorticity flux largely follows the flux of the upper layer, and is positive in midlatitudes and, to ensure that its latitudinal integral is zero, negative on either side. Then, using (12.83), a surface wind of similar pattern ensues (Fig. 12.12).

II. Potential vorticity flux

It is reasonable to infer that the dynamics of the upper layer is more linear than that of the lower because its potential vorticity gradient is larger. With a non-zero β, the steering level (the height where $\overline{u} = c$ where c is the Rossby wave speed) is moved to lower elevations and thus the critical latitude where $\overline{u} = c$ and Rossby waves break and dissipate will tend to be further from the source region than in the lower layer. The result of this is that the potential vorticity breaking, where the potential vorticity flux will be most negative, is far from the source region in the upper layer. In the lower layer the flux will be more concentrated near the source region and, because the integral of the potential vorticity flux sums to zero over the two layers, the flux will be large and positive in the lower layer, as illustrated in Fig. 12.12. Coupled with the mass flux distribution this gives a vorticity flux that is large and positive in the upper layer and weak and negative in the lower layer. The surface winds, being the vertical integral of the potential vorticity fluxes, are westerly in the baroclinic region and easterly to either side. The mean balance of forces in the lower layer is between the Coriolis force on the meridional wind and the frictional force on the zonal wind, with the vorticity fluxes being smaller than either.
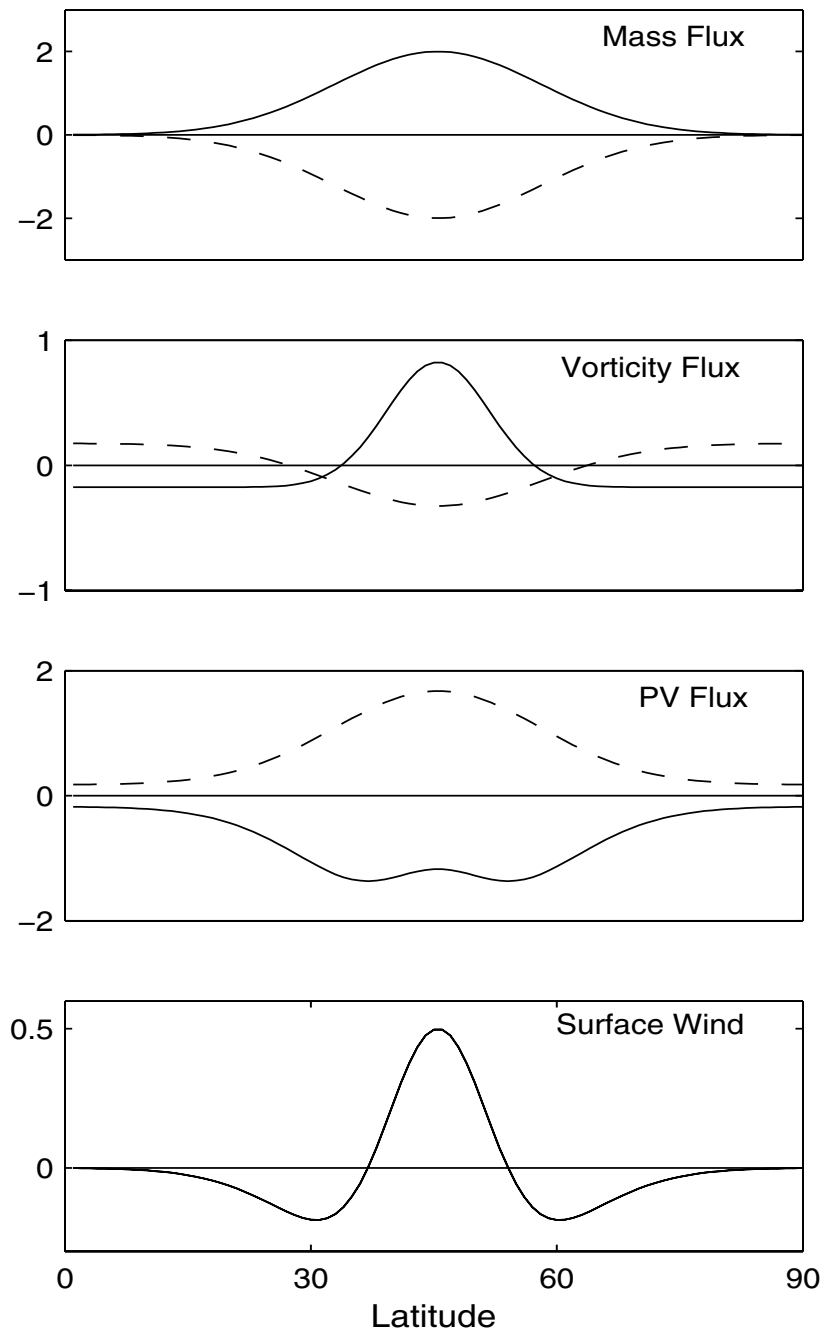
Fig. 12.12 Schema of the eddy fluxes in a two-layer model of an atmosphere with a single mid-latitude baroclinic zone. The upper layer fluxes are solid lines, the lower layer fluxes are dashed. The lowest panel shows the sum of the lower and upper layer vorticity fluxes (or, the same thing, the sum of the potential vorticity fluxes), which is proportional (when the surface friction is a linear drag) to the surface wind. The fluxes satisfy the various relationships and integral constraints of section 12.2.2 but are otherwise idealized.

Phenomenology of a Two-layer Mid-latitude Atmosphere: a Summary

A radiative forcing that heats low latitudes and cools high latitudes will lead to a interface that slopes upward with increasing latitude, and a poleward total mass flux in the upper layer and an equatorward flux in the lower layer. The interface implies a thermal wind shear between the two layers. Neglecting relative vorticity, the potential vorticity gradients in each layer are given by

$$\frac{\partial \overline{q}_1}{\partial y} = \beta - \frac{f_0}{H_1}\frac{\partial \overline{h}_1}{\partial y} > 0 \qquad \text{and} \qquad \frac{\partial \overline{q}_2}{\partial y} = \beta - \frac{f_0}{H_2}\frac{\partial \overline{h}_2}{\partial y} \lesssim 0. \qquad \text{(TL.1)}$$

The gradient is large and positive in upper layer and small and negative in the lower layer — the gradient must change sign if there is to be baroclinic instability which we assume to be the case. This baroclinic instability generates eddy fluxes that largely determine the surface winds and the meridional overturning circulation. The zonal momentum equation in each layer is

$$\frac{\partial \overline{u}_1}{\partial t} = f_0 \overline{v}_1 + \overline{v'_1 \zeta'_1} = f_0 \overline{v}_1^* + \overline{v'_1 q'_1} \qquad \text{(TL.2a)}$$

$$\frac{\partial \overline{u}_2}{\partial t} = f_0 \overline{v}_2 + \overline{v'_2 \zeta'_2} - r\overline{u}_2 = f_0 \overline{v}_2^* + \overline{v'_2 q'_2} - r\overline{u}_2 \qquad \text{(TL.2b)}$$

In steady state the potential vorticity flux will be equatorward in the upper layer and poleward in the lower layer. Because the mass flux in each layer is equal and opposite, the surface wind is given by the vertical integral of the vorticity or potential vorticity fluxes, namely

$$r\overline{h}_1\overline{u}_1 = \overline{h}_1\overline{v'_1 q'_1} + \overline{h}_2\overline{v'_2 q'_2} = \overline{h}_1\overline{v'_1 \zeta'_1} + \overline{h}_2\overline{v'_2 \zeta'_2} \qquad \text{(TL.3)}$$

Because the potential vorticity gradient in the upper layer is large, this layer is more linear than the lower layer and Rossby waves are better able to transport momentum. The vorticity flux is thus stronger in the upper layer than the lower and, using (TL.3), the surface winds are positive (eastward) in the mid-latitude baroclinic zone (see Fig. 12.12). To balance the upper level midlatitude momentum flux convergence a meridional overturning circulation (a Ferrel cell) is generated. In a steady state $f_0\overline{v}_1 = -\overline{v'_1 \zeta'_1}$ so that the zonally averaged upper level flow is equatorward. However, the total mass flux in the upper level is poleward; thus, the equatorward meridional velocity in the upper branch of the Ferrel cell is an product of an Eulerian zonal average and does not correspond to a net equatorward mass transport.

Overturning circulation

The residual circulation is 'direct', meaning that warm fluid rises in low latitudes, moves poleward aloft, and returns near the surface. In low latitudes, the zonally averaged Eulerian circulation circulates in the same way, for this is the Hadley Cell. In midlatitudes, in the upper layer where friction is small the zonal momentum equation is, in steady state,

$$- f_0 \overline{v}_1 \approx \overline{v'_1 \zeta'_1} \tag{12.87}$$

and because the right-hand side is positive the mean flow is equatorward, giving rise to the upper branch of the Ferrel cell. Because the total mass flux in the upper layer is poleward, the eddy mass flux must be poleward, and larger than that of the mean flow.

In the lower layer the balance in the zonal momentum equation is

$$- f_0 \overline{v}_2 \approx \overline{v'_2 \zeta'_2} - r \overline{u}_2 \tag{12.88}$$

and using (12.83) we obtain

$$f_0 \overline{v}_2 \approx \frac{H_1}{H_2} \overline{v'_1 \zeta'_1} = -\frac{H_1}{H_2} f_0 \overline{v}_1. \tag{12.89}$$

Thus, in the poloewards return flow of the Ferrel Cell there is a balance between the Coriolis force, friction, and eddy momentum fluxes. In the real atmosphere much of this return flow is confined to the planetary boundary layer.

12.3 * EDDY FLUXES AND NECESSARY CONDITIONS FOR INSTABILITY

In linear baroclinic instability problems, a necessary condition for instability (the Charney-Stern-Pedlosky, or CSP, condition) is that the potential vorticity change sign in the interior of the fluid, or that the potential vorticity gradient in the interior has a particular sign with respect to the buoyancy gradient at horizontal bounding surfaces, as discussed in chapters 6 and 7. These conditions don't apply in the statistical steady state of the forced-dissipative problem, but we may derive related conditions that do, although they are not completely general. We will focus on the interior condition and not the boundary conditions, as is appropriate in a layered model, but the argument may be extended to cover boundary issues explicitly.

The linear perturbation potential vorticity equation is

$$\frac{\partial q'}{\partial t} = -\overline{u} \frac{\partial q'}{\partial x} - v' \frac{\partial \overline{q}}{\partial y} - D' \tag{12.90}$$

where D' represents dissipative processes. From this we form the enstrophy equation

$$\frac{1}{2} \frac{\partial \overline{q'^2}}{\partial t} + \overline{D'q'} = -\overline{v'q'} \frac{\partial \overline{q}}{\partial y}. \tag{12.91}$$

In the standard linear problem we take $D = 0$ and then for growing waves the right-hand side is positive. But the integral of $\overline{v'q'}$ over latitude and height is zero, and thus

$\overline{v'q'}$ takes both positive and negative signs. Hence, $\partial \overline{q}/\partial y$ must also take both positive and negative signs, and we recover the CSP condition that $\partial \overline{q}/\partial y$ must change sign for an instability.

In a statistically steady state the production of variance by the terms on the right-hand-side is balanced a cascade of variance and dissipation at small scales. Just as in the linear instability problem the left-hand side is positive, now because $\overline{D'q'} > 0$, and therefore, once more, we see that $\partial \overline{q}/\partial y$ must change sign somewhere. Furthermore, the eddy flux must be downgradient everywhere, i.e., $\overline{v'q'}\partial \overline{q}/\partial y < 0$, because the left-hand-side is positive everywhere.

If we now include nonlinear terms the zonally-averaged perturbation enstrophy equation becomes

$$\frac{1}{2}\frac{\partial \overline{q'^2}}{\partial t} = -\overline{v'q'}\frac{\partial \overline{q}}{\partial y} - \frac{1}{2}\frac{\partial}{\partial y}\overline{v'q'^2} - \overline{D'q'}. \tag{12.92}$$

On integrating in y the third-order term vanishes and we obtain

$$\frac{1}{2}\int \left[\frac{\partial}{\partial t}\overline{q'^2} + \overline{D'q'}\right]\mathrm{d}y = -\int \overline{v'q'}\frac{\partial \overline{q}}{\partial y}\,\mathrm{d}y, \tag{12.93}$$

and so, if left-hand side is positive, the flux must still be downgradient in the integrated sense that

$$\int \overline{v'q'}\frac{\partial \overline{q}}{\partial y}\,\mathrm{d}y < 0. \tag{12.94}$$

If the flux is *locally* downgradient, and in the nonlinear case this is an additional physical assumption, then because $\overline{v'q'}$ has both positive and negative values (because its integral is zero) the mean potential vorticity gradient must also change sign. That is, when dissipation is present and if the potential vorticity fluxes are downgradient, a statistically steady state can only be maintained if the potential vorticity gradient changes sign somewhere. In the continuously stratified case, this condition is replaced by ones involving a combination of the interior potential vorticty gradient and the buoyancy gradient at the boundary, the conditions being the same as necessary conditions for instability.

12.4 † TOWARD A CLOSED MODEL

12.4.1 Equations of motion

In this section we construct a closed, two-layer model of the midlatitude circulation. Specifically, we invoke a potential vorticity closure, and then explicitly calculate the zonal winds and meridional circulation. With quasi-geostrophic scaling, the equations of motion are the momentum equations

$$\frac{\partial \overline{u}_1}{\partial t} = f_0\overline{v}_1^* + \overline{v'_1 q'_1} \tag{12.95a}$$

$$\frac{\partial \overline{u}_2}{\partial t} = f_0\overline{v}_2^* + \overline{v'_2 q'_2} - r\overline{u}_2 \tag{12.95b}$$

and the mass conservation equation for each layer which may be written as an equation for the interface height,

$$\frac{\partial \overline{\eta}}{\partial t} - H_1 \frac{\partial \overline{v}_1^*}{\partial y} = S, \tag{12.96}$$

where $\eta = h_1 - H_1 = H_2 - h_2$, with the notation of the previous sections. This can be written in terms of $\overline{v}_2^*$ because

$$H_1 \overline{v}_1^* + H_2 \overline{v}_2^* = 0. \tag{12.97}$$

The velocities and thickness of the layers are related by the thermal wind relation

$$f_0(\overline{u}_1 - \overline{u}_2) = g' \frac{\partial \eta}{\partial y} = -g' \frac{\partial h_1}{\partial y}. \tag{12.98}$$

Eliminating time derivatives between (12.95) and (12.96) reveals that the residual circulation satisfies

$$f_0^2 \frac{H}{H_2} \overline{v}_1^* - H_1 g' \frac{\partial^2 \overline{v}_1^*}{\partial y^2} = +g' \frac{\partial S}{\partial y} - f_0 \left(\overline{v_1' q_1'} - \overline{v_2' q_2'} \right) - f_0(F_1 - F_2), \tag{12.99}$$

Thus, *the residual circulation is driven by the potential vorticity fluxes,* plus the diabatic terms. We may derive a similar expression for the Eulerian mean meridional flow, namely

$$\begin{aligned} 2f_0^2 \frac{H}{H_2} \overline{v}_1 - H_1 g' \frac{\partial^2 \overline{v}_1}{\partial y^2} = g' \frac{\partial S}{\partial y} + g' \frac{\partial^2}{\partial y^2} \overline{v_1' h_1'} \\ - f_0 \left(\overline{v_1' \zeta_1'} - \overline{v_2' \zeta_2'} \right) - f_0(F_1 - F_2) \end{aligned} \tag{12.100}$$

However, the right-hand-side now involves *both* the eddy vorticity fluxes and the eddy mass fluxes. The above equations illustrate the natural way in which the potential vorticity fluxes proximately 'drive' the extratropical atmosphere (see box on page 548).

Potential vorticity equation

A single prognostic equation for each layer is obtained by eliminating the residual circulation from (12.95) and (12.96), giving

$$\frac{\partial \overline{q}_1}{\partial t} = -\frac{\partial \overline{v_1' q_1'}}{\partial y} + \frac{f_0}{H} \frac{\partial S}{\partial y} - \frac{\partial F_1}{\partial y} \tag{12.101a}$$

$$\frac{\partial \overline{q}_2}{\partial t} = -\frac{\partial \overline{v_2' q_2'}}{\partial y} - \frac{f_0}{H} \frac{\partial S}{\partial y} - \frac{\partial F_2}{\partial y} \tag{12.101b}$$

where the q_i are the quasi-geostrophic potential vorticities of each layer given by

$$\overline{q}_1 = -\frac{\partial \overline{u}_1}{\partial y} + f_0 \frac{\eta}{H_1}, \qquad \overline{q}_2 = -\frac{\partial \overline{u}_2}{\partial y} - f_0 \frac{\eta}{H_2}. \tag{12.102a,b}$$

12.4.2 Closure

If the potential vorticity fluxes can be expressed in terms of the mean fields then (12.101) is closed, and we solve for the potential vorticity in each layer and then, using (12.99), the residual circulation. One simple and rational closure is to assume that potential vorticity flux is transferred downgradient so that

$$\overline{v_i' q_i'} = -K_i \frac{\partial q_i}{\partial y} \qquad (12.103)$$

where K_i is an eddy diffusivity, or transfer coefficient, which here is just a scalar quantity.[4] Note that the model demands a closure of the potential vorticity flux — not momentum, vorticity or the mass flux — and potential vorticity, being a materially conserved variable, is also that field for which a diffusive closure is most applicable.

Such a closure has all of the features and problems associated with diffusive closures discussed in chapter 10, plus some of its own. One such is that a diffusive closure will not automatically respect the kinematic constraint that the volume integral of the potential vorticity flux must vanish, which for the two-layer model is expressed by (12.81). We may *choose* the vertical structure of the diffusivity in such a way that this constraint is satisfied, and in that case the model produces the results illustrated in Fig. 12.13. The diffusive closure does indeed then produce potential vorticity fluxes similar to the observed westward-eastward-westward surface wind pattern, and a residual circulation of the same sense as in Fig. 12.10, and constitutes perhaps the simplest closed model of the zonally-averaged atmospheric circulation. Note that the surface wind is produced by the integral of the potential vorticity flux and, because the fluxes are quite different in the two layers, two layers are needed to produce a realistic pattern of surface wind without oversimplification, as well as to represent the meridional overturning and residual circulations. However, the model should not be regarded as being quantitatively valid, and the results depend on the structure of the transfer coefficients and the boundary conditions chosen. Some of these difficulties will become apparent for readers who attempt problem 12.1.

12.5 A STRATIFIED MODEL AND THE REAL ATMOSPHERE

We now discuss, rather qualitatively, the dynamics of a stratified model and the real atmosphere. These dynamics are generally similar to that of the two-layer model, although a number of differences in interpretation arise. In particular, rather than the potential vorticity flux in the two layers, it is the potential vorticity flux in the interior and the buoyancy flux near the boundary that are key aspects in producing the mean circulation.

12.5.1 Potential vorticity and its fluxes

The observed zonally-averaged potential vorticity field is show in Fig. 12.14. Of import to us here is the fact that over most of the atmosphere, over most of the year, the potential vorticity gradient is monotonic, decreasing polewards. How, then, can the

Figure 12.13 Results from a diffusive closure in a two-layer zonally-averaged model. Upper layer quantities are solid lines, lower layer quantities are dashed. The specified zonally averaged zonal velocity (top panel) is large in the upper layer and zero in the lower layer. This produces the potential vorticity structure illustrated in the middle panel, in units in which $\beta = 1$, with a large positive PV gradient in the upper layer, and small negative one in the lower layer. A diffusive closure of the form (12.103) then produces the potential vorticity fluxes illustrated at bottom, where the sum of the fluxes in the two layers (which produces the tendency in the surface wind) is the dot-dashed line. The residual circulation is proportional to the negative of the PV flux, and so is poleward in the upper layer and equatorward in the lower layer. The vertical structure of the diffusivity is chosen such that (12.81) is satisfied.
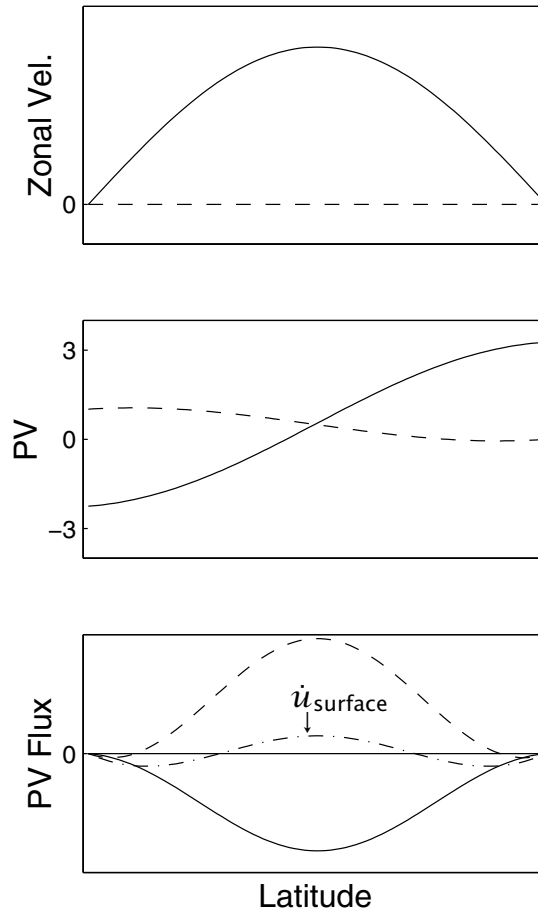
atmosphere be baroclinically unstable? It is because the surface buoyancy (or temperature) gradient also decreases polewards, and thus the atmosphere becomes unstable via the interaction of a surface edge wave with an interior Rossby wave (chapter 6). Thus, in a stratified atmosphere mid-latitude baroclinic instability excites Rossby waves which propagate meridionally, producing a momentum convergence and westward flow, much as described in section 12.1.

Surface winds

Consider the zonally-averaged, continuously stratified momentum equations with quasi-geostrophic scaling,

$$\frac{\partial \overline{u}}{\partial t} = \overline{v'\zeta'} + f_0\overline{v} + F = \overline{v'q'} + f_0\overline{v}^* + F. \tag{12.104}$$

where $F = \alpha \partial \tau / \partial z$ represents frictional effects and at the surface $\tau \approx r\overline{u}$, and the residual velocity $\overline{v}^*$ is given by

$$\overline{v}^* = -\frac{\partial \psi^*}{\partial z} = \overline{v} - \frac{\partial}{\partial z}\left(\frac{1}{N^2}\overline{v'b'}\right). \tag{12.105}$$

(a)

(b)
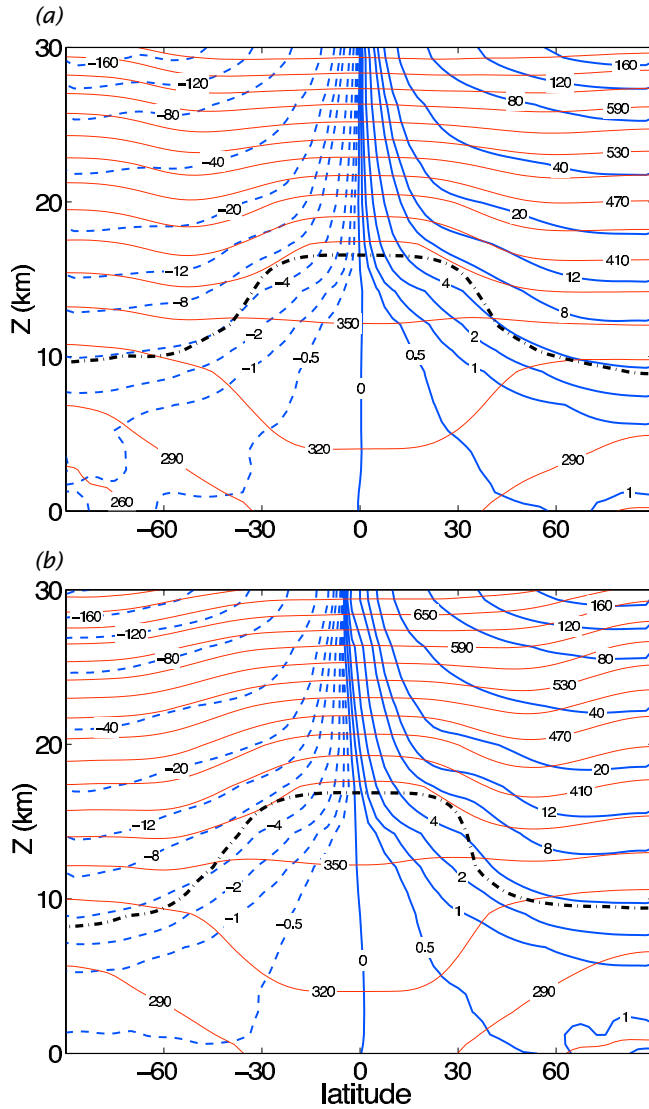
Figure 12.14 The observed zonally-averaged potential vorticity distribution (thicker, solid and dashed lines, peaking up at the equator) and the potential temperature (lighter lines) for (a) annual mean, (b) December-January-February. Also shown is the position of the WMO thermal tropopause (dot-dashed line). The potential vorticity is in 'PV units': $1\,\mathrm{PVU} \equiv 1.0 \times 10^{-6}\,\mathrm{m^2\,K\,s^{-1}\,kg^{-1}}$. Note the uneven contour interval for potential vorticity.

Vertically integrating (12.104) from the surface (where the stress is proportional to the wind) to the top of the atmosphere (where frictional stresses and the buoyancy flux both vanish) we find, in steady state,

$$r\overline{u}(0) = \left\langle \overline{v'\zeta'} \right\rangle = \left\langle \overline{v'q'} \right\rangle + \frac{f_0}{N^2}\overline{v'b'}(0) \qquad (12.106)$$

where the angle brackets denote a vertical integral and (0) denotes the surface value. Thus, the surface winds are determined, analogously to (12.83), by the vertically integrated relative vorticity fluxes, or equivalently by the integral of the interior potential vorticity fluxes and the buoyancy fluxes at the surface. The advantage of the latter representation is that both potential vorticity and buoyancy are materially conserved

variables and it may be easier to say something about their fluxes than it is about the
fluxes of relative vorticity. Compared to the two-layer formulation, the interior fluxes
are analogous to those of the upper layer whereas the surface fluxes are analogous to
those of the lower layer, especially as that lower layer becomes thin.

Potential vorticity and Eliassen-Palm fluxes

The potential vorticity flux may be written as the divergence of the Eliassen-Palm vec-
tor,

$$\overline{v'q'} = \nabla_x \cdot \boldsymbol{\mathcal{F}} \tag{12.107}$$

where $\nabla_x \cdot \equiv \mathbf{j}\, \partial/\partial y + \mathbf{k}\, \partial/\partial z$ and

$$\boldsymbol{\mathcal{F}} \equiv -\overline{u'v'}\, \mathbf{j} + \frac{f_0}{N^2}\overline{v'b'}\, \mathbf{k}. \tag{12.108}$$

In spherical and pressure coordinates we have

$$\boldsymbol{\mathcal{F}} = (\mathcal{F}^\vartheta, \mathcal{F}^p) = a\cos\vartheta \left(-\overline{u'v'}, \frac{f}{\partial_p \overline{\theta}}\overline{v'\theta'}\right) \tag{12.109}$$

and

$$\nabla_\lambda \cdot \boldsymbol{\mathcal{F}} = \frac{1}{a\cos\vartheta}\frac{\partial}{\partial\vartheta}(\mathcal{F}^\vartheta \cos\vartheta) + \frac{\partial\mathcal{F}^p}{\partial p} = \cos\vartheta\,\overline{v'q'}. \tag{12.110}$$

where $\nabla_\lambda \cdot$ is the divergence in the meridional plane. (See also the appendix to this
chapter.) The quasi-geostrophic expression retains a constant value of f, although a
varying value is often used in observational analyses. The EP vector as obtained from
an idealized GCM integration is illustrated in Fig. 12.15, and from observations in Fig.
12.16, and both show qualitatively similar properties — a generally upwards-pointing
vector in midlatitude, veering equatorwards aloft.

The upwards component represents the meridional transfer of heat, and this occurs
during the growth phase of the baroclinic life-cycle and is qualitatively captured by lin-
ear models — for example, in the Eady problem the EP flux is directed purely vertically
(Fig. 7.2), and resembles the vertical components of Fig. 12.15 and Fig. 12.16. But why
should the average over a complete baroclinic lifecycle (which the latter two figures rep-
resent) resemble that of the growing phase of the baroclinic lifecycle? It is because the
eddies do not decay baroclinically, and their lifecycle is not reversible. Rather, there is
an irreversible transfer to barotropic modes (as described in chapter 9) followed by a
barotropic decay. Thus, there is no downwards heat transfer in the cycle, and on average
the heat transfer balances the net atmospheric heating.

The lateral EP flux is a consequence of Rossby wave propagation, as described in
section 12.1. Baroclinic instability plays the role of the midlatitude wavemaker, and the
EP flux emanates laterally. The propagation is an irreversible process, with the Rossby
waves breaking some distance from their source, and it is this that breaks the non-
acceleration conditions and provides the mean flow acceleration and, consequentially,
the observed zonal wind.

The two components of the EP flux have rather different effects on the mean flow
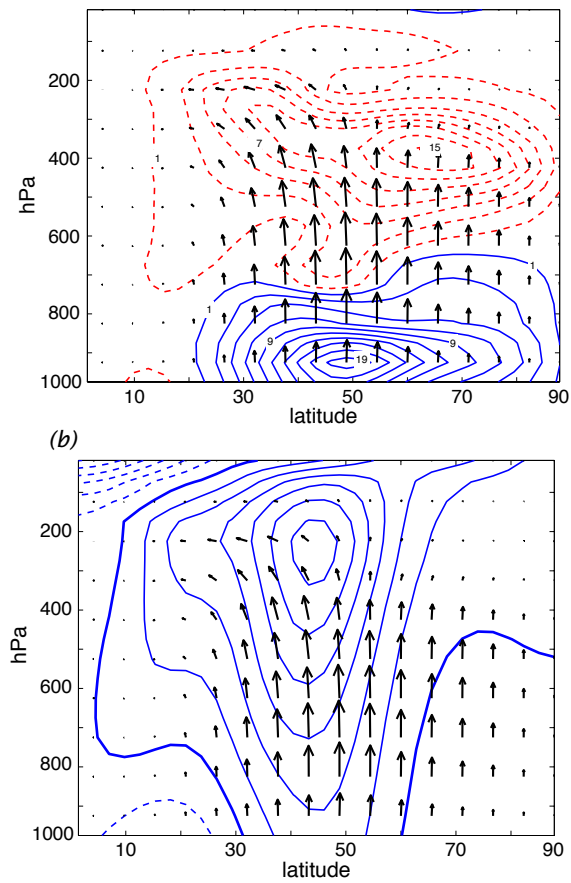
Fig. 12.15 The Eliassen-Palm flux in an idealized primitive equation of the atmosphere. (a) The EP flux (arrows) and its divergence (contours, with intervals of 2 m s^{-1}/day). (b) The EP flux (arrows) and the time- and zonally-averaged zonal wind (contours).

(a)   *(b)*
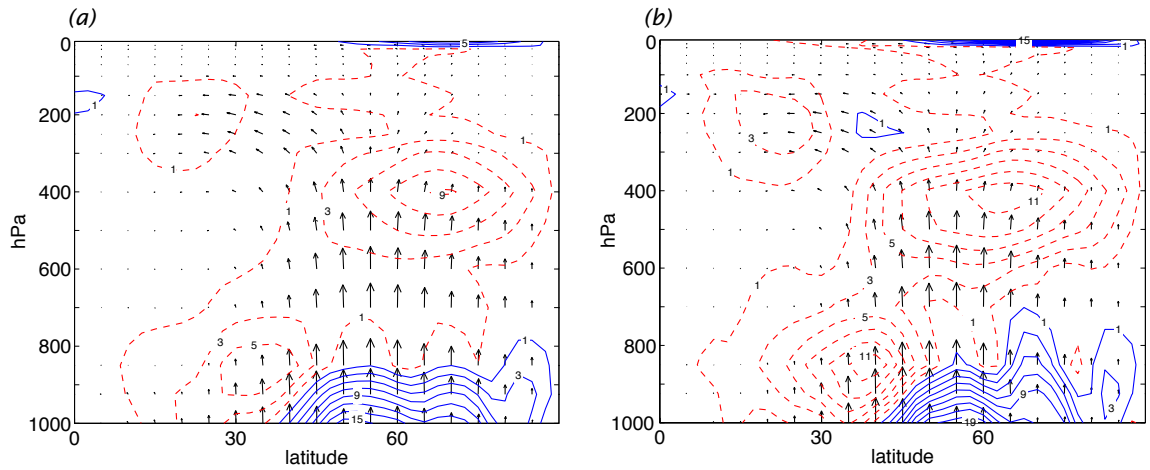
Fig. 12.16 The observed (i.e., re-analysed) Eliassen-Palm flux (arrows) and its divergence (contours, with intervals of $2\,\mathrm{m\,s}^{-1}$/day, zero contour omitted) in the Northern hemisphere. Solid contours denote divergence, a positive torque on the flow, and dashed contours denote convergence, a negative torque. (a) Annual mean, (b) DJF (December-January-February).

(a)   *(b)*
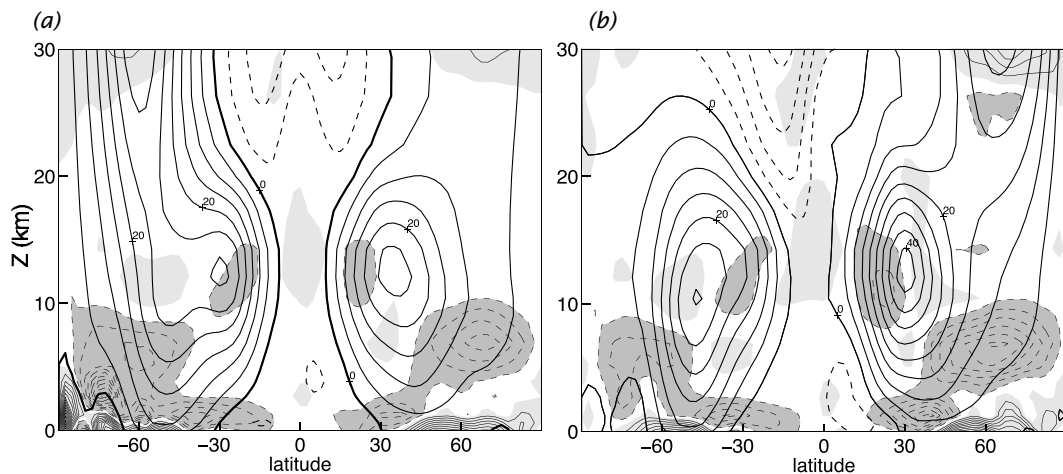
Fig. 12.17 The observed zonally-averaged zonal wind (thicker contours, interval $5\,\mathrm{m\,s}^{-1}$) superimposed on the Eliassen-Palm flux divergence (contour interval $2\,\mathrm{m\,s}^{-1}$/day, zero contour omitted). Regions of positive E-P flux divergence are lightly shaded; regions less than $-2\,\mathrm{m\,s}^{-1}$/day are more darkly shaded. (a) Annual mean, (b) DJF (December-January-February). The vertical coordinate is log pressure, $Z = -7.5\log(p/p_{00})\,\mathrm{km}$.

(a)   *(b)*
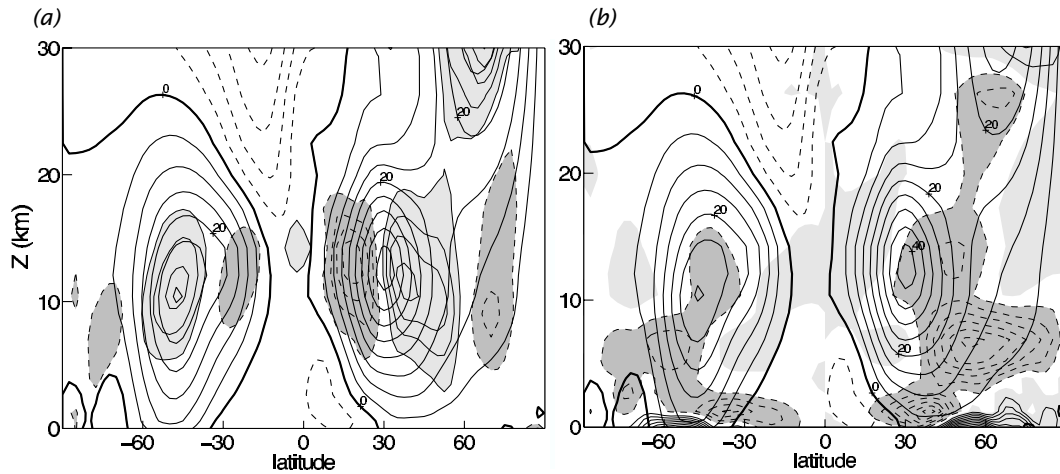
Fig. 12.18 The divergence of the two components of the EP flux for DJF: (a) The horizontal divergence $(\partial/\partial y)$ of (the negative of) the eddy momentum fluxes; contour interval is $1\,\mathrm{m\,s^{-1}/day^{-1}}$, light shaded for positive values > 1, dark shaded for negative values < -1. (b) Vertical divergence $(\partial/\partial z)$ of the buoyancy component, with contour interval and shading convention as in Fig. 12.17. Thicker contours are the zonally averaged zonal wind. The vertical coordinate is log pressure, $Z = -7.5\log(p/p_{00})$ km.

(Fig. 12.18). The horizontal component acts to extract momentum from the subtropics and deposit it, and so accelerate the flow, in mid-latitudes, producing a fairly barotropic eastward jet. The vertical component of the EP flux acts to reduce the intensity of the mid-latitude westerlies aloft, transferring momentum to the surface it may be balanced by friction, and producing the surface westerlies.

Two questions spring to mind:

(i) Why is the meridional wave-activity propagation predominantly in the upper atmosphere?

(ii) Why is the propagation predominantly equatorward?

It is in the upper atmosphere because it is here that the potential vorticity gradient is strongest, as can be seen from Fig. 12.14, and which can be understood on the basis of the two layer model (for example, Fig. 12.13). Thus, wave propagation is more efficient in the upper troposphere, whereas the lower troposphere is more nonlinear and so here the enstrophy cascade, and wavebreaking, occur locally and closer to the region of baroclinic instability itself. Regarding item *(ii)*, the proximate reason is that waves predominantly break on the equatorial side of the instability, and this in turn is for two possible reasons. One is that β increases toward the equator, so that linear propagation is more efficient. The other is that there is often a critical layer in the subtropics, where the speed of the waves equals that of the flow itself ($\overline{u} = c$), and here breaking can efficiently occur. However, we do not explore this problem further here.

12.5.2 Overturning circulation

The Eulerian overturning circulation (meaning the circulation from a conventional zonal average at constant height) in midlatitudes is a single indirect cell, the Ferrel Cell, with rising motion at high latitudes and sinking in the subtropics (Fig. 12.19). The residual circulation is direct and, consistent with the theory of section 7.3.3, resembles closely the thickness weighted circulation. Qualitatively these features are captured by the two-layer dynamics of section 12.2.2, but the continuously stratified case differs in some important respects.

One difference is that the return flows — both the lower branch of the Ferrel Cell and the equatorial branch of the residual circulation — is not distributed over the lower troposphere, but is confined to a relatively thin layer. In the lower branch of the Ferrel Cell the dynamical balance is between friction and the Coriolis force on the meridional flow, so that its thickness is that of a turbulent Ekman layer and about a kilometre.

To understand the residual circulation, consider it first from a quasi-geostrophic perspective. The mean potential vorticity gradient in the free atmosphere is nearly everywhere polewards and the potential vorticity flux is largely downgradient and equatorward. This means that the residual circulation is largely polewards, satisfying the balance

$$f \overline{v}^* \approx -\overline{v'q'} \tag{12.111}$$

In a multi-layer quasi-geostrophic model, the circulation is closed by return flow in the lowest model layer, as as the number of layers increases the return flow is carried in an ever-thinner layer, a delta-function in the conntinuous limit, just as in the example of residual flow in the Eady problem (section 7.5). In the real atmosphere, the return flow cannot be confined to a delta-function, but this argument suggest that it will occur close to the surface, regardless of frictional effects and this expectation is borne out in the lower panels of Fig. 12.19. In fact, the much of the equatorial return flow occurs at between isentropic surfaces that are, on average, below the level of the surface.

12.6 THE TROPOPAUSE AND THE STRATIFICATION OF THE ATMOSPHERE

As You Like It.
William Shakespeare, c. 1599.

The atmosphere may be divided by stratification into certain distinct regions, indicated in Fig. 12.20. The figure shows the so-called 'U.S. standard atmosphere', a rough average temperature profile and a sometimes-useful standard, as well as actual observed values in the lower atmosphere. In the lower 10 km or so of the atmosphere we have the *troposphere,* a dynamically active region wherein most of the weather and the vast predominace of heat transport occurs. The troposphere is capped by the *tropopause,* above which lies the *stratosphere,* a region of stable stratification extending upwards to about 50 km. (Troposphere means 'turning sphere', appropriately so as within it dynamical overturning is prevalent. Stratosphere means 'layered sphere', and here there is much less vertical motion.) The stratosphere is capped by the *stratopause,* above which are the mesosphere, thermosphere, and exosphere, regions of the upper atmosphere that do
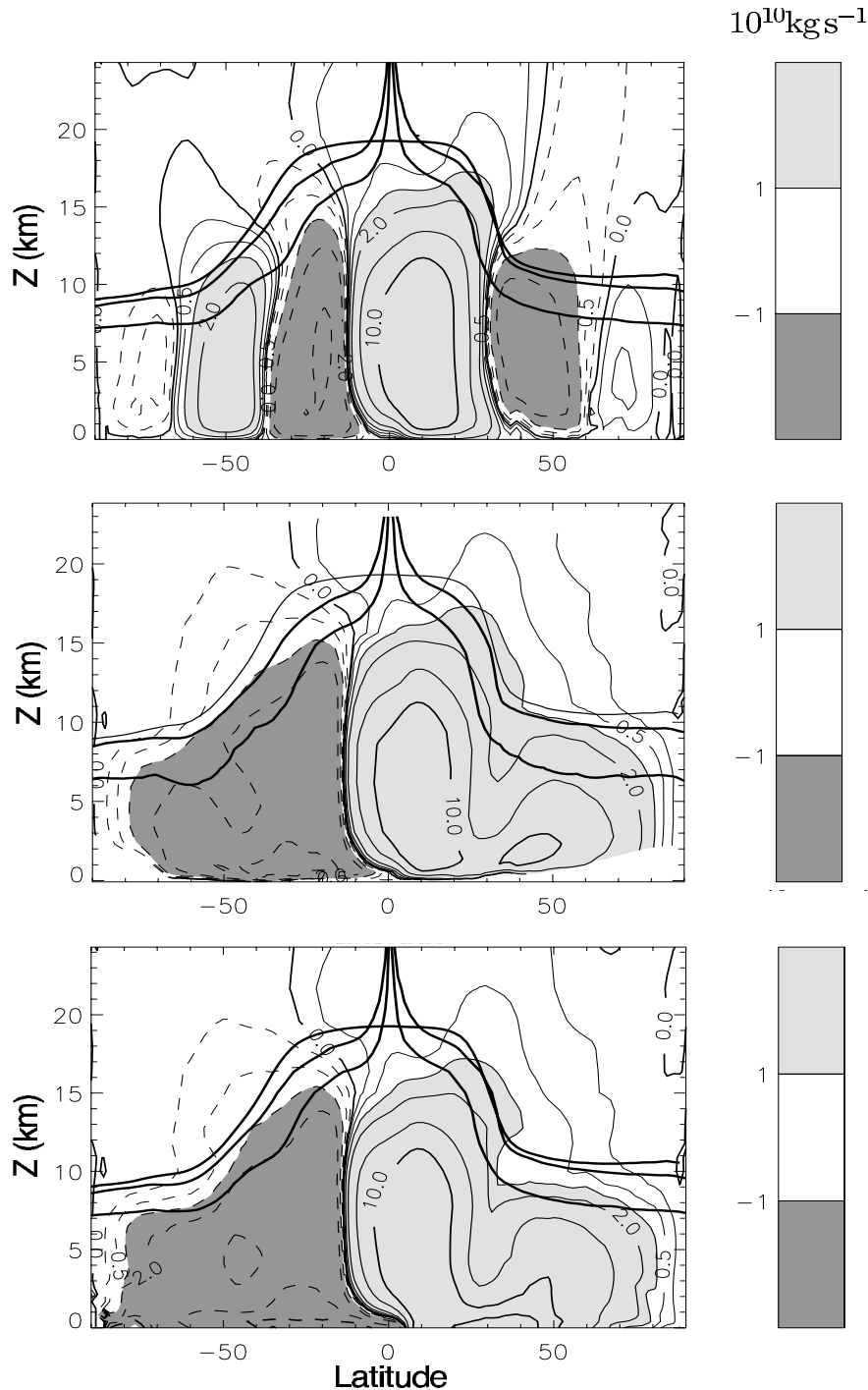
$$10^{10}\mathrm{kg\,s^{-1}}$$

Fig. 12.19 Top: The observed zonally averaged, Eulerian-mean, streamfunction in Northern Hemisphere winter (DJF, 1994–1997). Negative contours are dashed, and values greater or less than 10^{10} kg s^{-1} (10 Sv) are shaded, darker for negative values. The circulation is clockwise around the ligher shading, anticlockwise around dark shading. The three thick solid lines indicate various measures of the tropopause: the two that peak at the equator are isolines of potential vorticity, $Q = \pm 1.5, \pm 4$ PV units, and the flatter one is the WMO thermal tropopause (section 12.6) Middle: The thickness-weighted, or isentropic-mean, meridional mass streamfunction. After calculation in isentropic coordinates, the streamfunction is projected back onto log-pressure coordinates ($Z = -7.5 \log(p/p_{00})$ km) for display. Bottom: the residual, or transformed Eulerian

Potential Vorticity Fluxes and the Extra-Tropical Atmosphere

The extra-tropical circulation of the atmosphere is driven by the differential heating between equator and pole, mediated by fluxes of potential vorticity. Thus, in a layered model:

(i) *Zonal Winds:* At each level the acceleration of the zonal winds is governed by the potential vorticity fluxes:

$$\frac{\partial \overline{u}_i}{\partial t} = -\frac{\partial \overline{v_i q_i}}{\partial y} + f_0 \overline{v}_i^* + \text{friction} \tag{PV.1}$$

(ii) *Surface Winds:* In steady state, the surface winds are produced by the vertically integrated potential vorticity fluxes:

$$r H_s u_s = \sum_i H_i \overline{v_i q_i} \tag{PV.2}$$

where u_s is the surface wind, H_s the thickness of the lowest layer, and r is a frictional coefficient.

(iii) *Meridional Transport:* The total (or residual) meridional transport is, proximately, forced by the potential vorticity fluxes. For example, in a two-layer model

$$f_0^2 \frac{H}{H_2} \overline{v}_1^* - H_1 g' \frac{\partial^2 \overline{v}_1^*}{\partial y^2} = +g' \frac{\partial S}{\partial y} - f_0 \left(\overline{v_1' q_1'} - \overline{v_2' q_2'} \right) - f_0 (F_1 - F_2) \tag{PV.3}$$

where S is proportional to the diabatic forcing, and this equation holds at all times. In steady state the momentum equation gives simply

$$f_0 \overline{v}_1^* = \overline{v_1' q_1'} + \text{friction}. \tag{PV.4}$$

Above the surface layer friction is negligible and the meridional transport responds almost solely to the potential vorticity fluxes.

not concern us here. Our focus will be on the processes that determine the stratification of the lower atmosphere and the height of the tropopause.[6]

In the troposphere temperature generally falls with height, whereas in the stratosphere it increases with height, and this gives rise to a thermal definition of the tropopause:[7] *The tropopause is the lowest level at which the lapse rate decreases to $2\,K\,km^{-1}$ or less, provided also that the average lapse rate between this level and all higher levels within $2\,km$ does not exceed $2\,K\,km^{-1}$.* At any particular time there might also be a second
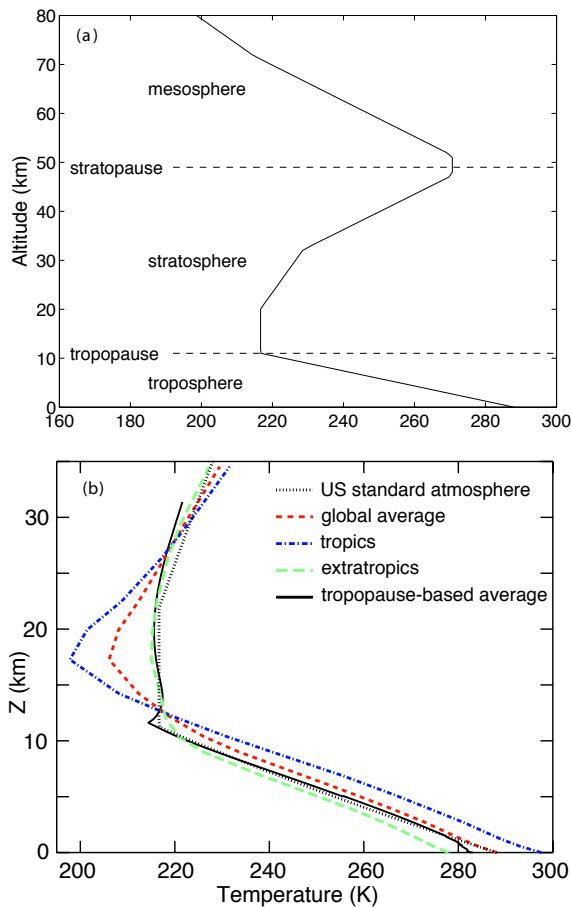
Figure 12.20 (a) The temperature profile of the 'U.S. Standard Atmosphere', marking the standard regions of the atmosphere below 80 km. In addition to the regions shown, the top of the mesosphere is marked by the mesopause, at about 80 km, above which lies the 'thermosphere', in which temperatures rise again into the 'exosphere', extending a few thousand kilometers and where the atmospheric temperature ceases to have useful meaning. (b) Observed, annually averaged profiles of temperature in the atmosphere, where the ordinate is log-pressure. 'Tropics' is the average from 30°S to 30°N, and the extratropics is the average over the rest of the globe. The observations are a from re-analysis over 1958–2003 that extends upward to about 35 km. See text for the meaning of 'tropopause-based average'.

tropopause: if above the first tropopause the average lapse rate between any level and all higher levels within 1 km exceed $3 \, \mathrm{K \, km^{-1}}$, then a second (higher) tropopause is defined by that same criterion. Finally, such definitions are presumed not to apply if they are satisfied below 500 mb. As so defined, the thermal tropopause typically varies in height from about 16 km in low latitudes to about 8 km near the poles.

One may wonder whether such statements reflect a robust property of the atmosphere, or are merely a practical definition of the tropopause, and certainly we should not expect these quantitative definitions to hold in a changed climate, but regardless of that the tropopause is a distinct boundary separating two differently-stratified regions, the troposphere and stratosphere. The thermal tropopause is marked in Fig. 12.19 and, as we see there and in Fig. 12.14, in the extra-tropics it is almost parallel to isolines of potential vorticity, and sometimes an isoline of potential vorticity (say $Q = 3$ or 4 PV units) is used as an *ad hoc* definition of the extra-tropical tropopause.

Finally, and interestingly, we note that the tropopause appears as a very sharp feature when viewed instantaneously, although this sharpness is often blurred when time or spatial averages are taken. The solid line in Fig. 12.20, denoted 'tropopause-based aver-

Figure 12.21 Schema of the radiative equilibrium profile (solid), and two profiles of a radiative-dynamical equilibrium in which the lower atmosphere is adjusted to some specified lapse rate N_1 or N_2. Here, $N_2 > N_1$ and $H(N_2) > H(N_1)$.
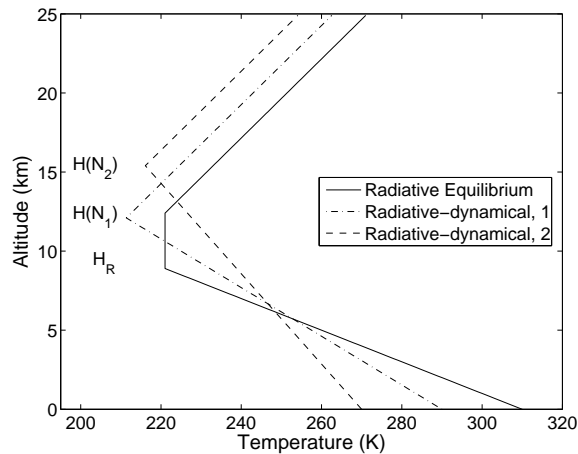
age', shows the profile obtained when the tropopause height itself is taken as a common reference level, using data from individual radiosonde ascents over the United States.[8]

12.6.1 A radiative-convective model

The radiative-equilibrium temperature is that temperature which arises from a pure radiative balance. Thus, a black body subject to a net incoming radiation of S (Watts per square meter) has a radiative-equilibrium temperature T_{rad} given by $\sigma T_{rad}^4 = S$ where $\sigma = 5.67 \times 10^{-8}\,\mathrm{W\,m^{-2}\,K^{-4}}$. For partially absorbing media like the earth's atmosphere the radiative equations are correspondingly more complicated, but nevertheless the vertical structure of the radiative equilibrium temperature may be calculated and its qualitative features are easy to understand. The atmosphere is largely transparent to solar radiation and thus it is largely heated from below by the ground, both through the latter's emission of infra-red radiation and by latent and sensible heat transfer. The atmosphere absorbs and re-emits infra-red radiation, and the upshot is that the radiative-equilibrium temperature falls rapidly in the lowest several kilometers of the atmosphere before rising again, this being in part as a consequence of a layer of ozone in the stratosphere, concentrated between 25 and 30 kilometers altitude, that absorbs solar radiation. A radiative-equilibrium profile is sketched in Fig. 12.21 and, although schematic, it illustrates an important point — the radiative equilibrium temperature falls so rapidly in the lower atmosphere that it would be convectively unstable. Detailed calculations show that $-\partial T_{rad}/\partial z$ is often greater than $10\,\mathrm{K\,km^{-1}}$, so exceeding even the dry adiabatic lapse rate and far exceeding the moist adiabatic lapse rate of about $6\,\mathrm{K\,km^{-1}}$ (depending on temperature).

This observation suggests a simple radiative-convective model of the structure of the stratification, as follows. Starting with a radiative-equilibrium profile, the temperature in the lower atmosphere is modified by convective overturning until it becomes statically neutral, when the lapse rate is equal to the dry or, if saturated, the moist adiabatic lapse rate. Such an adjustment will occur to such a height as is needed, above which the radiative-equilibrium temperature is maintained, and consequently there will

typically be a sharp transition between the two regimes which may be identified with the tropopause. As we see in Fig. 12.21 the height of the tropopause will depend on the lapse rate in the troposphere, a larger lapse rate (i.e., a more negative $\partial T/\partial z$) leading to a lower tropopause. This result does not depend on the adjustment mechanism being convective, meaning being due to small-scale essentially vertical motion. Any dynamical process that adjusts the lapse rate in the troposphere may produce a similar effect, and the consequent lapse-rate is called a radiative-dynamical profile.

The height of the tropopause can be calculated if we know how to calculate the radiative equilibrium temperature and if we are given the tropospheric lapse rate. The simplest calculation assumes that the radiative equilibrium temperature of the stratosphere is unaltered by the adjustment process. Then, suppose that the initial temperature profile is given as a function of height by

$$T_{\mathrm{i}}(z) = \begin{cases} T_{\mathrm{si}} - Az & z \leq z_1 \\ (T_{\mathrm{si}} - Az_1) + B(z - z_1) & z \geq z_1 \end{cases} \tag{12.112}$$

where the parameters A, B and T_{si} are given, z_1 is the height at which the radiative equilibrium temperature starts to increase, and below z_1 the profile is convectively unstable. If convection adjusts this profile to become

$$T_{\mathrm{f}}(z) = T_{\mathrm{sf}} - Cz \qquad z < H \tag{12.113}$$

until it intersects the stable profile at some height $H > z_1$, then we require

$$T_{\mathrm{sf}} - CH = (T_{\mathrm{si}} - Az_1) + B(H - z_1), \tag{12.114}$$

whence

$$H = \frac{T_{\mathrm{sf}} - T_{\mathrm{si}} + (A + B)z_1}{B + C}. \tag{12.115}$$

The final surface temperature is given by an energetic argument, that assuming there is no significant conversion to kinetic energy the internal energy plus the potential energy is conserved, or $\int_0^H \rho(c_v T + gz)\,\mathrm{d}z$ is fixed. (If condensation occurs there is an increase in energy equal to the latent heat released.)

The argument above is oversimplified in assuming that the radiative equilibrium temperature above the adjusted region is not altered by the adjustment process, but nevertheless there are a couple of robust conclusions:

(i) The mechanism produces a relatively sharp tropopause, the existence of which does not depend on the stratospheric temperature actually increasing with height. The tropopause is simply the boundary between radiative equilibrium temperatures aloft, and dynamically influenced temperatures below.

(ii) The smaller the lapse rate (i.e., the lower the value of $-\partial T/\partial z$, or equivalently the larger the stratification N^2) to which the lower atmosphere is adjusted, the higher and the warmer the tropopause.

12.6.2 Radiative and dynamical constraints

We assumed in our simple calculation that the radiative equilibrium temperature profile of the stratosphere was given, independently of the troposphere. This is not quite right, but if we can calculate the radiative equilibrium profile as a function of temperature then we can calculate the height of the tropopause if we are given the lapse rate in the troposphere and the surface (or average) temperature. The tropopause height is then the height at which the tropospheric temperature profile matches the radiative equilibrium temperature. The calculation can, at least in principle, be inverted: if the tropopause height is given (perhaps via purely dynamical reasoning), and the surface or average tropospheric temperature is also given, and one assumes a stratosphere in radiative equilibrium, then the tropospheric lapse rate follows. To illustrate this without the complication of a full radiative model, consider the heat balance at a particular latitude. The outgoing infra-red radiation, I, is in balance with the incoming solar radiation, S, the convergence of horizontal energy flux C and the flux from the surface, F. The temperature profile must adjust itself so that $I = S + F + C$, so that we may think of I as being effectively given — a radiative constraint. Suppose that the temperature profile has a constant lapse rate below some height H_t (the tropopause) and that above this radiative equilibrium holds. Given this, we may parameterize the outgoing infra-red radiation by a specification of the tropopause height H_t, the surface temperature T_s, and the temperature at the tropopause, T_t. If dynamical processes serve to specify the lapse rate and the surface temperature, then the tropospheric height is determined from the radiative constraint. Alternatively, if the tropospheric height and surface temperature are specified, the lapse rate follows.

It is clear from the above arguments that we don't need convection *per se* to produce a tropopause — a boundary will in general occur separating a dynamically influenced troposphere and a stratosphere in near radiative equilibrium. We may more generally think of the troposphere as that region of the atmosphere in which a redistribution of heat occurs, much of which may be *lateral*. This picture suggests itself naturally from the lower two panels of Fig. 12.19 where we see the height of the tropopause roughly co-inciding with the height attained by the overturning circulation, and the troposphere is then a kind of boundary layer to the atmosphere above (Fig. 12.22). The top of the boundary layer is the tropopause but, unlike purely dynamical boundary layers (including the oceanic thermocline) it is not marked by a discontinuity in potential temperature; this is not because potential temperature is not necessarily being mixed in the troposphere, but because radiation keeps the profile continuous. However, the vertical temperature gradient is (approximately) discontinuous.

If this large-scale overturning circulation and associated horizontal transport of heat is also able to transfer sufficient heat vertically so that a statically stable lapse rate can be maintained, then small-scale convective events and convective adjustment need play no role in determining the lapse rate of the troposphere and the height of the tropopause. In fact, it is generally believed that within the tropics moist convection is the dominant process determining the stratification and the height of the tropopause.[9] In contrast, the processes determining the extra-tropical stratification are still a matter of some debate, and in the next two sections we outline some of the dynamics relevant to this problem.
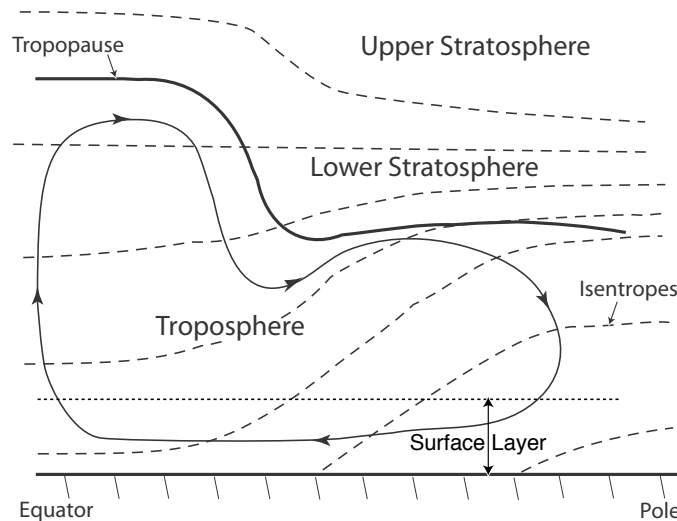
Fig. 12.22 A sketch of the stratification and overturning circulation in the lower atmosphere. The thick line marks the tropopause, the closed contour marks the residual overturning circulation and the dashed lines are isentropes. The overturning circulation has two distinct parts, a tropical Hadley Cell where most of the mass is carried by mean motions, and a shallower extra-tropical cell in which most of the mass transfer occurs via eddy motion. The equatorwards return flow is mostly confined to a shallow surface layer. The 'lower stratosphere' is ventilated by the troposphere along isentropic surfaces, whereas in the 'upper stratosphere' isentropes do not intersect the tropopause. The tropopause is the boundary between the partially-mixed troposphere and the near-radiative equilibrium stratosphere.

The theories fall into two general camps, one related to the redistribution of potential vorticity by baroclinic eddies, and the second related to convection, and we deal with them in turn.

12.7 † BAROCLINIC EDDIES AND POTENTIAL VORTICITY MIXING

The fundamental idea behind the arguments in this section is that the troposphere is that region in which a dynamical distribution of energy takes place, that that redistribution is effected by baroclinic eddies, and that potential vorticity dynamics then provides a natural height for these eddies and so of the tropopause.

In mid-latitudes baroclinic eddies transfer heat upwards, and if they do this efficiently enough there is no need for convection (meaning predominantly vertical convection occuring on small scales) to maintain a statically stable lapse rate (see Fig. 12.22). Nonetheless, the baroclinic eddies do not extend infinitely upwards, and so we expect a boundary (a tropopause) between a dynamical troposphere and a radiative stratosphere. How high is this tropopause, and what is its nature?

12.7.1 A linear argument

On the β-plane, linear baroclinic instability produces a height scale that is different from the height of any pre-existing 'lid' or from the density scale height. This height scale is (section 6.10.1)

$$h = \frac{\Lambda f^2}{\beta N^2} \tag{12.116}$$

where $\Lambda = \partial \overline{u}/\partial z$. That is to say, if $h < H$, where H is the scale height (or the height of some lid in a Boussinesq model), then the baroclinic eddies will extend upwards a height h. Thus (one may argue), below h the thermal structure is determined by the dynamical effects of baroclinic instability, whereas above h the atmosphere is more nearly in radiative equilibrium. Using $\Lambda = (15 \, \mathrm{m\,s^{-1}})/(10 \, \mathrm{km})$, $\beta = 1.6 \times 10^{-11} \, \mathrm{s^{-1} \, m^{-1}}$, $f = 1 \times 10^{-4} \, \mathrm{s^{-1}}$, and $N = 10^{-2} \, \mathrm{s^{-1}}$ gives $h \approx 10 \, \mathrm{km}$, which approximates the height of the tropopause in mid-latitudes, but this can only be a rough estimate, especially as our value of Λ is a little low.

Allowing the parameters f and β to vary with latitude, and using the thermal wind relation, (12.116) may be written in the form

$$h = s\frac{f}{\beta} = sa \tan \vartheta \tag{12.117}$$

where s is the isentropic slope, $-(\partial_y \theta)/(\partial_z \theta)$. This equation. especially when written as $s = h/(a \tan \vartheta)$, suggests that the isentropic slope is (roughly) such that isentropes extend from the surface at low latitudes to the tropopause at the poles, and this is roughly true in the present atmosphere (Fig. 12.14). This is still insufficient information to determine the lapse rate itself, for (12.116) or (12.117) provide only a single relationship between h and N^2, and a radiative or diabatic constraint is also needed, just as with the simple convective adjustment argument. However, a linear argument is incomplete for two reasons:

(i) The amplitude of meridional heat transfer, which determines the meridional temperature gradient, is determined by nonlinear effects.

(ii) The radiative equilibrium calculations typically indicate a radiative tropopause whose height is typically *less than* that calculated using (12.116), especially so if one uses in (12.116) the (rather small) value of N^2 that comes from the radiative equilibrium calculation. The radiative tropopause would then provide a lid on linear baroclinic waves, and above this their amplitude would fall rapidly (Fig. 6.21). In that case, h plays no significant role.

12.7.2 Mixing potential vorticity

Let us suppose that baroclinic eddies mix potential vorticity (a longer discussion of potential vorticity mixing is given in section 10.5). Such mixing will try to homogenize potential vorticity, or equivalently to expel potential vorticity gradients to the boundary, and the (extra-tropical) tropopause would then occur at an isoline of potential vorticity and be marked a near-discontinuity in the potential vorticity distribution. Because

$Q \approx (f/\rho)\partial\theta/\partial z$, the tropopause would also correspond to a discontinuity in stratification. Supporting this notion is the fact that potential distribution in the troposphere is indeed significantly more homogeneous than in the stratosphere (Fig. 12.14, noting the unequal contour intervals of PV). The correspondence is perhaps not so marked as to convince the skeptic, and the lower stratosphere is often locally charactererized by a more homogeneous potential vorticity that such Eulerian averages imply.[10] Putting such objections aside, let us conside to what height such potential vorticity mixing might occur.

Potential vorticity mixing will occur only so far as needed in order that the mean flow is stabilized. (We know that the meridional surface temperature gradient remains negative, so that if the flow is stabilized it must involve changes in the interior potential vorticity distribution.) Neglecting the contribution of relative vorticity, the quasi-geostrophic potential vorticity is given by

$$q = \beta y + \frac{\partial}{\partial z}\left(\frac{f_0^2}{N^2}\frac{\partial\psi}{\partial z}\right). \qquad (12.118)$$

so that

$$\frac{\partial\overline{q}}{\partial y} = \beta - \frac{\partial}{\partial z}\left(\frac{f_0^2}{N^2}\Lambda\right). \qquad (12.119)$$

We might hypothesize that this vertical extent is just sufficient to make the two terms on the right-hand side a similar size in order that potential vorticity can become homogeneous, or that it can change sign and be just unstable; that is

$$\beta \sim \frac{f_0^2\Lambda}{N^2 H_t} \qquad (12.120)$$

where H_t is the vertical extent of the instability, giving

$$H_t \sim \frac{f_0^2\Lambda}{N^2\beta} \qquad (12.121)$$

as in (12.116). Put another way, the troposphere extends vertically as far as baroclinic waves can alter the potential vorticity from its planetary value. (A similar depth scale occurs when evaluating the depth of the wind's influence in a ocean circulation model, section 14.8.1.) This height determines the tropopause, and the radiative constraint then determines the lapse rate within the tropopause. The shear itself is proportional to the horizontal temperature gradient, and the height of the tropopause and the meridional temperature gradient may adjust together to ensure the satisfaction of (12.121).

This kind of equilibration is closely related to a process known as *baroclinic adjustment*, by analogy with convective adjustment.[11] The essential idea is that baroclinic eddies seek to stabilize the mean flow by transferring heat polewards and upwards until the necessary condition for instability (the Charney-Stern-Pedlosky condition) is no longer satisfied, or that potential vorticity is homogenized. It is, however, unlikely that the atmosphere is able to completely homogenize potential vorticity, because in

a forced-dissipative, geostrophically turbulent fluid statistical equilibration can occur at supercritical values of the shear and so baroclinic adjustment in this 'strong' sense seems unlikely to occur.[12] Nevertheless, a weaker version may hold in which potential vorticity is imperfectly homogenized and (12.121) provides a plausible scaling, but not a precise prediction, for the height of the tropopause.

Diffusive potential vorticity mixing

A slightly different approach to the problem, albeit one with a similar basis, is to assume that potential vorticity is transported diffusively rather than being homogenized. Let us return to our two-layer model of the troposphere discussed in section 12.2.2, with a slight re-interpretation of the meaning of the layers: we let the upper layer be such as to carry all the polewards flow of the residual circulation and the lower layer carry all the equatorwards return flow, and consequently the upper layer is much thicker than the lower layer. We also noted previously the result that the eddy mass flux in each layer is equal and opposite, so that,

$$\overline{v_1' h_1'} = -\overline{v_2' h_2'}. \tag{12.122}$$

Further, using (12.65), in each layer the mass flux is related to the potential vorticity flux by

$$\overline{v_i q_i} \approx -\frac{f_0}{H_i} \overline{v_i h_i'} \tag{12.123}$$

if we neglect the fluxes of relative vorticity. Let us now assume that potential vorticity is diffused downgradient, and that the height of the tropopause is adjusted so that the constraint (12.122) is satisfied. Given these assumptions we have

$$\overline{v_1' h_1'} = -\frac{H_1}{f_0} \overline{v_1 q_1} = D_1 \frac{H_1}{f_0} \frac{\partial \overline{q}_1}{\partial y} = D_1 \frac{H_1}{f_0} \left(\beta - \frac{f_0}{H_1} \frac{\partial \overline{h}_1}{\partial y} \right) \tag{12.124a}$$

and similarly

$$\overline{v_2' h_2'} = D_2 \frac{H_2}{f_0} \left(\beta - \frac{f_0}{H_2} \frac{\partial \overline{h}_2}{\partial y} \right) \tag{12.124b}$$

where D_i is diffusivity of each layer. Applying (12.122) to (12.124) leads to

$$(D_1 H_1 + D_2 H_2)\beta = f_0 (D_2 - D_1)\partial \eta / \partial y. \tag{12.125}$$

where $\partial \eta / \partial y = \partial h_2 / \partial y = -\partial h_1 / \partial y$. Thus, assuming that $D_2 - D_1 \sim D_1$, and that $H_1 \gg H_2$ gives

$$H_1 \sim \frac{f_0 \partial \eta / \partial y}{\beta}. \tag{12.126}$$

Use of the thermal wind relation gives

$$H_1 \sim \frac{f_0^2 (\overline{u}_1 - \overline{u}_2)}{g' \beta}, \tag{12.127}$$

which is essentially the same as (12.121).

12.7.3 A few remarks

The essence of the PV mixing argument is that the troposphere is that part of the atmosphere within which energy is redistributed by dynamical mechanisms, and that the depth of the tropopause is determined by the constraints arising from the potential vorticity dynamics that effect that redistribution. We obtain a prediction of tropopause height (for a given meridional temperature gradient) if we assume either that:

(i) Potential vorticity is homogenized, or

(ii) The potential vorticity is redistributed diffusively, and the height of the tropopause adjusts to satisfy certain kinematic constraints.

The assumptions within item *(ii)* are particular to the derivation given above, and they are not self-evident. For example, one might suppose that the vertical distribution of diffusivity adjusts so that the constraints are satisfied, as in section 12.4.[13] We have also neglected relative vorticity which, although a reasonable assumption for the time-averaged state of the earth's atmosphere, may not generally hold. Nevertheless, given potential vorticity dynamics, the virtually equivalent scales (12.121) and (12.127) naturally and unavoidably arise.

12.8 † EXTRA-TROPICAL CONVECTION AND THE VENTILATED TROPOSPHERE

A contrasting point of view is to suppose that the mid-latitude tropospheric lapse rate is maintained by convection, the convection occurring predominantly in the warm sector of mature baroclinic waves.[14] First consider a dry atmosphere. In a given baroclinic zone the minimum potential temperature difference between the surface and the tropopause, $\Delta_z \theta = \theta_t - \theta_g$ is approximately zero. If the tropopause were colder than this the column would be convectively unstable, and the difference would become zero. The essential assumption is that within a baroclinic zone there generally *does* exist a region that is convectively unstable, and that convection then ensues with sufficient efficiency to partially fill the troposphere with air with that surface value of potential temperature. The process differs from that in the tropics because it is organized by baroclinic waves and, if we imagine a succesion of baroclinic waves around a latitude band the mean value of $\Delta_z \theta$ will be, approximately, its minimum (zero) plus half its variance. The variance in turn is a consequence of the pre-existing meridional temperature gradient and meridional advection across that gradient, and therefore

$$\text{Variance}(\Delta_z \theta) \propto \Delta_y \theta \qquad (12.128)$$

where the term on the right-hand side is the meridional temperature difference at the surface across the baroclinic zone. The mean potential temperature difference between the surface and tropopause is then proportional simply to the meridional temperature gradient at that latitude, with an undetermined constant of propotionality and so

$$\Delta_z \theta \propto \Delta_y \theta. \qquad (12.129)$$

Finally, if moisture is present (as it is!) the vertical potential temperature difference should be replaced by the 'equivalent potential temperature' difference — the equivalent

The Stratification of the Troposphere and Stratosphere

★ The troposphere is that region of the atmosphere where dynamics plays an important role in stratification, whereas the stratosphere is more nearly radiative equilibrium (although in winter in the lower stratosphere radiative equilibrium is not a very good approximation). The tropopause is the sharp change in stratification between the two regions.

★ The tropospheric lapse rate and the height of the tropopause are determined by a combination of dynamics and radiation. If a dynamical process predicts the height of the tropopause then, if the surface temperature is also given, the stratification follows via radiative considerations. Similarly, if the lapse rate is given, the tropopause height follows.

★ There are two general classes of theory for tropospheric stratification:

  (i) Potential vorticity mixing and its variants, including baroclinic adjustment. Baroclinic activity seeks to homogenize potential vorticity, although the homogenization may not be complete, and the depth to which the mixing occurs determines the position of the tropopause. This is related to the idea that baroclinic eddies are sufficiently efficient in transferring potential vorticity and heat that the atmosphere will be marginally critical to baroclinic instability.
  (ii) Moist convection, possibly organized by baroclinic activity. It is generally thought that moist convection does play the dominant role in determining tropical lapse rates, but in the extratropics the situation is less clear-cut.

In both of these, the troposphere is the region in which a dynamical redistribution of heat occurs.

★ In *(i)*, the constraints arising from potential vorticity dynamics suggest the importance of the height scale $H_t \sim (f^2 \Lambda)/(N^2 \beta)$, or equivalently that $s \sim \beta H_t / f$, where s is the isentropic slope, at least to the extent that relative vorticity gradients are much smaller than planetary vorticity gradients.

★ In *(ii)*, the lapse rate is bounded from below by the moist adiabatic lapse rate and, on average, the (equivalent) potential temperature difference between surface and troposphere is proportional to the meridional temperature difference across the baroclinic zone.

potential temperature being essentially the potential temperature achieved when all the water vapour in a parcel of air condenses and the latent heat of condensation is used to heat the parcel (section 2.9.3).

Put another way, the hypothesis is that within a baroclinic wave the advection of

warm air into a cold region *necessarily* leads to convection, and that this convection then efficiently fills the available volume, to the extent possible, with the warmest possible fluid. Oceanographers will find this a comfortable concept, for they are used to the notion of convection filling the domain with the densest available fluid (densest in the oceanic case because oceanic convection usually occurs from the top, with cold, dense water sinking). However, unlike the ocean in which the bottom of the container limits the volume of dense water that can be made, here it is tropopause that provides the upper lid; the height of this is determined by the dynamics itself, in conjunction with the radiative constraint discussed previously. Thus, the baroclinic zone becomes, in oceanographic parlance, *ventilated* by the warmest air at the surface. However, the entire baroclinic zone does not completely fill with this warm air because the convection is maintained by a meridional temperature gradient and it is necessarily intermittent: baroclinic instability would shut off if the entire baroclinic zone were filled with homogeneous warm fluid, and the zone would then meridionally restratify, and it is this maintenance of variance that leads to (12.129). The ultimate consequence then, is that the moist isentropic slope is proportional to that slope which would take an isentrope at the surface to the tropopause across a baroclinic zone. This contrasts with the potential vorticity mixing ideas, which suggest (at least in so far as relative vorticity fluxes are neglected) that the dry isentropic slope is proportional to the slope that goes from the ground to tropopause over a horizontal scale f/β, the equator-to-pole scale.

12.8.1 † Open questions, numerical and observational results

Details aside, the two general classes of theory for extra-tropical stratification are: (i) Potential vorticity mixing and its variants; (ii) Convection, and in particular moist convection organized by baroclinic activity. These are summarized in the shaded box on the facing page, and a number of numerical experiments and observational tests have been carried out to explore these.[15] Simulations with fairly complete atmospheric GCMs that include a realistic treatment of radiation do indicate that the tropopause height and stratification can be usefully considered to be set by a combination of a radiative and dynamical constraint. Furthermore, simulations with a dry atmospheric GCM *do* indicate that a realistic looking troposphere structure, and tropopause, can be maintained largely by the stirring effects of baroclinic eddies. Within the model troposphere potential vorticity is relatively well mixed, with the tropopause serving as a transport barrier. Given the potential vorticity distribution, the distribution of the velocity and potential temperature fields, including the lapse rate, follow by way of geostrophic invertibility. However, more detailed numerical tests do not unambiguously lend quantitative support to the predictions embodied in (12.121) or (12.126). The truth may well lie in some combination of our hypotheses, or elsewhere.

APPENDIX: ELIASSEN-PALM FLUX IN SPHERICAL COORDINATES

To obtain the plots of the Eliassen-Palm flux in figures 12.15, 12.16, 12.17 and 12.18 we make use of the following.[16] The zonal acceleration due to the EP flux, $\mathscr{F}$, is

approximately given by

$$\frac{\partial \overline{u}}{\partial t} + \cdots = \frac{1}{\cos \vartheta} \nabla \cdot \boldsymbol{\mathcal{F}} \tag{12A.1}$$

where

$$\boldsymbol{\mathcal{F}} = (\mathcal{F}^{\vartheta}, \mathcal{F}^{p}) = \left(-\cos \vartheta \, \overline{u'v'}, \, f \cos \vartheta \, \frac{\overline{v'\theta'}}{\partial_p \overline{\theta}} \right), \tag{12A.2}$$

where $f = 2\Omega \sin \vartheta$, $\partial_p \overline{\theta}$ takes its mean value, and

$$\nabla \cdot \boldsymbol{\mathcal{F}} = \frac{1}{a \cos \vartheta} \frac{\partial}{\partial \vartheta} (\mathcal{F}^{\vartheta} \cos \vartheta) + \frac{\partial}{\partial p} \mathcal{F}^{p}. \tag{12A.3}$$

From these we obtain

$$\nabla \cdot \boldsymbol{\mathcal{F}} = \frac{1}{a \cos \vartheta} \frac{\partial}{\partial \vartheta} \left(-\overline{u'v'} \cos^2 \vartheta \right) + \frac{\partial}{\partial p} \left(f \cos \vartheta \, \frac{\overline{v'\theta'}}{\partial_p \overline{\theta}} \right), \tag{12A.4}$$

and

$$\frac{\partial \overline{u}}{\partial t} + \cdots = \frac{1}{a \cos^2 \vartheta} \frac{\partial}{\partial \vartheta} \left(-\overline{u'v'} \cos^2 \vartheta \right) + \frac{\partial}{\partial p} \left(f \, \frac{\overline{v'\theta'}}{\partial_p \overline{\theta}} \right). \tag{12A.5}$$

In the figures that show the EP vectors, the arrows have a horizontal and vertical components proportional to $\mathcal{F}^{\vartheta}$ and $\mathcal{F}^{p}(a/1000)$ respectively, where the scaling factor on $\mathcal{F}^{p}$ makes it possible to see the divergence by eye. In the figures that show the EP flux divergence, we plot the right-hand side of (12A.5), namely the EP flux divergence divided by $\cos \vartheta$, this being the quantity that is equal to the acceleration of the zonal flow.

Notes

1 The modern view of the mid-latitude general circulation — the largely zonally asymmetric motion that provides the bulk of the meridional transport of heat and momentum in the extratropics — began to take form in the 1920s in papers by Defant (1921) and Jeffreys (1926). Defant regarded the mid-latitude circulation as turbulence on a large scale (geostrophic turbulence we might call it now) and actually calculated the horizontal eddy-diffusivities using Prandtl-like mixing length arguments. Soon after, Jeffreys presciently wrote of 'the dynamical necessity for a continual exchange of air between high and low latitude' and that 'no general circulation of the atmosphere without cyclones is dynamically possible when friction is taken into account.' This point of view slowly gained ground, with, for example, Starr (1948) advocating the point of view that large-scale eddies were responsible for the bulk of the meriodional transport of momentum in mid-latitudes, and Rossby (1949) eventually noting in a review article that 'One is forced to conclude that there no longer exists a compelling reason to build the theory of the maintenance of the general circulation exclusively on *meridional* solenoidal circulations'. Soon after this came a series of discussion papers by Eady (Eady 1950, Eady and Sawyer 1951, Eady 1954), that, setting the stage for the modern viewpoint, really struggle with the turbulent transport of mid-latitude eddies and the maintenance

of the surface currents — the importance of the enstrophy budget is discussed, for example, and Eady comes close to deriving wave activity conservation (p126 of Eady 1954). Another landmark is the influential monograph by Lorenz (1967) that summarized, clarified and added to progress to that date, noting (in his last paragraph) that the cause of the poleward eddy transport across mid-latitudes (and hence the cause of the surface eastward winds) had not at that time been properly explained. That explanation has come since then, by way of potential vorticity dynamics and the momentum transport in Rossby waves and with contributions from many scientists, as described in this chapter and in chapter 7.

2 Held (2000), Rhines and Holland (1979).

3 This technique is discussed in Lighthill (1965, 1978).

4 Models of the general circulation of this ilk were introduced by Green (1970).

5 Adapted from Juckes (2001).

6 Early evidence that the temperature increases above about 11 km came from the balloon measurements of Tesserenc De Bort (1902), who also suggested the names tropopause and stratosphere. More recently, radiative and dynamical issues relevant to this topic are discussed by, among others, Stone (1972), Held (1982), Juckes (2000) and Shepherd (2002).

7 Paraphrasing World Meteorological Organization (1957); also Lewis (1991).

8 I thank Thomas Birnir for the tropopause-based averages. See also Birner (2005).

9 However, it is often said that the height of the tropical tropopause is rather higher than the depth to which deep convection penetrates, and if true this is in need of explanation. Both convective overshooting and the influence of the Brewer-Dobson circulation may play a role.

10 Birner et al. (2002). Birnir (2005)

11 Stone (1978).

12 Salmon (1980), Vallis (1988).

13 As in Green (1970) and its immediate descendants, and Smith and Vallis (2002). See also Schneider (2004) for a related argument but one that is fundamentally non-quasigeostrophic.

14 Following Juckes (2000).

15 For example Thuburn and Craig (1997) and Haynes et al. (2001).

16 I am very grateful to E. Gerber for constructing these figures.

Further Reading

Green, J. S. A., 1999. *Atmospheric Dynamics.*
  A rather unique view of atmospheric dynamics, with a number of personal perspectives on how the atmosphere works.

Held, I., 2000. *The General Circulation of the Atmosphere.*
  These lecture notes, from a summer school in Woods Hole, present an informal synthesis of many modern ideas in atmospheric general circulation theory.

James, I., 1994. *An Introduction to Circulating Atmospheres.*
  An introductory book on the global circulation of the atmosphere, with discussions of theory, observations and models.

Problems

12.1 ◆ Construct a numerical model (e.g., in Fortran, C, or Matlab) that steps (12.101) forward in time, using a diffusive closure for the potential vorticity fluxes, a frictional term equivalent to a linear drag on velocity in the lower layer, and thermodynamic source term equivalent to a relaxation back to a temperature that monotonically decreases with latitude. Explore the effects of different lateral boundary conditions on the potential vorticity flux, the effects of satisfying or not the kinematic constraint (12.81), and the effects of various horizontal structures and amplitudes of the transfer coefficients. Discuss whether this is a useful model of the zonally averaged circulation.

Divide and conquer.

Zonally Asymmetries, Planetary Waves and the Stratosphere

IN TRYING TO BUILD A THEORY of the general circulation of the extra-tropical atmosphere it is useful to divide that task into two. The first task (chapters 11 and 12) is to understand the zonally averaged circulation and we suppose that, to a first approximation, this circulation is qualitatively the same as it would be if the boundary conditions were zonally symmetric, with no mountains or land-sea contrasts. Given the statistically zonally symmetric circulation, the second task is to understand the zonally asymmetric circulation by supposing that the latter is a perturbation on the former, and using a theory linearized about the zonally symmetric state. In practice, this involves calculating the forced, stationary Rossby waves that are generated by the interaction of surface topography and zonally asymmetric thermal forcing with that zonally averaged flow — that is, we compute the forced *stationary waves* of the system. Properly including the effects of transient eddies — equilibrated, finite amplitude baroclinic systems — is the most difficult aspect of such a calculation, although their effects may be included diagnostically by evaluating their associated heat and momentum fluxes from observations and adding them to the right-hand sides of the equations. However, we will find the calculations are quite revealing even if the effects of transient eddies are omitted entirely. We will focus first response to orography at the lower boundary and then consider thermodynamic forcing arising, for example, from a surface temperature field.[1] Because these waves propagate upwards as well as laterally, this will lead us into the second topic of this chapter, a brief discussion of stratospheric dynamics.

563

13.1 FORCED AND STATIONARY ROSSBY WAVES

13.1.1 A simple one-layer case

Many of the essential ideas can be illustrated by a one-layer quasi-geostrophic model, with potential vorticity equation

$$\frac{\mathrm{D}q}{\mathrm{D}t} = 0, \qquad q = \zeta + \beta y - \frac{f_0}{H}(\eta - h_b), \tag{13.1}$$

where H is the mean thickness of the layer, η is the height of free surface, h_b is the bottom topography, and the velocity and vorticity are given by $\boldsymbol{u} = (g/f_0)\nabla^\perp \eta$ and $\zeta = (\partial v/\partial x - \partial u/\partial y) = (g/f_0)\nabla^2 \eta$. Linearizing (13.1) about a flat-bottomed state with zonal flow $\overline{u}(y) = -(g/f_0)\partial\overline{\eta}/\partial y$ gives

$$\frac{\partial q'}{\partial t} + \overline{u}\frac{\partial q'}{\partial x} + v'\frac{\partial\overline{q}}{\partial y} = 0, \tag{13.2}$$

where $q' = \zeta' - (f_0/H)(\eta' - h_b)$ and $\partial\overline{q}/\partial y = \beta + \overline{u}/L_d^2$ with $L_d = \sqrt{gH}/f_0$, the radius of deformation. Eq. (13.2) may be written, after the cancellation of a term proportional to $\overline{u}\partial\eta'/\partial x$,

$$\frac{\partial}{\partial t}\left(\zeta' - \frac{\psi'}{L_d^2}\right) + \overline{u}\frac{\partial\zeta'}{\partial x} + \beta v' = -\overline{u}\frac{\partial\widehat{h}}{\partial x}. \tag{13.3}$$

where $\psi' = (g/f_0)\eta'$ and $\widehat{h} = (g/L_d^2 f_0)h_b$.

　　The solution of this equation consists of the solution to the homogeneous problem (with the right-hand-side equal to zero, as considered in section 5.7) and the particular solution. We proceed by decomposing the variables into their zonal Fourier components

$$(\zeta', \psi', \widehat{h}_b) = \operatorname{Re}(\widetilde{\zeta}, \widetilde{\psi}, \widetilde{h}_b)\sin ly\, e^{ikx}. \tag{13.4}$$

where such decomposition is appropriate for a channel, periodic in the x-direction and with no variation at its meridional boundaries at $y = (0, L)$. The full solution will be a superposition of such Fourier modes but, because the problem is linear, these modes do not interact. The free Rossby waves, the solution to the homogeneous problem, evolve according to

$$\psi = \operatorname{Re}\widetilde{\psi}\sin ly\, e^{i(kx-\omega t)}, \tag{13.5}$$

where ω is given by the dispersion relation [c.f., (5.187)]

$$\omega = k\overline{u} - \frac{\partial_y\overline{q}}{K^2 + k_d^2} = \frac{\overline{u}K^2 - \beta}{K^2 + k_d^2}. \tag{13.6a,b}$$

where $K^2 = k^2 + l^2$ and $k_d = 1/L_d$. Stationary waves occur at the wavenumbers where $K_s = \sqrt{\beta/\overline{u}}$.

　　To the free waves we add the solution to the steady problem,

$$\overline{u}\frac{\partial\zeta'}{\partial x} + \beta v = -\overline{u}\frac{\partial\widehat{h}}{\partial x}, \tag{13.7}$$

which gives, using the notation of (13.4)

$$\widetilde{\psi} = \frac{\widetilde{h}_b}{(K^2 - K_s^2)}. \tag{13.8}$$

Now, $\widetilde{h}_b$ is a complex amplitude; thus, for $K > K_s$ the streamfunction response is *in phase* with the topography. For $K^2 \gg K_s^2$ the steady equation of motion is

$$\overline{u}\frac{\partial \zeta'}{\partial x} \approx -\overline{u}\frac{\partial \widehat{h}}{\partial x}, \tag{13.9}$$

and the topographic vorticity source is balanced by zonal advection of relative vorticity. For $K^2 < k_s^2$ the streamfunction response is *out of phase* with the topography, and the dominant balance for very large scales is between the meridional advection of planetary advection, $v\partial f/\partial y$ or βv, and the topographic source. For $K = K_s$ the response is infinite, the stationary wave resonating with the topography. Now, any realistic topography can be expected to have contributions from *all* Fourier components. Thus, for *any* given zonal wind there will be a resonant wavenumber and an infinite response. This, of course, is not observed, and one reason is that the real system contains friction. The simplest way to include this is by adding a linear damping to the right-hand side of (13.3), giving

$$\frac{\partial}{\partial t}\left(\zeta' - \frac{\psi'}{L_d^2}\right) + \overline{u}\frac{\partial \zeta'}{\partial x} + \beta v = -r\zeta' - \overline{u}\frac{\partial \widehat{h}}{\partial x}. \tag{13.10}$$

The free Rossby waves all decay monotonically to zero (problem 13.12). However, the steady problem,

$$\overline{u}\frac{\partial \zeta'}{\partial x} + \beta v' = -r\zeta' - \overline{u}\frac{\partial \widehat{h}}{\partial x}, \tag{13.11}$$

now has solutions

$$\widetilde{\psi} = \frac{\widetilde{h}_b}{(K^2 - K_s^2 - iR)} \tag{13.12}$$

where $R = (rK^2/\overline{u}k)$, and the singularity has been removed. The amplitude of the response is still a maximum for the stationary wave, and for this wave the phase of the response is shifted by $\pi/2$ with respect to the topography (Fig. 13.1).[2] The upshot is that for a mountain range whose Fourier composition contains all wavenumbers, there is a minimum in the streamfunction a little downstream of the mountain ridge.

13.1.2 Application to Earth's atmosphere

Rather surprisingly, given the complexity of the real system and the simplicity of the model, when used with realistic topography a one-layer model gives reasonably realistic answers for the Earth's atmosphere. Thus, we calculate the stationary response to the earth's topography using (13.11), using a reasonably realistic representation of the earth's topography and, with qualification, the zonal wind. The zonal wind on the left-hand-side of (13.11) is interpreted as the wind in mid-troposphere, whereas the wind on
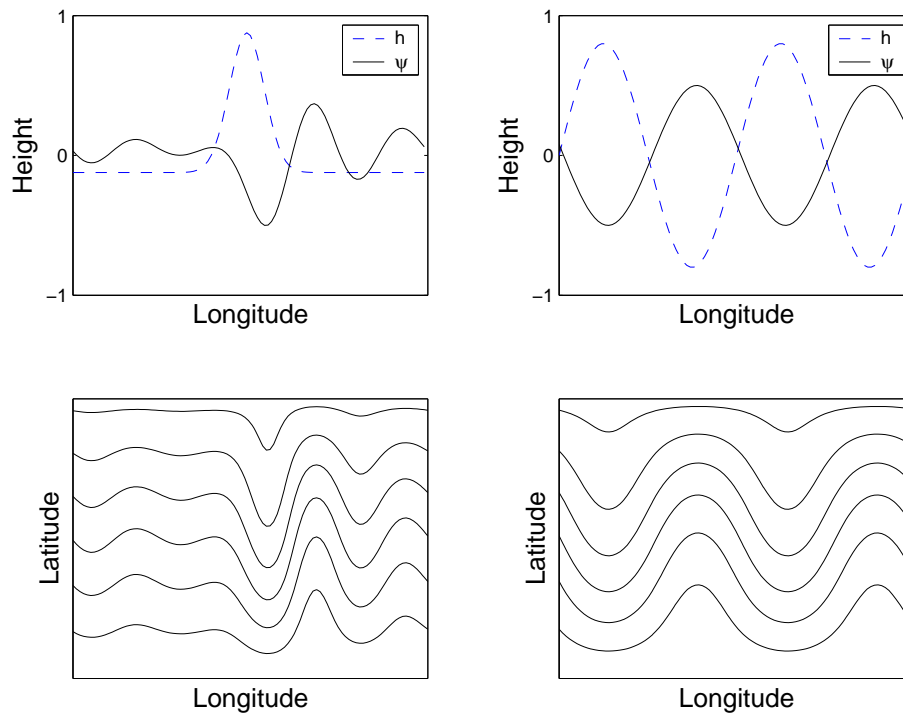
Fig. 13.1 The response to topographic forcing, i.e., the solution to (13.11), for topography consisting of an isolated Gaussian ridge (left panels) and a pure sinusoid (right panels). The wavenumber of the stationary wave is about 4, and $r/(\overline{u}k) = 1$. The upper panels show the amplitude of the topography (dashed curve) and the perturbation streamfunction response (solid curve). The lower panels are contour plots of the streamfunction, including the mean flow. With the ridge, the response is dominated by the resonant wave and there is a streamfunction minimum, a 'trough', just downstream of the ridge. In the case on the right, the flow cannot resonate with the topography, which consists only of wavenumber 2, and the response is exactly out of phase with the topography.

the right-hand-side is better interpreted as the surface wind, and so perhaps about 0.4 times the mid-troposphere wind. Since the problem is linear, this simply amounts to tuning the amplitude of the response. The results, obtained using a rather crude representation of the earth's topography, are plotted in Fig. 13.2. Also plotted is the observed time-averaged response of the real atmosphere (the 500 mb height field at 45° N). The agreement between model and observation is quite good, but this must be regarded as somewhat fortuitous if only because the other main source of the stationary wave field — thermal forcing — has been completely omitted from the calculation. Nevertheless, the calculation does suggest that the stationary, zonally asymmetric, features of the earth's atmosphere arise via the interaction of the zonally symmetric wind field and the
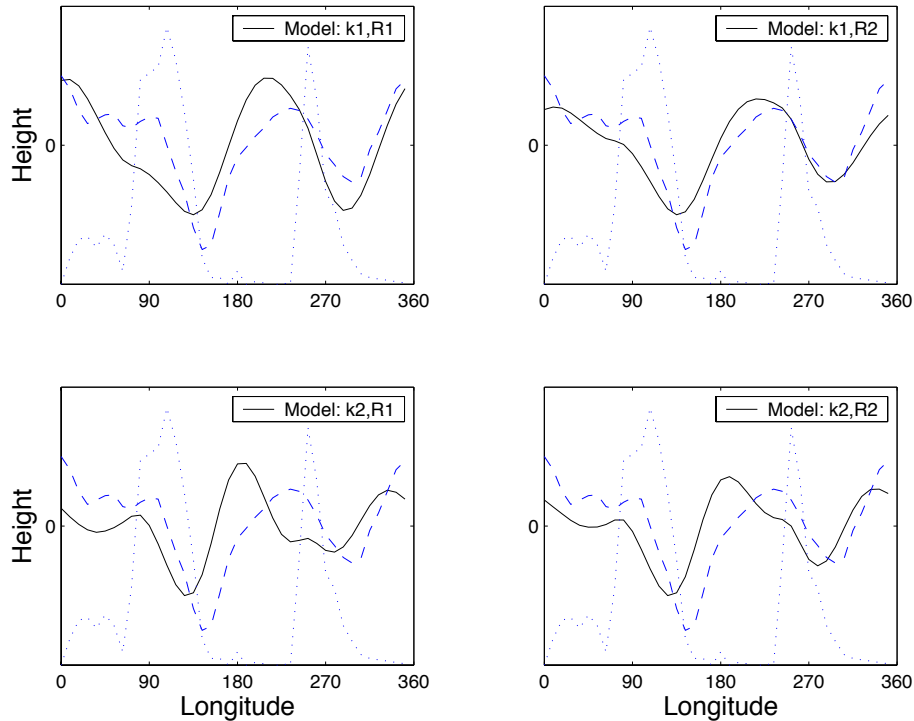
Fig. 13.2 Solutions of the Charney-Eliassen model. The solid lines are solution of (13.11) using the earth's topography at 45°N with two values of friction ($R1 \approx 6$ days, $R2 \approx 3$ days) and two values of resonant zonal wavenumber (2.5 for k1, 3.5 for k2), corresponding to zonal winds of approximately $17\,\mathrm{m\,s^{-1}}$ and $13\,\mathrm{m\,s^{-1}}$. The dashed line in each panel is the observed average height field at 500 mb at 45°N in January, and the dotted line is the topography used in the calculations.

zonally asymmetric lower boundary, and that these may be calculated to a reasonable approximation with a linear model.

13.1.3 * One-dimensional Rossby wave trains

Although the Fourier analysis above gives exact results, it is not particularly revealing of the underlying dynamics. We see from Fig. 13.1 response to the Gaussian ridge is largely downstream of the ridge, and this suggests that it will be useful to consider the Rossby as being due to Rossby *wavetrains* being excited by local features. This is also suggested by Fig. 13.3, which shows that the response to realistic topography is relatively local, and may be considered to arise from two relatively well-defined wavetrains each of finite extent one coming from the Rockies and the other from the Himalayas.

One way to analyse these wavetrains, and one which also brings up the concept of group velocity in a natural way, is to exploit (as in section 12.1.4) a connection between changes in wavenumber and changes in frequency. Consider the linear barotropic vor-

Figure 13.3 The solution of the upper left panel Fig. 13.2 (solid line), and the solution divided into two contributions (dashed lines), one due to the topography only of the western hemisphere (i.e., with the topography in the east set to zero) the other due to the topography only of the eastern hemisphere.
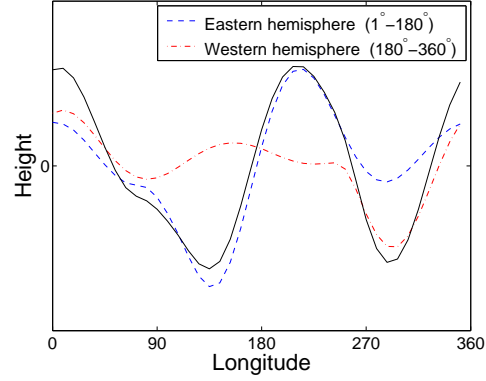
ticity equation in the form

$$\frac{\partial}{\partial t}(\zeta - k_d^2 \psi) + \overline{u}\frac{\partial \zeta}{\partial x} + \beta\frac{\partial \psi}{\partial x} = -r\zeta, \tag{13.13}$$

where r is a frictional coefficient, which we presume small. Setting $k_d = 0$ for simplicity, the linear dispersion relation is

$$\omega = \overline{u}k - \frac{\beta k}{K^2} - ir \equiv \omega_R(k,l) - ir, \tag{13.14}$$

where $K^2 = k^2 + l^2$ and $\omega_R(k,l)$ is the inviscid dispersion relation. Now, if there is a local source of the waves, for example an isolated mountain, we may expect to see a *spatial* attenuation of the wave as it moves away from the source. We thus regard the system as having a fixed, real frequency, but a changing, possibly complex, wavenumber. To determine this wavenumber for stationary waves (and so with $\omega = 0$), for small friction we expand the dispersion relation in a Taylor series about the inviscid value of ω_R at the stationary wavenumber k_s, where $k_s = (K_s^2 - l^2)^{1/2}$ and $K_s = \sqrt{\beta/\overline{u}}$. This gives

$$\omega + ir = \omega_R(k,l) \approx \omega_R(k_s,l) + \left.\frac{\partial \omega_R}{\partial k}\right|_{k=k_s} k' + \cdots. \tag{13.15}$$

Thus, $k' \approx ir/c_g^x$ where c_g^x is the zonal component of the group velocity evaluated at a fixed position and at the stationary wavenumber; using (5.185b) this is given by

$$c_g^x = \left.\frac{\partial \omega_R}{\partial k}\right|_{k=k_s} = \frac{2\overline{u}k_s^2}{k_s^2 + l^2}. \tag{13.16}$$

The solution then decays away from a source at $x = 0$ according to

$$\psi \sim \exp(ikx) \approx \exp(ik_s x - rx/c_g^x) \tag{13.17}$$

and, because $c_g^x > 0$, the response is east of the source. The approximate solution for the streamfunction (denoted ψ_δ) of (13.11) in an infinite channel, with the topography
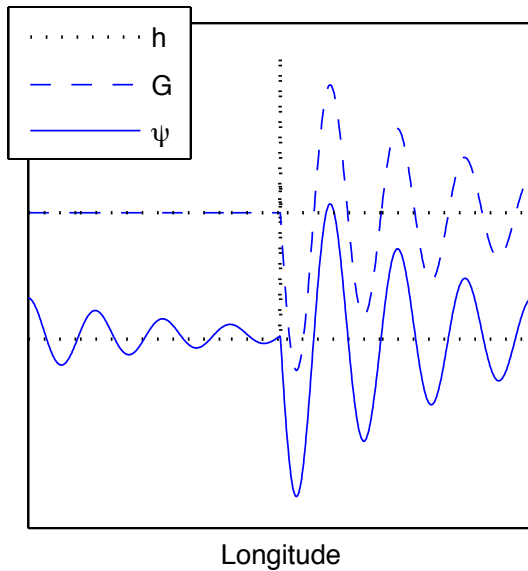
Figure 13.4 A one-dimensional Rossby wave train excited by a delta-function mountain ridge (h, dotted lines) in the center of the domain and a uniform eastward flow. The upper curve, G, shows the Green's function (13.18), whereas the lower curve shows the exact (linear) response, ψ, in a re-entrant channel numerically calculated using the Fourier method. The two solutions are both centered around zero and offset for clarity; the only noticeable difference is upstream of the ridge, where there is a finite response in the Fourier case because of the progression of the wavetrain around the channel. The stationary wavenumber is 7.5.

being a δ-function mountain ridge at $x = x'$ (and with all fields varying meridionally like $\sin ly$) is thus

$$\psi_\delta(x - x', y) \sim \begin{cases} 0 & x \le x' \\ -\dfrac{1}{k_s} \sin ly \, \sin[k_s(x - x')] \exp[-r(x - x')/c_g^x] & x \ge x'. \end{cases}$$
(13.18)

In the more general problem in which the topography is a general function of space, every location constitutes a separate source of wavetrains, and the complete (approximate) solution is given by the integral

$$\psi'(x, y) = \frac{1}{k_s} \int_{-\infty}^{\infty} \widehat{h}(x) \psi_\delta(x - x') \, dx'.$$
(13.19)

The field $\psi_\delta(x - x', y)$, is the 'Greens function' for the problem, and often denoted $G(x - x', y)$.

An example solution calculated using both the Fourier and Greens-function methods are illustrated in Fig. 13.4. As in Fig. 13.1 there is a trough immediately downstream of the mountain, a result that holds for a broad range of parameters. Here, the solution decays almost completely in one circumnavigation of the channel, and thus, downstream of the mountain, both methods give virtually identical results. Such a correspondence will not hold if the wave can circumnavigate the globe with little attenuation, for then resonance will occur and the Greens-function method will be inaccurate; thus, whether the resonant picture or the wavetrain picture is more appropriate depends largely on the frictional parameter. A frictional timescale of about 10 days is often considered to approximately represent the earth's atmosphere, in which case waves are only slightly damped on a global circumnavigation, and the Fourier picture is natural

with the possibility of resonance. However, the smaller (more frictional) value of 5 days seems to give quantitatively better results in the barotropic problem, and the solution is more evocative of wavetrains. The larger friction may perform better because it is crudely parameterizing the meridional propagation and dispersion of Rossby waves that is neglected in the one-dimensional model.[3]

13.2 * MERIDIONAL PROPAGATION AND DISPERSION

Rossby waves, of course, propagate meridionally as well as zonally. Furthermore, one of the major mountain ranges on the earth — the Himalayas — is fairly localized in the meridional direction, and even though the Rockies and Andes do form a convenient meridional ridge the Rossby waves they generate will still propagate both zonally and meridionally. Furthermore, the coefficients of the linear equations of motion vary with space: on the sphere β is a function of latitude and in general topography is a function of both latitude and longitude. Given this complexity, we cannot solve the full problem except numerically, but a few ideas from wave tracing illustrate many of features of the response, and indeed of the stationary wave pattern in the earth's atmosphere.[4]

13.2.1 Ray tracing

We will first, informally and without proof, go over some results about rays and ray tracing.[5] Roughly speaking, a *ray* is the trajectory in space along which certain properties of a wave propagate. The ray is perpendicular to the wave front, and in a homogeneous medium a wave propagates in a straight line. In a dispersive system, energy propagates at the group velocity, $c_g = \nabla_k \omega$, and rays are lines that are parallel to the group velocity. In non-homogeneous media the group velocity so defined will vary with position; however, if the medium varies only slowly, on a scale much larger than that that of the wavelength of the waves, the energy propagates along rays and, locally, the energy propagation velocity is still given by the group velocity. Let us represent a wave by

$$\psi(x_i, t) = \Psi(x_i, t) e^{i\theta(x_i, t)} \tag{13.20}$$

where the amplitude, Ψ, varies more slowly than the phase, θ. (We use subscripts to denote Cartesian axes, repeated subscripts are to be summed over, and (x_i, t) means (x, y, z, t) etc.) Locally, the phase is given by $\theta \approx k_i x_i - \omega t$, and the local frequency, ω, and wavenumber, k_i satisfy

$$k_i = \frac{\partial \theta}{\partial x_i}, \qquad \omega = -\frac{\partial \theta}{\partial t}, \tag{13.21a,b}$$

and these imply

$$\frac{\partial k_i}{\partial t} = -\frac{\partial \omega}{\partial x_i} \tag{13.22}$$

The frequency is, in general, a function of wavenumber and position, and a relation of the form $\omega = \omega(k_i, x_i)$ constitutes the dispersion relation. The local group velocity is then given by $c_{gi} \equiv \partial \omega / \partial k_i$.

Now, using (13.21) we can write the frequency as

$$\omega = \omega(k_i, x_i) = \omega(\partial\theta/\partial x_i, x_i). \tag{13.23}$$

Then, using (13.23), (13.22) becomes

$$\frac{\partial k_i}{\partial t} = -\left(\frac{\partial\omega}{\partial x_i}\right)_{k_i} - \left(\frac{\partial\omega}{\partial k_j}\right)_{x_i} \frac{\partial k_j}{\partial x_i} = -\left(\frac{\partial\omega}{\partial x_i}\right)_{k_i} - \left(\frac{\partial\omega}{\partial k_j}\right)_{x_i} \frac{\partial}{\partial x_i} \frac{\partial\theta}{\partial x_j}, \tag{13.24}$$

or, using the definition of the group velocity,

$$\frac{\partial k_i}{\partial t} + c_{gj} \frac{\partial k_i}{\partial x_j} = -\left(\frac{\partial\omega}{\partial x_i}\right)_{k_i}. \tag{13.25}$$

The left-hand side is the change in wavenumber along a ray. If the frequency is constant, the wavenumber is simply propagated at the group velocity. If the frequency is independent of a particular coordinate then the corresponding wavenumber is constant along the ray. If the frequency changes with position (as in general it will), then the wavenumber will change along a ray, and thus so will the direction of propagation — the wave is *refracted*. Note that we can write (13.25), and the definition of group velocity, in the compact forms:

$$\frac{\mathrm{D}_{c_g} k_i}{\mathrm{D}t} = -\frac{\partial\omega}{\partial x_i}, \qquad \frac{\mathrm{D}_{c_g} x_i}{\mathrm{D}t} = \frac{\partial\omega}{\partial k_i}. \tag{13.26a,b}$$

where $\mathrm{D}_{c_g}/\mathrm{D}t \equiv \partial/\partial t + (\boldsymbol{c}_g \cdot \nabla)$. One other consequence of these manipulations is that the frequency is constant along a ray. This follows by noting that frequency is a function both a space and wavenumber so that

$$\frac{\mathrm{D}_{c_g}\omega}{\mathrm{D}t} = \left(\frac{\partial\omega}{\partial k_i}\right)\frac{\mathrm{D}_{c_g} k_i}{\mathrm{D}t} + \left(\frac{\partial\omega}{\partial x_i}\right)\frac{\mathrm{D}_{c_g} x_i}{\mathrm{D}t} = 0, \tag{13.27}$$

where the second equality follows by use of (13.26). One practical result of all this that in problems of the form

$$\frac{\partial}{\partial t}\nabla^2\psi + \beta(y)\frac{\partial\psi}{\partial x} = 0, \tag{13.28}$$

the frequency and x-wavenumber are constant along a ray.

13.2.2 Rossby waves and Rossby rays

If the topography is localized, then ray theory provides a useful way of calculating and interpreting the response to a flow over that topography. On the β-plane and away from the orographic source the steady linear response to a zonally uniform but meridionally varying zonal wind will obey

$$\bar{u}(y)\frac{\partial}{\partial x}\left(\frac{\partial^2}{\partial x^2} + \frac{\partial^2}{\partial y^2}\right)\psi' + \beta\frac{\partial\psi'}{\partial x} = 0 \tag{13.29}$$

In fact, an equation of this form applies on the sphere. To see this, we transform the spherical coordinates (λ, ϑ) into Mercator coordinates with the mapping[6]

$$
x = a\lambda, \quad \frac{1}{a}\frac{\partial}{\partial\lambda} = \frac{\partial}{\partial x}, \qquad y = \frac{a}{2}\ln\left(\frac{1 + \sin\vartheta}{1 - \sin\vartheta}\right), \quad \frac{1}{a}\frac{\partial}{\partial\vartheta} = \frac{1}{\cos\vartheta}\frac{\partial}{\partial y}.
\tag{13.30}
$$

The spherical coordinate vorticity equation then becomes

$$
\overline{u}_M \frac{\partial}{\partial x}\left(\frac{\partial^2}{\partial x^2} + \frac{\partial^2}{\partial y^2}\right)\psi' + \beta_M \frac{\partial\psi'}{\partial x} = 0,
\tag{13.31}
$$

where $\overline{u}_M = \overline{u}/\cos\vartheta$ and

$$
\beta_M = \frac{2\Omega}{a}\cos^2\vartheta - \frac{\mathrm{d}}{\mathrm{d}y}\left[\frac{1}{\cos^2\vartheta}\frac{\mathrm{d}}{\mathrm{d}y}(\overline{u}_M\cos^2\vartheta)\right] = \cos\vartheta\left(\beta_s + \frac{1}{a}\frac{\partial\overline{\zeta}}{\partial\vartheta}\right),
\tag{13.32}
$$

where $\beta_s = 2a^{-1}\Omega\cos\vartheta$. Thus, β_M is the meridional gradient of the absolute vorticity, multiplied by the cosine of latitude. An advantage of Mercator coordinates over their spherical counterparts is that (13.31) has a Cartesian flavour to it, in that the metric coefficients are absorbed into the parameters $\overline{u}_M$ and β_M. Of course, unlike the case on the true β-plane, the parameter β_M is not a constant, but this is not a particular disadvantage if $\overline{u}$ is varying with y.

Having noted the spherical relevance we revert to the β-plane and seek solutions of (13.29) with the form $\psi' = \widetilde{\psi}(y)\exp(ikx)$, whence

$$
\frac{\mathrm{d}^2\widetilde{\psi}}{\mathrm{d}y^2} = \left(k^2 - \frac{\beta}{\overline{u}}\right)\widetilde{\psi} = \left(k^2 - k_s^2\right)\widetilde{\psi}.
\tag{13.33}
$$

where $k_s = (\beta/\overline{u})^{1/2}$. From this equation it is apparent that if $k < k_s$ the solution is harmonic in y and Rossby waves may propagate away from their source. On the other hand, wavenumbers $k > k_s$ are trapped near their source, and so waves are trapped by westward flow.

Without solving (13.33), we can expect an isolated mountain to produce two wavetrains, one for each meridional wavenumber $l = \pm(k_s^2 - k^2)^{1/2}$. These wavetrains will then propagate along a ray, and given the dispersion relation this trajectory can be calculated (usually numerically) using the expressions of the previous section. The local dispersion relation of Rossby waves is

$$
\omega = \overline{u}k - \frac{\beta k}{k^2 + l^2},
\tag{13.34}
$$

so that their group velocity is

$$
c_g^x = \frac{\partial\omega}{\partial k} = \overline{u} - \frac{l^2 - k^2}{(k^2 + l^2)^2} = \frac{\omega}{k} + \frac{2\beta k^2}{(k^2 + l^2)^2},
\tag{13.35a}
$$

$$
c_g^y = \frac{\partial\omega}{\partial l} = \frac{2\beta kl}{(k^2 + l^2)^2}.
\tag{13.35b}
$$
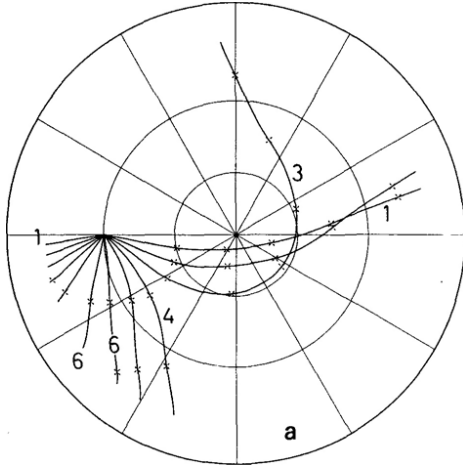
Figure 13.5 The rays emanating from a point source at 30°N and 180°, (nine o'clock), calculated using the observed value of the wind at 300 mb.[7] The crosses mark every 180° of phase, and mark the positions of successive positive and negative extrema. The numbers indicate the zonal wavenumber of the ray. The ray paths may be compared with the full linear calculation shown in Fig. 13.6.

The sign of the meridional wavenumber thus determines whether the waves propagate poleward (positive l) or equatorward (negative l). Also, because the dispersion relation (13.35) is independent of x and t, the zonal wavenumber and frequency in the wave group are constant along the ray, and the meridional wavenumber then adjusts to satisfy the local dispersion relation (13.34). Thus, from (13.33), the meridional scale becomes larger as k_s approaches k from above and an incident wavetrain wavetrain is reflected, its meridional wavenumber changes sign, and it continues to propagate eastward.

Stationary waves have $\omega = 0$, and the trajectory of a ray is parameterized by

$$\frac{\mathrm{d}y}{\mathrm{d}x} = \frac{c_g^y}{c_g^x} = \frac{l}{k}. \tag{13.36}$$

For a given zonal wavenumber the trajectory is then fully determined by this condition and that for the local meridional wavenumber which from (13.34) is

$$l^2 = k_s^2 - k^2. \tag{13.37}$$

Finally, from (13.35) the magnitude of the group velocity is

$$|c_g| = [(c_g^x)^2 + (c_g^y)^2]^{1/2} = 2\frac{k}{k_s}\overline{u}, \tag{13.38}$$

which is double the speed of the projection of the basic flow, $\overline{u}$, onto the wave direction. An example of rays are shown in Fig. 13.5.

* A JWKB solution

Information about the wave amplitudes along a ray can be obtained using a JWKB approach.[8] Let us write (13.33) as

$$\frac{\mathrm{d}^2 \widetilde{\psi}}{\mathrm{d}y^2} + l^2 \widetilde{\psi} = 0 \tag{13.39}$$

where

$$l^2(y) = k_s^2 - k^2. \tag{13.40}$$

If $l(y)$ is sufficiently slowly varying in y (i.e., if $|\mathrm{d}l^{-1}/\mathrm{d}y| < 1$) then we may seek a solution of the form

$$\widetilde{\psi} = Ae^{ig(y)}. \tag{13.41}$$

This leads to an approximate solution for $g(y)$, namely

$$g(y) = \int^y l(y)\,\mathrm{d}y + \frac{1}{2}i\ln l(y), \tag{13.42}$$

and the approximate solution for the stationary streamfunction is then

$$\psi(x, y) = Al^{-1/2}\exp\left[\left(kx + \int^y l(y)\,\mathrm{d}y\right)\right], \tag{13.43}$$

where A is a constant. Consider, for example, the disturbance excited by an isolated low-latitude peak, with $\overline{u}$ increasing, and so k_s decreasing, polewards of the source. Assuming that initially that there exists a zonal wavenumber k less than k_s then two eastward propagating wavetrains are excited. The meridional wavenumber of the polewards wavetrain diminishes according to (13.40), so that, using (13.36), the ray becomes more zonal. The latitude where $k = k_s$, the 'turning latitude' the wave is reflected but continues propagating eastward. The southward propagating wavetrain is propagating into a medium with smaller $\overline{u}$ and larger k_s. At the 'critical latitude', where $\overline{u} = 0$, $l \to \infty$ but c_g^x and c_g^y both tend to zero, but [using (13.35)] in such a way that $c_g^x/c_g^y \to 0$. That is, the rays become meridionally oriented and their speed tends to zero. At this latitude the waves may be absorbed, but the analysis is specialized and beyond our scope.[9] Finally, we mention without proof that for zonal flows with constant angular velocity the trajectories are great circles.

13.2.3 Application to an idealized atmosphere

We should best think of the remarks above as helping us interpret more complete numerical, but still linear, calculations of stationary Rossby waves — that is, solutions of the stationary barotropic vorticity equation,

$$\frac{\overline{u}}{a\cos\vartheta}\frac{\partial\zeta'}{\partial\lambda} + v'\left(\frac{1}{a}\frac{\partial\overline{\zeta}}{\partial\vartheta} + \beta\right) = -\frac{\overline{u}f_0}{a\cos\vartheta}\frac{\partial h_b}{\partial\lambda} - r\zeta', \tag{13.44}$$

written in spherical coordinates, with $[u, v] = a^{-1}[-\partial\psi/\partial\vartheta, (\partial\psi/\partial\lambda)/\cos\vartheta]$, $\beta = 2\Omega a^{-1}\cos\vartheta$ and $\zeta = \nabla^2\psi$. The last term in (13.44) crudely represents, as before, the effects of friction and generally reduces the sensitivity of the solutions to resonances. Such linear calculations, in turn, help us interpret the stationary wave pattern in the earth's atmosphere. Solutions to (13.44) may be obtained first by discretizing and then numerically inverting a matrix, and although the actual procedure is quite involved it is analogous to the Fourier methods used earlier for the simpler one-dimensional problem.
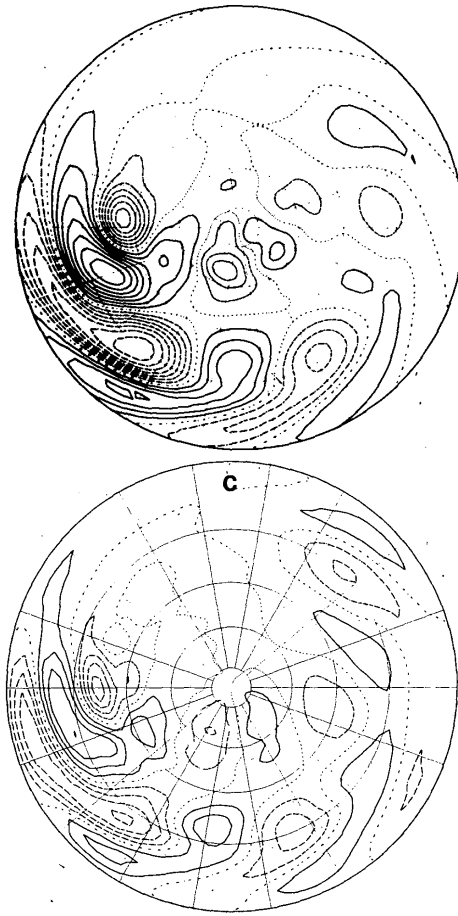
Fig. 13.6 The linear stationary response induced by circular mountain at 30°N and at 180° longitude (nine o'clock). The figure on the left uses a barotropic model, whereas the figure on the right uses a multi-layer baroclinic model.[10] In both cases the mountain excites a low wavenumber polar wavetrain and a higher wavenumber subtropical train.

Fig. 13.6 shows the stationary solution to the problem with a realistic Northern hemisphere zonal flow and an isolated, circular mountain at 30° N. The topography excites two wavetrains, both of which slowly decay downstream because of frictional effects, rather like the one dimensional wavetrain in Fig. 13.4. The polewards propagating wavetrain develops a more meridional orientation, corresponding to a smaller meridional wavenumber l, before moving southward again, developing a much more zonal orientation eventually to decay completely as it meets the equatorial westward flow. The equatorially propagating train decays a little more rapidly than its polewards moving counterpart because of its proximity to the critical latitude. More complicated patterns naturally result if a realistic distribution of topography is used, as we see later

Fig. **??**. We can see wavetrains emanating from both the Rockies and the Himalayas, but distinct polewards and equatorwards wavetrains are hard to discern.

13.3 * BAROCLINIC ROSSBY WAVES AND THEIR VERTICAL PROPAGATION

13.3.1 Forced and stationary waves in the atmosphere

Now consider the vertical propagation of Rossby waves in a stratified atmosphere. We will continue to use the stratified quasi-geostrophic equations, but we now allow the model to be compressible and semi-infinite, extending from $z = 0$ to ∞. The potential vorticity equation again describes motion in the fluid interior, with a surface boundary condition of vertical velocity being determined by the thermodynamic equation, and the upper boundary condition being determined by a radiation condition. Guided by the barotropic problem, we will allow for the possibility of Ekman friction and topography at the surface, but otherwise the flow is presumed inviscid and adiabatic. We will proceed using standard height coordinates.[11] The potential vorticity equation is

$$\frac{\partial q}{\partial t} + J(\psi, q) = 0, \qquad q = \nabla^2 \psi + f + \frac{f_0^2}{\rho_R} \frac{\partial}{\partial z}\left(\frac{\rho_R}{N^2}\frac{\partial \psi}{\partial z}\right), \qquad (13.45)$$

where we take $\rho_R = \rho_0 e^{-z/H}$ where H is a specified density scale height, typically $RT(0)/g$. We linearize this equation about a zonal wind that depends only on z; that is, we let

$$\psi = -\overline{u}(z)y + \psi', \qquad (13.46)$$

and obtain

$$\frac{\partial q'}{\partial t} + \overline{u}\frac{\partial q'}{\partial x} + v'\frac{\partial \overline{q}}{\partial y} = 0, \qquad \frac{\partial \overline{q}}{\partial y} = \beta - \frac{f_0^2}{\rho_R}\frac{\partial}{\partial z}\left(\frac{\rho_R}{N^2}\frac{\partial \overline{u}}{\partial z}\right). \qquad (13.47)$$

or equivalently, in terms of streamfunction,

$$\left(\frac{\partial}{\partial t} + \overline{u}\frac{\partial}{\partial x}\right)\left[\nabla^2 \psi' + \frac{f_0^2}{\rho_R}\frac{\partial}{\partial z}\left(\frac{\rho_R}{N^2}\frac{\partial \psi'}{\partial z}\right)\right]$$
$$+ \frac{\partial \psi'}{\partial x}\left[\beta - \frac{f_0^2}{\rho_R}\frac{\partial}{\partial z}\left(\frac{\rho_R}{N^2}\frac{\partial \overline{u}}{\partial z}\right)\right] = 0. \qquad (13.48)$$

The lower boundary is obtained using the thermodynamic equation,

$$\frac{\partial \psi}{\partial t} + J\left(\psi, \frac{\partial \psi}{\partial z}\right) + \frac{N^2}{f_0}w = 0, \qquad (13.49)$$

along with an equation for the vertical velocity, w, at the lower boundary. This is

$$w = \boldsymbol{u} \cdot \nabla h_b + r\zeta \qquad (13.50)$$

where two terms represent the kinematic contribution to vertical velocity due to flow over topography and the contribution from Ekman pumping, with r a constant, and

the effects are taken to be additive. Linearizing the thermodynamic equation about the zonal flow and using (13.50) gives

$$\frac{\partial}{\partial t}\left(\frac{\partial \psi'}{\partial z}\right) + \overline{u}\frac{\partial}{\partial x}\frac{\partial \psi'}{\partial z} - v'\frac{\partial \overline{u}}{\partial z} = -\frac{N^2}{f_0}\left(\overline{u}\frac{\partial h_b}{\partial x} + r\nabla^2\psi'\right), \qquad \text{at } z = 0. \quad (13.51)$$

Solution

We look for solutions of (13.47) and (13.51) in the form

$$\psi' = \text{Re }\widetilde{\psi}(z)\sin ly\,e^{ik(x-ct)}, \qquad\qquad\qquad (13.52)$$

Solutions must then satisfy

$$\left[\frac{f_0^2}{\rho_R}\frac{\partial}{\partial z}\left(\frac{\rho_R}{N^2}\frac{\partial \widetilde{\psi}}{\partial z}\right)\right] = \widetilde{\psi}\left(K^2 - \frac{\partial \overline{q}/\partial y}{\overline{u} - c}\right) \qquad\qquad (13.53)$$

in the interior, and the boundary condition

$$(\overline{u} - c)\frac{\partial \widetilde{\psi}}{\partial z} - \widetilde{\psi}\frac{\partial \overline{u}}{\partial z} + \frac{i\alpha N^2}{kf_0}\Psi = -\frac{N^2\overline{u}h_b}{f_0}, \qquad \text{at } z = 0, \qquad (13.54)$$

as well as a radiation condition at plus infinity (and we must have that $\rho_0\Psi^2$ be finite). Let us simplify by considering the case of constant $\overline{u}$ and N^2 and setting $r = 0$. We then let

$$\Phi(z) = \widetilde{\psi}(z)\left(\frac{\rho_R}{\rho_R(0)}\right)^{1/2} = \widetilde{\psi}(z)e^{-z/2H} \qquad\qquad (13.55)$$

and obtain the interior equation

$$\frac{d^2\Phi}{dz^2} + m^2\Phi = 0, \qquad \text{where} \quad m^2 = \frac{N^2}{f_0^2}\left(\frac{\beta}{\overline{u} - c} - K^2 - \gamma^2\right), \qquad (13.56\text{a,b})$$

and where $\gamma^2 = f_0^2/(4N^2H^2) = 1/(2L_d)^2$ where L_d is the deformation radius. The surface boundary condition is

$$(\overline{u} - c)\left(\frac{d\Phi}{dz} + \frac{\Phi}{2H}\right) = -\frac{N^2\overline{u}h_b}{f_0} \qquad \text{at } z = 0. \qquad (13.57)$$

Oscillating Waves

From (13.56b) we obtain the dispersion relation for Rossby waves, namely

$$\omega = \overline{u}k - \frac{\beta k}{K^2 + \gamma^2 + m^2 f_0^2/N^2}. \qquad\qquad (13.58)$$

The three components of the group velocity for these waves are:

$$c_g^x = \overline{u} - \frac{\beta[k^2 - (l^2 + m^2 f_0^2/N^2 + \gamma^2)]}{(K^2 + m^2 f_0^2/N^2 + \gamma^2)^2}, \qquad\qquad (13.59\text{a})$$

Figure 13.7 The boundary between propagating waves and evanescent waves as a function of zonal wind and wavenumber, using (13.61), for a couple of values of γ. With $N = 2 \times 10^{-2}\,\mathrm{s}^{-1}$, $\gamma = 1.6$ ($\gamma = 2$) corresponds to a scale height of 7.0 km (5.5 km) and a deformation radius NH/f of 1400 km (1100 km).
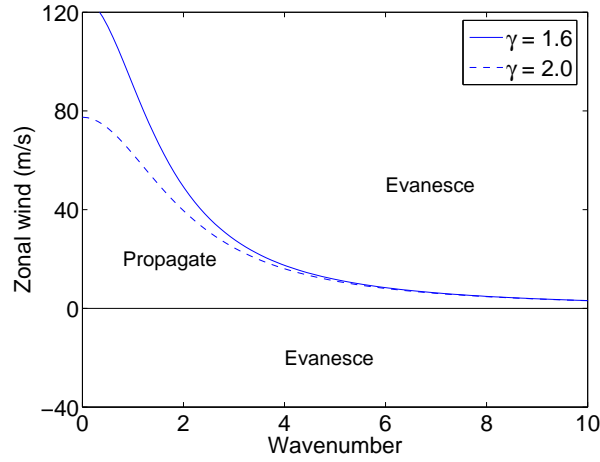
$$c_g^y = \frac{2\beta k l}{(K^2 + m^2 f_0^2/N^2 + \gamma^2)^2}, \tag{13.59b}$$

$$c_g^z = \frac{2\beta k m f_0^2/N^2}{(K^2 + m^2 f_0^2/N^2 + \gamma^2)^2}. \tag{13.59c}$$

The propagation in the horizontal is analogous to the propagation in a shallow water model, although note that higher baroclinic modes (bigger m) will have a more westward group velocity. The vertical group velocity is proportional to m, and therefore for waves that are excited at the surface we must choose m to be positive, for positive k.

Stationary waves

Stationary waves have $\omega = ck = 0$. In this case (13.56) has a solution $\Phi = \Phi_0 \exp(imz)$ provided m^2 is positive where

$$m = \pm \frac{N}{f_0}\left(\frac{\beta}{\overline{u}} - K^2 - \gamma^2\right)^{1/2}. \tag{13.60}$$

Furthermore, m itself must be positive. As we noted, for non-steady waves we must choose the sign of m to ensure that the group velocity, and hence the wave activity, is directed away from the energy source. This must still hold as $m \to 0$, and therefore the positive sign in (13.60) corresponds to the physically realizable solution.[12]

The condition $m^2 > 0$ holds if

$$\boxed{0 < \overline{u} < \frac{\beta}{K^2 + \gamma^2}}. \tag{13.61}$$

and this is illustrated in Fig. 13.7. Stationary, vertically oscillatory modes can exist only for zonal flows that are eastward and that are less than the critical velocity $U_c = \beta/(K^2 + \gamma^2)$. To interpret this condition, note that in a resting medium the Rossby

wave frequency has a minimum value (and maximum absolute value) when $m = 0$ of

$$\omega = -\frac{\beta k}{K^2 + \gamma^2}. \tag{13.62}$$

Note too that in a frame moving with the speed $\overline{u}$ our Rossby waves (stationary in the Earth's frame) have the frequency $-\overline{u}k$, and this is the forcing frequency arising from the now-moving bottom topography. Thus, (13.61) is equivalent to saying that for oscillatory waves to exist *the forcing frequency must lie within the frequency range of vertically propagating Rossby waves.*

For westward flow, or for sufficiently strong eastward flow, the waves decay exponentially as $\Phi = \Phi_0 \exp(-\alpha z)$ where

$$\alpha = \frac{N}{f_0} \left(K^2 + \gamma^2 - \frac{\beta}{\overline{u}} \right)^{1/2}. \tag{13.63}$$

Note that the critical velocity U_c is a function of wavenumber, and that it increases with horizontal wavelength. Thus, for a given eastward flow long waves may penetrate vertically when short waves are trapped.[13] One important consequence of this is that the stratospheric motion is typically of longer wavelength than that of the troposphere, because waves tend to be excited first in the troposphere (by baroclinic instability and by flow over topography, among other things), but the shorter waves are trapped and only the longer ones reach the stratosphere. In the summer, the stratospheric winds are often westward and all waves are trapped in the troposphere; the eastward stratospheric winds that favour vertical penetration occur in the other thee seasons, although very strong eastward winds can suppress penetration in mid-winter.

Finally, the surface boundary condition, (13.57) gives

$$\Phi_0 = \frac{N^2 h_b / f_0}{(\alpha, im) - (2H)^{-1}} \tag{13.64}$$

where $(\alpha, -im)$ refers to the (trapped, oscillatory) case. Equation (13.64) indicates that resonance is possible when $\alpha = 1/(2H)$, and from (13.63) this occurs when $K^2 = \beta/\overline{u}$, that is when barotropic Rossby waves are stationary. This wave resonates because the wave is a solution of the unforced (and inviscid) equations and, because $\Psi = \Phi \exp[z/(2H)]$, it has uniform vertical structure. If $K > K_S$ then $\alpha > 1/(2H)$ and the forced wave (i.e., the amplitude of Ψ) decays with height with no phase variation. If $\alpha < 1/(2H)$ then Ψ increases with height, and this occurs when $(K_s^2 - \gamma^2)^{1/2} < K < K_S$. If $(K_s^2 - \gamma^2)^{1/2} > K$ then the amplitude of Ψ is again independent of height; their vertical structure is oscillatory, like $\exp(imz)$. The complete solutions are collected for convenience in the box on page 580.

13.3.2 Properties of the solution

The various dynamical fields associated with the solution can all be easily constructed from (T.1), and a few simple properties of the solution are worth noting explicitly. In some cases the explicit calculation is left as a problem to the reader — see problems 13.6 and 13.7.

Stationary, Topographically Forced Solutions

Collecting the results in section 13.3.1, the stationary solutions of (13.47) and (13.51) are:

$$\psi'(x, y, z) = \text{Re}\, e^{imz} e^{z/2H} e^{ikx} \sin ly \frac{f_0 h_b \left[im - (2H)^{-1} \right]}{K_s^2 - K^2}, \quad m^2 > 0 \quad \text{(T.1a)}$$

$$\psi'(x, y, z) = \text{Re}\, e^{[(2H)^{-1} - \alpha]z} e^{ikx} \sin ly \frac{N^2 h_b}{f_0 \left[\alpha - (2H)^{-1} \right]}, \quad m^2 < 0 \quad \text{(T.1b)}$$

where

$$m = +\frac{N}{f_0} \left(\frac{\beta}{\bar{u}} - K^2 - \gamma^2 \right)^{1/2}, \tag{T.2}$$

and

$$\alpha = +\frac{N}{f_0} \left(K^2 + \gamma^2 - \frac{\beta}{\bar{u}} \right)^{1/2}. \tag{T.3}$$

and $\gamma = f_0/(2NH)$. If $m^2 > 0$ the solutions are propagating, or radiating, waves in the vertical. If $m^2 < 0$ the energy of the solution, $|\rho_R \psi'^2|$, is vertically evanescent. The condition $m^2 > 0$ is equivalent to

$$0 < \bar{u} < \frac{\beta}{K^2 + (f_0/2NH)^2}, \tag{T.4}$$

so that vertical penetration is favoured when the winds are weakly eastward, and the range of $\bar{u}$ values that allows this is larger for longer waves.

Amplitudes and phases: The decaying solutions have no vertical phase variations (they are 'equivalent barotropic') and the streamfunction is exactly in phase or out of phase with the topography according as $K > K_s$ and $\alpha > (2H)^{-1}$, or $K < K_s$ and $\alpha < (2H)^{-1}$. In the latter case case the amplitude of the streamfunction actually increases with height, but the energy, proportional to $\rho_R |\psi'^2|$ falls. The oscillatory solutions have constant energy with height but a shifting phase. The phase of the streamfunction at the surface may be in or out of phase with the topography, depending on m, but the potential temperature, $\partial \psi / \partial z$ is always out of phase with the topography. That is, positive values of h_b are associated with cool fluid parcels.

Vertical energy propagation: As noted, the energy propagates upward for the oscillatory waves. This may be verified by calculating $\overline{p'w'}$ where p' is the pressure perturbation, proportional to ψ' and w' is the vertical velocity perturbation. To

this end, linearize the thermodynamic equation (13.49) to give

$$\frac{\partial \psi'}{\partial t} + \overline{u}\frac{\partial}{\partial x}\frac{\partial \psi'}{\partial z} - \frac{\partial \overline{u}}{\partial z}\frac{\partial \psi'}{\partial x} + \frac{N^2}{f_0}w' = 0. \tag{13.65}$$

Then, multiplying by ψ' and integrating by parts gives a balance between the second and fourth terms,

$$N^2\overline{\psi'w'} = \overline{u}\,\overline{b'v'}, \tag{13.66}$$

where $b' = f_0\partial\psi'/\partial z$ and $v' = \partial\psi'/\partial x$. Thus, the upwards transfer of energy is proportional to the poleward heat flux.

Meridional heat transport: The meridional heat transport associated with a wave is

$$\rho_R\overline{v'b'} = \rho_R f_0 \overline{\frac{\partial \psi'}{\partial x}\frac{\partial \psi'}{\partial z}} \tag{13.67}$$

For an oscillatory wave this can readily be shown to be positive. In particular, it is proportional to $km/(K_s^2 - K^2)$, and this is positive because $km > 0$ is the condition that energy is directed upwards, and $K_s^2 > K^2$ for oscillatory solutions. The meridional transport associated with a trapped solution is identically zero.

Form Drag: If the waves propagate energy upward, there must be a surface interaction to supply that energy. There is a force due to *form drag* associated with this interaction, given by

$$\text{Form drag} = \overline{p'\frac{\partial h_b}{\partial x}} \tag{13.68}$$

(see chapter 3). In the trapped case, the streamfunction is either exactly in or out of phase with the topography, so this interaction is zero. In the oscillatory case

$$\overline{\psi'\frac{\partial h_b}{\partial x}} = \frac{f_0 h_b^2 km}{4(K_s^2 - K^2)} \tag{13.69}$$

where the factor of 4 arises from the x and y averages of the squares of sines and cosines. The rate of doing work is $\overline{u}$ times this.

13.4 * EFFECTS OF THERMAL FORCING

How does thermal forcing influence the stationary eddies? To give an accurate answer for the real atmosphere is a little more difficult than for the orographic case where the forcing can be included reasonably accurately in a quasi-geostrophic model with a term $\overline{u}\cdot\nabla h_b$ at the lower boundary. Anomalous (i.e., variations from a zonal or temporal mean) thermodynamic forcing typically also arises initially at the lower boundary through, for example, variations in the surface temperature. However, such anomalies may be felt throughout the lower troposphere on a relatively short time-scale by way

of such non-geostrophic phenomena as convection, so that the effective thermodynamic source that should be applied in a quasi-geostrophic calculation has a finite vertical extent. However, an accurate parameterization of this may depend on the structure of the atmospheric boundary layer and this cannot always be represented in a simple way.[14] Because of such uncertainties our treatment concentrates on the fundamental and qualitative aspects of thermal forcing.

The quasi-geostrophic potential vorticity equation, linearized around a uniform zonal flow, is [c.f., (13.48)]

$$
\left(\frac{\partial}{\partial t} + \overline{u} \frac{\partial}{\partial x} \right) \left[\nabla^2 \psi' + \frac{f_0^2}{\rho_R} \frac{\partial}{\partial z} \left(\frac{\rho_R}{N^2} \frac{\partial \psi'}{\partial z} \right) \right]
$$
$$
+ \frac{\partial \psi'}{\partial x} \left[\beta - \frac{f_0^2}{\rho_R} \frac{\partial}{\partial z} \left(\frac{\rho_R}{N^2} \frac{\partial \overline{u}}{\partial z} \right) \right] = \frac{f_0}{N^2} \frac{\partial Q}{\partial z} \equiv T \tag{13.70}
$$

where Q is the source term in the (linear) thermodynamic equation,

$$
\frac{\partial}{\partial t} \left(\frac{\partial \psi'}{\partial z} \right) + \overline{u} \frac{\partial}{\partial x} \frac{\partial \psi'}{\partial z} - v' \frac{\partial \overline{u}}{\partial z} + \frac{N^2}{f_0} w' = \frac{Q}{f_0} \tag{13.71}
$$

A particular solution to (13.70) may be constructed if $\overline{u}$ and N^2 are constant, and if Q has a simple vertical structure. If we again write $\psi' = \mathrm{Re}\, \widetilde{\psi}(z) \sin ly \exp(ikx)$ and let $\Phi(z) = \widetilde{\psi}(z) \exp(-z/2H)$ we obtain

$$
\frac{d^2 \Phi}{dz^2} + m^2 \Phi = \frac{T}{ik\overline{u}} e^{-z/2H}, \qquad \text{where} \quad m^2 = \frac{N^2}{f_0^2} \left(\frac{\beta}{\overline{u}} - K^2 - \gamma^2 \right). \tag{13.72}
$$

If we let $T = T_0 \exp(-z/H_Q)$, so that the heating decays exponentially away from the earth's surface, then the particular solution to the stationary problem is found to be

$$
\widetilde{\psi} = \mathrm{Re} \frac{i \hat{T} e^{-z/H_Q}}{k\overline{u} \left[(N/f_0)^2 (K_s - K^2) + H_Q^{-2}(1 + H_Q/H) \right]} \tag{13.73}
$$

where $\hat{T}$ is proportional to T. This solution does not satisfy the boundary condition at $z = 0$, which in the absence of topography and friction is

$$
\overline{u} \frac{\partial}{\partial x} \frac{\partial \psi'}{\partial z} - v' \frac{\partial \overline{u}}{\partial z} = \frac{Q(0)}{f_0}. \tag{13.74}
$$

A homogeneous solution must therefore be added, and just as in the topographic case this leads to a vertically radiating or a surface trapped response, depending on the sign of m^2. One way to calculate the homogeneous solution is to first use the linearized thermodynamic equation (13.71), or the linearized vorticity equation (13.76), to calculate the vertical velocity at the surface implied by (13.73), $w_p(0)$ say. We then notice that the homogeneous solution is effectively forced by an equivalent topography given by $h_e = -w_p(0)/(ik\overline{u(0)})$, and so proceed as in the topographic case. The complete solution is rather hard to interpret, and is in any case available only in special cases, so it is useful to take a more qualitative approach.

13.4.1 Thermodynamic balances

It is the properties of the particular solution that distinguish the response to thermodynamic forcing from that due to topography, because the homogeneous solutions of the two case are similar. And far from the source region, the homogeneous solution will dominate, giving rise to wavetrains as discussed previously.

We can determine many of the properties of the response to thermodynamic forcing by considering the balance of terms in the steady linear thermodynamic equation, which we write as

$$\overline{u} \frac{\partial}{\partial x} \frac{\partial \psi'}{\partial z} - \frac{\partial \psi'}{\partial x} \frac{\partial \overline{u}}{\partial z} + \frac{N^2}{f_0} w' = \frac{Q}{f_0} \equiv R \qquad (13.75a)$$

or

$$f_0 \overline{u} \frac{\partial v'}{\partial z} - v' \frac{\partial \overline{u}}{\partial z} + N^2 w' = Q. \qquad (13.75b)$$

The vorticity equation is

$$\overline{u} \frac{\partial \zeta'}{\partial x} + \beta v' = \frac{f_0}{\rho_R} \frac{\partial \rho_R w}{\partial z}. \qquad (13.76)$$

Assuming that the diabatic forcing is significant, we may imagine three possible simple balances in the thermodynamic equation:

(i) Zonal advection dominates, and $v' = \partial \psi'/\partial x \sim Q H_Q/(f_0 \overline{u})$

(ii) Meridional advection dominates, and $v' \sim Q H_u/(f_0 \overline{u})$.

(iii) Vertical advection dominates, and $w' \sim Q/N^2$. Then, for large enough horizontal scales the balance in the vorticity equation is $\beta v \sim f w_z$ and $v' \sim f Q/(\beta N^2 H_Q)$. For smaller horizontal scales advection of relative vorticity may dominate that of planetary vorticity, and β replaced by $\overline{u} K^2$.

Here, H_Q is the vertical scale of the source (so that $\partial Q/\partial z \sim Q/H_Q$) and H_u is the vertical scale of the zonal flow (so that $\partial \overline{u}/\partial z \sim \overline{u}/H_u$). We also assume that the vertical scale of the solution is is H_Q, so that $\partial v'/\partial z \sim v'/H_Q$. Which of the above three balances is likely to hold? Heuristically, we might suppose that the balance with the smallest v' will dominate, if only because meridional motion is suppressed on the β-plane. Then, zonal advection dominates meridional advection if $H_u > H_Q$, and vice versa. Defining $\hat{H} = \min(H_u, H_Q)$ then horizontal advection will dominate vertical advection if

$$\mu_1 = \frac{\beta N^2 H_Q \hat{H}}{\overline{u} f_0^2} \ll 1. \qquad (13.77)$$

More systematically, we can proceed in *reductio ad absurdum* fashion by first neglecting the vertical advection term in (13.75), and seeing if we can construct a self-consistent solution. If $\psi' = \operatorname{Re} \Psi_p(z) e^{ikx}$, and noting that $\overline{u} \partial \Psi_p/\partial z - \Psi_p \partial \overline{u}/\partial z = \overline{u}^2 (\partial/\partial z)(\Psi_p/\overline{u})$ we obtain

$$\Psi_p = \frac{i\overline{u}}{k f_0} \int_z^\infty \frac{\tilde{Q}}{\overline{u}^2} \, \mathrm{d}z \qquad (13.78)$$

where $\tilde{Q}$ denotes the Fourier amplitude of Q. Then, from the vorticity equation (13.76), we obtain the (Fourier amplitude of the) vertical velocity

$$W_p = \frac{-ik}{f_0 \rho_R} \int_z^{\infty} \rho_R \overline{u}(K_s^2 - K^2)\Psi_p \, \mathrm{d}z. \tag{13.79}$$

Using this one may, at least in principle, check whether the vertical advection in (13.75) is indeed negligible. If $\overline{u}$ is uniform (and so $H_u \gg H_Q$) then we find

$$\Psi \propto \frac{iQH_Q}{kf_0\overline{u}}, \qquad \text{and} \qquad W_p \propto \frac{QH_Q^2(K_s^2 - K^2)}{f_0^2}. \tag{13.80a,b}$$

Using this, vertical advection indeed makes a small contribution to the thermodynamic equation provided that

$$\mu_2 = \frac{N^2 H_Q^2 |K_s^2 - K^2|}{f_0^2} \ll 1 \tag{13.81}$$

If $K_s^2 \gg K^2$ and $H = H_Q$ then (13.81) is equivalent to (13.77). If $\overline{u}$ is not constant and if $H_u \ll H_Q$ then H_u replaces H_Q and the criterion for the dominance of horizontal advection becomes

$$\mu = \frac{N^2 \hat{H} H_Q |K_s^2 - K^2|}{f_0^2} \ll 1. \tag{13.82}$$

This is the condition that the first term in the denominator of (13.73) is negligible compared the second. For a typical tropospheric value of $N^2 = 10^{-4}\,\mathrm{s}^{-1}$ and for $K > K_S$ we find that $\mu \approx (H_Q/7\,\mathrm{km})^2$, and so we can expect $\mu < 1$ in extra-equatorial regions where the heating is shallow. In low latitudes f_0 is smaller and β is bigger and the $\mu \approx (H_Q/1\,\mathrm{km})^2$ and we can expect $\mu > 1$. However, there is both uncertainty and variation in these values.

Equivalent topography

In the case in which zonal advection dominates, the equivalent topography is given by

$$h_e = \frac{-W_p(0)}{ik\overline{u}(0)} = \frac{1}{u(0)f_0\rho_R(0)} \int_0^{\infty} \rho_R \overline{u}(K_s^2 - K^2)\Psi_p \, \mathrm{d}z \tag{13.83}$$

where Ψ_p is given by (13.78). The point to notice here is that if $K < K_s$ the equivalent topography is in phase with ψ_p.

13.4.2 Properties of the solution

In the tropics μ may be large for H_Q greater than a kilometer or so. Heating close to the surface cannot produce a large vertical velocity and will therefore produce a meridional velocity. However, away from the surface the heat source will be balanced by vertical advection. For scales such that $K < K_S$, a criterion that might apply at low latitudes for wavelengths longer than a few thousand kilometers, the associated vortex stretching $f \, \partial w/\partial z > 0$ is balanced by βv and a polewards meridional motion occurs. This

implies a trough west of the heating and/or a ridge east of the heating, although the use of quasi-geostrophic theory to draw tropical inferences may be a little suspect.

In midlatitudes μ is typically small and horizontal advection locally balances diabatic heating. In this case there is a trough a quarter-wavelength downstream from the heating, and equatorward motion at the longitude of the source. (To see this, note that if the heating has a structure like $\cos kx$ then from either (13.73) or (13.78) the solution goes like $\psi_p \propto -\sin kx$.) The trough may be warm or cold, but is often warm. If $H_Q \ll H_u$, as is assumed in obtaining (13.73), then θ is positive and warm. This is because zonal advection dominates and so the effect of the heating is advected downstream. If $H_Q \gg H_u$ and meridional advection is dominant, then the trough is still warm provided Q decreases with height. The vertical velocity can be inferred from the vorticity balance. If $f_0 \partial w/\partial z \approx \beta v$ and if $w = 0$ at the surface (in so the absence of Ekman pumping and any topographic effects) there is *descent* in the neighbourhood of a heat source. This counter-intuitive result arises because it is the horizontal advection that is balancing the diabatic heating. (Note that this result cannot be inferred from the particular solution alone.) If the advection of relative vorticity balances vortex stretching, the opposite may hold.

The homogeneous solution can be inferred from (13.83) and (T.1). Consider, for example, waves that are trapped ($m^2 < 0$) but still have $K < K_S$; that is $K^2 < K_S^2 < K^2 + \gamma^2$. The homogeneous solution forced by the equivalent topography is out of phase with that topography, and so out of phase with ψ_p, using (13.83). For still shorter waves, $K > K_s$, the homogeneous solution is in phase with the equivalent topography, and so again out of phase with ψ_p. Thermal sources produced by large-scale continental land masses may have $K^2 < K_s^2$ and, if $K^2 + \gamma^2 < K_S^2$ they will produce waves that penetrate up into the stratosphere and typically these solutions will dominate far from the source. Evidently though, the precise relationship between the particular and homogeneous solution is best dealt with on a case-by-case basis. A few more general points are summarized in the box on page 587.

13.4.3 Numerical Solutions

The response to an isolated heat source is illustrated in Fig. 13.8 and Fig. 13.9. The first figure shows the response to a 'deep' heating at $15°$ N. As the reasoning above would suggest, the vertical velocity field (not shown) is upward in the vicinity of the source. Away from the source, the solution is dominated by the homogeneous solutions in the form of wavetrains, as described in section 13.1.3, with a simple vertical structure. (In fact the pattern is quite similar to that obtained with a barotropic model.)

Fig. 13.9 shows the response to a perturbation at $45°$ N, and again the solutions are qualitatively in agreement with the reasoning above. The local heating is balanced by an equatorward wind, and there is a surface trough about $20°$ east of the source, and an upper level pressure maximum, or ridge, about $60°$ east. The scale height of the wind field, H_u is about 8 km, greater than that of the source, and the balance in the thermodynamic equation is between the zonal advection of the temperature anomaly
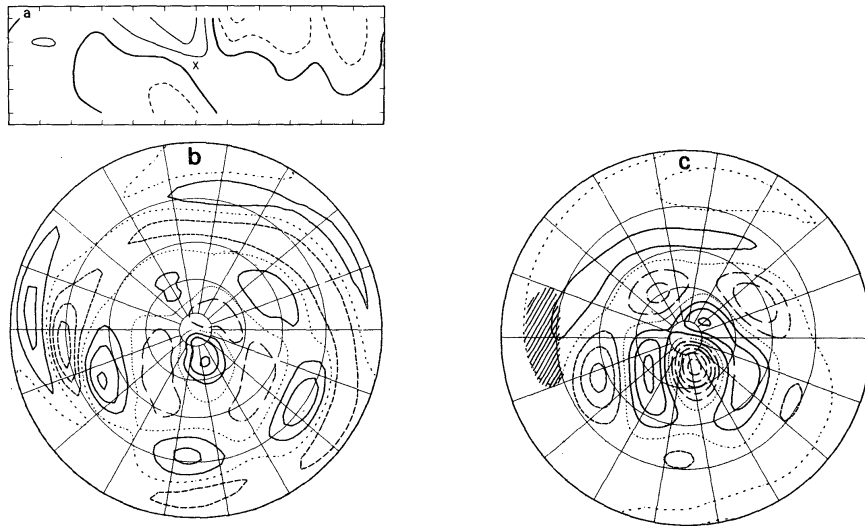
Fig. 13.8 Numerical solution of a baroclinic primitive equation model with a deep heat source at 15°N and a zonal flow similar to that of northern hemisphere winter. (a) height field in a longitude height at 18°N (vertical tick marks at 100, 300, 500, 700 and 900 mb); (b) 300 mb vorticity field; (c) 300 mb height field. The cross in (a) and the hatched region in (c) indicate the location of the heating. From Hoskins and Karoly (1981).
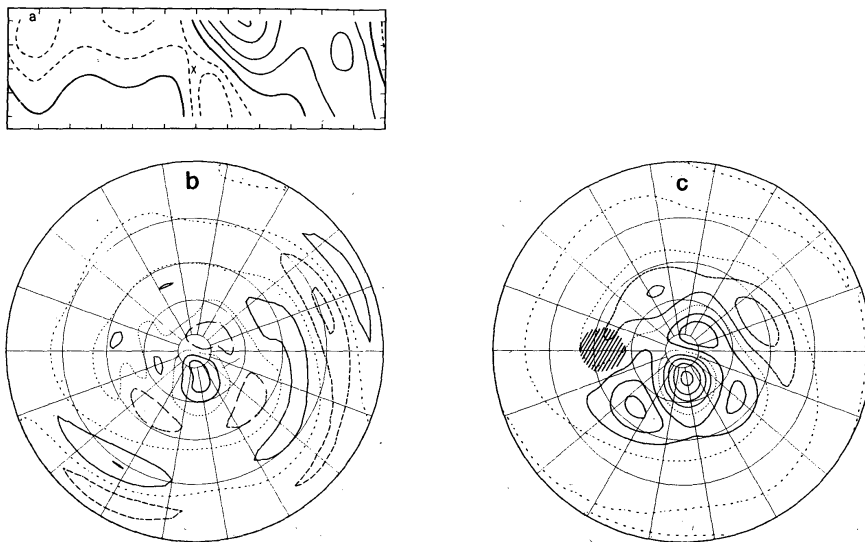
Fig. 13.9 As for Fig. 13.8, but now solution of a baroclinic primitive equation model with a deep heat source at 45°N. (a) height field in a longitude height at 18°N; (b) 300 mb vorticity field; (c) 300 mb height field. The cross in (a) and the hatched region in (c) indicate the location of the heating.[15]

> ## Thermal Forcing of Stationary Eddies: Salient Points
>
> *(i)* The solution is comprised of particular solution and a homogeneous solution.
>
> *(ii)* The homogeneous solution may be thought of as being forced by an 'equivalent topography', chosen so that the complete solution satisfies the boundary condition on vertical velocity at the surface.
>
> *(iii)* For a localized source, the far field is dominated by the homogeneous solution. This solution has the same properties as a solution forced by real topography. Thus, it may comprise waves that penetrate vertically into the stratosphere, and wavetrains propagating around the globe with an equivalent barotropic structure.
>
> *(iv)* In the extratropics, a diabatic heating is typically balanced by horizontal advection, producing a trough a quarter wavelength east (downstream) of a localized heat source. The heat source is balanced by advection of cooler air from higher latitudes, and there may be sinking air over the heat source. This can occur when $\mu \ll 1$ [see (13.82)].
>
> *(v)* In the tropics, a heat source may be locally balanced by vertical advection, that is adiabatic cooling as air ascends. This can occur when $\mu \gg 1$.
>
> *(vi)* In the real atmosphere, the stationary solutions must co-exist with the chaos of time-dependent, nonlinear flows. Thus, they are likely to manifest themselves only in time-averaged fields and in a modified form.

$\overline{u}\theta'_x$ and the heat source, so producing a temperature maximum downstream. Again, the far field is dominated by the wavetrain of the homoegeneous solution.

Finally, we show a calculation (Fig. 13.10) using realistic forcing from topography, heat sources and transient eddy flux convergences, and a realistic zonally averaged zonal flow, and a generally good agreement with the observed fields is found.[16] It is hard now to see the wavetrains emerging from isolated features like the Rockies or Himalayas, because they are combined with the responses from all the other sources included in the calculation. Indeed, on breaking up the forcing into separate contributions from orographic forcing, heating, and the time-averaged momentum and heat fluxes from transient eddies reveals that all of these forcings play a role. Nevertheless, the agreement does reveal the extent to which we might understand the zonally asymmetric circulation of the real atmosphere as the response due to the interaction of a zonally uniform zonal wind with the asymmetric features of the earth's geography.
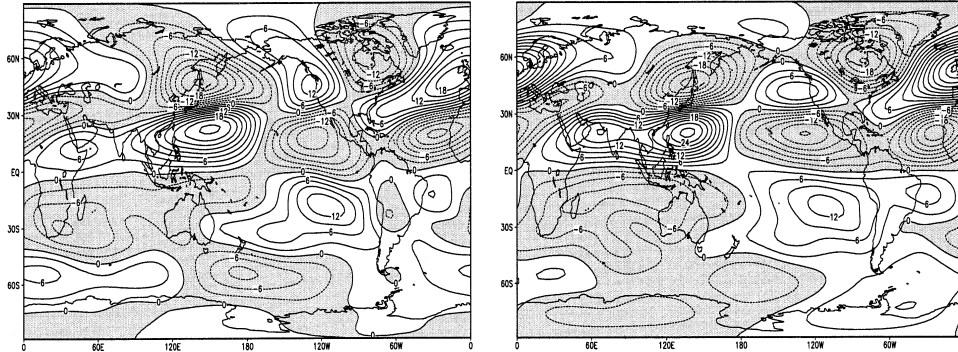
Fig. 13.10 Left: the observed stationary (i.e., time averaged) stream-function at 300 mb (about 7 km altitude) in Northern Hemisphere winter. Right: the steady, linear response to forcing by orography, heat sources and transient eddy flux convergences, calculated using a linear model with the observed height-varying zonally averaged zonal wind. Note the generally good agreement, and also the much weaker zonal asymmetries in the southern hemisphere.[17]

13.5 STRATOSPHERIC DYNAMICS

In our final topic of this chapter we look, all too briefly, at the circulation in the stratosphere. (We draw on results from earlier starred sections but the less technically-inclined reader who may have skipped them can simply refer back as needed.) Its convenenient to divide this circulation into two components: (i) the meridional overturning circulation; (ii) the quasi-horizontal circulation. There is also a region of the lower stratosphere that interacts directly with the troposphere and where fluid properties are exchanged; however, the dynamics of this region are complex and we shall not explore them here.

13.5.1 A descriptive overview

The radiative forcing of the stratosphere is effectively illustrated in Fig. 13.11, and the observed zonally-averaged temperature and zonal-wind structure are plotted in Fig. 13.12. From these we note:

★ The stratosphere is very stably stratified, with a lapse rate corresponding to $N \approx 2 \times 10^{-2}$ s, about twice that of the troposphere on average. This is in part due to the absorption of solar radiation by ozone between 20 km and 50 km.

★ In the summer the solar absorption at high latitudes leads to a reversed temperature gradient (warmer pole than equator) and a negative shear. The temperature distribution is, in fact, not far from the radiative equilibrium distribution. Consistently, by thermal wind balance, over much of the summer stratosphere the mean winds are negative (westward).
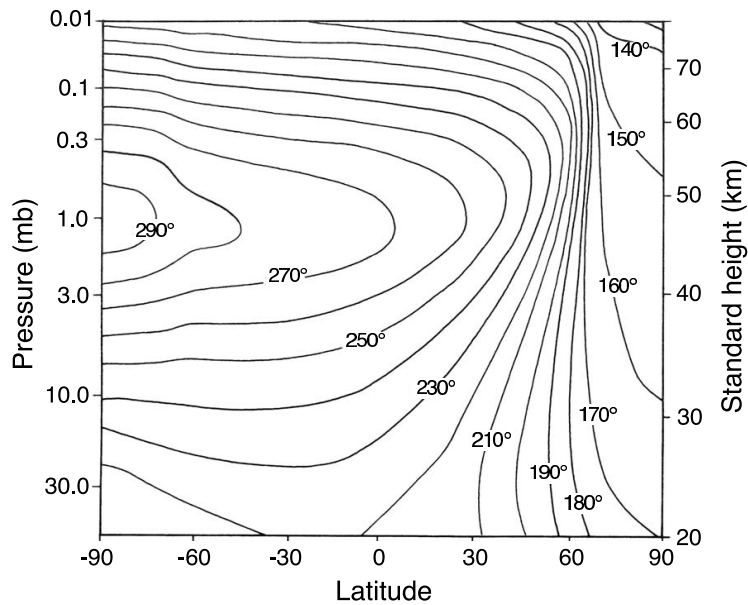
Fig. 13.11 The zonally-averaged radiative-equilibrium temperature in in January. The downwards solar radiation at the top of the atmosphere is given, and the upwards radiative flux into the stratosphere is based on observed properties, including temperature, of the troposphere.[18]
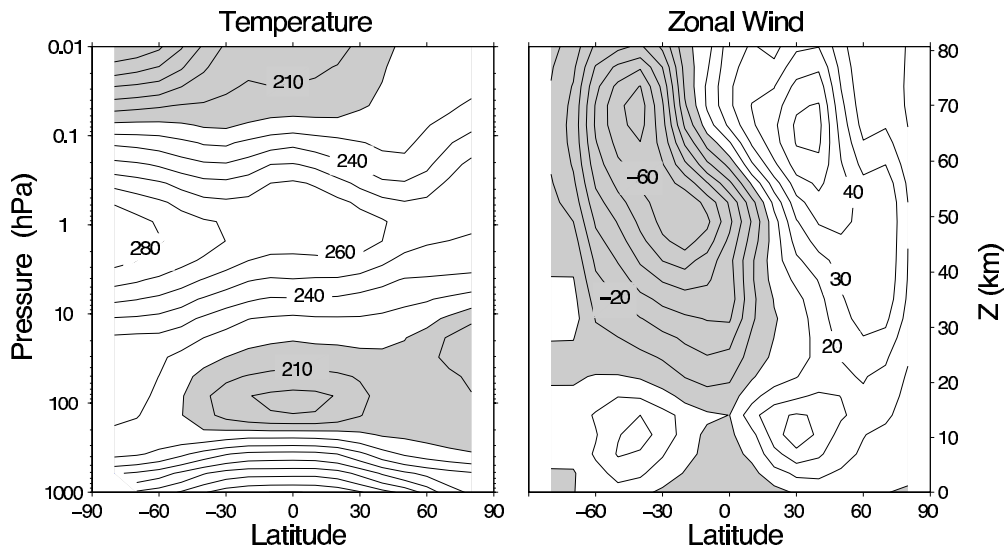
Fig. 13.12 The zonally averaged temperature and zonal wind in January. Temperature countour interval is 10 K, and values less than 220 K are shaded. Zonal wind contours are 10 m s^{-1} and negative (westward) values are shaded.[19]
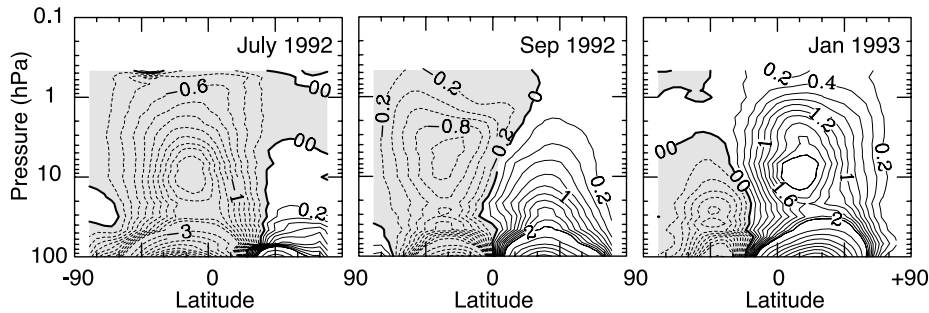
Fig. 13.13 The observed mass-weighted streamfunction in the stratosphere, in Sverdrups (10^9 kg s^{-1}). The circulation is clockwise where the contours are solid. Note the stronger circulation in the winter hemispheres, whereas the equinoctal circulation (September) is more interhemispherically symmetric.[21]

★ In winter high latitudes receive very little solar radiation and there is a strong meridional temperature gradient and consequently a strong vertical shear in the zonal wind. Nevertheless, this temperature gradient is significantly weaker than the radiative equilibrium temperature gradient, implying a poleward heat transfer by the fluid motions.

There must be, then, a circulation that keeps the stratosphere from radiative equilibrium, and one that is weakest in summer. In fact, a stratospheric meridional overturning circulation was inferred by A. Brewer and G. Dobson based on observations of water vapour and chemical transport, and is often called the *Brewer-Dobson circulation*.[20] It is depicted in Fig. 13.13; this shows the observed mass-weighted circulation, almost equivalent to the residual circulation, and so represents both the Eulerian mean and eddy-contributed components. It comprises a single, equator-to-pole cell in each hemisphere, stronger in the winter hemisphere where it goes high into the stratosphere. There is also a distinct lower branch to the circulation, present in all seasons although strongest in winter, that is confined to the lower stratosphere and is in some ways a vertical extension of (the residual circulation of) the tropospheric Ferrel Cell. Not all the upper circulation is ventilated by the troposphere — some of it recirculates within the stratosphere. This circulation and some of the associated dynamics is schematically illustrated in Fig. 13.14, and three three regions may usefully be delineated: (i) A tropical region; (ii) a mid-latitude region; (iii) the polar vortex. The tropical region is relatively quiescent, an area of generally upward motion where air is drawn up from the troposphere. In midlatitudes the residual flow is generally polewards before sinking at high latitudes. In winter the extreme cold leads to the formation of *polar vortex,* a strong cyclonic vortex that appears quite isolated from mid-latitudes although, especially in the Northern Hemisphere, it is not always centered over the pole.

13.5.2 Dynamics
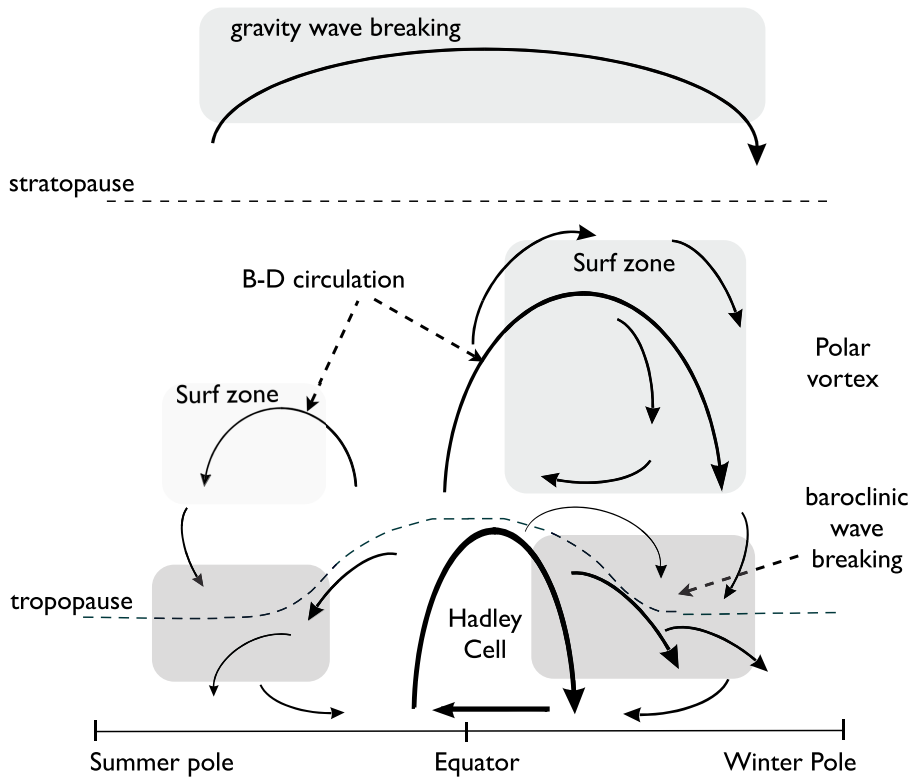
Fig. 13.14 A schema of the residual mean meridional circulation of the atmosphere. The solid arrows indicate the residual circulation (B-D for Brewer Dobson) and the shaded areas the main regions of wave breaking (i.e., enstrophy dissipation) associated with the circulation. In the surf zone the breaking is mainly that of planetary Rossby waves, and in the troposphere and lower stratosphere the breaking is that of baroclinic eddies. The surf zone and residual flow are much weaker in the summer hemisphere. Only in the Hadley Cell is the residual circulation comprised mainly of the Eulerian mean; elsewhere the eddy component dominates.[22]

Wave breaking and the residual circulation

Based on our discussion in the previous chapter of the wave-mean flow interaction and the (residual) Ferrel Cell, we might expect the Brewer-Dobson circulation to be a consequence of wave-breaking and enstrophy dissipation in the stratosphere. We ask:

  (i) What is the source of such waves?

 (ii) Does such wavebreaking give rise to a circulation of the right sense?

(iii) Why is the circulation weakest in summmer?

The equations of motion governing the mean fields are the zonally averaged momentum and thermodynamic equations, which in residual form may be written as

$$\frac{\partial \overline{u}}{\partial t} - f_0 \overline{v}^* = \nabla \cdot \boldsymbol{\mathcal{F}} + \overline{F}, \tag{13.84a}$$

$$\frac{\partial \overline{\theta}}{\partial t} + \frac{\partial \overline{\theta}}{\partial z} \overline{w}^* = \overline{J} \tag{13.84b}$$

where $\overline{F}$ represents frictional effects (for example, due to small scale turbulence) and $\overline{J}$ represents heating, and on the β-plane the residual velocities are related to the Eulerian means by

$$\overline{v}^* = \overline{v} - \frac{1}{\rho_R} \frac{\partial}{\partial z} \left(\rho_R \frac{\overline{v'\theta'}}{\partial_z \overline{\theta}} \right), \qquad \overline{w}^* = \overline{w} + \frac{\partial}{\partial y} \left(\frac{\overline{v'\theta'}}{\partial_z \overline{\theta}} \right). \tag{13.85}$$

The vector $\boldsymbol{\mathcal{F}}$ is the Eliassen-Palm flux, and this is related to the meridional flux of potential vorticity by $\nabla \cdot \boldsymbol{\mathcal{F}} = \overline{v'q'}$. The wave activity itself obeys the Eliassen-Palm relation

$$\frac{\partial \mathcal{A}}{\partial t} + \nabla \cdot \boldsymbol{\mathcal{F}} = \mathcal{D}, \tag{13.86}$$

where $\mathcal{A}$ is the wave activity, $\boldsymbol{\mathcal{F}}$ its flux and $\mathcal{D}$ its dissipation.

Now, in the stratosphere baroclinic instability is relatively weak, certainly compared to the troposphere (e.g., Fig. 6.21), and the main source of wave activity is upward propagation from the turbulent troposphere. From the autumn to the spring, the zonal wind in the stratosphere is generally receptive to planetary-scale Rossby waves propagating up from the troposphere (Fig. 13.7), although in at high latitudes in winter there may be a period when the eastward zonal winds are too strong for waves to propagate. If these waves break in the stratosphere then there will be an enstrophy flux to small scales and dissipation. In a quasi-statistically-steady state and with small frictional effects the dominant balance in the zonal momentum equation (13.84a) is

$$- f_0 \overline{v}^* \approx \overline{v'q'}, \tag{13.87}$$

where $\overline{v}^*$ is the residual velocity and the potential vorticity flux on the right-hand side is induced by the Rossby wave breaking. In dissipative regions the zonally-averaged potential vorticity flux will tend to be down its mean gradient and, if the potential vorticity gradient is polewards (largely because of the β-effect), the residual velocity will be positive if f_0 is positive. That is, the residual flow will be *polewards,* in both hemispheres, and the mechanism giving rise to this is called the 'Rossby wave pump.' Put another way, Rossby waves propagating up from the troposphere break and deposit westward momentum in the stratosphere, and this 'wave drag' is largely balanced by the Coriolis force on the residual meridional circulation.

This meridional circulation is weakest in summer mainly because linear Rossby waves cannot propagate upwards through the westward mean winds, as illustrated in Fig. 13.15. It is quite striking how the EP vectors avoid the region of westward winds in
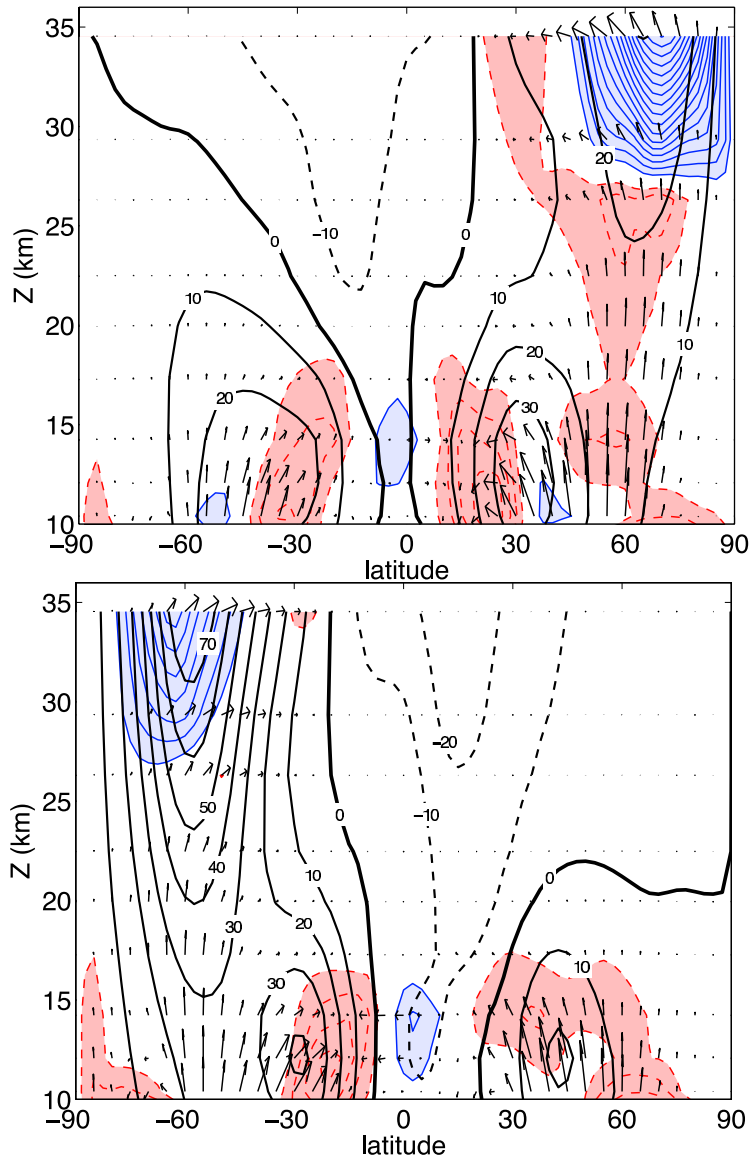
Fig. 13.15 The EP flux vectors (arrows), the EP flux divergence (shaded and light contours) and the zonally averaged zonal wind (heavy contours) for (a) Northern hemisphere winter; (b) Southern Hemisphere winter. Note the almost zero EP values in the summer hemispheres, and strong convergence at high latitudes in the winter hemispheres, leading to polewards residual flow and/or zonal flow acceleration. The EP divergence is shaded for values greater than $+1\,\mathrm{m\,s^{-1}}$/day, light solid contours) and for values less than $-1\,\mathrm{m\,s^{-1}}$/day (light dashed contours). The vertical coordinate is log pressure, extending between about 260 mb and 10 mb.

the summer hemisphere, even though the level of wave activity at low elevations is relatively similar in the summer and winter hemispheres (look between 10 km and 15 km in the figure). We can interpret this by noting that for nearly plane waves the EP flux obeys the group velocity property, meaning that $\mathcal{F} = \boldsymbol{c}_g$; however, as discussed in section 13.3, if the mean winds are westward the waves evanesce instead of propagating, and thus almost the entire summer hemisphere is shielded from upwardly propagating waves, leaving it in a near-radiative equilibrium state. In the other seasons, the EP flux is able to propagate into the stratosphere and a circulation is generated. This acts to weaken the pole-equator temperature gradient, as we see by inspection of the thermodynamic equation: if the heating is represented by a simple relaxation to a radiative equilibrium state, θ_E, then in a steady state we have

$$N^2 \overline{w}^* = \frac{\theta_E - \theta}{\tau}. \tag{13.88}$$

Polewards flow in midlatitudes must be supplied by rising air at low latitudes, and sinking air at high. Thus, from autumn to spring, at low latitudes we have $\theta < \theta_E$ and at high latitudes $\theta > \theta_E$.

Although cause and effect can be very difficult to disentangle in fluid dynamical problems, and the ultimate cause of nearly all fluid motions in the atmosphere is the differential heating from the sun, it is important to realize that the meridional overturning in the stratosphere is not a direct response to differential heating. We see this simply by noting that the most intense heating is over the summer pole, yet here there is little or no ascent. Rather, the circulation is more directly a response to potential vorticity fluxes which in turn are determined by the upward propagation of Rossby waves from the troposphere and polewards gradient of potential vorticity in the stratosphere.

The polar vortex and the quasi-horizontal circulation

Let us now shift our perspective and consider the quasi-horizontal circulation in the stratosphere. Stratospheric dynamics are, in fact, rather more two-dimensional than those in the troposphere because the high stratification inhibits vertical motion, and the vortex stretching term in the quasi-geostrophic potential vorticity equation is relatively small. In any case, because diabatic effects occur on a somewhat longer timescale than advective processes, the flow may be characterized by the advection of potential vorticity on more slowly evolving isentropic surfaces. In midlatitudes this flow is forced by wave propagagation from below, and the upshot is that the midlatitude stratospheric circulation is a good example of geostrophic turbulence, as illustrated in Fig. 13.16 and Fig. 13.17. Both the potential vorticity and tracer are evocative the flows in chapters 8 and 9. We see Rossby waves breaking and vortices stretched into filaments and tendrils — in short, a region of an enstrophy cascade. We also perceive some idea of the spectral nonlocality of the enstrophy transfer — a single large vortex overturns and breaks and there is little sense of an orderly cascade of enstrophy to dissipative scales. For this reason, the mid-latitude region is known as the *surf zone*. It is precisely this wave breaking that gives rise to the enstrophy flux to small scales and it dissipation, and which in turn gives rise to the residual flow that is the Brewer-Dobson circulation.
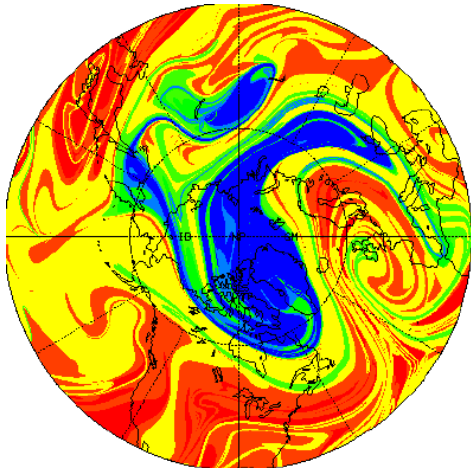
Figure 13.16 The tracer distribution in the Northern Hemisphere lower stratosphere on 28 January 1992. The tracer was initialized on January 16 by setting it equal to the potential vorticity field calculated from an observational analysis, and then advected for 12 days by the observed observed wind fields.[23]

This surf-zone does usually does not extend to the pole, and in winter dense cold air over the pole forms itself into a cyclonic vortex, the *polar vortex* (Fig. 13.17, Fig. 13.18). Although the vortex is diabatically forced, and has a preferred location, it is the tendency of quasi-two-dimensional flow to organize itself into vortices (as we see in Fig. 6.6 and Fig. 8.9) that undoubtedly contributes to its coherence and isolation from the rest of the hemisphere. The boundary of the vortex, as measure by potential vorticity
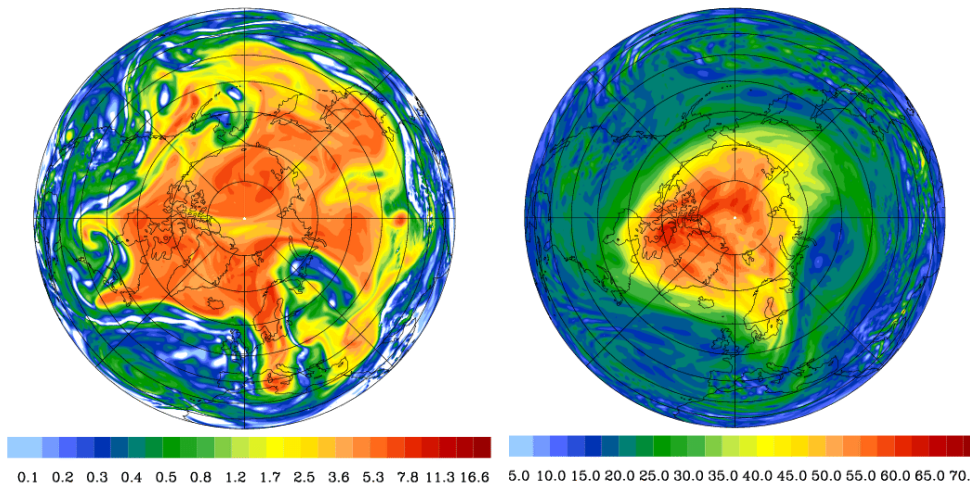
Fig. 13.17 The potential vorticity on two isentropic surfaces, the 310 K surface (left) and the 475 K surface (right), on January 19, 2005. The color bar is in PV units. The 310 K surface is mainly in the troposphere (see Fig. 12.14) where baroclinic instability is abundant. The 475 K surface is at about 20 km altitude, and on it we see a polar stratospheric vortex with a fairly sharp boundary where the PV gradient is high, and a mid-latitude region of smaller-scale features and wave breaking.[24]

Figure 13.18 The edge of the stratospheric polar vortex in 1984. Plotted is the 35 PVU isosurface of $Q^* = Q(\theta/\theta_0)^4.1$, where Q is Ertel PV. The vertical coordinate is potential temperature. Like Q, Q^* is materially conserved in adiabatic flow. It is approximately constant at the vortex edge, roughly compensating for the change in density with height that affects the Ertel PV. The left panel shows the vortex in a fairly usual state, and the right panel shows a split vortex following a stratospheric sudden warming.[25]
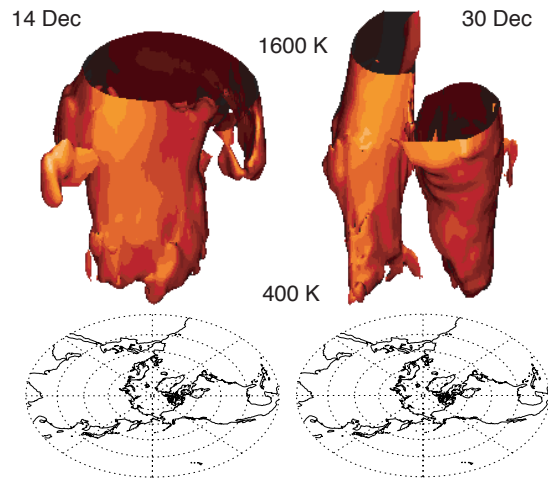
or tracer, is quite sharp with the value of PV often jumping by a factor of two or so, and the vortex is quite persistent — it is a near-permanent feature of the winter hemisphere. Within the vortex potential vorticity tends to homogenize, and once formed the main communication that the vortex has with the surf zone is via occasional wave breaking at its boundary. It is interesting that, although potential vorticity gradient is strong at the edge of the vortex, the exchange of properties is weak, implying a failure of notions of diffusion.

Stable as it is, the polar vortex is nevertheless sometimes disrupted by wave activity from below; this tends to occur when the wave activity itself is quite strong, and when the mean conditions are such as to steer that wave activity polewards. Occasionally, this activity is sufficiently strong so as to cause the vortex to break down, or to split into two smaller vortices, and so allow warm mid-latitude air to reach polar latitudes — an event known as a 'stratospheric sudden warming'.

Notes

1 Much of our basic understanding in this area stems from conceptual and numerical work on forced Rossby waves by Charney and Eliassen (1949), who looked at the response to orography using a barotropic model. This was followed by a study by Smagorinsky (1953) on the response to thermodynamic forcing using a baroclinic, quasi-geostrophic, model. Seeking more realism later studies have employed the primitive equations and spherical coordinates in studies that are at least partly numerical (e.g., Egger 1976, and a host of others) although most theoretical studies perforce still use the quasi-geostrophic equations. The description of the response in terms of wavetrains comes from Hoskins and Karoly (1981), with some earlier theoretical results having been derived by Longuet-Higgins (1964). There have been number of synthesis and review articles, among them Smith (1979), Dickinson (1980), Held (1983), Wallace (1983) and a collection in the *Journal of Climate,* (Volume 15, no. 16, 2002).

2 To obtain the figure, the topography is first specified in physical space. Its Fourier transform is taken and the streamfunction in wavenumber space is calculated using (13.12). The inverse Fourier transform of this gives the streamfunction in physical space.

3 Regarding the truly stationary (i.e., time-averaged) patterns of zonal asymmetry it may seem a little academic to try to differentiate between wavetrains emanating from an isolated topographic feature and a global resonant response, but the difference is relevant for intra-seasonal variability, which might considered a quasi-stationary response to slowly changing boundary conditions like the sea-surface temperature. If resonance is important, we might expect to see global-scale anomalies, whereas the viewpoint of damped wave-trains is more local. This whole area is one of continuing, active, research with deep roots going back to Namias (1959) and Bjerknes (1959) and beyond.

A different point of view, one that we do not explore in this book, is that the zonally asymmetric features of the earth's atmosphere are predominantly due to *nonlinear* effects. One possibility is that eddies might significantly modify (and perhaps amplify and sustain) stationary patterns through their large-scale turbulent transfers (see for example Green 1977, Shutts 1983). Different again is the notion, inspired by models of low-order dynamical systems, that the atmosphere might have have *regimes* of behaviour, and that the zonally asymmetric patterns are manifestations of the time spent in a particular regime before transiting to another. See for example Kimoto and Ghil (1993) and Palmer (1997).

4 Hoskins and Karoly (1981).

5 Following Lighthill (1978).

6 Steers (1962), Phillips (1973).

7 From Hoskins and Karoly (1981).

8 A description of JWKB methods can be found in Bender and Orszag (1978) and a number of other textbooks on approximate mathematical methods. 'JWKB' stands for Jeffreys, Wentzel, Kramers and Brillouin. The last three presented the technique in 1926 [G. Wentzel, Zeits. f. Phys. 38, 518; H. A. Kramers, Zeits. f. Phys. 39, 828; L. Brillouin, Comptes Rendus 183, 24] as a way to fing approximate solutions of the Schrödinger equation in quantum-mechanics and it is often referred to just as the WKB method, so affirming the notion that methods are often named for the last to discover them. Harold Jeffrey's, a mathematical geophysicist, had in 1923 [Proc. London Math. Soc. (2)23, 428] proposed a similar technique, and Lord Rayleigh in 1912 [Proc. Roy. Soc. A86, 207] had already addressed some aspects of the theory. The general mathematical matter was in fact treated by Joseph Liouville and George Green in the first half of the 19th century, so perhaps the method should really be called the LGRJWKB method!

9 At the critical latitude the JWKB analysis fails and both dissipative and nonlinear effects are likely to play a role. See Dickinson (1968) and Tung (1979).

10 From Grose and Hoskins (1979) and Hoskins and Karoly (1981).

11 Use of log-pressure coordinates, or the modified height coordinate set of White (1977), gives only a slightly different lower boundary condition. See 13.**??**.

12 This argument may seem like prestidigitation. If so, problem 13.6 provides an another approach that some may find more transparent.

13 Charney and Drazin (1961).

14 Because of such difficulties, understanding the effects sea-surface temperature anomalies, on the atmosphere has become largely the subject of GCM experiments, and one plagued with ambiguous results that depend in part on the particular configuration of the GCM. Some of the modelling issues are reviewed by Kushnir et al. (2002).

15 From Hoskins and Karoly (1981).

16 Such solutions are nearly always most easily obtained numerically. One way is to use a Fourier method described earlier. A related method is to write the equations in finite difference form, schematically as $AX = F$, where X is the vector of all the model fields, F represents the known forcing and A is a matrix obtained from the equations of motion and boundary conditions, and solve for X. A quite different method is to use a nonlinear time dependent model, such as a GCM: Prescribe or hold steady the zonally averaged zonal flow as well as all the zonally asymmetric forcing terms, but multiply the asymmetric terms by a small number (e.g., 0.01) to ensure the response is linear; then calculate by forward time integration the steady response, and then divide that solution by the small number to obtain the final solution.

17 Adapted from Held et al. (2002).

18 Adapted from Fels (1985), with the help of K. Hamilton.

19 Courtesty of J. Wilson of GFDL, using data from Fleming et al. (1988).

20 Brewer (1949), Dobson (1956). Brewer deduced upward motion into the stratosphere at low latitudes based on the water vapour distribution, while Dobson deduced a polewards transport within the stratosphere based on the ozone distribution — the circulation takes ozone from the low latitudes toward the poles. Although originally the Brewer-Dobson circulation was taken to mean the chemical transport circulation, it is now usually taken to mean the residual (mass) circulation. The two may differ if there is mixing of chemical without mixing of mass, and the chemical transport may differ among chemicals.

21 Adapted from Eluszkiewicz et al. (1996).

22 Modified from Plumb (2002).

23 Courtesy of D. Waugh.

24 Courtesy of A. Dörnbrack.

25 Courtesy of G. Esler. See also Lait (1994) for discussion of the alternative PV.

Problems

13.1 Consider the barotropic vorticity equation on the β-plane, with an uneven lower surface, satisfying the equation of motion

$$\frac{\mathrm{D}q}{\mathrm{D}t} = 0, \qquad q = \nabla^2 \psi + \beta y + h_b(x, y) \tag{P13.1}$$

where h_b is proportional to the bottom topography, assumed small. Linearize this about a constant zonal flow, U, and seek *steady state* solutions of the form $\psi = \mathrm{Re}\, \widetilde{\psi} e^{i(kx+ly)}$, with the topography similarly represented. (Re means take the real part of what follows.) Show that the response is infinite (a resonance) if its wavenumber is equal to that of stationary, free, barotropic Rossby waves.

Suppose that friction is introduced, so that the equation of motion becomes $\mathrm{D}q/\mathrm{D}t = -r\zeta$. Show that the response is now always finite. If the mountain is a single sinusoid, $h_b = H \sin kx$, sketch the response (i.e., the streamfunction field).

13.2 Explore the response the single-layer quasi-geostrophic system to flow over topography. Using Matlab, or otherwise, first obtain a response similar to that in Fig. 13.1. Then vary the frictional timescale, the wavenumber of the stationary Rossby wave, and the structure of the topography. Show that when the topography contains a resonant wavenumber that a trough in the streamfunction often occurs just downstream of the mountain peak, and that this is to be expected from the analytic solution.

13.3 ♦ Using an atlas, or obtaining the information from the literature or on-line, obtain rough representation of the earth's topography at 45° N and express it as a Fourier series. Then obtain (e.g., using Matlab) the barotropic stationary response to this topography — that is, the solution to (13.11). Explore the sensitivity of the solution to variations in $\overline{u}$, to using a different $\overline{u}$ on the left- and right-hand sides of (13.11), to the frictional parameter r, and to the deformation radius L_d. Artificially flatten the topography in the eastern and then the western hemisphere and comment on how the results vary. Finally, discuss whether your calculations are qualitatively and quantitatively in accord with observations. Optional: Repeat the entire problem for the southern hemisphere. [This problem develops a calculation similar to that of the well-known paper of Charney and Eliassen (1949).]

13.4 Obtain an expression analogous to (13.19) for the case with a finite deformation radius ($k_d \neq 0$). Compare the two results and explain the differences, if any.

13.5 Using log-pressure coordinates, show that the surface boundary condition analogous to (13.51) is

$$\frac{\partial}{\partial t}\left(\frac{\partial \psi'}{\partial Z} - \frac{N^2}{g}\psi'\right) + \overline{u}\frac{\partial}{\partial x}\frac{\partial \psi'}{\partial Z} - v'\frac{\partial \overline{u}}{\partial Z} = -\frac{N^2}{f_0}\left(\overline{u}\frac{\partial h_b}{\partial x} + \alpha\nabla^2\psi'\right) \quad \text{at } Z = 0,$$
(P13.2)

where here Z is proportional to log-pressure.

Hint: Note that the relation between $W = \mathrm{D}z/\mathrm{D}t$ and the real vertical velocity is $w = (f_0/g)\partial\psi/\partial t + RT/(gH)W$ and choose $H = RT(0)/g$.

13.6 The vertical energy flux in a radiating wave is proportional to $\rho_R \overline{p'w'}$ where the overline denotes a horizontal average and p' and w' are the pressure and vertical velocity.

(a) For the oscillatory solution, with $m^2 > 0$, show that if the energy flux is to be directed upwards then the product km must be positive, where k and m are the zonal and vertical wavenumbers.

(b) For the trapped solution with $m^2 < 0$, show that the vertical propagation of energy is zero.

N. B. In this problem and the next it is important to take the real part of each field properly before evaluating the averages. Thus, if $h = \mathrm{Re}\, h_b e^{ikx}$ where $h_b = h_{br} + ih_{bi}$ then $h_b = h_{br}\cos kx - h_{bi}\sin kx$. But with little loss of generality one may choose either h_{br} or h_{bi} equal to zero.

13.7 Obtain an expression for the meridional heat flux associated with the solutions (T.1). In particular, show that for $m^2 > 0$ it is proportional to $|h_b|^2 km/(K_s^2 - K^2)$ and therefore deduce that it is positive for an upwardly propagating wave. Show that for the trapped solutions the meridional heat flux is zero.

13.8 Evaluate the wave activity density (pseudo-momentum) associated with the solutions (T.1), and the associated EP flux. Show that the group velocity property is satisfied, and that the transport of wave activity is directed upwards for oscillatory solutions.

13.9 ♦ Obtain the homogeneous solution to (13.70) that, when added to the particular solution, properly satisfies the boundary condition (13.74). Discuss the solution, and in particular show that the total response remains bounded even as the denominator in (13.73) goes to zero.

Part IV

LARGE-SCALE OCEANIC CIRCULATION

To increase our knowledge the subject [oceanography] must be made attractive to men who do not mind facing up to the difficulties of fluid mechanics.

From *Nature,* 25 December 1954.

CHAPTER 14

Wind-Driven Gyres

U NDERSTANDING THE CIRCULATION OF THE OCEAN involves a combination of observations, comprehensive numerical modelling, and more conceptual modelling, or 'theory'. All have become essential, but in this chapter, and the ones following, our emphasis is on the last of the tripos. Its (continuing) role is not to explain every feature of the observed ocean circulation, nor to necessarily describe details best left to numerical simulations. It is to provide a conceptual and theoretical framework for understanding the circulation of the ocean, for interpreting observations and suggesting how new observations may best be made, and to aid the development and interpretation of experiments with numerical models.

The main currents of the worlds oceans are sketched in Fig. 14.1.[1] (Over most of the ocean, the vertically averaged currents have a similar sense as the surface currents, one exception being at the equator where the surface currents are mainly westwards but the vertical integral is dominated by the eastwards undercurrent.) Two seemingly dichotomous aspects stand out: (i) the complexity of the currents as they interact with topography and the geography of the continents; (ii) the simplicity and commonality of the large-scale structures in the major ocean basins, and in particular the ubiquity of subtropical and subpolar gyres. Indeed these gyres, sweeping across the great oceans carrying vast quantities of water and heat, are perhaps the single most conspicuous feature of the circulation. The subtropical gyres are anticyclonic, extending polewards to about 45°, and the subpolar gyres are cyclonic and polewards of this, primarily in the Northern Hemisphere. The existence of gyres, and that they are strongest in the west, has been known for centuries; this *western intensification* leads to such well-known currents as the Gulf Stream in the Atlantic (charted by Benjamin Franklin), the Kuroshio in the Pacific, and the Brazil Current in the South Atlantic. Although even today we barely have sufficient observations to produce a synoptic map of the ocean currents,
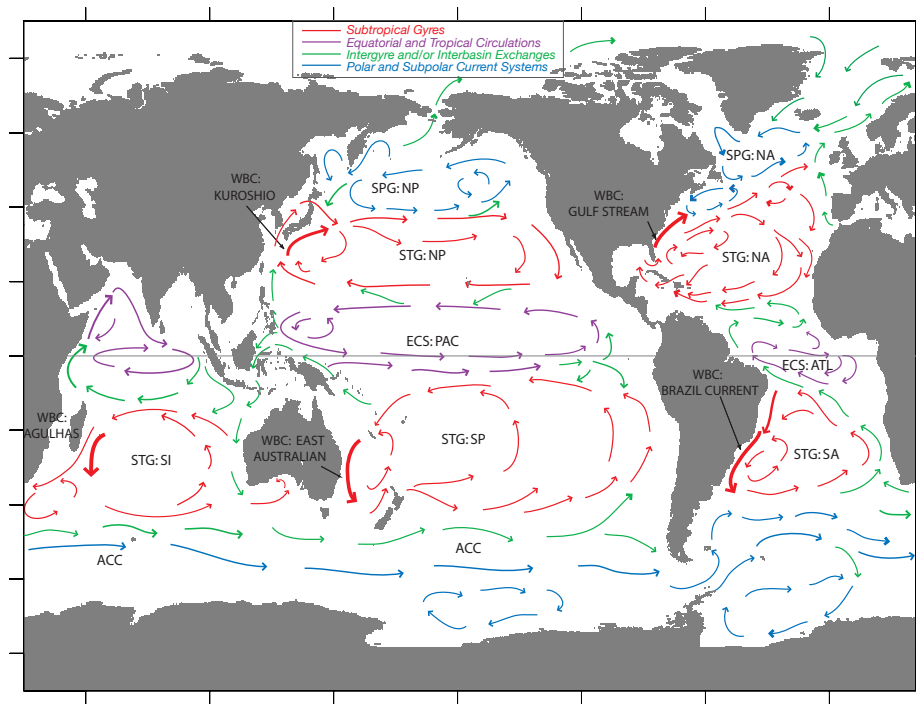
Fig. 14.1 A schema of the main currents of the global ocean. Key: STG – Sub-Tropical Gyre; SPG – Sub-Polar Gyre; WBC – Western Boundary Current; ECS – Equatorial Current System; NA – North Atlantic; SA – South Atlantic; NP – North Pacific; SP – South Pacific; SI – South Indian; ACC – Antarctic Circumpolar Current; ATL – Atlantic; PAC – Pacific.

except at the surface, the large-scale mean currents are fairly well mapped and Fig. 14.2 illustrates the average current pattern of the North Atlantic using a combination of observations and a numerical model, and the Gulf Stream is clearly visible.[2]

For much of this chapter we consider a model, and variations about it, that explains the large-scale features of ocean gyres and that lies at the core of ocean circulation theory — the steady, forced-dissipative, homogeneous model of the ocean circulation first formulated by Stommel.[4] Such models explain many of the zeroth-order features of the ocean, in particular the existence of gyres and the appearance of intense western boundary currents. In the later part of the chapter we examine the vertical structure of the wind-driven circulation, taking the stratification as given. In the two chapters following we consider the maintenance of that stratification.
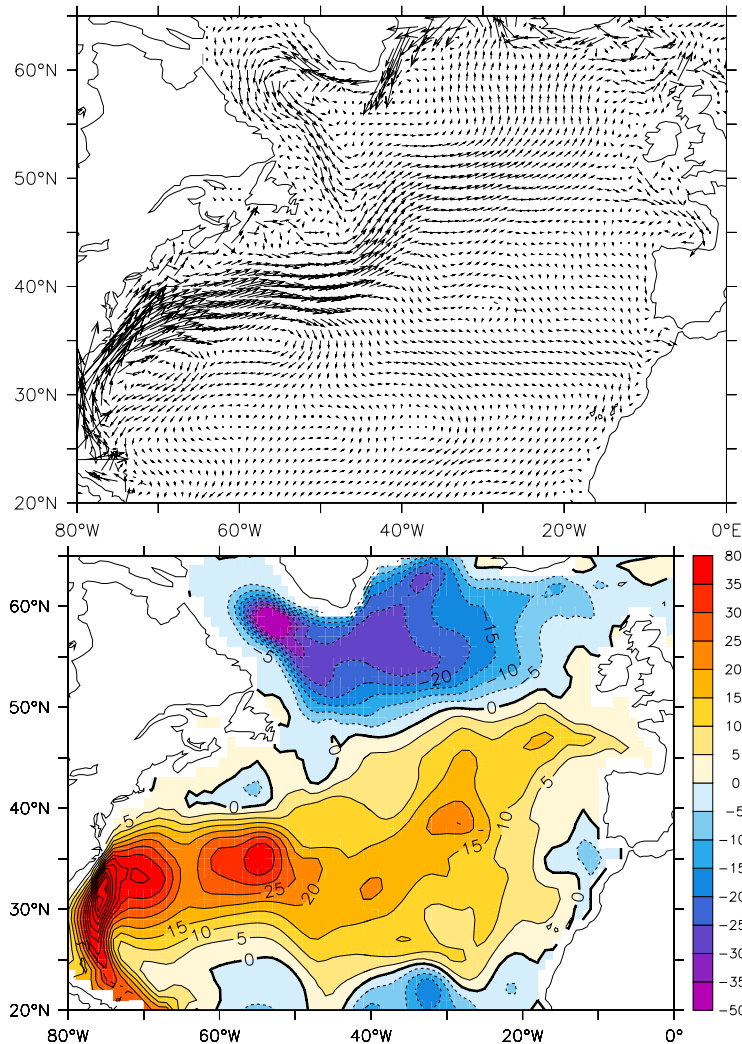
Fig. 14.2 Top: The time-averaged velocity field at a depth of 75 m in the North Atlantic, obtained by constraining a numerical model to hydrographic observations. Bottom: The streamfunction of the vertically integrated flow, in Sverdrups. Note the presence of an anticyclonic subtropical gyre, a cyclonic subpolar gyre, and intense western boundary currents.[3]

14.1 THE DEPTH INTEGRATED WIND-DRIVEN CIRCULATION

The equations that govern the large-scale flow in the oceans are the planetary-geostrophic equations. Greatly simplified as these are compared to the Navier-Stokes equations, or even the hydrostatic Boussinesq equations, they are still quite daunting: a prognostic equation for buoyancy is coupled to the advecting velocity via hydrostatic and geostrophic balance, and the resulting problem is formidably nonlinear. However, it turns out that thermodynamic effects can effectively be eliminated by the simple device

of vertical integration; the resulting equations are linear, and the only external forcing is that due to the wind-stress. The resulting model then, at the price of some comprehensiveness, gives a useful picture of the *wind-driven* circulation of the ocean.

14.1.1 The Stommel Model

The planetary geostrophic equations for a Boussinesq fluid are:

$$\frac{\mathrm{D}b}{\mathrm{D}t} = \dot{b}, \qquad \nabla \cdot \boldsymbol{v} = 0, \tag{14.1a,b}$$

$$\boldsymbol{f} \times \boldsymbol{u} = -\nabla \phi + \frac{1}{\rho_0} \frac{\partial \boldsymbol{\tau}}{\partial z}, \qquad \frac{\partial \phi}{\partial z} = b. \tag{14.2a,b}$$

These equations are, respectively, the thermodynamic equation (14.1a), the mass continuity equation (14.1b), the horizontal momentum equation (14.2a), (i.e., geostrophic balance, plus a stress term) and the vertical momentum equation (14.2b), (i.e, hydrostatic balance). These equations are derived more fully in chapter 5, but they are essentially the primitive equations with the advection terms omitted in the horizontal momentum equation, on the basis of small Rossby number. Take the curl of (14.2a) (that is, cross differentiate its x and y components) and integrate over the depth of the ocean to give

$$\int \boldsymbol{f} \nabla_z \cdot \boldsymbol{u} \, \mathrm{d}z + \frac{\partial f}{\partial y} \int v \, \mathrm{d}z = \mathrm{curl}_z(\widetilde{\boldsymbol{\tau}}_t - \widetilde{\boldsymbol{\tau}}_b) \tag{14.3}$$

where the operator curl_z is defined by $\mathrm{curl}_z \boldsymbol{A} \equiv \partial A^y / \partial x - \partial A^x / \partial y = \mathbf{k} \cdot \nabla \times \boldsymbol{A}$, and $\widetilde{\boldsymbol{\tau}}$ is the kinematic stress, $\widetilde{\boldsymbol{\tau}} = \boldsymbol{\tau}/\rho_0$. The divergence term vanishes if the vertical velocity is zero at the top and bottom of the ocean. Strictly, at the top of the ocean the vertical velocity is given by the material derivative of height of the ocean's surface, Dh/Dt, but on the large-scales that is negligible and setting it to zero is the rigid-lid approximation. At the bottom of the ocean the vertical velocity is only zero if the ocean in flat-bottomed; otherwise it is $\boldsymbol{u} \cdot \nabla \eta_b$, where η_b is the orographic height at the ocean floor. The neglect of this topographic term probably the most restrictive single approximation in the formulation of this model. Given this neglect, (14.3) becomes

$$\beta \overline{v} = \mathrm{curl}_z(\widetilde{\boldsymbol{\tau}}_t - \widetilde{\boldsymbol{\tau}}_b) \tag{14.4}$$

where henceforth, in this section, quantities with an overbar are understood to be the vertical integral over the depth of the ocean. If the stresses depend only on the velocity fields then thermodynamic variables evidently do not affect the vertically integrated flow.

At the top of the ocean, the stress is given by the wind. At the bottom, it is given by bottom friction, and we assume that this may be parameterized by a linear drag, or Rayleigh friction, as might be generated by an Ekman layer; it is this assumption that particularly characterizes this model as that due to Stommel. Eq. (14.4) then becomes

$$\beta \overline{v} = -r \overline{\zeta} + W(x, y) \tag{14.5}$$

> ### Formulation of the Stommel/Munk model
>
> ★ Vertically integrated planetary-geostrophic equations, or a homogeneous fluid with nonlinearity neglected.
>
> ★ Friction parameterized by a linear drag (Stommel model) or a harmonic Newtonian viscosity (Munk model) or both (Stommel-Munk model).
>
> ★ Flat bottomed ocean.
>
> Variations on the theme include allowing nonlinearity in the vorticity equation, posing the problem in domains of various shapes, and allowing bottom topography (in particular sloping sidewalls). The solutions are normally calculated in the boundary-layer approximation, but some exact solutions exist.

where W is proportional to the wind-stress curl at the top of the ocean and is a known function. Because the velocity is divergence-free, we can define a streamfunction ψ such that $\overline{u} = -\partial \psi / \partial y$ and $\overline{v} = \partial \psi / \partial x$. Eq. (14.5) then becomes

$$r \nabla^2 \psi + \beta \frac{\partial \psi}{\partial x} = W(x, y). \tag{14.6}$$

This equation is often referred to as the *Stommel problem* or *Stommel model,* and may be posed in a variety of two dimensional domains.

14.1.2 Alternative formulations

A number of alternative formulations, still leading to (14.6), are possible. None are perhaps as well justified as the derivation via the planetary-geostrophic equations but the differences in the specific assumptions made both give some indication of the robustness of the derivation, and show how the model might be extended to include topographic or nonlinear effects.

I. A Homogeneous Model

Rather than vertically integrating, we may suppose that the ocean is a homogeneous fluid obeying the shallow water equations (chapter 3). The potential vorticity equation is:

$$\frac{\mathrm{D}}{\mathrm{D}t} \left(\frac{\zeta + f}{h} \right) = \frac{F}{h}, \tag{14.7}$$

where F represents friction and forcing [c.f., (3.81)]. In an ocean with a rigid-lid and flat bottom then we obtain the barotropic vorticity equation,

$$\frac{\mathrm{D}\zeta}{\mathrm{D}t} + \beta v = F. \tag{14.8}$$

The forcing term F we again represent as a wind-stress curl, and a linear drag. Further, since the horizontal velocity is divergence-free (because of the flat-bottom and rigid-lid assumptions) we may represent it as a stream-function, whence we obtain the closed equation

$$\frac{\mathrm{D}}{\mathrm{D}t}\nabla^2\psi + \beta\frac{\partial\psi}{\partial x} = W_E(x,y) - r\nabla^2\psi. \tag{14.9}$$

This equation is the 'time-dependent nonlinear Stommel problem'. The steady nonlinear problem is sometimes of interest, too, and this is just

$$J(\psi, \nabla^2\psi) + \beta\frac{\partial\psi}{\partial x} = W_E(x,y) - r\nabla^2\psi. \tag{14.10}$$

To obtain the original Stommel model we just ignore the advective derivative, which will be valid if $|\zeta| \sim Z \ll \beta L$ where $Z = U/L$ is a representative value of vorticity. This condition is equivalent to

$$R_\beta \equiv \frac{U}{\beta L^2} \ll 1. \tag{14.11}$$

R_β is called the *beta-Rossby number*. On sufficiently large scales, $\beta \sim f/L$ so that (14.11) is then similar to a small Rossby number assumption. Given this, (14.9) reduces to (14.6).

II. Quasi-geostrophic formulation

In the PG formulation, the horizontal velocity is divergence-free only because we have vertically integrated, and the divergence-free aspect of the flow is crucial in our obtaining a solution. If the scales of motion are not too large the horizontal flow at every level is divergence-free for another reason: because it is in geostrophic balance. In reality, over a single oceanic gyre (say from 15° to 40° latitude), variations in Coriolis parameter are not large, and this prompts us to formulate the model in terms of the quasi-geostrophic equations. Formally, such a model would then be restricted to length-scales L no more than $\mathcal{O}(Ro^{-1})$ larger than the deformation radius, and for gyre scales this criterion is marginally satisfied if $L_{\mathrm{d}} = 100\,\mathrm{km}$. An advantage of the quasi-geostrophic equations is that it readily allows for the inclusion of both nonlinearity and stratification. [For a quick-and-dirty summmary of quasi-geostrophy, see the box on page 235.] The quasi-geostrophic potential vorticity equation for a Boussinesq system is:

$$\frac{\mathrm{D}}{\mathrm{D}t}\left[\zeta + \frac{\partial}{\partial z}\left(\frac{f_0^2}{N^2}\frac{\partial\psi}{\partial z}\right)\right] + \beta v = f_0\frac{\partial w}{\partial z} + \mathrm{curl}_z\frac{\partial\widetilde{\boldsymbol{\tau}}}{\partial z} \tag{14.12}$$

If we neglect the advective derivative, and vertically integrate, we obtain

$$\beta\int v\,\mathrm{d}z = f_0[w]_b^t + \mathrm{curl}_z[\widetilde{\boldsymbol{\tau}}]_b^t. \tag{14.13}$$

where t denotes the ocean top and b the bottom. We now make one of two virtually equivalent choices.

(i) We suppose that the integration is over the entire depth of the ocean, in which case the term $[w]_b^t$ vanishes given a rigid lid and a flat bottom. If the stress at the top of the ocean is given by the wind stress, and at the bottom of the ocean it is parameterized by a linear drag, then we obtain

$$\beta \overline{v} = W(x, y) - r\overline{\zeta} \tag{14.14}$$

just as in (14.5). The velocity is the integrated velocity over the depth of the ocean, and because the advecting velocity can be obtained from the streamfunction, (14.6) follows.

(ii) We suppose that the integration is between two thin Ekman layers at the top and bottom of the ocean. The stress is zero at the interior edge of these layers, but the vertical velocity is not. At the base of the upper Ekman layer it is given by:

$$w(x, y, -\delta_u) = \text{curl}_z(\widetilde{\tau}/f_0) \tag{14.15}$$

where the top of the ocean is at $z = 0$ and δ_u is the thickness of the upper Ekman layer. Similarly, at the top of the lower Ekman layer, the vertical velocity is:

$$w(x, y, -D + \delta_b) = \delta_b\zeta \tag{14.16}$$

where δ_b is the thickness of the bottom Ekman layer.

Neglecting the advective derivative, and integrating over the ocean between the two Ekman layers, (14.12) becomes

$$\beta \overline{v} = \text{curl}_z\widetilde{\tau} - f_0\delta_b\overline{\zeta}. \tag{14.17}$$

Defining the drag coefficient r by $r = f_0\delta_b$, we arrive at (14.14).

Because the flow is quasigeostrophic we may define a streamfunction such that $\overline{v} = \partial\psi/\partial x$ and $\overline{\zeta} = \nabla^2\psi$, and (14.14) becomes

$$r\nabla^2\psi + \beta\frac{\partial\psi}{\partial x} = \text{curl}_z\widetilde{\tau}, \tag{14.18}$$

which is the same as (14.6). Note that in all of these derivations, we have effectively parameterized the friction at the bottom of the ocean by a linear drag acting on the vertically integrated velocity (or vorticity) field. In reality, the bottom friction is produced by the velocity at the bottom of the ocean, but this wrinkle is beyond the scope of vertically integrated models.

14.1.3 Approximate solution of Stommel model

Sverdrup balance

Equation (14.6) is linear and it is possible to obtain an exact, analytic solution. However, it is more insightful to approach the problem perturbatively, by supposing that the

frictional term is small, meaning there is an approximate balance between wind-stress and the β-effect.[5] Friction is small if $|r\zeta| \ll |\beta v|$ or

$$\frac{r}{L} = \frac{f_0 \delta}{HL} \ll \beta \tag{14.19}$$

using $r = fd/H$ where δ is the thickness of the Ekman layer and L is the horizontal scale of the motion, and generally speaking this inequality is well satisfied for large-scale flow. The vorticity equation becomes

$$\beta \overline{v} \approx \text{curl}_z \widetilde{\boldsymbol{\tau}}, \tag{14.20}$$

or *Sverdrup balance*.[6] The observational support for Sverdrup balance is rather mixed, discrepancies arising not so much from failure of (14.19), but from the presence of small-scale eddying motion with concomitly large nonlinear terms, and the presence of non-negligible vertical velocities induced by the interaction with bottom topography.[7] Nevertheless, Sverdrup balance provides a useful, if not impregnable, foundation on which to build.

Boundary-layer solution

For simplicity, consider a square domain of side a and rescale the variables by setting

$$x = a\widehat{x}, \qquad y = a\widehat{y}, \qquad \widetilde{\tau} = \tau_0 \widehat{\tau}, \qquad \psi = \widehat{\psi}\frac{\tau_0}{\beta} \tag{14.21}$$

where τ_0 is the amplitude of the windstress. The hatted variables are nondimensional and, assuming our scaling to be sensible, these are $\mathcal{O}(1)$ quantities in the interior. Eq. (14.18) becomes

$$\frac{\partial \widehat{\psi}}{\partial \widehat{x}} + \epsilon_s \nabla^2 \widehat{\psi} = \text{curl}_z \widehat{\tau} \tag{14.22}$$

where $\epsilon_s = (r/a\beta) \ll 1$, in accord with (14.19). For the rest of this section we will drop the hats over nondimensional quantities

Over the interior of the domain, away from boundaries, the frictional term is small and an approximate solution may be obtained by simply dropping it, giving

$$\frac{\partial \psi_I}{\partial x} = \text{curl}_z \boldsymbol{\tau}, \tag{14.23}$$

where ψ_I is the interior streamfunction, or the 'Sverdrup flow'. The solution of this equation is

$$\psi_I(x, y) = \int_0^x \text{curl}_z \boldsymbol{\tau}(x', y) \, dx' + g(y), \tag{14.24}$$

where $g(y)$ is an arbitrary function of y, which thus gives rise to an arbitrary zonal flow. The corresponding velocities are

$$v_I = \text{curl}_z \boldsymbol{\tau}, \qquad u_I = -\frac{\partial}{\partial y} \int_0^x \text{curl}_z \boldsymbol{\tau}(x', y) \, dx' - \frac{\partial g(y)}{\partial y}. \tag{14.25}$$

Western Boundary Layer   Eastern Boundary Layer
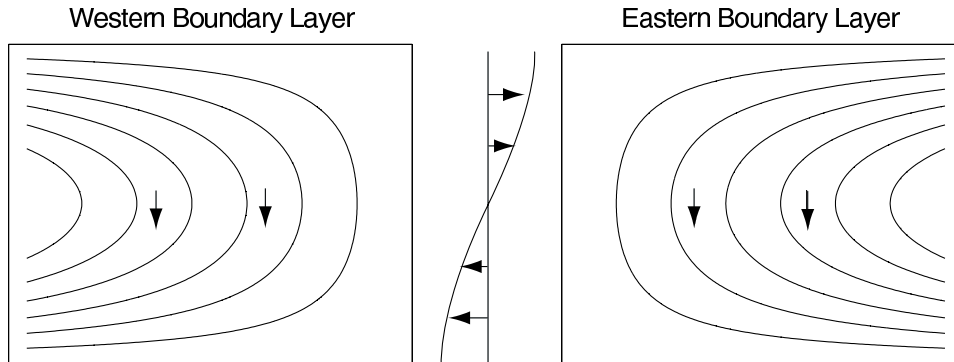
Fig. 14.3 Two possible Sverdrup flows, ψ_I, for the wind stress shown in the center. Each solution satisfies the no-flow condition at either the eastern or western boundary, and a boundary layer is therefore required at the other boundary. Both flows have the same, equatorward, meridional flow in the interior. Only the flow with the western boundary current is physically realizable, however, because only then can friction produce a torque that opposes that of the wind-stress, so allowing the flow to equilibrate.

The dynamics is most clearly illustrated if we now restrict attention to a windstress curl that is zonally uniform, and that vanishes at two latitudes, $y = 0$ and $y = 1$. An example is

$$\tau^y = 0, \qquad \tau^x = -\tau_0 \cos(\pi y), \tag{14.26}$$

for which $\mathrm{curl}_z \boldsymbol{\tau} = -\pi \sin(\pi y)$. The Sverdrup (interior) flow is then

$$\psi_I(x, y) = (x - C(y))\mathrm{curl}_z \boldsymbol{\tau} = \pi(C(y) - x) \sin \pi y. \tag{14.27}$$

Now, if we choose C to be a constant, then the arbitrary zonal flow is $C \, \mathrm{curl}_z \boldsymbol{\tau}$. Then we can satisfy $\psi = 0$ at *either* $x = 0$ (if $C = 0$) *or* $x = 1$ (if $C = 1$). These solutions are illustrated in Fig. 14.3 for the particular stress (14.26).

Regardless of our choice of C we cannot satisfy $\psi = 0$ at both zonal boundaries. We must choose one, and then construct a *boundary layer* solution to satisfy the other condition. Which choice do we make? On intuitive grounds it seems that we should choose the solution that satisfies $\psi = 0$ at $x = 1$ (the solution on the left in Fig. 14.3), for then the interior flow then goes round in the same direction as the wind: the wind is supplying a clockwise torque, and to achieve an angular momentum balance anticlockwise angular momentum must be removed by friction. We can imagine that this would be provided by the frictional forces at the western boundary layer if the interior flow is clockwise, but not by friction at an eastern boundary layer when the interior flow is anticlockwise. Note that this argument is not dependent on the sign of the windstress-curl: if the wind blew the other way a similar argument still implies that a western boundary layer is needed. We will now see if and how the mathematics reflects this intuitive but non-rigorous argument.

Asymptotic Matching

Let the complete solution be the sum of the Sverdrup interior solution plus a correction that we expect to be important only near the boundary. Thus we write

$$\psi(x, y) = \psi_I(x, y) + \phi(x, y), \tag{14.28}$$

where ϕ is the boundary layer correction, required to be small in the interior. At the boundary, the solution varies rapidly with x. To reflect this, let us *stretch* the x-coordinate near this point of failure (i.e., at $x = 0$ or $x = 1$) and let

$$x = \epsilon\alpha \qquad \text{or} \qquad x - 1 = \epsilon\alpha \tag{14.29a,b}$$

Here, α is the stretched-coordinate, which has values $\mathcal{O}(1)$ in the boundary layer, and ϵ is a small parameter, as yet undetermined. Then (14.22) becomes

$$\epsilon_S(\nabla^2\psi_I + \nabla^2\phi) + \frac{\partial\psi_I}{\partial x} + \frac{1}{\epsilon}\frac{\partial\phi}{\partial\alpha} = \text{curl}_z\tau \tag{14.30}$$

where $\phi = \phi(\alpha, y)$ and $\nabla^2\phi = \epsilon^{-2}\partial^2\phi/\partial\alpha^2 + \partial^2\phi/\partial y^2$. Now, by choice, ψ_I exactly satisfies Sverdrup balance, and so (14.30) becomes

$$\epsilon_S\left(\nabla^2\psi_I + \frac{1}{\epsilon^2}\frac{\partial^2\phi}{\partial\alpha^2} + \frac{\partial^2\phi}{\partial y^2}\right) + \frac{1}{\epsilon}\frac{\partial\phi}{\partial\alpha} = 0 \tag{14.31}$$

We now choose ϵ to obtain a physically meaningful solution. The obvious choice is $\epsilon = \epsilon_S$, for then the leading-order balance in (14.31) is

$$\frac{\partial^2\phi}{\partial\alpha^2} + \frac{\partial\phi}{\partial\alpha} = 0. \tag{14.32}$$

The solution of this equation is

$$\phi = A(y) + B(y)e^{-\alpha}, \tag{14.33}$$

Evidently, ϕ grows exponentially in the negative α direction. If this were allowed, it would violate our assumption that solutions are small in the interior, and we must eliminate this possibility by allowing α to take only positive values in the interior of the domain, and by setting $A(y) = 0$. We therefore choose $x = \epsilon\alpha$ so that $\alpha > 0$ for $x > 0$. The boundary layer is then at $x = 0$, that is, it is a *western boundary,* and it decays eastward in the direction of increasing α — that is, into the ocean interior. We then choose $C = 1$ in (14.27) to make $\psi_I = 0$ at $x = 1$ in (14.27) and then, for the windstress (14.26), the interior solution is given by

$$\psi_I = \pi(1 - x)\sin\pi y. \tag{14.34}$$

This alone satisfies the boundary condition at the eastern boundary. The function $B(y)$ is chosen to satisfy the additional condition that

$$\psi = \psi_I + \phi = 0 \qquad \text{at} \qquad x = 0, \tag{14.35}$$

and using (14.34) this gives

$$\pi \sin \pi y + B(y) = 0. \tag{14.36}$$

Thus, the boundary layer solution is:

$$\phi = -\pi \sin \pi y e^{-x/\epsilon_S}. \tag{14.37}$$

The composite (boundary layer plus interior solution) is

$$\psi = (1 - x - e^{-x/\epsilon_S})\pi \sin \pi y, \tag{14.38}$$

or, in full dimensional form,

$$\boxed{\psi = (1 - x/a - e^{-x/(a\epsilon_S)})\pi \sin(\pi y/a)}. \tag{14.39}$$

This is a 'single gyre' solution. Two or more gyres can be obtained with a different wind forcing, such as $\tau^x = -\tau_0 \cos(2\pi y)$, as in Fig. 14.4.

It is a relatively straightforward matter to generalize to more arbitrary wind-stresses, provided these also vanish at the two latitudes between which the solution is desired. It is left as a problem to show that in general

$$\psi_I = \int_{x_e}^{x} \text{curl}_z \boldsymbol{\tau}(x', y) \, dx', \tag{14.40}$$

and that the composite solution is

$$\psi = \psi_I - \psi_I(0, y)e^{-x/(x_e \epsilon_S)}. \tag{14.41}$$

14.2 USING VISCOSITY INSTEAD OF DRAG

A natural variation on on the Stommel problem is to use a harmonic viscosity, $\nu \nabla^2 \zeta$, in place of the drag term $-r\zeta$ in the vorticity equation, the argument being that the wind-driven circulation does not reach all the way to the ocean bottom so that an Ekman drag is not appropriate. This variation is called the Munk problem or Munk model,[8] and if both drag and viscosity are present we have the 'Stommel-Munk' model. The particular form of the lateral friction used in the Munk problem is still somewhat hard to justify because it relies on an ill-founded eddy diffusion of relative vorticity (chapter 10). Our treatment of this problem is relatively brief, concentrating only on those areas where the problem differs from the Stommel problem. The problem is to find and understand the solution to the (dimensional) equation

$$\beta \frac{\partial \psi}{\partial x} = \text{curl}_z \boldsymbol{\tau} + \nu \nabla^2 \zeta = \text{curl}_z \boldsymbol{\tau} + \nu \nabla^4 \psi \tag{14.42}$$

in a given domain, for example a square of side a. We need two boundary conditions at each wall to solve the problem uniquely, and as before for one of them we choose $\psi = 0$ to satisfy the no-normal-flow condition. For the other condition, two possibilities present themselves:

Streamfunction   Wind Stress
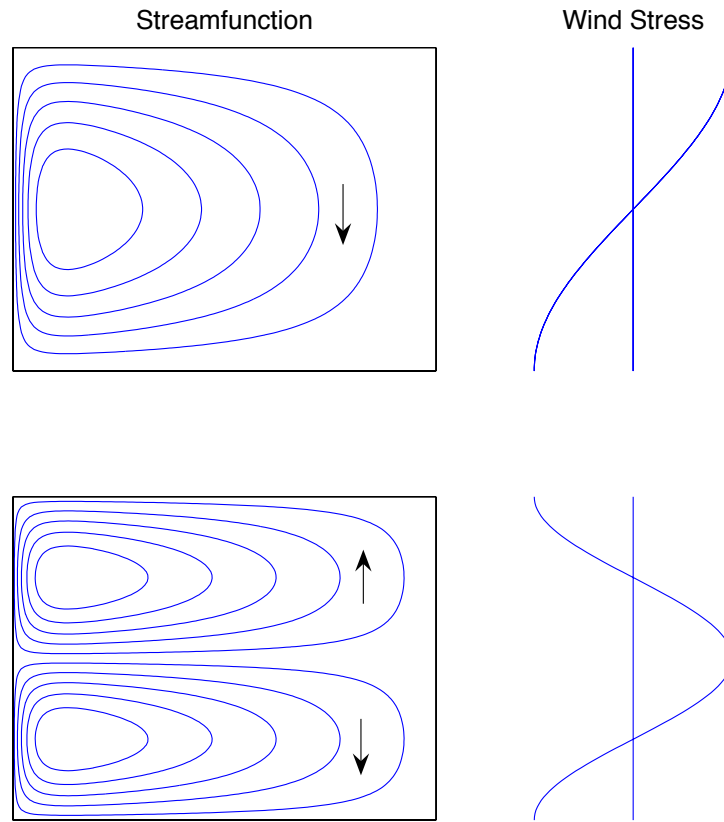
Fig. 14.4 Two solutions of the Stommel model. Upper panel shows the streamfunction of a single-gyre solution, with a windstress proportional to $-\cos(\pi y/a)$ (in a domain of side a), and the lower panel shows a two-gyre solution, with windstress proportional to $\cos(2\pi y/a)$. In both cases $\epsilon_s = 0.04$.

(i) Zero vorticity, or $\zeta = 0$. Since $\psi = 0$ along the boundary, this possibility is equivalent to $\partial^2\psi/\partial n^2 = 0$ where $\partial/\partial n$ denotes a derivative normal to the boundary. This is known as a 'free-slip' condition. At $x = 0$, for example, the condition becomes $\partial v/\partial x = 0$; that is, there is no horizontal shear at the boundary.

(ii) No flow along the boundary (the 'no slip' condition). That is $\psi_n = 0$ where the subscript denotes the normal derivative of the streamfunction. At $x = 0$ we have $v = 0$.

There is little *a priori* justification for choosing either of these. The second choice would be demanded if ν were a molecular viscosity, but then we would have to resolve a molecular boundary layer which perhaps would be a few millimeters thick. Instead, ν must be interpreted as some form of eddy viscosity, as we discuss in chapter 10. In that case, one might argue that the free-slip condition should be preferred, but in the

> ## Some Properties of the Stommel Model
>
> *(i)* The transport in the Sverdrup interior is equatorwards for an anti-cyclonic wind-stress curl. This transport is exactly balanced by the polewards transport in the boundary layer.
>
> *(ii)* There must be a boundary layer to satisfy mass conservation, and this must be a western boundary layer if the friction acts to provide a torque of opposite sign to the motion itself. As there is a balance between friction and the β-effect, it is a 'frictional boundary layer'. The western location does not depend on the sign of the wind-stress, nor on the sign of the Coriolis parameter, but it does depend on the sign of β, and so on the direction of rotation of the earth.
>
> *(iii)* The boundary layer width arises by noting that the terms $r\nabla^2\psi$ and $\beta\partial\psi/\partial x$ are in approximate balance in the western boundary layer, implying a length-scale of $L_w = (r/\beta)$. If r, the inverse frictional time, is $20\,\text{days}^{-1}$ then $L_w \approx 60\,\text{km}$, similar to the width of the Gulf Stream.

absence of a proper theoretical basis for such eddy viscosities there is no truly rational way to make the choice. We will solve the no-slip problem; see exercise 14.3 for the free-slip problem.

Let the wind stress be the canonical $\tau^x = -\tau_0\cos(\pi y/a)$. Then the interior (Sverdrup) flow is given by (14.34), as for the Stommel problem. This satisfies the free-slip boundary conditions at $y = 0, 1$, namely $\partial_x^2\psi = 0$, automatically. However, we will need boundary layers at both western and eastern boundaries, because the interior solution cannot satisfy all four boundary conditions required by (14.42). The eastern boundary layer will be relatively weak, and needed only to satisfy the no-slip or free-slip condition but, as in the Stommel problem, there will be a strong western boundary layer, needed to satisfy the no-normal flow condition. How thick will this be? Inspection of (14.42) suggests that the frictional term and the β term will balance in a boundary layer of thickness L_M where

$$L_M \sim \left(\frac{\nu}{\beta}\right)^{1/3} \tag{14.43}$$

and indeed this scale will result from a more formal analysis.

Nondimensionalizing (14.42) a similar way as for the Stommel problem yields

$$\epsilon_M\nabla^4\psi + \frac{\partial\psi}{\partial x} = \text{curl}_z\boldsymbol{\tau} \tag{14.44}$$

where $\epsilon_M = (\nu/\beta a^3)$. Considering for now only the western boundary layer correction we let the solution be the sum of an interior (Sverdrup) streamfunction plus a boundary

layer correction:

$$\psi = \psi_I + \phi_w(\alpha, y) \tag{14.45}$$

where, as before, ϵ is a small parameter and α is a stretched coordinate such that $x = \epsilon\alpha$. Similarly, may we add a correction to the eastern edge with a stretched coordinate α' such that $x - 1 = \epsilon\alpha'$. Substituting (14.45) into (14.44) and subtracting the Sverdrup balance gives

$$-\epsilon_M \left(\frac{1}{L_w^4} \frac{\partial^4 \phi_w}{\partial \alpha^4} \right) + \frac{1}{L_w} \frac{\partial \phi_w}{\partial \alpha} = 0 \tag{14.46}$$

As expected from the simpler dimensional analysis, a nontrivial balance is obtained when $L_w = L_M = (\nu/\beta)^{1/3}$. The boundary conditions on this are that:

(i) $\phi_w \to 0$ as $\alpha \to \infty$. This states that the perturbation decays as it extends into the interior.

(ii) $\phi_w = -\psi_I$ at $x = \alpha = 0$. This is the no-normal-flow condition on the meridional boundary.

(iii) $\partial_x \phi_w = -\partial_x \psi_I$ at $x = \alpha = 0$. (The no-slip condition.)

Solving (14.46) is a standard albeit non-trivial algebraic exercise and, omitting the weak zonal boundary layers at $y = 0, 1$ but including the eastern boundary layer correction, the solution of (14.44) is found to be

$$\psi = \psi_I - \psi(0, y)e^{-x/(2\epsilon_M)} \left[\cos\left(\frac{\sqrt{3}}{2} \frac{x}{\epsilon_M} \right) + \frac{1}{\sqrt{3}} \sin\left(\frac{\sqrt{3}}{2} \frac{x}{\epsilon_M} \right) \right]$$
$$- \epsilon_M e^{(x-1)/\epsilon_M} \frac{\partial}{\partial x} \psi_I(1, y) \tag{14.47}$$

With the canonical windstress this solution becomes

$$\psi = (1 - x)\pi \sin(\pi y) - \pi \sin(\pi y)e^{-x/(2\epsilon_M)} \left[\cos\left(\frac{\sqrt{3}}{2} \frac{x}{\epsilon_M} \right) + \frac{1}{\sqrt{3}} \sin\left(\frac{\sqrt{3}}{2} \frac{x}{\epsilon_M} \right) \right]$$
$$+ \epsilon_M \pi \sin(\pi y)e^{(x-1)/\epsilon_M} \tag{14.48}$$

The solutions of this are plotted in Fig. 14.5. Note how the Munk layers bring the tangential as well as the normal velocity to zero. The eastern boundary layer has similar thickness to the western boundary layer, but is not as dynamically important since its *raison d'etre* is to enable the no-slip condition to be satisfied, a relatively weak frictional constraint that manifests itself by a boundary layer in which the flow parallel to the boundary is slowed down. On the other hand the western boundary layer exists in order that the no-normal flow condition can be satisfied, which causes a qualitative change in the flow pattern. It should be emphasized that neither the Stommel nor Munk models are quantitative descriptors of the real ocean, but taken together the similarities of their solutions are a powerful argument for the relative insensitivity of the qualitative form of the solution to the detailed form of the friction. The models do in fact produce qualitatively realistic patterns of large-scale flow in the major basins of the world, as illustrated in Fig. 14.6.
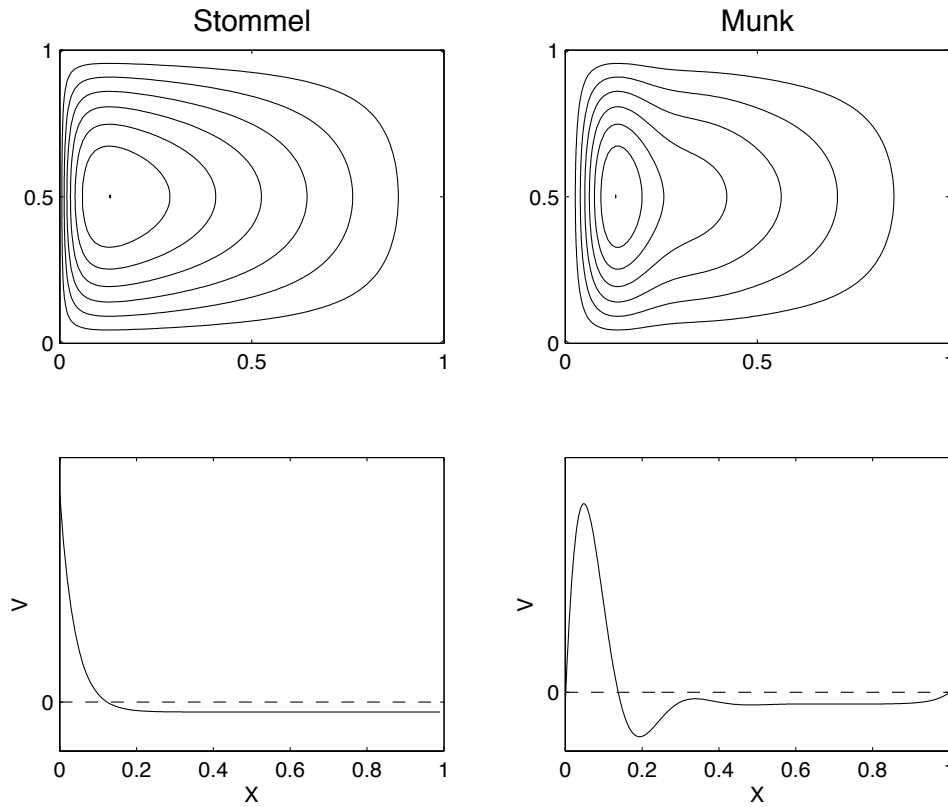
Fig. 14.5 The Stommel and Munk solutions, (14.48) with $\epsilon_S = \epsilon_M = 0.04$], with the windstress $\tau = -\cos \pi y$, for $x, y \in (0, 1)$. Upper panels are contours of streamfunction in the x-y plane, and the flow is clockwise. The lower panels are plots of meridional velocity as a function of x, in the center of the domain ($y = 0.5$). The Munk solution can satisfy both no-normal flow and one other boundary condition at each wall, here chosen to be no-slip.

14.3 ZONAL BOUNDARY LAYERS

The canonical wind stress $[\tau^x = -\tau_0 \cos(\pi y/a)]$ is special because the its curl vanishes at $y = 0, a$, and so the interior solution satisfies $\psi_I = 0$ at $y = 0, 1$. We cannot expect the real wind to be so forthcoming. Consider the linear wind profile,

$$\tau^x = \frac{\tau_0}{a} \left(y - \frac{a}{2} \right). \tag{14.49}$$

Then, scaling the variables in the usual way leads to the problem

$$\epsilon_S \nabla^2 \psi + \frac{\partial \psi}{\partial x} = -1 \tag{14.50}$$

We now suppose the solution is the sum of five parts,

$$\psi = \phi_I + \phi_w + \phi_e + \phi_n + \phi_s \tag{14.51}$$
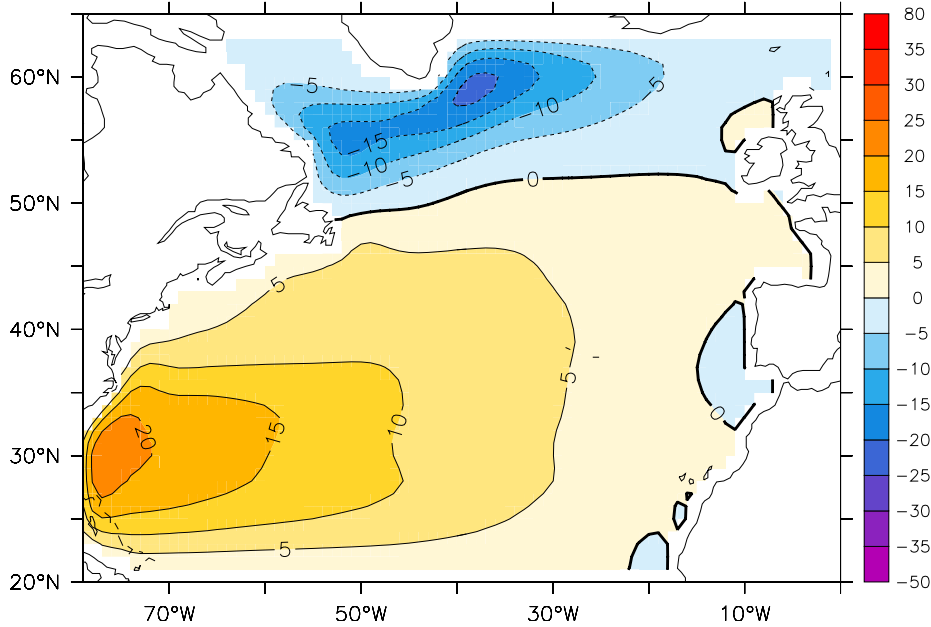
Fig. 14.6 The solution to the Stommel-Munk problem numerically calculated for the North Atlantic, using the observed wind field. The model ocean has realistic geometry, but is flat-bottomed. The calculation reproduces well the large-scale patterns, including the subtropical and subpolar gyre and the western intesification of both. However, the separation of the Gulf Stream from the coast is a little too far North, and that is likely due to the absence of baroclinic effects, topography, and mesoscale eddies. Compare with Fig. 14.2.[9]

where the notation is self-explanatory. The interior solution is simply the solution of $\partial \psi_I / \partial x = -1$ so that a solution satisfying $\psi_I = 0$ at $x = 1$ is $\psi_I = (1 - x)$ and, as before, there is no need for an eastern boundary layer. The western boundary layer solution is straightforwardly found to be

$$\phi_w = -\mathrm{e}^{-\alpha} = -\mathrm{e}^{-x/\epsilon_S}. \tag{14.52}$$

The interior solution alone does not satisfy $\psi = 0$ at either $y = 0$ or $y = 1$ (the interior flow is $v_I = -1$ everywhere) and we must again find these through a boundary layer analysis. Consider the solution at $y = 1$, and introduce the stretched coordinate

$$\epsilon_n \alpha = y - 1. \tag{14.53}$$

Substituting this into (14.22) we find

$$\epsilon_S \left(\nabla^2 \psi_I + \frac{\partial^2 \phi_n}{\partial x^2} + \frac{1}{\epsilon_n^2} \frac{\partial^2 \phi_n}{\partial \alpha^2} \right) + \frac{\partial \psi_I}{\partial x} + \frac{\partial \phi_n}{\partial x} = -1 \tag{14.54}$$

We may neglect the small contributions from the other boundary layer streamfunctions
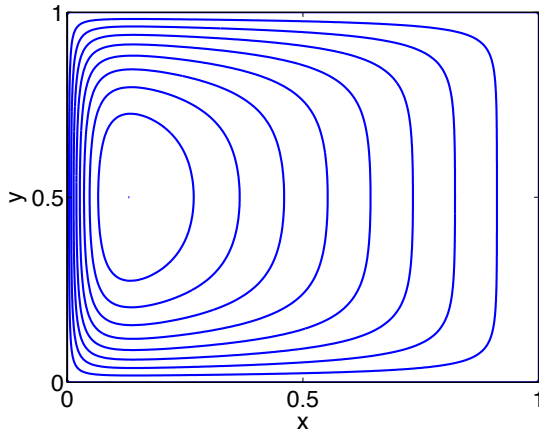
Figure 14.7 Solutions to the Stommel problem with a wind-stress that increases linearly from $y = 0$ to $y = 1$, as in (14.49). The interior solution is $\psi_I = (1 - x)$, or $v_I = -1$, necessitating zonal boundary layers at $y = 0$ and $y = 1$, as well as the western boundary current at $x = 0$.

(such as ϕ_s). To obtain a nontrivial balance we choose $\epsilon_n^2 = O(\epsilon_S)$ and obtain the dominant balance

$$\frac{\partial^2 \phi_n}{\partial \alpha^2} + \frac{\partial \phi_n}{\partial x} = 0 \tag{14.55}$$

(noting that the interior solution already satisfies $\partial \psi_I / \partial x = -1$). The boundary conditions necessary to complete the solution are:

(i) The total streamfunction (interior plus boundary correction) must vanish at the northern boundary. That is, $\phi_n(x, \alpha = 0) = -\psi_I(x, y = 1) = -(1 - x)$.

(ii) The boundary solution should match to the interior streamfunction far from the boundary. That is $\phi_n(x, \alpha \to \infty) = 0$.

(iii) At the eastern boundary ϕ_n should also vanish, else it would provide a velocity into the eastern wall. Thus, $\phi_n(1, \alpha) = 0$.

The solution at the southern boundary is obtained in an analogous way (the details are complicated, however), and the complete solution is illustrated in Fig. 14.7. The nondimensional thickness, L_n, of the northern (and southern) boundary layers is $L_n \sim \epsilon_S^{1/2} a$, which, because it scales like the half power of a small number, is much thicker than the western boundary current. This thickness arises from the dimensional equations that dominate at the boundary, namely

$$r \frac{\partial^2 \psi}{\partial y^2} + \beta \frac{\partial \psi}{\partial x} = 0. \tag{14.56}$$

This follows from (14.18) by noting that the Laplacian operator must be dominated by the derivatives in the y−direction, and the β term has an (interior) component that anihilates the wind-stress-curl, plus a boundary layer correction to balance the Laplacian. Inspection of (14.56) yields a dimensional thickness $L_n \sim \sqrt{ra/\beta}$, where a is the length-scale in the x-direction.

14.4 THE NONLINEAR PROBLEM

In the nonlinear problem we seek solutions to

$$\frac{\partial \zeta}{\partial t} + J(\psi, \zeta) + \beta \frac{\partial \psi}{\partial x} = -r\nabla^2 \psi + \text{curl}_z \boldsymbol{\tau} + \nu \nabla^2 \zeta, \qquad (14.57)$$

which we have written in dimensional form. In the Stommel problem we set $\nu = 0$ and in the Munk problem we set $r = 0$. In general solutions will be time-dependent and turbulent and this will create motion on small scales, so that ν cannot be neglected. The 'steady nonlinear Stommel-Munk problem' is

$$J(\psi, \zeta) + \beta \frac{\partial \psi}{\partial x} = -r\nabla^2 \psi + \text{curl}_z \boldsymbol{\tau} + \nu \nabla^2 \zeta. \qquad (14.58)$$

We can scale this by first supposing that the leading order balance is Sverdrupian (i.e., $\beta \partial \psi / \partial x \sim \text{curl}_z \boldsymbol{\tau}$), from which we obtain the scales $\Psi = |\tau|/\beta$ and $U = |\tau|/(\beta L)$. Equation (14.58) may then be nondimensionalized to yield

$$R_\beta J(\widehat{\psi}, \widehat{\zeta}) + \frac{\partial \widehat{\psi}}{\partial \widehat{x}} = -\epsilon_S \nabla^2 \widehat{\psi} + \text{curl}_z \widehat{\boldsymbol{\tau}} + \epsilon_M \nabla^2 \widehat{\zeta} \qquad (14.59)$$

where $R_\beta = U/\beta L^2 = |\tau|/(\beta^2 L^3)$, the β-Rossby number for this problem, is a measure of the nonlinearity. Evidently, the nonlinear term increases in importance with increasing wind-stress and for a smaller domain.

If the nonlinearity were a priori expected to be of leading order importance, we might assume the nonlinear balance

$$J(\psi, \zeta) \sim \text{curl}_z \boldsymbol{\tau} \qquad (14.60)$$

which suggests the scaling $U = (|\tau|L)^{1/2}$. The nondimensional version of (14.58) would then be

$$J(\widehat{\psi}, \widehat{\zeta}) + \gamma \frac{\partial \widehat{\psi}}{\partial \widehat{x}} = \epsilon_S' \nabla^2 \widehat{\psi} + \text{curl}_z \widehat{\boldsymbol{\tau}} + \epsilon_M' \nabla^2 \widehat{\zeta} \qquad (14.61)$$

where $\gamma = \beta L^2 / U = \beta / (|\tau|L^5)^{1/2}$ and $\epsilon_S' = r(L/|\tau|)^{1/2}$. This implies that the friction becomes less important as the wind-stress increases but, because it is a high-order term, it will remain important near the boundaries and the details of the solution may still depend on its particular form.

14.4.1 A perturbative approach

A direct attack on the full nonlinear problem (14.58) is is possible only through numerical methods, so first we shall explore the problem perturbatively, assuming the nonlinear term to be small; the analysis is straightforward. We begin with the Stommel problem, (14.59) with $\epsilon_M = 0$, and expand the streamfunction in terms of R_β,

$$\psi = \psi_0 + R_\beta \psi_1 + \cdots . \qquad (14.62)$$

Now substitute this into (14.59) and equate powers of R_β. The lowest order problem is simply

$$\epsilon_S \nabla^2 \psi_0 + \frac{\partial \psi_0}{\partial x} = \text{curl}_z \boldsymbol{\tau} \qquad (14.63)$$

which is the Stommel problem we have already solved. At next order,

$$\epsilon_S \nabla^2 \psi_1 + \frac{\partial \psi_1}{\partial x} = J(\psi_0, \zeta_0) \qquad (14.64)$$

This equation has precisely the same form as the Stommel problem, with the known nonlinear term on the right playing the part of the wind-stress. The algebra to obtain the solution is rather tedious, because the right-hand side varies with both x and y, but this is much ameleriated by the use of computer algebraic manipulation languages. For the canonical wind stress $\tau^x = -\tau_0 \cos(\pi y/a)$ the corrected solution, in the boundary layer approximation and ignoring any corrections at the zonal boundaries, is found to be:[10]

$$\psi \approx \sin(\pi y)(1 - x - e^{-x/\epsilon_S}) - \frac{R_\beta \pi^3}{2\epsilon_S^3} \sin(2\pi y) x e^{-x/\epsilon_S}. \qquad (14.65)$$

The solution is illustrated in Fig. 14.8. The perturbation is antisymmetric about $y = 1/2$, being positive for $y > 1/2$ and negative for $y < 1/2$. This tends to move the center of the gyre polewards, narrowing and intensifying the flow in the polewards half of the western boundary current, whereas the western boundary current equatorwards of $y = 1/2$ is broadened and weakened. The net effect is that the center of the gyre is pushed polewards. This occurs because the western boundary current is advecting the vorticity of the gyre polewards. In the perturbation solution the advection is both by and of the linear Stommel solution; thus, negative vorticity is advected polewards, intensifying the gyre in its polewards half, weakening it in its equatorward half. The solution illustrated in Fig. 14.8 has $\epsilon = 0.04$ and $R_\beta = 0.0001$; for larger values of R_β the perturbation itself starts to dominate.

The problem with this perturbative approach is that boundary layer solution to the Stommel problem does not calculate derivatives accurately, so that the nonlinear term $J(\psi, \nabla^2 \psi)$ is poorly approximated in the western boundary layer; however, in the interior where the errors are small the perturbative correction is negligible. A more accurate perturbative approach begins with the *exact* solution to the Stommel problem, and proceeds in the same way. However, the analytic effort is considerable, and the intuitive sense of the way nonlinearities affect the solution is not apparent. (See problem 14.6.)

14.4.2 A numerical approach

Fully nonlinear solutions show qualitatively similar effects to those seen in the perturbative solutions, as we see in Fig. 14.9, where the solution to (14.59) for the Stommel and Munk problems are obtained numerically by a Newton's method.[11] Just as with the perturbative procedure, for both the Stommel and Munk problems small values of nonlinearity lead to the poleward advection of the gyre's anticyclonic vorticity in the western boundary current, strengthening and intensifying the boundary current in the
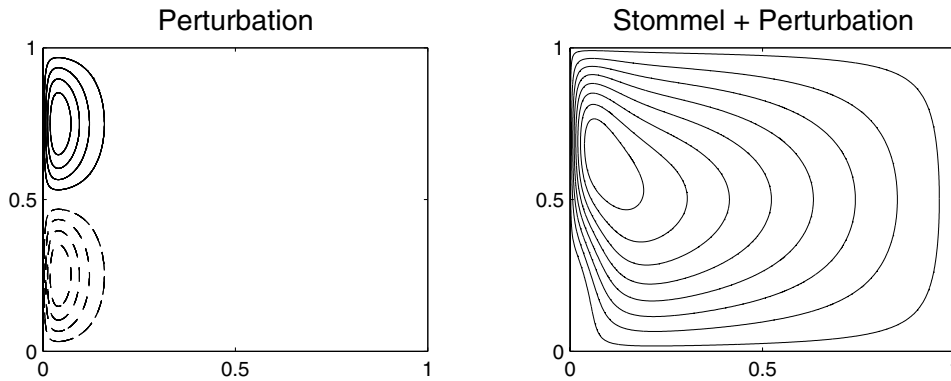
Fig. 14.8 The nonlinear perturbation solution of the Stommel problem, calculated according to (14.65). On the left is the perturbation, $-R_\beta \pi^3/(2\epsilon_S^2)\sin(2\pi y)xe^{-x/\epsilon_S}$, and on the right is the reconstituted solution, using $R_\beta = 10^{-4}$ and $\epsilon = 0.04$. Dashed contours are negative.

northwest corner. A higher level of nonlinearity results in a strong recirculating regime in the upper westward quadrant, and ultimately much of the gyre's transport is confined to this regime. The western boundary current itself becomes less noticeable as nonlinearity increases, the more nonlinear solutions have a much greater degree of E-W symmetry than the linear ones, just as the fully nonlinear Fofonoff solutions (section 14.5.3).

Such qualitative effects do not depend on the precise formulation of the model, but the boundary conditions do play an important role in the detailed solution. For example, for a given value of R_β, nonlinearity has a stronger effect in the Munk problem with slip boundary conditions than with no-slip, because in the latter the velocity is reduced to zero at the boundary with a corresponding reduction in the advection term. However, these solutions themselves are unlikely to be relevant for larger values of nonlinearity, because then the flow becomes hydrodynamically unstable.

14.5 * THE INERTIAL WESTERN BOUNDARY CURRENT

In this section we ask: might purely inertial effects be sufficient to satisfy boundary conditions at the Western boundary? Can we envision a purely inertial gyre circulation? Now, the steady wind-driven, Rayleigh damped quasi-geostrophic equation is,

$$J(\psi, \nabla^2\psi) + \beta\frac{\partial\psi}{\partial x} = W_E - r\nabla^2\psi \qquad (14.66)$$

$$\frac{U^2}{L^2} \qquad \beta U \quad |W_E| \quad r\frac{U}{L} \qquad (14.67)$$

where W_E is the wind forcing and the second line indicates the magnitude of the various terms. Since the inertial (advective) terms are higher order than the linear terms, indeed they are higher order than the Rayleigh drag, it is natural to wonder if they themselves
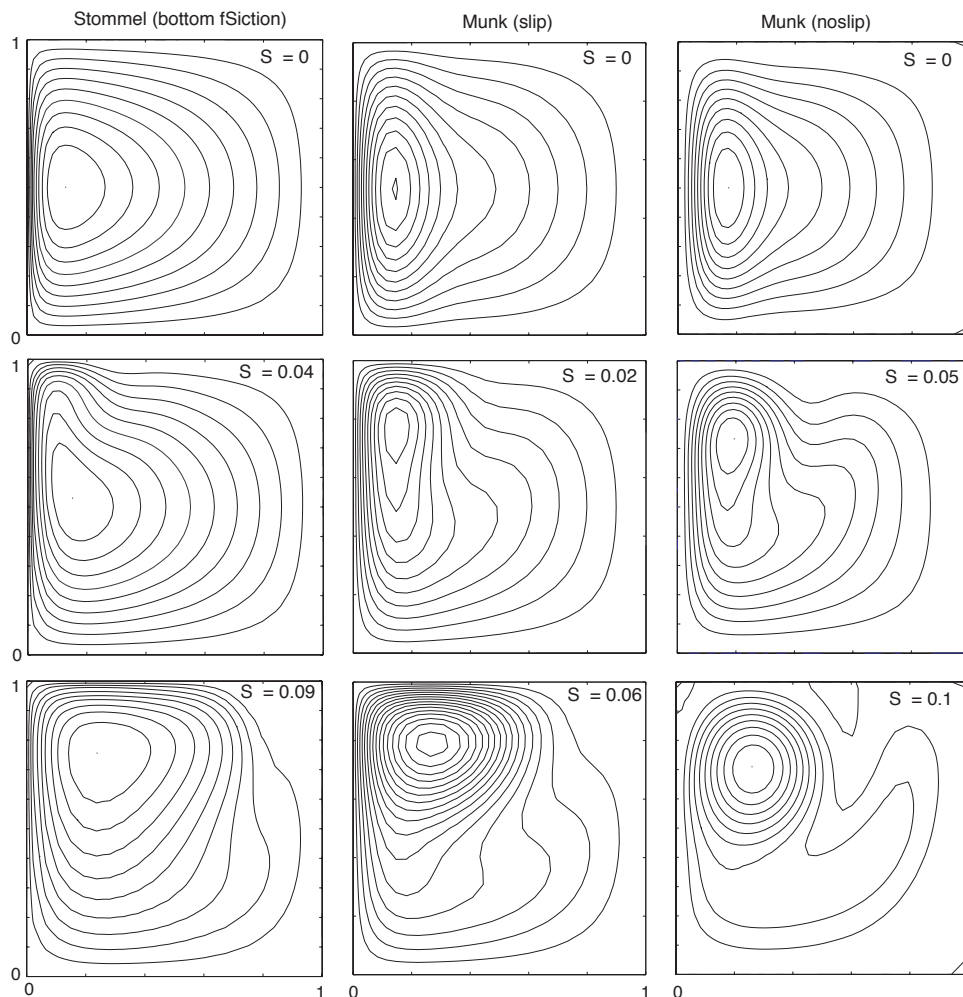
Fig. 14.9 Streamfunctions in solutions of the nonlinear Stommel and Munk problems, obtained numerically with a Newton's method, for various values of the nonlinearity parameter $S = R_\beta^{1/2}$. As in the perturbation solution, for small values of nonlinearity the center of the gyre moves polewards, strengthening the boundary current in the north-western quadrant (for a northern-hemisphere solution). As nonlinearity increases, the recirculation of the gyre dominates, and the solutions become increasingly inertial.

might serve to satisfy the no-normal flow condition on the western boundary, without recourse to rather ill-defined frictional terms. The answer is no, as we see below, but nevertheless nonlinear effects are likely to be important in the Western boundary layer even if they are small in the interior.

14.5.1 The need for friction

Consider the steady barotropic flow satisfying

$$\boldsymbol{u} \cdot \nabla q = \text{curl}_z \tau + F \tag{14.68}$$

where $q = \nabla^2 \psi + \beta y$ and F represents frictional effects. Noting that $\boldsymbol{u}$ is divergence-free and integrating the left-hand side of (14.68) over the area, A, between two closed streamlines (ψ_1 and ψ_2, say) and using the divergence theorem we find

$$\int_A \nabla \cdot (\boldsymbol{u} q) \, \mathrm{d}A = \oint_{\psi_1} \boldsymbol{u} q \cdot \boldsymbol{n} \, \mathrm{d}l - \oint_{\psi_2} \boldsymbol{u} q \cdot \boldsymbol{n} \, \mathrm{d}l = 0. \tag{14.69}$$

Here, $\boldsymbol{n}$ is the unit vector normal to the streamline so that $\boldsymbol{u} \cdot \boldsymbol{n} = 0$. The integral of the wind-stress curl over the same area will not in general be zero. Now, we can take these two streamlines as close together as we wish; thus, a balance in (14.68) can only be achieved if *every* closed contour passes through a region where frictional effects are non-zero. This does not mean that nonlinear terms may not locally dominate the friction, just that friction must be somewhere important. In the Stommel and Munk problems, it means that every streamline must pass through the frictional western boundary layer.

The ratio of the size of the nonlinear terms to the linear terms is given by the the beta Rossby number,

$$R_\beta = \frac{U}{\beta L^2}. \tag{14.70}$$

In the western boundary layer the length scales can be expected to be much smaller than the basin scale. Indeed, if the balance in the western boundary layer were between the nonlinear and beta term, perhaps being of the form

$$u \frac{\partial}{\partial x} \nabla^2 \psi \sim \beta \frac{\partial \psi}{\partial x} \tag{14.71}$$

then the *inertial boundary layer thickness*, δ_I, is given by

$$\delta_I = \left(\frac{U}{\beta} \right)^{1/2}, \tag{14.72}$$

which of course gives $R_\beta = 1$ if $L = \delta_I$. The more energetic the flow, the wider the region where nonlinearity is important, and the corresponding scale is sometimes called the Charney thickness.[12]

The linearized Stommel equation has a boundary layer of thickness $\delta_S \sim (r/\beta)$, obtained by equating $\beta \partial \psi / \partial x$ and $r \nabla^2 \psi$. This thickness is equal to the inertial boundary layer thickness when $U = (r^2/\beta)$. If $\delta_I > \delta_S$, i.e., if $U > (r^2/\beta)$ then nonlinearity *must* be important in the western boundary layer, because the nonlinear terms are at least as important as the beta term in (14.66). On the other hand, if the Stommel boundary layer is wider than the inertial boundary layer, there is no obvious need for nonlinearity to be important, since the Stommel boundary layer generates no length scales smaller than δ_I and R_β remains small.

14.5.2 A perturbative approach

Although friction must be important, it is instructive to try to find an inertial solution using the familiar boundary layer methods we used for the Stommel and Munk problems. The relevant dimensional equation of motion is

$$J(\psi, \zeta) + \beta \frac{\partial \psi}{\partial x} = W_E \tag{14.73}$$

and we may seek a solution as the sum of two parts $\psi = \psi_I + \phi$ where ψ_I is Sverdrup interior solution that satisfies

$$\beta \frac{\partial \psi_I}{\partial x} = W_E. \tag{14.74}$$

In the boundary layer it is now convenient to consider the equation for the full streamfunction, ψ rather than the perturbation ϕ, and this is

$$J(\psi, \nabla^2 \psi + \beta y) = 0. \tag{14.75}$$

and this must tend to ψ_I for $x \gg \delta_I$. Equation (14.75) has the general solution

$$\nabla^2 \psi + \beta y = G(\psi) \tag{14.76}$$

where G is an arbitrary function of its argument. We determine a special form of G, by considering flow entering the boundary layer with a local velocity $-U$ (i.e., westward). That is, $\psi_I = Uy$. The potential vorticity in the interior region is $Q_I = \beta y$. Thus, the relation between potential vorticity and streamfunction is,

$$Q_I = \frac{\beta \psi_I}{U} \tag{14.77}$$

and thus, in this particular case

$$G(\psi) = \frac{\beta \psi}{U}. \tag{14.78}$$

Because we are assuming the flow is inviscid, the fluid will preserve this relationship between potential vorticity and streamfunction even as it moves through the western boundary layer. Thus, using (14.76) and (14.78), the flow in the interior *and* in the boundary layer are given by solutions of

$$\nabla^2 \psi + \beta y = \frac{\beta \psi}{U}. \tag{14.79}$$

The appropriate boundary conditions are determined by matching the flow in the boundary layer to that in the interior, and the no-normal-flow condition at the western edge. Since $\psi_I = Uy$ the boundary layer flow is determined by solutions of

$$\nabla^2 \phi - \frac{\beta \phi}{U} = 0. \tag{14.80}$$

In the western boundary layer, length-scales in the x-direction are much smaller than length-scales in the y-direction, and so (14.80) becomes approximately

$$\frac{\partial^2 \phi}{\partial x^2} - \frac{\beta \phi}{U} = 0 \tag{14.81}$$

Solutions of this are $\phi = -\psi_I e^{-x/\delta_I}$, where $\delta_I = (U/\beta)^{1/2}$, and thus the full solution (interior plus boundary layer) is

$$\psi = \psi_I (1 - e^{-x/\delta_I}) \tag{14.82}$$

it is easily checked that this satisfies the no-flow condition at the western boundary, and smoothly transitions into the interior solution for large x.

What about solutions exiting the boundary layer? We attempt a similar procedure, but now the interior boundary condition that we must match is that of westward flow, namely

$$\psi_I = -Uy. \tag{14.83}$$

Thus, we seek solutions to the problem,

$$\nabla^2 \psi + \beta y = -\frac{\beta \psi}{U} \tag{14.84}$$

[c.f. (14.79)], for which the homogeneous (boundary layer) equation is

$$\frac{\partial^2 \phi}{\partial x^2} + \frac{\beta \phi}{U} = 0 \tag{14.85}$$

Solutions of (14.85) are also of the form

$$\psi = \psi_I (1 - e^{-x/\delta_I}) \tag{14.86}$$

except that now $\delta_I = i(U/\beta)^{1/2}$. The solution is wavelike, and does not transition smoothly to the interior flow.[13] Physically, we can see that we appear to be attempting the impossible, in that flow in the westward flowing region of the interior flow has a different potential vorticity–streamfunction ($q - \psi$) relationship than does the eastward flowing interior. If these are to be connected by a boundary layer flow, that flow must be viscous or unsteady since the value of potential vorticity on mean streamlines must change. The western boundary layers of a flat-bottomed ocean are irreducibly frictional.

14.5.3 A fully inertial approach: the Fofonoff model

Rather than attempt to match an inertial boundary layer with an interior Sverdrup flow, we may look for a purely inertial solution that holds basinwide, and such a construction is known as the 'Fofonoff model'.[14] That is, we seek global solutions to the inviscid, unforced problem,

$$J(\psi, \nabla^2 \psi + \beta y) = 0 \tag{14.87}$$

We should not regard this problem as representing even a very idealised wind-driven ocean; rather, we may hope to learn about the properties of purely inertial solutions that might, in turn, tell us something about the ocean circulation.

The general solution to (14.87) is

$$\nabla^2 \psi + \beta y = Q(\psi) \tag{14.88}$$

where $Q(\psi)$ is an arbitrary function of its argument. For simplicity we choose the linear form,

$$Q(\psi) = A\psi + B, \tag{14.89}$$

where $A = \beta/U$ and $B = \beta y_0$, where U and y_0 are arbitrary constants. Thus, (14.88) becomes

$$\left(\nabla^2 - \frac{\beta}{U}\right)\psi = \beta(y_0 - y). \tag{14.90}$$

We will further choose $\beta/U > 0$, which we anticipate will provide a westward flowing interior flow, but which (from our experience in the previous section) is more likely to provide a meaningful solution than an eastward interior, and we will use boundary-layer methods to find a solution. A natural scaling for ψ is UL, where L is the domain size, and with this the nondimensional problem is

$$(\epsilon\nabla^2 - 1)\widehat{\psi} = \widehat{y}_0 - \widehat{y} \tag{14.91}$$

where $\epsilon = U/(\beta L^2)$ and we presume this to be small. The interior solution is just

$$\widehat{\psi}_I = \widehat{y} - \widehat{y}_0 \tag{14.92}$$

or, in dimensional form,

$$\psi_I = U(y - y_0). \tag{14.93}$$

A boundary layer is required on each wall. Thus we write

$$\widehat{\psi} = \widehat{\psi}_I + \phi \tag{14.94}$$

where ϕ, the boundary layer correction, satisfies

$$\epsilon\frac{\partial^2\phi}{\partial x^2} - \phi = 0. \tag{14.95}$$

Just as in the Stommel and Munk problems, we stretch the coordinate in the region of failure, although a priori we do not know how much to stretch it. Thus, at the western boundary ($x = 0$) we write $\alpha = (x/\epsilon)^\gamma$ and obtain

$$\epsilon\left(\frac{\partial^2\phi}{\partial x^2} + \left(\frac{1}{\epsilon}\right)^n \frac{\partial^2\phi}{\partial\alpha^2}\right) - \phi = 0 \tag{14.96}$$

By choosing $\gamma = 1/2$ we obtain a nontrivial balance, and obtain the boundary layer correction

$$\phi = B(y)e^{-\alpha} = B(y)e^{-x/\delta_f} \tag{14.97}$$

where $\delta_f = \sqrt{U/\beta}$ and $B(y)$ is chosen to satisfy $\psi = 0$ at $x = 0$. Note that if $U < 0$ the boundary layer solution is oscillatory, and does not decay in the interior. We follow a similar procedure at each boundary to obtain the full solution, and in dimensional form this is

$$\psi = U(y - y_0)\left(1 - e^{-x/\delta_f} - e^{-(x-x_e)/\delta_f}\right)$$
$$- U(y_n - y_o)e^{-(y_n-y)/\delta_f} + Uy_0 e^{-y/\delta_f}. \tag{14.98}$$

Figure 14.10 The Fofonoff solution. Plotted are contours (streamlines) of (14.98) in the plane $0 < x < x_e$, $0 < y < y_n$ with $U = 1$, $y_n = 1$, $x_e = y_n = 1$, $y_0 = 0.5$ and $\delta_f = 0.05$. The interior flow is westward everywhere, and $\psi = 0$ at $y = y_0$. In addition, boundary layers of thickness $\delta_f = \sqrt{U/\beta}$ bring the solution to zero at $x = (0, x_e)$ and $y = (0, y_n)$, excepting small regions at the corners.
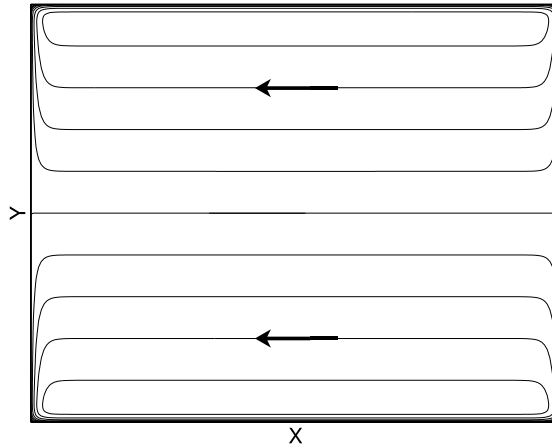
By construction this satisfies $\psi = 0$ at $x = (0, x_e)$ and at $y = (0, y_n)$.

A typical solution is illustrated in Fig. 14.10. On approaching the western boundary layer, the interior flow bifurcates at $y = y_0$. The western boundary layer, of width δ_f, accelerates away from this point, being constantly fed by the interior flow. The westward return flow occurs in zonal boundary layers at the northern and southern edges, also of width δ_f. Flow along the eastern boundary layers is constantly being decelerated, because it is feeding the interior. If one of the zonal boundaries corresponds to y_0 (e.g., if $y_n = y_0$) there would be no boundary layer along it, since ψ is already zero at $y = y_0$. Rather, there would be westward flow along it, just as in the interior. Indeed, a slippery wall placed at $y = 0.5$ would have no effect on the solution illustrated in Fig. 14.10

14.5.4 Connection between boundary layer and interior

We have seen that solutions with a boundary layer character that transition smoothly to a flow interior exist only for westward interior flow ($u_I = -U < 0$). If the interior flow were eastward, wavelike solutions would be required, just as are needed to satisfy flow emerging from a western boundary current in section 14.5. That is to say, *inertial western boundary layers on a beta-plane cannot smoothly release fluid into the interior and still conserve potential vorticity,* and the underlying reason is illustrated in Fig. 14.11.

Conservation of potential vorticity demands that $v_x - u_y + \beta y$ is a constant on streamlines. Now, in the interior relative vorticity is zero, and in the meridional boundary layers it is effectively v_x. Consider first the case with westward flow in the interior (upper panel of Fig. 14.11). Fluid from the irrotational interior approaches the western boundary and if it is polewards of the bifurcation latitude y_0 it will be deflected polewards, generating negative relative vorticity. Potential vorticity is conserved because this can be exactly balanced by the reduced value of f. Similarly, flow deflected southwards generates positive relative vorticity, which is compensated for by the reduced value of f. In the eastern boundary layer, southwards (northwards) moving flow has
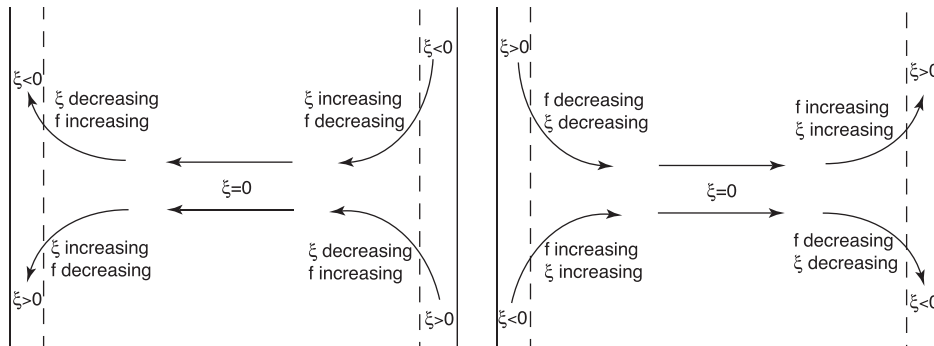
Fig. 14.11 Putative inertial boundary layers connected to a westward flowing internal flow (left panel) or eastward flowing internal flow (right panel), in the Northern Hemisphere. Westward flow into the western boundary layer, or flow emerging from an eastern boundary layer, is able to conserve its potential vorticity through a balance between changes in relative vorticity and Coriolis parameter. But flow cannot emerge smoothly from a western boundary layer into an eastward flowing interior and still conserve its potential vorticity. The right panel thus has inconsistent dynamics.

negative (positive) relative vorticity. As it emerges into the interior its relative vorticity increases (decreases), this being balanced by a fall (rise) in the value of f. Thus, we see that the Fofonoff solution with a westward flowing interior can indeed conserve potential vorticity.

On the other hand suppose the interior flow were eastward (right panel of Fig. 14.11). Flow moving polewards in the western boundary layer has negative relative vorticity. It cannot be freely released into an irrotational ($\zeta = 0$) interior because f and ζ would then both need to increase, violating potential vorticity conservation. Flow moving southwards with positive relative vorticity similarly is trapped within the western boundary current, unless it meets a zonal boundary which allows a eastward moving boundary current with positive relative vorticity. Similar arguments show that an eastern boundary current cannot entrain fluid from an eastward flowing, irrotational interior.

Finally, one might ask, why we cannot simply reverse the trajectory of all the fluid parcels in an inviscid flow and thereby obtain a solution with an eastward-flowing interior? The answer is that such a flow will only be a solution if we also reverse the direction of the earth's rotation, and so reverse the sign of β. With negative β, an eastward flowing interior is indeed the solution to the Fofonoff problem.

14.6 TOPOGRAPHIC EFFECTS ON WESTERN BOUNDARY CURRENTS

The above sections have emphasized the role of friction in satisfying the boundary conditions in the west. However, we should not think of friction as being the *cause* of the western boundary layer and in this section we shall show that if there are sloping sidewalls the role of friction is significantly different, and the western bouundary current may even be largely invisicid![15] The key point is that the flow may be inviscid if it is

able to follow potential vorticity contours. Now, in a flat-bottomed western boundary layer the flow is moving to larger values of f (and not as a direct response to the wind forcing) and so the flow *must* be frictional. However, if the sidewalls are sloping, then the flow may preserve its value of potential vorticity (essentially its value of f/h) if it moves offshore as it moves polewards. We will focus on homogeneous fluids, noting that the interaction of topography and stratification is a subtle and rather complex problem.

14.6.1 Homogeneous model

The potential vorticity evolution equation for a homogeneous model with topography and a rigid lid [c.f., (14.7)] may be written as:

$$\frac{\mathrm{D}q}{\mathrm{D}t} = \frac{F}{h}. \tag{14.99}$$

where $h = h(x, y)$ is the depth of the fluid and F represents all forcing and frictional terms. Because h is given, the relative vorticity may be obtained from this by $\zeta = qh - f$. The advecting velocity is determined by noting that the mass conservation equation is just $\nabla \cdot [\boldsymbol{u} h(x, y)] = 0$, which allows us define the mass-transport streamfunction ψ such that

$$u = -\frac{1}{h}\frac{\partial \psi}{\partial y}, \qquad v = \frac{1}{h}\frac{\partial \psi}{\partial x}. \tag{14.100}$$

The streamfunction is obtained from the vorticity by solving the elliptic equation,

$$\nabla \cdot \left(\frac{1}{h}\nabla\psi\right) = \zeta = qh - f. \tag{14.101}$$

The system — equations (14.99), (14.101) and (14.100) — is then closed. Note that, unlike in quasi-geostrophy, neither the Rossby number nor the topography need be small for the validity of the model. Including finite size topography but not stratification is not especially realistic vis a vis the real ocean, but nevertheless this model is physically realizable and a useful tool.

The 'topographic Stommel problem' is obtained by neglecting relative vorticity in (14.99), which on expanding the advective term and omitting time dependence gives

$$J\left(\psi, \frac{f}{h}\right) = -\nabla \cdot \left(\frac{r}{h}\nabla\psi\right) + \mathrm{curl}_z(\boldsymbol{\tau}/h), \tag{14.102}$$

where the boundary conditions are $\psi = 0$ at the domain edges.

14.6.2 Advective dynamics

An illuminating way to begin to study the problem is to write (14.102) in the form:[16]

$$J(\Psi, \psi) = +\nabla \cdot \left(\frac{r}{h}\nabla\psi\right) - \mathrm{curl}_z(\boldsymbol{\tau}/h) \tag{14.103}$$
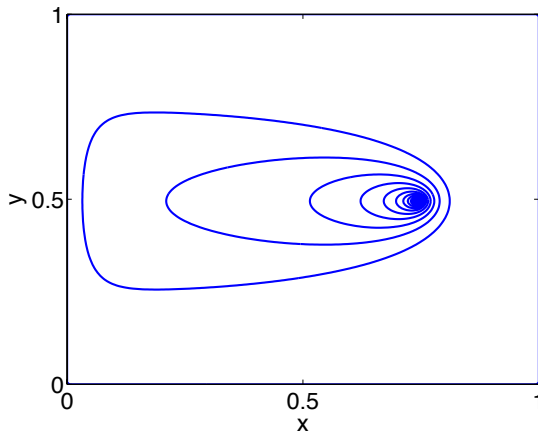
Figure 14.12 The β-plume, namely the Green's function for the Stommel problem. Specifically we plot the solution of (14.104) with $\psi = 0$ at the walls, and a delta-function source at $x = 0.75$, $y = 0.5$. The streamfunction trails westward from the source, as if it were a tracer being diffused while being advected westward along lines of constant f.

where $\Psi \equiv f/h$. Thus, noting that $J(\Psi, \psi) = \boldsymbol{U} \cdot \nabla\psi$ where $\boldsymbol{U} = \mathbf{k} \times \nabla(f/h)$, we regard ψ as being advected by the pseudo-velocity $\boldsymbol{U}$. This advection is along f/h contours and is quasi-westward, meaning that high values of potential vorticity lie to the right. Eq. (14.103) is then an advection-diffusion equation for the tracer ψ, with the advection occuring along f/h contours. The 'source' of ψ is the wind-stress curl, and ψ is diffused by the first term on the right-hand side of (14.103). This same interpretation applies to the original Stommel problem, of course, where the pseudo-velocity, $-\beta\mathbf{i}$, is purely westward, and it is useful to revisit this problem.

Consider, then, a flat-bottomed ocean, where the wind is only a point source at $\boldsymbol{x}_0$. Eq. (14.103) becomes

$$r\nabla^2\psi + \beta\frac{\partial\psi}{\partial x} = \delta(\boldsymbol{x} - \boldsymbol{x}_0). \tag{14.104}$$

This can be transformed to a Helmholtz equation by writing $\phi = \psi\exp(\beta x/2r)$, giving $\nabla^2\phi - [\beta/(2r)]^2\phi = \delta(\boldsymbol{x} - \boldsymbol{x}_0)$. This may then be solved exactly, and the solution (for ψ) is illustrated in Fig. 14.12 — this is the Greens function for the Stommel problem. The tracer ψ is 'advected' westwards along f/h contours — lines of latitude in this case — spreading diffusively as it goes; the resulting structure is a simple example of a 'β-plume'. The western boundary layer results as a consequence of the f/h contours colliding with the western boundary, along with the need to satisfy the boundary condition $\psi = 0$. If there is no diffusion at all, ψ just propagates westwards from the source, and if the source is spatially distributed, for example as $\sin \pi y$, we obtain the Sverdrup interior flow.

Now consider the case with a sloping sidewall on the western boundary. The f/h contours (the dashed lines in Fig. 14.13b) tend to converge at the southwest corner of the domain, and only where f/h contours intersect the boundary is a diffusive boundary layer required. The solution to (14.104) with $r = 0$ with a conventional 'two-gyre' wind-stress are also illustrated in that figure; this is the Sverdrup flow for this problem and it evidently satisfies $\psi = 0$ on the western boundary. In terms of the interpretation above, wind-stress provides a source for the streamfunction ψ and the latter is advected *pseudo-westward* — i.e., along potential vorticity contours, with higher values to the

Figure 14.13 The two-gyre Sverdrup flow (solid contours) for (a) a flat-bottomed domain and (b) a domain with sloping sidewalls. The f/h contours are dashed.[17]
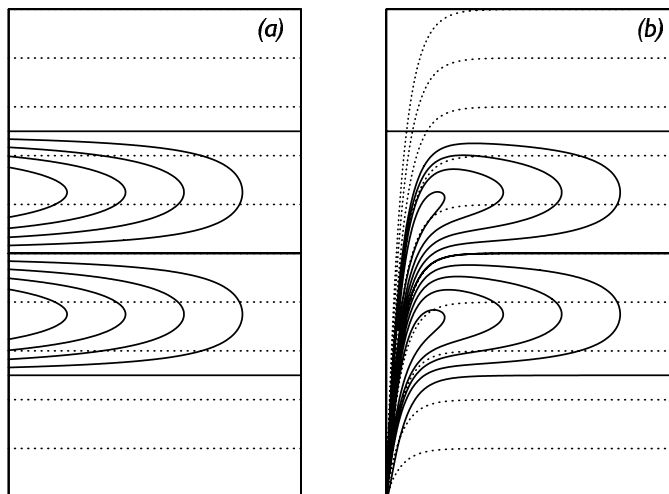
right. The source in this case is distributed over the entire domain, but the contours all converge in the southwest corner. The (numerically obtained) solution to the associated Stommel problem is illustrated in Fig. 14.14, and the western boundary current in this case is no longer a frictional boundary layer. Friction is necessarily important where the flow crosses f/h contours; linear theory suggests that this will occur at the southwest corner. It also occurs on the western boundary where the f/h contours are densely packed and the vorticity in the topographic Sverdrup flow is large, and the friction enables the flow to move across the f/h contours. (In the flat bottomed case the f/h contours are zonal and friction allows the flow to move meridionally.)

14.6.3 Bottom pressure torques and form drag

In the homogeneous problem f and h appear only in the combination f/h, and we may solve the problem entirely without considering pressure effects. It is nevertheless informative to think about how the pressure interacts with the topography to produce meridional flow. The geostrophic momentum equation is

$$\boldsymbol{f} \times \boldsymbol{u} = -\nabla\phi + \boldsymbol{F} \qquad (14.105)$$

where $\boldsymbol{F}$ represents both wind forcing and frictional terms. Integrating this over the depth of the ocean (with $z = 0$ at the top), and using Leibnitz's rule ($\nabla \int_{\eta_b}^{0} \phi \, dz = \int_{\eta_b}^{0} \nabla\phi \, dz - \phi_b \nabla\eta_b$) to evaluate the pressure term, gives

$$\boldsymbol{f} \times \overline{\boldsymbol{u}} = -\nabla\overline{\phi} - \phi_b \nabla\eta_b + \overline{\boldsymbol{F}}. \qquad (14.106)$$

Here, the overbar denotes a vertical integral (e.g., $\overline{\boldsymbol{u}} = \int_{\eta_b}^{0} \boldsymbol{u} \, dz$), ϕ_b is the pressure at $z = \eta_b$ and η_b is the z-coordinate of the bottom topography. We take the top of the ocean at $z = 0$, and note that $\nabla\eta_b = -\nabla h$ where h is the fluid thickness. Taking the curl of (14.106) gives

$$\beta\overline{v} = -J(\phi_b, \eta_b) + \text{curl}_z \overline{\boldsymbol{F}} \qquad (14.107)$$
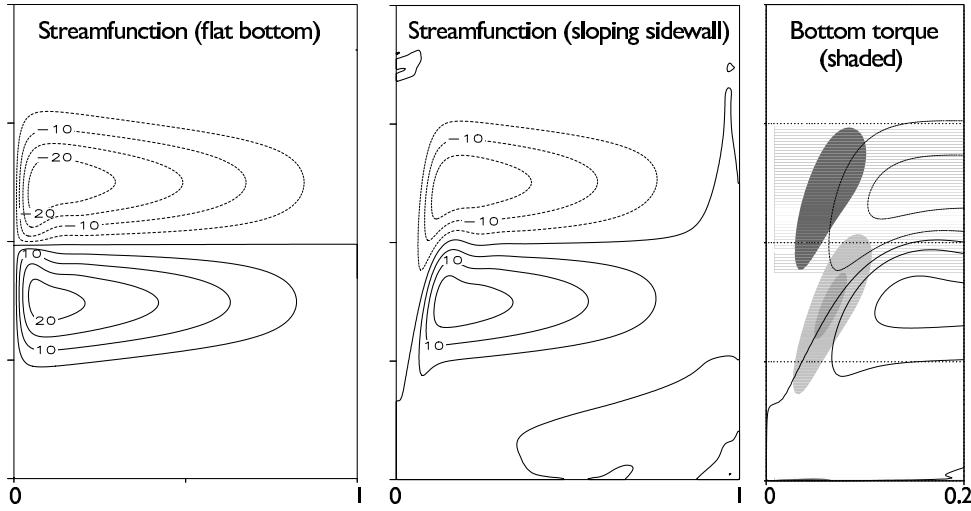
Fig. 14.14 The numerically obtained steady solution to the homogenous problem with a two-gyre forcing and friction, for a flat-bottomed doman and a domain with sloping western sidewall. The shaded regions in the right panel show the regions where bottom pressure torque is important, in the meridional flow of the western boundary currents.[18]

This equation holds for both a stratified and homogeneous fluid. The first term on the right-hand side is the *bottom pressure torque, B*, discussed more below.

Equation (14.107) is similar to (14.102), in that both arise from (14.106). To derive a equation with the same form as (14.102) but valid for a stratified fluid, we write the vertical integral of the pressure as

$$\int_{-h}^{0} \phi \, \mathrm{d}z = \int_{-h}^{0} [\mathrm{d}(\phi z) - z(\partial \phi / \partial z) \, \mathrm{d}z] = \int_{-h}^{0} [\mathrm{d}(\phi z) - zb \, \mathrm{d}z] = h\phi_b + \Gamma, \quad (14.108)$$

using hydrostatic balance, and where $\Gamma \equiv -\int_{-h}^{0} zb \, \mathrm{d}z$. Using (14.108) in (14.106) we obtain:

$$\boldsymbol{f} \times \overline{\boldsymbol{u}} = -h\nabla\phi_b + \nabla\Gamma + \overline{\boldsymbol{F}}. \quad (14.109)$$

The curl of this equation just gives back (14.107), but if we divide by h before taking the curl we obtain

$$J(\psi, f/h) + J(h^{-1}, \Gamma) = \mathrm{curl}_z(\boldsymbol{F}/h). \quad (14.110)$$

If the stratification vanishes we may take $\Gamma = 0$ and the equation reprises (14.102), given an appropriate choice of $\boldsymbol{F}$. The second term in (14.110) equation is known as the JEBAR term — joint effect of baroclinicity and relief — and it serves to couple the depth integrated flow with the baroclinic flow.

Bottom pressure torque in a homogeneous gyre

The first term on the right-hand side of (14.107) is the *bottom pressure torque, B*. It be written as the curl of a form stress τ_b; that is, $B\mathbf{k} = \nabla \times \tau_b = -\nabla \times (\phi_b \nabla \eta_b) = -\nabla \phi_b \times \nabla \eta_b$, and so is non-zero whenever the pressure gradient has a component parallel to the topographic contour. Note that for unforced and inviscid flow we have both $J(\psi, f/h) = 0$ and, from (14.107), $\beta v = B$. That is, flow along f/h contours is equivalent to meridional flow balanced by a bottom pressure torque and, of course, if the domain is flat-bottomed, all meridional flow is viscid.

However, unlike viscosity, the bottom pressure torque cannot balance the effects of the wind-stress curl when integrated over the whole domain, or indeed when integrated over an area bounded by a line of constant ϕ_b or constant η_b, because its integral over such an area vanishes and (14.102) cannot be balanced if $r = 0$. Locally, however, bottom pressure torque can be as or more important than either the wind forcing or friction. In the numerical simulations shown in Fig. 14.14, it is the bottom pressure torque term that largely balances the polewards flow (βv) in the vorticity equation in parts of western boundary current, with friction acting in the opposite sense. That is, over some regions where the flow is crossing f/h contours we have the balance

$$[\beta v] \approx [\text{Bottom pressure torque}] - [\text{Friction}], \qquad (14.111)$$

where the terms in square brackets are positive, and friction is small. In contrast, in the flat-bottomed case in the western boundary layer we have the classical balance $[\beta v] \approx +[\text{Friction}]$, with both terms positive.

Now consider the balance of momentum, integrated zonally across the domain. We write the vorticity equation (14.107) in the form

$$\nabla \cdot (f \overline{\boldsymbol{v}}) = -\text{curl}_z(\phi_b \nabla \eta_b) + \text{curl}_z \tau_w - \text{curl}_z \tau_f, \qquad (14.112)$$

where τ_w represents the wind stress and τ_f represents frictional effects. Integrate (14.112) over the area of a zonal strip bounded by two nearby lines of latitude, y_1 and y_2, and the coastlines at either end. The term on the left-hand side vanishes by mass conservation and using Stokes's theorem we obtain:

$$\int_{y_1} \phi_b \frac{\partial \eta_b}{\partial x} \, dx - \int_{y_2} \phi_b \frac{\partial \eta_b}{\partial x} \, dx = \int_{y_1} (\tau_w^x - \tau_f^x) \, dx - \int_{y_2} (\tau_w^x - \tau_f^x) \, dx. \quad (14.113)$$

If the topography is non-zero, there is nothing in this equation to prevent the wind-stress being balanced by the form stress terms, with the friction being a negligible contribution. If, for example, friction were to be confined to the southwest corner, then bottom pressure torque is the proximate driver of fluid polewards in the western boundary current. This may hold only if the scale of the sloping sidewall is greater than the thickness of the Stommel layer; if the converse holds, the sidewalls appear to be essentially vertical to the flow. If the sidewalls are truly vertical, then the form stress is confined to delta-functions at the walls. Friction must then be important even in the zonal balance, because if we restrict the integral in (14.113) to a strip that does not quite reach the sidewalls, the left-hand side vanishes identically and the wind-stress can only be balanced by friction.

To conclude this discussion, we note that the effects of topography are likely greater in homogeneous fluids than in stratified fluids, because the stratification may partially shield the wind-driven upper ocean from feeling the topography, but we leave the exploration of that topic for another day.

14.7 * VERTICAL STRUCTURE OF THE WIND-DRIVEN CIRCULATION

We now examine the vertical structure of the wind-driven flow. We pose the problem in the framework of the quasi-geostrophic equations, taking the overall stratification of the ocean as a given. Of course the production of the stratification itself one of the most important problems of physical oceanography, but we will leave that to subsequent chapters.

14.7.1 A Two-Layer Quasi-Geostrophic Model

Scales of motion

We will concern ourselves with scales that are sufficiently larger than the deformation radius that we can ignore relative vorticity relative to vortex stretching and the β-effect. We must be careful in so doing, because quasi-geostrophic scaling applies only to scales that are not significantly larger than the deformation scale; thus, our analysis will be formally valid under the following set of inequalities.

$$\beta L \ll f_0 \qquad \text{(small variations in Coriolis parameter)}$$

$$\beta L > U/L \qquad \text{(to ignore relative vorticity compared to planetary vorticity)}$$

$$L^2 > L_d^2 \qquad \text{(to ignore relative vorticity compared to vortex stretching)}$$

$$Ro\, L^2 \ll L_d^2 \qquad \text{(to keep the variations in stratification small)}$$

where L_d is the deformation radius and L the scale of the motion. Since in the midlatitude ocean $L_d \approx 10^5$ m, then the above inequalities are reasonably well satisfied for $L \approx 10^6$ m and $U \approx 0.1\,\mathrm{m\,s^{-1}}$ with $\beta = 10^{-11}\,\mathrm{m^{-1}\,s^{-1}}$ and $f_0 = 10^{-4}\,\mathrm{s^{-1}}$. The first and last of the inequalities are standard quasi-geostrophic requirements, with the '$\gg$' symbol denoting the asymptotic ordering. The middle two inequalities are taken within the quasi-geostrophic dynamics, and are needed in order to ignore relative vorticity and give a balance between the β-effect and vortex stretching. The simultaneous satisfaction of all these conditions may seem restrictive, but the plangent dynamics contained within the quasi-geostrophic equations and the generality of the method employed below will suggest that the principle results obtained may transcend the particular limitations of the equations used.

Constructing the model

We now make the following simplifications for our model ocean.
  (i) We use the two-layer quasi-geostrophic equations, with layers of equal thickness.
  (ii) We seek only statistically-steady solutions.

(iii) We include a frictional term derived by assuming potential vorticity is fluxed downgradient. Given the neglect of relative vorticity, this is equivalent to an interfacial drag.

(iv) We will neglect the western boundary layer.

Because of the equal-layer-thickness assumption, which we make primarily for algebraic simplicity, it is best considered as model for the upper ocean above a level where the vertical velocity is approximately zero. The equations of motion are then

$$J(\psi_1, q_1) = \frac{1}{H_0} \text{curl}_z \boldsymbol{\tau} - \nabla \cdot \boldsymbol{T}_1, \qquad J(\psi_2, q_2) = -\nabla \cdot \boldsymbol{T}_2 \qquad \text{(14.114a,b)}$$

where

$$q_1 = \beta y + F(\psi_2 - \psi_1), \qquad q_2 = \beta y + F(\psi_1 - \psi_2). \qquad \text{(14.115a,b)}$$

Here, $F = f_0^2/(g' H_0) = 1/L_d^2$ is a measure of the stratification, where H_0 is the thickness of either layer, and the $\nabla \cdot \boldsymbol{T}$ terms are represent interfacial eddy stresses, which we parameterize by by a downgradient flux of potential vorticity: are given by

$$\boldsymbol{T}_1 = -\kappa \nabla q_1 = -R \nabla(\psi_2 - \psi_1), \qquad \boldsymbol{T}_2 = -\kappa \nabla q_2 = -R \nabla(\psi_1 - \psi_2), \quad \text{(14.116)}$$

where R and κ are constants, and $R = \kappa F$. We will be interested in the limit of small R, or more specifically $UFL/R \gg 1$, which is a large Péclet number condition. (The Péclet number is similar to a Reynolds number, but with the diffusivity replacing the kinematic viscosity.) So first consider the case when R is identically zero. An *exact* solution to (14.114) has $\psi_2 = 0$, so that (14.114a) becomes $\beta \partial \psi_1/\partial x = H_0^{-1} \text{curl}_z \boldsymbol{\tau}$, with solution

$$\psi_1 = -\frac{1}{H_0 \beta} \int_x^{x_e} \text{curl}_z \boldsymbol{\tau} \, dx. \qquad \text{(14.117)}$$

That is, there is no flow in the lower layer, and the upper layer solution is given by Sverdrup balance. The solution satisfies $\psi_1 = 0$ at $x = x_e$ and, because $\psi_2 = 0$, the nonlinear term on the left-hand side of (14.114a) vanishes identically.

General Solution

We now construct the solution without assuming $\psi_2 = 0$. Although the equations are nonlinear, we obtain a linear equation for the lower-layer streamfunction by adding (14.114a) and (14.114b), giving

$$J(\psi_1, \beta y + F(\psi_2 - \psi_1)) + J(\psi_2, \beta y + F(\psi_1 - \psi_2)) = \frac{1}{H_0} \text{curl}_z \boldsymbol{\tau}. \qquad \text{(14.118)}$$

The nonlinear terms cancel leaving

$$J(\overline{\psi}, \beta y) = \frac{1}{H_0} \text{curl}_z \boldsymbol{\tau}, \qquad \text{where} \quad \overline{\psi} = \psi_1 + \psi_2, \qquad \text{(14.119a,b)}$$

with solution [c.f., (14.117)]

$$\overline{\psi} = -\frac{1}{H_0 \beta} \int_x^{x_e} \text{curl}_z \boldsymbol{\tau} \, dx'. \qquad \text{(14.120)}$$
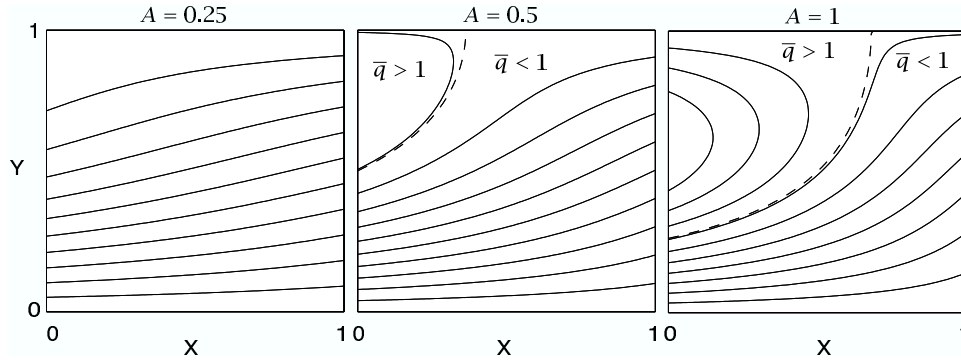
Fig. 14.15 Contours of $\overline{q} = \beta y + A \sin \pi y (1 - x)$, with $\beta = 1$. The dashed line is $\overline{q} = 1$, which separates the blocked region to the east ($\overline{q} < 1$) from the closed region to the west ($\overline{q} > 1$). See Fig. 14.16 for plots of the other fields.

This simply says that the vertically integrated flow obeys Sverdrup balance. For the canonical windstress

$$\boldsymbol{\tau} = -\tau_0 \cos \pi y \, \mathbf{i} \tag{14.121}$$

we obtain $\overline{\psi} = (\pi \tau_0 / \beta H_0)(x_e - x) \sin \pi y$. It is useful to define

$$\overline{q} \equiv (\beta y + F\overline{\psi}), \tag{14.122}$$

and then $\overline{q} = \beta[y + A(1 - x) \sin \pi y]$, where $A = \pi \tau_0 / (\beta H_0)$ parameterizes the wind strength, and this is plotted in Fig. 14.15. For $\overline{q} < 1$ (below and to the right of the dashed line) all the geostrophic contours intersect the eastern boundary and the flow is 'blocked'. For $\overline{q} > 1$ the flow is 'closed'.

Lower layer

Although the full equations are nonlinear, using (14.122) we can obtain a linear equation for the lower layer. Because the Jacobian of a field with itself vanishes, (14.114b) and (14.115b) imply that

$$J(\psi_2, \overline{q}) = -\nabla \cdot \boldsymbol{T}_2, \tag{14.123}$$

and this is useful because $\overline{q}$ is a function of the wind, using (14.122). If $\nabla \cdot \boldsymbol{T}_2 = 0$ then

$$J(\psi_2, \overline{q}) = 0. \tag{14.124}$$

As well as the possibility that $\psi_2 = 0$ we now have the more general solution

$$\psi_2 = G(\overline{q}) \tag{14.125}$$

where G is an *arbitrary* function of its argument. Isolines of ψ_2 and $\overline{q}$ are then co-incident. (Contours that are isolines of both streamfunction and potential vorticity are generally known as geostrophic contours.)

Consider a blocked isoline of $\overline{q}$; that is, one that intersects the eastern boundary

(see again Fig. 14.15). The ψ_2 contour coincident with this has value zero at the eastern boundary (by the no-normal flow condition). Thus $\psi_2 = 0$ *everywhere* in the blocked region, and $q_2 = \overline{q}$. In this region the Sverdrup transport is carried everywhere by the upper layer, and the lower layer is at rest. This region is called a 'shadow zone', for the fluid is in the shadow of the eastern boundary, and it will re-appear in a model of the thermocline in chapter 16. In the region of closed contours, ψ_2 cannot be given by this argument. But if R is small, we can expect (14.124) to approximately hold, and that the presence of a small amount of dissipation will determine the functional relationship between ψ_2 and $\overline{q}$. Thus, in summary, there are two regions of flow:

  (i) The blocked region in which $\psi_1 \approx \overline{\psi} \gg \psi_2$ and ψ_1 is approximately given by (14.117).

  (ii) A closed region in which $\psi_2 = G(\overline{q}) + \mathcal{O}(R)$.

14.7.2 The form of $G(\overline{q})$

A general argument

In chapter 10 we showed that, within a region of closed contours, the values of tracer that is materially conserved except for the effects of a small diffusion would become *homogeneous*. In the case at hand, potential vorticity is that tracer so that within potential vorticity contours or closed streamlines potential vorticity will become homogenized. If we can determine the value of q_2 within the region of closed contours, then from (14.115) ψ_2 is given by

$$\psi_2 = (1/2F)(\overline{q} - q_2) \tag{14.126}$$

and the solution would be complete. Now, outside the closed region $\psi_2 \ll \psi_1$, so that the outermost contour of the closed region must be characterized by $q_2 \approx \overline{q}$, for this makes ψ_2 continuous between closed and blocked regions. Thus, the value of q_2 within the closed homogeneous region is that of $\overline{q}$ (i.e., $\beta y + F\overline{\psi}$) on its boundary. Since this contour intersects the poleward edge of the domain, where $\overline{\psi}$ is zero, the value of this contour is just βy at $y = L$; that is, βL. Thus, within the closed region,

$$q_2 = \beta L. \tag{14.127}$$

A specific calculation

Now consider the steady, lower-layer potential vorticity equation (14.114b); since $J(\psi_2, F(\psi_1 - \psi_2)) = J(\psi_2, F(\psi_1 + \psi_2))$, (14.114b) may be written as

$$J(\psi_2, \overline{q}) = -\nabla \cdot \boldsymbol{T}_2 \tag{14.128}$$

Integrating around a closed contour of $\overline{q}$ the left-hand side vanishes and

$$R \int (\nabla\psi_1 - \nabla\psi_2) \cdot \boldsymbol{n} \, \mathrm{d}l = 0 \tag{14.129}$$

or

$$\oint \boldsymbol{u}_1 \cdot \mathrm{d}\boldsymbol{l} = \oint \boldsymbol{u}_2 \cdot \mathrm{d}\boldsymbol{l} \tag{14.130}$$

Summary of Wind-driven, Two-layer Solution

The vertically integrated flow in a wind-driven two-layer quasi-geostrophic model is determined by Sverdrup balance. The effects of eddies may be crudely parameterized by a downgradient diffusion of potential vorticity. If this is identically zero, then the lower layer flow is identically zero and the upper layer flow carries all the transport. If the diffusion is small but non-zero, the lower layer streamfunction approximately satisfies $J(\psi_2, \overline{q}$, where $\overline{q}$ is given by (14.122), and therefore ψ_2 is a function of $\overline{q}$ — that is, $\psi_2 \approx G(\overline{q})$. For a typical subtropical wind, contours of $\overline{q}$, and therefore contours of ψ_2, are naturally divided into two regions (Fig. 14.15):

(i) A blocked region (the shadow zone), in which contours of $\overline{q}$ intersect the eastern boundary, the lower layer flow is zero and the upper layer carries all the Sverdrup transport.

(ii) A closed region in which (if we envision a nearly inviscid western boundary current) the flow recirculates. In this region we posit that the lower layer potential vorticity becomes homogeneous, with a value determined by the value at the region's boundary, and this is in turn is determined by tracing $\overline{q}$ back to the domain boundary.

To satisfy a circulation constraint the function $G(\overline{q})$ must be a linear function, and given this the entire solution may be determined. If, for example, the wind is zonal and a function of y only, and $\text{curl}_z \tau = g(y)$ then, in both regions:

$$\overline{\psi} \equiv \psi_1 + \psi_2 = -\frac{1}{\beta H_0} g(y)(x_e - x), \qquad \overline{q} \equiv \beta y + F\overline{\psi} \qquad \text{(OC.1a,b)}$$

In the blocked region:

$$\psi_2 = 0, \qquad\qquad \psi_1 = -\frac{1}{\beta H_0}(x_e - x)g(y), \qquad \text{(OC.2a)}$$

$$q_1 = \beta y + F(\psi_1 - \psi_2), \qquad q_2 = \beta y + F(\psi_2 - \psi_1). \qquad \text{(OC.2b)}$$

In the closed region:

$$q_2 = \beta L \quad \text{(by homogenization)}, \qquad \text{(OC.3a)}$$

$$\psi_2 = \frac{1}{2F}(\overline{q} - \beta L), \qquad \psi_1 = \overline{\psi} - \psi_2, \qquad \text{(OC.3b)}$$

$$q_1 = \beta y + F(\psi_2 - \psi_1) = 2\beta y - \beta L. \qquad \text{(OC.3c)}$$

For $g(y) = -\sin \pi y$ these solutions are illustrated in Fig. 14.15 and Fig. 14.16.

This approach provides a solution to the conundrum of what drives the lower ocean ocean, for if there are no eddy effects at all [i.e., $\boldsymbol{T}_1 = \boldsymbol{T}_2 = 0$ in (14.116))], then the lower layer flow is stationary. This seems unrealistic, for the upper layer flow could be made quite shallow. Another solution to this issue is provided in section 16.4, wherein it is assumed that the lower layers may outcrop and so feel the wind directly.

thus, the deep circulation around a mean geostrophic contour (i.e., isoline of $\overline{q}$) is equal to the upper level circulation.

Now, previously we argued that

$$\psi_2 = G(\overline{q}) = G(\beta y + F(\psi_1 + \psi_2)). \tag{14.131}$$

where G is an arbitrary function of its argument. In order to satisfy (14.130), G must clearly be a linear function, and so we write

$$\psi_2 = C\left[\frac{\beta y}{F} + (\psi_1 + \psi_2)\right] + B, \tag{14.132}$$

where C and B are constants. This may be re-arranged to give

$$\psi_1 = -C\frac{\beta y}{F} + (\psi_1 + \psi_2)(1 - C) - B. \tag{14.133}$$

This is consistent with (14.130) if $C = 1/2$. With this, (14.132) gives

$$\overline{q} = 2F(\psi_2 - B) \tag{14.134}$$

and the potential vorticity in the closed contour region of the lower layer is

$$q_2 = \beta y + F\overline{\psi} - 2F\psi_2 = -2FB. \tag{14.135}$$

That is, it is constant. Outside the closed contours $\psi_2 \ll \psi_1$ so that $q_2 \approx \overline{q} = \beta y + F\psi_1$. If we trace this contour to the edge of the domain where $\psi_1 = 0$ and $y = L$ then we see that the value of $\overline{q}$ on the contour, and hence q_2 in the closed region, is βL, as in (14.127), and $B = -\beta L/(2F)$. Using (14.134) then gives

$$\psi_2 = (2F)^{-1}(\overline{q} - \beta L). \tag{14.136}$$

Given ψ_2 and q_2 [from (14.127)], we obtain q_1 and ψ_1 using (14.115) and (14.119b), giving

$$q_1 = 2\beta y - \beta L, \qquad \psi_1 = \overline{\psi} - \psi_2. \tag{14.137}$$

All these fields are illustrated in Fig. 14.16, and see the shaded box on the preceding page for a summary.

14.8 * A MODEL WITH CONTINUOUS STRATIFICATION

We now look the dynamics of the continuously stratified circulation by way of an extension of our two-layer procedure.[19] Let us first consider how deep the wind's influence is.
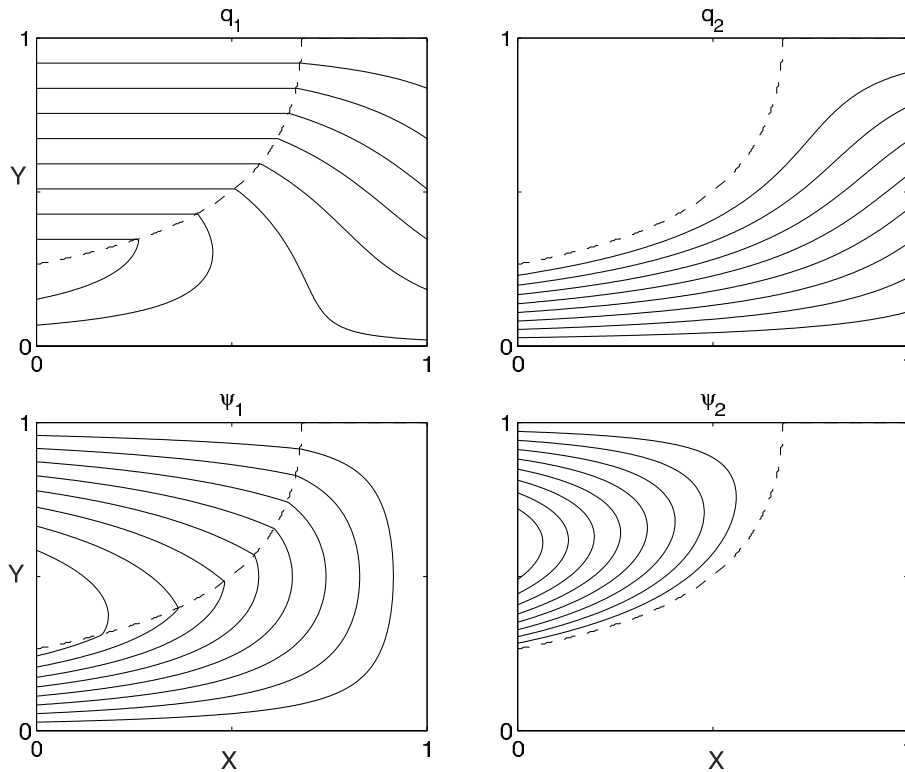
Fig. 14.16 Upper and lower level potential vorticity and streamfunction for the canonical windstress (14.121). The field of $\bar{q}$ is that of Fig. 14.15 with $A = 1$. The dashed line divides the blocked region from the closed region. The lower layer streamfunction ψ_2 is non-zero only in the closed region, and here $q_2 = \beta L$) and $q_1 = 2\beta y - \beta L$. In the blocked region the upper layer carries all of the Sverdrup transport. Both streamfunction and potential vorticity are continuous at the divide: $\psi_2 = 0$ and $q_2 = \bar{q} = \beta L$.

14.8.1 Depth of the Wind's Influence

The thermal wind-relationship in the form $f \, \partial u / \partial z = \partial b / \partial y$ implies a vertical scale H given by

$$H = \frac{fUL}{\Delta b} \tag{14.138}$$

where Δb is a typical magnitude of the horizontal variation of the buoyancy. We can relate this to the Ekman pumping velocity using the linear geostrophic vorticity equation, $\beta v = f \, \partial w / \partial z$, which, (assuming that the horizontal components of velocity are roughly similar, i.e., $V = U$), implies that

$$U = \frac{fW_E}{\beta H}, \tag{14.139}$$

Equations (14.138) and (14.139) may be combined to give an estimate of the depth of the wind-driven circulation, namely

$$H = \left(\frac{f^2 W_E L}{\beta \, \Delta b} \right)^{1/2}, \tag{14.140}$$

where L may be interpreted as the gyre scale. We now use quasi-geostrophic scaling to relate the horizontal temperature gradient to the stratification using the thermodynamic equation,

$$\frac{\mathrm{D}b}{\mathrm{D}t} + wN^2 = 0, \tag{14.141}$$

with implied scaling

$$\Delta b = \frac{W_E N^2 L}{U} = \frac{N^2 \beta H L}{f_0}, \tag{14.142}$$

where the second equality uses (14.139). Using (14.140) and (14.142) gives

$$\boxed{H = \left(\frac{W_E f^3}{\beta^2 N^2} \right)^{1/3}.} \tag{14.143}$$

Potential vorticity interpretation

The estimate (14.143) can be obtained and interpreted more directly: *the wind-driven circulation penetrates as far as it can alter the potential vorticity q from its planetary value βy.* Recall that, ignoring relative vorticity,

$$q = \beta y + \frac{\partial}{\partial z} \left(\frac{f_0^2}{N^2} \frac{\partial \psi}{\partial z} \right). \tag{14.144}$$

The two terms are comparable if

$$\frac{f_0^2}{N^2 H^2} UL \approx \beta L \tag{14.145}$$

or

$$H^2 \approx \frac{f_0^2 U}{N^2 \beta}. \tag{14.146}$$

Using (14.139) to eliminate U in favour W_E recovers (14.143). Thus, for a given stratification, we have an estimate of the depth of the wind-driven circulation, or at least a scaling for depth of the vertical influence of the wind.

14.8.2 The complete solution

Armed with an estimate for the depth of the wind's influence, we can obtain a solution for the continuously stratified case analogous to that found in the two-layer case section 14.7. Our assumptions are:

(i) In the limit of small dissipation streamfunction and potential vorticity have a functional relationship with each other.

(ii) Potential vorticity is homogenized within closed isolines of q or ψ. The value of q within the homogenized pool is that of the outermost contour, which here is the value of q at the poleward edge of the barotropic gyre.

(iii) Outside of the pool region, (i.e., below the depth of the wind's influence) the streamfunction is zero, and the potential vorticity is given by the planetary value, i.e., βy.

Given these, finding a solution is not difficult. If N^2 is constant and neglecting relative vorticity, the expression for potential vorticity is

$$q = \frac{\partial^2}{\partial z^2}\left(\frac{f_0^2}{N^2}\psi\right) + \beta y \qquad (14.147)$$

We nondimensionalize by writing

$$z = \left(\frac{f_0^2 U}{N^2 \beta}\right)^{1/2}\widehat{z}, \quad q = \beta L \widehat{q}, \quad \psi = \widehat{\psi} U L, \quad y = L \widehat{y}, \quad w = \frac{U^2 f_0}{N^2 H}\widehat{w}, \qquad (14.148)$$

where the hatted variables are nondimensional, and the scaling for w arises from the thermodynamic equation $N^2 w \sim J(\psi, f_0 \psi_z)$. With this, (14.147) becomes

$$\widehat{q} = \frac{\partial^2 \widehat{\psi}}{\partial \widehat{z}^2} + \widehat{y}, \qquad (14.149)$$

The flow is then given by solving the following equations:

$$\psi_{zz} + y = y_0, \qquad -D(x, y) < z < 0, \qquad (14.150\text{a})$$
$$\psi = 0, \qquad z \leq -D(x, y), \qquad (14.150\text{b})$$

where D is the (to-be-determined) depth of the bowl, y_0 is a constant, and we have dropped the hats over the nondimensional variables. The solution in $D(x, y) < z < 0$ corresponds to the closed region of the two-layer model, and the solution $z \leq -D(x, y)$ corresponds to the blocked region of zero lower-layer flow. The constant y_0 is the nondimensional value of potential vorticity within the pool region, and following our reasoning in the two-layer case this is the value of the potential vorticity at the northern boundary. Dimensionally this is βL, so that in nondimensional units $y_0 = 1$.

The lower boundary conditions on (14.150a) is that $\psi = \psi_z = 0$ at $z = -D$, because in the abyss $\psi = \partial\psi/\partial z = 0$ and we require that both ψ and $\partial\psi/\partial z$ be
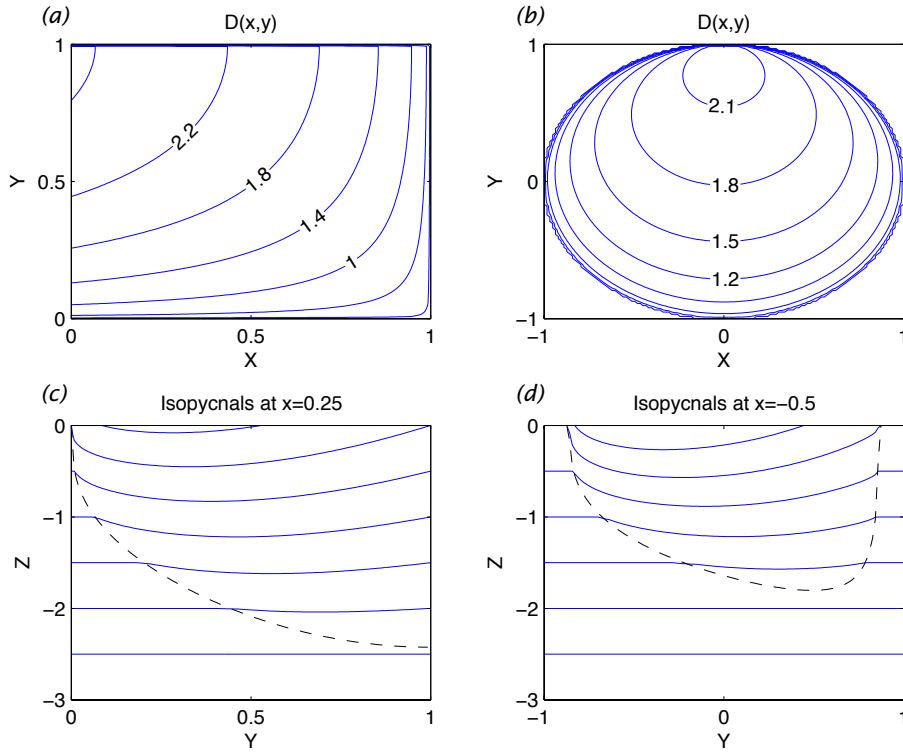
Fig. 14.17 Solutions of (14.122) for two different barotropic streamfunctions. On the left $\psi_B = (1-x)\sin\pi y$ and on the right $\psi_B = 1 - (x^2 + y^2)$ for $x^2 + y^2 < 1$, zero elsewhere. The upper panels show contours of the depth of the wind-influenced region (solutions of (14.155)). The depth increases to the northwest in the left panel, and to the north in the right panel, so that in both cases the area of the bowl shrinks with depth. The lower panels are contours of $z + (\beta L/f_0)\psi_z/2$, with $\beta L/f_0 = 1/2$, obtained from (14.151) or (14.156), at $x = 0.25$ and $x = -0.5$ in the two cases. These are isopycnal surfaces, with a rather large value of $\beta L/f_0$ to exaggerate the displacement in the bowl region. The dashed lines indicate the boundary of the bowl region, outside of which the isopycnals are flat.

continuous (note that the buoyancy perturbation is proportional to $\partial\psi/\partial z$). The solution that satisfies this

$$\psi = \frac{1}{2}(z+D)^2(y_0 - y), \tag{14.151}$$

and $\psi = 0$ for $z < D$ To obtain an expression for D we first note that the nondimensional vertical velocity at $z = 0$ is given by

$$w = -J(\psi, \psi_z), \tag{14.152}$$

which, using (14.151), gives

$$w = \frac{1}{2}(z+D)^2(y_0 - y)\frac{\partial D}{\partial x}. \tag{14.153}$$
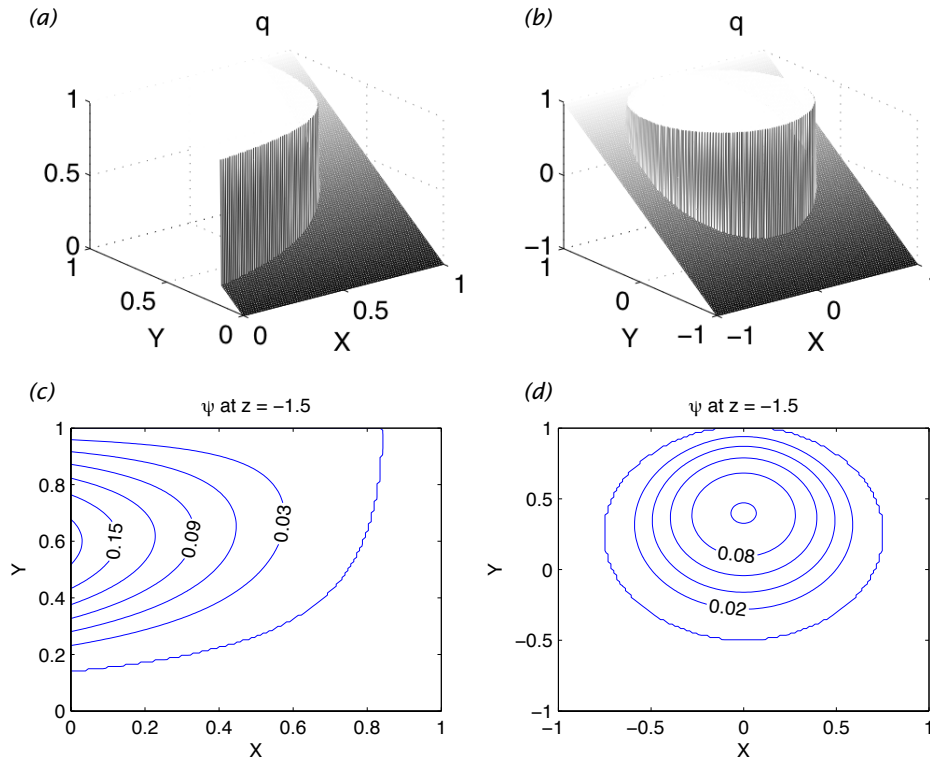
Fig. 14.18 As for Fig. 14.17, but now a perspective of potential vorticity (upper panels, obtained from (14.157)) and contours of streamfunction (lower panels, from (14.156)), at a nondimensional depth of $z = -1.5$. Within the bowls the circulation is clockwise within the bowls and the potential vorticity is uniform. Outside the bowls the fluid is stationary and the potential vorticity has the planetary value βy. The value of potential vorticity within the bowl is the planetary value at the poleward edge of the gyre, and is the same value at all depths.

At $z = 0$ the vertical velocity is the Ekman pumping velocity and (14.153) becomes

$$D^2 \frac{\partial D}{\partial x} = \frac{2 w_E}{(y_0 - y)} \tag{14.154}$$

But the Ekman pumping velocity is related to the barotropic streamfunction, ψ_B, by the Sverdrup relationship, so that integrating (14.154) gives

$$\boxed{D^3 = \frac{6 \psi_B}{(y_0 - y)} = -\frac{6(x_e - x) w_E}{(y_0 - y)}} \tag{14.155}$$

where the second equality holds if w_e is not a function of x. This is a solution for the depth of moving region, the bowl in which potential vorticity is homogenized. An expression for the streamfunction is then obtained by using (14.155) in (14.151), and is

found to be

$$\psi = \begin{cases} \frac{1}{2}\left[z(y_0 - y)^{1/2} + (6\psi_B)^{1/3}(y_0 - y)^{1/6}\right]^2 & -D < z < 0, \\ 0 & z < -D. \end{cases} \quad (14.156)$$

The potential vorticity corresponding to this solution is

$$q = \begin{cases} y_0 & -D < z < 0, \\ y & z < -D. \end{cases} \quad (14.157)$$

Solutions are illustrated in Fig. 14.17 and Fig. 14.18 for two different barotropic streamfunctions.

It is possible to extend models such as the one described above by appending a western boundary layer, and indeed the homognization of potential vorticity depends upon presence of such layer in allowing the flow to recirculation. However, as we saw in section 14.5.3, it is difficult for flow leave a western boundary layer without the help of friction, and a neutrally stable, damped, stationary Rossby wave typically forms. The critical issue then is whether the presence of dissipation in the western boundary layer affects the homogenization of potential vorticity in the gyre itself. Numerical solutions with a quasi-geostrophic model do show that potential vorticity is able to homogenize under such circumstances. Homgenization in the real ocean has been observed in the Pacific and, somewhat less compellingly, in the Atlantic.[20]

Notes

1 This figure is based in part on earlier drawings by W. Schmitz and L. Talley that are largely based on observations, as well as on output from numerical models constrained to the observations at GFDL. However, it is highly schematic and not quantitative.

2 The climatological data set of Conkright et al. (2001) was assimilated into a primitive equation numerical model (MOM) by strongly relaxing the model temperature and salinity fields to those of the data set, a method arcanely known as 'robust diagnostics' or 'nudging'. Larger scale features are broadly representative of reality but smaller scale feature may be inaccurate.

3 Courtesy of R. Zhang. See also Zhang and Vallis (2006).

4 Henry Stommel (1920–1992) was one of the most creative and influential physical oceanographers of the 20'th century. Spending most of his career at Woods Hole Institute of Oceanography, his enduring contributions include the first essentially correct theory of western intensification (and so of the Gulf Stream), some of the first models of abyssal flow and the thermohaline circulation (chapter 15), and his foundational work on the thermocline. His *forté* was in constructing elegantly simple models of complex phenomena — often models that were physically realizable in the laboratory — while at the same time encouraging the testing of the models against observations. This chapter might have been entitled 'Variations on a theme of Stommel'.

5 The asymptotic solution to this boundary value problem was obtained by Wasow

(1944), a few years prior to Stommel's work, and further investigated by Levinson (1950). However, it seems unlikely these two investigators were motivated by the oceanographic problem.

6 Harald Sverdrup (1888–1957) was a Norwegian meteorologist/oceanographer who is most famous for the balance that now bears his name, but he also played a leadership role in scientific policy and was the director of Scripps Institution of Oceanography from 1936–1948. The Sverdrup unit is also named for him. Originally defined as a measure of volume transport, with $1\,\mathrm{Sv} \equiv 10^6\,\mathrm{m^3\,s^{-1}}$, it is more generally thought of as a mass transport with $1\,\mathrm{Sv} \equiv 10^9\,\mathrm{kg\,s^{-1}}$, in which case it can also be used as a measure of transport in the atmosphere. The Hadley Cell, for example, has an average transport of about 100 Sv (Fig. 11.3 and Fig. 12.19).

7 Leetmaa et al. (1977) and Wunsch and Roemmich (1985) offer somewhat different views on the matter.

8 After Munk (1950).

9 Courtesy of R. Zhang. See also Zhang and Vallis (2006).

10 Hendershott (1987), Veronis (1966a).

11 Veronis (1966b) investigated nonlinear effects in the Stommel and Munk problems. I am grateful to B. Fox-Kemper for providing the solutions shown in Fig. 14.9, and for many comments on this chapter. See also Fox-Kemper and Pedlosky (2003).

12 After Charney (1955).

13 A more general discussion is given by Greenspan (1962). Il'in and Kamenkovich (1964) and Ierley and Ruehr (1986) show numerically that the friction must in fact be sufficiently strong for steady boundary-layer solutions to exist, and in particular that the Munk boundary layer width must be greater than twice the inertial boundary layer width, $\delta_M > 2\delta_I$. If this does not hold, Ierley (1987) suggests that an inertial 'recirculation gyre' may form, whose strength may be controlled by transient eddy fluxes Fox-Kemper (2004).

14 After Fofonoff (1954).

15 Hughes and de Cuevas (2001), Jackson et al. (2005).

16 Welander (1968).

17 Figure kindly provided by Laura Jackson.

18 From Jackson et al. (2005).

19 Following Rhines and Young (1982b). Young and Rhines (1982) also considered the problem of a western boundary layer.

20 See Rhines and Young (1982a) for a numerical example of PV homogenization (numerical simulation by W. Holland). See Keffer (1985), Talley (1988) and Lozier et al. (1996) for some observed PV fields. See Holland et al. (1984) for some of both.

Further Reading

Abarbanel H. D. I. and W. R. Young (eds) 1987. *General Circulation of the Ocean.*
     This book contains several useful articles on the oceanic general circulation. Particularly relevant to this chapter is the article by Hendershott on homogeneous single-layer models.

Pedlosky, J. 1996. *Ocean Circulation Theory.*
    As well as covering the theory of wind-driven gyres, this book discusses cross-gyre flows and equatorial dynamics.

Salmon, R. 1998. *Lectures on Geophysical Fluid Dynamics.*
    This book provides a discussion of topographic effects (including the effects of stratification), as well as a discussion of thermocline theory relevant to the material of our chapter 16.

Problems

14.1 ♦ Obtain the exact analytic solution to the Stommel problem (14.6) in a rectangular basin, and not by way of a boundary-layer approximation.

14.2 ♦ Obtain the exact analytic solution to the Munk problem (14.42) in a rectangular basin, and not by way of a boundary-layer approximation. You may use a simple, single-gyre, zonal wind-stress.

14.3 Obtain a boundary-layer solution of the Munk problem, (14.44), but with 'free-slip' boundary conditions instead of no-slip boundary conditions. Thus, instead of setting the normal derivative of ψ to be zero at the boundaries ($\partial\psi/\partial n = 0$), set the relative vorticity at the boundary to be zero, and thus $\partial^2\psi/\partial n^2 = 0$.

14.4 Obtain a solution of either the Stommel or Munk problems in a triangular domain (or a circular domain).

14.5 What is the formal asymptotic accuracy of derivatives in the boundary-layer solution to the Stommel problem? Show that the nonlinear term $J(\psi_s, \nabla^2\psi_s)$, where ψ_s is the streamfunction, is estimated to $\mathcal{O}(1/\delta_S^3)$ accuracy, where δ_S is the width of the western boundary layer.

14.6 ♦ (a) Using regular perturbation theory explicitly obtain the nonlinear corrections to the Stommel solutions for a single gyre flow, and show that (14.65) is an appropriate approximation of this. Discuss the properties of the solution, and in particular, show where are the errors largest. Optional: Repeat this calculation using the exact solution to the Stommel problem, and compare the solutions to those obtained using the boundary-layer approximation. [This problem may be made easier by using algebraic manipulation software.]

   ♦ (b) Suggest a better approach to this problem that is still semi-analytic or that at least gives some insight into the nonlinear solution.

14.7 ♦ Do problem 14.6, but with lateral viscosity instead of bottom drag, as in the Munk problem.

14.8 Consider the two-dimensional, non-divergent flow in a box of side L, as pictured. The equatorward flow, of magnitude U, is weak and spread over a lateral scale L, whereas the poleward flow is concentrated in a layer of width $d \ll L$. Suppose the

initial condition is a spot of tracer, as shown.
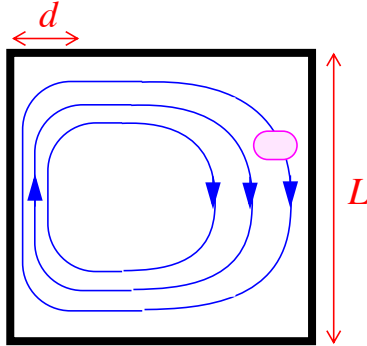
Estimate how long it takes to homogenize the tracer in terms of U, L, κ and d. *Hint:* Consider the advection-diffusion equation,

$$\frac{\partial \phi}{\partial t} + \boldsymbol{u} \cdot \nabla \phi = \kappa \nabla^2 \phi. \qquad \text{(P14.1)}$$

and estimate advective and diffusive times in the western boundary layer and the interior.

14.9 For a two-layer wind-driven quasi-geostrophic model, obtain an expression for the minimum strength of the wind that leads to closed contours of $\overline{q} = \beta y + F \overline{\psi}$. In particular, for the solution illustrated in Fig. 14.15, at what values of A do closed contours first form?
(*Answer:* $A = \pi^{-1}$.)

14.10 Show by differentiating (14.156) that potential vorticity is uniform in the pool region. What is its value?

CHAPTER 15

The Buoyancy Driven Circulation

O UR GOAL in this chapter and the next is to gain a rudimentary understanding of the three-dimensional dynamics and structure of the ocean circulation. In this chapter we focus on the *meridional overturning* and the associated *abyssal* circulation of the ocean, treating them as if they were solely driven by buoyancy forces, and in chapter 16 we look at the combined effects of wind and buoyancy forcing.

The meridional overturning circulation (MOC) is so-called because it is associated with sinking at high latitudes and upwelling elsewhere, although as we shall see even such a seemingly simple matter as this is not wholly settled. The circulation is also sometimes known as the 'thermohaline' circulation, reflecting a belief that it is driven by gradients in temperature and salinity, but because other mechanisms are also important that name is not appropriate as a general descriptor. In fact, the theory explaining the MOC is not in as satisfactory a state as it is for the quasi-horizontal wind-driven circulation discussed in chapter 14. In the theory of the wind-driven circulation, a rational series of approximations from the governing Navier-Stokes equations leads to a sequence of simple models (e.g., the homogeneous models of the wind-driven circulation, layered quasi-geostrophic models, etc.) whose foundations are thus reasonably secure, whose shortcomings are understood, and whose behaviour can be fairly completely analyzed. Attempts to proceed in a similar fashion with overturning circulation have been less successful; the reason is that the approximations required in order that a tractable conceptual model be constructed are unavoidably severe and, from a fluid-dynamicist's perspective, unjustifiable. Thus, although the large-scale overturning flow is well-described by the planetary geostrophic equations whose complexity is similar to that of the quasi-geostrophic equations, there is no rational simplification of these that leads to a model that is both as simple and informative as the homogeneous Stommel model of the quasi-horizontal, wind-driven circulation. Nevertheless, progress *has* been

Figure 15.1 The mean meridional overturning circulation in the North Atlantic, obtained with a combination of observations and a model. The contours are the streamfunction of the zonally averaged meridional flow. The units are Sverdrups, and the circulation is mostly clockwise, with sinking at high latitudes.[2]
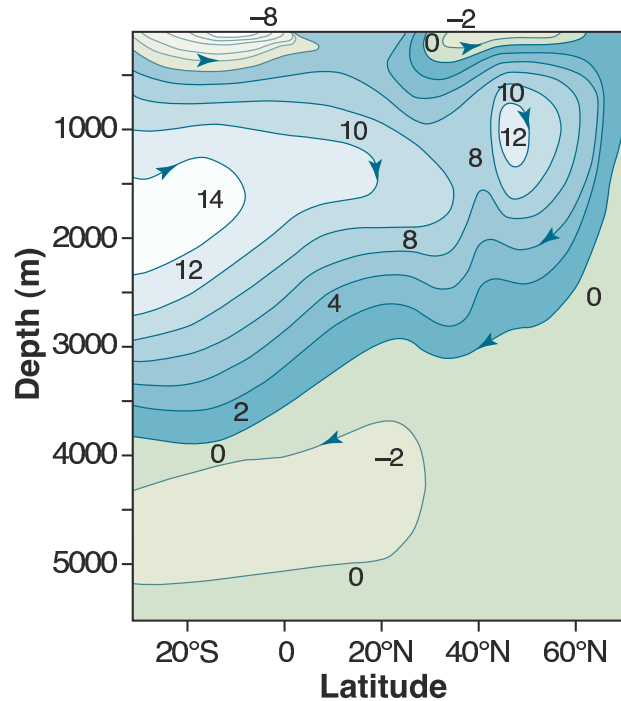
made, both numerically and through the use of very simple models, and in this chapter we concentrate on the foundations underlying these.

15.1 A BRIEF OBSERVATIONAL OVERVIEW

That there *is* a deep circulation has been known for a long time, largely from observations of tracers such as temperature, salinity and constituents such as dissolved oxygen and silica.[1] We can also take advantage of numerical models that are able to assimilate hydrographic and other observations and produce an estimate of the overturning circulation that is consistent with both the observations and the equations of motion, as illustrated in Fig. 15.1.

Associated with the overturning circulation is a stratification that has a quite distinctiv structure, as illustrated in Fig. 15.2. Most of the stratification is evidently concentrated in the upper kilometre or so of the ocean, with a relatively (although not completely) unstratified abyss full of dense water that has originated from high latitudes — the isopycnals shown in Fig. **??** all outcrop (i.e., intersect the surface) in the North Atlantic subpolar gyre and/or in the Antarctic Cicumpolar Current (ACC). The region of high stratification near the surface is known as the *thermocline* ('thermo' for temperature, 'cline' for changing); it is effectively synonymous with the *pycnocline* (for changing density), although the latter could exist without the former if there were a *halocline*, in which salinity changed rapidly. What is the cause of this circulation and the associated stratification?
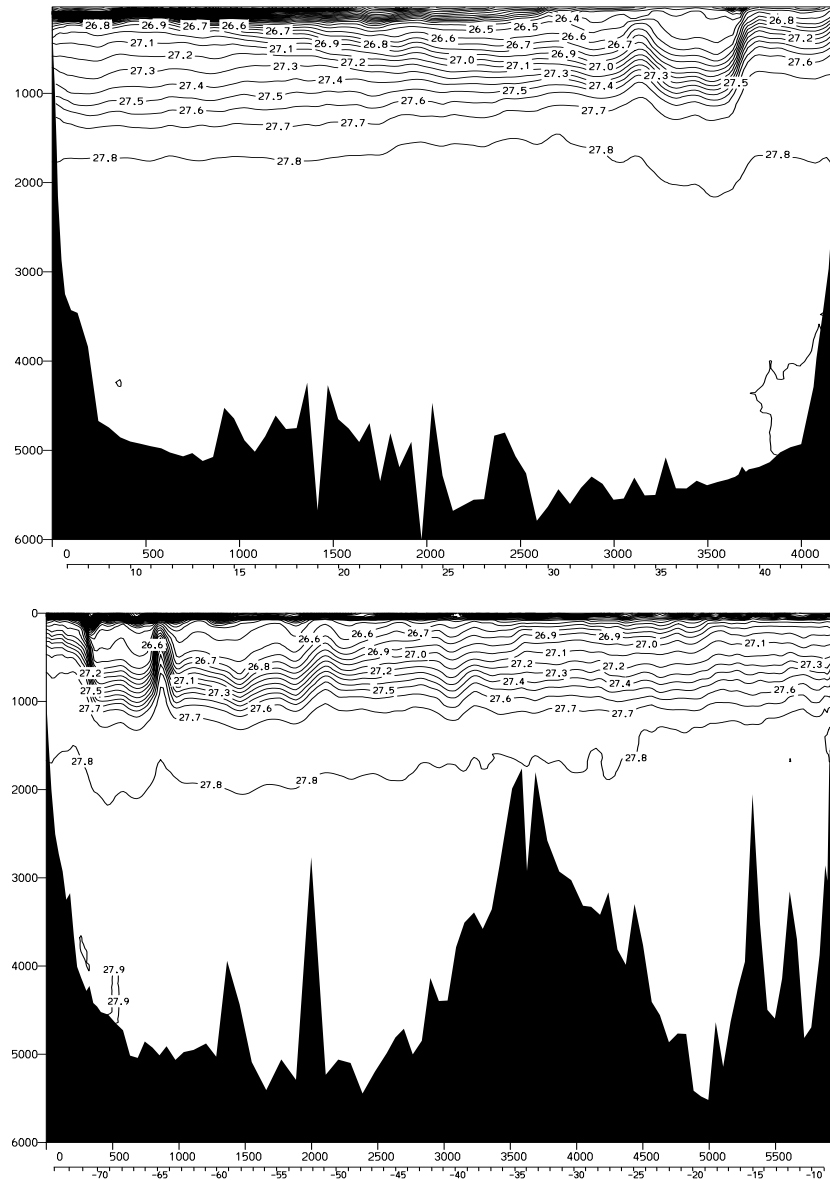
Fig. 15.2 Sections of potential density (σ_θ) in the North Atlantic: Upper panel: meridional section at 53°W, from 5°N to 45°N, across the subtropical gyre. Lower panel: zonal section at 36°N, from about 75°W to 10°W. The region of rapid change of density (and temperature) is concentrated in the upper kilometer, in the *main thermocline,* below which the ocean has a much more uniform density. A front is associated with the western boundary current and its departure from the coast near 40°N. In the upper northwestern region of subtropical thermocline there is a region of low stratification known as MODE water: isopycnals above this outcrop in the subtropical gyre and are 'ventilated'; isopycnals below the MODE water outcrop in the subpolar gyre.[3]
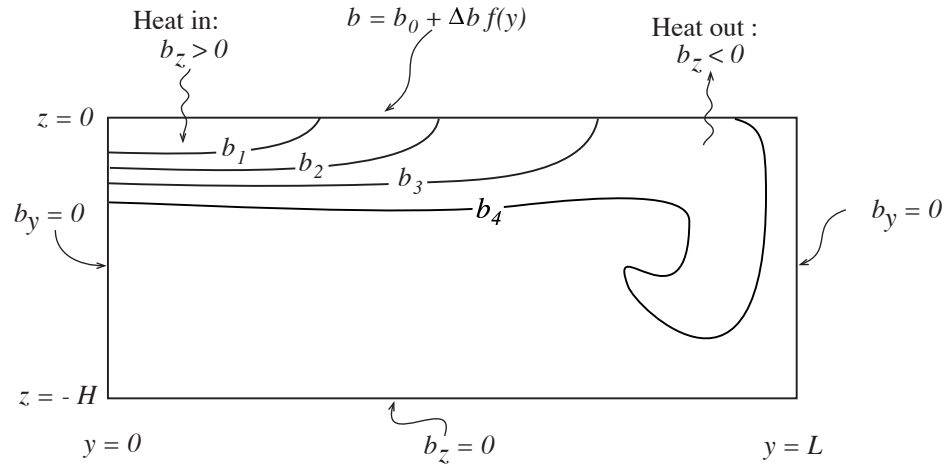
Fig. 15.3 A schema of 'sideways convection'. The y-axis represents latitude and the z-axis represents depth. The fluid is differentially heated and cooled along its top surface, whereas all the other walls are insulating. The result is, typically, a small region of convective instability and sinking near the coldest boundary, with generally upwards motion elsewhere.[4]

15.2 SIDEWAYS CONVECTION

Perhaps the simplest and most obvious fluid dynamical model of the overturning circulation is that of *sideways* or *horizontal convection.* The physical situation is sketched in Fig. 15.3. A fluid (two- or three-dimensional) is held in a container that is insulated on all its sides and bottom, but its upper surface is non-uniformly heated and cooled. In the purest fluid dynamical problem the heat enters the fluid solely by conduction at the upper surface, and one may suppose that here the temperature is imposed. Thus, for a simple Boussinesq fluid the equations of motion are

$$\frac{Dv}{Dt} + f \times v = -\nabla\phi + b\mathbf{k} + \nu\nabla^2 v, \tag{15.1a}$$

$$\frac{Db}{Dt} = \kappa\nabla^2 b, \tag{15.1b}$$

$$\nabla \cdot v = 0, \tag{15.1c}$$

with boundary conditions

$$b(x, y, 0, t) = f(x, y), \tag{15.2a}$$

where $f(x, y)$ is a specified field, and $\partial_n b = 0$ on the other boundaries, meaning that the derivative normal to the boundary, and so the buoyancy flux, is zero. An alternative upper boundary condition is to impose a flux condition whereby

$$\kappa\frac{\partial}{\partial z}b(x, y, 0, t) = g(x, y), \tag{15.2b}$$

where $g(x, y)$ is given. The oceanographic relevance of and (15.2) should be clear: the ocean is heated and cooled from above, and although the thermal forcing in the real

ocean may differ in detail (being in part a radiative flux, and in part a sensible and latent heat transfer from the atmosphere), (15.2) is a useful idealization. In some numerical models of the ocean, the heat input at the top is parameterized by way of a relaxation to some specified temperature. This is a form of flux condition in which

$$\text{Flux} = \kappa \frac{\partial b}{\partial z} = C(b^* - b), \tag{15.3}$$

and C is an empirical constant.[5] Although this may be a little more realistic than (15.2a) it will not affect the arguments below.

15.2.1 Two-dimensional convection

We may usefully restrict attention to the two-dimensional problem, in latitude and height. The two-dimensional flow may then loosely be thought of as representing the statistically steady zonally averaged flow of the ocean, valid only for large spatial scales. The zonally-averaged zonal flow is then small, and concomitantly so is the Coriolis force. The incompressibility of the flow then allows one to define a streamfunction such that

$$v = -\frac{\partial \psi}{\partial z}, \qquad w = \frac{\partial \psi}{\partial y}, \qquad \zeta = \nabla_x^2 \psi = \left(\frac{\partial^2 \psi}{\partial y^2} + \frac{\partial^2 \psi}{\partial z^2} \right) \tag{15.4}$$

where ζ is the vorticity in the meridional plane. We will neglect the subscript x on the Laplacian operator where there is no ambiguity. Taking the curl of Boussinesq equations of motion (15.1) then gives

$$\frac{\partial \nabla^2 \psi}{\partial t} + J(\psi, \nabla^2 \psi) = \frac{\partial b}{\partial y} + \nu \nabla^4 \psi \tag{15.5a}$$

$$\frac{\partial b}{\partial t} + J(\psi, b) = \kappa \nabla^2 b \tag{15.5b}$$

where $J(a, b) \equiv (\partial_y a)(\partial_z b) - (\partial_z a)(\partial_y b)$.

Nondimensionalization and scaling

We non-dimensionalize (15.5) by formally setting

$$b = \Delta b \, \hat{b}, \qquad \psi = \Psi \hat{\psi}, \qquad x = L \hat{x}, \qquad z = H \hat{z}, \qquad t = \frac{LH}{\Psi} \hat{t}, \tag{15.6}$$

where the hatted variables are non-dimensional, Δb is the temperature difference across the surface, L is the horizontal size of the domain, and Ψ, and ultimately the vertical scale H, are to be determined. Substituting into (15.6) gives

$$\frac{\partial \hat{\nabla}^2 \hat{\psi}}{\partial \hat{t}} + J(\hat{\psi}, \nabla^2 \hat{\psi}) = \frac{H^3 \Delta b}{\Psi^2} \frac{\partial \hat{b}}{\partial \hat{y}} + \frac{\nu L}{H} \hat{\nabla}^4 \hat{\psi} \tag{15.7a}$$

$$\frac{\partial \hat{b}}{\partial \hat{t}} + J(\hat{\psi}, \hat{b}) = \frac{\kappa L}{\Psi H} \hat{\nabla}^2 \hat{b} \tag{15.7b}$$

where $\widehat{\nabla}^2 = (H/L)^2 \partial^2/\partial\widehat{y}^2 + \partial^2/\partial\widehat{z}^2$ and the Jacobian operator is also appropriately non-dimensional. If we now use (15.7b) to choose Ψ as

$$\Psi = \frac{\kappa L}{H} \tag{15.8}$$

so that $t = H^2\widehat{t}/\kappa$, then (15.6) become

$$\frac{\partial \widehat{\nabla}^2 \widehat{\psi}}{\partial \widehat{t}} + J(\widehat{\psi}, \nabla^2 \widehat{\psi}) = Ra\,\sigma\alpha^5 \frac{\partial \widehat{b}}{\partial \widehat{y}} + \sigma\widehat{\nabla}^4\widehat{\psi} \tag{15.9}$$

$$\frac{\partial \widehat{b}}{\partial \widehat{t}} + J(\widehat{\psi}, \widehat{b}) = \widehat{\nabla}^2\widehat{b} \tag{15.10}$$

and the three non-dimensional parameters that govern the behaviour of the system are

$$Ra = \left(\frac{\Delta b L^3}{\nu\kappa}\right), \qquad \text{(the Rayleigh number)}, \tag{15.11a}$$

$$\sigma = \frac{\nu}{\kappa}, \qquad \text{(the Prandtl number)}, \tag{15.11b}$$

$$\alpha = \frac{H}{L}, \qquad \text{(the aspect ratio)}. \tag{15.11c}$$

The Rayleigh number is a measure of the strength of the buoyancy forcing relative to the viscous term, and in the ocean it will be very large indeed, perhaps $\sim 10^{24}$ if molecular values are used. (Sometimes H is used instead of L in the Rayleigh number definition; we use L here because it is an external parameter.)

For steady non-turbulent flows (or conceivably statistically steady flows in which ν and κ are an eddy viscosity and an eddy diffusivity) then we can demand that the buoyancy term in (15.9) is $\mathcal{O}(1)$. If it is smaller then the flow is not buoyancy driven, and if it is larger there is nothing to balance it. This can only hold if the vertical scale of the motion appropriately adjusts, and for $\sigma = \mathcal{O}(1)$, this leads to the possible scalings[6]

$$H = L\sigma^{-1/5}Ra^{-1/5}, \qquad \Psi = Ra^{1/5}\sigma^{-4/5}\nu. \tag{15.12a,b}$$

Note that the vertical scale arises as a consequence of the scaling analysis, and the vertical size of the domain plays no direct role. (For $\sigma \gg 1$ we might expect the nonlinear terms to be small and if the buoyancy term balances the viscous term in (15.9) the right-hand sides of (15.12) are multiplied by $\sigma^{1/5}$ and $\sigma^{-1/5}$. For seawater $\sigma \approx 7$ with the molecular values of κ and ν. If small scale turbulence exists, then the eddy viscosity will likely be similar to the eddy diffusivity and $\sigma \approx 1$.)

Numerical experiments (Fig. 15.4 and Fig. 15.5) do provide some support for this scaling, and although the range of Rayleigh numbers that has been achieved is limited a few simple and robust points that have relevance to the real ocean do emerge, namely:

⋆ Most of the box fills up with the densest available fluid, with a boundary layer in temperature near the surface required in order to satisfy the top boundary condition. The boundary gets thinner with decreasing diffusivity, consistent with (15.12). This is a diffusive prototype of the oceanic thermocline.
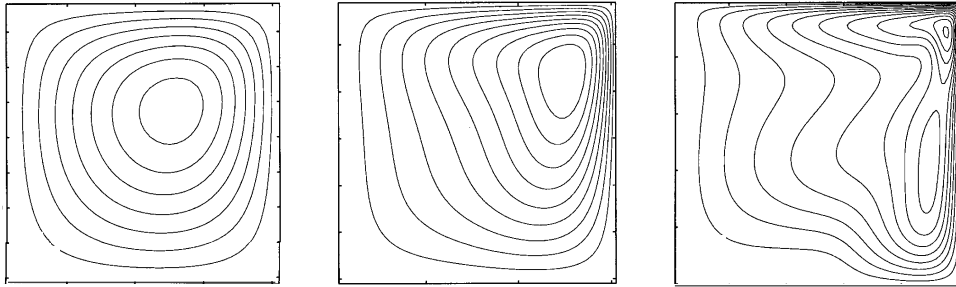
Fig. 15.4 The streamfunction in a numerical simulation of two-dimensional sideways convection. The circulation is clockwise, and the imposed temperature at the top linearly decreases from left to right, and the other walls are insulating. From left to right the Rayleigh numbers are 10^4, 10^6 and 10^8, and the contour interval is 1, 4 and 10 in arbitrary units. The Prandtl number is 10.[7]

★ The horizontal scale of the overturning circulation is large, being at or near the scale of the box.

★ The downwelling regions (the regions of active convection) tend to be of smaller horizontal scale than the upwelling regions, especially as the Rayleigh number increases.

Let us now try to explain some of these features in a simple and heuristic way.

15.2.2 Phenomenology of the overturning circulation

No water can be denser (or, more accurately, have a greater potential density) than the densest water at the surface, and if the subsurface water is a little lighter than this the surface water will be convectively unstable and sink in a plume.[8] The plume slowly entrains the warmer water that surrounds it, and then spreads horizontally when it reaches
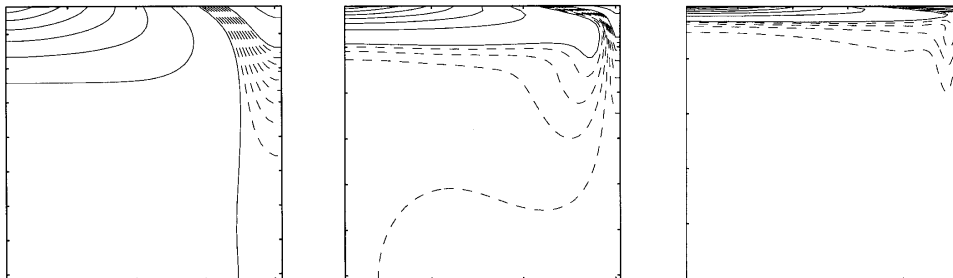
Fig. 15.5 The temperature or buoyancy field corresponding to the streamfunction fields shown in Fig. 15.4. Note an increasingly sharp gradient (a thermocline) near the top as the Rayleigh number increases, and that the bulk of the domain is filled with the densest available fluid.

the bottom or when density becomes similar to that of its surroundings. The presence of water denser than its surroundings creates a pressure gradient, and the ensuing flow will displace any adjacent lighter fluid, and so the domain fills with the densest available fluid. This process is a continous one: the plumes take cold water into the interior, where the water slowly warms by diffusion, and the source of cold water at the surface is continuously replenished. If diffusion is small, the end result is that density of the fluid in the interior will be almost the same as (in fact just slightly less than) that of the densest fluid formed at the surface. (Because diffusion can act only to reduce extrema, no fluid in the interior can be colder than the coldest fluid formed at the surface.) However, the value at the surface is given by the boundary condition $b(x, y, z = 0) = f(x, y)$. Thus, the interior cannot fill all the way to the surface with this cold water and there must be a boundary layer connecting the cold, dense interior with the surface; its thickness δ is given by the height scale of (15.12a), that is

$$\delta \sim L\sigma^{-1/5}Ra^{-1/5} = \left(\frac{L^2\nu\kappa}{\sigma\,\Delta b}\right)^{1/5}. \tag{15.13}$$

Such a strong boundary layer will not necessarily be manifest in the velocity field, however, because the no-normal flow boundary condition on the velocity field is satisfied by setting $\psi = 0$ as a boundary condition to the elliptic problem $\nabla^2\psi = \zeta$, where ζ is the prognostic variable in (15.5a), and this boundary condition has a global effect on the velocity field.

   Why is the horizontal scale of the circulation large? The circulation transfers heat meridionally, and it is far more efficient to do this by a single overturning cell than by a multitude of small cells, so although we cannot entirely eliminate the possibility that some instability will produce such small scales of motion, it seems likely the horizontal scale of the mean circulation will be determined by the domain scale. Indeed, at low Rayleigh number we can explicitly calculate an approximate analytic solution to the problem.[9] To do this we define $\mathcal{R} \equiv Ra\alpha^5$ and, with an eye to the nondimensional equations (15.9), we try

$$\hat{\psi} = \mathcal{R}\psi_1 + \mathcal{R}^2\psi_2 + \mathcal{O}(\mathcal{R}^3), \qquad \hat{b} = b_0 + \mathcal{R}b_1 + \mathcal{O}(\mathcal{R}^2). \tag{15.14}$$

We also suppose that the aspect ratio is sufficiently small that $\widehat{\nabla}^2 = \partial^2/\partial\hat{z}^2$. Substituting into (15.9) gives at zeroth order

$$\frac{\partial^2 b_0}{\partial\hat{z}^2} = 0, \tag{15.15}$$

whence $b_0 = f(x, y)$, which satisfies the boundary conditions at both top and bottom. Proceeding a little further reveals that

$$\frac{\partial^4\psi_1}{\partial\hat{z}^4} = -\frac{\partial f}{\partial\hat{y}}, \qquad J(\psi_1, f) = \frac{\partial^2 b_1}{\partial\hat{z}^2}. \tag{15.16a,b}$$

These equations can be solved, but it is clear without explicitly doing so that $\psi_1(y, z) = (\partial f/\partial y)A(z)$ and $b_1(y, z) = (\partial f/\partial y)^2 B(z)$, and therefore that horizontal form of the

solution is determined by the surface forcing, provided there are no meridional walls that force ψ to zero where $\partial f / \partial y \neq 0$. It is important to realise that *even for large diffusion and viscosity there is no stationary solution:* as soon as we impose a temperature gradient at the top the fluid begins to circulate, a manifestation of the dictum that a baroclinic fluid is a moving fluid, encountered in section 4.2. For higher Rayleigh number the perturbation analysis fails and we must resort to numerical solutions; these (e.g., Fig. 15.4), do show the circulation dominated by a single overturning circulation rather than many small convective cells. We cannot rigorously prove that this will always be the case, but a general energetic argument that shows that the flow cannot in fact break up into a succession of ever smaller cells in a turbulent cascade is given in the next section.

15.3 ENERGETICS OF SIDEWAYS CONVECTION

This section is a slight extension of section 2.4.3, but now with a starring role for diffusion and the boundary conditions. Let us write the equations of motion as

$$\frac{\partial \boldsymbol{v}}{\partial t} + (\boldsymbol{f} + 2\boldsymbol{\omega}) \times \boldsymbol{v} = -\nabla B + b\mathbf{k} + \nu \nabla^2 \boldsymbol{v} \qquad (15.17\text{a})$$

$$\frac{\partial b}{\partial t} + \nabla \cdot (b\boldsymbol{v}) = Q = J + \kappa \nabla^2 b \qquad (15.17\text{b})$$

$$\nabla \cdot \boldsymbol{v} = 0. \qquad (15.17\text{c})$$

where B is the Bernoulli function and $Q \ (= \dot{b})$ is the total heating, with J its non-diffusive component.

15.3.1 The energy budget

To obtain an energy budget we follow the procedure of section 2.4.3. First take the dot product of (15.17a) with $\boldsymbol{v}$ to give

$$\frac{1}{2} \frac{\partial \boldsymbol{v}^2}{\partial t} = -\nabla \cdot (\boldsymbol{v} B) + wb + \nu \boldsymbol{v} \cdot \nabla^2 \boldsymbol{v}. \qquad (15.18)$$

Integrating over a domain bounded by rigid walls gives the kinetic energy equation

$$\frac{\mathrm{d}}{\mathrm{d}t} \left\langle \frac{1}{2} \boldsymbol{v}^2 \right\rangle = \langle wb \rangle - \varepsilon, \qquad (15.19)$$

where angle brackets denote a volume integration and $\varepsilon = -\nu \langle \boldsymbol{v} \cdot \nabla^2 \boldsymbol{v} \rangle = \nu \langle \boldsymbol{\omega}^2 \rangle$ is the total dissipation of kinetic energy, a positive definite quantity. Thus, in a statistically steady state in which the left-hand side vanishes after time-averaging, the dissipation of kinetic energy is maintained by the buoyancy flux; that is, by a release of potential energy with light fluid ascending and dense fluid descending.

We obtain a potential energy budget by using (15.17b) to write

$$\frac{\mathrm{D}bz}{\mathrm{D}t} = z \frac{\mathrm{D}b}{\mathrm{D}t} + b \frac{\mathrm{D}z}{\mathrm{D}t} = zQ + bw, \qquad (15.20)$$

and integrating this over the domain gives the potential energy equation

$$\frac{\mathrm{d}}{\mathrm{d}t} \langle bz \rangle = \langle zQ \rangle + \langle bw \rangle.$$

(15.21)

Subtracting (15.21) from (15.19) gives the energy equation

$$\frac{\mathrm{d}}{\mathrm{d}t} \left\langle \frac{1}{2} \boldsymbol{v}^2 - bz \right\rangle = -\langle zQ \rangle - \varepsilon.$$

(15.22)

15.3.2 The maintenance of a circulation and Sandström's theorem

In a statistically steady state the left-hand side of (15.22) vanishes and the kinetic energy dissipation is balanced by the buoyancy source terms; that is

$$\boxed{\langle zQ \rangle = -\varepsilon}.$$

(15.23)

The right-hand side is negative definite, and to balance this the heating must be negatively correlated with height. (Note also that $\langle Q \rangle = 0$ if the fluid is not being heated or cooled overall, and the origin of the z-coordinate is immaterial.) Thus, *in order to maintain a circulation in which kinetic energy is dissipated, the heating must occur, on average, at lower levels than the cooling.* Results resembling this are sometimes called, albeit unjustifiably, 'Sandström's theorem'.[10] In the ocean the non-diffusive heating occurs predominantly at the surface, except for the negligible effects of hydrothermal vents. (In fact, the heating at low latitudes occurs at a slightly higher elevation than the cooling at high latitudes, because sea-level is on average a little higher there.) Thus, $\langle Jz \rangle \approx 0$ and a kinetic-energy-dissipating circulation can *only* be maintained, in the absence of mechanical forcing, if the diffusion is non-zero — in that case heat may be diffused from the surface to depth so effectively providing a deep heat source. In the atmosphere, the heating is mostly at the surface and the cooling is higher up, at lower pressure, so that (15.23) does not provide any particularly useful information.

There are a couple of ways to think intuitively about this result. If the heating is below the cooling, then the heated fluid will expand and become buoyant and rise, and a steady circulation between heat source and heat sink can readily be imagined. But if the heating is above the cooling, there is no obvious pathway between source and sink. Another point of view, more appropriate for a compressible fluid, is in terms of work: if the heating is to do work, as it must because this is the source of the energy that is ultimately dissipated, then the heating and concomitant expansion must occur at a higher pressure than the cooling and concomitant compression.

Surface fluxes, diffusion and diffusivity

Suppose that the only heating to the fluid is via diffusion through the upper surface; that is $J = 0$ in (15.17b). We will show that as $\kappa \to 0$ the kinetic energy dissipation does indeed go to zero.[11] Assuming a statistically steady state, integrating (15.17b) horizontally gives

$$\frac{\partial \overline{bw}}{\partial z} = \kappa \frac{\partial^2 \overline{b}}{\partial z^2},$$

(15.24)

where an overbar indicates a horizontal and time average. Integrating this equation up from the bottom (where there is no flux) to a level z gives

$$\overline{wb} - \kappa \overline{b}_z = 0, \tag{15.25}$$

at every level in the fluid. The two terms on the left-hand-side together comprise the total buoyancy flux through the level z, and this vanishes because there is no buoyancy input except at the surface. If we integrate this vertically we have

$$\langle wb \rangle = H^{-1}\kappa \left[\overline{b}(0) - \overline{b}(-H) \right], \tag{15.26}$$

where the angle brackets denote an average over the entire volume. In the limit $\kappa \to 0$, the integrated advective buoyancy flux will vanish, because the term $\overline{b}(0) - \overline{b}(-H)$ remains finite. (This follows because b is conserved on parcels, except for the effects of diffusion which can only act to reduce the value of extrema in the fluid — see also section 10.5.1. Thus, $\overline{b}(0) - \overline{b}(-H)$ can only be as large as the temperature difference at the surface, which is set by the boundary conditions.)

Now consider the kinetic energy budget. Using (15.22) and (15.26) we have in a statistically steady state

$$\varepsilon = H^{-1}\kappa \left[\overline{b}(0) - \overline{b}(-H) \right]. \tag{15.27}$$

The right-hand side is bounded by the maximum difference of b at the surface, so that kinetic energy dissipation goes to zero if the thermal diffusivity goes to zero; that is, $\varepsilon \to 0$ as $\kappa \to 0$ and in particular $\varepsilon < \kappa b_0/H$ where b_0 is the maximum temperature difference at the surface. We may also consider the limit $(\kappa, \nu) \to 0$ with fixed Prandtl number $\sigma \equiv \nu/\kappa$, and in this limit also the energy dissipation vanishes with κ.

Finally, let us see how the surface temperature is related to the buoyancy flux, for any value of κ. Multiplying (15.17b) by b and integrating over the domain gives the buoyancy variance equation,

$$\frac{1}{2} \frac{\mathrm{d}\langle b^2 \rangle}{\mathrm{d}t} = \kappa \left[\overline{b \frac{\partial b}{\partial z}}\bigg|_{z=0} - \left\langle |\nabla b|^2 \right\rangle \right]. \tag{15.28}$$

We have assumed that the normal derivative of b vanishes on all surfaces except the top one ($z = 0$) and an overbar denotes a horizontal integral. In a statistically steady state,

$$\overline{b \frac{\partial b}{\partial z}}\bigg|_{z=0} = \left\langle |\nabla b|^2 \right\rangle, \tag{15.29}$$

where the overbar and angle brackets now also imply a time average. The right-hand side is positive definite, and thus there must be a positive correlation between b and $\partial b/\partial z$, meaning there is a heat flux into the fluid where it is hot, and a heat flux out of the fluid where it is cold. This result holds no matter whether the upper boundary condition is a condition on b or on $\partial b/\partial z$.

15.3.3 Interpretation

The result encapsulated by (15.27) means that, for a fluid forced only at the surface by buoyancy forcing, as the diffusivity goes to zero so does the energy dissipation. One immediate result, for a fluid of finite viscosity, is that the vorticity in the fluid must go to zero, because $\varepsilon = \nu \langle \omega^2 \rangle$; this in turn means that the flow cannot be baroclinic, because baroclinicity generates vorticity, even in the presence of viscosity (section 4.2). An even more interesting result follows for a fluid with small viscosity. In turbulent flow, the energy dissipation at high Reynolds number is not a function of the viscosity; if the viscosity is reduced, the cascade of energy to smaller scales merely continues to still smaller scale, generating vorticity at these smaller scales, and the energy dissipation is unaltered, remaining finite even in the limit $\nu \rightarrow 0$. In contrast, for a fluid heated and cooled only the upper surface, the energy dissipation *tends to zero* as $\kappa \rightarrow 0$, whether or not one is in the high Reynolds number limit. This means that vorticity cannot be generated at the viscous scales by the action of a turbulent cascade, for that would lead to energy dissipation. Effectively, the result prohibits an ocean that is forced only at the surface by a buoyancy flux from having an 'eddy viscosity' that would enable the fluid to efficiently dissipate energy, and if there is no small scale motion producing an eddy viscosity there can be no eddy diffusivity either. This is a rather different picture from that which describes the real ocean, where there is some dissipation of energy in the interior because of breaking gravity waves, and dissipation at the boundary in Ekman layers, and the eddy diffusivity is needed for there to to be a non-negligible buoyancy-driven meridional overturning circulation.

Of course, thermal forcing in the ocean is in part an imposed flux, coming from radiation among other things, and this penetrates below the surface. However, this makes little real physical difference, provided that this forcing remains confined to the upper ocean. If so, then for any level below this forcing we still have the result (15.25), and the final result (15.27) holds, assuming that the range of temperatures produced by the forcing is still finite.

15.3.4 The importance of mechanical forcing

The real ocean *does* have a deep circulation, so something is missing. Suppose we add a mechanical forcing, $\boldsymbol{F}$, to the right-hand-side of (15.17a); this might represent wind forcing at the surface, or tidess. The kinetic energy budget becomes

$$\varepsilon = \langle wb \rangle + \langle \boldsymbol{F} \cdot \boldsymbol{v} \rangle = H^{-1}\kappa[\overline{b}(0) - \overline{b}(-H)] + \langle \boldsymbol{F} \cdot \boldsymbol{v} \rangle. \tag{15.30}$$

In this case even for $\kappa = 0$ there is a source of energy and turbulence (i.e., a dissipative circulation) can be maintained. We emphasize that the results of (15.23) and (15.27) do not prohibit there being a thermal circulation, with fluid sinking at high latitudes and rising at low. However, in the absence of any mechanical forcing this circulation must be laminar as $\kappa \rightarrow 0$, even at high Rayleigh number, and the flow is not allowed to break in such a way that energy can be dissipated — a very severe constraint that most flows cannot satisfy. The solution most likely adopted by the fluid is for the flow to

become confined to a very thin layer at the surface, with no abyssal motion at all, which is completely unrealistic vis-a-vis the observed ocean.

Now, turbulent motion at small scales provides a mechanism of mixing and so can effectively generate an 'eddy diffusivity' of buoyancy. *Given* such an eddy diffusivity, it is by no means self-evident that wind forcing is subsequently important for the overturning circulation. That is to say, it is useful to think of mechanical forcing as having two distinct effects:

(i) The wind provides a stress on the surface that may directly drive the large-scale circulation, including the overturning circulation. (An explicit example of this is discussed in section 16.5.)

(ii) Both tides and the wind provide a mechanical source of energy to the system that allows the flow to become turbulent and so provides a source for an eddy diffusivity and eddy viscosity.

In either case, we may conclude that presence of mechanical forcing is necessary for there to be an overturning circulation in the world's oceans of the kind observed. In the remainder of this chapter we ignore the first of these effects, and we suppose that the most important effect of the wind is that it provides an eddy diffusivity to the ocean that is much larger than the molecular value; this then allows large volumes of the ocean to become mixed, so allowing a substantial buoyancy-driven overturning circulation (sometimes called a thermohaline circulation). We first consider extremely simple models of this circulation, so-called box models.

15.4 SIMPLE BOX MODELS

Even though they are far simpler than the real ocean, the fluid dynamical models of the previous section are still quite daunting. The analysis that can be performed is either very specific and of little generality, for example the construction of solutions at low Rayleigh number, of it is a very general form, being of the form of scaling or energetic arguments at high Rayleigh number. Models based on the fluid dynamical equations do not easily allow for the construction of explicit solutions in the parameter regime — high Rayleigh and Reynolds numbers — of interest. It is therefore useful to consider an extreme simplification of the overturning circulation, *box models*. These are very simple caricatures of the circulation, constructed by dividing the ocean into a very small number of boxes with simple rules determining the transport of fluid properties between them.[12] The purist may consider this section a diversion away from a consideration of the fluid dynamical properties of the ocean, but such box models have been quite fecund and an evident source of qualitative understanding, and thus find a place in our discussion.

15.4.1 A Two-Box Model

Consider two boxes as illustrated in Fig. 15.6. Each box is well-mixed and has a uniform temperature and salinity, T_1, T_2 and S_1, S_2. The boxes are connected with a capillary tube at the bottom along which the flow is viscous, obeying Stokes' Law. That
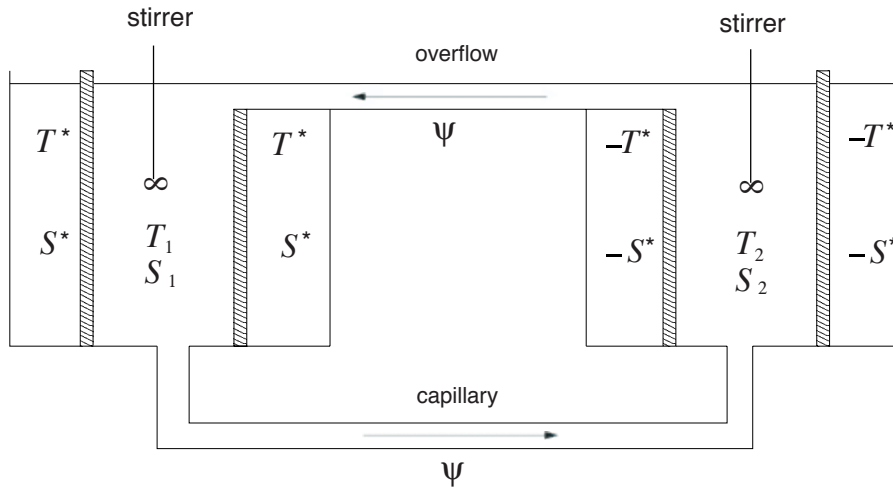
Fig. 15.6 A two-box model of relevance to the overturning circulation of the ocean. The shaded walls are porous, and each box is well-mixed by its stirrer. Temperature and salinity evolve by way of fluid exchange between the boxes via the capillary tube and the overflow, and by way of relaxation with the two infinite reservoirs at $(+T^*, +S^*)$ and $(-T^*, -S^*)$.

is, the flow along the tube is proportional to the pressure gradient which, because the flow is hydrostatic, is proportional the density difference between the two boxes. An overflow at the top keeps the upper surfaces of the two boxes at the same level. Thus, the circulation is given by

$$\Psi = A(\rho_1 - \rho_2), \tag{15.31}$$

where Ψ is proportional to the flow in the pipe, ρ_1 and ρ_2 are the densities of the fluids in the two boxes and A is a constant. The boxes are enclosed by porous walls beyond which are reservoirs of constant temperature and salinity, and we are at liberty to choose the origin of the temperature scale such that the two reservoirs are at $+T^*$ and $-T^*$, and similarly for salinity. Thus, heat and salinity are transferred into and out of the boxes as represented by simple linear laws and we have

$$\frac{dT_1}{dt} = c(T^* - T_1) - 2|\Psi|(T_1 - T_2), \quad \frac{dT_2}{dt} = c(-T^* - T_2) - 2|\Psi|(T_2 - T_1),$$

$$\frac{dS_1}{dt} = d(S^* - S_1) - 2|\Psi|(S_1 - S_2), \quad \frac{dS_2}{dt} = d(-S^* - S_2) - 2|\Psi|(S_2 - S_1).$$

$$\tag{15.32}$$

Note that the advective transfer is independent of the sign the circulation, because it occurs through both the capillary tube and the overflow.

From these equations it is apparent that the sum of the temperatures, $T_1 + T_2$ decays to zero and is uncoupled from the difference, and similarly for salinity. Defining $\widehat{T} =$

$(T_1 - T_2)/(2T^*)$ and $\widehat{S} = (S_1 - S_2)/(2S^*)$ then gives

$$
\begin{aligned}
\frac{d\widehat{T}}{dt} &= c(1 - \widehat{T}) - 2|\Psi|\widehat{T} \\
\frac{d\widehat{S}}{dt} &= d(1 - \widehat{S}) - 2|\Psi|\widehat{S}
\end{aligned}
\tag{15.33}
$$

Using a linear equation of state of the form $\rho = \rho_0(1 - \beta_T T + \beta_S S)$ (where the variables are dimensional) the circulation (15.31) becomes

$$
\Psi = 2\rho_0 T^* \beta_T A \left(-\widehat{T} + \frac{\beta_S S^*}{\beta_T T^*} \widehat{S} \right).
\tag{15.34}
$$

Finally, nondimensionalizing time using $\tau = ct$, the equations of motion become

$$
\frac{d\widehat{T}}{d\tau} = (1 - \widehat{T}) - |\Phi|\widehat{T},
\tag{15.35a}
$$

$$
\frac{d\widehat{S}}{d\tau} = \delta(1 - \widehat{S}) - |\Phi|\widehat{S},
\tag{15.35b}
$$

$$
\Phi = -\gamma(\widehat{T} - \mu\widehat{S}),
\tag{15.35c}
$$

where the three parameters that determine the behaviour of the system are

$$
\gamma = \frac{4\rho_0 T^* \beta_T A}{c}, \qquad \delta = \frac{d}{c}, \qquad \mu = \frac{\beta_S S^*}{\beta_T T^*}.
\tag{15.36}
$$

The parameter γ measures the overall strength of the forcing in determining the strength of the circulation, and is the ratio of a relaxation to an advective timescale. The parameter δ is the ratio of the reciprocal time constants of temperature and salinity relaxation, and μ is a measure of the ratio of the effect of the salinity and temperature forcings on the density. Salinity transfer will normally be much slower than heat transfer so that $\delta \ll 1$, whereas if salinity and temperature are both to play a role in the dynamics we need $\mu = \mathcal{O}(1)$. We also might expect both advection and relaxation to be important if $\gamma = \mathcal{O}(1)$, and this will depend on the properties of the capillary tube.

Interpretation

The above model describes a potentially real system, one that might be constructed in the laboratory, and one with relevance to aspects of the ocean circulation. One box then represents the entire high-latitude ocean and the other the entire low-latitude ocean, and the capillary tube and the overflow carry the overturning circulation between them. The reservoirs at $\pm T^*$ and $\pm S^*$ represent the atmosphere. Typically, we would choose the low latitudes to be both heated and salted (the latter because of the low rainfall and high evaporation in the subtropics) and the high latitudes to be cooled and freshened by rainfall. Thus, T^* and S^* have the same sign, and they force the circulation in opposite directions. Given the common fluid-dynamical experience that the behaviour of highly-truncated systems often has little resemblance to that of the complete system,

this may only be a cartoon of the ocean circulation. For example, we have restricted the circulation to be of basin scale, and the parameterization of the intensity of the overturning circulation by (15.35c) must be regarded with caution, because it represents a frictionally controlled flow rather than a nearly inviscid geostrophic flow. However, observations and numerical simulations do indicate that the overturning circulation does have a relatively simple vertical and horizontal structure: the circulation in the North Atlantic is similar to that of a single cell, for example, indicating that an appropriate low-order model may be useful.

One might also question the oceanic appropriateness of the linear relaxation terms. For temperature, the bulk ærodynamic formulae often used to parameterize air-sea transport do have a similar form, but the freshening of sea-water by rainfall is more akin to an imposed (negative) flux of salinity, and evaporation is a function of temperature. An alternative might be to impose a salt flux so that

$$\frac{\mathrm{d}}{\mathrm{d}t}(S_1 - S_2) = 2E - 2|\Psi|(S_1 - S_2) \tag{15.37}$$

where E is an imposed, constant, rate of salt exchange with the atmosphere. After nondimensionalization, using E/c to nondimensionalize salt, (15.35b) is replaced by

$$\frac{\mathrm{d}S}{\mathrm{d}\tau} = 1 - |\Phi|S. \tag{15.38}$$

Another aspect of the model that is oceanographically questionable is that it assumes that the water masses can be mixed below the surface. Thus, when water enters one box from the other it immediately mixes with its surroundings. Without the stirrer to ensure this this would not occur and the equations of box model would not represent a real system. In the real ocean, most of the mixing of water masses seems to happen near the surface (in the mixed layer) and near lateral boundaries or possibly regions of steep topography. Elsewhere in the ocean mixing is quite small, and likely far from sufficient to mix a large volume of water in the advective or relaxation times of the box model. We will defer consideration of this and continue with an analysis of the model.

Solutions

Perhaps the most interesting aspect of the set (15.35) is that it exhibits *multiple equilibria;* that is, there are multiple steady solutions with the same parameters. Equilibria occur when the time-derivatives vanish, and the circulation satisfies

$$\Phi = \phi(\Phi) \equiv \gamma \left(\frac{-1}{1 + |\Phi|} + \frac{\mu}{1 + |\Phi|/\delta} \right). \tag{15.39}$$

A graphical solution of this is obtained as the intercept of the right-hand side with the left-hand side, the latter being a straight line through the origin at an angle of 45°, and this is plotted in Fig. 15.7.

Evidently, for a range of parameters three solutions are possible, whereas for others only one solution exists. Although a fairly complete analysis of the nature of the steady solutions is possible, it is instructive to consider the special case with $\gamma \gg 1$ and
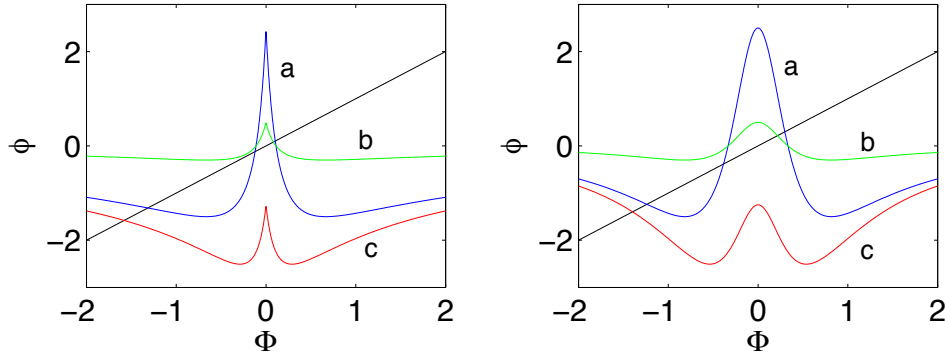
Fig. 15.7 Left panel: Graphical solution of the two-box model. The straight line has unit slope and passes through the origin, and the curved lines plot the function $\phi(\Phi)$ as given by the right-hand-side of (15.39). The intercepts of the two are solutions to the equation. The parameters for the three curves are: a, $\gamma = 5$, $\delta = 1/6$, $\mu = 0.1.5$; b, $\gamma = 1$, $\delta = 1/6$, $\mu = 1.5$; c, $\gamma = 5$, $\delta = 1/6$, $\mu = 0.75$. Right panel: same except with Φ^2 in place of $|\Phi|$ on rhs of (15.39).

$\delta \ll 1$. This corresponds to the situation in which the advective timescale is shorter than the diffusive one and temperature relaxation is much faster than salt relaxation. Two of the solutions are then close to the origin, with $\Phi \ll 1$ and satisfying

$$\Phi = \phi(\Phi) \equiv \gamma \left(-1 + \frac{\mu\delta}{\delta + |\Phi|} \right). \tag{15.40}$$

giving for small $|\Phi|$

$$\Phi \approx \pm[\delta(\mu - 1)]. \tag{15.41}$$

Only the positive solution will be stable, and this solution is driven by the density gradient in salinity; the high salinity of box 1 outweighs (so to speak) the compensating fact that it is also warmer, leading to a flow along the capillary tube from box 1 to box 2. Solving for temperature and salinity we find that $T \approx 1$ (i.e., it is close to its relaxation value and hardly altered by advection), and $S \approx 2 - \mu$ or μ, for $\mu < 2$ and $\mu > 2$ respectively. The saline contribution to density can therefore be larger than that of temperature, and indeed is so for this solution.

The other solution has a circulation far from the origin, and the balance in (15.39) is between the left-hand-side and the first term on the right. In the limiting case we find

$$\Phi \approx -\sqrt{\gamma}. \tag{15.42}$$

This solution has a density gradient dominated by the temperature effect: the temperature difference is $T \approx 1/\sqrt{\gamma}$ whereas the salinity difference is $S \approx \delta/\sqrt{\gamma}$, and thus its effect on density is much smaller.
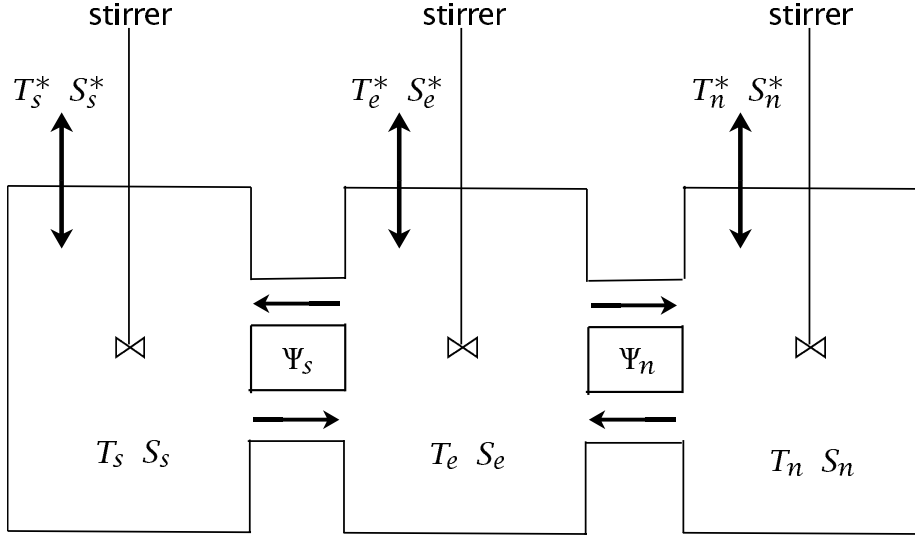
Fig. 15.8 A three-box model. Each box has a constant value of temperature and salinity within it, each exchanges fluid with its neighbour, and in each the temperature and salinity are relaxed back to fixed atmospheric values.

15.4.2 More boxes

More boxes can be added in a variety of ways and, now forgoing an easy relevance to a laboratory apparatus, one such is illustrated in Fig. 15.8. The three boxes represent the mid- and high-latitude northern hemisphere, the mid- and high-latitude southern hemisphere, and the equatorial regions. Each of the three boxes can exchange fluid with its neighbour, and each is also in contact with a reservoir and subject to a relaxation to a fixed value of temperature and salinity, (T_s^*, S_s^*), (T_e^*, S_e^*), (T_n^*, S_n^*). (A variation on this theme allows direct communication between the two poleward boxes.) Then, with obvious notation, we infer the equations of motion:

$$\frac{dT_s}{dt} = c(T_s^* - T_s) - 2|\Psi_s|(T_s - T_e), \qquad \frac{dT_n}{dt} = c(T_n^* - T_s) - 2|\Psi_n|(T_n - T_e),$$

$$\frac{dT_e}{dt} = c(T_e^* - T_e) - |\Psi_s|(T_e - T_s) - |\Psi_n|(T_e - T_n),$$

$$\frac{dS_s}{dt} = d(S_s^* - S_s) - 2|\Psi_s|(S_s - S_e), \qquad \frac{dS_n}{dt} = d(S_n^* - S_s) - 2|\Psi_n|(S_n - S_e),$$

$$\frac{dS_e}{dt} = d(S_e^* - S_e) - |\Psi_s|(S_e - S_s) - |\Psi_n|, (S_e - S_n),$$

$$(15.43)$$

with flow rates given by the density differences.

$$\Psi_s = A\rho_0[-\beta_T(T_s - T_e) + \beta_S(S_s - S_e)], \quad \Psi_n = A\rho_0[-\beta_T(T_n - T_e) + \beta_S(S_n - S_e)].$$

$$(15.44)$$

These equations may be nondimensionalized and reduced to four prognostic equations for the quantities $T_e - T_n$, $T_e - T_s$, $S_e - S_n$, $S_e - S_s$. Not surprisingly, multiple equi-
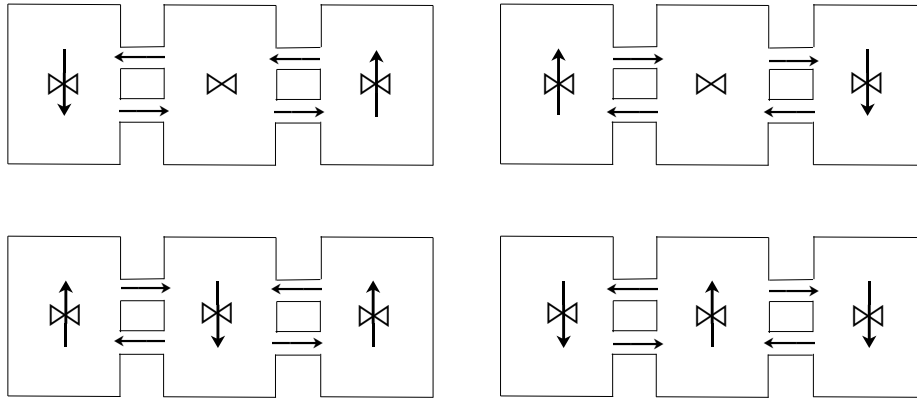
Fig. 15.9 Schematic of four solutions to the three box model with the symmetric forcing $S_s^* = S_n^*$ and $T_n^* = T_s^*$. The two solutions on the top row have an asymmetric, 'pole-to-pole', circulation whereas the solutions on the bottom row are symmetric.[13]

libria can again be found. One particularly interesting aspect is that stable asymmetric solutions arise with symmetric forcing ($T_s^* = T_n^*$, $S_s^* = S_n^*$). These effectively have a pole-to-pole circulation, illustrated in the upper row of Fig. 15.9. Such a circulation can be thought of as the superposition of a thermal circulation in one hemisphere and a salinity-driven circulation in the other.

The box models are useful because they are suggestive of behaviour that might occur in real fluid systems, and because they provide a means of interpreting behaviour that does occur in more complete numerical models, and perhaps in the real world. But without other supporting evidence the solutions found in box models should not be regarded as representing real solutions of the fluid equations for the world's oceans.[14]

15.5 A LABORATORY MODEL OF THE ABYSSAL CIRCULATION

We now return to a more fluid dynamical description of the deep ocean circulation, and consider two simple, closely related, models that are relevant to aspects of the deep circulation. The first, which we consider in this section, is a laboratory model that, although originally envisioned as being a prototype for the deep circulation, is also illustrative of the principles of the wind-driven circulation. The second model, considered in the sections following, is explicitly a model of the deep circulation. Both models are severe idealizations that describe only limited aspects of the circulation.

15.5.1 Set-up of the laboratory model

Let us consider flow in a rotating tank, as illustrated in Fig. 15.10. The fluid is confined by vertical walls to occupy a sector, and the entire tank rotates anti-clockwise when viewed from above, like the Northern Hemisphere. When the fluid is stationary in the
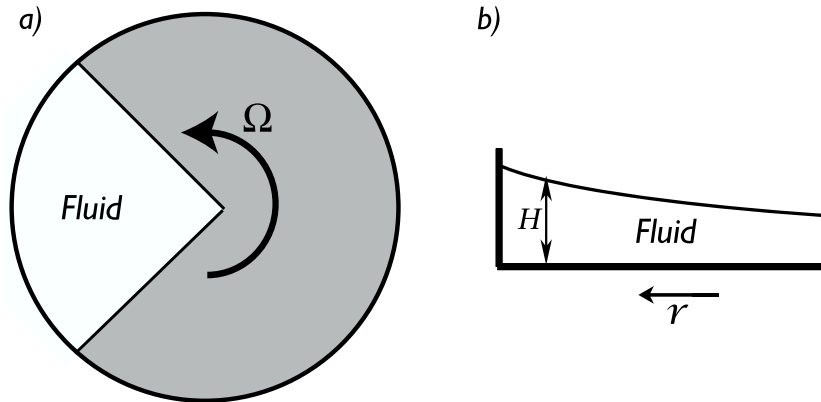
Fig. 15.10 The experimental set-up in the Stommel-Arons-Faller rotating tank experiment. (a) A plan view of the apparatus. The fluid is contained in the sector at left. (b) Side view. The free surface of the fluid slopes up with increasing radius, giving a balance (in the rotating frame) between the centrifugal force pointing outwards and the pressure force pointing inwards. Small pipes may be introduced into the fluid to provide mass sources and sinks.

rotating frame, the fluid slopes up toward the outer edge of the tank and the balance of forces in the rotating frame is between a centrifugal force pointing outwards and the pressure gradient due to the sloping fluid pointing inwards. In the inertial frame of the laboratory itself, the pressure gradient pointing inwards provides a centripetal force that causes the fluid to accelerate toward the center of the tank, resulting in a circular motion. (Recall that steady circular motion is always accompanied by an acceleration toward the center of the circle.) This set-up, and the accompanying theory, is known as the *Stommel-Arons-Faller* model.[15] The motivation of this construct is clear, in that the sector represents an ocean basin. However, rather than driving the fluid with wind or by differential heating, we drive it with localized mass sources and sinks, for example from a small pipes inserted into the tank.

15.5.2 Dynamics of flow in the tank

Let us assume that motion of the fluid in the tank is sufficiently weak that its Rossby number is small, and that it obeys the shallow water planetary geostrophic equations, namely

$$f_0 \times u = -g\nabla h + \Omega^2 r\,\hat{\mathbf{r}} + F, \qquad (15.45a)$$

$$\frac{\partial h}{\partial t} + \nabla \cdot (uh) = S \qquad (15.45b)$$

where $\hat{\mathbf{r}}$ is a unit vector in the direction of increasing r, $\boldsymbol{F}$ represents frictional terms and S represents mass sources. These two equations yield the potential vorticity equation,

$$\frac{\mathrm{D}}{\mathrm{D}t}\left(\frac{f_0}{h}\right) = \frac{\mathrm{curl}_z \boldsymbol{F}}{h} - \frac{f_0 S}{h^2}. \tag{15.46}$$

Let us write the height field as

$$h = H(r,t) + \eta(r,\theta,t) \tag{15.47}$$

where $H(r,t)$ is the height field corresponding to the rest state of the fluid (in the rotating frame) and η the perturbation. Thus, from (15.45a)

$$0 = -g\nabla H + \Omega^2 r\hat{\mathbf{r}}, \tag{15.48}$$

which gives

$$H = \frac{\Omega^2 r^2}{2g} + \widehat{H}(t), \tag{15.49}$$

where $\widehat{H}$ is a measure of the overall mass of the fluid. Its rate of change is determined by the mass source

$$\frac{\mathrm{d}\widehat{H}}{\mathrm{d}t} = \langle S \rangle, \tag{15.50}$$

the angle brackets indicating a domain average. The equations of motion (15.45a), and (15.45b) become

$$\boldsymbol{f}_0 \times \boldsymbol{u} = -g\nabla\eta + \boldsymbol{F}, \tag{15.51a}$$

$$\frac{\partial}{\partial t}(\eta + H) + \nabla \cdot [\boldsymbol{u}(\eta + H)] = 0. \tag{15.51b}$$

Eq. (15.51a) tells us that, away from frictional regions, the velocity is in geostrophic balance with the pressure field due to the perturbation height η.

Let us now suppose $|\eta| \ll H$, which holds if the mass source is small and gentle enough. Then (15.51b) may be written

$$\frac{\partial H}{\partial t} + \nabla \cdot (\boldsymbol{u}H) = 0. \tag{15.52}$$

In this approximation, the potential vorticity equation (15.46) becomes, away from friction and mass sources,

$$\frac{\mathrm{D}}{\mathrm{D}t}\left(\frac{f_0}{H}\right) = 0 \quad \text{or} \quad \frac{\mathrm{D}H}{\mathrm{D}t} = 0. \tag{15.53a,b}$$

where the second equation follows because f_0 is a constant. (This equation also follows directly from (15.52), because the velocity is geostrophic and divergence-free where friction is absent; however, it is better thought of as a potential vorticity equation, not a mass conservation equation.) Eq. (15.53b) means that fluid columns change position

in order to keep the same value of H. Further, because H only varies with r, (15.53b) becomes

$$\frac{\partial H}{\partial t} + v_r \frac{\partial H}{\partial r} = 0, \tag{15.54}$$

which, using (15.49) and (15.50), gives

$$\boxed{v_r = -\frac{g}{\Omega^2 r} \langle S \rangle}. \tag{15.55}$$

This is a remarkable result, for it implies that, if $\langle S \rangle$ is positive the flow if is *toward* the apex of the dish except at the location of the mass sources and in frictional boundary layers, *no matter where the mass source is actually located*. The explanation of this counterintuitive result is simple enough: if $\langle S \rangle > 0$ the overall height of the fluid is increasing with time. Thus, in order that a given material column of fluid may keep its height fixed, it must move toward the apex of the dish. The full velocity field may be obtained, away from the frictional regions, using the divergence-free nature of the velocity:

$$\nabla \cdot \boldsymbol{u} = \frac{\partial (r v_r)}{\partial r} + \frac{\partial v_\theta}{\partial \theta} = 0. \tag{15.56}$$

Then, using (15.55), $\partial v_\theta / \partial \theta = 0$ except at a source or sink, or in a frictional boundary layer. Assuming there is only one frictional boundary layer, $v_\theta = 0$ except at those latitudes (i.e., values of r) that contain a mass source or sink.

Suppose then, that we introduce a localized mass source somewhere in the domain, and a localized mass sink of equal strength somewhere else. According to our heuristic theory, there is no flow in the interior of the domain that can provide a passage from the mass source to the sink. Thus, there must be *boundary layers* in which frictional effects are important, and which set themselves up in such a way to satisfy mass conservation. But mass conservation alone is insufficient to determine where the boundary layers might be — for this we need some vorticity dynamics. Now, away from the mass source, but including friction, the potential vorticity equation is

$$\frac{\mathrm{D}}{\mathrm{D}t}\left(\frac{f_0}{H}\right) = \frac{\mathrm{curl}_z \boldsymbol{F}}{H}, \tag{15.57}$$

and the free surface of the water slopes downward toward the apex, as illustrated in Fig. 15.10. Now, suppose that there are mass source and a sink of equal maginudes, with the source further from the apex than the sink, as in the panel at the bottom right of Fig. 15.11. The flow from source to sink must be along either the left of right boundary of the container. This flow is toward smaller values of H, and therefore the left-hand side of (15.57) is positive (just as for poleward flow in the ocean on a sphere or β-plane). To balance this the friction in the boundary current must import a positive vorticity to the flow (i.e., $\mathrm{curl}_z \boldsymbol{F} > 0$), implying a *western* boundary layer, i.e., a boundary layer on the left of the container, for then the flow itself then has an anticyclonic (clockwise) sense and friction will normally oppose this. For example, if $\boldsymbol{F} = -\lambda \boldsymbol{u}$ the right hand side of (15.57) is $-(\lambda/H)\mathrm{curl}_z \boldsymbol{u}$ and this is positive if the flow is clockwise. A little more
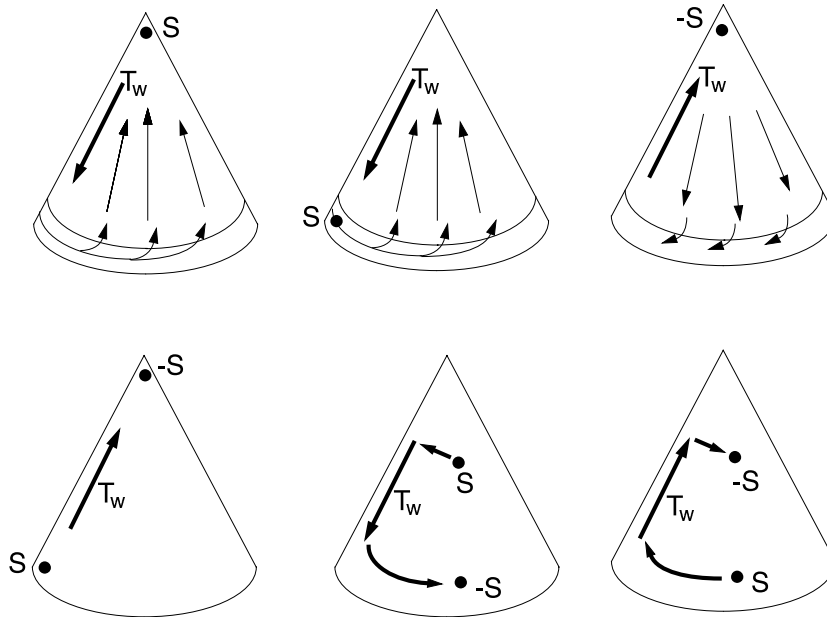
Fig. 15.11 Idealized examples of the flow in the rotating sector experiments, with various locations of a source (S) or sink ($-S$) of mass

thought will reveal that a western boundary layer is general feature of the flow, and is not dependent on the placement of mass sources or sinks. If there is only a net source of mass, as for example in the upper left example of Fig. 15.11, then the interior mass flow will be toward the apex, the flow in the boundary layer away from the apex, but again requiring a western boundary layer to achieve a balance in the potential vorticity equation. It is clear that this flow is in some ways analogous to flow on the β-plane, and that in particular:

   (i) The r-dependence of the height field provides a background potential vorticity gradient, analogous to the β-effect.

  (ii) The time-dependence of H is analogous to a wind curl, for it is this that ultimately drives the fluid motion.

The analogies are drawn out explicitly in shaded box on the next page; the box also includes a column for abyssal flow in the ocean, discussed in the next two sections.

15.6 A MODEL FOR OCEANIC ABYSSAL FLOW

We will now extend the reasoning applied to the rotating tank to the rotating sphere, and so construct a model — the *Stommel-Arons model* — of the abyssal flow in the ocean.[16] The basic idea is simple: we will model the deep ocean as a single layer of homogeneous fluid in which there is a localized injection of mass at high latitudes, representing convection (Fig. 15.12). However, unlike the rotating dish, mass is extracted from this layer by upwelling into the warmer waters above it, keeping the average thickness of

Analogies between a rotating dish, wind-driven and abyssal flows

Consider homogeneous models of (i) rotating dish, (ii) wind-driven flow on the β-plane, and (iii) abyssal flow on the the β-plane. We model all with a single layer of homogeneous fluid satisfying the planetary geostrophic equations. In (i) the mass source, $\langle S \rangle$, is localized and the total depth of the fluid layer changes with time; fluid columns move to keep their depth constant. In (ii) there is no mass source and depth of the fluid layer is constant; the fluid motion is determined by the wind stress curl, $\mathrm{curl}_z \boldsymbol{\tau}$, and by β. In (iii) the fluid source (convection) is localized at high latitudes and exactly balanced by a mass loss, S_u, due to upwelling everywhere else, so that layer depth is constant and S_u is uniform and negative nearly everywhere. The equations below then apply away from frictional boundary layers and localized mass sources:

(i) Rotating dish	*(ii) Wind-driven flow*	*(iii) Abyssal flow*

PV Conservation

$$\frac{\mathrm{D}}{\mathrm{D}t}\left(\frac{f_0}{H}\right) = 0 \qquad \frac{\mathrm{D}}{\mathrm{D}t}\left(\frac{f}{H_0}\right) = \frac{1}{H_0}\mathrm{curl}_z\boldsymbol{\tau} \qquad \frac{\mathrm{D}}{\mathrm{D}t}\left(\frac{f}{h}\right) = -\frac{f S_u}{h^2}$$

This leads to

$$v_r\frac{\partial H}{\partial r} = -\frac{\partial H}{\partial t} \qquad \frac{v}{H_0}\frac{\partial f}{\partial y} = \frac{1}{H_0}\mathrm{curl}_z\boldsymbol{\tau} \qquad \frac{v}{h}\frac{\partial f}{\partial y} = -\frac{f S_u}{h^2}$$

and

$$v_r = -\frac{g}{\Omega^2 r}\langle S\rangle \qquad v = \frac{1}{\beta}\mathrm{curl}_z\boldsymbol{\tau} \qquad v = -\frac{f S_u h}{\beta}$$

$\langle S\rangle$ is localized mass source	$\mathrm{curl}_z\boldsymbol{\tau}$ is wind-stress curl	S_u is upwelling mass loss

Meridional mass flow away from boundaries is thus determined by:

Sign (and not location) of localized mass source, $\langle S\rangle$.	Sign of wind-stress curl, $\mathrm{curl}_z\boldsymbol{\tau}$.	Upwelling and sign of f, so polewards if $S_u < 0$ (upwelling).
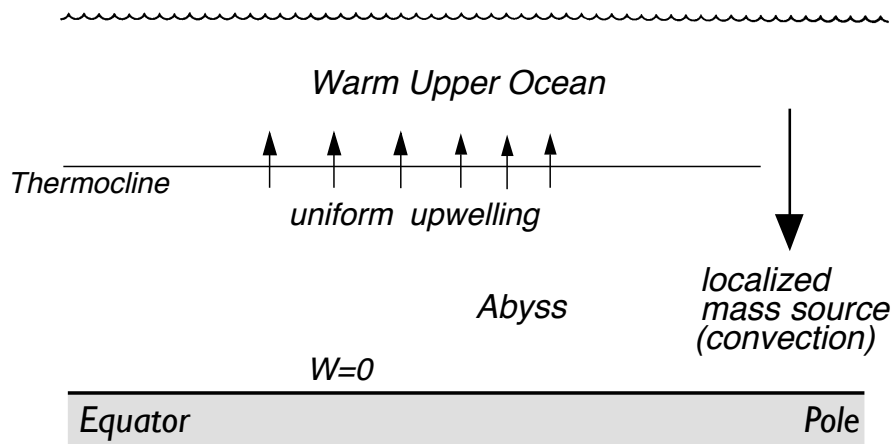
Fig. 15.12 The structure of simple Stommel-Arons ocean model of the abyssal circulation. Convection at high latitudes provides a localized mass-source to the lower layer, and upwelling through the thermocline provides a more uniform mass sink.

the abyssal layer constant. We assume that this upwelling is nearly uniform, that the ocean is flat-bottomed, and that a passive western boundary current may be invoked to satisfy mass conservation, and which does not affect the interior flow. Obviously, these assumptions are very severe and the model can at best be a conceptual model of the real ocean. Given that, we will work in Cartesian coordinates on the β-plane, and use the planetary geostrophic approximation. Our treatment in this section is physically based but quite heuristic; in section 15.7 we are a little more mathematical and a little more formal.

The momentum and mass continuity equations are

$$\boldsymbol{f} \times \boldsymbol{u} = -\nabla\phi \quad \text{and} \quad \nabla \cdot \boldsymbol{u} = -\frac{\partial w}{\partial z}, \tag{15.58}$$

which together yield the familiar balance,

$$\beta v = f\frac{\partial w}{\partial z}. \tag{15.59}$$

Except in the localized regions of convection, the vertical velocity is, by assumption, positive and uniform at the top of the lower layer, and zero at the bottom. Thus (15.59) becomes

$$v = \frac{f}{\beta}\frac{w_0}{H}. \tag{15.60}$$

where w_0 is the uniform upwelling velocity and H the layer thickness. Thus, the flow is *polewards* everywhere (including the Southern hemisphere), vanishing at the equator.
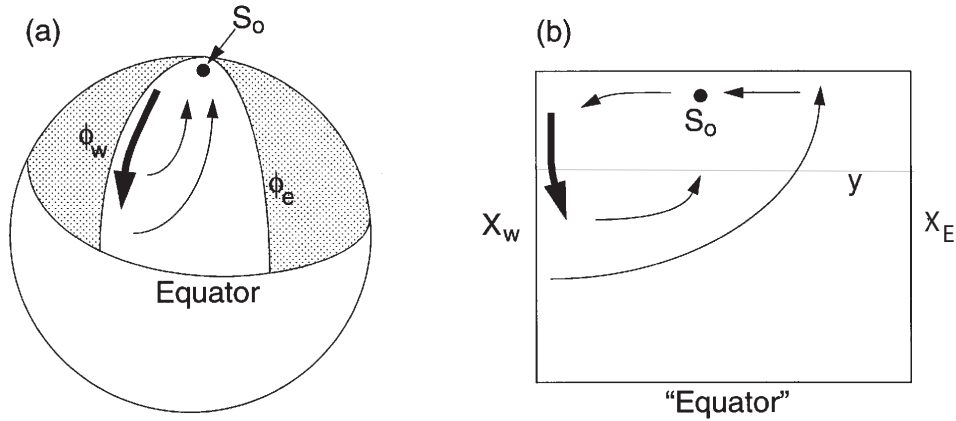
Fig. 15.13 Abyssal circulation in a spherical sector (left) and in a corresponding Cartesian rectangle (right).

15.6.1 Completing the solution

Since $v = f^{-1}(\partial\phi/\partial x)$, the pressure is given by

$$\phi = \int_{x_0}^{x} \left(\frac{f^2 w_0}{\beta H} \right) dx' \tag{15.61}$$

where x_0 is a constant of integration, to be determined by the boundary conditions. Because there no flow into the Eastern boundary, x_e we set $\phi = $ constant at $x = x_e$, and because this is a one-layer model we are at liberty to set that constant equal to zero. Thus,

$$\phi(x) = -\int_{x}^{x_e} \left(\frac{f^2 w_0}{\beta H} \right) dx' = -\frac{f^2}{\beta H} w_0 (x_e - x). \tag{15.62}$$

The zonal velocity follows using geostrophic balance,

$$u = \frac{1}{f} \frac{\partial \phi}{\partial y} = \frac{2}{H} w_0 (x_e - x), \tag{15.63}$$

where we have also used $\partial f/\partial y = \beta$ and $\partial \beta/\partial y = 0$. Thus the velocity is eastward in the interior, and independent of f and latitude, provided x_e is not a function of y.

Using (15.60) and (15.63) we can confirm mass conservation is indeed satisfied:

$$\frac{\partial u}{\partial x} + \frac{\partial v}{\partial y} + \frac{\partial w}{\partial z} = -\frac{2w_o}{H} + \frac{w_0}{H} + \frac{w_0}{H} = 0 \tag{15.64}$$

15.6.2 Application to the ocean

Let us consider a rectangular ocean with a mass source at the northern boundary, balanced by uniform upwelling (see figures 15.13 and 15.14). Since the interior flow will
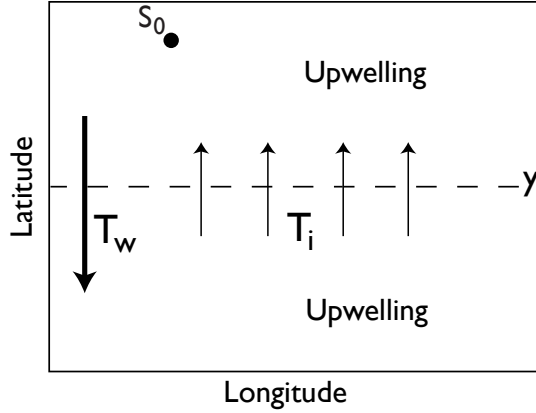
Figure 15.14 Mass budget in an idealized abyssal ocean. Polewards of some latitude y, the mass source (S_0) plus the polewards mass flux across y (T_i) are equal to sum of the southwards mass flux in the western boundary current (T_w) and the integrated loss due to upwelling (U) polewards of y. See (15.65).

be northwards, we anticipate a southwards flowing western boundary current to balance mass. Conservation of mass in the area poleward of the latitude y demands that

$$S_0 + T_i(y) = -T_w(y) + U(y) \tag{15.65}$$

where S_0 is the strength of the source, T_w the transport in the western boundary current (positive if polewards), T_i the (polewards) transport in the interior, and U is the integrated loss due to upwelling polewards of y. Then, using (15.60),

$$T_i = \int_{x_w}^{x_e} vH \, dx = \int_{x_w}^{x_e} \frac{f w_o}{\beta} \, dx = \frac{f}{\beta} w(x_e - x_w). \tag{15.66}$$

The upwelling loss is given by

$$U = \int_{x_w}^{x_e} \int_y^{y_n} w \, dx = w_0(x_e - x_w)(y_n - y) \tag{15.67}$$

Assuming the source term is known, then using (15.65) we obtain the strength of the western boundary current,

$$-T_w(y) = S_0 + T_i - U = S_0 + \frac{f}{\beta} w(x_e - x_w) - w_0(x_e - x_w)(y_n - y). \tag{15.68}$$

To close the problem we note that over the entire basin mass must be balanced, which gives a relationship between w and S_0,

$$S_0 = w_0 \Delta x \, \Delta y, \tag{15.69}$$

where $\Delta x = x_e - x_w$ and $\Delta y = y_n - y_s$. where y_s is the southern boundary of the domain. Using (15.69), (15.68) becomes

$$\begin{aligned} -T_w(y) &= -w_0 \left(\Delta x(y_n - y) - \frac{f}{\beta} \Delta x - \Delta x \Delta y \right) \\ &= w_0 \Delta x \left(y - y_s + \frac{f}{\beta} \right). \end{aligned} \tag{15.70}$$

Figure 15.15 Schematic of a Stommel-Arons circulation in a single sector. The transport of Western boundary current is greater than that provided by the source at the apex, illustrating the property of *recirculation.* The transport in the western boundary current T_w decreases in intensity equatorwards, as it loses mass to the polewards interior flow, and thence to upwelling. The integrated sink, due to upwelling, U, exactly matches the strength of the source, S.
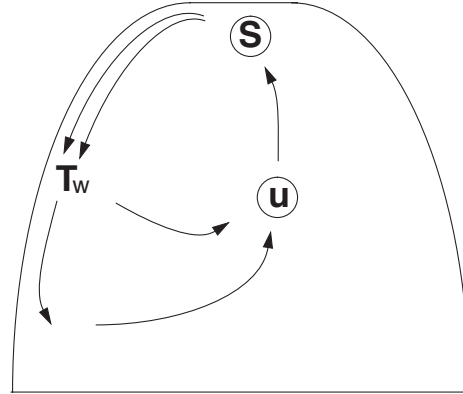
With no loss of generality we will take $y_s = 0$ and $f = f_0 + \beta y$. Then (15.70) becomes

$$- T_w(y) = w_0 \Delta x \left(2y + f_0/\beta \right) \tag{15.71}$$

or, using $S_0 = w_0 \Delta x \, y_n$,

$$- T_w(y) = \frac{S_0}{y_n} \left(2y - \frac{f_0}{\beta} \right). \tag{15.72}$$

With a slight loss of generality (but consistent with the spirit of the planetary geostrophic approximation) we take $f_0 = 0$, which is equivalent to supposing that the equatorial boundary of the domain is at the equator, and finally obtain

$$\boxed{T_w(y) = -2S_0 \frac{y}{y_n}.} \tag{15.73}$$

At the northern boundary this becomes

$$T_w(y) = -2S_0, \tag{15.74}$$

which means that the flow southwards from the source is twice the strength of the source itself. We also see that:
  (i) The western boundary current is equatorwards everywhere;
  (ii) At the northern boundary the equatorwards transport in the western boundary current is equal to *twice* the strength of the source;
 (iii) The northwards mass flux at the northern boundary is equal to the strength of the source itself.
We may check this last point directly: from(15.66)

$$T_I(y_n) = \frac{\beta y_n}{\beta} w_0 \Delta x = S. \tag{15.75}$$

The fact that convergence at the 'pole' balances T_w and S_0 does not of course depend on the particular choice we made for f and y_s.

The flow pattern evidently has the property of *recirculation* (see Fig. 15.15): this is one of the most important properties of the solution, and one that is likely to transcend all the limitations inherent in the model. This single-hemisphere model may be thought of as a crude model for aspects of the abyssal circulation in the North Atlantic, in which convection at high latitudes near Greenland is at least partially associated with the abyssal circulation. In the North Pacific there is, in contrast, little if any deep convection to act as a mass source. Rather, the deep circulation is driven by mass sources in the opposite hemisphere, and we now consider a simple model of this.

15.6.3 A two hemisphere model

Our treatment now is even more obviously heuristic, since our domain crosses the equator yet we continue to use the planetary geostrophic equations, invalid at the equator. We also persist with Cartesian geometry, even for these global-scale flows. In our defense, we note that the value of the solutions lies in their qualitative structure, not in their quantitative predictions. Let us consider a situation with a source in the Southern Hemisphere but none in the Northern Hemisphere. For later convenience we take the Southern Hemisphere source to be of strength $2S_0$, and we suppose the two hemispheres have equal area. As before, the upwelling is uniform, so that to satisfy global mass balance

$$S_0 = w_0 \Delta x \Delta y \tag{15.76}$$

where $\Delta x \Delta y$ is the area of each hemisphere. Then, given w_0, the zonally integrated polewards interior flow in each hemisphere, away from the equator, follows from Sverdrup balance,

$$T_i(y) = \frac{f}{\beta} w_0 (x_e - x_w) = S_0 \frac{y}{y_p} \tag{15.77}$$

where y_p is either y_n (the northern boundary) or y_s. The western boundary current is assumed to 'take up the slack,' that is to be able to adjust its strength to satisfy mass conservation. Thus, since $T_i(y_n) = S_0$, where S_0 is half the strength of the source in the *southern* hemisphere, it is plain that there must be a southwards flowing western boundary current near the northern end of the northern hemisphere, even in the absence of any deep water formation there!

In the northern hemisphere, the total loss due to upwelling polewards of a latitude y is given by

$$U(y) = w_0 \Delta x |y_n - y| \tag{15.78}$$

The strength of the western boundary current is then given by

$$T_w(y) = U - T_i = w_0 \Delta x (y_n - y) - \frac{f}{\beta} w_0 \Delta x = w_0 \Delta x (y_n - 2y) \tag{15.79}$$

using $f = \beta y$. Thus, at $y - y_n$,

$$T_w(y_n) = -w_0 \Delta x y = -S. \tag{15.80}$$

The boundary current changes sign halfway between equator and pole, at $y = y_n/2$. (In

Figure 15.16 Schematic of a Stommel-Arons circulation in a two-hemisphere basin. There is only one mass source, and this is in the Southern hemisphere and for convenience it has a strength of 2. Although there is no source in the Northern Hemisphere, there is still a western boundary current and a recirculation. The integrated sinks due to upwelling exactly match the strength of the source.
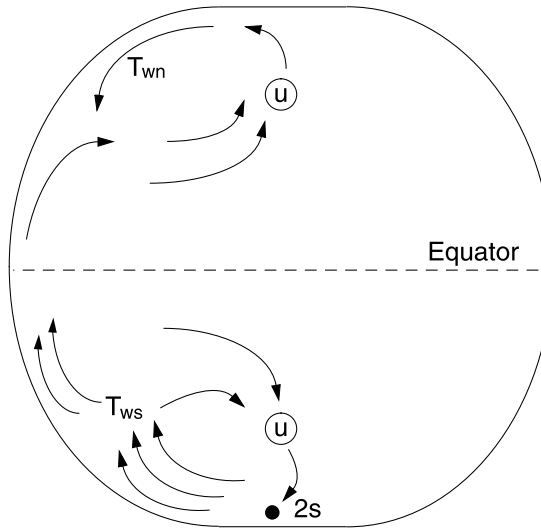
spherical coordinates, the analogous critical latitude turns out to be at $\theta = \sin^{-1}(1/2)$.) The solution is illustrated schematically in Fig. 15.16. We can (rather fancifully) imagine this to represent the abyssal circulation in the Pacific Ocean, with no source of deep water at high northern latitudes.

15.7 * A SHALLOW WATER MODEL OF THE ABYSSAL FLOW

We can obtain a more complete solution of the flow that explicitly includes the western boundary current by constructing a shallow water Stommel-Arons type model of the abyssal circulation.[17] However, the essential dynamics is the same as that of the previous section. The model is similar to that illustrated in Fig. 15.12 and comprises a single moving layer of homogeneous fluid lying underneath a lighter, stationary layer. The lower fluid is forced by a mass source at its polewards end that represents convection, and by a uniform mass sink everywhere else that represents diffusive upwelling into the upper layer. The mass source and sink are specified — that is, they are not functions of the flow — and are equal and opposite, so that there is no net mass source. The motion of the lower layer is then governed by the planetary geostrophic reduced-gravity shallow water equations (sections 3.2 and 5.2), to wit:

$$-fv = -g'\frac{\partial h}{\partial x} - ru, \qquad fu = -g'\frac{\partial h}{\partial y} - rv, \tag{15.81a}$$

$$\frac{\partial h}{\partial t} + \nabla \cdot (\boldsymbol{u}h) = S, \tag{15.81b}$$

Here h is the thickness of the lower layer (below the thermocline of Fig. 15.12), g' is the reduced gravity between the two layers, and r is a constant frictional coefficient; we will assume this is small, and in particular that $r \ll f$. The mass source term S on the right-hand side of the mass continuity equation represents both upwelling and

a localized convective source at the polewards end of the domain. We will suppose the upwelling is uniform and that, when integrated over area, it exactly balances the convective mass source. Thus, we write $S = S_0 + S_u$ where S_u is uniform and negative, S_0 is the localized convective source, and $\int_A S \, dA = 0$.

15.7.1 Potential vorticity and polewards interior flow

Straightforward manipulation of (15.81) gives the potential vorticity equation

$$\frac{D}{Dt}\left(\frac{f}{h}\right) = -\frac{r}{h}\text{curl}_z \boldsymbol{u} - \frac{fS_u}{h^2}. \tag{15.82}$$

Away from boundaries the first term on the right-hand side is negligible, and so, away from the convective source and in a steady state (15.82) becomes

$$\frac{\beta v}{h} + \frac{f}{h^2}\boldsymbol{u} \cdot \nabla h = -\frac{fS_u}{h^2}. \tag{15.83}$$

However, the second term on the left-hand side is small if friction is small, for then the flow is nearly in geostrophic balance and, using (15.81a) with $r = 0$, it follows that

$$f\boldsymbol{u} \cdot \nabla h = -g'\frac{\partial h}{\partial y}\frac{\partial h}{\partial x} + g'\frac{\partial h}{\partial x}\frac{\partial h}{\partial y} = 0. \tag{15.84}$$

The potential vorticity equation is then just

$$\beta v = -fS_u/h, \tag{15.85}$$

and because $S_u < 0$ the flow is polewards, regardless of the location of the convective mass source. From the perspective of the continuously stratified equations, the corresponding potential vorticity equation is just

$$\beta v = f\frac{\partial w}{\partial z} \tag{15.86}$$

Upwelling from the abyss into the upper ocean corresponds to a postive value of the stretching term $f\,\partial w/\partial z$, and again the interior flow is polewards.

15.7.2 The solution

It is convenient to deal with mass transports rather than velocities and we define $\boldsymbol{U} \equiv U\mathbf{i} + V\mathbf{j} \equiv uh\mathbf{i} + vh\mathbf{j}$. Away from the convective source equations of motion, (15.81), become, in steady state,

$$-fV = -\frac{\partial \Phi}{\partial x} - rU, \qquad fU = -\frac{\partial \Phi}{\partial y} - rV, \tag{15.87a}$$

$$\nabla \cdot \boldsymbol{U} = S_u, \tag{15.87b}$$

where $\Phi = g'h^2/2$. For small friction ($r \ll f$) we may write (15.87a) as

$$V = \frac{1}{f}\frac{\partial \Phi}{\partial x} - \frac{r}{f^2}\frac{\partial \Phi}{\partial y}, \qquad U = -\frac{1}{f}\frac{\partial \Phi}{\partial y} - \frac{r}{f^2}\frac{\partial \Phi}{\partial x}, \qquad (15.88\text{a,b})$$

which, after differentiation and use of (15.87b), combine to give

$$\frac{\beta}{f}\frac{\partial \Phi}{\partial x} = -fS_u - f\nabla \cdot \left(\frac{r}{f^2}\nabla\Phi\right). \qquad (15.89)$$

In the interior where the effects of friction are small (15.89) becomes $\beta V = -fS$, so recovering (15.85) and imlying polewards interior flow. However, by mass conservation, the flow cannot be polewards at all longitudes, for reasons similar to those articulated in section 14.1.1 we expect there to be a frictional western boundary current. We thus let $\Phi = \Phi_I + \Phi_b$, where Φ_I is the interior field and Φ_b the boundary layer correction. The interior field obeys $\partial\Phi_I/\partial x = -(f^2/\beta)S$ and therefore given by, for constant S,

$$\Phi_I(x, y) = \frac{f^2}{\beta}S_u(x_e - x) + \Phi_e \qquad (15.90)$$

where Φ_e is the value of Φ_I at the eastern boundary, x_e. This does not affect the solution and may be set to zero.

In the western boundary layer the the dominant balance in (15.89) is

$$\beta\frac{\partial \Phi_b}{\partial x} = -r\frac{\partial^2 \Phi_b}{\partial x^2}, \qquad (15.91)$$

with solution

$$\Phi_b = P(y)\exp(-\beta x/r), \qquad (15.92)$$

where $P(y)$ is to be determined by mass conservation: the southwards mass flux at a latitude y in the western boundary current must be equal to the sum of the polewards mass flux in the interior at that latitude, plus the total mass lost to upwelling equatorwards of y (see Fig. 15.14). These fluxes are:

$$\text{Upwelling flux} = \int_0^{x_e}\int_0^y S_u\,\mathrm{d}x\,\mathrm{d}y = S_u x_e y, \qquad (15.93)$$

using the definition of S;

$$\text{Interior flux} = \int_0^{x_e} V\,\mathrm{d}x = \frac{1}{f}\int_0^{x_e}\frac{\partial \Phi_I}{\partial x}\,\mathrm{d}x = \frac{1}{f}[\Phi_e - \Phi_I(0, y)] = -\frac{f}{\beta}S x_e, \qquad (15.94)$$

using (15.90); and

$$\text{Boundary flux} = \int_0^{\infty}\frac{1}{f}\frac{\partial \Phi_b}{\partial x}\,\mathrm{d}x = P(y), \qquad (15.95)$$
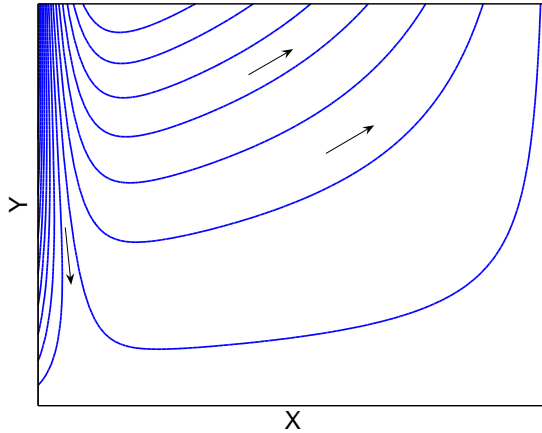
Figure 15.17 The pressure field Φ for the shallow-water Stommel-Arons model, as given by (15.98) with $r/\beta = 0.04x_e$, $f = \beta y$, and $y = 0$ at the equatorwards edge of the domain. The arrows indicate the flow direction, with the western boundary current diminishing in intensity as it moves equatorwards. The convective mass source is, implicitly, just polewards of the domain. (Note that the pressure field is not exactly a streamline.)

using (15.88a), neglecting the very small term $r\partial\Phi/\partial y$, and (15.92). By mass conservation we have

$$P(y) = S_u x_e y + \frac{f}{\beta} S_u x_e, \qquad (15.96)$$

and if $f = \beta y$ and the domain goes from $y = 0$ to $y = y_n$ this becomes

$$P(y) = 2S_u x_e y = -2S_0 \frac{y}{y_n}, \qquad (15.97)$$

where the second equality follows because the integrated upwelling balances the mass source. Consistent with our earlier heuristic treatment, the western boundary curren: there

 (i) is equatorwards, away from the convective mass source;
 (ii) diminishes in intensity as it moves equatorwards, as it feeds the interior;
 (iii) has a maximum mass flux of twice that of the convective source; that is, the flow
      recirculates.
Using (15.90) and (15.97) the complete (western boundary layer plus interior) solution is thus given by

$$\Phi = \Phi_I + \Phi_b = \frac{f^2}{\beta} S_u(x_e - x) + 2S_u x_e y e^{-\beta x/r}, \qquad (15.98)$$

and this is plotted in Fig. 15.17. This solution does not, of course, include the flow in the neighbourhood of the convective source itself, nor does it satisfy no-normal flow conditions at the polewards edge of the domain.

15.8 SCALING FOR THE BUOYANCY-DRIVEN CIRCULATION

Thus far, we have taken the strength of the upwelling as a given. In reality, this is a consequence of the presence diapycnal diffusion, because in its absence the flow is along isopycnals. In section 15.2 we estimated the upwelling for a non-rotating model;

we now do the same for a fluid obeying the steady planetary geostrophic equations,
namely

$$\boldsymbol{v} \cdot \nabla b = \kappa \nabla^2 b, \qquad \nabla \cdot \boldsymbol{u} + \frac{\partial w}{\partial z} = 0 \qquad (15.99\text{a,b})$$

$$\boldsymbol{f} \times \boldsymbol{u} = -\nabla \phi, \qquad b = \frac{\partial \phi}{\partial z}. \qquad (15.100\text{a,b})$$

On the first line we have the thermodynamic equation and the mass continuity equation,
and on the second line we have the momentum equations, that is geostrophic and hydro-
static balance, respectively. We use the continuously stratified equations rather than the
corresponding shallow water equations because the former allow for a straightforward
representation of diapycnal diffusion.

The momentum and mass continuity equations combine to give the linear geostrophic
vorticity equation and the thermal wind equation and associated scales as follows:

$$\beta v = f \frac{\partial w}{\partial z} \quad \rightarrow \quad \beta U = \frac{f_0 W}{\delta}, \qquad (15.101\text{a})$$

$$f \frac{\partial \boldsymbol{u}}{\partial z} = \mathbf{k} \times \nabla b \quad \rightarrow \quad f \frac{U}{\delta} = \frac{\Delta b}{L}. \qquad (15.101\text{b})$$

We use uppercase to denote scaling variables, except that the vertical scale is denoted δ
and the scaling for buoyancy variations is denoted Δb. We will take Δb is given, and
equal to the buoyancy difference at the surface that is ultimately driving the motion. We
also assume that the horizontal scales are isotropic, with $U = V$ and $X = Y = L$. The
thermodynamic relation gives a relationship between W, κ and δ if we assume a broad
upwelling region with a balance between upwards advection and diffusion:

$$w \frac{\partial b}{\partial z} = \kappa \frac{\partial^2 b}{\partial z^2} \quad \rightarrow \quad W = \frac{\kappa}{\delta}. \qquad (15.102)$$

Eliminating U from (15.101) gives

$$W = \frac{\delta^2 \beta \, \Delta b}{f^2 L}. \qquad (15.103)$$

and using this with (15.102) gives scalings for the vertical velocity and δ:

$$W = \kappa^{2/3} \left(\frac{\beta \, \Delta b}{f^2 L} \right)^{1/3} \qquad \delta = \kappa^{1/3} \left(\frac{f^2 L}{\beta \, \Delta b} \right)^{1/3}. \qquad (15.104\text{a,b})$$

These scalings mean that (in so far as (15.100) describes the flow) the upwelling strength,
and the circulation more generally, are dependent on a finite value of the diffusivity, and
scale as the 2/3 power of that diffusivity. The upwelling water is cold but the water at
the surface is warm, and (15.104b) is a measure of the depth of the transition region —
that is, the thickness of the thermocline, a topic we return to in more detail in the next
chapter. We will make one important point now though: In order for the scales given
in (15.104) to be at all representative of those observed in the real ocean, we must use
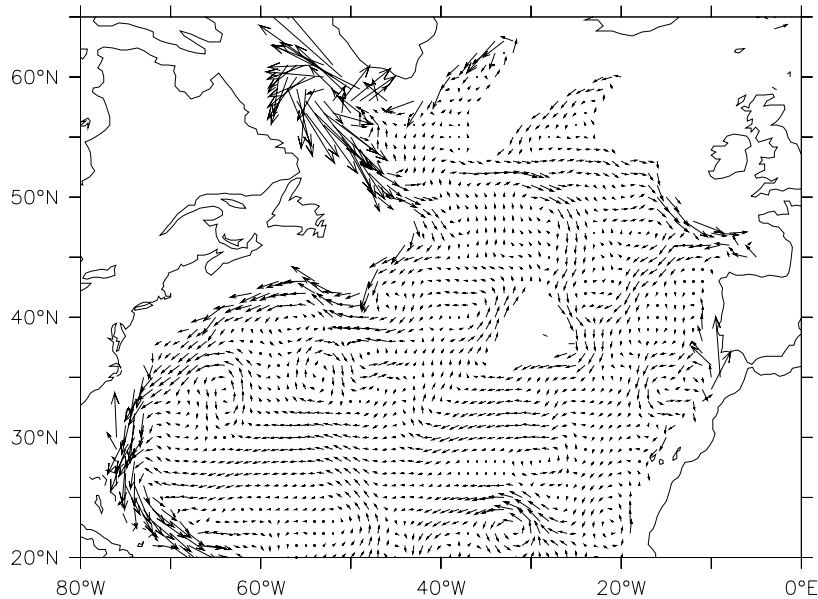
Fig. 15.18 The ocean currents at a depth of $2500\,\mathrm{m}$ in the North Atlantic, obtained using a combination of observations and model (as in Fig. 14.2). Note the southwards flowing *deep western boundary current.*

an eddy diffusivity for κ. Using $f = 10^{-4}\,\mathrm{s^{-1}}$, $\beta = 10^{-11}\,\mathrm{m^{-1}\,s^{-1}}$, $L = 5 \times 10^6\,\mathrm{m}$, $g = 10\,\mathrm{m\,s^{-2}}$, $\kappa = 10^{-5}\,\mathrm{m^2\,s^{-1}}$, $\Delta b = -g\Delta\rho/\rho_0 = g\beta_T\Delta T$ and $\Delta T = 10\,\mathrm{K}$ we find $\delta \approx 150\,\mathrm{m}$ and $W = 10^{-7}\,\mathrm{m\,s^{-1}}$, not unreasonable values albeit δ is rather smaller than the thickness of the observed thermocline. However, if we take the molecular value of $\kappa \approx 10^{-7}\,\mathrm{m^2}$ the values of W and δ are much smaller, and unrealistically so. Evidently, if the deep circulation of the ocean is buoyancy driven, it must take advantage of turbulence that enhances the small scale mixing and produces an eddy diffusivity.

15.8.1 Summary remarks on the Stommel-Arons model

If we were given the location and strength of the sources of deep water in the real ocean, the Stommel-Arons model could give us a global solution for the abyssal circulation. The solution for the Atlantic, for example, resembles a superposition of Fig. 15.15 and Fig. 15.16 (with deep water sources in the Weddell Sea and near Greenland), and that for the Pacific resembles Fig. 15.16 (with a deep water source emanating from the Antarctic Circumpolar Current). Perhaps the greatest success of the model is that it introduces the notions of deep western boundary currents and recirculation — enduring concepts of the deep circulation that remain with us today. For example, the North Atlantic does have a well-defined deep western boundary current running south along the Eastern seaboard of Canada and the United States, as seen in Fig. 15.18.[18] However, in other important aspects the model is found to be in error, in particular it is found that there is little upwelling through the main thermocline — much of the water formed by

deep convection in the North Atlantic in fact upwells in the Southern Hemisphere.[19] Are there fundamental problems with the model, or just discrepancies in details that might be corrected with a slight reformulation? To help answer that we summarize the assumptions and corresponding predictions of the model, and distinguish the essential aspects from what is merely convenient.

(i) A foundational assumption is that of linear geostrophic vorticity balance in the ocean abyss, represented by $\beta v \approx f \partial w/\partial z$, or its shallow water analog.

— The effects of mesoscale eddies are thereby neglected. As discussed in chapter 9, in their mature phase mesoscale eddies seek to barotropize the flow, and so create deep eddying motion that might dominate the deep flow.

(ii) A second important assumption is that of uniform upwelling, across isopycnals, into the upper ocean, and that $w = 0$ at the ocean bottom. When combined with (i) this gives rise to polewards interior flow, and by masss conservation a deep western boundary current. The upwelling is a consequence of a finite diffusion, which in turn leads to deep convection as in the model of sideways convection of section 15.2.

— The uniform-upwelling assumption might be partially relaxed, while remaining within the Stommel-Arons framework, by supposing (for example) that the upwelling occurs near boundaries, or intermittently, with corresponding detailed changes to the interior flow.

— If bottom topography is important, then $w \neq 0$ at the ocean bottom. This effect may be most important if mesoscale eddies are present, for then in an attempt to maintain its value of potential vorticity the abyssal flow will have a tendency to meander nearly inviscidly along contours of constant topography. In the presence of a mid-ocean ridge, some of the deep western boundary current might travel meridionally along the eastern edge of the ridge instead of along the coast.

— The deep water may not upwell across isopycnals at at all, but may move along isopycnals that intersect the surface (or are connected to the surface by convection). If so, then in the presence of mechanical forcing a deep circulation could be maintained even in the absence of a diapycnal diffusivity. The circulation might then be qualitatively different from the Stommel-Arons model, although a linear vorticity balance might still hold, with deep western boundary currents. This is discussed in section 16.5.

Note that, even if Stommel-Arons picture were to be essentially correct, we should not consider the deep flow is being driven by deep convection at the source regions. It is a *convenience* to specify the strength of these regions for the calculations but, just as in the models of sideways convection considerer in section 15.2, the overall strength of the circulation (insofar as it is thermally driven) is a function of the size of the diffusivity and the meridional temperature gradient at the surface.

Notes

1 See, for example, Warren (1981) who provides a review and historical background and Schmitz (1995) who surveys the observations and provides an interpretation of the deep global circulation.

2 From Wunsch (2002).

3 Courtesy of L. Talley

4 Adapted from Paparella and Young (2002).

5 As in Haney (1971). Only the value of C, and not the value of κ, is material to the boundary condition written in this form, because we are parameterizing only the flux at the surface. The parameter C is often taken to be such that the heat flux is of order $30\,\mathrm{W\,m^{-2}\,K^{-1}}$, but it is not a universal constant.

6 Rossby (1965).

7 Adapted from Rossby (1998).

8 Ocean convection is reviewed by Marshall and Schott (1999).

9 I am grateful to W. R. Young for some useful comments on this.

10 Sandström (1908, 1916). However, Sandström did not prove the result encapsulated by (15.23); his discussion was thermodynamic, in terms of a Carnot cycle, and the dissipation of kinetic energy played no role in his argument. Since that time various related statements with varying degrees of generality and preciseness have been given (see e.g., Huang 1999). The more rigorous result (15.23) is a statement about a kinetic-energy dissipating circulation, and it does not prove that unless the heating occurs at a lower level than the height then no circulation at all can be maintained.

11 Following Paparella and Young (2002).

12 The original box model is due to Stommel (1961), and many studies with variations around this have followed. Rooth (1982) developed the idea of a buoyancy-driven pole-to-pole overturning circulation, and Welander (1986) discussed, among other things, the role of boundary conditions on temperature and salinity at the ocean surface. Thual and McWilliams (1992) systematically explored how box models compare with two-dimensional fluid models of sideways convection, Quon and Ghil (1992) explored how multiple equilibria arise in related fluid models, and Dewar and Huang (1995) discussed the problem of flow in loops. Cessi and Young (1992) tried to derive simple models systematically from the equations of motion, obtaining various nonlinear amplitude equations. Our discussion is of just a fraction of all this; see also Whitehead (1995), Cessi (2001) and Dijkstra (2002) for reviews and more discussion.

13 Adapted from Welander (1986) and Dijkstra (2002).

14 Bryan (1986), Manabe and Stouffer (1988) and Marotzke (1989) did find evidence of multiple equilibria in various three-dimensional numerical models.

15 After Stommel et al. (1958).

16 Following Stommel and Arons (1960).

17 Motivated by Cessi (2001).

18 A global Stommel-Arons-like solution was presented by Stommel (1958). The dis-

covery of deep western boundary currents, by Swallow and Worthington (1961), was motivated by the theoretical model. Using neutrally-buoyant floats underneath the Gulf Stream they found a robust equatorwards-flowing undercurrent with typical speeds of $9-18\,\mathrm{m\,s^{-1}}$. Relevant observations of the deep circulation are summarized by Hogg (2001).

19 For example, Toggweiler and Samuels (1995).

Problems

15.1 *(a)* Obtain an expression analogous to (15.23) for the anelastic equations.

    (b) ♦ Obtain, if possible, an expression analogous to (15.23) for a compressible gas (which you may suppose to be ideal, if needed). Interpret the result.

15.2 ♦ Consider a model of sideways convection in which the boundary condition at the top is the relaxation, or Haney, condition $b_z = A(b^*(y) - b)$ where A (a constant) and $b^*(y)$ are given, b is the buoyancy, proportional to the temperature, the other boundaries are insulating, and the flow is statistically steady.

    (a) Is it still the case that on average the fluid is heated (i.e., there is a heat flux into the fluid through the upper surface) where it is already warm? If so, how may this be reconciled with the intuition that if the ocean surface is anomalously warm it will cool by way of a heat flux from the ocean to the atmosphere?

    (b) Show that if $A < 0$ a statistically steady state cannot be reached.

    (c) Suppose that b^* varies monotonically with latitude. Show that if κ is non-zero, the average surface temperature gradient will be less than that of b^*.

15.3 Consider a variation of the Stommel box model in which the equation of motion (15.35) is replaced by

$$\frac{\mathrm{d}T}{\mathrm{d}\tau} = (1 - T) - \Phi^2 T, \quad \frac{\mathrm{d}S}{\mathrm{d}\tau} = \delta(1 - S) - \Phi^2 S, \quad \Phi = -\gamma(T - \mu S). \quad \text{(P15.1)}$$

The interbox flow equations now depends on the density difference squared, so allowing continuous equations. Show that multiple equilibria are possible, and that one is thermally driven and one salinity driven. Obtain approximate expressions for the temperature and salinity for these equilibria, in the limit of large γ and small δ if you wish. If δ is large, what changes about these solutions?

15.4 *(a)* In the Stommel two-box problem, show physically that when three solutions are present, the middle one is generally unstable. One way to do this is to suppose that the system is perturbed slightly from that equilibrium, and argue qualitatively that the forces on the system will then take it farther from that state. By use of similar arguments, show that the other solutions are generally stable.

    (b) ♦ Alternatively, linearize the equations about the equilibrium points and show that small perturbations will grow if the solution is that of the middle equilibrium state, but will be damped in the other two cases.

15.5 ♦ Obtain the solution to (15.16) at lowest order. Take the solution to higher order and show that the sinking region is narrower than the upwelling region.

No fairer destiny [has] any physical theory, than that it should of itself point out the way to the introduction of a more comprehensive theory, in which it lives on as a limiting case.
Albert Einstein, *Relativity, the Special and the General Theory,* 1916.

The Wind and Buoyancy Driven Circulation

I N THIS CHAPTER we try to understand the combined effect of wind and buoyancy forcing in setting the three-dimensional structure of the ocean. There are three main topics we will consider:

(i) The *main thermocline*, the region in the upper 1 km or so of the ocean where density and temperature changes most rapidly.

(ii) The 'wind-driven' overturning circulation. More precisely, we look into whether and how the ocean might maintain a deep overturning circulation that owes its existence to the direct effects of wind at the surface, and that persists even as the diapycnal diffusivity in the ocean interior goes to zero.

(iii) The circulation of the flow in a channel, as a model of the Antarctic Circumpolar Current (ACC).

16.1 THE MAIN THERMOCLINCE: AN INTRODUCTION

In the previous chapter we saw that a fluid that is differentially heated from above will develop both an overturning circulation and a region near the surface where the temperature changes rapidly. We now examime this in more detail, and to begin we consider the circulation in a closed, single hemispheric basin, and again suppose that there is a net surface heating at low latitudes and a net cooling at high latitudes which maintains a meridional temperature gradient at the surface. We also presume, *ab initio,* that there is a single overturning cell, with water rising at low latitudes before returning to polar regions, illustrated schematically in Fig. 16.1.

At lower latitudes the surface water is warmer than the cold water in the abyss.
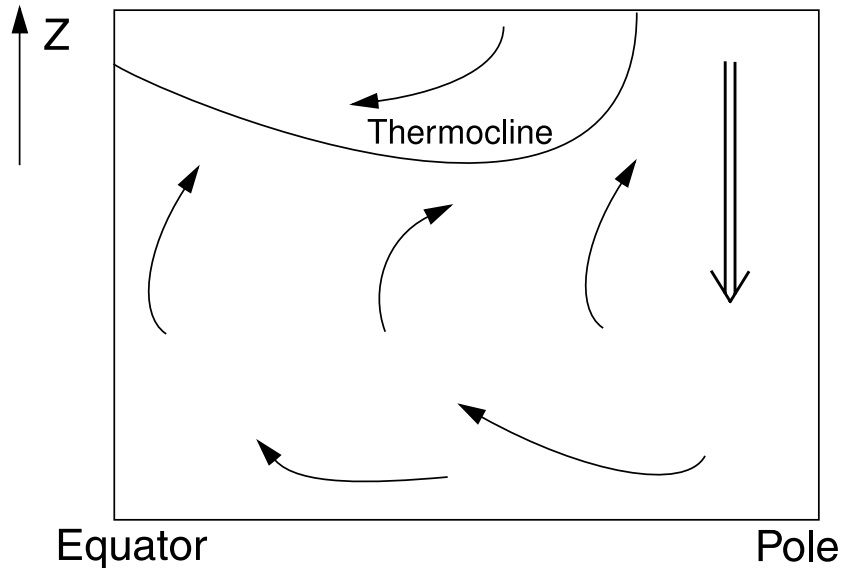
Fig. 16.1 Cartoon of a single-celled meridional overturning circulation. Sinking is concentrated at high latitudes and upwelling spread out over lower latitudes. The thermocline is the boundary between the cold abyssal waters that have polar origins, and the warmer near-surface subtropical water. Wind forcing in the subtropical gyre may also mechanically push the warm water down, deepening the thermocline.

Thus there must be a vertical temperature gradient everywhere except possibly at the highest latitudes where the cold dense water sinks. This temperature gradient is called the *thermocline*. In purely bouyancy-driven flows the thickness of the thermocline is determined by way of an advective-diffusive balance, and proportional to (some power of) the thermal diffusivity, and we first consider a simple model of this.

16.1.1 A simple kinematic model

The fact that cold water with polar origins upwells into a region of warmer water suggests that we consider the simple one-dimensional advective-diffusive balance,

$$w\frac{\partial T}{\partial z} = \kappa \frac{\partial^2 T}{\partial z^2}.$$
(16.1)

where w is the vertical velocity, κ is a diffusivity and T is temperature. In mid-latitudes, where this might hold, w is positive and the equation represents a balance between the upwelling of cold water and the downward diffusion of heat. If w and κ are given constants, and if T is specified at the top ($T = T_T$ at $z = 0$) and if $\partial T/\partial z = 0$ at great depth ($z = -\infty$) then the temperature falls exponentially away the surface according to

$$T = (T_T - T_B)e^{wz/\kappa} + T_B.$$
(16.2)

where T_B is a constant. This expression cannot be used to estimate how the thermocline depth scales with either w or κ, because the magnitude of the overturning circulation depends on κ (section 15.8). However, it is reasonable to see if the observed ocean is broadly consistent with this expression. The diffusivity κ can be measured; it is an eddy diffusivity, maintained by small-scale turbulence, and measurements produce values that range between $10^{-5}\,\mathrm{m^2\,s^{-1}}$ in the main thermocline to $10^{-4}\,\mathrm{m^2\,s^{-1}}$ in abyssal regions over rough topography and in and near continental margins, with still higher values locally.[1] The vertical velocity is too small to be measured directly, but various estimates based on deep water production suggest a value of about $10^{-7}\,\mathrm{m\,s^{-1}}$. Using this and the smaller value of κ in (16.2) gives an e-folding vertical scale, κ/w, of just 100 m, beneath which the stratification is predicted to be almost uniform. Using the larger value of κ increases the vertical scale to 1000 m, which is probably closer to the observed value for the total thickness of the thermocline (look at Fig. 15.2), but using such a large value of κ in the main thermocline is probably not supported by the observations. Similarly, the deep stratification of the ocean is rather larger than that given (16.1), except with values of diffusivity on the large side of those observed.[2] Thus, there are two conclusions to be drawn:

(i) The observed thickness of the thermocline is somewhat larger than what one might infer from observed values of the diffusivity and overturning circulation.

(ii) The observed deep stratification is somewhat larger than what one might infer from the advective-diffusive balance (16.1) with observed values of diffusivity and overturning circulation.

Of course the model itself, (16.1), is overly simple but these conclusions suggest that we look for additional physical factors, and Mechanical forcing, and in particular the wind, is one such. As regards the thermocline, the wind stress curl forces water converges in the subtropical Ekman layer, thereby forcing relatively warm water to downwell and therefore to meet the upwelling colder abyssal water at some finite depth, thereby deepening the thermocline from its purely diffusive value. Indeed, in so far as we can separate these two effects of wind and diffusion, we can say that the strength of the wind influences the *depth* at which the thermocline occurs, whereas the strength of the diffusivity influences the *thickness* of the thermocline. The influence of the wind on the abyssal circulation is not quite as straightforward, but we find in section 16.5 that it will enable both a stronger circulation, and deep stratification, to persist even in the absence of diffusion.

16.2 SCALING AND SIMPLE DYNAMICS OF THE MAIN THERMOCLINE

We now begin to consider the dynamics that produce an overturning circulation and a thermocline. The Rossby number of the large-scale circulation is small and the scale of the motion large, and the flow obeys the planetary geostrophic equations:

$$\boldsymbol{f} \times \boldsymbol{u} = -\nabla\phi, \qquad \frac{\partial\phi}{\partial z} = b, \qquad\qquad (16.3\text{a,b})$$

$$\nabla \cdot \boldsymbol{v} = 0, \qquad \frac{\mathrm{D}b}{\mathrm{D}t} = \kappa\frac{\partial^2 b}{\partial z^2}. \qquad\qquad (16.4\text{a,b})$$

We suppose that these equations hold below an Ekman layer, so that the effects of a wind stress may be included by specifiying a vertical velocity at the top of the domain. The diffusivity, κ, is, as we noted above, an eddy diffusivity, but since its the precise form and magnitude are uncertain we must proceed with due caution, and a useful practical philosophy is to try ignore dissipation and viscosity where possible, and to invoke them only if there is no other way out. Let us therefore scale the equations in two ways, with and without diffusion; these scalings will be the central to our theory.

16.2.1 An advective scale

As usual we denote (with one or two exceptions) scaling values with capital letter and non-dimensional values with a hat, so that for example $u = U\hat{u}$ and $u = \mathcal{O}(U)$. Let us ignore the diffusive term in (16.4b) and try to construct a scaling estimate for the depth of the wind's influence.

If there is upwelling ($w > 0$) from the abyss, and Ekman downwelling ($w < 0$) at the surface, there is some depth D_a at which $w = 0$. By cross-differentiating (16.3a) we obtain $\beta v = -f\nabla_z \cdot \boldsymbol{u}$, and combining this with (16.4a) gives the familiar geostrophic vorticity equation and corresponding scaling

$$\beta v = f\frac{\partial w}{\partial z}, \qquad \rightarrow \qquad \beta V = f\frac{W}{D_a}. \tag{16.5}$$

Here, D_a is the unknown depth scale of the motion, L is the horizontal scale of the motion, which we take as the gyre or basin scale, and V is a horizontal velocity scale. (It is reasonable to suppose that $V \sim U$, where U is the zonal velocity scale, and henceforth we will denote both by U.) The appropriate vertical velocity to use is that due to Ekman pumping, W_E; we will assume (and demonstrate later) that this is much larger than the abyssal upwelling velocity, which in any case is zero by assumption at $z = -D_a$, and this leads to the Sverdrup-balance estimate

$$U = \frac{f}{\beta}\frac{W_E}{D_a}. \tag{16.6}$$

We may determine an appropriate value of U using the thermal wind relation, which from (16.3) is

$$\boldsymbol{f} \times \frac{\partial \boldsymbol{u}}{\partial z} = -\nabla b, \qquad \rightarrow \qquad \frac{U}{D_a} = \frac{1}{f}\frac{\Delta b}{L}, \tag{16.7}$$

where Δb is the magnitude of variations (i.e., the scaling value) of buoyancy in the horizontal. Assuming the vertical scales are the same in (16.6) and (16.7) then eliminating U gives

$$D_a = W_E^{1/2}\left(\frac{f^2 L}{\beta\,\Delta b}\right)^{1/2}. \tag{16.8}$$

[This is in fact the same as the estimate (14.140).] If we relate U and W_E using mass conservation, $U/L = W_E/D_a$, instead of using Sverdrup balance, then we write L in

place of f/β and (16.8) becomes $D_a = \left(W_E f L^2 / \Delta b\right)^{1/2}$, which is not qualitatively different for large scales. The important aspect of these equations is that the of depth wind-influenced region increases with the strength of the wind-stress (as $W_E \sim \mathrm{curl}_z \tau$) and decreases with the meridional temperature gradient. The former dependence is reasonably intuitive, and the latter arises because as the temperature gradient increases, the associated thermal wind-shear U/D_a correspondingly increases. But the horizontal transport (the product UD_a) is fixed by mass conservation; the only way that these two can remain consistent is for the vertical scale to decrease. Taking $W_E = 10^{-6}\,\mathrm{m\,s^{-1}}$, $\Delta b = g\Delta\rho/\rho_0 = g\beta_T \Delta T \sim 10^{-2}\,\mathrm{m\,s^{-2}}$, $L = 5000\,\mathrm{km}$ and $f = 10^{-4}\,\mathrm{s^{-1}}$ gives $D_a = 500\,\mathrm{m}$. Such a scaling argument cannot be expected to give more than an estimate of depth of the wind-influenced region; nevertheless, it does indicate that the wind-driven circulation is predominantly an upper-ocean phenomenon.

16.2.2 A diffusive scale

The estimate (16.8) cares nothing about the thermodynamic equation, and if we include this, with nonzero diffusivity, we recover the model of section 15.8. Thus, briefly, the scaling follows from advective-diffusive balance in the thermodynamic equation, the linear geostrophic vorticity equation, and thermal wind balance:

$$w\frac{\partial b}{\partial z} = \kappa\frac{\partial^2 b}{\partial z^2}, \qquad \beta v = f\frac{\partial w}{\partial z}, \qquad f\frac{\partial \boldsymbol{u}}{\partial z} = \mathbf{k} \times \nabla b, \qquad (16.9\text{a,b,c})$$

with corresponding scales

$$\frac{W}{\delta} = \frac{\kappa}{\delta^2}, \qquad \beta U = \frac{fW}{\delta}, \qquad \frac{U}{\delta} = \frac{\Delta b}{fL}. \qquad (16.10\text{a,b,c})$$

where δ is the vertical scale. Because there is now one more equation than in the advective scaling theory we cannot take the vertical velocity as a given, else the equations are overdetermined. We therefore take it to be the abyssal upwelling velocity, which then becomes part of the *solution,* rather than being imposed. From (16.10) we obtain diffusive vertical scale,

$$\boxed{\delta = \kappa^{1/3}\left(\frac{f^2 L}{\beta\,\Delta b}\right)^{1/3}.} \qquad (16.11)$$

Using $\kappa = 10^{-5}\,\mathrm{m^2\,s^{-2}}$ this gives $\delta \approx 150\,\mathrm{m}$ and $W \approx 10^{-7}\,\mathrm{m\,s^{-1}}$, an order of magnitude smaller than W_E.

A modified diffusive scaling

The scaling above assumes that the length scale over which thermal wind balance holds is the gyre scale itself. In fact there is another length scale that is more appropriate, and this leads to a slightly different scaling for the thickness of the thermocline. Note that the depth of the subtropical thermocline is not constant: it shoals up to the east because of Sverdrup balance, and it may shoals up polewards as the curl of the wind

Figure 16.2 Schema of a scaling for the thermocline. The diagonal lines mark the diffusive thermocline of thickness δ and depth $D(y)$. The advective scaling for $D(y)$, i.e., D_a, is given by (16.8), and the diffusive scaling for δ is given by (16.13).
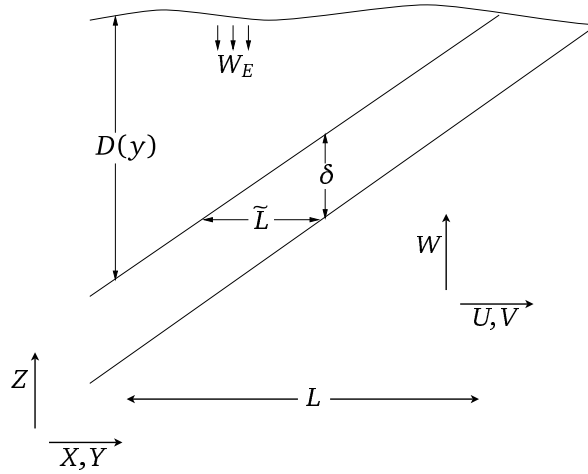
stress falls (and is zero at the polewards edge of the gyre). Thus, referring to Fig. 16.2, the appropriate horizontal length scale $\widetilde{L}$ is not the basin scale itself, but is given by

$$\widetilde{L} = \delta \frac{L}{D_a}. \tag{16.12}$$

This is no longer an external imposed parameter, but must be determined as part of the solution. Using $\widetilde{L}$ instead of L as the length scale in the thermal wind equation (16.10c) gives, using (16.8), the modified diffusive scale

$$\delta = \kappa^{1/2} \left(\frac{f^2 L}{\Delta b\, \beta D_a} \right)^{1/2} = \kappa^{1/2} \left(\frac{f^2 L}{\Delta b\, \beta W_e} \right)^{1/4}. \tag{16.13}$$

Substituting values of the various parameters results in a thickness of about 100–200 m. The thermocline thickness now scales as $\kappa^{1/2}$. The interpretation of this scale and that of (16.11) is that the thickness of the thermocline scales as $\kappa^{1/3}$ in the absence of a wind stress, but scales as $\kappa^{1/2}$ if a wind stress is present that can provide a finite slope the the depth of the thermocline that is independent of κ, and this is confirmed by numerical simulations[3] The vertical velocity, and hence the meridional overturning circulation, now scales as

$$W = \frac{\kappa}{\delta_w} \propto \kappa^{1/2} \tag{16.14}$$

rather than $\kappa^{2/3}$.

16.2.3 Summary of the physical picture

What do the vertical scales derived above represent? The wind-influenced scaling, D_a, is the depth to which the directly wind-driven circulation can be expected to penetrate.

Thus, over this depth we can expect to see wind-driven gyres and associated phenomena. At greater depths lies the abyssal circulation, and this is not wind-driven in the same sense. Now, in general, the water at the base of the wind-driven layer will not have the same thermodynamic properties as the upwelling abyssal water — this being cold and dense, whereas the water in the wind-driven layer is warm and subtropical (look again at Fig. 16.1). The thickness δ characterizes the diffusive transition region between these two water masses and in the limit of very small diffusivity this becomes a *front*. One might say that D_a is the *depth* of the thermocline, while δ is the *thickness* of the thermocline. In the diffusive region, no matter how small the diffusivity κ is in the thermodynamic equation, the diffusive term is important. Of course if the diffusion is sufficiently large, the thickness will be as large or larger than the depth, and the two regions will blur into each other, and this may indeed be the case in the real ocean. (The real world is also complicated by the effects of mesoscale eddies.) Nevertheless, these scales are a useful foundation on which to build.[4]

16.3 THE INTERNAL THERMOCLINE

We now try to go beyond simple scaling arguments and investigate in more detail the dynamics of the thermocline. In this section we consider the diffusive, or internal, thermocline and in section 16.4 we consider the advective, or ventilated, thermocline. Such an investigation requires trying to actually solve the equations of motion, but the advective term in the thermodynamic equation makes this extremely difficult; indeed this prevents us from constructing wholly analytic models, but not from constructing informative models. We begin by expressing the planetary geostrophic equations as an equation in a single unknown.

16.3.1 The M-equation

The planetary geostrophic equations can be written as a single partial differential equation in a single variable, although the resulting equation is of quite high order and nonlinear. We write the equations of motion as

$$- fv = -\frac{\partial \phi}{\partial x}, \qquad fu = -\frac{\partial \phi}{\partial y}, \qquad b = \frac{\partial \phi}{\partial z}, \qquad (16.15\text{a,b,c})$$

$$\nabla \cdot \boldsymbol{v} = 0, \qquad \frac{\partial b}{\partial t} + \boldsymbol{v} \cdot \nabla b = \kappa \nabla^2 b, \qquad (16.16\text{a,b})$$

where we take $f = \beta y$. Cross differentiating the horizontal momentum equations and using (16.16a) gives the linear geostrophic vorticity relation $\beta v = f \partial w / \partial z$ which, using (16.15a) again, may be written as

$$\frac{\partial \phi}{\partial x} + \frac{\partial}{\partial z} \left(-\frac{f^2}{\beta} w \right) = 0. \qquad (16.17)$$

This equation is the divergence in (x, z) of $(\phi, -f^2 w / \beta)$ and is automatically satisfied if

$$\phi = M_z \qquad \text{and} \qquad \frac{f^2 w}{\beta} = M_x. \tag{16.18a,b}$$

where the subscripts on M denote derivatives. Then straightforwardly

$$u = -\frac{\partial_y \phi}{f} = -\frac{M_{zy}}{f}, \qquad v = \frac{\partial_x \phi}{f} = \frac{M_{zx}}{f}, \qquad b = \partial_z \phi = M_{zz}. \tag{16.19a,b,c}$$

The thermodynamic equation, (16.16b) becomes

$$\frac{\partial M_{zz}}{\partial t} + \left(\frac{-M_{zy}}{f} M_{zzx} + \frac{M_{zx}}{f} M_{zzy} \right) + \frac{\beta}{f^2} M_x M_{zzz} = \kappa M_{zzzz} \tag{16.20}$$

or

$$\frac{\partial M_{zz}}{\partial t} + \frac{1}{f} J(M_z, M_{zz}) + \frac{\beta}{f^2} M_x M_{zzz} = \kappa M_{zzzz}. \tag{16.21}$$

where J is the usual horizontal Jacobian. This is the *M-equation*,[5] somewhat analogous to the potential vorticity equation in quasi-geostrophic theory in that it expresses the entire dynamics of the system in a single, nonlinear, advective-diffusive partial differential equation, although note that M_{zz} is materially conserved (in the absence of diabatic effects) by the three-dimensional flow. Because of the high differential order and nonlinearity of the system analytic solutions of (16.21) are very hard to find, and from a numerical perspective it is easier to integrate the equations in the form (16.15) and (16.16) than in the form (16.21). Nevertheless, it is possible to move forward by approximating the equation to one or two dimensions, or by *a priori* assuming a boundary-layer structure.

A one-dimensional model

Let us consider an illustrative one-dimensional model (in z) of the thermocline.[6] Merely setting all horizontal derivatives in (16.21) to zero is not very useful, for then all the advective terms on the left-hand side vanish. Rather, we look for steady solutions of the form $M = M(x, z)$, and the M-equation then becomes

$$\frac{\beta}{f^2} M_x M_{zzz} = \kappa M_{zzzz}, \tag{16.22}$$

which represents the advective-diffusive balance

$$w \frac{\partial b}{\partial z} = \kappa \frac{\partial^2 b}{\partial z^2}. \tag{16.23}$$

(We must also suppose that the value of κ varies meridionally in the same manner as does β / f^2; without this technicality M would be a function of y, violating our premise.) If the ocean surface is warm and the abyss is cold, then (16.22) represents a balance between the upward advection of cold water and the downward diffusion of warm water. The horizontal advection terms vanish because the zonal velocity (u) and

the meridional temperature gradient (b_y) are each zero. Let us further consider the special case

$$M = (x - x_e)W(z) \qquad (16.24)$$

where the domain extends from $0 \leq x \leq x_e$, so satisfying $M = 0$ on the eastern boundary. Equation (16.22) becomes the ordinary differential equation

$$\frac{\beta}{f^2} W W_{zzz} = \kappa W_{zzzz}, \qquad (16.25)$$

where W has the dimensions of (velocity)^2. We nondimensionalize this by setting

$$z = H\hat{z}, \qquad \kappa = \hat{\kappa}(HW_S), \qquad W = \left(\frac{f^2 W_S}{\beta}\right)\hat{W} \qquad (16.26)$$

where the hatted variables are nondimensional and W_S is a scaling value of the dimensional vertical velocity, w (e.g., the magnitude of the Ekman pumping velocity W_E). Eq. (16.25) becomes

$$\hat{W}\hat{W}_{zzz} = \hat{\kappa}\hat{W}_{zzzz}, \qquad (16.27)$$

(omitting the hats on the subscripted, nondimensional, z). The parameter $\hat{\kappa}$ is a nondimensional measure of the strength of diffusion in the interior, and the interesting case occurs when $\hat{\kappa} \ll 1$; in the ocean, typical values are $H = 1\,\mathrm{km}$, $\kappa = 10^{-5}\,\mathrm{m\,s^{-2}}$ and $W_S = W_E = 10^{-6}\,\mathrm{m\,s^{-2}}$ so that $\hat{\kappa} \approx 10^{-2}$, which is indeed small.

The time-dependent form of (16.27), namely $\hat{W}_{zzt} + \hat{W}\hat{W}_{zzz} = \hat{\kappa}\hat{W}_{zzzz}$, is similar to Burger's equation, $V_t + VV_z = \nu V_{zz}$, which is known to develop fronts. (To see this, note that the inviscid Burger's equation has the form $DV/Dt = 0$, where the advective derivative is one-dimensional, and therefore the velocity of a given fluid parcel is preserved on the line. Suppose that the velocity of the fluid is positive but diminishes in the positive z-direction, so that a fluid parcel will catch-up with the fluid parcel in front of it — there no pressure force to keep the fluid parcels apart. But since the velocity of a fluid parcel is fixed, then a singularity must form. In presence of viscosity, the singularity is tamed to a front.) Thus, we might similarly expect (16.27) to produce a front, but because of the extra derivatives the argument is not as straightforward and it is simplest to obtain solutions numerically.

Equation (16.27) is fourth order, so four boundary conditions are needed, two at each boundary. Appropriate ones are a prescribed buoyancy and a prescribed vertical velocity at each boundary, for example

$$\begin{aligned}
\hat{W} &= \hat{W}_E, & -\hat{W}_{zz} &= T_0, & &\text{at top} \\
\hat{W} &= 0, & -\hat{W}_{zz} &= 0, & &\text{at bottom}
\end{aligned} \qquad (16.28)$$

where $\hat{W}_E$ is the (nondimensional) vertical velocity at the base of the top Ekman layer, which is negative for Ekman pumping in the subtropical gyre, and T_0 is a constant, representative of the buoyancy difference across the domain. We obtain solutions numerically by Newton's method,[7] and these are shown in Fig. 16.3 and Fig. 16.4. The solutions do indeed display fronts, or boundary layers, for small diffusivity. If the wind
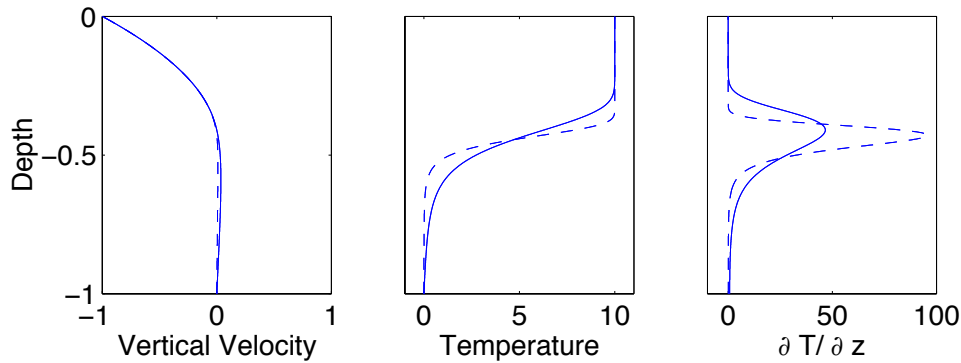
Fig. 16.3 Solution of the one-dimensional thermocline equation, (16.27), with boundary conditions (16.28), for two different values of the diffusivity: $\hat{\kappa} = 3.2 \times 10^{-3}$ (solid line) and $\hat{\kappa} = 0.4 \times 10^{-3}$ (dashed line), in the domain $0 \leq z \leq -1$. 'Vertical velocity' is W, 'temperature' is $-W_{zz}$, and all units are the nondimensional ones of the equation itself. A negative vertical velocity, $\hat{W}_E = -1$, is imposed at the surface (representing Ekman pumping) and $T_0 = 10$. An internal boundary layer forms within the fluid interior, separating the warm near surface fluid from the cold abyssal fluid. The boundary layer thickness increases as $\hat{\kappa}^{1/3}$, so doubling in thickness for an eightfold increase in $\hat{\kappa}$. The upwelling velocity also increases with $\hat{\kappa}$, (as $\hat{\kappa}^{2/3}$), but this is barely noticeable on the graph because the downwelling velocity, above the internal boundary layer, is much larger and almost independent of $\hat{\kappa}$. The depth of the boundary layer increases as $\hat{W}_E^{1/2}$, so if $\hat{W}_E = 0$ the boundary layer is at the surface, as in Fig. 16.4.

forcing is non-zero, the front is an internal boundary layer with an adiabatic layer above; if the wind forcing is zero, the boundary layer is at the top of the fluid. In the real ocean, wind forcing is non-zero and the frontal region is known as the *internal thermocline*.

16.3.2 * Boundary layer analysis

The reasoning and the numerical solutions of the above sections all suggest that the internal thermocline has a boundary layer structure whose thickness decreases with κ. If the Ekman pumping at the top of the ocean is non-zero, the boundary layer is internal to the fluid. This suggests that we might be able to learn something about the solution by performing a boundary layer analysis, much as we did when investigating western boundary currents in section 14.1.3. The nonlinearity precludes a complete solution of the equation, but we can obtain useful information about the thickness of the boundary layer itself.[8]

One-dimensional model

Let us now *assume* a steady two-layer structure of the form illustrated in Fig. 16.5. The temperature varies rapidly only in an internal boundary layer of thickness δ located at $z = -h$; above and below this the temperature is assumed to be only very slowly vary-
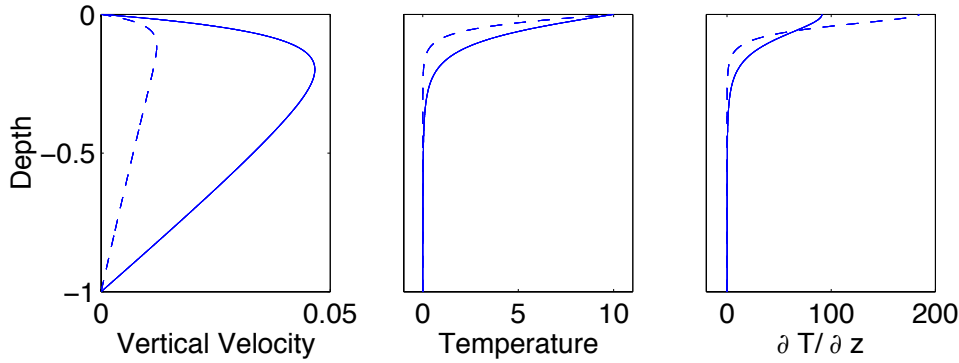
Fig. 16.4 As for Fig. 16.3, but with no imposed Ekman pumping velocity at the upper boundary ($\widehat{W}_E = 0$), again for two different values of the diffusivity: $\widehat{\kappa} = 3.2 \times 10^{-3}$ (solid line) and $\widehat{\kappa} = 0.4 \times 10^{-3}$ (dashed line). The boundary layer now forms at the upper surface. The boundary thickness again increases with diffusivity and, even more noticeably, so does the upwelling velocity — this scales as $\widehat{\kappa}^{2/3}$, and so increases fourfold for an eightfold increase in $\widehat{\kappa}$.

ing. Following standard boundary layer procedure, we introduce a stretched boundary layer coordinate ζ, where

$$\zeta = \frac{z + h}{\delta}. \tag{16.29}$$

This is the distance from $z = -h$, scaled by the boundary layer thickness δ. Thus, within the boundary layer, ζ is an order one quantity. We also let

$$\widehat{W}(z) = \widehat{W}_I(z) + \widetilde{W}(\zeta) \tag{16.30}$$

where $\widehat{W}_I$ is the solution away from the boundary layer and $\widetilde{W}$ is the boundary layer correction. Because the boundary layer is presumptively thin, $\widehat{W}_I$ is effectively constant in it and, furthermore, for $z < -h$, $\widehat{W}$ vanishes in the limit as $\kappa = 0$. We thus take $\widehat{W}_I = 0$ throughout the boundary layer. (The small diffusively-driven upwelling below the boundary layer is part of the boundary layer solution, not the interior solution.) Now, temperature varies rapidly in the boundary layer but it remains an order one quantity throughout. To satisfy this we explicitly scale $\widetilde{W}$ in the boundary layer by writing

$$\widetilde{W}(\zeta) = \delta^2 T_0 A(\zeta) \tag{16.31}$$

where T_0 is proportional to the temperature difference across the boundary layer and A is an order one field. (Again, $-W_{zz}$ is the 'temperature'.) The derivatives of W are

$$\begin{aligned}
\frac{\partial \widehat{W}}{\partial z} &= \frac{1}{\delta} \frac{\partial \widetilde{W}}{\partial \zeta} = \delta T_0 \frac{\partial A}{\partial \zeta} \\
\frac{\partial^2 \widehat{W}}{\partial z^2} &= T_0 \frac{\partial^2 A}{\partial \zeta^2},
\end{aligned} \tag{16.32}$$

so that $\widehat{W}_{zz}$ is an order one quantity. Far from the boundary layer the solution must be able to match the external conditions on temperature and velocity. On temperature we require that $T \to T_0$ as $\zeta \to +\infty$ and $T \to 0$ as $\zeta \to -\infty$. Thus,

$$A_{\zeta\zeta} \to \begin{cases} 1 & \text{as } \zeta \to +\infty \\ 0 & \text{as } \zeta \to -\infty. \end{cases} \tag{16.33}$$

On vertical velocity we require that $W \to (z/h+1)W_E$ as $\zeta \to +\infty$, and $W \to$ constant as $\zeta \to -\infty$. The first matches the Ekman pumping velocity above the boundary layer, and the second condition produces the abyssal upwelling velocity, which as noted vanishes for $\kappa \to 0$.

Substituting (16.30) and (16.31) into (16.27) we obtain

$$T_0 A A_{\zeta\zeta\zeta} = \frac{\widehat{\kappa}}{\delta^3} A_{\zeta\zeta\zeta\zeta}. \tag{16.34}$$

which implies that $\delta \sim (\widehat{\kappa}/T_0)^{1/3}$. Restoring the dimensions gives

$$\delta' \sim \left(\frac{\kappa f^2 L}{\Delta b \, \beta} \right) \tag{16.35}$$

where $\delta' = H\delta$ is the dimensional boundary layer thickness and Δb is the buoyancy difference across the boundary layer. (To obtain this we use $\kappa = \widehat{\kappa}(HW_S)$ and $T_{\text{dim}} = T_0 \times f^2 W_S/(\beta H^2)$ and $\Delta b \sim LT_{\text{dim}}$, because $b = M_{zz} = (x-1)W_{zz} \sim LT$.) The vertical velocity scales as

$$\widehat{W} \sim \frac{\kappa}{\delta} \sim \kappa^{2/3} T_0^{1/3}. \tag{16.36}$$

This is the strength of the upwelling velocity at base of the thermocline and, more generally, the strength of the diffusively-driven component of meridional overturning circulation of the ocean. The scalings for thickness and upwelling velocity are the same as that obtained previously by more heuristic reasoning.

Somewhat different one-dimensional thermocline models may be constructed (see problem 16.3), and these have slightly different scaling properties. However, their qualitative features transcend their detailed construction, and in particular:

★ The thickness of the internal thermocline increases with increasing diffusivity, and decreases with increasing temperature difference across it. In particular, as the diffusivity tends to zero the thickness of the internal thermocline tends to zero.

★ The strength of the upwelling velocity, and hence the strength of the meridional overturning circulation, increases with increasing diffusivity and increasing temperature difference.

The three-dimensional equations

We can apply the same boundary-layer techniques to the three-dimensional M-equation. The main difference is that the depth of the boundary layer is now a function of x and y, so that the stretched coordinate ζ is now given by
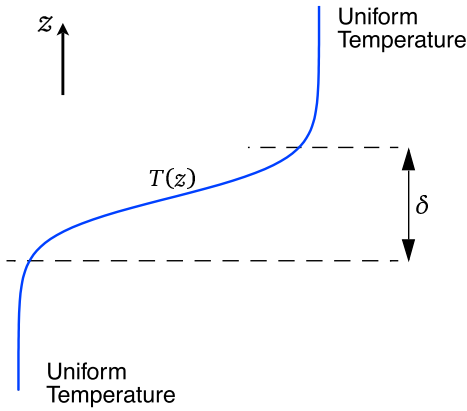
$$\delta\zeta = z + h(x, y). \tag{16.37}$$

Figure 16.5 The simplified boundary-layer structure of the internal thermocline. In the limit of small diffusivity the internal thermocline forms a boundary layer, of thickness δ in the figure, in which the temperature changes rapidly. The internal boundary layer lies below the ventilated thermocline, so that in reality the temperature above the internal boundary layer is not uniform.

Just as in the one-dimensional case we rescale M in the boundary layer and write

$$M = T_0 \delta^2 \widehat{A}(x, y, \zeta), \tag{16.38}$$

where the scaling factor δ^2 again ensures that the temperature remains an order-one quantity. In the boundary layer the derivatives of M become

$$\frac{\partial M}{\partial z} = \frac{1}{\delta} \frac{\partial A}{\partial \zeta}, \tag{16.39}$$

and

$$\frac{\partial M}{\partial x} = \delta^2 T_0 \left(\frac{\partial A}{\partial \zeta} \frac{\partial \zeta}{\partial x} + \frac{\partial A}{\partial x} \right) = \delta^2 T_0 \left(\frac{\partial A}{\partial \zeta} \left(\frac{1}{\delta} \frac{\partial h}{\partial x} \right) + \frac{\partial A}{\partial x} \right) \tag{16.40}$$

Substituting these into (16.20) we obtain, omitting the time-derivative,

$$\delta \left[\frac{1}{f} \left(A_{\zeta x} A_{\zeta\zeta y} - A_{\zeta y} A_{\zeta\zeta x} \right) + \frac{\beta}{f^2} A_x A_{\zeta\zeta\zeta} \right] + \frac{\beta}{f^2} h_x A_\zeta A_{\zeta\zeta\zeta}$$
$$+ \frac{1}{f} \left[h_x \left(A_{\zeta\zeta} A_{\zeta\zeta y} - A_{\zeta y} A_{\zeta\zeta\zeta} \right) + h_y \left(A_{\zeta x} A_{\zeta\zeta\zeta} - A_{\zeta\zeta} A_{\zeta\zeta x} \right) \right] \tag{16.41}$$
$$= \frac{\kappa}{T_0 \delta^2} A_{\zeta\zeta\zeta\zeta},$$

where the subscripts on A denote derivatives. (The horizontal advective terms of order δ^{-1} vanish identically.) If $h_x = h_y = 0$, that is if the base of the thermocline is flat, then (16.41) becomes

$$\frac{1}{f} \left[A_{\zeta x} A_{\zeta\zeta y} - A_{\zeta y} A_{\zeta\zeta x} \right] + \frac{\beta}{f^2} A_x A_{\zeta\zeta\zeta} = \frac{\kappa}{T_0 \delta^3} A_{\zeta\zeta\zeta\zeta}. \tag{16.42}$$

Since all the terms in this equation are, by construction, order one, we immediately see that the boundary layer thickness δ scales as

$$\delta \sim \left(\frac{\kappa}{T_0} \right)^{1/3}, \tag{16.43}$$

just as in the one-dimensional model. On the other hand, if h_x and h_y are order one quantities then the dominant balance in (16.41) is

$$\frac{1}{f}\left[h_x(A_{\zeta\zeta}A_{\zeta\zeta y} - A_{\zeta y}A_{\zeta\zeta\zeta}) + h_y(A_{\zeta x}A_{\zeta\zeta\zeta} - A_{\zeta\zeta}A_{\zeta\zeta x})\right] = \frac{\kappa}{T_0\delta^2}A_{\zeta\zeta\zeta\zeta} \quad (16.44)$$

and

$$\delta \sim \left(\frac{\kappa}{T_0}\right)^{1/2}, \quad (16.45)$$

confirming the heuristic scaling arguments. Thus, if the isotherm slopes are fixed independently of κ (for example by the wind stress), then as $\kappa \to 0$ an internal boundary layer will form whose thickness is proportional to $\kappa^{1/2}$. We expect this to occur at the base of the main thermocline, with purely advective dynamics being dominant in upper part of the thermocline, and determining the slope of the isotherms (i.e., the form of h_x and h_y), as in Fig. 16.2. Interestingly, the balance in the three-dimensional boundary layer equation does not in general locally correspond to $wT_z \approx \kappa T_{zz}$. Both at $\mathcal{O}(1)$ and $\mathcal{O}(\delta)$ the horizontal advective terms in (16.41) are of the same asymptotic size as the vertical advection terms. In the boundary layer the thermodynamic balance is thus $\boldsymbol{u} \cdot \nabla_z T + wT_z \approx \kappa T_{zz}$, whether the isotherms are sloping or flat. We might have anticipated this, because the vertical velocity passes through zero within the boundary layer.

What are the dynamics above the diffusive layer, presuming that it does does not extend all the way to the surface? Answering this leads us into our next topic, the 'ventilated thermocline.'

16.4 THE VENTILATED THERMOCLINE

We now consider the nature of the dynamics *above* the diffusive layer, presuming that the diffusivity is sufficiently small that there is a meaningful separation of the internal boundary layer and the advective dynamics above. In this advective region there is no general reason that the temperature profile should be uniform, and we envision an essentially adiabatic region that is both wind-driven and stratified. This region of the thermocline has become known, for reasons that will become apparent, as the *ventilated thermocline*. The main thermocline is comprised of the internal thermocline plus a ventilated region, and to set our bearings it may be useful to refer now to the overall picture sketched in Fig. 16.6, and to come back to it again later on. To elucidate the structure of the ventilated thermocline we will assume:[10]

 (i) The motion satisfies the ideal, steady, planetary geostrophic equations.

 (ii) The surface temperature, and the vertical velocity due to Ekman pumping, are given. (These surface conditions are, in reality, influenced by the ocean's dynamics, but we assume that we can calculate a solution with specified surface conditions.) At the base of the wind-influenced region we will impose $w = 0$.

(iii) Rather than use the continuously stratified equations, we will assume the solution can be adequately represented by a small number of layers, each of constant density. The abyss is represented by a single stationary layer.
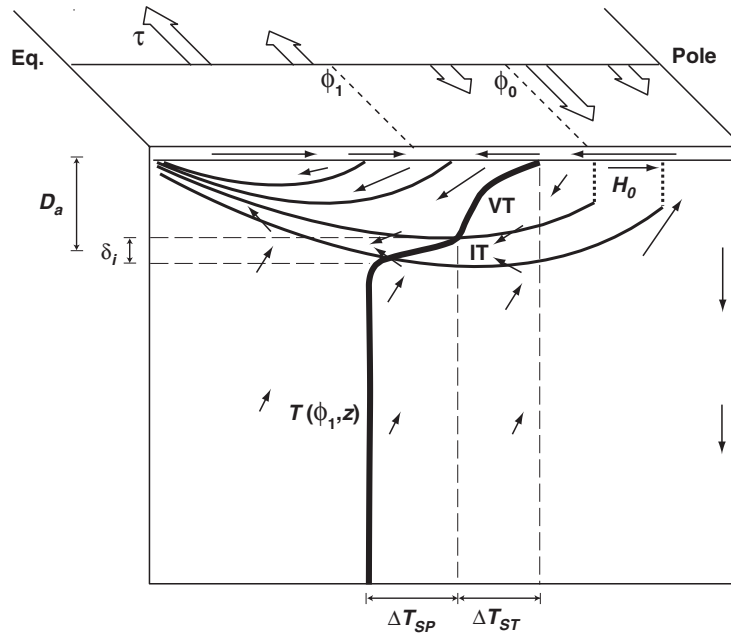
Fig. 16.6 Schema of the large-scale circulation and structure of the main thermocline, in a single-hemisphere ocean driven by wind-stress (broad arrows) and a meridional gradient of heating at the surface. The subtropical-subpolar gyre boundary is a constant latitude ϕ_0, where the wind-stress curl changes sign. 'VT' denotes the ventilated thermocline, an advective regime of thickness D_a, and 'IT' denotes the internal thermocline, a diffusive internal boundary layer of thickness Δ_I. The thin arrows indicate the meridional overturning circulation and the flow in the Ekman layer near the ocean surface. The thick line is a temperature profile at latitude ϕ_1: The temperature drop across the internal thermocline is ΔT_{SP}, equal to the meridional temperature difference across the subpolar gyre; the temperature drop across the ventilated thermocline is Δ_{ST}, the temperature difference across the subtropical gyre.[9]

(iv) We will not take into account the possible effects of a western boundary current. In that sense the model is extension of the Sverdrup interior of homogeneous models.

The model is thus not a complete one, yet we may hope that is revealing about the structure of the real ocean.

16.4.1 A reduced gravity, single-layer model

The simplest possible model along these lines is to suppose the ocean is composed of just two layers, as illustrated in Fig. 16.7. The upper layer of density ρ_1 is wind-driven, whereas the lower layer of density ρ_2 is assumed stationary; this is called a 'one-and-a-half-layer' model or a 'reduced gravity single-layer' model. Pertinent questions are: *(i)* How deep is the upper layer? *(ii)* What is the velocity field in it?

In the planetary geostrophic approximation, the momentum and mass conservation

Figure 16.7 A reduced gravity, single layer model. A single moving layer lies above a deep, stationary layer of higher density. The upper surface is rigid. A thin Ekman layer may be envisioned to lie on top of the moving layer, providing a vertical velocity boundary condition.
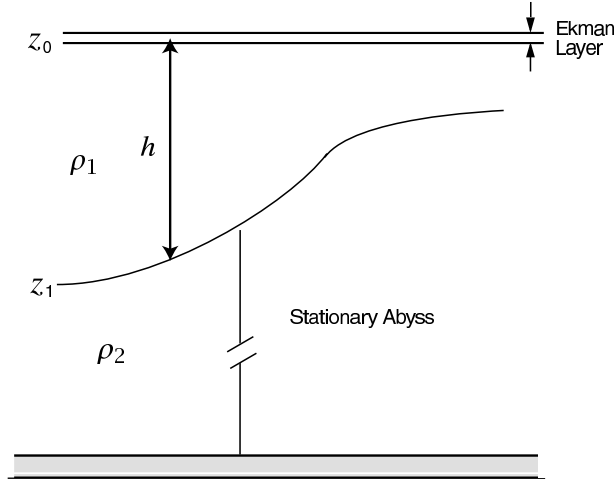
equations of the reduced gravity shallow water model may be written as:

$$f \times \mathbf{u} = -g' \nabla h, \qquad \nabla \cdot \mathbf{u} = -\frac{\partial w}{\partial z}, \qquad (16.46\text{a,b})$$

where ∇ is a two dimensional operator (as it will be for the rest of this section) and $g' = g(\rho_2 - \rho_1)/\rho_0$ is the *reduced gravity*. Taking the curl of (16.46a) gives the geostrophic vorticity equation, $\beta v + f \nabla \cdot \mathbf{u} = 0$, and integrating this over the depth of the layer and using mass conservation gives

$$h \beta v = f(w_E - w_b), \qquad (16.47)$$

where w_E is the velocity at the top of the layer, due mainly to Ekman pumping, and w_b is the vertical velocity at the layer base. If the flow is steady, w_b is zero for then

$$w_b = \mathbf{u} \cdot \nabla h = -\frac{g'}{f} \frac{\partial h}{\partial y} \frac{\partial h}{\partial x} + \frac{g'}{f} \frac{\partial h}{\partial x} \frac{\partial h}{\partial y} = 0. \qquad (16.48)$$

Using this result and geostrophic balance, (16.47) becomes

$$\frac{g'}{f} \beta h \frac{\partial h}{\partial x} = f w_E \qquad (16.49)$$

which integrates to

$$\boxed{h^2 = -2\frac{f^2}{g'\beta} \int_x^{x_e} w_E \, \mathrm{d}x' + H^2} , \qquad (16.50)$$

where H is the (unknown) value of h at the eastern boundary x_e, and this is a constant to satisfy the no-normal flow condition. This apart, the equation contains complete information about the solution. We note:
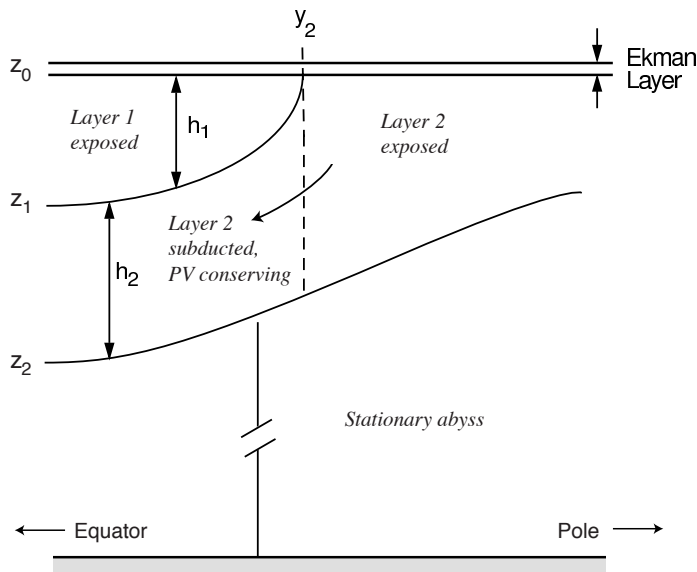
Figure 16.8 A two-layer model of the ventilated thermocline. Two moving layers lie above an infinitely deep, stationary layer of higher density. Models with more moving layers may be constructed by straightforward extension.

★ The depth of the moving layer scales as the magnitude of the wind stress (or Ekman pumping velocity) to the one-half power.

★ The horizontal solution is very similar to the simpler Sverdrup interior solution previously obtained in section 14.1.3.

★ There is no solution if w_E is positive; that is, if there is Ekman upwelling.

★ The solution depends on the unknown parameter H, the layer depth at the eastern boundary.[11]

16.4.2 A two-layer model

If there is a meridional temperature gradient at the surface then isopycnals *outcrop*, or intersect the surface. Thus, at some latitude (say $y = y_2$) layer 2 passes underneath layer 1, which is of lower density (and higher temperature), as sketched in Fig. 16.8. Thus, polewards of y_2 the dynamics are just those of a single layer discussed above, whereas equatorwards of y_2 layer 2 does not feel the wind directly, and its dynamics are are governed by two principles:

(i) Sverdrup balance. This still applies to the vertically integrated motion, and thus to the sum of layer 1 and layer 2.

(ii) Conservation of potential vorticity. The motion in layer 2 is shielded from the wind forcing, and the effects of dissipation are (assumed) negligible. Thus, the fluid parcels in the layer will conserve their potential vorticity.

These two principles are sufficient to provide a complete description of the dynamics. We first use potential vorticity conservation to obtain an expression for the depths of

each layer in terms of the total depth of the moving fluid, h, and then use Sverdrup balance to obtain h.

Use of potential vorticity conservation

Conservation of potential vorticity in the region equatorwards of y_2 is, for steady flow,

$$\boldsymbol{u}_2 \cdot \nabla q_2 = 0 \qquad (y < y_2). \tag{16.51}$$

where $q_2 = f/h_2$. Now, the velocity field in layer 2 is given by $\boldsymbol{u}_2 = (g_2'/f)\mathbf{k} \times \nabla h$ where $h = h_1 + h_2$ is the total depth of the fluid (see the appendix to this chapter). Thus, (16.51) becomes

$$-\frac{g_2'}{f}\frac{\partial h}{\partial y}\frac{\partial}{\partial x}\left(\frac{f}{h_2}\right) + \frac{g_2'}{f}\frac{\partial h}{\partial x}\frac{\partial}{\partial y}\left(\frac{f}{h_2}\right) = \frac{g_2'}{f}J\left(\frac{f}{h_2}, h\right) = 0. \tag{16.52}$$

This is an equation relating h and h_2 and it has the general solution

$$q_2 = \frac{f}{h_2} = G_2(h) \tag{16.53}$$

where G_2 is an *arbitrary* function of its argument. However, we *know* what the potential vorticity of layer 2 is at the moment it is subducted; it is just

$$q_2(y_2) = \frac{f(y_2)}{h_2} = \frac{f_2}{h}. \tag{16.54}$$

where $f_2 \equiv f(y_2)$, and $h_2 = h$ because $h_1 = 0$. This relationship must therefore hold everywhere in layer 2, equatorwards of y_2. That is,

$$G_2(h) = \frac{f_2}{h} = \frac{f_2}{-z_2}. \tag{16.55}$$

Thus, in the subducted region,

$$\frac{f}{z_1 - z_2} = -\frac{f_2}{z_2} \tag{16.56}$$

whence

$$z_1 = \left(1 - \frac{f}{f_2}\right)z_2 = -\left(1 - \frac{f}{f_2}\right)h. \tag{16.57}$$

From this we obtain expressions for the layer depths as functions of the total depth, h, namely

$$h_2 = z_1 - z_2 = \frac{f}{f_2}h \quad \text{and} \quad h_1 = -z_1 = \left(1 - \frac{f}{f_2}\right)h. \tag{16.58}$$

Note that because potential vorticity, f/h_2, is conserved, as a fluid column moves equatorward its height must decrease.

Use of Sverdrup balance

Equations (16.58) contain the unknown total depth h, and we now use Sverdrup balance to find this and close the problem. Because the velocity at the base of layer 2 is zero, this may be written as

$$\beta(h_1 v_1 + h_2 v_2) = f w_E \tag{16.59}$$

where the velocities in each layer are given by [see (16A.18)]

$$f v_1 = \frac{\partial}{\partial x}(g_2' h + g_1' h_1) \quad \text{and} \quad f v_2 = \frac{\partial}{\partial x}(g_2' h). \tag{16.60}$$

Thus the Sverdrup relationship becomes,

$$\beta h_1 \frac{\partial}{\partial x}(g_2' h + g_1' h_1) + \beta(h - h_1)g_2' \frac{\partial h}{\partial x} = f^2 w_E, \tag{16.61}$$

or

$$\frac{\partial}{\partial x}\left(g_2' h^2 + g_1' h_1^2\right) = \frac{2f^2}{\beta} w_E. \tag{16.62}$$

On integrating this gives

$$\left(h^2 + \frac{g_1'}{g_2'} h_1^2\right) = D_0^2 + C. \tag{16.63}$$

where

$$D_0^2(x, y) = -\frac{2f^2}{\beta g_2'} \int_x^{x_e} w_E(x', y)\, \mathrm{d}x' \tag{16.64}$$

which by construction vanishes at the eastern wall ($x = x_e$). The constant of integration C may be interpreted as follows. We write $C = H^2 + (g_1'/g_2')H_1^2$ where H is the (unknown) total depth of layers 1 and 2 at the eastern boundary, and H_1 is the depth of layer 1. These must both be constants in order to satisfy the no normal flow condition. However, H_1 must be zero, because at the outcrop line $h_1 = 0$. Thus, H_1 is zero at $y = y_2$, and therefore zero everywhere, and $C = H^2$.

Using (16.58) and (16.63) we obtain a closed expression for h, namely

$$\boxed{h = -z_2 = \frac{(D_0^2 + H^2)^{1/2}}{\left[1 + (g_1'/g_2')(1 - f/f_2)^2\right]^{1/2}}.} \tag{16.65}$$

Using (16.57) and (16.58) the depths in each layer, and the corresponding geostrophic velocities, can be obtained.

A typical solution is shown in Fig. 16.9. The upper layer exists only equatorwards of the outcrop latitude, $y_2 = 0.8$, and isolines of total thickness correspond to streamlines of the lower layer. We see, as expected, the overall shape of a subtropical gyre, with the circulation beng closed by an implicit western boundary current that is not part of the calculation. Two regions are shaded in the figure, the 'pool' region in the west and the 'shadow zone' in the south-east. The solutions above do not apply to these, and they require special attention.
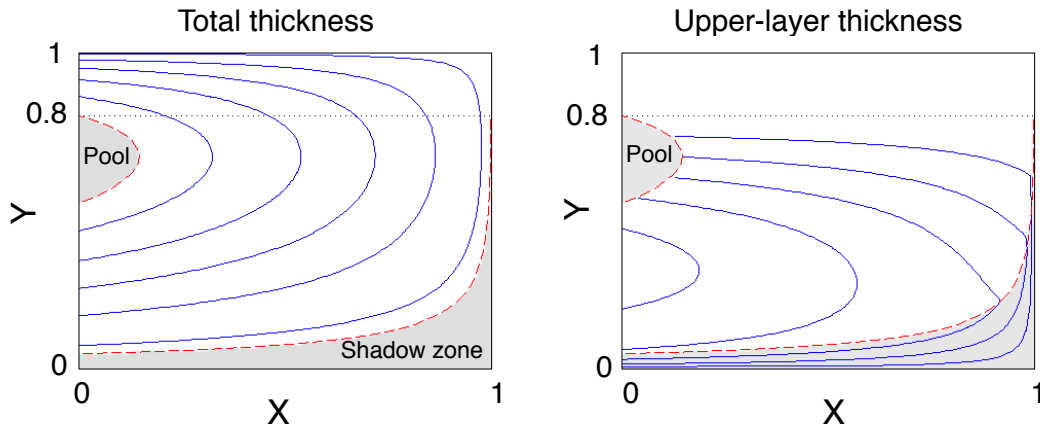
Fig. 16.9 Contour plots of total thickness and upper layer thickness in a two-layer model of the ventilated thermocline. The thickness generally increases westward, and the flow is clockwise. The shadow zone and the western pool are shaded, and no contours are drawn in the latter. The outcrop latitude, $y_2 = 0.8$, is marked with a dotted line. [Parameters are $g'_1 = g'_2 = 1$, $\beta = 1$, $f_0 = 0.5$, $H = 0.5$, and $w_E = -\sin(\pi y)$.]

16.4.3 The shadow zone

In the fluid interior the potential vorticity of a parcel in layer 2 is determined by tracing its trajectory back to its outcrop latitude where the potential vorticity is given. That trajectory is determined by its velocity, and this turn is determined by inverting the potential vorticity. Now, parcels subducted at y_2 sweep equatorwards and westwards, so that a parcel, labelled '*a*' say, subducted at the eastern boundary will in general leave the eastern boundary tracing a southwestern trajectory. Consider another parcel, '*b*' say, in the interior that lies eastward of the subducted position of *a*, in the shaded region of Fig. 16.10. It is impossible to trace *b* back to the outcrop line without trajectories crossing, and this is forbidden in steady flow. Rather, it seems as if the trajectory of *b* would emanate from the eastern wall. What is the potential vorticity there?

At the eastern boundary the condition of no normal flow at the boundary demands that h be constant (so that $u_2 = 0$), and h_1 be constant (so that $u_1 = 0$). But if a parcel in layer 2 moves *along* the boundary potential vorticity conservation demands that f/h_2 is constant, and therefore h_2 must change, contradicting the no-normal flow requirement. Thus, there can be no motion at all along the boundary, and so we cannot trace parcels in the shaded region back to the wall. Rather, in the absence of closed trajectories (for example, eddying motion), we may assume that the shaded region is stagnant, and h is constant. Of course, potential vorticity is everywhere given by f/h_2, which varies spatially, but since there is no motion potential vorticity is still, rather trivially, conserved along trajectories. This region is aptly called the *shadow zone,* since the region falls under the shadow of the eastern boundary; an analogous region arose in the quasi-geostrophic discussion of section 14.7.

To obtain an expression for the fields within the shadow zone, first note that because
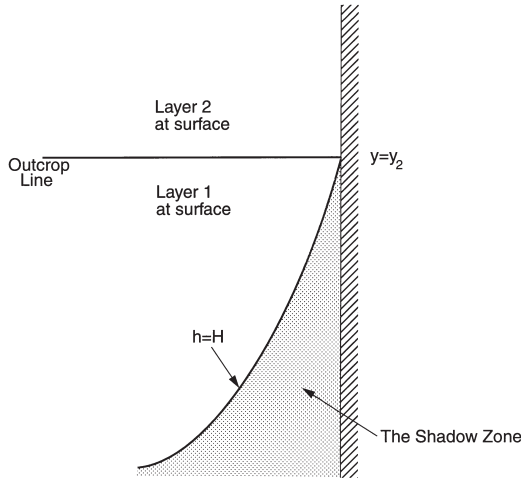
Figure 16.10 The shadow zone in the ventilated thermocline. Layer 2 outcrops at $y = y_2$. A column moving equatorwards along the eastern boundary in layer 2 is subducted at y_2. It cannot remain against the eastern wall and both preserve its potential vorticity, which implies the column shrinks, at the same time that the no-normal flow condition is satisfied, as by geostrophy this implies the layer depth is constant. Thus, the column must move westward, along the boundary of a 'shadow zone' within which is there is no motion. The streamline it follows is the isoline of constant total thickness of the two moving layers [see (16A.18) or (16A.20c)].

h is constant, its values is equal to that on the eastern wall; that is, $h = H$. The wind forcing must then all be taken up by the upper layer, and Sverdrup balance then implies

$$\beta v_1 h_1 = f w_E, \tag{16.66}$$

and using (16.60) we obtain an expression for h_1, to wit:

$$h_1^2 = -\frac{2 f^2}{\beta g_1'} \int_x^{x_e} w_E(x', y) \, dx' = \frac{g_2'}{g_1'} D_0^2, \tag{16.67}$$

which is zero at the eastern wall. In the lower layer the thickness is just $h_2 = H - h_1$. The boundary of the shadow zone is given by the trajectory of a fluid parcel in layer 2 that emanates from the eastern boundary at the outcrop line where $h_1 = 0$ and $h = h_2 = H$. Since the flow is steady, the trajectory is an isoline of h. Thus, from (16.65) we have

$$h^2 = \frac{(D_0^2(x_s, y_s) + H^2)}{\left[1 + g_1'/g_2' \, (1 - f/f_2)^2 \right]} = H^2. \tag{16.68}$$

where (x_s, y_s) denotes the boundary of the shadow zone. (Note that $x_s = x_e$ at $y = y_2$.) From this

$$D_0^2(x_s, y_s) = H^2 \left[\frac{g_1'}{g_2'} \left(1 - \frac{f}{f_2} \right)^2 \right] \tag{16.69}$$

which, given the wind-stress, is an equation for the shadow zone boundary x_s as a function of y.

16.4.4 † The western pool

Polewards of the outcrop latitude the fluid of layer 2 feels the wind directly and the layer thickness is determined by Sverdrup balance. Equatorwards of the outcrop latitude the properties of this layer are determined by potential vorticity conservation, with the potential vorticity being determined by the layer thickness at the outcrop. However, just as there is a region in the east where trajectories cannot be traced back to the outcrop, there is a 'pool' region in the west that is bounded by the trajectory that emerges from the western boundary at the outcrop latitude. Within the pool, trajectories cannot be traced back to the outcrop (Fig. 16.9), and one might imagine that they emerge from the western boundary current. In the context of ventilated themocline theory, there are two plausible hypotheses for determining the layer depths within this region:

  (i) Within layer 2, potential vorticity is homogenized;

  (ii) Because there is no source for layer 2 water, layer 2 water does not exist and the pool consists solely of ventilated, layer 1 water.

Note the analogy between these two hypotheses and those for the stratification of the troposphere summarized on page 558.

(i) Potential vorticity homogenization

The pool region is a region of recirculation, receiving water from and depositing water into the western boundary current. Thus, following the ideas described in chapter 10 and employed in section 14.7, we hypothesize that the potential vorticity within this region becomes homogenized. The value of potential vorticity within the pool is just the value of potential vorticity at its boundary, and this is given by $f_2/h_2(w)$, where $h_2(w)$ is the thickness of layer 2 at the western boundary at the outcrop latitude. This is given using (16.50) with $f = f_2$ and $g' = g'_2$, and thus the potential vorticity in the pool is given by

$$q_{\text{pool}} = \frac{f_2}{D_w^2 + H^2} \tag{16.70}$$

where $D_w^2 = -2(f_2^2/g'_2\beta)\int_{x_w}^{x_e} w_E(x', y_2)\, dx'$. The thickness of layer 2 in the pool must be consistent with this, and so is given by

$$h_2 = \frac{f}{q_{\text{pool}}}. \tag{16.71}$$

The thickness of layer 1 is determined by using Sverdrup balance, (16.59), which, given h_2 and geostrophy, reduces to an equation for h_1.

(ii) The ventilated pool

> *'I came for the waters.' 'What waters?' 'I was misinformed.'*
> From *Casablanca* (1942).

The homogenization hypothesis, although plausible, depends on the assumption of downgradient diffusion of potential vorticity by eddies. Also, because there is no source of layer-2 water in the pool, we must suppose that it is ventilated by eddy pathways that
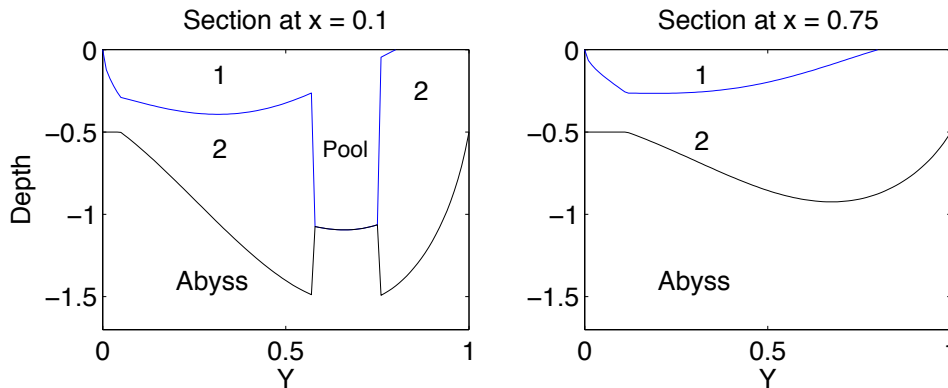
Fig. 16.11 Two north-south section of layer thickness, at different longitudes, from the same solution as Fig. 16.9 and assuming a ventilated western pool. The numbers refer to the fluid layer. The section on the left passes through the western ventilated pool region, where all the Sverdrup transport is taken up by the top layer. The region near $y = 0$ in both plots where the total depth of the thermocline is constant is the shadow zone.

meander down from the surface. An alternative hypothesis, and one that does not rely on the properties of mesoscale eddies, is to suppose that the western pool is filled with water that is directly ventilated from the surface. That is, if there is no surface source for a water mass, we simply suppose that that water mass does not exist. In the two-layer model, this means that the western pool is filled entirely with layer-1 fluid. If a nonventilated (e.g., layer 2) fluid is present initially, then we hypothesize that it is slowly expunged by the continuous downwards Ekman pumping of layer-1 water into the pool.[12]

Because layer-2 fluid is absent, layer-1 fluid extends all the way down to the stagnant abysss; it takes up all the Sverdrup transport, and this determines the depth of the ventilated pool. Thus, rounding up the usual equations, we set $h = h_1$ in (16.63) to give

$$h_1^2 = D_1^2 + g_2' H^2 \tag{16.72}$$

where

$$D_1^2(x, y) = -\frac{2f^2}{\beta g_{1a}'} \int_x^{x_e} w_E(x', y)\, dx' \tag{16.73}$$

and $g_{1a}' = g_1' + g_2'$ is the reduced gravity between layer 1 and the abyss and H, as before, is the thickness of layer 2 at the eastern boundary. Because $g_{1a}' > g_2'$ this pool will generally be shallower than the total depth of moving fluid $(h_1 + h_2)$ just outside, but the depth of layer-1 fluid alone will be much greater; that is, there will be a discontinuities in layer depths at the pool boundary. A section through the pool region is shown in Fig. 16.11.

Although the reader may be shocked by the appearance of discontinuities in layer depths in a fluid model, the model does provide a simple mechanism for the appearance

of *mode water*. This is a distinct mass of weakly stratified, low potential vorticity water appearing in the northwest corner of the North Atlantic subtropical gyre (where it is sometimes called '18 degree water'), with analogs in the other gyres of the world's oceans, and so-called because it appears as a distinct mode in a census of water properties. The proximate mechanism for mode water formation is convection in winter, but for such convection to occur the large-scale ocean circulation must maintain a weakly stratified region, and it is the ventilated pool that enables this, and sets the formation in the context of thermocline structure. In reality, the vertical isopycnals predicted by the simple model will, of course, be highly baroclinically unstable, and the ensuing mesoscale eddies will erode the pool interface and cause the isopycnals to slump, so that the discontinuities in layer depths will be manifest only as rapid changes or fronts.

We conclude by emphasizing that both the ventilated pool theory and the potential vorticity homogenization theory rely on hypotheses that cannot be derived from the governing equations of motion without making additional physical assumptions that are neither *a priori* true nor obvious. For an overview of the entire thermocline, refer to the shaded box on the facing page.

16.5 † A MODEL OF DEEP WIND-DRIVEN OVERTURNING

Our goal in this section is to construct a model that illustrates that the overturning circulation of the ocean, and a concomitant deep stratification, may have a wind-driven component that persists even as the diffusivity goes to zero.[13]

How might deep stratification be maintained in the absence of a diapycnal diffusivity? In that case, no upwelling can occur through the stratification, because that is a diabatic process. Rather, the deep water must be directly connected to surface, perhaps by a convective pathway. Let us recall two *de facto* principles that were useful in our discussion of the overturning circulation and the thermocline:

(i) A basin will, in the of absence mechanical forcing, tend to fill up with the densest available fluid.

(ii) Light fluid forced down by wind may displace the cold fluid, so producing stratification.

A completely closed ocean thus fills completely with dense polar water, except in the upper several hundred meters where the main thermocline forms, and whose thickness is the sum of wind-driven and diffusive components. However, suppose that the polewards part of the basin is not fully enclosed but is periodic, as illustrated in Fig. 16.12, with a sill across it at mid-depth, and suppose too that the surface bondary conditions are such that the surface temperature decreases monotonically polewards. A fully enclosed basin exists only beneath the level of the sill, and we may expect the densest water in the basin, formed at the polewards edge of the domain, to fill the basin only below the level of the sill, and that above this may lie warmer water with origins at lower latitudes. Furthermore, suppose that an eastward wind blows over the channel that produces a equatorial flow in the Ekman layer. Then mass conservation demands that there must exist a *subsurface* return flow, and thus a meridional overturning circulation is set up. Note the essential role of the channel in this: if the gap were closed, then the return

Thermocline Dynamics — a Summary and Overview

The model of the main thermocline that we have constucted in sections 16.1 to 16.4 is schematically illustrated in Fig. 16.6. Some of the features, and limitations, of this model are listed below.

⋆ The main subtropical thermocline consists of an advective upper region overlying a diffusive base.

   – The diffusive base forms forms the *internal thermocline,* and in limit of small diffusivity this is an internal boundary layer. The advective region forms the *ventilated thermocline.* The separation of the two regions may, in reality, not be sharp.

   – The relative thicknesses of these layers is a function of various parameters, notably the strength of the wind and the magnitude of the diffusivity.

⋆ Above the ventilated thermocline there may be a mixed layer with a seasonally varying depth. In certain regions, for example at the polewards edge of the subtropical gyre, convection may deepen the mixed layer as far as the base of the thermocline.

⋆ A western boundary layer is needed to close the circulation and the heat budget.

⋆ The single-hemisphere model assumes that the water that sinks at high latitude either upwells through the main thermoline or returns to the subpolar gyre beneath the main thermocline. In reality some of this water may cross into the other hemisphere, so that, for example, the deep water in the North Atlantic may upwell in the Antarctic Circumpolar Current.

   – In this case, the diffusion-dependent overturning circulation represents only part of the overall meridional overturning circulation.

   – Nevertheless, there would remain a diffusive internal thermocline, because there is still a boundary between the warm subtropical water and cold abyssal water.

⋆ Within the ventilated thermocline there are two regions — the shadow zone and the western pool — whose dynamics are not determined without additional assumptions. A plausible assumption for the western pool, namely that all the water within it is ventilated, leads to a model of mode water.

⋆ Mesoscale eddies may play an important role in thermocline dynamics. Numerical simulations and some observations suggest that eddies may be particularly important in the internal thermocline, and they may provide a tendency for potential vorticity to homogenize.

Figure 16.12 Idealized geometry of the Southern Ocean: a re-entrant channel, partially blocked by a sill, is embedded within a closed rectangular basin; thus, the channel has periodic boundary conditions, whereas elsewhere there is no normal flow. The channel is a crude model of the Antarctic Circumpolar Current, with the area over the sill analagous to the Drake Passage.
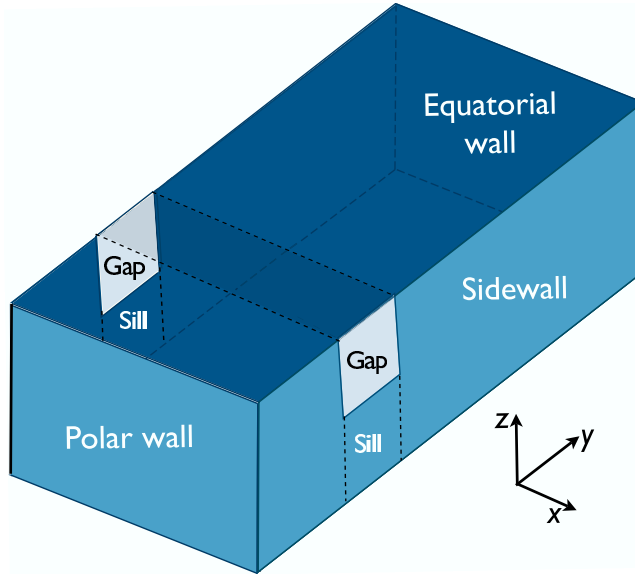
flow could take place at the surface via a western boundary current, as in a conventional subpolar gyre, and no overturning circulation need be set up.

16.5.1 A single hemisphere model

We consider first a single-hemisphere basin with a periodic channel near its polewards edge. We suppose it to be in the southern hemisphere, so the channel represents the Antactic Circumpolar Current (ACC), and that the dynamics are Boussinesq and planetary-geostrophic. We will choose extremely simple forms of wind and bouyancy forcing to allow us to obtain an analytic solution, and then later discuss how the qualitative forms of these solutions might more generally apply.

Wind and buoyancy forcing

Thermodynamic forcing is imposed by fixing the surface bouyancy. South of the gap we suppose the bouyancy is constant, then that it linearly increases across the gap, and is constant again polewards of the gap. Thus, there is no temperature gradient across the subtropical gyre, focussing attention on the influence of the channel. Thus, referring to Fig. 16.13:

$$b_s = \begin{cases} b_1, & 0 \le y \le y_1 \\ \dfrac{(b_2 - b_1)(y - y_1)}{y_2 - y_1}, & y_1 \le y \le y_2 \\ b_2, & y \ge y_2. \end{cases} \qquad (16.74)$$

where $b_2 > b_1$, and both are constants, and we make take $b_1 = 0$.

The wind forcing is purely zonal, and it is convenient to express this in terms of the Ekman transport and associated pumping (refer to section 2.12). In the channel the Ekman transport is chosen to be (realistically) equatorwards and (less realistically)
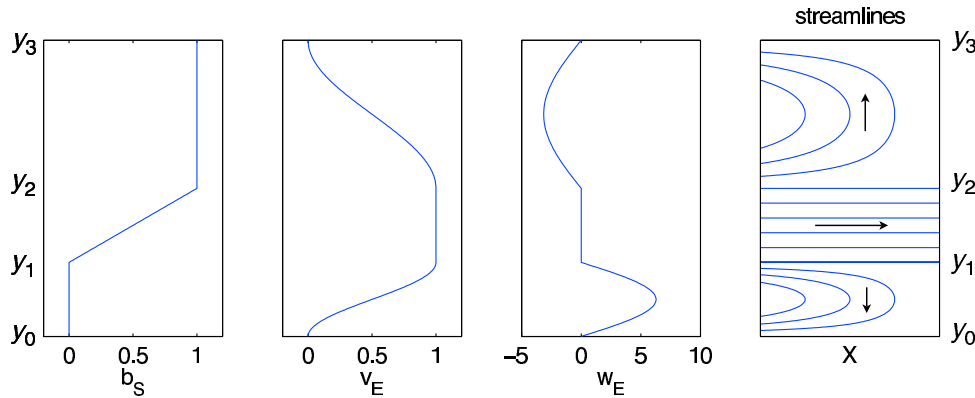
Fig. 16.13 The surface temperature b_s, merdional Ekman velocity v_E, vertical Ekman velocity w_E and the solution streamlines for the geostrophic horizontal flow, omitting the western boundary currents. The ordinate in all plots is latitude, with the pole at the bottom, and the four fields are given by, respectively, (16.74), (16.75a), (16.75b), and (16.76), with purely zonal flow given by (16.79) in the channel.

constant, a simplification that avoids complications of wind-driven upwelling in the channel. South (polewards) of the channel there is a conventional subpolar gyre, with an Ekman upwelling and an equatorwards Ekman transport that joins smoothly to that of the channel. Equatorwards of the channel there is conventional subtropical gyre, with Ekman downwelling. All this may be achieved by specifying:

$$
v_E = \begin{cases} \dfrac{V}{2}\left[1 - \cos\left(\dfrac{\pi y}{\Delta y_1}\right)\right] \\ V \\ \dfrac{V}{2}\left[1 + \cos\left(\dfrac{\pi(y - y_2)}{\Delta y_2}\right)\right] \end{cases} \qquad w_E = \begin{cases} W_1 \sin\left(\dfrac{\pi y}{\Delta y_1}\right) & 0 \le y < y_1 \\ 0 & y_1 \le y < y_2 \\ -W_2 \sin\left(\dfrac{\pi(y - y_2)}{\Delta y_2}\right) & y_2 \le y < y_3. \end{cases}
$$

$$(16.75\text{a,b})$$

where $\Delta y_1 = y_1$ and $\Delta y_2 = y_3 - y_2$. The meridional Ekman transport, v_E, is related to the Ekman pumping by $w_E = \partial v_E / \partial y$, so that $W_i = \pi V / (2\Delta y_i)$. If f were constant, the wind stress curl would be proportional to the w_E field above. The precise details of the forcing do not affect the qualitative form of the solution — they merely allow an analytic solution to be obtained — but there are two essential aspects to it:

  (i) The surface is cold south of the channel, warm north of the channel, and there is a temperature gradient across the channel.

 (ii) The Ekman flow is equatorwards within the channel, with a conventional gyres to either side.

The meridional extent of the region south of the channel and the wind forcing within it are relatively unimportant, and this region could be shrunk to nearly zero.

Solution in the gyres

Figure 16.14 Cross section of the structure of the single-hemisphere ocean model described in section 16.5.1. The domain is zonally closed equatorwards of y_2 and polewards of y_1, with a zonall-perioidic channel between latitudes y_1 and y_2 and above the sill, which has height η_{sill}. The arrows indicate the fluid flow driven by the equatorwards Ekman transport in the channel, and the solid lines are isopycnals.
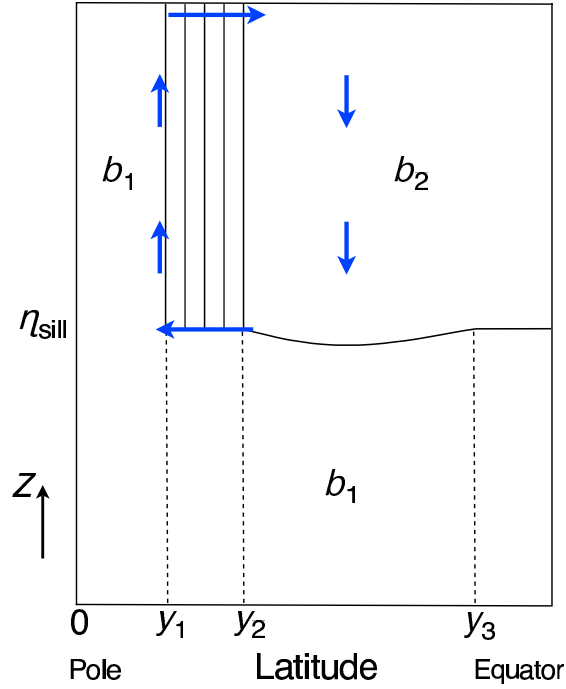
Below the depth of the sill the basin is fully enclosed, and therefore up to that level the basin will fill with the densest available water (much as described in section 15.2), except where it may be displaced by warmer fluid polewards of the gap that is pumped down below the level of the sill by the wind (Fig. 16.14). Thus, all of the domain south of the channel, and nearly everywhere below the sill the water has buoyancy b_1. Polewards of the channel, then, the fluid is barotropic and its vertically integrated horizontal circulation is given by Sverdrup balance, $\beta V = f w_E / H$, where V is the vertically integrated flow. With the wind-stress of (16.75) we get a conventional barotropic subpolar gyre (and associated western boundary current) by the same methods as we employed in chapter 14.

Above the sill, net meridional geostrophic transfer is forbidden in the channel region, because $\overline{v}_g = \partial \overline{\phi} / \partial x = 0$, where the overbar denotes a zonal average. Equatorwards of the channel the region above the sill will therefore tend to fill with the densest water available to it, and this is water with buoyancy equal to b_2. However because of the presence of wind forcing, the base of this layer is not flat; rather, this fluid obeys the dynamics of the one-layer ventilated thermocline model discussed in section 16.4.1. In such a model the depth of the fluid on the eastern boundary is constant, and this must be specified. Here, this is given by the height of the sill, and therefore $h(x = x_e, y) = h_e = H - \eta_{\text{sill}}$, where H is the total thickness of the fluid and η_{sill} is the sill height. Then, using (16.50), the thickness of the moving layer equatorwards of the sill is given by, for $y_2 < y < y_3$.

$$h^2 = (D^2(x, y) + h_e^2)^{1/2} \tag{16.76}$$

where

$$D^2 = -\frac{2f^2}{g'\beta} \int_x^{x_e} w_E \, \mathrm{d}x' = \frac{2f^2}{g'\beta} W(x_e - x) \sin\left(\frac{\pi(y - y_3)}{\Delta y}\right) \qquad (16.77)$$

where $g' = b_2 - b_1$. The solution is closed by the addition of a western boundary current. Note that because $h > h_e$, the light fluid is pushed below the level of the sill in the subtropical gyre.

Solution in the channel

In the channel, the fluid in the Ekman layer flows equatorwards, and therefore there must be a compensating polewards flow at depth. This will occur at and just below the level of the sill: it cannot be deeper, because here the basin is full of denser, b_1 fluid, and in the absence of eddying or ageostrophic flow it cannot be shallower because of the geostrophic constraint. Now, because of the temperature gradient across the channel the polewards flowing fluid is warmer than the fluid at the surface, and therefore convectively unstable. Convection ensues, the result of which is the entire column of fluid between the top of the sill and the surface takes on the temperature of the surface. Thermal wind demands that there be a zonal flow associated with this meridional temperature gradient, so this temperature distribution is advected eastwards into the interior of the channel. Because the interior is presumed to to be adiabatic, this temperature fields extends zonally throughout the channel. Thus, in steady state, the temperature *everywhere* in the channel above the level of the sill is given by:

$$b(x, y, z) = b_s(y) = \frac{(b_2 - b_1)(y - y_1)}{y_2 - y_1}, \qquad y_1 \leq y \leq y_2, \ z > \eta_{\text{sill.}} \qquad (16.78)$$

Note that convective mixing does not rely on a diapycnal diffusivity other than a molecular one: Convective plumes are generally turbulent, generating small scales in the fluid interior where mixing and entrainment may occur; failing that, the lighter fluid is displaced to the surface where it cools by way of interaction with the atmosphere. The zonal velocity within the channel is then given by thermal wind balance, so that

$$u(x, y, z) = -\frac{1}{f}\left(\frac{b_2 - b_1}{y_2 - y_1}\right)(z - \eta_{\text{sill}}). \qquad (16.79)$$

(Note that $f < 0$ so that the shear is positive.)

Regarding the depth-integrated zonal momentum budget, the wind-stress at the surface is balanced by a pressure force against the sill walls. This pressure gradient arises through the meridional circulation, for the southwards return flow just below the level of the sill is associated with a zonal pressure gradient that is exactly equal, but opposite, to the stress exerted by the wind. That is to say, in the Ekman layer the wind stress is balanced by the Coriolis force on the equatorwards flow in the Ekman layer, which by mass conservation is equal and opposite to the Coriolis force on the deep polewards flow, which by geostrophy is equal to the net pressure force on the sill walls. The wind-stress plays no role in determining the zonal transport of the channel: if the wind increases the meridional overturning, and the pressure force, increase but with no

change to the transport. This is a somewhat unrealistic feature of the model, for in reality the form stress induced by the flow over bottom topography, and that balances the wind stress, is a likely to be a function of the zonal transport as well as the meridional transport.

A qualitative summary

The circulation of the model may described as follows. The entire basin polewards of the channel fills with dense, b_1, water. Below the sill this fluid extends equatorward, filling the channel and the subtropical basin up to the level of the sill. Now, Ekman pumping in the channel forces near-surface fluid equatorwards, which warms as it goes, entering the subtropical basin at with buoyancy b_1. This fluid fills the basin down to the level of the sill, where it encounters the dense, b_1, fluid. The subtropical basin is wind-driven, and it forms a subtropical gyre with a single moving layer. Its dynamics are completely determined by specifying the wind, the reduced gravity ($g' = b_2 - b_1$), and the depth of the fluid at the eastern boundary (the sill depth). Because of the requirements of mass conservation, there must be a polewards return flow at depth, and so at the level of the sill warm water flows polewards. This flow is convectively unstable (because the water is lighter than that at the surface), and so the entire column of fluid mixes and its density takes on the value at the surface. The meridional temperature gradient gives rise to a eastwards flow, and this temperature field is advected zonally, and in steady state the temperature distribution is zonally symmetric and given by (16.78). The overturning circulation within the ACC is known as the Deacon cell, and this is a crude model of it. It is considered further in section 16.6.

If we were to add some diapycnal diffusivity to this situation, the sharp boundary between the two fluid masses at the sill height would be diffused to a front of finite thickness, with some upwelling and water mass transformation occurring across the front. This diffusive loss of dense fluid would be compensated by water-mass formation at the surface, polewards of the channel, leading to a deep, diffusively-driven circulation. That is, the deep water mass of b_1 fluid would circulate: this is a crude model of the 'Antarctic Bottom Water' cell.

Suppose now that the wind were everywhere zero, and the diffusivity small but non-zero. The cold, b_1 fluid would still quickly completely fill the basin polewards of the channel, and would fill the basin equatorwards of the channel up to the level of the sill. However, with no wind to drive an overturning circulation dense b_1 water would slowly drift ageostrophically across the channel, displacing warmer water until the *entire basin* were filled with the dense fluid, except for a thin boundary layer at the top needed to satisfy the upper boundary condition. The final state would be one of no motion, and no stratification, below this boundary layer. The important conclusion to the drawn is the following: *A deep meridional circulation, and a deep stratification, can be maintained, even as the diapycnal diffusivity goes to zero, in the presence of a wind forcing and a circumpolar channel.* Of course there are a number of idealised or unrealistic aspects to this model, perhaps the most egregious being:

  ★ The vertical isopycnals in the channel will be highly baroclinically unstable. This

will cause the isopycnals to slump, as well as (potentially) setting up a eddy-induced circulation. We consider this in section 16.6.

★ There is no surface temperature gradient across the subtropical gyre. If present it would lead to the formation of a 'main' subtropical thermocline, a full treatment of which would require determining its eastern boundary conditions. This would, however, be unlikely to qualitatively affect the presence of a deep, wind-driven overturning circulation.

★ The wind stress in the model channel is chosen so that the meridional Ekman transport is constant. (This means the wind-stress is chosen to vary in the same fashion as the Coriolis parameter, and if f were constant, the wind-stress curl would vanish.) Thus, there is no wind-driven downwelling or upwelling in the channel, and this simplifies the solution. Numerical simulations suggest that this choice does not affect the qualitative nature of the overturning circulation or temperature distribution.

16.5.2 A cross-equatorial wind-driven circulation

Let us now qualitatively and heuristically extend the above model to consider flow across the equator. The essential addition is that we suppose that the ocean basin extends to high northern latitudes, where there is, potentially, another source of cold deep water. To keep the model simple and tractable we will assume a very simple temperature structure:

$$
b_s = \begin{cases}
b_1, & 0 \leq y \leq y_1 \\
\dfrac{(b_2 - b_1)(y - y_1)}{y_2 - y_1}, & y_1 \leq y \leq y_2 \\
b_2, & y_2 \leq y \leq y_4 \\
b_3 & y > y_4.
\end{cases}
\tag{16.80}
$$

where the geometry is illustrated in Fig. 16.15. Given that $b_2 > b_1$, there are three cases to consider:

(i) $b_3 > b_2$. This is not oceanographically relevant to today's climate, nor does it provide another potential deep water source.

(ii) $b_3 < b_1$. The northern water is now the densest in the ocean, and would fill up the entire basin north of the channel (except near the surface in regions where some b_2 water is pushed down by the wind), and so provide no mid-depth stratification.

(iii) $b_1 < b_3 < b_2$. This is the most interesting and relevant case, and the only one we explore further.

As regards the wind, we will assume that that the south of the equator this is given by (16.75). North of the equator the wind forcing does not affect the qualitative nature of the overturning circulation, and may be taken to be zero.

Descriptive solution

In case (iii), the entire basin below the sill fills with b_1 water, except where wind forcing forces warmer fluid below the sill level, as before. However, unlike the earlier case, the

Figure 16.15 As for Fig. 16.14, but now for a two hemisphere ocean with a source of dense water, b_3, at high northern latitudes. The solid lines are isopycnals, and here the wind is zero in the Northern Hemisphere.
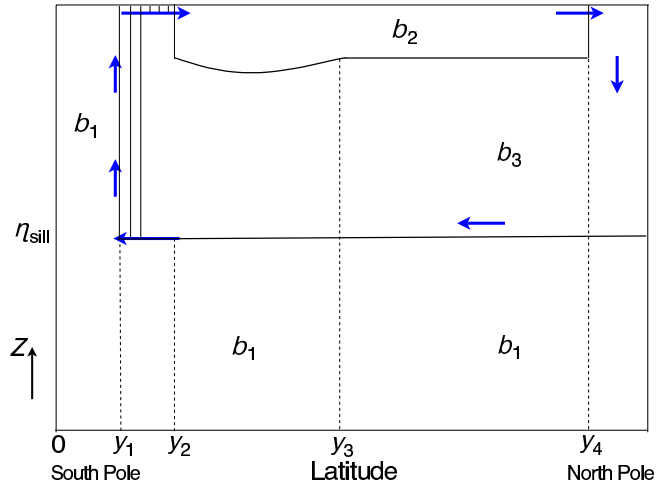
fluid above the sill is predominantly b_3 water from high northern latitudes. This forms in high polar latitudes and fills most of the basin above the sill, from the basin boundary in the north to the channel in the south (as discussed more below). However, except at latitudes where the b_3 is formed, it does not reach the surface because of the presence of b_2 water. That water is pushed down by the wind in the southern hemisphere to some as yet undetermined depth (discussed below), the boundary between b_2 and b_3 water then forming the upper ocean thermocline.

These water masses circulate because of the wind forcing in the channel. As in the single hemisphere case, northwards flowing water emerges from the channel with buoyancy b_2. This emerges into a region of Ekman downwelling, with a northwards transport carried by a western boundary current. This transport crosses the equator finally reaching the latitudes where b_3 water is formed where it sinks and returns equatorwards, again in a western bundary current. (Away from the western boundary layer there is no meridional flow in the absence of diffusion, because the flow satisfies $\beta v = f \, \partial w / \partial z$ and there is no upwelling.) This water then crosses the sill. However, unlike in the single hemisphere case, in the northern part of the sill this water is denser than the surface water; no convection occurs and so the b_3 water extends upwards to the surface, where it warms by contact with the atmosphere and advected equatorwards to become b_2 water. Further south the surface buoyancy in the channel is less than b_3, and the column now convectively mixes, much as in the single-hemisphere case. The solution is completed by specifying the thickness of the layer of b_2 water at the surface. Now, if the circulation is in steady state, the meridional transport between the gyres must equal that of the northwards Ekman flow at the northern edge of the circumpolar channel, and given the wind forcing, this is determined by the depth of the layer at the eastern boundary, a constant. Thus, in this model, global constraints determine the depth of the eastern boundary of the thermocline.

Suppose that the wind were everywhere zero. Then, as in the single-hemisphere case, the circulation would eventually die. Again, though, slow ageostrophic motion across the channel would first allow the entire basin, within and on both sides of the

channel, to fill with the densest available water, and in the final steady state there would be no stratification (and no motion) below a thin surface layer.

Suppose that a small amount of diffusion were added to the (wind-driven) model above. Then there would be mass exchange between the layers and, in particular, the deep cell of b_1 water would begin to diffusively circulate. In addition, the middepth cell would begin to upwell through the b_2–b_3 interface, and develop a diffusively driven circulation, in much the same way as is illustrated in Fig. 16.6.

Summary remarks

The key result of this model is that, as the diffusivity falls and the interior of the ocean becomes more and more adiabatic, a meridional cross-hemispheric circulation can be maintained, provided that the wind across the circumpolar channel remains finite. The diabatic water mass transformations all occur at the surface or in convection: these processes require a finite diffusivity, but this diffusivity can be the molecular one because the associated mixing involves turbulence, which can generate arbitrarily small scales. (Note that the convection that occurs in the circumpolar channel reduces the potential energy of the column, and requires no mechanical input of energy.) Aside from the region of the ACC, the meridional transport will occur (in this model) in western boundary layers. Indeed, we may still expect to see a southwards flowing deep western boundary current south of y_4 and below the b_2 water in Fig. 16.15, just as in the implicitly diffusive Stommel-Arons model. In the ACC itself, the the meridional transport occurs in a sub-surface current, nestled against the sill.

Although the overturning circulation in this model is 'wind-driven', the possibility that it may be cross-equatorial depends upon the thermodynamic forcing; in particular, if there is no source of dense water in the northern hemisphere, then the basin above the sill simply fills with b_2 water, as in the model of section 16.5.1, and there need be little or no inter-hemispheric flow. We emphasize, too, that our model of interhemispheric flow is quite heuristic: we have essentially *posited* that b_2 water may continuously flow across the equator, without examining the equatorial dynamics in any detail. Finally, we note that the simple model we have discussed, the overturning circulation is equal to that of the Ekman pumping in the channel. In reality, the ACC is a complex beast, and some of this water most likely recirculates within the channel, and this leads us into our next topic.

16.6 † FLOW IN A CHANNEL, AND THE ANTARCTIC CIRCUMPOLAR CURRENT

We now take a closer look at the Antarctic Circumpolar Current (ACC) itself, with less of a focus on how the ACC connects the rest of the worlds ocean and more of a focus on its own internal dynamics. This current system, sketched in Fig. 16.16, differs from other oceanic regimes primarily in that the flow is, like that of the atmosphere, predominantly zonal and re-entrant. The two obvious influences on the circulation are the strong, eastward winds (the 'roaring forties', the 'furious fifties', and the 'screaming sixties') and the buoyancy forcing associated with the meridional gradient of atmospheric temperature and radiative effects which cause ocean cooling at high latitudes

Figure 16.16 Schema of the major currents in the Southern Ocean. Shown are the South Atlantic subtropic gyre, and the two main cores of the ACC, associated with the Polar front and the sub-Antarctic front.[14]
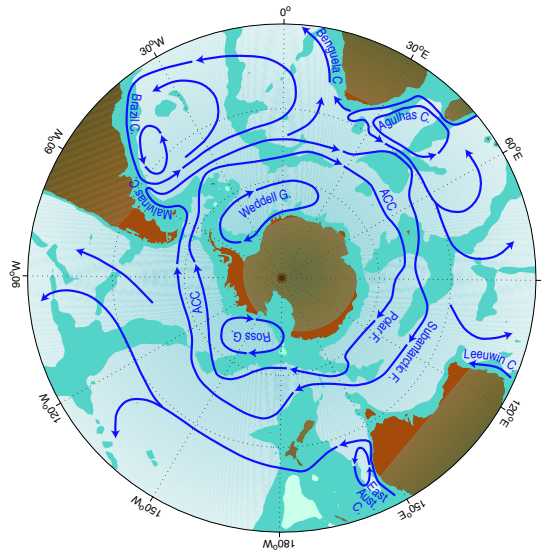
and warming at low. Providing a detailed description of the resulting flow is properly the province of numerical models, and here our goals are much more modest, namely to describe some of the basic dynamical mechanisms that determine the structure and transport of the system.[15]

16.6.1 Steady and eddying flow

Consider again the simplified geometry of the Southern Ocean as sketched in Fig. 16.12. The ocean floor is flat, except for a ridge (or 'sill') at the same longitude as the the gyre walls; this is a crude representation of the topography across the Drake Passage, that part of the ACC between the tip of South America and the Antarctic Peninsula. In the planetary geostrophic approximation, the steady response is that of nearly vertical isopycnals in the area above the sill, as illustrated in Fig. 16.14. Below the sill a meridional flow can be supported and the isotherms spread polewards, as illustrated in numerical solutions using the primitive equations (Fig. 16.17).[16]

The stratification of the non-eddying simulation is similar to that predicted by the idealized model illustrated in Fig. 16.14. However, the steep isotherms within the channel contain a huge amount of available potential energy (APE), and the flow is highly baroclinically unstable, and if baroclinic eddies are allowed to form, the solution is dramatically different: the isotherms slump, releasing that APE and generating mesoscale eddies. An important conclusion is that *baroclinic eddies are of first order importance in the dynamics of the ACC.* A dynamical description of the ACC without eddies would be *qualitatively* in error, in much the same way as would a similar description of the mid-latitude troposphere (i.e., the Ferrel Cell). (However, it is less clear whether these eddies are important in the interaction of the ACC with the rest of the worlds oceans.)
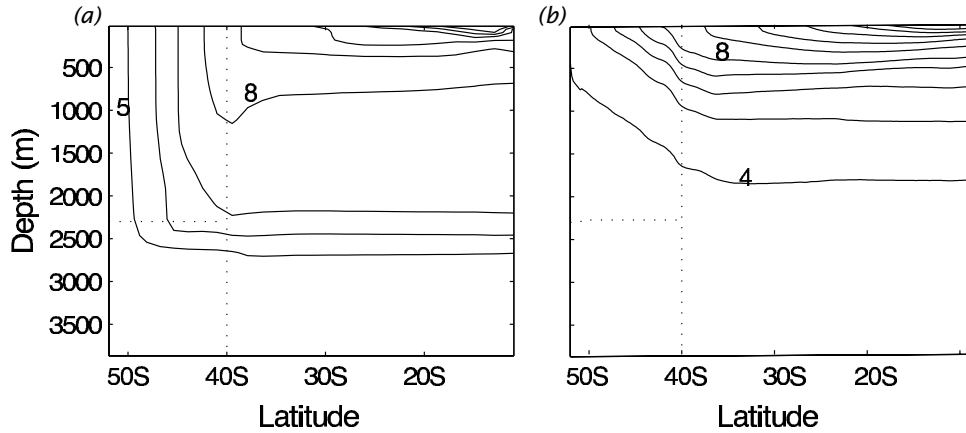
Fig. 16.17 The zonally-averaged temperature field in numerical solutions of the primitive equations in a domain similar to that of Fig. 16.12. Panel (a) shows the steady solution of a diffusive model with no baroclinic eddies, and (b) shows the time-averaged solution in a higher resolution model that allows baroclinic eddies to develop. The dotted lines show the channel boundaries and the sill.[17]

These eddies transfer both heat and momentum, and much of the rest of our description will focus on their effects.

16.6.2 Vertically integrated momentum balance

The momentum supplied by the strong eastward winds must somehow be removed. Presuming that lateral transfers of momentum are small the momentum must be removed by fluid contact with the solid earth at the bottom of the channel. Thus, let us first consider the vertically integrated momentum balance in a channel, without regard to how the momentum might be vertically transferred. We begin with the frictional-geostrophic balance

$$\boldsymbol{f} \times \boldsymbol{u} = -\nabla\phi + \frac{\partial \widetilde{\boldsymbol{\tau}}}{\partial z}, \tag{16.81}$$

where $\widetilde{\boldsymbol{\tau}}$ is the kinematic stress (and henceforth we drop the tilde). Integrating over the depth of the ocean gives [c.f. (14.106)]

$$\boldsymbol{f} \times \widehat{\boldsymbol{u}} = -\nabla\widehat{\phi} - \phi_b \nabla\eta_b + \boldsymbol{\tau}_w - \boldsymbol{\tau}_f, \tag{16.82}$$

where $\boldsymbol{\tau}_w$ is the stress at the surface (due mainly to the wind), and $\boldsymbol{\tau}_f$ is the frictional stress at the bottom. A hat denotes a vertical integral and ϕ_b is the pressure at $z = \eta_b$, where η_b is the z-coordinate of the bottom topography.

The x-component of this equation is just

$$f\widehat{v} = -\frac{\partial \widehat{\phi}}{\partial x} - \phi_b \frac{\partial \eta_b}{\partial x} + \tau_w^x - \tau_f^x, \tag{16.83}$$

and on integrating around a line of latitude the term on the left-hand side vanishes by mass conservation and we are left with

$$\oint [\phi_b \frac{\partial \eta_b}{\partial x} + \tau_w^x - \tau_f^x] \, dx = 0. \tag{16.84}$$

The first term is the form drag, encountered in sections 3.5 and 14.6, and observations and numerical simulations indicate that it is this, rather than the frictional term τ_f^x, that predominantly balances the wind stress in the zonally and vertically integrated momentum balance.[18] We return to the question of why this should be so later.

The vorticity balance is also dominated by a balance between bottom pressure torque and wind stress curl. Taking the curl of (16.82) gives

$$\beta \hat{v} = \mathbf{k} \cdot \nabla \phi_b \times \nabla \eta_b + \mathrm{curl}_z \boldsymbol{\tau}_w - \mathrm{curl}_z \boldsymbol{\tau}_f. \tag{16.85}$$

Now, on integrating over an area bounded by a latitude circle and applying Stokes's theorem the β term vanishes by mass conservation and we regain (16.84). This means that Sverdrup balance, in the usual sense of $\beta v \approx \mathrm{curl}_z \boldsymbol{\tau}_w$, cannot hold in the zonal average: the left-hand side vanishes but the right-hand side does not. The same could be said for the zonal integral of (16.85) across a gyre, but the two cases do differ: In a gyre Sverdrup balance can (in principle) hold over most of the interior, with mass balance being satisfied by the presence of an intense western boundary current. In contrast, in a channel where the dynamics are zonally homogeneous then v must be, on average, zero at *all* longitudes and form drag and/or frictional terms must balance the wind-stress curl in a given water column. Sverdrup balance is thus a less useful foundation for channel dynamics (at least zonally homogeneous ones) than it is for gyres. Of course, the real ACC is *not* zonally homogeneous, and may contain regions of polewards Sverdrup flow balanced by equatorwards flow in boundary currents along the eastern edges of sills and continents, and the extent to which Sverdrup flow is a leading-order descriptor of its dynamics is partly a matter of geography.

We cannot in general completely neglect nonconservative frictional terms, on two counts. First, they are the means whereby kinetic energy is dissipated. Second, if there is a contour of constant orographic height encircling the domain (i.e., encircling Antartica) then the form drag will vanish when integrated along it. However, the same integral of the wind stress will not vanish, and therefore must be balanced by something else. To see this explicitly, write the vertically integrated vorticity equation, (16.85), in the form

$$\beta \hat{v} + J(\phi_b, \eta_b) = \mathrm{curl}_z \boldsymbol{\tau}_w - \mathrm{curl}_z \boldsymbol{\tau}_f. \tag{16.86}$$

If we integrate over an area bounded by a contour of constant orographic height (i.e., constant η_b) then both terms on the left-hand side vanish, and the wind-stress along that line must be balanced by friction. In the real ocean there may be no such contour that is confined to the ACC — rather, any such contour would meander through the rest of the ocean; indeed, no such confined contour exists in the idealized geometry of Fig. 16.12.

16.6.3 Form drag and baroclinic eddies

How does the momentum put in at the surface by the wind stress make its way to the bottom of the ocean where it may be removed by form drag? We saw in section 16.5.1 that one mechanism is by way of a mean meridional overturning circulation, with an upper branch in the Ferrel cell and a lower branch at the level of the sill, with no meridional flow between. However, the presence of baroclinic eddies changes things in two related ways:

 (i) Eddy form drag can pass momentum vertically within the fluid
 (ii) Eddies can allow a net meridional mass flux.

Momentum dynamics of layers

Let us first model the channel as a finite number of fluid layers, each of constant density and lying one on top of the other — a 'stacked shallow water' model, equivalent to a model expressed in isopycnal coordinates. The wind provides a stress on the upper layer which sets it into motion, and this in turn, via the mechanism of form drag, provides a stress to the layer below, and so on until the bottom is reached. The lowest layer then equilibrates via form drag with the bottom topography or via Ekman friction, and the general mechanism is illustrated in Fig. 16.18.

Recalling the results of section 3.5, the form drag at a layer interface is given by

$$\tau_i = -\overline{\eta_i \frac{\partial p_i}{\partial x}} = -\rho_0 f \overline{\eta_i v_i} \tag{16.87}$$

where p_i is the pressure and η_i the displacement at the i'th interface (i.e., between the i'th and $i + 1$ layer as in Fig. 16.19), and the overbar denotes a zonal average. If we define the averaged meridional transport in each layer by

$$V_i = \int_{\eta_i}^{\eta_{i-1}} \rho_0 v \, \mathrm{d}z \tag{16.88}$$

then, neglecting the meridional momentum flux divergence (as explained in the next subsection), the time- and zonally-averaged zonal momentum balance for Boussinesq layers of fluid are:

$$-f\overline{V}_1 = \tau_w - \tau_1 = \overline{\eta_1 \frac{\partial p_1}{\partial x}} + \tau_w, \tag{16.89a}$$

$$-f\overline{V}_i = \tau_{i-1}^x - \tau_i = -\overline{\eta_{i-1} \frac{\partial p_{i-1}}{\partial x}} + \overline{\eta_i \frac{\partial p_i}{\partial x}}, \tag{16.89b}$$

$$-f\overline{V}_N = \tau_{N-1} - \tau_N = -\overline{\eta_{N-1} \frac{\partial p_{N-1}}{\partial x}} + \overline{\eta_b \frac{\partial p_b}{\partial x}} - \tau_f, \tag{16.89c}$$

where the subscripts 1, i and N refer to the top layer, an interior layer, and the bottom layer, respectively. Also, η_b is the height of bottom topography and τ_w is the zonal stress imparted by the wind which, we assume, is confined to the uppermost layer. The term τ_f represents drag at the bottom due to Ekman friction, but we have neglected any other viscous terms or friction between the layers.
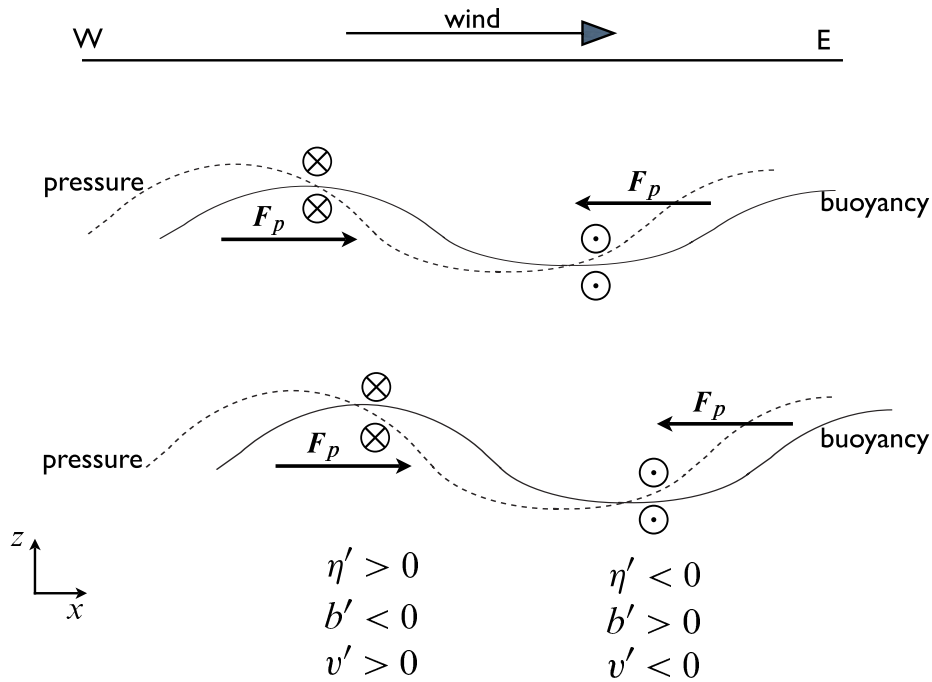
Fig. 16.18 Eddy fluxes and form drag in a Southern Hemisphere channel, viewed from the south. In this example, cold (less buoyant) water flows equatorwards and warm water polewards, so that $\overline{v'b'} < 0$. The pressure field associated with this flow (dashed lines) provides a form-drag on the successive layers, $\boldsymbol{F}_p$, shown. At the ocean bottom the westward form drag on the fluid arising through its interaction with the orography of the sea-floor is equal and opposite to that of the eastward wind-stress at the top. The mass fluxes in each layer are given by $\overline{v'h'} \approx -\partial_z(\overline{v'b'}/N^2)$. If the magnitude of buoyancy displacement increases with depth then $\overline{v'h'} < 0$, providing a polewards mass flux that could balance the equatorwards mass flux in the Ekman layer.

The vertically integrated meridional mass transport must vanish, and thus summing over all the layers (16.89) becomes

$$0 = \tau_w - \tau_f - \tau_N \tag{16.90}$$

or, noting that $\tau_N = -\overline{\eta_b \partial p_b/\partial x}$,

$$\boxed{\tau_w = \tau_f - \overline{\eta_b \frac{\partial p_b}{\partial x}}} \; . \tag{16.91}$$

Thus, the stress imparted by the wind (τ_w) may be communicated vertically through the fluid by form drag, and ultimately balanced by the sum of the bottom form stress (τ_N) and bottom friction (τ_f). Note that it is also a type of form drag that leads to the

momentum balance in the steady model of section 16.5; in that case, the southwards return flow is nestled against the sill, and the associated Coriolis force is balance by a pressure force against the sill.

Momentum dynamics in height coordinates

We now look at these same dynamics in height coordinates, using the quasi-geostrophic TEM formalism (it may be helpful to review section 7.3 before proceeding). We write the zonally-averaged momentum equation in the form

$$-f_0 \overline{v}^* = \nabla_m \cdot \boldsymbol{\mathcal{F}} + \frac{\partial \tau}{\partial z} \tag{16.92}$$

where $\overline{v}^*$ is the residual meridional velocity, τ is the zonal component of the kinematic stress (wind induced and frictional) and $\boldsymbol{\mathcal{F}}$ is the Eliasssen-Palm flux, which satisfies

$$\nabla_m \cdot \boldsymbol{\mathcal{F}} = -\frac{\partial}{\partial y} \overline{u'v'} + \frac{\partial}{\partial z} \left(\frac{f_0}{N^2} \overline{v'b'} \right) = \overline{v'q'}. \tag{16.93}$$

The stress is typically important only in an Ekman layer at the surface and in a frictional layer at the bottom. Now, if the horizontal velocity and buoyancy perturbations are related by $v' \sim b'/N$ (see chapter 9) then the two terms comprising the potential vorticity flux scale as

$$\frac{\partial}{\partial y} \overline{u'v'} \sim \frac{v'^2}{L_e}, \qquad \frac{\partial}{\partial z} \left(f_0 \frac{\overline{v'b'}}{\overline{b}_z} \right) \sim \frac{v'^2}{L_d} \tag{16.94}$$

where L_e is the scale of the eddies and L_d is the deformation radius. If the former is much larger than the latter, as we might expect in a field of developed geostrophic turbulence (and as is indeed observed in the ACC), then the potential vorticity flux is dominated by the buoyancy flux [so also justifying the neglect of the lateral momentum fluxes in (16.89)] and (16.92) becomes

$$-f_0 \overline{v}^* \approx \frac{\partial \tau}{\partial z} + \frac{\partial}{\partial z} \left(f_0 \frac{\overline{v'b'}}{\overline{b}_z} \right). \tag{16.95}$$

If we integrate this equation over the depth of the channel the term on the left-hand side vanishes and we have

$$\tau_w = \tau_f - \left[f_0 \frac{\overline{v'b'}}{\overline{b}_z} \right]_{-H}^{0}, \tag{16.96}$$

where τ_w is the wind stress and τ_f is the frictional stress at the bottom. As we noted in section 7.4.3, the vertical component of the EP flux is equivalent to a form stress acting on a fluid layer, and (16.96) expresses essentially the same momentum balance as (16.91) (where it was assumed that the stress at the top arises from the wind). Thus, the EP flux expresses the passage of momentum vertically through the water column, and it is removed at the bottom through frictional stresses and/or form drag with the orography.
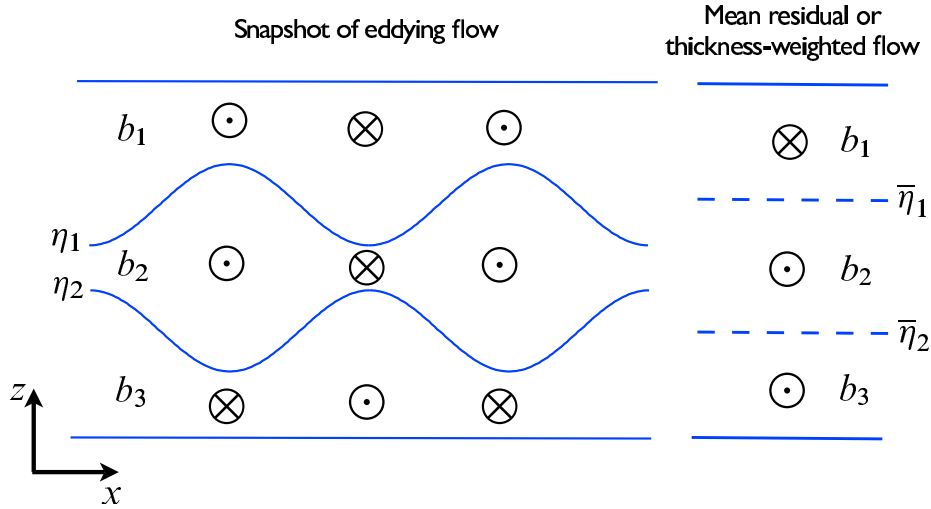
Fig. 16.19 A schema of the meridional flow in an eddying channel. The eddying flow may be organized (for example by baroclinic instability) such that, even though at any given level the Eulerian meridional flow may be small, there is a net flow in a given isopycnal layer. The residual ($\overline{v}^*$) and Eulerian ($\overline{v}$) flows are related by $\overline{v}^* = \overline{v} + \overline{v'h'}/\overline{h}$; thus, the thickness-weighted average of the eddying flow on the left gives rise to the residual flow on the right, where $\overline{\eta}_i$ denotes the mean elevation of the isopycnal η_i.

Mass fluxes and thermodynamics

Associated with the form drag is a meridional mass flux, which in the layered model appears as V_i in each layer. The satisfaction of the momentum balance at a particular latitude goes hand-in-hand with the satisfaction of the mass balance. Above any topography the Eulerian mean momentum equation is (with quasi-geostrophic scaling and neglecting eddy momentum fluxes),

$$f_0 \overline{v}_a = \tau \tag{16.97}$$

where $\overline{v}_a$ is the ageostrophic meridional velocity and τ the zonal stress. That is, all the zonally-averaged meridional flow is ageostrophic and, in this approximation, it is non-zero only near the surface (i.e., equatorwards Ekman flow) and below the level of the topography, where it can be supported by friction and/or form drag. Even in an eddying flow, the Eulerian circulation is primarily confined to the upper Ekman layer and a frictional or topographically interupted layer at the bottom, as illustrated in Fig. 16.20. This is a perfectly acceptable description of the flow, and is not an artifact in any way. However, and analogously to the atmospheric Ferrel Cell (section 11.6 and 12.2.2), if the flow is unsteady this circulation does not necessarily represent the flow of water parcels, nor does it imply that water parcels cross isopycnals, as might be suggested by the leftmost panel of Fig. 16.20. That flow is better represented by the residual flow, or the thickness weighted flow, and as sketched in Fig. 16.19 there can be
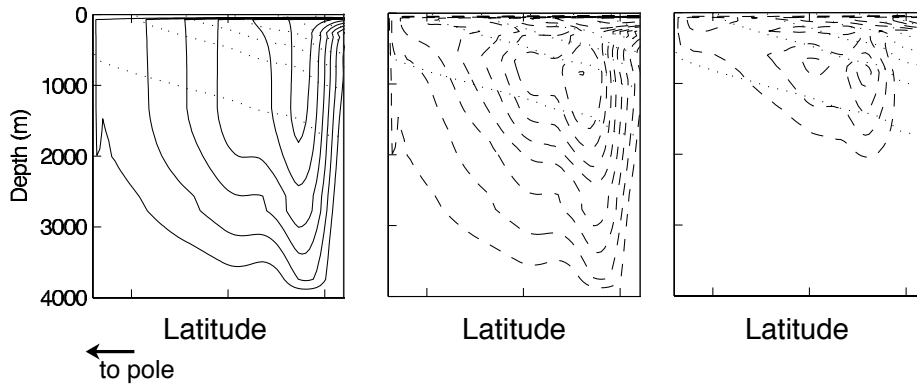
Fig. 16.20 The meridional circulation in the re-entrant channel of an idealized, eddying numerical model of the ACC (as in Fig. 16.17, but showing only the region south of 40°S). Left panel, the zonally averaged Eulerian circulation. Middle panel, the eddy induced circulation. Right panel, the residual circulation. Solid lines represent a clockwise circulation and dashed lines, anticlockwise. The faint dotted lines are the mean isopycnals. Over much of the channel the model ocean is losing buoyancy (heat) to the atmosphere and so the net, or residual, flow at the surface is polewards.

a net meridional flow in a given layer (i.e., of a given water mass type) *even when the net meridional Eulerian flow at the level of mean height of the layer is zero.*

The vertically integrated mass flux must of course vanish, and even though one component of this — the equatorwards Ekman flow — is determined mechanically, the overall sense of the residual circulation cannot be determined by the momentum balance alone: thermodynamic effects play a role. As in (7.93), the thermodynamic equation may be written in TEM form as

$$\frac{\partial \overline{b}}{\partial t} + J(\psi^*, \overline{b}) = Q[b] \tag{16.98}$$

where $J(\psi^*, \overline{b}) = (\partial_y \psi^*)(\partial_z b) - (\partial_z \psi^*)(\partial_y b) = \overline{v}^* \partial_y b + \overline{w}^* \partial_z b$, ψ^* is the streamfunction of the residual flow and $Q[b]$ represents heating and cooling, which occurs mainly at the surface. In the ocean interior and in statistically steady state we therefore have

$$J(\psi^*, \overline{b}) = 0, \tag{16.99}$$

the general solution of which is $\psi^* = G(\overline{b})$ where G is an arbitrary function. That is, the residual flow is along isopycnals, and this is approximately satisfied by the numerical solution shown in Fig. 16.20.

At the surface, however, the flow is generally not adiabatic, because of heat exchange with the atmosphere. In the simulations shown there is a net heat flux, and consequent buoyancy loss, from the ocean to the atmosphere at the polewards edge of the domain. Heat balance is then achieved by a polewards residual flow of warmer fluid at the surface and sinking at the the highest latitudes. If there were no surface fluxes,

and the flow were everywhere adiabatic, then we can expect the residual circulation to vanish. Note that the sense of the subsurface circulation determines how the form drag varies with depth; if the residual flow were zero for example then, either from (16.89) or from (16.95), we see that the form drag must be constant with depth.

16.6.4 † An idealized adiabatic model

We finally consider a simple model of the ACC that, although very idealized, provides a starting point for understanding more complete numerical models and the system itself.[19] The simplifying assumption we make is that the flow is adiabatic everywhere; it then follows that the net overturning, as given by the residual circulation, is zero. We can see this by first noting that in a statistically steady state the flow satisfies (16.99), implying that the residual flow is along isopycnals. However, if there is a meridional buoyancy gradient at the surface there can be no surface residual flow (because this would be cross-isopycnal); it then follows that there can be no net flow along isopycnals in the interior, because if these outcrop there would be a net fluid source, and hence diapycnal flow, at the surface. This idealized, and rather unrealistic, limit has thus led to the 'vanishing of the Deacon Cell'.

The zonal momentum equation in this limit follows from (16.95), which with $\overline{v}^* = 0$ gives

$$\frac{\partial \tau}{\partial z} \approx -\frac{\partial}{\partial z}\left(f_0 \frac{\overline{v'b'}}{\overline{b}_z}\right), \tag{16.100}$$

In this balance the equatorwards flow in the Ekman layer is balanced by a polewards eddy mass flux, and in the ocean interior where the stress is small the meridional buoyancy flux is constant with height. This situation is unlikely to hold in reality, but Fig. 16.20 shows that in a numerical simulation the residual flow is weaker than either the Eulerian or the eddy-induced flow.

Integrating (16.100) from the surface (where $\tau = \tau_w$) to a stress-free level in the interior gives

$$\tau_w = f_0 \frac{\overline{v'b'}}{\overline{b}_z}, \tag{16.101}$$

if the bouyancy flux at the surface is small. If we are now willing to parameterize the eddy fluxes in terms of the mean flow, then we can predict the stratification. Thus, let $\overline{v'b'} = -\kappa \partial \overline{b}/\partial y$, and noting that $s = -\overline{b}_y/\overline{b}_z$ is the slope of the isopycnals, or using thermal wind balance, we find

$$\tau_w = \kappa f_0 s \approx \kappa \frac{f_0^2}{N^2}\frac{\partial \overline{u}}{\partial z} \tag{16.102}$$

Thus, given κ, we can predict the isopcynal slope and, potentially, the total transport of the ACC as a function of the wind stress. Further progress then depends on making a specific choice for κ, as described in chapter 10, but our reach has already exceeded our grasp. In a more realistic diabatic model, the sense of the residual circulation can be inferred if the diabatic fluxes at the surface are known, but at the same time these fluxes

depend in a complicated way on both the lateral eddy fluxes and the general circulation itself.

16.6.5 Form stress and Ekman stress at the ocean bottom

Earlier, we noted that the stress at the ocean bottom is observed to be dominated by form stress, rather than Ekman friction. A simple scaling argument helps understand why this should be. The form stress scales like

$$\tau_{\text{form}} \sim \eta_b \frac{\partial p_b}{\partial x} \sim \eta_b V f, \tag{16.103}$$

where V is a scaling for the horizontal velocity. The frictional stress due to an Ekman layer scales like

$$\tau_{\text{Ekman}} \sim A \frac{\partial u}{\partial z} \sim \frac{AV}{d} \sim dVf \tag{16.104}$$

where A is a coefficient of viscosity and $d = \sqrt{A/f}$ is the Ekman layer thickness. The ratio of these two stresses thus scales as

$$\frac{\tau_{\text{form}}}{\tau_{\text{Ekman}}} \sim \frac{\eta_b}{d}. \tag{16.105}$$

We therefore expect the form stress to dominate the Ekman stress if the variations in topography are greater than the Ekman layer thickness, and if the flow goes *over* the topography rather than around it. In the ACC, and indeed in many regions of the ocean, the topography is hundreds or even thousands of meters high whereas the bottom Ekman layer may be of order tens of meters, and furthermore the predominantly westward flow must (unlike the siutation in gyre circulations) go over the topography. Thus, form stress dominates the frictional, Ekman layer, stress at the bottom of the ocean.

16.6.6 Differences between gyres and channels

In the dynamics of the ACC, the wind stress itself seems to play an important role, whereas in our discussion of gyres in chapter 14 the wind stress *curl* was dominant. What is the root of this difference?[20] Suppose that we change the wind stress, but not its curl, in a closed basin. The vertically integrated gyral flow, as given for example by the Stommel solution (14.39) or its two-gyre counterpart, does not change at all. However, the vertical structure of this flow will in general change; for example, if the wind is made uniformly more eastward, there will be a corresponding increase in the equatorward flux in the Ekman layer that must return polewards at depth (note that the western boundary current balances only the Sverdrup flow). At the same time, the added force from the wind must be balanced by a increased pressure difference between the western and eastern boundaries. This may be achieved if the the sea-surface tilts upward to the east, so producing a net (vertically integrated) northwards geostrophic flow. The subsurface isopycnal slopes must then adjust in order to reduce this southwards flow to near zero in the abyss. This added force provided by the by the basin walls on the fluid

in the basin is a kind of form drag (rather like the force provided by the sill in section 16.5), and integrated around the basin this force must be equal and opposite to the force supplied by the wind. In a channel, adding a constant wind produces a direct change in its zonal transport. This is because the wind-stress is balanced by form drag and bottom friction (with the former likely dominating), and both of these, in practice, depend on the zonal flow at the channel bottom.

APPENDIX: MISCELLANEOUS RELATIONSHIPS IN A LAYERED MODEL

Here for convenience we collect various expressions relating pressure, density and velocity in a geostrophic and Boussinesq layered model. The layers and the interfaces are numbered, increasing downwards, as in Fig. 16.21, and the bottom layer is stationary.

16.A.1 Hydrostatic balance

Hydrostatic balance is:

$$\frac{\partial p}{\partial z} = -\rho g \tag{16A.1}$$

Thus, in each layer we can represent the velocity as

$$p_n = -\rho_n g z + p'_n(x, y) \tag{16A.2}$$

and

$$p_{n-1} = -\rho_{n-1} g z + p'_{n-1}(x, y) \tag{16A.3}$$

Since pressure is continuous, at $z = z_{n-1}$ these two expressions are equal so that

$$-\rho_n g z_{n-1} + p'_n = p_{n-1} = -\rho_{n-1} g z_{n-1} + p'_{n-1} \tag{16A.4}$$

whence

$$(\rho_n - \rho_{n-1}) g z_{n-1} = p'_n - p'_{n-1}. \tag{16A.5}$$

or

$$g'_{n-1} z_{n-1} = \frac{1}{\rho_0}(p'_n - p'_{n-1}) \tag{16A.6}$$

where $g'_n = g(\rho_{n+1} - \rho_n)/\rho_0$ is the *reduced gravity*, and ρ_0 is the constant, reference, value of the density used in the Boussinesq approximation.

16.A.2 Geostrophic and thermal wind balance

Geostrophic balance is:

$$\rho_0 f \boldsymbol{u}_n = \mathbf{k} \times \nabla p_n \tag{16A.7}$$

where we use a constant value of the density, consistent with the Boussinesq approximation. Using this with (16A.6) gives

$$\boldsymbol{u}_{n+1} - \boldsymbol{u}_n = \frac{g'_n}{f}\mathbf{k} \times \nabla z_n \tag{16A.8}$$
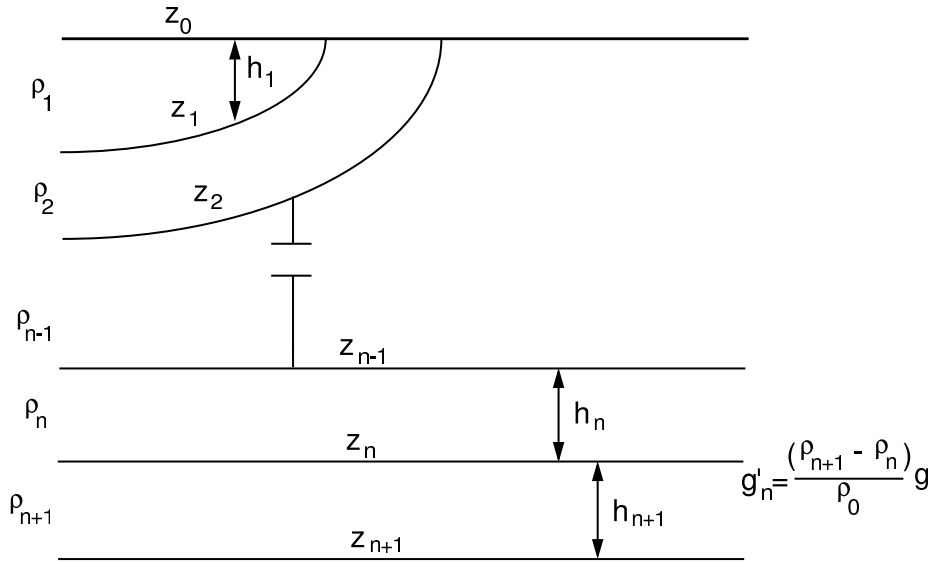
Fig. 16.21 Structure and notational conventions used here for a multi-layered model.

which is the appropriate form of thermal wind balance for this system.

Let us suppose that at sufficient depth there is no motion, and in particular that layer $N+1$ is stationary and contains no pressure gradients. That is, $p'_{N+1} = 0$ and so, from (16A.5),

$$p'_N = -(\rho_{N+1} - \rho_N)gz_N = -g'_N\rho_0 z_N. \tag{16A.9}$$

Integrating upwards we obtain the pressure in each layer,

$$p'_n = -\rho_0 \sum_{i=n}^{i=N} g'_i z_i \tag{16A.10}$$

where $n \leq N$. Thus, the geostrophic velocities in each layer are given by

$$f\boldsymbol{u}_n = -\mathbf{k} \times \nabla \left(\sum_{i=n}^{i=N} g'_i z_i \right). \tag{16A.11}$$

The quantity in brackets on the right-hand side is not, strictly, a streamfunction because it is $f\boldsymbol{u}_n$, and not $\boldsymbol{u}_n$ that is given by its curl. Nevertheless, the velocity is normal to its gradient, and therefore its isolines define streamlines.

The upper surface of the ocean is assumed to be fixed; this is the 'rigid-lid' approximation. Thus, $z_0 = 0$ and $h_1 = -z_1$. More generally, the layer thicknesses and the interfaces between the layers are related by

$$z_n = -\sum_{i=M}^{i=n} h_i \tag{16A.12}$$

where M is the index of the uppermost layer, and $n \geq M$. If there is no outcropping, then $M = 1$.

The geostrophic velocity in the lowest moving layer is given by

$$f\boldsymbol{u}_N = -g'_N \mathbf{k} \times \nabla z_N = g'_N \mathbf{k} \times \nabla h. \qquad (16A.13)$$

This means that lines of constant depth of the lowest layer are also streamlines; the velocity moves parallel to the depth contours. The vertical velocity at the base of the lowest layer is given by

$$w(z = -h) = \boldsymbol{u}_N \cdot \nabla h = \frac{1}{f} g'_N (\mathbf{k} \times \nabla h) \cdot \nabla h = 0. \qquad (16A.14)$$

That is, there is no vertical motion at the base of the moving layers if the flow is steady.

16.A.3 Explicit cases

A one-layer reduced-gravity model

The perturbation pressure in the moving layer (layer 1) is

$$p'_1 = -\rho_0 g'_1 z_1 = \rho_0 g'_1 h_1 \qquad (16A.15)$$

The geostrophic velocity is given by

$$f\boldsymbol{u}_1 = \frac{1}{\rho_0} \mathbf{k} \times \nabla p'_1 = g'_1 \mathbf{k} \times \nabla h_1. \qquad (16A.16)$$

(In a single layer model, the subscripts are often omitted.)

A two-layer model

The perturbation pressure in the upper and lower moving layers are given by

$$p_1 = -\rho_0 (g'_2 z_2 + g'_1 z_1) = \rho_0 (g'_2 h + g'_1 h_1) \qquad (16A.17a)$$

$$p'_2 = -\rho_0 g'_2 z_2 = \rho_0 g'_2 (h_1 + h_2) = \rho_0 g'_2 h \qquad (16A.17b)$$

(c.f. (16A.9)), where $h = h_1 + h_2 = -z_2$.

The corresponding geostrophic velocities are

$$f\boldsymbol{u}_1 = \mathbf{k} \times \nabla(g'_2 h + g'_1 h_1) \qquad (16A.18a)$$

$$f\boldsymbol{u}_2 = \mathbf{k} \times \nabla(g'_2 h). \qquad (16A.18b)$$

A three-layer model

The perturbation pressures in the three moving layers are

$$p_1 = -\rho_0[g_3'z_3 + g_2'z_2 + g_1'z_1]$$
$$= \rho_0[g_3'h + g_2'(h_1 + h_2) + g_1'h_1] \tag{16A.19a}$$

$$p_2 = -\rho_0[g_2'z_2 + g_3'z_3] = \rho_0[g_2'(h_1 + h_2) + g_3'h] \tag{16A.19b}$$

$$p_3 = -\rho_0 g_3'z_3 = \rho_0 g_3'h. \tag{16A.19c}$$

where $h = h_1 + h_2 + h_3 = -z_3$. The corresponding geostrophic velocities are:

$$f\boldsymbol{u}_1 = \mathbf{k} \times \nabla[g_3'h + g_2'(h_1 + h_2) + g_1'h_1] \tag{16A.20a}$$
$$f\boldsymbol{u}_2 = \mathbf{k} \times \nabla[g_2'(h_1 + h_2) + g_3'h] \tag{16A.20b}$$
$$f\boldsymbol{u}_3 = \mathbf{k} \times \nabla[g_3'h]. \tag{16A.20c}$$

Notes

1 For measurements of the diapycnal diffusivity in various parts of the worlds oceans, see (among others) Gregg (1998), Toole et al. (1994), Polzin et al. (1997), Ledwell et al. (1998).

2 For estimates of the strength of the overturning circulation in the ocean, and its relation to diapycnal diffusivity and the observed stratification, see Munk (1966), revisited by Munk and Wunsch (1998). See also Huang (1999) and, for a review, Wunsch and Ferrari (2004).

3 Vallis (2000).

4 The modern development of the theory of the thermocline began with two back-to-back papers in 1959 in the journal *Tellus*. Welander (1959) suggested an adiabatic model, based on the ideal-fluid thermocline equations (i.e., the planetary geostrophic equations, with no diffusion terms in the buoyancy equation), whereas Robinson and Stommel (1959) proposed a model that is intrinsically diffusive. In this model [developed further by Stommel and Webster (1963), Salmon (1990), and others] the thermocline is an internal boundary layer or front that forms at the convergence of two different homogeneous water types, warm surface fluid above and cold abyssal fluid below. Meanwhile, the adiabatic model continued its own development (see Veronis 1969), culminating in the ventilated thermocline model of Luyten et al. (1983) and its continuous extensions (e.g., Huang 1988). As time passed, Welander (1971b) and Colin De Verdiere (1989) realized that the diffusion might become important below an adiabatic near-surface flow, and Samelson and Vallis (1997) suggested a model in which the upper thermocline is adiabatic, as in the ventilated thermocline model, but has a diffusive base, constituting an internal boundary layer. The role of mesoscale eddies in all of this is still unclear. However, numerical simulations do suggest they do play a role in determining the structure of the thermocline, at least in its diffusive base and perhaps everywhere. Further,

the fact that the some of the deep overturning circulation may be wind-driven, and inter-hemispheric, will also affect the dynamics of the diffusive layer, so the story is not over.

5 Welander (1971a).

6 Drawing from Salmon (1990).

7 Newton's method is an iterative way to numerically solve certain types of differential equations. The solutions here are obtained using about 1000 uniformly spaced grid points to span the domain, taking just a few seconds of computer time. Because of the boundary layer structure of the solutions employing a nonuniform grid would be still more efficient for this problem, but there is little point in designing a streamlined hat to reduce the effort of walking.

8 Samelson (1999b).

9 Adapted from Samelson and Vallis (1997).

10 Following Luyten et al. (1983).

11 That the eastern boundary depth is undetermined is perhaps the main incomplete aspect of the theory. It may be that the depth is determined by global thermodynamic and/or mass constraints. For example, there must be a given polewards transport across the boundary of the subtropical-subpolar gyre to balance the equatorward transport in the Ekman layer and that of the meridional overturning circulation.

12 Dewar et al. (2005). This paper also discusses the nature of discontinuities at the pool boundaries, and their treatment via shock conditions.

In the shadow zone, layer-2 fluid also has no direct surface source, so one may wonder why is this not also expunged. However, the shadow zone is not a recirculating regime and the Ekman induced displacement will be much less efficient. More directly, the eastern boundary condition $h_1(x = x_e) = 0$ precludes the vanishing of layer-2 water there, and this boundary condition is propagated westward into the interior.

13 Drawing from the numerical and conceptual models of Toggweiler and Samuels (1995, 1998), Döös and Coward (1997), Vallis (2000), Webb and Suginohara (2001), Nof (2003) and simplifying the analytic model of Samelson (1999a, 2004).

14 From Rintoul et al. (2001).

15 See Rintoul et al. (2001) and Olbers et al. (2004) for reviews.

16 These simulations, described in Henning and Vallis (2005), solve the primitive equations in a domain similar to Fig. 16.12. The wind forcing produces a polewards Ekman drift across the channel, as well as a subtropical gyre, and there is a meridional temperature gradient across the whole domain, so giving rise to a subtropical thermocline.

17 Adapted from Henning and Vallis (2005).

18 Munk and Palmén (1951), Gille (1997), Stevens and Ivchenko (1997).

19 Models if the ilk derive from Johnson and Bryden (1989). Straub (1993), Hallberg and Gnanadesikan (2001), Karsten et al. (2002), Marshall and Radko (2003), Henning and Vallis (2005), and others, consider related issues and extensions.

20 See also Warren et al. (1996) and Hughes (2002).

Further Reading

Siedler, G., Church, J. and Gould, J. 2001. *Ocean Circulation and Climate.*
    A comprehensive collection of review articles, with a general emphasis on observations and modelling of the large-scale circulation and its role in the climate system.

Problems

16.1 Show that the height of the upper layer in a model of the ventilated thermocline is continuous at the edge of the shadow zone, although the gradient normal to the shadow zone boundary need not be. [Hint: In the ventilated region $h_1 = (1 - f/f_2)h$, and in the shadow zone $g'_1/g'_2 h_1^2 = D_0^2$. Show that these lead to a shadow zone boundary that is the same as (16.69).]

16.2 Obtain an expression for the boundary of the western pool in a two-layer model of the ventilated thermocline.

16.3 ♦ A one-dimensional equation similar to (16.27) was put forward by Stommel and Webster (1963) as a simple model of the thermocline. The equation is

$$\left(2W - z\frac{\partial W}{\partial z}\right)\frac{\partial^3 W}{\partial z^3} = \kappa\frac{\partial^4 W}{\partial z^4}. \tag{P16.1}$$

Perform a boundary layer analysis on this equation, and show that if the downwards vertical velocity at the surface $z = 0$ is non-zero then the thickness of an internal boundary layer scales as $\kappa^{1/2}$. How does the vertical velocity scale with κ in this case? Why do these differ from the corresponding scalings for (16.27)? How does the boundary layer thickness scale if it is at the surface ($z = 0$)?

16.4 Construct a one-dimensional thermocline boundary layer equation by simply ignoring the variations in x and y in A, so by substituting $A(x, y, \zeta) = B(\zeta)$ in (16.41). Show that this leads to an equation of the form

$$C\frac{\mathrm{d}B}{\mathrm{d}\zeta}\frac{\mathrm{d}^3 B}{\mathrm{d}\zeta^3} = \frac{\kappa}{\delta^2}\frac{\mathrm{d}^4 B}{\mathrm{d}\zeta^4}, \tag{P16.2}$$

where C depends on β, f, h_x and T_0. If C were independent of x and y, show that this equation is essentially the same as the boundary layer equation that emerges from (P16.1). Is C in fact constant (i.e., not a function of x) in general?

16.5 If the Ekman pumping velocity at the surface, W_E, is zero then we cannot use it to non-dimensionalize W in (16.27). In this case what would be an appropriate choice for the scaling value of W, W_S? Does this choice affect whether $\hat{\kappa}$ is 'small' and $\hat{W}$ is $\mathcal{O}(1)$ in (16.27)?

REFERENCES

ABARBANEL, H. D. I. & YOUNG, W. R., Eds., 1987. *General Circulation of the Ocean.* Springer-Verlag, 291 pp.

ALLEN, J. S., 1993. Iterated geostrophic intermediate models. *J. Phys. Oceanogr.*, **23**, 2447–2461.

ALLEN, J. S., BARTH, J. A. & NEWBERGER, P. A., 1990a. On intermediate models for barotropic continental shelf and slope flow fields. Part I: formulation and comparison of exact solutions. *J. Phys. Oceanogr.*, **20**, 1017–1042.

ALLEN, J. S., BARTH, J. A. & NEWBERGER, P. A., 1990b. On intermediate models for barotropic continental shelf and slope flow fields. Part II: Comparison of numerical model solutions in doubly periodic domains. *J. Phys. Oceanogr.*, **20**, 1043–1082.

ALLEN, J. S., HOLM, D. D. & NEWBERGER, P. A., 2002. Extended-geostrophic Euler-Poincaré models for mesoscale oceanographic flow. In J. Norbury and I. Roulstone, Eds., *Large-Scale Atmosphere-Ocean Dynamics I*. Cambridge University Press.

ANDREWS, D. G., HOLTON, J. R. & LEOVY, C. B., 1987. *Middle Atmosphere Dynamics*. International Geophysics Series, Vol. 40, Academic Press, 489 pp.

ANDREWS, D. G. & MCINTYRE, M. E., 1976. Planetary waves in horizontal and vertical shear: The generalized Eliassen-Palm relation and the mean zonal acceleration. *J. Atmos. Sci.*, **33**, 2031–2048.

ANDREWS, D. G. & MCINTYRE, M. E., 1978. Generalized Eliassen-Palm and Charney-Drazin theorems for waves on axisymmetric mean flows in compressible atmospheres. *J. Atmos. Sci.*, **35**, 175–185.

ARBIC, B., FLIERL, G. & SCOTT, R., 2005. A cascade inequality in geostrophic turbulence. *(Unpublished).*

ARNOLD, V. I., 1965. Conditions for nonlinear stability of stationary plane curvilinear flows of an ideal fluid. *Dokl. Akad. Nauk SSSR*, **162**, 975–978. Engl. transl.: *Sov. Math.* **6,** 773–777, (1965).

ARNOLD, V. I., 1966. On an a priori estimate in the theory of hydrodynamic stability. *Izv. Vyssh. Uchebn. Zaved. Math.*, **54**, 3–5. Engl. transl.: *Am Mat. Soc. Transl. Ser.,* 2, **79,** 267–289, (1969).

AUBIN, D. & DAHAN DALMEDICO, A., 2002. Writing the history of dynamical systems and chaos: *Longue durée* and revolution, disciplines and cultures. *Historia Mathematica*, **29**, 1–67.

BANNON, P. R., 1995. Potential vorticity conservation, hydrostatic adjustment, and the anelastic approximation. *J. Atmos. Sci.*, **52**, 2301–2312.

BANNON, P. R., 1996. On the anelastic equation for a compressible atmosphere. *J. Atmos. Sci.*, **53**, 3618–3628.

BARNIER, B., HUA, B. L. & PROVOST, C. L., 1991. On the catalytic role of high baroclinic modes in eddy-driven large-scale circulations. *J. Phys. Oceanogr.*, **21**, 976–997.

BARTELLO, P. & WARN, T., 1996. Self-similarity of decaying two-dimensional turbulence. *J. Fluid Mech.*, **326**, 357–372.

BATCHELOR, G. K., 1949. Diffusion in a field of homogeneous turbulence. *Aust. J. Sci. Res.*, **A2**, 437–450.

BATCHELOR, G. K., 1953. The conditions for dynamical similarity of motions of a frictionless perfect-gas atmosphere. *Quart. J. Roy. Meteor. Soc.*, **79**, 224–235.

BATCHELOR, G. K., 1959. Small-scale variation of convected quantities like temperature in turbulent fluid. Part 1: General discussion and the case of small conductivity. *J. Fluid Mech.*, **5**, 113–133.

BATCHELOR, G. K., 1967. *An Introduction to Fluid Dynamics*. Cambridge University Press, 615 pp.

BATCHELOR, G. K., 1969. Computation of the energy spectrum in homogeneous two-dimensional turbulence. *Phys. Fluids Suppl*, **12**, II–233–II–239.

BATCHELOR, G. K., 1986. Geoffrey Ingram Taylor, 7 March 1886 – 27 June 1975. *J. Fluid Mech.*, **173**, 1–14.

BATCHELOR, G. K., HOWELLS, I. D. & TOWNSEND, A. A., 1959. Small-scale variation of convected quantities like temperature in turbulent fluid. Part 2: The case of large conductivity. *J. Fluid Mech.*, **5**, 134–139.

BATCHELOR, G. K. & TOWNSEND, A. A., 1956. Turbulent diffusion. In G. K. Batchelor and R. M. Davies, Eds., *Surveys in Mechanics*, pp. 352–399. Cambridge University Press.

BAUMERT, H. Z., SIMPSON, J. & SÜNDERMANN, J., Eds., 2005. *Marine Turbulence: Theories, Observations and Models*. Cambridge University Press, 630 pp.

BENDER, C. M. & ORSZAG, S. A., 1978. *Advanced Mathematical Methods for Scientists and Engineers*. McGraw-Hill, 593 pp.

BIRNER, T., 2005. Tropopause (placeholder). *Geophys. Res. Lett.*, **32**, doi xxx.

BIRNER, T., DÖRNBRACK, A. & SCHUMANN, U., 2002. How sharp is the tropopause at midlatitudes? *Geophys. Res. Lett.*, **29**, 1700, doi: 10.1029/2002GL015142.

BJERKNES, J., 1919. On the structure of moving cyclones. *Geofys. Publ*, **1**(2), 1–8.

BJERKNES, J., 1959. Atlantic air-sea interaction. In *Advances in Geophysics*, Vol. 10, pp. 1–82. Academic Press.

BJERKNES, J., 1969. Atmospheric teleconnections from the equatorial Pacific. *Mon. Wea. Rev.*, **97**, 163–172.

BJERKNES, V., 1898. Über die bildung von circulationsbewegungen und wirdeln in reibunglosen flüssigkeiten. *Skr. Nor. Vidensk.-Akad. 1: Mat.-Naturvidensk. Kl.*, **5**, 1–29.

BJERKNES, V., 1902. Cirkulation relativ zu der erde (Circulation relative to the Earth). *Meteor. Z.*, **37**, 97–108.

BJERKNES, V., 1904. Das problem der wettervorhersage, betrachtet vom standpunkte der mechanik und der physic. *Meteorologische Zeitschrift*, January, 1–7. Engl. trans. by Y.

Mintz: The problem of weather forecasting as a problem in mathematics and physics, in Shapiro and Grønas (1999), pp. 1–7.

BLUMEN, W., 1968. On the stability of quasi-geostrophic flow. *J. Atmos. Sci.*, **25**, 929–933.

BOER, G. J. & SHEPHERD, T. G., 1983. Large-scale two-dimensional turbulence in the atmosphere. *J. Atmos. Sci.*, **40**, 164–184.

BOUSSINESQ, J., 1903. Théorie analytique de la chaleur (analytic theory of heat). *Tome, Paris, Gauthier-Villars*, II, 170–172.

BOYD, J. P., 1976. The noninteraction of waves with the zonally averaged flow on a spherical earth and the interrelationships of eddy fluxes of energy, heat and momentum. *J. Atmos. Sci.*, **33**, 2285–2291.

BRANSCOME, L. E., 1983. The Charney baroclinic stability problem: Approximate solutions and modal structures. *J. Atmos. Sci.*, **40**, 1393–1409.

BRETHERTON, C. S. & SCHÄR, C., 1993. Flux of potential vorticity substance: A simple derivation and a uniqueness property. *J. Atmos. Sci.*, **50**, 1834–1836.

BRETHERTON, F. P., 1966. Critical layer instability in baroclinic flows. *Quart. J. Roy. Meteor. Soc.*, **92**, 325–334.

BREWER, A. W., 1949. Evidence for a world circulation provided by the measurements of helium and water vapour distribution in the stratosphere. *Quart. J. Roy. Meteor. Soc.*, **75**, 251–363.

BRYAN, F., 1986. High-latitude salinity effects and interhemispheric thermohaline circulations. *Nature*, **323**, 301–304.

BRYDEN, H. L., 1973. New polynomials for thermal expansion, adiabatic temperature gradient and potential temperature gradient of sea water. *Deep Sea Res.*, **20**, 401–408.

BURGER, A., 1958. Scale considerations of planetary motions of the atmosphere. *Tellus*, **10**, 195–205.

CALLEN, H. B., 1985. *Thermodynamics and an Introduction to Thermostatistics*. John Wiley & Sons, 493 pp.

CESSI, P., 2001. Thermohaline circulation variability. In *Conceptual Models of the Climate, 2001 Program in Geophysical Fluid Dynamics* (2001). http://gfd.whoi.edu/proceedings/2001/PDFvol2001.html.

CESSI, P. & YOUNG, W. R., 1992. Multiple equilibria in two-dimensional thermohaline circulation. *J. Fluid Mech.*, **241**, 291–309.

CHANDRASEKHAR, S., 1961. *Hydrodynamic and Hydromagnetic Stability*. Oxford University Press, 652 pp. Reprinted by Dover Publications, 1981.

CHAPMAN, S. & LINDZEN, R. S., 1970. *Atmospheric Tides*. Gordon and Breach, 200 pp.

CHARNEY, J. G., 1947. The dynamics of long waves in a baroclinic westerly current. *J. Meteor.*, **4**, 135–162.

CHARNEY, J. G., 1948. On the scale of atmospheric motion. *Geofys. Publ. Oslo*, **17**(2), 1–17.

CHARNEY, J. G., 1955. The Gulf Stream as an inertial boundary layer. *Proc. Nat. Acad. Sci.*, **41**, 731–740.

CHARNEY, J. G., 1971. Geostrophic turbulence. *J. Atmos. Sci.*, **28**, 1087–1095.

CHARNEY, J. G. & DRAZIN, P. G., 1961. Propagation of planetary scale disturbances from the lower into the upper atmosphere. *J. Geophys. Res.*, **66**, 83–109.

CHARNEY, J. G. & ELIASSEN, A., 1949. A numerical method for predicting the perturbations of the mid-laitude westerlies. *Tellus*, **1**, 38–54.

CHARNEY, J. G. & ELIASSEN, A., 1964. On the growth of the hurricane depression. *J. Atmos. Sci.*, **21**, 68–75.

CHARNEY, J. G., FJØRTOFT, R. & NEUMANN, J. V., 1950. Numerical integration of the barotropic vorticity equation. *Tellus*, **2**, 237–254.

CHARNEY, J. G. & STERN, M. E., 1962. On the stability of internal baroclinic jets in a rotating atmosphere. *J. Atmos. Sci.*, **19**, 159–172.

CHARNOCK, H., GREEN, J., LUDLAM, F., SCORER, R. & SHEPPARD, P., 1966. Dr. e. t. eady, b. a. (obituary). *Quart. J. Roy. Meteor. Soc.*, **92**, 591–592.

CHASNOV, J. R., 1991. Simulation of the inertial-conductive subrange. *Phys. Fluids A*, **3**, 1164–1168.

CHELTON, D. B., DE SZOEKE, R. A., SCHLAX, M. G., NAGGAR, K. E. & SIWERTZ, N., 1998. Geographical variability of the first-baroclinic Rossby radius of deformation. *J. Phys. Oceanogr.*, **28**, 433–460.

COLIN DE VERDIERE, A., 1980. Quasi-geostrophic turbulence in a rotating homogeneous fluid. *Geophys. Astrophys. Fluid Dyn.*, **15**, 213–251.

COLIN DE VERDIERE, A., 1989. On the interaction of wind and buoyancy driven gyres. *J. Mar. Res.*, **47**, 595–633.

CONKRIGHT, M. E., ANTONOV, J., BARANOVA, O., BOYER, T. P., GARCIA, H., GELFELD, R., JOHNSON, D., LOCARNINI, R. A., MURPHY, P., O'BRIEN, T. D., SMOLYAR, I. & STEPHENS, C., 2001. World ocean database 2001, vol. 1. In S. Levitus, Ed., *NOAA Atlas NESDIS 42*, pp. 167. US Government Printing Office, Washington D. C.

CORIOLIS, G. G., 1832. Mémoire sur le principe des forces vives dans les mouvements relatifs des machines (On the principle of kinetic energy in the relative movement of machines). *J. Ec. Polytech*, **13**, 268–301.

CORIOLIS, G. G., 1835. Mémoire sur les équations du mouvement relatif des systèmes de corps (On the equations of relative motion of a system of bodies). *J. Ec. Polytech*, **15**, 142–154.

CORRSIN, S., 1951. On the spectrum of isotropic temperature fluctuations in an isotropic turbulence. *J. Appl. Phys.*, **22**, 469–473. Erratum: *J. Appl. Phys.* **22**, 1292, (1951).

CRESSMAN, G. P., 1996. The origin and rise of numerical weather prediction. In J. R. Fleming, Ed., *Historical Essays on Meteorology 1919–1995*, pp. 617. Am. Meteor. Soc.

CUSHMAN-ROISIN, B., 1994. *Introduction to Geophysical Fluid Dynamics*. Prentice Hall, 320 pp.

DANIELSEN, E. F., 1990. In defense of Ertel's potential vorticity and its general applicability as a meteorological tracer. *J. Atmos. Sci.*, **47**, 2353–2361.

DANILOV, S. & GURARIE, D., 2001. Quasi-two-dimensional turbulence. *Uspekhi Fizicheskikh Nauk.*, **170**, 921–968.

DAVIES-JONES, R., 2003. Comments on "a generalization of Bernoulli's theorem". *J. Atmos. Sci.*, **60**, 2039–2041.

DAVIS, R. E., DE SZOEKE, R., HALPERN, D. & NIILER, P., 1981. Variability in the upper ocean during MILE. Part I: The heat and momentum balances. *Deep-Sea Res.*, **28**, 1427–1452.

DE SZOEKE, R., 2003. A prototype equation of state for seawater. Preprint.

DE SZOEKE, R. & BENNETT, A. F., 1993. Microstucture fluxes across density surfaces. *J. Phys. Oceanogr.*, **24**, 2254–2264.

DEFANT, A., 1921. Die zirkulation der atmosphäre in den gemäßigten breiten der Erde. Grundzüge einer theorie der klimaschwankungen (the circulation of the atmosphere in the earth's midlatitudes. basic features of a theory of climate fluctuations). *Geograf. Ann.*, **3**, 209–266.

DEWAR, W. K. & HUANG, R. X., 1995. Fluid flow in loops driven by freshwater and heat fluxes. *J. Fluid Mech.*, **297**, 153–191.

DEWAR, W. K., SAMELSON, R. S. & VALLIS, G. K., 2005. The ventilated pool: a model of subtropical mode water. *J. Phys. Oceanogr.*, **35**, 137–150.

DICKINSON, R. E., 1968. Planetary Rossby waves propagating vertically through weak westerly wind wave guides. *J. Atmos. Sci.*, **25**, 984–1002.

DICKINSON, R. E., 1980. Planetary waves: Theory and observation. In *Orographic Effects on Planetary Flows*, Number 23 in GARP Publication Series. W.M.O., Geneva.

DIJKSTRA, H. A., 2002. *Nonlinear Physical Oceanography*. Kluwer, 456 pp.

DIMA, I. & WALLACE, J. M., 2003. On the seasonality of the Hadley Cell. *J. Atmos. Sci.*, **60**, 1522–1527.

DOBSON, G. M. B., 1956. Origin and distribution of the polyatomic molecules in the atmosphere. *Proc. Roy. Soc. Lond. A*, **236**, 187–193.

DÖÖS, K. & COWARD, A., 1997. The Southern Ocean as the major upwelling zone of the North Atlantic. *Int. WOCE Newsletter* 27, 3–4.

DRAZIN, P. G. & REID, W. H., 1981. *Hydrodynamic Stability*. Cambridge University Press, 527 pp.

DRIJFHOUT, S. S. & HAZELEGER, W., 2001. Eddy mixing of potential vorticity versus temperature in an isopycnic ocean model. *J. Phys. Oceanogr.*, **31**, 481–505.

DRITSCHEL, D. G., 1989. On the stabilization of a two-dimensional vortex strip by adverse shear. *J. Fluid Mech.*, **45**, 193–221.

DUNKERTON, T. J., 1980. A Lagrangian-mean theory of wave, mean-flow interaction with applications to non-acceleration and its breakdown. *Rev. Geophys. Space Phys.*, **18**, 387–400.

DURRAN, D. R., 1989. Improving the anelastic approximation. *J. Atmos. Sci.*, **46**, 1453–1461.

DURST, C. S. & SUTCLIFFE, R. C., 1938. The effect of vertical motion on the "geostrophic departure" of the wind. *Quart. J. Roy. Meteor. Soc.*, **64**, 240.

EADY, E. T., 1949. Long waves and cyclone waves. *Tellus*, **1**, 33–52.

EADY, E. T., 1950. The cause of the general circulation of the atmosphere. In *Cent. Proc. Roy. Meteor. Soc. (1950)*, pp. 156–172.

EADY, E. T., 1954. The maintenance of the mean zonal surface currents. *Proc. Toronto Meteor. Conf. 1953*, **138**, 124–128. Published by Roy. Meteor. Soc.

EADY, E. T. & SAWYER, J. S., 1951. Dynamics of flow patterns in extra-tropical regions. *Quart. J. Roy. Meteor. Soc.*, **77**, 531–551.

EGGER, J., 1976. Linear response of a two-level primitive equation model to forcing by topography. *Mon. Wea. Rev.*, **104**, 351–364.

EINSTEIN, A., 1916. *Relativity: The Special and the General Theory*. Random House, 188 pp.

EKMAN, V. W., 1905. On the influence of the earth's rotation on ocean currents. *Arch. Math. Astron. Phys.*, **2**, 1–52.

ELIASSEN, A. & PALM, E., 1961. On the transfer of energy in stationary mountain waves. *Geofys. Publ.*, **22**, 1–23.

ELUSZKIEWICZ, J., CRISP, D., ZUREK, R., ELSON, L., FISHBEIN, E., FROIDEVAUX, L., WATERS, J., GRAINGER, R. G., LAMBERT, A., HARWOOD, R. & PECKHAM, G., 1996. Residual circulation in the stratosphere and lower mesosphere as diagnosed from microwave limb sounder data. *J. Atmos. Sci.*, **53**, 217–240.

ER-EL, J. & PESKIN, R., 1981. Relative diffusion of constant-level balloons in the Southern Hemisphere. *J. Atmos. Sci.*, **38**, 2264–2274.

ERTEL, H., 1942a. Ein neuer hydrodynamischer Wirbelsatz (A new hydrodynamic eddy theorem). *Meteorolol. Z.*, **59**, 277–281.

ERTEL, H., 1942b. Über des verhältnis des neuen hydrodynamicshen Wirbelsatzes zum zirculationssatz von V. Bjerknes (on the relationship of the new hydrodynamic eddy theorem to the circulation theorem of V. Bjerknes). *Meteorol. Z.*, **59**, 385–387.

ERTEL, H. & ROSSBY, C.-G., 1949. A new conservation theorem of hydrodynamics. *Geofis. Pura Appl.*, **14**, 189–193. Also 'Ein neuer Erhaltungs-satz der Hydrodynamik' in *Sitzung Deutschen Akad. Wissenschaften Berlin*, vol. 1, pp3-11, 1949.

FANG, M. & TUNG, K. K., 1996. A simple model of nonlinear Hadley circulation with an ITCZ: Analytic and numerical solutions. *J. Atmos. Sci.*, **53**, 1241–1261.

FANG, M. & TUNG, K. K., 1999. Time-dependent nonlinear Hadley circulation. *J. Atmos. Sci.*, **56**, 1797–1807.

FARRELL, B., 1984. Modal and non-modal baroclinic waves. *J. Atmos. Sci.*, **41**, 668–673.

FARRELL, B. F. & IOANNOU, P. J., 1996. Generalized stability theory. part i: Autonomous operators. *J. Atmos. Sci.*, **53**, 2025–2040.

FEISTEL, R. & HAGEN, E., 1995. On the Gibbs thermodynamic potential of seawater. *Prog. Oceanogr.*, **36**, 249–347.

FELS, S., 1985. Radiative-dynamical interactions in the middle atmosphere. In S. Manabe, Ed., *Adv. Geophys. Vol 28, Part A, Issues in Atmospheric and Oceanic Modeling*, pp. 27–300. Academic Press.

FERREL, W., 1856a. An essay on the winds and currents of the ocean. *Nashville J. Med. & Surg.*, **11**, 287–301.

FERREL, W., 1856b. The problem of the tides. *Astron. J*, **4**, 173–176.

FERREL, W., 1858. The influence of the earth's rotation upon the relative motion of bodies near its surface. *Astron. J.*, **V**, No. 13 (109), 97–100.

FJØRTOFT, R., 1950. Application of integral theorems in deriving criteria for laminar flows and for the baroclinic circular vortex. *Geophys. Publ.*, **17**, 1–52.

FJØRTOFT, R., 1953. On the changes in the spectral distribution of kinetic energy for two-dimensional nondivergent flow. *Tellus*, **5**, 225–230.

FLEMING, E. L., CHANDRA, S., SCHOEBERL, M. R. & BARNETT, J. J., 1988. Monthly mean global climatology of temperature, wind, geopotential height, and pressure for 0-120 km. Technical report, NASA/Goddard Space Flight Center, Greenbelt, MD. NASA Tech. Memo. 100697.

FOFONOFF, N. P., 1954. Steady flow in a frictionless homogeneous ocean. *J. Mar. Res.*, **13**, 254–262.

FOFONOFF, N. P., 1985. Physical properties of seawater: A new salinity scale and equation of state for seawater. *J. Geophys. Res.*, **90**(C), 3332–3342.

FOSTER, T. D., 1972. An analysis of the cabbeling instability in sea water. *J. Phys. Oceanogr.*, **2**, 294–301.

FOX-KEMPER, B., 2004. Re-evaluating the role of eddies in multiple barotropic wind-driven gyres. *J. Phys. Oceanogr.*, **34**, (in press).

FRIEDMAN, R. M., 1989. *Appropriating the weather: Vilhelm Bjerknes and the Construction of a Modern Meteorology*. Cornell University Press, 251 pp.

FRISCH, U., 1995. *Turbulence: The Legacy of A. N. Kolmogorov*. Cambridge University Press, 296 pp.

FU, L. L. & FLIERL, G. R., 1980. Nonlinear energy and enstrophy transfers in a realistically stratified ocean. *Dyn. Atmos. Oceans*, **4**, 219–246.

GAGE, K. S. & NASTROM, G. D., 1986. Theoretical interpretation of atmospheric wavenumber spectra of wind and temperature observed by commercial aircraft during GASP. *J. Atmos. Sci.*, **43**, 729Ð740.

GARDINER, C. W., 1985. *Handbook of Stochastic Methods.* Springer.

GENT, P. R. & MCWILLIAMS, J. C., 1990. Isopycnal mixing in ocean circulation models. *J. Phys. Oceanogr.*, **20**, 150–155.

GENT, P. R., WILLEBRAND, J., MCDOUGALL, T. J. & MCWILLIAMS, J. C., 1995. Parameterizing eddy-induced transports in ocean circulation models. *J. Phys. Oceanogr.*, **25**, 463–474.

GILL, A. E., 1982. *Atmosphere-Ocean Dynamics.* Academic Press, 662 pp.

GILL, A. E., GREEN, J. S. A. & SIMMONS, A. J., 1974. Energy partition in the large-scale ocean circulation and the production of mid-ocean eddies. *Deep-Sea Res.*, **21**, 499–528.

GILLE, S. T., 1997. The Southern Ocean momentum balance: evidence for topographic effects from numerical model output and altimeter data. *J. Phys. Oceanogr.*, **27**, 2219–2232.

GODSKE, C. L., BERGERON, T., BJERKNES, J. & BUNDGAARD, R. C., 1957. *Dynamic Meteorology and Weather Forecasting.* Am. Meteor. Soc., 864 pp.

GOUGH, D. O., 1969. The anelastic approximation for thermal convection. *J. Atmos. Sci.*, **216**, 448–456.

GRANT, H. L., HUGHES, B. A., VOGEL, W. M. & MOILLIET, A., 1968. The spectrum of temperaure fluctuation in turbulent flow. *J. Fluid Mech.*, **344**, 423–442.

GRANT, H. L., STEWART, R. W. & MOILLIET, A., 1962. Turbulent spectra from a tidal channel. *J. Fluid Mech.*, **12**, 241–268.

GREATBATCH, R. J., 1998. Exploring the relationship between eddy-induced transport velocity, vertical momentum transfer, and the isopycnal flux of potential vorticity. *J. Phys. Oceanogr.*, **28**, 422–432.

GREEN, J. S. A., 1960. A problem in baroclinic stability. *Quart. J. Roy. Meteor. Soc.*, **86**, 237–251.

GREEN, J. S. A., 1970. Transfer properties of the large-scale eddies and the general circulation of the atmosphere. *Quart. J. Roy. Meteor. Soc.*, **96**, 157–185.

GREEN, J. S. A., 1977. The weather during July 1976: Some dynamical considerations of the drought. *Weather*, **32**, 120–128.

GREEN, J. S. A., 1999. *Atmospheric Dynamics.* Cambridge University Press, 213 pp.

GREENSPAN, H., 1962. A criterion for the existence of inertial boundary layers in oceanic circulation. *Proc. Nat. Acad. Sci.*, **48**, 2034–2039.

GREGG, M. C., 1998. Estimation and geography of diapycnal mixing in the stratified ocean. In J. Imberger, Ed., *Physical Processes in Lakes and Oceans*, pp. 305–338. American Geophysical Union.

GRIFFIES, S. M., 1998. The Gent-McWilliams skew flux. *J. Phys. Oceanogr.*, **28**, 831–841.

GRIFFIES, S. M., 2004. *Fundamentals of z-coordinate ocean modelling.* Princeton University Press, 496 pp.

GROSE, W. & HOSKINS, B., 1979. On the influence of orography on large-scale atmospheric flow. *J. Atmos. Sci.*, **36**, 223–234.

HADLEY, G., 1735. Concerning the cause of the general trade-winds. *Phil. Trans. Roy. Soc.*, **29**, 58–62.

HALLBERG, R. & GNANADESIKAN, A., 2001. An exploration of the role of transient eddies in determining the transport of a zonally reentrant current. *J. Phys. Oceanogr.*, **31**, 3312–3330.

HANEY, R. L., 1971. Surface thermal boundary condition for ocean circulation models. *J. Phys. Oceanogr.*, **1**, 241–248.

HAYES, M., 1977. A note on group velocity. *Proc. Roy. Soc. Lond.*, **A354**, 533–535.

HAYNES, P. H. & MCINTYRE, M. E., 1987. On the evolution of vorticity and potential vorticity in the presence of diabatic heating and frictional or other forces. *J. Atmos. Sci.*, **44**, 828–841.

HAYNES, P. H. & MCINTYRE, M. E., 1990. On the conservation and impermeability theorem for potential vorticity. *J. Atmos. Sci.*, **47**, 2021–2031.

HAYNES, P. H., SCINOCCA, J. F. & GREENSLADE, M., 2001. Formation and maintenance of the extratropical tropopause by baroclinic eddies. *Geophys. Res. Lett.*, **28**, 4179–4182.

HELD, I. M., 1982. On the height of the tropopause and the static stability of the troposphere. *J. Atmos. Sci.*, **39**, 412–417.

HELD, I. M., 1983. Stationary and quasi-stationary eddies in the extratropical troposphere: Theory. In B. Hoskins and R. P. Pearce, Eds., *Large-Scale Dynamical Processes in the Atmosphere*, pp. 127–168. Academic Press.

HELD, I. M., 2000. *The General Circulation of the Atmosphere*. Proc. Woods Hole Summer School on GFD, 66 pp.

HELD, I. M. & HOU, A. Y., 1980. Nonlinear axially symmetric circulations in a nearly inviscid atmosphere. *J. Atmos. Sci.*, **37**, 515–533.

HELD, I. M. & LARICHEV, V. D., 1996. A scaling theory for horizontally homogeneous, baroclinically unstable flow on a beta-plane. *J. Atmos. Sci.*, **53**, 946–952.

HELD, I. M. & SCHNEIDER, T., 1999. The surface branch of the zonally averaged mass transport circulation in the troposphere. *J. Atmos. Sci.*, **56**, 1688–1697.

HELD, I. M., TANG, M. & WANG, H., 2002. Northern winter stationary waves: Theory and modeling. *J. Climate*, **15**, 2125–2144.

HELMHOLTZ, H., 1868. Über discontinuirliche flüssigkeitsbewegungen. *Monats. Königl. Preuss. Akad. Wiss. Berlin*, **23**, 215–228. Eng. trans. by F. Guthrie, 'On discontinuous movements of fluids', *Phil. Mag.*, **36**, 337-346, (1868).

HENDERSHOTT, M., 1987. Single layer models of the general circulation. In H. Abarbanel and W. R. Young, Eds., *General Circulation of the Ocean*, pp. 202–267. Springer-Verlag.

HENNING, C. C. & VALLIS, G. K., 2005. The effects of mesoscale eddies on the stratification and transport of an ocean with a circumpolar channel. *J. Phys. Oceanogr.*, **35**, 880–896.

HIDE, R., 1969. Dynamics of the atmospheres of major planets with an appendix on the viscous boundary layer at the rigid boundary surface of an electrically conducting rotating fluid in the presence of a magnetic field. *J. Atmos. Sci.*, **26**, 841–853.

HOCKNEY, R., 1970. The potential calculation and some applications. In *Methods of Computational Physics, vol. 9*, pp. 135–211. Academic Press.

HOGG, N., 2001. Quantification of the deep circulation. In G. Siedler, J. Church, and J. Gould, Eds., *Ocean Circulation and Climate: Observing and Modelling the Global Ocean*, pp. 259–270. Academic Press.

HOLLAND, W. R., KEFFER, T. & RHINES, P. B., 1984. Dynamics of the oceanic circulation: the potential vorticity field. *Nature*, **308**, 698–705.

HOLLOWAY, G. & HENDERSHOTT, M. C., 1986. Stochastic closure for nonlinear rossby waves. *J. Fluid Mech.*, **82**, 747–765.

HOLM, D. D., MARSDEN, J. E., RATIU, T. & WEINSTEIN, A., 1985. Nonlinear stability of fluid and plasma equilibria. *Phys. Rep.*, **123**, 1–116.

HOLTON, J. R., 1974. Forcing of mean flows by stationary waves. *J. Atmos. Sci.*, **31**, 942–945.

HOLTON, J. R., 1992. *An Introduction to Dynamic Meteorology*. 3rd ed. Academic Press, 507 pp.

HOSKINS, B. J. & KAROLY, D. J., 1981. The steady linear response of a spherical atmosphere to thermal and orographic forcing. *J. Atmos. Sci.*, **38**, 1179–1196.

HUA, B. L. & HAIDVOGEL, D. B., 1986. Numerical simulations of the vertical structure of quasi-geostrophic turbulence. *J. Atmos. Sci.*, **43**, 2923–2936.

HUANG, R. X., 1988. On boundary value problems of the ideal-fluid thermocline. *J. Phys. Oceanogr.*, **18**, 619–641.

HUANG, R. X., 1998. Mixing and available potential energy in a Boussinesq ocean. *J. Phys. Oceanogr.*, **28**, 669–678.

HUANG, R. X., 1999. Mixing and energetics of the oceanic thermohaline circulation. *J. Phys. Oceanogr.*, **29**, 727–746.

HUGHES, C. W., 2002. Sverdrup-like theories of the Antarctic Circumpolar Current. *J. Mar. Res.*, **60**, 1–17.

HUGHES, C. W. & DE CUEVAS, B., 2001. Why western boundary currents in realistic oceans are inviscid: A link between form stress and bottom pressure torques. *J. Phys. Oceanogr.*, **31**, 2871–2885.

IERLEY, G. R., 1987. On the onset of inertial recirculation in barotropic general circulation models. *J. Phys. Oceanogr.*, **17**, 2366–2374.

IERLEY, G. R. & RUEHR, O. G., 1986. Analytic and numerical solutions of a nonlinear boundary value problem. *Stud. Appl. Math.*, **75**, 1–36.

IL'IN, A. M. & KAMENKOVICH, V. M., 1964. The structure of the boundary layer in the two-dimensional theory of ocean currents. (in Russian). *Okeanologiya*, **4**(5), 756–769.

IWAYAMA, T., SHEPHERD, T. G. & WATANABE, T., 2002. An 'ideal' form of decaying two-dimensional turbulence. *J. Fluid Mech.*, **456**, 183–198.

JACKSON, L., HUGHES, C. & WILLIAMS, R., 2005. Inviscid western boundary currents in qg models (placeholder). *J. Phys. Oceanogr.*, **xx**, xx.

JAMES, I. N., 1994. *Introduction to Circulating Atmospheres*. Cambridge University Press, 422 pp.

JEFFREYS, H., 1926. On the dynamics of geostrophic winds. *Quart. J. Roy. Meteor. Soc.*, **51**, 85–101.

JOHNSON, G. C. & BRYDEN, H. L., 1989. On the size of the Antarctic Circumpolar Current. *Deep-Sea Res.*, **36**, 39–53.

JUCKES, M. N., 2000. The static stability of the midlatitude troposphere: The relevance of moisture. *J. Atmos. Sci.*, **57**, 3050–3057.

JUCKES, M. N., 2001. A generalization of the transformed Eulerian-mean meridional circulation. *Quart. J. Roy. Meteor. Soc.*, **127**, 147–160.

KALNAY, E., 1996. The NCEP/NCAR 40-year reanalysis project. *Bull. Amer. Meteor. Soc.*, **77**, 437–471.

KALNAY, E., 2003. *Atmospheric modeling, data assimilation and predictability*. Cambridge University Press, 341 pp.

KARSTEN, R., JONES, H. & MARSHALL, J., 2002. The role of eddy transfer in setting the stratification and transport of a circumpolar current. *J. Phys. Oceanogr.*, **32**, 39–54.

KEFFER, T., 1985. The ventilation of the world's oceans: maps of potential vorticity. *J. Phys. Oceanogr.*, **15**, 509–523.

KIBEL, I., 1940. Priloozhenie k meteorogi uravnenii mekhaniki baroklinnoi zhidkosti. *SSSR Ser. Geogr. Geofiz.*, **5**, 627–637.

KILLWORTH, P. D., 1997. On the parameterization of eddy transfer. Part I: Theory. *J. Marine Res.*, **55**, 1171–1197.

KIMOTO, M. & GHIL, M., 1993. Multiple flow regimes in the northern hemisphere winter. Part 1: Methodology and hemispheric regimes. *J. Atmos. Sci.*, **50**, 2625–2643.

KOLMOGOROV, A. N., 1941. The local structure of turbulence in incompressible viscous fluid for very large Reynolds numbers. *Dokl. Acad. Sci. USSR*, **30**, 299–303.

KOLMOGOROV, A. N., 1962. A refinement of previous hypotheses concerning the local structure of turbulence in a viscous incompressible fluid at high Reynolds numbers. *J. Fluid Mech.*, **13**, 82–85.

KOPKA, H. & DALY, P. W., 1999. *A Guide to LaTeX*. 3rd ed. Addison-Wesley, 600 pp.

KRAICHNAN, R., 1967. Inertial ranges in two-dimensional turbulence. *Phys. Fluids*, **10**, 1417–1423.

KRAICHNAN, R. & MONTGOMERY, D., 1980. Two-dimensional turbulence. *Rep. Prog. Physics*, **43**, 547–619.

KUNDU, P., ALLEN, J. S. & SMITH, R. L., 1975. Modal decomposition of the velocity field near the Oregon coast. *J. Phys. Oceanogr.*, **5**, 683–704.

KUNDU, P. & COHEN, I. M., 2002. *Fluid Mechanics*. Academic Press, 730 pp.

KUSHNIR, Y., ROBINSON, W. A., BLADÉ, I., HALL, N. M. J., PENG, S. & SUTTON, R., 2002. Atmospheric GCM response to extratropical SST anomalies: synthesis and evaluation. *J. Climate*, **15**, 2233–2256.

LACASCE, J. H. & OHLMANN, C., 2003. Relative dispersion at the surface of the Gulf of Mexico. *J. Mar. Res.*, **65**, 285–312.

LAIT, L. R., 1994. An alternative form for potential vorticity. *J. Atmos. Sci.*, **51**, 1754–1759.

LANCZOS, C., 1970. *The Variational Principles of Mechanics*. University of Toronto Press, Reprinted by Dover Publications 1980, 418 pp.

LANDAU, L. D., 1944. On the problem of turbulence. *Dokl. Akad. Nauk SSSR*, **44**, 311–314.

LARICHEV, V. D. & HELD, I. M., 1995. Eddy amplitudes and fluxes in a homogeneous model of fully developed baroclinic instability. *J. Phys. Oceanogr.*, **25**, 2285–2297.

LEDWELL, J. R., WATSON, A. J. & LAW, C. S., 1998. Mixing of a tracer in the pycnocline. *J. Geophys. Res.*, **103**, 21499–21529.

LEE, M.-M., MARSHALL, D. P. & WILLIAMS, R. G., 1997. On the eddy transfer of tracers: Advective or diffusive? *J. Mar. Res.*, **55**, 483–595.

LEE, T. D., 1951. Difference between turbulence in a two-dimensional fluid and in a three-dimensional fluid. *J. Appl. Phys.*, **22**, 524.

LEETMAA, A., NIILER, P. & STOMMEL, H., 1977. Does the Sverdrup relation account for the mid-Atlantic circulation? *J. Mar. Res.*, **35**, 1–10.

LEITH, C. E., 1968. Diffusion approximation for two-dimensional turbulence. *Phys. Fluids*, **11**, 671–672.

LESIEUR, M., 1997. *Turbulence in Fluids: Third Revised and Enlarged Edition*. Kluwer Academic Publishers, 515 pp.

LEVINSON, N., 1950. The 1st boundary value problem for $\epsilon \Delta U + A(x, y)U_x + B(x, y)U_y + C(x, y)U = D(x, t)$ for small epsilon. *Ann. Math.*, **51**, 429–445.

LEWIS, R. P. W., Ed., 1991. *Meteorological Glossary*. 6 ed. Her MajestyÕs Stationer's Office, 335 pp.

LIGHTHILL, J., 1978. *Waves in Fluids*. Cambridge University Press, 504 pp.

LIGHTHILL, M. J., 1965. Group velocity. *J. Inst. Math. Appl.*, **1**, 1–28.

LILLY, D. K., 1969. Numerical simulation of two-dimensional turbulence. *Phys. Fluid Suppl. II*, **12**, 240–249.

LINDBORG, E., 1999. Can the atmospheric kinetic energy spectrum be explained by two-dimensional turbulence? *J. Fluid Mech.*, **388**, 259–288.

LINDBORG, E. & ALVELIUS, K., 2000. The kinetic energy spectrum of the two-dimensional enstrophy turbulence cascade. *Phys. Fluids*, **12**, 945–947.

LINDZEN, R. S. & FARRELL, B., 1980. The role of the polar regions in global climate, and a new parameterization of global heat transport. *Mon. Wea. Rev.*, **108**, 2064–2079.

LINDZEN, R. S. & HOU, A. Y., 1988. Hadley circulation for zonally averaged heating centered off the equator. *J. Atmos. Sci.*, **45**, 2416–2427.

LINDZEN, R. S., LORENZ, E. N. & PLAZMAN, G. W., Eds., 1990. *The Atmosphere — a Challenge: the Science of Jule Gregory Charney.* Americal Meteorological Society, 321 pp.

LIPPS, F. B. & HEMLER, R. S., 1982. A scale analysis of deep moist convection and some related numerical calculations. *J. Atmos. Sci.*, **39**, 2192–2210.

LONGUET-HIGGINS, M. S., 1964. Planetary waves on a rotating sphere, I. *Proc. Roy. Soc. Lond.*, **A279**, 446–473.

LORENZ, E. N., 1955. Available potential energy and the maintenance of the General Circulation. *Tellus*, **7**, 157–167.

LORENZ, E. N., 1963. Deterministic nonperiodic flow. *J. Atmos. Sci.*, **20**, 130–141.

LORENZ, E. N., 1967. *The Nature and the Theory of the General Circulation of the Atmosphere.* WMO Publications, Vol. 218, World Meteorological Organization.

LOZIER, S., OWENS, W. B. & CURRY, R. G., 1996. The climatology of the North Atlantic. *Prog. Oceanog.*, **36**, 1–44.

LUYTEN, J. R., PEDLOSKY, J. & STOMMEL, H., 1983. The ventilated thermocline. *J. Phys. Oceanogr.*, **13**, 292–309.

MAHRT, L., 1986. On the shallow motion approximations. *J. Atmos. Sci.*, **43**, 1036–1044.

MAJDA, A. J., 2003. *Introduction to PDEs and Waves for the Atmosphere and Ocean.* American Math. Society, 234 pp.

MALTRUD, M. E. & VALLIS, G. K., 1991. Energy spectra and coherent structures in forced two-dimensional and beta-plane turbulence. *J. Fluid Mech.*, **228**, 321–342.

MANABE, S. & STOUFFER, R. J., 1988. Two stable equilibria of a coupled ocean-atmosphere model. *J. Climate*, **1**, 841–866.

MARGULES, M., 1903. Über die energie der stürme. *Jahrb. Kais.-kön Zent. für Met., Vienna.* Translation by C. Abbe in Smithson. Misc. Coll, v51, 1910.

MAROTZKE, J., 1989. Instabilities and multiple steady states of the thermohaline circulation. In D. L. T. Anderson and J. Willebrand, Eds., *Oceanic Circulation Models: Combining Data and Dynamics*, pp. 501–511. NATO ASI Series, Kluwer.

MARSHALL, D. P., WILLIAMS, R. G. & LEE, M.-M., 1999. The relation between eddy-induced transport and isopycnic gradients of potential vorticity. *J. Phys. Oceanogr.*, **29**, 1571–1578.

MARSHALL, J. & RADKO, T., 2003. Residual-mean solutions for the Antarctic Circumpolar Current and its associated overturning circulation. *J. Phys. Oceanogr.*, **22**, 2341–2354.

MARSHALL, J. & SCHOTT, F., 1999. Open-ocean convection: observations, theory, and models. *Rev. Geophys.*, **37**, 1–64.

MARSHALL, J. C., 1981. On the parameterization of geostophic eddies in the ocean. *J. Phys. Oceanogr.*, **11**, 257–271.

MARSHALL, J. C. & NURSER, A. J. G., 1992. Fluid dynamics of oceanic thermocline ventilation. *J. Phys. Oceanogr.*, **22**, 583–595.

MCCOMB, W. D., 1990. *The Physics of Fluid Turbulence.* Clarendon Press, 572 pp.

MCDOUGALL, T. J., JACKETT, D. R., WRIGHT, D. G. & FEISTEL, R., 2002. Accurate and compuationally efficient formulae for potential temperature and density of seawater. *J. Atmos. Ocean. Tech.*, **20**, 730–741.

MCINTOSH, P. C. & MCDOUGALL, T. J., 1996. Isopycnal averaging and the residual mean circulation. *J. Phys. Oceanogr.*, **26**, 1655–1660.

MCINTYRE, M. E. & NORTON, W. A., 1990. Dissipative wave-mean interactions and the transport of vorticity or potential vorticity. *J. Fluid Mech.*, **212**, 403–435.

MCINTYRE, M. E. & NORTON, W. A., 2000. Potential vorticity inversion on a hemisphere. *J. Atmos. Sci.*, **57**, 1214–1235.

MCINTYRE, M. E. & SHEPHERD, T. G., 1987. An exact local conservation theorem for finite-amplitude disturbances to nonparallel shear flows, with remarks on Hamiltonian structure and on Arnol'd's stability theorems. *J. Fluid Mech.*, **181**, 527–565.

MCWILLIAMS, J. C., 1984. The emergence of isolated coherent vortices in turbulent flow. *J. Fluid Mech.*, **146**, 21–43.

MELLOR, G. L., 1991. An equation of state for numerical models of oceans and estuaries. *J. Atmos. Ocean. Tech.*, **8**, 609–611.

MIHALJAN, J. M., 1962. A rigorous exposition of the Boussinesq approximations applicable to a thin layer of fluid. *Astrophysical J.*, **136**, 1126–1133.

MITTELBACH, F., GOOSSENS, M., BRAHMS, J., CARLISLE, D. & ROWLEY, C., 2004. *The LATEX Companion.* 2nd ed. Addison-Wesley, 1087 pp.

MOREL, P. & LARCHEVEQUE, M., 1974. Relative dispersion of constant-level balloons in the 200 mb general circulation. *J. Atmos. Sci.*, **31**, 2189–2196.

MUNDT, M., VALLIS, G. K. & WANG, J., 1997. Balanced models for the large- and meso-scale circulation. *J. Phys. Oceanogr.*, **27**, 1133–1152.

MUNK, W., 1966. Abyssal recipes. *Deep-Sea Res.*, **13**, 707–730.

MUNK, W. & WUNSCH, C., 1998. Abyssal recipes II: energetics of tidal and wind mixing. *Deep-Sea Res.*, **45**, 1976–2009.

MUNK, W. H., 1950. On the wind-driven ocean circulation. *J. Meteorol*, **7**, 79–93.

MUNK, W. H., GROVES, G. W. & CARRIER, G. F., 1950. Note on the dynamics of the Gulf Stream. *J. Mar. Res.*, **9**, 218–238.

MUNK, W. H. & PALMÉN, E., 1951. Note on dynamics of the Antarctic Circumpolar Current. *Tellus*, **3**, 53–55.

NAMIAS, J., 1959. Recent seasonal interaction between North Pacific waters and the overlying atmospheric circulation. *J. Geophys. Res.*, **64**, 631–646.

NOF, D., 2003. The Southern Ocean's grip on the northward meridional flow. In *Progress in Oceanography*, Vol. 56, pp. 223–247. Pergamon.

NOVIKOV, E. A., 1959. On the predictability of synoptic processes. *Izv. An. SSSR Ser. Geophys.*, **11**.

NURSER, A. G. & LEE, M.-M., 2004. Isopycnal averaging at constant height. Part I: The formulation and a case study. *J. Phys. Oceanogr.*, **34**, 2721–2739.

OBERBECK, A., 1879. Über die wärmeleitung der flüssigkeiten bei berücksichtigung der strömungen infolge vor temperaturdifferenzen (On the thermal conduction of liquids taking into account flows due to temperature differences). *Ann. Phys. Chem., Neue Folge*, **7**, 271–292.

OBERBECK, A., 1888. Über die bewegungserscheinungen der atmosphaere. *Sitzb. K. Preuss. Akad. Wiss*, **7**, 383–395 and 1129–1138. Translated in Smithsonian Misc. Coll. 1891. [English trans., 'On the phenomena of motion in the atmosphere', in *Theory of Thermal Convection*, B. Saltzman, Ed., Dover, 162–183].

OBUKHOV, A. M., 1941. Energy distribution in the spectrum of turbulent flow. *Izv. Akad. Nauk. SSR, Ser. Geogr. Geofiz.*, **5**, 453–466.

OBUKHOV, A. M., 1949. Structure of the temperature field in turbulent flows. *Izv. Akad. Nauk. SSR, Ser. Geogr. Geofiz.*, **13**, 58–63.

OBUKHOV, A. M., 1962. On the dynamics of a stratified liquid. *Dokl. Akad. Nauk SSSR*, **145**, 1239–1242. Eng. transl. in *Soviet Physics–Dokl.* 7, 682–684.

OETZEL, K. & VALLIS, G. K., 1997. Strain, vortices, and the enstrophy inertial range in two-dimensional turbulence. *Phys. Fluids*, **9**, 2991–3004.

OF CHICAGO PRESS, U., 2003. *The Chicago Manual of Style*. 15th ed. Univ. Chicago Press, 956 pp.

O'GORMAN, P. A. & PULLIN, D. I., 2005. Effect of Schmidt number of the velocity-scaler cospectrum. *J. Fluid Mech.*, **(submitted)**, xxxx.

OGURA, Y. & PHILLIPS, N. A., 1962. Scale analysis of deep and shallow convection in the atmosphere. *J. Atmos. Sci.*, **19**, 173–179.

OLBERS, D., BOROWSKI, D., VÖLKER, C. & WOLFF, J.-O., 2004. The dynamical balance, transport and circulation of the Antarctic Circumpolar Current. *Antarctic Science*, **xxx**, xxx.

PALMER, T. N., 1997. A nonlinear dynamical perspective on climate prediction. *J. Climate*, **12**, 575–591.

PAPARELLA, F. & YOUNG, W. R., 2002. Horizontal convection is non-turbulent. *J. Fluid Mech.*, **466**, 205–214.

PARES-SIERRA, A. & VALLIS, G., 1989. A fast semi-direct method for the numerical solution of non-separable elliptic equations in irregular domains. *J. Comp. Physics*, **82**, 398–412.

PEDLOSKY, J., 1964. The stability of currents in the atmosphere and ocean: Part i. *J. Atmos. Sci.*, **21**, 201–219.

PEDLOSKY, J., 1987. *Geophysical Fluid Dynamics*. 2nd ed. Springer, 710 pp.

PEDLOSKY, J., 1996. *Ocean Circulation Theory*. Springer, 453 pp.

PEIXOTO, J. P. & OORT, A. H., 1992. *Physics of Climate*. American Institute of Physics, 520 pp.

PERSSON, A., 1998. How do we understand the Coriolis force? *Bull. Am. Meteor. Soc.*, **79**, 1373–1385.

PHILANDER, S. G., 1990. *El Niño, La Niña, and the Southern Oscillation*. Academic Press, 289 pp.

PHILLIPS, N. A., 1963. Geostrophic motion. *Rev. Geophysics*, **1**, 123–176.

PHILLIPS, N. A., 1966. The equations of motion for a shallow rotating atmosphere and the traditional approximation. *J. Atmos. Sci.*, **23**, 626–630.

PHILLIPS, N. A., 1973. Principles of large-scale numerical weather prediction. In P. Morel, Ed., *Dynamic Meteorology*, pp. 1–96. Riedel.

PIERINI, S. & VULPIANI, A., 1981. Nonlinear stability analysis in multi-layer quasi-geostrophic system. *J. Phys. A*, **14**, L203–L207.

PIERREHUMBERT, R. T. & SWANSON, K. L., 1995. Baroclinic instability. *Annu. Rev. Fluid Mech.*, **27**, 419–467.

PLUMB, R. A., 1979. Eddy fluxes of conserved quantities by small-amplitude waves. *J. Atmos. Sci.*, **36**, 1699–1704.

PLUMB, R. A., 1990. A nonacceleration theorem for transient quasi-geostrophic eddies on a three-dimensional time-mean flow. *J. Atmos. Sci.*, **47**, 1825–1836.

PLUMB, R. A., 2002. Stratospheric transport. *J. Meteor. Soc. Japan*, **80**, 793–809.

PLUMB, R. A. & FERRARI, R., 2005. Transformed Eulerian-mean theory. Part I: non-quasigeostrophic theory for eddies on a zonal mean flow. *J. Phys. Oceanogr.*, **35**, 165–174.

POINCARÉ, H., 1893. *Leçons sur la Théorie des Tourbillons (Lessons on the theory of vortices [swirls])*. Paris.

POINCARÉ, H., 1908. *Science and Method*. Random House. Reprinted in *The Value of Science: Essential Writings of Henri Poincaré,* Ed. S. J. Gould.

POLZIN, K. L., TOOLE, J. M., LEDWELL, J. R. & SCHMIDT, R. W., 1997. Spatial variability of turbulent mixing in the abyssal ocean. *Science*, **276**, 93–96.

PRICE, J. F., WELLER, R. A. & SCHUDLICH, R. R., 1987. Wind-driven ocean currents and Ekman transport. *Science*, **238**, 1534–1538.

PROUDMAN, J., 1916. On the motion of solids in liquids. *Proc. Roy. Soc. Lond. A*, **92**, 408–424.

QUON, C. & GHIL, M., 1992. Multiple equilibria in thermosolutal convection due to salt-flux boundary conditions. *J. Fluid Mech.*, **245**, 449–484.

READ, P. L., 2001. Transition to geostrophic turbulence in the laboratory, and as a paradigm in atmospheres and oceans. *Surveys in Geophys.*, **33**, 265–317.

REIF, F., 1965. *Fundamentals of Statistical and Thermal Physics*. McGraw-Hill, 651 pp.

RHINES, P. B., 1975. Waves and turbulence on a β-plane. *J. Fluid. Mech.*, **69**, 417–443.

RHINES, P. B., 1977. The dynamics of unsteady currents. In E. A. Goldberg, I. N. McCane, J. J. O'Brien, and J. H. Steele, Eds., *The Sea*, Vol. 6, pp. 189–318. J. Wiley and Sons.

RHINES, P. B. & HOLLAND, W. R., 1979. A theoretical discussion of eddy-driven mean flows. *Dyn. Atmos. Oceans*, **3**, 289–325.

RHINES, P. B. & YOUNG, W. R., 1982a. Homogenization of potential vorticity in planetary gyres. *J. Fluid Mech.*, **122**, 347–367.

RHINES, P. B. & YOUNG, W. R., 1982b. A theory of wind-driven circulation. I. Mid-ocean gyres. *J. Mar. Res. (Suppl)*, **40**, 559–596.

RICHARDSON, L. F., 1920. The supply of energy from and to atmospheric eddies. *Proc. Roy. Soc. Lond. A*, **97**, 354–373.

RICHARDSON, L. F., 1922. *Weather Prediction by Numerical Process.* Cambridge University Press, 236 pp. Reprinted by Dover Publications.

RICHARDSON, L. F., 1926. Atmospheric diffusion on a distance-neighbour graph. *Proc. Roy. Soc. Lond. A*, **110**, 709–737.

RICHARDSON, P. L., 1983. Eddy kinetic-energy in the North Atlantic from surface drifters. *J. Geophys. Res.*, **88**, NC7, 4355–4367.

RINTOUL, S. R., HUGHES, C. & OLBERS, D., 2001. The Antarctic Circumpolar Current system. In G. Siedler, J. Church, and J. Gould, Eds., *Ocean Circulation and Climate*, pp. 271–302. Academic Press.

ROBINSON, A. R., Ed., 1984. *Eddies in Marine Science*. Springer-Verlag, 609 pp.

ROBINSON, A. R. & MCWILLIAMS, J. C., 1974. The baroclinic instability of the open ocean. *J. Phys. Oceanogr.*, **4**, 281–294.

ROBINSON, A. R. & STOMMEL, H., 1959. The oceanic thermocline and the associated thermohaline circulation. *Tellus*, **11**, 295–308.

ROOTH, C., 1982. Hydrology and ocean circulation. *Prog. Oceanogr.*, **11**, 131–149.

ROSSBY, C.-G., 1936. Dynamics of steady ocean currents in the light of experimental fluid dynamics. *Papers in Phys. Oceanog. and Meteor.*, **5**, 1–43.

ROSSBY, C.-G., 1938. On the mutual adjustment of pressure and velocity distributions in certain simple current systems. *J. Mar. Res.*, **5**, 239–263.

ROSSBY, C.-G., 1940. Planetary flow patterns in the atmosphere. *Quart. J. Roy. Meteor. Soc.*, **66,** suppl., 68–87.

ROSSBY, C.-G., 1949. On the nature of the general circulation of the lower atmosphere. In G. P. Kuiper, Ed., *The Atmospheres of the Earth and Planets*, pp. 16–48. University of Chicago Press.

ROSSBY, H. T., 1965. On thermal convection driven by non-uniform heating from below: an experimental study. *Deep-Sea Res.*, **12**, 9–16.

ROSSBY, H. T., 1998. Numerical experiments with a fluid heated non-uniformly from below. *Tellus*, **50A**, 242–257.

RUDNICK, D. L. & WELLER, R. A., 1993. Observations of superinertial and near-inertial wind-driven flow. *J. Phys. Oceanogr.*, **23**, 2351–2359.

RUELLE, D. & TAKENS, F., 1971. On the nature of turbulence. *Comm. Math. Phys.*, **20**, 167–192.

SALMON, R., 1980. Baroclinic instability and geostrophic turbulence. *Geophys. Astrophys. Fluid Dyn.*, **10**, 25–52.

SALMON, R., 1983. Practical use of Hamilton's principle. *J. Fluid Mech.*, **132**, 431–444.

SALMON, R., 1990. The thermocline as an internal boundary layer. *J. Mar. Res.*, **48**, 437–469.

SALMON, R., 1998. *Lectures on Geophysical Fluid Dynamics*. Oxford University Press, 378 pp.

SALTZMAN, B., 1962. Finite amplitude free convection as an initial value problem. *J. Atmos. Sci.*, **19**, 329–341.

SAMELSON, R. M., 1999a. Geostrophic circulation in a rectangular basin with a circumpolar connection. *J. Phys. Oceanogr.*, **29**, 3175–3184.

SAMELSON, R. M., 1999b. Internal boundary layer scaling in "two-layer" solutions of the thermocline equations. *J. Phys. Oceanogr.*, **29**, 2099–2102.

SAMELSON, R. M., 2004. Simple mechanistic models of middepth meridional overturning. *J. Phys. Oceanogr.*, **34**, 2096–2103.

SAMELSON, R. M. & VALLIS, G. K., 1997. Large-scale circulation with small diapycnal diffusion: The two-thermocline limit. *J. Mar. Res.*, **55**, 223–275.

SANDSTRÖM, J. W., 1908. Dynamische versuche mit meerwasser (Attempting dynamics with seawater). *Annal. Hydrogr. Marit. Meteorol.*, **36**, 6–23.

SANDSTRÖM, J. W., 1916. Meteologische studien in Schwedischen hochgebirge (Meteological studies in Swedish high mountains). *Goteborgs Kungl. Vetenskaps-och Vitterhets-Samhalles, Handingar*, **27**, 1–48.

SCHÄR, C., 1993. A generalization of Bernoulli's theorem. *J. Atmos. Sci.*, **50**, 1437–1443.

SCHMITZ, W. J., 1995. On the interbasin-scale thermohaline circulation. *Rev. Geophysics*, **33**, 151–173.

SCHNEIDER, E. K., 1977. Axially symmetric steady-state models of the basic state for instability and climate studies. Part II: Nonlinear calculations. *J. Atmos. Sci.*, **34**, 280–297.

SCHNEIDER, T., 2004. The tropopause and the thermal stratification of the extratropics of a dry atmosphere. *J. Atmos. Sci.*, **61**, 1317–1349.

SCHNEIDER, T., HELD, I. & GARNER, S. T., 2003. Boundary effects in potential vorticity dynamics. *J. Atmos. Sci.*, **60**, 1024–1040.

SCHUBERT, W. H., HAUSMAN, S. A., GARCIA, M., OOYAMA, K. V. & KUO, H.-C., 2001. Potential vorticity in a moist atmosphere. *J. Atmos. Sci.*, **58**, 3148–3157.

SCINOCCA, J. F. & SHEPHERD, T. G., 1992. Nonlinear wave-activity conservation laws and Hamiltonian structure for the two-dimensional anelastic equations. *J. Atmos. Sci.*, **49**, 5–28.

SHAPIRO, M. & GRØNAS, S., Eds., 1999. *The life cycles of extratropical cyclones*. American Meteorological Society, 359 pp.

SHEPHERD, T. G., 1983. Mean motions induced by baroclinic instability in a jet. *Geophys. Astrophys. Fluid Dyn.*, **27**, 35–72.

SHEPHERD, T. G., 1990. Symmetries, conservation laws, and Hamiltonian structure in geophysical fluid dynamics. *Adv. Geophys.*, **32**, 287–338.

SHEPHERD, T. G., 1993. A unified theory of available potential energy. *Atmosphere-Ocean*, **31**, 1–26.

SHEPHERD, T. G., 2002. Issues in stratosphere-troposphere coupling. *J. Meteor. Soc. Japan*, **80**, 769–792.

SHUTTS, G. J., 1983. Propagation of eddies in diffluent jet streams: Eddy vorticity forcing of blocking flow fields. *Quart. J. Roy. Meteor. Soc.*, **109**, 737–761.

SIEDLER, G., CHURCH, J. & GOULD, J., 2001. *Ocean Circulation and Climate: Observing and Modelling the Global Ocean*. Academic Press, 715 pp.

SILBERSTEIN, L., 1896. O tworzeniu sie wirow, w plynie doskonalym (On the creation of eddies in an ideal fluid). *W Krakaowie Nakladem Akademii Umiejetnosci (Proc. Cracow Acad. Sci.)*, **31**, 325–335. Also published as Über die Entstehung von Wirbelbewegungen in einer reibungslosen Flüssigkeit in *Bull. Int. l'Acad. Sci. Cracovie, Compte Rendue Scéances Année,* 280–290, 1896. Eng. translation by M. Ziemiánski available on this books web site.

SIMMONS, A. & HOSKINS, B., 1978. The life-cycles of some nonlinear baroclinic waves. *J. Atmos. Sci.*, **35**, 414–432.

SMAGORINSKY, J., 1953. The dynamical influences of large-scale heat sources and sinks on the quasi-stationary mean motions of the atmosphere. *Quart. J. Roy. Meteor. Soc.*, **79**, 342–366.

SMITH, K. S., BOCALLETTI, G., HENNING, C. C., MARINOV, I., TAM, F., HELD, I. & VALLIS, G., 2002. Turbulent diffusion in the geostrophic inverse cascade. *J. Fluid Mech.*, **469**, 13–48.

SMITH, K. S. & VALLIS, G. K., 1998. Linear wave and instability properties of extended range geostrophic models. *J. Atmos. Sci.*, **56**, 1579–1593.

SMITH, K. S. & VALLIS, G. K., 2001. The scales and equilibration of mid-ocean eddies: freely evolving flow. *J. Phys. Oceanogr.*, **31**, 554–571.

SMITH, K. S. & VALLIS, G. K., 2002. The scales and equilibration of mid-ocean eddies: forced-dissipative flow. *J. Phys. Oceanogr.*, **32**, 1669–1721.

SMITH, R. B., 1979. The influence of mountains on the atmosphere. In B. Saltzman, Ed., *Advances in Geophysics,* vol. 21, pp. 87–230. Academic Press.

SPALL, M. A., 2000. Generation of strong mesoscale eddies by weak ocean gyres. *J. Mar. Res.*, **58**, 97–116.

SPIEGEL, E. A. & VERONIS, G., 1960. On the Boussinesq approximation for a compressible fluid. *Astrophys. J.*, **131**, 442–447. (Correction: **135,** 655–656).

STAMMER, D., 1997. Global characteristics of ocean variability estimated from regional TOPEX/Poseidon altimeter measurements. *J. Phys. Oceanogr.*, **27**, 1743–1769.

STARR, V. P., 1948. An essay on the general circulation of the earth's atmosphere. *J. Meteor.*, **78**, 39–43.

STEERS, J. A., 1962. *An Introduction to the Study of Map Projections*. Univ. of London Press, 288 pp.

STEVENS, D. P. & IVCHENKO, V. O., 1997. The zonal momentum balance in an eddy-resolving general-circulation model of the southern ocean. *Quart. J. Roy. Meteor. Soc.*, **123**, 929–951.

STEWART, G. R., 1941. *Storm.* Random House, 349 pp.

STIPS, A., 2005. Dissipation measurement: theory. In H. Z. Baumert, J. Simpson, and J. Sündermann, Eds., *Marine Turbulence*. Cambridge University Press.

STOMMEL, H., 1958. The abyssal circulation. *Deep-Sea Res.*, **5**, 80–82.

STOMMEL, H., 1961. Thermohaline convection with two stable regimes of flow. *Tellus*, **13**, 224–230.

STOMMEL, H. & ARONS, A. B., 1960. On the abyssal circulation of the world ocean—i. Stationary planetary flow patterns on a sphere. *Deep-Sea Res.*, **6**, 140–154.

STOMMEL, H., ARONS, A. B. & FALLER, A. J., 1958. Some examples of stationary planetary flow patterns in bounded basins. *Tellus*, **10**, 179–187.

STOMMEL, H. & MOORE, D. W., 1989. *An Introduction to the Coriolis Force*. Columbia University Press, 297 pp.

STOMMEL, H. & WEBSTER, J., 1963. Some properties of the thermocline equations in a subtropical gyre. *J. Mar. Res.*, **44**, 695–711.

STONE, P. H., 1972. A simplified radiative-dynamical model for the static stability of rotating atmospheres. *J. Atmos. Sci.*, **29**, 405–418.

STONE, P. H., 1978. Baroclinic adjustment. *J. Atmos. Sci.*, **35**, 561–571.

STRAUB, D. N., 1993. On the transport and angular momentum balance of channel models of the Antarctic Circumpolar Current. *J. Phys. Oceanogr.*, **23**, 776–782.

SUTCLIFFE, R. C., 1939. Cyclonic and anticylonic development. *Quart. J. Roy. Meteor. Soc.*, **65**, 518–524.

SUTCLIFFE, R. C., 1947. A contribution to the problem of development. *Quart. J. Roy. Meteor. Soc.*, **73**, 370–383.

SWALLOW, J. C. & WORTHINGTON, V., 1961. An observation of a deep countercurrent in the western North Atlantic. *Deep-Sea Res.*, **8**, 1–19. Observations motivated by and consistent with Stommel Arons theory.

TALLEY, L., 1988. Potential vorticity distribution in the North Pacific. *J. Phys. Oceanogr.*, **18**, 89–106.

TAYLOR, G. I., 1921a. Diffusion by continuous movements. *Proc. London Math. Soc.*, **2 (20)**, 196–211.

TAYLOR, G. I., 1921b. Experiments with rotating fluids. *Proc. Roy. Soc. Lond. A*, **100**, 114–121.

TENNEKES, H. & LUMLEY, J. L., 1972. *A First Course in Turbulence*. The MIT Press, 330 pp.

TESSERENC DE BORT, L. P., 1902. Variations de la température de l'air libre dans la zone comprise 8 km et 13 km d'altitude (variations in the temperature of the free air in the zone between 8 km and 13 km of altitude). *C. R. Hebd. Sea. Acad. Sci.*, **134**, 987–989.

THOMPSON, P. D., 1957. Uncertainty of initial state as a factor in the predictability of large scale atmospheric flow patterns. *Tellus*, **9**, 275–295.

THOMSON, W. (LORD KELVIN), 1871. Hyrdokinetic solutions and observations. *Phil. Mag.*, **42**, 362–377.

THOMSON, W. (LORD KELVIN), 1879. On gravitational oscillations of rotating water. *Proc. Roy. Soc. Edinburgh*, **10**, 92–100.

THORPE, A. J., VOLKERT, H. & ZIEMIANSKI, M. J., 2003. The Bjerknes' circulation theorem: A historical perspective. *Bull. Am. Meteor. Soc.*, **84**, 471–480.

THUAL, O. & MCWILLIAMS, J. C., 1992. The catastrophe structure of thermohaline convection in a two-dimensional fluid model and a comparison with low-order box models. *Geophys. Astrophys. Fluid Dyn.*, **64**, 67–95.

THUBURN, J. & CRAIG, G. C., 1997. GCM tests of theories for the height of the tropopause. *J. Atmos. Sci.*, **54**, 869–882.

TOGGWEILER, J. R. & SAMUELS, B., 1995. Effect of Drake Passage on the global thermohaline circulation. *Deep-Sea Res.*, **42**, 477–500.

TOGGWEILER, J. R. & SAMUELS, B., 1998. On the ocean's large-scale circulation in the limit of no vertical mixing. *J. Phys. Oceanogr.*, **28**, 1832–1852.

TOOLE, J. M., POLZIN, K. L. & SCHMITT, R. W., 1994. Estimates of diapycnal mixing in the abyssal ocean. *Science*, **264**, 1120–1123.

TREGUIER, A. M., HELD, I. M. & LARICHEV, V. D., 1997. Parameterization of quasi-geostrophic eddies in primitive equation ocean models. *J. Phys. Oceanogr.*, **29**, 567–580.

TRITTON, D. J., 1988. *Physical Fluid Dynamics*. Oxford University Press, 519 pp.

TRUESDELL, C., 1951. Proof that Ertel's vorticity theorem holds in average for any medium suffering no tangential acceleration on the boundary. *Geofis Pura Appl.*, **19**, 167–169.

TRUESDELL, C., 1954. *The Kinematics of Vorticity*. Indiana University Press, 232 pp.

TUNG, K. K., 1979. A theory of stationary long waves. Part III: Quasi-normal modes in a singular wave guide. *Mon. Wea. Rev.*, **107**, 751–774.

UNESCO, 1981. The practical salinity scale 1978 and the international equation of state of seawater 1980. Tenth report of the joint panel on oceanographic tables and standards. Technical report, UNESCO Technical Papers in Marine Science No. 36, Paris.

VALLIS, G. K., 1982. A statistical dynamical climate model with a simple hydrology cycle. *Tellus*, **34**, 211–227.

VALLIS, G. K., 1985. Instability and flow over topography. *Geophys. Astrophys. Fluid Dyn.*, **34**, 1–38.

VALLIS, G. K., 1988. Numerical studies of eddy transport properties in eddy-resolving and parameterized models. *Quart. J. Roy. Meteor. Soc.*, **114**, 183–204.

VALLIS, G. K., 1996. Potential vorticity and balanced equations of motion for rotating and stratified flows. *Quart. J. Roy. Meteor. Soc.*, **122**, 291–322.

VALLIS, G. K., 2000. Large-scale circulation and production of stratification: effects of wind, geometry and diffusion. *J. Phys. Oceanogr.*, **30**, 933–954.

VALLIS, G. K., 2005. *Atmospheric and Oceanic Fluid Dynamics*. Cambridge University Press. This book, draft available from www.princeton.edu/~gkv/aofd.

VALLIS, G. K. & MALTRUD, M. E., 1993. Generation of mean flows and jets on a beta plane and over topography. *J. Phys. Oceanog.*, **23**, 1346–1362.

VERONIS, G., 1966a. Wind-driven ocean circulation, part 1: Linear theory and perturbation analysis. *Deep-Sea Res.*, **13**, 17–29.

VERONIS, G., 1966b. Wind-driven ocean circulation, part 2: Numerical solutions of the non-linear problem. *Deep-Sea Res.*, **13**, 30–55.

VERONIS, G., 1969. On theoretical models of the thermocline circulation. *Deep-Sea Res.*, **31** Suppl., 301–323.

VISBECK, M., MARSHALL, J., HAINE, T. & SPALL, M., 1997. Specification of eddy transfer coefficients in coarse-resolution ocean circulation models. *J. Phys. Oceanogr.*, **27**, 381–402.

WALKER, C. & SCHNEIDER, T., 2005. Response of idealized Hadley circulations to seasonally varying heating. *Geophys. Res. Lett.*, **32**, L06813, doi:10.1029/2004GL022304.

WALLACE, J. M., 1983. The climatological mean stationary waves: observational evidence. In B. Hoskins and R. P. Pearce, Eds., *Large-Scale Dynamical Processes in the Atmosphere*, pp. 27–63. Academic Press.

WARN, T., BOKHOVE, O., SHEPHERD, T. G. & VALLIS, G. K., 1995. Rossby number expansions, slaving principles, and balance dynamics. *Quart. J. Roy. Meteor. Soc.*, **121**, 723–739.

WARREN, B. A., 1981. Deep circulation of the world ocean. In B. A. Warren and C. Wunsch, Eds., *Evolution of Physical Oceanography*, pp. 6–41. MIT Press.

WARREN, B. A., LaCASCE, J. H. & ROBBINS, P. E., 1996. On the obscurantist physics of form drag in theorizing about the circumpolar current. *J. Phys. Oceanogr.*, **26**, 2297–2301.

WASOW, W., 1944. Asymptotic solution of boundary value problems for the differential equation $\Delta U + \lambda(\partial/\partial x)U = \lambda f(x, y)$. *Duke Math J.*, **11**, 405–415.

WATANABE, T., IWAYAMA, T. & FUJISAKA, H., 1998. Scaling law for coherent vortices in decaying drift rossby wave turbulence. *Phys. Rev. E*, **57**, 1636–1643.

WEBB, D. J. & SUGINOHARA, N., 2001. Vertical mixing in the ocean. *Nature*, **409**, 37.

WEINSTOCK, R., 1952. *Calculus of Variations*. McGraw-Hill, Reprinted by Dover Publications 1980, 328 pp.

WELANDER, P., 1959. An advective model of the ocean thermocline. *Tellus*, **11**, 309–318.

WELANDER, P., 1968. Wind-driven circulation in one-and two-layer oceans of variable depth. *Tellus*, **20**, 1–15.

WELANDER, P., 1971a. Some exact solutions to the equations describing an ideal-fluid thermocline. *J. Mar. Res.*, **29**, 60–68.

WELANDER, P., 1971b. The thermocline problem. *Phil. Trans. Roy. Soc. Lond. A*, **270**, 415–421.

WELANDER, P., 1973. Lateral friction in the ocean as an effect of potential vorticity mixing. *Geophys. Fluid Dyn.*, **5**, 101–120.

WELANDER, P., 1986. Thermohaline effects in the ocean circulation and related simple models. In J. Willebrand and D. L. T. Anderson, Eds., *Large-scale transport processes in oceans and atmospheres*, pp. 163–200. Reidel.

WHITE, A. A., 1977. Modified quasi-geostrophic equations using geometric height as vertical co-ordinate. *Quart. J. Roy. Meteor. Soc.*, **103**, 383–396.

WHITE, A. A., 2002. A view of the equations of meteorological dynamics and various approximations. In J. Norbury and I. Roulstone, Eds., *Large-Scale Atmosphere-Ocean Dynamics I*, pp. 1–100. Cambridge University Press.

WHITE, A. A., 2003. The primitive equations. In J. Holton, J. Pyle, and J. Curry, Eds., *Encyclopedia of Atmospheric Science*, pp. 694–702. Academic Press.

WHITEHEAD, J. A., 1995. Thermohaline ocean processes and models. *Ann. Rev. Fluid Mech.*, **27**, 89–113.

WHITHAM, G. B., 1974. *Linear and Nonlinear Waves*. Wiley-Interscience, 656 pp.

WORLD METEOROLOGICAL ORGANIZATION, 1957. Meteorology: A three dimensional science. Second session of the Commission for Aerology. *WMO Bulletin*, **IV**, 134–138.

WRIGHT, D. G., 1997. An equation of state for use in ocean models: Eckart's formula revisited. *J. Atmos. Ocean. Tech.*, **14**, 735–740.

WUNSCH, C., 2002. What is the thermohaline circulation? *Science*, **298**, 1179–1180.

WUNSCH, C. & FERRARI, R., 2004. Vertical mixing, energy, and the general circulation of the oceans. *Ann. Rev. Fluid Mech.*, **36**, 281–314.

WUNSCH, C. & ROEMMICH, D., 1985. Is the North Atlantic in Sverdrup balance? *J. Phys. Oceanogr.*, **15**, 1876–1880.

WYRTKI, K., MAGAARD, L. & HAGER, J., 1976. Eddy energy in oceans. *J. Geophys. Res.*, **81**, 15, 2641–2646.

YAGLOM, A. M., 1994. A. N. Kolmogorov as a fluid mechanician and founder of a school in turbulence research. *Ann. Rev. Fluid Mech.*, **26**, 1–22.

YOUNG, W. R. & RHINES, P. B., 1982. A theory of the wind-driven circulation II. Gyres with western boundary layers. *J. Mar. Res.*, **40**, 849–872.

ZDUNKOWSKI, W. & BOTT, A., 2003. *Dynamics of the Atmosphere: A Course in Theoretical Meteorology.* Cambridge University Press, 719 pp.

ZHANG, R. & VALLIS, G. K., 2006. The role of the deep western boundary current in the gulf stream path and northern recirculation gyre. *J. Phys. Oceanogr.*, (submitted).